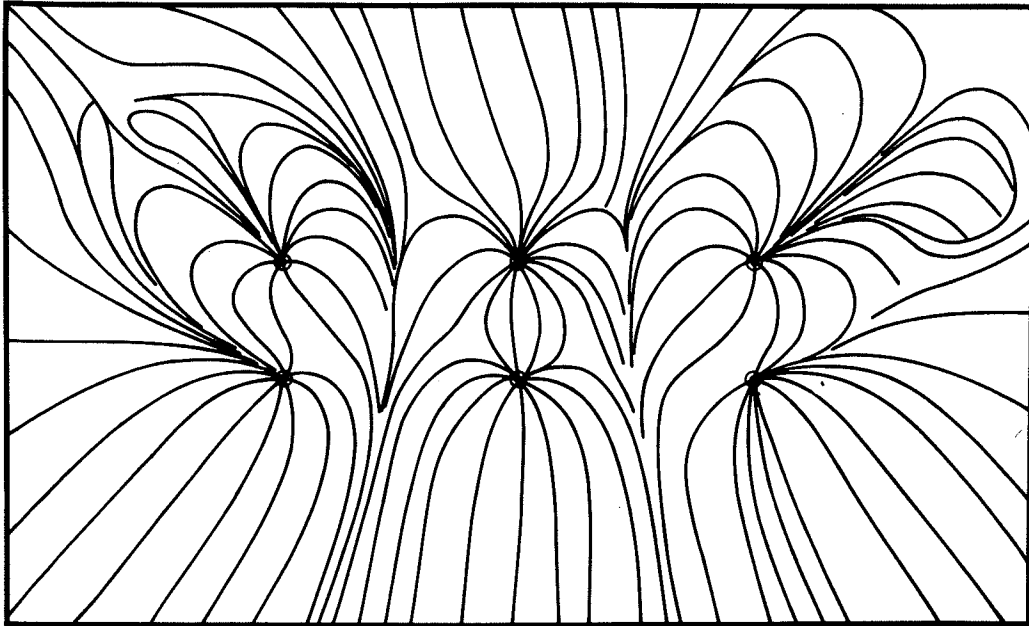
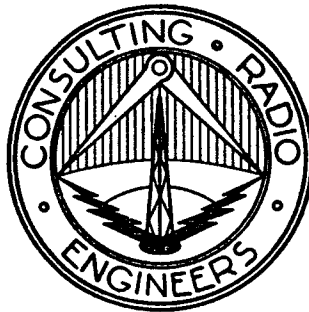


# THE DESIGN OF NON-RADIAL GROUND SYSTEMS FOR MEDIUM-WAVE DIRECTIONAL ANTENNAS



COHEN AND DIPPELL  
RECEIVED  
APR 26 1978  
WASHINGTON, D.C.



OGDEN PRESTHOLDT  
1978 NAB ENGINEERING CONFERENCE

---

A. D. RING & ASSOCIATES

WASHINGTON, D. C.

---

THE DESIGN OF NON-RADIAL GROUND SYSTEMS  
FOR MEDIUM-WAVE DIRECTIONAL ANTENNAS

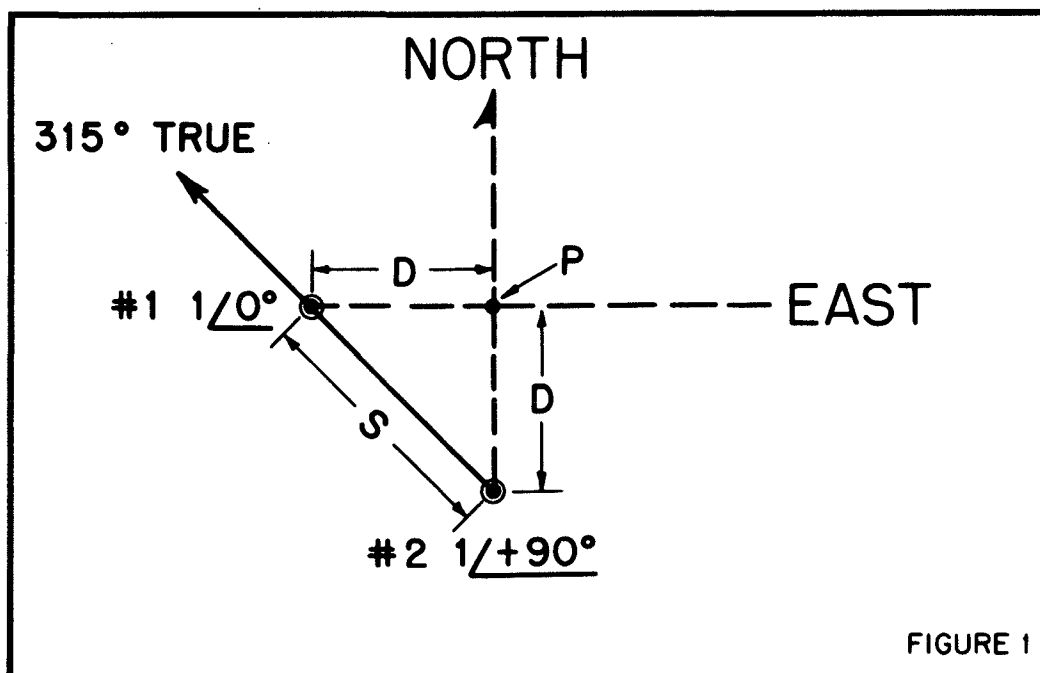
By Ogden Prestholdt

A. D. Ring and Associates

I. Introduction

It is well known that the ground currents in the immediate vicinity of a medium-wave nondirectional vertical transmitting antenna flow along radial lines to and from the base of the antenna. It also has been customary to install buried radial wires as the principal part of the ground system of medium-wave directional antennas. An example will demonstrate that in general the ground currents from a directional antenna do not follow such simple radial paths.

Consider the simple directional antenna shown in Figure 1.

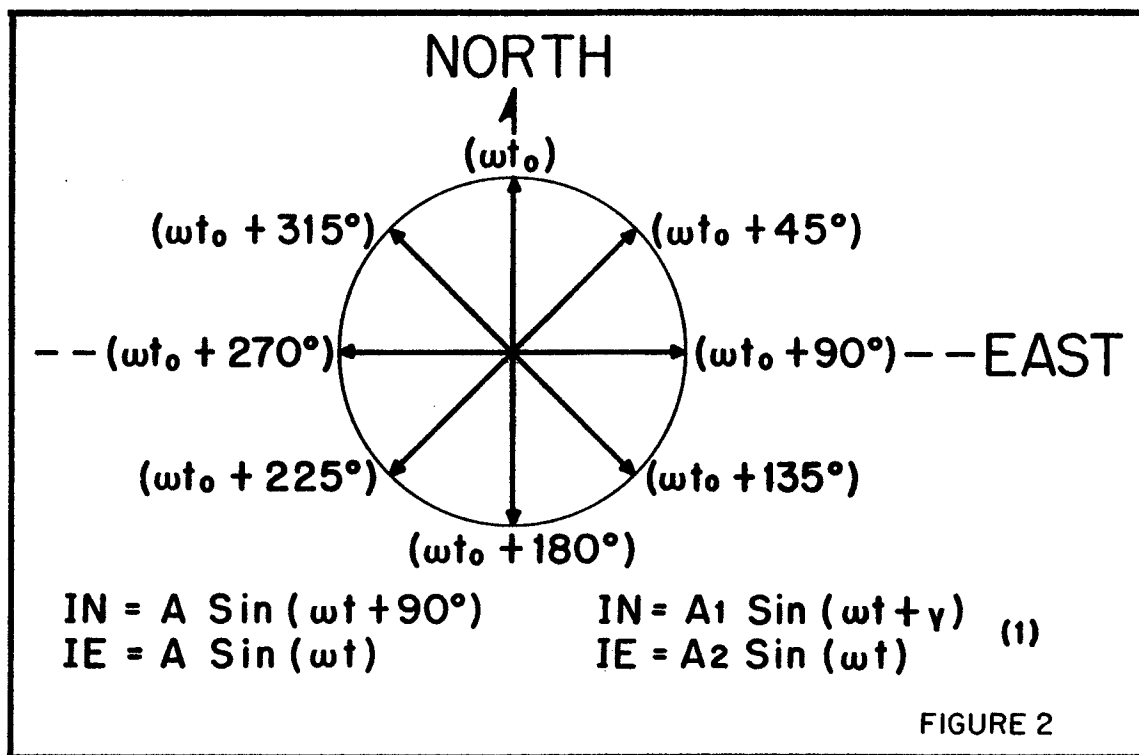




The antenna system consists of two identical antennas oriented along a line whose bearing is  $315^\circ$  true. Antenna No. 1 has a field ratio of 1.0 and a relative phase of  $0^\circ$ , antenna No. 2 also has a field ratio of 1.0 but with a relative phase of  $+90^\circ$ . The spacing, chosen to be  $180^\circ$ , is not important for the example. Select a point (P) such that it is directly east of antenna No. 1 and north of antenna No. 2. Because of the orientation of the array it is also equidistant from the two antennas.

Now, if we excite only antenna No. 1 the ground current at point (P) will be an alternating current flowing east and west with a time phase corresponding to the phase of the current in antenna No. 1 at some earlier time. Similarly, if we excite only antenna No. 2, the ground current at point (P) will flow north and south, its time phase will be delayed from the current in antenna No. 2 by the same delay as that which occurred for antenna No. 1.

Let us now excite the directional antenna as depicted by Figure 1 and examine the resulting ground current flowing at point (P). At some specific time ( $t_0$ ) during the R.F. cycle the east-west current at point (P) will have zero amplitude in its flow cycle. At that same instant of time the ground current from antenna No. 2 at point (P) will be advanced in time phase by  $90^\circ$  since the phase of the current in that antenna is advanced by  $90^\circ$ . Thus at time ( $t_0$ ) the instantaneous current from antenna No. 2 at point (P) will be at its maximum value and will be flowing north.



The north directed vector identified by  $(\omega t_0)$  on Figure 2 represents the ground current at time  $(t_0)$ . One eighth of an R. F. cycle later  $(45^\circ)$  the ground current from antenna No. 1 will be  $\sqrt{2}/2$  times its maximum value and will be flowing east. The ground current from antenna No. 2 will be reduced to  $\sqrt{2}/2$  times its maximum value and will still be flowing north. The resultant of these two currents is an instantaneous linear current of unity amplitude or the  $\sqrt{2}$  times each component and is flowing toward the northeast. Another eighth cycle later  $(90^\circ)$  after time  $(t_0)$ , the instantaneous ground current from antenna No. 1 is at maximum value and is flowing eastward while the contribution from antenna No. 2 has reduced to zero.

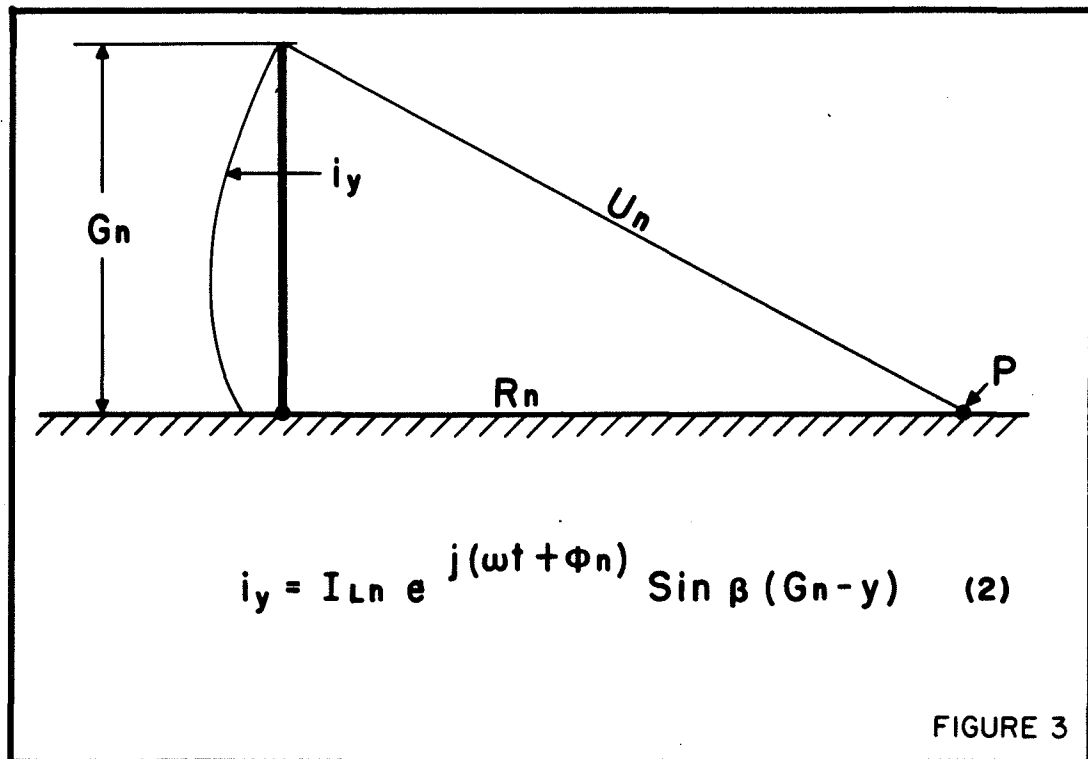
Continuing through the R.F. cycle and plotting the vector representing the direction and magnitude of the instantaneous ground current for each eighth of the cycle at point (P) we arrive at the full display shown on Figure 2. We see that locus of the tip of this ground current vector at point (P) is a circle and at any time during the R.F. cycle the amplitude and direction of the ground current can be found from the parametric equations shown as the left pair of equations on Figure 2.

If the field ratio of the directional antenna in Figure 1 is changed from unity and if the phase relationship is altered we obtain the general parametric equations identified as (1) on Figure 2. These are the general parametric equations of an ellipse centered in the coordinate system but with arbitrary orientation. In general, the locus of the tip of ground current vector at any point (P) in the near field of a directional antenna is an ellipse.

## II. Calculation of Ground Currents.

Assuming perfectly conducting ground at the site of the directional antenna, the ground current at a specific point on the site may be deduced from the magnetic field strength at that point. Figure 3 depicts a base fed vertical antenna, the subscript (n) is used to denote that it is the nth antenna in the directional system.

Figure 4 defines the various terms in equation (2) and on Figure 3.



$G_n$  = Height of antenna, meters

$R_n$  = Distance from (P) to base of antenna, meters

$U_n$  = Distance from (P) to top of antenna, meters

$\lambda$  = Wavelength, meters

$\beta$  =  $2\pi / \lambda$

$I_{Ln}$  = Peak loop current, amperes

$\Phi_n$  = Relative phase of ( $I_{Ln}$ ), radians

FIGURE 4

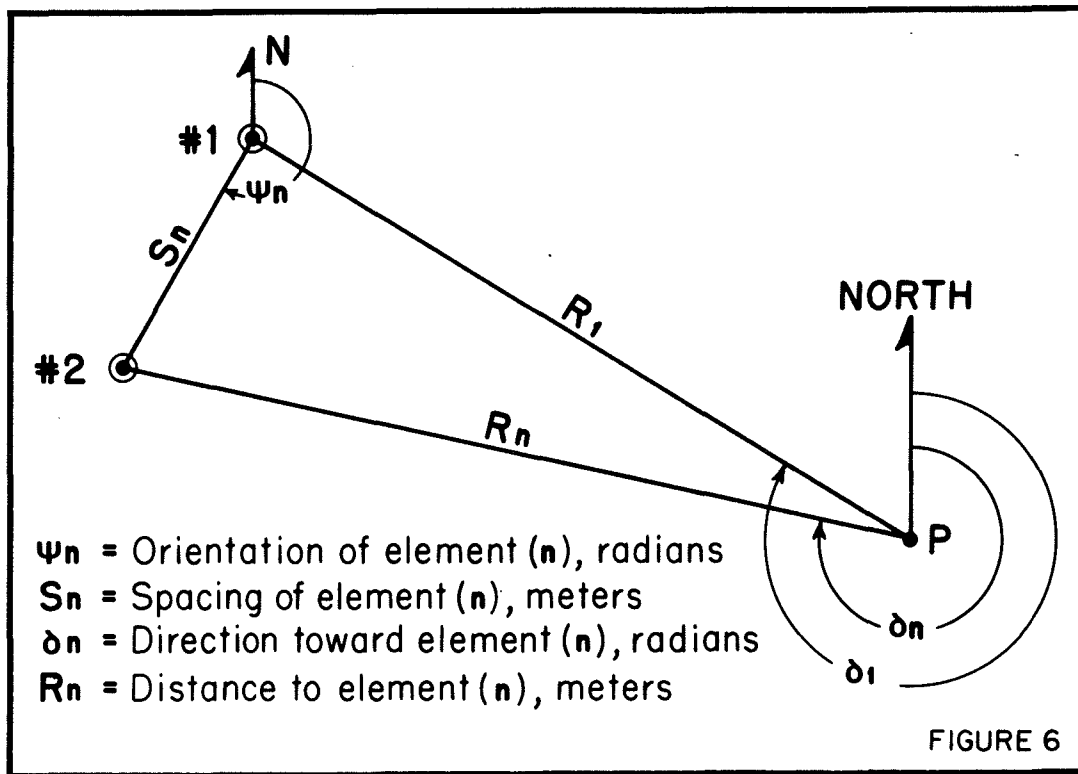
$$B_{\psi} = j \frac{2 \cdot 10^{-9} I_{Ln} e^{j(\omega t + \Phi_n)}}{R_n} \left[ e^{-j\beta U_n} - (\cos \beta G_n) e^{-j\beta R_n} \right] \quad (3)$$

$$I_{Gn} = j \frac{I_{Ln} e^{j(\omega t + \Phi_n)}}{R_n} \left[ e^{-j\beta U_n} - (\cos \beta G_n) e^{-j\beta R_n} \right] \quad (4)$$

FIGURE 5

The magnetic field strength at ground level may be found by taking the Curl of Vector Potential of the current  $i_y$  throughout the antenna.  $\beta\psi$ , shown on Figure 5 as equation (3) is the magnetic field strength on the ground and follows counter clockwise circles concentric to the antenna when  $I_{Ln}$  is assumed to be flowing upward. The corresponding ground current  $I_{Gn}$  is shown as equation (4) on Figure 5.  $I_{Gn}$  is the instantaneous ground current in amperes per meter of arc, flowing toward antenna (n), its time phase with respect to  $I_{Ln}$  is as indicated by the exponentials. It is important to note that  $I_{Gn}$  represents only the amplitude and time phase of the ground current. It is incomplete in that it does not specify the direction of the current flow; it infers that it is toward

the  $n$ th antenna. Thus, we see that the ground current at a specific point must be described by three kinds of numbers, one representing direction, one representing amplitude and one representing time (or phase). We can completely describe the ground current by resolving  $I_{Gn}$  into two components, one in the north-south direction and the other in the east-west direction, each with appropriate amplitude and phase.

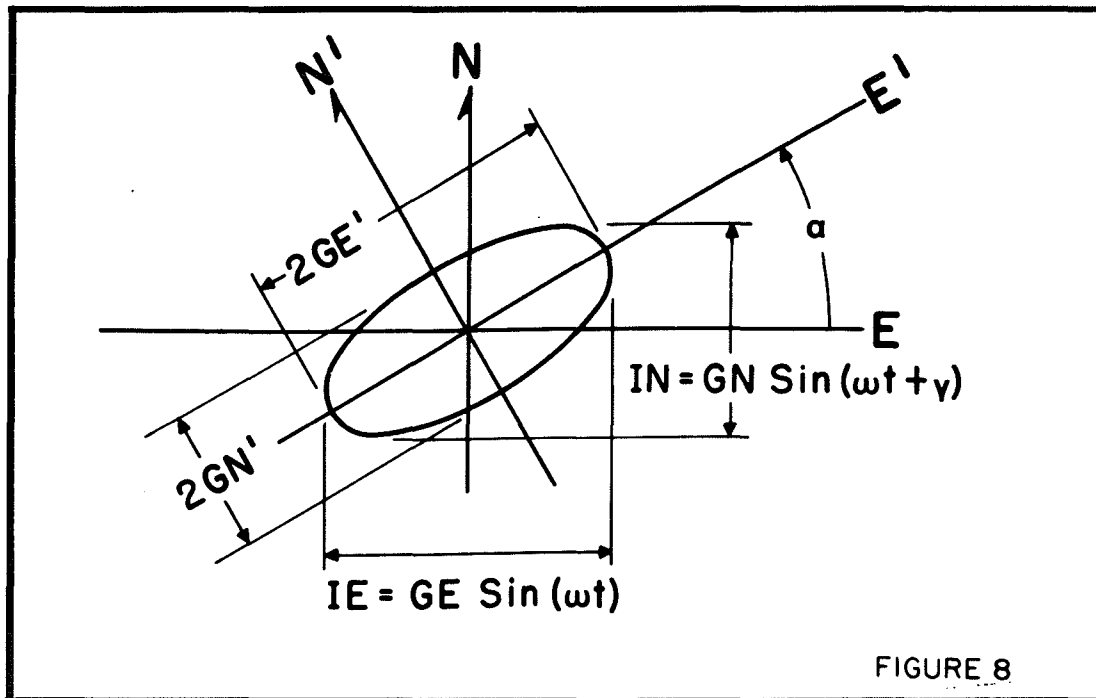


The total ground current at point (P) in the near field of a directional antenna may be found by summing up the components from the various antennas with the aid of the geometry shown in Figure 6.

$$IN = \sum_{n=1}^{n=m} j \frac{(\cos \delta_n) I_{Ln} e^{j(\omega t + \phi_n)}}{R_n} \left[ e^{-j\beta U_n} - (\cos \beta G_n) e^{-j\beta R_n} \right] \quad (5)$$

$$IE = \sum_{n=1}^{n=m} j \frac{(\sin \delta_n) I_{Ln} e^{j(\omega t + \phi_n)}}{R_n} \left[ e^{-j\beta U_n} - (\cos \beta G_n) e^{-j\beta R_n} \right] \quad (6)$$

FIGURE 7



The total ground current at point (P) consists of two orthogonal components which are shown as equations (5) and (6) on Figure 7. These are the parametric equations of the ellipse

which is the locus of the tip of the ground current vector at point (P) throughout the R.F. cycle.

Figure 8 shows how these parametric equations describe the general ellipse and the orientation of the new coordinate system in which we can identify the magnitude of the current along the semi-axes of the ellipse.

In order to determine the orientation and magnitude of the current component along the major and minor axes of the ellipse we start with the modified parametric equations (7) and (8) shown on Figure 9. These equations are obtained by appropriate expansion of the exponentials in equations (5) and (6) and by collecting real and imaginary terms. For simplicity  $M_1$ ,  $N_1$ ,  $M_2$ , and  $N_2$  are substituted for the lengthy expressions which result from the foregoing steps.

$$IN = M_1 + jN_1 = \sqrt{M_1^2 + N_1^2} \angle \tan^{-1}(N_1/M_1) \quad (7)$$

$$IE = M_2 + jN_2 = \sqrt{M_2^2 + N_2^2} \angle \tan^{-1}(N_2/M_2) \quad (8)$$

$$IN = GN \sin(\omega t + \gamma) \quad (9)$$

$$IE = GE \sin(\omega t) \quad (10)$$

$$\gamma = \tan^{-1}(N_1/M_1) - \tan^{-1}(N_2/M_2) \quad (11)$$

FIGURE 9



We then eliminate the parameter ( $\omega t$ ) from the parametric equations and obtain the equation of the ellipse in rectangular coordinates. That equation is then transformed into a similar equation in a coordinate system that has been rotated counter-clockwise through an angle  $\alpha$  from the original coordinate system. Now by equating to zero the coefficient of the  $IN'xIE'$  term and solving for  $\alpha$  we obtain the necessary angle of rotation. From the coefficient of the  $(IN')^2$  and  $(IE')^2$  terms we obtain the magnitude of the two orthogonal current components in the new coordinate system. The angle of rotation and the two magnitudes are the three parameters we are looking for.

Figure 10 shows the values, at the point (P), of the three ellipse parameters  $\alpha$ ,  $GN'$ , and  $GE'$  in terms of the parameters of the general ellipse equations (9), (10) and (11).

$$\alpha = \frac{1}{2} \tan^{-1} \left( \frac{2 GN \cdot GE \cos \gamma}{GE^2 - GN^2} \right) \quad (12)$$

$$GN' = \left| \frac{\sin \gamma}{\sqrt{\left(\frac{\cos \alpha}{GN}\right)^2 + \left(\frac{\sin \alpha}{GE}\right)^2 + \frac{\cos \gamma \sin 2\alpha}{GN \cdot GE}}} \right| \quad (13)$$

$$GE' = \left| \frac{\sin \gamma}{\sqrt{\left(\frac{\sin \alpha}{GN}\right)^2 + \left(\frac{\cos \alpha}{GE}\right)^2 - \frac{\cos \gamma \sin 2\alpha}{GN \cdot GE}}} \right| \quad (14)$$

FIGURE 10

### III. Computer Program

It can be readily seen from equations 5 and 6 that the calculations of the various components of the ground current at each point within the ground system of a multi-element directional array is a lengthy and tedious process. It is necessary to use modern computer techniques to permit one to make a sufficient number of calculations to understand the nature of the ground current throughout the ground system of the directional antenna. A computer program for this analysis has been written which provides three different types of printout. A description of the various types of printouts with examples will provide an insight into the nature of the ground currents in directional antennas.

The inputs to the program include the transmitter power, operating frequency, the loop current and phase in each tower and the spacing and orientation of each tower from the reference tower. The scale and coordinates of the reference tower are also selectable.

The amplitude, phase and direction of the ground current from each tower is computed at the selected point. Then the complete analysis previously described is performed to arrive at a set of three numbers, one of which represents the amplitude of the ground current in the major semi-axis direction, one of which represents the amplitude of the ground current in the minor semi-axis direction and a third which represents the orientation of the ellipse axes with respect to true north.

The first printout format is one which shows the magnitude of the principal component of the current,  $IN'$  or  $IE'$ , whichever is the larger, at each location in the printout field. The actual computed ground currents are compared to the ground current at a specified distance from a standard tower with specified height and power. The reference is changeable within the program at the user's option. The standard tower normally used is a  $1/4$  wave tower driven with the power which is feeding the antenna array under consideration and the ground current at a distance of  $1/8$  wave length from the standard tower is the selected reference.

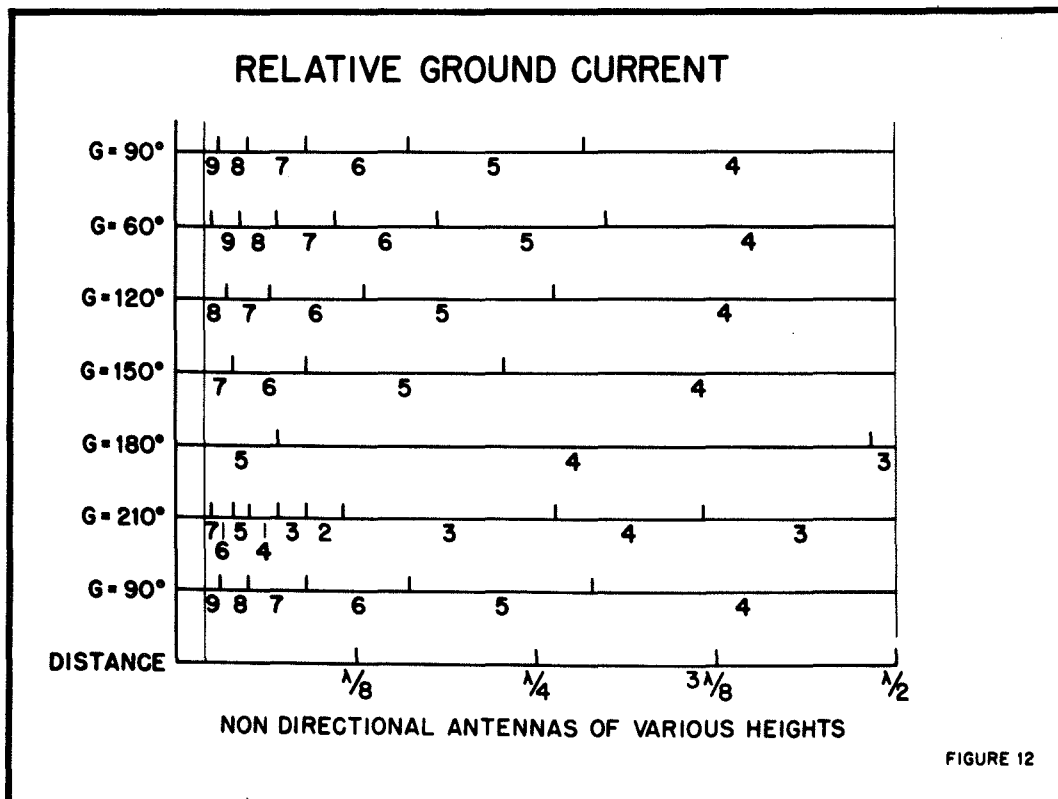
Each amplitude is ratioed to the reference ground current from the standard tower. In order to convert these ratios to a simple printout format a stepped function is used which has

<u>CHARACTER PRINTED</u>	<u>RELATIVE GROUND CURRENT</u>	
	<u>RATIO</u>	<u>dB</u>
+	10.000	20
9	5.623	15
8	3.162	10
7	1.778	5
6	1.000	0
5	0.5623	-5
4	0.3162	-10
3	0.1778	-15
2	0.1000	-20
1	0.0562	-25
0	0.	

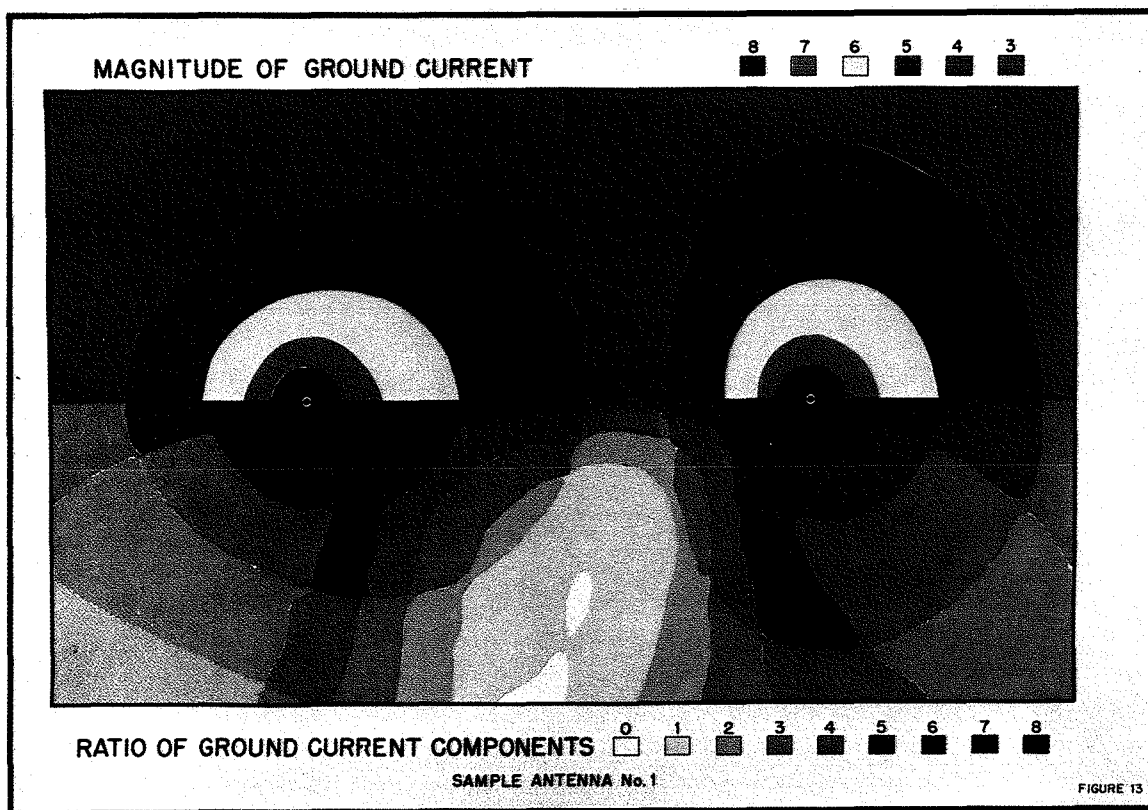
FIGURE 11

the ratio of successive steps being equivalent to the fourth root of ten. Figure 11 shows the ratios and the equivalence of these ratios to a one digit number to be used in the print-out. The chosen scale has a dynamic range of more than 40 dB which is sufficient to display the current amplitudes in any array yet tested.

As a demonstration of the use of this ground current amplitude indication scheme we have prepared an analysis of the ground current from single towers of varying heights. A one-line printout for each of six different tower heights (60°, 90°, 120°, 150°, 180°, 210°) is shown on Figure 12.



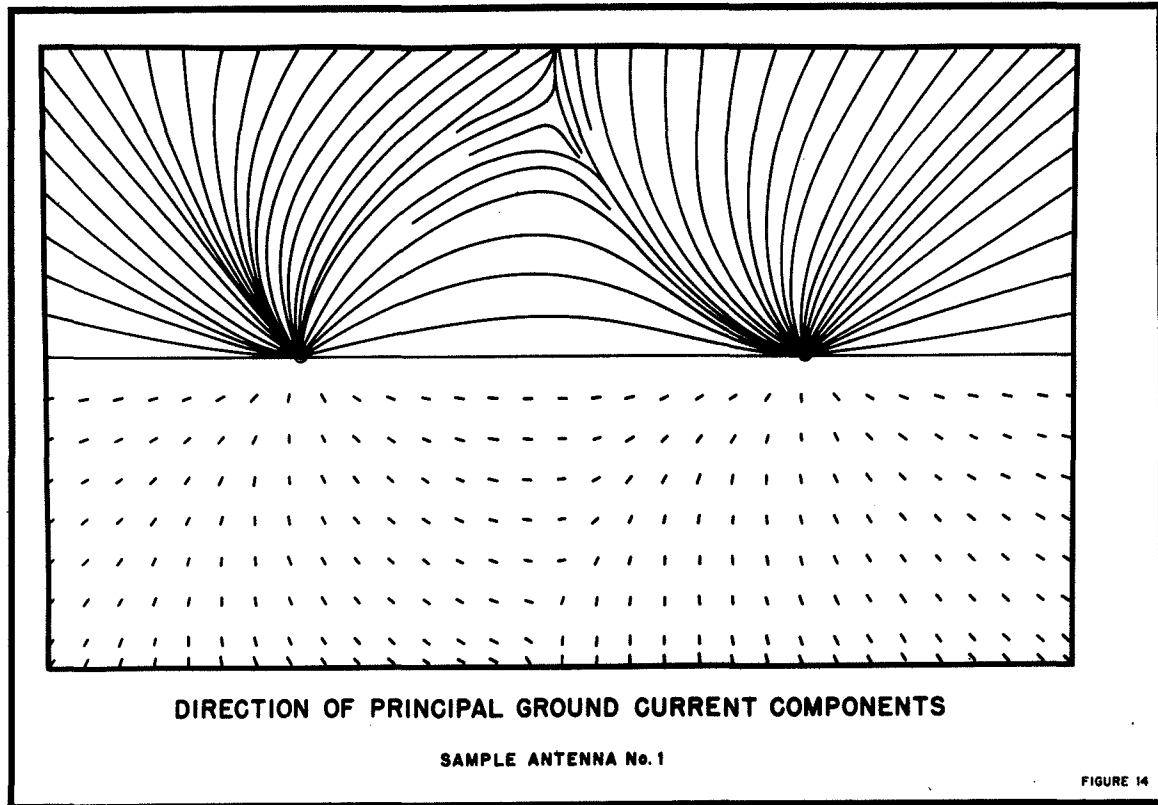
Now let us apply that analysis to a simple directional antenna. The upper half of Figure 13 shows the ground currents in the two element antenna used in the opening example. It was derived by this process but rather than printout the individual numbers in Figure 13 we have used a different color to represent each step of current amplitude. The legend shows the current ratio key for each color.



The second important concept to be mapped is the ratio of the two components. We wish to know where the current is changing direction throughout the R.F. cycle or where it is not changing direction during the cycle. If the two orthogonal components are approximately equal in magnitude, the

current is continuously changing in direction at that point. Since both of the components are scaled to a simple integer series we can determine the relative circularity or eccentricity of the ellipse by subtracting the integer magnitude of one component from the integer magnitude of the other component. If the absolute value of the difference is zero the locus of the tip of the current vector is approximately a circle, whereas, if it differs by three or four units the current is essentially in the same direction at all times. The lower half of Figure 13 is a printout generated by this process. The legend shows the ratio of the two components as found by this process.

The third form of printout is one which specifies the direction of the principal component of the ground current at each point. For this printout a two character word was devised, the first character identifies the 45° sector within which the major component of current is directed and the second character defines a 5° increment with that sector. The upper half of Figure 14 was prepared from such a printout and shows the directions of flow for the principle components of current in the same two element directional antenna. The lower half of the figure shows the direction of the major current component at selected points in the field.



#### IV. Some Typical Examples

We have chosen three directional antennas to demonstrate the unusual nature of the ground currents for directional antennas which provide deep suppression over wide angles.

Sample antenna No. 2 consists of three half wave-length antennas spaced approximately  $90^\circ$ . It produces a cardioid pattern typical of that used by many class I-B stations.

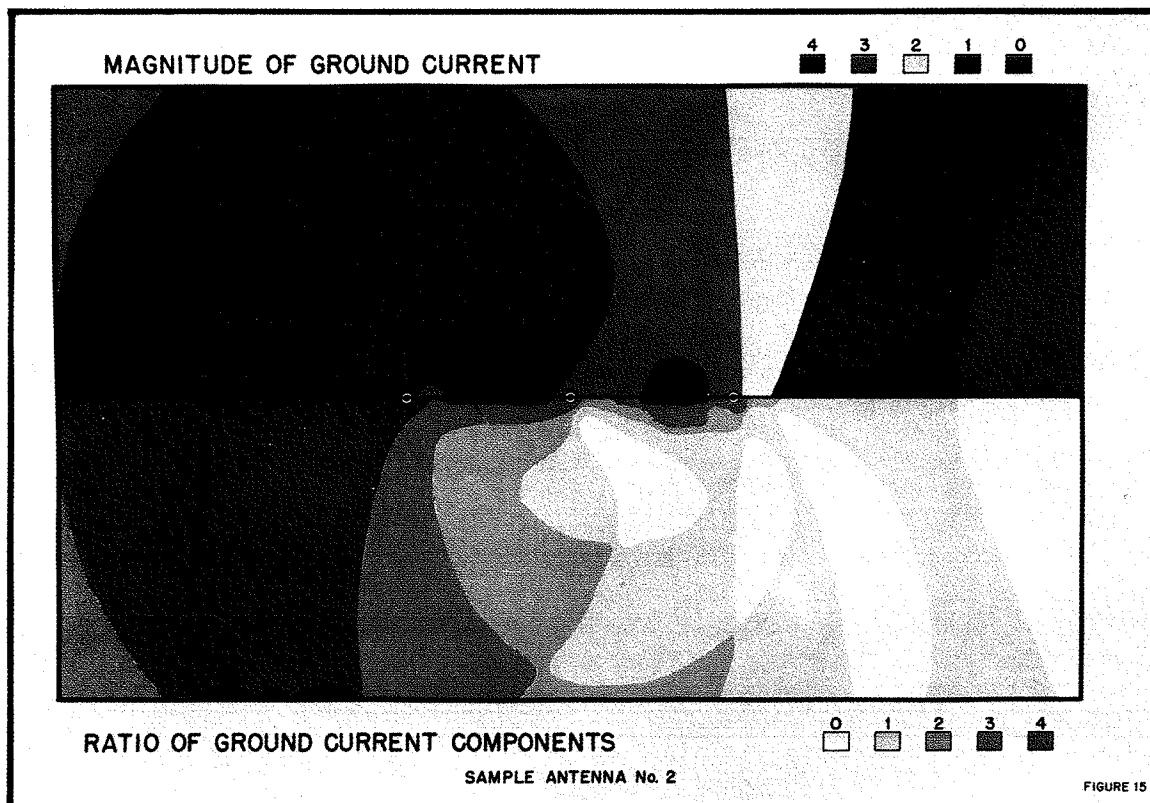
Sample antenna No. 3 consists of a four element parallelogram with  $90^\circ$  and  $180^\circ$  spacings, the antennas are of intermediate height. Its suppression is comparable to that of many class II stations.

Sample antenna No. 4 consists of a six element array in a three by two configuration. The spacing is  $180^\circ$  in the three

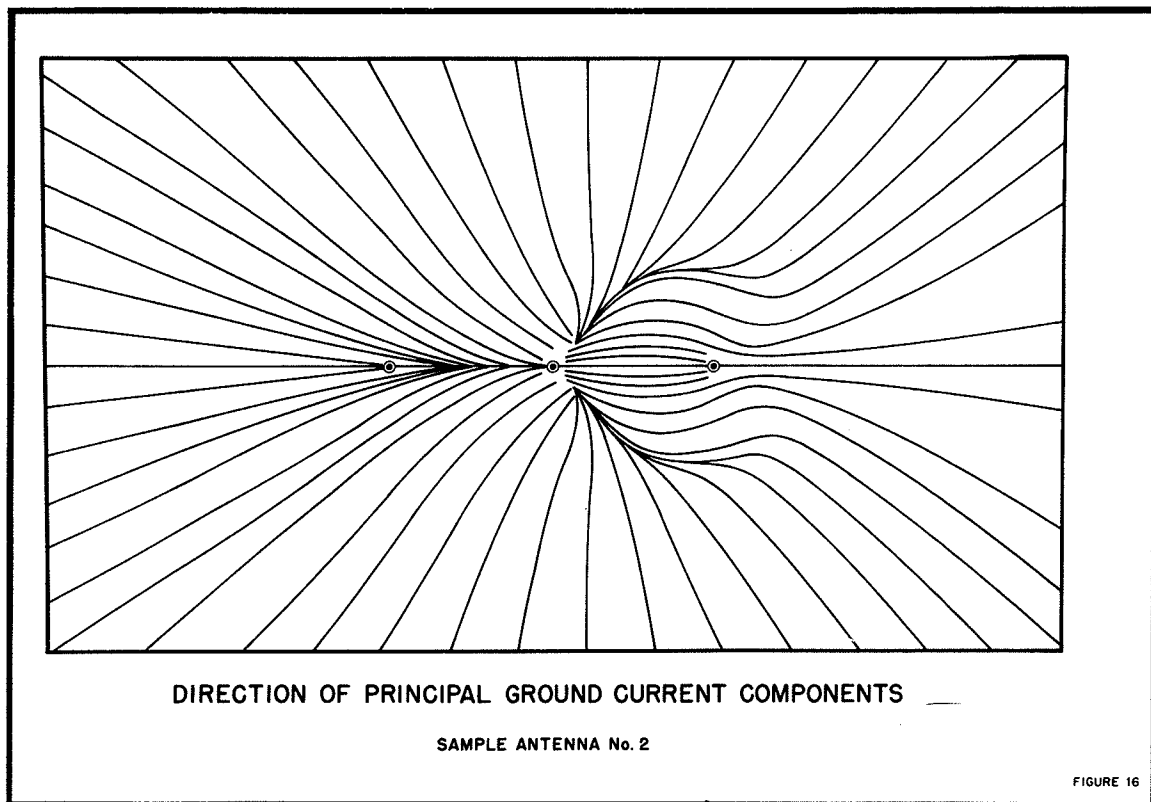
in line dimension and  $90^\circ$  in the other direction. The antenna elements are approximately  $90^\circ$  in height.

Two figures have been prepared to show the nature of the ground currents for the three in line antenna. They are the same two formats that were used to demonstrate the procedure using our introductory two element antenna.

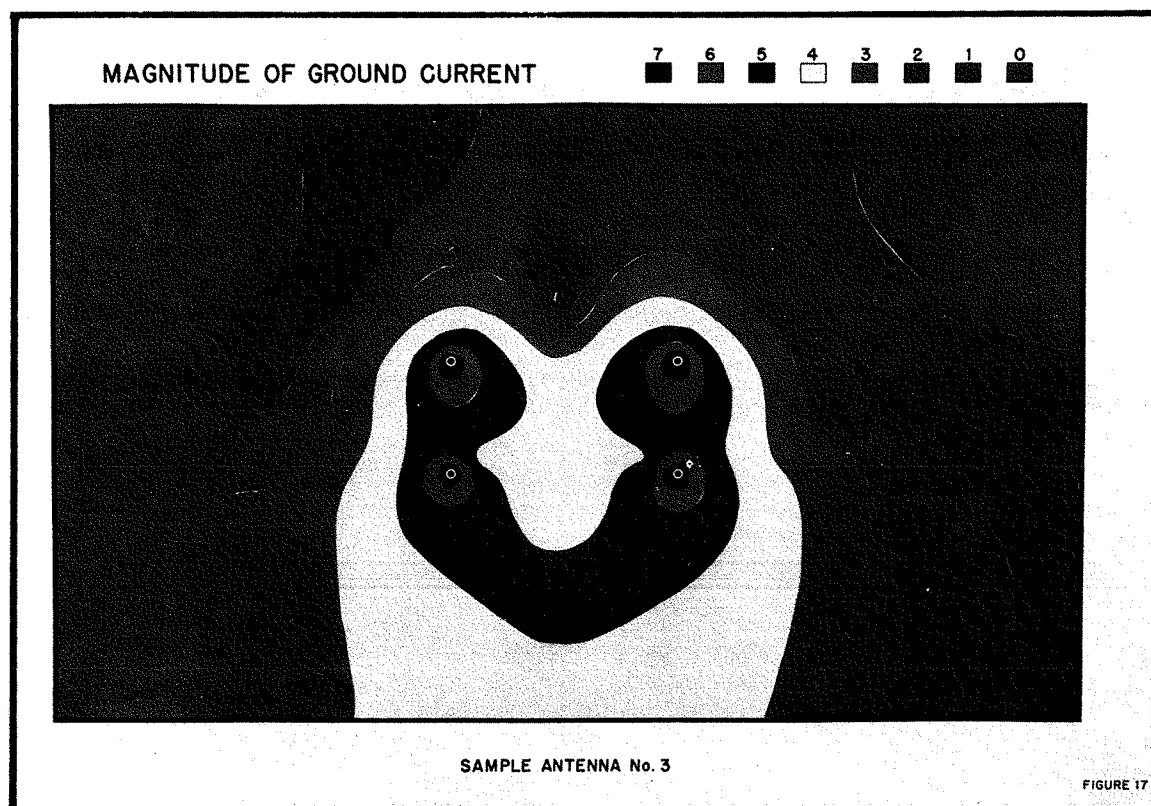
The upper half of Figure 15 shows by the colored sectors the relative amplitude of the ground current for antenna No. 2 and by the shading in the lower half the ratio of the two ground current components. Figure 16 shows the direction of the principal component of the ground current.







Figures 17 and 18 show the ground current density and ratio of the two components of the ground currents in antenna No. 3.



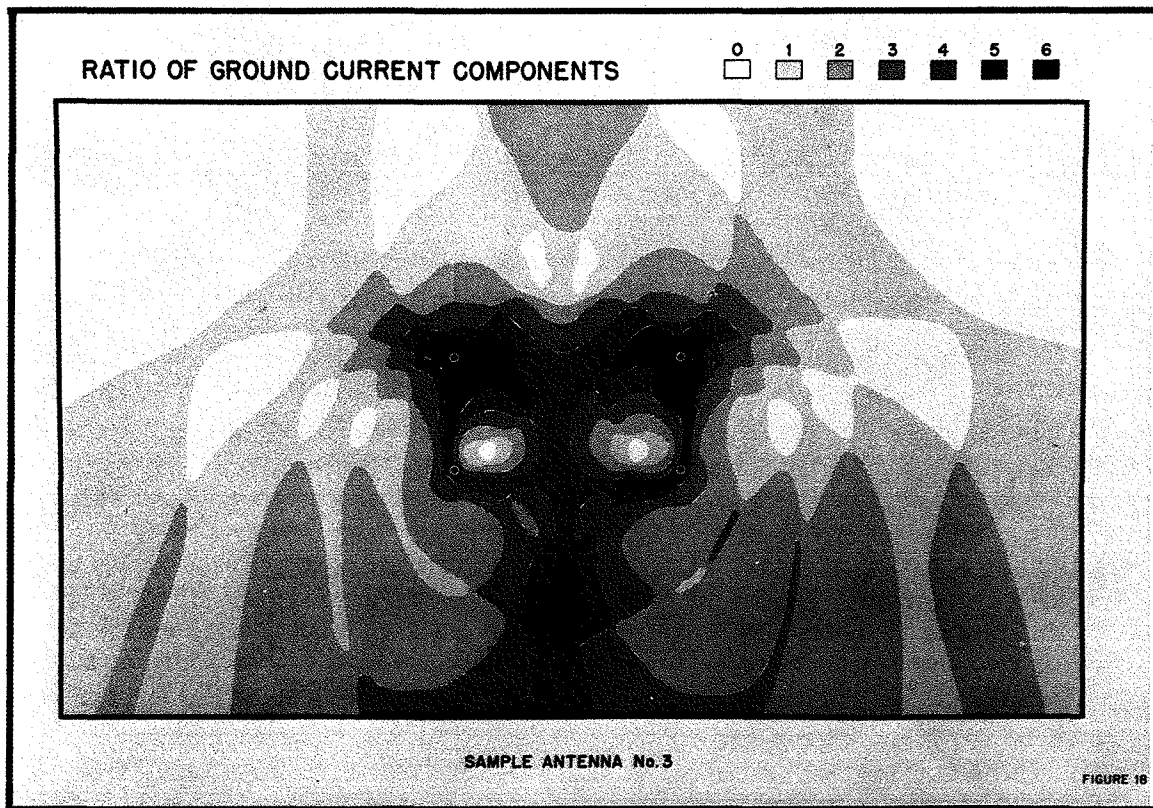
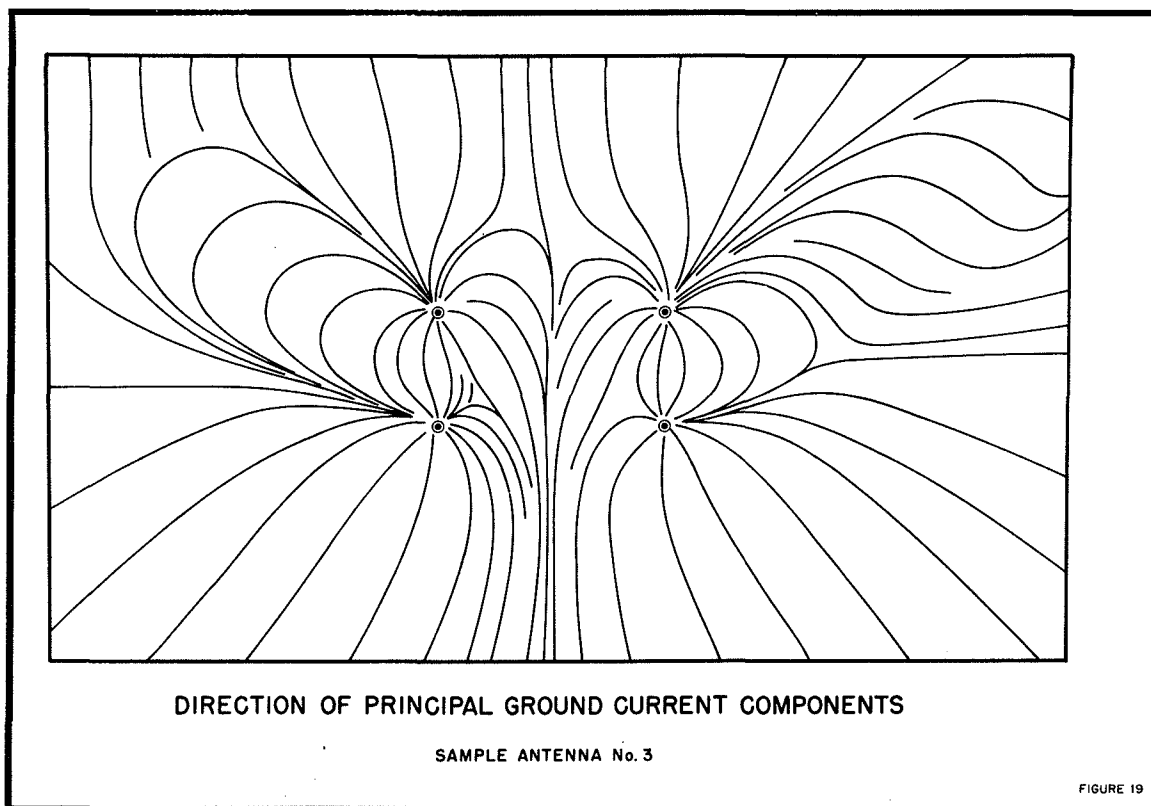
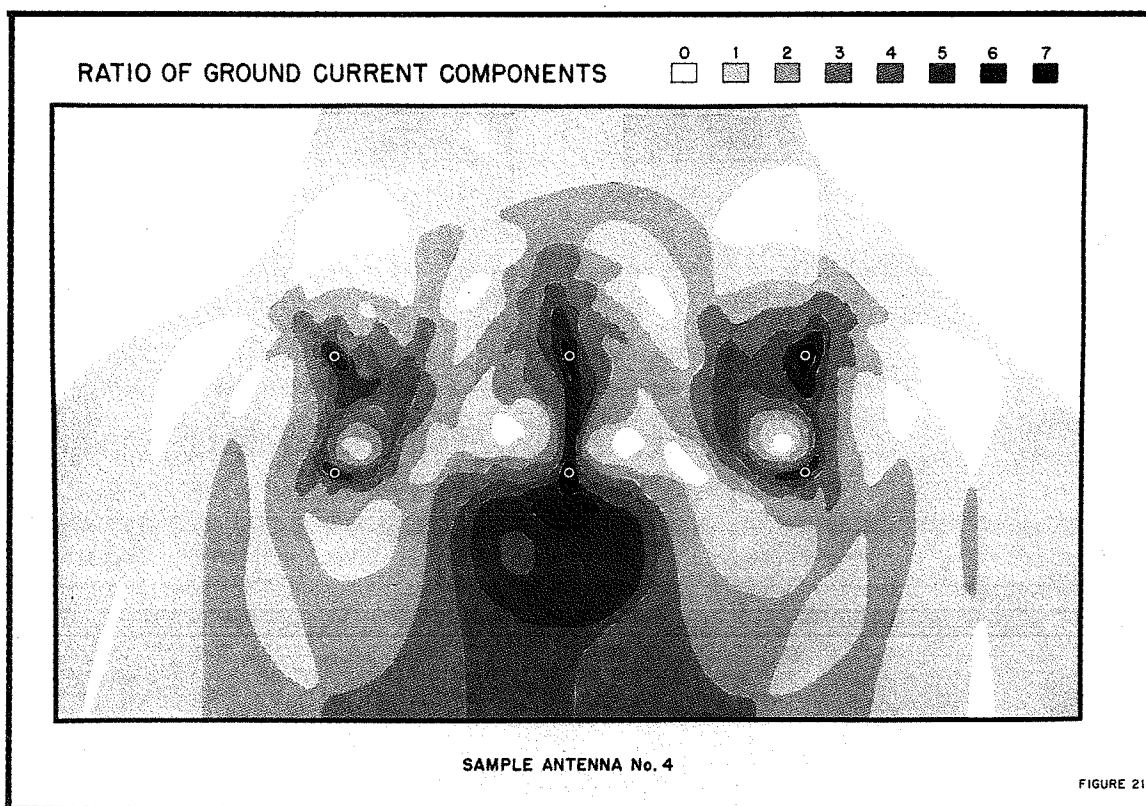
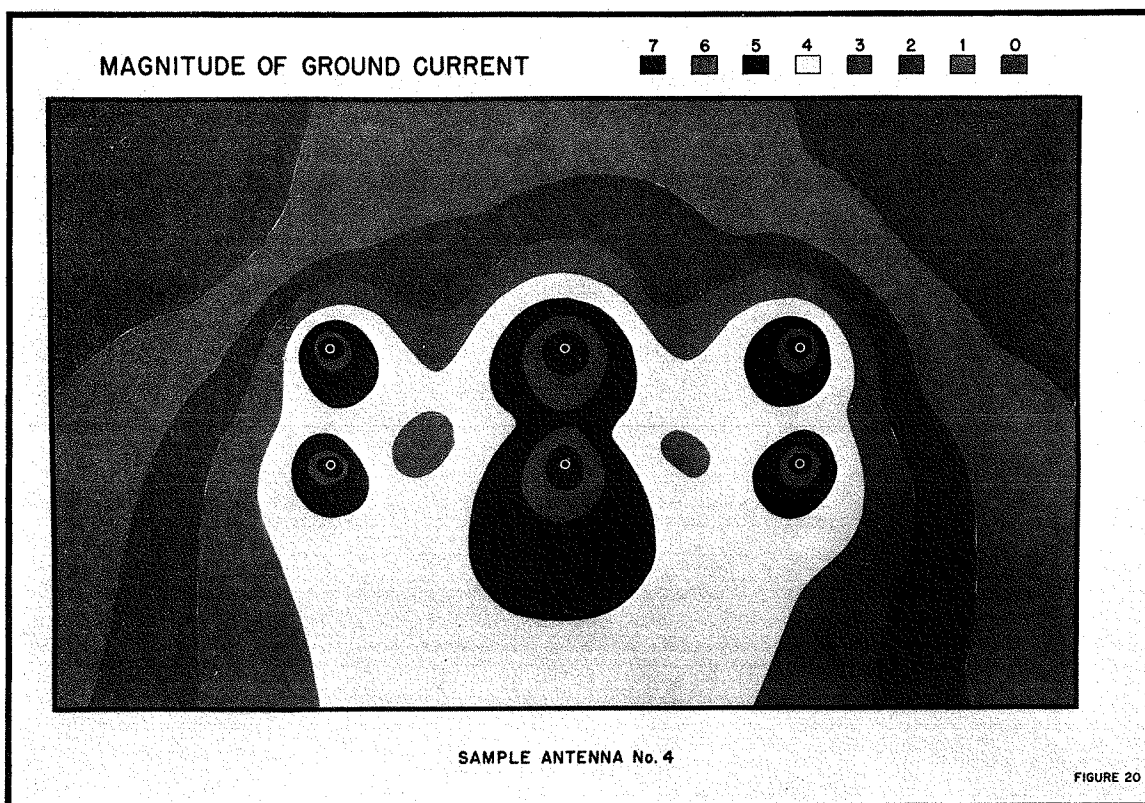
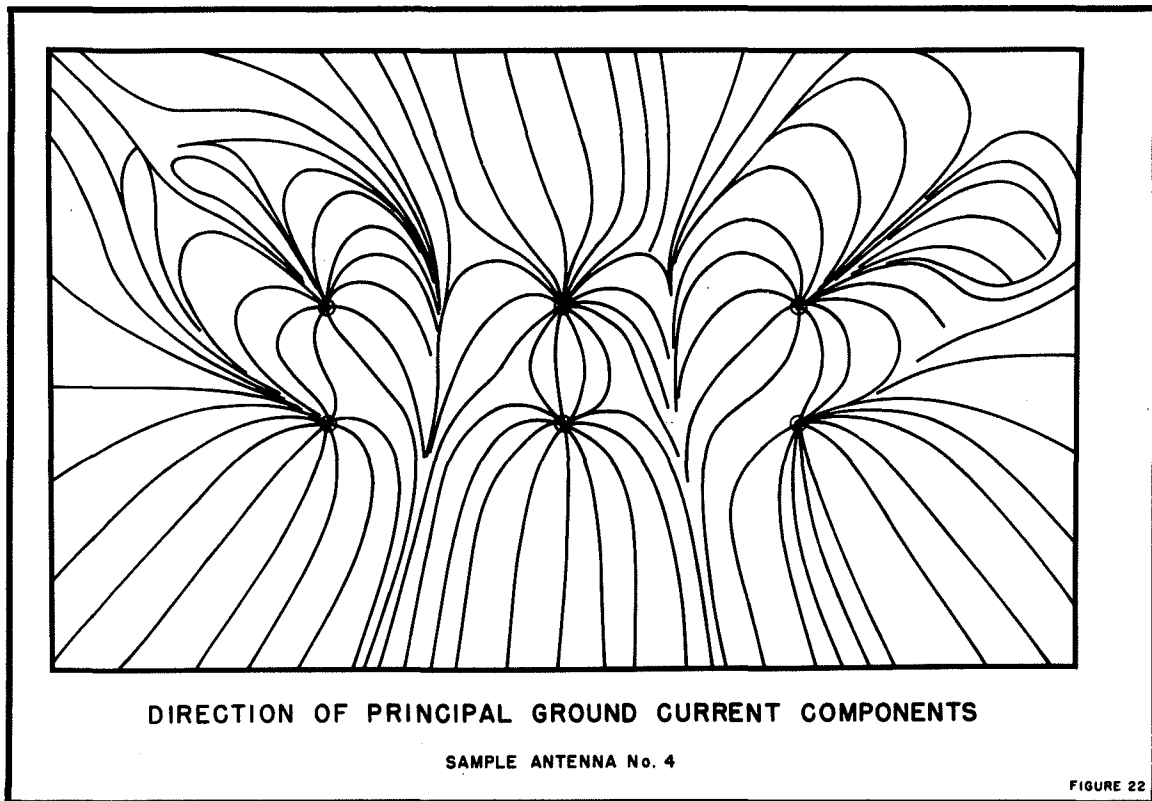


Figure 19 shows the direction of the principle component of the ground current for antenna No. 3. Figures 20, 21 and 22 demonstrate the nature of the ground currents for antenna No. 4.







## V. Conclusion

We have shown that the ground currents in many medium wave directional antennas do not flow along simple radial paths surrounding the antenna elements. We have provided a method of demonstrating the actual nature of these ground currents. Our work on this project has led us to speculate that the use of conventional ground systems, rather than ground systems designed to support the actual ground currents, may explain inefficiency in some arrays, instability in other arrays and may be a major contributor to some annual variations in still other arrays. We feel that use of these principles can provide a significant improvement in the operating characteristics of medium wave directional antennas.

I wish to acknowledge the enthusiastic assistance of John Lundin in the preparation of the computer program used in this analysis.

0870W  
WRMR

OFFICE MEMORANDUM

TO: Don

FROM: Warren

SUBJECT: IEEE Broadcast Symposium Talk on Reduced Skywave  
AM Antennas

DATE: October 6, 1986

---

The fourth session on Thursday, September 18, 1986, concerned a computer modeling study of the two new reduced skywave antenna systems proposed by Dick Biby and Ogden Prestholt. The horizontal plane efficiency of both antenna systems was computed to be significantly reduced below the theoretical efficiency for a simple 90 degree vertical antenna.

A model of the Dick Biby antenna, assuming a desired 40 dB null at a vertical elevation angle of approximately 25 to 30 degrees above the horizontal plane, oriented at one horizontal angle towards a hypothetical station to be protected, resulted in a horizontal plane efficiency of approximately 200 mV/m/km (125 mV/m per mile). The Biby antenna system appeared to be extremely critical with respect to the current amplitude fed to the short towers around the main radiating structure. A change in relative amplitude from 1.002 to 0.998 resulted in the 40 dB null becoming a 20 dB null. Discussions that followed the talk indicated that the computer model was based on ideal ground conditions and that the system should work better under non-idealized ground conductivity conditions. Note to Don: Seasonal variations in ground conductivity values could ~~destabilize~~ destabilize the desired radiation characteristics of the Biby antenna system.

The Ogden Prestholt antenna model incorporates a 190 vertical radiator with an associated horizontal radiating element, 90 degrees long and 145 degrees above ground level.

The horizontally polarized component aimed at vertical angles above approximately 70 degrees is virtually equal to the vertically polarized field in the horizontal plane. Accordingly, excessive skywave interference can be expected to be reflected back down from the ionosphere, to interfere with primary ground wave coverage. The predicted ground wave efficiency of the Prestholt system is approximately 240 mV/m/km (150 mV/m at a mile). It should be noted that the predicted effective field for a simple 190 degree vertical radiator is 394 mV/m/km (245 mV/m/mile).

My impression from the lectures was that a suitable antenna which restricts skywave radiation in favor of horizontal plane (ground wave) efficiency cannot be expected from either of the above two described systems within the <sup>near</sup>~~immediate~~ future.

Harmon  
8/17/82

# ANTENNAS (AM)

## PERFORMANCE OF SECTIONALIZED BROADCASTING TOWERS

C. E. Smith<sup>†</sup>, Fellow Member, IRE, D. B. Hutton<sup>‡</sup>, Associate Member, IRE,  
and W. G. Hutton<sup>§</sup>, Senior Member, IRE.

**Summary**--With a sectionalized tower high angle radiation can be minimized to give better ground wave performance than is possible with a simple vertical radiator. A study of theoretical conditions in conjunction with physical limitations reveals that it is necessary to maximize the current distribution on any given tower construction to obtain the maximum ground plane field intensity. Several sectionalized towers and a variety of current distributions on each tower are treated theoretically and tested experimentally. The results obtained are compared with the findings of several other writers treating similar problems.

### I. Introduction

The problem of increasing the ground wave coverage of a radio broadcasting station by improved antenna design dates back to the early days of broadcasting. Ballantine<sup>1</sup> published a classical article in 1924 showing  $225^\circ$  ( $5/8\lambda$ ) to be the optimum height for a simple vertical radiator. For antennas less than this height top loading has been successfully used to improve the performance. For short antennas Smith and Johnson<sup>2</sup> show that loading accomplishes this improved performance by simultaneously increasing the radiation resistance and decreasing the capacitive reactance at the base input terminals. A practical application of this theory was made on the antenna system of a Million Watt Broadcasting Station in Europe<sup>3</sup>.

In the early 1930's a number of people gave consideration to sectionalized antennas as a method of increasing the ground wave. Harmon<sup>4</sup> in 1936 proposed and tested a sectionalized antenna with essentially constant current distribution and showed it to be more efficient than sinusoidal current distribution. Brown<sup>5</sup> published a critical study of numerous current distributions in an effort to find combinations most likely to be useful. Also in 1936 Smith<sup>6,7</sup> completed a critical study of several antennas designed to increase the primary coverage of a radio broadcasting station. For the most part these tests involved vertical radiators with improved current distributions within  $90^\circ$  ( $\lambda/4$ ) of height as shown in Fig. 1. Due to extremely low values of radiation resistance in these antennas the circulating currents required were quite high and the efficiency prohibitively low. However, this work gives a clue as to how to improve the current distribution to obtain the best theoretical results. It will be noted that the

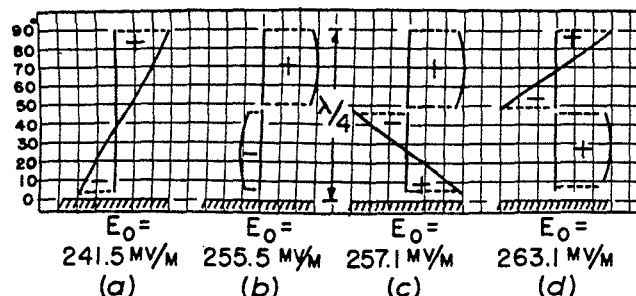


Fig. 1 - Four improved current distributions.

maximum theoretical horizontal field intensity is largest for the current distribution in Fig. 1(d).

With this background, the problem is to discover a method for producing a more efficient antenna system. This can be accomplished by using taller sectionalized towers and maximize current distributions. In some cases the radiation possibilities are enhanced by top loading.

### II. General Theory

For a simple vertical radiator the radiation characteristic can be improved by increasing the height of the tower or employing top loading. This in effect raises the position of the current loop with respect to the ground. This principle can also be applied to the top section of a sectionalized tower.

The purpose of sectionalizing a tower is to provide a means of further controlling the current distribution. Sectionalizing the tower controls the current distribution on the lower section only. Considering efficiency and stability it is usually possible to achieve a more favorable radiation characteristic of the whole tower by employing top loading and sectionalization. In the case of a tall tower used to support an FM or a TV antenna it may not be practical to employ top loading. Depending on the height of the tower in wavelengths the tower can be sectionalized at one or more points to accomplish the highest efficiency consistent with good operating stability.

As is well known,<sup>6,7,8</sup> the tower currents must be in phase or  $180^\circ$  out of phase to produce maximum ground plane radiation. This can theoretically be accomplished by properly driving each section of the tower independently to produce the desired current distribution on that section. For vertical sectionalized towers, driven at the base, current continuity will be assumed across the sectionalizing insulators.

The top section will be assumed to have a sinusoidal current distribution with the current node at or above the top of the tower depending on whether or not top loading is applied. This will

<sup>†</sup>Carl E. Smith Consulting Radio Engineers, Cleveland, Ohio.

<sup>‡</sup>Federal Communications Commission, Washington, D. C.

<sup>§</sup>Goodyear Aircraft Corporation, Akron, Ohio.

Recently joined Carl E. Smith Consulting Radio Engineers, Cleveland, Ohio.



also fix the location of the current loop on the top section of the tower. The top section with its top loading if any will serve as top loading for the next lower section.

For the remainder of this paper the next lower section will be termed the bottom section since only a two section tower will be considered. The current on the bottom section will also be assumed to be sinusoidal with the height of the current node as a variable. When the height of the current node is fixed the radiation characteristics of the tower is fixed. Therefore, the operation of the tower can be maximized with respect to the height of the node of the current for the bottom section. The selection of the final operating condition must, however, take into account the stability and efficiency of the system.

### Sectionalized Tower Theory

Figure 2 illustrates the current distribution on the top and bottom sections of a sectionalized

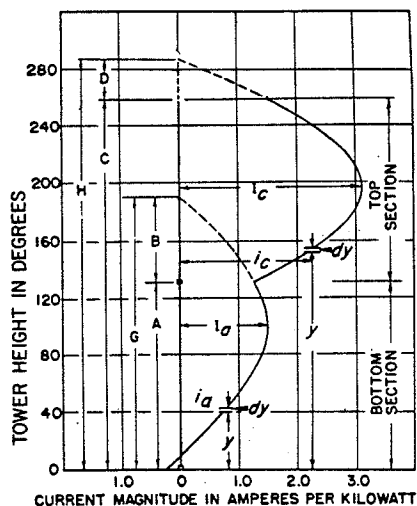


Fig. 2 - Theoretical current distribution on top loaded sectionalized tower.

tower having top loading on the top section. The radiating portions of the sine waves are shown as solid curves and the instantaneous current values  $i_c$  and  $i_a$  are illustrated on each of the upper and lower sections. Pertinent tower heights and dimensions of the sine waves are shown by the letters A, B, C, D, G, H,  $I_c$  and  $I_a$ .

Figure 3 illustrates the geometrical considerations for determination of the Vector Potential at any point P in space at a great distance from the antenna due to the elements of instantaneous current  $i_c$  and  $i_a$  shown in Fig. 2. The total Vector Potential derived from the radiation of the tower over the entire radiating space above the earth is given by the equation,

$$\vec{A} = \int_{vol} \frac{i(t + \frac{d}{c})}{cd} dv \quad (1)$$

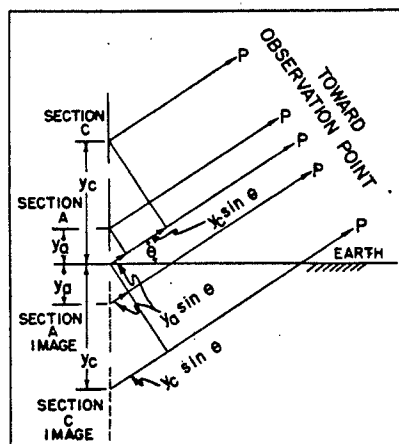


Fig. 3 - Sectionalized tower with images.

where  $\vec{A}$  = retarded electromagnetic vector potential

$i$  = instantaneous current element, amp

$t$  = time, sec

$d$  = distance from current element, meters

$c$  = velocity of light, meters per sec

$dv$  = increment of volume, cubic meters.

Substituting in this equation the values of instantaneous current  $i$  for both top and bottom sections plus their respective images and letting  $d$ , the distance from the antenna base to the point P, be used in the amplitude term but  $d + y \sin \theta$  be used in the phase terms of the images and  $d - y \sin \theta$  be used in the phase terms of the antenna sections as shown in Fig. 3 results in

$$\begin{aligned} \frac{\vec{A} c d 2\pi}{\lambda} = & I_a \int_{a_1}^{a_2} \sin(G-y) \sin \left[ \omega(t - \frac{d}{c}) \right. \\ & \left. + y \sin \theta \right] dy \\ & + I_a \int_{a_1}^{a_2} \sin(G-y) \sin \left[ \omega(t - \frac{d}{c}) \right. \\ & \left. - y \sin \theta \right] dy \\ & + I_c \int_{c_1}^{c_2} \sin(H-y) \sin \left[ \omega(t - \frac{d}{c}) \right. \\ & \left. - \psi + y \sin \theta \right] dy \\ & + I_c \int_{c_1}^{c_2} \sin(H-y) \sin \left[ \omega(t - \frac{d}{c}) \right. \\ & \left. - \psi - y \sin \theta \right] dy \end{aligned} \quad (2)$$

where the first and third terms are for the images and the second and fourth terms are for the antenna sections. The  $2\pi/\lambda$  term was introduced when the  $y$  term was changed to degrees. The  $y$  subscripts of Fig. 3 are not used since the limits of integration indicate which section is involved.

The right hand member of Eq. (2) is readily integrated so that after substituting the limits  $a_1 = 0$ ,  $A_2 = C_1 = A$ ,  $C_2 = C$  and  $G - A = B$  Eq. (2) becomes

$$\frac{\dot{A} c d \pi}{\lambda} = -I_a \sin \left\{ \omega \left( t - \frac{d}{c} \right) \right\}$$

$$\left[ \begin{array}{l} \cos B \cos (A \sin \theta) - \cos G \\ + \frac{\sin B \cos (H-C) \cos (C \sin \theta)}{\sin (H-A)} \\ - \frac{\sin B \sin \theta \sin (H-C) \sin (C \sin \theta)}{\sin (H-A)} \\ - \frac{\sin B \cos (H-A) \cos (A \sin \theta)}{\sin (H-A)} \end{array} \right] \frac{1}{\cos^2 \theta} \quad (3)$$

The Electric Field Intensity is

$$E_\theta = \frac{\partial A}{\partial d} \cos \theta \quad (4)$$

where  $E_\theta$  = field intensity at any point P

d = distance of point P from antenna, meters

$\theta$  = elevation angle of point P, degrees.

Applying the differentiation indicated in Eq. (4) to A of Eq. (3) we have

$$E_\theta = \frac{60 I_a}{d} \left[ \begin{array}{l} \cos B \cos (A \sin \theta) - \cos G \\ + \frac{\sin B \cos (H-C) \cos (C \sin \theta)}{\sin (H-A)} \\ - \frac{\sin B \sin \theta \sin (H-C) \sin (C \sin \theta)}{\sin (H-A)} \\ - \frac{\sin B \cos (H-A) \cos (A \sin \theta)}{\sin (H-A)} \end{array} \right] \frac{1}{\cos \theta} \quad (5)$$

This equation gives the field intensity at the point P produced by the sectionalized tower for various amounts of top loading on both the top and bottom sections with the restriction of holding the currents in or out of phase and having current continuity across the sectionalizing insulator.

The Vertical Radiation Characteristic can be derived from Eq. (5) by evaluating the quantity inside the brackets for  $\theta = 0$  and using this as the denominator with the bracket quantity itself as the numerator.

$$f(\theta) = \frac{\left[ \begin{array}{l} \cos B \cos (A \sin \theta) - \cos G \\ + \frac{\sin B \cos (H-C) \cos (C \sin \theta)}{\sin (H-A)} \\ - \frac{\sin B \sin \theta \sin (H-C) \sin (C \sin \theta)}{\sin (H-A)} \\ - \frac{\sin B \cos (H-A) \cos (A \sin \theta)}{\sin (H-A)} \end{array} \right]}{\left[ \begin{array}{l} \cos \theta \{ \cos B - \cos G \} \\ + \frac{\sin B}{\sin (H-A)} (\cos H-C - \cos H-A) \end{array} \right]} \quad (6)$$

If the Vertical Radiation Characteristic,  $f(\theta)$ , is squared and multiplied by  $\cos \theta$  the Power Flow Characteristic is obtained thus,

$$p(\theta) = f^2(\theta) \cos \theta \quad (7)$$

The ground wave radiation will be a maximum when the area under the curve,  $p(\theta)$  plotted against  $\theta$ , is a minimum. A family of  $p(\theta)$  curves for various heights of the current node on the bottom section is drawn in order to select the minimum area curve. No losses are taken into account since  $p(\theta)$  is theoretical.

A rigorous evaluation of the efficiency involves a determination of the radiation resistance. This is determined by performing the following integration,

$$R = 60 \int_0^{\frac{\pi}{2}} \left[ \begin{array}{l} \cos B \cos (A \sin \theta) - \cos G \\ + \frac{\sin B \cos (H-C) \cos (C \sin \theta)}{\sin (H-A)} \\ - \frac{\sin B \sin \theta \sin (H-C) \sin (C \sin \theta)}{\sin (H-A)} \\ - \frac{\sin B \cos (H-A) \cos (A \sin \theta)}{\sin (H-A)} \end{array} \right]^2 \cos \theta d\theta \quad (8)$$

R the radiation resistance can be determined by applying the trapezoidal rule. When R is found the current  $I_a$  of Eq. (5) is then given by the relation

$$I_a = \sqrt{\frac{P_r}{R}} \quad (9)$$

Where  $I_a$  = bottom section loop current

$P_r$  = power radiated, watts

R = total radiation resistance referred to the bottom section current loop, ohms,

The efficiency of the tower can be predicted from the equation

$$\eta = \frac{100 P_r}{P_r + P_L} \quad (10)$$

Where  $\eta$  = power efficiency, percent

$P_r$  = power radiated, watts

$P_L$  = power lost, watts

and where  $P_L$  can be determined from the equation

$$P_L = I_a^2 R_L = \frac{P_r}{R} R_L \quad (11)$$

Where  $R_L$  = total loss resistance referred to the bottom section current loop, ohms.

Finally the horizontal field intensity with loss can be obtained from

$$E_{OL} = E_O \sqrt{\eta} \quad (12)$$

Where  $E_{OL}$  = horizontal r-m-s field with loss, mv/m

$E_O$  = horizontal r-m-s field without loss, mv/m.

#### Theoretical Examples

1. 258° Sectionalized Tower with Top Loading. Figure 2 illustrates this type of sectionalized tower. For the special case approximating a tower built in Linz, Austria the following substitutions were made in Eq. (8):

A = 130° height of lower section above ground, degrees

B = variable top loading of lower section, degrees

G = A + B = 130° + B height of current node for lower section above ground, degrees

C = 258° height of upper section above ground, degrees

D = 28° top loading of upper section, degrees

H = C + D = 286° height of current node for upper section above ground, degrees

These substitutions give

Where R = resistance in ohms.

The lower section loop radiation resistance value, R, was determined by applying the trapezoidal rule to the above equation as follows,

$$R = 10.4720 \left\{ \frac{[ ]^2}{2} + \sum_{n=1}^{n=8} \left[ \frac{[ ]^2}{10n} \cos 10n \right] \right\} \quad (14)$$

Where [ ] = bracket term in Eq. (13)

n = integers from 1 to 8 which multiplied by 10 gives the elevation angle  $\theta$  in degrees.

B = 15 degrees, then 30, 60, 90 and 120 degrees for 5 determinations of R.

The corresponding 5 values of the loop current,  $I_a$ , for the bottom section were then determined from Eq. (9) for the power,  $P_r$ , of 1000 watts. Hence

$$I_a = \sqrt{\frac{1000}{R}} \quad (15)$$

Where  $I_a$  = amperes per kw of power radiated.

Since d = 1609.4 meters per mile Eq. (5) can be written

$$E_\theta = 0.37281 I_a [ ] \quad (16)$$

Where  $E_\theta$  = mv/m at one mile

[ ] = the quantity inside the bracket of Eq. (13).

The vertical radiation characteristic also can be written

$$f(\theta) = \frac{[ ]}{\cos B - \cos (130 + B) + 4.4170 \sin B} \quad (17)$$

and the power flow characteristic,  $p(\theta)$  is most simply expressed by Eq. (7). The 5 vertical radiation characteristic curves corresponding to the above 5 loop current values were found in accordance with Eq. (17) and plotted in Fig. 4. Likewise the 5 power flow characteristic curves were determined by Eq. (7) and plotted in Fig. 5. The area under each power flow characteristic curve was planimeted and plotted in Fig. 6 as the curve labeled 258° tower. Equations (10) to (12)

$$R = 60 \int_0^{\frac{\pi}{2}} \left[ \frac{(\cos B + 2.2461 \sin B) \cos (130 \sin \theta) - \cos (130 + B) + 2.1708 \sin B \cos (258 \sin \theta) - 1.1544 \sin B \sin \theta \sin (258 \sin \theta)}{\cos \theta} \right]^2 \cos \theta d\theta \quad (13)$$

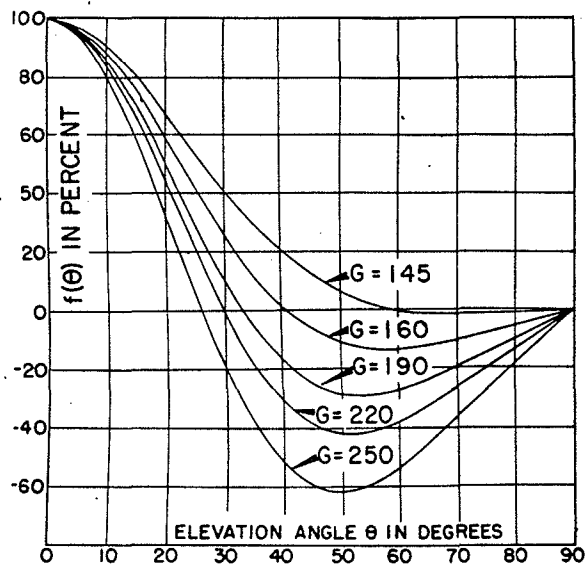


Fig. 4

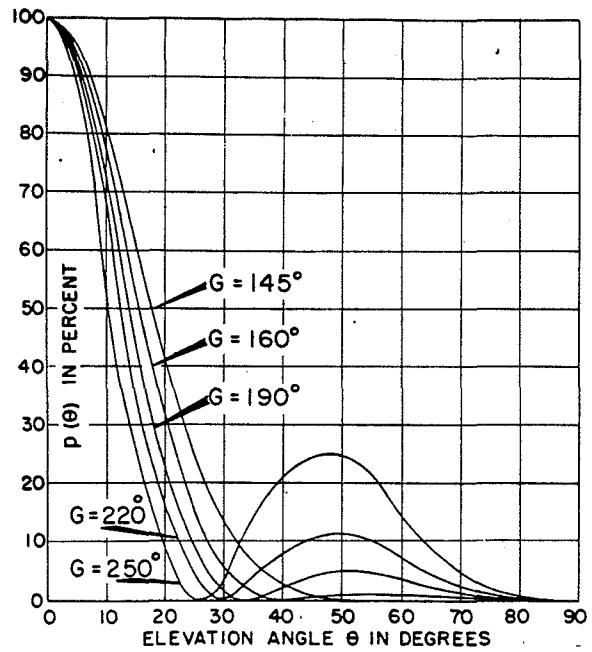


Fig. 5

Fig. 4 - Vertical radiation characteristic for 258° top loaded sectionalized tower.  
 Fig. 5 - Vertical power flow characteristics for 258° top loaded sectionalized tower.  
 Fig. 6 - Relative total power flow per unit field radiated. Fig. 7 - Bottom section loop radiation resistance and unattenuated horizontal field intensity for 258° sectionalized top loaded tower.

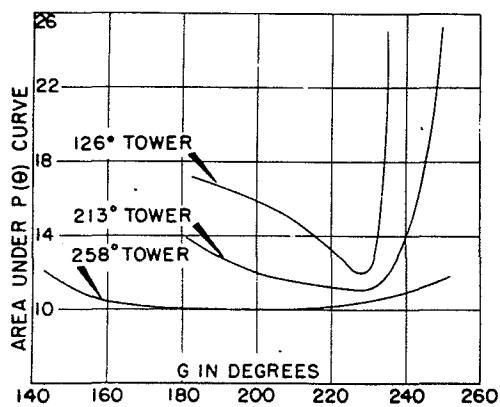


Fig. 6

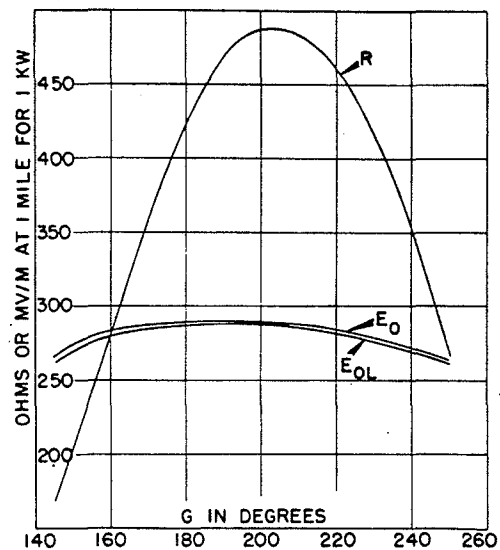


Fig. 7

can be manipulated to give

$$E_{OL} = E_O \sqrt{\frac{R}{R + R_L}} \quad (18)$$

where  $E_{OL}$  = horizontal r-m-s field with loss, mv/m.

$E_O$  = horizontal r-m-s field without loss, mv/m.

$R$  = lower section loop radiation resistance. Eq. (14) ohms.

$R_L$  = total loss resistance referred to bottom section current loop, ohms.

Employing the above 5 current values to find  $E_C$  from Eq. (16) for  $\theta = 0$  the effective horizontal plane field intensity of the tower was determined for each current condition assuming loop resistance losses referred to the lower section,  $R_L$  of 0 and 4 ohms. Figure 7 shows the lower section loop radiation resistance  $R$ , horizontal r-m-s field without loss  $E_O$  and horizontal r-m-s field  $E_{OL}$  with 4 ohms lower section loop loss resistance.

2. 213° Sectionalized Tower. Figure 2 would illustrate this type of tower if the top loading were absent and the current node for the top section were shown to fall at the exact top of the tower.

For the special case, approximating a tower built in Cleveland, Ohio the following substitutions were made in Eq. (8):

$A = 96^\circ$  height of lower section above ground, degrees

$B =$  variable top loading of lower section, degrees

$G = A + B = 96^\circ + B$  height of current node for lower section above ground, degrees

$C = 213^\circ$  height of upper section above ground, degrees

$D = 0$  top loading of upper section, degrees

$H = C + D = 213^\circ$  height of current node for upper section above ground, degrees.

Calculations corresponding to those referred to in Section A above were relatively simple by virtue of the fact the formulas simplify when  $H=C$  as happens in this case. The resulting  $p(\theta)$  curves are shown in Fig. 8 and the area under these curves is plotted to give the curve of Fig. 6 labeled 213° tower.

Figure 9 shows  $R$ ,  $E_O$  and  $E_{OL}$  for  $R_L = 1, 2$ , and 4 ohms.

3. 126° Sectionalized Tower with Top Loading. This example resembles the case of Section B above except that the top section of the tower is so short that it supplies a very small portion of the total radiation of the tower. The top loading on the top section is not considered as altering the current distribution on the top section, but it is looked upon as a means of absorbing a large current contributed by the lower section into non-radiating top loading.

The special case approximates a tower built in Vienna, Austria. The following substitutions were made in Eq. (8):

$A = 112.7$

$B =$  variable

$C = 126^\circ$

$D = 0$

$H = C + D = 126^\circ$

where each term is defined in Section B above.

The calculations were similar to those involved in Section B. The resulting  $p(\theta)$  are shown in Fig. 10 and the area under these curves is plotted to give the curve of Fig. 6 labeled 126° tower. Figure 11 shows the  $R$ ,  $E_O$  and  $E_{OL}$  for  $R_L = 1, 2, 4$  and 8 ohms.

### III. Experimental Results

#### Basic Procedure

The experimental work covered in this article was conducted according to common engineering practice as follows:

1. The driving point impedance of the antenna was measured after the antenna system was completely installed.
2. An r-f ammeter was used to measure the current into the measured driving point from which the input power to the antenna was determined.
3. Field intensity measurements were made according to "The FCC Standards of Good Engineering Practice", to establish the unattenuated field intensity at one mile for one kw of input power.
4. Measurements were made to determine the current and phase distribution along the tower in order to check theory against experimental results.

#### 258° Sectionalized Top Loaded Tower

1. Base Driven with Center Tuning. A transmission line messenger cable inside the 130° (450 foot) bottom section of the tower was supported on stand-off insulators at regular intervals plus strain insulators at both top and bottom. The characteristic impedance of this transmission line with respect to the tower was determined to be,

$$Z_O = 190 \text{ ohms.}$$

Tuning at the center of the tower was accomplished by varying the location of a shorting strap between the transmission line messenger cable and the tower when the top end of the transmission line was connected to the top section of the tower just above the sectionalizing insulator.

Base impedance measurements of the tower as a function of location of the shorting strap are shown in Fig. 12 along with a sketch of the bottom section of the tower drawn to scale.

Current and phase distribution measurements along the 258° tower as a function of shorting locations of the transmission line are shown

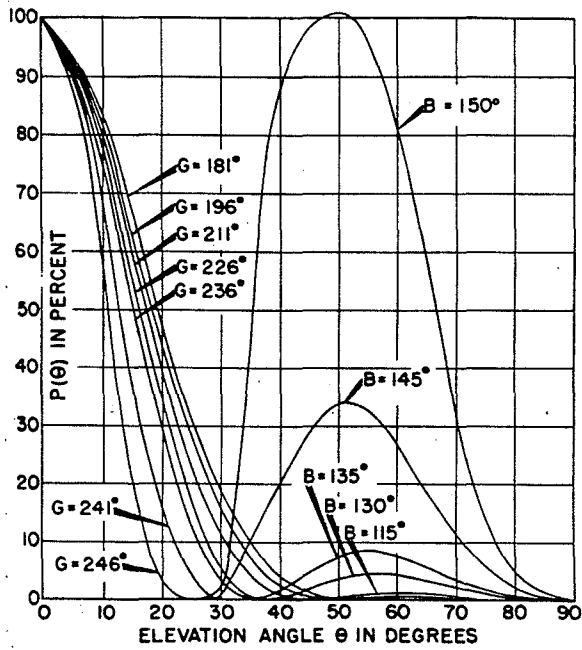


Fig. 8 - Vertical power flow characteristics for 213° sectionalized tower.

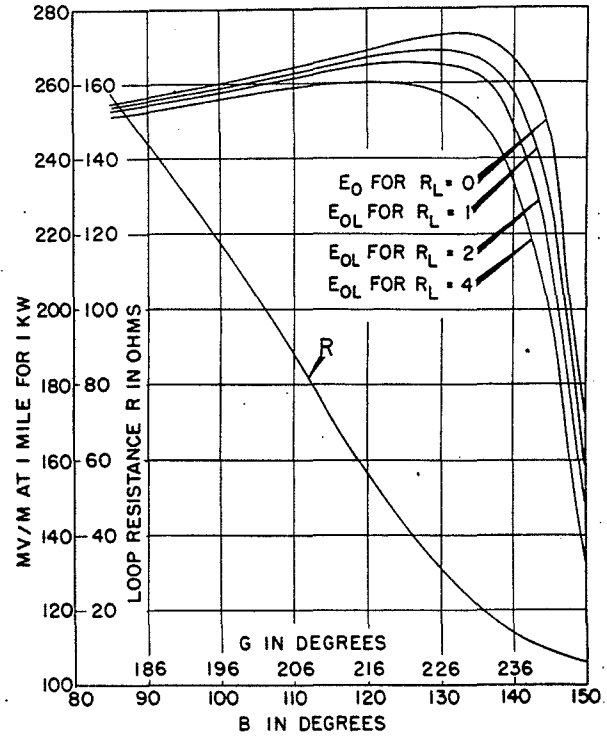


Fig. 9 - Bottom section loop radiation resistance and unattenuated field intensity for 213° sectionalized tower.

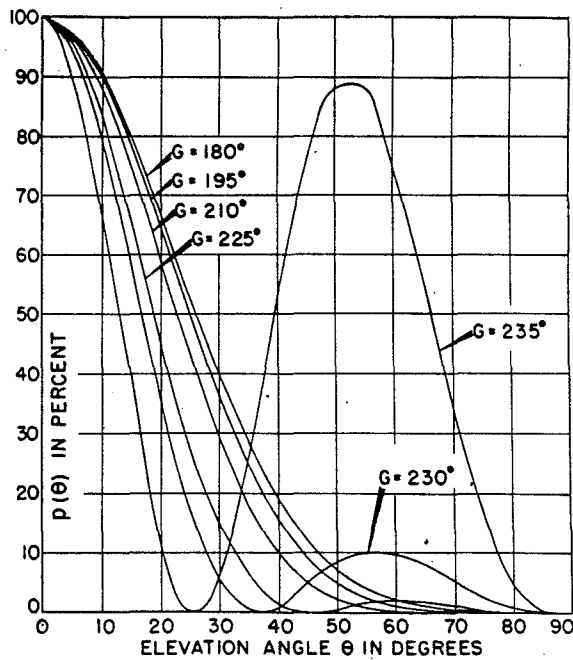


Fig. 10 - Vertical power flow characteristics for 126° top loaded sectionalized tower.

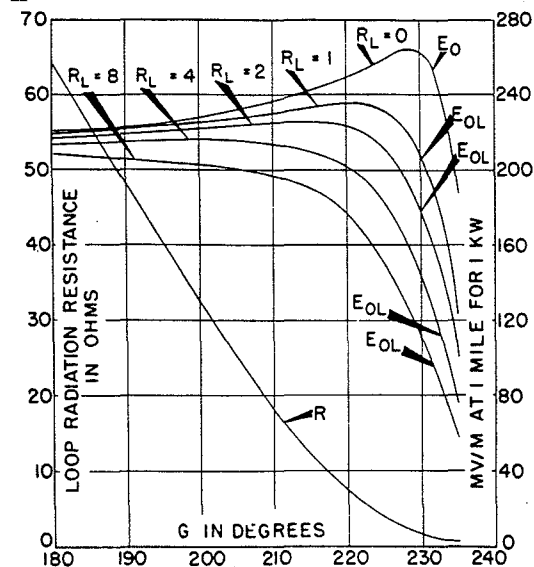


Fig. 11 - Bottom section loop radiation resistance and unattenuated field intensity for 126° top loaded sectionalized tower.

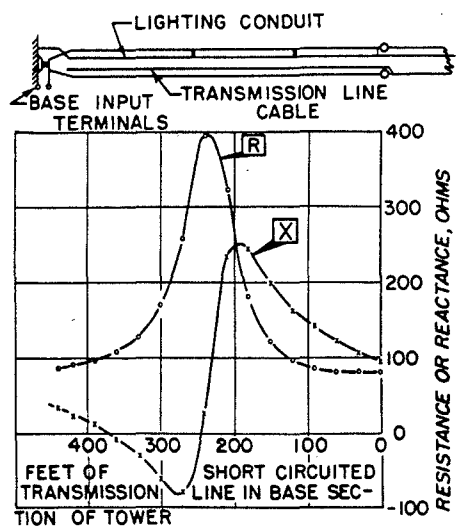


Fig. 12 - Base impedance of 258° tower as a function of loading reactance across sectionalizing insulator.

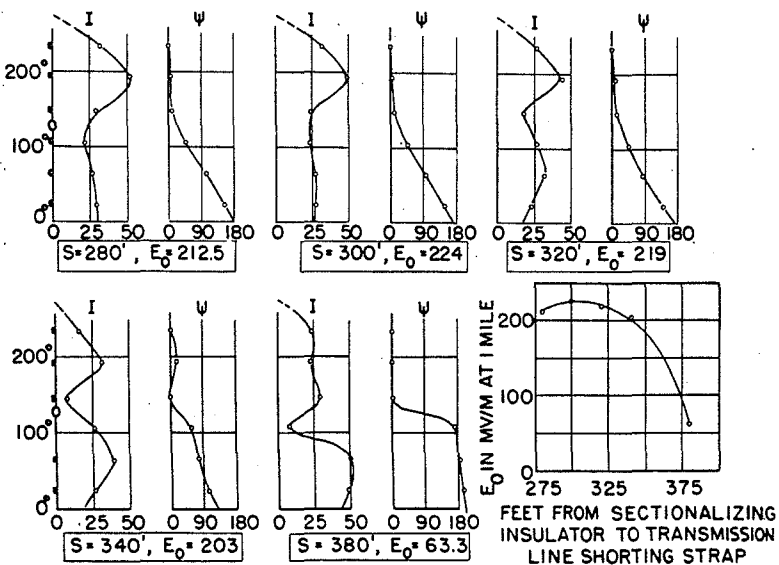


Fig. 13 - Current and phase distribution on 258° tower as function of loading reactance across sectionalizing insulator in terms of shorted transmission line lengths.

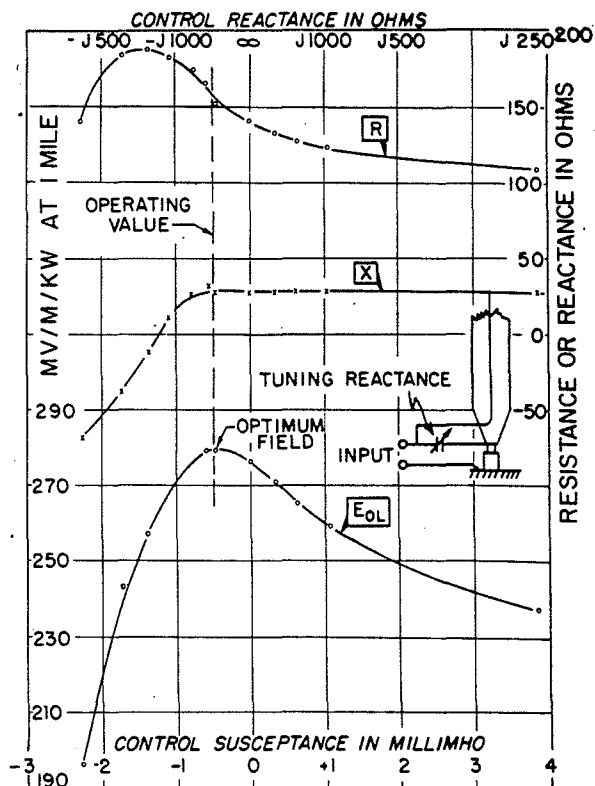


Fig. 14 - Input impedance and field intensity of top loaded sectionalized 258° tower as function of tuning reactance.

in Fig. 13 along with a plot of the unattenuated field intensity at one mile for one kilowatt of input power to the antenna. It will be noted that the maximum field intensity occurs for the condition when the short is placed approximately 300 feet below the sectionalizing insulator which corresponds to 170 ohms base resistance. The maximum or optimum unattenuated field intensity for the method of center tuning described was approximately 224 mv/m per kw at one mile.

**2. Center Driven with Base Tuning.** Input impedances to the transmission line messenger cable at the base of the tower were measured for various values of a capacitive tuning reactance between the messenger cable and the base of the tower. Figure 14 shows the base tuning diagram along with the resistance, reactance and field intensity curves as a function of tuning reactance. Since the tuning reactance was high the major part of the power was fed up the transmission line and thus drove the 258° tower across its center sectionalizing insulator.

The optimum field intensity as shown on the  $E_{OL}$  curve was approximately 279 mv/m for one kw at one mile.

Current and phase distribution measurements along the 258° tower as a function of base tuning reactance are shown in Fig. 15.

It is interesting to note in Fig. 13 for the maximum field intensity when  $S = 300$  feet that a standing wave of zero phase is located on the top section of the tower. This standing wave is fed with energy from a traveling wave of constant magnitude and steadily progressing phase shift from the base of the tower. Now referring to Fig. 15 for optimum field intensity when  $X = -j1680$  it will be noted that the top section has a standing wave of zero phase, but that the bottom section has a traveling wave of variable magnitude such that when the phase is in quadrature the amplitude is a minimum. This may account for the higher radiation efficiency since it is known that for maximum efficiency the radiation currents must be minimized at quadrature phase.

### 213° Sectionalized Tower

Since the 213° two section tower, without top loading, has considerable radiation resistance in each section it was possible to secure enough radiation efficiency to make a worthwhile improvement in the ground wave signal. Because this tower supports an f-m antenna it was necessary to insulate the concentric transmission line mounted in this case on the outside of the tower as shown in Fig. 16. Quarter wave shorting straps above the center and base insulators made it possible to retain the insulator properties at the operating frequency.

The top section is fed by a single copper clad steel cable mounted on stand off insulators inside the bottom section. This terminal plus a connection to the ground system and the bottom section gives a three terminal network which can be properly fed at the base.

The top section, if the cross-section is uniform, would under all normal conditions of operation have essentially a sinusoidal current distribution with a current loop approximately 90° below the top of the antenna. Due to the decrease of cross-section area where the f-m antenna is located the current does not build up as rapidly. See Fig. 18. The phase and magnitude of the current on the top section is determined by one phase monitor sampling loop mounted as shown in Fig. 16. In this installation it was necessary to adjust the vertical plane of the loop to minimize the induction field produced by the quarter-wave length of f-m concentric transmission line mounted on the outside of the tower.

The bottom section of the tower also has essentially a sinusoidal current distribution. However, in order to determine the magnitude, phase and also obtain some idea of the placement of the current distribution two phase monitor sampling loops were provided as shown in Fig. 16. Again, on the bottom section it was necessary to adjust the vertical plane of the middle and bottom phase monitor sampling loops to cancel the induction field produced by the f-m concentric transmission line mounted on the outside of the tower.

In order to properly feed power into the three terminal network at the tower base it was necessary to have a power division and phase shifting network. The network in Fig. 17 has impedance matching, power dividing and phase shifting properties.

The three terminal network at the tower base can be driven in a number of ways. If for example, a generator is placed between terminals 1 and 2 in Fig. 17 the effect is the same as placing the generator across the center insulator and floating the tower at the base. This produces an in phase current distribution similar to the Franklin with sinusoidal current distribution on each section and current nodes at the top and bottom of the tower. This condition approximates the results of a constant current distribution and does not give as strong a ground wave as other conditions of operation.

Another way to drive the tower is to produce a current distribution on the bottom section such that the middle loop in Fig. 16 gives approximately a minimum magnitude and a quadrature phase with respect to the top loop. This is in good agreement with the experimental results as shown in Fig. 18 for the optimum condition of operation.

The unattenuated field intensity at one mile turned out to be only 246 mv/m for 1 kw. This is attributed to the fact that this tower was not provided with its own ground system and furthermore the transmitter and garage buildings at its base account for considerable loss. The theoretical value without loss and with current continuity across the sectionalizing insulator is  $E_O = 273$  mv/m for 1 kw. For the theoretical case of current discontinuity across the sectionalizing insulator and optimized sinusoidal current



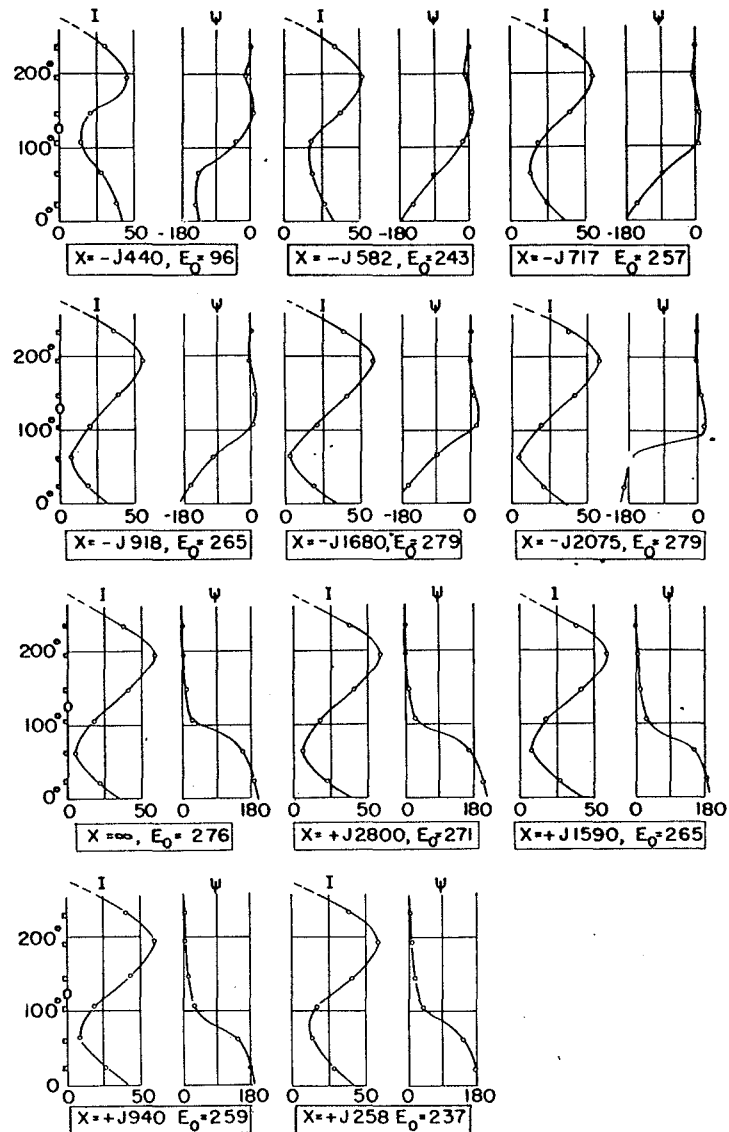


Fig. 15 - Current and phase distribution on 258° tower as function of tuning reactance at base of tower.

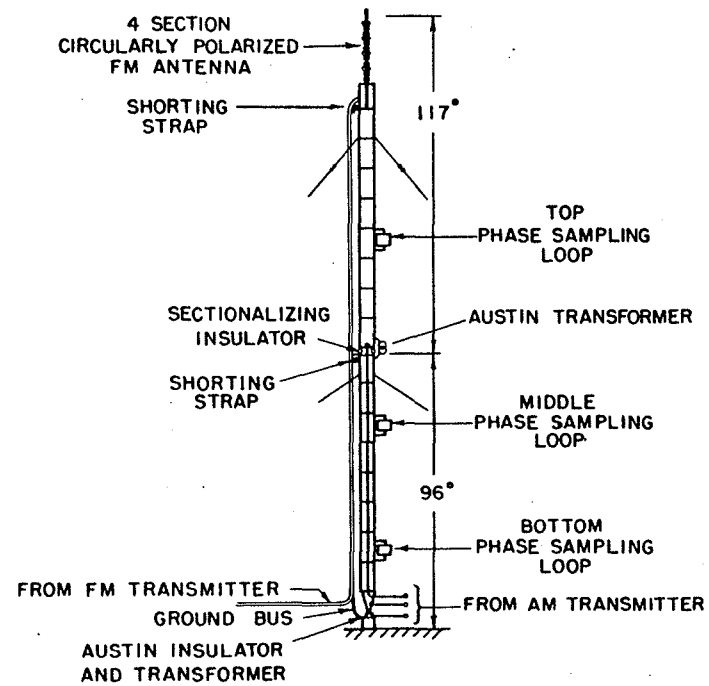


Fig. 16 - 213° sectionalized tower.

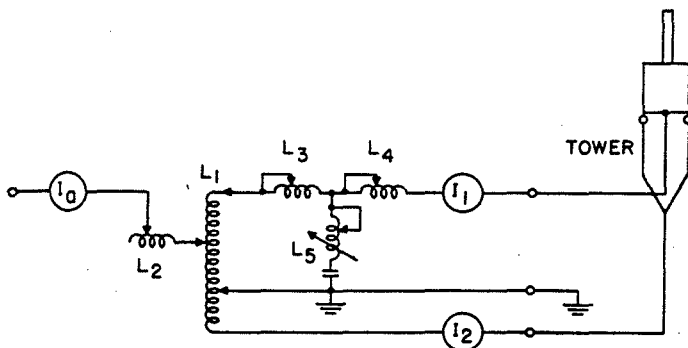


Fig. 17 - Network to feed 213° sectionalized tower.

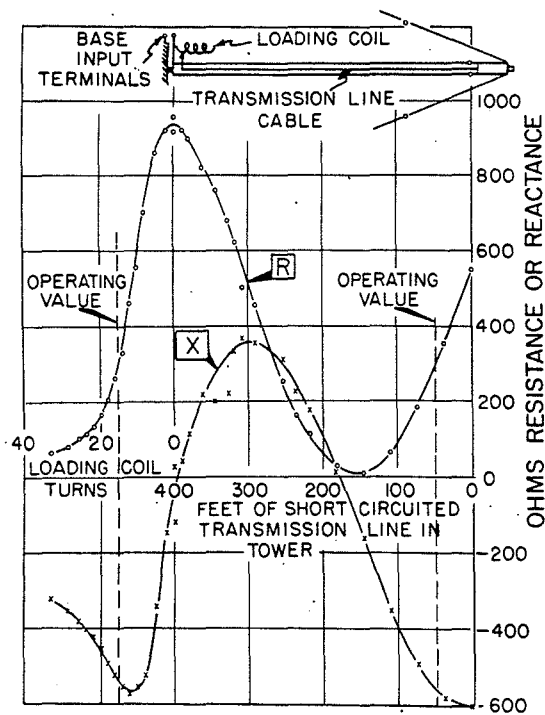


Fig. 19 - Base impedance of 126° tower as function of loading reactance.

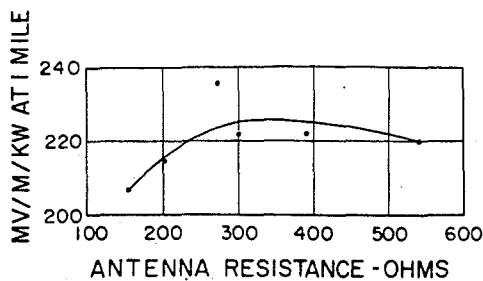


Fig. 20 - Field intensity curve for top loaded sectionalized 126° tower.

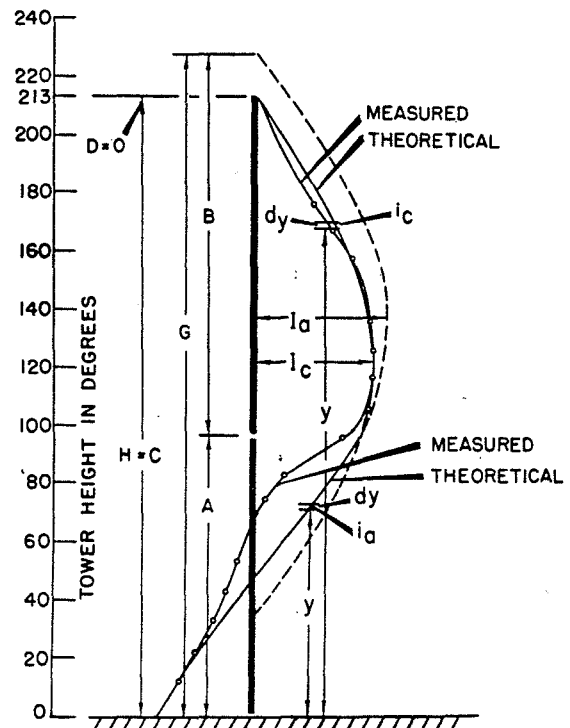


Fig. 18 - Current distribution on 213° sectionalized tower.

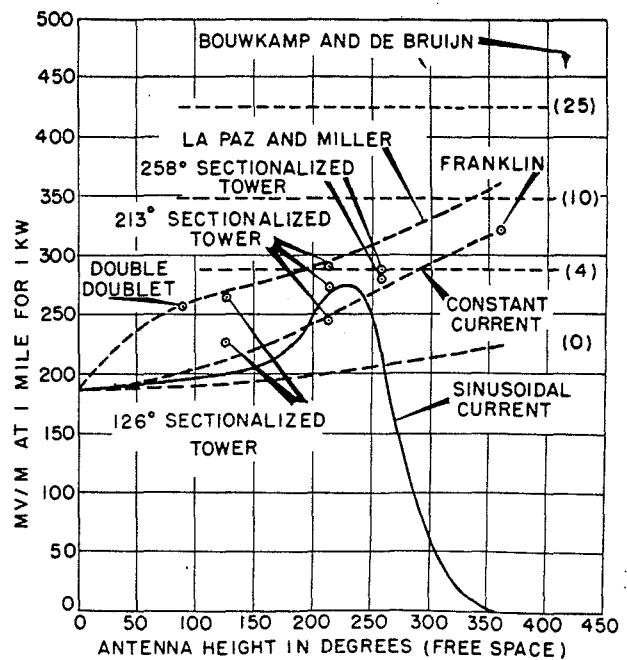


Fig. 21 - Ground wave field intensity as function of antenna height.

distribution on the bottom section with a node at the center of the section  $E_0 = 291$  mv/m for 1 kw. These values are shown in Fig. 21 for comparison purposes.

#### 126° Sectionalized Top Loaded Tower

A transmission line messenger cable inside the 112.7° (400 foot) bottom section of the tower was supported on stand-off insulators at regular intervals plus strain insulators at both the top and bottom. The characteristic impedance between the transmission line messenger cable and the tower was measured to be;

$$Z_0 = 168 \text{ ohms.}$$

The top end of the messenger cable was connected to the top section of the tower, just above the sectionalizing insulator. Base impedance measurements were made on the tower as a function of the location of a shorting strap between the transmission line cable and the tower. To extend the electrical length of the transmission line cable at the base of the tower a coil was added as shown in Fig. 19. The base impedance measurement curves along with a sketch of the tower, drawn to scale, are also shown in this figure.

Measured field intensities were plotted as a function of the base resistance as shown in Fig. 20. From the curve in Fig. 20 it was determined that optimum performance would be achieved when the base input resistance measured 300 ohms and the reactance component was  $-j 540$  ohms. It will also be noted in Fig. 19 that the same base impedance exists for two conditions, first when 15 turns of coil are used and secondly when the transmission line cable is shorted to the tower approximately 47 feet below the sectionalizing insulator.

The coil condition was used during tune up procedure for ease of adjustment and the short at 47 feet on the messenger cable was used for the final adjustment in order to eliminate the maintenance of the coil and the insulators below the shorting strap and secure some improvement in efficiency. Optimum unattenuated field intensity was approximately 225 mv/m for 1 kw at 1 mile.

#### IV. Comparison of Various Current Distributions and Efficiencies

Figure 21 was prepared to compare the performance of various kinds of vertical radiators as a function of antenna height. The sinusoidal current distribution curve is from Ballantine and shows good performance at 225°. The constant current distribution gives better performance at the higher antenna heights. The Franklin antenna theoretical value falls on this curve. The computations on the double doublet from Fig. 1 are close to the optimum curve predicted by LaPaz and Miller.<sup>8</sup>

More recently Bouwkamp and DeBruijn<sup>9</sup> published an article on the problem of optimum

antenna current distribution showing theoretically there is no upper bound in the improvement of antenna performance assuming no loss in the system. The prototype curve marked (0) is the ground wave field intensity when the current distribution is the well known Gaussian error-distribution. The curves marked (4), (10) and (25) are for more complicated derived current distributions. There is no evidence to date that such current distributions can be easily accomplished in practice let alone doing it efficiently enough to make the scheme worth while.

The theoretical and experimental results of the authors are also shown in Fig. 21 for comparison purposes.

#### V. Conclusions

From this theoretical study and experimental field work it is evident that top loaded and sectionalized towers can be used to improve the performance of vertical tower radiators. The tower height need not be limited in order to secure superior performance. With reasonably good design the performance will be better than for constant current or sinusoidal current distribution.

A very worthwhile application today is to use high television towers to increase the coverage of associated standard broadcast stations. This can be done by incorporating top loading and sectionalizing the tower. There are several ways to achieve such results.

#### VI. Acknowledgment

The source material for this paper was obtained principally from work done for the United Broadcasting Company in Cleveland, Ohio and from a contract project handled by the authors for the United States Department of State, now the United States Information Agency, involving high powered radio stations in Linz and Vienna, Austria.

Portions of this paper was presented before the Professional Group on Broadcast Transmission Systems at the 1951 IRE National Convention in New York and as a conference paper prepared for the Television and Aural Broadcasting Committee of the AIEE and presented at the 1955 Winter General Meeting of the AIEE in New York.

#### References

- <sup>1</sup>Stuart Ballantine, "On the Optimum Transmitting Wavelength for a Vertical Antenna Over Perfect Earth", Proc. I.R.E., Vol. 12, pp. 833-839; December, 1924.
- <sup>2</sup>Carl E. Smith and Earl M. Johnson, "Performance of Short Antennas", Proc. I.R.E., Vol. 35, pp. 1026-1038; October, 1947.
- <sup>3</sup>Carl E. Smith, John R. Hall and James O. Weldon, "Very High-Power Long-Wave Broadcasting Station", Proc. I.R.E., Vol. 42, No. 8, pp. 1222-1235; August, 1954.

<sup>4</sup>Ralph N. Harmon, "Some Comments on Broadcast Antennas", Proc.I.R.E., Vol. 24, pp. 36-47; January, 1936.

<sup>5</sup>George H. Brown, "A Critical Study of the Characteristics of Broadcast Antennas as Affected by Current Distribution", Proc. I.R.E., Vol. 24, pp. 48-81; January, 1936.

<sup>6</sup>Carl E. Smith, "A Critical Study of Several Antennas Designed to Increase the Primary Coverage of a Radio Broadcasting Transmitter", Professional Thesis at Ohio State University, Columbus, Ohio.

<sup>7</sup>Carl E. Smith, "A Critical Study of Two Broadcast Antennas", Proc.I.R.E., Vol. 24, pp.1329-1341; October, 1936.

<sup>8</sup>Lincoln La Paz and Geoffrey Miller, "Optimum Current Distributions on Vertical Antennas", Proc. I. R. E., Vol. 31, pp. 214-232, May, 1943.

<sup>9</sup>C. J. Bouwkamp and N. G. DeBruijn, "The Problem of Optimum Antenna Current Distribution", Philips Res. Reports, Vol. 1, No. 2.2; 1946.

IRE

TRANSACTIONS

ON BROADCAST TRANSMISSION SYSTEMS

GEORGE C. DAVIS  
RECEIVED  
DEC 21 1955  
WASHINGTON, D. C.



PGBTS-2

DECEMBER, 1955

## TABLE OF CONTENTS

*Papers Presented at the Third Annual Broadcast Symposium  
Philadelphia, Pennsylvania  
November 16, 1953*

Television Station Construction.....	B. Eichwald	1
Power Amplifiers for Television.....	G. E. Hamilton	5
One Kilowatt uhf Television Transmitter.....	T. P. Tissot and W. N. Wylde	17

### *Contributed Papers*

Performance of Sectionalized Broadcasting Towers		
	C. E. Smith, D. B. Hutton and W. G. Hutton	22
Dual-Frequency Operation of a Loaded Vertical Medium-Frequency Radiator		
	A. J. McKenzie, W. H. Hatfield and V. F. Kenna	35
A Precision Deflection Yoke.....	H. J. Benzuly	43
<hr/>		
1955 Directory of Membership of PGBTS.....		49

PUBLISHED BY THE

PROFESSIONAL GROUP ON BROADCAST TRANSMISSION SYSTEMS

JAMES B. HATFIELD, PE  
BENJAMIN F. DAWSON III, PE  
THOMAS M. ECKELS, PE

PAUL W. LEONARD, PE  
L.S. CHRISTIANE ENSLOW  
STEPHEN S. LOCKWOOD, EIT

HATFIELD & DAWSON  
CONSULTING ELECTRICAL ENGINEERS  
4226 SIXTH AVE. N.W.  
SEATTLE, WASHINGTON 98107

TELEPHONE  
(206) 783-9151  
FACSIMILE  
(206) 789-9834

MAURY L. HATFIELD, PE  
CONSULTANT  
Box 1326  
ALICE SPRINGS, NT 5950  
AUSTRALIA

## **A STUDY OF AM TOWER BASE IMPEDANCE**

By James B. Hatfield

Presented At The 42nd Annual  
IEEE Broadcast Symposium

September 17, 1992

## THE PROBLEM IN HISTORICAL PERSPECTIVE

The design of matching networks and power division networks for non-directional and directional antennas used for medium wave (standard broadcast) stations depends upon knowledge of the load impedance of the antenna system. Over the years many attempts have been made to predict the impedance of the conventional monopole over a radial wire ground screen. Many published computations were referenced to measurements made at high frequencies, where the center conductor of the feed line was extended through a copper ground plane as an antenna (Figure 1)[1,2]. A medium wave tower antenna has a much more complicated base geometry than this and its impedance is demonstrably different. For example, 50 Ohms or so is typical for a base driven tower, while 37 Ohms is shown in [2] R.W.P. King's *"The Theory of Linear Antennas"*.

S. A. Schelkunoff [3] treated antennas as a transmission line problem in terms of characteristic impedance. Some workers have used his theory to good advantage in predicting AM tower impedance. Until recently use of his methods resulted in the most accurate predictions of measured base impedance.

In an effort to achieve more realistic estimations of tower impedances several empirical curves have been developed over the years. One such curve appeared in the NAB Engineering Handbook [4] through several revisions (Figure 3). The information for this curve was compiled by my father, J.B. Hatfield. This curve was incorrectly labeled as to electrical height and, as a result, was never very useful or accurate. The correctly labeled curve (Figure 4) gives results that are a closer match to experience (i.e. 50 Ohms resistance for a 90 degree tower).

George Mather, in his June 1952 article in *Electronics*, page 143, and in a paper prepared for the Canadian Ministry of Transportation [5] presented curves of the tower impedance based upon measurements of more than 150 towers. I have used this curve with some success in calibrating various calculation techniques.

## PROBLEMS IN MEASUREMENTS AND COMPUTATIONS OF TOWER IMPEDANCE

Several writers, including R.W.P. King, [2] have dealt with the effect of the tower base capacitance upon the measured impedance. The interaction can be quite large for towers with a high reactance. Most empirical curves of measured impedances ignore base capacitance effects.

Another factor that affects base impedance is the inductance of the feedline from the Antenna Tuning Unit (ATU) to the tower. Long feedlines can have more inductance than the output leg of the matching "T" network. I measure the resistance and reactance at the tower base and then repeat the measurement at the output of the ATU. A slight impedance transformation can occur due to transmission line effects.

When the reactive component of the tower impedance is large the base capacitance must be taken into account when computations are made. The average tower, using the most commonly available brand of base insulator, has from 75 to 100 pF capacitance from the base plate to ground. Austin ring transformers used for lighting can double this capacitance. Static drain coils, isocouplers, and lighting chokes can also affect the measured base impedance.

## RECENT ADVANCES IN COMPUTATIONAL METHODS

These days many engineers use some sort of "Method of Moments" program to compute tower impedance. MININEC and its various clones are relatively "user friendly". Various tricks must be employed if one is to get useful answers; however, computed results must be verified by measurements.

In the last decade two papers treating this subject [1,6] have been published in "IEEE Transactions On Broadcasting". The 1983 paper by Wright, Klock and Jubera [1] studied the effect of guy wires, guy wire insulators, and base capacitance upon tower base impedance. The reference impedance data (used as a benchmark for the measured and calculated impedances



presented in the paper.), however, was measured using an antenna geometry similar to Figure 1 and does not include the effects of the base geometry of an actual tower. The 1989 article by Chiodini [6] demonstrated that their moment method results agreed well with his measurements for towers of  $96^\circ$  and  $105^\circ$  physical height.

Ron Rackley, of du Treil, Lundin, & Rackley, increases the electrical length of the towers used in the computation so that measured results are matched. Adding about 6.7% to the tower height gives 50 Ohms for a quarter wave tower. Radiation efficiency is increased about 3% by this change in tower height. The results of this computation, shown as data points on Mather's 1952 "Electronics" empirical curve, are depicted in Figure 5. The computed impedances, using the technique, diverge from the empirical curve for taller towers and other correction factors must be applied to the tower height.

For a thick (8 foot face) guyed tower (120 electrical degrees) Rackley increased the height by 12.5% and added two reactances to the base of his MININEC tower model. The model and a computed vs measured curve are shown in Figure 6. There is good agreement between measured and computed impedances as a function of frequency. This apparent increase in tower height is, in all probability, due to the large cross section of the tower and the accompanying increase in capacitive coupling to ground relative to thinner towers.

A good match to the 1952 Mather experience curve can be made with MININEC using the model shown in Figure 7. The tower height is unmodified while the tower base is modeled as a thin filament with a lumped capacitance of 100 pF. The tower feed is modeled as a horizontal two meter length of tubing. To properly match the 1952 empirical curve,  $5 + j43$  Ohms must be added to all the computed impedances. The result (Figure 8) is a good approximation to the impedances shown in the empirical curve over the range of tower heights shown.

## APPLICATIONS TO FIELD WORK

The measured self impedances of the towers in an array can be used to correct the driving point impedances computed by MININEC. Moment method programs like MININEC compute AM tower mutual impedances more accurately than self impedances. This is due to the fact that the self impedance can be considered to be sensitive to the conditions at the base of the towers (a situation difficult to model using moment method programs) while mutual impedance involves coupling along the entire tower length. The difference between the measured self impedance and the self impedance computed by MININEC is added to the driving point impedances computed by MININEC.

When this technique is applied to a specific case the results are mixed. The networks in a three tower array at the low end of the band were adjusted to drive point impedances calculated from measured self and mutual impedances. When the array was initially powered up the magnitudes of the impedances of the terminations for the lines were within the following percentages of 50 Ohms: Tower #1 +20%; Tower #2 +4%; Tower #3 (with a negative resistance) -27% at the bus. These results give one confidence in the accuracy of the measured self and mutual impedances. A successful D. A. Proof of Performance was made on this antenna system without any further adjustments.

The measured self impedances were also used to adjust the drive point impedances computed by MININEC. The results of both procedures are shown below for comparison.

Adjusted MININEC Drive Points		Drive Points From Measured Selfs & Mutuals
$Z_1 =$	38 + j62	37 + j71
$Z_2 =$	24 + j36	21 + j41
$Z_3 =$	-7 + j11	-22 + j11

The impedances for the first two towers given by the two methods are in reasonable agreement but the results for the third tower are much more problematical.

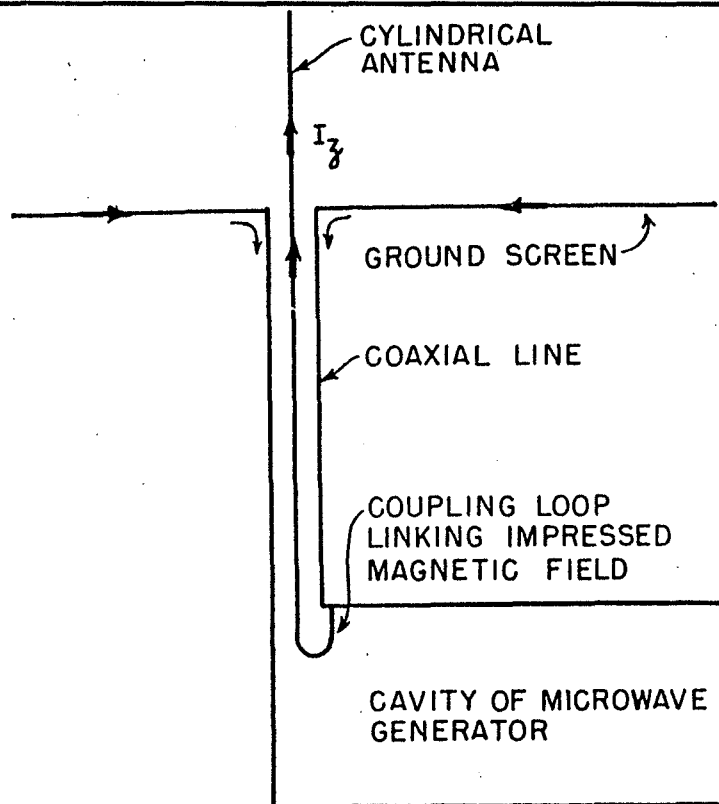
Tower heights that are not near resonance (i.e.  $90^\circ$  or  $180^\circ$ ) have base impedances that are well predicted by MININEC. A 70 degree self supporting tower, for example, measured 24 -j41 Ohms while the MININEC self impedance for this tower was 25 -j47 Ohms. This resistance is predicted by the radiation resistance curve (Figure 2 of this paper) in the 1937 Brown, Lewis & Epstein paper. A 64.4 degree guyed tower, on the other hand, measured 19 -j103 Ohms and MININEC predicted 15 -j137 Ohms. The resistance of the self supporting tower and the reactance of the guyed tower are both well outside the confines of the empirical curves of Figure 5.

## CONCLUSION

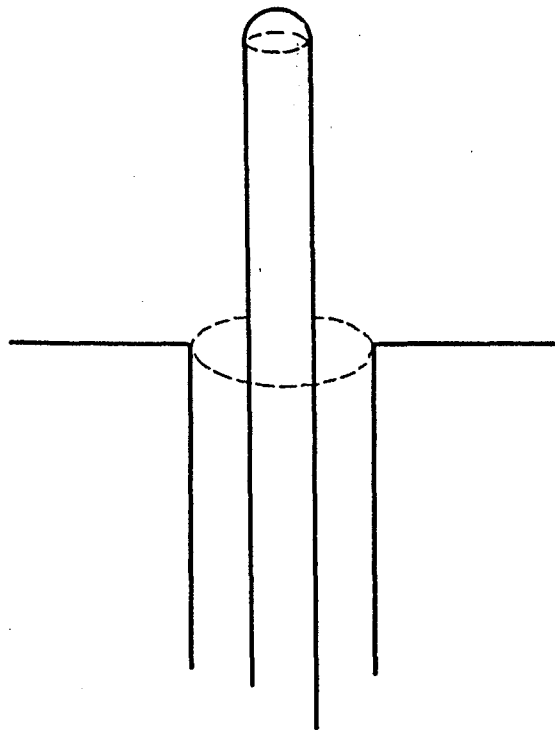
While newer prediction methodology using method of moments for determining AM tower impedance is in closer agreement with measured values than older methods, measurements must be relied upon in critical situations to accurately determine self and drive point impedances. In any case, because of the substantial variation in the electrical characteristics of ostensibly similar towers within and between different installations, it is vitally important that computations be calibrated by measured impedances.

## REFERENCES

- [1] S.M. Wright, P.W. Klock, J.D. Jubera, "The Impedance of the Guyed Quarter Wave Monopole", IEEE Transactions on Broadcasting, Vol. BC-29, No.1, March 1983.
- [2] R.W.P. King, "*The Theory of Linear Antennas*", Harvard University Press Cambridge, Mass., 1956.
- [3] S.A. Schelkunoff, H.T. Friis, "*Antennas: Theory and Practice*", John Wiley & Sons, Inc., New York, 1966.
- [4] A.P.Walker, G.W. Bartlett, "NAB Engineering Handbook", McGraw-Hill Book Company, Inc., New York, 1960.
- [5] "Vertical Radiator Characteristics Uniform Cross Section Base Insulated Guyed Tower", George Mather & Associates, October 1982.
- [6] T. Chiodini, "Moment Method Predicted Impedances Compared to Actual Measured Impedances of Directional Arrays", IEEE Transactions on Broadcasting, Vol.35, No. 2, June 1989.



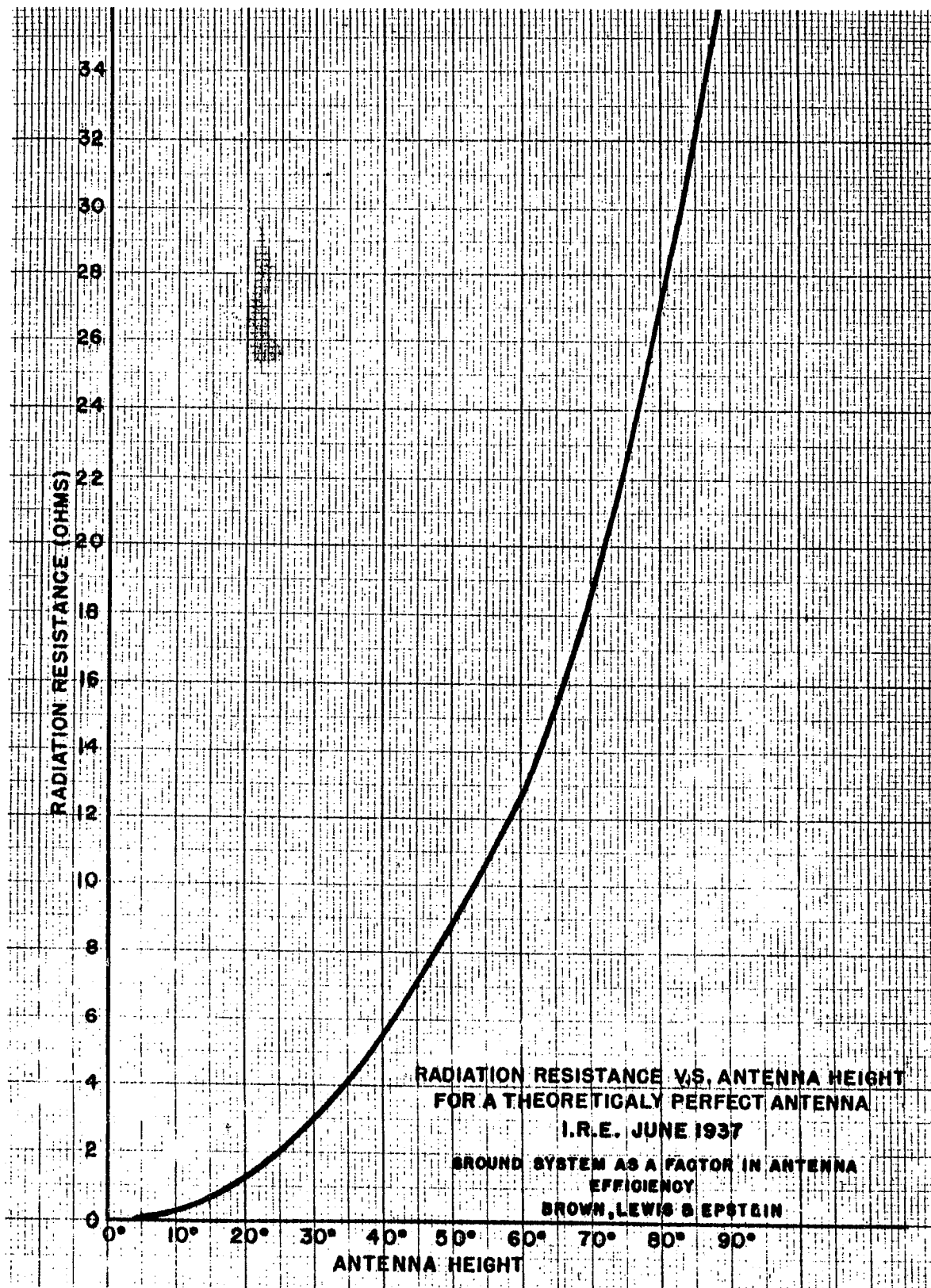
Transmitting system with coaxial line.



Coaxial drive.

HATFIELD & DAWSON  
CONSULTING ENGINEERS

FIGURE 1  
FROM "THE THEORY OF LINEAR ANTENNAS"  
BY R.W.P. KING pg. 845



HATFIELD & DAWSON  
CONSULTING ENGINEERS

FIGURE 2

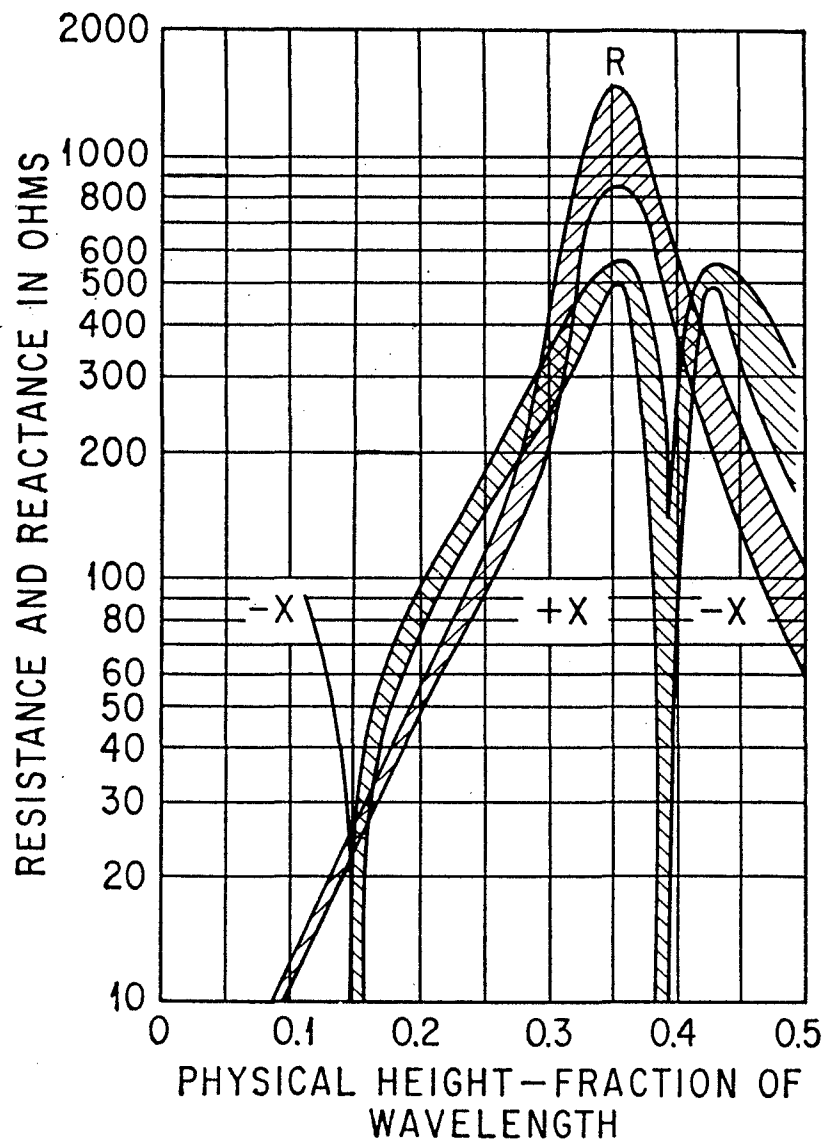
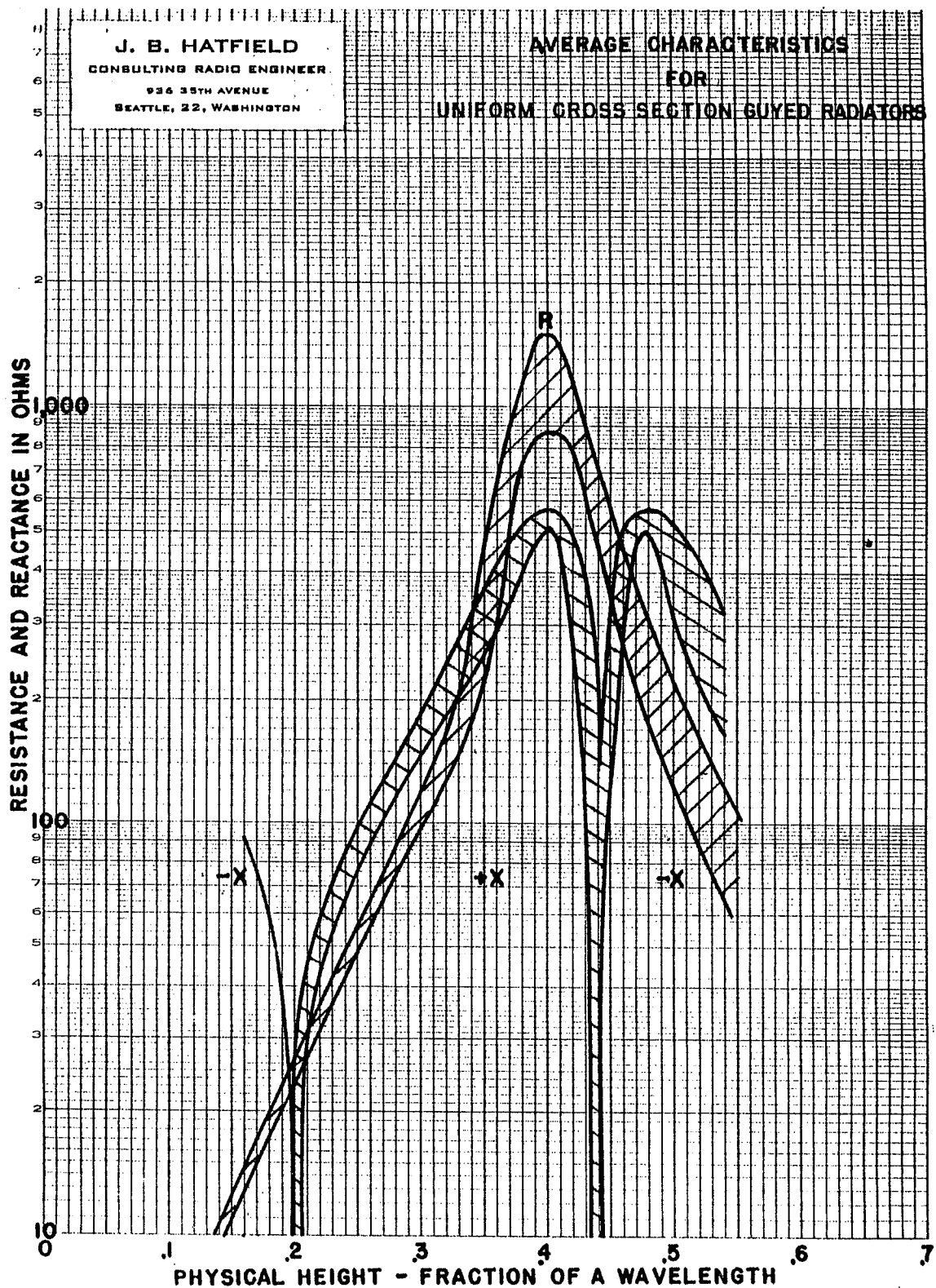


FIG. 9-15. Average characteristics for guyed radiators of uniform cross section. Data compiled from measurements of KNX and KIRO's 4-ft triangular radiators and a large number of 12- to 18-in. triangular radiators. (Prepared by J. B. Hatfield.)

HATFIELD & DAWSON  
CONSULTING ENGINEERS

FIGURE 3

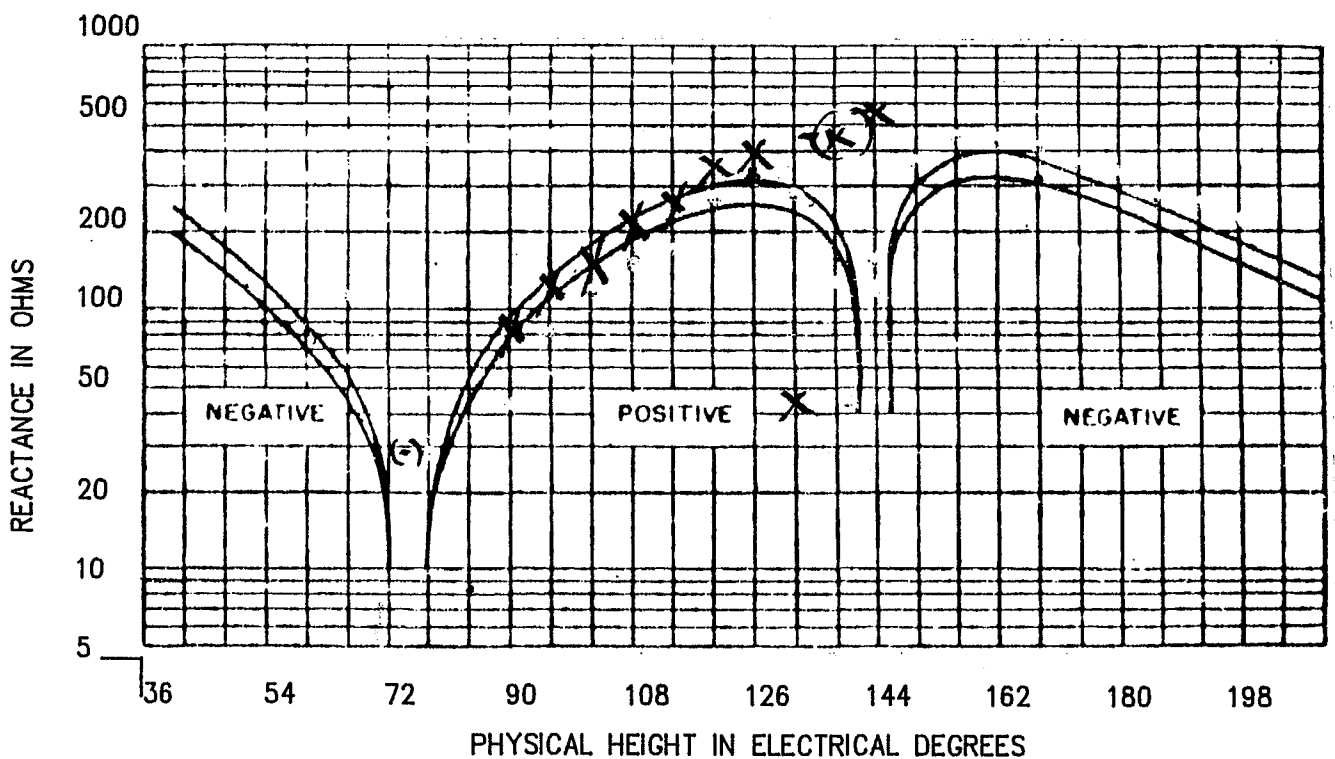
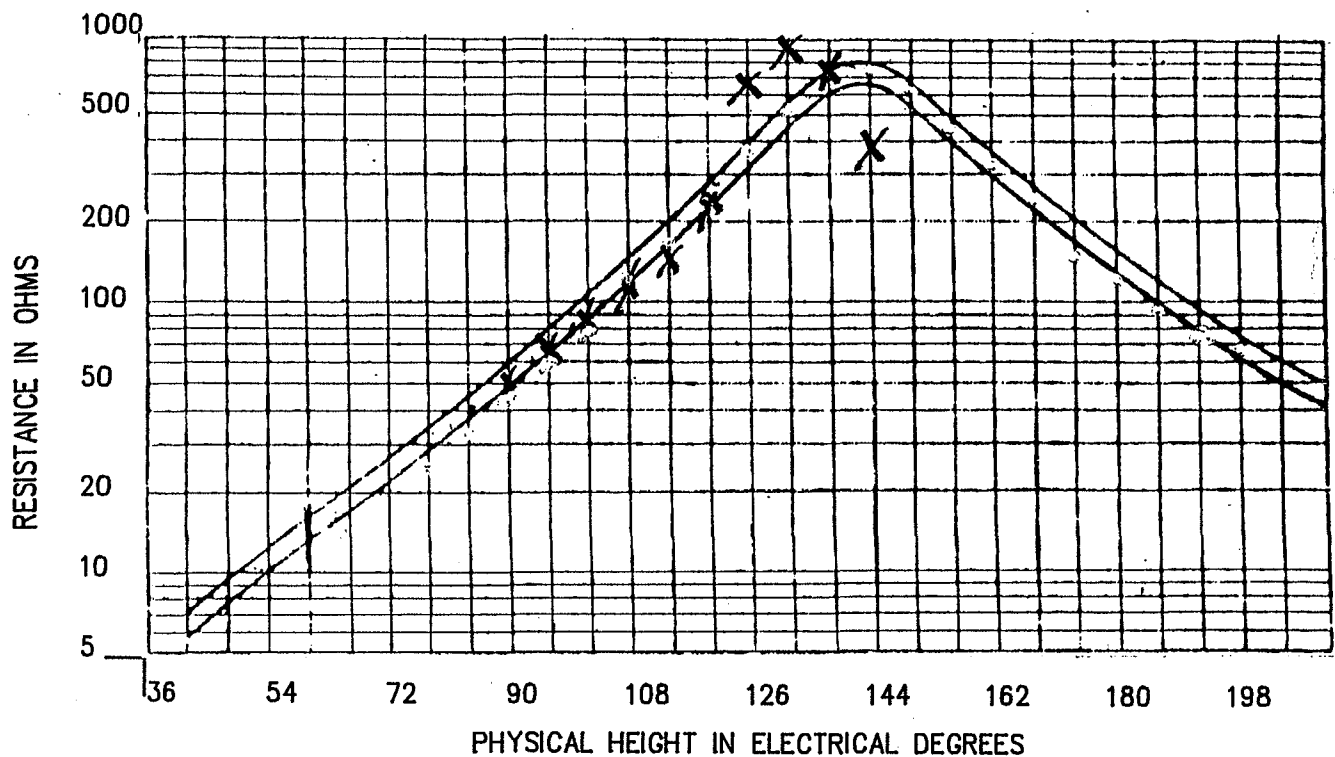
J.B. HATFIELD EMPIRICAL TOWER IMPEDANCE CURVES  
AS SHOWN IN 5TH EDITION (1960)  
"NAB ENGINEERING HANDBOOK"  
WITH PHYSICAL HEIGHTS INCORRECTLY LABELED.



**HATFIELD & DAWSON**  
CONSULTING ENGINEERS

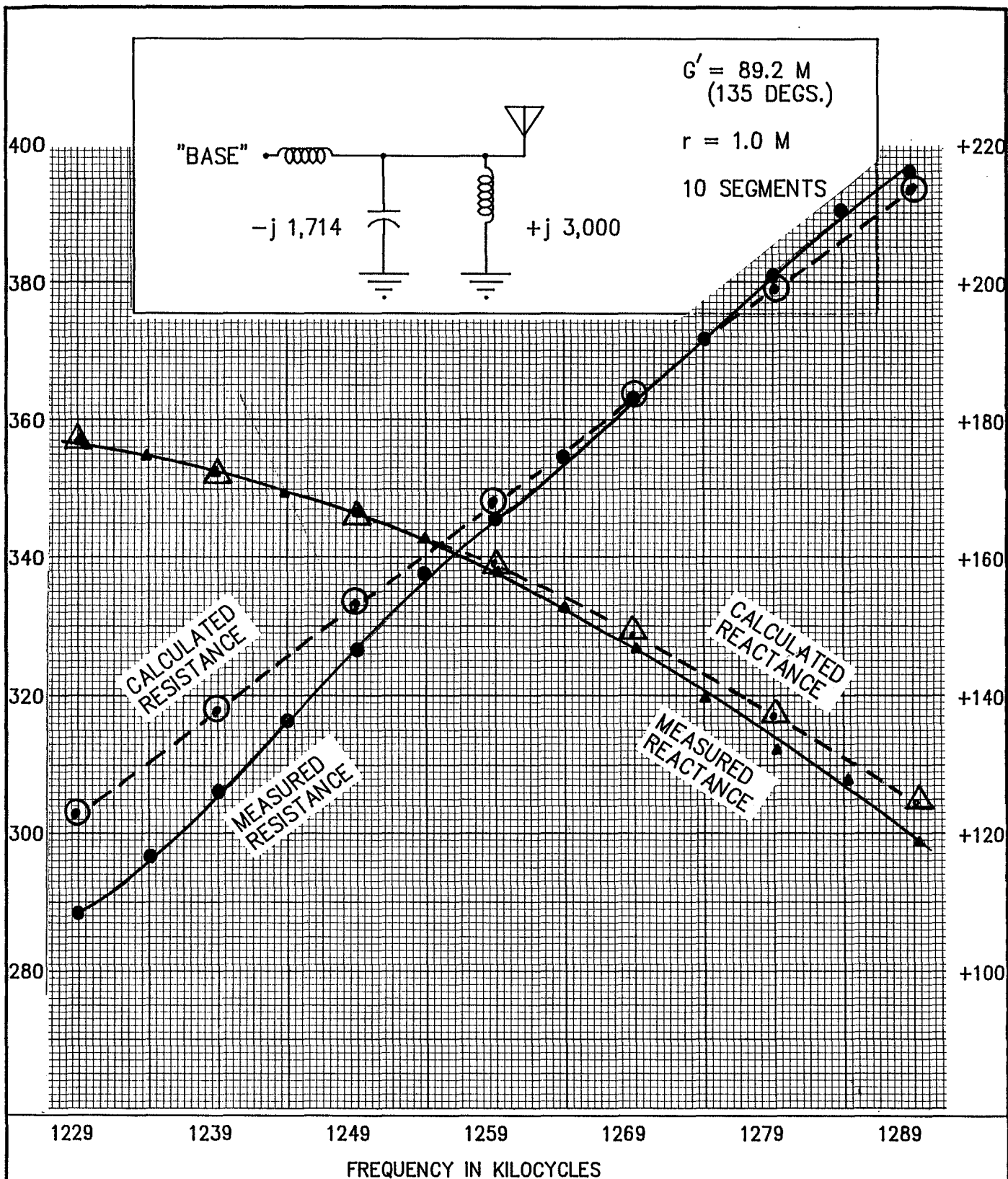
**FIGURE 4**  
CORRECT VERSION OF J.B. HATFIELD  
EMPIRICAL TOWER IMPEDANCE CURVES





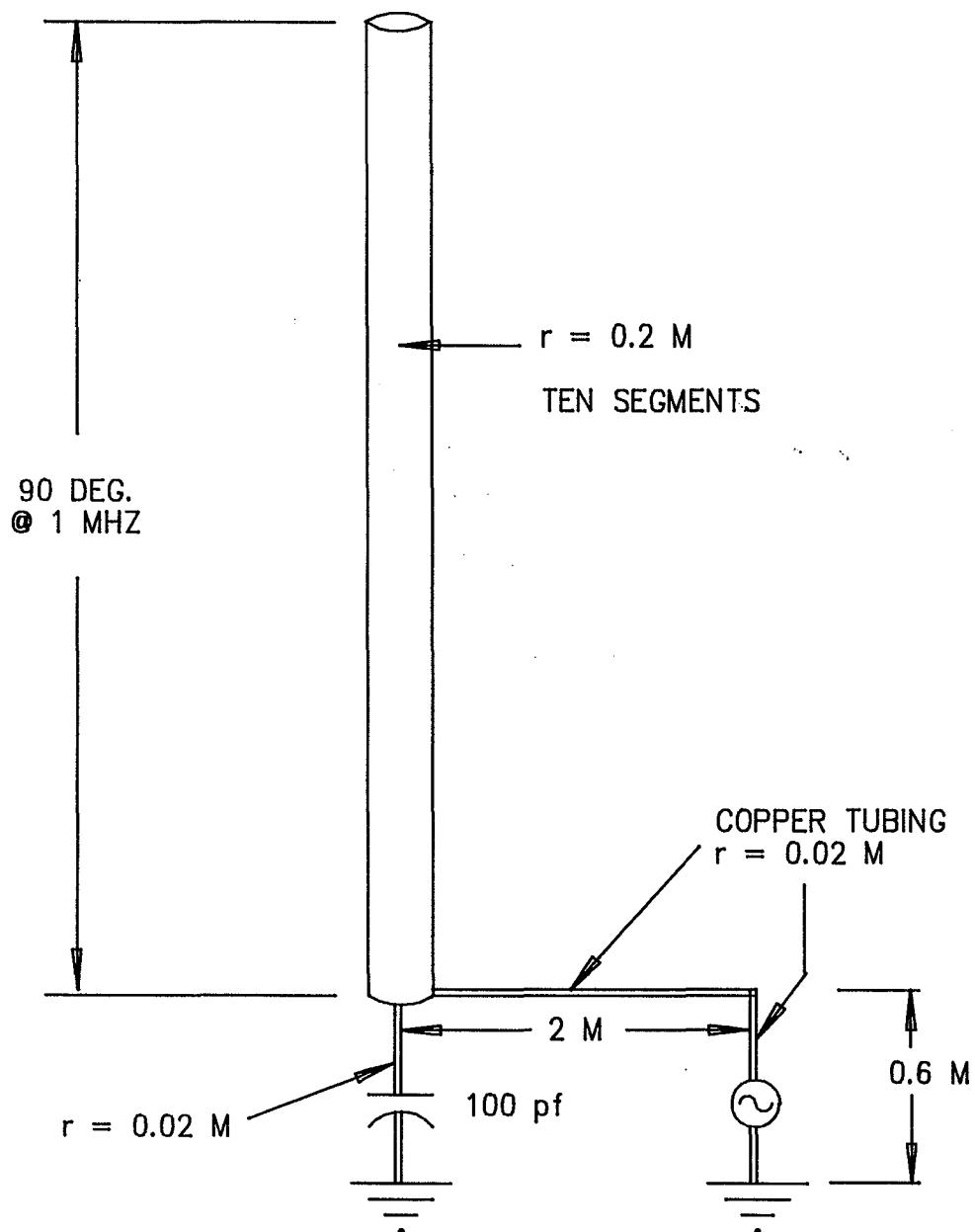
**HATFIELD & DAWSON**  
CONSULTING ENGINEERS

FIGURE 5  
TOWER SELF IMPEDANCE COMPUTED BY INCREASING PHYSICAL HEIGHT BY 6.7%. "X"s ARE COMPUTED VALUES PLOTTED ON EMPIRICAL MEASUREMENT CURVES. THIS HEIGHT INCREASE YIELDS A MININEC COMPUTED RESISTANCE OF 50 OHMS FOR A 90 DEG. TOWER.



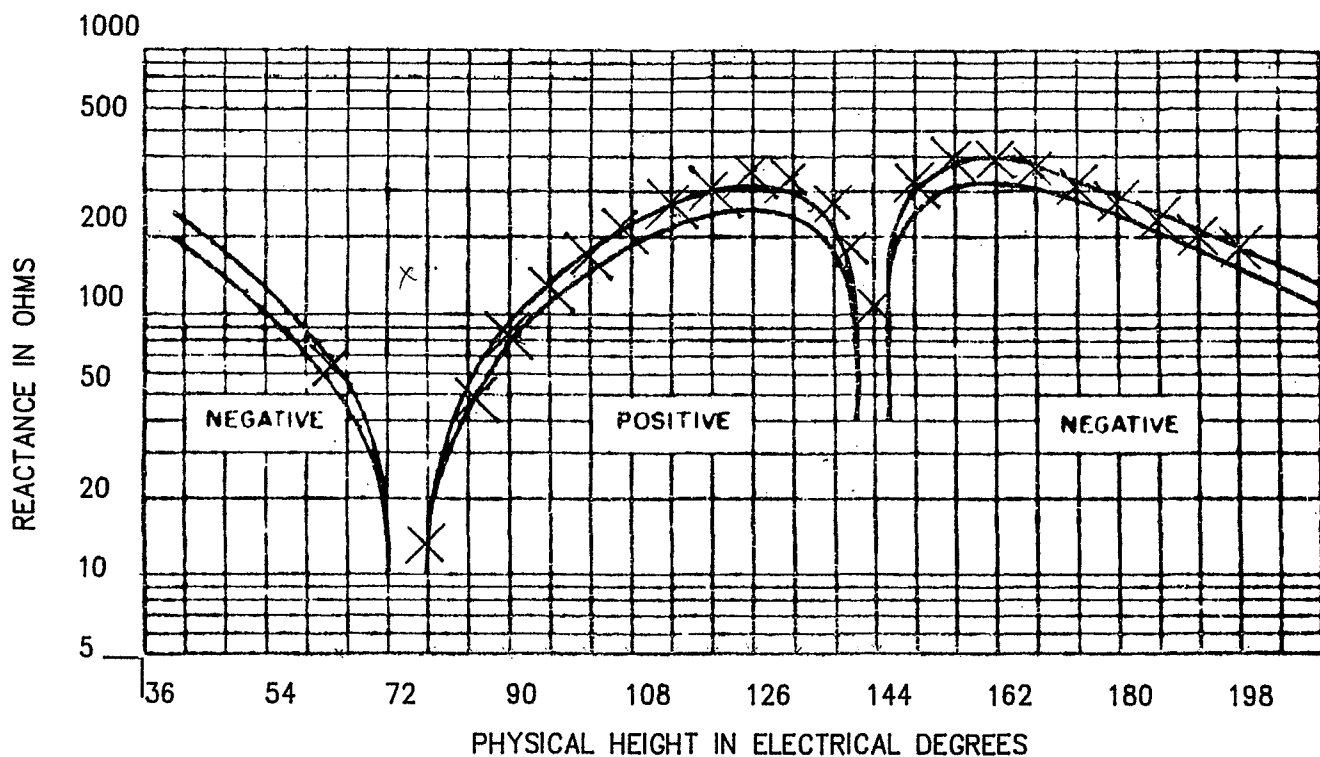
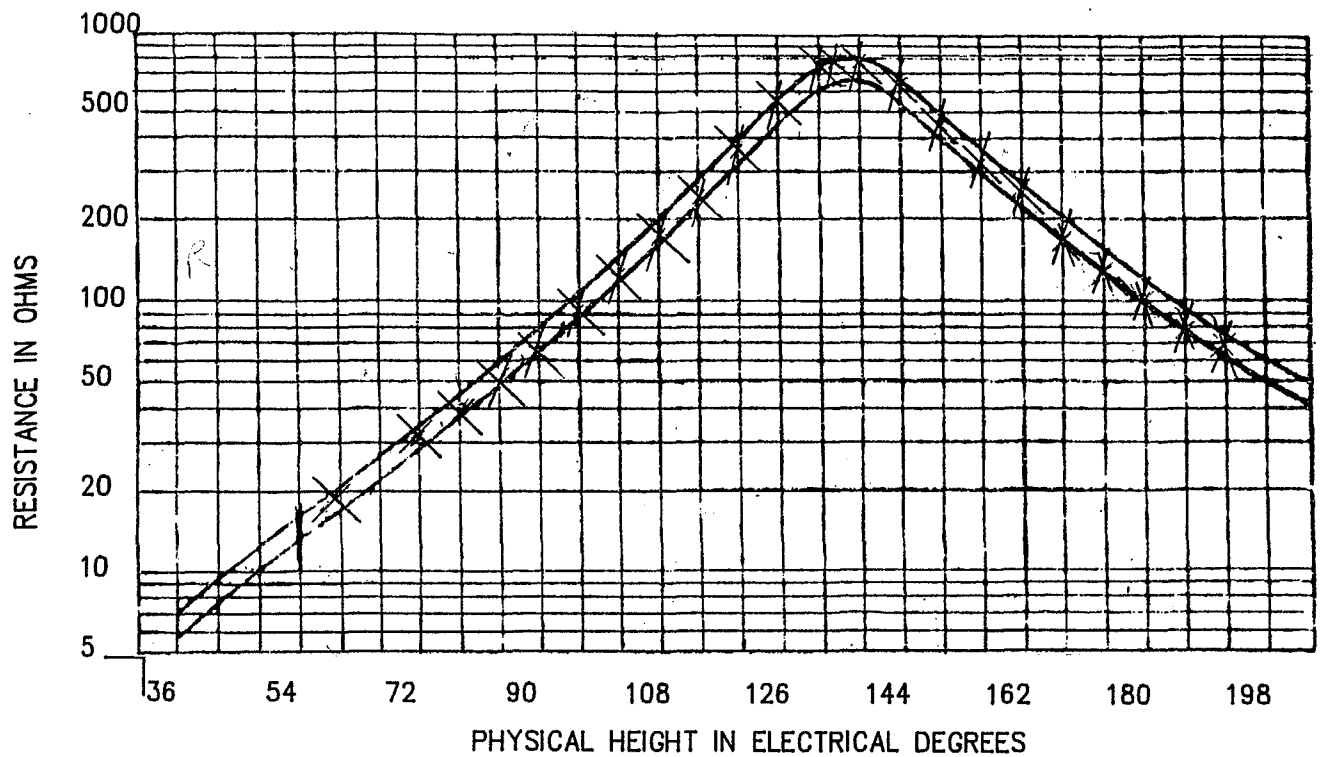
**HATFIELD & DAWSON**  
CONSULTING ENGINEERS

FIGURE 6  
RHODES, GREECE  
TOWER MODEL  
MEASUREMENT AND ANALYSIS BY RON RACKLEY



HATFIELD & DAWSON  
CONSULTING ENGINEERS

FIGURE 7  
TOWER & FEED MODEL  
FOR MININEC IMPEDANCE COMPUTATIONS



**HATFIELD & DAWSON**  
CONSULTING ENGINEERS

FIGURE 8  
SELF IMPEDANCE OF MONOPOLE OVER A RADIAL WIRE GROUND  
SCREEN. MODELED BY MININEC (SEE FIGURE 7) AND  
CORRECTED BY ADDING  $5 + j43$  TO COMPUTED IMPEDANCE.  
COMPUTED DATA POINTS PLOTTED ON EMPIRICAL CURVES FROM  
ELECTRONICS MAGAZINE ARTICLE (JUNE 1952 pg.143)

RESEARCH DEPARTMENT

THE DESIGN OF COMBINING CIRCUITS FOR MEDIUM-FREQUENCY TRANSMITTERS  
WORKING INTO A COMMON AERIAL

Research Department Report No. 1969/6  
UDC 621.396.673  
621.372.622

This Report may not be reproduced in any  
form without the written permission of the  
British Broadcasting Corporation.

It uses SI units in accordance with B.S.  
document PD 5686.

R.D.C. Thoday, M.I.E.R.E.  
P. Knight, B.A., M.I.E.E.

*D. Maurice*  
Head of Research Department

THE DESIGN OF COMBINING CIRCUITS FOR MEDIUM-FREQUENCY TRANSMITTERS  
WORKING INTO A COMMON AERIAL

Section	Title	Page
	SUMMARY . . . . .	1
1.	INTRODUCTION . . . . .	1
2.	THE DESIGN OF THE REJECTOR CIRCUITS . . . . .	2
	2.1. Impedance at the Rejection Frequency . . . . .	2
	2.2. Circuit Magnification Factor ( $Q$ ) . . . . .	2
	2.3. Component Values and Ratings . . . . .	4
3.	THE DESIGN OF THE MATCHING CIRCUITS . . . . .	4
4.	COMBINING CIRCUITS FOR MORE THAN TWO TRANSMITTERS . . . . .	5
5.	CONCLUSIONS . . . . .	6
	REFERENCE . . . . .	6
	APPENDIX I: THE IMPEDANCE OF A REJECTOR CIRCUIT . . . . .	6
	APPENDIX II: AN EXAMPLE ILLUSTRATING THE DESIGN OF A COMBINING CIRCUIT . . . . .	7

## THE DESIGN OF COMBINING CIRCUITS FOR MEDIUM-FREQUENCY TRANSMITTERS WORKING INTO A COMMON AERIAL

### SUMMARY

*Two or more m.f. transmitters separated in frequency by as little as 3% may be operated into a common aerial provided its impedance is first transformed to a fairly high resistance. Rejector circuits are used to isolate the transmitters from each other and prevent excessive cross-modulation and intermodulation occurring in their output stages. A satisfactory performance can be obtained using rejector circuits with normal components, but the maximum powers which can be fed to a common aerial may be limited by the voltage ratings of the capacitors in the combining circuit.*

### 1. INTRODUCTION

It is common practice at low-power m.f. transmitting stations for up to four transmitters to feed a single aerial. While this presents no difficulty when the individual frequency separations exceed 10%, complications may arise if the separations are smaller. This report describes the design and performance of combining circuits for frequency separations of less than 10%. Separations less than about 20 kHz (2% at 1 MHz) are not likely to be used, however, because of limitations imposed by receiver selectivity.

When two transmitters are combined into a common aerial, an arrangement similar to that shown in Fig. 1 is usually adopted. If more than two transmitters are connected to the point A, additional rejector circuits have to be inserted in the feeders from the transmitters but the principle remains the same. The rejector circuits ensure that the greater part of the transmitter power reaches the aerial and they also prevent excessive cross-modulation and intermodulation\* occurring

in the output stages of the transmitters. In the design of the rejector circuits the suppression of the modulation products is the overriding consideration. Although cross-modulation and intermodulation levels are difficult to calculate, experience has shown that acceptable levels result if the unwanted voltage which reaches the anode of the output valve of a transmitter is less than 10 volts r.m.s. when the e.h.t. supply to the valve is removed. Rejector circuits are therefore designed with this criterion in mind.

Frequency separations as low as 3% are now being considered and calculations have shown that very-high- $Q$  rejector circuits are required for certain aerial impedances if the criterion stated above is to be satisfied. The difficulty of using high- $Q$  circuits can be overcome by inserting an additional matching network between the point A of Fig. 1 and the aerial, to transform the aerial impedance to one which is considerably greater than the transmitter load impedance and predominantly resistive. The majority of low-power transmitters are designed for load impedances between 50 and 80 ohms and calculations have shown that practicable rejectors can be used if the impedance at A is approximately equal to  $500 + j0$  ohms. If this impedance is made exactly 500 ohms midway between the two frequencies, it will be sufficiently close to 500

\* Cross-modulation is the transfer of modulation from one carrier frequency to another. Intermodulation is the generation of spurious frequencies such as the sum and difference of two carrier frequencies.

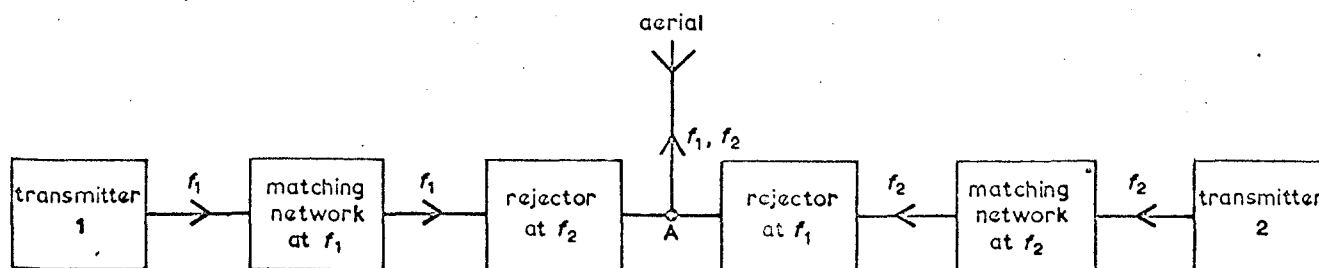


Fig. 1 - General arrangement of networks

ohms at both  $f_1$  and  $f_2$  for the performance of rejector circuits designed for 500 ohms to be almost unaffected. The matching circuits in the transmitter branches are designed to transform the true impedance at A, seen through the rejector circuit, to the load impedance required by the transmitter (usually 80 ohms).

This arrangement is shown in more detail in Fig. 2. It is assumed that the two transmitters and the point A are close together, i.e. in the same building. If the aerial is less than  $0.1\lambda$  from the transmitters (where  $\lambda$  is the wavelength) the primary matching circuit may be situated either in the transmitter building or below the aerial. If the aerial is more than  $0.1\lambda$  from the transmitters, the aerial should be matched to the feeder and the impedance transformed to 500 ohms in the transmitter building. Whatever arrangement is adopted, care should be taken to ensure that the impedance at A is as close to 500 ohms as possible at both  $f_1$  and  $f_2$ .

The detailed design of the combining circuit is considered in the sections which follow and an example of the design procedure is given in Appendix II.

## 2. THE DESIGN OF THE REJECTOR CIRCUITS

Each rejector circuit must satisfy the following requirements:

- (i) the impedance at the rejection frequency must be high enough to prevent the unwanted r.m.s. voltage at the valve anode exceeding 10
- (ii) the rejector circuit must not introduce excessive loss at the pass frequency
- (iii) the  $Q$  must not be too high or the rejection at the sideband frequencies will be poor and the tuning of the circuit will be critical.

The design of circuits which satisfy these requirements will now be discussed.

### 2.1. Impedance at the Rejection Frequency

When the  $f_1$  transmitter radiates, a small fraction of the voltage at A (Fig. 2) appears at the anode of the output stage of the  $f_2$  transmitter. This fraction depends partly on the impedance of the  $f_1$  rejector (a pure resistance  $R_D$  at  $f_1$ ) and partly on the design of the output circuit of the transmitter. With low-power transmitters,  $\pi$ -networks are commonly used in place of conventional tank circuits and coupling coils. The equivalent circuit of the  $f_2$  transmitter branch therefore takes the form shown in Fig. 3 at  $f_1$ ; a similar circuit may be drawn for the  $f_1$  transmitter branch at  $f_2$ .

Anode voltages have been computed for a range of values of  $R_D$  for frequency separations between 2 and 10%. In every case, the matching circuit com-

ponents were assumed to be adjusted so as to present the idle transmitter with a resistive impedance of 80 ohms at its working frequency. Values of  $R_D$  which give exactly 10 volts at the anode of one transmitter as a result of the other transmitter radiating 1 kW were then found by interpolation and are shown in Fig. 4. Values of  $R_D$  for other powers may be obtained by multiplying by  $\sqrt{P}$ , where  $P$  is the power of the rejected transmitter in kW.

In general, the component values of the output circuit of a transmitter are chosen to give efficient power transfer into the load, without considering requirements for rejection of power from other transmitters; Fig. 4 therefore shows curves for three values of output-circuit loaded  $Q$  ( $Q_L$ ). In practice  $X_1$  has a fixed value and  $X_2$  and  $X_3$  are adjusted for maximum power transfer;  $Q_L$  may then be calculated from the measured values of  $X_2$  and  $X_3$ .<sup>\*</sup> For the computations,  $X_1$  was specified as -160 ohms, since further computations indicated that very high values of  $R_D$  might be required if  $|X_1|$  was less than 80 ohms. Although Fig. 4 was calculated for a load impedance of 80 ohms it may be applied with little error to a load of  $80n$  ohms (where  $n$  is a scaling factor) provided  $X_1$  is made equal to  $-160n$  ohms and the value of  $R_D$  obtained from curves is also multiplied by  $n$ . The  $Q$  of the rejector circuit was assumed to be 400 but Fig. 4 is reasonably accurate for  $Q$  values between 200 and 800. The actual choice of  $Q$  value is governed by factors discussed in the next section.

### 2.2. Circuit Magnification Factor ( $Q$ )

The  $Q$  of the rejector circuit must exceed a minimum value or the loss at the pass frequency will be excessive. In this report the maximum permissible pass loss is taken to be 0.5 dB, i.e. 11% of transmitter power is lost in the rejector.

The pass loss  $L$  is given by

$$L = 10 \log_{10}(1 + R_S/R_A) \text{ dB} \quad (1)$$

where  $R_A$  is the series resistance of the load at A in Fig. 2 (nominally 500 ohms) and  $R_S$  is the resistive part of the rejector impedance at the pass frequency. For losses under 1 dB,  $L$  may be expressed in the form

$$L = 4.34 \log(1 + R_S/R_A) \simeq 4.34 R_S/R_A \text{ dB} \quad (2)$$

In Appendix I it is shown that, for frequencies more than 2% but less than 10% from the resonant frequency,  $R_S$  is given approximately by

$$R_S \simeq R_D/(2Q\nu)^2 \quad (3)$$

<sup>\*</sup> If the load presented to the transmitter is 80 ohms and  $X_1 = -160$  ohms, the values of  $X_2$  and  $X_3$  are  $64Q_L$  and  $-64(Q_L - 0.25)$  ohms respectively.



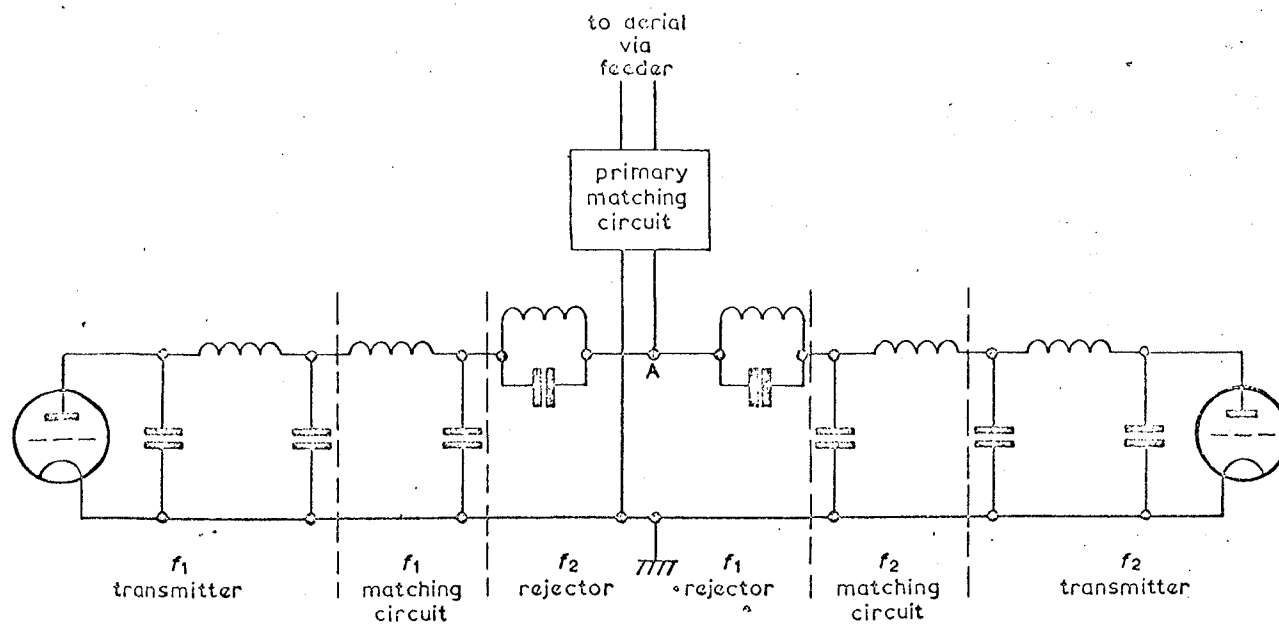


Fig. 2 - Combining network for two transmitters separated in frequency by less than 10%

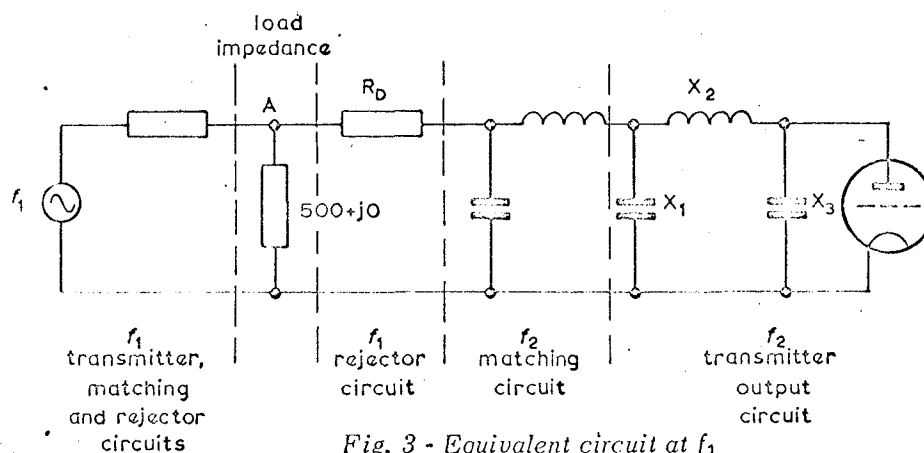
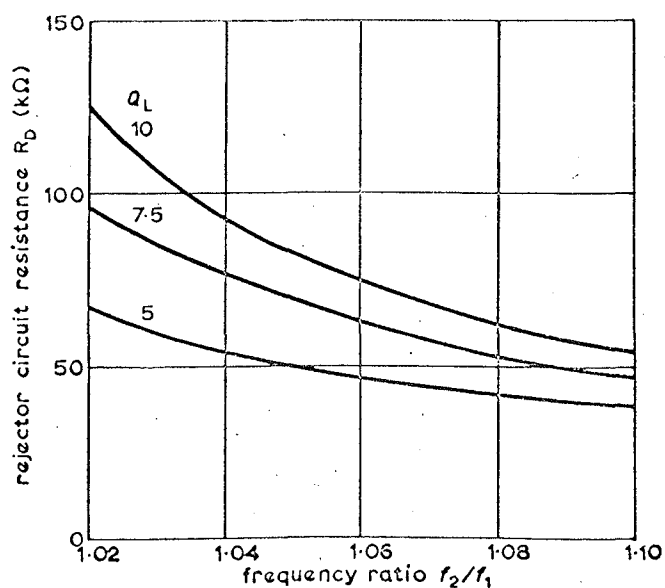
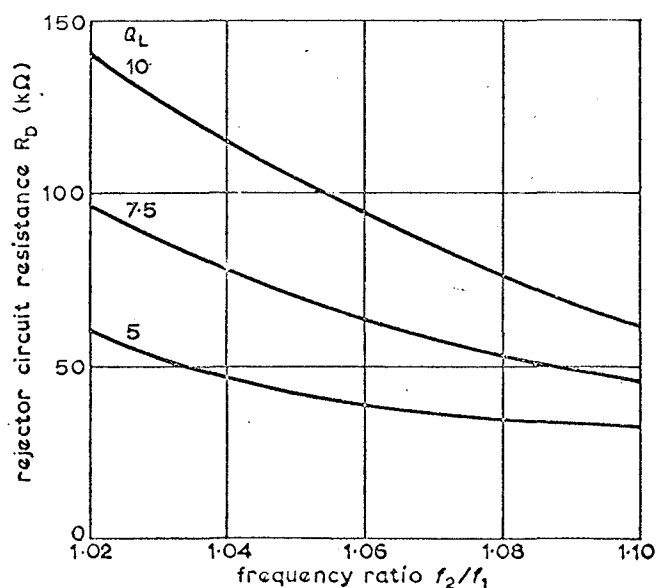


Fig. 3 - Equivalent circuit at  $f_1$



(a)



(b)

Fig. 4 - Values of rejector circuit resistance which give 10 volts r.m.s. at the valve anodes

(a) Rejector circuit in the  $f_1$  transmitter branch (b) Rejector circuit in the  $f_2$  transmitter branch

$Q_L$  is the loaded  $Q$  of the output circuit of the idle transmitter

Power of rejected transmitter, 1 kW

where  $\nu = (f - f_0)/f_0$  is the fractional deviation from the resonant frequency  $f_0$ . The pass loss is therefore given approximately by

$$L \simeq \frac{1.08 R_D}{(Q\nu)^2 R_A} \text{ dB} \quad (4)$$

From this it follows that the loss will be less than 0.5 dB provided

$$Q > \frac{(2R_D/R_A)^{1/2}}{\nu} \quad (5)$$

Equation (5) specifies the lower limit for  $Q$ . For example, if  $\nu = 0.04$  (4%),  $R_D = 100,000$  ohms and  $R_A = 500$  ohms, then  $Q$  must exceed 500.

Although a higher value of  $Q$  will give a lower pass loss, it may lead to inadequate rejection of sideband frequencies. A reasonable criterion to adopt is that the rejection should be within 6 dB of that at the carrier over a bandwidth of  $\pm 1$  kHz, since most of the power in an amplitude-modulated wave is contained within this band. Poorer rejection may, however, be tolerated outside the band.

The cause of poor rejection at sideband frequencies with high- $Q$  circuits is the rapid reduction of the rejector circuit impedance which occurs away from resonance. Equation (8) of Appendix I shows that the modulus of the impedance falls to  $0.7R_D$  when  $\nu = \pm 1/2Q$ ; the unwanted voltage at the transmitter would then be expected to be 3 dB greater than that at the carrier frequency. There is, however, a possibility that the series reactance of the rejector circuit may resonate with the matching circuit, in which case the unwanted voltage would be 6 dB greater than at the carrier frequency. Thus if  $\nu = \pm 1/2Q$  is made to correspond to  $\pm 1$  kHz, the 6 dB criterion is bound to be satisfied at all frequencies within 1 kHz of the carrier. Now for  $\pm 1$  kHz,  $\nu = \pm 1/f_0$ , where  $f_0$  is the carrier frequency in kHz. It follows therefore that the criterion is satisfied if  $Q$  is less than  $f_0/2$ . Thus the highest  $Q$  value which will be required in the m.f. band (at 1.6 MHz) is 800 and this can be achieved with normal components. At the low-frequency end of the band (0.530 MHz)  $Q$  should not exceed 265 for adequate sideband rejection. This value may, however, conflict with the minimum  $Q$  required for low pass loss and a compromise may be necessary; the use of the  $Q$  value which gives exactly 0.5 dB pass loss is then recommended. A compromise is unlikely to be required above 1 MHz, assuming a transmitter frequency difference of not less than 3%.

To summarize, the  $Q$  of the rejector circuit should, if possible, lie within the range

$$\frac{(2R_D/R_A)^{1/2}}{\nu} < Q < \frac{f_0}{2} \quad (6)$$

However, if the  $Q$  of an available coil is  $r$  times greater than the value desired it may be used with advantage provided  $R_D$  is increased to  $r^2 R_D$ . The rejection at both carrier and sideband frequencies will then be improved and the pass loss will be unchanged. If  $R_D$  were not increased the pass loss would be reduced but the rejection at the sidebands would be degraded.

### 2.3. Component Values and Ratings

Having determined the values of  $R_D$  and  $Q$  which give the required performance, the rejector circuit reactances ( $X_L$  and  $X_C$ ) are calculated from the relationship  $X_L = -X_C = R_D/Q$ . If a variable capacitor cannot be used, a fixed capacitor whose reactance is greater, rather than less, than  $R_D/Q$  should be chosen, since this ensures that the specified anode voltage is not exceeded. In general, tapped rejector circuits do not offer any advantage.

Circulating currents flow in the rejector circuit at both the rejection and pass frequencies. The maximum voltage across the capacitor is the arithmetic sum of the voltages at the two frequencies, since these will periodically add in phase.

At the rejection frequency  $f_1$ , the voltage  $V_1$  across the capacitor is essentially the same as that across the load and is therefore equal to  $(P_1 R_1)^{1/2}$ , where  $P_1$  is the power the  $f_1$  transmitter delivers to the load and  $R_1$  is the parallel resistance of the load at  $f_1$ . At the pass frequency  $f_2$  the impedance of the rejector is predominantly reactive and equal to  $\pm jR_D/2Q\nu$ . Thus the voltage at  $f_2$  across the capacitor is

$$V_2 = \frac{R_D}{2Q\nu} \left( \frac{P_2}{R_{A2}} \right)^{1/2} \quad (7)$$

where  $P_2$  is the power delivered by the  $f_2$  transmitter to the load and  $R_{A2}$  is the series resistance of the load at  $f_2$ . The total peak voltage when both transmitters are modulated 100% is  $2.82(V_1 + V_2)$ . If the frequency separation is small the peak voltage will be large even for moderate powers; in the example given in Appendix II it is of the order of 10 kV for two 1 kW transmitters separated by 3.4%.

### 3. THE DESIGN OF THE MATCHING CIRCUITS

The impedance of the rejector circuit at the pass frequency is given approximately by Equation (9) in Appendix I. This impedance must be added to the series impedance of the load and transformed to a resistive value (usually 80 ohms) with a simple matching network.

If  $f_1$  is less than  $f_2$ , the  $f_1$  rejector will look like a capacitance at  $f_2$ . The impedance presented to the  $f_2$  transmitter is then most conveniently matched by

mean  
as s  
the n  
mitte  
acita  
use  
conc  
quel  
and

is c  
beca  
freq  
volta  
wher  
part  
is v

means of a shunt capacitance and series inductance, as shown in the right-hand arm of Fig. 2. Conversely the most convenient matching network for the  $f_1$  transmitter would be a shunt inductance and a series capacitance. Calculations have shown, however, that the use of the latter network may lead to a resonance condition in the  $f_1$  transmitter at the unwanted frequency  $f_2$ ; the alternative network (shunt capacitance and series inductance) is therefore used instead.

The voltage across the matching circuit capacitor is comparable with that across the rejector circuit because of the high reactance of the latter at the pass frequency. If the impedance to be matched is  $Z$ , the voltage across the capacitor is given by  $|Z|(P/R)^{1/2}$ , where  $P$  is the transmitter power and  $R$  is the real part of  $Z$ . The voltage due to the rejected transmitter is very small and may be neglected.

#### 4. COMBINING CIRCUITS FOR MORE THAN TWO TRANSMITTERS

The principles described may be extended to three or more transmitters feeding a common aerial, the exact arrangement depending mainly on their frequency separations. Thus three transmissions separated in frequency by more than 10% would be fed directly to the aerial, as shown in Fig. 5(a), and each transmitter branch would contain a matching circuit and two rejectors. If two closely-spaced transmitters are to be combined with one which is more widely spaced, an arrangement of the type shown in Fig. 5(b) would be used. Here the transmitter with the more widely spaced frequency ( $f_1$ ) feeds the aerial directly via rejectors while the more closely spaced pair feed a nominal 500-ohm impedance derived from a primary

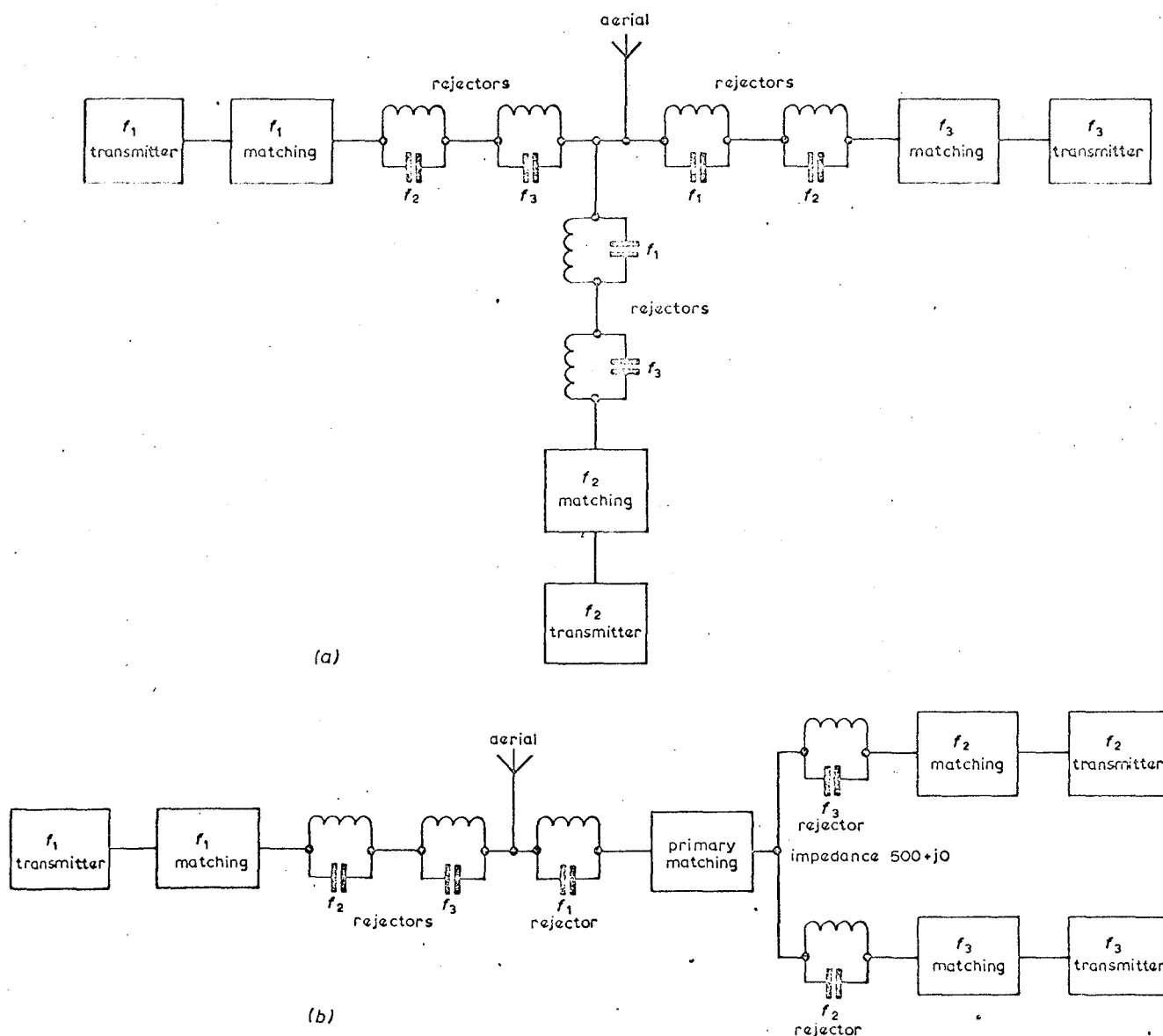


Fig. 5 - Three transmitters fed to a common aerial

(a) Three widely-spaced frequencies

(b) One widely-spaced frequency ( $f_1$ ) and two closely-spaced frequencies

matching circuit. Three transmitters with closely-spaced frequencies would be combined as in Fig. 5(a), but with the aerial impedance transformed to 500 ohms at the central frequency.

Whichever arrangement is adopted, the design of the rejector circuits follows the principles described in Section 2. Although two or more rejectors in series will have a higher pass loss than one rejector, some of the rejectors will inevitably be tuned to frequencies well away from the pass frequency and will have correspondingly lower losses. Thus the total pass loss in many cases may not be much greater than that occurring when only two transmitters are combined.

## 5. CONCLUSIONS

It has been shown theoretically that two m.f. transmissions separated in frequency by as little as 3% may be combined in a common aerial provided the latter is first matched to 500 ohms. The use of rejector circuits having a  $Q$ -factor less than 800 gives satisfactory suppression of cross-modulation and intermodulation products at both carrier and sideband frequencies, while the pass loss does not generally

exceed 0.5 dB. The principles described can be extended to three or more transmitters operating into a common aerial.

With such small frequency separations, however, the peak voltages across the capacitors in the combining circuit may be quite large; for example with 1 kW transmitters they may be as much as 10 kV. Thus the voltage ratings of commercially-available capacitors may impose an upper limit on the powers of transmitters which can be combined in the manner described.

The principal applications for close frequency combining will probably be at low-power stations. Nevertheless the design principles set out in this report can be used for high-power stations although the peak voltages encountered may present a difficulty.

## 6. REFERENCE

1. CCIR Documents of the XIth Plenary Assembly, Oslo 1966, Rec. 499.

## APPENDIX I

### *The Impedance of a Rejector Circuit*

A simple rejector circuit consists of an inductance  $L$  in parallel, with a capacitance  $C$ , as shown in Fig. 6. Providing the circuit has a high  $Q$  value, losses may be represented by a parallel resistance  $R_D = \omega_0 L Q$ , where  $\omega_0$  is the angular frequency at which the circuit resonates. At resonance,  $\omega_0^2 LC = 1$  and the reactances of the inductance and capacitance are equal and opposite. The impedance of the circuit is then equal to  $R_D$ .

At an angular frequency  $\omega$ , the admittance  $Y$  of the circuit is

$$Y = \frac{1}{R_D} + j \left( \omega C - \frac{1}{\omega L} \right)$$

$$= \frac{1}{R_D} + \frac{jC}{\omega} (\omega^2 - \omega_0^2)$$

If the deviation from the resonant frequency is less than 10%,  $\omega_0 + \omega \approx 2\omega$  and consequently

$$Y \approx \frac{1}{R_D} + j2\omega C\nu = \frac{1}{R_D} \left[ 1 + j2Q\nu \right]$$

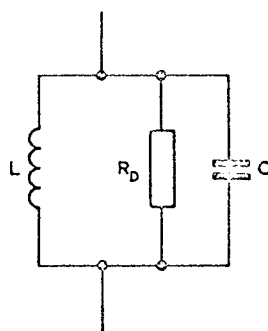


Fig. 6 - Equivalent circuit of a rejector

where  $\nu = (f - f_0)/f_0$  is the fractional deviation from the resonant frequency. The impedance of the rejector is therefore

$$Z_S = R_S + jX_S = \frac{R_D(1 - j2Q\nu)}{1 + (2Q\nu)^2} \quad (8)$$

If  $Q > 200$  and  $\nu > 0.01$  (1%)

$$Z_S \approx \frac{R_D}{2Q\nu} \left[ \frac{1}{2Q\nu} - j \right] \quad (9)$$

since  $(2Q\nu)^2 \gg 1$ .

### An Example Illustrating the Design of a Combining Circuit

An example is given of the design of a combining circuit for two 1kW transmitters operating on 1052 and 1088 kHz. These two frequencies, used by the BBC, are separated by 3.4%.

The aerial will be assumed to be the standard type used at BBC low-power stations; this consists of a T suspended between two 38 m (126 ft) masts spaced 61 m (200 ft). Measured impedances of a typical aerial are given in Table 1:

TABLE 1

Aerial Impedance

Frequency kHz	Impedance (ohms)
1052	$23.2 + j40$
1070	$24.2 + j50$
1088	$25.4 + j60$

In designing the combining circuit, shown in Fig. 7, the aerial is first matched to 500 ohms at the mid-frequency, 1070 kHz. This requires a series inductance  $L_1$  and a shunt capacitance  $C_1$ ; their reactances at 1070 kHz are 57.2 and -113 ohms respectively. The impedance at A then has the values given in Table 2.

Fig. 4 shows that, if the transmitter output circuits have a loaded  $Q$  of 5, rejector circuit impedances of 60,000 ohms will be adequate for both transmitter branches. Equation (6) then shows that the rejector circuit  $Q$ s must lie within the range  $455 < Q < 535$ ; a value of 500 will be chosen. The rejector circuit reactances, equal to  $\pm R_D/Q$  are therefore  $\pm 120$  ohms at their resonant frequencies.\*

\* This would require rejector circuit capacitances of 1220 and 1260  $\mu\text{F}$ . In practice standard values of 1200 or  $5 \times 250 \mu\text{F}$  could be used with negligible change in performance.

TABLE 2

Impedance at the point A, Fig. 7

Frequency (kHz)	Series Impedance (ohms)	Parallel Impedance (ohms)
1052	$347 + j168$	$423    j909$
1070	$500 + j0$	$500    j\infty$
1088	$451 - j239$	$575    -j1084$

Note: || signifies 'in parallel with'

The matching circuits in the transmitter branches are now designed. At 1052 kHz the impedance of the 1088 kHz rejector is  $52 + j1765$  ohms and the impedance at the point B (Fig. 7) is therefore  $399 + j1930$  ohms. This is matched to 80 ohms with a shunt reactance of -615 ohms and a series reactance of 879 ohms. At 1088 kHz the impedance of the 1052 kHz rejector is  $52 - j1765$  ohms and the impedance at C is  $503 - j2000$  ohms. This is matched to 80 ohms with a shunt reactance of -1350 ohms and a series reactance of 819 ohms.

This completes the design of the combining circuit apart from the calculation of the voltage ratings of the capacitors. Its performance may now be verified.

**Pass Loss.** The series resistance of both rejectors is 52 ohms at the pass frequency and the series resistance of the load is given in Table 2. Equation (1) gives the pass losses, which are 0.61 and 0.47 dB at 1052 and 1088 kHz respectively.

**Unwanted Voltages at the Valve Anodes.** The 1052 kHz transmitter delivers 870 watts to the load and the voltage at A is 608 volts. This voltage is attenuated by the rejector circuit, the 1088 kHz matching circuit and the output circuit of the 1088 kHz transmitter and

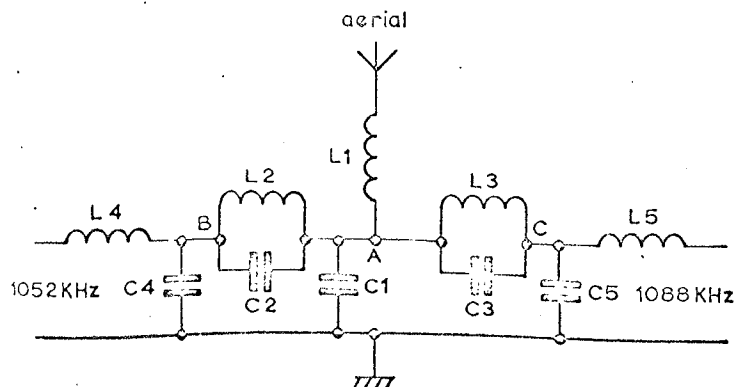


Fig. 7 - Combining circuit for 1052 and 1088 kHz

component values

$L_1$	8.5 $\mu\text{H}$	$C_1$	1320 $\mu\text{F}$ , 3.7 kV
$L_2$	17.6 $\mu\text{H}$	$C_2$	1220 $\mu\text{F}$ , 10 kV
$L_3$	18.1 $\mu\text{H}$	$C_3$	1260 $\mu\text{F}$ , 8.7 kV
$L_4$	133 $\mu\text{H}$	$C_4$	246 $\mu\text{F}$ , 8.8 kV
$L_5$	120 $\mu\text{H}$	$C_5$	103 $\mu\text{F}$ , 8.2 kV

Voltage ratings are peak values for two 1 kW transmitters simultaneously modulated 100%

computation shows that the unwanted voltage reaching the anode is 7.7 volts. The reactances of the output circuit components are required for this computation; values for 1088 kHz are given by the formulae in the footnote on page 2 and must be modified by the frequency ratio to obtain values for 1052 kHz. A similar computation shows that the unwanted voltage at the anode of the 1052 kHz transmitter is 7.5 volts.

**Sideband Rejection.** The amount by which the rejection at the sidebands falls below that at the carrier is calculated by assuming the unwanted transmitter to be detuned. Unwanted voltages for the  $\pm 1$  kHz sideband frequencies, calculated in this way, are given in Table 3.

TABLE 3

*Unwanted Voltages at Sideband Frequencies*

Frequency kHz	Voltage
1051	10.5
1053	11.2
1087	10.9
1089	10.4

These voltages are about 3 dB greater than the voltages at the carrier frequencies. The circuit therefore satis-

fies all the design requirements except that for pass loss, which is slightly exceeded at 1052 kHz.

Finally the voltage ratings of the capacitors are calculated as follows. The powers delivered to the aerial by the 1052 and 1088 kHz transmitters are 870 and 896 watts respectively. The impedances at A given in Table 2 enable the voltages at this point to be calculated; they are 606 and 717 volts at 1052 and 1088 kHz respectively. When both transmitters are modulated 100% the peak voltage at A is the sum of these voltages multiplied by  $2\sqrt{2}$ . Thus the voltage rating of  $C_1$  is 3.7 kV.

The voltage across  $C_2$  at 1088 kHz is almost the same as that across  $C_1$  at this frequency, i.e. 717 volts. At 1052 kHz the current through the rejector is 1.58 amps and its impedance is  $52 + j1765$  ohms; thus the voltage across  $C_2$  at this frequency is 2.80 kV. Addition as before gives the voltage rating of  $C_2$  as 10 kV. The voltage rating of  $C_3$  is 8.7 kV.

The voltage across  $C_4$  at 1088 kHz is negligible. The impedance at B is  $399 + j1930$  at 1052 kHz and the current is 1.58 amps. Thus the voltage at B at 1052 kHz is 3.11 kV. The peak voltage across  $C_4$ , for 100% modulation, is therefore 8.8 kV. The voltage rating of  $C_5$ , calculated in the same way, is 8.2 kV.

A table of component values and voltage ratings is given below Fig. 7.

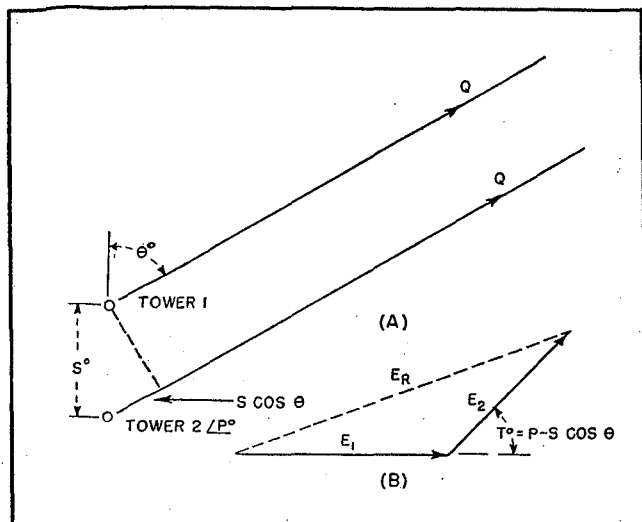


FIG. 1—Basic relationships used in setting up tower equations with spatial relationships shown at (A) and vector addition in (B)

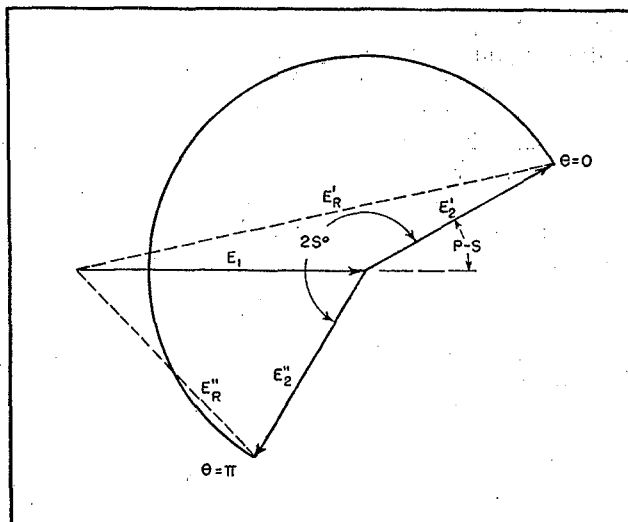


FIG. 2—Vector diagram to show how, if the spacing  $S$  between the antenna towers remains fixed, the arc subtended by  $E_2$  can be calibrated in  $\theta$

# Pattern Calculator for A-M

Graphical method useful for original design work on a pair of a-m broadcast antenna towers is also particularly applicable if a new pattern or change in frequency is necessary. Requires only dividers and transparent overlay

By **GEORGE R. MATHER**

*Radio Engineer  
Department of Transport  
Ottawa, Ontario, Canada*

**T**HE CALCULATION of directional antenna patterns is often a long and tedious job and is usually at best a laborious exercise in trigonometry. The graphical calculator to be described is readily applicable to two-tower arrays and once the antenna spacing has been established it is a simple matter to observe the change in pattern shape with variations of phasing angle and antenna-current ratios. Although this graphical calculator can be used in original designs its obvious merit is evident when the towers are already installed but perhaps a change in operating frequency is necessitated.

The determination of the shape of a pattern is accomplished by the addition of the field vectors from each of the towers in an array. Figure 1A is a graphical illustration of the geometry involved and is used to establish the notation used.

## Development

Tower 1 is used as a reference while tower 2 is considered to be spaced at  $S$  degrees from tower 1 with a phase angle of  $P$  degrees. Movable point  $Q$  is sufficiently remote from the array so that the lines from  $Q$  to tower 1 and  $Q$  to tower 2 are considered as being parallel. The angle  $\theta$  is subtended between the line of the towers and a

line from the movable point  $Q$  to tower 1. Thus for any position of point  $Q$  the total phase displacement between the field vectors of tower 1 and tower 2 is  $T$  degrees where  $T = P - S \cos \theta$ .

The resultant field at some angle  $\theta$  is determined by the use of a vector diagram as shown in Fig. 1B where  $E_1$  and  $E_2$  are proportional to the field of towers 1 and 2 respectively. Note that as the angle  $\theta$  is varied the phase displacement angle  $T$  changes and as a result the position of  $E_2$  with reference to  $E_1$  is dependent on the angle  $\theta$ . Actually the radius vector  $E_2$  describes the arc of a circle.

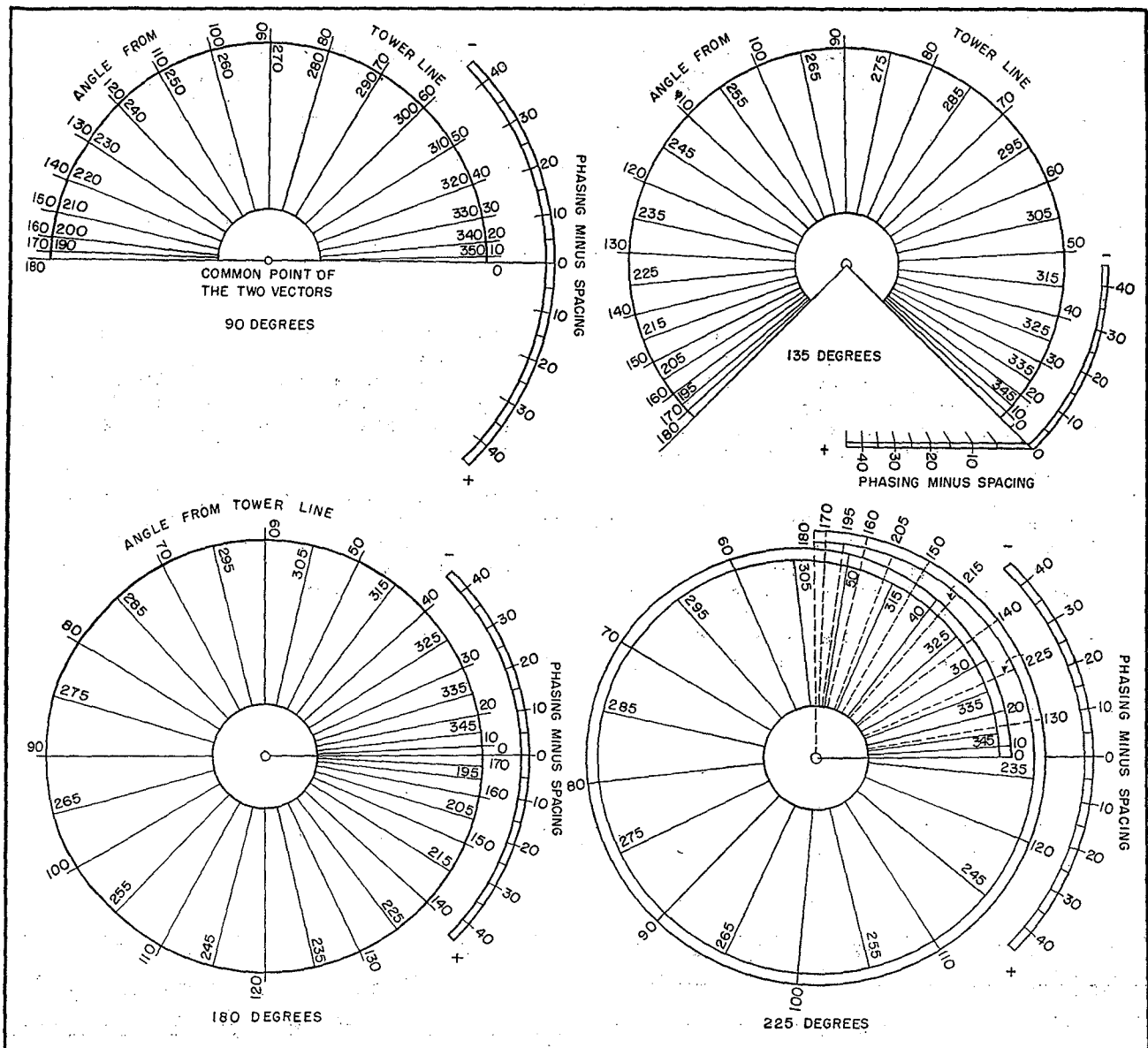


FIG. 3—Patterns can be computed to slide-rule accuracy using enlargements of these calculators. They are given for antenna spacings of 90, 135, 180 and 225 degrees

In Fig. 2 the following relationships become evident. When  $T = P - S \cos \theta$ , and when  $\theta = 0$ ,  $T = P - S$ , also when  $\theta = 180$ ,  $T = P + S$ .

Thus the arc subtended by the rotation of the vector  $E_2$  is  $(P + S) - (P - S) = 2S$  degrees. Therefore if the spacing  $S$  remains fixed, any such arc whose circumference is calibrated in  $\theta$  may be used with any combination of current ratio and phasing angle. This calibration of the circumference in  $\theta$  is also accomplished by solution of the equation  $T = P - S \cos \theta$ , where  $\theta$  is the variable.

For purpose of illustration, graphical calculators have been com-

puted for spacing angles 90, 135, 180 and 225 degrees.

### Example

In a determination of the shape of a pattern all that is necessary is a pair of dividers and a transparent overlay sheet. Suppose, for example, we have the following array:  $E_1 = 1.0$ ,  $\angle 0^\circ$ ;  $E_2 = 0.5$ ,  $\angle +60^\circ$ ;  $S = 90$  degrees. Note that the phasing angle minus the spacing angle is equal to  $60 - 90 = -30$  degrees.

First a straight line is drawn on the transparency that is then placed in register on the pattern calculator (90 degrees) so that the line passes through the common point of the

two vectors and through a phasing - spacing angle of  $-30$  degrees.

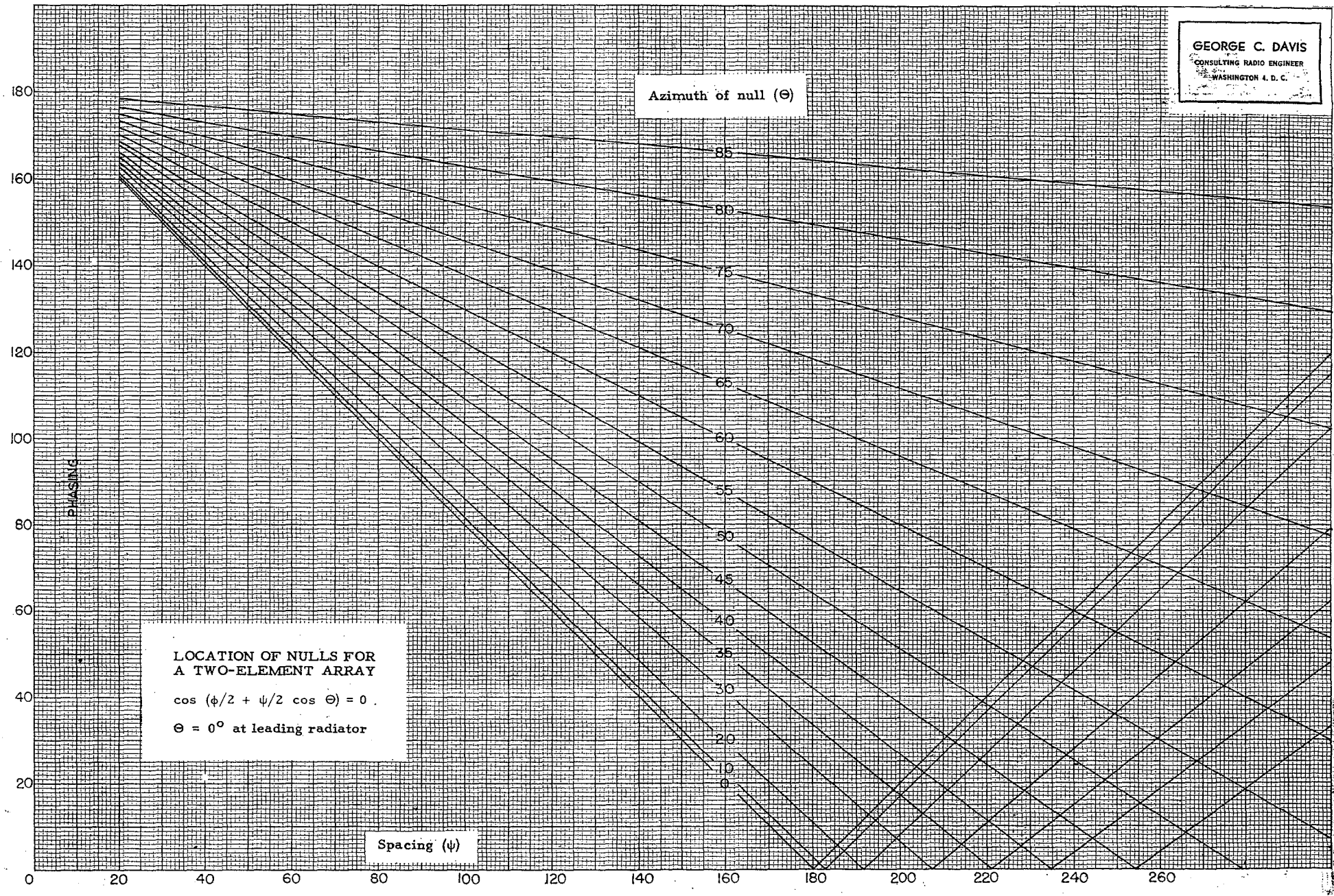
From the common point measure a distance to the left on the line that is proportional to  $E_1$ . With the common point as center, draw a circle with a radius proportional to  $E_2$ . The resultant for any angle from the tower line is then the sum of the vectors  $E_1$  and  $E_2$ , it being recognized that the position of  $E_2$  at any angle is the intersection of the circle described by  $E_2$  with the line representing that angle from the tower line.

The resultant vector will be in the same units as were used for  $E_1$  and  $E_2$ .



GEORGE C. DAVIS  
CONSULTING RADIO ENGINEER  
WASHINGTON 4, D. C.

SCUFFEL & ESSER CO., N. Y. NO. 386-111  
20 X 20 to the inch, with lines heavy.  
MADE IN U. S. A.



TO: THE REAL BOB GUILL

FROM: INGENIERO CONSULTOR RINALDO RACKLE'  
HABANA Y SARASOTA

TOTAL  
PAGES: 13

DEAR ANN: I have a problem. I have two brothers. One brother is in yadio, the other was put to death in the electric chair for murder. My mother died from insanity when I was three years old. My two sisters are both prostitutes, and my father sells narcotics to high school students. Recently I met a girl who was just released from a reformatory where she served time for smothering her illegitimate child to death, and I want to marry her.

My problem is: if I marry this girl, how do I tell her about my brother who is in radio?

LOOK AT THE EFFICIENCY COMPARISONS  
OF THESE TWO PAPERS FOR  
45° SLOPING AND STRAIGHT-WIRE  
GROUNDS.

HAPPY THANKSGIVING

  
11-24-93

USING ELEVATED RADIALS IN CONJUNCTION WITH DETERIORATED  
BURIED-RADIAL GROUND SYSTEMS

by

Al Christman  
Grove City College  
100 Campus Drive  
Grove City, PA 16127-2104

R. Paul Zeineddin  
ECE Department  
Ohio University  
Athens, OH 45701-2979

with

Roger Radcliff  
ECE Department  
Ohio University  
Athens, OH 45701-2979

Jim Breakall  
Pennsylvania State University  
EE Department  
306 EE East  
University Park, PA 16802

**Abstract**

In the US, medium-wave broadcast stations utilize ground-mounted vertical monopole antennas with extensive buried-radial ground systems. Over a period of time, these radials may deteriorate, leading to a decrease in the radiated field strength of the antenna. Computer modeling studies indicate that, in such a situation, the addition of four elevated radials can restore performance to a level which is equal to or better than the original installation. Several different configurations for the elevated radials were investigated, including variations in their orientation, length, and height above ground. The computer software used for this work was the Numerical Electromagnetics Code (NEC) [1].

**Background**

Previous computer-modeling exercises have shown that an elevated vertical monopole antenna with four elevated radials can perform as well as a conventional ground-mounted tower with 120 buried radials [2]. Also, other studies reveal that a ground-mounted tower may be used with four elevated radials (and no buried radials) to produce radiated field intensities which are equivalent to that of a standard buried-radial system [3]. The integrity of a ground screen composed of buried radial wires may be compromised in a variety of ways, but the damage will be manifested as a decrease in the magnitude of the radiated field strength and a change in the driving-point impedance. This study examines the feasibility of adding elevated radials to a pre-existing conventional AM broadcast antenna in an effort to counteract the loss in field intensity caused by a deteriorating buried-radial ground system.

As in our earlier papers, a classic ground-mounted series-fed tower with 120 buried radials was modeled initially, to serve as a standard reference [4]. An operating frequency of 1 MHz was selected, and the radii of all conductors were set at 3 millimeters. In the NEC model, the tower is made of aluminum and rests upon a two-meter-long buried steel ground rod. All radials are copper and are buried to a depth of six inches in "average" soil with a conductivity of 0.004 Siemens per

meter and a dielectric constant of 15. The tower and the radials are all 90° in length, which is equal to 75 meters at 1 MHz. A drawing of this antenna is shown in Figure 1, which illustrates all of the metallic conductors in the system and the segmentation that was utilized in the computer model. NEC predicts an input impedance of  $40.52 + j 23.40$  Ohms for this antenna, with a field strength of 267.91 millivolts per meter. This is the magnitude of the "theta" component of the radiated electric field intensity ( $E_\theta$ ), monitored at a distance of 1 kilometer from the antenna, at a height of 50 inches (1.27 meters) above the ground, when the input power is 1000 watts.

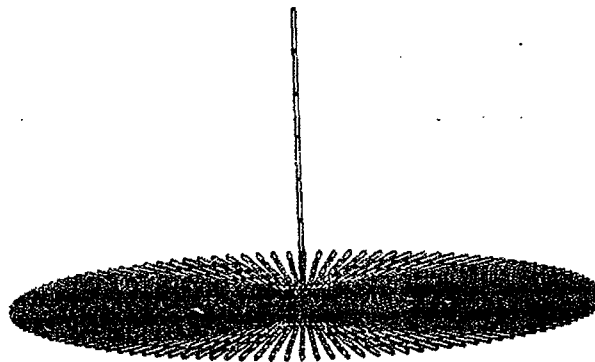


Figure 1. A conventional ground-mounted tower with 120 buried radials.

In order to ascertain the minimum field-strength values which could be expected, a similar antenna with only four buried radials was also examined. This computer-modeled antenna produced a field intensity of 225.56 mV/m, which is a reduction of almost 15% (about 1.5 dB) from the 120-radial reference level. As a result, one would expect that conventional antennas with deteriorating ground systems should yield field-strength values between 225 and 267 mV/m/kW at 1 km. (A note of interest at this point: with only a two-meter-long ground rod and no radials at all, the predicted field intensity is 125.57 mV/m, which is about 6.6 dB below the reference.)

### Deteriorated Ground Systems

It was decided that a "typical" group of deteriorated radials would appear as depicted in Figure 2. Here we see a top view of five adjacent radials, all of which were originally 90° in length. The first radial is completely intact and remains bonded to the central ground rod at the tower base, which is located at the top of this figure. The second radial is still connected to the grounding node, but its outer portion is gone. The third (middle) radial is missing entirely. Neither the fourth nor fifth radials are joined to the ground node, and various portions of their inner sections have disappeared.

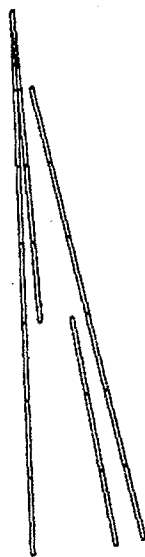


Figure 2. Top view of a "typical" group of five "deteriorated" radials.

This group of five radials, as described above, was then rotated 24 times about the tower axis (5 X 24 = 120) in order to produce the "deteriorated ground system model" shown in Figure 3.

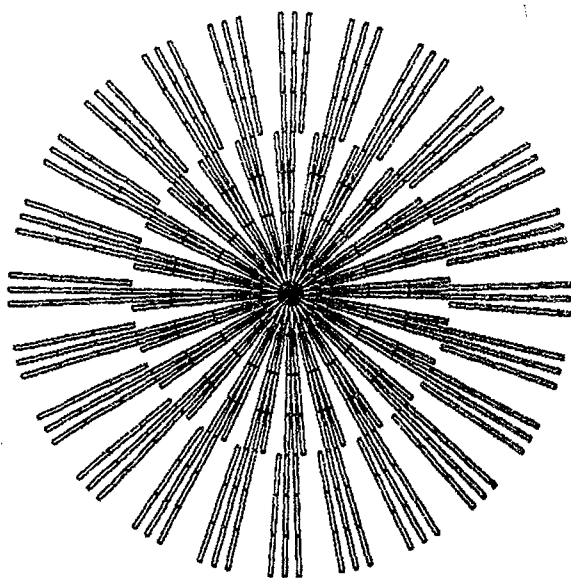


Figure 3. Top view of the "deteriorated ground system model."

In addition, a "very deteriorated ground system model" was constructed, and is illustrated in Figure 4. Here, the "typical" five-radial group which was shown earlier is spaced evenly at 120-degree intervals around the base of the tower. This particular model could represent a worst-case scenario.

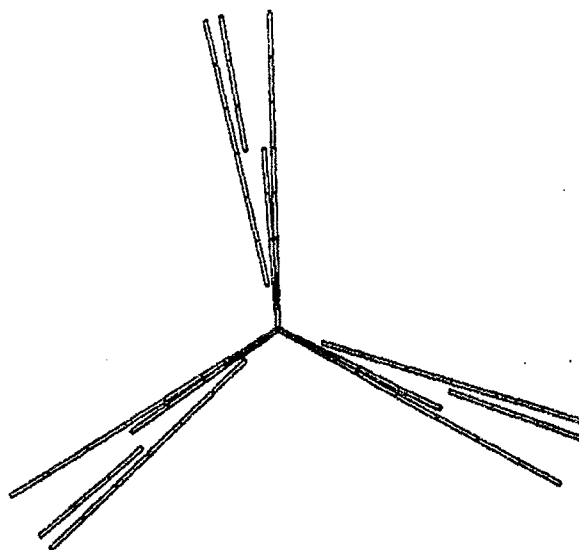


Figure 4. Top view of the "very deteriorated ground system model."

### Elevated-Radial Configurations

After designing two separate "damaged" buried-radial ground systems, the next step was to add four elevated radials to each of these pre-existing structures and take note of the effects. A large number of different test configurations for the elevated radials were modeled. In order to minimize confusion, an abbreviated symbol was adopted for each of these permutations, which are explained below:

- 435 - quarter-wave (75 m) radials which slope upward from the base of the tower at a 45-degree angle until reaching a height of five meters above ground; the remaining portion of each radial is horizontal
- 455K - same as above, except the radial lengths are extended from 75 meters to 80 meters, so that each radial has a total length of .25λ plus its height above ground
- 4310 - quarter-wave (75 m) radials which slope upward from the base of the tower at a 45-degree angle until reaching a height of ten meters above ground; the remaining portion of each radial is horizontal; (see Figure 5)

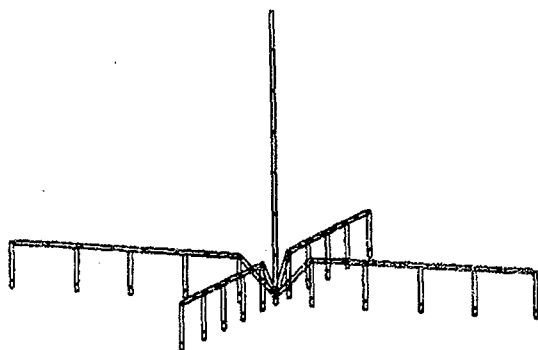


Figure 5. This is configuration "4510" as described in the text. The 4 elevated radials slope upward from the tower base at a 45° angle to a height of 10 meters, and then extend horizontally outward. They are supported atop metallic masts set on steel ground rods. All buried radials are omitted for clarity.

4510E - same as above, except the radial lengths are extended from 75 meters to 85 meters, so that each radial has a total length of  $.25\lambda$  plus its height above ground

S5 - quarter-wave (75 m) radials which slope steeply upward from the base of the tower until reaching a height of five meters above ground; at this height, the radial is displaced laterally from the tower by only one-half meter; the remaining portion of each radial is horizontal

S5E - same as above, except the radial lengths are extended from 75 meters to 80 meters, so that each radial has a total length of  $.25\lambda$  plus its height above ground

S10 - quarter-wave (75 m) radials which slope steeply upward from the base of the tower until reaching a height of ten meters above ground; at this height, the radial is displaced laterally from the tower by only one-half meter; the remaining portion of each radial is horizontal; (see Figure 6)

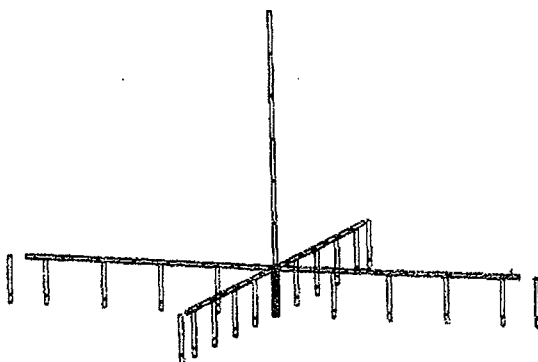


Figure 6. This is configuration "S10" as described in the text. The 4 elevated radials slope steeply upward from the tower base to a height of 10 meters, and then extend horizontally outward. They are supported atop metallic masts set on steel ground rods. All buried radials are omitted for clarity.

S10E - same as above, except the radial lengths are extended from 75 meters to 85 meters, so that each radial has a total length of  $.25\lambda$  plus its height above ground

H5 - quarter-wave (75 m) radials which are completely horizontal; the tower is fed against these four radials at a height of five meters above ground; note that the tower is now being fed above its base; for this configuration, the base of the tower was raised one-half meter above the ground to isolate it from the buried radials

H10 - same as above, except the radials are located at a height of ten meters above ground (see Figure 7)

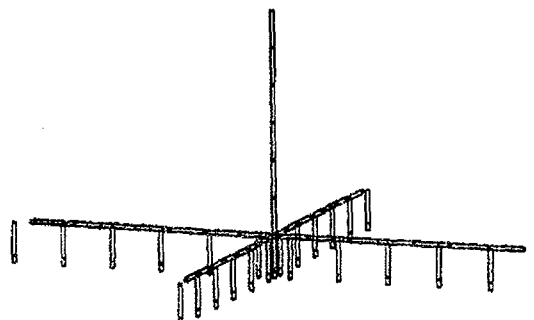


Figure 7. This is configuration "H10" as described in the text. The 4 elevated radials extend outward horizontally from the tower at a height of 10 meters. They are supported atop metallic masts set on steel ground rods. The tower base is 1/2 meter above the ground. All buried radials are omitted for clarity.

In addition, each of the ten configurations listed above was modeled using either metallic or non-metallic masts to support the elevated radials. When metallic (steel) masts are used, these rest upon two-meter-long buried steel ground rods, and extend to within one-half meter of the height of the radial. The outer-most masts are the same height as the elevated radials, but are laterally displaced from them by a short distance. In every case, the elevated radials are positioned at the four cardinal points of the compass, where  $\phi = 0^\circ, 90^\circ, 180^\circ, \text{ and } 270^\circ$ .

## Results

Table I includes all of the differing values of radiated field strength which are predicted by NEC, when various arrangements of elevated radials are added to a "deteriorated" buried-radial ground system. The first two data entries reveal that, even though 35 to 40 percent of the buried copper has been removed from the radial ground system, the field intensity drops only by about 2%, from 268 to 262 mV/m (roughly 0.2 dB).

An examination of the remainder of the table indicates that some of the elevated-radial configurations actually lead to a decrease in the radiated field intensity, so that "more is less" in these instances. Other configurations produce values of field strength which are well above the standard reference, and the five best performers are numbered in their order of precedence. Notice that all five of these structures utilize radials which are elevated to a height of ten meters above ground.

If the buried-radial ground screen is "very deteriorated," then the addition of different configurations of elevated radials will produce the results displayed in Table II. Here, NEC indicates that the removal of nearly all of the buried radials will cause the transmitted field strength to drop almost 14%, from 268 to 231 mV/m, a loss of about 1.3 dB.

A review of the other data in Table II shows that, as before, some elevated-radial structures do more harm than good, and thus should be avoided. However, several of the configurations allow the antenna system to perform "better than new", and the top five are again indicated numerically.

Comparing the results from both tables, one can see that the same five configurations came out in the "top five" in both cases. In fact, "number one" and "number two" were identical in both instances, while the next three positions were interchanged among the remaining trio of contenders.

All of the data in both tables indicates that the radiation patterns have excellent circularity in every instance, even when most of the buried radials have been removed.

The information contained in Tables I and II is also presented pictorially in Figures 8 and 9 respectively. These bar charts show very clearly the relative field-strength amplitudes for each of the elevated-radial structures, as well as the standard reference antenna. The consistent first- and second-place finishers both stand out "head-and-shoulders" above the crowd. The computer modeling indicates that, whether metallic or non-metallic masts are used, extended radials which slope steeply upward to a height of ten meters above the ground always provided the best performance.

Table I. Radiated Field Intensity for a Vertical Monopole Antenna when Various Configurations of Elevated Radials are added to a "Deteriorated" Buried-Radial Ground System (see Figure 3).

Ground System	$E_r$ (mV/m @ 1 km for 1 kW)	
	$\phi = 0^\circ$	$\phi = 45^\circ$
Reference Standard	267.91	267.91
"Deteriorated"	262.19	262.19
<hr/>		
455 (met)	254.26	254.15
(non-met)	246.86	246.65
455E (met)	270.84	270.77
(non-met)	265.39	265.33
4510 (met)	187.06	186.41
(non-met)	216.74	216.47
4510E (met)	5 279.67	279.65
(non-met)	267.98	267.98
S5 (met)	203.40	203.26
(non-met)	215.82	215.69
S5E (met)	220.46	220.37
(non-met)	225.32	225.27
S10 (met)	275.64	275.41
(non-met)	3 294.25	294.14
S10E (met)	1 312.24	312.09
(non-met)	2 308.88	308.82
H5 (met)	254.18	254.03
(non-met)	267.82	267.68
H10 (met)	4 293.21	292.96
(non-met)	269.85	269.68

$\phi = 0^\circ$  corresponds to a point located directly off the end of an elevated radial, while  $\phi = 45^\circ$  is midway between two elevated radials; met = metallic masts used to support the elevated radials, and non-met = non-metallic support masts

Table II. Radiated Field Intensity for a Vertical Monopole Antenna when Various Configurations of Elevated Radials are added to a "Very Deteriorated" Buried-Radial Ground System (see Figure 4).

Ground System	$E_r$ (mV/m @ 1 km for 1 kW)	
	$\phi = 0^\circ$	$\phi = 45^\circ$
Reference Standard	267.91	267.91
"Very Deteriorated"	231.12	231.49
<hr/>		
455 (met)	250.42	250.60
(non-met)	247.20	247.63
455E (met)	264.48	264.69
(non-met)	260.34	260.66
4510 (met)	216.26	215.68
(non-met)	226.54	226.28
4510E (met)	4 277.10	277.40
(non-met)		264.00
S5 (met)	193.26	193.80
(non-met)	196.83	197.56
S5E (met)	216.24	216.44
(non-met)	220.78	221.00
S10 (met)	269.47	269.24
(non-met)	5 270.11	270.42
S10E (met)		308.61
(non-met)	2 304.60	304.91
H5 (met)	249.39	249.55
(non-met)	263.07	263.48
H10 (met)	3 289.78	289.87
(non-met)		266.79

$\phi = 0^\circ$  corresponds to a point located directly off the end of an elevated radial, while  $\phi = 45^\circ$  is midway between two elevated radials; met = metallic masts used to support the elevated radials, and non-met = non-metallic support masts

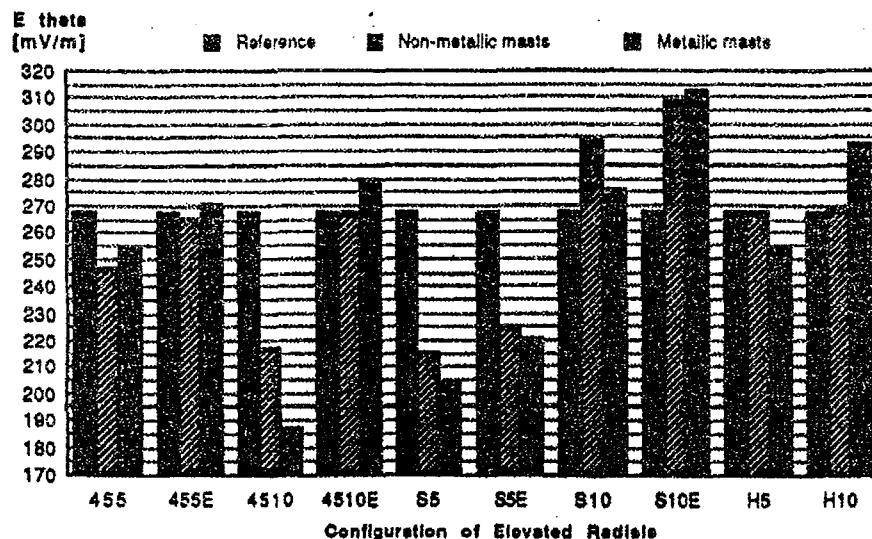


Figure 8. Radiated electric field intensity for all elevated-radial configurations when installed above a "deteriorated" conventional ground system. In each case, the performance of the reference-standard buried-radial ground system is shown for comparison (267.91 mV/m at 1 km for 1 kW).

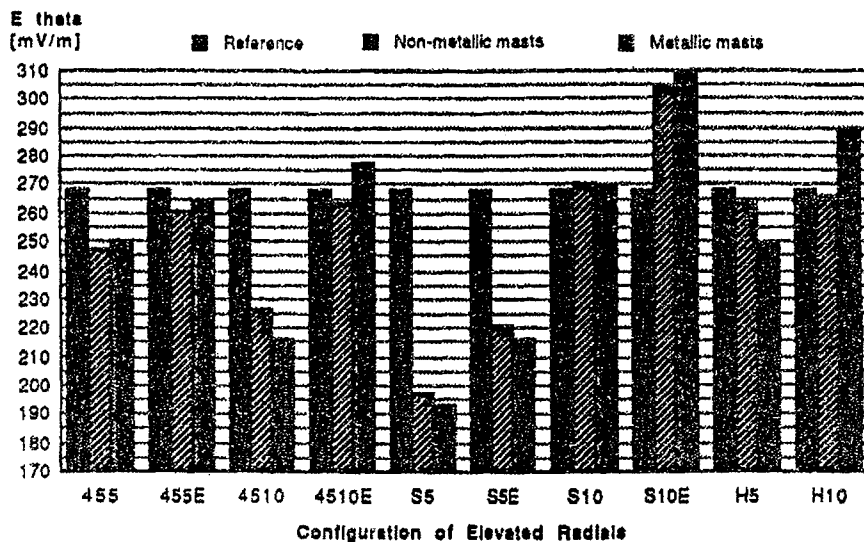


Figure 9. Radiated electric field intensity for all elevated-radial configurations when installed above a "very deteriorated" conventional ground system. In each case, the performance of the reference-standard buried-radial ground system is shown for comparison (267.91 mV/m at 1 km for 1 kW).

#### Conclusions

Computer-modeling exercises indicate that it is possible to add a group of four elevated radials to a pre-existing conventional AM-broadcast vertical monopole antenna system in order to restore performance to its original level (or better) in situations where the buried-radial ground system has been damaged. A wide variety of different configurations for the elevated radials have been examined, and clear-cut winners were determined. As always, extensive outdoor testing should be performed in order to verify these computer predictions.

The choice of whether to replace those radials which are damaged with new buried radials, or to add elevated radials, must be made by the station's management personnel, and would depend upon the particular circumstances at each individual installation.

#### Acknowledgements

The authors would like to express their appreciation to Al Resnick for providing important technical information [5], and to Suzanne Vazzano for her expert word processing of this report. Thanks go also to Richard Piccard and Karen Hostetler of Ohio University's Computing and Technology Services for assisting with software implementation.

#### References

- [1] G. J. Burke and A. J. Foggio, "Numerical Electromagnetics Code (NEC) - Method of Moments", Naval Ocean Systems Center, San Diego, CA, January 1981.
- [2] A. M. Christman, R. D. Radcliff, et al, "AM Broadcast Antennas with Elevated Radial Ground Systems", *IEEE Transactions on Broadcasting*, Vol. 34, No. 1, March 1988.
- [3] A. M. Christman and R. D. Radcliff, "Using Elevated Radials with Ground-Mounted Towers", *IEEE Transactions on Broadcasting*, Vol. 37, No. 3, September 1991.
- [4] G. H. Brown, R. F. Lewis, and J. Epstein, "Ground Systems as a Factor in Antenna Efficiency", *Proceedings of the Institute of Radio Engineers*, Vol. 25, No. 6, June 1937.
- [5] A. E. Resnick, Vice President and Director of Engineering, Capital Cities/ABC Inc, New York. Private communication.



## USING ELEVATED RADIALS WITH GROUND-MOUNTED TOWERS

Al Christman  
EE Department  
Grove City College  
Grove City PA 16127

Roger Radcliff  
ECE Department  
Ohio University  
Athens OH 45701

Abstract

Computer-modeling studies indicate that elevated radials may be used in conjunction with a conventional ground-mounted tower to produce radiated field strength which is equivalent to that emitted by a similar monopole using 120 buried radials. Several different methods of attaching the radials to the tower were investigated, along with variations in radial height, radial length, and tower height. Limited field testing, performed by William Culpepper, appears to confirm the results of the computer analysis.

Background

The elevated vertical-monopole antenna system would be more attractive to potential users if it were not necessary to raise the tower base (and its accompanying insulator) several meters into the air. With this in mind, a number of computer-modeling studies were performed to investigate the possibility of combining a ground-mounted tower with elevated radials. A double-precision version of the method-of-moments code NEC-GS [1] was used as the principal research tool.

A classic [2] ground-mounted series-fed tower with 120 buried radials was modeled initially, to serve as a standard reference. An operating frequency of 1 MHz was selected, and the radii of all conductors was set at 3 millimeters. The tower is made of aluminum and rests upon a two-meter-long buried steel ground rod. All radials are copper and are buried to a depth of six inches in soil with a conductivity of 0.004 Siemens per meter and a dielectric constant of 15. The tower and the radials are all 90° in length, which is equal to 75 meters at 1 MHz. NEC-GS predicts an input impedance of  $40.52 + j 23.40$  Ohms for this antenna, with a field strength of 267.91 millivolts per meter rms. This is the magnitude of the vertical component of the electric field intensity monitored at a distance of 1 kilometer away from the monopole at a height above ground of 50 inches (1.27 meters), when the input power is 1000 watts.

Elevated-Radial Configurations

At first, two separate methods for positioning the radials were investigated in detail. In both instances the interior ends of the radials were placed near ground level, adjacent to the tower base. From that point, the radials slope upwards until reaching the desired height above ground level, which is either  $h = 5$  or  $h = 10$  meters. Once the target height is reached, the remaining portion of each radial extends outward horizontally at constant height. The radials are supported at 15-meter intervals on insulators mounted atop steel masts which rest upon two-meter-long buried steel ground rods.

For the first case, the angle of inclination for the sloping part of the radials was set at 45°, as shown in Figure 1. In the second permutation, illustrated in Figure 2, the interior ends of the radials were made to slope very steeply upward, so that the final elevation height was reached at a point located only 0.5 meters (laterally) from the tower.

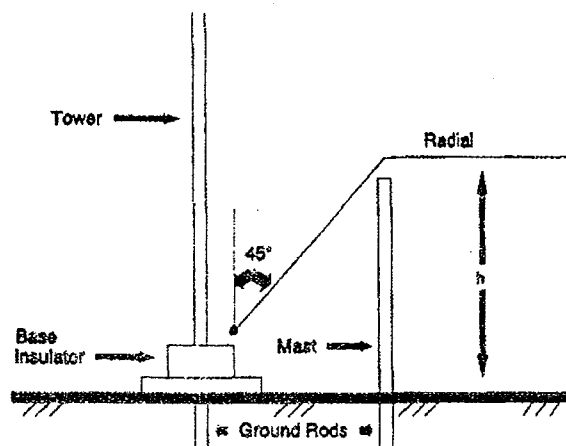


Figure 1. Vertical monopole antenna system; the inner ends of the elevated radials slope upward at 45° from the tower base until the desired height is reached.

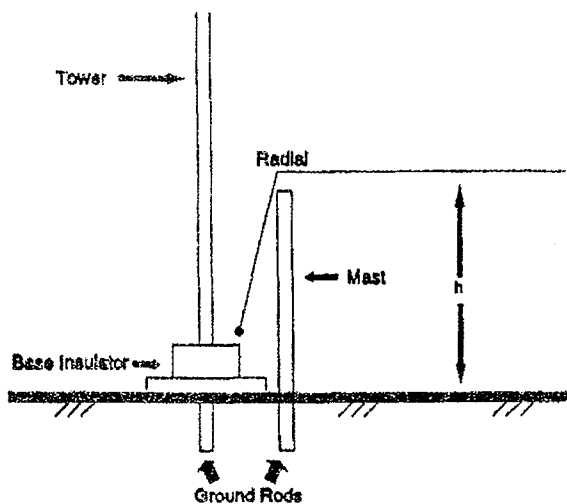


Figure 2. Vertical monopole antenna system; the inner ends of the elevated radials slope very steeply upward from the tower base until the desired height is reached.

The resulting combinations, which were then modeled on the computer, are:

- (1) four horizontal radials, 45°-slope at the feed-point, final elevation height = 5 meters
- (2) four horizontal radials, 45°-slope at the feed-point, final elevation height = 10 meters
- (3) four horizontal radials, very steep slope at the feed-point, final elevation height = 5 meters
- (4) four horizontal radials, very steep slope at the feed-point, final elevation height = 10 meters.

Because the radials are always located above the ground, it was decided to lengthen the tower height incrementally to determine if the lower portion of the vertical monopole was being "shielded" by the elevated radials. And, along a similar line of reasoning, the radials were also lengthened slightly. As a result, there are 25 combinations of tower height and radial length for each of the antenna configurations which were examined.

#### Radials with 45°-Sloping Ends, at a Height of 5 Meters

Figure 3 shows the computer-predicted values of radiated field intensity for the case when radials with inner ends that have a 45° slope are installed at a height of five meters. It can be seen that, for a specific tower height, longer radials always produce larger field strengths, although the incremental change is not constant. On the other hand, if the length of the radials is held fixed, then increasing the height of the tower will yield a small but consistent increase in the field. A few of these combinations actually generate as much radiated field intensity as the standard reference antenna. Table I lists the input impedance for each of the antennas studied. Note that the base resistance is generally around 30 to 40 ohms. When the metallic masts which support the elevated radials are removed (or replaced with non-conductive masts), the radiated field strength increases by about 3%.

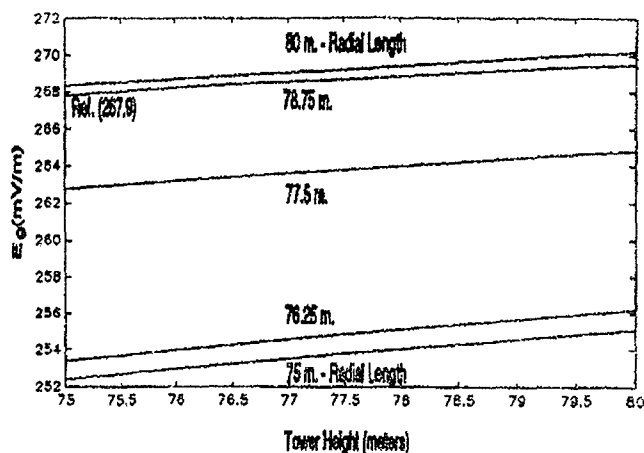


Figure 3. Field strength versus tower height and radial length, 4 elevated radials (45° slope) at h = 5 meters

#### Radials with 45°-Sloping Ends, at a Height of 10 Meters

Figure 4 is a similar graph which displays the results for the same antenna, only now the radials are installed 10 meters above ground. As before, an increase in the height of the tower always leads to a slightly higher field intensity, for a given radial length. However, when the tower height is fixed, longer radials do not necessarily produce increases in the strength of the fields. As the length of the radials is increased beyond 0.25λ (75 meters), the field intensity initially builds, but then falls off, only to increase once more as the radials are lengthened still further. In this case, then, longer radials are not always better! With the radials now elevated twice as far above the earth, many of the listed radial-length/tower-height combinations provide performance which is superior to the standard reference antenna. The input impedance values are given in Table II, which indicates that the feed-point resistances now span the range between 22 and 40 ohms. Removing the conductive radial-support masts leads to a decrease in field strength of one to two percent.

Table I. Input impedance as a function of tower height and radial length. The four radials slope upward from the tower base at an angle of 45°, to an elevation of 5 meters. The entire remaining portion of the radial is horizontal (f = 1 MHz, λ = 300 meters, σ = 0.004 S/m, ε<sub>r</sub> = 15).

Input Impedance (Ohms)					
	75 m. tower	76.25 m. tower	77.5 m. tower	78.75 m. tower	80 m. tower
75 m. radials	35.12 - j 1.63	36.82 + j 13.65	38.59 + j 28.92	40.43 + j 44.18	42.35 + j 59.46
76.25 m. radials	34.79 + j 2.73	36.47 + j 18.01	38.22 + j 33.27	40.04 + j 48.54	41.94 + j 63.81
77.5 m. radials	32.17 - j 9.40	33.78 + j 5.75	35.46 + j 20.88	37.21 + j 36.01	39.03 + j 51.15
78.75 m. radials	30.86 - j 8.33	32.43 + j 6.77	34.06 + j 21.86	35.77 + j 36.95	37.55 + j 52.05
80 m. radials	30.73 - j 1.21	32.28 + j 13.92	33.90 + j 29.04	35.59 + j 44.15	37.35 + j 59.28

Table II. Input impedance as a function of tower height and radial length. The four radials slope upward from the tower base at an angle of  $45^\circ$ , to an elevation of 10 meters. The entire remaining portion of the radial is horizontal ( $f = 1$  MHz,  $\lambda = 300$  meters,  $c = 0.004$  S/m,  $\epsilon_r = 15$ ).

	Input Impedance (Ohms)				
	75 m. tower	77.5 m. tower	80 m. tower	82.5 m. tower	85 m. tower
75 m. radials	24.65 - j 32.90	27.47 - j 3.50	30.55 + j 25.87	33.94 + j 55.34	37.65 + j 85.00
77.5 m. radials	23.58 - j 21.34	26.37 + j 8.28	29.42 + j 37.87	32.77 + j 67.55	36.46 + j 97.43
80 m. radials	24.26 - j 8.82	27.06 + j 21.03	30.13 + j 50.86	33.49 + j 80.79	37.19 + j 110.92
82.5 m. radials	27.06 + j 4.54	29.91 + j 34.64	33.03 + j 64.71	36.45 + j 94.89	40.20 + j 125.27
85 m. radials	22.02 + j 0.07	24.59 + j 29.99	27.41 + j 59.89	30.53 + j 89.89	33.96 + j 120.10

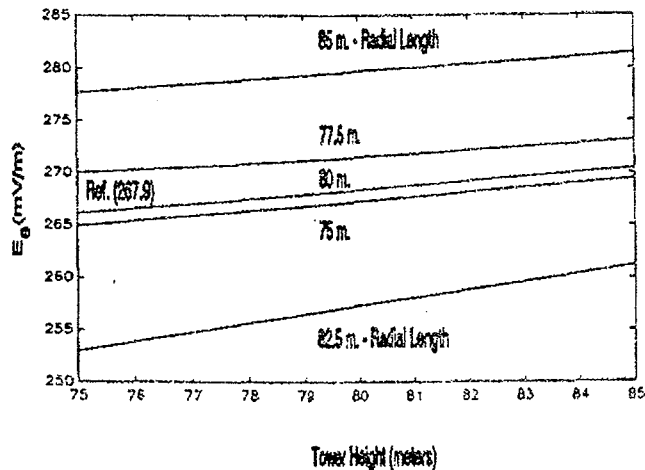


Figure 4. Field strength versus tower height and radial length, 4 elevated radials ( $45^\circ$  slope) at  $h = 10$  meters

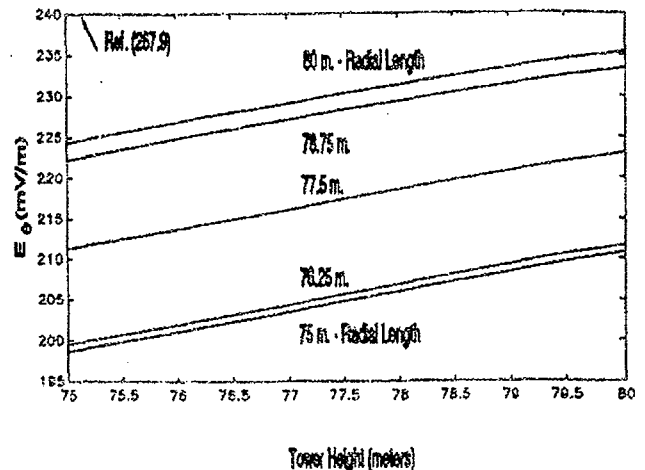


Figure 5. Field strength versus tower height and radial length, 4 elevated radials (steeply sloping) at  $h = 5$  meters

#### Radials with Steeply-sloping Ends, at a Height of 5 Meters

Figure 5 shows the results of the field-strength analysis for antennas with steeply-sloping radials, whose horizontal portion is 5 meters off the ground. If the length of the radials is fixed, increasing the tower height produces a higher value of field intensity, and this result also holds true when the tower height is held constant while the radials are made longer. Notice that the field strength here is always inferior to that of the reference antenna, so this particular configuration is not desirable. The corresponding values for input impedance are displayed in Table III. If the metal masts which hold up the radials are omitted, the field strength values improve by around 13%, but this is still well below the standard reference.

#### Radials with Steeply-sloping Ends, at a Height of 10 Meters

Lifting the elevated radials further, to a height of 10 meters above ground, produces a dramatic improvement in performance. Figure 6 shows the results, and indicates other changes in the behavior of the antenna system as well. Notice that continually making the tower taller no longer guarantees a correspondingly higher field-strength reading. Similarly, increasing the length of the radials can often reduce the radiated field intensity. On the positive side, though, every one of the combinations which were investigated here proved to be far superior to the standard reference antenna. Table IV lists the feed-point impedances, whose real parts span the interval between 14 and 26 ohms. The use of non-conductive masts in this situation leads to a reduction in radiated field strength of about 11%, which is significant, but not sufficient to bring the performance down to the level of the reference antenna.

Table III. Input impedance as a function of tower height and radial length. The four radials slope very steeply upward from the tower base to an elevation of 5 meters. The entire remaining portion of the radial is horizontal ( $f = 1$  MHz,  $\lambda = 300$  meters,  $\sigma = 0.004$  S/m,  $\epsilon_r = 15$ ).

	Input Impedance (Ohms)				
	75 m. tower	76.25 m. tower	77.5 m. tower	78.75 m. tower	80 m. tower
75 m. radials	57.02 - j 64.73	58.34 - j 40.60	59.63 - j 16.76	60.95 + j 5.45	62.35 + j 28.90
76.25 m. radials	56.40 - j 51.23	57.74 - j 27.31	59.03 - j 3.87	60.34 + j 18.85	61.74 + j 40.79
77.5 m. radials	50.17 - j 73.43	51.39 - j 49.50	52.67 - j 25.73	54.04 - j 2.50	55.53 + j 20.01
78.75 m. radials	45.23 - j 93.14	46.35 - j 59.31	47.62 - j 35.50	49.03 - j 12.16	50.58 + j 10.52
80 m. radials	44.31 - j 65.99	45.44 - j 42.40	46.71 - j 19.08	48.12 + j 3.66	49.66 + j 25.70

Table IV. Input impedance as a function of tower height and radial length. The four radials slope very steeply upward from the tower base to an elevation of 10 meters. The entire remaining portion of the radial is horizontal ( $f = 1$  MHz,  $\lambda = 300$  meters,  $\sigma = 0.004$  S/m,  $\epsilon_r = 15$ ).

	Input Impedance (Ohms)				
	75 m. tower	77.5 m. tower	80 m. tower	82.5 m. tower	85 m. tower
75 m. radials	15.39 - j 42.52	17.10 - j 20.43	19.12 + j 1.53	21.49 + j 23.64	24.26 + j 46.13
77.5 m. radials	15.54 - j 33.73	17.25 - j 11.65	19.27 + j 10.29	21.64 + j 32.36	24.40 + j 54.78
80 m. radials	16.06 - j 26.42	17.78 - j 4.33	19.81 + j 17.60	22.18 + j 39.64	24.93 + j 62.02
82.5 m. radials	17.56 - j 16.99	19.31 + j 5.09	21.35 + j 27.01	23.73 + j 49.01	26.48 + j 71.33
85 m. radials	14.41 - j 19.24	16.01 + j 2.72	17.91 + j 24.51	20.15 + j 46.41	22.78 + j 68.62

*referee*  
5/88

## Elevated Vertical Antennas on 80 Meters

by

Al Christman  
Department of Electrical and Computer Engineering  
Ohio University  
Athens, OH 45701

### INTRODUCTION

Computer modeling studies indicate that an elevated vertical monopole antenna with four elevated horizontal radials provides more power gain at low elevation angles than does a conventional ground-mounted monopole with 120 buried radials. For this analysis, the frequency of operation was fixed at 3.8 MHz in the 80-meter band, and ground constants  $\sigma$  (conductivity) and  $\epsilon_r$  (relative permittivity) were used which simulated "average" soil electrical parameters. The computer program used for this work was NEC-GSD, a "Method of Moments" code developed by engineers at the Lawrence Livermore National Laboratory.

### BACKGROUND

For many years, radio stations in the US standard broadcast band have utilized vertical monopoles (towers) as transmit antennas. These monopoles are required by the FCC to have extensive ground systems, usually consisting of 120 or more buried radial wires which are used to simulate a perfectly-conducting image plane beneath the monopole.

The length of the radials is usually  $0.25 \lambda$ , although taller towers often have longer radials. Electromagnetic energy leaving the radiator travels through space until reaching the earth's surface, where it flows through the soil to the radials and then back to the antenna feed-point.

The FCC mandate requiring the use of many buried radials is apparently based upon the findings of three RCA engineers—Brown, Lewis, and Epstein. These men carried out extensive tests on buried-wire radial ground systems in the mid-1930's and published their results in a now-classic paper in the *Proceedings of the Institute of Radio Engineers*. [1] In this 1937 paper, a single test was performed where the radials were laid upon the surface of the earth rather than buried in the soil. The conclusion was that "this ground system is about as good as an equal number of buried wires". [2] Their normal procedure was to bury the wires to a depth of about six inches. [3] Although this work was done at a frequency of 3 MHz, the results were quickly applied by AM broadcasters to their own part of the spectrum (540-1600 kHz), and buried radials have been used ever since.

It is the author's belief that the use of elevated, rather than buried, radials would provide superior performance, allowing the collection of electromagnetic energy in the form of displacement currents rather than forcing it to flow through lossy earth in the form of conduction currents.

## COMPUTER ANALYSIS

The first step was to determine what effects, if any, would be caused

by changing the depth at which the ground radials were buried. The computer code NEC-GSD was used to model a  $0.25 \lambda$  vertical monopole with 120 buried  $0.25 \lambda$  radials. The operating frequency was 3.8 MHz, and "average ground" ( $\sigma = 0.003 \text{ S/m}$  and  $\epsilon_r = 13$ ) was used.[4] For the NEC model, the antenna was constructed of number 12 AWG wire (radius = 1 mm) and metal conductivities were adjusted to simulate an aluminum monopole with copper radials on a 2-foot steel ground stake. As the burial depth of the radials was increased from 2 inches to 6 inches, the power gain of the antenna decreased only slightly (see Table I), as did the ground-wave field strength. (Note that the input reactance may be altered by adjusting the length of the monopole or by making it thicker in relation to the radials.) Throughout the remainder of this paper, the vertical monopole antenna system with 120 radials buried 2 inches deep will be used as a "standard reference" with which all other antennas will be compared.

The procedure described above was repeated using 4 buried radials rather than 120, with the results given in Table II. As before, slightly lower power gains and field strengths are measured as the radials are moved downward away from the surface of the earth. Compared to the 120-radial cases, monopoles with only 4 buried radials have much higher ground losses, as evidenced by the reductions in gain and field strength, and by the increase in the input resistance values. Much of the power which was radiated by the 120-radial antennas is now wasted heating the soil in the 4-radial systems. Azimuthal variations in gain were negligible,

TABLE I. POWER GAIN AND ELECTRIC FIELD STRENGTH FOR VERTICAL MONOPOLE ANTENNAS WITH BURIED RADIALS.  
 Each system has 120 radials, with the burial depth being varied between 2 and 6 inches.  
 Electric field strength values are given for a power input of 1 kW to the antenna,  
 and are measured at a height of 5 feet above the ground at a distance of 1 mile.  
 Input impedances are given for #12 AWG conductors:  
 aluminum monopole, steel ground stake, and copper radials.

ELEVATION ANGLE (degrees)	POWER GAIN (dBi)		
	120 RADIALS BURIED 2 "	120 RADIALS BURIED 4 "	120 RADIALS BURIED 6 "
0	-∞	-∞	-∞
5	-6.14	-6.15	-6.16
10	-2.40	-2.41	-2.42
15	-0.86	-0.87	-0.88
20	-0.17	-0.18	-0.19
25	+0.06	+0.04	+0.03
30	-0.02	-0.03	-0.04
40	-0.83	-0.84	-0.85
50	-2.37	-2.37	-2.37
60	-4.68	-4.69	-4.69
70	-8.13	-8.14	-8.14
80	-14.13	-14.14	-14.14
90	-158.38	-158.45	-158.51
VERTICAL ELECTRIC FIELD STRENGTH (mV/m)	33.16	33.10	33.06
INPUT IMPEDANCE (ohms)			
R	39.87	40.18	40.44
X	22.00	22.49	23.02



TABLE II . POWER GAIN AND ELECTRIC FIELD STRENGTH FOR VERTICAL MONOPOLE ANTENNAS WITH 4 BURIED RADIALS.

Each system has 4 radials, with the burial depth being varied between 2 and 6 inches.

Radials are located at  $\phi = 0, 90, 180, \text{ and } 270$  degrees.

All gain and electric field values are given at  $\phi = 0$  degrees.

Concerning azimuthal variations, gain differences at  $\phi = 45$  degrees are 0.01 dB or less,

and electric field differences at  $\phi = 45$  degrees are 0.03 mV/m or less.

Electric field strength values are given for a power input of 1 kW to the antenna,

and are measured at a height of 5 feet above the ground at a distance of 1 mile.

Input impedances are given for #12 AWG conductors:

aluminum monopole, steel ground stake, and copper radials.

ELEVATION ANGLE (degrees)	POWER GAIN (dBi)		
	4 RADIALS BURIED 2 "	4 RADIALS BURIED 4 "	4 RADIALS BURIED 6 "
0	- $\infty$	- $\infty$	- $\infty$
5	-8.82	-8.84	-8.85
10	-5.08	-5.10	-5.11
15	-3.54	-3.56	-3.58
20	-2.85	-2.87	-2.89
25	-2.62	-2.65	-2.66
30	-2.70	-2.72	-2.74
40	-3.52	-3.54	-3.55
50	-5.06	-5.08	-5.10
60	-7.37	-7.40	-7.42
70	-10.83	-10.86	-10.87
80	-16.84	-16.86	-16.88
90	-169.74	-169.99	-170.17
VERTICAL ELECTRIC FIELD STRENGTH (mV/m)	24.37	24.31	24.27
INPUT IMPEDANCE (ohms)			
R	74.48	74.73	74.93
X	33.69	34.04	34.39

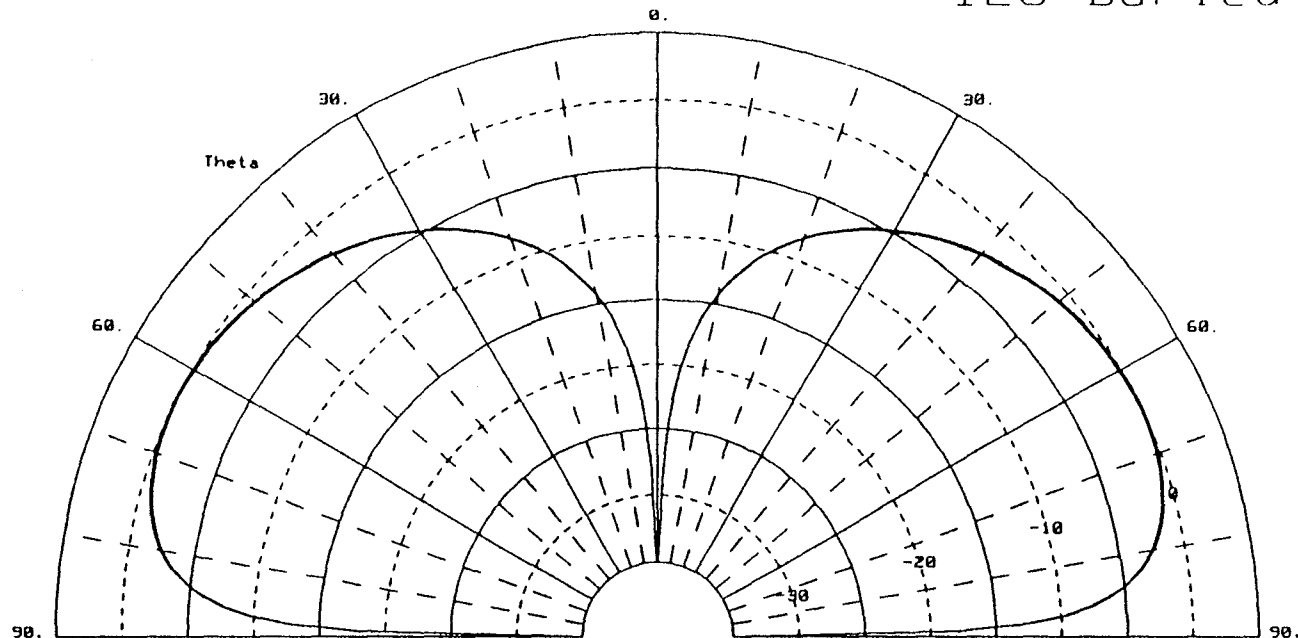
amounting to 0.01 dB or less. Figure 1 shows the elevation-plane power patterns for vertical monopole antennas with 120 radials, 4 radials, and no radials (ground stake only). The pattern shape remains essentially constant, but the pattern size (gain) depends upon the quality of the ground system. All of the vertical electric field strengths in the Tables were normalized for a power input of 1000 Watts to the antenna, and were measured at a distance of 1 mile and a height of 5 feet. At this height, the electric field is almost entirely surface wave ("ground wave") rather than sky wave. The conclusion drawn from this section is that if radials must be buried, it is better to use a lot of them rather than just a few, in order to minimize losses, and it is helpful to keep them close to the surface.

Next, vertical monopole antenna systems were modeled in which the radiator and four horizontal radials were raised above the earth's surface. As the height of the antenna system was increased, its low-angle power gain and field strength also increased steadily, although the gain at somewhat higher angles was attenuated more and more as the antenna was raised further (see Table III). Notice that the power gain at take-off angles of  $15^\circ$  (or less) increases continually as the antenna height is raised from 5 feet to 30 feet, but the gain at a take-off angle of  $20^\circ$  reaches a maximum value at a height of around 10 feet, and then tapers off as the antenna is moved still higher. Compared with the "reference standard" 120-buried-radial system, the 4-radial elevated antenna reaches "parity", or equivalent low-angle performance, at a height of about 15 feet above

NEC Elevation Plot:

Full-Size Elements

120 Buried Radials



Maximum Gain:

0.06 dBi

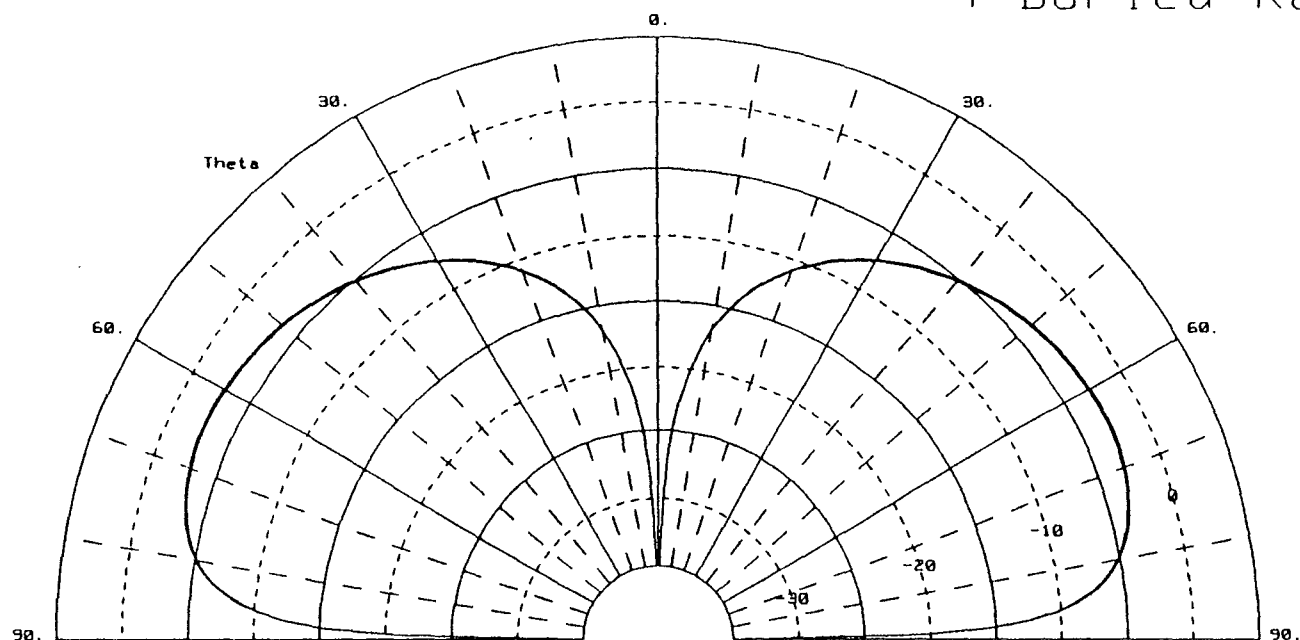
Phi: 0.00

Figure 1 (a)

NEC Elevation Plot:

Full-Size Elements

4 Buried Radials



Maximum Gain:

-2.61 dBi

Phi: 0.00

NEC Elevation Plot:

Full-Size Element  
Ground Stake ONLY

Maximum Gain:  
-9.66 dBi

Phi: 0.00

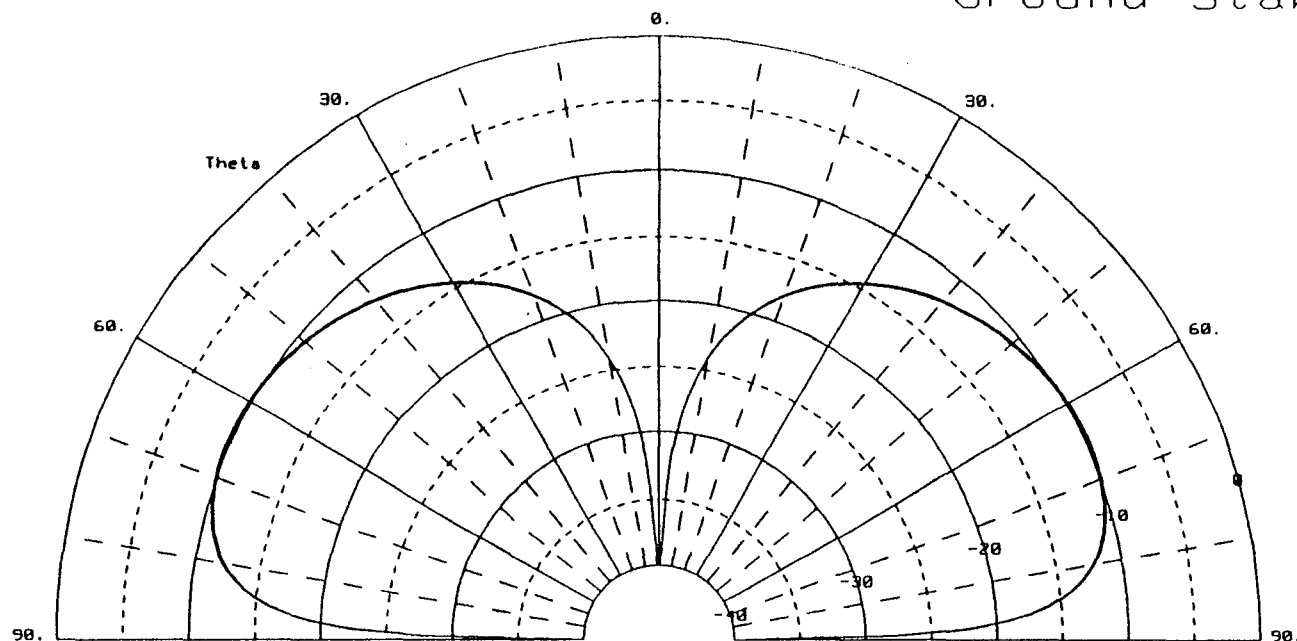


Figure 1 (a)

TABLE III. POWER GAIN AND ELECTRIC FIELD STRENGTH FOR ELEVATED VERTICAL MONOPOLE ANTENNA SYSTEMS.

All systems have 4 radials, with the base height being varied between 5 and 30 feet.

Radials are located at  $\phi = 0, 90, 180$ , and  $270$  degrees.

The gain and electric field values are given at  $\phi = 0$  degrees.

Concerning azimuthal variations, gain differences at  $\phi = 45$  degrees are 0.06 dB or less,  
and electric field differences at  $\phi = 45$  degrees are 0.05 mV/m or less.

Electric field strength values are given for a power input of 1 kW to the antenna,  
and are measured at a height of 5 feet above the ground at a distance of 1 mile.

Input impedances are given for #12 AWG conductors:

aluminum monopole, steel masts and ground stakes, and copper radials.

ELEVATION ANGLE (degrees)	POWER GAIN (dBi)					
	4 RADIALS HEIGHT = 5 FT	4 RADIALS HEIGHT = 10 FT	4 RADIALS HEIGHT = 15 FT	4 RADIALS HEIGHT = 20 FT	4 RADIALS HEIGHT = 25 FT	4 RADIALS HEIGHT = 30 FT
0	$-\infty$	$-\infty$	$-\infty$	$-\infty$	$-\infty$	$-\infty$
5	-6.40	-6.22	-6.09	-5.97	-5.82	-5.60
10	-2.69	-2.53	-2.43	-2.34	-2.23	-2.06
15	-1.19	-1.08	-1.03	-1.00	-0.96	-0.85
20	-0.56	-0.50	-0.53	-0.59	-0.64	-0.64
25	-0.41	-0.43	-0.54	-0.71	-0.89	-1.02
30	-0.57	-0.68	-0.91	-1.22	-1.56	-1.87
40	-1.59	-1.93	-2.45	-3.13	-3.92	-4.71
50	-3.38	-3.99	-4.88	-6.05	-7.46	-8.87
60	-5.94	-6.85	-8.15	-9.92	-12.06	-13.72
70	-9.61	-10.80	-12.50	-14.87	-17.55	-18.05
80	-15.77	-17.15	-19.16	-21.97	-24.67	-23.45
90	-157.37	-154.72	-152.32	-150.20	-148.37	-146.88
VERTICAL ELECTRIC FIELD STRENGTH (mV/m)	32.19	32.94	33.49	34.00	34.66	35.55
INPUT IMPEDANCE (ohms)						
R	38.64	36.06	33.77	31.35	28.82	26.51
X	8.60	3.37	0.59	-1.17	-2.05	-2.08

the surface of the earth. If the antenna is raised further, and its height approaches  $0.25 \lambda$ , a secondary high-angle lobe will develop, although extreme low-angle gain will continue to build. Azimuthal gain variations again are quite small, even though only 4 radials are used.

## GEOMETRY

The physical layout of a typical elevated-radial antenna system is shown in Figure 2. The monopole and the outer ends of the radials are supported by conductive masts. The height of the end masts is equal to the elevation of the radials above ground, but these masts are separated laterally from the tips of the radials by 6 inches. The central mast supports the monopole, and its height is also equal to the elevation of the radials. Each mast is attached to a 2-foot-long ground stake which is driven full-length into the earth. The masts and ground stakes are made of steel, the radials are copper, and the monopole is constructed of aluminum, as before, and all conductors are number 12 AWG. The four radials are bonded directly to the top of the central mast, but are insulated from all other support structures. The outer conductor of the coax is also bonded to the four radials at the top of the center mast.

The arrangement described above allows significant current to flow on the central mast, so an alternate feed-point design was modeled. In the second technique, the central mast was isolated from the radials in order to reduce current flow on its vertically-oriented structure. As shown in Table IV, these "isolated" antenna systems yielded a small improvement

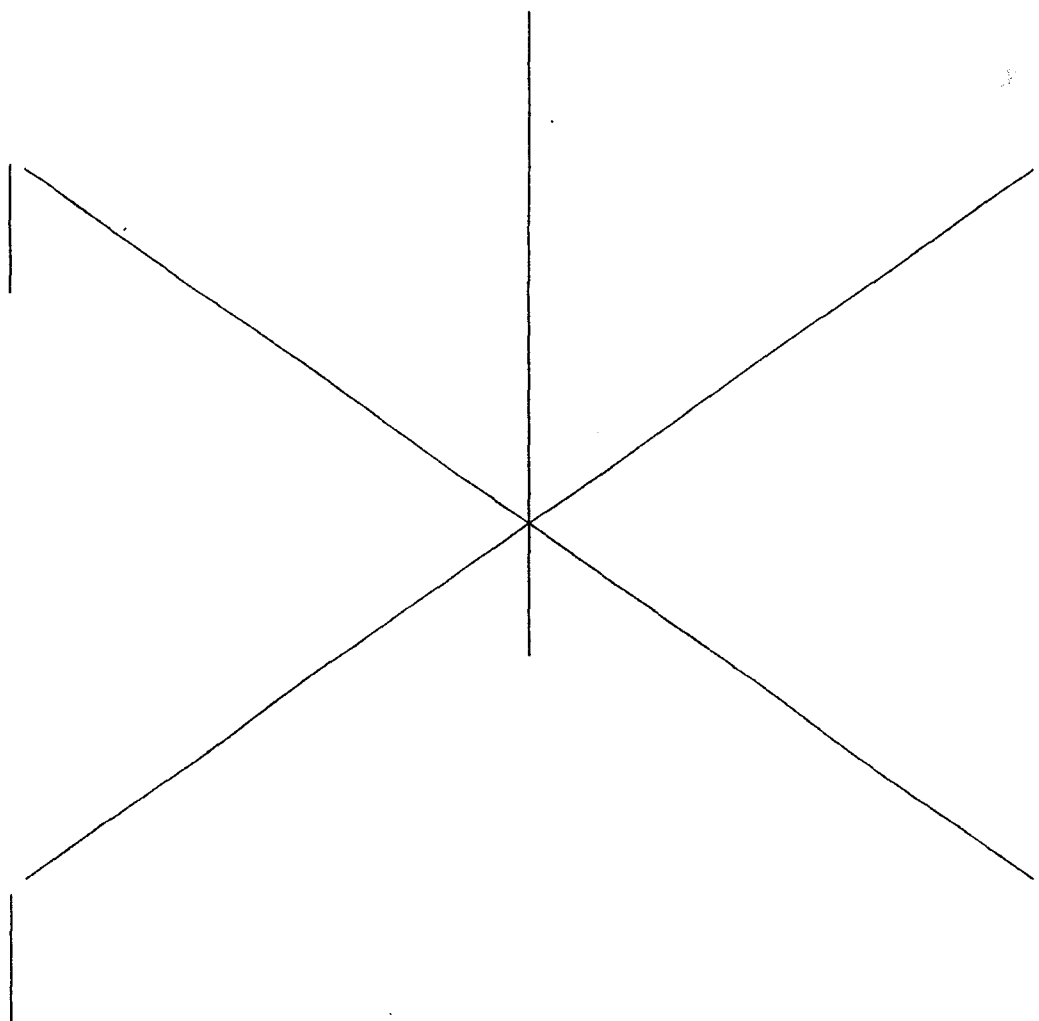




TABLE IV. POWER GAIN AND ELECTRIC FIELD STRENGTH FOR "ISOLATED" ELEVATED VERTICAL MONOPOLE ANTENNA SYSTEMS.

All systems have 4 radials, with the base height being varied from 5 to 30 feet.

Radials are located at  $\phi = 0, 90, 180$ , and  $270$  degrees.

The gain and electric field values are given at  $\phi = 0$  degrees.

Concerning azimuthal variations, gain differences at  $\phi = 45$  degrees are 0.04 dB or less, and electric field differences at  $\phi = 45$  degrees are 0.04 mV/m or less.

Electric field strength values are given for a power input of 1 kW to the antenna, and are measured at a height of 5 feet above the ground at a distance of 1 mile.

Input impedances are given for #12 AWG conductors:

aluminum monopole, steel masts and ground stakes, and copper radials.

ELEVATION ANGLE (degrees)	POWER GAIN (dBi)					
	4 RADIALS HEIGHT = 5 FT	4 RADIALS HEIGHT = 10 FT	4 RADIALS HEIGHT = 15 FT	4 RADIALS HEIGHT = 20 FT	4 RADIALS HEIGHT = 25 FT	4 RADIALS HEIGHT = 30 FT
0	$-\infty$	$-\infty$	$-\infty$	$-\infty$	$-\infty$	$-\infty$
5	-6.33	-6.01	-5.74	-5.50	-5.27	-5.06
10	-2.62	-2.32	-2.08	-1.87	-1.67	-1.50
15	-1.12	-0.87	-0.67	-0.51	-0.37	-0.26
20	-0.49	-0.30	-0.16	-0.07	-0.02	+0.01
25	-0.33	-0.21	-0.16	-0.17	-0.22	-0.32
30	-0.49	-0.46	-0.52	-0.64	-0.82	-1.08
40	-1.51	-1.70	-2.01	-2.44	-2.99	-3.66
50	-3.29	-3.74	-4.37	-5.20	-6.23	-7.48
60	-5.85	-6.58	-7.57	-8.85	-10.43	-12.21
70	-9.52	-10.50	-11.83	-13.55	-15.58	-17.30
80	-15.67	-16.84	-18.41	-20.44	-22.65	-23.65
90	-157.35	-154.72	-152.47	-150.61	-149.07	-147.80
VERTICAL ELECTRIC FIELD STRENGTH (mV/m)	32.47	33.71	34.82	35.86	36.86	37.82
INPUT IMPEDANCE (ohms)						
R	38.19	35.06	32.59	30.54	28.74	27.15
X	8.46	3.52	1.38	0.26	-0.35	-0.64

in ground-wave field strength values and more power gain at low elevation angles, with only slight changes in feed-point impedance. Figure 3 shows elevation- and azimuthal-plane power patterns for an "isolated" 4-radial antenna system at a height of 15 feet; notice the excellent circularity of the radiation pattern. Since the coaxial transmission line feeding power to the antenna must also extend vertically along the center mast, some means of preventing the flow of antenna current on the outer surface of the coax shield must be utilized in order to actually achieve isolation of the vertical support structure. This could be accomplished by using a transformer at the feed-point, or by placing suitable ferrite material around the outside of the transmission line (a "choke" balun) to eliminate the flow of undesired currents on the outer surface of the coax.

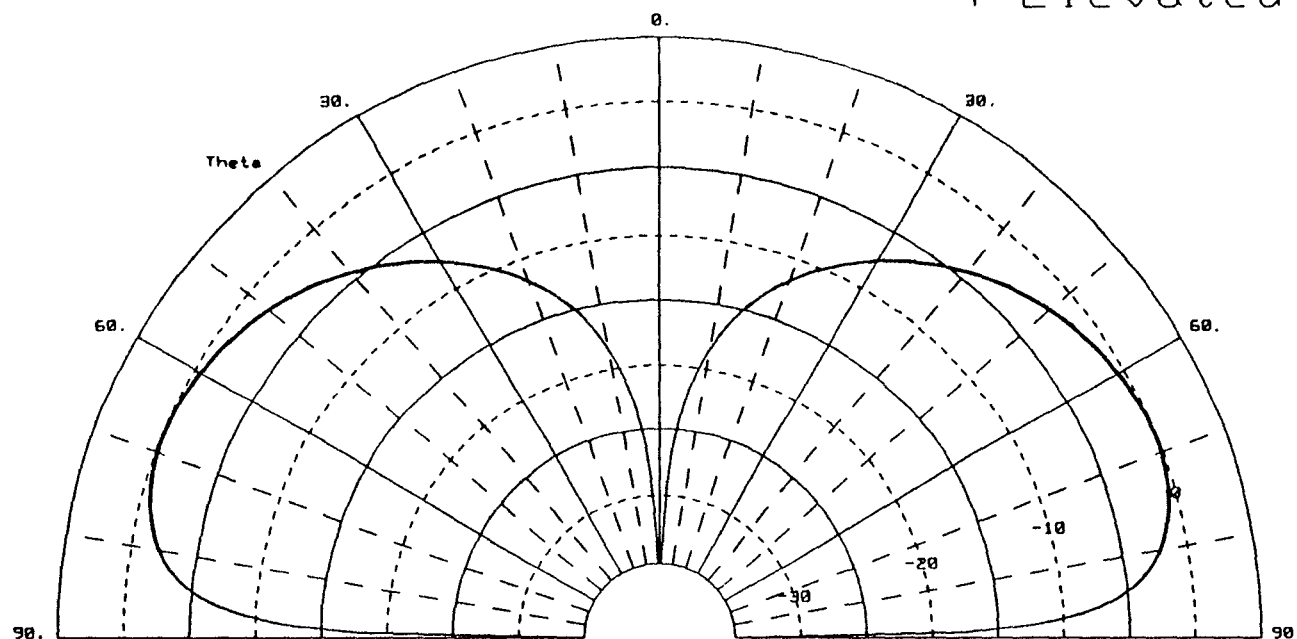
#### MODIFICATIONS TO THE BASIC ELEVATED-RADIAL SYSTEM

As has been demonstrated, the full-size "isolated" elevated antenna system, consisting of a  $0.25 \lambda$  monopole and four  $0.25 \lambda$  radials at a height of 15 feet, is competitive with a conventional 120-buried-radial ground-mounted antenna. This section describes the results of experiments which were conducted with various combinations of shortened monopoles and/or radials. Table V shows what can be achieved with a mixture of  $0.25 \lambda$  and  $0.125 \lambda$  elements. Surprisingly perhaps, the best performer of the group is a  $0.25 \lambda$  monopole with four  $0.125 \lambda$  radials, which provides more signal strength than the other permutations and has a more favorable input impedance as well.

NEC Elevation Plot:

Full-Size Elements

4 Elevated Radials



Maximum Gain:

-0.03 dBi

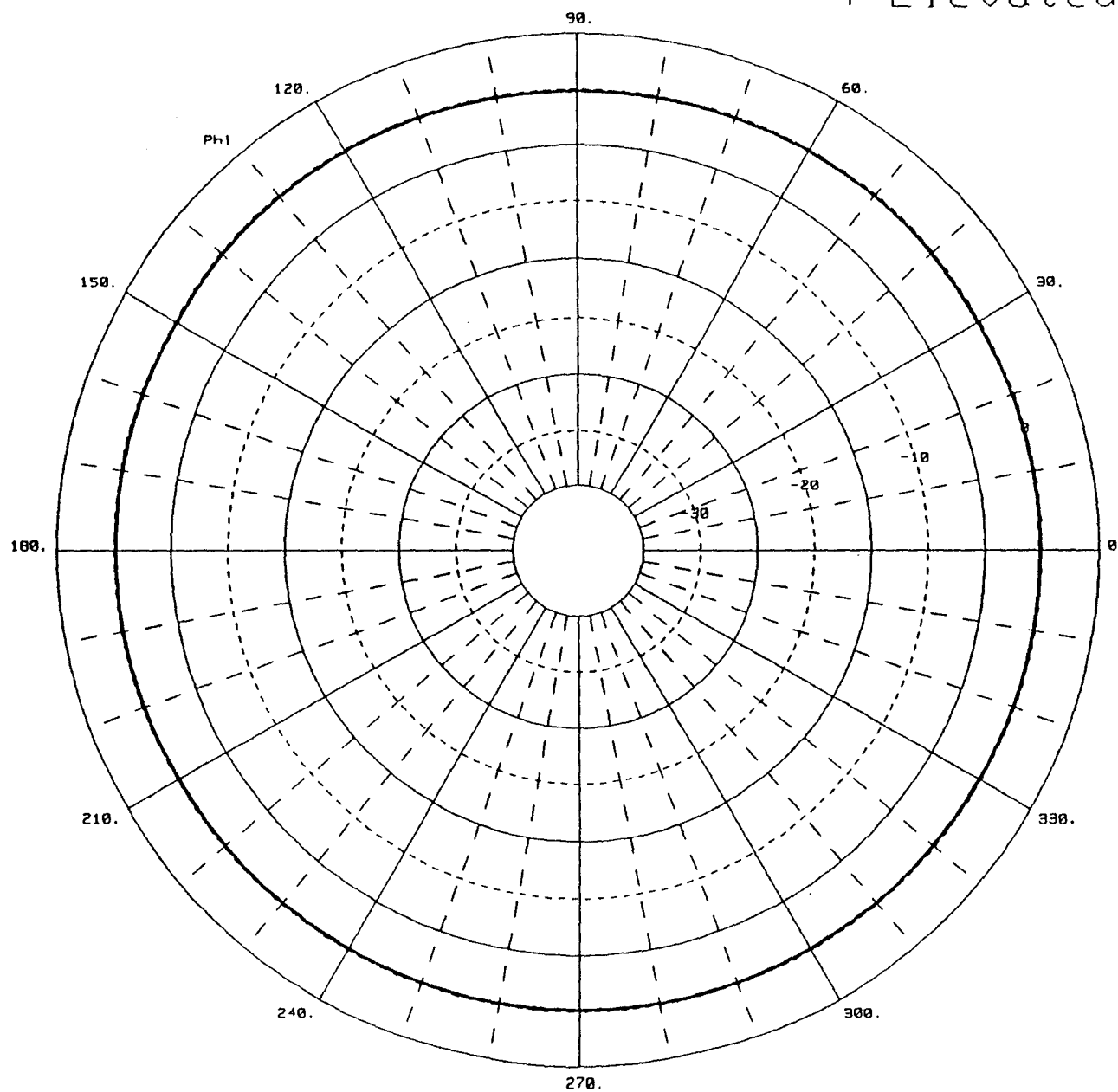
Phi: 0.00

Figure 5 (a)

NEC Azimuth Plot:

Full-Size Elements

4 Elevated Radials



Maximum Gain:

-0.08 dBi

Theta: 70.00

Page 5(b)

TABLE V. POWER GAIN AND ELECTRIC FIELD STRENGTH FOR "ISOLATED" VERTICAL ANTENNA SYSTEMS WITH SHORTENED RADIALS AND/OR SHORTENED MONOPOLES.

Each system has 4 radials, and is elevated to a base height of 15 feet above ground.

Radials are located at  $\phi = 0, 90, 180,$  and  $270$  degrees.

All gain and electric field values are given at  $\phi = 0$  degrees.

Concerning azimuthal variations, gain differences at  $\phi = 45$  degrees are  $0.05$  dB or less, and electric field differences at  $\phi = 45$  degrees are  $0.05$  mV/m or less.

Electric field strength values are given for a power input of  $1$  kW to the antenna, and are measured at a height of  $5$  feet above the ground at a distance of  $1$  mile.

Input impedances are given for #12 AWG conductors:

aluminum monopole, steel masts and ground stakes, and copper radials.

ELEVATION ANGLE (degrees)	POWER GAIN (dBi)		
	$0.125-\lambda$ monopole $0.125-\lambda$ radials	$0.125-\lambda$ monopole $0.25-\lambda$ radials	$0.25-\lambda$ monopole $0.125-\lambda$ radials
0	$-\infty$	$-\infty$	$-\infty$
5	-6.88	-6.44	-6.20
10	-3.15	-2.74	-2.53
15	-1.62	-1.27	-1.09
20	-0.95	-0.67	-0.54
25	-0.74	-0.55	-0.49
30	-0.84	-0.77	-0.77
40	-1.71	-1.94	-2.09
50	-3.32	-3.93	-4.22
60	-5.72	-6.75	-7.14
70	-9.25	-10.66	-11.13
80	-15.31	-17.01	-17.51
90	-154.24	-146.52	-160.29
VERTICAL ELECTRIC FIELD STRENGTH (mV/m)	30.44	32.05	33.02
INPUT IMPEDANCE (ohms)			
R	8.25	7.00	36.32
X	-653.45	-541.76	-136.61

In an effort to reduce a voluminous three-dimensional structure to two dimensions, elevated-radial systems were next modeled in which only two radials were used. The outcome is listed in Tables VI and VII. The  $0.25 \lambda$  monopole with two  $0.25 \lambda$  radials appears to be the best of the pack, and is actually superior to the best of the 4-radial "half-pints" which were detailed in the previous paragraph. The patterns for this antenna are given in Figure 4.

Jack Belrose, VE2CV, suggested that I model some "Field-Day Special" antennas using an elevated monopole with just a single radial; the results are presented in Tables VIII and IX. These hybrids put out a mix of vertical and horizontal polarization; they produce both low- and high-angle radiation, and exhibit maximum "front-to-back" ratios of 12 to 15 dB at certain take-off angles. The full-size version ( $0.25 \lambda$  elements) appears to work the best, and its feed-point impedance is much easier to live with than the rest of the bunch. Figure 5 illustrates the patterns generated by this antenna.

## ARRAYS

Many hams use phased vertical arrays for 80-meter DX-ing, and the elevated-radial antenna system lends itself nicely to such applications. Table X lists the power gain and field strength values for both the 2-element end-fire (cardioid) array and the very popular 4-square array, when constructed from individual 4-elevated-radial "building blocks". Line drawings appear in Figures 6 and 7, while the patterns are shown

TABLE VI. POWER GAIN AND ELECTRIC FIELD STRENGTH FOR "ISOLATED" VERTICAL ANTENNA SYSTEMS WITH A HALF-SIZED MONOPOLE AND RADIALS OF VARIOUS LENGTHS

Each system has 2 radials, and is elevated to a base height of 15 feet above ground.

Radials are located at  $\phi = 0$  and 180 degrees.

Electric field strength values are given for a power input of 1 kW to the antenna, and are measured at a height of 5 feet above the ground at a distance of 1 mile.

Input impedances are given for #12 AWG conductors:

aluminum monopole, steel masts and ground stakes, and copper radials.

ELEVATION ANGLE (degrees)	POWER GAIN (dBi)					
	0.125- $\lambda$ monopole 0.125- $\lambda$ radials			0.125- $\lambda$ monopole 0.25- $\lambda$ radials		
	$\phi = 0$	$\phi = 45$	$\phi = 90$	$\phi = 0$	$\phi = 45$	$\phi = 90$
0	$-\infty$	$-\infty$	$-\infty$	$-\infty$	$-\infty$	$-\infty$
5	-7.13	-7.05	-6.96	-7.75	-7.59	-7.32
10	-3.41	-3.31	-3.22	-4.09	-3.87	-3.58
15	-1.89	-1.78	-1.67	-2.68	-2.37	-2.04
20	-1.24	-1.11	-0.98	-2.17	-1.74	-1.35
25	-1.05	-0.90	-0.74	-2.18	-1.59	-1.11
30	-1.18	-0.99	-0.81	-2.54	-1.77	-1.18
40	-2.13	-1.86	-1.60	-4.09	-2.83	-1.98
50	-3.83	-3.46	-3.13	-6.52	-4.66	-3.51
60	-6.32	-5.85	-5.43	-9.75	-7.26	-5.83
70	-9.93	-9.37	-8.88	-13.96	-10.95	-9.28
80	-16.05	-15.42	-14.88	-20.41	-17.11	-15.29
90	-151.54	-151.54	-151.54	-144.30	-144.30	-144.30
VERTICAL ELECTRIC FIELD STRENGTH (mV/m)	29.61	29.87	30.16	27.59	27.96	28.88
INPUT IMPEDANCE (ohms)						
R		8.63			9.20	
X		-780.88			-544.24	

TABLE VII. POWER GAIN AND ELECTRIC FIELD STRENGTH FOR "ISOLATED" VERTICAL ANTENNA SYSTEMS WITH A FULL-SIZED MONOPOLE AND RADIALS OF VARIOUS LENGTHS  
Each system has 2 radials, and is elevated to a base height of 15 feet above ground.  
Radials are located at  $\phi = 0$  and  $180$  degrees.  
Electric field strength values are given for a power input of 1 kW to the antenna, and are measured at a height of 5 feet above the ground at a distance of 1 mile.  
Input impedances are given for #12 AWG conductors:  
aluminum monopole, steel masts and ground stakes, and copper radials.

ELEVATION ANGLE (degrees)	POWER GAIN (dBi)					
	$0.25-\lambda$ monopole $0.125-\lambda$ radials			$0.25-\lambda$ monopole $0.25-\lambda$ radials		
	$\phi = 0$	$\phi = 45$	$\phi = 90$	$\phi = 0$	$\phi = 45$	$\phi = 90$
0	$-\infty$	$-\infty$	$-\infty$	$-\infty$	$-\infty$	$-\infty$
5	-6.29	-6.25	-6.21	-6.12	-6.03	-5.90
10	-2.61	-2.57	-2.53	-2.48	-2.36	-2.22
15	-1.18	-1.13	-1.09	-1.10	-0.95	-0.78
20	-0.64	-0.58	-0.53	-0.64	-0.43	-0.22
25	-0.60	-0.53	-0.46	-0.69	-0.42	-0.16
30	-0.90	-0.81	-0.73	-1.12	-0.77	-0.44
40	-2.26	-2.13	-2.00	-2.81	-2.22	-1.72
50	-4.43	-4.25	-4.07	-5.43	-4.53	-3.81
60	-7.41	-7.16	-6.93	-8.90	-7.63	-6.68
70	-11.45	-11.14	-10.86	-13.40	-11.78	-10.63
80	-17.87	-17.52	-17.19	-20.11	-18.26	-16.97
90	-157.65	-157.65	-157.65	-149.71	-149.71	-149.71
VERTICAL ELECTRIC FIELD STRENGTH (mV/m)	32.72	32.84	32.97	33.35	33.67	34.15
INPUT IMPEDANCE (ohms)						
R		36.81			34.92	
X		-263.26			0.83	



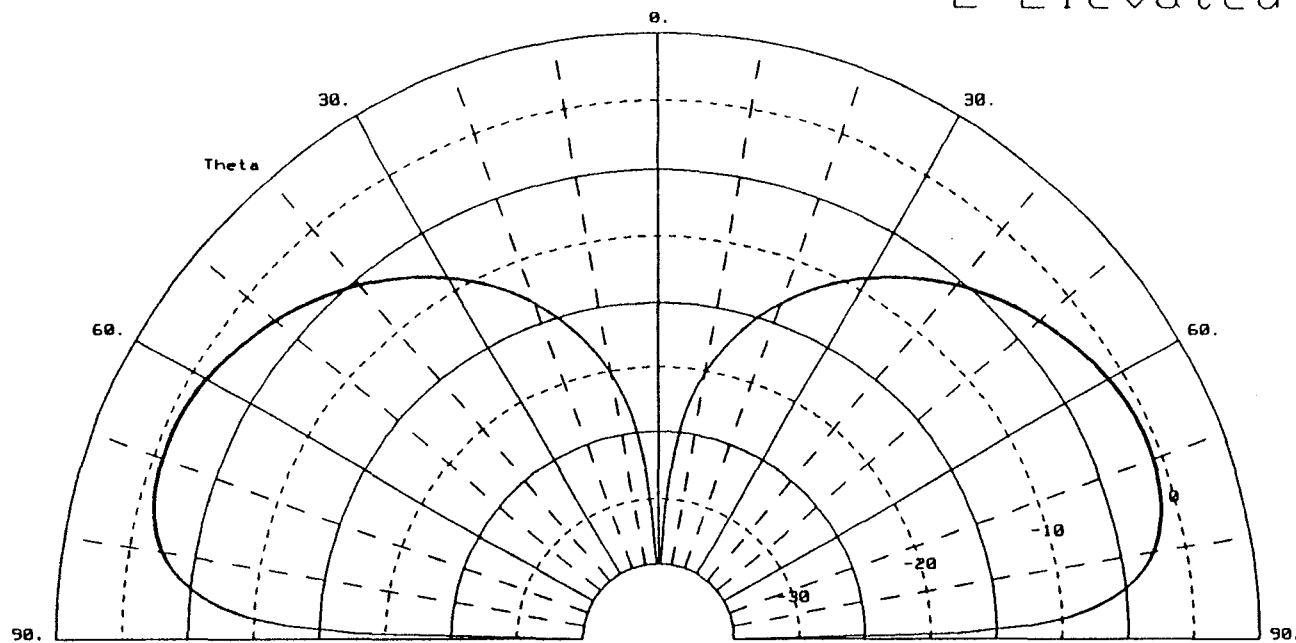
TABLE VII. POWER GAIN AND ELECTRIC FIELD STRENGTH FOR "ISOLATED" VERTICAL ANTENNA SYSTEMS WITH A FULL-SIZED MONOPOLE AND RADIALS OF VARIOUS LENGTHS  
Each system has 2 radials, and is elevated to a base height of 15 feet above ground.  
Radials are located at  $\phi = 0$  and 180 degrees.  
Electric field strength values are given for a power input of 1 kW to the antenna, and are measured at a height of 5 feet above the ground at a distance of 1 mile.  
Input impedances are given for #12 AWG conductors:  
aluminum monopole, steel masts and ground stakes, and copper radials.

ELEVATION ANGLE (degrees)	POWER GAIN (dBi)					
	$0.25-\lambda$ monopole $0.125-\lambda$ radials			$0.25-\lambda$ monopole $0.25-\lambda$ radials		
	$\phi = 0$	$\phi = 45$	$\phi = 90$	$\phi = 0$	$\phi = 45$	$\phi = 90$
0	$-\infty$	$-\infty$	$-\infty$	$-\infty$	$-\infty$	$-\infty$
5	-6.29	-6.25	-6.21	-6.12	-6.03	-5.90
10	-2.61	-2.57	-2.53	-2.48	-2.36	-2.22
15	-1.18	-1.13	-1.09	-1.10	-0.95	-0.78
20	-0.64	-0.58	-0.53	-0.64	-0.43	-0.22
25	-0.60	-0.53	-0.46	-0.69	-0.42	-0.16
30	-0.90	-0.81	-0.73	-1.12	-0.77	-0.44
40	-2.26	-2.13	-2.00	-2.81	-2.22	-1.72
50	-4.43	-4.25	-4.07	-5.43	-4.53	-3.81
60	-7.41	-7.16	-6.93	-8.90	-7.63	-6.68
70	-11.45	-11.14	-10.86	-13.40	-11.78	-10.63
80	-17.87	-17.52	-17.19	-20.11	-18.26	-16.97
90	-157.65	-157.65	-157.65	-149.71	-149.71	-149.71
VERTICAL ELECTRIC FIELD STRENGTH (mV/m)	32.72	32.84	32.97	33.35	33.67	34.15
INPUT IMPEDANCE (ohms)						
R		36.81			34.92	
X		-263.26			0.83	

NEC Elevation Plot:

Full-Size Elements

2 Elevated Radials



Maximum Gain:

-0.55 dBi

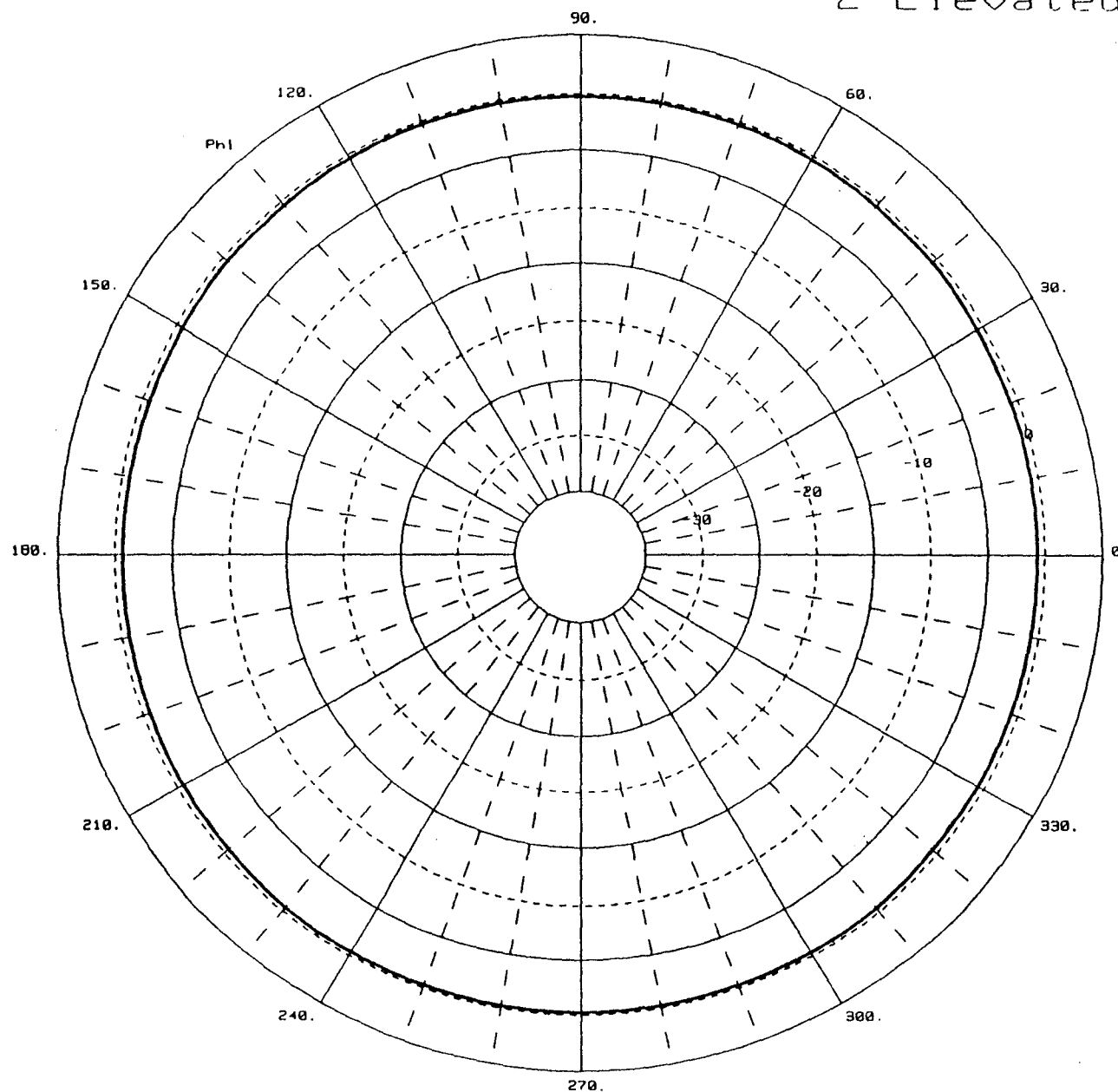
Phi: 0.00

Figure 4 (a)

NEC Azimuth Plot:

Full-Size Elements

2 Elevated Radials



Maximum Gain:

-0.17 dBi

Theta: 70.00

TABLE VIII. POWER GAIN AND ELECTRIC FIELD STRENGTH FOR "ISOLATED" VERTICAL ANTENNA SYSTEMS WITH A FULL-SIZED MONOPOLE AND A SINGLE RADIAL OF VARIABLE LENGTH

Each system has 1 radial, and is elevated to a base height of 15 feet above ground.

The radial is located at  $\phi = 0$  degrees.

Electric field strength values are given for a power input of 1 kW to the antenna, and are measured at a height of 5 feet above the ground at a distance of 1 mile.

Input impedances are given for #12 AWG conductors:

aluminum monopole, steel masts and ground stakes, and copper radials.

ELEVATION ANGLE (degrees)	POWER GAIN (dBi)							
	0.25- $\lambda$ monopole 0.25- $\lambda$ radial				0.25- $\lambda$ monopole 0.125- $\lambda$ radial			
	$\phi = 0$	$\phi = 45$	$\phi = 90$	$\phi = 180$	$\phi = 0$	$\phi = 45$	$\phi = 90$	$\phi = 180$
0	$-\infty$	$-\infty$	$-\infty$	$-\infty$	$-\infty$	$-\infty$	$-\infty$	$-\infty$
5	-6.07	-6.25	-7.30	-9.52	-5.91	-6.08	-6.60	-7.53
10	-2.36	-2.52	-3.55	-5.96	-2.21	-2.38	-2.90	-3.88
15	-0.87	-1.00	-2.01	-4.75	-0.74	-0.91	-1.44	-2.49
20	-0.23	-0.33	-1.33	-4.54	-0.14	-0.30	-0.86	-2.02
25	-0.05	-0.11	-1.09	-4.97	-0.01	-0.17	-0.76	-2.08
30	-0.14	-0.16	-1.14	-5.92	-0.19	-0.36	-0.99	-2.51
40	-0.76	-0.71	-1.69	-9.36	-1.17	-1.36	-2.12	-4.24
50	-1.55	-1.49	-2.49	-13.82	-2.70	-2.93	-3.89	-7.02
60	-2.19	-2.20	-3.20	-11.80	-4.54	-4.85	-6.07	-10.72
70	-2.64	-2.77	-3.65	-7.82	-6.55	-6.94	-8.37	-14.10
80	-3.12	-3.28	-3.86	-5.35	-8.69	-9.08	-10.31	-13.70
90	-3.92	-3.92	-3.92	-3.92	-11.12	-11.12	-11.12	-11.12
VERTICAL ELECTRIC FIELD STRENGTH (mV/m)	33.21	32.43	28.69	22.90	33.98	33.35	31.49	28.52
INPUT IMPEDANCE (ohms)								
R		49.56				40.65		
X		16.56				-485.47		

TABLE IX. POWER GAIN AND ELECTRIC FIELD STRENGTH FOR "ISOLATED" VERTICAL ANTENNA SYSTEMS WITH  
A HALF-SIZED MONOPOLE AND A SINGLE RADIAL OF VARIABLE LENGTH

Each system has 1 radial, and is elevated to a base height of 15 feet above ground.

The radial is located at  $\phi = 0$  degrees.

Electric field strength values are given for a power input of 1 kW to the antenna,  
and are measured at a height of 5 feet above the ground at a distance of 1 mile.

Input impedances are given for #12 AWG conductors:

aluminum monopole, steel masts and ground stakes, and copper radials.

POWER GAIN (dBi)

ELEVATION ANGLE (degrees)	0.125- $\lambda$ monopole 0.25- $\lambda$ radial				0.125- $\lambda$ monopole 0.125- $\lambda$ radial			
	$\phi = 0$	$\phi = 45$	$\phi = 90$	$\phi = 180$	$\phi = 0$	$\phi = 45$	$\phi = 90$	$\phi = 180$
0	- $\infty$	- $\infty$	- $\infty$	- $\infty$	- $\infty$	- $\infty$	- $\infty$	- $\infty$
5	-8.54	-8.88	-10.84	-17.05	-6.96	-7.28	-8.33	-10.58
10	-4.76	-5.01	-6.79	-13.72	-3.19	-3.50	-4.54	-6.90
15	-3.13	-3.29	-4.88	-12.93	-1.61	-1.90	-2.92	-5.47
20	-2.31	-2.36	-3.75	-13.42	-0.85	-1.12	-2.14	-4.93
25	-1.86	-1.80	-3.00	-14.95	-0.52	-0.77	-1.79	-4.90
30	-1.63	-1.46	-2.48	-17.44	-0.46	-0.69	-1.71	-5.21
40	-1.41	-1.10	-1.82	-17.11	-0.83	-1.03	-2.08	-6.55
50	-1.19	-0.87	-1.42	-10.19	-1.58	-1.78	-2.88	-8.36
60	-0.88	-0.69	-1.16	-5.93	-2.52	-2.75	-3.89	-9.51
70	-0.59	-0.56	-0.99	-3.32	-3.56	-3.82	-4.91	-8.99
80	-0.52	-0.59	-0.89	-1.72	-4.68	-4.92	-5.68	-7.49
90	-0.85	-0.85	-0.85	-0.85	-5.97	-5.97	-5.97	-5.97

VERTICAL ELECTRIC FIELD STRENGTH (mV/m)	24.75	23.45	18.09	9.90	29.95	28.79	25.48	20.18
---	-------	-------	-------	------	-------	-------	-------	-------

INPUT  
IMPEDANCE  
(ohms)

R	23.49	12.22
X	-527.41	-1004.27

TABLE X. POWER GAIN AND ELECTRIC FIELD STRENGTH FOR "ISOLATED" PHASED-ARRAY VERTICAL ANTENNA SYSTEMS

Each monopole has 4 radials, although it may share one or more radials with any adjacent monopoles. All antennas are elevated to a base height of 15 feet above ground. Electric field strength values are given for a power input of 1 kW to the antenna, and are measured at a height of 5 feet above the ground at a distance of 1 mile.

Input impedances are given for #12 AWG conductors:  
aluminum monopole, steel masts and ground stakes, and copper radials.

ELEVATION ANGLE (degrees)	POWER GAIN (dBi)							
	2-element cardioid array				4-element "4-square" array			
	front	45 deg	side	back	front	45 deg	side	back
0	-∞	-∞	-∞	-∞	-∞	-∞	-∞	-∞
5	-2.45	-2.96	-6.18	-32.85	-0.50	-3.29	-13.87	-37.32
10	+1.23	+0.69	-2.53	-27.61	+3.16	+0.39	-9.94	-33.19
15	2.66	2.07	-1.16	-23.74	4.54	1.82	-8.15	-31.06
20	3.20	2.55	-0.70	-20.42	5.03	2.36	-7.17	-29.65
25	3.23	2.51	-0.76	-17.68	5.00	2.40	-6.61	-28.67
30	2.92	2.10	-1.20	-15.51	4.63	2.11	-6.33	-28.00
40	+1.51	+0.47	-2.91	-12.70	3.17	+0.85	-6.33	-26.44
50	-0.76	-2.06	-5.57	-11.57	+1.08	-0.94	-6.71	-22.02
60	-3.87	-5.40	-9.11	-11.93	-1.29	-2.89	-7.10	-16.70
70	-8.01	-9.69	-13.60	-13.99	-3.61	-4.66	-7.35	-12.58
80	-14.06	-15.65	-19.44	-19.06	-5.65	-6.17	-7.48	-9.66
90	-25.00	-25.00	-25.00	-25.00	-7.53	-7.53	-7.53	-7.53
VERTICAL ELECTRIC FIELD STRENGTH (mV/m)	51.39	48.35	32.99	1.89	64.86	46.34	12.90	0.81
INPUT IMPEDANCE (ohms)								
R	19.61	51.07			9.68	36.80	36.80	66.62
X	7.41	33.71			2.78	-4.47	-4.47	47.29

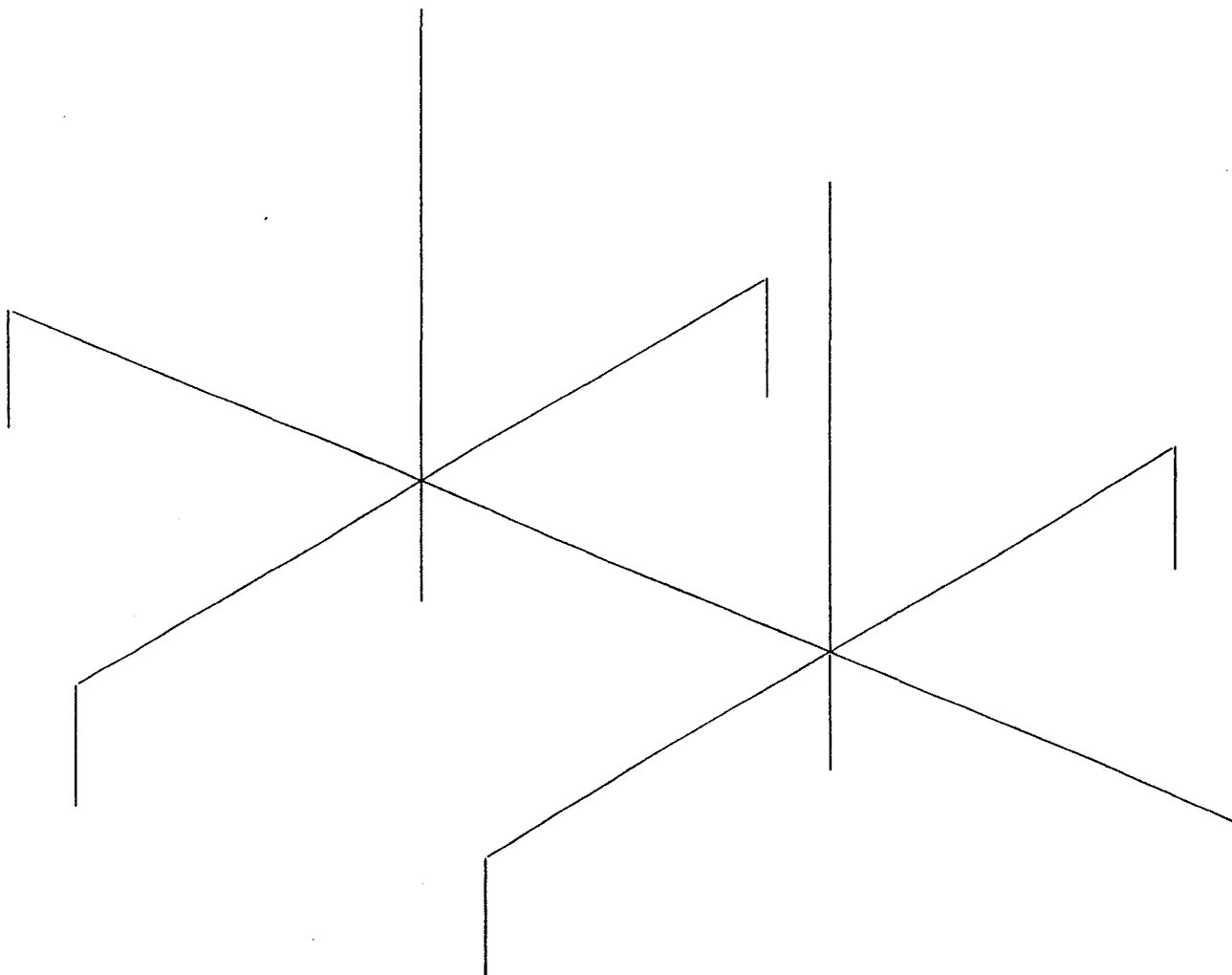


Figure 6

in Figures 8 and 9.

## OTHER TYPES OF SOIL

For those amateurs who do not live in a region with "average" ground constants, the following guidelines are suggested. As the electrical quality of the soil becomes worse, an elevated-radial antenna system must be raised progressively higher above the earth in order to reach "parity" with a conventional 120-buried-radial vertical monopole; if the soil is very conductive, the reverse is true. At AM broadcast frequencies (1 MHz) the author has found that a height of 5 meters is adequate for average soil, 3 meters for very good soil, and 7 meters for very poor soil. This statement reveals another aspect of the elevated-radial technique: as the transmitted wavelength gets longer, the "parity height" also increases, if the quality of the soil remains constant. In other words, an elevated-radial 160-meter antenna would have to be higher above the earth than would a similar 80-meter antenna, in order to obtain equivalent performance over the same ground.

## CONCLUSION

Studies on vertical monopole antennas using the NEC-GSD computer code indicate that a radiator elevated 10 to 20 feet above ground and having only 4 elevated horizontal radials can outperform a ground-mounted monopole with 120 buried radials. On 80 meters (for average soil) an elevation height of about 15 feet is adequate, while a lower height would be satisfactory for shorter wavelengths. Higher elevation above



ground is necessary for locations with poorer soil electrical characteristics. Field studies will be carried out to verify the computer predictions, although preliminary tests during Field Day showed very promising results. If the computer output from NEC is correct, then the construction cost and complexity of vertical monopole antenna systems can be greatly reduced, while installation flexibility and low-angle gain will be increased. The elevated-radial technique appears to be equally valid at AM broadcast frequencies as well as in the lower part of the HF band, so that perhaps the "ground plane" vertical monopole is the "antenna for all bands".

#### REFERENCES

1. Brown, G. H., R. F. Lewis, J. Epstein. "Ground Systems as a Factor in Antenna Efficiency", *Proceedings of the Institute of Radio Engineers*, Volume 25, Number 6, June 1937, pages 753-787.
2. *Ibid*, page 784.
3. *Ibid*, page 769.
4. Hagn, G. SRI International, Arlington, VA., Private communication.
5. Christman, A. M., "Vertical Monopoles with Elevated Ground Systems", *Proceedings of the Third Annual Review of Progress in Applied Computational Electromagnetics*, Naval Postgraduate School, Monterey, CA, March 1987.

# The Fields Due to a Small Loaded Loop in Free Space

Miles E. G. Upton, *Member, IEEE*, and Andrew C. Marvin, *Member, IEEE*

**Abstract**—A theoretical analysis of a resistively loaded, electrically small loop is presented which shows the variations of the transverse-wave impedance close to the loop as the resistive loading is altered. The theoretical results are compared with those obtained from a numerical simulation using Numerical Electromagnetics Code (NEC). Depending upon the loading, the loop exhibits electric (high wave impedance) or magnetic (low wave impedance) dipole properties, or intermediate wave impedances. These changes in wave impedance are closely related to variations in the far-field radiation pattern, and simulations are used to demonstrate this. Measured results are used to demonstrate that the variations predicted in wave impedance actually occur in practice. These results have bearing on the interpretation of emission measurements and on the design of circuits to minimize interference to other neighboring circuits.

## I. INTRODUCTION

THERE ARE many international specifications which exist for regulating the maximum electromagnetic radiation emitted by electronic devices. Radiated emission measurements are normally carried out in the far field of a radiating source, but the Federal German VDE specification [1] requires that measurements be made at frequencies down to 150 kHz. The defined test antenna to equipment-under-test (EUT) spacing of 30 m means that the antenna is within a region much less than a wavelength from the radiating equipment. This region is defined as the induction-field region. One of the main characteristics of the induction-field region is the divergence of the wave impedance (defined as the ratio of electric to magnetic field) from  $377 \Omega$ . Generally, the wave impedance becomes greater than  $377 \Omega$  for electric-dipole-like sources and less than  $377 \Omega$  for magnetic-dipole-like sources. The wave impedance implies the dominant energy transfer mechanism from the source in the induction-field region; magnetic field for magnetic-dipole sources and electric field for electric-dipole sources. However, the VDE specifications do not enforce the measurement of both electric and magnetic field and this leads to potentially large errors in predicted radiation, as will be shown.

The radiating geometry discussed in this paper is a resistively loaded, electrically small, square loop in free space. The emphasis in our paper is upon the variation of the induction-field wave impedance as a function of the load. The load is a lumped element at one point on the loop, which is intended to represent the typical situation encountered with

a printed-circuit board (PCB) track. Similar geometries have been considered previously for two main applications:

- 1) simple broadband antennas [9], [10]
- 2) modeling the radiation from PCB's [2]–[8].

The first of these applications concentrates upon the far-field radiation pattern and the radiation efficiency of a loop with distributed resistive loading. The second set of papers are specific to PCB's and do not consider the general characteristics of the radiation from a loaded loop.

This paper will show the dependency of both the induction-field transverse-wave impedance and the far-field radiation pattern upon the resistive loop loading. The results will highlight the link between the induction-field and the far-field effects. Practical measurements of wave impedance will be shown, in order to demonstrate the physical existence of these effects.

Two methods are used to model the loaded loop behavior. The first is analytical and relies upon an equivalent circuit analysis to deduce loop currents and hence radiated fields. The second technique solves for the fields numerically using Numerical Electromagnetics Code—Version Three (NEC) [11]. Note that the term “wave impedance” as used in this paper is not the total wave impedance at a point. Instead, results presented are of “transverse wave impedance,” the ratio of the transverse components of electric and magnetic field ignoring any components in the direction of propagation.

## II. EQUIVALENT CIRCUIT MODEL OF LOADED LOOP

The first analytical solution for the fields radiated by a loaded loop considers the square geometry of Fig. 1(a) with excitation and load at the center of opposite sides of the loop. Provided the loop is electrically small, then it can be shown that a square loop radiates the same fields as a magnetic dipole [12, p. 155]. The square loop can also be broken down into four electric dipoles as in Fig. 1(b) and it can be shown that these also behave as a magnetic dipole if each electric dipole has the same current (both magnitude and phase).

The analytical model developed in this section assumes that the addition of loading to the loop destroys the equality between the electric dipole currents in Fig. 1(b). A simple lumped-component equivalent circuit is used to deduce the current in each dipole and dipole radiation equations then give the fields due to these currents. Superposition of the fields from each dipole gives the total field.

A better understanding of the effect of loop loading is achieved by first considering very high loop loading, where dipole 3 is effectively an open circuit at the center. In this case, the only current that flows is the reactive displacement current through the capacitance between the top and the bottom

Manuscript received December 5, 1991; revised June 13, 1993.

M. E. G. Upton was with the Department of Electronics, University of York, Heslington, York, England. He is now with the Cambridge Consultants Ltd., Science Park, Milton Road, Cambridge, England.

A. C. Marvin is with the Department of Electronics, University of York, Heslington, York, England.

IEEE Log Number 9214323.

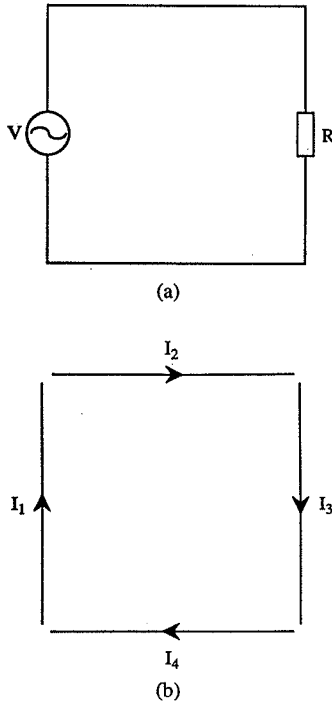


Fig. 1. (a) Square loop with excitation and load at opposite sides. (b) The same loop represented as a four electric dipoles each with an excitation current.

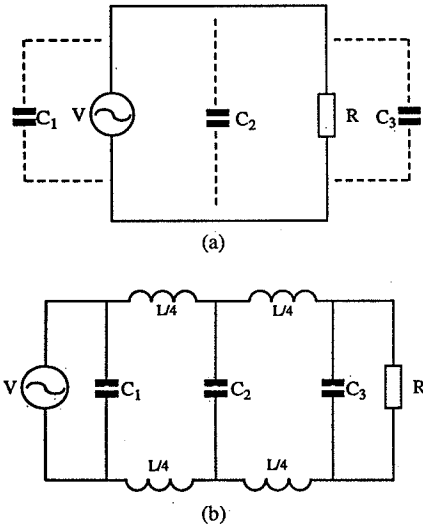


Fig. 2. (a) Loop geometry showing capacitances between top and bottom of loop. (b) Circuit equivalent model including partial inductances.

of the loop, with a small real component due to radiation. This current is similar to the displacement current across an electric dipole and will give rise to electric dipole radiation. Hence, a highly loaded loop acts like an electric dipole.

Fig. 2(a) shows the loaded loop with the notional capacitances between the top and the bottom of the loop through which the displacement current flows. This is redrawn in Fig. 2(b) as a circuit equivalent model where the loop is modeled as the three capacitances given in Fig. 2(a) and four separate inductances (each a quarter of the total loop inductance). These "partial" inductances are discussed in Paul's paper on PCB radiation [18]. The effect of loop loading upon the loop

currents can be envisaged from this model. Under conditions of no load, the loop current is only limited by the loop inductance which is small for an electrically small loop. The displacement current exists but it is relatively small compared to the current circulating in the loop and hence its effect is negligible. Increasing the loop loading limits the total loop current and increases the significance of the displacement current. Once the loop loading is larger than the loop impedance, the currents flowing through  $C_1$ ,  $C_2$ , and  $C_3$  are approximately constant, being mainly related to the loop geometry and excitation. Therefore, at high loading the displacement current dominates as the circulating current becomes smaller.

$C_1$  and  $C_3$  are equal and equivalent to the input capacitance of a short dipole antenna (ignoring any end effects due to the presence of  $C_2$ ). The input reactance of a dipole is given in [13, p. 547] as

$$X = \frac{-30}{\sin^2 \beta \ell} \left\{ \sin(2\beta \ell) \left[ -U + \ln \left( \frac{\ell}{\beta a^2} \right) + 2 \text{Ci}(2\beta \ell) - \text{Ci}(4\beta \ell) \right] - \cos(2\beta \ell) [2 \text{Si}(2\beta \ell) - \text{Si}(4\beta \ell)] - 2 \text{Si}(2\beta \ell) \right\} \quad (1)$$

where  $U$  = Euler's constant,  $\ell$  = length of wire,  $a$  = wire radius and

$$\text{Si}(x) = \int_0^x \frac{\sin x}{x} \quad \text{Ci}(x) = \int_x^\infty \frac{\cos x}{x}.$$

The functions  $\text{Si}(x)$  and  $\text{Ci}(x)$  (the sine and cosine integrals) cannot be evaluated analytically and are normally solved using numerical techniques. However, the following approximations from [12, pp. 145–146] are valid:

$$\text{Si}(x) = x \quad \text{Ci}(x) = U + \ln x$$

provided  $x < 0.2$  to give a maximum 0.1% error in the solution. The resulting input reactance of a dipole is thus

$$X = \frac{-30}{\sin^2 \beta \ell} \left[ 2 \sin(2\beta \ell) \ln \left( \frac{\ell}{a} \right) - 4\beta \ell \right]. \quad (2)$$

Also from Fig. 2(a) it can be seen that  $C_2$  is equivalent to the capacitance between two parallel cylindrical conductors. The capacitance per unit length is given in [13, p. 53] as

$$C = \frac{10^{-9}}{36 \ln \left( \frac{\ell}{b} \right)} \text{ F} \cdot \text{m}^{-1} \quad (3)$$

where  $b$ , the separation between the two conductors, is in this case equal to  $\ell$  the length of the perpendicular side of the loop. Note that a more complex model for the loop capacitances could be used, but the three capacitances used in this model account for the dominant effects within the loop.

The inductance of a small circular loop is given in [14, p. 311] as

$$L = R\mu \left[ \ln \left( \frac{8R}{a} \right) - 2 \right] \quad (4)$$

where  $R$  = radius of loop. It has already been mentioned that a small square loop is identical to a small circular loop provided

the areas are the same. Hence  $R = \sqrt{A/\pi}$  where  $A$  = area of square loop.

The limitations of this theoretical model are

- the approximations for  $L$  and  $C$ , the effects of which will be seen later, and
- the simplifications for  $\text{Si}(x)$  and  $\text{Ci}(x)$ .

The latter approximations limit the frequency range for which the model can be applied. The simplifications for  $\text{Si}(x)$  and  $\text{Ci}(x)$  assumes the largest value of  $x$  is less than 0.2, which implies  $4\beta l < 0.2$  and in turn implies  $\lambda > 40\pi\ell$ . Therefore, the maximum loop dimension must be less than 1/125 of a wavelength.

Once the current in each dipole of the loop has been deduced, the radiated field is calculated from the following equations [15, pp. 285–290]:

$$E_\rho = -\frac{jZ_0}{4\pi\beta} I_e \rho \left[ (1 + j\beta R) \frac{G}{R^2} \right]_{z_1}^{z_2} \quad (5)$$

$$E_z = -\frac{jZ_0}{4\pi\beta} I_e \left\{ \left[ (1 + j\beta R)(z - z') \frac{G}{R^2} \right]_{z_1}^{z_2} + \beta^2 \int_{z_1}^{z_2} G dz' \right\} \quad (6)$$

$$H_\phi = \frac{I_e \rho}{4\pi} \int_{z_1}^{z_2} \left( \frac{1 + j\beta R}{R^2} \right) G dz' \quad (7)$$

where the dipole is oriented in a cylindrical polar coordinate system as shown in Fig. 3(a),  $z_1 = -\ell/2$ ,  $z_2 = \ell/2$ ,  $z'$  is the variable distance along the dipole length, and

$$G = \frac{e^{-j\beta R}}{R} \quad R = \sqrt{\rho^2 + (z - z')^2}.$$

The above equations for the radiation from a finite-length dipole are used as opposed to the Hertzian dipole equations because the lengths of the dipoles are significant when compared with the distance at which the fields are calculated.

The integrals in the solution of  $E_z$  and  $H_\phi$  are not analytically solvable and these are derived using a proprietary numerical analysis package called NAG [16]. The routine used evaluates a series of increasingly accurate rules for the integral until the error difference between two successive evaluations is less than a specified relative accuracy. An accuracy of 0.1 % was chosen for the purposes of this program.

### III. NEC MODEL OF LOADED LOOP

The loop being modeled is 4 cm square with source and load at the center of opposite sides. The orientation of the loop in a Cartesian coordinate system is shown in Fig. 3(b). The excitation frequency is 10 MHz and the optimum segment length was found to be 0.8 cm (i.e., five segments per side), this being the smallest number of segments for which the current solution converges. The double-precision version of NEC was needed to support such fine segmentation ( $\equiv \lambda/3750$ ). The loop is made of 0.5-mm-radius wire.

### IV. INDUCTION-FIELD WAVE IMPEDANCE RESULTS

The variation of wave impedance with distance (the “wave impedance response”) is plotted in Figs. 4–6 for loads of 0

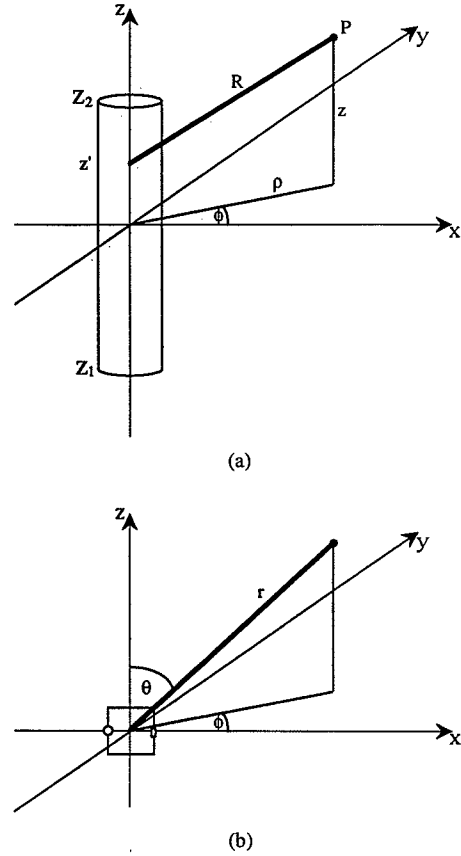


Fig. 3. (a) Orientation of finite-length dipole in cylindrical polar coordinate system. (b) Orientation of square loop in Cartesian and polar coordinate systems.

$\Omega$ , 100  $\Omega$ , 300  $\Omega$ , 330  $\Omega$ , 350  $\Omega$ , 1 k $\Omega$ , and 5 k $\Omega$ . The wave impedance response is really a function of distance in wavelengths from the radiating source, the product  $\beta R$  in (5)–(7). In this case, we are varying distance ( $R$ ) at fixed frequency, i.e., fixed ( $\beta$ ). Later, for the measured results, we will fix the distance and vary the frequency to produce the same effect. In each response, distance is measured along a line through the source and load (the  $x$ -axis in Fig. 3(b)) and the distance varies from 50 cm to 30 m logarithmically. In wavelength terms this corresponds to a variation from  $\lambda/60$  (which is well within the induction field) up to  $1\lambda$ , which is approximately far-field conditions. In the discussion that follows  $\Omega_{WI}$  is used to denote wave impedance in order to differentiate from resistive load  $\Omega$ .

The wave-impedance response varies from that of a magnetic dipole for the unloaded loop in Fig. 4 to that of an electric dipole for the loop loaded with 5 k $\Omega$  in Fig. 6. In between these two extremes, the variation can be considered in two regions:

- the region up to 0.1 wavelengths, at which the curve crosses the  $377\Omega_{WI}$  axis, and
- the region beyond this where the response goes through a peak or trough before becoming asymptotic to  $377\Omega_{WI}$ .

Note that all the responses cross through the  $377\Omega_{WI}$  axis at exactly the same point.

The response for 100- $\Omega$  load in Fig. 4 shows a large increase in the wave impedance close to the antenna in region a), with

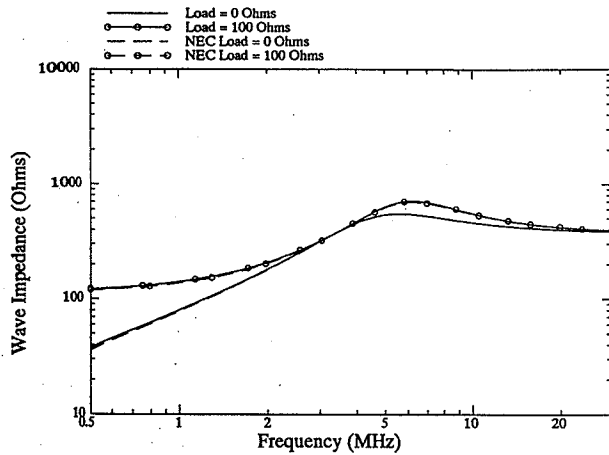


Fig. 4. Comparison of theoretical (solid line) and NEC (dashed line) wave impedance responses for loop in free space unloaded and with 100-Ω load.

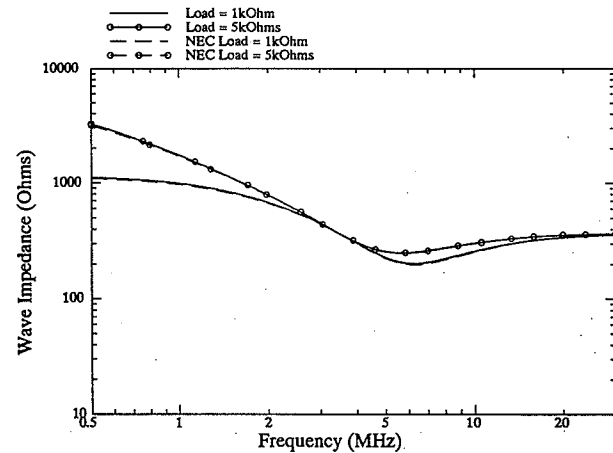


Fig. 6. Comparison of theoretical (solid line) and NEC (dashed line) wave impedance responses for loop in free space with 1- and 5-kΩ loads.

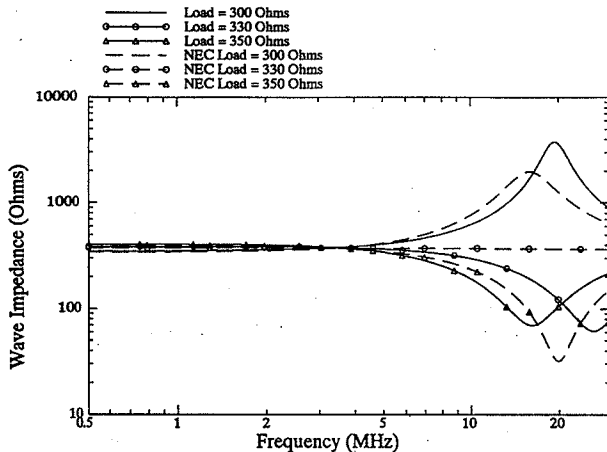


Fig. 5. Comparison of theoretical (solid line) and NEC (dashed line) wave impedance responses for loop in free space with 300-, 330-, and 350-Ω loads.

a small increase in height and movement outwards of the peak in region b). At 300 Ω (Fig. 5) the response close to the loop is very close to being flat at 377  $\Omega_{WI}$ , with very little change in this region as the load is increased through 330 Ω (Fig. 5) and 350 Ω (Fig. 5). The response in region b) changes drastically, however. The peak is now at 20 MHz and 3750  $\Omega_{WI}$  for the 300-Ω load (analytical). When the load is increased to 330 and 350 Ω, the peak in region b) flattens out and becomes a trough of 70  $\Omega_{WI}$  at 16 MHz (analytical). As load is increased to 1 kΩ (Fig. 6) and 5 kΩ (Fig. 6), the response close to the loop quickly approaches that of the electric dipole. The trough in region b) also comes into line with that for the electric dipole.

The overall trend in the wave impedance response as load is increased is for the peak to increase and move away from the loop until the electric dipole response starts to dominate, when the peak flips to a trough and moves back towards the loop. Hence, not only is the height of the peak/trough a definition of the relative electric or magnetic dipole type behavior, but also the position of the peak/trough with respect to that of a pure electric or magnetic dipole. This behavior forms the basis of extensions to this work in other areas which will be published in a later paper.

In terms of agreement between the analytical solution and NEC, the responses for 0 and 100 Ω are almost indistinguishable from the theoretical results. However, at 300-Ω load there is a noticeable difference in the position and height of the peak in the response. The NEC response exhibits the more magnetic dipole nature of the two responses. This difference is more accentuated at 330 Ω where NEC gives a flat-wave-impedance response. The trough at 350-Ω load is at 32  $\Omega_{WI}$  and 20 MHz from NEC, which compares with 70  $\Omega_{WI}$  and 16 MHz from theory. Note, however, that the NEC response is still tending to be the more magnetic dipole. The 1- and 5-kΩ responses show negligible difference between the two sets of results.

The discrepancies demonstrated are not as significant as they might first appear. This is because they occur when the response is very sensitive to loop loading. (Note the large change in the response encompassed by the 300–350 Ω load change.) A particular example of this is the flat response which occurs at 330-Ω load for the NEC solution. It is possible to demonstrate this flat response using the theoretical model, but in this case it occurs at 319.35-Ω load. In general, decreasing the resistance slightly (by 3%) in the analytical model will lead to much better agreement between the two sets of responses.

The main reason for the discrepancy is the simplified model of the loop capacitances used in the analytical model, whereas NEC allows for all the interactions within the loop. At 10 MHz the input capacitance of the open-circuit loop is 0.55 pF from NEC compared with 0.91 pF from the theoretical analysis. This difference will lead to a greater displacement current across the loop in the analytical model and a correspondingly larger contribution from the electric dipole effect. It is only significant at intermediate loads where neither dipole is dominant. Reference [17] gives an equation for the average input capacitance per unit length along the circumference for a circular loop as (symbols are the same as defined in (4))

$$C_{av} = \frac{\pi\epsilon}{\log(R/a)}$$

which, if the present square loop is equated to a circular loop of

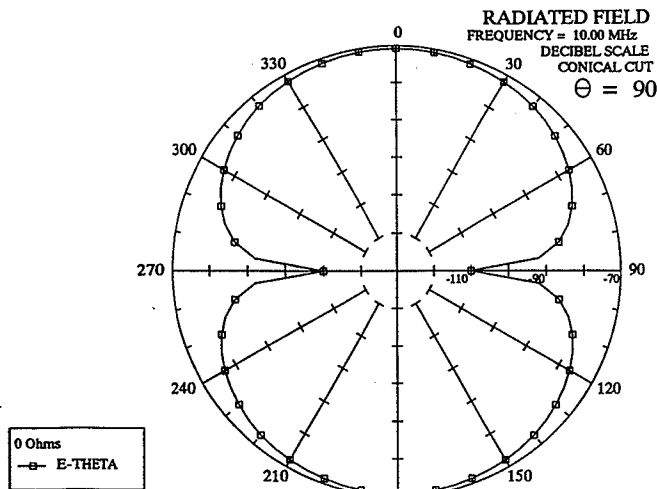
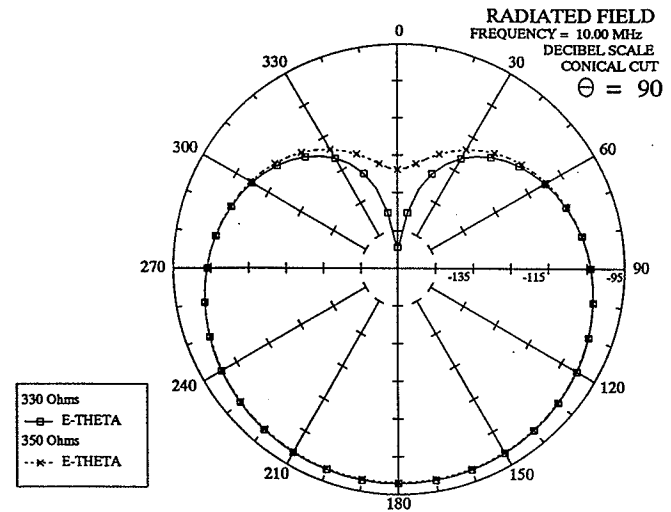
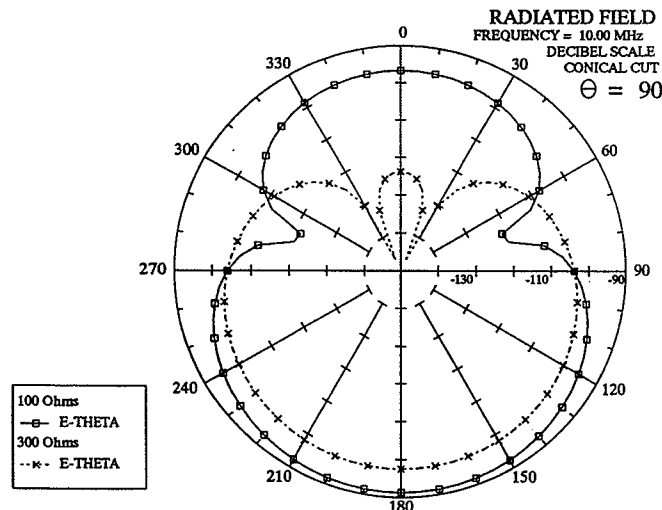
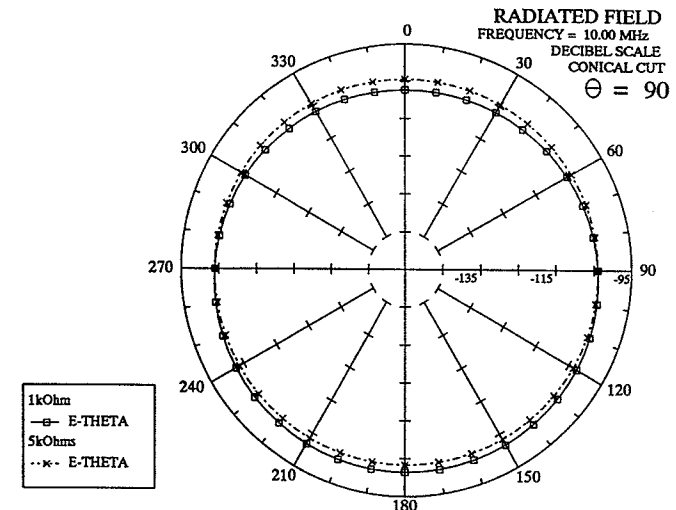


Fig. 7. Radiation pattern for unloaded loop in free space.


 Fig. 9. Radiation pattern for loop in free space loaded with 330- and 350- $\Omega$  loads.

 Fig. 8. Radiation pattern for loop in free space loaded with 100- and 300- $\Omega$  loads.

 Fig. 10. Radiation pattern for loop in free space loaded with 1- and 5-k $\Omega$  loads.

equal area, gives an input capacitance of 0.58 pF. Therefore, NEC seems to be giving a more accurate prediction of the input capacitance.

## V. FAR-FIELD RADIATION PATTERN RESULTS

Radiation patterns are plotted in Figs. 7–10 for the same set of resistances as in the previous section (0  $\Omega$ , 100  $\Omega$ , 300  $\Omega$ , 330  $\Omega$ , 350  $\Omega$ , 1 k $\Omega$ , and 5 k $\Omega$ ). In each case, the pattern is plotted as a function of angle from the  $x$ -axis in the  $x$ - $y$  plane of Fig. 3(b) (i.e., for  $\phi$  varying,  $\theta = 90^\circ$  in cylindrical polar coordinates). NEC alone is used to produce these results and the units of the plots are dBV/m. Note that all the plots use a 60-dB range, but that the unloaded loop pattern is in the range  $-70$  dBV/m to  $-130$  dBV/m; Fig. 8 uses the range  $-90$  dBV/m to  $-150$  dBV/m; and Figs. 9 and 10 use the range  $-95$  dBV/m to  $-155$  dBV/m. This is because the unloaded loop radiates all its input power, whereas the load absorbs the majority of the power for the other cases.

The radiation pattern for 0- $\Omega$  load (Fig. 7) is the “figure-of-eight” pattern expected from an electrically small loop ([15, p. 180]), with peaks at  $0^\circ$  and  $180^\circ$ , and nulls along the  $\pm 90^\circ$ -axis. The peak-to-null ratio is 40 dB which agrees with that given in [15, p. 180]. The results for loaded loops can be divided into two types; those below 330  $\Omega$ , where the radiation pattern has two nulls, and those above where it has only one null. At 100- $\Omega$  load (Fig. 8) the figure-of-eight has become lopsided, with two nulls at  $70^\circ$  and  $290^\circ$  and the lobe at  $180^\circ$  being 5 dB higher than that at  $0^\circ$ . Increasing the load to 300  $\Omega$  (Fig. 8) moves the two nulls to  $25^\circ$  and  $335^\circ$  with the difference between the two lobes in the pattern being 26 dB. The two nulls in the pattern join up at 330- $\Omega$  load (Fig. 9) to form a “cardioid” type radiation pattern. The peak-to-null ratio now reaches its maximum at 52 dB.

The cardioid-type response is maintained as load is increased further to 350  $\Omega$  (Fig. 9), 1 k $\Omega$  (Fig. 10), and 5 k $\Omega$  (Fig. 10). The only change is in the peak-to-null ratio, which is 30 dB at 350  $\Omega$ , dropping to only 1 dB at 5 k $\Omega$ . The response at 5

k $\Omega$  is approaching an omnidirectional (in this plane) radiation pattern, which would be expected from an electric dipole.

It can be seen that the radiation pattern changes with load reflect the changes in the induction-field wave impedance, with the responses between the two extremes of loading being a composite response made up of the two basic dipole components of the radiation pattern (the figure-of-eight and the omnidirectional). Note that the transition from figure-to-eight, magnetic-dipole-type patterns to cardioid, electric-dipole-type patterns occurs at 330  $\Omega$ , which is the point at which the induction-field response is flat, halfway between the two extremes of dipole behavior.

These results can be compared with [9, fig. 8] of Smith which plots the same far-field radiation pattern as a function of the normalized, distributed resistance around the loop. It can be seen that the variation in radiation pattern is very similar with the move from figure-of-eight for the unloaded loop to almost omnidirectional for the highly loaded loop, passing through a cardioid pattern at intermediate loads.

## VI. MEASURED WAVE IMPEDANCE RESULTS

In order to demonstrate that the predicted variations in wave impedance are achievable in practice, the wave-impedance response of a small square loop has been measured. Details of the sensor for measuring wave impedance are described separately in [19]. The radiating loop is fed from beneath the ground plane via a BNC connector. The radiating loop is 4 cm square and mounted on a BNC connector which raises it to 3.8 cm above the ground plane. The use of the unbalanced loop as a radiating source rather than the loop in free space is a matter of practical convenience. The single-loop sensor is placed 50 cm from the radiating loop, and both are mounted upon a 2.4 m by 1.2 m aluminum ground plane. The excitation frequency range is 10 to 400 MHz which implies that the source-sensor separation varies from  $\lambda/60$  to  $2\lambda/3$ . The orientation of the radiating loop is such that the sensor is in the plane of the loop. The wave-impedance response using a frequency scan with the fields measured at a fixed distance is easier to implement in practice and gives a similar variation in distance measured in wavelengths to that described for the theoretical results.

Wave-impedance responses are plotted in Fig. 11 for two different loop loads, 0  $\Omega$  and 1.5 k $\Omega$ . In each case, the response is compared with that from a NEC simulation of the practical situation. When the loop is unloaded the wave-impedance response is similar to that of the unloaded loop in free space, but the lower frequency portion (below 80 MHz) is consistently offset slightly higher in this case. This is due to the interaction of the loop with the ground plane. There is also a slight ripple on the linear part of the measured response (around 30 MHz) which arises from imperfections in the "open-field" test site used for these measurements. The agreement between the measured response and that predicted from NEC is excellent, except in the region around 80 MHz where the NEC response peaks at 1200  $\Omega_{WI}$  as opposed to 800  $\Omega_{WI}$  for the practical response. The reason these discrepancies occur is the difference between NEC, which calculates the magnetic field at a point in space, and the practical measure-

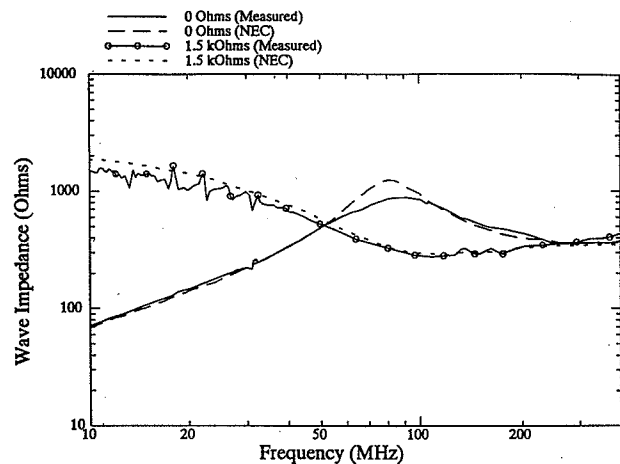


Fig. 11. Comparison of measured (solid line) and NEC (dashed line) wave impedance responses for loop above a ground plane with no load and 1.5-k $\Omega$  load.

ment which in order to obtain a measurable signal, covers an area of space. Therefore, the measured quantity is really the average field over the breadth of the sensor (4 cm) which implies that the response will be "smoothed," as is happening in this case. This effect and the errors it introduces in the magnetic-field measurement are discussed in more detail in [20].

The 1.5-k $\Omega$  responses shows a trend towards electric-dipole behavior. The practical response has developed a small trough at 100 MHz and the lower frequency portion of the curve is becoming asymptotic to the linear response of the monopole. The agreement between the measured and NEC responses is very good, except at low frequencies where some ripple is present on the measured responses.

## VII. CONCLUSIONS

It has been shown that the induction-field wave impedance of the fields generated by a resistively loaded, electrically small loop are critically dependent upon the loop loading. In the limits, the loop can be made to exhibit either electric-dipole or magnetic-dipole behavior. Between these two extremes the loop exhibits a complex, composite response with elements of both dipole types. Over the range from 300- to 350- $\Omega$  load a large peak (3750  $\Omega_{WI}$ ) in the wave impedance response becomes a trough of 70  $\Omega_{WI}$ . Such a large change in wave impedance demonstrates that these effects need to be taken into account when considering coupling between circuits. Judicious placement of loading in a loop on a PCB track, for example, may be all that is needed to drastically reduce coupling to other circuit tracks.

This paper has also demonstrated a link between the changes in induction-field wave impedance as load varies and corresponding changes in the far-field radiation pattern. Measured results have been used to demonstrate that these effects exist in practice.

From the viewpoint of EMC emission measurements, interpretation of measurements of either magnetic or electric fields may be complicated by the effects predicted. In particular, the

prediction of fields at distances other than the measurement distance will be affected. Thus requirement of the VDE specifications that the highest value of radiated electric field obtained from measurements of both electric field and "converted" magnetic field merits further examination.

# REFERENCES

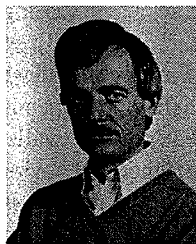
- [1] EMACO EMC Consultants translation of *VDE Specification Radio Frequency Interference Suppression of Electrical Appliances and Systems*, VDE 0875/6.77.
- [2] D. White, "Electromagnetic shielding: Materials and performance," Don White Consulting Rep., 1980, p. 1.6.
- [3] D. J. R. White and M. Mardiguian, "EMC design of printed circuit boards and backplanes," in *Proc. 4th Annu. Int. Printed Circuits Conf.* (New York, June 2-4, 1991), pp. 1-9.
- [4] B. Cooperstein, "Radiation from printed wiring boards," in *1982 IEEE Int. EMC Symp.* (Santa Clara, CA, Sept. 8-10), pp. 103-106.
- [5] H. W. Ott, "Controlling EMI by proper printed circuit board layout," in *EMC 1985, 6th Symp. and Tech. Exhibition* (Zurich, Switzerland, Mar. 1985), pp. 127-132.
- [6] M. Costa, T. K. Sarkar, B. J. Strait, and S. Bennett, "On radiation from printed circuit boards," in *IEEE Int. EMC Symp.* (Boulder, CO, Aug. 18-20), pp. 246-249.
- [7] R. Raut, W. J. Steenart, and G. I. Costache, "A note on the optimum layout of electronic circuits to minimize the radiated electromagnetic field strength," *IEEE Trans. Electromagn. Compat.*, vol. 30, pp. 88-89, 1988.
- [8] T. H. Hubing and J. F. Kaufman, "Modeling the electromagnetic radiation from electrically small table-top products," *IEEE Trans. Electromagn. Compat.*, vol. 31, no. 1, pp. 74-84, 1989.
- [9] G. S. Smith, "A note on the imperfectly conducting circular-loop antenna," *Radio Sci.*, vol. 9, no. 1, pp. 35-41, 1974.
- [10] J. L. Lin, "The imperfectly conducting circular-loop antenna," *Radio Sci.*, vol. 8, no. 3, pp. 251-257, 1973.
- [11] G. J. Burke and A. J. Poggio, "Numerical electromagnetics code (NEC)—Method of moments," Lawrence Livermore Nat. Lab. Rep. UCID-18834, Jan. 1981.
- [12] J. D. Kraus, *Antennas*. New York: McGraw-Hill, 1950.
- [13] E. C. Jordan and K. G. Balmain, *Electromagnetic Waves and Radiating Systems: Second Edition*. Englewood Cliffs, NJ: Prentice-Hall, 1968.
- [14] S. Ramo, J. R. Whinnery, and T. Van Duzer, *Fields and Waves in Communication Electronics*. New York: Wiley, 1965, p. 311.
- [15] C. A. Balanis, *Antenna Theory, Analysis and Design*. New York: Wiley, 1982.
- [16] *The NAG Fortran Library—Mark 13*, Routine DO1AHF, Numerical Algorithms Group, Ltd., 1988.
- [17] S. K. Schelkunoff and H. T. Friis, *Antennas: Theory and Practice*. New York: Wiley, 1952, p. 322.

- [18] C. R. Paul, "Modelling and prediction of ground shift on printed circuit boards," in *IERE 5th Int. Conf. on EMC* (York, England, Oct. 1-3, 1986), pp. 37-46.
- [19] M. E. G. Upton, "Investigation of the wave impedance radiated by a loaded loop," D. Phil. dissertation, Dept. Electronics, University of York, England, 1990.
- [20] S. Iskra and I. P. Macfarlane, "H-field sensor measurement errors in the near-field of a magnetic dipole source," *IEEE Trans. Electromagn. Compat.*, vol. 31, pp. 306-311, Aug. 1989.



**Miles E. G. Upton** (M'92) graduated from the University of York in 1986 with the B.Sc. degree in electronic engineering, and received the D.Phil. degree in 1990 from the same university. For his doctorate he specialized in electromagnetic modeling of antennas and other structures.

He spent a year working for an electronics research company in the security industry, designing electromagnetic object detection systems, before being awarded a SERC/NATO Postdoctoral Fellowship to study EMC and numerical modeling at Concordia University in Montreal, Que., Canada. Since January 1992 he has been employed by Cambridge Consultants Ltd, Cambridge, England as an EMC consultant. He specializes in designing EMC and Tempest into products for a wide variety of clients, and gives guidance on implementing the European EMC Directive. His current interests are in time-domain electromagnetic modeling techniques and in the applications of ultrawide-bandwidth radar.



**Andrew C. Marvin** (M'85) was born in Brierley Hill, England, in 1950. He was at the University of Sheffield between 1969 and 1977 where he received the B.Eng., M.Eng., and Ph.D. degrees in electrical and electronic engineering.

After working in the EMC Department at British Aerospace, Filton, Bristol he moved to the University of York, England as their first lecturer in Electronics late in 1979. He is, at present, Senior Lecturer in Electronics in the Electronics Department of the University of York where he is the founder member and Leader of the Applied Electromagnetics Research Group and Course Director for the M.Sc. degree in EMC. His research interests lie in the development of improved EMC measurement techniques and in the production of CAD tools incorporating EMC into equipment design.



## MEDIUM-WAVE AERIALS FOR SIMULTANEOUS TRANSMISSION OF BROADCAST PROGRAMMES

621.396.67

After explaining the manner in which a medium-wave aerial is used for transmitting a single wavelength, the author examines the possibilities of simultaneous transmission, taking as examples installations which Brown Boveri have carried out or have on hand. The article is confined to the most important practical case, in which two transmitters are concerned; for more than two transmitters to radiate at the same time is exceedingly rare, although feasible, using the same means as for double transmissions.

WHEN a transmitting station is required to radiate the same or several programmes over a number of transmitters operating at different frequencies, an obvious solution is to utilize one aerial for several transmissions. Indeed such problems frequently have to be faced, and solved, by radio engineers.

For example, in television the problem is quite normal; the picture and sound transmitters feed into a common aerial. But in the medium-wave band conditions are different to those in the v.h.f. band as used for television. The nature of the r.f. circuits and aerials themselves are fundamentally different, as are the modulation systems. The two television transmitters have adjacent frequencies, since picture and sound must be inseparable. Medium-wave transmitters, on the other hand, are completely independent of one another, a fact which the aerial system must take into account; faults in the channel belonging to one transmitter must not affect the other.

### Single Aerial Feed

Medium-wave aerials of modern design may be either self-radiating guyed masts or self-supporting towers, the r.f. energy being conducted asymmetrically to the base in most conventional cases. Unhindered radiation

in all directions and the radial earthing system necessitate the aerial being a fair distance from the transmitter building. Then there are safety conditions to be considered, which usually stipulate that the distance must be at least equal to the height of the tower.

The r.f. power must therefore be conveyed from the transmitter to the aerial by a feeder. To avoid the difficulty of transforming symmetries to asymmetries, the feeder is most conveniently arranged asymmetrically, like the aerial, using overhead lines with earthed return (with a characteristic impedance of 200-300  $\Omega$ ) or coaxial r.f. cable (50-70  $\Omega$ ). The feeder must be matched. Therefore suitable equipment has to be provided at the base of the aerial, mostly housed in a cabin.

The main parts in a transmitter installation are given in Fig. 1. The matching circuit is shown as T-shaped; but equally well the  $\Pi$  formation could have been used. Fundamentally it is sufficient to have an L section, which can be obtained from the T or  $\Pi$  formations. Merely the longitudinal reactance  $X_3$  on the aerial side, or  $X_1$  on the feeder side, is omitted.

The relationship between the three quantities of the T formation matching the impedance at the base of the antenna  $Z_A = R_A + jX_A$  to the purely resistive input impedance  $R_E$ , which itself is equal to the characteristic impedance of the feeder, is given by the following formulae.

$$\frac{(X_A + X_3)^2}{R_A} - \frac{X_1^2}{R_E} = R_E - R_A \quad (1a)$$

$$-\frac{X_A + X_3}{R_A} + \frac{X_1}{R_E} = \frac{X_3(R_E - R_A)}{R_E R_A} \quad (1b)$$

It will be seen from equation (1a) that when  $R_E > R_A$  there is always a real solution for  $X_A + X_3$ , to which we give the same value as  $X_1$ . If, on the other hand  $R_E < R_A$  a real solution is obtained for any value of  $X_3$ . Thus the L formation is sufficient, provided the longitudinal section is arranged on the side having the lower resistance.

A special case is when the two components are equal ( $R_A = R_E$ ). Then it is sufficient if the longitudinal reactance  $X_3 = -X_A$ , thus compensating for the reactive

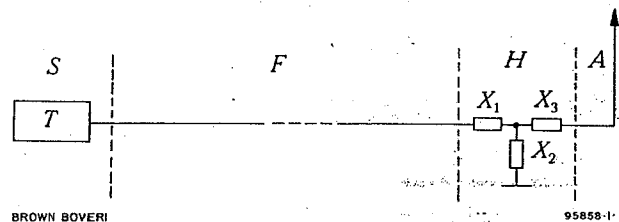


Fig. 1. — Connection between a transmitter and an aerial

S = Transmitter building      H = Aerial matching cabin  
T = Transmitter      A = Aerial  
F = Feeder       $X_1, X_2, X_3$  = Matching elements

component of the base impedance. The transverse section thus has infinite reactance. A symmetrical T formation may also be employed. If the matching network is suitable for use over a range of frequencies, at one of which  $R_E$  and  $R_A$  are equal, it is advisable to adopt the full T formation (or alternatively  $\Pi$ ) because with the L formation, very high, impracticable values of  $X_2$  would be necessary for those frequencies at which  $R_A$  and  $R_E$  were not quite equal, but differed very little from one another.

### Simultaneous Operation by Two Transmitters over a Single Aerial

The system carrying the signals between two transmitters operating simultaneously must contain wave-traps in order to prevent appreciable voltages at the frequency of the one transmitter from reaching the anodes of the other. The tubes are the non-linear element in which the superposed voltages of the two frequencies can produce combination oscillations and cross-talk. The levels of the latter must therefore be kept below the interference limit by effective wave-traps.

The circuits between the anodes of the output stage and the aerial are composed of linear impedances in which the superposed voltages cannot exert any harmful effects. There are a number of positions in which the wave-traps can be situated. For practical reasons it is preferable not to encumber the anode circuits of the transmitter with wave-traps because it is desirable not to change transmitters of established design.

Let us therefore consider the chain of elements between the transmitter output terminals, matched to the characteristic impedance, and the base of the aerial. Of the available alternatives, two fundamentally different systems are picked out and illustrated side by side in Fig. 2. That in Fig. 2a includes the matching circuit  $N$ . This circuit must be selective, i.e. it must transform the base impedance, which is different for the two frequencies, to conform to the characteristic impedance. A common feeder links the matching circuit with the transmitter building, where the frequencies are separated by means of the wave-traps  $B_1$  and  $B_2$ . The matching circuits  $M_1$  and  $M_2$  transform to the transmitter outputs.

In the system shown in Fig. 2b, the two frequencies are immediately separated at the base of the aerial by the wave-traps  $B_1$  and  $B_2$ . From the input to each trap there are two independent normal line systems back to the transmitter. The only special feature is that the matching

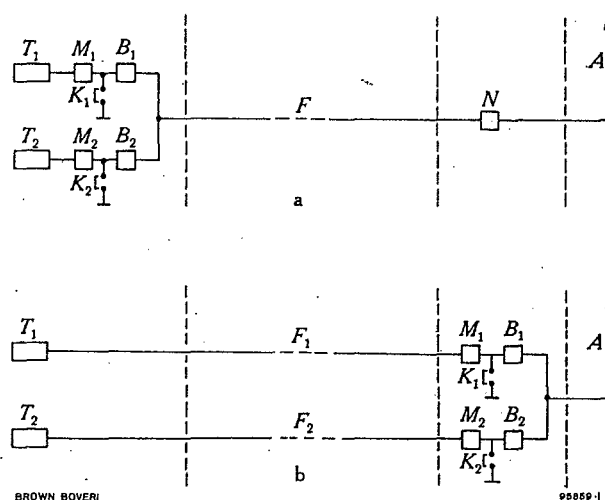


Fig. 2. — Connection of two transmitters to one aerial

- a = With separation in transmitter building
- b = With separation in aerial matching cabin
- T = Transmitter
- M = Matching circuit
- N = Matching circuit for two frequencies
- B = Wave-trap
- K = Shorting switch
- F = Feeder
- A = Aerial

circuits in this case do not transform from the characteristic impedance of the feeders to the base impedance of the aerial, but to the input impedance of the wave-trap.

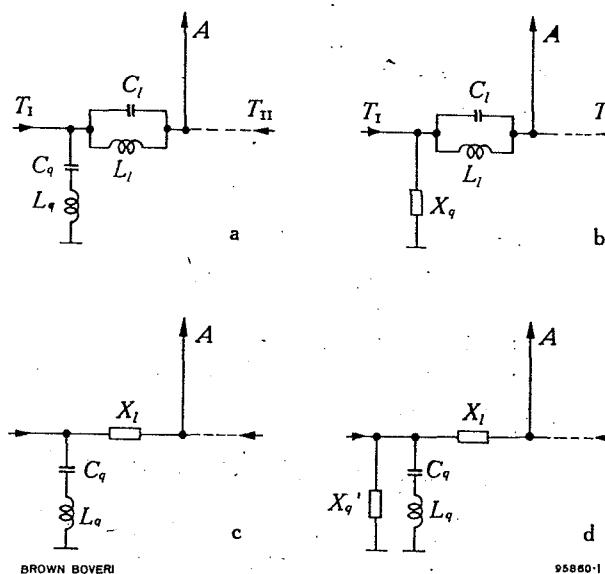


Fig. 3. — Alternative arrangements for wave-traps

- $T_I$  = Transmitter I
- $T_{II}$  = Transmitter II
- $C_l$  = Longitudinal capacitance
- $C_q$  = Transverse capacitance
- $L_l$  = Longitudinal inductance
- $L_q$  = Transverse inductance
- $X_l$  = Longitudinal reactance
- $X_q$  = Transverse reactance
- $X_q'$  = Supplementary transverse reactance for matching

### Wave-Traps

An L-shaped section can be used as a wave-trap if the longitudinal arm is in the form of a parallel resonance circuit and the transverse arm a series resonance circuit (Fig. 3 a). It is also permissible to use a simple reactance (Fig. 3 b or c) for one of the two arms.

Since, for the frequency to be excluded (alien frequency)  $\omega_{II}$  and its sidebands, the transverse reactance  $X_q$  must be very small compared with the longitudinal  $X_l$ , the ratio  $v$  of the voltage divider, which governs the blocking effect of the trap, can be approximated to

$$v = \frac{X_q}{X_l + X_q} \approx \frac{X_q}{X_l}$$

The resonance circuits are tuned to the alien carrier frequency  $\omega_{II}$ . In circuits with no losses  $v$  is zero at this frequency; if losses are taken into account  $v$  is extremely small. The deciding factor is therefore the  $v$  of the sideband frequencies, produced by modulation of the second transmitter by the audio frequency  $\omega_n$  of the first.

In the parallel resonance circuit, for the sideband frequencies  $\omega_{II} + \omega_n$  the value of  $X_l$  becomes approximately

$$X_l \approx \mp \frac{\omega_{II}^2 L_l}{2 \omega_n}$$

and for the series circuit

$$X_q \approx \pm 2 \omega_n L_q$$

(The approximation is sufficient because in the medium-wave band  $\omega_n$  is very small in comparison to  $\omega_{II}$ .) The division of the voltage in the wave-traps shown in Fig. 3 is therefore as follows.

$$\text{Fig. 3a} \quad v = -4 \frac{\omega_n^2}{\omega_{II}^2} \cdot \frac{L_q}{L_l} \quad (2a)$$

$$\text{Fig. 3b} \quad v = \mp 2 \frac{\omega_n}{\omega_{II}} \cdot \frac{X_q}{\omega_{II} L_l} \quad (2b)$$

$$\text{Fig. 3c} \quad v = \pm 2 \frac{\omega_n}{\omega_{II}} \cdot \frac{\omega_{II} L_q}{X_l} \quad (2c)$$

The effect of the trap in Fig. 3a corresponds to the square of the ratio of the audio frequency  $\omega_n$  to the carrier frequency  $\omega_{II}$ ; in the traps b and c the effect is only as the first power of this ratio. It is, however, possible by a cascade connection of two traps corresponding to Fig. 3b or c to achieve the greater effect gained with the trap in Fig. 3a. The number of filters is the same; the elements in the non-selective branches become useful if the traps are also employed for matching.

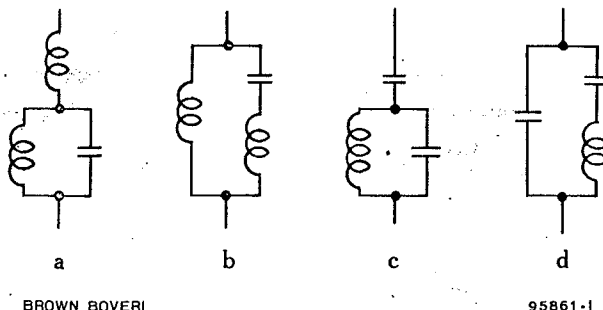


Fig. 4. — Alternative arrangements for circuits with two resonance frequencies

a, b = Parallel < series resonance frequency  
c, d = Series < parallel resonance frequency

With a definite voltage division, the trap only admits of one degree of freedom. A combined trap, evolved from the type in Fig. 3c, as chosen to illustrate the point, must therefore contain an additional element  $X'_q$ , producing the circuit as in Fig. 3d. The value of  $X_l$  is that necessary for matching to the "own" frequency. For the "alien" frequency,  $X_l$  has a given value, which defines  $L_q$  as in equation (2c), and  $C_q$  to produce the resonance with the alien frequency. The series resonance remains permanently set, whereas the match can be accurately adjusted by varying  $X_l$  and  $X'_q$ , without noticeably changing the blocking effect.

### Frequency Separation in the Transmitter Building

The special problem which has to be faced in the system in which the frequencies are separated in the transmitter building is the matching circuit  $N$  for the two frequencies. It is possible to start from an arrangement corresponding to the basic T or  $\Pi$  formations, and to make the various branches selective circuits, as far as necessary. But series or parallel resonance circuits are not always able to produce the desired reactance ratio. At the higher frequencies the inductive reactance of such circuits is always larger, while the capacitive reactance is smaller. Therefore, if reactances of the same sign are desired, but of opposite proportions, these are only obtainable by using more complicated arrangements, such as networks with three reactances, possessing a series and a parallel resonance (Fig. 4).

Matching to two frequencies is also feasible by means of a circuit in which each leg only contains simple reactances. But then a certain number of legs must be used to ensure that there are sufficient degrees of freedom available.

$$\text{for } 10 \text{ KHz } \omega_n \approx 1.257 \cdot 10^5$$

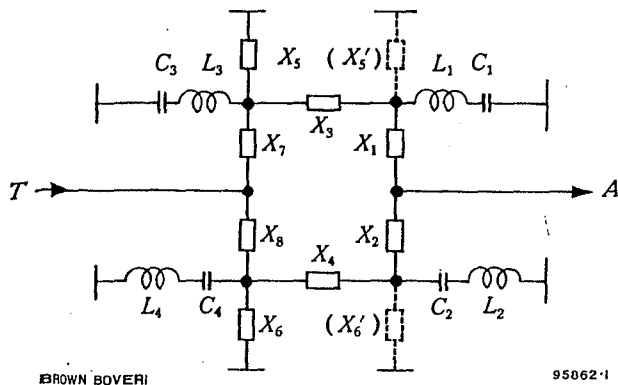


Fig. 5. — Matching circuit for two frequencies with independent control of matching

A feature common to the arrangements described so far is that matching to the two frequencies used is not performed independently. This makes the matching procedure considerably more difficult. Furthermore, all elements are subjected to both frequencies, which greatly increases the amount of material involved. A fault in any one element puts both transmitters out of action.

A system possessing the advantage of mutually independent matching is shown in Fig. 5. It is nevertheless very expensive, requiring four wave-traps ( $X_1$ ,  $C_1$ ,  $L_1$ , etc.) and two matching circuits ( $X_3$ ,  $X_5$  and  $X_4$ ,  $X_6$ ). After the wave-traps have been set, any frequency can be matched, independent of another.

The common feeder must be dimensioned for the sum of the powers. Since there can always be moments in which the voltages of like phases of the two transmitters can be added, the line must be dimensioned for the algebraic sum of the voltages of the two transmitters.

#### Frequency Separation at the Base of the Aerial

According to the foregoing remarks, it is evident that the system of frequency separation at the base of the aerial (Fig. 2b) is clearly superior. Although this method necessitates the laying of two separate feeders, Brown Boveri prefer it, because it offers the following advantages:

All elements between the transmitter output terminals and the ends of the matching circuits  $M_1$  and  $M_2$  are completely free from the alien frequency. The adjustment of the match is just as simple as it is with solo operation. Changes on the part of one frequency do not affect the other.

Should a fault occur in the feeder or matching circuit on one side, the operation of the other transmitter can continue uninterrupted and unaffected.

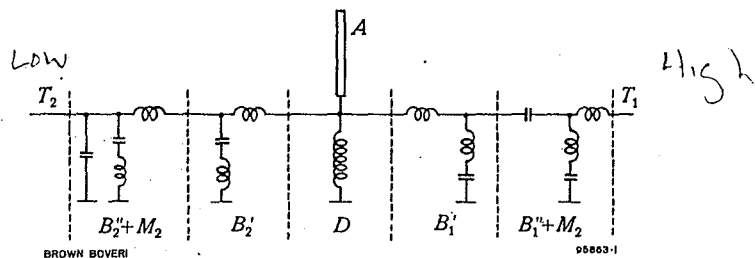


Fig. 6. — Schematic diagram of the aerial of the Castanheira transmitting station near Lisbon of "Emissora Nacional de Radiodifusão", designed for simultaneous radiation of 135 kW at frequencies of 665 and 755 kc/s

$T_1$  = From 755-kc/s transmitter

$T_2$  = From 665-kc/s transmitter

$A$  = Aerial

$B'$  = First wave-trap

$B' + M$  = Second wave-trap, combined with matching circuit

$D$  = Feed choke for obstruction lights

Even if the transverse element of one wave-trap should break down, the other transmission can be continued. It is only necessary to take the affected element out of service by closing the shorting switch  $K$ . For the other channel, only the longitudinal element of the trap needs to be in order, thus assuring the maximum degree of independence.

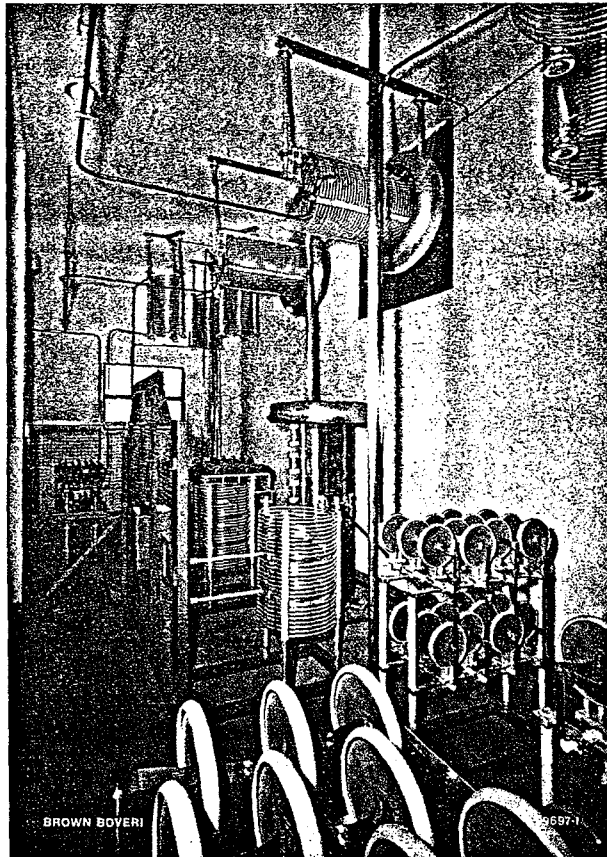
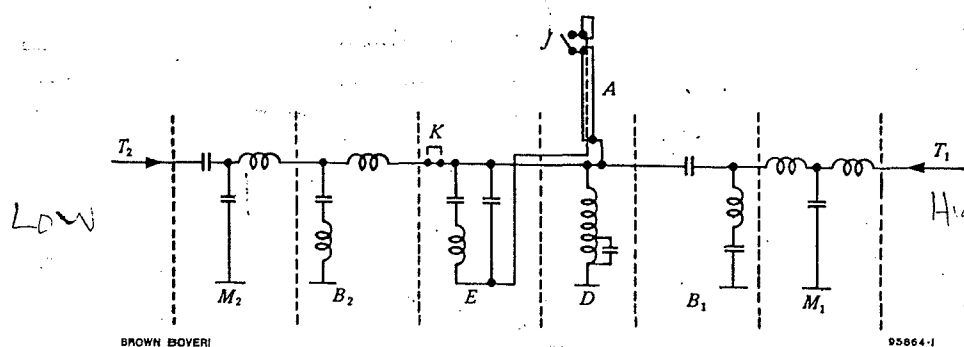


Fig. 7. — View of part of the installation shown in Fig. 6



There is a second trap for each transmitter in the transmitter building.

Fig. 8. — Schematic diagram of a subdivided aerial mast as employed in the Austrian Radio transmitting station at Bisamberg near Vienna. This may radiate 240 kW at 1475 kc/s alone, or 120 kW operating simultaneously at 1475 and 584 kc/s

$T_1$  = From 1475-kc/s transmitter  
 $T_2$  = From 584-kc/s transmitter  
 $A$  = Aerial  
 $J$  = Separating point with bypass switch  
 $D$  = Lighting choke with capacitance  
 $E$  = Selective circuit  
 $K$  = Switch  
 $B$  = Wave-trap  
 $M$  = Matching circuit

In order to gain full benefit from the last of the above advantages, the longitudinal element of the trap is made robust and as simple as possible. An ideal solution is given by the circuit in Fig. 3c, the longitudinal element in which is a simple reactance.

#### Installations Completed or On Hand

The main elements of an aerial system for simultaneous transmission at 665 kc/s and 755 kc/s, with 135 kW carrier power in each case, are shown schematically in Fig. 6. This arrangement, which presented considerably difficulty because the interval between transmission frequencies was only 90 kc/s, has now been operating successfully for some time. Fig. 7 depicts the room containing the first wave-traps and the feed chokes for the obstruction lights. The series resonance circuit was arranged as a quadruple sequence of inductances and capacitances (simplified in the diagram). In a single circuit the voltages would be so large, on account of the small frequency interval at such a high power, that ordinary means would be incapable of coping with them. The second wave-traps are accommodated in two adjacent rooms, where they are carefully screened.

Fig. 8 shows the basic layout of an aerial system at present under construction, where various forms of operation must be possible. The transmitting equipment consists of two transmitters, each of which comprises a pair of 120-kW units. Normally one double transmitter radiates 240 kW carrier power at 584 kc/s over its own aerial (the equipment for which does not concern this article). The second double transmitter supplies the same output at 1475 kc/s to a subdivided aerial via the equipment shown schematically in the illustration. The lower part of the aerial for 1475 kc/s is about  $0.53\lambda$ , while the total height is  $0.63\lambda$  (in which  $\lambda$  is the wavelength).

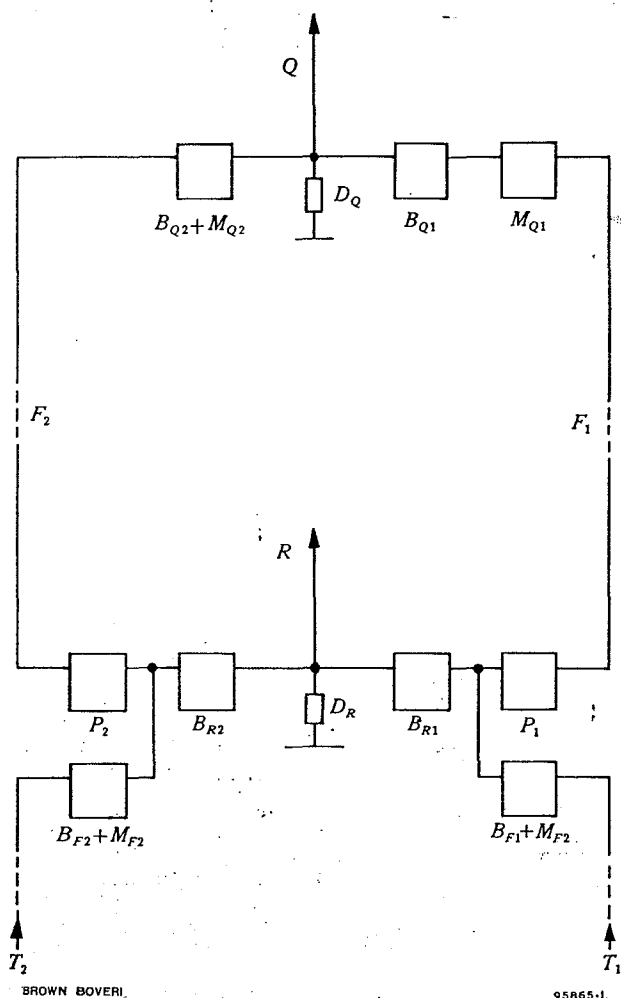


Fig. 9. — Block diagram of a directional aerial system for simultaneous transmission of 50 kW at 1061 and 719 kc/s, employed at the San Salvador station of "Emissora Nacional de Radiodifusão"

$T_1$  = 1061-kc/s transmitter  
 $T_2$  = 719-kc/s transmitter  
 $Q$  = Radiator  
 $R$  = Reflector  
 $D$  = Lighting choke  
 $B$  = Wave-trap  
 $B + M$  = Wave-trap combined with matching circuit  
 $P$  = Phase control and power distribution

Depending on requirements, it will be possible to radiate with either of these two effective heights. The switch at the separating point allows the two parts to be connected together. When radiating from the lower part alone, the upper part must be decoupled. Therefore above the central conductor shown dotted it is linked with a selective circuit which also has to fulfil other tasks.

If necessary, the aerial array may also have to radiate simultaneously at both frequencies, in which case the alternative operating features for 1475 kc/s, i.e. using part or all of the mast height, must be retained. The total height must be used in any case for 584 kc/s. This necessitates a special layout for the selective circuit.

In this case it proved helpful to connect part of the lighting feed choke in parallel with a capacitance, enabling the base impedance to be varied individually for each fre-

quency. The traps and matching circuits conform to the principle described. The independence of the match at each frequency is most important in this instance because the 1475-kc/s side may be changed over from partial or total mast height. Repercussion on the 584-kc/s side would be an almost intolerable complication.

A directional aerial installation (Fig. 9) for simultaneous operation at 719 and 1061 kc/s, each with 50 kW output, is at present being built. The radiator and reflector masts are 120 m apart. At both frequencies the energy has to be concentrated in the same direction. As can be seen from the diagram, with the arrangement chosen, the equipment for matching, phase adjustment and load distribution at each frequency has been devised as if the other frequency were completely non-existent.

MS 596 (KME)

L. Leng

## SPECIAL SPOT WELDING METHODS

621.791.763.1

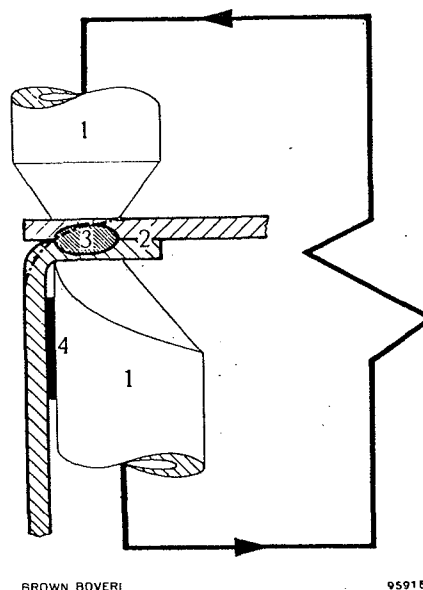
Resistance spot welding depends on a combination of pressure and heat, the latter being produced directly by the resistance heating effect of an electric current. The article describes some cost-saving spot welding methods suitable for the batch- and mass-production of steel components. Examples of work produced are illustrated and hints are given for the use of these versatile processes.

**M**ANUFACTURERS of pressed metal components in large quantities are particularly interested in improving quality and increasing output while keeping labour costs as low as possible. They have, therefore, a special need for improved methods of joining metals.

When, for example, pressed, stamped or drawn parts—or even machined parts—have to be permanently joined together, the experienced designer always tries to use the most economical process, namely resistance welding; and above all, spot welding. Where the type of work is suitable, spot welding can offer the following advantages:

- (a) Expensive forming processes (e.g. deep drawing) are avoided.
- (b) Expensive materials are saved (e.g. stainless steel need only be used where, for hygienic reasons or in order to resist corrosion, it is essential).
- (c) Less economical methods of fastening such as riveting, brazing, gas welding or arc welding are superseded.

To ensure success in spot welding it is, however, necessary to allow for the special peculiarities of the process, which require a shape of workpiece fundamentally



BROWN BOVERI

95915-1

Fig. 1. — Diagram of spot welding

Smooth sheet surfaces and sufficient overlap are necessary for good spot welding.

The dotted line shows the shape of a watertight stitch-welded lap joint finished by grinding (e.g. a stainless steel sink).

- 1 = Electrodes
- 2 = Workpiece
- 3 = Weld nugget
- 4 = Insulation (to prevent shunting of the welding current)

*Mather*  
JULY 1, 1987

VERTICAL RADIATOR CHARACTERISTICS

UNIFORM CROSS SECTION

BASE INSULATED

GUYED TOWER

Prepared by;

GEORGE MATHER & ASSOCIATES

October 1982.

## VERTICAL RADIATOR CHARACTERISTICS

The majority of standard band broadcast antenna systems, in Canada, are comprised of one or more vertical radiators. These vertical elements are usually guyed, uniform cross section, base insulated structures, centered on an appropriate ground screen. The ground screen consists of 120 equally spaced radials, one-quarterwavelength, or more, in length.

A knowledge of the electrical characteristics of the vertical radiators will facilitate array design and the performance predictions. In addition, a determination of impedances will enable the design of suitable transmission systems and networks for operation of a broadcast array.

The information in this report has been collated from measured antenna data and its interpretation is based on judgement and experience.

- M -



## VERTICAL RADIATOR CHARACTERISTICS

### Table of Contents

1. Base Input Impedances
  - 1.1 base resistance versus physical height
  - 1.2 base reactance versus physical height
  - 1.3 base reactance versus base resistance
2. Electrical Length and Voltage Standing Wave Ratio
  - 2.1.1 Smith chart plot of self impedance
  - 2.1.2 impedance circle diagram
  - 2.2.1 derivation of electrical height
  - 2.2.2 derivation of electrical height
  - 2.2.3 derivation of electrical height
  - 2.3.1 derivation of VSWR
  - 2.3.2 derivation of VSWR
  - 2.3.3 derivation of VSWR
3. Antenna Current Relative Magnitude and Phase
  - 3.1 incremental relative current and phase
  - 3.2 incremental relative current and phase
4. Vertical Plane Relative Field Strength
  - 4.1 relative field versus vertical angle
  - 4.2 relative field versus vertical angle
5. Theoretical Horizontal Field Intensity at One Mile
  - 5.1 radiation efficiency versus height
  - 5.2 loop amps for 100 Mv/m versus height
6. Resistive Component of Mutual Impedance
  - 6.1 mutual resistance versus spacing
7. Mutual Impedance Magnitude and Phase for Reference Tower
  - 7.1 mutual impedance, spacing 000 to 180 degrees
  - 7.2 mutual impedance, spacing 180 to 360 degrees
  - 7.3 mutual impedance, spacing 360 to 540 degrees

## VERTICAL RADIATOR CHARATERISTICS

### Table of Contents

7.4	mutual impedance, spacing 540 to 720 degrees
7.5	mutual impedance, spacing 720 to 900 degrees
7.6	mutual impedance, spacing 900 to 1080 degrees
7.7	mutual impedance, spacing beyond 1080 degrees
8.	Derivation of Base Operating Impedance, Current & Power
8.1.1	form for derivation routine
8.1.2	form for derivation routine
8.2	sample array
8.3.1	impedance circle diagram
8.3.2	impedance circle diagram
8.4.1	base impedance derivation
8.4.2	base impedance derivation
8.4.3	base impedance derivation
8.4.4	base impedance derivation

### Acknowledgements

## VERTICAL RADIATOR CHARACTERISTICS

### 1. Base Input Impedance

The observed base input impedance of a vertical radiator is directly related to the tower height. While other features such as type of cross section and height to cross section area ratio will have some influence, the primary controlling factor is the height at the frequency utilized.

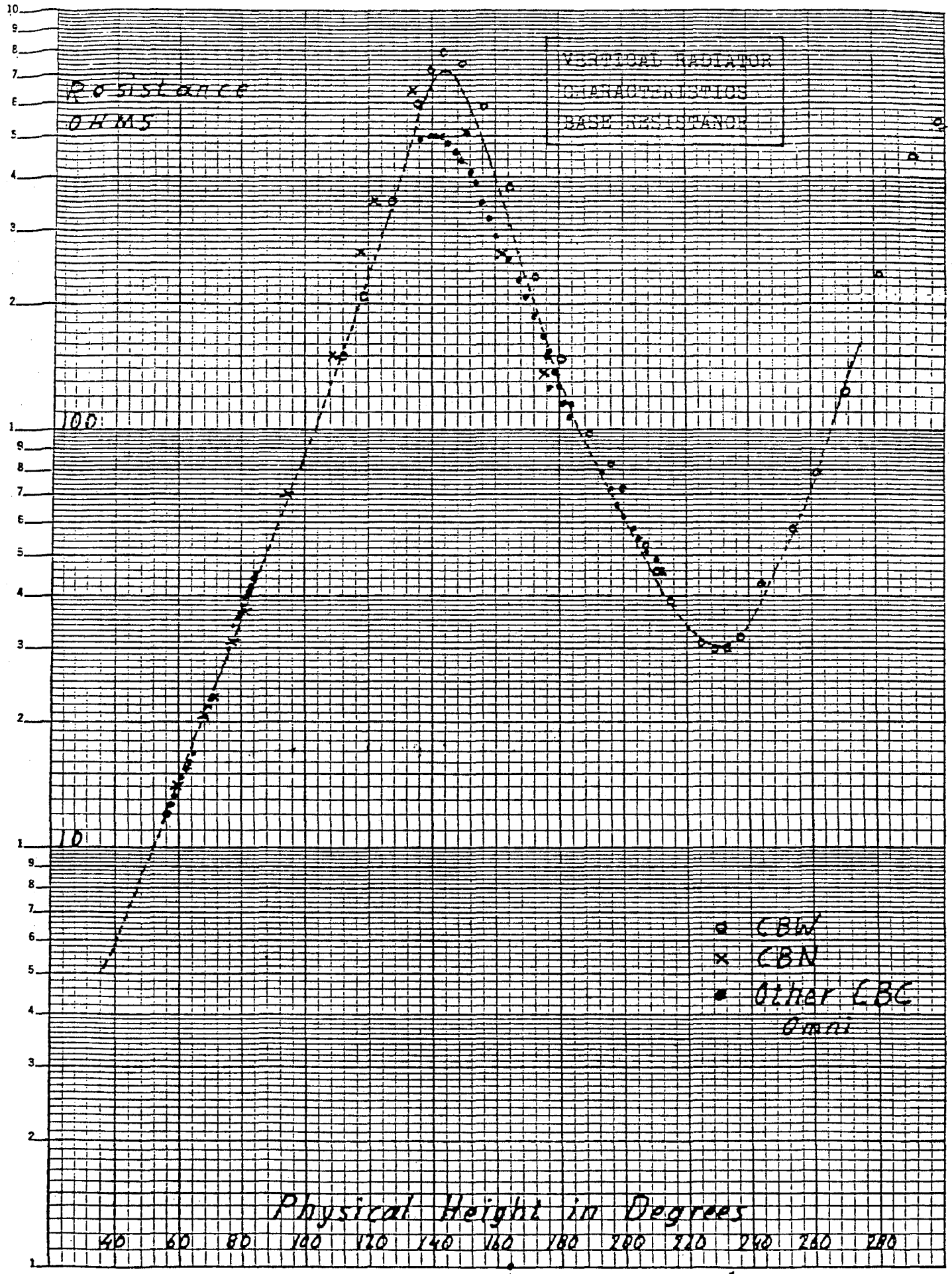
In order to establish the impedance characteristics of a vertical radiator, the measurements should ideally be predicated on a single isolated tower without influence from other metallic structures. In this regard the Canadian Broadcasting Corporation employs a number of single tower systems upon which a most comprehensive set of impedance measurements has been executed. The self impedance derivations in this report are based on the CBC measurement data which has been made available.

A plot of base resistance versus physical tower height is shown in Figure 1.1 and a plot of reactance versus physical tower height is depicted in Figure 1.2. The lines drawn to show the trends of resistance and reactance, versus physical height, are "judgement" lines drawn without benefit of a statistical or mathematical fit. It is expected, however, that these "judgement" lines are generally representative of the impedance characteristics of vertical radiators.

Figure 1.3 is a plot of reactance versus resistance for vertical radiators. The Figure 1.3 plot is based on the "judgement" lines derived from Figures 1.1 and 1.2, with the physical height indicated for each data point. The spiral curve shown in Figure 1.3 suggests an approach for further evaluation which will be examined in subsequent sections of this report.

- M -

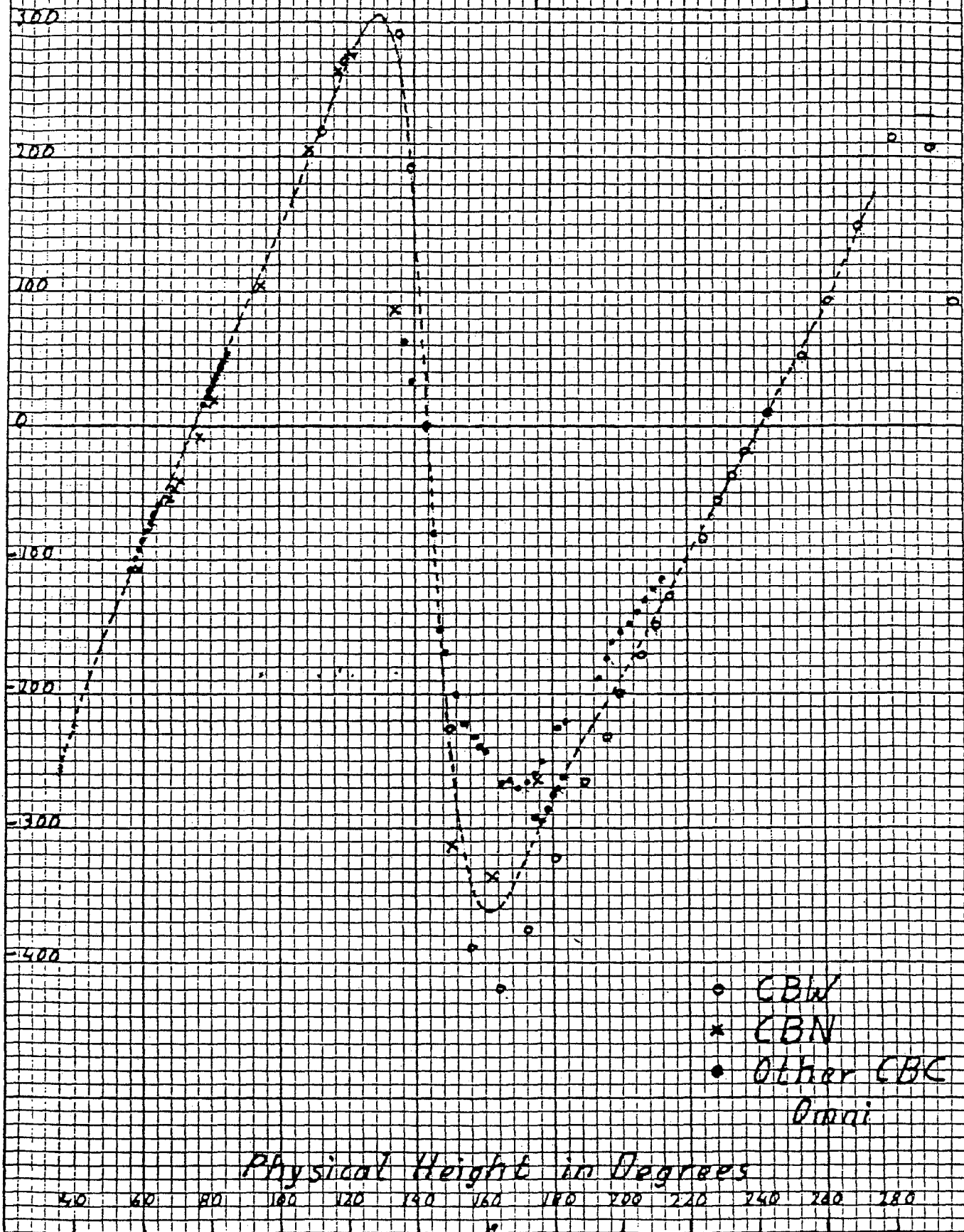
K-2 3 CYCLES X 70 DIVISIONS 300 H.P.S.A.  
KEUFFEL & ESSER CO.



Reactance

OHMS

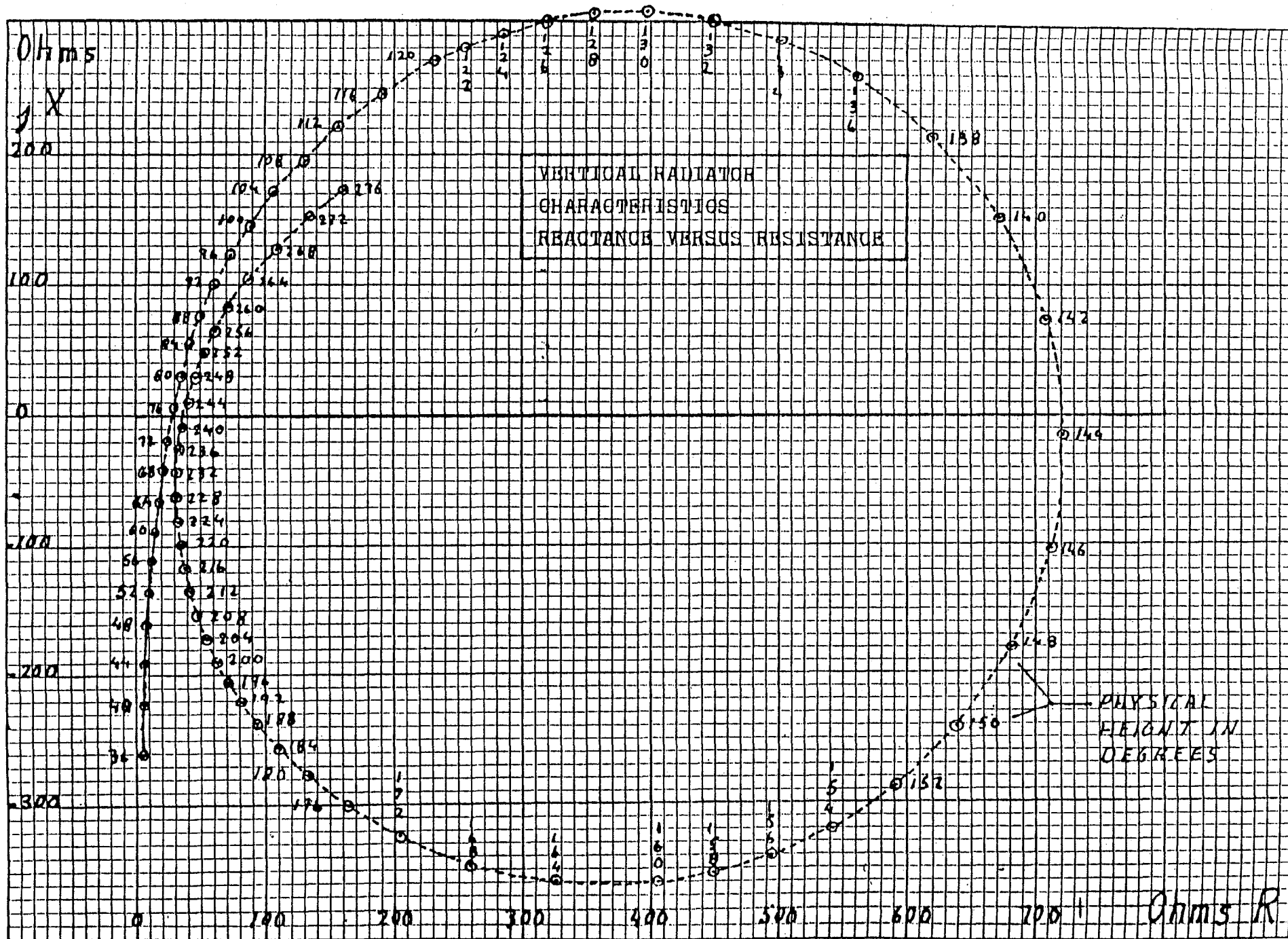
VERTICAL RADIATOR  
CHARACTERISTICS  
BASE REACTANCE



○ CBW  
× CBN  
• Other CBC  
Dashed line

Physical Height in Degrees

K&E  
10 x 10 INCH 40 0/03  
7 x 10 INCHES  
MADE IN U.S.A.  
KRUPP & ESSER CO.



## VERTICAL RADIATOR CHARACTERISTICS

### 2. Electrical Length and Voltage Standing Wave Ratio

A plot of reactance versus resistance, normalized with a characteristic impedance of 200 ohms, is shown on the impedance circle diagram of Figure 2.1. The nature of the curve on Figure 2.1 suggests that it may be of interest to derive the Electrical Length (G) and the Voltage Standing Wave Ratio (V) for the spiral curve which is evident.

The Electrical Length (G) and the Voltage Standing Wave Ratio (V) may be scaled from the curve plotted on Figure 2.1. However, calculated values of G and V derived from the Resistance and Reactance plots of Figures 1.1 and 1.2 may afford improved accuracy. Accordingly, the derivation of G and V are based on the following;

R = resistance                      X = reactance

r = R ÷ 200                          x = X ÷ 200

a = (r<sup>2</sup> + x<sup>2</sup> + 1) ÷ (2r)

$\delta = \frac{-2x \pm (x^2 + r^2 - 1)}{2}$

n = an integer dependent on the quadrant

then G =  $\frac{1}{2}(180^\circ n + \arctan \frac{-2x \pm (x^2 + r^2 - 1)}{2})$

and V = a + (a<sup>2</sup> - 1)<sup>1/2</sup>

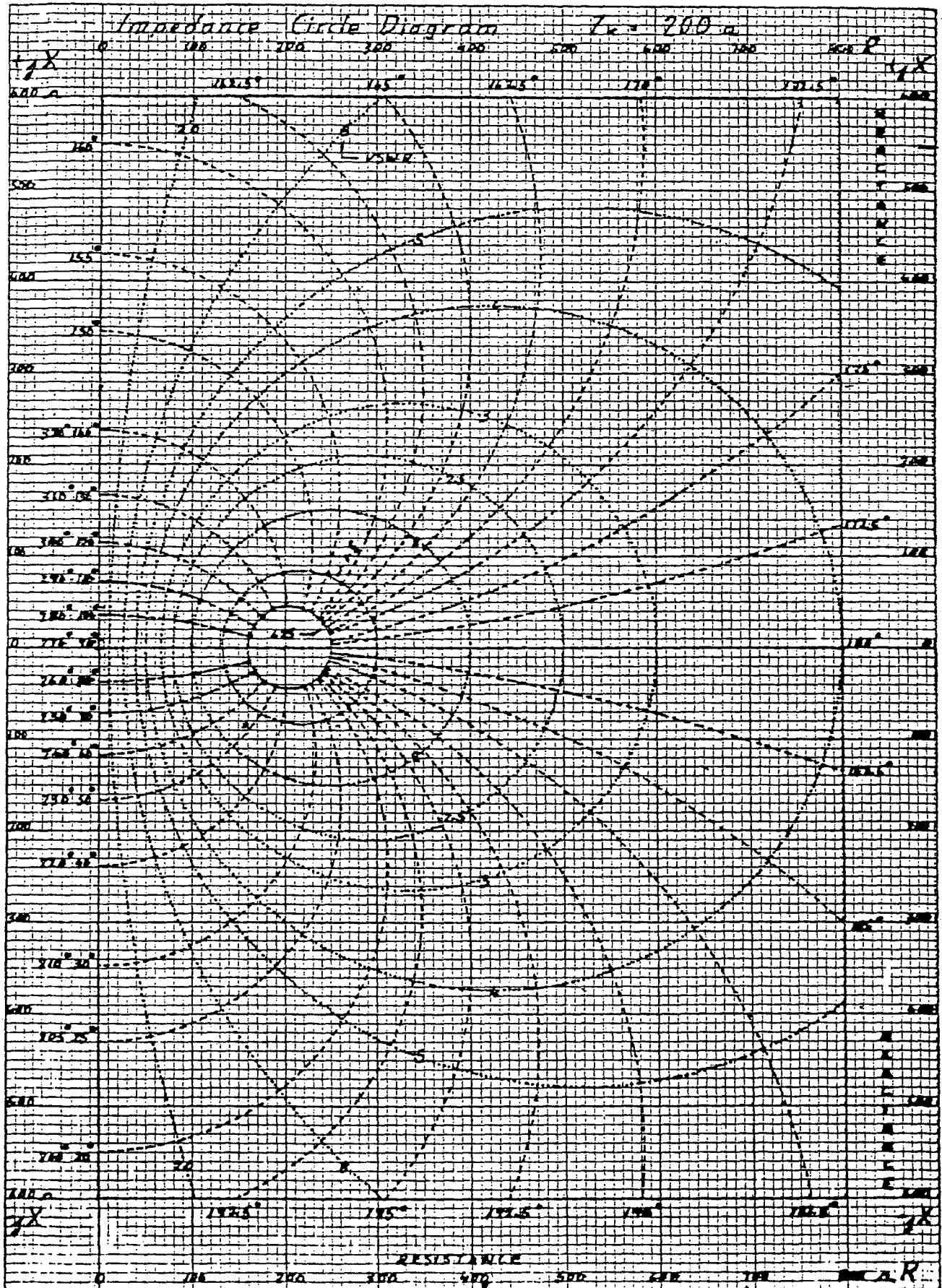
The results of these derivations are shown in the following graphs. Figure 2.2 shows a plot of G/H versus the physical height H. Figure 2.3 shows a plot of M versus the electrical height G where M = (V + 1) ÷ (V - 1) or conversely V = (M + 1) ÷ (M - 1).

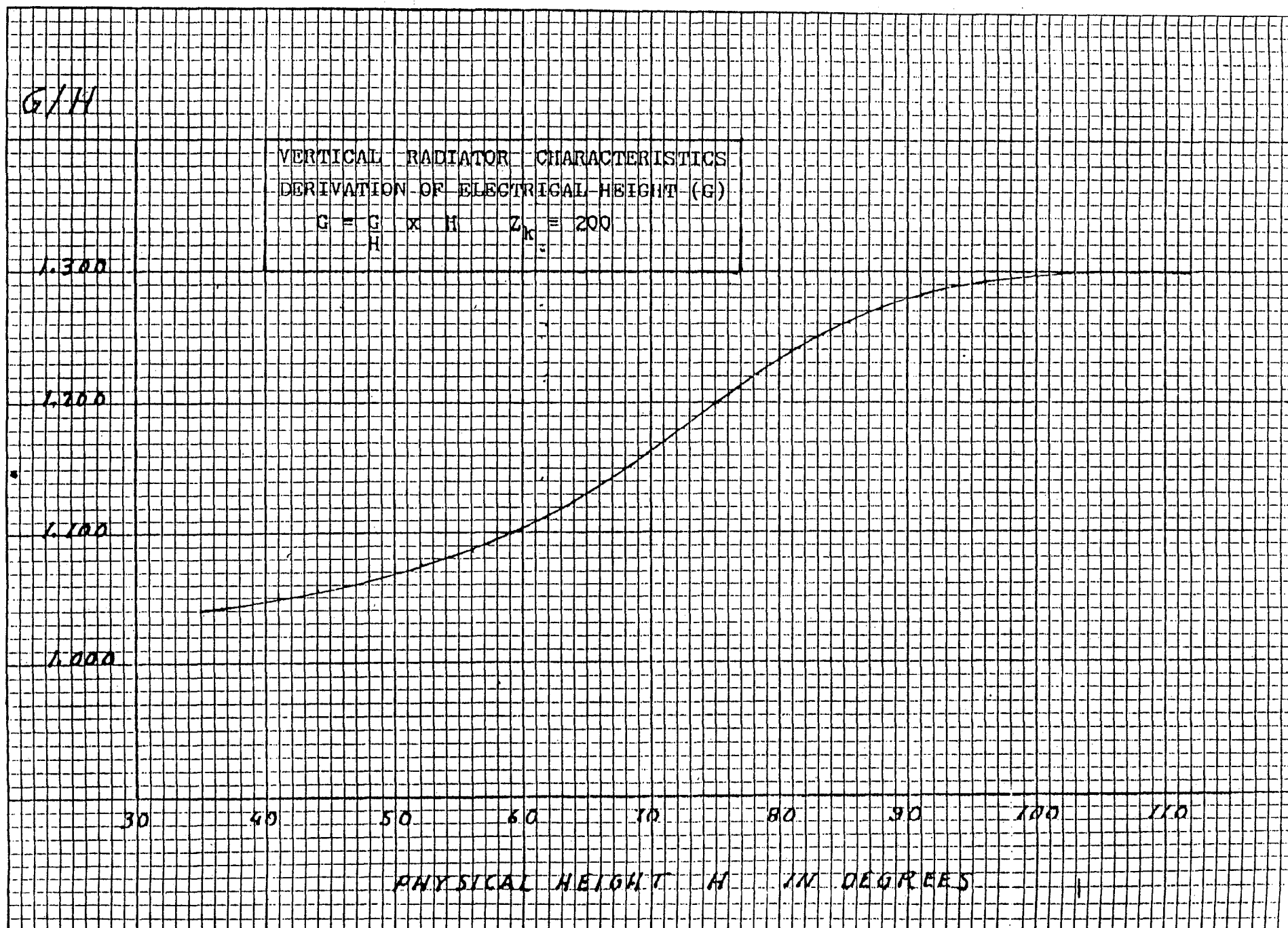
It follows from the foregoing that for a given physical height H the value of G/H and M or V may be found from the graphs of Figures 2.2 and 2.3 respectively. When G and V are known the impedance may be determined from;

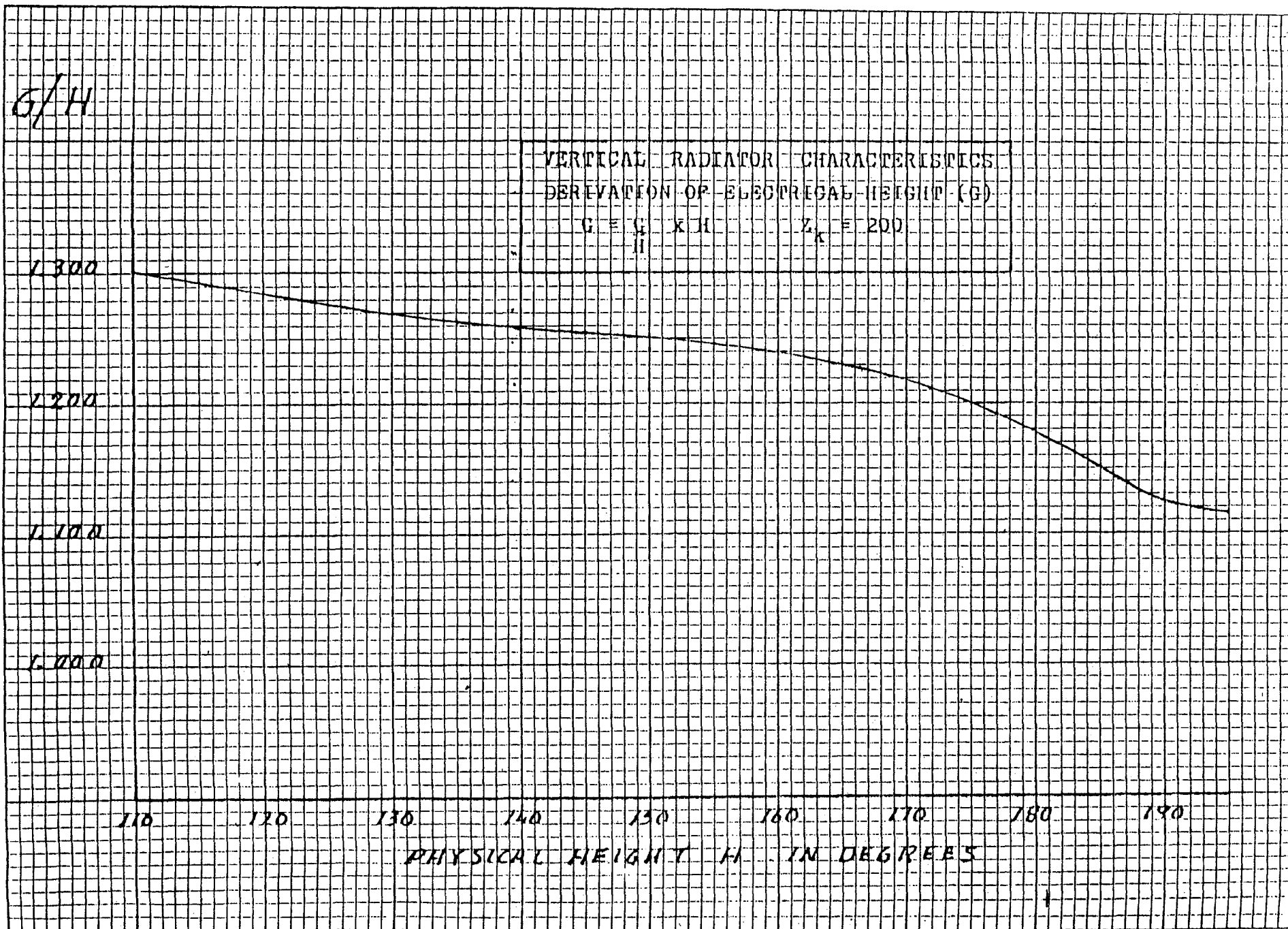
$$R + jX = Z_k (1 - jV \cot G) + (V - j \cot G)$$











$G/H$

VERTICAL RADIATOR CHARACTERISTICS  
DERIVATION OF ELECTRICAL HEIGHT (G)

$$G = \frac{G}{H} \times H \quad Z_K = 200$$

1.300

1.200

1.100

1.000

190

200

210

220

230

240

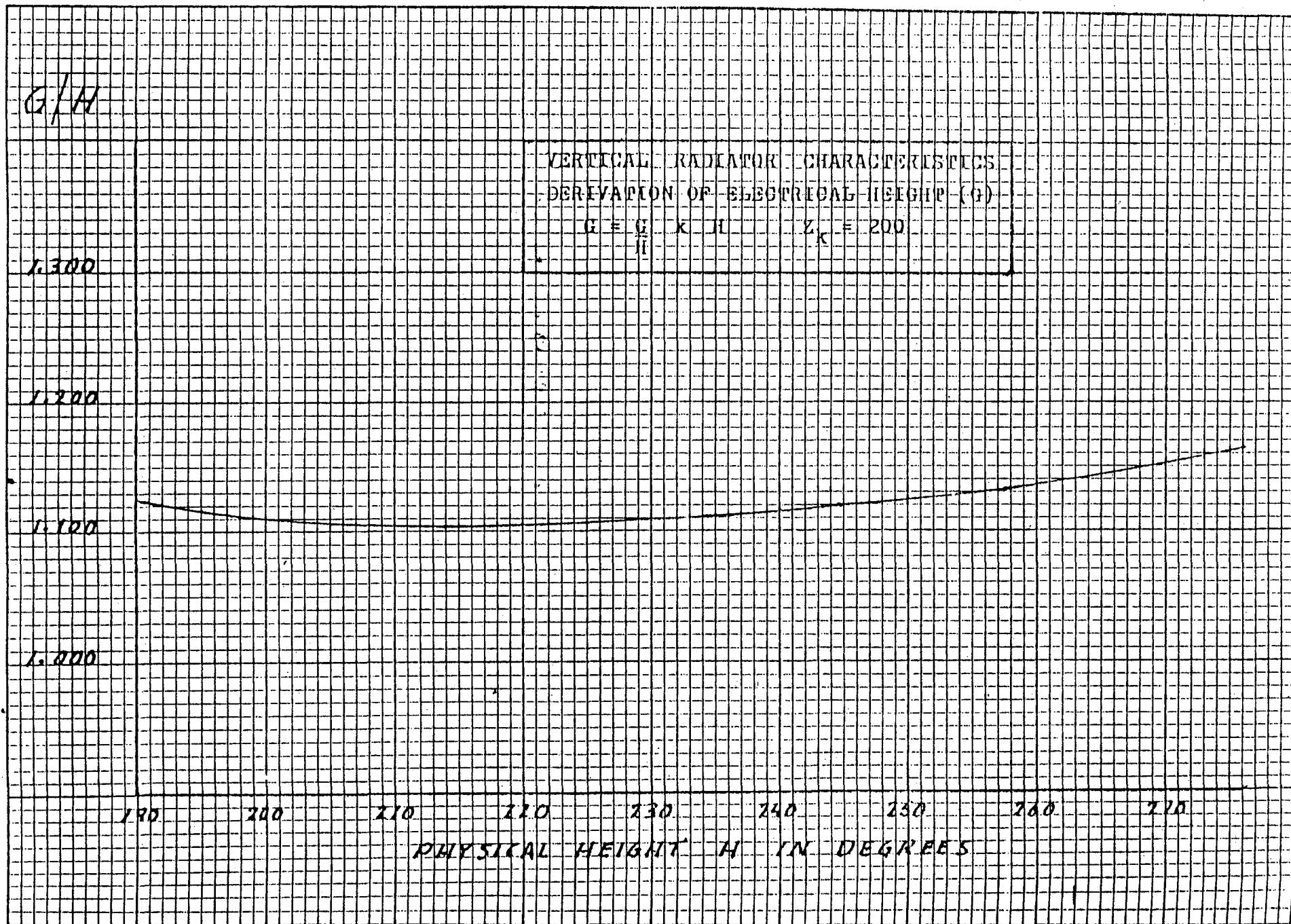
250

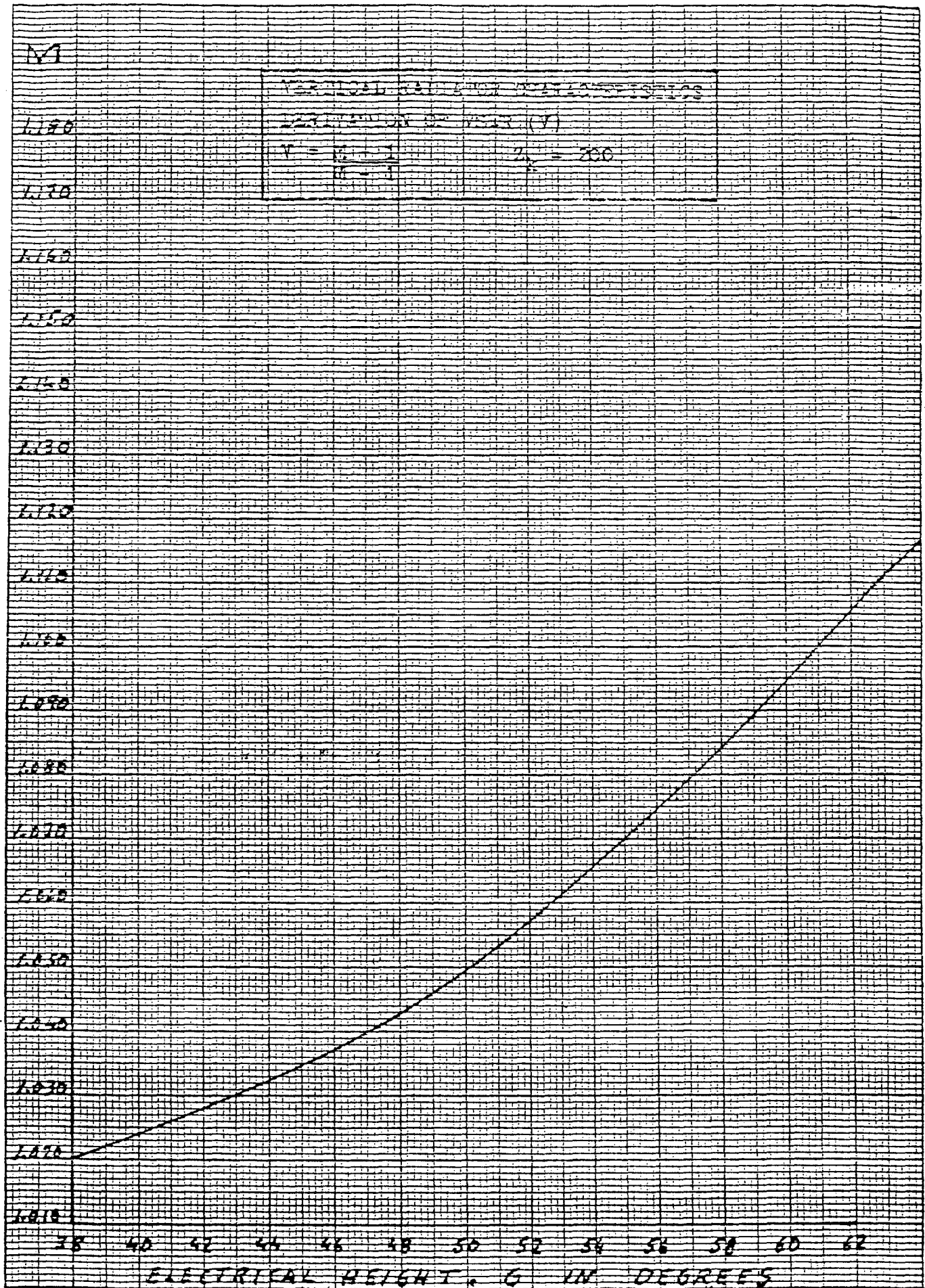
260

270

PHYSICAL HEIGHT H IN DEGREES

2.2.3







M

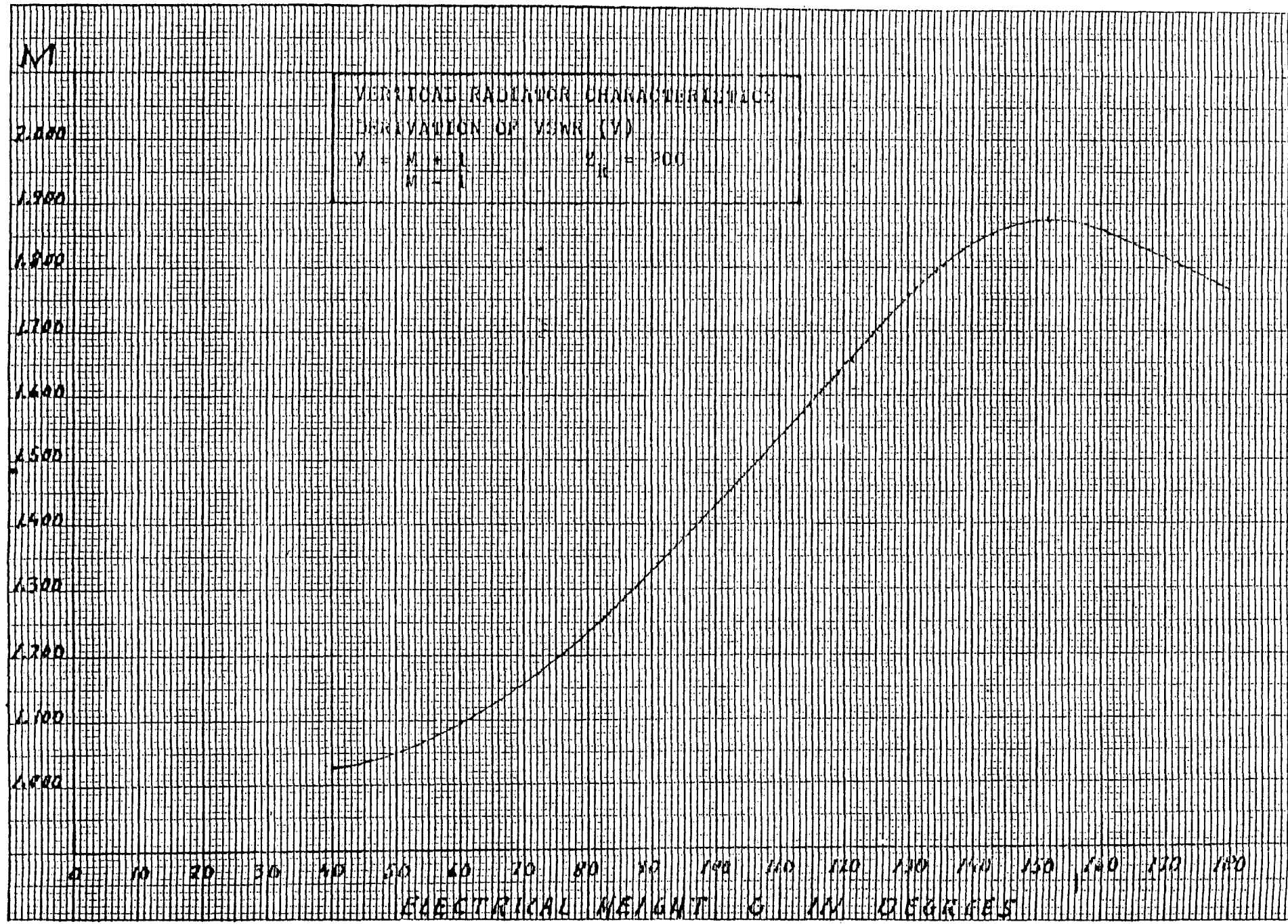
VERTICAL RADIATOR CHARACTERISTICS  
 DERIVATION OF VSWR (V)

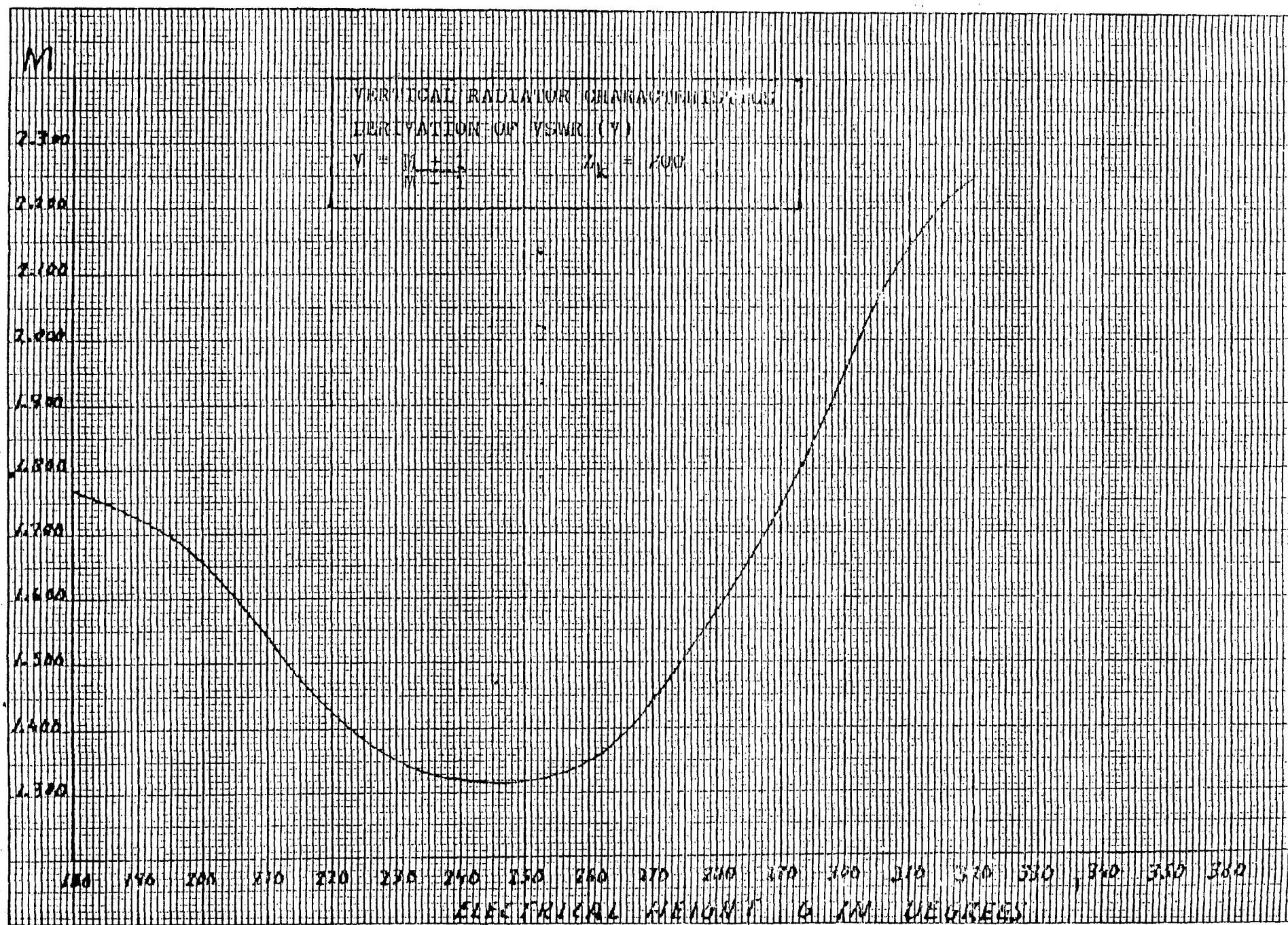
$$V = \frac{M + 1}{M - 1} \quad Z_R = 200$$

2.000  
 1.900  
 1.800  
 1.700  
 1.600  
 1.500  
 1.400  
 1.300  
 1.200  
 1.100  
 1.000

0 10 20 30 40 50 60 70 80 90 100 110 120 130 140 150 160 170 180  
 ELECTRICAL HEIGHT  $\theta$  IN DEGREES

2.3.2





## VERTICAL RADIATOR CHARACTERISTICS

### 3. Antenna Current Relative Magnitude and Phase

The plot of antenna impedance on an impedance circle diagram resembles a plot of impedance for an open circuit transmission line. Assuming the appropriate formulae for an open circuit transmission line are applicable, it is of interest to derive the relative magnitude and phase for the antenna current.

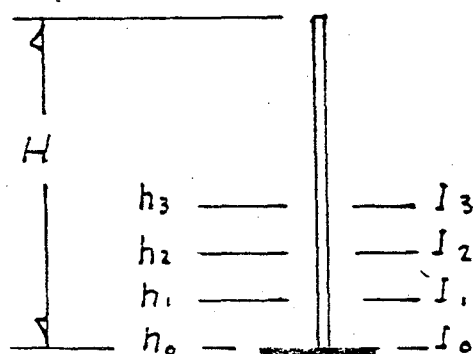
Where  $G = H G/H$        $g = h G/H$   
 let  $a = (10 \log M) + (8.686) \times (G - g) + G$   
 $b = (G - g)$   
 $E_r =$  receiving end voltage

Then  $E = E_r \cosh (a + jb)$

or  $E = E_r ((\cos b \frac{1}{2}(e^a + e^{-a})) + j(\sin b \frac{1}{2}(e^a - e^{-a})))$

and  $I = E_r/Z_0 \sinh (a + jb)$

or  $I = \frac{E_r}{Z_0} ((\cos b \frac{1}{2}(e^a - e^{-a})) + j(\sin b \frac{1}{2}(e^a + e^{-a})))$



The results derived by the foregoing approach are tabulated, for a number of physical heights, in the following tables.





VERTICAL RADIATOR CHARACTERISTICS ANTENNA CURRENT RELATIVE MAGNITUDE & PHASE

$h^\circ$	H = 150° Rel I	H = 165° Rel I	H = 180° Rel I	H = 195° Rel I	H = 210° Rel I	H = 225° Rel I	H = 240° Rel I
0	0.2991	0.4164	0.5632	0.6880	0.8158	0.9417	1.0000
H/15	0.2822	0.2602	0.3582	0.4820	0.6288	0.8002	0.9412
2 H/15	0.3990	0.2541	0.1903	0.2596	0.4005	0.5496	0.7943
3 H/15	0.5584	0.4038	0.2483	0.1436	0.1657	0.3446	0.5745
4 H/15	0.7124	0.5837	0.4444	0.3216	0.1854	0.1100	0.3085
5 H/15	0.8418	0.7475	0.6404	0.5417	0.4223	0.2601	0.1169
6 H/15	0.9364	0.8772	0.8051	0.7350	0.6462	0.5164	0.3394
7 H/15	0.9899	0.9630	0.9243	0.8827	0.8260	0.7374	0.6005
8 H/15	0.9987	0.9991	0.9891	0.9731	0.9466	0.8990	0.8103
9 H/15	0.9619	0.9827	0.9953	0.9997	0.9983	0.9865	0.9439
10 H/15	0.8810	0.9146	0.9418	0.9605	0.9773	0.9923	0.9871
11 H/15	0.7593	0.7978	0.8319	0.8579	0.8846	0.9157	0.9357
12 H/15	0.6025	0.6388	0.6722	0.6986	0.7273	0.7631	0.7942
13 H/15	0.4179	0.4458	0.4719	0.4931	0.5166	0.5469	0.5761
14 H/15	0.2139	0.2290	0.2432	0.2550	0.2682	0.2854	0.3027
$h^\circ$	H = 150° Rel $\phi$	H = 165° Rel $\phi$	H = 180° Rel $\phi$	H = 195° Rel $\phi$	H = 210° Rel $\phi$	H = 225° Rel $\phi$	H = 240° Rel $\phi$
0	116.5	148.7	164.8	171.8	175.9	178.7	181.7
H/15	71.5	118.5	152.0	165.3	172.7	176.1	178.7
2 H/15	39.8	63.7	111.9	140.5	165.1	172.4	175.5
3 H/15	24.8	32.3	44.4	74.9	138.0	164.2	170.7
4 H/15	16.8	19.5	21.3	24.4	36.5	115.1	159.0
5 H/15	11.9	13.0	12.9	12.8	14.0	21.8	81.1
6 H/15	8.6	9.0	8.5	8.0	7.9	9.7	18.8
7 H/15	6.2	6.4	5.8	5.3	5.0	5.6	9.1
8 H/15	4.4	4.5	4.0	3.6	3.3	3.6	5.3
9 H/15	3.0	3.1	2.7	2.4	2.2	2.3	3.3
10 H/15	2.0	2.0	1.8	1.5	1.4	1.4	2.0
11 H/15	1.2	1.2	1.1	0.9	0.8	0.8	1.2
12 H/15	0.6	0.6	0.6	0.5	0.4	0.4	0.6
13 H/15	0.2	0.2	0.2	0.2	0.2	0.2	0.2
14 H/15	0.0	0.0	0.0	0.0	0.0	0.0	0.0

## VERTICAL RADIATOR CHARACTERISTICS

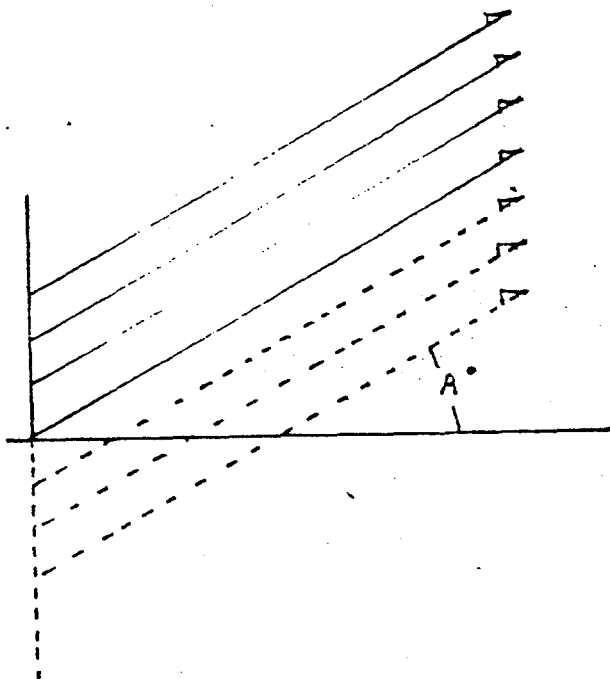
### 4. Vertical Plane Relative Field Strength Pattern

The vertical plane relative field strength pattern is derived assuming the radiator is comprised of a series of equal finite elements and then summing the contribution of each finite element. The finite elements are assigned current magnitude and phase according to the results from the previous section of this report.

Where "A" is the angle in degrees, from the horizontal, the relative field at angle "A" may be represented by:

$$\begin{aligned} \text{Relative Field} = \cos A \left( \frac{1}{2} I_0 \cos \phi_0 + I_1 \cos (\phi_1 + h_1 \sin A) \right. \\ \left. + I_2 \cos (\phi_2 + h_2 \sin A) \right. \\ \left. + I_3 \cos (\phi_3 + h_3 \sin A) \right. \\ \left. + \text{-----} \right) \end{aligned}$$

$$\begin{aligned} h_3 &= I_3 L \phi_3 & - \\ h_2 &= I_2 L \phi_2 & - \\ h_1 &= I_1 L \phi_1 & - \\ h_0 &= I_0 L \phi_0 & - \\ -h_1 &= I_1 L \phi_1 & - \\ -h_2 &= I_2 L \phi_2 & - \\ -h_3 &= I_3 L \phi_3 & - \end{aligned}$$



The vertical plane relative field patterns, for a range of tower heights, are listed in the following tables.

VERTICAL RADIATOR CHARACTERISTICS VERTICAL PLANE RELATIVE FIELD STRENGTH PATTERN

Vertical Angle A Degrees	H = 45° G=47.52° Rel Fld	H = 60° G=66.24 Rel Fld	H = 75° G=90.00 Rel Fld	H = 90° G=115.11 Rel Fld	H = 105° G=136.50 Rel Fld	H = 120° G=154.32 Rel Fld	H = 135° G=170.51 Rel Fld
00	1.0000	1.0000	1.0000	1.0000	1.0000	1.0000	1.0000
05	0.9958	0.9952	0.9941	0.9919	0.9887	0.9853	0.9817
10	0.9832	0.9815	0.9782	0.9725	0.9645	0.9553	0.9451
15	0.9624	0.9590	0.9529	0.9427	0.9283	0.9114	0.8921
20	0.9337	0.9282	0.9187	0.9032	0.8815	0.8557	0.8255
25	0.8976	0.8897	0.8764	0.8553	0.8260	0.7907	0.7490
30	0.8544	0.8440	0.8270	0.8004	0.7636	0.7191	0.6661
35	0.8048	0.7920	0.7716	0.7399	0.6964	0.6437	0.5807
40	0.7492	0.7344	0.7110	0.6752	0.6263	0.5670	0.4962
45	0.6883	0.6720	0.6465	0.6077	0.5551	0.4915	0.4156
50	0.6228	0.6056	0.5789	0.5386	0.4843	0.4188	0.3409
55	0.5532	0.5358	0.5090	0.4689	0.4150	0.3503	0.2737
60	0.4802	0.4634	0.4376	0.3993	0.3482	0.2869	0.2146
65	0.4044	0.3889	0.3653	0.3305	0.2841	0.2288	0.1638
70	0.3262	0.3127	0.2924	0.2626	0.2230	0.1759	0.1207
75	0.2462	0.2355	0.2194	0.1957	0.1645	0.1275	0.0842
80	0.1648	0.1574	0.1462	0.1299	0.1083	0.0828	0.0531
85	0.0826	0.0788	0.0731	0.0647	0.0537	0.0407	0.0256

VERTICAL RADIATOR CHARACTERISTICS    VERTICAL PLANE RELATIVE FIELD STRENGTH PATTERN

Vertical Angle A Degrees	H = 150° G=186.15 Rel Fld	H = 165° G=199.32 Rel Fld	H = 180° G=211.68 Rel Fld	H = 195° G=221.91 Rel Fld	H = 210° G=233.52 Rel Fld	H = 225° G=248.85 Rel Fld	H = 240° G=268.08 Rel Fld
00	1.0000	1.0000	1.0000	1.0000	1.0000	1.0000	1.0000
05	0.9774	0.9727	0.9685	0.9637	0.9564	0.9415	0.9032
10	0.9323	0.9174	0.9021	0.8843	0.8578	0.8080	0.6921
15	0.8673	0.8382	0.8063	0.7687	0.7139	0.6145	0.3929
20	0.7867	0.7406	0.6886	0.6273	0.5392	0.3823	0.0420
25	0.6952	0.6313	0.5580	0.4722	0.3502	0.1358	-0.3202
30	0.5980	0.5171	0.4240	0.3155	0.1631	-0.1015	-0.6557
35	0.5002	0.4049	0.2951	0.1684	-0.0077	-0.3101	-0.9346
40	0.4062	0.3002	0.1785	0.0396	-0.1515	-0.4759	-1.1376
45	0.3196	0.2074	0.0794	-0.0650	-0.2615	-0.5916	-1.2567
50	0.2430	0.1295	0.0009	-0.1423	-0.3349	-0.6555	-1.2938
55	0.1779	0.0679	-0.0558	-0.1918	-0.3726	-0.6707	-1.2578
60	0.1249	0.0277	-0.0912	-0.2149	-0.3776	-0.6435	-1.1617
65	0.0837	-0.0070	-0.1072	-0.2147	-0.3547	-0.5815	-1.0195
70	0.0530	-0.0230	-0.1063	-0.1948	-0.3090	-0.4927	-0.8446
75	0.0314	-0.0275	-0.0918	-0.1594	-0.2459	-0.3844	-0.6479
80	0.0169	-0.0233	-0.0669	-0.1124	-0.1705	-0.2629	-0.4378
85	0.0072	-0.0131	-0.0352	-0.0581	-0.0871	-0.1333	-0.2205

## VERTICAL RADIATOR CHARACTERISTICS

### 5. Theoretical Horizontal Field Intensity at One Mile

The theoretical horizontal field intensity at one mile is determined by a simulated integration of the vertical plane relative field intensity pattern. The routine is shown by the following example where the physical height is 75 degrees ( $G = 90^\circ$ ), with an input power of 1000 watts.

Vertical Angle A	Relative Field K	$K^2 \cos A$
0°	1.0000	1.0000
5	0.9941	0.9844
10	0.9782	0.9424
15	0.9529	0.8771
20	0.9187	0.7931
25	0.8764	0.6962
30	0.8270	0.5924
35	0.7716	0.4877
40	0.7110	0.3873
45	0.6465	0.2955
50	0.5789	0.2154
55	0.5090	0.1486
60	0.4376	0.0958
65	0.3653	0.0564
70	0.2924	0.0292
75	0.2194	0.0125
80	0.1462	0.0037
85	0.0731	0.0005
Sum of $K^2 \cos A$		7.6182
$\frac{1}{2} K^2 \cos 0$		0.5000
Difference		7.1182
Square Root		2.6680
Multiply by $(\pi/36)^{\frac{1}{2}}$		0.7881
Reciprocal		1.2688
Multiply by 152.1 for field at 1 mile		192.9836 Mv/m

The theoretical one mile horizontal field has been calculated for a range of tower heights. The results of these calculations are illustrated in Figure 5.1.

An alternative method of illustrating radiator efficiency is to show the loop antenna current required for

... 2

100 Mv/m at 1 mile. In this regard an element of physical height of 75 degrees ( $G = 90^\circ$ ) is utilized as a reference. In this case the input resistance is 28.373 ohms and the current for 1000 watts is 5.9367 amps. Therefore, for any element;

Amps per 100 Mv/m =  $100 \times 5.9367 \div \text{RMS Field (1 kw - 1 mile)}$

Figure 5.2 shows the amps for 100 Mv/m at one mile over a range of antenna heights.

My/m

at 1

Mile

210

240

250

240

230

220

210

200

190

180

170

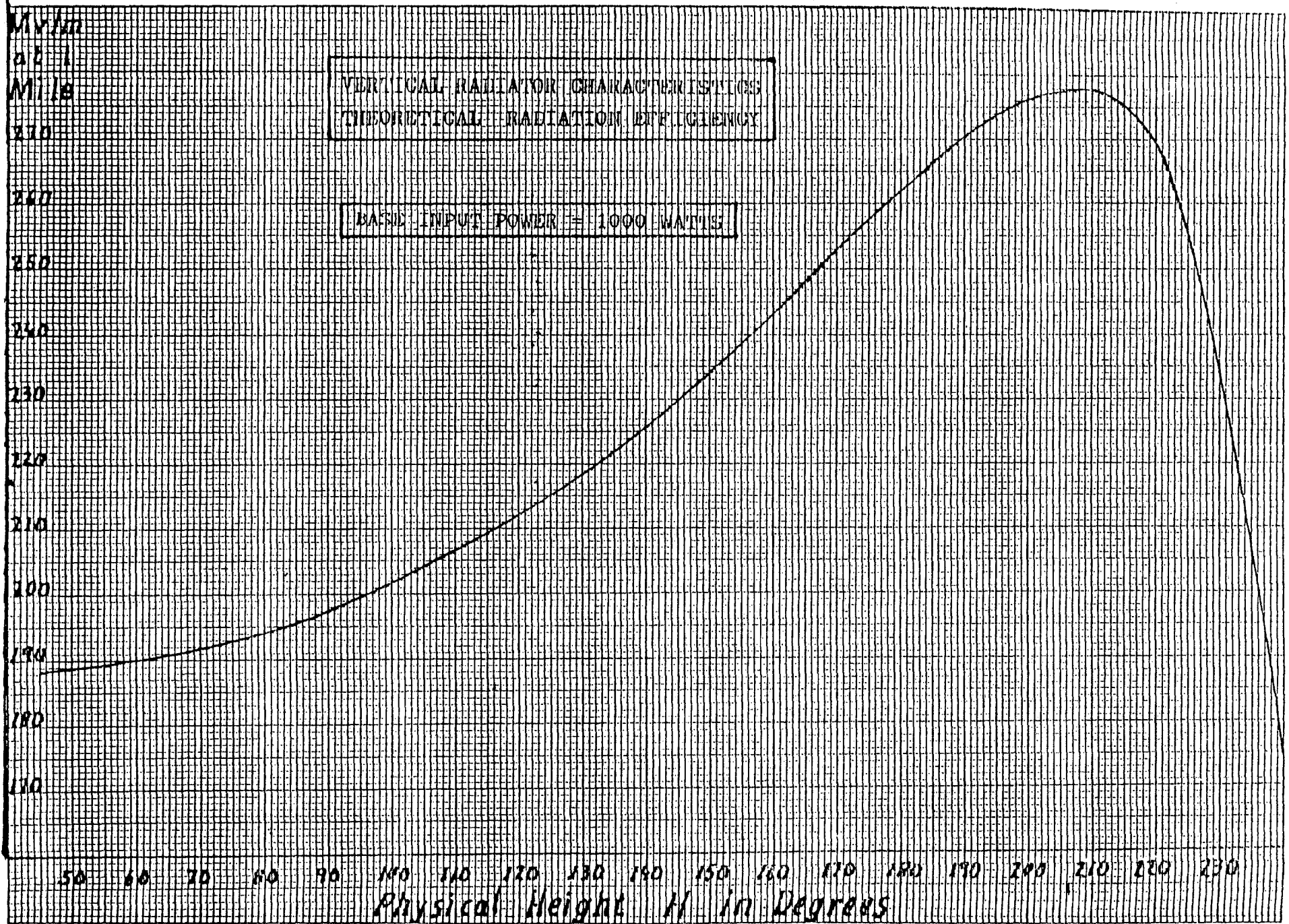
VERTICAL RADIATOR CHARACTERISTICS  
THEORETICAL RADIATION EFFICIENCY

BASIC INPUT POWER = 1000 WATTS

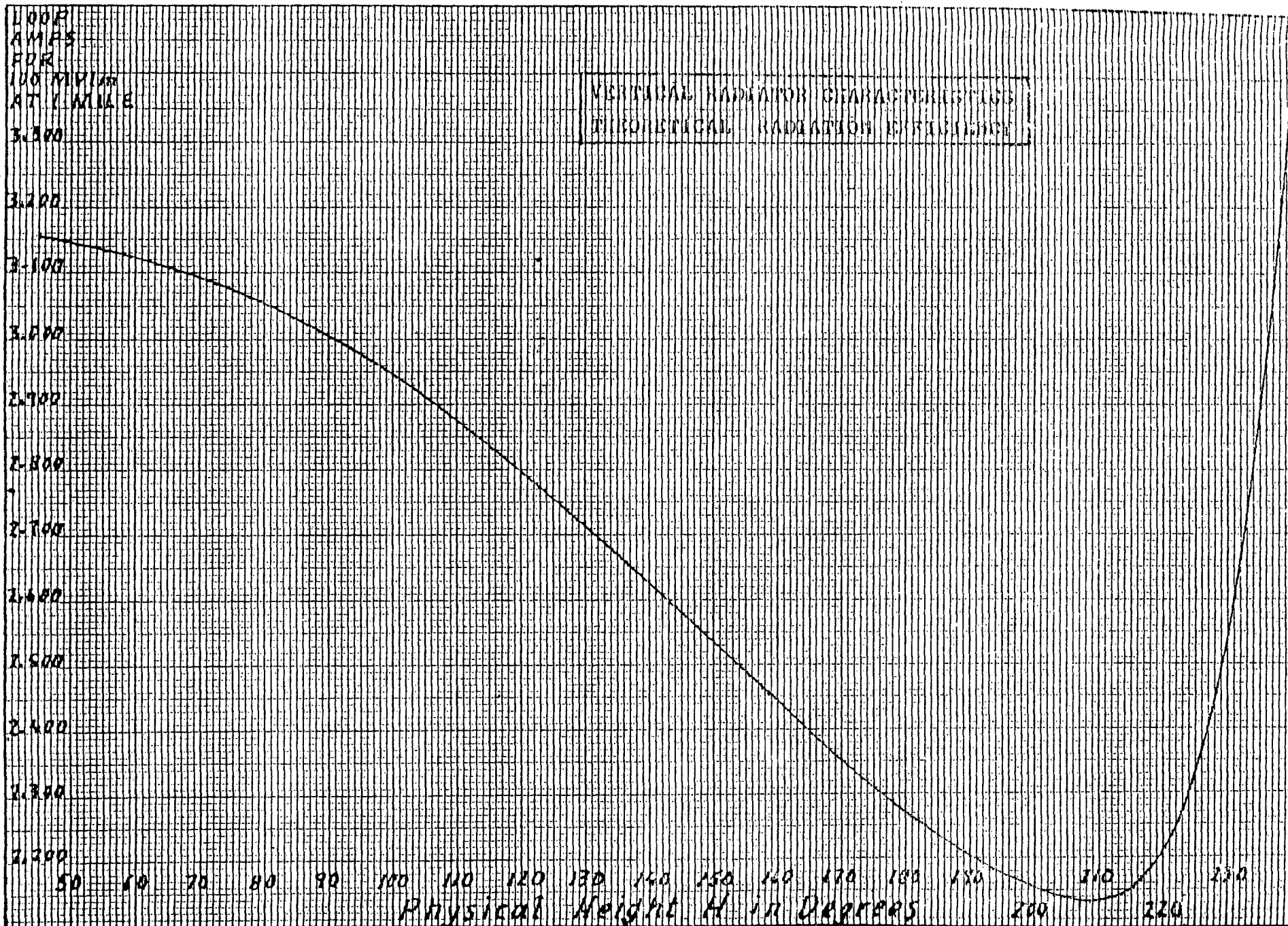
Physical Height  $H$  in Degrees

151

50 60 70 80 90 100 110 120 130 140 150 160 170 180 190 200 210 220 230







## VERTICAL RADIATOR CHARACTERISTICS

### 6. Resistive Component of Mutual Impedance

Mutual Impedance describes the interaction between radiators and is dependent on the spacing between radiators. The resistive component of mutual impedance is calculated by solving for element current, derived from antenna array root-mean-square computations, and then substituting in the array impedance formulas.

A radiator of physical height 75 degrees ( $G = 90^\circ$ ) is utilized as a reference element in these determinations. This reference element has a resistance of 28.373 ohms and for 1000 watts input the current is 5.9367 amps. The field at one mile, per kilowatt is 192.9836 Mv/m or 32.5067 Mv/m per ampere of input current.

If an array is comprised of two reference elements, separated by S degrees, with equal field ratio and fed in phase, the relative root-mean-square is;

$$RMS = (2 + 2 J_0(S \cos A))^{\frac{1}{2}}$$

The impedance relationship for an array comprised of the two reference elements, with equal fields and fed in phase, is as follows;

$$Z_1 = Z_{11} + \frac{I_2}{I_1} Z_m \angle \phi_m \quad \text{and} \quad Z_2 = Z_{22} + \frac{I_1}{I_2} Z_m \angle \phi_m$$

$$\text{Since } Z_{11} = Z_{22} \text{ and } I_1 = I_2$$

$$\text{Then } Z_1 = Z_2 = Z_{11} + Z_m \angle \phi_m$$

$$\text{Or } R_1 = R_{11} + Z_m \cos \phi_m = R_{11} + R_m$$

When the power is 1000 watts,

$$\text{Then } 1000 = I_1^2 R_1 + I_2^2 R_2 = 2 I_1^2 R_1$$

$$\text{or } R_1 = (500/I_1^2) \quad \text{and} \quad R_m = R_1 - 28.373$$

... 2

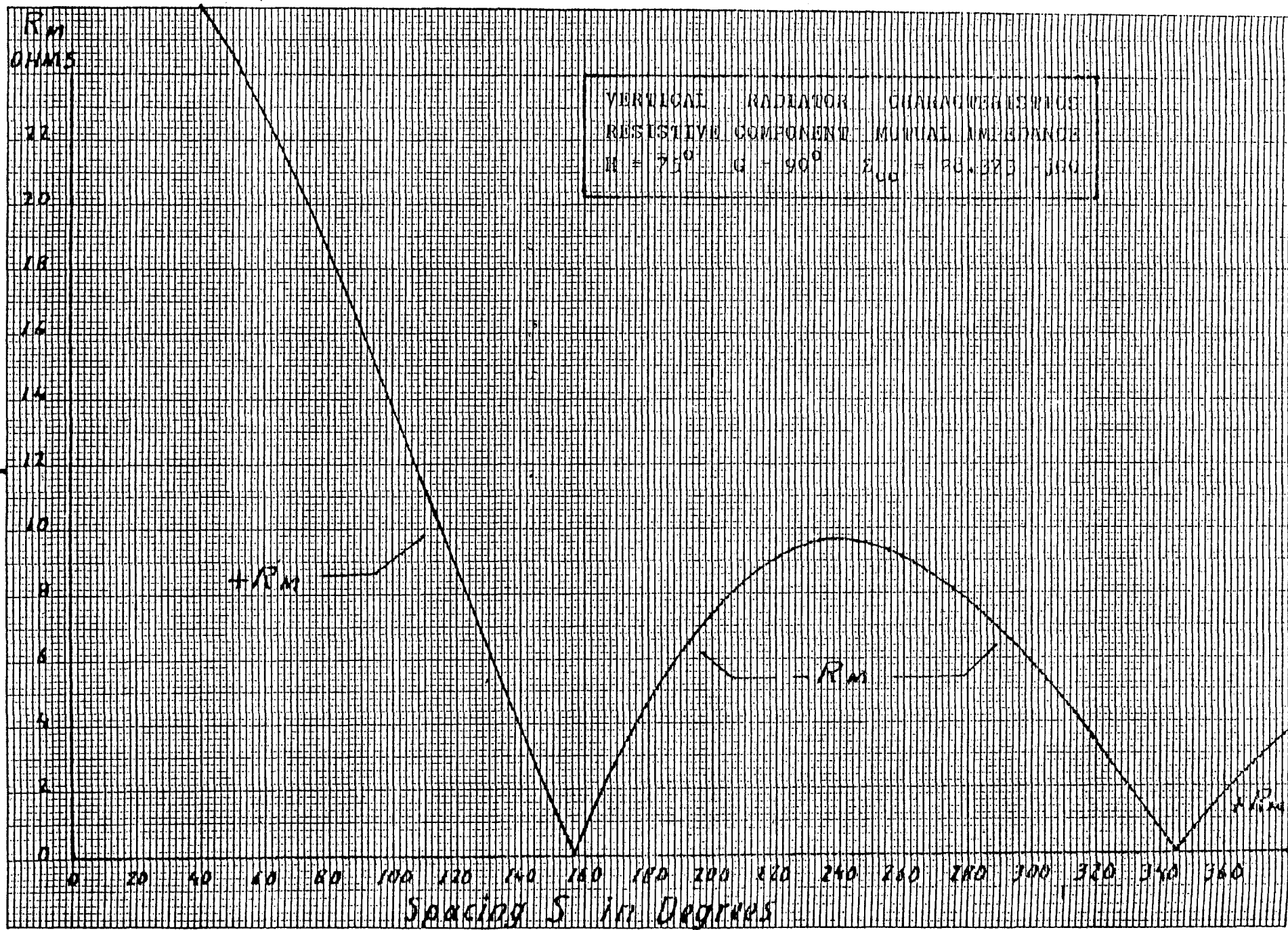
For purposes of illustration, assuming the spacing S is 90 degrees, the results are as follows;

Vertical Angle A	Relative Field K	R M S	$(RMS)^2 K^2 \cos A$
0	1.0000	1.7158	2.9440
5	0.9941	1.7178	2.9050
10	0.9782	1.7237	2.7998
15	0.9529	1.7333	2.6350
20	0.9187	1.7465	2.4192
25	0.8764	1.7630	2.1636
30	0.8279	1.7822	1.8813
35	0.7716	1.8039	1.5870
40	0.7110	1.8273	1.2930
45	0.6465	1.8518	1.0135
50	0.5789	1.8767	0.7587
55	0.5090	1.9011	0.5371
60	0.4376	1.9244	0.3546
65	0.3653	1.9457	0.2135
70	0.2924	1.9642	0.1128
75	0.2194	1.9794	0.0488
80	0.1462	1.9907	0.0147
85	0.0731	1.9977	0.0019
Sum of $(RMS)^2 K^2 \cos A$			23.6835
$\frac{1}{2}$ of $(RMS)^2 K^2 \cos A$ at $A = 00^\circ$			1.4720
Difference			22.2115
Square Root			4.7129
Multiply by $(\pi/36)^{\frac{1}{2}}$			1.3922
Reciprocal			0.7183
Multiply by 152.1 = $F_1 = F_2 =$			109.2488
Divide by 32.5067 = $I_1 = I_2 =$			3.3608

$$R_1 = 500 \div (3.3608)^2 = 44.267$$

$$R_m = 44.267 - 28.373 = 15.894$$

The value of  $I_1$  was determined from pattern integration and substitution of  $I_1$  in the impedance formulae will solve for  $R_m$ , the resistive component of the mutual impedance. Figure 6.1 illustrates a plot of mutual resistance over a range of spacings between elements.



1.9

## VERTICAL RADIATOR CHARACTERISTICS

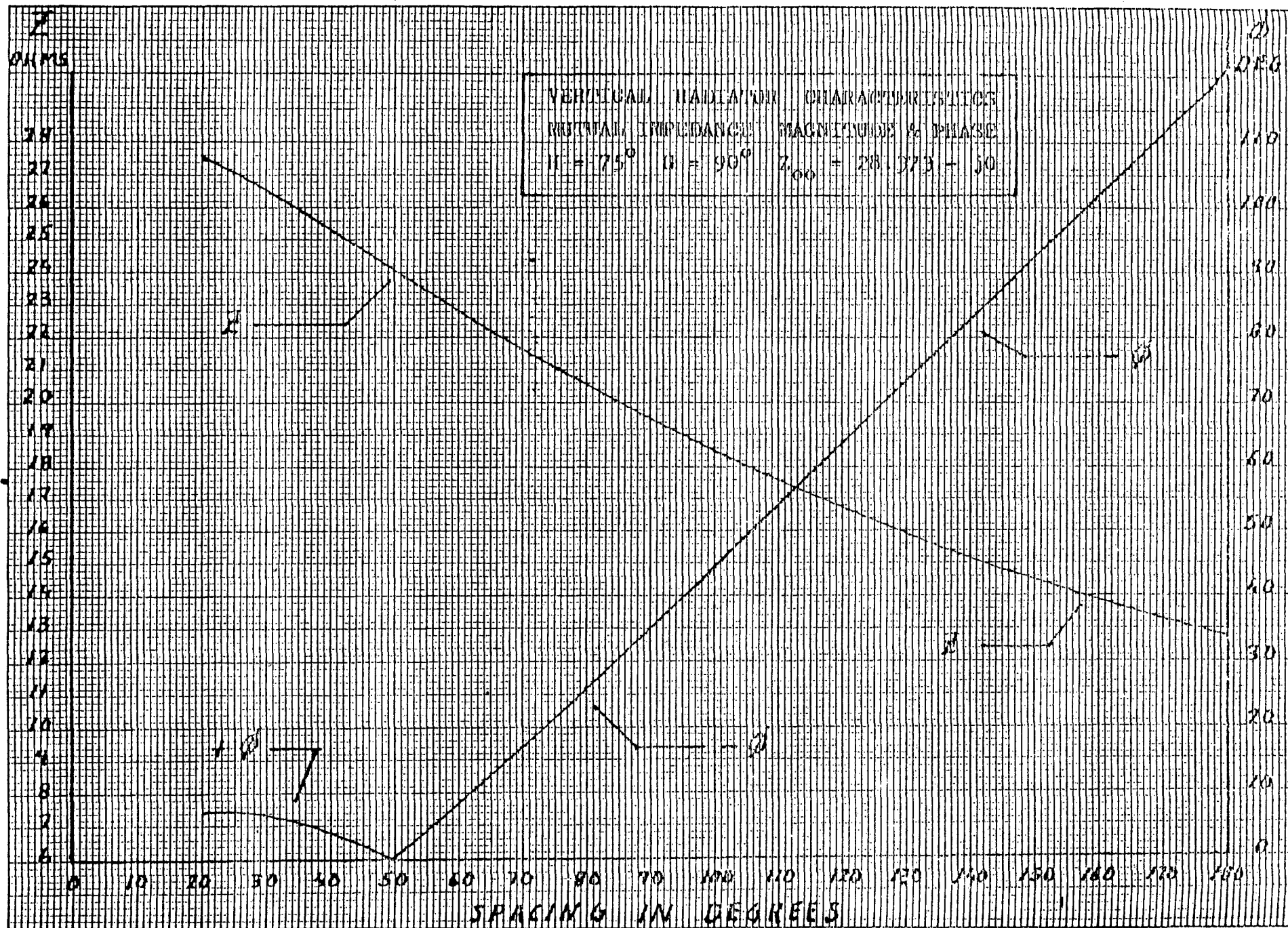
### 7. Derivation of Mutual Impedance

The magnitude and phase of mutual impedance is derived from the values calculated for the resistive component of mutual impedance. A radiator with a physical height of 75 degrees ( $C = 90^\circ$ ) is utilized as a standard reference element and mutual impedance is computed only for the reference element.

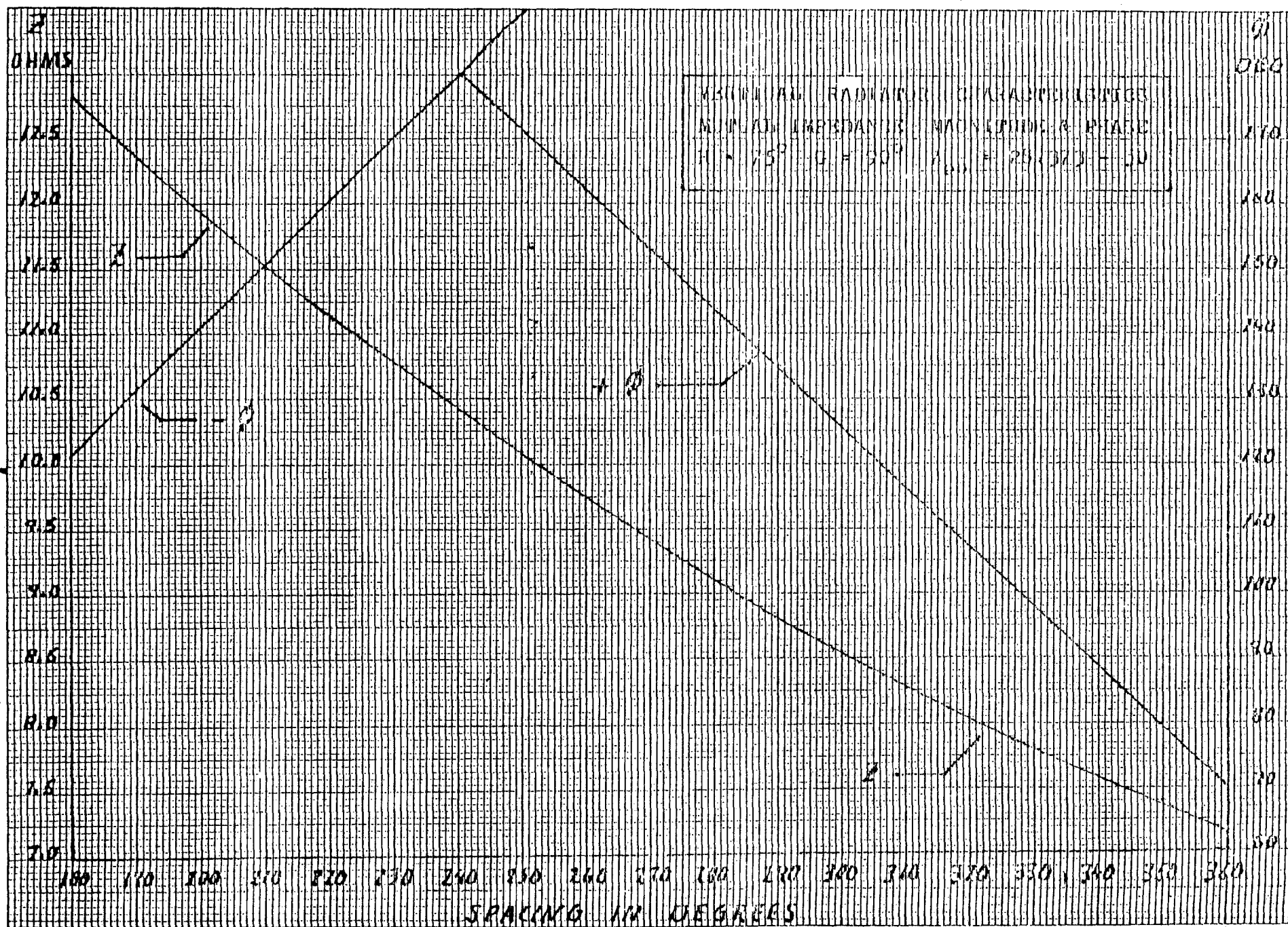
To some extent the derivation of magnitude and phase of mutual impedance is a trial and error procedure. However, it is evident with regard to phase that the angle is an odd multiple of 90 degrees when the value of mutual resistance is zero. Furthermore, for large spacings, the relationship between phase and spacing appears to be linear. In addition, for large spacings, the relationship between the reciprocal of the magnitude and spacing also appears to be linear.

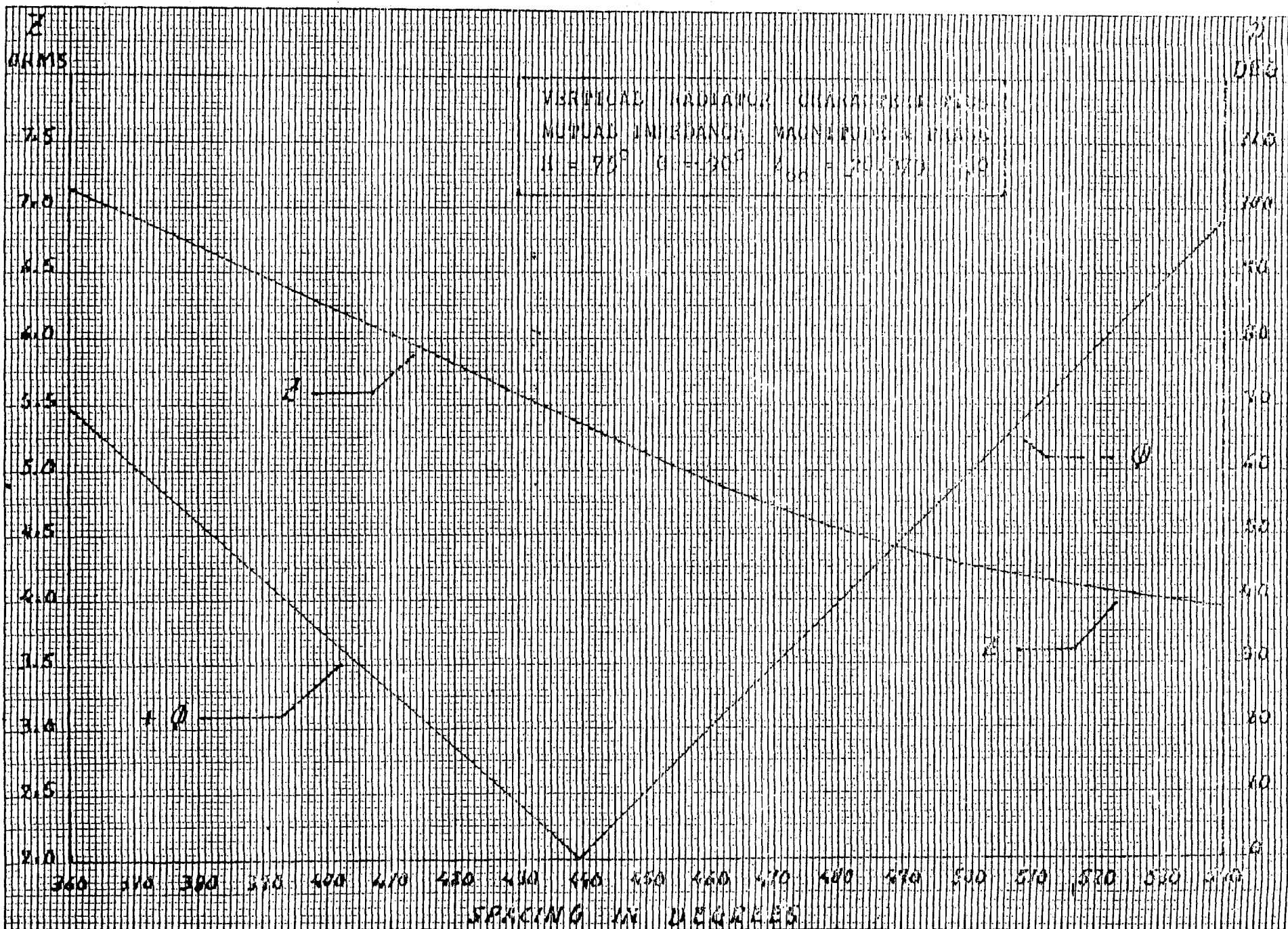
On the basis of the foregoing the magnitude and phase of mutual impedance has been derived for the reference radiator. The results of these derivations are illustrated in the following Figures 7.1 through to 7.7.

- M -



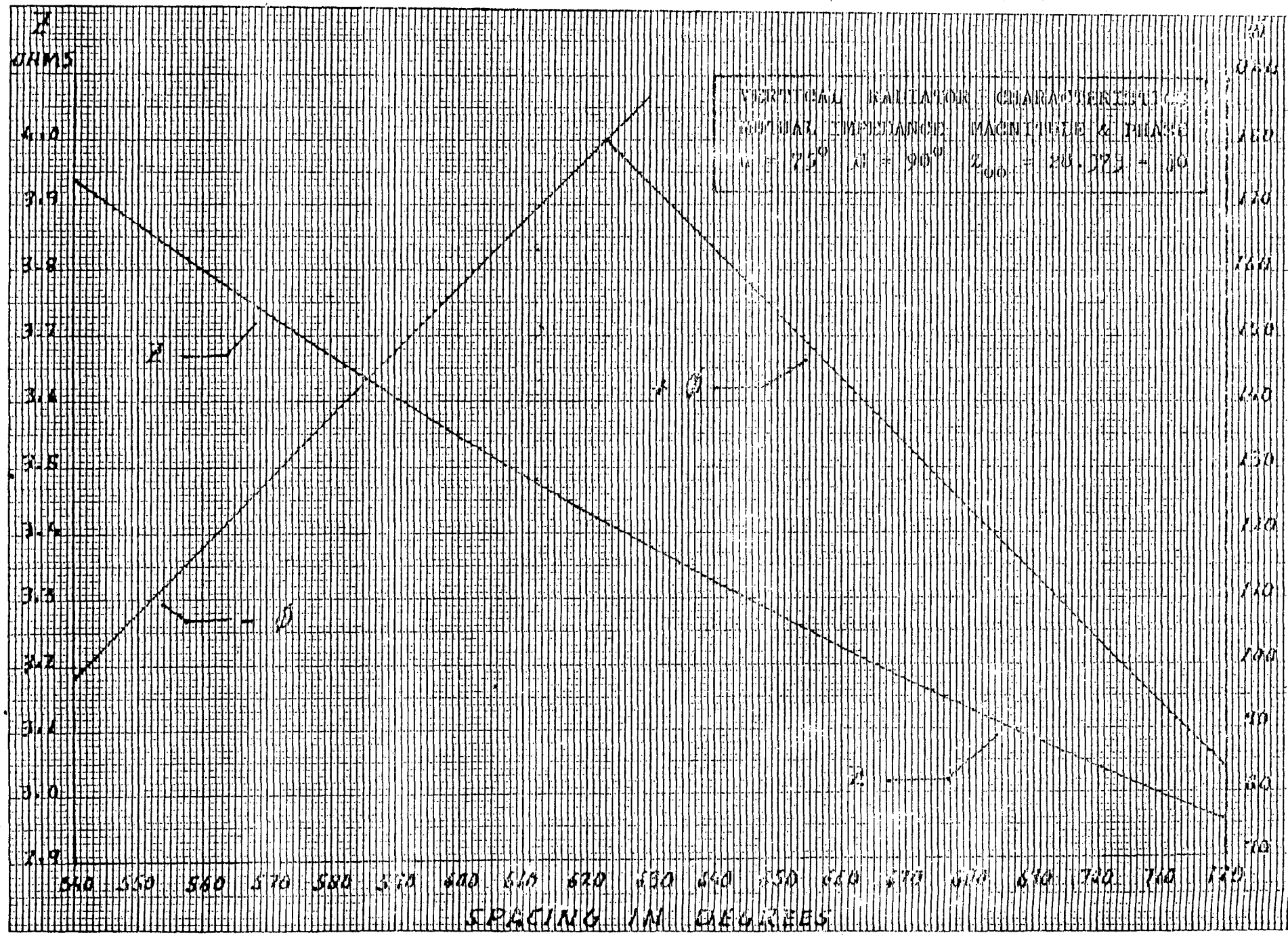






7.3





7.4

VERTICAL RADIATOR CHARACTERISTICS  
MUTUAL IMPEDANCE MAGNITUDE & PHASE  
 $H = 75^\circ$   $G = 90^\circ$   $Z_{00} = 28.373 - j0$

Spacing (S) Between Elements Greater Than 1080 Degrees

$$\text{Magnitude } Z = \frac{75 \times 28.373}{S^\circ}$$

$$\text{Phase } \phi^\circ = 86 - S^\circ$$

## VERTICAL RADIATOR CHARACTERISTICS

### 8. Derivation of Base Operating Impedances, current & power

Base operating impedances are determined in order to facilitate the design of appropriate matching networks. If a single tower system is to be utilized, the input impedance at the tower base, may be determined by reference to Figure 1.1 and Figure 1.2 for the desired element height.

Where two or more towers are involved in an array the situation is more complex because of the mutual coupling between towers. In these instances radiators with a physical height of 75 degrees ( $G = 90^\circ$ ) are utilized as a standard reference to derive an impedance, current and power analysis. The values thus determined are referred to as the "Loop" impedance, current and power.

When element heights other than the "reference" heights are involved an adjustment is required to estimate the base operating impedances. The routine developed is predicated on employment of the Impedance Circle Diagram and the "Spiral" curve depicted in Figure 2.1.1.

The initial analysis is based on the "reference" height, however, the "Loop" impedances are rotated on the Impedance Circle Diagram to allow for a difference in electrical height between the reference element and the desired element. In addition it is assumed that the VSWR (Voltage Standing Wave Ratio) at the desired height is proportional to the ratio of the calculated VSWR, for the Loop operating impedance, and the nominal VSWR (Figure 2.3) for the electrical length calculated from the Loop operating impedance. Finally, it is assumed that the base input power is equivalent to the Loop power.

Figure 8.1.1 summarizes the routine that is employed

... 2

to adjust from "Loop" values of operating impedance, current and power to values for the "Base" operating impedance, current and power, at the desired element height. If data based on measurement is available, a further adjustment of the estimates may be undertaken by utilization of the routine summarized in Figure 8.1.2.

In order to illustrate the foregoing a sample array has been analyzed and the results derived for several element height combinations. The derivations are shown in Figure 8.4 for these height combinations.

# 00 CIRCLE DIAGRAM VERTICAL RADIATOR IMPEDANCE ANALYSIS

- 01 Station
- 02 Array
- 03 Element
- 04 Physical Height H
- 05 G/H from Fig 2.2
- 06 Electrical Height G
- 07  $\Delta G = G - 90$
- 08 Loop Field Ratio
- 09 Loop Amps @ 100 Mv/m Fig 5.2
- 10 Loop Current Ratio
- 11  $R_L$  Loop Operating Resistance
- 12  $X_L$  Loop Operating Reactance
- 13  $I_L$  Loop Operating Amps
- 14  $W_L$  Loop Operating Watts
- 15  $r = R_L / 200$
- 16  $x = X_L / 200$
- 17  $b = -2x \div (xx + rr - 1)$
- 18  $a = (rr + xx + 1) \div (4rr)^{\frac{1}{2}}$
- 19  $V = VSWR = a + (aa - 1)^{\frac{1}{2}}$
- 20 n = an integer
- 21  $G_1 = \frac{1}{2} (180n + \text{arc tan } b)$
- 22  $G_2 = G_1 + \Delta G$
- 23  $M_2$  from Fig 2.3 for  $G_2$
- 24  $M_1$  from Fig 2.3 for  $G_1$
- 25  $V_1 = (M_1 + 1) \div (M_1 - 1)$
- 26  $V_2 = (M_2 + 1) \div (M_2 - 1)$
- 27  $V_3 = (V)(V_2) \div (V_1)$
- 28  $Z/\theta = (1 - jV_3 \cot G_2) \quad Z_b =$
- 29  $(V_3 - j \cot G_2) \quad \theta_b =$
- 30  $R_b = \text{Base Resis} = Z_b \cos \theta_b =$
- 31  $X_b = \text{Base React} = Z_b \sin \theta_b =$
- 32  $W_b = \text{Base Watts} = W_L$
- 33  $I_b = \text{Base Amps} = (W_b \div R_b)^{\frac{1}{2}}$
- 34 Base Current Ratio
- 35  $R_o$  Measured Operating Base R
- 36  $X_o$  Measured Operating Base X

# CIRCLE DIAGRAM VERTICAL RADIATOR IMPEDANCE ANALYSIS

01	Station				
02	Array				
03	Element				
04	Physical Height H				
05	G/H from Fig 2.2				
06	Electrical Height G				
07	$\Delta G = G - 90$				
.....					
08	Loop Field Ratio				
09	Loop Amps for 100 Mv/m Fig 5.2				
10	Loop Current Ratio				
.....					
11	$R_L$ Loop Operating Resistance				
12	$X_L$ Loop Operating Reactance				
13	$I_L$ Loop Operating Amps				
14	$W_L$ Loop Operating Watts				
.....					
15	$r = R_L \div 200$				
16	$x = X_L \div 200$				
17	$b = -2x \div (xx + rr - 1)$				
*18	$a = (rr + xx + 1) \div 2r_1$				
19	$V = VSWR = a + (aa - 1)^{1/2}$				
.....					
20	$n = \text{an integer}$				
21	$G_1 = \frac{1}{2} (180n + \text{arc tan } b)$				
22	$G_2 = G_1 + \Delta G$				
.....					
23	$M_2$ from Fig 2.3 for $G_2$				
24	$M_1$ from Fig 2.3 for $G_1$				
.....					
25	$V_1 = (M_1 + 1) \div (M_1 - 1)$				
26	$V_2 = (M_2 + 1) \div (M_2 - 1)$				
27	$V_3 = (V)(V_2) \div V_1$				
.....					
28	$Z/\phi = (1 - jV_3 \cot G_2) - Z_b =$				
29	$(V_3 - j \cot G_2) \phi_b =$				
30	$R_b = \text{Base Resis} = Z_b \cos \phi_b$				
31	$X_b = \text{Base React} = Z_b \sin \phi_b$				
.....					
32	Predicted Base Self $R = R_p$				
33	Predicted Base Self $X = X_p$				
34	Measured Base Self $R = R_m$				
35	Measured Base Self $X = X_m$				
*36	$R_B = (R_b)(R_m) \div R_p$				
37	$X_B = X_b + X_m - X_p$				
.....					
38	$W_B = \text{Base Watts} = W_L \div R_B$				
39	$I_B = \text{Base Amps} = (W_B \div R_B)^{1/2}$				
40	Base Amps Ratio				
.....					
41	$R_o$ Measured Operating Base R				
42	$X_o$ Measured Operating Base X				
43	$I_o$ Measured Operating Base I				
44	$W_o$ Measured Operating Base W				
45	$W_o$ Measured Base Amps Ratio				
.....					
NB	At line 18 use "r" as positive to determine "a"				
	At line 36 when $R_L$ (line 11) is negative then $R_B = (R_b)(R_p) \div R_m$				

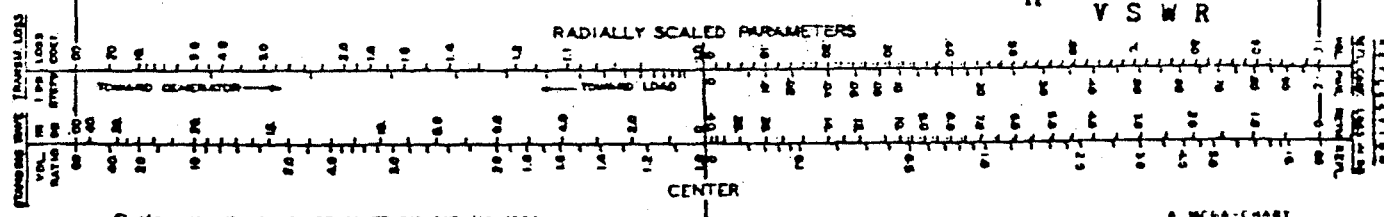
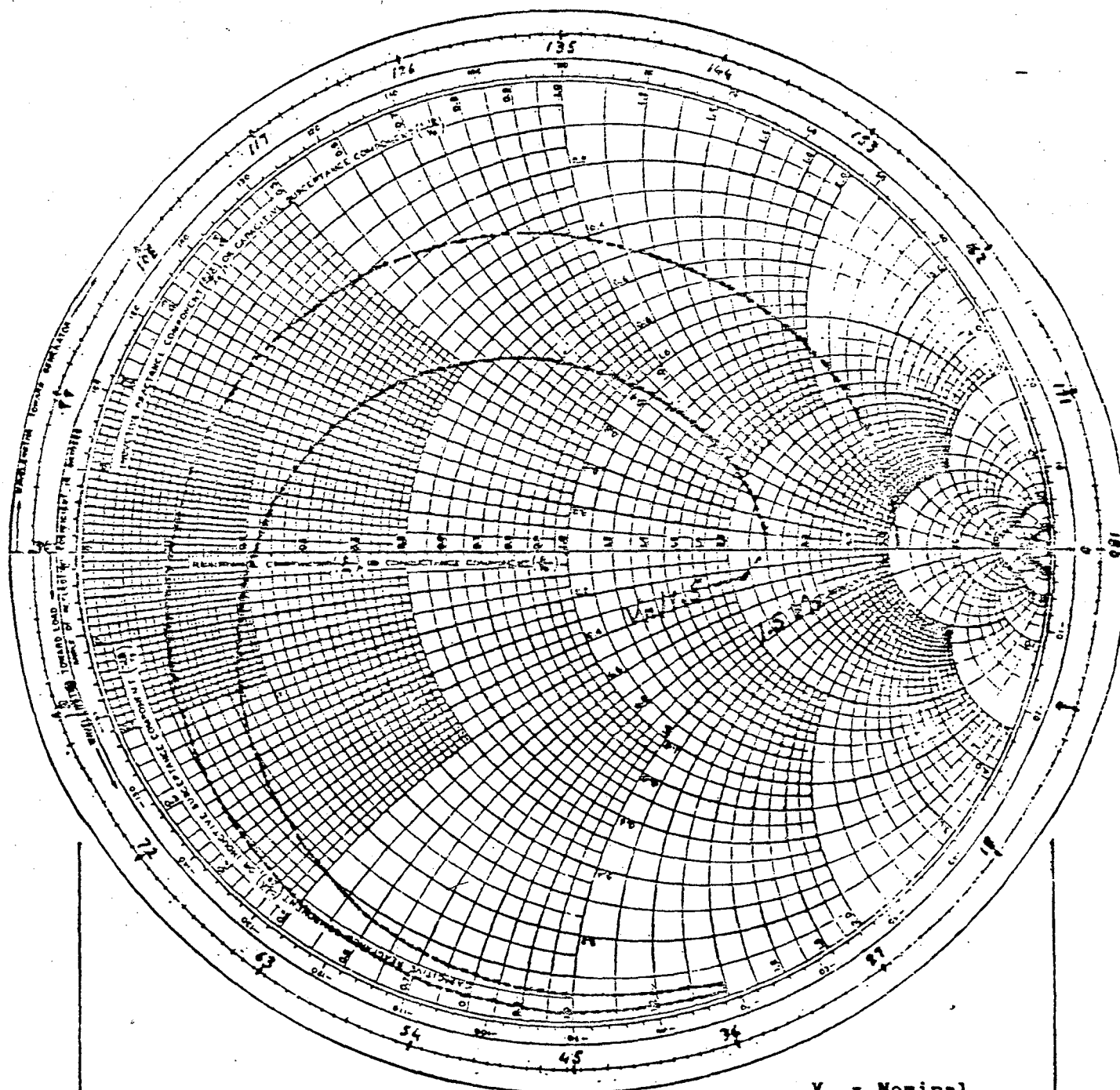
# SAMPLE DERIVATION OF OPERATING IMPEDANCE

Element	1	2
Loop Field Ratio	1.000	0.760
Loop Phase	00°	-90°
Spacing	ref	110°
Loop Resistance	28.37	28.37
Loop Reactance	0	0
Magnitude of Mutual Impedance		17.6
Phase of Mutual Impedance		-54°
$R_L$ Loop Operating Resistance	17.55	47.11
$X_L$ Loop Operating Reactance	-7.86	13.61
$I_L$ Loop Operating Amps	4.727	3.592
$W_L$ Loop Operating Watts	392	608
$r = R_L / 200$	0.08755	0.23555
$x = X_L / 200$	-0.0393	0.06805
$b = -2x \div (xx + rr - 1)$	-0.0793	0.1448
$a = (rr + xx + 1) \div 2r$	5.7507	2.2506
$V = VSWR = a + (aa - 1)^{\frac{1}{2}}$	11.414	4.267
$n = \text{an integer}$	1	1
$G_1 = \frac{1}{2} (180n + \text{arc tan } b)$	87.73	94.12
$M_1$ from Fig 2.3 for $G_1$	1.306	1.369
$V_1 = (M_1 + 1) \div (M_1 - 1)$	7.536	6.420
$V / V_1$	1.515	1 / 1.505

To convert from Loop Values refer to Figure 8.3.1 or Figure 8.3.2 and follow appropriate Spiral Curve to the desired Electrical Height.

NAME $Z_k = 200$	TITLE VERTICAL RADIATOR CHARACTERISTICS	DWG NO.
DATA CHART FORM 3525 (2-49) NAT. ELECTRIC COMPANY, PINE BROOK, N.J. 07640 PRINTED IN U.S.A.		DATE Jan 1983

# IMPEDANCE OR ADMITTANCE COORDINATES



Electronics - VOL 17, NO 1, PP 120-122, 310-325, JAN 1983

A MEGA-CHART





# 00 CIRCLE DIAGRAM VERTICAL RADIATOR IMPEDANCE ANALYSIS

01 Station				
02 Array				
03 Element	1	2	1	2
04 Physical Height H	60	60	90	90
05 G/H from Fig 2.2	1.104	1.104	1.279	1.279
06 Electrical Height G	66.24	66.24	115.11	115.11
07 $\Delta G = G - 90$	-23.76	-23.76	25.11	25.11
08 Loop Field Ratio	1.00	0.76	1.00	0.76
09 Loop Amps @ 100 Mv/m Fig 5.2	3.123	3.123	3.005	3.005
10 Loop Current Ratio	1.00	0.76	1.00	0.76
11 $R_L$ Loop Operating Resistance	17.55	47.11	17.55	47.11
12 $X_L$ Loop Operating Reactance	-7.86	13.61	-7.86	13.61
13 $I_L$ Loop Operating Amps	4.727	3.592	4.727	3.592
14 $W_L$ Loop Operating Watts	392	608	392	608
15 $r = R_L / 200$	.08775	.23555	.08775	.23555
16 $x = X_L / 200$	-.03930	.06805	-.03930	.06805
17 $b = -2x + (xx + rr - 1)$	-.0793	.1448	-.0793	.1448
*18 $a = (rr + xx + 1) + 2r$	5.7507	2.2506	5.7507	2.2506
19 $V = VSWR = a + (aa - 1)^{1/2}$	11.414	4.267	11.414	4.267
20 $n = \text{an integer}$	1	1	1	1
21 $G_1 = \frac{1}{2} (180n + \arctan b)$	87.73	94.12	87.73	94.12
22 $G_2 = G_1 + \Delta G$	63.97	70.36	112.84	119.23
23 $M_2$ from Fig 2.3 for $G_2$	1.117	1.160	1.365	1.635
24 $M_1$ from Fig 2.3 for $G_1$	1.306	1.369	1.306	1.369
25 $V_1 = (M_1 + 1) + (M_1 - 1)$	7.536	6.420	7.536	6.420
26 $V_2 = (M_2 + 1) + (M_2 - 1)$	15.094	13.506	4.540	4.150
27 $V_3 = (V)(V_2) + (V_1)$	27.405	8.973	6.876	2.758
28 $Z/\eta = (1 - jV_3 \cot G_2)$ $Z_b =$	98.70	74.71	88.96	130.69
29 $(V_3 - j \cot G_2)$ $\beta_b =$	-24.73°	-70.38°	67.45°	45.59°
30 $R_b = \text{Base Resis} = Z_b \cos \beta_b =$	9.06	25.09	34.12	91.46
31 $X_b = \text{Base React} = Z_b \sin \beta_b =$	-98.28	-70.38	82.15	93.36
32 $W_b = \text{Base Watts} = W_L$	392	608	392	608
33 $I_b = \text{Base Amps} = (W_b + R_b)^{1/2}$	6.578	4.923	3.390	2.578
34 Base Amps Ratio	1.000	0.748	1.000	0.761

\* At line 18 use "r" as positive to determine "a"

# 00 CIRCLE DIAGRAM VERTICAL RADIATOR IMPEDANCE ANALYSIS

01 Station				
02 Array				
03 Element	1	2	1	2
04 Physical Height H	180	180	225	225
05 G/H from Fig 2.2	1.177	1.177	1.106	1.106
06 Electrical Height G	211.86	211.86	248.85	248.85
07 $\Delta G = G - 90$	121.86	121.86	158.85	158.85
08 Loop Field Ratio	1.00	0.76	1.00	0.76
09 Loop Amps @ 100 Kv/m Fig 5.2	2.270	2.270	2.333	2.333
10 Loop Current Ratio	1.00	0.76	1.00	0.76
11 $R_L$ Loop Operating Resistance	17.55	47.11	17.55	47.11
12 $X_L$ Loop Operating Reactance	-7.86	13.61	-7.86	13.61
13 $I_L$ Loop Operating Amps	4.727	3.592	4.727	3.592
14 $W_L$ Loop Operating Watts	392	608	392	608
15 $r = R_L / 200$	.08775	.23555	.08775	.23555
16 $x = X_L / 200$	-.03930	.06805	-.03930	.06805
17 $b = -2x + (xx + rr - 1)$	-.0793	.1448	-.0793	.1448
*18 $a = (rr + xx + 1) + 2r$	5.7507	2.2506	5.7507	2.2506
19 $V = VSWR = a + (a^2 - 1)^{1/2}$	11.414	4.267	11.414	4.267
20 $n = \text{an integer}$	1	1	1	1
21 $G_1 = \frac{1}{2} (180n + \arctan b)$	87.73	94.12	87.73	94.12
22 $G_2 = G_1 + \Delta G$	209.59	215.98	246.58	252.97
23 $M_2$ from Fig 2.3 for $G_2$	1.545	1.465	1.314	1.322
24 $M_1$ from Fig 2.3 for $G_1$	1.306	1.369	1.306	1.369
25 $V_1 = (M_1 + 1) + (M_1 - 1)$	7.536	6.420	7.536	6.420
26 $V_2 = (M_2 + 1) + (M_2 - 1)$	4.670	5.301	7.369	7.211
27 $V_3 = (V)(V_2) + (V_1)$	7.073	3.523	11.161	4.793
28 $Z_b = (1 - jV_3 \cot G_2)$	338.20	261.96	88.39	73.97
29 $\theta_b = \arctan \frac{V_3 - j \cot G_2}{V_3}$	-71.56°	-57.46°	-76.09°	-57.08°
30 $R_b = \text{Base Resis} = Z_b \cos \theta_b$	106.99	142.67	21.25	45.46
31 $X_b = \text{Base React} = Z_b \sin \theta_b$	-320.83	-219.70	-85.80	-58.36
32 $W_b = \text{Base Watts} = W_L$	392	608	392	608
33 $I_b = \text{Base Amps} = (W_b + R_b)^{1/2}$	1.914	2.064	4.295	3.657
34 Base Amps Ratio	1.000	1.078	1.000	0.851

\* At line 18 use "r" as positive to determine "a"

# 00 CIRCULAR DIAGRAM VERTICAL RADIATOR IMPEDANCE ANALYSIS

01 Station				
02 Array				
03 Element	1	2	1	2
04 Physical Height H	75	60	75	90
05 G/H from Fig 2.2	1.200	1.104	1.200	1.279
06 Electrical Height G	90.00	66.24	90.00	115.11
07 $\Delta G = G - 90$	0.00	-23.76	0.00	25.11
08 Loop Field Ratio	1.000	0.748	1.000	0.777
09 Loop Amps @ 100 Wv/m Fig 5.2	3.074	3.123	3.074	3.005
10 Loop Current Ratio	1.000	0.760	1.000	0.760
11 $R_L$ Loop Operating Resistance	17.55	47.41	17.55	47.11
12 $X_L$ Loop Operating Reactance	-7.86	12.61	-7.86	13.61
13 $I_L$ Loop Operating Amps	4.727	3.592	4.727	3.592
14 $W_L$ Loop Operating Watts	392	608	392	608
15 $r = R_L / 200$	.08775	.23555	.08775	.23555
16 $x = X_L / 200$	-.03930	.06805	-.03930	.06805
17 $b = -2x + (xx + rr - 1)$	-.0793	.1448	-.0793	.1448
*18 $a = (rr + xx + 1) + 2r$	5.7507	2.2506	5.7507	2.2506
19 $V = VSWR = a + (aa - 1)^{1/2}$	11.414	4.267	11.414	4.267
20 n = an integer	1	1	1	1
21 $G_1 = \frac{1}{2} (180n + \arctan b)$	87.73	94.12	87.73	94.12
22 $G_2 = G_1 + \Delta G$	87.73	70.36	87.73	119.23
23 $M_2$ from Fig 2.3 for $G_2$	1.306	1.160	1.306	1.635
24 $M_1$ from Fig 2.3 for $G_1$	1.306	1.369	1.306	1.369
25 $V_1 = (M_1 + 1) + (M_1 - 1)$	7.536	6.420	7.536	6.420
26 $V_2 = (M_2 + 1) + (M_2 - 1)$	7.536	13.508	7.536	4.150
27 $V_3 = (V) (V_2) + (V_1)$	11.414	8.973	11.414	2.758
28 $Z_b = (1 - jV_3 \cot G_2) / (V_3 - j \cot G_2)$	19.23	74.71	19.23	130.69
29 $\theta_b =$	-24.13°	-78.38°	-24.13°	45.57°
30 $R_b = \text{Base Resis} = Z_b \cos \theta_b$	17.55	25.09	17.55	91.46
31 $X_b = \text{Base React} = Z_b \sin \theta_b$	-7.86	-70.38	-7.86	93.36
32 $W_b = \text{Base Watts} = W_L$	392	608	392	608
33 $I_b = \text{Base Amps} = (W_b + R_b)^{1/2}$	4.727	4.923	4.727	2.578
34 Base Amps Ratio	1.000	1.041	1.000	0.545

\* At line 18 use "r" as positive to determine "a"

# 00 CIRCLE DIAGRAM VERTICAL RADIATOR IMPEDANCE ANALYSIS

01 Station				
02 Array				
03 Element	1	2	1	2
04 Physical Height H	75	180	90	225
05 G/H from Fig 2.2	1.200	1.177	1.279	1.106
06 Electrical Height G	90.00	211.86	115.11	248.85
07 $\Delta G = G - 90$	0.00	121.86	25.11	158.85
08 Loop Field Ratio	1.000	1.029	1.000	0.979
09 Loop Amps @ 100 Mv/m Fig 5.2	3.074	2.270	3.005	2.733
10 Loop Current Ratio	1.000	0.760	1.000	0.760
11 $R_L$ Loop Operating Resistance	17.55	47.11	17.55	47.11
12 $X_L$ Loop Operating Reactance	-7.86	13.61	-7.86	13.61
13 $I_L$ Loop Operating Amps	4.727	3.592	4.727	3.592
14 $W_L$ Loop Operating Watts	392	608	392	608
15 $r = R_L / 200$	.08775	.23555	.08775	.23555
16 $x = X_L / 200$	-.03930	.06805	-.03930	.06805
17 $b = -2x + (xx + rr - 1)$	-.0793	.1448	-.0793	.1448
*18 $a = (rr + xx + 1) + 2r$	5.7507	2.2506	5.7507	2.2506
19 $V = VSWR = a + (aa - 1)^{1/2}$	11.414	4.267	11.414	4.267
20 $n = \text{an integer}$	1	1	1	1
21 $G_1 = \frac{1}{2} (180n + \arctan b)$	87.73	94.12	87.73	94.12
22 $G_2 = G_1 + \Delta G$	87.73	215.98	112.84	252.97
23 $M_2$ from Fig 2.3 for $G_2$	1.306	1.465	1.565	1.322
24 $M_1$ from Fig 2.3 for $G_1$	1.306	1.369	1.306	1.369
25 $V_1 = (M_1 + 1) + (M_1 - 1)$	2.536	6.420	2.536	6.420
26 $V_2 = (M_2 + 1) + (M_2 - 1)$	2.536	5.301	4.540	7.211
27 $V_3 = (V)(V_2) + (V_1)$	11.414	3.523	6.876	4.793
28 $Z/\theta = (1 - jV_3 \cot G_2)$ $Z_b =$	19.23	261.96	88.96	73.97
29 $(V_3 - j \cot G_2)$ $\theta_b =$	-24.13°	-57.00°	67.45°	-52.08°
30 $R_b = \text{Base Resis} = Z_b \cos \theta_b$	17.55	142.67	34.12	45.46
31 $X_b = \text{Base React} = Z_b \sin \theta_b$	-7.86	-219.70	82.15	-58.36
32 $W_b = \text{Base Watts} = W_L$	392	608	392	608
33 $I_b = \text{Base Amps} = (W_b + R_b)^{1/2}$	4.727	2.064	3.390	3.657
34 Base Amps Ratio	1.000	0.437	1.000	1.079

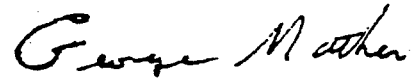
\* At line 18 use "r" as positive to determine "a"

## ACKNOWLEDGEMENTS

The self impedance derivations in this report are based on Canadian Broadcasting Corporation single tower measurement data which has been made available.

D. E. M. Allen & Associates Ltd. has made a worthy contribution to this study by using the routines to compare theoretical derivations with measured results they have compiled.

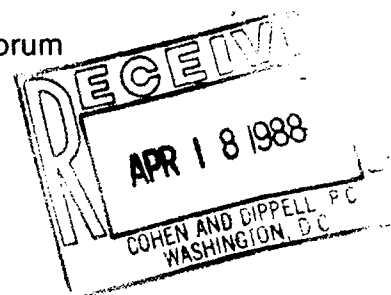
February 1983.



George Mather, P.Eng.,  
Consultant.

# A NEW LOW PROFILE ANTI-SKYWAVE ANTENNA FOR AM BROADCASTING

Basil F. Pinzone, James F. Corum, Ph.D. and Kenneth L. Corum  
Pinzone Communications Products, Inc.  
Newbury, Ohio



## ABSTRACT

A new technique for controlling the elevation plane pattern of broadcast antennas is presented. Practical results, measurements and theoretical predictions are evaluated and discussed. It is concluded that the new Corum structure is a viable candidate for solving skywave problems and for providing low profile radiators where traditional antennas are impractical.

## Introduction

A novel technique for the control of the elevation plane pattern of broadcast antennas has been developed at Pinzone Communications Products' Newbury, Ohio laboratory and the antenna test range at its rural Windsor, Ohio engineering experimental station. This remarkable new technology makes possible the practical implementation of anti-fade and anti-skywave antennas.

Nighttime skywave interference has continued to be a major plague for the AM broadcast service since the early days of radio. For most broadcasters, skywave radiation presents two problems. First, it represents wasted radiated power. Secondly, because of the legally protected contours of existing stations, high angle radiation severely limits a broadcast station's market place, or primary coverage area. From a pragmatic point of view, if the interference-causing high angle radiation could be significantly reduced, in many cases, the transmitter power and ground wave coverage could be dramatically increased with no additional interference to other stations. The potential market place economic impact is obvious.

High angle radiation is also a plague to clear channel broadcast stations. The groundwave daylight service area, for a clear channel station, may exist out to a

considerable range. However, the nighttime skywave signal can be greater than the groundwave signal well within the daytime coverage area. When the groundwave and skywave signals are of the same magnitude, they can phase out one another, resulting in serious fading and irritating audio distortion in the detected signal at the consumer's receiver. The outer edge of the primary service area, caused by this self-interference phenomenon, is called the "fading wall". Its physical elimination is only possible by the reduction of high angle radiation.

## Historical Perspective

The history of the anti-skywave problem makes for fascinating reading. Stuart Ballantine, in the second of his two historic papers from Harvard in the 1920's, according to Laport, "... disclosed a hitherto unknown fact: there was an optimum height for a vertical radiator for obtaining maximum groundwave field strength."<sup>1</sup>

Laport continues, "Further study of the optimum height antenna disclosed eventually that the conditions of maximum groundwave and best antifading characteristics were not obtained with the same height. . . . The optimum choice for antifading over land was experimentally established at about 190 degrees."<sup>1</sup> The 225 degree tower gives the maximum groundwave but its high angle lobe produces a non-negligible fading wall.

Laport, in his fascinating 1952 publication, observes that, "By 1934, the modern broadcast radiator had evolved to its present state."<sup>1</sup>

Summarizing the state of affairs in the early 1950's Laport concludes, "Diligent research and experiments have been conducted for other possible broadcast principles that might equal or surpass those disclosed by Ballantine."<sup>1</sup> As we know

today, the results (though often significant) have been of marginal utility.

### Practical Requirements

Over the past several years a renewed interest in anti-skywave antennas has been exhibited by broadcasters, the NAB and consulting engineers. The noteworthy papers publishing the separate approaches of Biby and Prestholdt indicate the creative effort put forth to arrive at acceptable alternatives to expensive radiators of heroic proportions.<sup>2,3</sup>

Perhaps the clearest verbalization of the necessary technical requirements which challenge the creation of any realistic Anti-Skywave Antenna was put forth by Richard Biby in his 1986 NAB Engineering Conference technical paper:

"In order to be really economically viable, an 'Anti-Skywave' antenna design concept must be able to take the typical 90 degree vertical tower, with a conventional buried copper wire ground system, make minimal changes thereto, and end up with decreased nighttime interference and improved groundwave signal strength. All the while, the system should remain non-directive, but still offer the possibility of being made directive in the horizontal plane if such were needed."<sup>2</sup>

To this we would also add, because of the Sommerfeld attenuation function, the structure must produce only a vertically polarized groundwave. What is needed is some way to increase the vertical current moment of the radiating system (the integral of  $i \cdot dl$ ).

This has been done, and Pinzone Communications Products, Inc. has just such a solution available.

The patented Corum Antenna provides a splendid candidate to simultaneously surmount all of the above engineering requirements.

It can be used to retrofit existing towers, at ground level, and produce an enhanced elevation plane directivity previously unavailable to design engineers.

### Elementary Considerations

Normal mode helices have been of interest since Pocklington's famous 1897 paper. One particularly intriguing idea is to take a self resonant normal mode helix, pull it around into a closed multiply connected region and let the resulting structure, which has been called a "Corum Ele-

ment", combine the tuning and matching networks with the radiating structure itself.<sup>4,5</sup> The radiation resistance is now in series with the coil inductance, and this combination is shunted by the helix turn-to-turn capacitance. The impedance transforming nature of this lumped circuit equivalent is well known, and it also has the advantage of transforming a relatively small feedpoint current into a stepped up current passing through the radiation resistance.

There exist a variety of techniques available to predict the behavior of simple antennas. Because of the geometrical complexity of our structure, traditional moment methods are not only cumbersome, but require inordinate computer time and yield little insight into the physics of the antenna. We have found the Kron/Gobau Diakoptic technique much more promising. We can attest to the oft heard complaint that, "The method of moments is little more than a numerical experiment. It generates no analytical formula or expression by which to gauge how the result might change with a change in configuration . . . insight can only be gained by running the experiment again and again." Consequently, we favor an analytical model for the physical insight which it provides.

The field theory analysis of the basic Corum element is fairly straightforward. Since the structure is a slow wave self resonant helix, it is reasonable to assume a superposed sinusoidal distribution of electric and magnetic current, where the electric current is given by

$$(1) J(r') = I_0 \sin(n\phi') \delta(\cos \theta') \frac{\delta(r'-a)}{a} \hat{\phi}'$$

the coordinates having their usual meanings (see figure 1), and the magnetic current is found from

$$(2) I_m = \mu\omega(\pi b^2/s) I_0 \cos(n\phi')$$

where  $a$  is the major radius of the torus,  $b$  is the helix radius (the minor radius of the torus) and  $s$  is the turn-to-turn spacing. In these expressions,  $n$  is a mode number for the current distribution on the structure. The radiated fields are determined in Reference 4 as:

$$(3a) E_{\theta}^e = -\frac{\beta_g a Z_0 I_0}{2r} \cos n\phi J_n(\beta_g a \sin \theta) e^{j(n\pi/2)}$$

$$(3b) E_{\phi}^e = \frac{n\beta_g a Z_0 I_0}{2r} \sin n\phi \frac{J_n(\beta_g a \sin \theta)}{\beta_g a \tan \theta} e^{j(n\pi/2)}$$



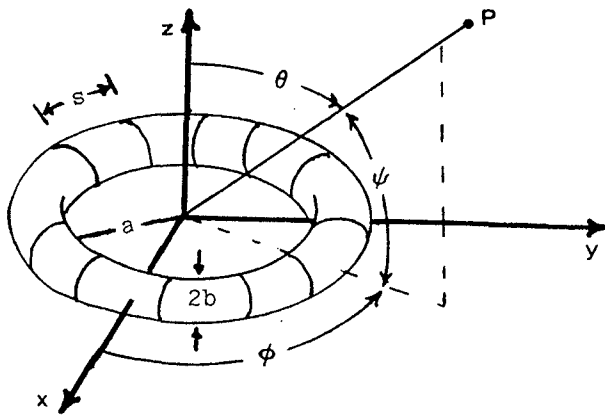


Fig. 1. Geometrical configuration.

$$(3c) \quad E_{\theta}^m = -\frac{\beta_g a I_m}{2r} \cos n\phi \quad J_n'(\beta_g a \sin \theta) \quad e^{j(n\pi/2)}$$

$$(3d) \quad E_{\phi}^m = -\frac{n\beta_g a I_m}{2r} \sin n\phi \quad \frac{J_n(\beta_g a \sin \theta)}{\beta_g a \tan \theta} \quad e^{j(n\pi/2)}$$

The superscript  $e$  indicates a field component attributable to the electric current and  $m$  to the magnetic current.  $J_n(x)$  is the usual Bessel function of order  $n$  and  $\beta_g$  is the phase constant appropriate for the slow wave helix.

It should be clear that the structure is basically a low  $Q$  leaky resonator. The resonator loss resistance arises from the radiation resistance, the skin effect and proximity effect losses. The skin and proximity effect losses may be calculated in the usual manner for coils. The radiation resistance may be gotten by a Poynting integration of the radiated fields.

These fields are not unlike those produced by the superposition of a resonant electric loop and a "magnetic frill" or circular slot antenna. [Neither of which is really practical for AM broadcasting - the loop produces a horizontally polarized ground wave and the slot requires the construction of a heroic ground plane. The theory of these structures is of present interest.] However, because of the slow wave nature of the Corum helix, the physical size of a self resonant structure has been considerably reduced. The self resonant electric loop and annular slot require a circumference on the order of a free space wavelength. The Corum Helix is self resonant at only a fraction of this size.

Several variations of the basic configuration are now possible. Note the presence of the azimuthally directed (or horizontally polarized) electric field components. These must be eliminated for groundwave AM broadcasting. By contrawinding the helix [References 4,5,7], the azimuthal component of electric current is cancelled out and one is simply left with what is commonly known as a poloidal flow of electric current. (See figures 2 and 3.) A toroidal flow of electric current would be in the azimuthal direction (parallel to a thread in the center of the doughnut), while a poloidal flow is up over and around the anchor ring, or minor axis of the torus. This produces the  $\phi$ -directed effective magnetic current of equation (2) above. Occasionally, this is called a caduceus winding.

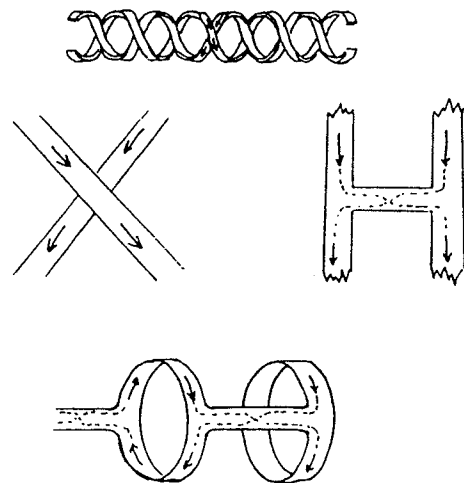


Fig. 2. Fundamental structure for the rings in a contrawound helix.

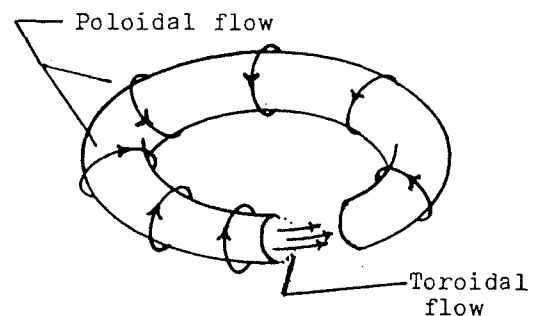


Fig. 3. A "poloidal" flow of electric current is equivalent to a "toroidal" flow of effective magnetic current.

The radiated fields are then described only by expressions 3(c) and 3(d). Note that "Figure Eight" patterns can be obtained. Further, and this is important, if one divides the toroidal helix into 4 or more segments, it can be fed as Smith's omnidirectional cloverleaf antenna, so familiar in FM broadcasting. [See references 4 and 8.] The resultant magnetic current distribution will be uniform, ( $n = 0$ ), and the radiated field is described simply by equation (3c). See figure 4.

#### THE CORUM ELEMENT

We now have a Low Profile, slow wave vertically polarized, self resonant, omnidirectional (in the azimuthal plane) radiator with a substantial feedpoint impedance. Consequently, the structure has considerable desirability as a stand alone electrically small antenna at frequencies where ground wave propagation or ground effects are important.

For example, in the fundamental mode ( $n=0$ ), a power flow calculation gives the predicted vertically polarized elevation plane field pattern, in RMS mV/m at 1 mile, per kilowatt radiated, as the expression

$$(4) E_{\theta} = -412.7 \sqrt{P_{KW}} J_1(\beta_g a \sin \theta) .$$

In order to experimentally test the validity of the analytical model above, a variety of structures have been fabricated at frequencies from 150 KHz to several GHz. Typical measured and calculated elevation plane electric field strength patterns are shown in figure 5. The measured vertically polarized azimuthal plane pattern is displayed in figure 6. The theoretical and measured feedpoint impedances are shown in figure 7.

Needless to say, we have considerable confidence in the relatively simple analytical model presented in the previous section. And now we come to the exciting news concerning anti-skywave antennas.

#### THE CORUM ANTENNA

The above element, when used alone, may produce rather high angle radiation. See figure 8. This fact, however may be used to great advantage. In order to produce low angle radiation, a standard tower may be surrounded with the Corum Element and phased to produce increased groundwave and decreased skywave radiation. See figure 9.

This new structure is now marketed under the name "Corum Antenna". Since the

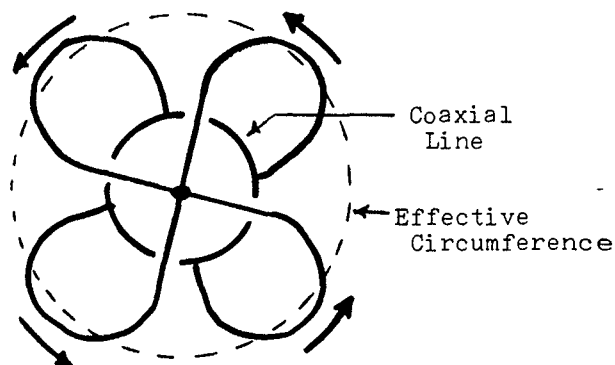


Fig. 4. Smith's "cloverleaf" arrangement for producing a uniform azimuthal current distribution.

system's phase center is at the tower's spatial position, the resultant radiation pattern is simply the sum of the Corum Element pattern, above, and that of a vertical conductor of height  $G$ , given by the well known expression

$$(5) E_{\theta} = E_0 \frac{\cos(G \sin \Psi) - \cos G}{(1 - \cos G) \cos \Psi} \text{ mV/m @ 1 mi}$$

where  $E_0$  is the RMS field intensity produced by the tower in mV/m at 1 mile, per kilowatt radiated (186.5 for a stub; 194.5 for a quarter wave tower; 236.2 for a half wave tower; 275 for a 5/8 wave tower; etc.). In practice, a multiplicative efficiency factor would be employed to account for ground system and structure losses.

#### Elevation Plane Patterns

This remarkable structure provides the design engineer with a new flexibility in pattern synthesis. The element may be used in a variety of applications to dramatically tailor the shape of radiated patterns.

As a demonstration of the utility and flexibility of this new technology, let us plot the elevation plane patterns of several configurations. In the following we let

$K$  = the electrical circumference of the Corum Element in wavelengths ( $K = \beta_g a$ )

$P$  = the fraction of the total power radiated by the central element

$G$  = the electrical height of the central element ( $G = \beta_0 H$ ).

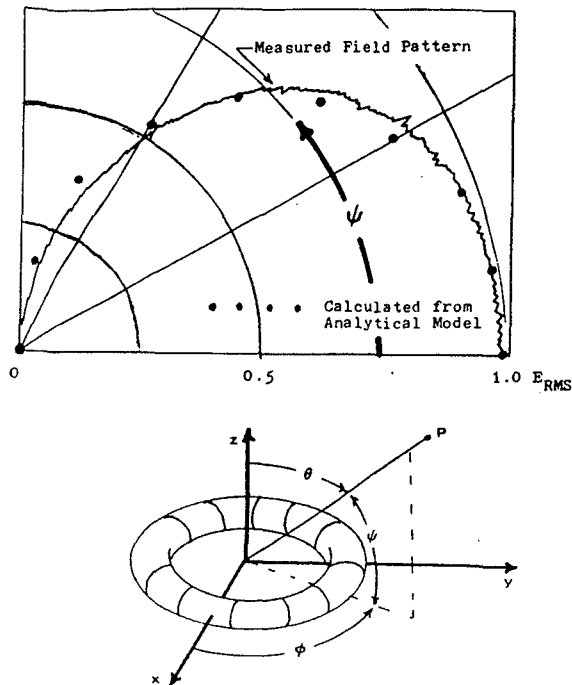


Fig. 5. Experimentally measured electric field strength pattern (vertical polarization) from a contrawound Corum Element lying in the x-y plane. The black dots are the values calculated from the theoretical model. The pattern is omnidirectional in the azimuthal plane.

In figure 10, we calculate and plot the elevation plane electric field pattern for the case where the electrical circumference of the Corum element is  $1 \lambda_g$  and the power is split 55% to the tower and 45% to the Corum element. The radiated power is 1 KW. The Corum element is constructed of 2 inch diameter copper tubing and produces a vertically polarized omnidirectional pattern in the azimuthal plane. The RMS field strength at one mile is 241.5 mV/m when losses are included (256.0 mV/m @ 1 mile in the loss less case), or equivalently, 388.6 mV/m @ 1 Km including losses (411.9 mV/m @ 1 Km for the loss less case).

In figure 11, we compare Gihring and Brown's optimum antifade tower (190 degrees high), the standard 225 degree tower, and a new antenna made possible by combining the 225 degree tower and a cophasal Corum element with

$$K = 4.25$$

$$P = 0.945$$

The new antenna is clearly superior at all critical skywave angles.

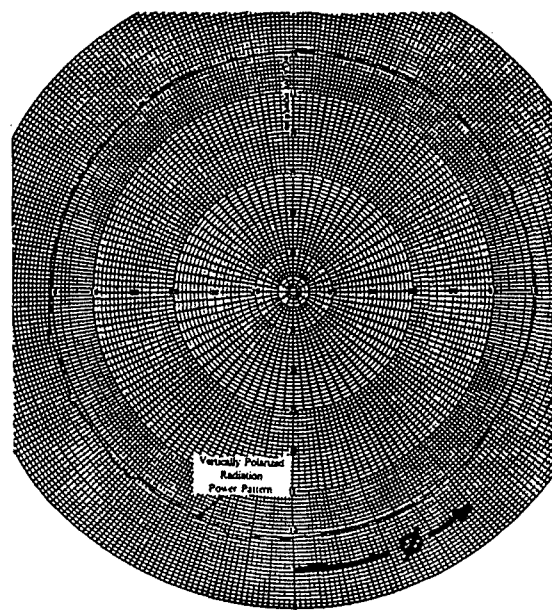


Fig. 6. Measured azimuthal plane radiation power pattern. The Corum element was in the x-y (azimuthal) plane and the polarization state was vertical.

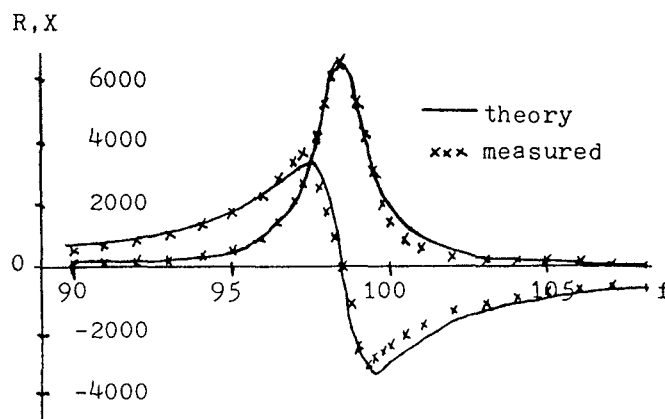


Fig. 7. A comparison of the measured and theoretical impedance versus frequency for a single Corum helix antenna designed for 98.5 MHz.

In figure 12, we present a comparison of the optimum antifade tower (190 degrees), the standard Quarter wave tower (90 degrees), and a short stub (12 degrees, in this example) surrounded by a Corum element with

$$K = 1.0$$

$$P = 0.54$$

fed 180 degrees out of phase with respect to the stub. Losses are neglected.

Table 1 gives the actual numerical values of the various elevation plane patterns and compares the classical performance with what the new technology makes possible.

Remember to compare apples with apples. The results are very dramatic at angles above (and below) 30 degrees. These numbers are only typical, and have not even been optimized.

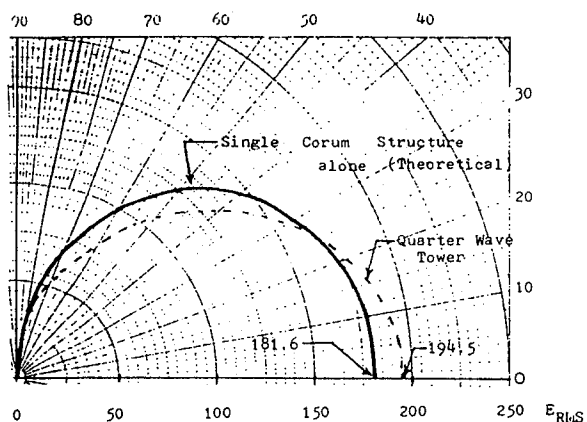


Fig. 8. Theoretical elevation plane of a single Corum element alone. (Elevation plane pattern of a quarter wave tower for reference.)  $E_{RMS}$  in mV/m at 1 mile for 1 KW radiated.

Is there any reason why the center tower is even necessary? As with concentric annular slot arrays at microwave frequencies, one may array concentric Corum elements. In figure 13, we show just such an array. In this example, we portray the case where the inner element has  $K = 1$  and the outer element has  $K = 2$ . The radiated power is 1 KW and the calculation is at a frequency of 620 KHz. There are 52 rings in the outer element displaced 10 feet apart, with a major radius of 80 feet. The wire diameter on the outer

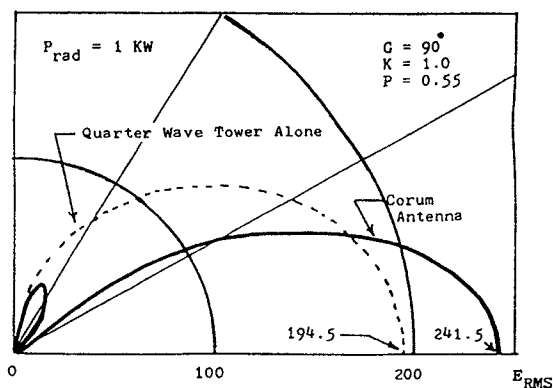


fig. 10. Elevation plane pattern for a quarter wave tower surrounded by a Corum element (losses included). In the loss free case, the RMS field strength rises to 256 mV/m at 1 mile, per kilowatt radiated.

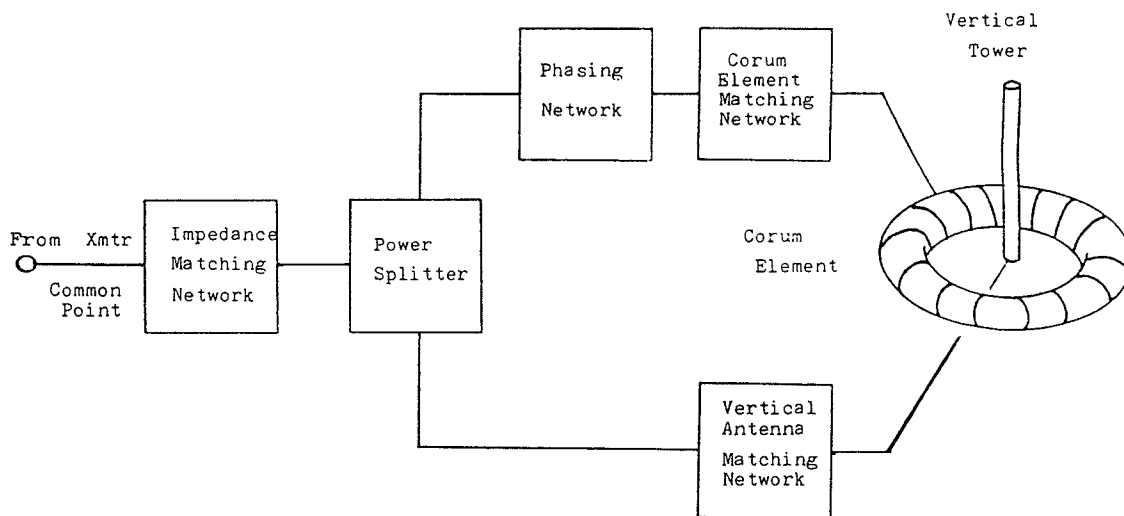


Figure 9 . Block diagram of Corum array feed system.

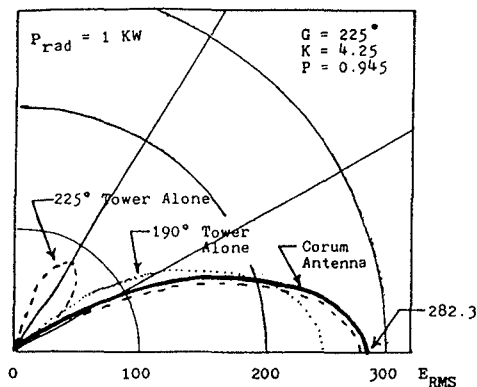


Fig. 11. Elevation plane pattern comparing the optimum antifade tower (190 degrees), Ballantine's optimum ground wave tower (225 degrees), and a 225 degree tower surrounded by a Corum Element. Note that the high angle lobe of the 5/8 wave tower can be phased out. Other combinations of K and P are also effective.

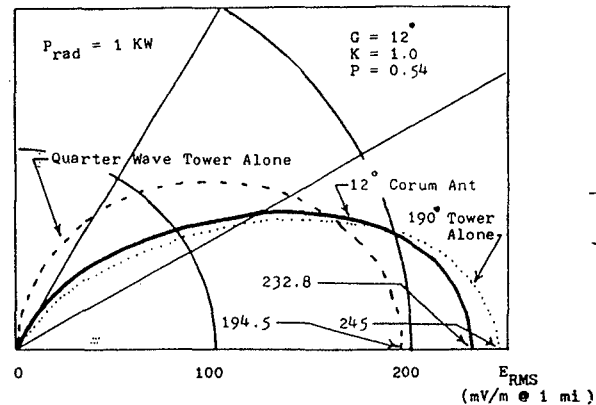
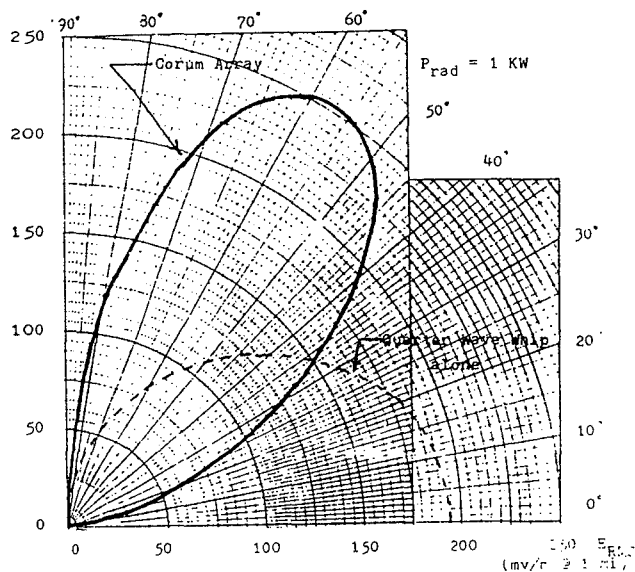


Fig. 12. A remarkable configuration in which a Corum Element surrounding a 12 degree tower not only out performs a quarter wave tower, but is competitive with a full sized optimum antifade tower (190 degrees).



Corum Array

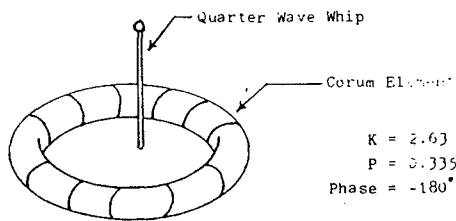


Fig. 14. Utilization of a Corum Element to produce high angle radiation from a standard quarter wave whip antenna.

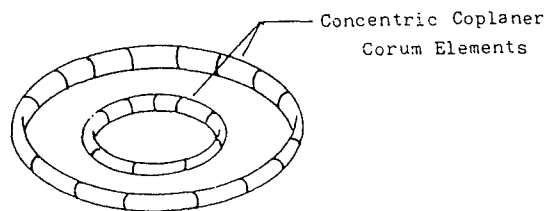
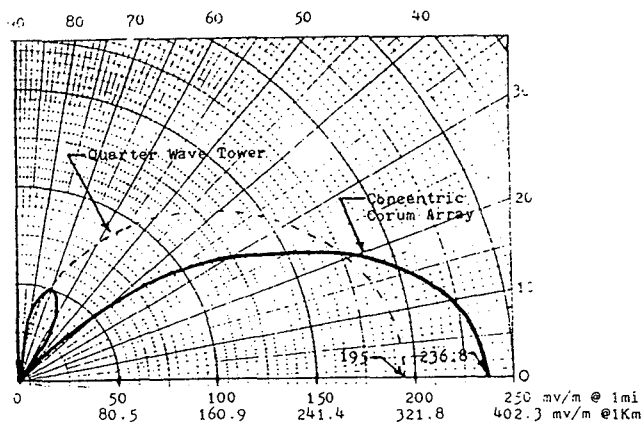


Fig. 13. A new element available for antenna design. At 620 KHz the structure is less than 60 feet high and 80 feet in radius. The ground wave field strength is comparable to that of a half wave Tower.

element is taken as 0.75 inches. The RMS field strength at one mile (including structural losses) is 236.8 mV/m (249 mV/m in the loss less case). The power is split 55% radiated by the inner element and 45% by the outer element. The electric field pattern is omnidirectional and vertically polarized. A variety of elevation plane patterns may be obtained by varying the electrical circumferences and power division. And, of course, this element may be used in a larger phased array.

Occasionally, one desires high angle radiation. In figure 14, we present the case where a Corum element may be fabricated to produce high angle radiation from a standard quarter wave whip antenna. In this case the appropriately fed surrounding element elevates the pattern maxima to about 60 degrees above the horizon. The pattern may even be made switchable for mixed high/low angle radiation for communication with elevated platforms and with other ground stations. Again, the figure has not been optimized, and superior configurations may exist for this application.

By the way, it should now be obvious how we have been able to increase the current moment without adding more tower height.

$$(6) \quad E_z \sim i \cdot dl = i_z^e dz + i_\phi^m a d\phi$$

As with a monopole and an annular slot, the vertical electric field is increased by the equivalent magnetic current.

What about ground screens and counterpoises? Certainly, one may employ a Corum Element in place of an extensive ground system to produce the same ground wave signal. This comes about simply because more signal is pulled out of the sky and concentrated along the earth. This latter technique might be of interest to stations lacking sufficient real estate for a full sized ground screen.

### Conclusions

All this sounds too good to be true. One should always be on guard against extravagant claims made by theoreticians and antenna manufacturers. Common sense and past experience should provide some guidance, even with a new technology.

In this regard, one must bear in mind the fundamental limits associated with antennas. One does not get something for nothing. Chu's fundamental limit, which relates the lowest achievable Q of a loss less structure to its maximum physical dimension, is still in force. The Corum Element is a remarkable structure, but it

has been wrestled from Nature at the price of reduced bandwidth. Fortunately, even at the low end of the AM broadcast band, we are in that happy state of affairs where it is possible to operate with Q's as high as 20, and practical configurations can be fabricated. The problem is not as acute at higher frequencies.

In summary, then, we believe that our patented structure is not only the best available candidate for an anti-skywave antenna, but is, perhaps, the only viable alternative for many situations.

It satisfies the pragmatic requirements placed above on an anti-skywave antenna. It has five significant advantages:

1. The Corum Element is constructed at or near ground level.
2. It may be used to retrofit most existing arrays.
3. Each element of the phased array now has a much narrower elevation plane pattern.
4. Arrays of concentric Corum Elements may be used, trading off going out in horizontal extent for going up in tower height, to achieve directivity.
5. It permits pattern tailoring which would otherwise be impossible with traditional radiators.

Unless we have committed serious error, we believe that by finding an alternative to the annular slot, we have brought to light broadcast principles that "equal or surpass those disclosed by Ballantine".

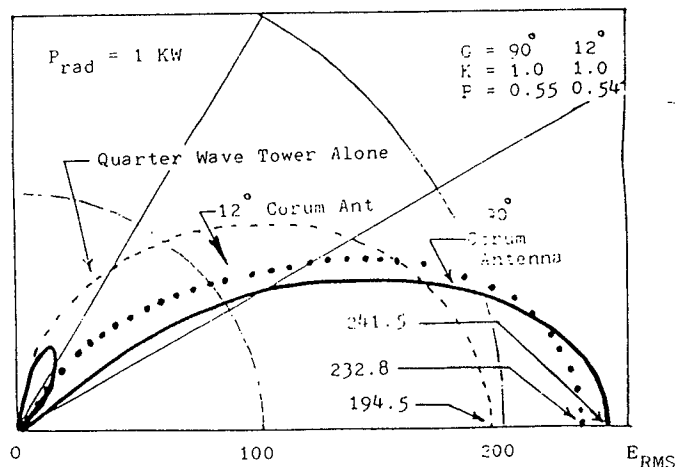


Fig. 15. A comparison of a quarter wave tower, a 12 degree Corum antenna and a 90 degree Corum antenna.

TABLE 1 COMPARISON OF ANTENNAS FOR ANTI-FADE OPERATION

PSI	12 Degree Tower	90 Degree Tower	180 Degree Tower	190 Degree Tower	225 Degree Tower
0	186.500	194.500	236.200	245.000	275.000
10	183.646	190.199	222.438	228.567	242.664
20	175.178	177.824	185.528	184.915	159.922
30	161.367	158.809	136.374	127.950	60.359
40	142.652	135.108	87.312	72.996	-22.758
50	119.622	108.715	47.438	30.771	-71.163
60	92.994	81.261	20.619	5.182	-83.583
70	63.581	53.791	6.182	-5.362	-68.034
80	32.272	26.727	0.776	-5.326	-37.941

## CORUM ELEMENTS:

G = 12°	90°	225°
K = 1.00	1.25	4.25
P = 0.54	0.63	0.945
Phase = -180	-180	0

F(psi)	F(psi)	F(psi)
232.823	235.148	282.310
221.004	222.595	249.530
188.022	187.798	167.628
140.717	138.534	74.942
88.686	85.329	7.791
42.019	38.626	-18.585
8.603	6.118	-13.362
-7.602	-9.080	1.086
-8.372	-8.988	6.364

Comments: K is the electrical circumference of the slow wave Corum element in velocity inhibited wavelengths.  
P is the fraction of the total input power supplied to the center element.

REFERENCES

1. RADIO ANTENNA ENGINEERING, BY E. A. Laport, McGraw-Hill, 1952, pp. 77-82, 102-104. (Reprinted by Mei Ya Publications, Inc., P.O. Box 22555, Taipei, Taiwan, 1967)
2. "The Anti-Skywave Antenna", by R.L. Biby, Proceedings of the 1986 NAB Engineering Conference, pp. 7-13.
3. "New Dimensions for the Design of Medium Wave Antennas", by O.L. Prestholdt, Proceedings of the 1986 NAB Engineering Conference, pp. 14-17.
4. J.F. Corum, US Patent # 4,623,558; Canadian Patent # 1,186,049; Australian Patent # 548,541. Other foreign and domestic patents pending.
5. "Toroidal Helix Antenna", by J.F. Corum, IEEE AP-S International Symposium Digest, 1987, pp.832-835.
6. "A Novel Structure for Improved Directivity", by B.F. Pinzone, J.F. Corum and K.L. Corum, Submitted to the 1988 IEEE AP-S International Symposium at Syracuse University.
7. "Experimental Test Program on the New Corum Anti-Skywave Antenna", by C.E. Smith, prepared for the FCC on behalf of Pinzone Communications Products, Inc., January 25, 1988.
8. "Cloverleaf Antenna for FM Broadcasting", by P.H. Smith, Proc. IRE, Vol. 35, No. 12, December, 1947, pp. 1556-1563.
9. "Fundamental Limitations of Small Antennas", by H.A. Wheeler, Proc. IRE, Vol. 35, No. 12, December, 1947, pp. 1479-1488.
10. "Physical Limitations of Omni-Directional Antennas", by L.J. Chu, Jour. Applied Physics, Vol. 19, No. 12, December, 1948, pp.1163-1175.

BASIL F. PINZONE, JR.  
PRESIDENT  
SYSTEMS ENGINEER

PINZONE COMMUNICATIONS  
PRODUCTS, INC.

COMMUNICATIONS PRODUCTS, INC.  
40, NEWBURY, OHIO U.S.A. 44065  
216-564-9093

POST OFFICE BOX 540  
14850 CROSS CREEK PARK  
NEWBURY, OHIO 44065

(216) 564-9093  
TELEX 3714400 PINZONE UR  
FAX 216-564-8066

COMMUNICATIONS PRODUCTS, INC.

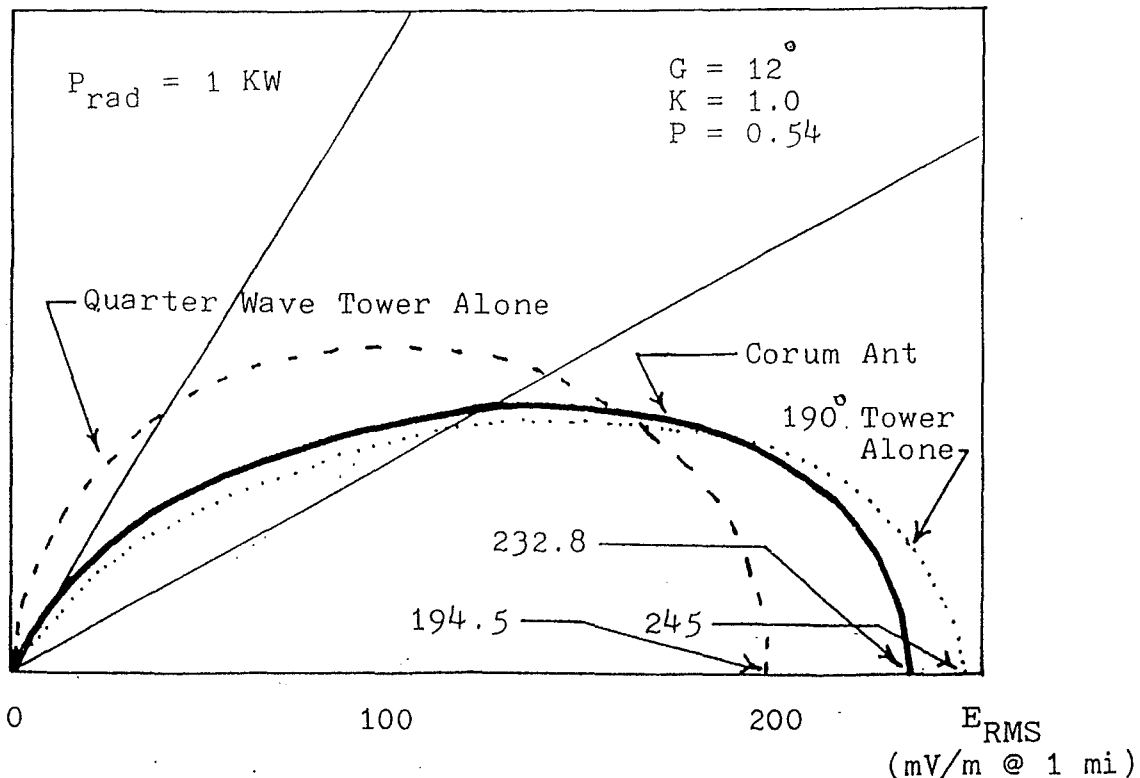
NAB 88

(RADIO INDUSTRY)

NEW TECHNOLOGY PRESS RELEASE

PINZONE COMMUNICATIONS OFFERS CORUM ANTI-SKYWAVE AM ANTENNA

PINZONE COMMUNICATIONS will display a model of its newest technology development, the CORUM Anti-Skywave/Anti-Fading AM Broadcast Antenna, at NAB '88. The CORUM ANTENNA is a low profile structure (30 - 50' height) that yields a pattern nearly equal to that of a 190 degree tower (835 feet at 620 KHz). More information will be available at PINZONE COMMUNICATIONS NAB Booth # 1119.





ANTENNAS (AM)  
M.F.

A NEW ANTENNA FOR AM BROADCASTERS

by  
James F. Corum, Ph.D.  
CPG Communications, Inc.  
Rt. 9 Box 207-B  
Morgantown, WV 26505

SMITH ELECTRONICS, INC.

AUG 10 1987  
ATT: SP 614

Kenneth L. Corum  
Pinzone Communications Products, Inc.  
14850 Cross Creek Park - PO Box 540  
Newbury, Ohio 44065

Basil F. Pinzone, Jr.  
Pinzone Communications Products, Inc.  
14850 Cross Creek Park - PO Box 540  
Newbury, Ohio 44065

ABSTRACT

An analytical and experimental evaluation and design has recently been performed on an extensive series of new low profile structures appropriate for AM broadcast antennas. These new omnidirectional radiating elements may be fed either in phased array fashion or parasitically.

When configured as a concentric halo about a previously existing vertical tower, there is a considerable increase in the groundwave field strength, along with a comenserate decrease in the skywave radiation.

Consequently, the new vertically polarized Toroidal Helix Antenna, as developed at Pinzone Communications, has emerged as an attractive and practical canadate for broadcasters either desiring an anti-skywave antenna, or an efficient, low profile, alternative to conventional low frequency radiators.

June 15th-19th 1987

Virginia Polytechnic Institute & State University  
Blacksburg, Virginia 24061

IEEE ANTENNAS AND PROPAGATION SOCIETY  
87CH2435-6

1987 IEEE AP-S INTERNATIONAL  
SYMPOSIUM DIGEST

AP21-3

TOROIDAL HELIX ANTENNA

James F. Corum  
Department of Electrical  
and Computer Engineering  
West Virginia University  
Morgantown, WV 26505-6101

Kenneth L. Corum  
CPG Communications, Inc.  
158 Salem St.  
Wilmington, Mass. 01887

Introduction

The design and operation of Low Profile and Electrically Small Antennas has traditionally centered around the properties of efficiency and bandwidth for these structures. Over the years a variety of significant theoretical studies and experimental efforts have been performed by many well known investigators. Wheeler's monumental work of over 40 years, summarized in Ref.1, is worthy of special note. He has provided one of the most splendid practical techniques for characterizing and predicting the behavior of these small antennas. (Small, in this context, means that the entire antenna, and its images, fit within the radian sphere - a sphere of radius  $\lambda_0/2\pi$ . Small at VLF or ELF, of course, may entail substantial real estate.) Clearly, the bottom line on all this is that remarkable performance is certainly practical, provided only that one does not become too greedy in the size-efficiency-bandwidth tradeoff.

Electrically Small Antennas have always represented one of the major challenges to the RF engineering profession. (Indeed, the topic seems to reappear in regular cycles.) Traditionally, acceptable performance has been coaxed and tweaked out of these devices by either (1) reducing system losses (use thick wires on the antennas and low loss elements in the matching networks) or by (2) increasing the radiation resistance (say, by top loading short towers). Newmann has devised a third line of attack which is viable when a small antenna is to be located on a larger conducting support structure. The technique, apparently, is to (3) use the small antenna as a coupler to excite characteristic modes on the support. The method is especially useful if the small antenna, by itself, is not very efficient. Unfortunately, only the first two techniques are of value to AM broadcasters or for VLF/ELF communications.

Small Antennas at Low Frequencies

At these lower frequencies, another major electromagnetic factor is of considerable significance. Traditional small antenna analysis is usually formulated in a free space environment. At these lower frequencies, however, one must also contend with the Sommerfeld attenuation function. (In

this regard, consult the remarkable work of Norton, who reduced the calculation of ground wave losses to a practical form appropriate for use by AM broadcasters in this country. Ref. 3) Simply put, at these lower frequencies the problem with electrically small antennas is not only to reduce system losses, but simultaneously to produce vertical polarization. At AM broadcast frequencies, horizontal polarization attenuates so rapidly as to be of no practical significance. Any radiated HP, in fact, represents a serious degradation of system performance. A simple coil, multiturn loop or helix, no matter how efficient, will produce elliptical polarization. No matter how well constructed, these electrically small antennas are of no commercial value whatsoever to AM broadcasters since the inherent horizontal component of the radiation represents wasted power, and must not appear in the numerator of the radiation efficiency expression. This genus of electrically small antennas would be of significant value at low frequencies if they could also be made self-resonant and exclusively vertically polarized, while at the same time either requiring a ground system no larger than conventional short vertical towers, or none at all.

#### The Toroidal Helix Approach

One particularly intriguing idea is to take a self resonant normal mode helix, pull it around into a closed torus and let the resulting structure combine the tuning and matching networks with the radiating element itself. (See Ref.4). The radiation resistance is now in series with the coil inductance, and this combination is shunted by the helix turn-to-turn capacitance. The impedance transforming nature of this lumped circuit equivalent is well known, and it also has the advantage of transforming a relatively small feedpoint current into a stepped up current passing through the radiation resistance. The circuit equivalent used to be called a "current amplifier" in the old books on network theory.

The field theory analysis of the antenna is fairly straightforward. Since the structure is a slow wave self resonant helix, it is reasonable to assume a superposed sinusoidal distribution of electric and magnetic current, where the electric current is given by

$$(1) \quad J(r') = I_0 \cos(n\phi') \delta(\cos \theta') \frac{\delta(r'-a)}{a} \hat{\phi}'$$

the coordinates having their usual meanings, and the magnetic current is found from

$$(2) \quad I_m = 2 \pi f \mu (\pi b^2/s) I_0$$

where  $b$  is the helix radius and  $s$  is the turn-to-turn spacing. In these expressions,  $n$  is a mode number for the

current distribution. The radiated fields are determined in Ref.4 as:

$$(3a) \quad E_{\theta}^e = - \frac{\beta_g a Z_o I_o}{2r} \cos n\theta \quad J'_n(\beta_g a \sin \theta) e^{j(n\pi/2)}$$

$$(3b) \quad E_{\theta}^e = \frac{n\beta_g a Z_o I_o}{2r} \sin n\theta \quad \frac{J_n(\beta_g a \sin \theta)}{\beta_g a \tan \theta} e^{j(n\pi/2)}$$

$$(3c) \quad E_{\theta}^m = - \frac{\beta_g a I_m}{2r} \cos n\theta \quad J'_n(\beta_g a \sin \theta) e^{j(n\pi/2)}$$

$$(3d) \quad E_{\theta}^m = - \frac{n\beta_g a I_m}{2r} \sin n\theta \quad \frac{J_n(\beta_g a \sin \theta)}{\beta_g a \tan \theta} e^{j(n\pi/2)}$$

The superscript e indicates a field component attributable to the electric current and m to the magnetic current.  $J_n(x)$  is the usual Bessel function and  $\beta_g$  is the phase constant appropriate for the helix. These fields are not unlike those produced by the superposition of a resonant loop and a circular slot. However, because of the slow wave nature of the toroidal helix, the physical size has been considerably reduced.

Several variations of the basic configuration are now possible. By contrawinding the helix (Refs.4,5,6), the azimuthal component of electric current is cancelled out and one is simply left with what is commonly known as a poloidal flow of electric current. This is occasionally called a caduceus winding. The radiated fields are then given by only expressions (3c) and (3d). Further, and this is important, if one divides the Toroidal Helix into 4 or more segments it can be fed as Smith's cloverleaf antenna, so familiar from FM broadcasting. (See Refs.4,7). The resultant magnetic current distribution will be uniform, ( $n = 0$ ), and the radiated field is described simply by equation (3c).

We now have a Low Profile, slow wave, vertically polarized, self resonant, omni-directional (in the azimuthal plane) radiator with a substantial feed-point impedance. Consequently, the structure has considerable desirability as an Electrically Small Antenna at frequencies where ground-wave propagation or ground effects are important.

One does not get something for nothing, however. Chu's fundamental limit, which relates the lowest achievable Q of a lossless Electrically Small Antenna to its maximum physical dimension, is still in force. The Toroidal Helix is a remarkable structure, but it has been bought at the price of reduced bandwidth. Of course, one may make a trade-off between operational bandwidth and efficiency, if one so desires.

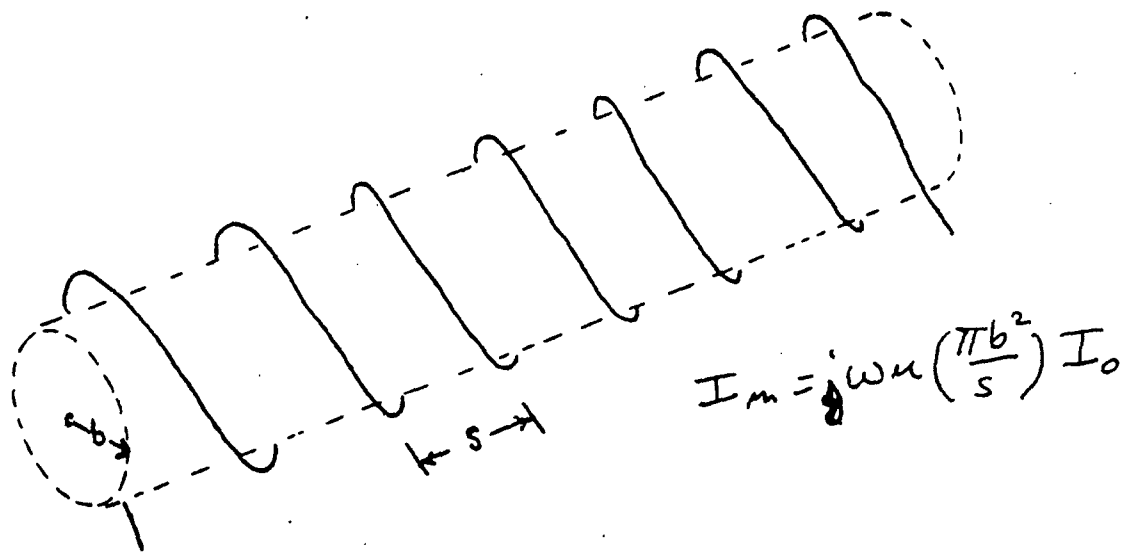
Lastly, several experimentally measured electrical properties should be reported. A typical structure consisting of 32 contrawound rings  $1/60^{\text{th}}$  of a wavelength in diameter, arranged in a torus of radius  $1/21^{\text{th}}$  of a wavelength had a resonant feed-point impedance on the order of 1500 ohms (purely resistive). The Toroidal Helix produced purely vertical polarization. (The horizontal component was at least 35 dB, or more, down from the vertical component.) The structure had a Q on the order of 35, as determined from impedance measurements. The measured field intensity was within 3 dB of a quarter wave monopole above 36 radials one quarter-wavelength long.

#### REFERENCES

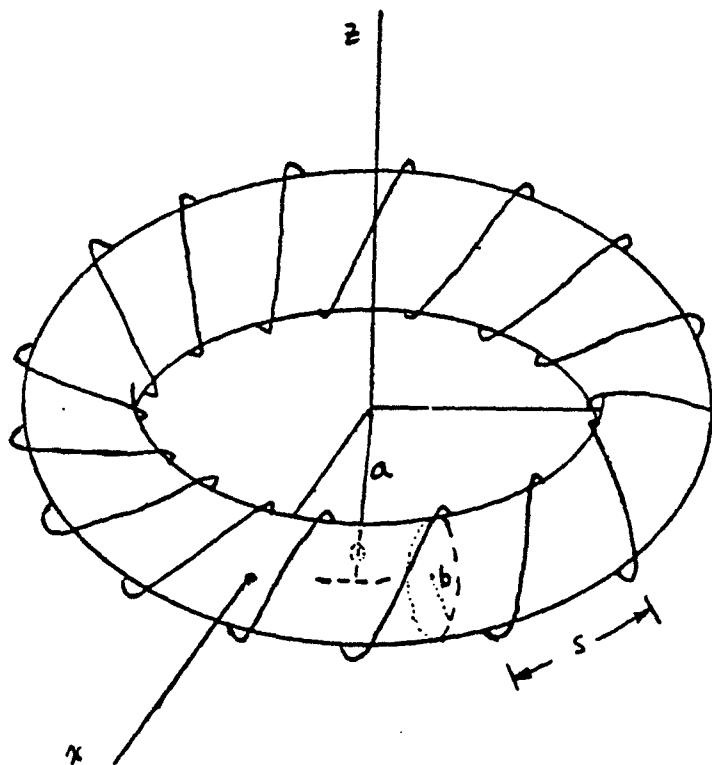
1. "Small Antennas", by H.A. Wheeler, (chapter 6 in Antenna Engineering Handbook, H. Jasik, 2<sup>nd</sup> edition, 1984). Consult the many references listed.
2. "Small Antenna Location Using Characteristic Modes", by E.H. Newman, IEEE Trans. on Ant. and Prop., Vol. AP-27, No. 4, July 1979, PP. 530-531.
3. "The Calculation of Ground-Wave Field Intensity Over a Finitely Conducting Spherical Earth", by K.A. Norton, Proc. IRE, Vol. 29, Dec., 1941, PP. 623-639.
4. "Toroidal Antenna", J.F. Corum, U.S. Patent #4,623,558; Canadian Patent #1,186,049; Australian Patent #548,541. Other Patents Pending.
5. "Modified Contrawound Helix Currents for High Power Traveling Wave Tubes", by C.K. Birdsall and T.E. Everhart, IRE Trans. on Electron Devices, ED-3, Oct. 1956, Pg. 190.
6. Electromagnetic Slow Wave Systems, by R.M. Bevensee, John Wiley, 1964, PP. 188-190.
7. "Cloverleaf Antenna for FM Broadcasting", by P.H. Smith, Proc. IRE, Vol. 35, Dec. 1947, PP. 1556-1563.

Corl: These are the overhead transparencies to go with the 20 min lecture.

6



(a)



(b)

Slow Wave  
Self Resonant Structure  
which combines the  
tuning & matching

networks with the  
radiating element itself.

Fig. 3. (a) A spiral helix or solenoid.  
(b) A toroidal helix.

"old Ref Data for Radio Engineers"

$$V_f = \frac{R}{Z} = \frac{1}{\sqrt{1 + 20 \left( \frac{D}{s} \right)^{1/2} \left( \frac{D}{\lambda_0} \right)^{1/2}}}$$

(D/λ<sub>0</sub>)

for  $\frac{D^2}{s \lambda_0} < 0.2$   
 $V_f = 2 \cdot 4 = \frac{2}{\lambda_0}$  for  $\frac{D^2}{s \lambda_0} > 0.4$

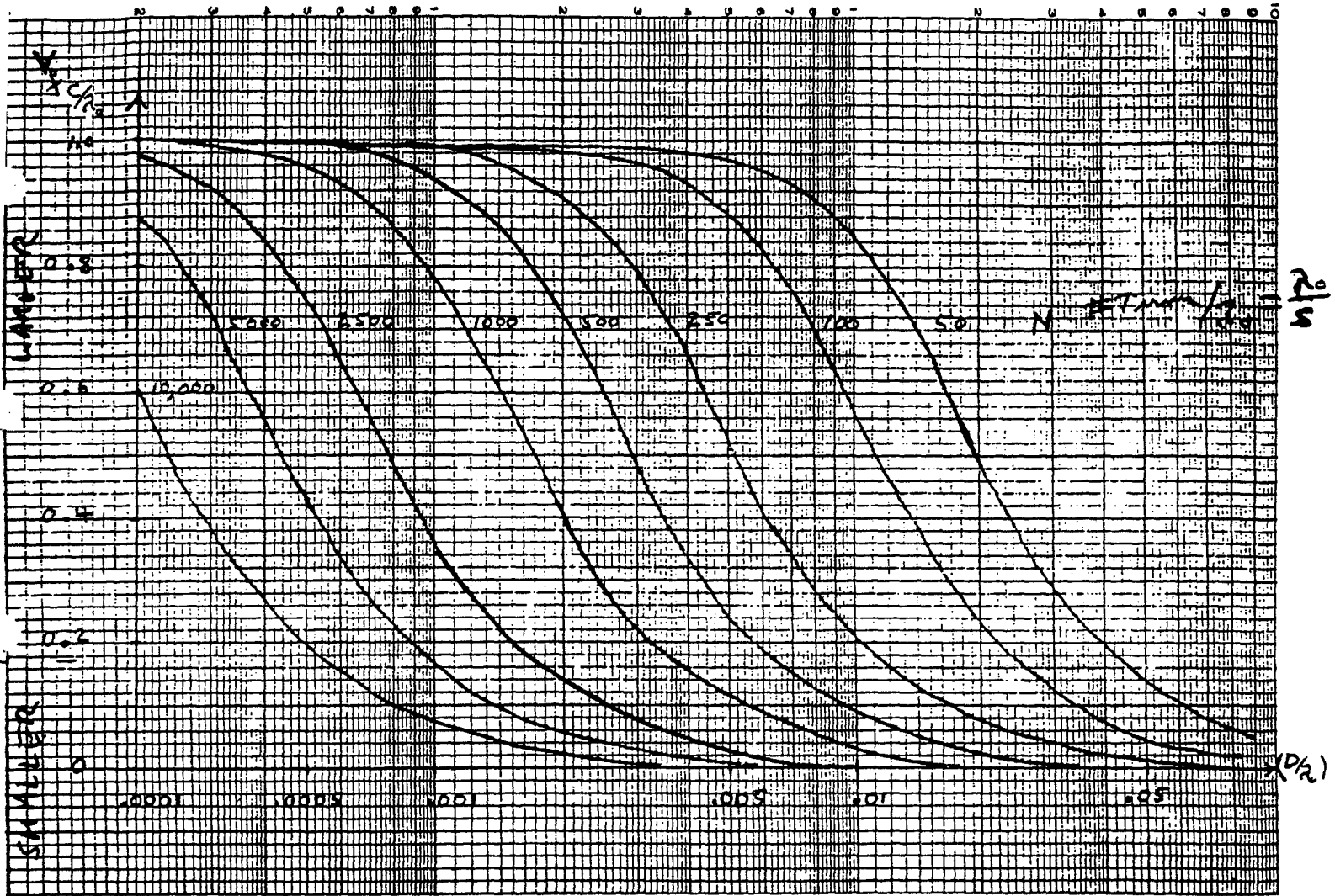


Fig. 6. A graph of equation 7, showing the effects on the velocity factor of varying the number of turns and diameter of a helix.

Pope "Hope Springs Eternal in the Human Breast."

H.A. Wheeler (1947): "A small antenna free of dissipation can extract from a radio-wave and deliver to a load an amount of power independent of the size of the antenna."

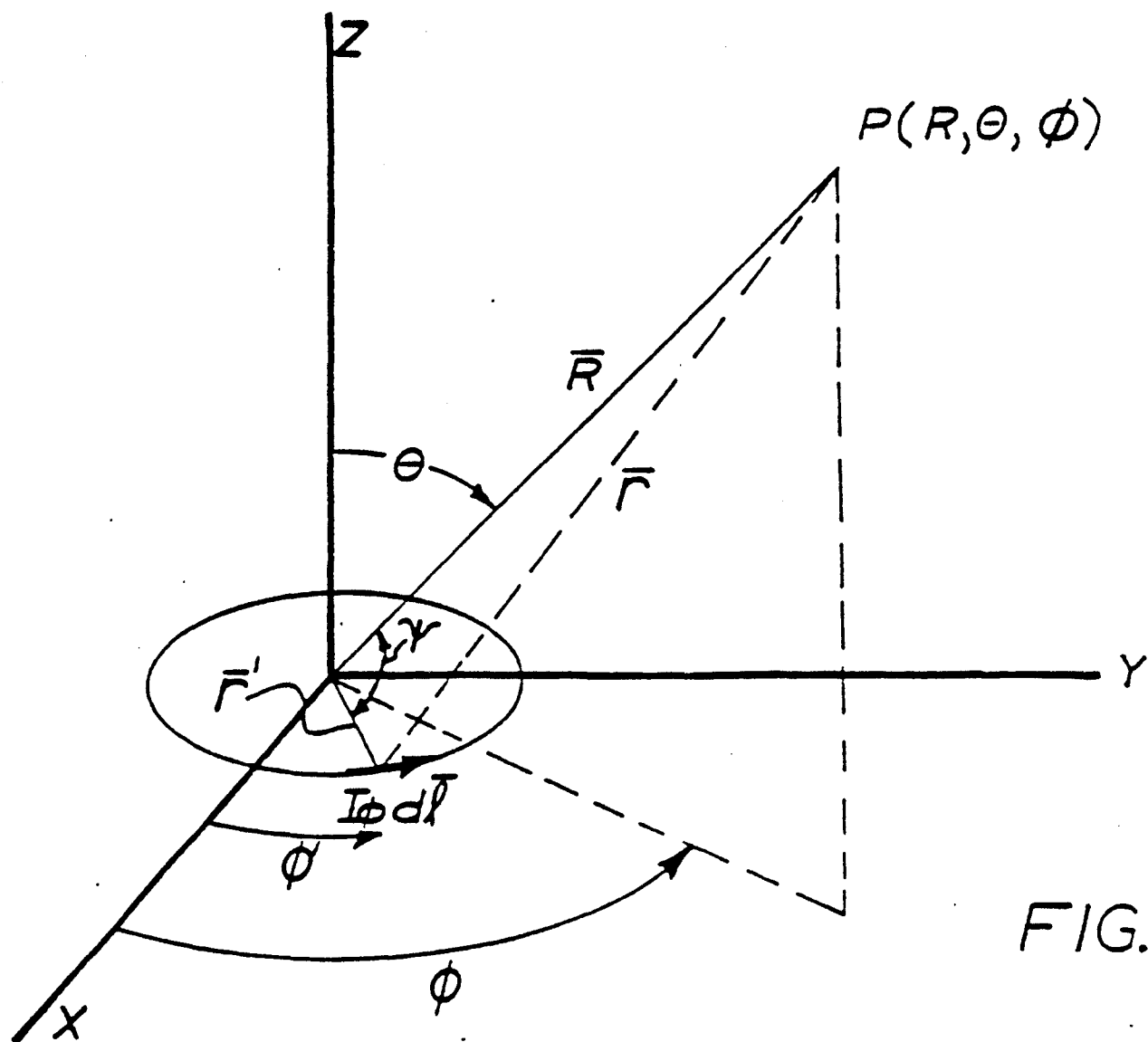
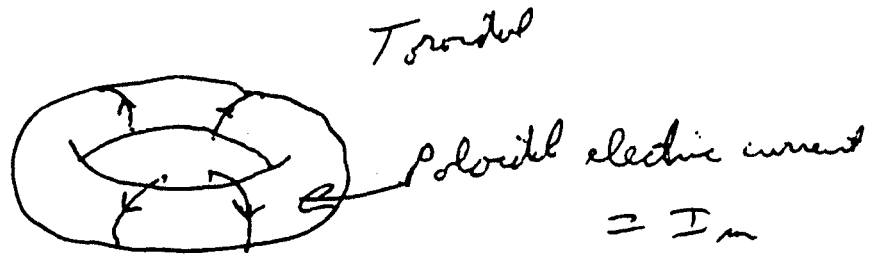


FIG.

$$\begin{aligned}\vec{r}' &= a\hat{r} \\ \vec{r} &= \vec{R} - \vec{r}'\end{aligned}$$





$$(3a) \quad E_{\phi}^e = - \frac{\beta_g a^2 I_o}{2r} \cos n\phi \quad J'_n (\beta_g a \sin \theta) e^{j(n\pi/2)}$$

$$(3b) \quad E_{\theta}^e = \frac{n\beta_g a^2 I_o}{2r} \sin n\phi \quad \frac{J_n (\beta_g a \sin \theta)}{\beta_g a \tan \theta} e^{j(n\pi/2)}$$

$$(3c) \quad E_{\phi}^m = - \frac{\beta_g a I_m}{2r} \cos n\phi \quad J'_n (\beta_g a \sin \theta) e^{j(n\pi/2)}$$

$$(3d) \quad E_{\theta}^m = - \frac{n\beta_g a I_m}{2r} \sin n\phi \quad \frac{J_n (\beta_g a \sin \theta)}{\beta_g a \tan \theta} e^{j(n\pi/2)}$$

The superscript e indicates a field component attributable to the electric current and m to the magnetic current.

Can wiggle the parameters and get figure 8 patterns

# Contrawound Winding

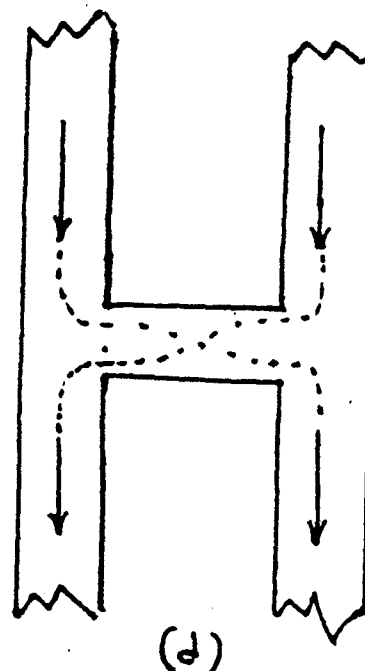
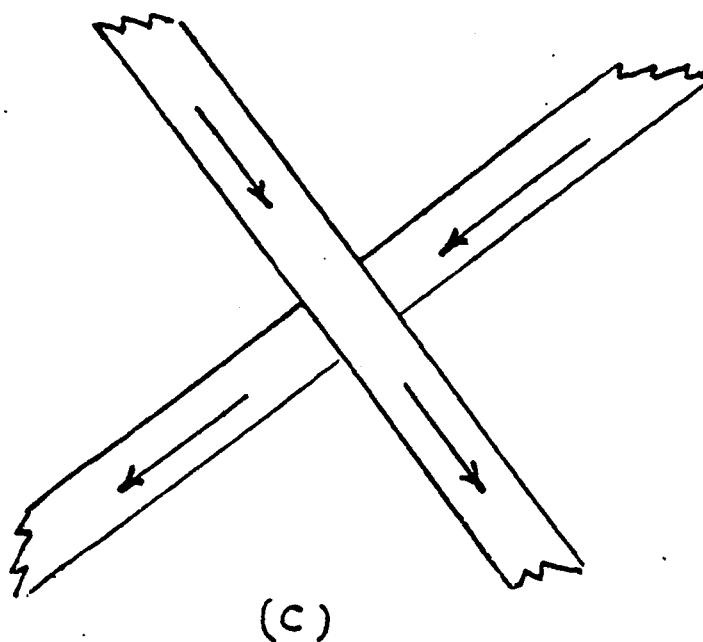
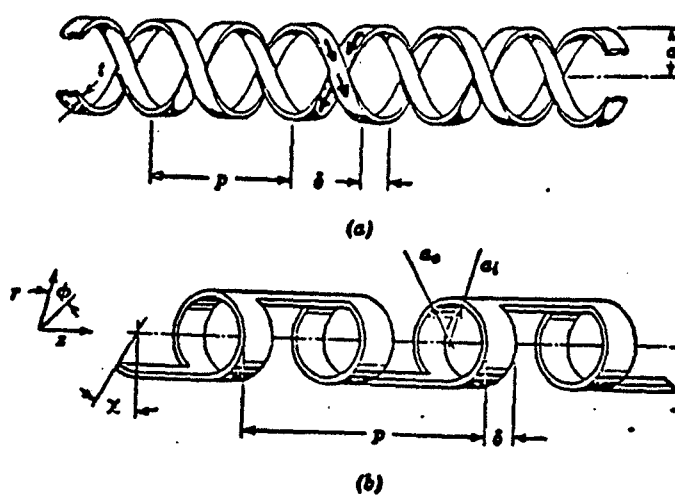


Figure 6. Contrawound Helices. (a), Structure analyzed by Chodrow and Chu. (b), Structure studied by Birdsall and Everhart. (c) and (d), Current paths on the contrawound helices of (a) and (b). In both cases, the longitudinal axis component of the electric current cancels out. When the structure is drawn into a closed torus, one is left with only a poloidal current flow.

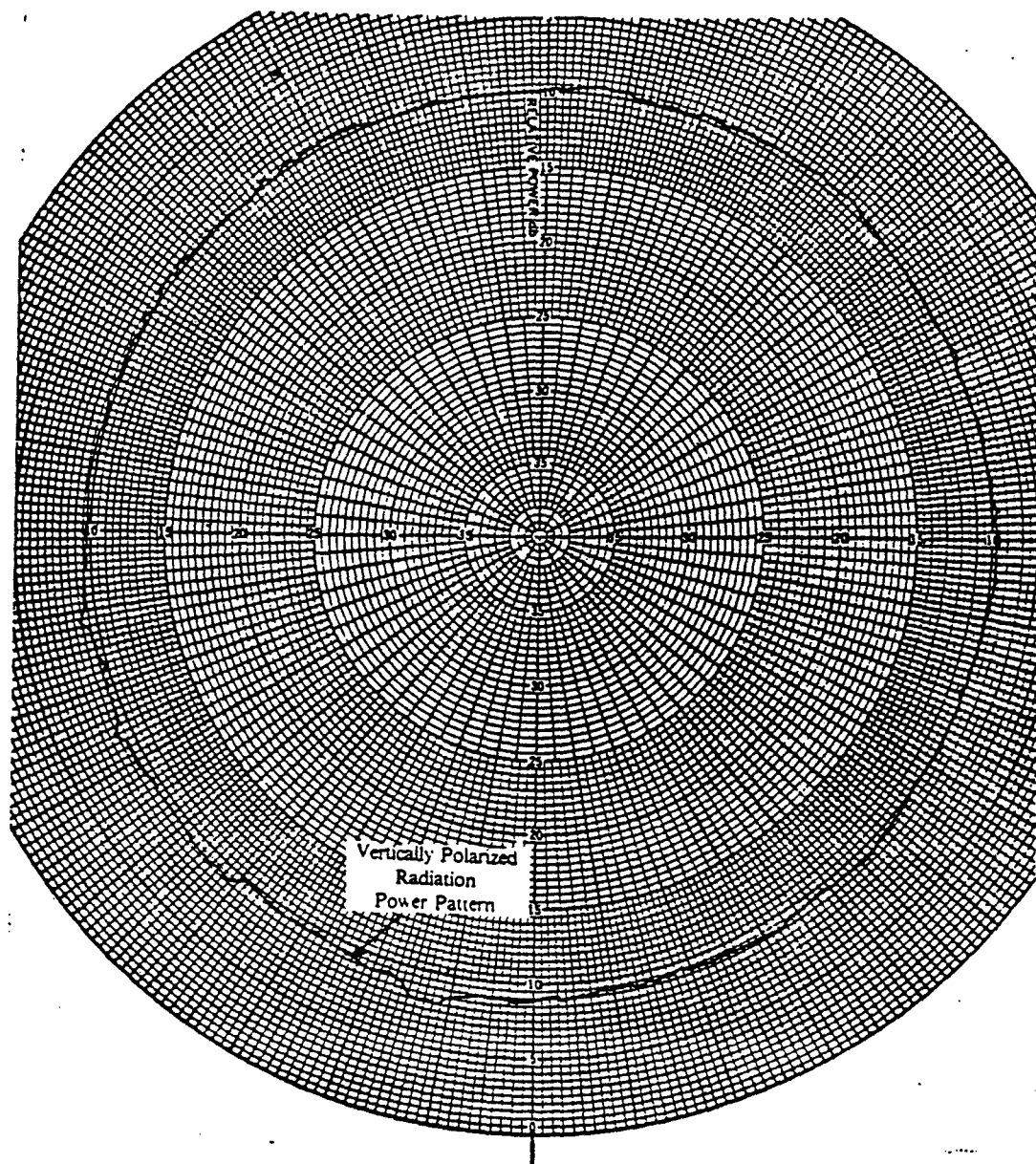


Figure . Measured radiation power pattern for an omnidirectional vertically polarized CPG antenna structure. The maximum physical dimension of this scaled model antenna was 0.075 wavelengths and the pattern was measured at a frequency of 70 MHz.

---

Use or disclosure of proposal data is subject to the restriction on the Title Page of this Proposal (1966 DEC).

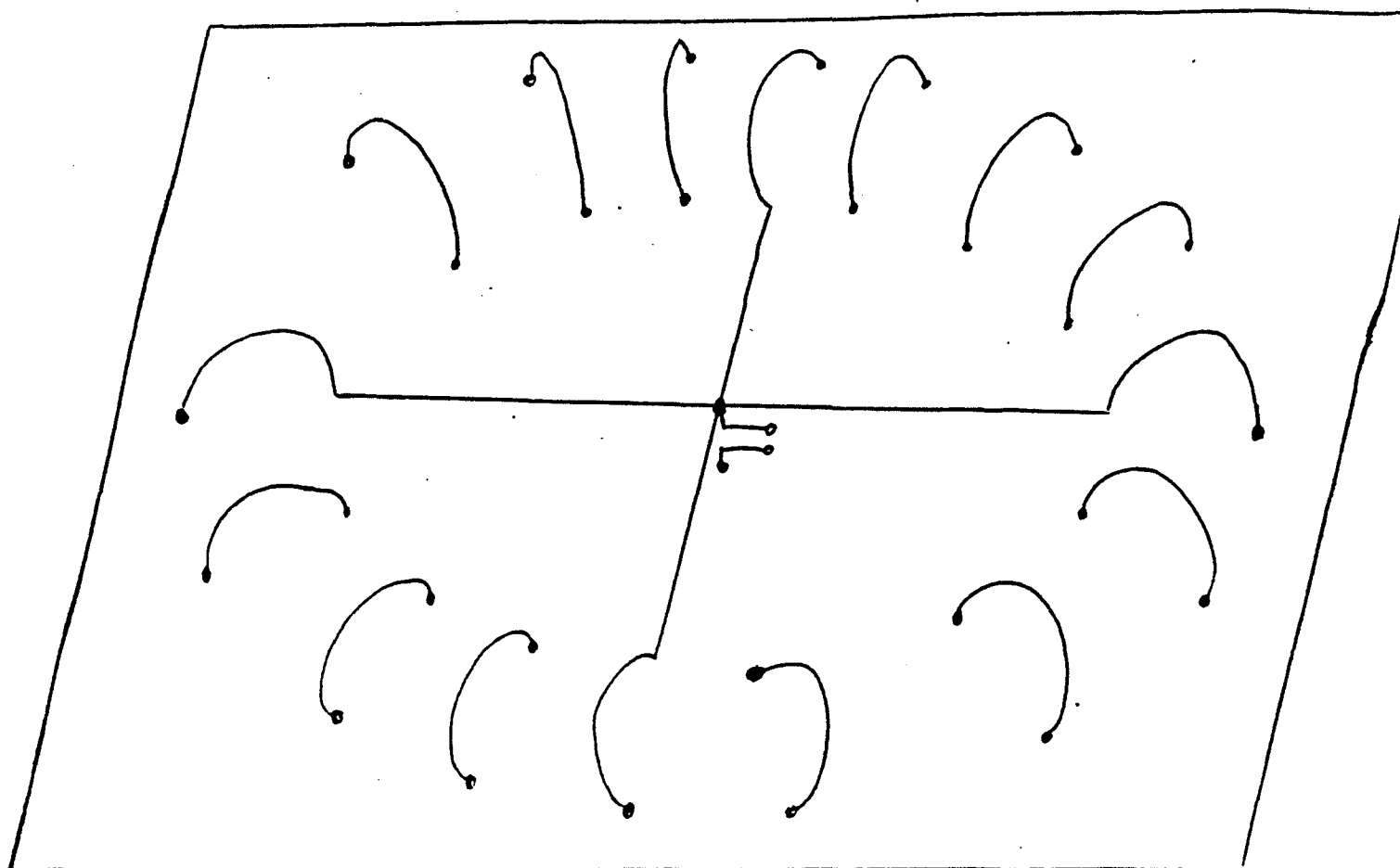
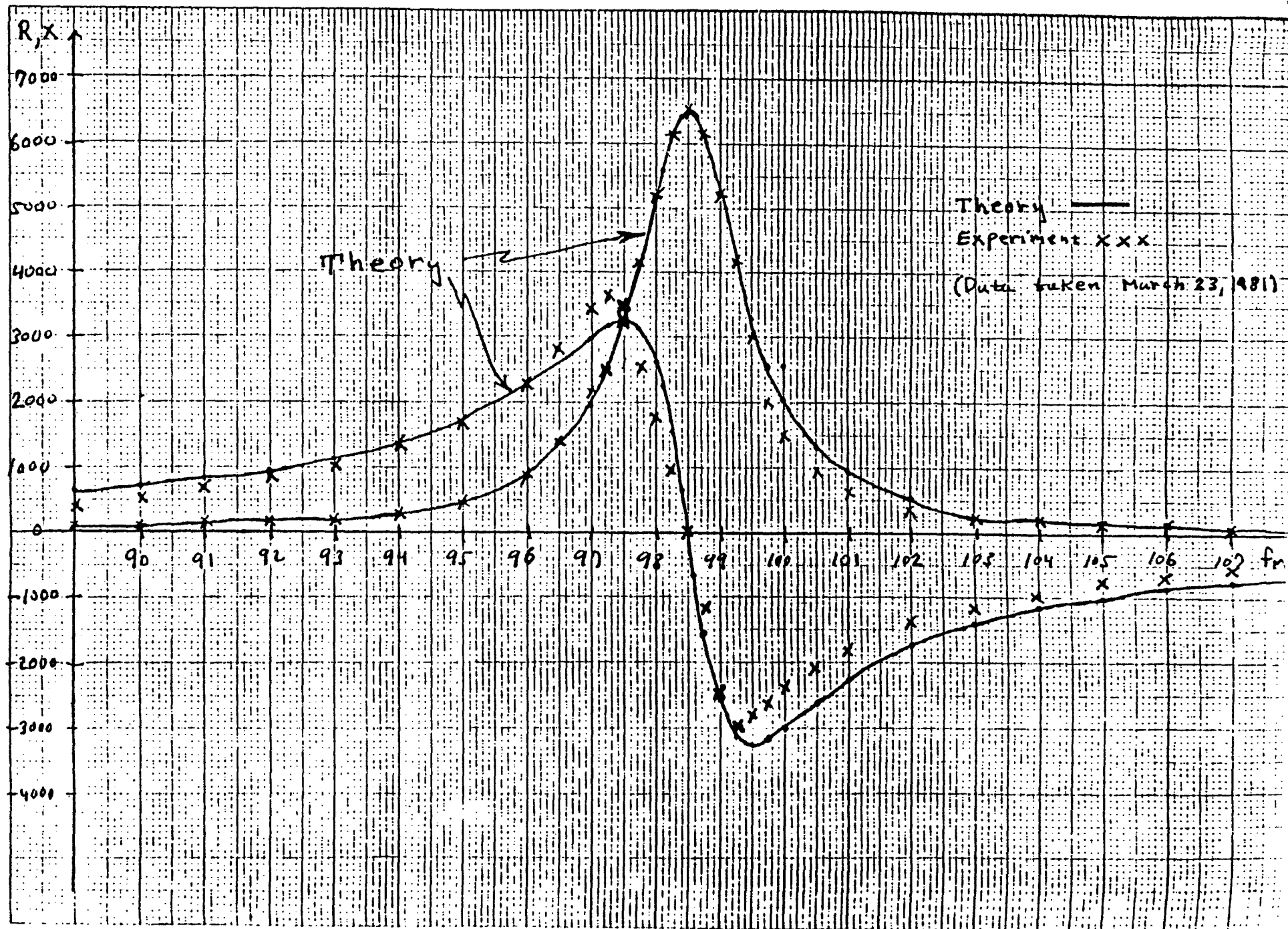


Fig.2. A contrawound toroidal helix above a large electrically conducting plane (with feed for producing the  $n = 0$  omnidirectional radiation pattern).

"A coupled resonator"  $\therefore$  Z-Matching



PLANE TOROIDAL HELIX

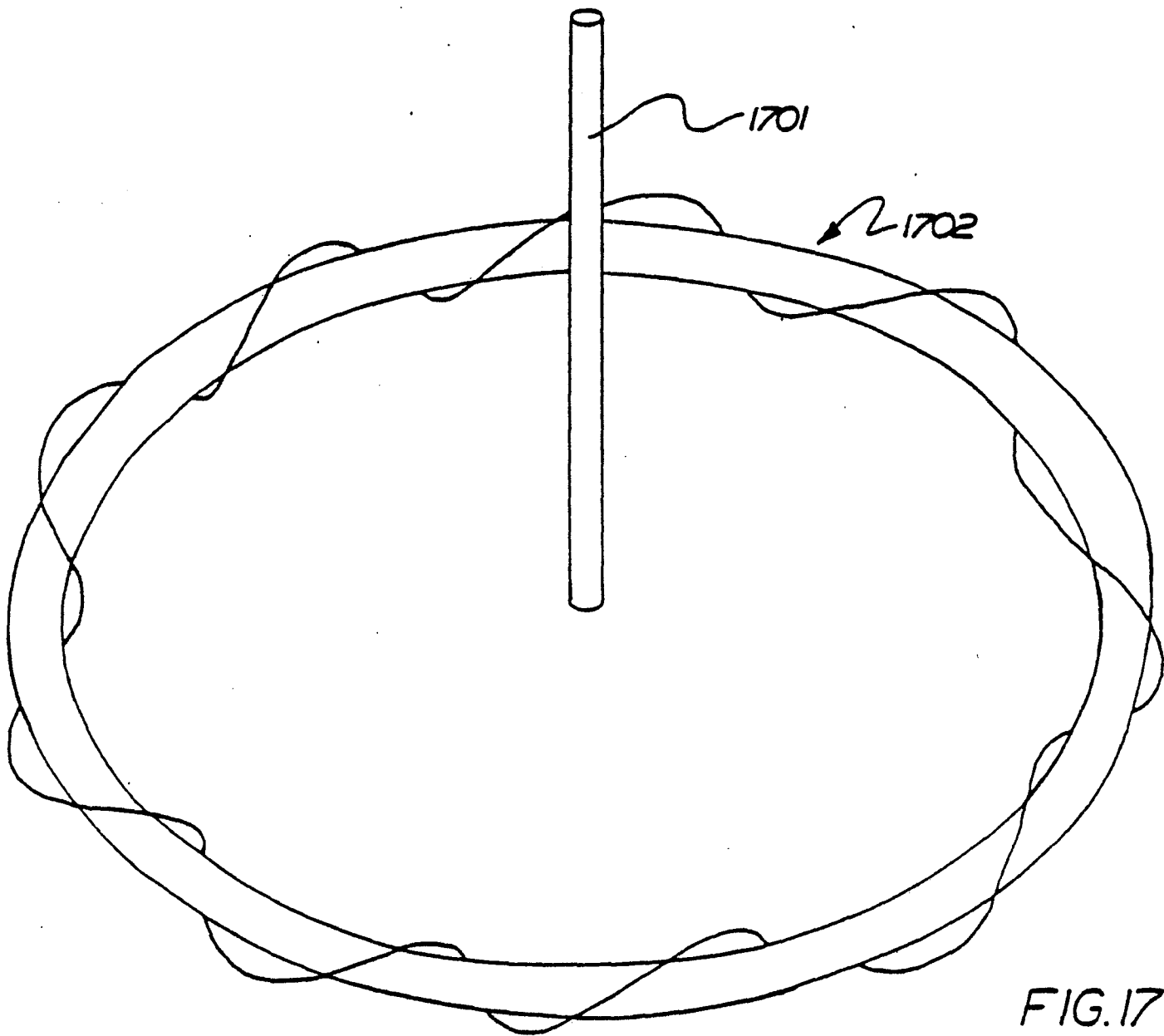


FIG.17

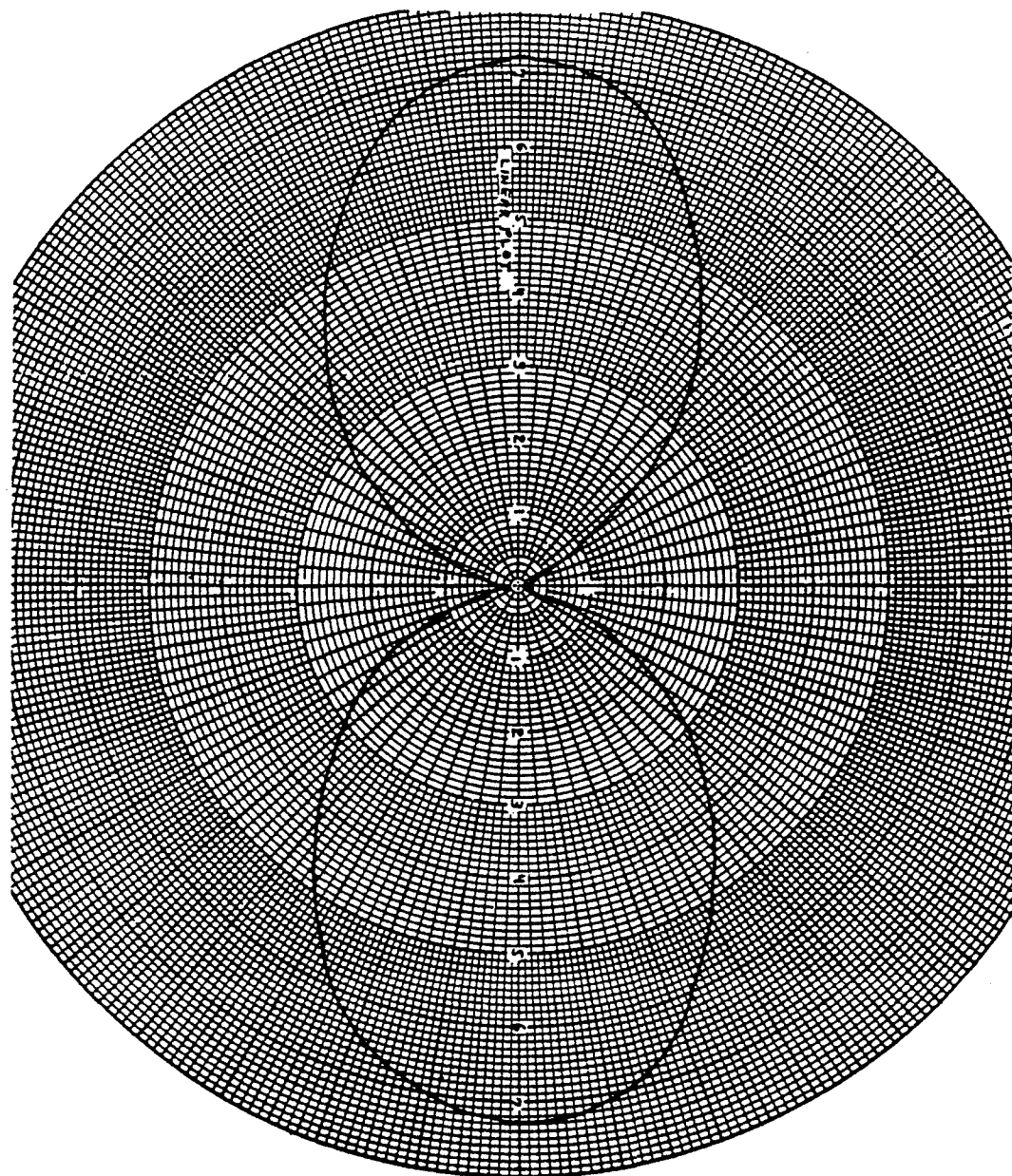


Figure 2. Measured *vertically polarized* azimuthal plane electric field pattern. The maximum dimension of the scaled model is less than 14 inches. The measurement was performed at 80 MHz.

## [54] TOROIDAL ANTENNA

[76] Inventor: James F. Corum, Rte. 9, Box 207-B,  
Morgantown, W. Va. 26505

[21] Appl. No.: 795,721

[22] Filed: Nov. 7, 1985

## Related U.S. Application Data

[63] Continuation of Ser. No. 514,176, Jul. 15, 1983, abandoned, which is a continuation-in-part of Ser. No. 167,329, Jul. 9, 1980, abandoned.

[51] Int. Cl.<sup>4</sup> ..... H01Q 11/14

[52] U.S. Cl. .... 343/742; 343/744

[58] Field of Search ..... 343/742, 743, 744, 856,  
343/895, 908

## [56] References Cited

## U.S. PATENT DOCUMENTS

3,278,937	10/1966	Leydorf	343/856
3,365,721	1/1968	Bittner	343/856
3,646,562	2/1972	Acker et al.	343/720

## FOREIGN PATENT DOCUMENTS

1751249 8/1957 Fed. Rep. of Germany .

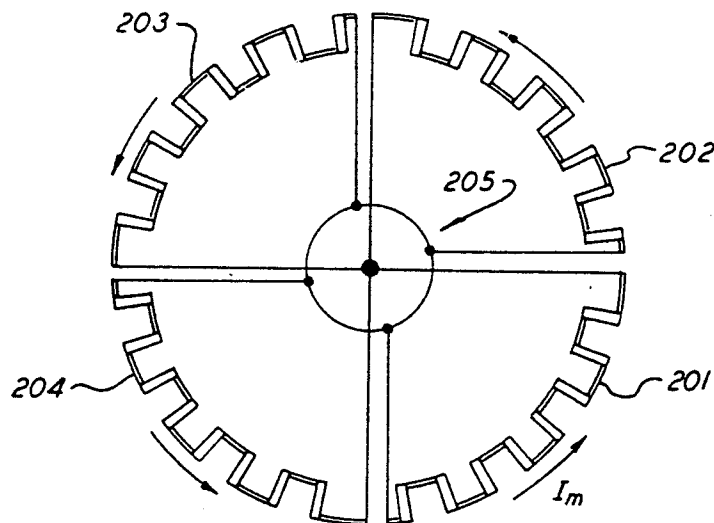
Primary Examiner—Eli Lieberman

Attorney, Agent, or Firm—Jeffrey A. Wyand

## [57] ABSTRACT

An electrically small, efficient electromagnetic structure, that may be used as an antenna or waveguide probe, having an electromagnetically closed, velocity-inhibiting conducting path, for supporting a standing, inhibited-velocity wave in response to the flow of an electrical current through the path and a process for establishing the standing wave. Use of the structure is particularly advantageous at the lower end of the electromagnetic spectrum, where various embodiments produce purely vertically polarized radiation in directional and omnidirectional patterns. Various embodiments of the structure include multiple conducting paths and image means to complete the conducting path.

22 Claims, 29 Drawing Figures





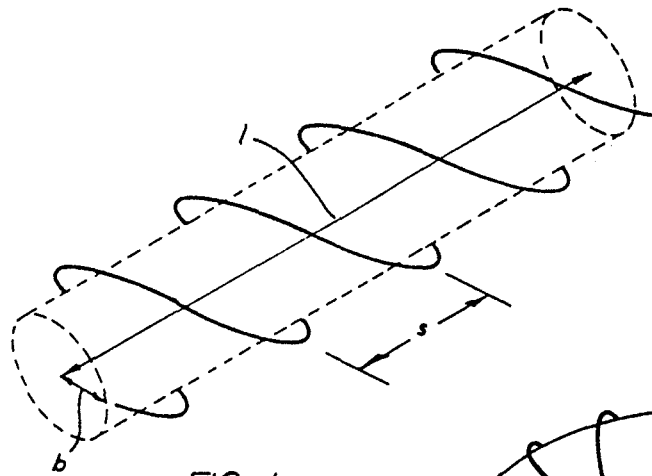


FIG. 1  
Prior Art

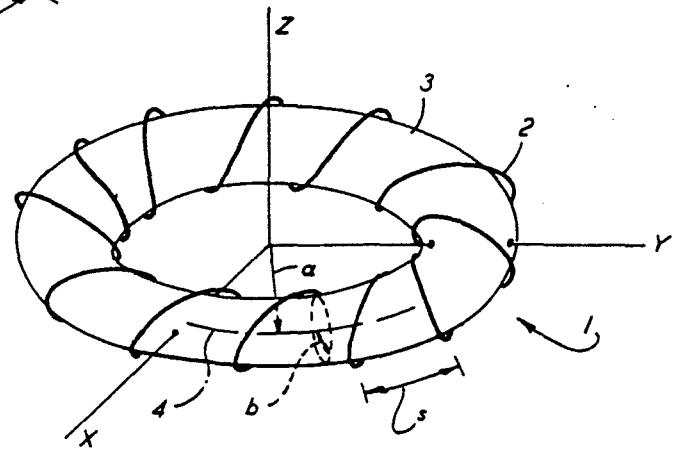


FIG. 2

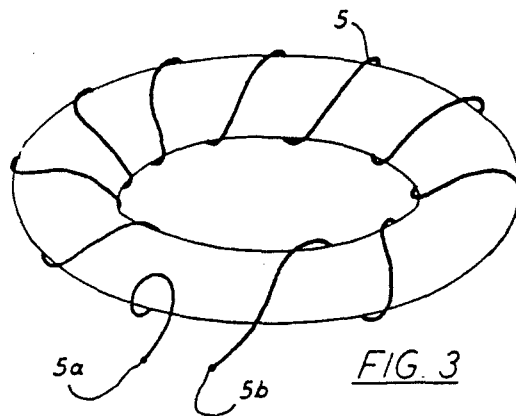


FIG. 3

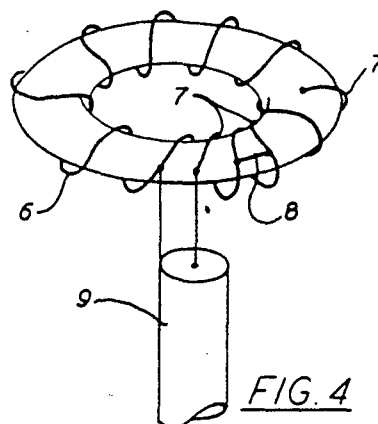


FIG. 4

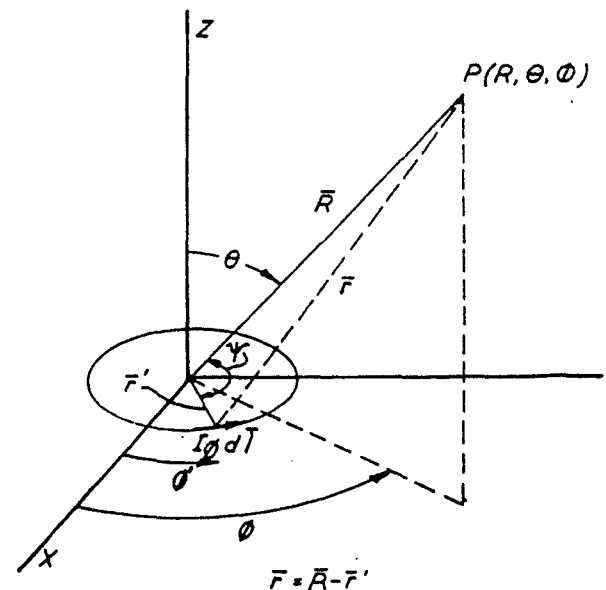
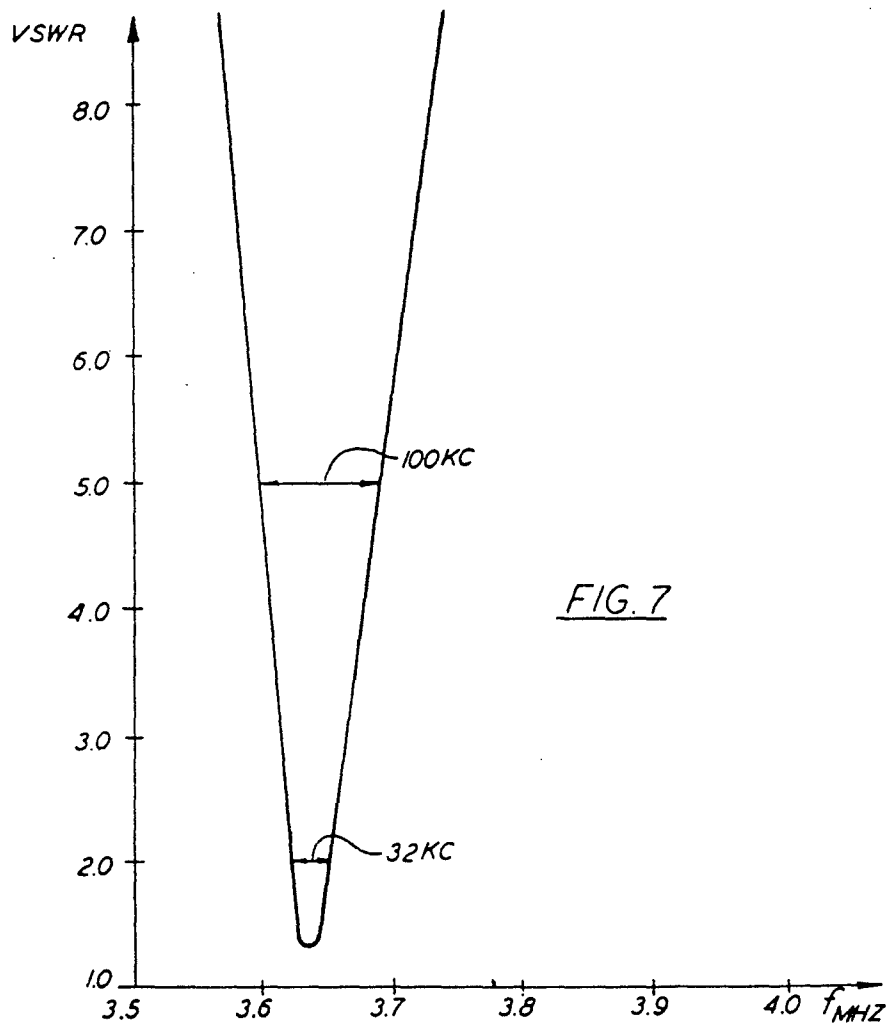
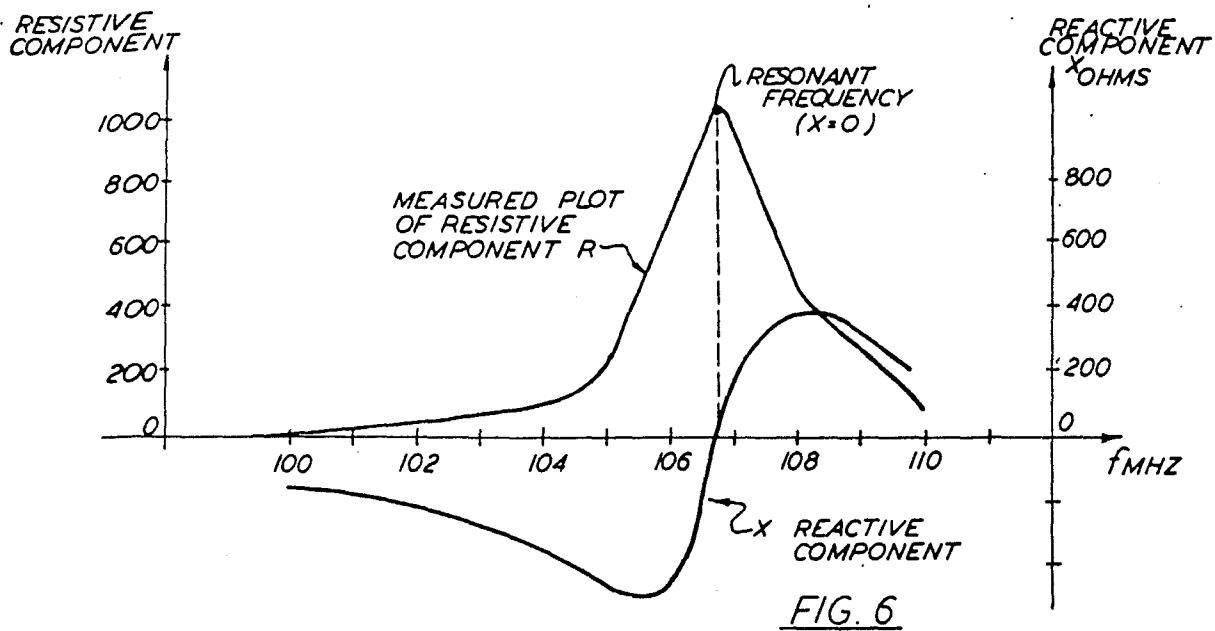


FIG. 5



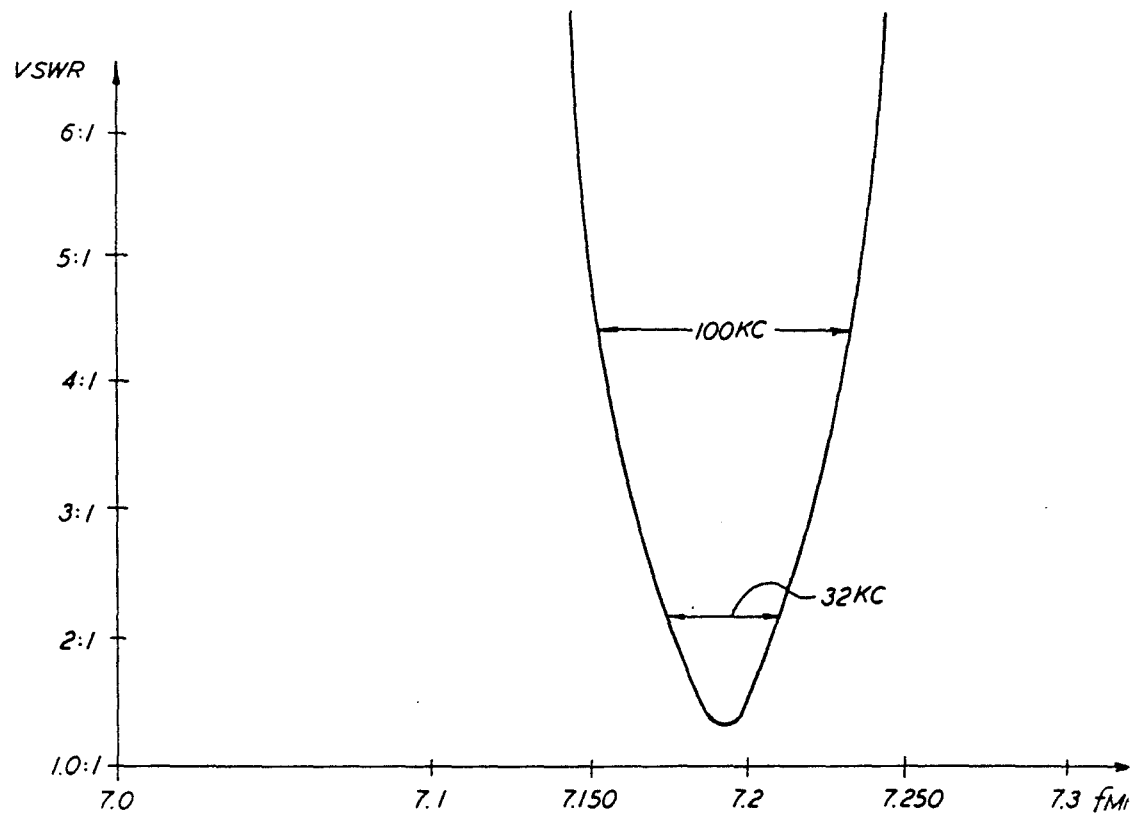


FIG. 8

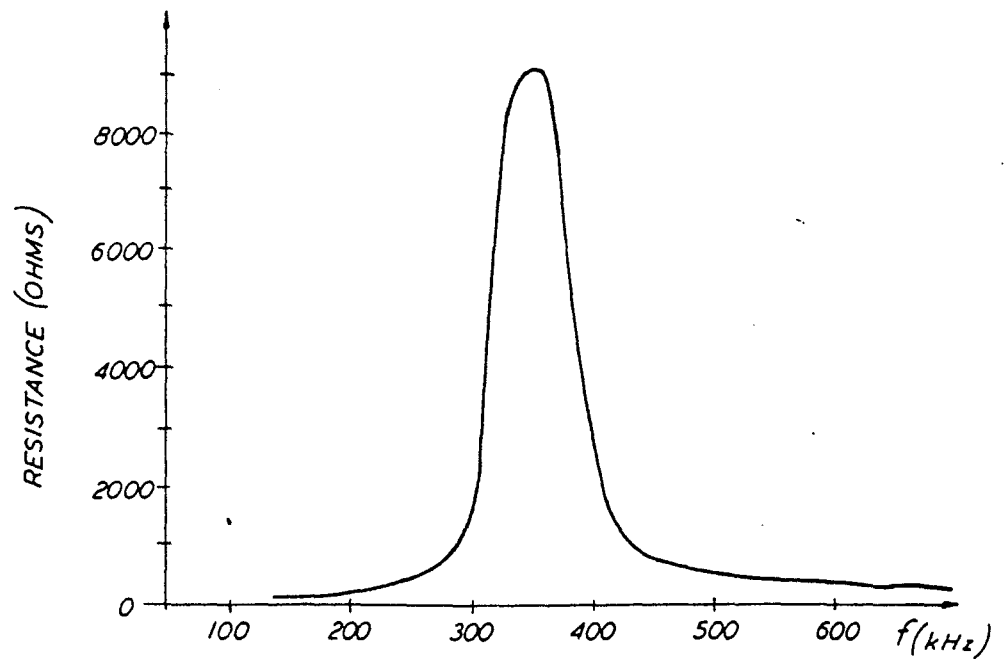


FIG. 9

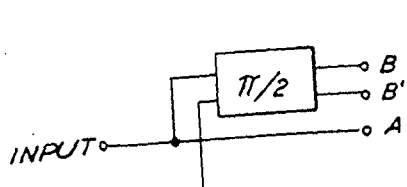


FIG. 12b

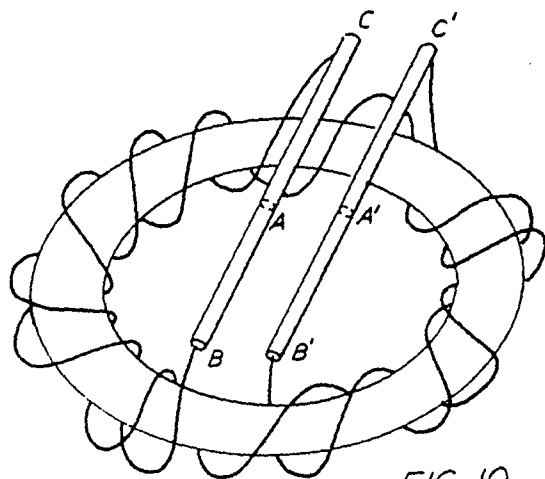


FIG. 10

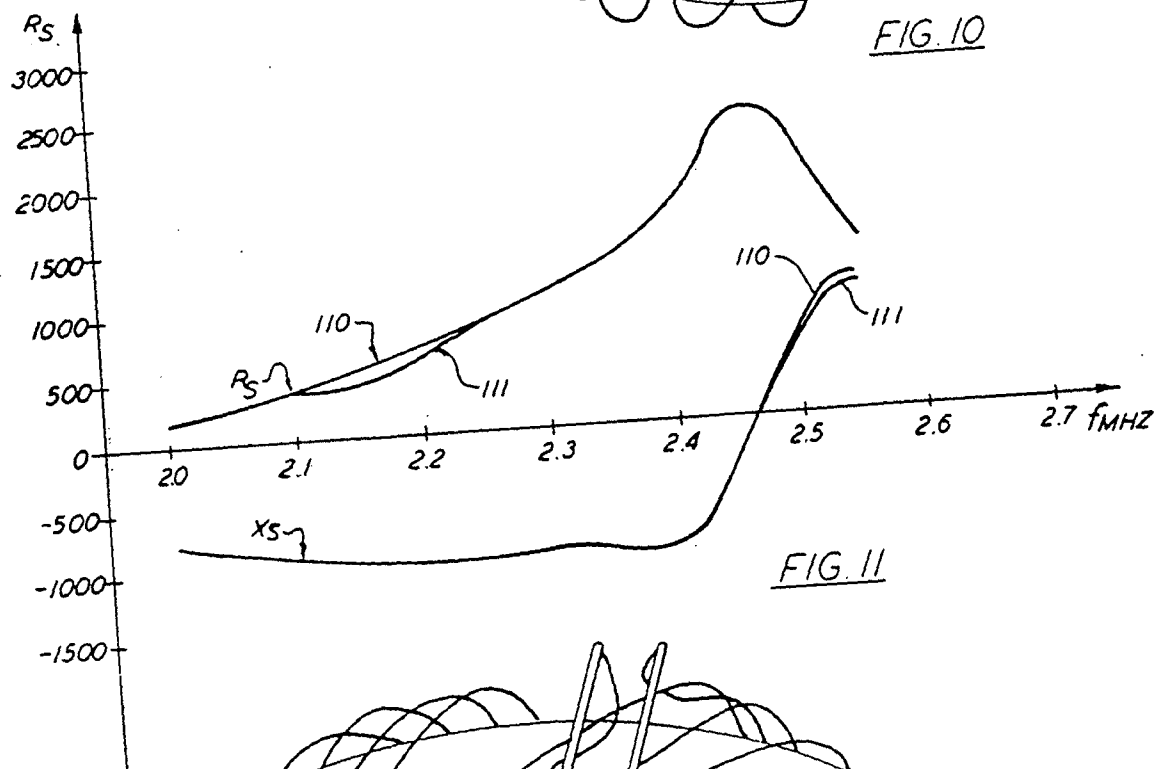


FIG. 11

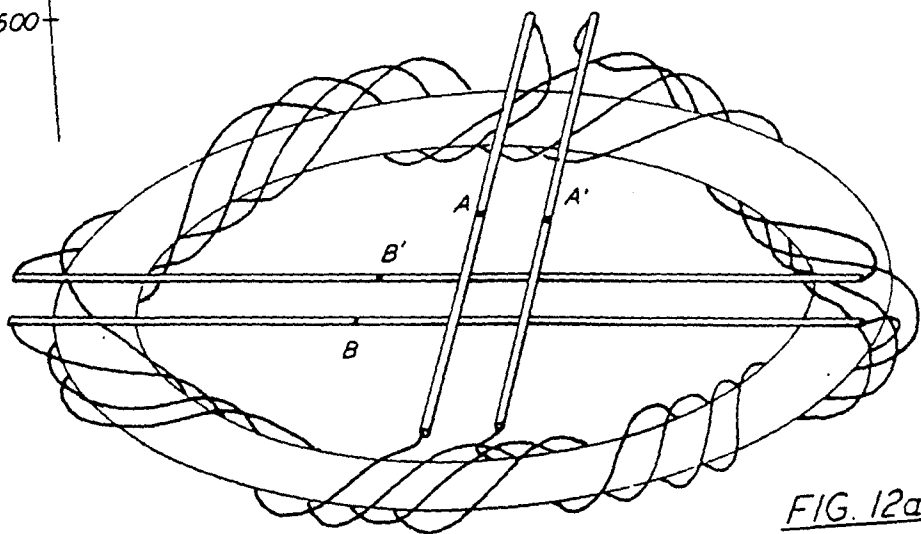


FIG. 12a

FIG. 13

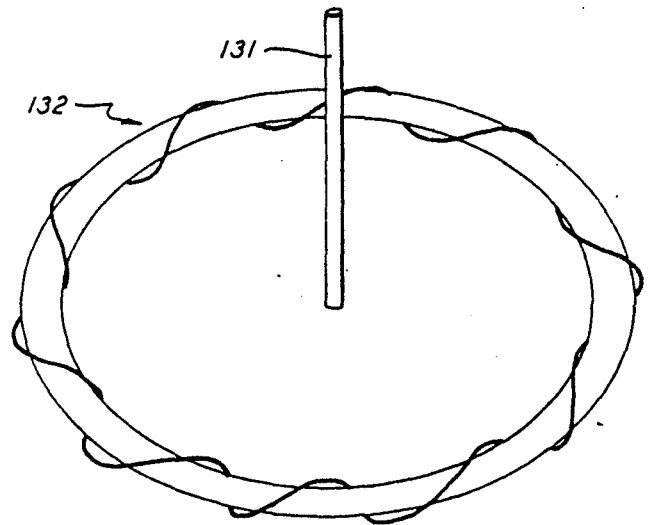


FIG. 14

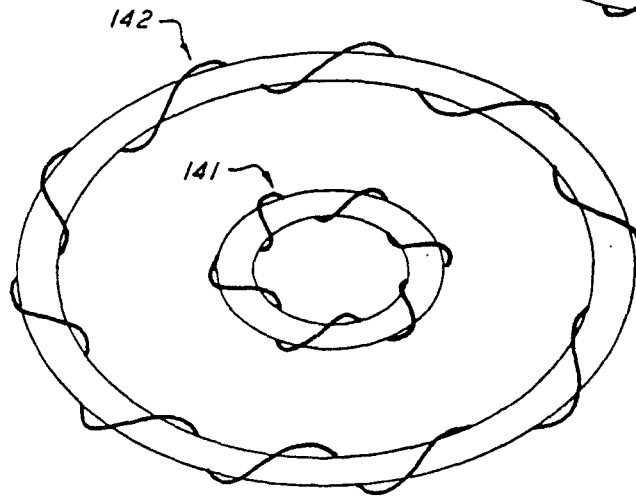
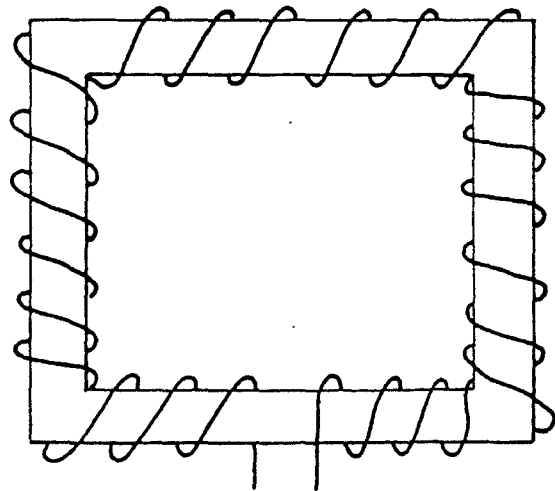


FIG. 15



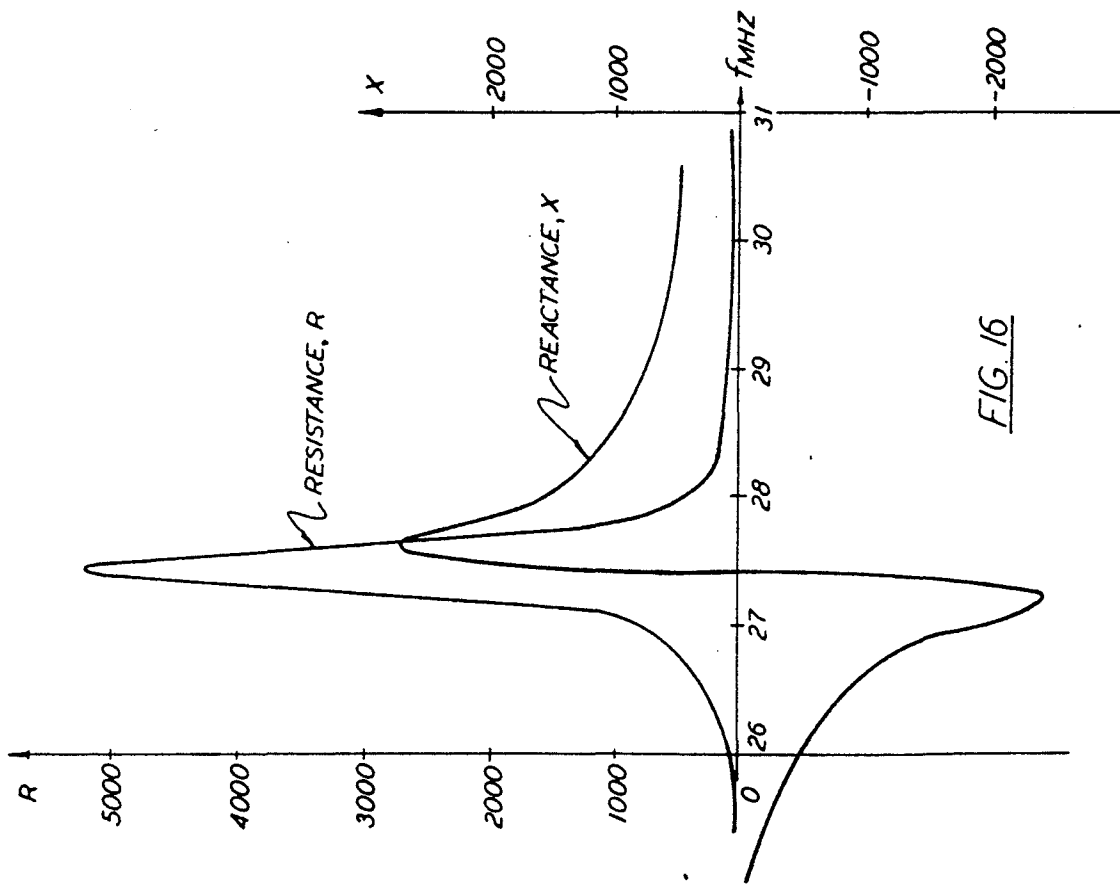


FIG. 16

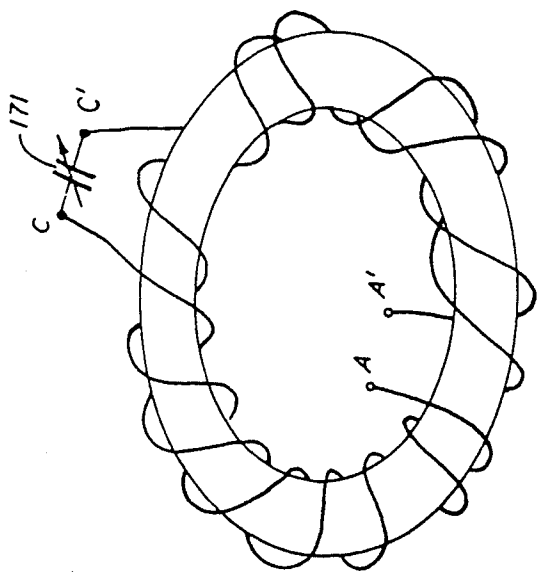


FIG. 17



FIG. 18a

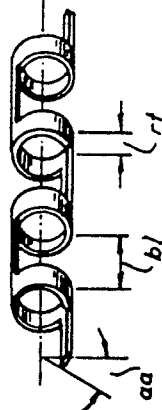


FIG. 18b  
Prior Art

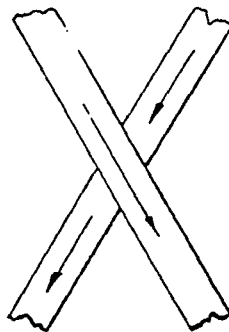


FIG. 19a

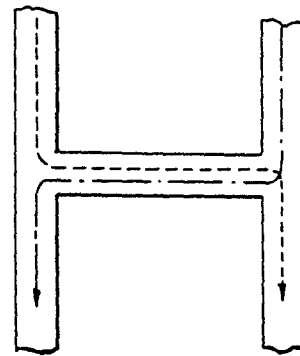


FIG. 19b

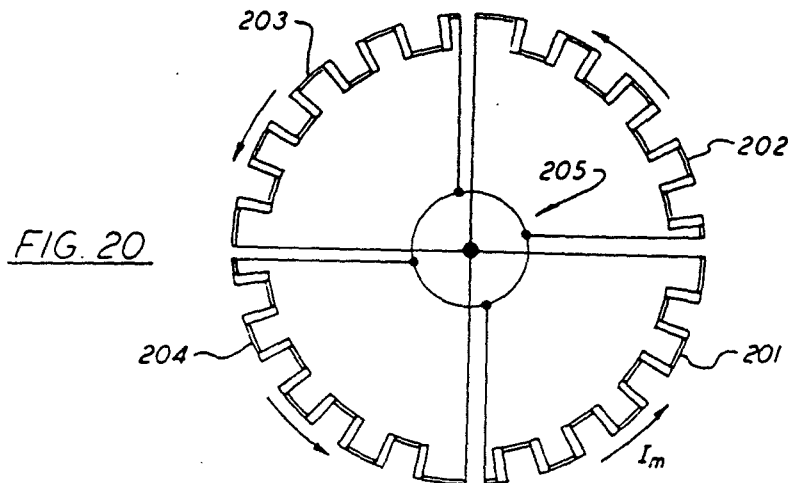


FIG. 20

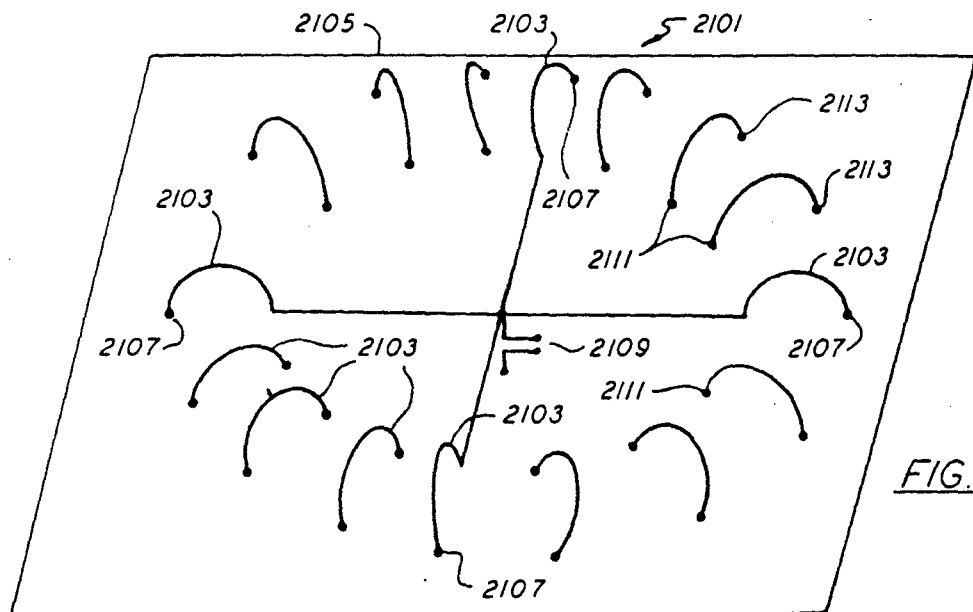


FIG. 21

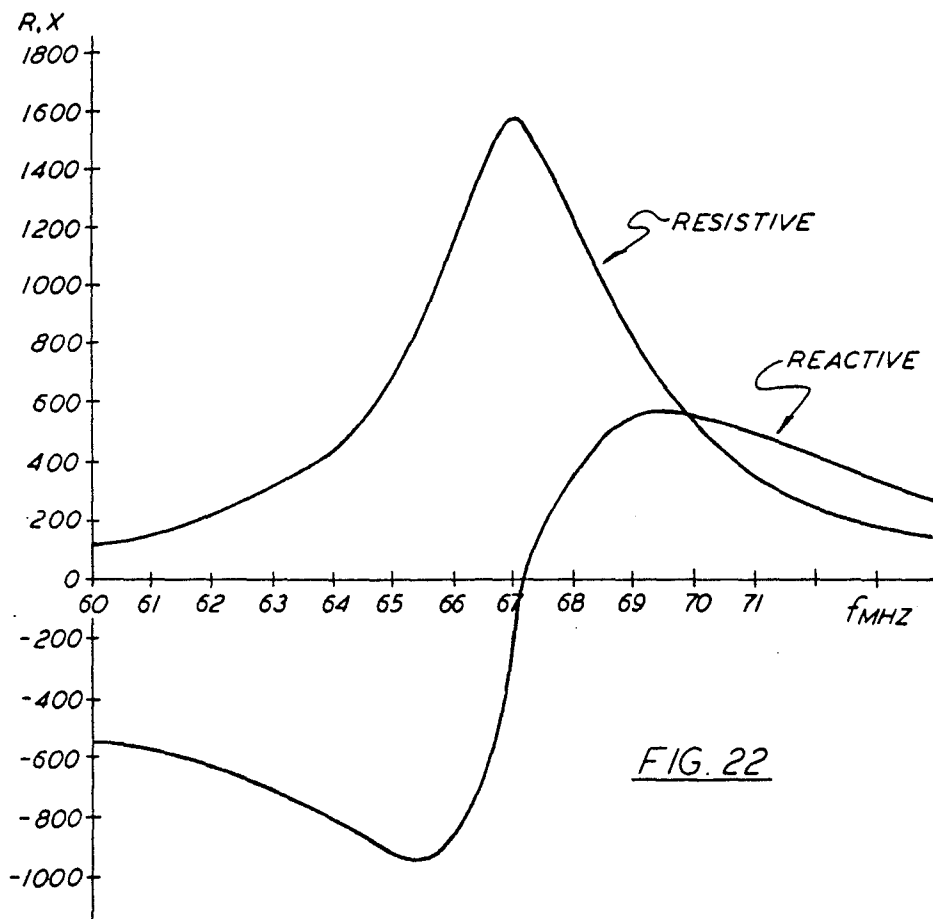


FIG. 22

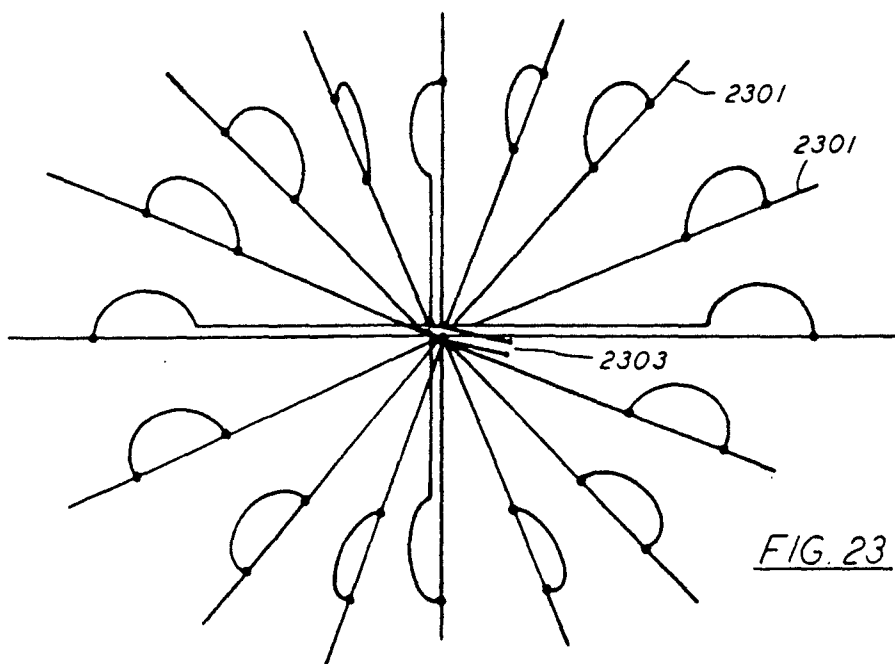
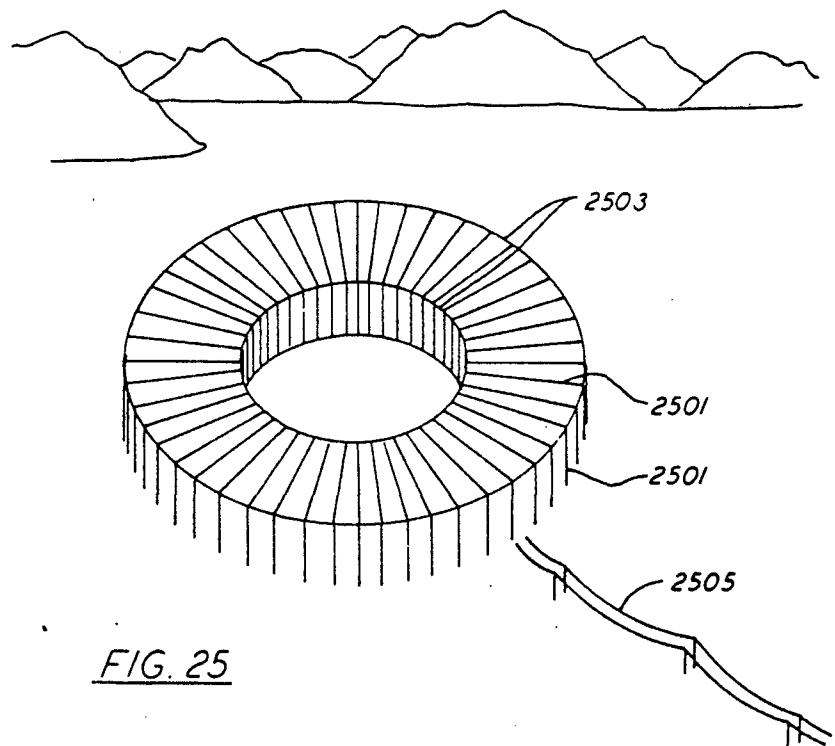
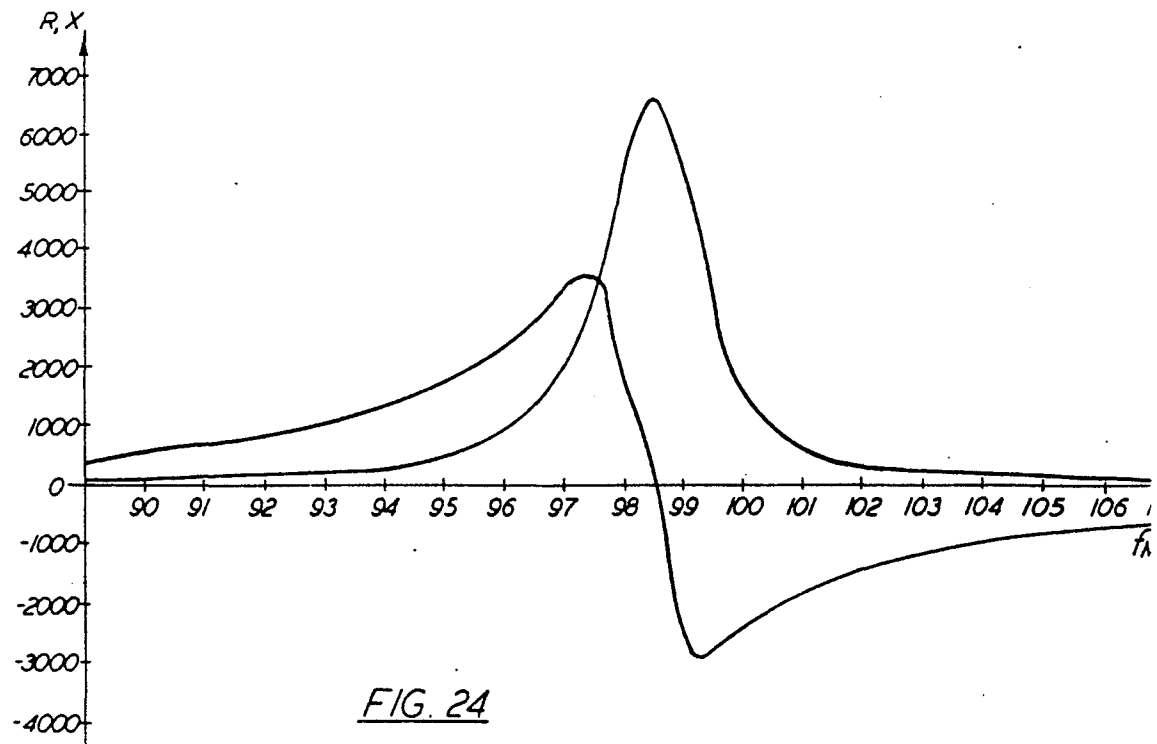


FIG. 23





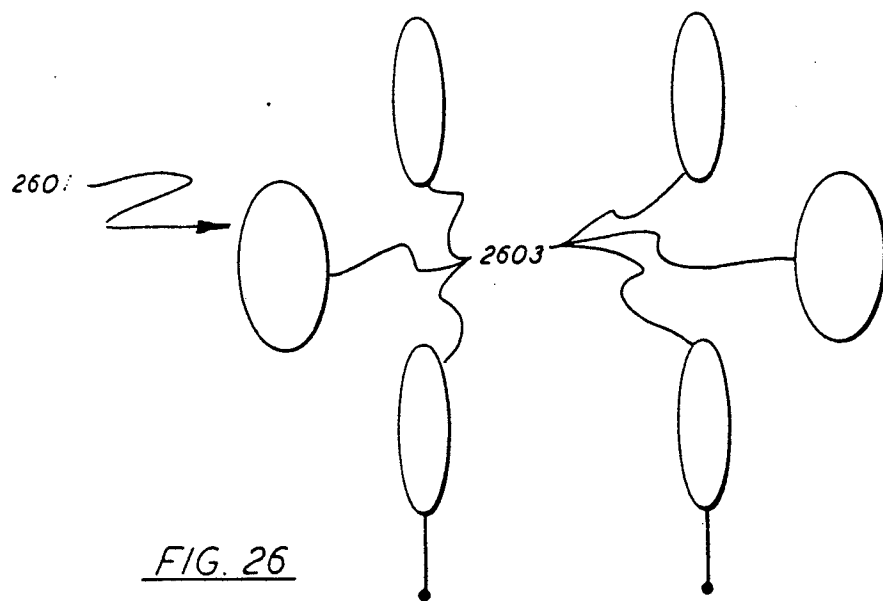


FIG. 26

## TOROIDAL ANTENNA

This application is a continuation of U.S. patent application Ser. No. 514,176 filed July 15, 1983, now abandoned, which is a continuation-in-part application of U.S. patent application Ser. No. 167,329 filed July 9, 1980, now abandoned.

## BACKGROUND OF THE INVENTION

The present application relates to electromagnetic structures that can function as antennas for transmitting or receiving electromagnetic energy and as waveguide probes in cavities for injection or extraction of electromagnetic energy.

It is well known in the electromagnetic arts that efficient, linear antennas are usually constructed from elements having lengths that are significant portions of a free-space wavelength at the operating frequency. It is also known that if those lengths are made equal to integer multiples of one quarter wavelength, standing waves may be induced in the antenna. It is also understood that operation of an antenna at one of its self-resonance frequencies, if possible, is desirable to increase antenna efficiency. At the self-resonant frequencies, standing waves are produced on antennas and the reactive component of the feedpoint impedance is zero. This efficient operation contrasts with the familiar "matched" operation where the impedance of an antenna is conjugately matched by an external network to the impedance of a transmitter or receiver to improve performance. Reactive power losses are experienced both in the antenna and in the matching network, when a matching network is used, so that overall system efficiency is not maximized. It is also established that horizontally polarized electromagnetic waves suffer greater ground wave propagation losses than do vertically polarized waves. Therefore, vertically polarized waves are preferred over horizontally polarized waves for communication over the surface of the earth.

It is recognized that a vertical antenna having a length equal to one quarter of a wavelength at the operating frequency provides a desirable vertically polarized, omnidirectional radiation pattern. However, because wavelength increases inversely with operating frequency, the length, i.e., the height, of such an antenna becomes unmanageably long at frequencies below about 1 MHz. As a consequence of the long wavelengths below 1 MHz, various antenna structures have been employed at those frequencies. Generally, those antenna structures are physically large, may not necessarily produce the desired vertically polarized signal, and are not self-resonant. Therefore they are inherently inefficient as well as being unwieldy.

The goal of constructing a physically small, but self-resonant (and therefore efficient) antenna or waveguide probe has eluded electromagnetic arts specialists for over three-quarters of a century. An antenna or other electromagnetic structure is electrically small when its physical size is small relative to the free-space wavelength at which it operates. Thus, at the lower end of the radio frequency spectrum where wavelengths are relatively long, a physically large electromagnetic structure may still be electrically small. As used here, the term "electrically small" means that the physical dimensions of an electromagnetic structure, measured in terms of free-space wavelengths, at the operating

frequency, are small, whether or not the structure may be electromagnetically self-resonant.

## SUMMARY OF THE INVENTION

In the present invention electrically small, yet self-resonant and, therefore, efficient, electromagnetic structures are disclosed. These structures may be used as antennas or waveguide probes. By employing a slow wave structure including an electromagnetically closed path and by operating the structure at one of the frequencies at which an inhibited-velocity standing wave is established along the closed path, a small, yet self-resonant, i.e., efficient, antenna or probe may be achieved. These structures are not only self-resonant (i.e., have a nonreactive input impedance), but also possess relatively large radiation resistances.

A particularly useful embodiment of the inventive structure, and one that may be used as a building block to build more complex structures, includes a toroidal helical electrically conducting path. In a simple case the structure has a single conductive path, such as a copper wire or other electrical conductor, disposed on the surface of a torus in uniformly spaced turns. The axis of the helical path lies on a circle which is described by the major radius of the torus. (A toroidal surface is generated by the rotation of a closed planar figure about a rotational axis lying outside the figure. When the figure is a circle, the surface generated is a torus. For a torus, the distance between the rotational axis and the center of the rotated circle is the torus' major radius. When the conducting path on the toroidal surface is electrically excited in a pre-selected frequency range, a pair of slow electromagnetic waves, i.e., ones with propagation velocities less than the speed of light, propagates along the path. At the resonance frequencies of the toroidal path, an inhibited-velocity standing wave is established along the electromagnetically-closed path which in this elementary example is approximately equal to the circumference of the torus. Because of the inhibited-velocity propagation, i.e., the slow wave effects imparted by the structure, the standing wave that is established has an inhibited or guide wavelength. That wavelength is shorter than a free-space wavelength at the frequency of resonance. Therefore, at the primary resonance frequency, the toroidal structure behaves electrically as if its circumference were or free-space wavelength long when that circumference actually physically smaller than one free-space wavelength. Thus an electrically small, resonant structure is achieved. The structure also has higher mode resonance frequencies. When it is operated at one of those frequencies the structure is electrically larger than at the primary resonance frequency.

By combining a number of the toroidal conducting paths just described and by controlling the relative phases of the electromagnetic energy supplied to each path, various embodiments of the inventive structure and various antenna radiation patterns may be created. In some embodiments of the invention including a plurality of toroidal conducting paths, the conducting paths have opposing senses, i.e., are contrawound. appropriately feeding the contrawound paths, an electrically small, self-resonant antenna providing purely vertically polarized radiation having an omnidirectional radiation pattern may be realized. This is an especially important and useful achievement in the lower frequency ranges, an achievement that has totally eluded others in the electromagnetic arts. Other embodiments

of the invention may be used to produce the same radiation patterns as known antennas, such as the turnstile antenna, but in an electrically small volume. By appropriately combining conducting paths, embodiments of the invention producing nearly any antenna polarization and radiation pattern may be realized.

Other embodiments of the inventive electromagnetic structures may be constructed having helical and non-helical electrical conducting paths disposed on other toroidal and non-toroidal surfaces. (Those surfaces may be physically existing coil forms or mathematical, conceptual surfaces not physically present in a particular embodiment of the inventive structure.) For example, the surface may include corners and/or have a cross section including corners and convolutions. An important element of the invention is that the path inhibit propagation, thereby creating slow waves, and provide an electromagnetically closed path so that a standing inhibited-velocity wave, meaning resonant operation, can be established in response to the flow of an electrical current through the path.

One half of the electrically conducting path may be eliminated in embodiments of the structure by employing the image theory technique. In these embodiments, a conducting image surface electrically supplies the missing portion of the path. The image surface may be a conducting sheet, a screen or wires arranged to act electrically as a conducting sheet, or may be the earth, in accordance with the disclosed improvement in known electromagnetic technology.

While the achievements of the invention are usable over a wide range of the radio frequency spectrum, they are particularly useful at the lower end of the spectrum where wavelengths are very long. Known antennas operating in that region of the spectrum are exceedingly large and inefficient. According to the invention, antennas no larger than a few thousandths of a free space wavelength at their primary resonance frequency may be constructed and may be operated efficiently at a resonance frequency or sufficiently close to a resonance frequency so as to be within the resonance frequency bandwidth. With such antennas reliable communication to deeply submerged submarines is possible and practicable.

A particularly intriguing application of the structure is the construction and operation of a waveguide probe at the primary or higher mode resonance frequencies of the waveguide formed by the surface of the earth and ionosphere. Because these resonance frequencies, the so-called Schumann resonances, are so low, e.g., about 8, 14 and 30 Hz, it has not heretofore been practical even to attempt to build a self-resonant structure to operate at any of the frequencies. Although a waveguide probe according to the invention resonantly operating at one of the Schumann resonance frequencies would be physically large, it would still be electrically small and therefore realizable, as well as efficient. Because propagation losses are so low at the primary Schumann resonance frequency (below 0.25 dB per Mm according to published data), signals at that frequency may be transmitted to any point on the earth without significant attenuation.

The invention may be more clearly understood from the detailed description that follows, particularly when taken in conjunction with the appended drawing figures.

#### BRIEF DESCRIPTION OF THE DRAWINGS

FIG. 1 is a perspective view of a prior art linear helical slow wave structure.

FIG. 2 is a perspective view of an embodiment of an electromagnetic structure according to the invention.

FIG. 3 shows an embodiment of an electromagnetic structure according to the invention adapted for a balanced feed.

FIG. 4 shows an embodiment of an electromagnetic structure according to the invention adapted for an unbalanced feed.

FIG. 5 shows a reference polar coordinate system used in the mathematical analysis of the embodiment of the invention shown in FIG. 2.

FIG. 6 shows the measured feed point impedance as a function of frequency of a very high frequency antenna constructed according to the embodiment of the invention depicted in FIG. 3.

FIG. 7 shows the measured voltage standing wave ratio as a function of frequency measured in the vicinity of the primary resonance frequency of a high frequency antenna constructed according to the embodiment of the invention depicted in FIG. 2.

FIG. 8 shows the measured voltage standing wave ratio as a function of frequency measured in the vicinity of the secondary resonance frequency of a high frequency antenna constructed according to the embodiment of the invention depicted in FIG. 2.

FIG. 9 shows the resistive component of the measured feed point impedance as a function of frequency of a medium frequency antenna constructed according to the embodiment of the invention depicted in FIG. 2.

FIG. 10 shows a perspective view of an embodiment of an electromagnetic structure according to the invention including bifilar electrically conducting paths.

FIG. 11 shows the measured impedance as a function of frequency of a medium frequency antenna constructed according to the embodiment of the invention depicted in FIG. 10.

FIG. 12a shows a perspective view of an embodiment of an electromagnetic structure according to the invention including quadrifilar electrically conducting paths and FIG. 12b shows, schematically, a phase shifting network for use with the electromagnetic structure of FIG. 12a.

FIG. 13 shows a perspective view of an embodiment of an electromagnetic structure according to the invention.

FIG. 14 shows a perspective view of an embodiment of an electromagnetic structure according to the invention.

FIG. 15 shows a top view of an embodiment of an electromagnetic structure according to the invention having a rectangular form.

FIG. 16 shows the measured feed point impedance as a function of frequency of a high frequency antenna constructed according to the embodiment of the invention depicted in FIG. 15.

FIG. 17 is a perspective view of an embodiment of an electromagnetic structure according to the invention including a frequency adjustment means.

FIG. 18a is a perspective view of a prior art contrawound helix; and FIG. 18b is a perspective view of a prior art structure electrically equivalent to the contrawound helix of FIG. 18a.

FIG. 19a is a view of the crossover current paths of the contrawound helical structure of FIG. 18a and FIG. 19b is a view of the crossover current paths of the contrawound helical structure of FIG. 18b.

19b is a view of the current crossover paths of the electrically equivalent structure of FIG. 18b.

FIG. 20 is a top view of an embodiment of an electromagnetic structure according to the invention including a modified form of the structure of FIG. 18(b).

FIG. 21 is a perspective view of an embodiment of an electromagnetic structure according to the invention including an electrically conducting surface as an image path means.

FIG. 22 shows the measured feed point impedance as a function of frequency of a very high frequency antenna constructed according to the embodiment of the invention depicted in FIG. 21.

FIG. 23 is a perspective view of an embodiment of an electromagnetic structure according to the invention including electrically conducting radial wires as an image charge means.

FIG. 24 shows the measured feed point impedance as a function of frequency of a very high frequency antenna constructed according to the embodiment of the invention depicted in FIG. 23.

FIG. 25 is a perspective view of an embodiment of an electromagnetic structure according to the invention including the earth as an image path means.

FIG. 26 is a perspective view of an embodiment of an electromagnetic structure according to the invention.

#### DETAILED DESCRIPTION OF PREFERRED EMBODIMENTS

A slow wave structure forms an essential part of the invention. It is well known that in a slow wave structure electromagnetic waves propagate with a velocity less than the speed of light, the free-space propagation velocity. The relation between these velocities may be expressed as

$$V_p = V_f c$$

where

$V_p$  = slow wave propagation velocity

$V_f$  = velocity factor, and

$c$  = speed of light.

The velocity factor may be on the order of 0.1 or less in many slow wave structures. In propagating along a slow wave structure, an alternating electric current has a guide wavelength,  $\lambda_g$ , that is related to other variables as

$$\lambda_g = \frac{V_p}{f} = V_f \lambda_o$$

where the additional variables are

$f$  = frequency, and

$\lambda_o$  = a free-space wavelength at the frequency  $f$ .

Numerous slow wave structures are known in the art. Many have been used in microwave electron tubes. In the present invention slow wave structures are used to radiate electromagnetic energy, whereas in microwave tubes every attempt is made to suppress radiation by the slow wave structures. A particularly convenient slow wave structure for mathematical analysis and for construction of some preferred embodiments of the present invention is the helix.

Linear Helix. A linear helical conductor of length 1, radius  $b$  and "turn" spacing  $s$  is shown in FIG. 1. A useful formula for calculating the velocity factor,  $V_f$ , in a linear helix appears in *Reference Data for Radio Engineers* (Howard W. Sams Co., 1972) 25-11 ff.

$$V_f = \frac{1}{\left[ 1 + 20 \left( \frac{2bn}{l} \right)^{5/2} \left( \frac{2b}{\lambda_o} \right)^4 \right]^{1/2}} \quad (1)$$

where  $N$  = the number of turns ( $N = l/s$ ), the other terms are as previously defined and it is assumed that

$$\frac{4b^2}{s\lambda_o} < \frac{1}{5}$$

Elementary Toroidal Embodiment. The advantages of the invention are achieved when a standing wave is established, in response to the flow of current through a slow wave structure, along an electromagnetically closed wave path provided by a slow wave structure. An electromagnetically closed wave path may be created from the linear helix of FIG. 1 by conceptually bending the helix into a circle. A toroidal form 1, in this instance a torus, shown in FIG. 2, is then described. In FIG. 2, torus 1 is shown disposed along orthogonal Cartesian axes. A helical conducting path 2, which may be a copper wire, a metal tube, a metallic film or the like, is disposed on toroidal form 1. A surface 3 on which the path is disposed is a torus having two circular cross sections in each plane containing the Z axis. Those cross sections have the radius  $b$ , the minor radius of the torus. The centers of those cross-sectional circles describe a circle 4 lying in the XY plane and having a radius  $a$ , the major radius of the torus. The toroidal surface may be a dielectric form or it may be an imaginary surface if the conducting path 2 is self supporting. Alternately, the toroidal surface might be considered not as a bent cylinder, but as generated by rotating a circle of radius  $b$  about the Z axis which is spaced from the center of the circle by the distance  $a$ . Toroidal surfaces, other than a torus, are useful in the invention as surfaces for supporting a conducting path and may be similarly created by rotating a non-circular closed figure about an axis lying outside the figure. Still other surfaces, not the production of rotation of a closed figure may also be similarly used in embodiments of the invention. Likewise, the conducting path need not be helical, but could be spiral, that is, the "turns" of the path need not be equally spaced, i.e., of the same pitch, and the minor and major radii need not be constant. The toroidal, helical embodiment of FIG. 2 is, however, particularly useful for mathematical analysis as well as being a preferred embodiment. Torus 1 is one form of a multiply connected surface. The circle described by major radius  $a$  is a closed figure forming a central axis of torus 1. Several different kinds of circumferences can be drawn on surface 3 of torus 1. For example, the circle described by minor radius  $b$  is circumferential. That circle of radius  $b$  is planar and its plane lies transverse to and intersects that central axis. I refer here to such circumferences, which need not be planar, that describe a surface that intersects the central axis of the torus as transverse or as being disposed transversely. Other circumferential lines may be drawn on surface 3. For example, a circle drawn on surface 3 concentric to the central axis of radius  $a$ , is circumferential. Those kinds of circumferences describe surfaces that do not intersect the central axis of the torus. I refer here to such circumferences, which need not be planar, as longitudinal or as longitudinally disposed. Still other circumferential

lines lying on surface 3, such as the helical path described by conductor 2, are neither circumferentially transverse nor longitudinal, but only circumferential.

Applying Equation 1 to the torus of FIG. 2, it is noted that the length of the linear helix is now the circumference described by the major radius, i.e.,  $l=2\pi a$ . The number of turns  $N$  is then,

$$N = \frac{2\pi a}{s}$$

Equation 1 becomes

$$V_f = \frac{1}{\left[ 1 + 20 \left( \frac{2b}{s} \right)^{5/2} \left( \frac{2b}{\lambda_0} \right)^4 \right]^{1/2}} \quad (2)$$

where all the variables have been previously defined.

I have found Equation 2 very useful for designing elementary and multifilar helical, toroidal embodiments of my invention. The velocity factor,  $V_f$ , can be varied by changing the size of the torus and the pitch of the helical path. When the structure of FIG. 2 is driven with a current at a frequency such that the circumference,  $2\pi a$ , is approximately equal to an integer number of guide wavelengths,  $n\lambda_g$ , self-resonance is achieved. That is, a standing wave is established along the electromagnetically closed path formed by bending the slow wave structure, the linear helix, to form a closed geometric figure, in this case a circle. It follows, as the mathematical analysis and measured, experimental results below demonstrate, that an electrically small antenna, which is efficient because it is self-resonant, is achieved in the invention. The circumference of the toroidal structure at the primary resonance frequency ( $N=1$ ) is equal to one guide wavelength,  $\lambda_g$ , which is shorter than a free-space wavelength by the factor  $V_f$ . The diameter of the antenna is approximately  $2a$ . If, for example, the velocity factor is 0.1, then the overall dimension of the antenna at the primary resonance frequency will be less than one thirtieth of a free-space wavelength, making it electrically small. In addition to the advantage of remarkably small electrical size, the invention enables simple achievement of special electromagnetic radiation properties not previously obtainable.

In practice, the electrically conducting path of the structure must be electromagnetically excited and some means of supplying or extracting the energy must be provided. FIG. 3 shows the embodiment of FIG. 2 with a helical conducting path 5 cut to form two terminals 5a and 5b for a balanced feed. These terminals are sufficiently close to each other and are of the proper phase so as to appear, electromagnetically, to be closed. Thus the standing wave may still be established even though the path is not continuous on the toroidal surface. Similarly, in FIG. 4, the conducting path 6 is continuous and includes a short interleaved, discontinuous toroidal path 7. A sliding tap 8 connects conductors 6 and 7 so that an unbalanced feed, a coaxial cable 9, may be connected across conductors 6 and 7. Adjustment of the position of tap 8 permits variation of the impedance to permit impedance matching, if necessary. Obviously, embodiments of antennas according to the invention may operate either to radiate or receive electromagnetic energy.

Mathematical Analysis. An approximate mathematical analysis of the radiation fields of the structure of FIG. 2 aids in understanding its performance and that of

more complex embodiments of the inventive electromagnetic structure. In the mathematical analysis, it is convenient to use the polar coordinate system of FIG. 2 as a frame of reference. In the analysis it is assumed that (a) the radiation pattern is observed in the far field of the structure; (b) the helical conducting path is excited with a current non-uniformly distributed along the azimuthal angle,  $\phi$ , of FIG. 3; and (c) the helix can be decomposed into a continuous circular loop of sinusoidally distributed electrical current of the form  $I_\phi^e(\phi') = I_0 \cos n\phi' e^{j\omega t}$  and a continuous circular loop of sinusoidally distributed "magnetic current" of the form  $I_\phi^m(\phi') = \sin(n\phi' + \alpha) e^{j\omega t}$  where  $\alpha$  represents a phase angle shift between the currents and  $n$  is an integer representing the resonance mode of the structure. Assuming that electric and magnetic currents are in phase quadrature  $\alpha=0$ . When  $n=1$ , the structure is operating at its primary resonance frequency and  $2\pi a = \lambda_g$ . Beginning with the source density of the field from the electric current as

$$J(\vec{r}) = I_0 \cos(n\phi) e^{j\omega t} \delta(\cos \theta) \frac{\delta(r-a)}{a} \hat{\phi}$$

and applying Maxwell's equations with the usual far field assumption, the intensity of the incremental magnetic field produced by the electrical current may be calculated. Neglecting negligible quantities, the  $\theta$  and  $\phi$  magnetic field intensity components may be calculated by direct integration. Then, from Maxwell's equations the  $\theta$  and  $\phi$  components of the electric field attributable to the electric current may be determined. Similarly, the electric and magnetic fields generated by the loop "magnetic" current may be determined beginning with a similar source density expression for the "magnetic" current. The results for "magnetic" and electric currents are then combined, according to the principle of superposition, to predict the fields produced by the structure of FIG. 2 at the distance  $R$  from the origin in the coordinate system. These fields are predicted by equations 3.

$$E_\phi^e = -\frac{\beta_0 a Z_0 I_0}{2R} \cos n\phi J_n(\beta_0 a \sin \theta) e^{j(\omega t - \beta_0 R + \frac{n\pi}{2})}$$

$$E_\theta^e = \frac{n\beta_0 a Z_0 I_0}{2R} \sin n\phi \frac{J_n(\beta_0 a \sin \theta)}{\beta_0 a \tan \theta} e^{j(\omega t - \beta_0 R + \frac{n\pi}{2})}$$

$$E_\phi^m = -\frac{\beta_0 a I_m}{2R} \cos n\phi J_n(\beta_0 a \sin \theta) e^{j(\omega t - \beta_0 R + \frac{n\pi}{2})}$$

$$E_\theta^m = -\frac{n\beta_0 a I_m}{2R} \sin n\phi \frac{J_n(\beta_0 a \sin \theta)}{\beta_0 a \tan \theta} e^{j(\omega t - \beta_0 R + \frac{n\pi}{2})}$$

The superscript  $e$  indicates a field component attributable to the electric current, whereas the superscript  $m$  indicates a field component attributable to the "magnetic current".  $\beta$  is the phase constant equal to  $2\pi/\lambda_0$ ;  $\beta_0$  is calculated with  $\lambda$  equal to the free-space wavelength at the frequency of operation,  $\lambda_0$ , while  $\beta$  is calculated using the guide wavelength,  $\lambda_g$ .  $Z_0$  is the characteristic impedance of free space,  $\omega = 2\pi f$  are the usual Bessel functions. The magnitude of "magnetic current" is

$$I_m = \omega \mu \frac{\pi b^2}{s} I_o$$

where the new terms are  $\mu$ , the permeability of free space, and  $I_o$ , the magnitude of the electric current flowing in the conducting path. In the azimuthal, i.e., horizontal, plane,  $\theta = 90^\circ$ . When  $n=1$ , the fundamental resonance frequency, the magnitudes of the fields reduce to:

$$E_\phi = -\frac{\beta_g a Z_o I_o}{2R} J_1(\beta_g a) \cos \phi \quad (4a)$$

$$E_\theta = -\frac{\beta_g a I_m}{2R} J_1(\beta_g a) \cos \phi \quad (4b)$$

**Monofilar Toroidal Embodiments.** Equation 2 may be used to design circular toroidal embodiments of the inventive structure. The simplest embodiments are referred to as monofilar since they have a single electrically conducting path.

a. Conceptual embodiment of a receiving antenna for FM broadcast. Assume a primary resonance frequency of 100 MHz, and the following parameters:

$b = 0.5$  inches = 1.27 cm.

$s = 0.5$  inches = 1.27 cm.

Applying equation 2,  $V_f = 0.296 = \lambda_g / \lambda_o$ , so that the major radius  $a$  is 14.1 cm. = 5.55 inches. From Equations 4, it can be seen that the azimuthal  $\theta$  and  $\phi$  fields of this antenna will vary and have different magnitude ratios in different directions. Therefore, this antenna has an elliptically polarized characteristic. The maximum dimension of this embodiment is 0.1 free-space wavelengths at the primary self-resonance frequency.

b. Conceptual embodiment of a low frequency (LF) antenna. Assume a primary resonance frequency of 150 kHz and let:

$b = 10$  feet = 3.05 m.

$s = 2$  feet = 0.61 m.

Solving equation 2,  $V_f = 0.053$ , so that  $a = 55.8$  feet = 17 m. Although this structure is physically large, its maximum dimension is only about 0.02 free-space wavelengths at the primary self-resonance frequency.

c. Measured embodiment of a very high frequency (VHF) antenna. This embodiment of my invention was constructed on a plastic torus form as shown in FIG. 3 with the following parameters:

$a = 6.25$  inches = 15.87 cm.

$b = 0.5$  inches = 1.27 cm.

$N = 70$  turns (of 16 gauge copper wire)

$s = 0.56$  inches = 1.42 cm.

According to Equation 2, the velocity factor at the primary resonance frequency of 100 MHz is 0.336. The measured value was 0.332 at a resonance frequency of about 106.8 MHz. A measured plot of the input impedance as a function of frequency of this embodiment is shown in FIG. 6. The resonance frequency, at which the reactive component of the impedance is zero, is readily identified. The measured characteristic shows a relatively narrow bandwidth and an input impedance at resonance of 1000 ohms. As with all embodiments of the invention, the zero reactive impedance component means that there is no need to use a matching component to attempt to achieve a conjugate match between the receiver or transmitter impedance and the antenna impedance in order to maximize system efficiency. The resistive components of the structures described here

are readily matched in a receiver or transmitter by known circuit design techniques.

d. Measured embodiment of a high frequency (HF) antenna. This embodiment had the following parameters:

$a = 2.74$  feet = 0.834 m.

$b = 0.925$  inches = 2.35 cm.

$N = 1000$  turns (of 18 gauge wire)

$s = 0.2$  inches = 0.5 cm.

The voltage standing wave ratio (VSWR) of this antenna was measured through a 4 to 1 balun transformer and a 50 ohm coaxial cable. In FIG. 7, the measured VSWR is plotted versus frequency in the vicinity of the primary resonant frequency,  $n=1$ , of about 3.63 MHz. In FIG. 8, the measured VSWR as a function of frequency is plotted in the vicinity of the secondary resonant frequency,  $n=2$ , of about 7.19 MHz. FIGS. 7 and 8 illustrate two important properties of embodiments of the invention. First, the various resonance frequencies of an embodiment of the invention do not have the familiar integer multiple, harmonic relationship of a simple linear antennas. The absence of this relationship is evident from the non-linear wavelength relationship of Equation 2. Second, although operation of this embodiment of the invention at higher modes increases its electrical size, it also broadens its bandwidth. This increase in electrical size is particularly useful at higher frequencies, where embodiments of the inventive antenna may be undesirably physically small if operated at their primary frequencies. The broadened bandwidth may be important at any frequency. In the present embodiment, at the primary resonant frequency, the maximum dimension is 0.01 free-space wavelengths and at the secondary resonant frequency the maximum dimension is 0.02 free-space wavelengths.

e. Measured embodiment of a medium frequency (MF) antenna. This embodiment had the following parameters:

$a = 12$  feet = 3.66 m.

$b = 9.7$  feet = 2.96 m.

$N = 120$  turns

The feed point impedance was measured with a General Radio 916-AL impedance bridge with the antenna placed four feet above sandy soil. As expected with the simple toroidal embodiment of the invention, elliptically polarized radiation was observed. A plot of the measured resistive component of the feed point impedance as a function of frequency is shown in FIG. 9. The resonant frequency was 339 kHz at an impedance of approximately 9100 ohms. At the measured resonant frequency, the maximum dimension of the antenna is about 0.015 free-space wavelengths.

The "crossed-field" properties of the toroidal embodiment of the invention are particularly useful in mobile communications typically operated in the VHF and UHF frequency ranges. The typical whip receiving antenna used in these applications responds to the electrical field component aligned with it. In metropolitan areas, particularly, a communications transmitter located between buildings, fences or the like, produces standing electrical and magnetic wave components that are spatially displaced by one quarter wavelength with respect to each other. Therefore, the amplitude of the received signal at the antenna terminals varies depending upon the location of the antenna, much like the response of a waveguide probe moving along a slotted waveguide supporting a standing wave. The same result is obtained regardless of whether an antenna sensitive

the electrical or magnetic components of the wave is used.

Because the toroidal embodiment of the inventive antenna, particularly, responds to both electrical and magnetic components of an electromagnetic wave, it can be used to avoid these standing wave effects. Therefore, this embodiment could be referred to as an energy antenna since it responds to the energy in the transmitted wave rather than to one of the components of the transmitted wave. In addition, as shown by Equations 3 and the discussion that follows, embodiments of the inventive structure may be designed to maximize response to electrical or magnetic field components to take advantage of the phenomenon of transmitted standing waves.

**Multifilar Toroidal Embodiments.** By combining the fields of Equations 4, various azimuthal radiation patterns can be generated. The physical achievement of the combinations is made by using several helical conducting paths on a toroidal form and establishing a fixed phase relationship between the currents in each helical conducting path. These embodiments of the invention are referred to as multifilar since they have multiple electrical conducting paths. An embodiment of a bifilar structure used as an antenna is shown in FIG. 10. The bars BC and B'C are phasing lines for controlling the relative phases of the current in each path and provide input terminals for the feed. One conducting path runs from B to B' and the other from C to C'. The paths do not intersect since they are wound with the same sense and pitch. When the windings are fed at terminals AA', in the middle of the phasing bars, the currents flow in opposite directions in the windings and the field produced by one of the electric current loops is reversed with respect to the other. Therefore, the  $E_\phi$  components, from Equation 4a, of the two windings are 180° out of phase and cancel. As a result, a vertically polarized field in the horizontal plane is produced. The antenna pattern has a "figure 8" shape. If B and B' or C and C' are interchanged, reversing the current in one winding with respect to the other in comparison to the previous embodiment, then the  $E_\theta$  components, from Equation 4a, of the two windings cancel and a horizontally polarized field with the same antenna pattern as before is produced.

a. Measured embodiment of a bifilar VHF antenna. A bifilar antenna such as shown in FIG. 10 and driven at terminals AA' to produce vertically polarized radiation had the following parameters:

- a=12.5 inches=31.75 cm.
- b=0.5 inches=1.27 cm.
- s=0.26 inches=0.63 cm.

The observed radiation was predominantly vertical; the vertical to horizontal field strength ratio was 46. The velocity factor calculated from Equation 2 was 0.153 compared to a measured value of 0.156 at 46 MHz. A "figure 8" radiation pattern was observed. At the resonant frequency, this embodiment is about 0.1 free-space wavelengths across.

b. Measured embodiment of a bifilar MF antenna. This bifilar antenna had the following parameters:

- a=5.95 feet=1.81 m.
- b=0.95 feet=29.0 cm.
- s=4 inches=10.2 cm.
- N=106 turns (of  $\frac{3}{8}$ " copper tubing)

The structure was placed 3.5 feet above soil having a measured conductivity of 2 millimhos/meter. The structure was fed and the impedance measured at points

AA' of FIG. 10. The measured results are plotted in FIG. 11 as a function of frequency. The calculated velocity factor was 0.103 while the measured value was 0.094 at about 2.46 MHz. The larger variation between the calculated and measured velocity factor in this embodiment compared with other measured embodiments may be attributable to mutual coupling effects of the conducting paths. In order to determine the magnitude of the effects, if any, of the earth on the antenna, 4 twenty foot long conducting rods were disposed radially and symmetrically on the ground beneath the antenna. The feed point impedance shifted very little from the lines marked 110 in FIG. 11 to the line marked 111. The small change suggests the major field are produced by the "magnetic current." This embodiment, at its primary resonance, had a maximum dimension of 0.03 free-space wavelengths.

If two of the embodiments of FIG. 10 are combined to form a quadrifilar embodiment as in FIG. 12(a) with their two pairs of windings fed in quadrature, as indicated by the phasing means shown in FIG. 12(b), an omnidirectional antenna pattern may be produced. Both pairs of windings in the quadrifilar embodiment are arranged to produce vertical polarization; that is, the  $E_\phi$  field components are cancelled, leaving an  $E_\theta$  component proportional to  $\sin wt \sin \phi + \cos \phi \sin wt = \sin(\phi + wt)$ . Because of the phase relationship of the field produced by the two pairs of conducting paths, the "figure 8" radiation pattern of the quadrifilar embodiment rotates at a rate equal to the frequency of operation, yielding an effectively omnidirectional azimuthal pattern. This is the same pattern produced by the turnstile antenna, Brown, "The Turnstile Antenna," Electronics (April 1936) 14, but produced in a different way. I have found experimentally that operation of this embodiment at its higher order modes results in increasing the horizontally radiated field at the expense of vertically radiated field. This embodiment offers particular promise for standard AM broadcast transmission which the customary very tall, vertical transmitting antenna tower may be eliminated with no loss of, or even an increase in, the field strength at receiving location.

By interchanging the path connections at one end of each pair of bars, a similar omnidirectional rotational radiation pattern may be achieved, but with horizontal polarization. This result is entirely analogous to the previously described for the structures of FIG. 12. Other polarization mixtures may be obtained by varying the phase relationships of the feeds and currents and a great variety of desirable radiation phenomena produced.

c. Measured embodiment of a quadrifilar omnidirectional VHF antenna. A quadrifilar antenna of the construction shown in FIG. 12 was constructed on a plastic torus with the following parameters:

- a=4 inches=10.2 cm.
- b=0.3 inches=0.76 cm.
- s=0.4 inches=1.02 cm.
- N=64 turns

The structure had a primary resonance frequency 93.4 MHz and the ratio of vertically polarized to horizontally polarized field strengths was 76.4. The antenna spanned 0.07 free-space wavelengths at the primary resonant frequency.

All of the multifilar embodiments shown and discussed had toroidal, helical paths of the same sense and pitch so that the paths do not cross. As used here,



term multifilar means having more than one conducting path, regardless of whether or not the paths intersect.

Antenna Array Embodiments. Antenna arrays employing driven and parasitic elements to produce directed radiation patterns are known in the art. Inventive arrays incorporating the advantages of my invention may be constructed. In FIG. 13, a driven linear element 131 excites a parasitic toroidal element 132. More complex arrays may be constructed using additional toroidal elements appropriately physically spaced and having currents phased to increase the directivity of the radiation pattern or to generate different radiation patterns. Known or novel phased array techniques may also be employed.

a. Measured embodiment of VHF array antenna. A VHF array antenna as shown in FIG. 13 was constructed. Element 131 was a quarter wavelength stub, at 450 MHz, disposed above a ground plane two free space wavelengths in diameter. Element 132 was a toroidal loop having a major radius of approximately one tenth of a free-space wavelength (approximately  $2\frac{1}{2}$  inches) and tuned to resonate at about 495 MHz. The maximum measured gain was 4 dB over that of the linear element alone.

In FIG. 14 another array according to the invention is shown. In that array a toroidal element 141 is resonant at the transmitting frequency. A toroidal element 142 is tuned as a parasitic director at a frequency about 10 percent above that of the resonant frequency of element 141. Element 142 has a diameter about one tenth of a free-space wavelength larger than the diameter of element 141.

Non-toroidal Embodiments of The Invention. As already mentioned, the surface (real or imaginary) on which the conducting path for creating slow waves is disposed need not be toroidal. In fact, it may not be a real surface at all. But it is convenient to construct mentally a mathematical surface on which the conducting path is disposed for purposes of describing the inventive structure. A toroidal surface is a surface of rotation, but may for example, include corners. I have constructed toroidal embodiments of my invention having rectangular and triangular cross sections. Other closed tube-like, but non-toroidal surfaces, can also provide forms for constructing embodiments of my invention. Virtually any multiply connected surface, as that term is used in the mathematical specialty of topology, may be used as a form upon which a conducting path may be disposed to construct an embodiment of my invention. As used generally and herein, the term multiply connected surface, includes toroidal surfaces and the particular toroidal surface referred to as a torus, as well as far more complex surfaces. That is, electromagnetic structures within the scope of my invention are not limited in form to toruses or even to more general toroidal forms.

a. Measured non-toroidal embodiment of an HF antenna. An HF antenna was constructed on a form having a rectangular shape as shown in the top view of FIG. 15. The form was prepared from plastic pipe having a circular cross section and a  $2\frac{1}{2}$  inch outside diameter. The rectangle was a square 27 inches on a side with its feedpoint at the center of one of the legs. The conductive path was constructed from 116 equally spaced turns of 18 gauge copper wire. The measured feedpoint impedance of this structure is plotted in FIG. 16 as a function of frequency and shows a resonance at 27.42 MHz.

Frequency Tuneable Embodiment. A characteristic of the measured results presented above for various embodiments of the inventive structure is a relatively high Q at the fixed resonance frequencies of each structure. In FIG. 17 an embodiment of a structure according to the invention is shown including a continuous monofilar conducting path and a shorter, discontinuous interleaved conductor. The shorter conductor has the same sense as the continuous conductor on the toroidal form. One path ends in the feed terminal A, A'. A variable reactance, capacitor 171, is connected across the terminals C, C' of the other path. By varying the capacity of capacitor 171, the resonant frequency of the structure may be adjusted. Similarly, a variable inductance may be used to tune the resonant frequency of the structure.

Contrawound Embodiments. Certain specialized forms of multifilar helical embodiments of the inventive structure achieve extremely important results. All of the multifilar embodiments previously discussed have toroidal helical conducting paths having the same sense and pitch. In those embodiments the conducting paths do not cross each other. By contrast, when two or more helical paths on a toroidal form have opposite senses, the paths repeatedly cross. Structures with multiple paths having opposite senses or its electrical equivalent are referred to here as being contrawound. Contrawound helices, such as shown in FIG. 18(a), and related structures, such as the ring and bridge structure shown in FIG. 18(b), have been used as slow wave structures in microwave tubes. See, Birdsall et al., "Modified Contrawound Helix Circuits for High Power Traveling Wave Tubes," ED-3, *I.R.E. Trans. on Electron Devices*, 190 (1956). These contrawound slow wave structures may be conceptually bent into a closed, toroidal form to produce embodiments of my inventive structure. In the structure resulting from "bending" of the structure of FIG. 18(b), the "bridges" are aligned with the circle described by the major radius of the torus and the "rings" are transverse to that circle. Both the bridges and rings lie on the same toroidal surface. The current flows at the crossovers of electrical paths of the slow wave structures shown in FIGS. 18(a) and 18(b) are shown in FIGS. 19(a) and 19(b), respectively. An important feature of the ring and bridge structure of FIG. 18(b) is shown in FIG. 19(b). In that structure, since the currents of the waves propagating in opposite directions on the structure are constrained to flow in opposite directions along the "bridges", i.e., at the crossover paths, if those counterflowing currents are equal they cancel each other. For an inventive toroidal structure employing the slow wave conducting path of FIG. 18(b), the crossover cancellation means that, effectively, the only net electric current flowing in the structure flows around the rings lying transverse to the circle described by the major radius of the torus. That is, no net electric current flows along the circle described by the major radius of the torus. The electric current that does flow in the structure, sometimes referred to as a poloidal flow, in contrast to the cancelled toroidal flow, is equivalent to a toroidal "magnetic current" flow. Since no net toroidal electric current flows, the conducting bridges are unnecessary to this mode of operation of the toroidal ring and bridge structure embodiment of the invention. In fact, such an embodiment may be readily constructed by omitting the bridges and allowing the ring widths to be so narrow that the rings are no more than loops of wire disposed on a multiply con-

nected surface. A view of an embodiment 2601 of such a structure is shown in FIG. 26 where wire loops 2603 are disposed on toroidal surface. Applying Equations 3 to this mode of operation of the ring and bridge embodiment and its equivalents,  $I_0=0$  and  $\alpha=\pi/2$  so that the  $E_{\phi}^e$  and  $E_{\theta}^e$  equations equal zero. The  $E_{\phi}^m$  and  $E_{\theta}^m$  equations remaining predict that elliptically polarized fields will be produced by this structure.

a. Measured embodiment of contrawound antenna. A contrawound toroidal structure of the form shown in FIG. 18(b) was constructed with the following dimensions as defined in that figure.

ring thickness (rt)=0.5 inches=1.27 cm.

bridge length (bl)=0.25 inches=0.63 cm.

$N=78$  turns.

The resulting structure performed as an antenna with a resonance at 85 MHz and a radiation resistance of about 300 ohms.

It is particularly desirable to construct an antenna according to the invention producing only vertically polarized radiation and having an omnidirectional radiation pattern in the azimuthal plane. Such a pattern is produced by a loop of continuous "magnetic current" uniform in amplitude and phase, or its equivalent. With respect to Equations 3, the desired operation would correspond to operation of the contrawound structure just described with  $E_{\phi}^m$  equal to zero, i.e., with  $n$  effectively equal to zero.

The known cloverleaf antenna employs, effectively, a uniform loop of electric current to produce a horizontally polarized field that is omnidirectional in the azimuthal plane. Smith, "Cloverleaf Antenna For FM Broadcasting," 35 *Proc. I.R.E.* 1556 (1947). The cloverleaf antenna succeeds in approximating a current flow uniform in phase and amplitude around a large loop through use of four radiators each bent into a smaller loop occupying a quadrant of a large, imaginary loop. The radiators are connected in parallel to achieve, effectively, the desired current flow.

An embodiment of the inventive structure, in this case a magnetic analog of Smith's cloverleaf antenna, is shown in top view in FIG. 20. There, the "ring and bridge" slow wave structure of FIG. 18(b) has been bent into a circle and the structure divided into four opposing portions each occupying a quadrant—201, 202, 203 and 204. Each of the quadrants is connected in parallel across a coaxial feed 205 so that a "magnetic feed current" simultaneously flows in the same direction in each quadrant and, thereby, around the circle. This embodiment of the structure acts as an antenna with a uniform "magnetic current" loop, thereby producing vertical polarization in an omnidirectional radiation pattern. That is,  $n$  in Equations 3 is effectively equal to zero. Only Equation 3(c) has a non-zero value for the electromagnetic fields produced by this embodiment.

b. Measured embodiment of VHF antenna producing vertically polarized, omnidirectional radiation. An embodiment of the antenna shown in the top view of FIG. 20 was constructed. The slow wave structure was fabricated from 32 turns of 10 gauge copper wire. The major radius was  $4\frac{1}{2}$  inches and the minor radius was  $11\frac{1}{16}$  inches. The bridge length ("bl" of FIG. 18) was  $\frac{3}{4}$  inches and the ring thickness ("rt" of FIG. 18) was  $\frac{1}{4}$  inches. The structure was electrically, but not physically, divided into four quadrants which were fed in parallel from a coaxial line. The resonant frequency of the structure, operating as an antenna, was 125 MHz, and the

radiation produced was vertically polarized and omnidirectional.

Image Embodiments. It is well known in the electromagnetic arts that the fields produced by an electric current above a perfectly conducting plane are the same as if an equal, oppositely directed current were flowing in mirror image, on the opposite side of the plane and the plane were absent. In this principle, an image current flows along an image path. If the physically existing path is in electrical contact with the image plane, an electrically conducting circuit is completed—partly by the existing path and partly by the image path. This principle can be advantageously applied to construct many additional embodiments of my inventive structures. Other embodiments are "sliced," preferably in half along a plane of symmetry, such as an equatorial plane, removing the conducting path on one side of the plane and replacing it with the electromagnetic equivalent of a perfectly conducting plane. It is known in the art that such an image plane need not be a solid conductor, but that a screen or a set of wires disposed so that the spaces between them are much less than a wavelength will suffice.

In FIG. 21 an embodiment of a structure electromagnetically equivalent to that shown in FIG. 20 is depicted. The structure 2101 includes a plurality of conducting half circles 2103 each lying in a plane. All of the planes containing a half circle 2103 commonly intersect along a line which forms the Z axis of the embodiment. The missing portion of each conducting half circle or ring is replaced by an electrically conducting planar sheet 2105. Sheet 2105 may be a piece of copper or some other highly conducting metal. Half circles 2103 are disposed in a circle on sheet 2105. Four of half circles 2103, which are equally spaced from each other around the circle, have their outer ends 2107 electrically connected to sheet 2105. The inner ends of those four half circles are connected together at the Z axis of the embodiment to form one feed terminal 2109. Sheet 2105 is the other feed terminal. All of other half circles 2103 are equally spaced from each other around the circle described on sheet 2105. Other than the four feed point half circles, each half circle has each of its ends 2111 and 2113 electrically connected to sheet 2105. The image currents electrically complete each of the half circles 2103. In addition, sheet 2105 furnishes bridge connections between loops. Therefore, the embodiment of FIG. 21 is equivalent to the bridge and ring contrawound embodiment of FIG. 20 with narrow ring widths.

a. Measured embodiment of a VHF contrawound image antenna. I constructed an antenna embodiment of the type shown in FIG. 21 having a solid copper image plane and 32 half circles, each having a 2 inch (5.1 cm) diameter. The centers of the half circles were disposed on a 12 inch diameter circle. The measured feedpoint impedance of the structure is plotted in FIG. 22 and shows a resonance at 67.25 MHz at a resistance of nearly 1600 ohms. A coaxial line was used to feed the antenna. The polarization of the radiation was vertical and the radiation had a maximum value in the azimuthal plane.

In FIG. 23, an embodiment identical to that of FIG. 21 is shown, except that the solid conducting sheet has been replaced by radial conducting wires 2301. The spacing of those radial wires must be much less than a free space wavelength in order that the electromagnetic equivalent of a solid sheet is achieved. In general, be-

cause the inventive antenna embodiments are much smaller than a free space wavelength at the primary resonance frequency, conducting radial wires may nearly always be substituted in the embodiment for a solid image plane. I have found it useful to cut each of the radials 2301 to a length of one quarter of a free space wavelength at the operating frequency so that the image plane formed by the radials spans a half wavelength. This practice follows that used for minimum dimensioning of horizontal linear reflector elements used as a ground plane with vertical whip antennas. In FIG. 23 an embodiment of an antenna similar to that of FIGS. 20 and 21 is shown with four quadrant sections of the slow wave structures connected in parallel to a feed point 2303. The embodiment of FIG. 23 lacks the bridge elements of the bridge and ring structure. However, as already described for the embodiment of FIG. 26, which does not include an image path, and as confirmed by experiment for an embodiment including an image path, those "bridgeless" structures still behave as if they are contrawound, bridge and ring toroidal embodiments operated so that there is not net toroidal electric current flow.

b. Measured embodiment of a VHF antenna having image radials. An antenna embodiment like that shown in FIG. 23 was constructed. The embodiment had 32 half circles, each half circle having a diameter of 2 inches. The major radius of the "torus" was 10 inches. The four quadrants were fed in parallel through a short coaxial transmission line. The measured feedpoint impedance is plotted in FIG. 24 versus frequency and indicates a resonance at 98.5 MHz with a resistive impedance of about 6500 ohms. The structure produced vertically polarized radiation with a maximum in the XY plane and a minimum along the Z axis.

The earth may also be used as an image plane. Antenna embodiments of my invention generally grow physically larger (though electrically smaller) for descending frequencies. In the larger embodiments effects of the earth are important and unavoidable, so it is advantageous to use the earth as an image source. Such an embodiment is shown in FIG. 25. There, a very large "toroidal" embodiment of the invention has conducting paths 2501 that are rectangular in cross section supported on dielectric circular forms 2503. The ends of each "half loop" are in electrical contact with the earth. A transmission line 2505 feeds the antenna. This structure behaves like a contrawound structure since it has a series of "rings" joined by earthen "bridges." In this embodiment, the rings are again narrow, are made complete rings by the image path and do not have a circular cross section, but a "ring and bridge" slow wave structure is still realized. It may even be desirable that the physical portions of the rings be greater or lesser than one-half the total effective ring cross section depending on the application. For example, when the earth provides the image path the rings might be varied in cross section to compensate for varying topography.

Such large antennas are still electrically small and efficient. Therefore they offer great promise in the lower frequency ranges such as the extra low frequency (ELF) range. It is well known that frequencies in that range deeply penetrate sea water enabling reliable communication transmissions to submerged submarines. For some time the U.S. Navy has been attempting to build an ELF antenna for submarine communication at 78 Hz. See, OE-2 *IEEE J. of Oceanic Eng.* 161 (1977). The proposed Navy antenna, a slight variation of the Bever-

age wave antenna devised in the 1920's (see, 42 *Trans. AIEE* 215 (1923)), covers an area 100 miles by 100 miles and is atrociously inefficient. At 78 Hz, a free space wavelength is 3.85 Mm long. An antenna according to the invention having a maximum dimension of 0.003 free space wavelengths, a dimension believed attainable at 78 Hz, would be about 11.5 km (seven miles) across, would be self-resonant and would have a high radiation efficiency. While ohmic losses might be a significant consideration in such a large structure, it is obvious that an antenna occupying less than one tenth the area taken up by the Navy's Project Sanguine/Seafarer antenna will have much reduced ohmic losses if the same size conductors are used. Since no antenna embodiment of the inventive structure has yet been built to operate in the ELF region, it is not known how small such an antenna can be made. But it is believed that it could be even smaller than 0.003 free space wavelengths, with no sacrifice in directive gain. Harrington, *Time Harmonic Electromagnetic Fields* (McGraw-Hill 1961) 278-79 and 307-11, points out that there is no theoretical limit to antenna size reduction for a specified gain. My conclusion is based on measurements of a structure according to the invention having a resonant frequency at 138 KHz and a resistive feedpoint impedance of 900 ohms at that resonance. The maximum overall dimension of this embodiment was 0.007 free space wavelengths at the resonance frequency. This performance compares very well with the U.S. Navy's 15 KHz transmitter at Cutler, Maine which occupies over a square mile, is about 0.1 free space wavelength overall, and operates at only 50 percent efficiency, largely because of its non-resonant operation.

The Inventive Structure As A Waveguide Probe. It is known that the earth's surface and the ionosphere form a cavity has certain natural resonant frequencies. The resonances of this cavity are regularly excited by lightning. These resonance phenomena were apparently first analytically described in two articles by Schumann in 1952, 72 *Z. Naturforsch.* 149 and 250 (1952). Measurements of the cavity resonance frequencies indicate they occur at about 8, 14 and 20 Hz, as well as at higher frequencies. Galejs, *Terrestrial Propagation of Long Electromagnetic Waves*, 241 (1972). Although the theoretical attenuation with distance of electromagnetic waves at the cavity resonance frequencies varies depending upon the propagation model used and atmospheric assumptions, it is known that the attenuation is quite small. See, Galejs, *ibid.*, at 254. For example, the attenuation at 8 Hz is less than 0.25 dB/per million meters. Since half the circumference of the earth is approximately 20 million meters, propagation at 8 Hz using the earth-ionosphere cavity from any point on the earth to any other point on the earth with a loss no greater than 5.0 dB appears to be possible.

However, no one has yet built a practical waveguide probe capable of exciting the earth-ionosphere cavity at 8 Hz where the wavelength is about 37.5 million meters. This failure is attributable to the poor radiation efficiency and physical size limitations for such probes in the previously known technology. However, with my invention, a waveguide probe of reasonable size can be built which can efficiently excite the earth-ionosphere cavity at the primary Schumann resonance frequency. An embodiment of my inventive contrawound structure employing the earth as an image current source and having a maximum dimension of 0.001 free space wavelengths, and probably much smaller, can be built to

launch vertically efficiently into the frequency. While physically large, produces less than Sanguine/Seafarer at a frequency.

My invention contains certain preferred modifications. The invention will include, among other things, the following claim:

1. An electrically closed, image plane spaced from a toroidal surface.
2. The invention including a toroidal surface connecting said image plane.
3. The invention including a ring and bridge structure having four substantial elements, said elements arranged in parallel.
4. A probe for detecting energy transmitted through a ring and bridge structure, the probe being disposed in response to the electric wave resonance.
5. The probe including a plurality of elements disposed on the electrically closed image plane.
6. The probe including a plurality of elements divided into four sections in parallel.
7. An electrically closed, second substantially wound toroidal surface.
8. The invention including a connected relative phase and conductance.
9. The invention including a justment means for adjusting the resonance.
10. The invention including an adjustment means.
11. A probe for detecting energy

(see, 42 Trans miles by 100 miles Hz, a free space antenna according to dimension of 0.003 (miles) across, a high radiation be a significant it is obvious that with the area taken Seafarer antenna if the same size a embodiment of built to operate in w small such an that it could be lengths, with no Time Harmonic 1961) 278-79 and etical limit to . My conclu- ture according frequency at 138 e of 900 ohms at dimension of this elengths at the e compares very mitter at Cutler, ile, is about 0.1 tes at only 50 on-resonant

uide Probe. It is onosphere form equencies. The excited by light- apparently first y Schumann in 1952). Measure- indicate they is at higher n of Long Elec- the theoretical netic waves at epend upon heric assump- uite small. See, ttenuation at 8 ers. Since half mately 20 mil- e earth-ionos- h to any other r than 5.0 dB

cal waveguide here cavity at million meters. radiation effi- uch probes in ver, with my le size can be ionosphere e frequency. ound struc- ent source and e space wave- n be built to

launch vertically polarized, omnidirectional energy efficiently into the cavity at its primary resonant frequency. While the embodiment of the structure is physically large, perhaps 10 to 20 miles across, it still occupies less than four percent of the area of the Project Sanguine/Seafarer antenna which is supposed to operate at a frequency ten times higher.

My invention has been described with respect to certain preferred embodiments. Various additions and modifications without departing from the spirit of the invention will occur to those of skill in the art. Accordingly, the scope of my invention is limited solely by the following claims.

I claim:

1. An electromagnetic antenna including a plurality of closed, interconnected conducting ring elements spaced from each other and transversely disposed on a toroidal surface.
2. The invention of claim 1 further including conducting bridge elements longitudinally disposed on said toroidal surface, said bridge elements electrically connecting said ring elements.
3. The invention of claim 2 wherein said conducting ring and bridge elements are electrically divided into four substantially identical sections of ring and bridge elements, said sections being electrically connected in parallel.
4. A process for radiating or receiving electromagnetic energy comprising conducting an electrical current through a path of closed, interconnected conducting ring elements spaced from each other and transversely disposed on a toroidal surface, and establishing, in response to the flow of said current, an electromagnetic wave along said surface in a condition of resonance.
5. The process of claim 4 wherein said path includes a plurality of conducting bridge elements longitudinally disposed on said toroidal surface, said bridge elements electrically connecting said ring elements.
6. The process of claim 5 including the steps of electrically dividing said conducting ring and bridge elements into four substantially identical sections of ring and bridge elements and electrically connecting said sections in parallel before conducting said current.
7. An electromagnetic antenna including first and second substantially closed, elongated conductors helically wound and disposed in bifilar relation on the same toroidal surface.
8. The invention of claim 7 including phasing means connected to said first conductor for controlling the relative phases of currents flowing in said first and second conductors.
9. The invention of claim 7 including frequency adjustment means connected to said first conductor for adjusting the frequencies at which said antenna may resonate.
10. The invention of claim 9 wherein said frequency adjustment means comprises a variable reactance.
11. A process for radiating or receiving electromagnetic energy comprising conducting first and second

electrical currents, respectively, through first and second substantially closed, elongated conductors helically wound and disposed in bifilar relation on the same toroidal surface and establishing, in response to the flow of said currents, an electromagnetic wave along said surface in a condition of resonance.

12. The process of claim 11 including controlling the relative phases of said first and second currents.

13. The process of claim 11 including altering the frequencies at which said electromagnetic wave may be established along said surface in a condition of resonance.

14. The process of claim 13 wherein said altering step comprises altering the reactance of a variable reactance connected to said first conductor.

15. An electromagnetic antenna comprising a plurality of ring elements, each ring element including a conducting ring element portion and an image means for electromagnetically completing each ring element, said conducting ring element portions being spaced from each other and transversely disposed on a toroidal surface.

16. The invention of claim 15 wherein said image means comprises a plurality of radially disposed, conducting linear elements, one of said conducting linear elements being electrically connected to each of said conducting ring element portions.

17. The invention of claim 15 wherein said image means comprises the earth and each said conducting ring element portion is in contact with the earth.

18. The invention of claim 15 wherein said conducting ring element portions are divided into four substantially identical sections of conducting ring element portions, said sections being electrically connected in parallel.

19. A process for radiating or receiving electromagnetic energy comprising conducting an electrical current through a path of ring elements, each ring element including a conducting ring element portion and an image means for electromagnetically completing each said ring element, said conducting ring element portions being spaced from each other and transversely disposed on a toroidal surface, and establishing, in response to the flow of said current, an electromagnetic wave along said surface in a condition of resonance.

20. The process of claim 19 wherein said image means includes a plurality of radially disposed, conducting linear elements, one of said conducting linear elements being electrically connected to each of said conducting ring element portions.

21. The process of claim 19 wherein said image means includes the earth and each of said conducting ring element portion is in contact with the earth.

22. The process of claim 19 including dividing said conducting ring element portions into four substantially identical sections of conducting ring element portions and electrically connecting said sections in parallel before conducting said current.

\* \* \* \* \*

## VERTICAL RADIATORS FOR BROADCASTING STATIONS<sup>1</sup>

J. H. DEWITT, JR.

CHIEF ENGINEER, STATION WSM, NASHVILLE

Until a few years ago development work on radio broadcasting stations was confined to the transmitting equipment, little study being given to the antenna system or radiator. It was generally believed that a radiator supported by two towers 100 to 300 feet in height was all that would be required for stations operating within the frequency band set aside for broadcasting. This conception was an outgrowth of both the economies of design and lack of knowledge of signal coverage and fading. The development of high power transmitters has made it much easier to justify the expenditure of relatively large sums on the radiating system, hence the study of this phase of broadcasting has been renewed.

In 1924, Stuart Ballentine<sup>2</sup> worked out the equations for radiation from antennae of various heights. He was able to show that an antenna having a height equal to  $.58 \lambda$  ( $\lambda$  being the transmitting wavelength) would produce the maximum signal along the ground for a given power input. This is undoubtedly the optimum condition for a broadcasting station interested in giving the maximum signal within its primary area. By this is meant the area in which the day and night signals are practically equal.

At the time this theoretical work was done very little was known about the Heaviside layer and the degree to which radio signals were refracted to earth by it. Therefore, it was impossible to determine whether or not this antenna of  $.58 \lambda$  in height would be the most desirable from the standpoint of national coverage. Measurements during the last five years or so made by many observers have established the average effective height of the Heaviside layer at between 60 and 100 miles, depending upon the time of day. Assuming these

<sup>1</sup>Read before the Tennessee Academy of Science at the Nashville meeting, Nov. 24, 1932.

<sup>2</sup>Ballentine, Stuart. 1924. *Proceedings of Institute of Radio Engineers*, p. 837.

ured fading pattern from a typical antenna of about  $.25 \lambda$  in height is shown in figure 3. Here we see that fading becomes measurable at a distance of 35 miles. At 80 miles the variation is such as to make reception rather poor.

It is difficult to form a very definite picture of the fading pattern to be expected from an antenna having a height equal to  $.58 \lambda$ . One would naturally expect the fading area to be pushed well out from the station because of the large component of radiation along the

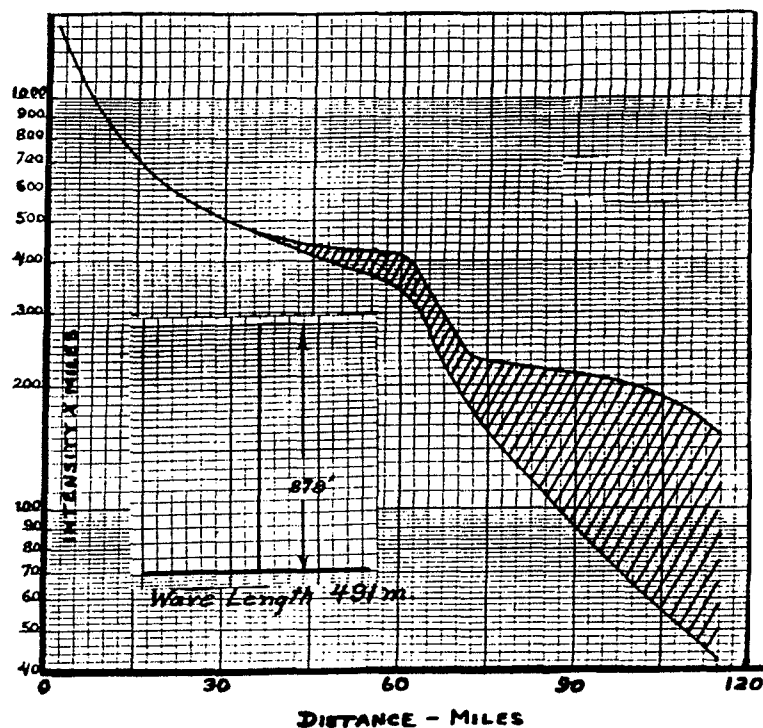
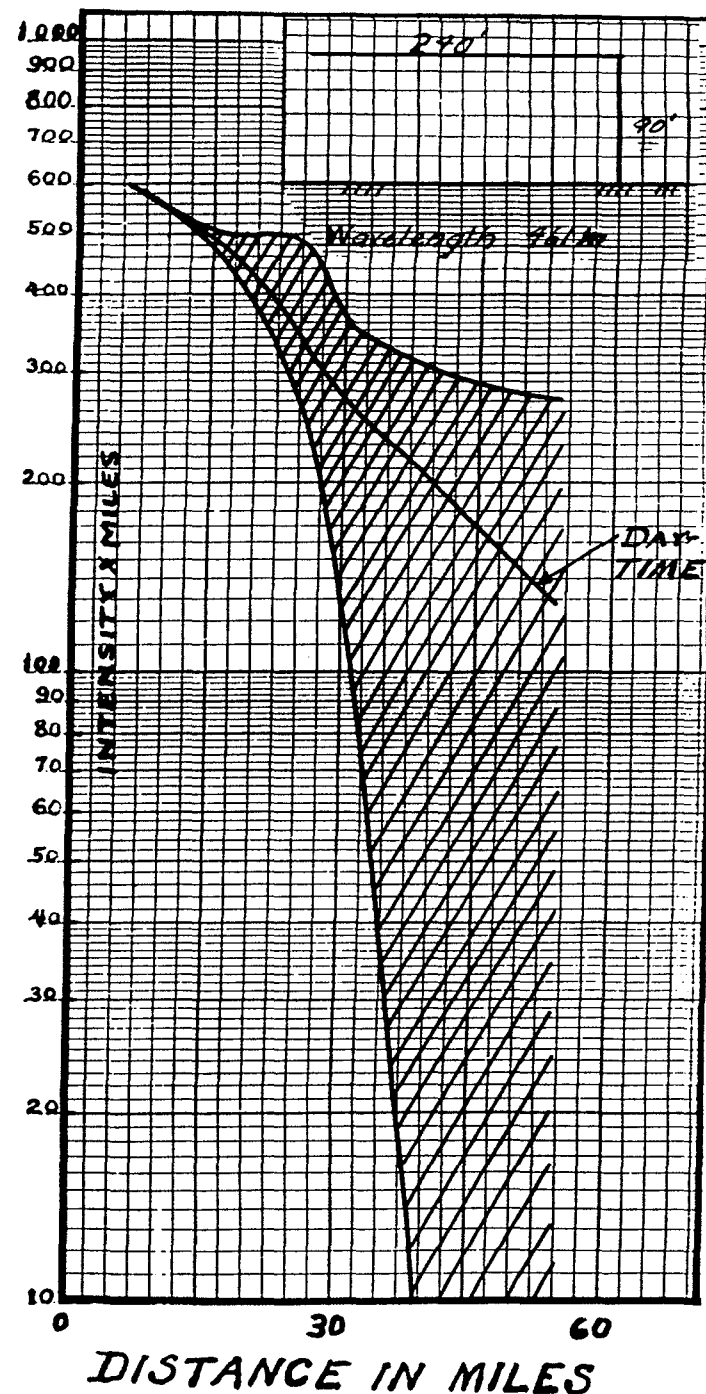


Fig. 4. Wave Intensity at Various Distances from the Antenna. The upper and lower curves indicate actual measured wave intensity with a vertical 878' antenna. The shaded area indicates fading. The lower figure indicates antenna length in relation to wave length. The wave length is erroneously given in the figure as 491 m. It should be 461 m.

ground. Since there are two angles of maximum radiation it is possible that energy from the second lobe shown at about 55 degrees with respect to the horizontal will return to earth at such a distance as to cause trouble. Our measurements, which so far are incomplete, do not bear this out.

In figure 4 is shown the result of measurement of this antenna over the same country as that of figure 1. The difference in the fading



heights, it is easy to show graphically that energy radiated from an antenna at high angles will be returned to earth by the layer at moderate distances from the station. If at these distances the ground wave has been so attenuated or is of such magnitude that the energy in the two paths is comparable, violent fading will result due to phasing effects between the two signals. This type of fading is of the most objectionable nature as frequently the quality of transmission is seriously affected.

In figure 1 is shown an antenna of the type used a number of years ago for broadcasting. This antenna radiates a large amount of energy at high angles. The fact that this high angle radiation is extremely harmful to signal coverage is demonstrated by the intensity curve shown at the lower part of the same figure. In this curve, as in the ones following, signal strength multiplied by the distance at which it is measured is plotted against distance. This is done for convenience as in this way the degree to which the signal is attenuated in passing over the earth is indicated by the slope of the curve. The procedure in making these measurements was to read the signal strength for some time at a given place until it was certain that both the maximum and minimum values had been observed. It will be seen that fading set in at a distance of about 15 miles from the station. At 33 miles the variation in intensity was such as to make reception rather poor. At 40 miles the signal faded to zero at times indicating that the sky wave and ground wave were of equal intensity and varying in phase relation. Here the signal not only varied in intensity, but the fading was of the selective type which caused rather serious quality impairment. It is the author's opinion that the horizontally polarized waves radiated from the horizontal portion of the antenna contributed to the trouble as their plane of polarization was probably shifted in the process of refraction from the ionized layer.

At the top of figure 2 is shown the current distribution on antennae having heights of  $.25 \lambda$  and  $.58 \lambda$ . As before,  $\lambda$  is the transmitting wave length. Below these figures is shown the corresponding distribution of power in space around the antenna calculated by Ballentine on the assumption of a perfectly reflecting earth. It is further assumed that the current is distributed sinusoidally along the wire.<sup>3</sup> In the case of the antenna of height  $.25 \lambda$  it will be seen that quite a lot of energy is radiated at relatively high angles at the expense of radiation in the horizontal direction. Since the degree of fading is determined by the ratio of ground wave to the reflected wave, we would expect fading to set in fairly close to the antenna. The meas-

Fig. 1. Wave Intensity at Various Distances from the Antenna. The upper and lower curves show actual measured wave intensity at night and the curve marked "Daytime" the actual measured intensity in the daytime. Thus the shaded area represents fading. The small figure above shows the length of the horizontal antenna (240') and the height of the tower (90'). Wave length 461 meters.

<sup>3</sup>Op. cit.

pattern of these two antennae is remarkable, and in this respect demonstrates the improvement to be derived by concentrating the energy along the ground rather than radiating it upward into space. For a station interested in national coverage the same holds true because the energy radiated at low angles will be reflected well away from the transmitter to return to earth at a great distance. As yet no measurements have been made at any distance greater than 200 miles, but it is expected that future observations will bear this out.

The antenna shown in figure 1 was erected at station WSM and was used prior to the completion of the permanent structure. The measurements set down in figure 4 were taken on the 878-foot antenna erected at the same place, a photograph of which is shown in figure 5.

In conclusion the author wishes to express his thanks to Messrs. A. C. Omberg and W. C. Montgomery for valuable assistance.

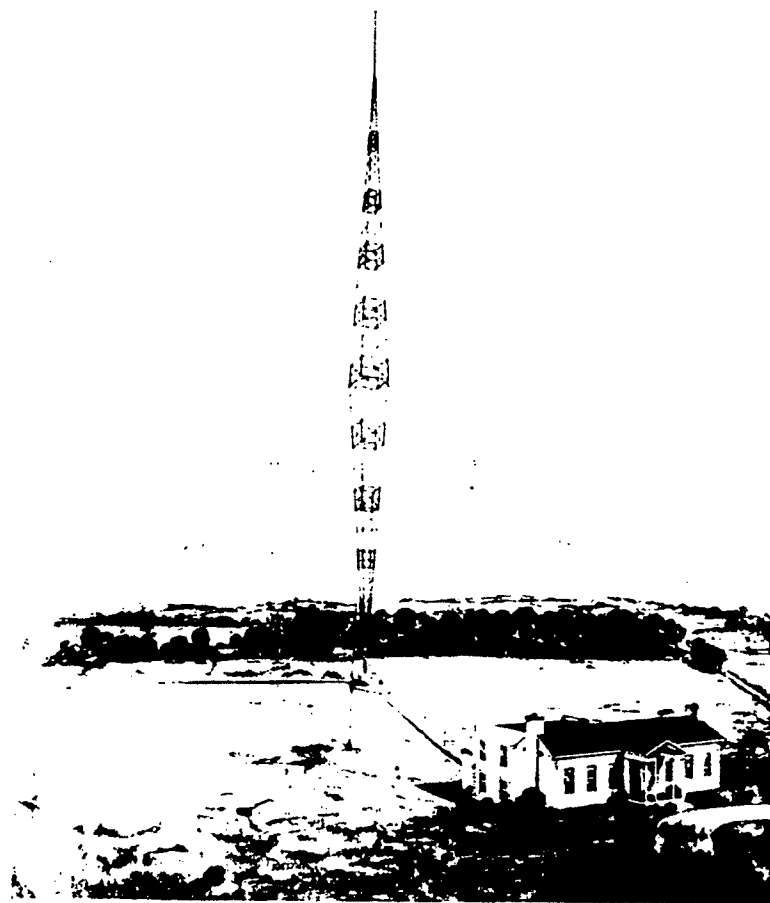


Fig. 5. The New 878' Antenna of Radio Station WSM



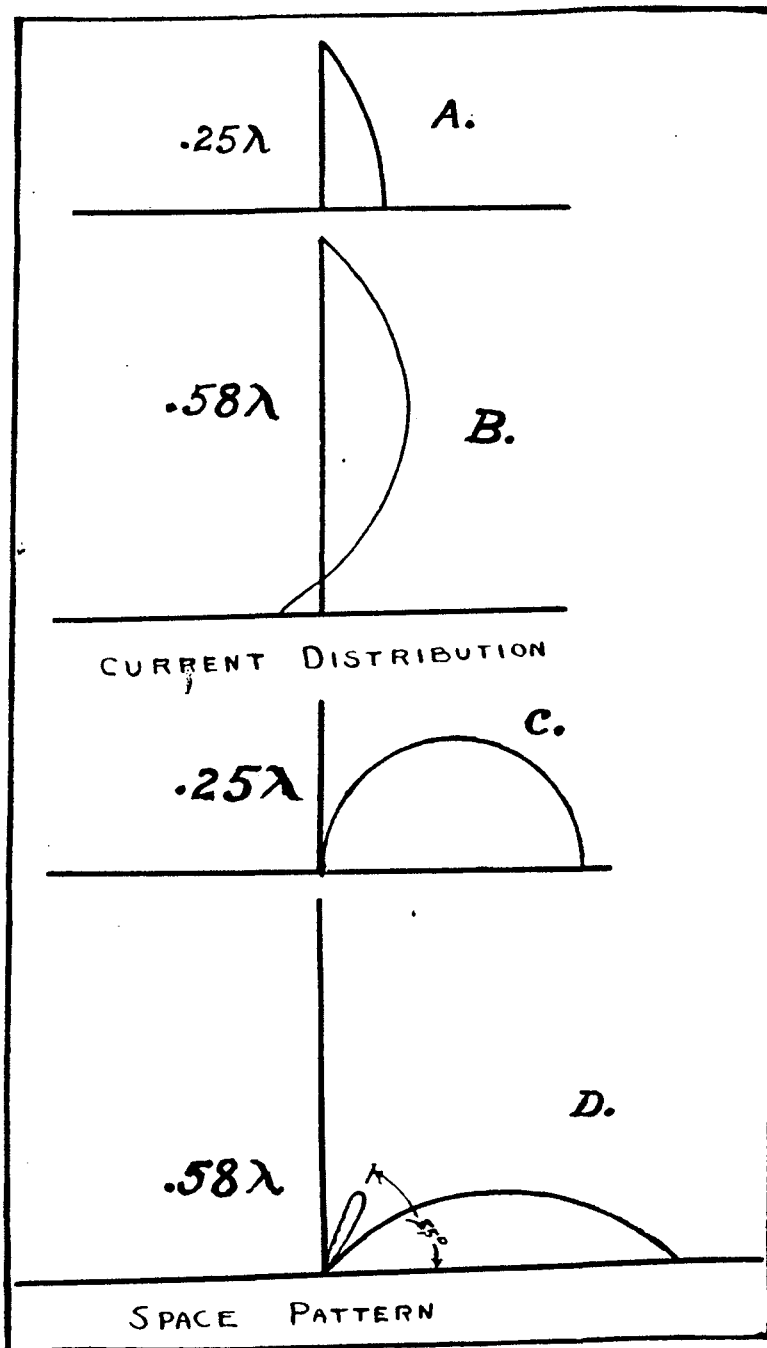


Fig. 2. Current Distribution and Space Pattern for Antennae of Different Heights. A. and B., Current Distribution; C. and D., Space Pattern; A. and C., Antennae with a height of  $.25\lambda$ ; B. and D., Antennae with a length of  $.58\lambda$ .

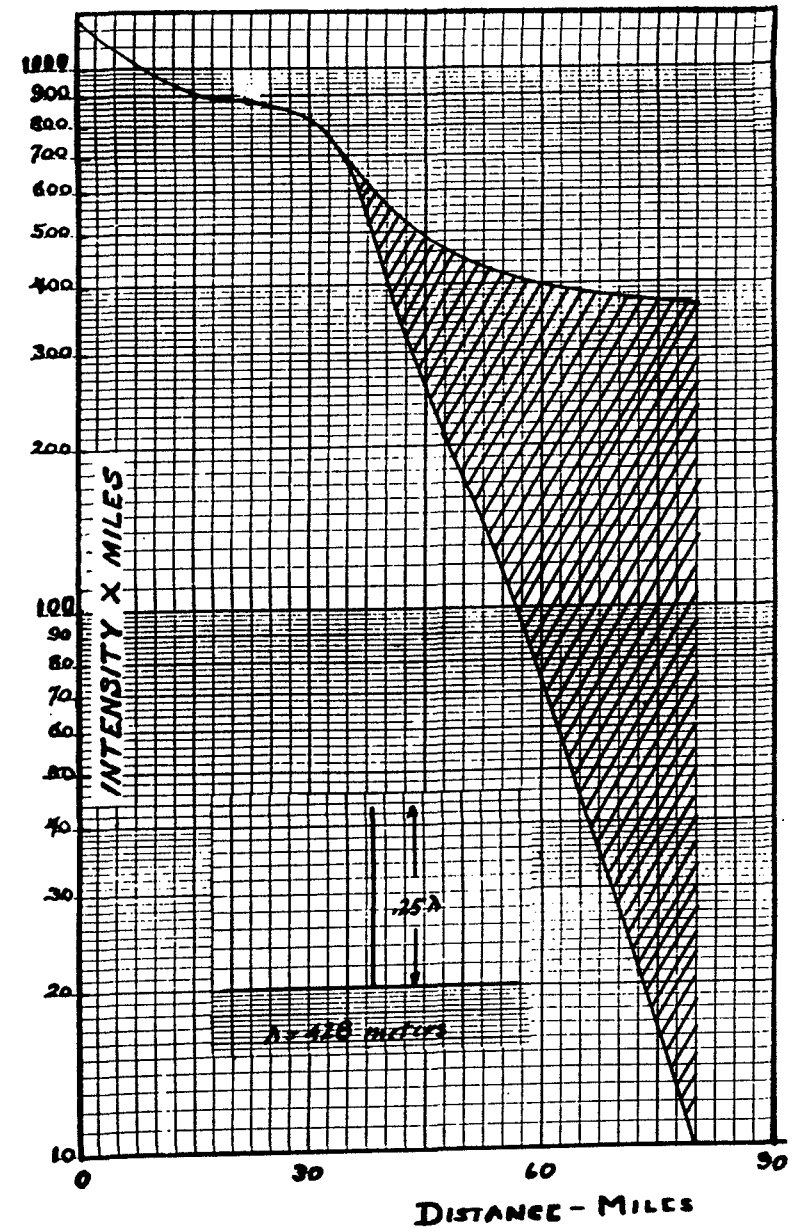


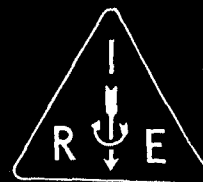
Fig. 3. Wave Intensity at Various Distances from the Antenna. The upper and lower curves represent actual measured wave intensity. As before, the shaded area indicates fading. The lower figure indicates the length of the antenna ( $.25\lambda$ ) in relation to wave length ( $\lambda = 428 \text{ m.}$ ).



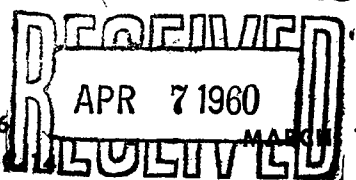
# IRE TRANSACTIONS

## ON BROADCASTING

AM  
Antennas



GEORGE C. DAVIS



Volume BC-6  
Follows PGB

MARCH 1960

Number 1

WASHINGTON, D. C.

### TABLE OF CONTENTS

A Resonant Coaxial-Stub as an Automatic Equalizer.....	G. V. Rao
Television Antenna System Measurements Based on Pulse Techniques...	D. W. Peterson
New Equipment for Measuring Envelope Delay.....	E. N. Luddy
Reactivation of Image Orthicons under Low Temperatures.....	B. Wolfe
Some Color Slide and Color Television Experiments Using the Land Technique	W. L. Hughes
Design and Performance Measurements on a New Anti-Fade Antenna for Radio Station WOAI.....	C. L. Jeffers and S. W. Kershner

PUBLISHED BY THE  
PROFESSIONAL GROUP ON BROADCASTING

# DESIGN AND PERFORMANCE MEASUREMENTS ON A NEW ANTI-FADE ANTENNA FOR RADIO STATION WOAI

Charles L. Jeffers  
Southland Industries, Inc.  
San Antonio, Texas  
And  
Stephen W. Kershner  
A. D. Ring & Associates  
Washington, D.C.

## Summary

A new anti-fade type radiator for Station WOAI is described. Vertical radiation patterns are presented on the basis of computations from predicted current distributions. Measurements on a model antenna generally confirm the performance predicted by the computations. Skywave measurements using pulse techniques were made on the full scale antenna to determine the optimum tuning and the suppression of skywave signals. These measurements show skywave signals transmitted by both the E and F layers of the ionosphere. Final performance data are presented, including current distribution measurements, the vertical radiation pattern and groundwave field intensity measurements.

## Manuscript

Radio Station WOAI is authorized by the Federal Communications Commission to operate in San Antonio, Texas, on the clear channel frequency of 1200 kc with a power of 50 kw unlimited time. Both groundwave and skywave signals are protected from interference from other stations. The most efficient use of the assignment requires maximum groundwave signal during daytime hours. During nighttime hours, the groundwave signal should be free from selective fading out to the distance where the signal is just adequate to overcome noise, then the skywave signal should rise rapidly so as to provide maximum secondary service. These requirements call for an antenna having a carefully controlled vertical radiation pattern.

In April, 1956, the WOAI antenna tower was struck by an Air Force plane, and plans were made for installing a new antenna of optimum design at a location creating less air hazard. A new transmitter site was selected some 17 miles

southeast of San Antonio, and a location for the tower was chosen some 3,000 feet from the 1531-foot tower which supports the television antennas of WOAI-TV and KENS-TV.

Several workers, including one of the authors, have reported on various aspects of anti-fade antennas for broadcasting applications.<sup>1-6</sup> A new type of anti-fade antenna was reported by Jeffers in 1948<sup>3</sup>, but in view of recent advances in the knowledge of antenna performance, it was decided to reexamine the possibilities.

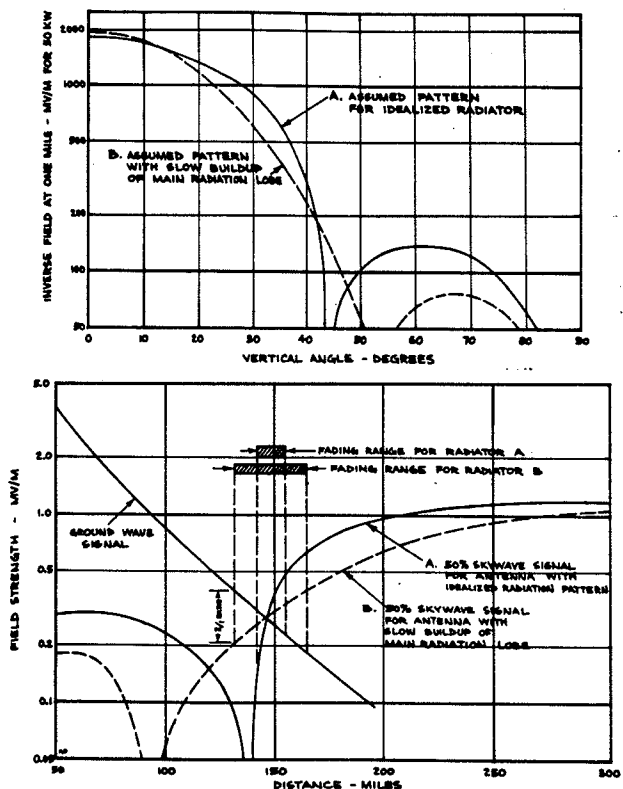


FIGURE 1. VERTICAL RADIATION PATTERN AND SKYWAVE SIGNAL FOR IDEALIZED RADIATOR

## DESIGN CONSIDERATIONS

The first task was to undertake to outline in general terms the radiation pattern requirements for providing optimum nighttime service. Figure 1 shows vertical radiation patterns and signal vs. distance curves for two assumed radiators. The solid lines represent the performance obtained from an idealized radiator, and the dashed lines illustrate an antenna with less desirable characteristics.

In the zone where the groundwave and skywave signals are of approximately the same intensity, rapid or selective fading will occur. Periodic cancellation of the carrier signal takes place, creating the effect of over-modulation and causing serious distortion. For optimum design this fading zone should occur just beyond the limits of useful groundwave service as limited by noise. Furthermore, the skywave signal should increase rapidly with distance as shown by Curve A, Fig. 1. Curve B shows that a slow build-up of skywave signal is undesirable as it results in a wider fading zone. Also, the suppression of skywave signals at closer distances as influenced by high angle lobes must be adequate to prevent an extension of the fading zone. These factors necessitate a vertical radiation pattern tailored to the frequency of operation, ground conductivity and minimum field strength for satisfactory groundwave service.

Figure 2 shows the vertical radiation patterns for three types of radiators. These patterns were computed on the basis of the simple sinusoidal current distributions shown, with the phase velocity assumed equal to the velocity of light. Pattern A is for a con-

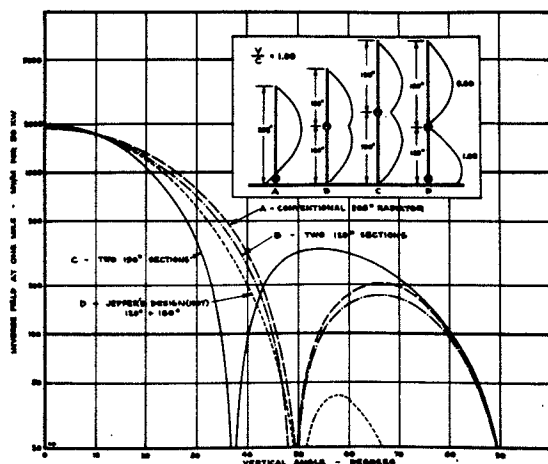


FIGURE 2. VERTICAL RADIATION PATTERNS BASED ON SIMPLE SINUSOIDAL CURRENT DISTRIBUTION

ventional base-fed radiator with a height of  $205^\circ$ . Patterns B and C are for sectionalized antennas insulated at the center with current distributions as shown. Pattern D is for the sectionalized antenna designed by Jeffers in 1947. This design results in almost complete suppression of the high angle radiation. Patterns A, B and D have very nearly the desired characteristics for the WOAI application. It is well known, however, that the current distribution in an actual antenna of practical dimensions does not correspond closely to the assumed simple sinusoidal current distribution. An investigation of radiation patterns based on practical current distributions was therefore undertaken.

Figure 3 shows the predicted current distribution for four types of radiators. The prediction of current distribution was based on a modification and extension of a method outlined by Schelkunoff and Friis<sup>7</sup> for determining the approximate current distribution of cylindrical radiators of anti-resonant length. The total current  $I_0$  is composed of an  $I'$  "in phase" component and a quadrature component,  $I''$ . The  $I'$  component may be thought of as representing the power component of the current, while the quadrature component is responsible for most of the radiation from the antenna. The constant  $k_1$  is simply the ratio  $I_{\text{max}}'/I_{\text{max}}$  and the constant  $\gamma$  is the ratio of the velocity of the light to the phase velocity on the radiator.

The constants  $k_1$  and  $\gamma$  were determined by reference to base impedances for cylindrical antennas of anti-resonant length. Complete details, including equations, for obtaining the current distributions are given in the Appendix.

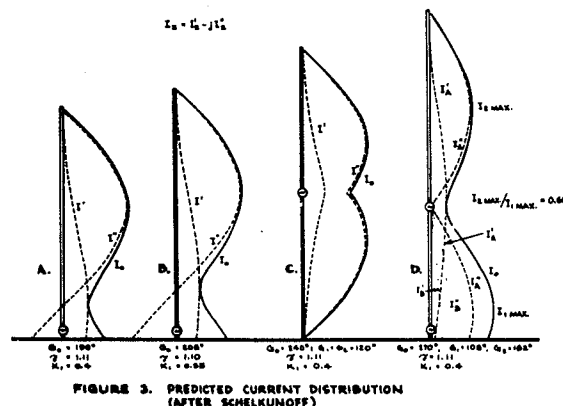


FIGURE 3. PREDICTED CURRENT DISTRIBUTION (AFTER SCHELKUNOFF)

The method used to predict the current distributions is reasonably simple and provides an adequate approximation for this application. It should be noted that considerable information is available concerning more advanced methods of establishing the current distribution of cylindrical radiators,<sup>8,9,10</sup> but unfortunately the methods which yield the most accurate results are quite complex and require tedious computations.

Current distributions A and B of Figure 3 show that the minimum of the current distribution is filled in by the in-phase component of current. The amount of the fill increases as the effective diameter of the radiator is increased.

Current distribution C of Figure 3 is based on the assumption that both the in-phase and quadrature components of current will be symmetrical with respect to the sectionalizing level, where power is applied. Such symmetrical current distribution would be expected if the radiator were removed from the ground plane; thus it is apparent that the effect of the ground plane on the current distribution has been neglected.

Current distribution D shows the predicted current distribution for the Jeffers antenna. The length of the upper section length was adjusted to be anti-resonant, and the current predicted for the bottom section is based on two sets of components as indicated. Components  $I_B$  and  $I_C$  are predicted in the same manner as for the simple base-fed radiator. The sum of these components provides the total current and the desired loop current ratios.

Figure 4A shows the vertical radiation patterns for three types of antennas computed on the basis of the predicted current distributions shown by Figure 3. All vertical patterns presented are based on the usual assumption of a flat infinitely conducting ground plane and the details, including the equations used, are given in the Appendix. Note the large amount of null fill in the A and B patterns for conventional base-fed radiators. The relatively large amount of high angle radiation obviously makes this type antenna unsuitable for anti-fade applications.

Pattern C has the desired characteristics for the WOAI application, and Pattern D also exhibits desirable characteristics with very effective suppression of high angle radiation.

Figure 4B shows the predicted WOAI groundwave and 50 percent skywave signals computed for antennas providing the vertical patterns shown by Figure 4A. The skywave signals are based on the "latitude" 50% skywave curves developed for the clear channel hearing at the FCC. The skywave signals shown for the conventional base-fed radiators are undesirable because of inadequate close-in suppression of the skywave signal. The Jeffers antenna provides the best suppression of close-in skywave signal, but the build-up of the skywave signal in a range from 125 to 175 miles is relatively slow, and undesirable, as it increases the depth of the fading zone.

The antenna consisting of two 120° sections was selected as the optimum design because of the rapid build-up of skywave signal between 125 and 175 miles. While the close-in skywave suppression is not as good as the Jeffers antenna, it is still considered adequate. Consideration of the several vertical patterns explored shows that the desired rapid build-up of

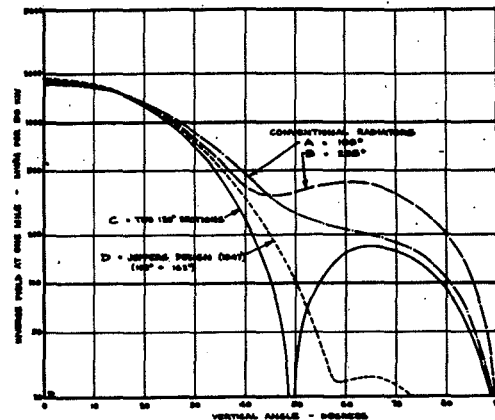


FIGURE 4A. VERTICAL RADIATION PATTERNS BASED ON PREDICTED CURRENT DISTRIBUTION (AFTER SCHUCKHOFF)

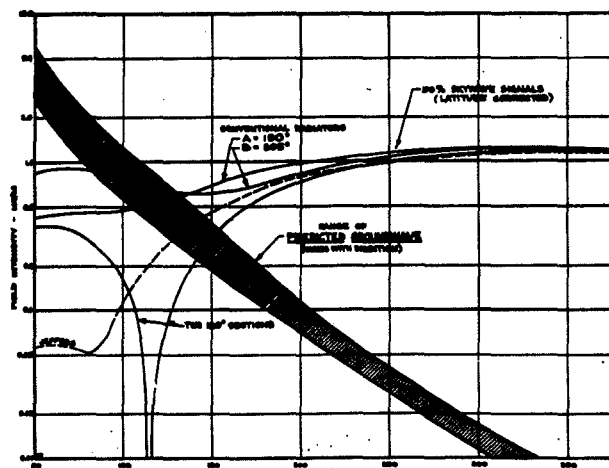


FIGURE 4B. PREDICTED GROUNDWAVE AND SKYWAVE SIGNALS

skywave signal in the region of the fading zone can be obtained only with an antenna having a sharp null in the vertical pattern and a high angle lobe of appreciable size.

### MODEL TESTS

A model of the proposed antenna was constructed to permit a further evaluation of the performance. Figure 5 is a sketch of the model antenna as scaled for measurements at a frequency of 755 mc. The model was constructed of 1/8 inch brass tubing with insulated spacers provided as indicated. A miniature coaxial line was used to transfer power to the sectionalizing insulator. The outer conductor of the coaxial line was insulated from the lower section of the antenna as indicated, and the position of the shorting plug was adjusted to obtain the required base isolation.

Figure 6 shows the arrangement of measuring equipment employed to measure the amplitude and phase of the currents on the model antenna. The model was mounted on a copper-covered wall of a special test room, with the wall simulating the ground in the case of the actual antenna. The other surfaces of the room were covered with R.F. absorbing material so as to make an anechoic chamber simulating an infinite ground plane in free space. One miniature balanced shielded sampling loop was employed to sample the current on the antenna, and a second loop was used to obtain a reference signal. Choke coils were used to minimize currents on the sampling lines. The loops were coupled to a receiver through a variable attenuator and a terminated slotted coaxial

line, as shown by Figure 6. One loop was maintained at a fixed position and the other loop was moved along the model antenna to measure the current distribution. At each position the variable attenuator and slotted line probe were adjusted to produce minimum signal at the receiver input. The relative amplitude and phase of the current were then computed as a function of the location of the pick-up probe on the slotted line and the attenuator setting.

Figure 7 shows three sets of current distribution measurements made for three conditions of base tuning. The tuning was accomplished by adding short capacitive stubs of wire just above the base insulator. Analysis of Figure 7 shows that the amplitude of current in the lower element of the antenna can be controlled by base tuning. A completely symmetrical current distribution could not be obtained due to coupling from the image antenna, but the current distribution obtained with the 1.2 centimeter stub is reasonably close to the assumed symmetrical distribution.

Figure 8 shows vertical radiation patterns for the model antenna computed from the current distribution measurements. These patterns were computed by a graphical integration process. The results show that the base tuning may be used to control the angle of minimum radiation. The efficiency figures (inverse field strength at one mile) shown by Figure 8 were determined by integration of the radiation patterns.

Figure 9 shows the 50 percent sky-wave signals based on the vertical radiation patterns computed from the

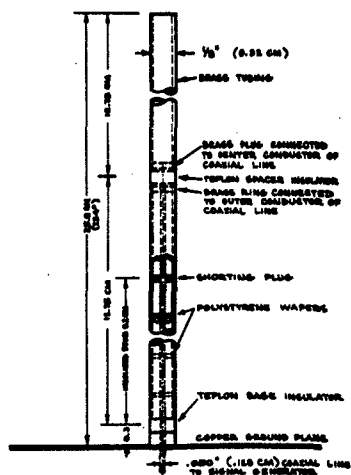


FIGURE 5. SKETCH OF MODEL ANTENNA

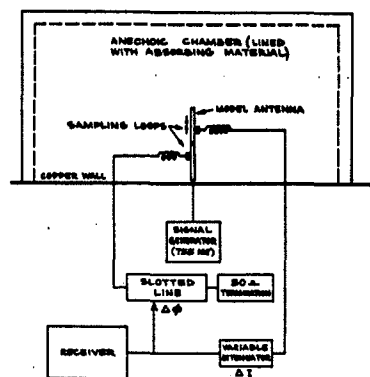


FIGURE 6. TEST EQUIPMENT USED FOR CURRENT DISTRIBUTION MEASUREMENTS

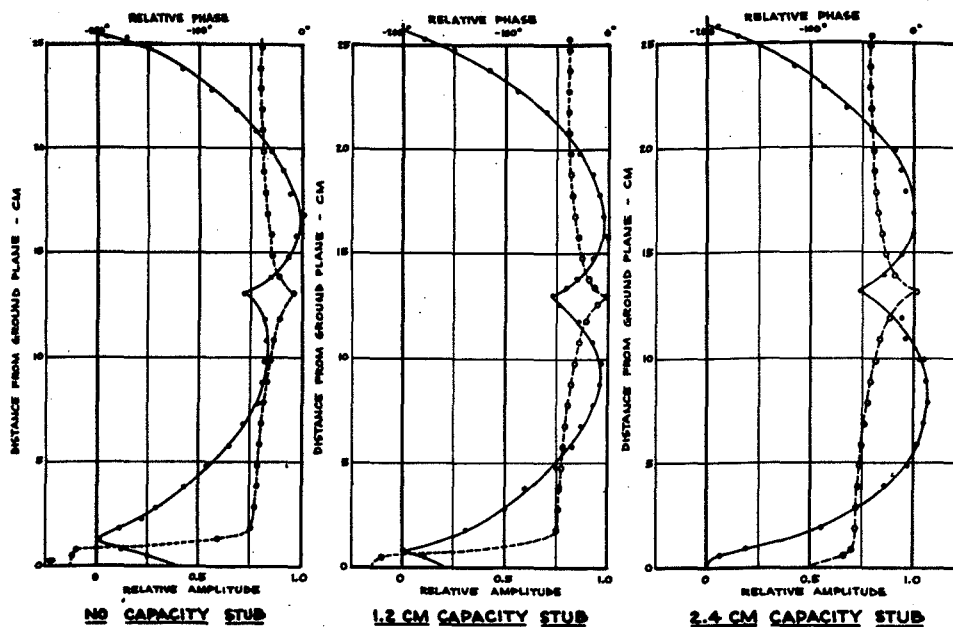


FIGURE 7. CURRENT DISTRIBUTION OBTAINED ON MODEL ANTENNA (755 MC)

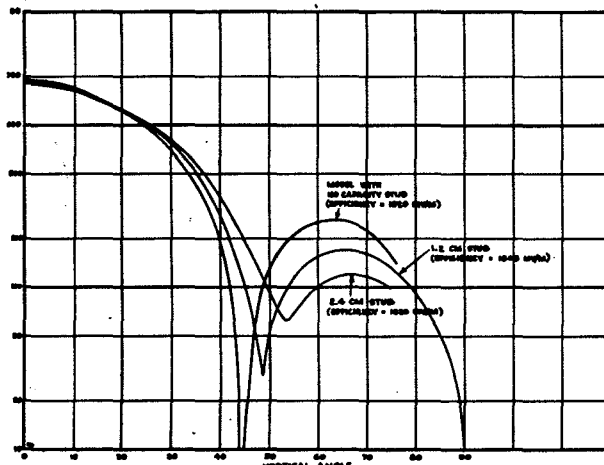


FIGURE 8. VERTICAL RADIATION PATTERNS FOR MODEL ANTENNA AS COMPUTED FROM MEASURED CURRENT DISTRIBUTION

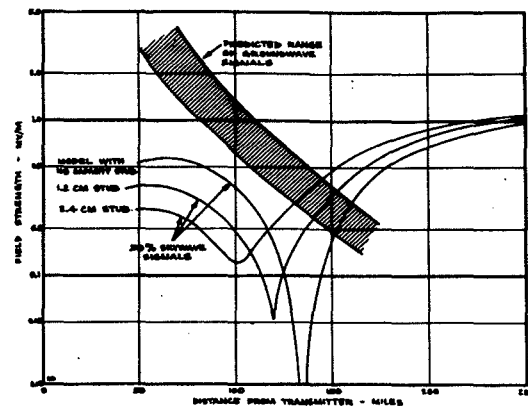


FIGURE 9. GROUNDWAVE AND SKYWAVE SIGNALS PREDICTED FROM MODEL MEASUREMENTS

model measurements. The model with the 1.2 centimeter stub provides the required suppression of high angle skywave signal and exhibits the desired rapid build-up of signal in the region from 125 to 175 miles.

#### ADJUSTMENTS AND PERFORMANCE MEASUREMENTS

Figure 10 is a sketch showing details of the antenna as constructed at the new transmitter site of Station WOAI.

The overall height is 540 feet, or approximately  $240^\circ$ , at 1200 kc. The tower is insulated at the base and at the mid-point, 270 feet above ground level. The tower was manufactured by Stainless, Inc. and is a uniform triangular cross-section guyed structure, with a side dimension of 5 feet. The isolation required at the sectionalizing insulator level and the base is obtained by using insulated stub sections formed by the tower legs and the insulated transmission line and wiring

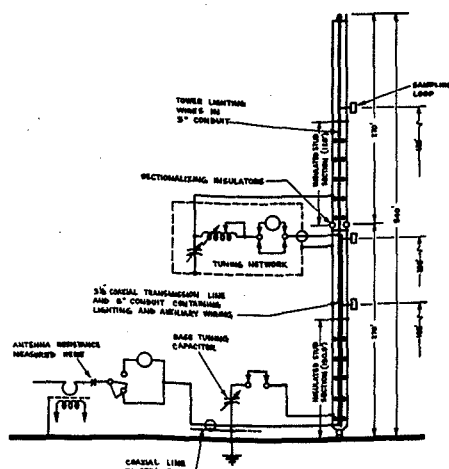


FIGURE 10. DETAILS OF WOAI ANTENNA

conduit. All wiring is housed in a single 5-inch galvanized steel conduit which is centered in the tower cross-section and insulated from the tower where required. The 3-1/8 inch transmission line required to transfer power to the sectionalizing insulator level is attached to the center conduit. An L network is utilized to match the transmission line to the impedance presented across the sectionalizing insulators. The base of the antenna is tuned by a variable capacitor employed in conjunction with the inductive stub section. Three sampling loops are located on the tower as shown by Figure 10 and the coaxial lines from these loops are connected to a phase monitor located at the base.

Figure 11 shows the results of measurements made to determine the effect of base tuning on the groundwave efficiency. Current ratios as provided by the sample loop signals are also shown. Field measurements were made at two clear locations at distances of 2.6 and 5.1 miles, and the results were adjusted for equal power input to the antenna. A base tuning susceptance of 1.4 mmhos provided maximum groundwave efficiency.

Observations of the suppression of sky-wave signals were then made by employing pulse transmissions during the experimental period and observing the results at significant distances. The Continental transmitter of WOAI was modified for pulse operation by keying one of the low-power stages with a pulse generator of special construction. The pulse repetition rate was approximately 200 per second and the width of the pulse was approximately 100 micro-seconds. Observations were made at three locations where the signal was picked up by a wide-

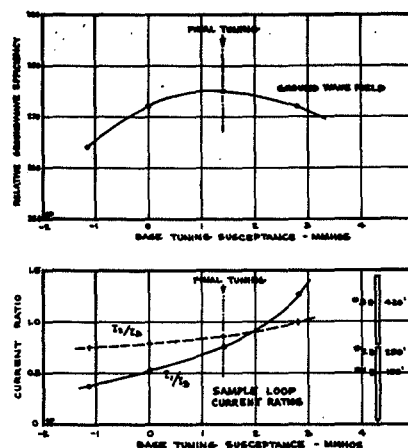


FIGURE 11. GROUND WAVE EFFICIENCY AND SAMPLE LOOP CURRENT RATIOS VS. BASE TUNING SUSCEPTANCE

band receiver and displayed on a Tektronix oscilloscope. A large single-turn loop antenna was used to pick up the signals, as it was believed this type of antenna would offer minimum directivity in the vertical plane.

Figure 12 shows photographs of pulse signals as received near Austin on October 29, 1958. Photograph A shows an F layer pulse with a delay of 1,100 micro-seconds and two pulses of greater delay which are probably two and three-hop F pulses. The groundwave pulse extends well beyond the lower edge of the photographs. Photograph B shows a small E layer pulse and an F layer pulse. During most of the night, no E layer signals were present, but just before daybreak some weak E layer signals as shown by photograph B were observed.

Figure 13 shows photographs of pulse signals received at Temple. Photograph A shows E layer and F layer pulses along with a weak two-hop E layer pulse. Several other weak pulses are also evident. The interference evident in the groundwave pulse was caused by pickup of R.F. signals generated by the oscilloscope sweep circuits. Photograph B shows the groundwave pulse only with no skywave signals evident. This condition was typical of the night of November 5 when no F layer signals were observed and E layer signals, when observed, were relatively weak.

Figure 14 shows photographs of signals received at Waco on October 28, 1959. Photograph A shows E layer and F layer pulses and photograph B shows one-hop and two-hop E layer pulses and

also an F layer pulse. The one-hop E layer pulse is considerably wider than the transmitted pulse, indicating a considerable spread of effective virtual heights.

Figure 15 shows two unusual conditions observed at Waco. Photograph A shows E layer and F layer pulses followed by several pulses having a large delay. The largest of these pulses has a delay of approximately 2,500 microseconds indicating a two-hop F layer mode. Photograph B shows a double pulse with the larger peak occurring at the correct time delay for E layer transmission. The smaller pulse indicates a time delay of 150 microseconds corresponding to a virtual height of only 80 km. The interference apparent on Photograph B was caused by an adjacent channel station.



A. GROUNDWAVE, F LAYER, (1100  $\mu$ s) AND TWO PULSES OF GREATER DELAY (3000 AND 4000  $\mu$ s).  
B. GROUNDWAVE, E LAYER, (340  $\mu$ s) AND F LAYER (1000  $\mu$ s)

FIGURE 12. PHOTOGRAPHS OF PULSE SIGNALS RECEIVED AT AUSTIN (84 MILES) ON OCTOBER 29, 1958



A. GROUNDWAVE, E LAYER (360  $\mu$ s) TWO HOP E LAYER (700  $\mu$ s) AND F LAYER (1100  $\mu$ s) PULSES. OCT. 28, 1958  
B. GROUNDWAVE PULSE ONLY NOV. 5, 1958

FIGURE 13. PHOTOGRAPHS OF PULSE SIGNALS RECEIVED AT TEMPLE (135 MILES)

Figure 16 shows the results of a time delay analysis of the pulse observations made at the three locations. The observed time delays are plotted as a function of the distance from the transmitter. The experimental data are compared to computed time delay curves based on virtual ionosphere heights of 100 km for E layer transmission and 240 km for F layer transmission. There appears to be little question but what the pulses having the greatest time delay were transmitted by the F layer of the ionosphere.

Figure 17 shows the results of pulse amplitude observations made just north of Austin on the night of October 29, 1958. The base tuning of the antenna was varied and the ratios of skywave to groundwave pulses were observed over a period of approximately two hours. A number of observations were made for each tuning condition and the average results are shown. During most of the night the F layer pulse was the only skywave pulse evident. As daybreak approached some weak E layer signals were observed. It was evident from the observations that during most of the time the skywave signals completely penetrated the E layer and were reflected by the F layer. The results show the base tuning for minimum E and F layer signals.

Figure 18 shows the pulse amplitude



A. GROUNDWAVE, E LAYER (320  $\mu$ s) AND F LAYER (900  $\mu$ s) PULSES.  
B. GROUNDWAVE, ONE HOP E LAYER (350  $\mu$ s), TWO HOP E LAYER (700  $\mu$ s) AND F LAYER (900  $\mu$ s) PULSES

FIGURE 14. PHOTOGRAPHS OF PULSE SIGNALS RECEIVED AT WACO (170 MILES) ON OCTOBER 28, 1958



A. GROUNDWAVE, E LAYER (310  $\mu$ s) AND F LAYER (930  $\mu$ s) PULSES. NOTE ADDITIONAL LARGE PULSE WITH DELAY OF 2500  $\mu$ s.  
B. GROUNDWAVE, POSSIBLE D LAYER (180  $\mu$ s) AND E LAYER (340  $\mu$ s) PULSES.

FIGURE 15. PHOTOGRAPHS OF SOME UNUSUAL PULSE SIGNALS RECEIVED AT WACO (170 MILES) ON OCT. 28, 1958

results obtained at a location near Temple, Texas, 135 miles from the transmitter site. Observations were made at this location on two nights as indicated. E layer signals were observed on both occasions, but F layer signals were observed only on the night of October 28. The E layer signal was substantially higher on October 28 than on November 5, but in both cases minimum E layer signal was obtained with a base tuning susceptance of approximately 1.3 mmhos.



Figure 19 shows pulse amplitude results obtained at a location near Waco, Texas, some 170 miles from the transmitter site. E layer signals were observed on October 28 and November 5, and on October 28 F layer signals were also present. The results show minimum E layer signal with a base tuning susceptance of zero and minimum F layer signal with 3.0 mmhos.

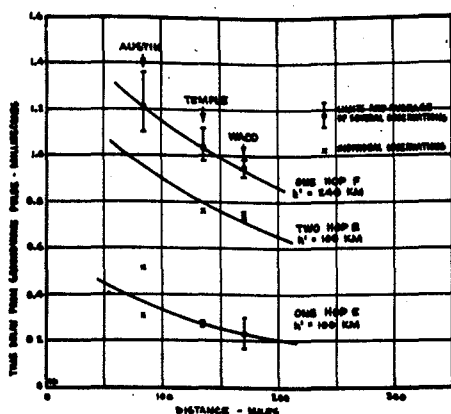


FIGURE 16. RESULTS OF PULSE DELAY MEASUREMENTS

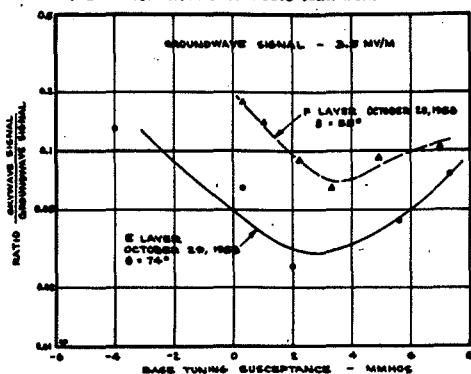


FIGURE 17. RESULTS OF AMPLITUDE ANALYSIS OF PULSE MEASUREMENTS  
AUSTIN - 64 MILES

Figure 20 shows the relation between base tuning susceptance and the vertical angle of minimum radiation as deduced from the data shown by Figures 17, 18, and 19. The angle of minimum radiation may be varied from  $38^\circ$  to  $74^\circ$  by varying the base tuning. The final tuning selected provides minimum vertical radiation at an angle of approximately  $42^\circ$ .

The strong F layer skywave signals observed on the nights of October 28 and October 29 indicate that F layer transmission may be an important factor in the design of anti-fade antennas for use in the higher frequency portion of the

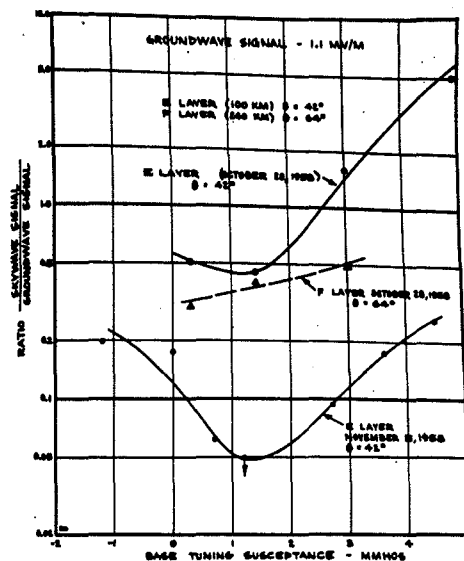


FIGURE 18. RESULTS OF AMPLITUDE ANALYSIS OF PULSE MEASUREMENTS - TEMPLE - 126 MILES

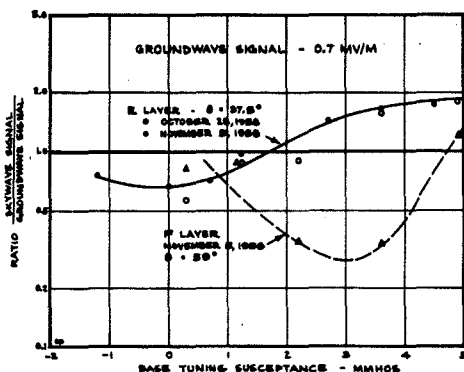


FIGURE 19. RESULTS OF AMPLITUDE ANALYSIS OF PULSE MEASUREMENTS - WACO - 170 MILES

broadcast band. The presence of F layer signals has also been reported by DeWitt and Ring,<sup>11</sup> who made measurements at a frequency of 1410 kc. The observations made at Austin on the night of October 29 show that the signal completely penetrated the E layer except toward daybreak when weak E layer signals were observed. Time was not available to make further pulse observations to establish whether the F layer transmission observed on

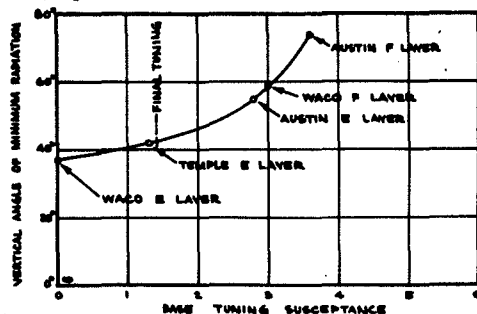


FIGURE 20. EFFECT OF BASE TUNING ON ANGLE OF MINIMUM RADIATION

October 28 was an isolated instance or occurred for an appreciable percentage of the time. The results obtained clearly indicate the need for obtaining more measurements of this type so that the mechanics of skywave propagation for this frequency range will be more fully understood.

Figure 21 shows the current distribution measured on the full scale antenna with the final base tuning adjustment. A movable sampling loop was connected to one of the regular sampling lines so that amplitude and phase measurements could be made by employing the phase monitor at the base of the antenna. The sampling loop was spaced several feet from the center of the tower to minimize pick-up from stub currents. It can be seen that the current distribution obtained on the full scale antenna closely approximates the current distribution shown by the dashed lines as obtained on the model with no capacity stub.

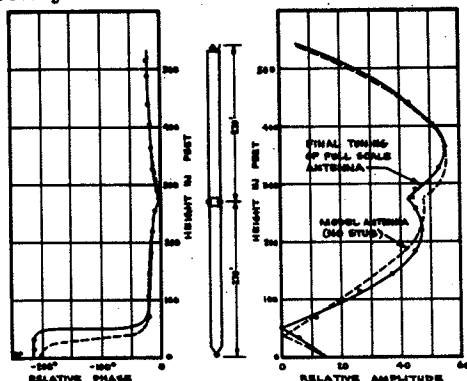


FIGURE 21. CURRENT DISTRIBUTION MEASUREMENTS FOR FINAL TUNING - ( $b = 1.4$  mmhos)

Figure 22 shows the vertical radiation pattern for the final tuning of the antenna compared with the vertical pattern obtained for the model with no capacity stub. The vertical patterns were computed from the current distribution measurements by a mechanical integration process. Further integration of the vertical pattern for the full scale antenna indicates a no loss inverse field strength at one mile of 1950 mv/m for a power of 50 kw.

Figure 23 shows the groundwave and skywave signals for the final adjustment of the antenna as compared with the originally intended tuning of the

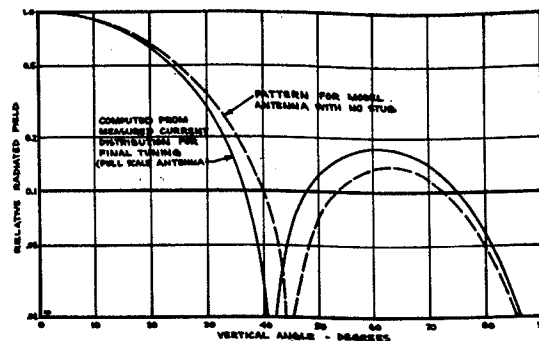


FIGURE 22. VERTICAL RADIATION PATTERN FOR FINAL TUNING ( $b = 1.4$  mmhos)

antenna. The measured groundwave signal on the route through Austin and Temple is also shown, and it is evident that the measured groundwave field strength was considerably higher than predicted. In view of the higher than expected groundwave signal, it was decided to select the final tuning condition shown rather than the tuning condition which would most closely approximate the originally intended performance. The final tuning provides minimum radiation at a vertical angle of approximately  $42^\circ$ , which corresponds to a distance of 150 miles for E layer transmission. Skywave signals computed for an F layer virtual height of 240 km are also shown by Figure 23. Further observations, including field strength measurements to establish the limit of groundwave service in several directions, are now being made to determine whether any change in tuning may be desirable.

Radial groundwave field strength measurements were made in 8 radial directions to establish the efficiency of the WOAI antenna. The RMS inverse field

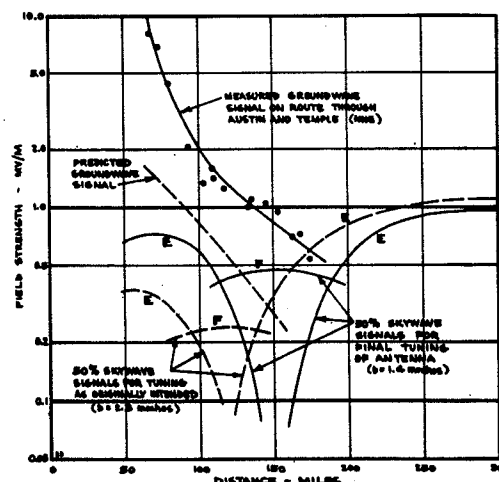


FIGURE 23. GROUNDWAVE AND SKYWAVE SIGNALS FOR FINAL AND ORIGINALLY INTENDED TUNING OF ANTENNA

at one mile was found to be approximately 1890 mv/m. This value is in good agreement with the expected values of 1845 mv/m based on the original design pattern and 1950 mv/m obtained by integration of the radiation pattern as based on the current distribution measurements.

The antenna input impedance at the sectionalizing level for the final base tuning was measured to be  $110 + j 200$  ohms. The impedance value was determined by measuring the input impedance at the lower end of the transmission line with the output end connected directly across the sectionalizing insulators. The impedance was then transferred to the output end of the line by means of a Smith chart.

The authors wish to acknowledge the considerable help provided by A. D. Ring who actively participated in establishing the design criteria and selecting the optimum radiation pattern.

#### CONCLUSION

The design of an anti-fade antenna for broadcasting purposes requires careful consideration of all pertinent factors, including the frequency of operation and the ground conductivity. A rapid build-up of skywave signal just beyond the primary service area is required to minimize the rapid fading zone. For best results the design should incorporate a range of control of the vertical radiation pattern. The effect of practical current distributions on the vertical radiation patterns must be considered. Measurements on a model of the proposed antenna performance form a good basis for making a final evaluation of the performance before constructing the full scale antenna.

After the actual antenna has been constructed, careful measurements are required to insure that the optimum performance is obtained. The suppression of skywave signals may be checked by employing pulse transmissions, and limited measurements indicate that F layer transmissions are sometimes predominant. Finally, the current distribution (both amplitude and phase) of the full scale antenna should be measured and the vertical radiation pattern computed from the current distribution data.

#### REFERENCES

1. G.H. Brown, "A Critical Study of the Characteristics of Broadcast Antennas as Affected by Antenna Current Distribution," Proc. I.R.E., Vol. 24, pp. 48-81, Jan., 1948.
2. H. Page, "Anti-Fading Series-Loaded Mast Radiators," B.B.C. Quarterly Vol. 2, pp. 165-176, Oct., 1947
3. C. L. Jeffers, "An Antenna for Controlling the Non-fading Range of Broadcasting Station," Proc. I.R.E., Vol. 36, pp. 1426-1431, Nov., 1948
4. H. Brueckmann, "Anti-fading Broadcast Antenna," Electronics, Vol. 23, pp. 82-85, May, 1950
5. J. D. Tillman, W. T. Patton, C. E. Blakely, and F. V. Schultz, "The Use of a Ring Array as a Skip Range Antenna," Proc. I.R.E., Vol. 43, pp. 1655-1660, Nov., 1954
6. H. Page and G. D. Monteath, "The Vertical Radiation Patterns of Medium-Wave Broadcasting Aerials," Proc. I.E.E. Part B, Vol. 102, pp. 279-297, May, 1955
7. S. A. Schelkunoff and H. T. Friis, "Antennas, Theory and Practice," John Wiley and Sons, Inc., New York, 1952.
8. R. King and D. Middleton, "The Cylindrical Antenna, Current and Impedance," Quart. Appl. Math., Vol. III, pp. 302-339, Jan., 1946
9. T. Morita, "Current Distributions on Transmitting and Receiving Antennas," Proc. I.R.E., Vol. 38, pp. 898-904, Aug., 1950
10. B. Storm, "Cylindrical Aerials," Wireless Engineer, Vol. 29, pp. 174-176, July, 1952
11. J. H. DeWitt and A. D. Ring, "Significant Radiation from Directional Antennas of Broadcast Stations for Determining Skywave Interference at Short Distances," Proc. I.R.E., Vol. 32, pp. 668-673, Nov., 1944

## APPENDIX

### METHOD OF DETERMINING CURRENT DISTRIBUTIONS AND VERTICAL RADIATION PATTERNS OF CYLINDRICAL RADIATORS

#### A. Conventional Radiators (Power Applied at Base)

Schelkunoff and Friis<sup>7</sup> have shown a method for determining the current distribution on a cylindrical radiator of a given diameter where the length is such as to make the radiator anti-resonant. In the case of a radiator above a ground plane, the anti-resonant length is defined as the length (near  $\lambda/2$ ) where the base input reactance is zero and the resistance is at or near the maximum value. For our purpose the equation for current distribution given by Schelkunoff and Friis has been rearranged so as to permit an extension to radiators of other lengths.

The current may be expressed as:

$$I_z = I_z' - j I_z'' \quad (1)$$

$$I_z' = \frac{I_{\max}'}{2} [1 - \cos \gamma (G_0 - z)] \quad (2)$$

$$I_z'' = I_{\max}'' \sin \gamma (G_0 - z) \quad (3)$$

where:

$I_z$  = current at height  $z$ ,

$z$  = height in degrees above ground plane,

$I_z'$  = real or "in-phase" component of current,

$I_z''$  = imaginary or quadrature component of current,

$I_{\max}'$  and  $I_{\max}''$  = maximum values of  $I_z'$  and  $I_z''$

$v = \frac{c}{v}$  or the ratio of the velocity of light to the phase velocity of the antenna,

and  $G_0$  = overall height of radiator.

For an antenna of anti-resonant length the current at  $z = 0$  is equal to  $I_{\max}'$ , thus

$$I_{\max}' = \sqrt{\frac{P}{R_0}} \quad (4)$$

where  $P$  is the power and  $R_0$  is the base input resistance of the anti-resonant length radiator.

The value of  $\gamma$  can then be determined from

$$\gamma = \frac{180}{l_0} \quad (5)$$

where  $l_0$  is the length of the anti-resonant radiator in degrees. Appropriate values of  $R_0$  and  $l_0$  may be determined from graphs or equations given by Schelkunoff<sup>7</sup> or others.<sup>8,9,10</sup>

The value of  $I_{\max}''$  is determined so as to satisfy the required relationship between current and groundwave efficiency for a given power input. For the current distribution of equations 1 - 3 and assuming anti-resonant length ( $\gamma G_0 = 180^\circ$ ) it can be shown that:

$$E_0 = 0.651 G_0 \sqrt{(I_{\text{avg}}')^2 + (I_{\text{avg}}'')^2} \quad (6)$$

$$I_{\text{avg}}' = \frac{I_{\max}'}{2} \quad (7)$$

$$I_{\text{avg}}'' = \frac{2 I_{\max}''}{\pi} \quad (8)$$

Where  $E_0$  is the inverse field strength in mv/m, at a distance of one mile along the ground plane, and  $I_{\text{avg}}'$  and  $I_{\text{avg}}''$  are the respective average currents in amperes along the radiator. It follows that  $I_{\max}''$  is given by

$$I_{\max}'' = \frac{\pi}{2} \sqrt{\left(\frac{E_0}{0.651 G_0}\right)^2 + \left(\frac{I_{\max}'}{2}\right)^2} \quad (9)$$

The value of  $E_0$  to be used in equation (9) may be taken from data given by Brown<sup>1</sup>, which shows the ground plane radiation efficiency of vertical radiators with reduced velocity, sinusoidal current distribution. This approximate method of determining  $E_0$  amounts to neglecting the influence of the  $I'$  component of current on the radiation efficiency of the antenna. It can be shown, however, that this method yields

results which are quite accurate for the range of effective radiator diameters generally in use for standard broadcast station antennas.

For radiators of other than anti-resonant length an approximate current distribution may be obtained from

$$\frac{I_z}{k_0} = \frac{k_1}{2} [1 - \cos \gamma (G_0 - z)] - j \sin \gamma (G_0 - z) \quad (10)$$

Where  $k_0$  is a constant to relate the absolute current to the relative current distribution and  $k_1 = I'_{\max} / I''_{\max}$ . The values of  $I'_{\max}$ ,  $I''_{\max}$  and  $\gamma$  are based on the solution for a radiator of anti-resonant length and the given effective diameter. This method yielded current distributions A and B shown by Figure 3. The results appear to be reasonable as long as the length of the radiator is not much greater than the anti-resonant length.

The vertical radiation patterns for non-sectionalized radiators such as A and B of Figure 3 were computed by the usual integration of the current distribution:

$$f(\theta) = \frac{\cos \theta}{\int_0^{G_0} I_z dz} \int_0^{G_0} I_z \cos(z \sin \theta) dz \quad (11)$$

where  $f(\theta)$  is the vertical radiation at angle  $\theta$  above the ground plane, normalized with respect to the ground plane radiation.

Solution of this integral expression yields

$f(\theta) = N/D$  where:

$$N = \frac{2\gamma \cos \theta}{\gamma^2 - \sin^2 \theta} [\cos \gamma G_0 - \cos S_0] - j k_1 \cos \theta \left[ \frac{\sin S_0}{\sin \theta} + \frac{\gamma}{\gamma^2 - \sin^2 \theta} \left[ \frac{\sin \theta \sin S_0}{\gamma} \sin \gamma G_0 \right] \right] \\ D = \frac{2}{\gamma} (\cos \gamma G_0 - 1) - j k_1 \left( \frac{G_0}{57.3} - \frac{\sin \gamma G_0}{\gamma} \right) \quad (12)$$

and where:  $S_0 = G_0 \sin \theta$

#### B. Sectionalized Radiators with Current Distribution Symmetrical about Sectionalizing Insulator.

The current distribution shown for radiator C of Fig. 3 is based on a radiator sectionalized at the midpoint with the current distribution assumed to be symmetrical about the feed point. The approximate current distribution for a sectionalized radiator with the current symmetrical about the feed point may be expressed by dividing the radiator into lower and upper sections of lengths  $G_1$  and  $G_2$  respectively.

For the lower section

$$\frac{I_{1z}}{k_0} = \frac{k_1}{2} [1 - \cos \gamma (G_2 - G_1 + z)] - j \sin \gamma (G_2 - G_1 + z) \quad (13)$$

and for the upper section

$$\frac{I_{2z}}{k_0} = \frac{k_1}{2} [1 - \cos \gamma (G_0 - z)] - j \sin \gamma (G_0 - z) \quad (14)$$

As before the constants  $k_1$  and  $\gamma$  were determined from the solution for a radiator of anti-resonant length.

The integration of the current distribution expressed by equations (13) and (14) may be performed in parts to yield

$f(\theta) = N/D$  where

$$N = \frac{2\gamma \cos \theta}{\gamma^2 - \sin^2 \theta} [2 \cos \gamma G_2 \cos S_1 - \cos \gamma(G_2 - G_1) - \cos S_0] - jk_1 \cos \theta \left[ \frac{\sin S_0}{\sin \theta} + \frac{\gamma}{\gamma^2 - \sin^2 \theta} [\sin \gamma (G_2 - G_1) - 2 \sin \gamma G_2 \cos S_1 + \frac{\sin \theta \sin S_0}{\gamma}] \right]$$

$$D = \frac{2}{\gamma} [2 \cos \gamma G_2 - \cos \gamma(G_2 - G_1) - 1] - jk_1 \left[ \frac{G_0}{57.3} - \frac{1}{\gamma} [\sin \gamma(G_2 - G_1) - 2 \sin \gamma - G_2] \right] \quad (15)$$

where  $S_n = G_n \sin \theta$

C. Sectionalized Radiator with Power Applied Both at the Base and at the Sectionalizing Level.

The current distribution for a modified Jeffers antenna as shown for radiator D of Figure 3 was predicted by combining two current distributions predicted by the methods outlined above. Current Components  $I_A'$  and  $I_A''$  represent a symmetrical distribution about the upper feed point as determined from equations (13) and (14). Current components  $I_B'$  and  $I_B''$  represent the expected current distribution on the lower section due to the power applied at the base as determined from equation (10). The total current is simply the sum of the A and B

components with the ratio adjusted to produce the desired loop current ratio. The length of the upper section was made equal to the anti-resonant length in order to simplify this simulation of the current distribution.

The vertical radiation pattern for the modified Jeffers antenna was computed by adding the two radiation patterns produced by the two sets of current components with appropriate constants inserted to maintain the proper relative magnitude of the two patterns. The individual patterns were determined from equations (12) and (15).

D. Evaluating the Equivalent Cylindrical Cross Section of a Tower with Uniform Cross Section.

The equivalent cylindrical diameter of a tower may be determined by computing the effective cylindrical diameter of the three tower legs. Generally the effect of cross and diagonal bracing members may be neglected. Schelkunoff and Friis<sup>7</sup> have shown that

$$a_{\text{eff}} = a \left( \frac{n a_0}{a} \right)^{1/n} \quad (16)$$

Where  $a_{\text{eff}}$  = radius of equivalent cylinder.

$A_0$  = radius of tower legs

$n$  = number of tower legs

$a$  = distance from center of tower legs to center of tower cross section.

AM  
ANTENNAS

# 1958 IRE National Convention Record

## PART 7

Sessions Sponsored by  
IRE Professional Groups on

**Audio**  
**Broadcast Television Receivers**  
**Broadcast Transmission Systems**

at  
the IRE National Convention, New York, N. Y.  
March 24-27, 1958

The Institute of Radio Engineers

## USE OF A SECTIONALIZED TV TOWER IN AM BROADCAST SERVICE

A. C. Goodnow  
Westinghouse Broadcasting Company, Inc.  
New York, New York

### Summary

The 905 foot antenna structure of KYW-TV has been adapted to use as a two-element Franklin antenna at 1100 kc/s, the standard broadcast frequency of station KYW. The TV lines, FM line, and power conduit are insulated within the tower over portions of its length in such a manner as to function as coupling elements at 1100 kc/s. Insulated power transformers or phase monitor isolation coils are not required across the sectionalizing and base insulators, and the tower has a single driving point at the base. Construction details and tuning procedures are discussed; the results of performance measurements show that a horizontal field intensity of 301 mV/m for one kilowatt is realized.

### Introduction

Over the years, considerable attention has been given to the problem of developing antenna designs yielding optimum values of horizontal radiation in the standard broadcast band. As a result of early investigations<sup>1</sup> pointing to the desirability of use of vertical radiators in the vicinity of one-half wavelength or slightly greater in height, and further work<sup>2, 3, 4</sup> emphasizing the allied problem of suppression of high-angle lobes of radiation, the 190 degree radiator (or a top-loaded equivalent) had during the thirties come into wide use in high power broadcasting stations as representing an economically feasible approach to an ideal antenna. With but few exceptions<sup>5, 6</sup>, the use of towers of appreciably greater height was not undertaken because of the rapid increase in cost with increasing height.

Within the past decade, however, construction of towers to decidedly greater heights has become commonplace in the television broadcasting service. The possibility of adapting these taller structures to use as standard broadcast radiators also, where practicable, has aroused considerable interest, and methods of

accomplishing this have been proposed<sup>7, 8</sup>. This paper describes the manner in which the KYW-TV tower in Cleveland, Ohio has recently been put into service as a radiator for KYW.

The FCC authorization for the KYW operation stipulates reduction of the field in northerly directions by approximately 4 db, in order not to increase the previously existing field in the service area of adjacent channel Canadian stations. The required pattern was obtained through use of a parasitically excited reflector in the form of a cable suspended from one of the guys of the tower. Reference to directional operation, however, will be made herein only where it has significance in considering performance of the main tower.

### The KYW Antenna; Choice of Operating Mode

The KYW-TV tower is a uniform-section, triangular guyed tower, 805.5 feet in height and 6 feet in width between corner members. An FM antenna is side-mounted on the tower 753 feet above ground. Atop the tower is mounted a 6-bay superturnstile television antenna, increasing the over-all height of the structure to 905.5 feet. This height corresponds to 364 electrical degrees, or slightly in excess of a full wavelength at the KYW frequency (1100 kc/s).

With the radiator height thus established at approximately one wavelength, operation with the two halves in phase in the Franklin arrangement immediately suggests itself, although consideration of other possible modes of operation was not neglected.

In the quest for maximum values of horizontal radiation, many types of current distribution along vertical radiators have been proposed. Some of these are difficult to realize physically, and none seems to have any great advantage (in this particular application) over



an approximate sine function distribution. Brown<sup>4</sup> points out that the horizontal field of a two-element full-wave Franklin antenna is the same as that of an antenna of the same height having a hypothetical uniform current distribution. The "optimum" distribution of La Paz and Miller<sup>9</sup> for this height (developed to determine the maximum possible horizontal radiation, without regard to whether the indicated distribution is realizable) yields as a theoretical limit a field only slightly higher than that of the Franklin.

These considerations, together with the results of experience with a similar arrangement in the three-fourths wave antenna at KDKA, made firm the decision to operate the KYW radiator as a two-element Franklin antenna, with approximately equal and in-phase currents in the two halves.

#### Details of Coupling and Isolation Sections

The tower is insulated at the center and the base, and insulated cross-bars at thirteen-foot intervals are provided up to the three-fourths wave elevation for supporting the TV and FM lines and a power conduit within the tower. Permanently installed current sampling loops are provided at the one-fourth and three-fourth wave levels, and the cables coupling these to the remote phase monitor are enclosed within the power conduit. The latter, since it may carry an appreciable amount of radio frequency current, is a copper conduit made up of the outer conductor only of the same type of coaxial line (3-1/8 inch) employed for the TV and FM circuits.

The unavoidable presence of TV and FM transmission lines within the tower at first appears to be an annoying complication in the consideration of means of driving the tower as an 1100 kc/s radiator. It soon becomes apparent, however, that in so disposing these lines as to permit the desired voltage and current relations to be developed on the tower, they can themselves be utilized to function as coupling elements between the sections, so that the tower need be driven only at the base. Moreover, by suitably fitting the power conduit into this arrangement, the need for insulated power transformers at the center and the base (along with sampling line isolation coils) is eliminated, and a feed system of gratifying simplicity results.

As shown schematically in Fig. 1 and in greater detail in Fig. 2, the TV lines, FM line, and power conduit are grounded at the base and insulated within the tower to a point one-fourth wavelength above ground. This is a well-known means of isolating such lines so that the tower may be series fed at the base. Both below and above the insulated half-wave level, the lines are similarly disposed as quarter-wave sections in a mechanical arrangement permitting take-off of power, sampling, TV and FM circuits at appropriate points along the tower. Inasmuch as the quarter-wave line sections so formed are connected with their open-circuited ends across the center insulators, they act as a resonant circuit and thus are the means of reversing voltage phase and exciting the upper half of the tower.

The method of excitation bears a superficial resemblance to that of Wheeler's coaxial cable antenna, but the need for a metallic connection (for power and sampling circuits) between the lines and the lower tower element prevents it from functioning in the manner described by Wheeler<sup>10</sup>. Rather it is equivalent to the method shown by Smith and the Huttons<sup>8</sup> in their example of a 258 degree sectionalized top-loaded tower, although in the latter case TV and FM circuits were not considered and a steel cable within the tower functioned as a coupling section.

#### Tuning Procedure

It was anticipated that the mechanical length of the line sections would require reduction by means of shorting straps between the central lines and the tower structure at points in the vicinity of the one-fourth and three-fourths wavelength levels, principally because of the loading effect of insulator capacitance at the base and the center of the tower. In the process of adjustment, as the shorting straps were moved over a range of positions, measurements were made of base impedance, field intensity, and loop current ratio and phase (as indicated by the phase monitor). During the preliminary adjustments, equal active line lengths were maintained in the three sections involved. (The length of short-circuited section below the three-quarter wave point was maintained approximately 10 ft. greater than the other short-circuited portions with the intention of compensating for the lengthening effect of expansion loops formed in the

central lines above the sectionalizing insulators.) Final "trimming" adjustments were made by varying the length of active line section below the half-wave level only.

The measured values of loop current ratio and phase versus active length of coupling line sections are shown in Fig. 3. Inspection of the curves of this figure shows that as the active length of the coupling lines is varied between approximately 168 and 158 feet, the ratio of the loop currents in the upper and lower elements varies from 0.2 to 1.6, while the phase difference varies relatively slowly between approximately 40 and 115 degrees. Apparently over this range the reactance of the coupling sections passes through the point of resonance with the capacity of the tower gap, and it is in this region that the desired mode of tower excitation is approached. On either side of this range of adjustments, the tower gap is bridged by rapidly decreasing values of reactance, and a distinct reversal of phase in the currents of the two elements occurs; this condition is an approach to what should be expected were the tower gap non-existent. With the active length of coupling line sections at a little greater than 162 feet and approximately unity current ratio, the indicated phase lead of the upper element loop current is approximately 83 degrees. Although some rotation of phase is to be expected along the length of the tower, the measured amount is greater than anticipated; as discussed later on, this measurement is believed to be not representative of the phase relation over any considerable portion of the tower length.

A more detailed investigation of the distribution of current amplitude along the tower was made by use of an exploring loop and meter assembly. The measurements were made at a power level of approximately 10 KW. Two-way UHF communication sets were used to facilitate recording the measurements and de-energizing the transmitter while the tower team changed positions.

A set of measurements was made on each of the three tower legs at corresponding positions on the structural sections along the tower; the vertical interval between measuring points was 26 feet in most instances. The results of these measurements, with readings for the three tower legs averaged, are shown in Fig. 4. The discontinuities in the measured leg currents at elevations corresponding to the shorting strap levels are indicative of the functioning of the line sections; at these levels the tower legs begin to carry not only the "antenna" current but also

"transmission line" current in their role as the outer conductor of the line sections. Although the transmission line current in the legs is balanced out in the far-field region by the out-of-phase current in the central conductors, it shows up in the loop measurements because of the closer proximity of the loop to the tower legs. The probable distribution of the antenna current component over pertinent tower sections is indicated by dashed lines in Fig. 4.

The measured distribution is a reasonable approximation of the sine function distribution shown by the dotted line in Fig. 4, although exhibiting somewhat more triangular maxima and broad minima; some reduction of velocity is apparent, particularly in the lower element.

#### Measured Performance

In the process of completing the adjustments and measurements requisite for putting the system into service, a logical work sequence could not always be followed because of prevailing conditions of high wind or icing which made tower work difficult and hazardous. A period of severe weather interrupted work on the tower after it has been tuned approximately to the condition shown by Fig. 4, but before the current ratio indicated by the phase monitor could be verified by measurements with the exploring loop. At this time, however, in the interest of completing the work as rapidly as possible, an extended set of non-directional field intensity measurements (in accordance with the procedure set forth in the FCC Rules and Regulations) was made forthwith. The measured RMS value of the essentially circular pattern resulting was 2070 mV/m, as compared to a value of 2150 mV/m calculated with a 5% allowance for expected system losses.

Subsequently, as a result of the distribution measurements along the tower, it was found that the discrepancy between the readings of the permanently installed sampling loops and the exploring loop measurements was approximately 27%. In the belief that the exploring loop measurements (involving a number of readings averaged over the three tower legs) are less subject to error than the remote readings from the sampling loops, a readjustment of the coupling section lengths was made, to yield the distribution shown in Fig. 4. The field intensity as monitored at a single check point showed no sensible change during this readjustment; the field intensity remains nearly constant on a broad maximum as the current ratio approaches unity. It is probable,

however, that a slight improvement in the horizontal radiation was obtained, since a similar field survey made after the change but with the system operating directionally resulted in an RMS field value only 1% less than a similarly computed value. Accordingly, this is believed to reflect an improvement in the horizontal field of the tower itself that would result in an RMS value of 2130 mV/m in non-directional operation, corresponding to 301 mV/m for one kilowatt.

The apparent error in sampling loop ratio readings may be attributable to a difference in active areas of the loops or their relation to the tower members, although every effort was made to preserve symmetry in their mounting. As mentioned in Section IV above, the approximate quadrature phase relation in loop currents indicated by the phase monitor may also be questionable. Sources of error such as differences in lengths of sampling lines, instrumental inaccuracy etc., were eliminated by appropriate checks, and the fact that the sampling loops are located on portions of the tower which do not carry "transmission line" currents should eliminate any complication associated with effects of the coupling sections. On the other hand, a calculation of the RMS value of the horizontal field assuming quadrature phase difference throughout both elements yields a figure of 1780 mV/m, or 16% less than the value realized. It may therefore be concluded, giving due weight to the measured amplitude distribution of Fig. 4, that the currents are substantially in phase throughout the greater portion of the tower length.

An estimate of the base impedance to be expected was made by assuming that the calculated loop resistance of the upper section (100 ohms) could in this case of half-wave elements be considered to be transferred unmodified to the loop of the lower element and there added to the calculated loop resistance of the latter (127 ohms) the tower then being treated as a fictitious 182 degree radiator with the resultant loop resistance of 227 ohms. These values were used in Schelkunoff's modification<sup>11</sup> of the Siegel and Labus formulae, and yielded a calculated base impedance of  $319-j264$  ohms. The measured base impedance was  $606-j50$  ohms. The actual base impedance, however, may assume any value on a circular locus through the origin, depending on the selected value of the shunting reactance of the lower isolation section. The calculated value, if shunted by a reactance of  $j650$  ohms, for example, becomes  $537+j0$  ohms, a reasonably close approximation of the measured value. It is evident, therefore, that by some device similar to that described, the base impedance in application

such as this can be predicted closely enough for system design purposes.

### Operational Advantages

The operational advantages realized through adaptation of the KYW-TV tower to AM service may be summarized as follows:

1. An increase in horizontal field intensity was obtained equivalent to that corresponding approximately to a 50% increase in power with a conventional antenna.
2. For non-directional operation in Cleveland, an increase of approximately 26% in area and 27% in population served within the primary service area would result.
3. For the actual directional operation authorized in Cleveland, an increase of approximately 34% in area and 53% in population served within the primary service area was realized.

### Acknowledgements

Throughout the planning and completion of the project, the cooperation of the KYW engineering staff, in particular Messrs: R. J. Plaisted and A. H. Butler, was invaluable.

Portions of this material have been included in Applications and Proof of Performance submitted to the Federal Communications Commission.

### References

1. Stuart Ballantyne, "On the Optimum Transmitting Wavelength for a Vertical Antenna Over Perfect Earth," Proc. I.R.E., Vol. 12, pp. 833 - 839; December, 1924.
2. P. O. Pedersen, "Radiation From a Vertical Antenna Over Flat Perfectly Conducting Earth," Danmarks Naturvidenskabelige Samfund, Copenhagen, 1935.
3. A. B. Chamberlain and W. B. Lodge, "The Broadcast Antenna," Proc. I.R.E., Vol. 24, pp. 11 - 35; January, 1936.
4. George H. Brown, "A Critical Study of the Characteristics of Broadcast Antennas as Affected by Current Distribution," Proc. I.R.E., Vol. 24, pp. 48 - 81; January, 1936.

5. Ralph N. Harmon, "Some Comments on Broadcast Antennas," Proc. I.R.E., Vol. 24, pp. 36 - 47; January, 1936.

6. Ralph N. Harmon, "KDKA Low-Angle Antenna Array," presented at I.R.E. National Convention, June 16, 1938.

7. Charles L. Jeffers, "An Antenna for Controlling the Non-Fading Range of Broadcast Stations," Proc. I.R.E., Vol. 36, pp. 1426-1431; November, 1948.

8. C. E. Smith, D. B. Hutton, and W. G. Hutton, "Performance of Sectionalized

Broadcasting Towers," I.R.E. Transactions PGBTS, January 10, 1955.

9. Lincoln La Paz and Geoffrey Miller, "Optimum Current Distributions on Vertical Antennas," Proc. I.R.E., Vol. 31, pp. 214 - 232; May, 1943.

10. Harold A. Wheeler, "A Vertical Antenna Made of Transposed Sections of Coaxial Cable," I.R.E. Convention Record, Vol. 4, Part 1, pp. 160 - 164; March, 1956.

11. S. A. Schelkunoff, "Antenna Theory and Experiment," Jour. Appl. Physics, Vol. 15, pp. 54 - 60; January, 1944.

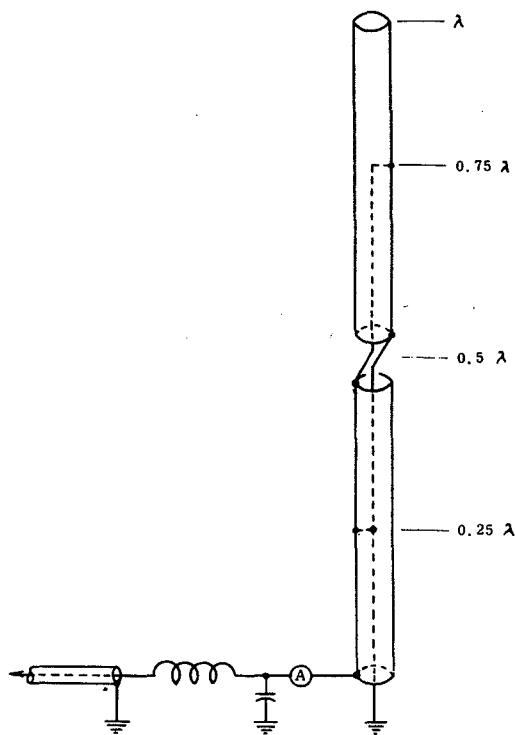


Fig. 1 Schematic diagram of antenna and coupling and isolation sections.

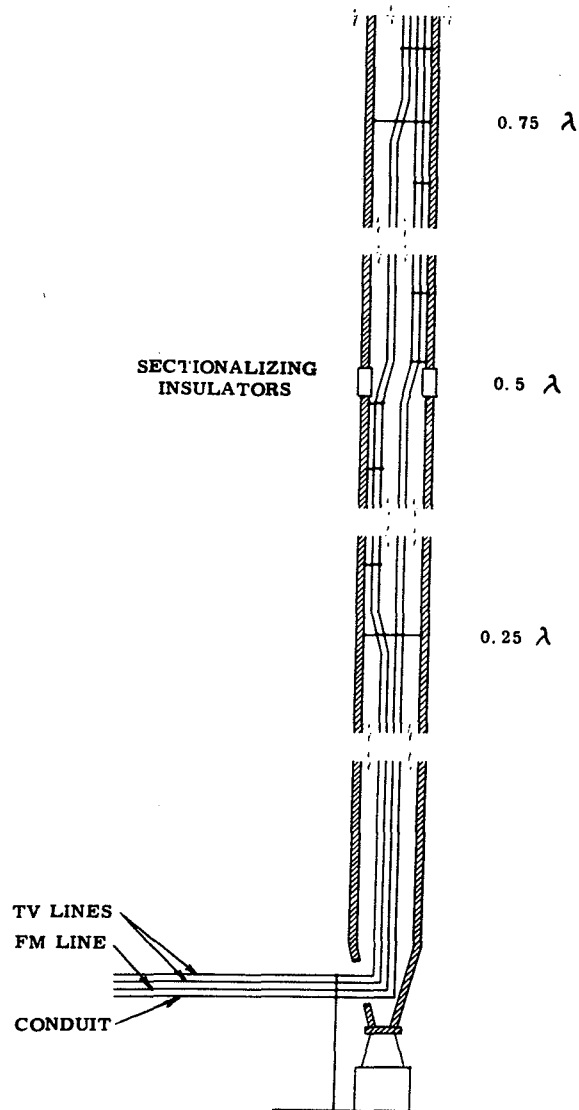


Fig. 2 Detailed schematic of coupling and isolation line sections.

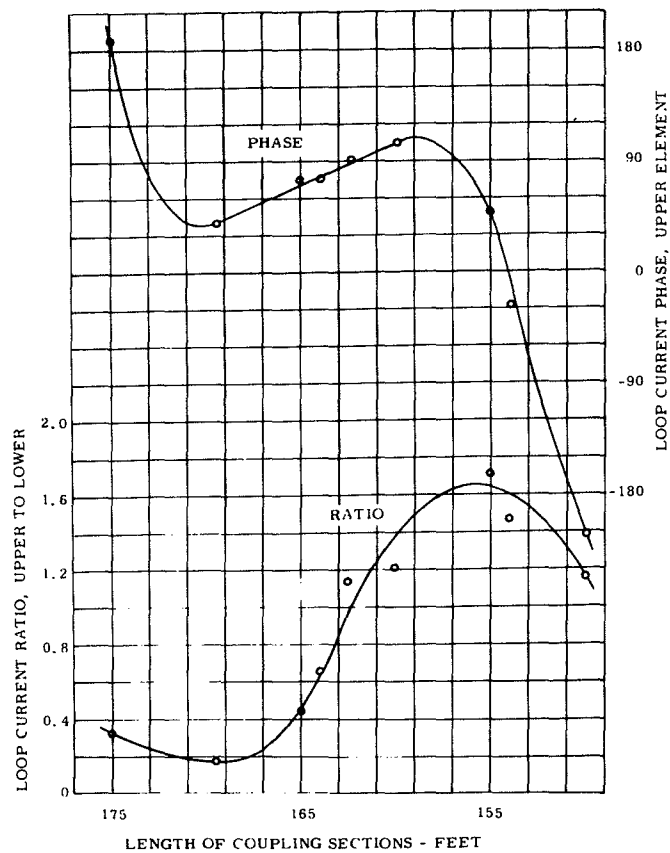


Fig. 3 Measured loop-current amplitude and phase relations vs. coupling-line length.

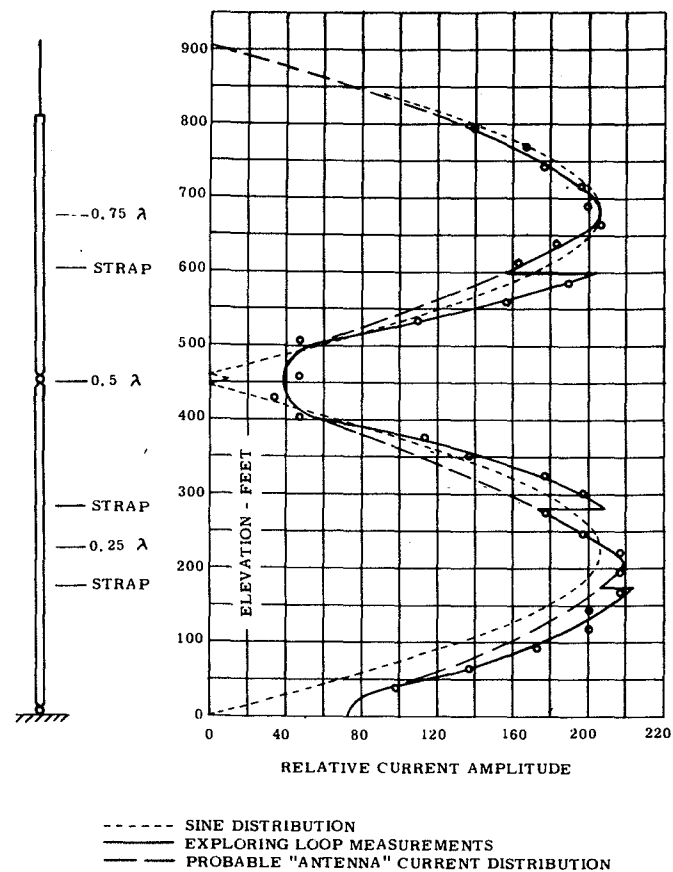


Fig. 4 Measured current amplitude distribution.

DON: Re WMC tall tower problem:-  
 thought this may be usefull.

Warren 10/18/82

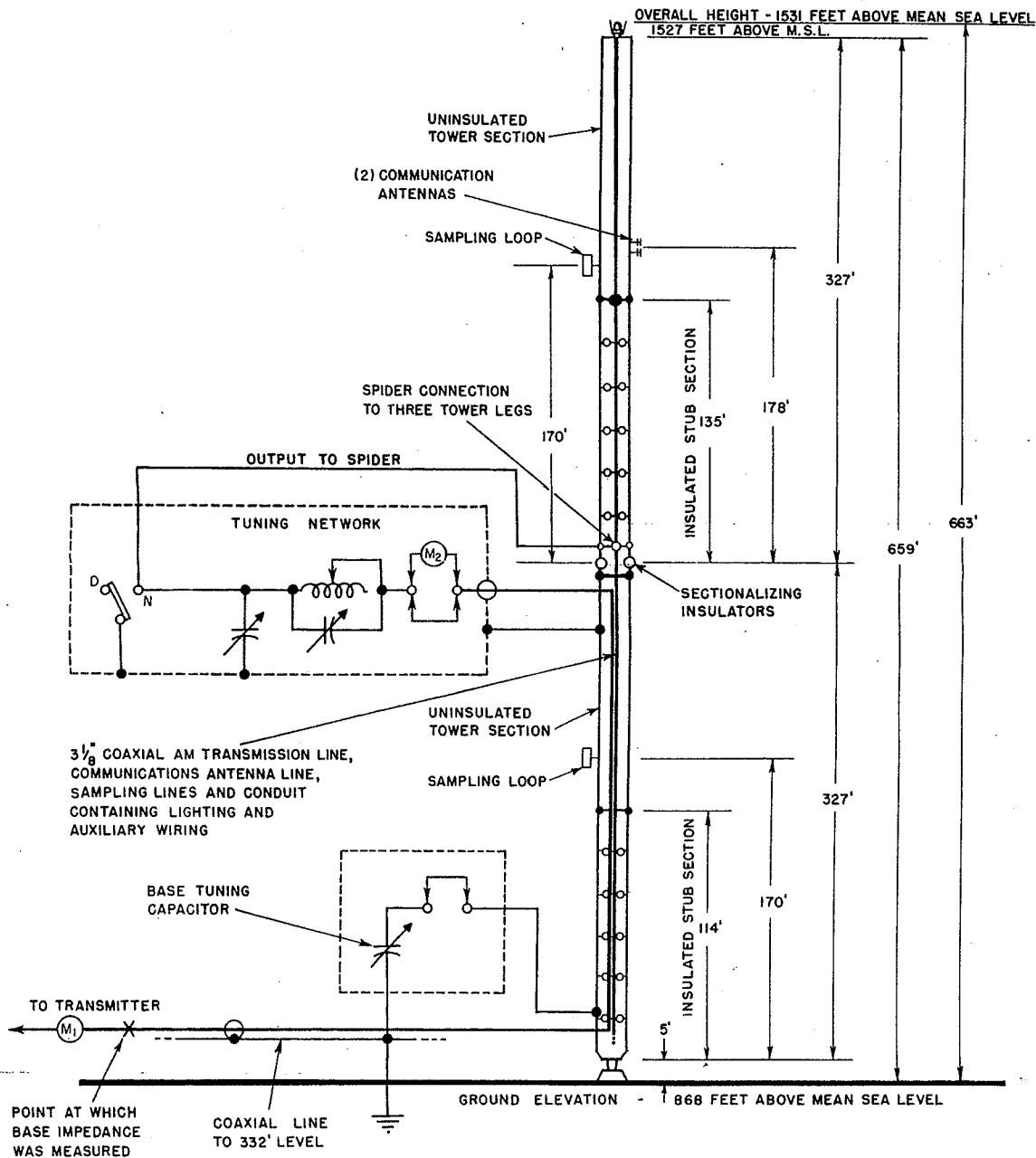


Figure 8

SCHEMATIC DIAGRAM OF DAYTIME  
 FRANKLIN NON-DIRECTIONAL RADIATOR &  
 COUPLING AND TUNING CIRCUITS  
 Station KSTP  
 Hubbard Broadcasting, Inc.  
 St. Paul, Minnesota  
 1500 kc 50 kw-U DA-N

A. D. RING & ASSOCIATES  
 CONSULTING RADIO ENGINEERS  
 WASHINGTON, D. C.

RMS AND RADIATION PROGRAM

The FCC RMS and Radiation program has been designed specifically to meet the needs of FCC engineers processing proposals for broadcast facilities in the standard broadcast band. Using an IBM 704 computer the program first computes the pattern size of the directional array for checking the proposed RMS. It then computes the radiation in the various directions. The pattern size for the computed radiations is ordinarily based upon the value of the radiation specified for a particular direction in the major lobe. If this figure is not supplied to the computer, it uses the applicant's RMS figure. Lacking this, the computer will base the computed pattern size upon the RMS previously computed in the program for the antenna array.

The program uses the vector addition formulae for all types of antenna systems. For some antenna types, certain diagonal spacings and orientations required by the vector addition formulae are not ordinarily supplied by the applicant. It invariably happens however that the towers may be listed in such an order on the coding form that the orientation and spacing of each tower is known either with respect to a common reference point or with respect to the last tower listed. The input form is arranged so that this information may be supplied in either manner. A "1" must be inserted in column 49 of the coding form when the data is given with respect to the last tower listed, as a signal to the computer to make the necessary extra calculations. Formulae 1-4 are used for this purpose and are skipped for towers not having a "1" in column 49.

$$(1) \text{ TEMP } 1 = D_I \cos \theta_I + D_{(I-1)} \cos (I-1)$$

$$(2) \text{ TEMP } 2 = D_I \sin \theta_I + D_{(I-1)} \sin (I-1)$$

$$(3) D_I = [( \text{TEMP } 1 )^2 + ( \text{TEMP } 2 )^2]^{1/2}$$

$$(4) \theta_I = \tan^{-1} \left[ \frac{\text{TEMP } 2}{\text{TEMP } 1} \right]$$

Where:

$D_I$  = distance of tower I from (I-1)<sup>th</sup> tower (temporarily)

$\theta_I$  = orientation of tower I from (I-1)<sup>th</sup> tower (temporarily)

$D_I$  = distance of tower I from reference point

$\theta_I$  = orientation of tower I from the reference point with respect to true north

It should be noted that the  $D_I$  and  $\phi_I$  at the left of the equal sign are with respect to the arbitrary reference point whereas the same symbols to the right of the equal sign have a special temporary meaning and are the spacing and orientation with respect to the  $(I-1)^{th}$  tower for those towers with a 1 in column 49.

The no loss rms is next determined. In this program, this is done by summing calculated values of the "little rms's" at vertical elevation angle increments of ten degrees, using zero order bessel functions for getting the individual little rms's and the trapezoidal rule for summing the little rms's over the hemisphere. (Formulae 6 and 7) Note the use of small letters for little rms's based upon the field ratios, and the use of capital letters for the big RMS which, of course, is a function of the transmitter power. The no loss constant for getting the no loss RMS from the little rms on the ground at theta equal zero is obtained by the relationship between the transmitted power and the summation of the little rms's. (formula 8) Formula 5 gives the vertical radiation characteristic for conventional towers.

$$(5) f_p(\theta) = \frac{\cos(G_p \sin \theta) - \cos G_p}{(1 - \cos G_p) \cos \theta}$$

$$(6) rms_\theta = \left[ \sum_{p=1}^n \sum_{q=1}^n F_p F_p(\theta) F_q(\theta) \cos \psi_{pq} \int_0^{S_{pq} \cos \theta} (S_{pq} \cos \theta) \right]^{1/2}$$

$$(7) rms = \frac{4}{18} \left[ \frac{rms_\theta^2}{2} + \sum_{n=1}^8 rms_{10n}^2 \cos 10n \right]^{1/2}$$

$$(8) K' = \frac{152.1 (P)^{1/2}}{rms}$$

$\theta$  = Vertical angle of the direction of radiation measured from the horizon.

$f_p(\theta)$  = Function of theta defining the vertical radiation pattern of tower p.

$G_p$  = Height of Tower p in degrees.

$F_p$  = Field ratio of the  $p^{th}$  tower.

$rms_\theta$  = Little rms at vertical angle  $\theta$ .

$rms$  = Summation of little rms's over a hemisphere; this is also called total little rms.

$\psi_{pq}$  = Difference in phasing between towers p and q.

$S_{pq}$  = Spacing between towers p and q.



$RMS_R$  Calculated RMS at theta equals zero assuming loss resistance R.

$J_0$  Zero order Bessel function of the first kind.

$F_p$  Field ratio of tower p.

$K'$  Multiplying constant for obtaining hypothetical value of field strengths from field ratio values or hypothetical  $RMS'_q$  from the little rms at theta equals zero.

$RMS'$  Calculated RMS at theta equals zero assuming no loss.

The hypothetical radiated field strengths and tower currents are next determined by formulae 9, 10 and 11.

The adjusted constant, the adjusted tower currents, and the adjusted RMS are next computed by taking into account the power loss in the individual towers of the array. (formulae 12 and 13)

$$(9) \quad E'_q = F_q K'$$

$$(10) \quad I'_q(\theta) = \frac{E'_q \sin G_p}{37.25(1 - \cos G_p)}$$

$\text{if } G \geq 90^\circ$

$$(11) \quad I'_q(\theta) = \frac{E'_q}{37.25(1 - \cos G_p)}$$

$$(12) \quad P'_L(q) = R_q I_q'^2$$

$$(13) \quad P'_L = \sum_{q=1}^n P'_L q$$

Where:

$R_q$  Assumed loss resistance in the  $q^{\text{th}}$  tower.

$G_p$  Antenna height of  $p^{\text{th}}$  tower.

$E'_q$  Hypothetical field strength at one mile from tower q. This is the same as the no loss field strength.

$I'_q(\theta)$  Hypothetical base current of  $q^{\text{th}}$  tower. This is the same as the no loss current.

$I'_q(\theta)$  Hypothetical loop current of  $q^{\text{th}}$  tower. This is the same as the no loss current.

$P'_L(q)$  Hypothetical power loss in  $q^{\text{th}}$  tower.

Hypothetical values of transmitter power output, and tower currents are useful in making this computation. The hypothetical values are defined for this purpose as those which would exist if the no loss field strengths and no loss tower currents were assumed to prevail despite the presence of the assumed loss resistances in the individual towers. The hypothetical values of the currents, power loss, the radiated field strengths, and the constant are the same as the no loss values. The hypothetical values of transmitter power (which includes hypothetical power loss) are greater than the rated transmitter power. In the formulae, the hypothetical values are differentiated from the no loss values by a prime.

The hypothetical values of tower current  $I_p'$ , constant  $K'$ , Field Strengths  $E_p'$  and total power loss  $P_L'$  as well as the value of RMS' are adjusted downwards to predicted values by an amount corresponding to the decrease in transmitter power from the hypothetical value to the operating value. The operating value of transmitter output power is P. The hypothetical transmitter output power  $P'$  is equal to P plus  $P_L'$ .

Power values are adjusted downward by the ratio  $P/P + P_L$ .  $K'$ , RMS, and radiation values are adjusted downward by a factor  $\sqrt{P/(P + P_L)}$ .

Tower current values are also adjusted by the factor  $\sqrt{P/(P + P_L)}$  and these are the values shown on the printout:

$$(14) I_q = I_q' (P/P + P_L)^{1/2}$$

$$(15) P_L(q) = P_L'(q) (P/P + P_L)$$

$$(16) K_{ADJ} = K' (P/P + P_L)^{1/2}$$

$$(17) RMS = RMS' (P/P + P_L)^{1/2}$$

Where:

$I_q$  = predicted current in tower q.

$P_L(q)$ : predicted power loss in tower q.

$K_{ADJ}$  = predicted constant considering losses.

RMS predicted RMS considering losses.

The radiated fields in all required direction is found from the vector sum of the field radios from all towers multiplied by  $K_{ADJ}$ .

$$(18) E_{\theta} = \sum_{p=1}^N E_p F_p(\theta) / \beta_p$$

$$(19) \beta_p = S_p \cos \theta \cos(\phi_p - \phi) + \psi_p$$

Where:

$K_{adj}$  : Adjusted Constant.

$F_p$  Field ratio of the  $P^{th}$  tower.

$\theta$  Vertical angle above horizon.

$\phi_p$  Orientation of tower P.

$S_p$  Spacing of tower P.

$\psi_p$  Relative phasing of tower P.

The pertinent vertical radiation characteristics (function of theta) for the particular type of towers is selected by an 0, 1 or 2 in column 50 of the input card for that tower.

$f_p(\theta)_0$  previously supplied for conventional towers (see  $f_p(\theta)$ ).

The formula for top loaded towers is as follows:

$$f_p(\theta)_1 = \frac{\cos B \cos(A \sin \theta) - \cos A - \sin B \sin \theta \sin(A \sin \theta)}{\cos \theta (\cos B - \cos A)}$$

The vertical function of theta for sectionalized antennas is quite long and was taken from page 2-112 of the NAB Handbook (5th edition). For top loaded towers, the following formulae should be used to find tower current in lieu of Formulae 10 and 11:

$$(20) \text{ if } G_g < 90^\circ I_g'(\theta) = \frac{K' F_g \sin(A+B)}{37.25(\cos B - \cos(A+B))}$$

$$(21) \text{ if } G_g \geq 90^\circ I_g'(\theta) = \frac{K' F_g}{37.25(\cos B - \cos(A+B))}$$

IMPLEMENTATION OF ANTISKYWAVE ANTENNA  
TECHNOLOGY BY EXTREME TOP LOADING OF SHORT  
ANTENNAS IN A DIRECTIONAL ARRAY

Timothy C. Cutforth  
Vir James Consulting Radio Engineers  
Denver, Colorado

ABSTRACT

Top loading of short vertical antennas is usually limited to groundwave field enhancement. A successful method of top loading to achieve antiskywave properties is detailed. The allocation criteria of the KNWZ Thousand Palms, California nighttime directional array includes protection of a station in the direction of the major population center in the service area making antiskywave design essential. The high radiation efficiency achieved in the KNWZ nighttime array is also attributable to the antiskywave characteristics in the antenna design. A similar nondirectional toploading implementation at KIAM Nenana, Alaska achieved dramatic improvement in fringe reception both daytime and nighttime.

ANTI SKYWAVE ANTENNA

The well known  $5/8$  wavelength tower is in effect a gain vertical colinear array because of the current distribution. The gain and the change in vertical section is largely due to the phasing of the currents along the tower. In the far field a  $5/8$  wavelength tower and its ground reflection behave as a 3 element broadside array.

The additional gain clearly comes from the suppression of the otherwise wasted high angle radiation. A similar broadside vertical array can be created with a rather wide range of "element" spacings (or tower height) while retaining significant gain and desirable improvement in the vertical section characteristics. This can be achieved by shifting the normal current distribution with top loading on towers shorter than  $5/8$  wavelength. As the tower becomes considerably shorter than  $5/8$  wavelength the method of top loading becomes more important. In the case of KNWZ Thousand Palms, California the deepest required protection was to XEAZ Tijuana, Mexico at 52 degree vertical angle in the direction of Palm Springs. Top loading from 93 degrees of physical height to 216 degrees electrical height provided the needed high angle skywave suppression while increasing gain for the KNWZ array.

#### MEASURED PERFORMANCE

Measured gain beyond theoretical for the ND and DA-2 arrays indicated gain of 1.5, 1.2 and 3 db was actually achieved at KNWZ. A similar toploading installation was done at KIAM. The KIAM ND tower in Nenana, Alaska achieved 1 db measured gain as constructed when toploaded from 68 degrees physical height to 208 degrees electrical height. KIAM has regular listeners and FM translators as much as 200 miles distant in areas with signal strengths of as little as 25 microvolts per meter. Before installation of the toploading the signal strength at the Tanana translator was S7 on the receiver and varied downward to S5. Since the toploading installation the receiver indication is S8 with no visible fading day or night. Other fringe locations indicate a dramatic improvement in reception with some locations reporting full time listenable signal where there was

little or no discernable signal before. This is clearly greater improvement than can be attributed to the measured 1 dB signal strength increase as measured in the nondirectional proof of performance. We attribute the much larger fringe reception increase to changes in the high angle skywave interference to the groundwave. There was also some increase in the actual transmitter modulation ability resulting from the excellent antenna bandwidth.

#### DEFINING THE ANTENNA

The tower characteristic and the amount of top loading is defined most clearly by the location of the current null on the tower. Measurement of the current is facilitated by the construction of a shielded torroidal loop of coaxial cable which can encompass the tower section. This type of loop is much more tightly coupled to the actual tower current than a conventional sample loop or field meter antenna loop and will easily define the current null location with accuracy of better than one degree. After setting the current null at the exact location desired the loop is moved up and down the tower at convenient increments to measure the actual current distribution. Relative current distributions measured were not sinusoidal but appeared to have the approximately the same current area under the curve that should result from a theoretical sinusoidal current distribution.

The large degree of top loading was accomplished using a relatively small capacity to ground. The KNWZ array used 5m of the top guy wires. The KIAM tower used a 20 ft diameter capacitance hat. The resulting capacitance is insulated from the top of the tower in each case but attached via a coaxial transmission line to lumped reactances at the bottom of the tower for ease of adjustment. An adjustable reactance at the tower base allows for easy adjustment of the current distribution over a wide nearly infinitely variable range of current null locations.

#### METHOD OF ADJUSTMENT

The most practical method of adjustment is to place the current sample loop at the desired tower elevation and then to adjust the loading reactance for a minimum sample current. Sample current nulls as much as 30 db below the current maximum have been observed. The severely top loaded antenna is relatively broadband with driving point resistances considerably higher than the standard tower of the same physical height and have a rather low base reactance resulting in a low Q driving impedance. The KNWZ daytime and nighttime directional arrays both exhibited good bandwidth without specific effort going into field adjustment of the bandwidths of the common point networks or antenna tuning units. The KIAM antenna characteristic provided 10 kHz sideband VSWR's of 1.7 and 2.0 at the tower and was reduced to 1.04 and 1.50 using a standard three component "T" network from parts on hand. The resulting measured KIAM modulation sideband symmetry was down 2 db at 622 kHz relative to 638 kHz with 8 kHz tone modulation and the plate of the Collins 21E transmitter tuned just slightly on the high efficiency side of the dip as is customary. Overall, these antennas have been successful in all respects.

## A SHORT BROADCAST ANTENNA FOR RESTRICTED HEIGHT LOCATIONS

Homer A. Ray

Continental Electronics Mfg. Co., Dallas, Texas

There is a continuing need for the development of small antennas which perform as well as large antennas in current use. This is particularly true at medium and low frequencies where structural height and available sites are fractions of one wavelength. The antenna to be described was developed for very low frequency communications and Loran. It is useful throughout the frequency range where the vertically polarized ground wave is the principle means for radiation.

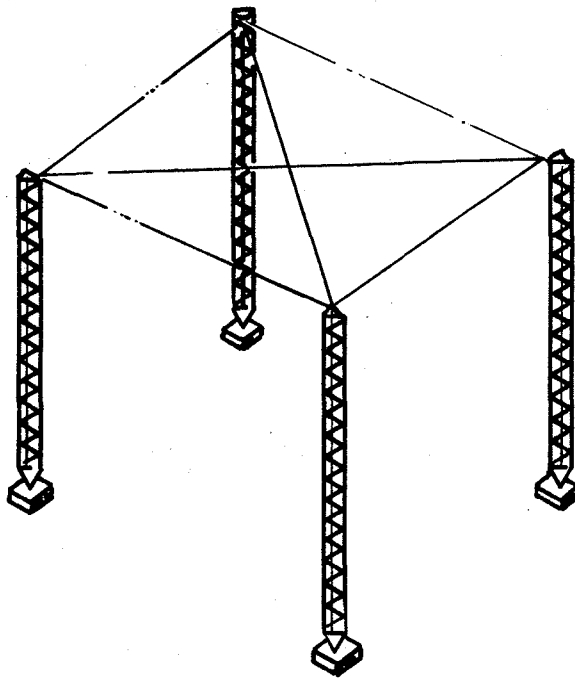
It has evolved that the maximum bandwidth x efficiency product will be achieved for a given site volume if a current sheet of constant amplitude flows vertically at the site perimeter to the total height of the system. This accounts for the name PARAN or "Perimeter Current Antenna". A useful configuration for broadcast applications is shown in Figure 1.

Where FAA height restrictions prevail it can be used at heights as low as 50 to 100 feet. Low heights tend to restrict the charge or induction fields of low radiators to smaller areas and ground systems may therefore be smaller without excessive losses. It is structurally easier to harden small grounded towers as opposed to tall ones so that survival in hurricane areas can be achieved more readily. Small size allows its use as an on-site emergency antenna in the event of damage to the main radiator.

A pictorial diagram of the components in a monopole tower system as used in broadcasting is shown in Figure 2. In all of the discussion which follows a very short tower is visualized and the impedance is predominantly the capacitance



**THE PARAN ANTENNA  
LOW HEIGHT – HIGH EFFICIENCY**



**BROADCAST APPLICATIONS**

1. FAA RESTRICTED HEIGHT LOCATIONS
2. SITES WITH LIMITED GROUND AREA
3. HARDENED FOR HURRICANE AREAS
4. ON - SITE EMERGENCY ANTENNA

**Figure 1 Broadcast Paran Antenna**

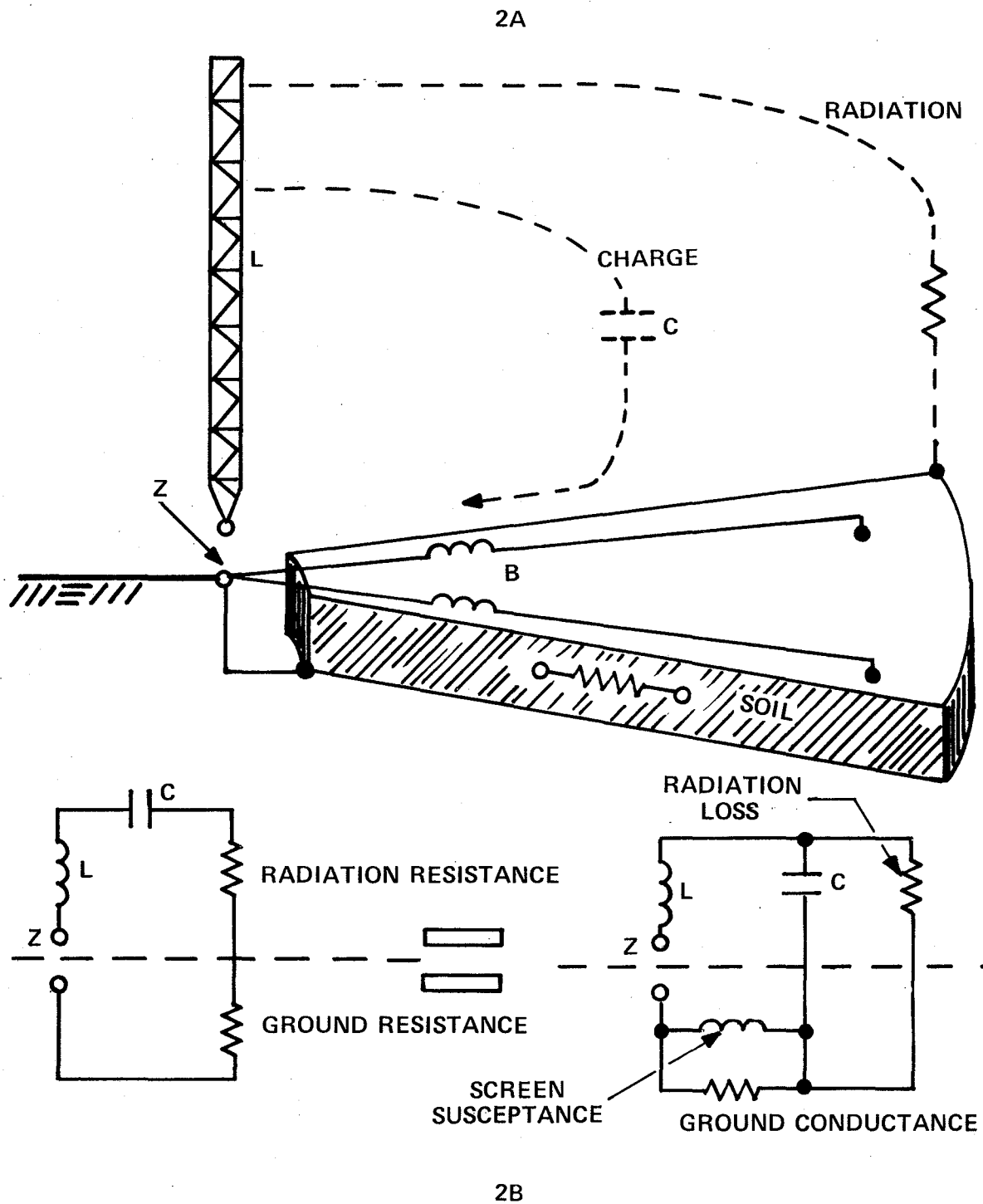


Figure 2 The Monopole Antenna System

of the tower to ground. When power is applied to the terminals Z the predominant current flow during each alternation of the cycle is charging and discharging this capacitance C. Its path includes the tower inductance, plus the inductance of the ground screen and the soil resistance in parallel.

In addition to the local charge through C there is energy propagated beyond a radian length from the tower. This energy due to its distance cannot return to the circuit as an in-phase component on each cycle and is therefore lost to the circuit as radiated power. If there were no soil or conductor losses in the antenna circuit the total loss would be due to radiation and the system would be one hundred percent efficient. We must therefore address ourselves to the ratio of the circuit losses versus the radiation loss. The circuit as seen from Terminal Z is the left diagram of Figure 2B.

It is neither economical or practical to reduce the ground resistance to zero. For the moment we will consider it fixed and equal to one ohm which is a familiar value to broadcasters. A tower 20 electrical degrees high will have a one ohm radiation resistance and the efficiency of this system will be

$$\eta = \frac{100 R_a}{R_a + R_g} = \frac{100}{2} = 50\%$$

If the efficiency of this system is to be improved it must be done by increasing the radiation resistance. Radiation resistance increases as the square of the height and where height is not a limitation is the usual approach. With height limited we have two other options:

1. Current distribution on the tower.
2. Mutual impedance with other towers.

It turns out that each of these options provides a possible four-to-one improvement or a total of sixteen-to-one in the radiation resistance without increasing the tower height.

The current distribution on a single short tower conforms to the first few degrees of a sinewave as shown in Figure 3A. For small angles the sine is equal to its argument and the current distribution is a linear function of height. The field intensity from the tower is the integral of the current over the total height which in this case is simply the area of the triangle A. If the tower is 20 degrees high and the base current is one ampere the area A is

$$A = \frac{1 \times 20}{2} = 10 \text{ ampere degrees.}$$

The field intensity is

$$E = KA \quad \text{Mv/m at 1 mile}$$

where  $K = 0.65$ .

By simple manipulation of ohms law it follows that the radiation resistance at the base of the tower where one ampere is flowing is

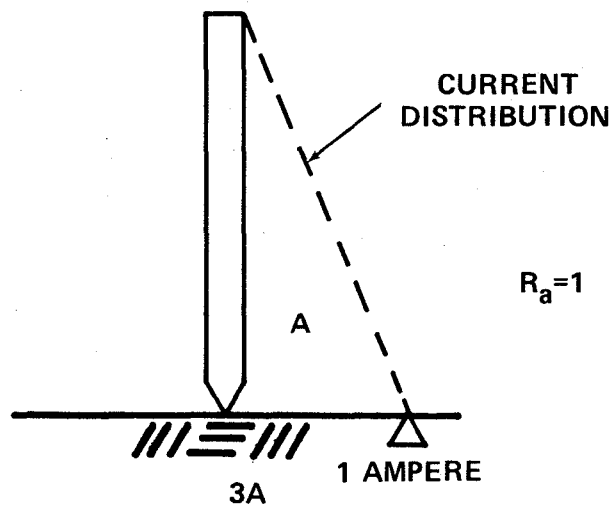
$$R_a = kA^2$$

where  $k = 1,215 \times 10^{-5}$

If A can be doubled as shown in Figure 3B then the radiation resistance will be quadrupled. This calls for constant current throughout the tower height.

One way to achieve constant current is to put a large top hat on the tower so that it becomes quarter wave resonant as shown in Figure 4A. The current distribution on the vertical tower is a few degrees of sine wave but now near 90 degrees and is almost constant throughout the tower height. The top hat can be shortened without affecting the current distribution by inserting a tuning coil as shown in Figure 4B.

A coil at the top of the tower is cumbersome and can be placed at the base by using the tower as a coaxial line to effectively connect it at the top as shown in Figure 4C.



FIELD INTENSITY =  $KA \propto I$

POWER =  $I^2 R_a$

RADIATION RESISTANCE =  $KA^2$

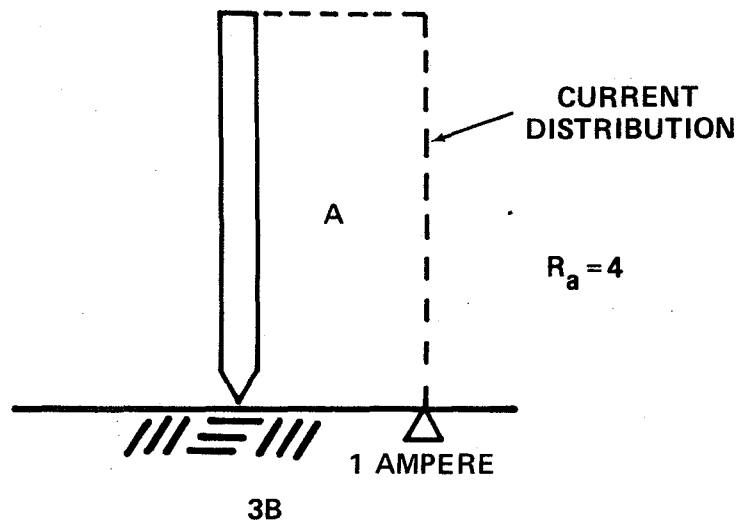
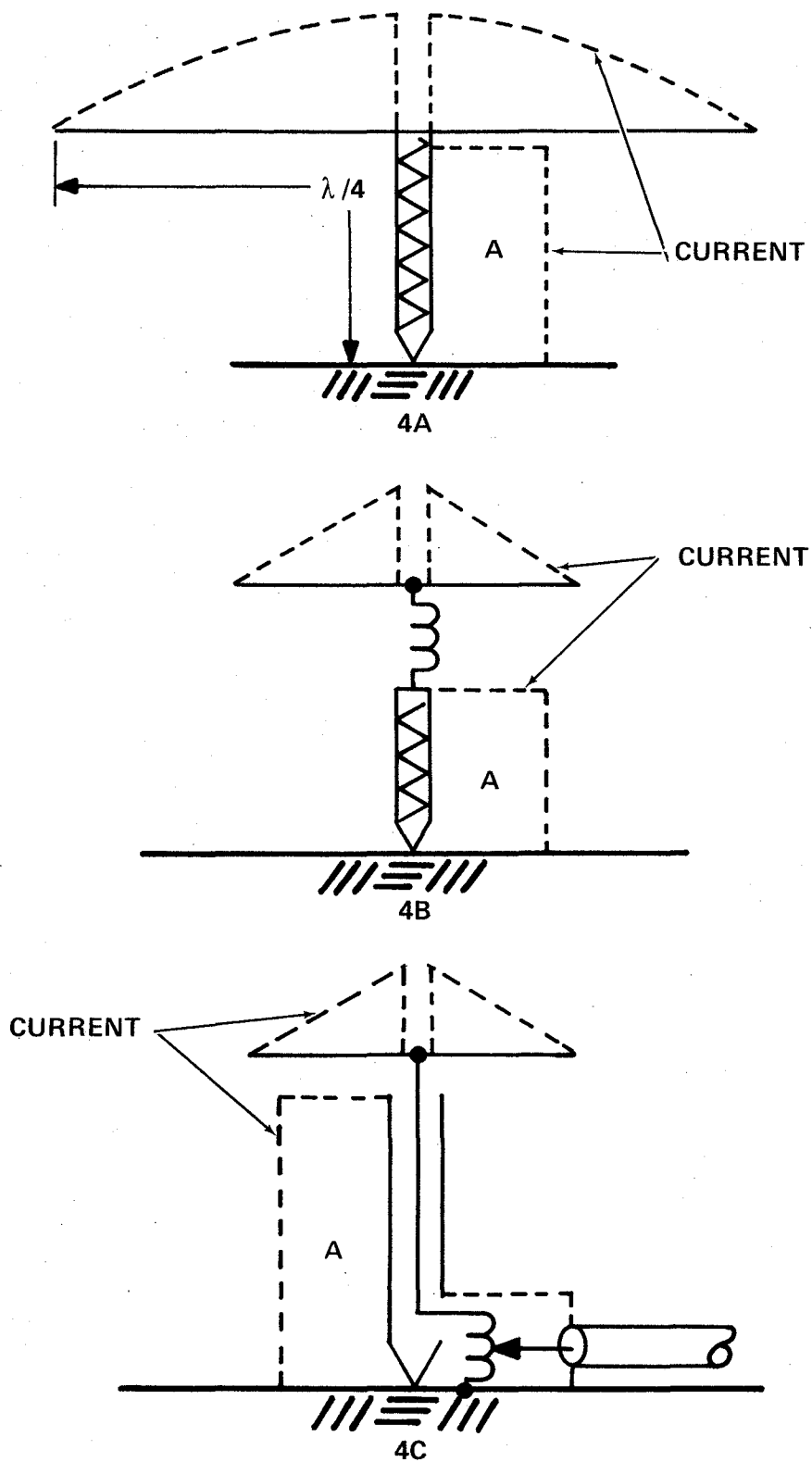


Figure 3 Current Distributions On Monopoles



M4-3(4)

Figure 4 Current Distribution On The Parantenna

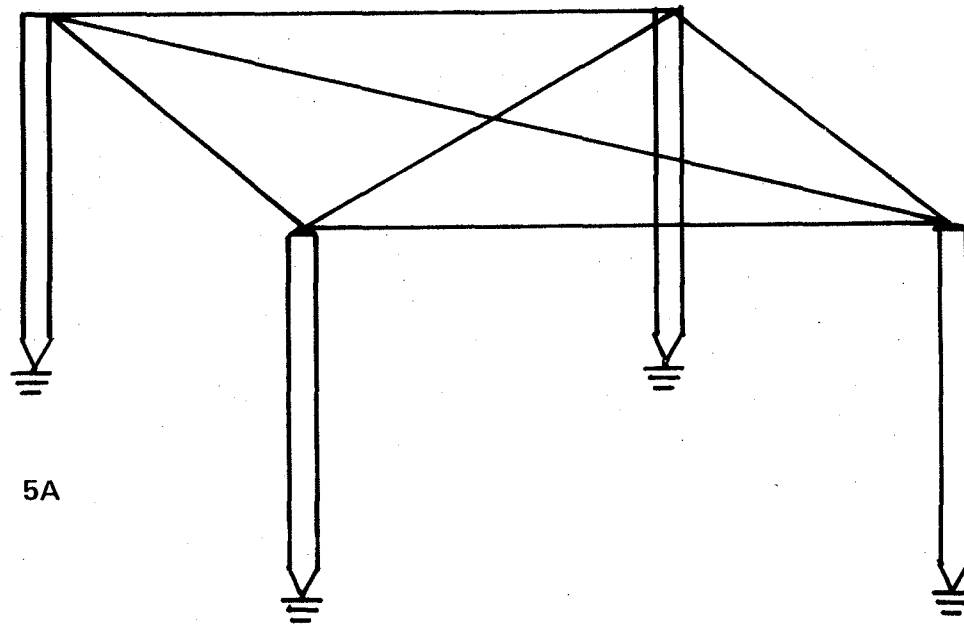
An advantage is that a convenient feed point is now provided on the grounded coil. The tower is effectively fed between the top hat and the top of the tower and the current distribution is unchanged. This practical configuration then supplies a four-to-one increase in radiation resistance for the single tower.

Since the top hat must be supported by additional towers it is desirable to use these towers as additional radiators and examine the mutual impedance between them. A circuit for that configuration is shown in Figure 5. Four towers as shown are an economical compromise for broadcasting use. Since there is a common connection between these four elements in the top hat only one needs to be fed by the transmitter. Tuning of this system is simple in that the four inductors are made to contain the same number of turns at all times and the taps are moved until the system is resonant at the frequency of operation.

Experience shows that the currents in the four towers will be matched to within ten percent without any additional adjustment. The match is not critical to operation or efficiency. The ratio of the mutual resistance to the antenna's radiation resistance is shown in Figure 6. A typical spacing is one tower height or from 10 to 20 electrical degrees. Here it can be seen that the mutual resistance is within 95% of the radiation resistance of each element.

The mutual reactance as shown in Figure 7 where the spacing between towers is one tower height is insignificant. This mutual reactance is not to be confused with the mutual reactance component from Figure 6. Figure 6 is a vector which rotates in proportion to spacing and in fact will be a pure reactance at 140 degrees electrical spacing. Figure 7 is a close-in component which falls rapidly with spacing. We will return to it later when discussing bandwidth.

The resulting radiation resistance of each tower when operating with unity phase and amplitude is shown in Figure 8. We have the self radiation resistance of a constant current element which is four times that for a linear current element plus three coupled mutual resistances which are almost equal



4 ELEMENT PARAN ANTENNA

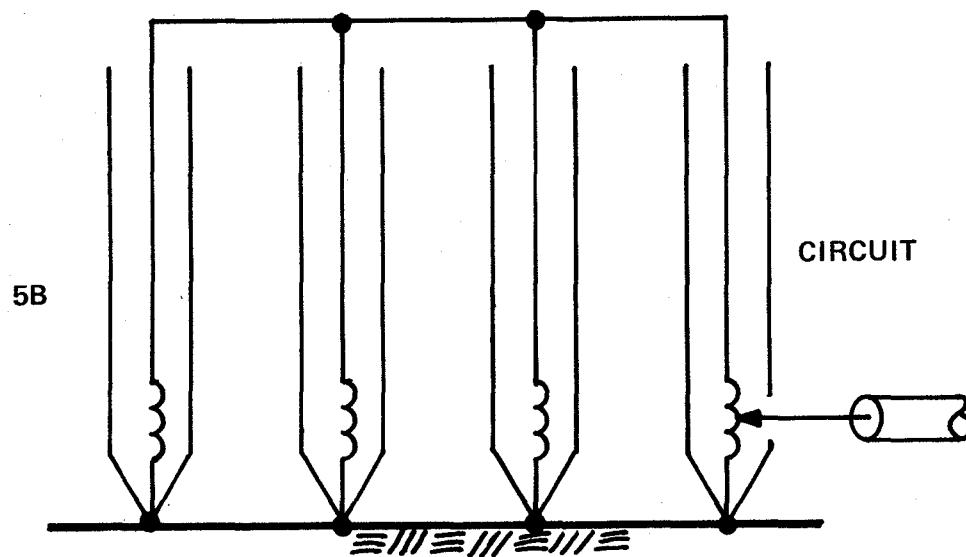


Figure 5 Circuit Of Paran Antenna



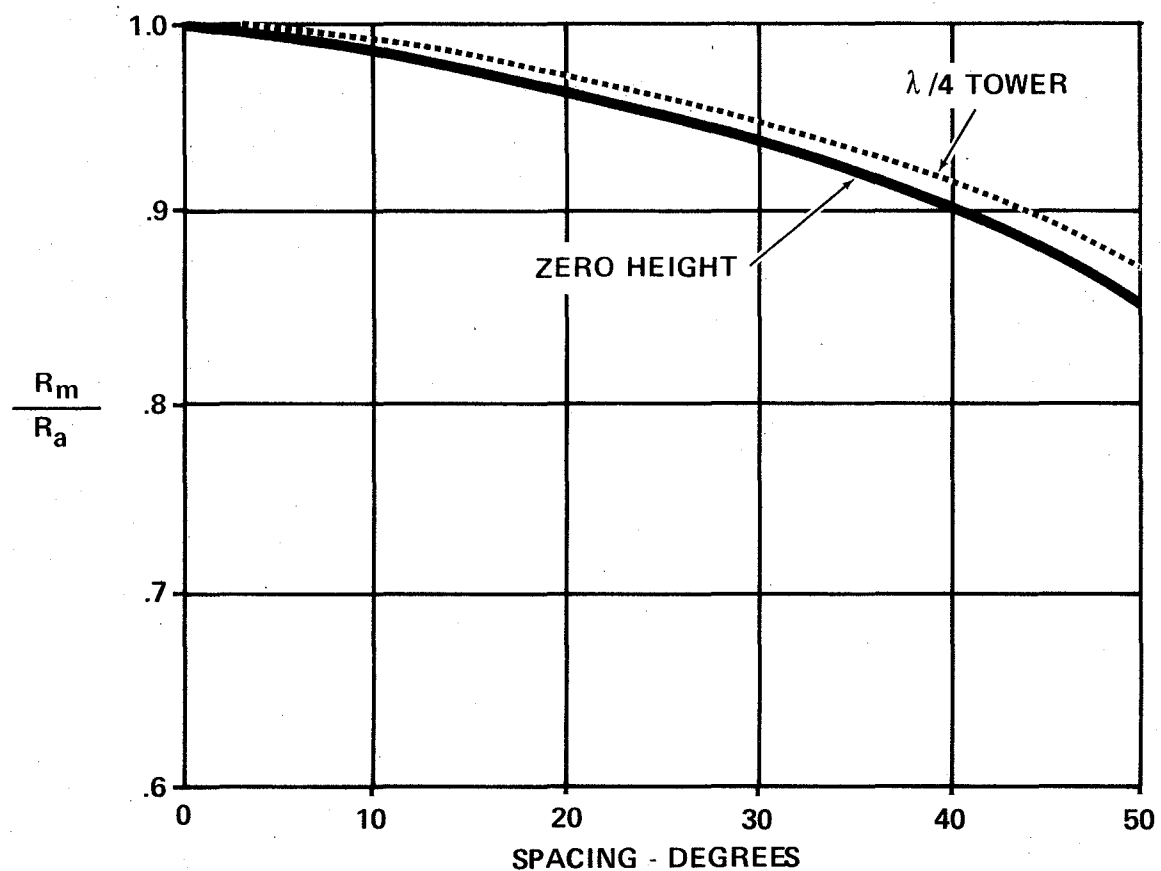


Figure 6 Mutual Resistance Close Spaced Monopoles

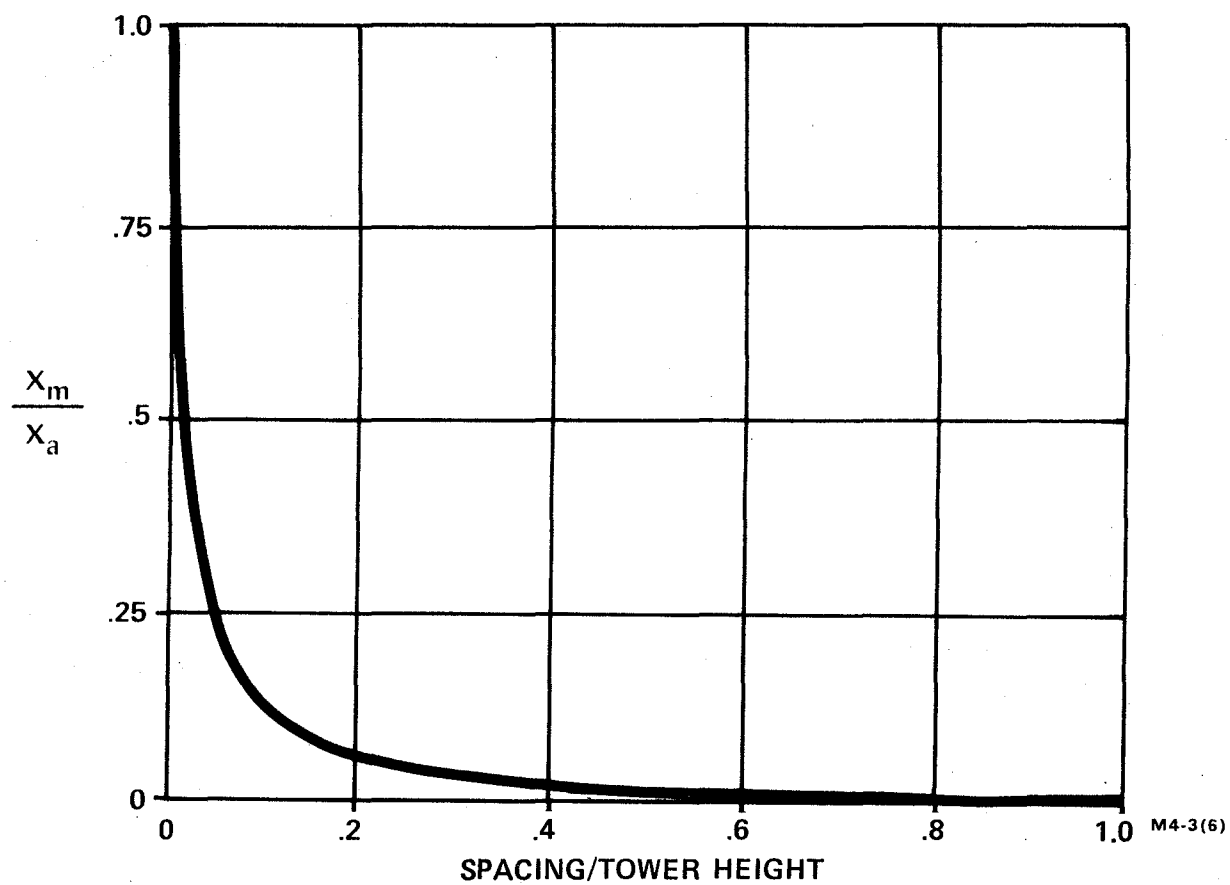


Figure 7 Mutual Reactance Close Spaced Monopoles

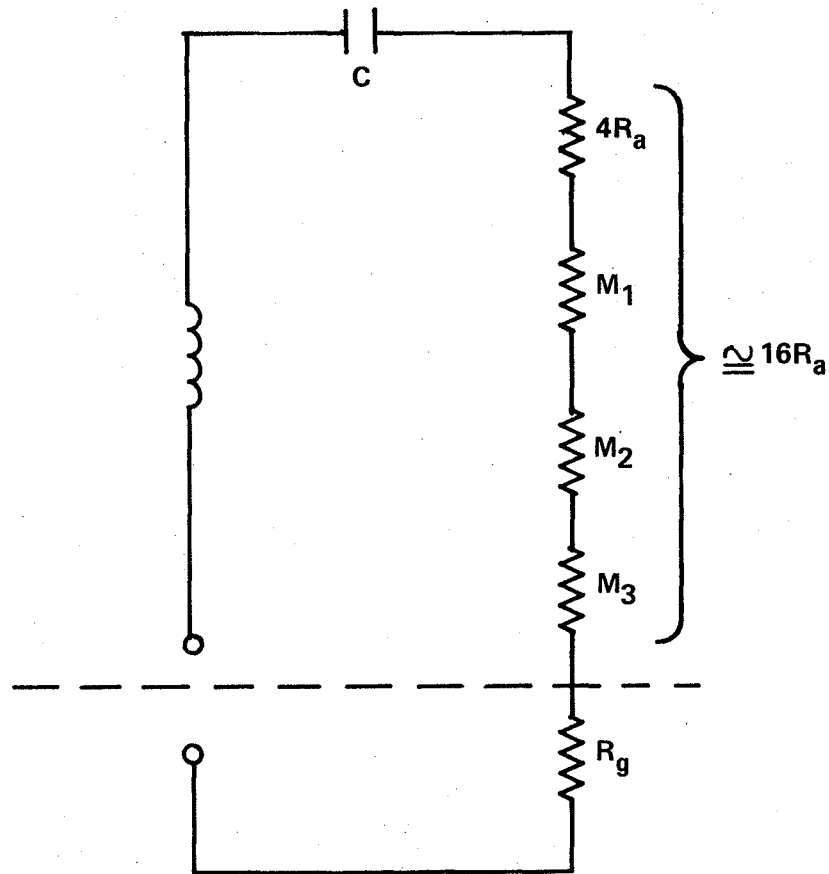


Figure 8 Circuit Diagram Of One Paran Element

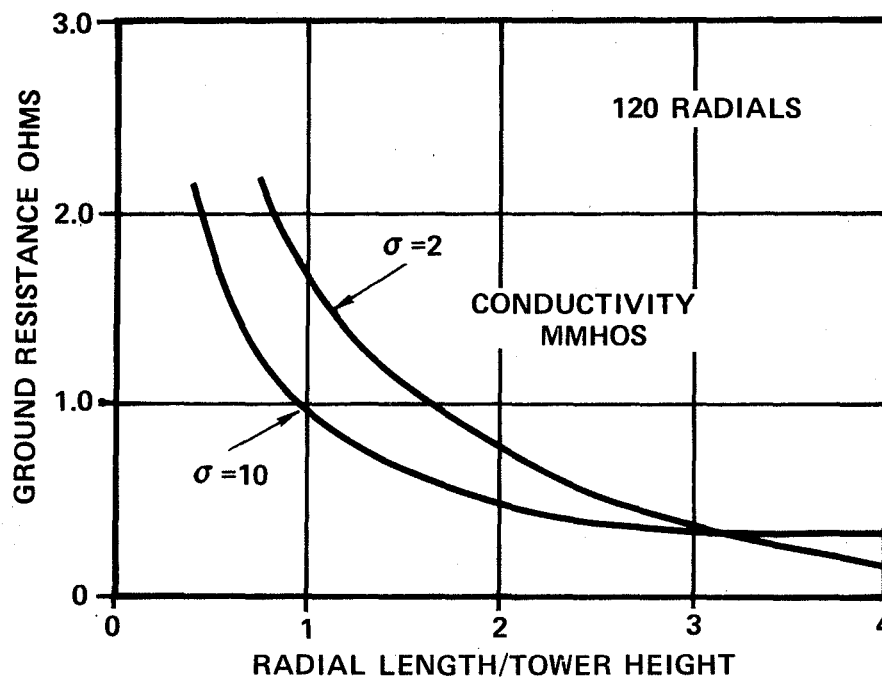


Figure 9 Paran Ground System Requirements

to the radiation resistance, and their sum approaches sixteen times the radiation resistance for a single tower. To the extent that the ground currents to each tower overlap, there will be a mutual ground resistance component which must be added to  $R_g$ . With one tower height spacing this overlap of ground currents is minor.

The efficiency of our first example which was 50% with one ohm ground resistance and one ohm radiated resistance now approaches

$$\eta \cong \frac{100 \times R_a}{R_a + R_g} = \frac{100 \times 16}{17} = 94\%$$

This example represents a 50 foot antenna at one megahertz or a 100 foot antenna at 500 kilohertz.

The size of the ground system to achieve one ohm or less of ground loss with these antennas is shown in Figure 9. There are many ways to configure the ground system but it is shown with 120 radials and their length is in terms of tower height. With that many radials in a small area the loss resistance within the confines of the radials themselves is very low and the loss is mostly due to the soil beyond the end of the ground system.

With a conductivity of ten millimhos a length equal to one tower height will produce one ohm and with a conductivity to two millimhos the length required will be closer to two tower heights. The radiation resistance developed in the PARAN elements for broadcasting is shown in Figure 10. The resulting efficiency with one ohm of ground loss is shown in Figure 11. Here a comparison is made with the efficiency of a single tower under the same conditions. It shows the very large improvement obtained at low heights. It also shows that there is little to be gained where the height of both antennas approaches one quarter wavelength.

The radiation intensity for fifty and one hundred foot PARANs using one ohm ground loss is shown in Figure 12. With a perfect ground system the radiation for one kilowatt

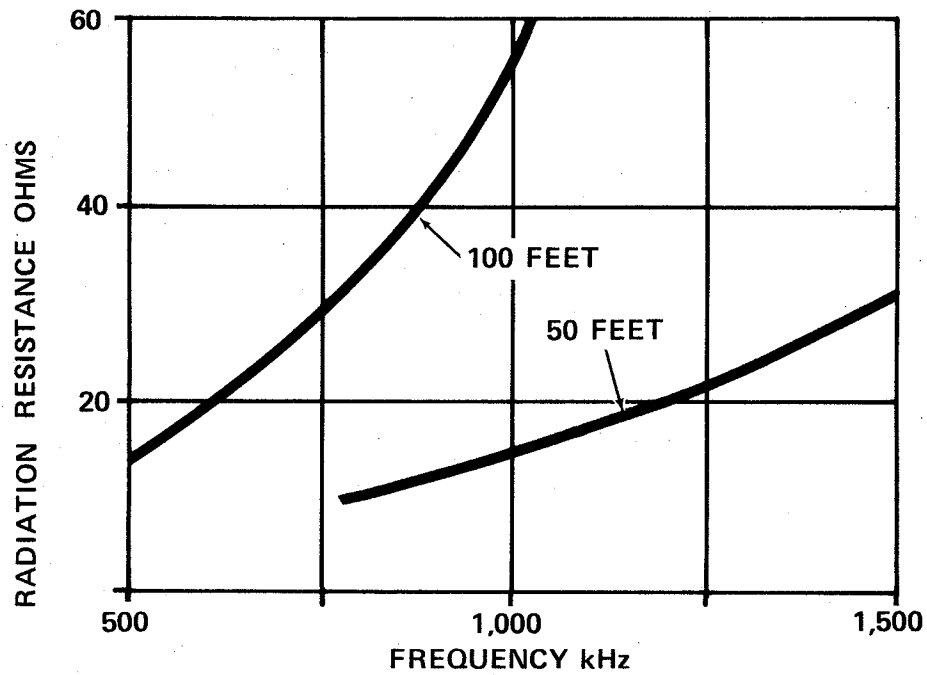


Figure 10 Parant Element Radiation Resistance

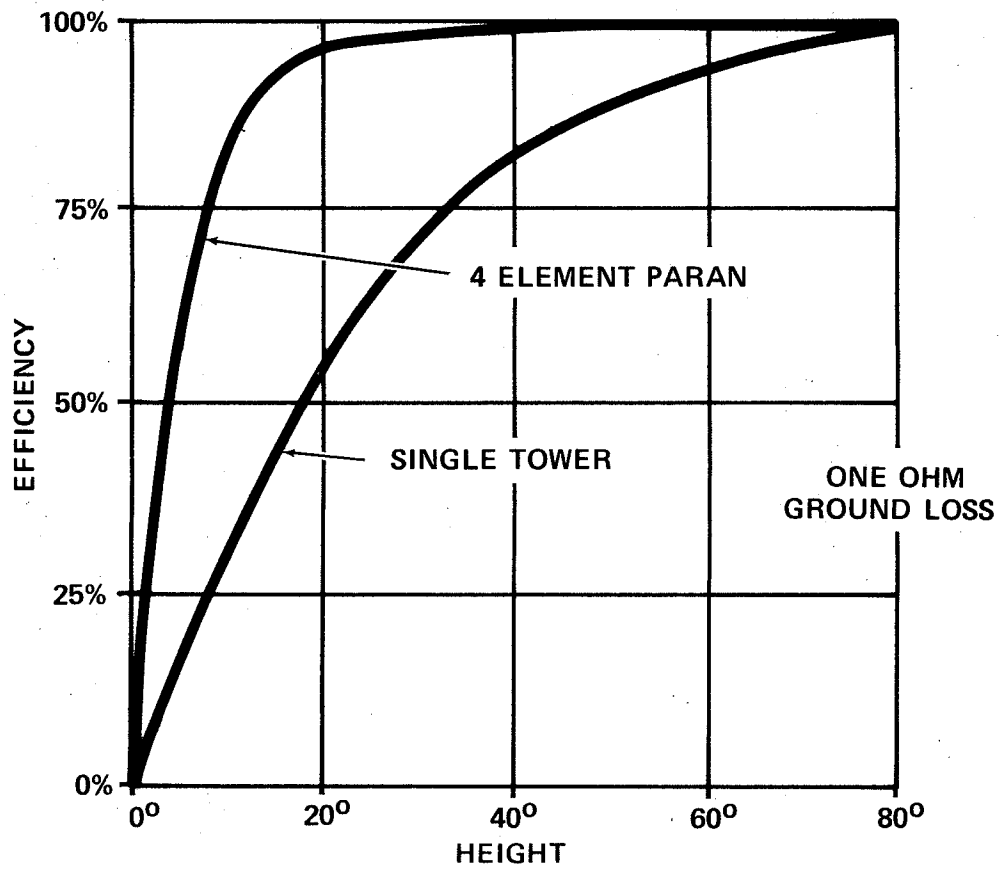


Figure 11 Comparison Of Radiating Efficiency

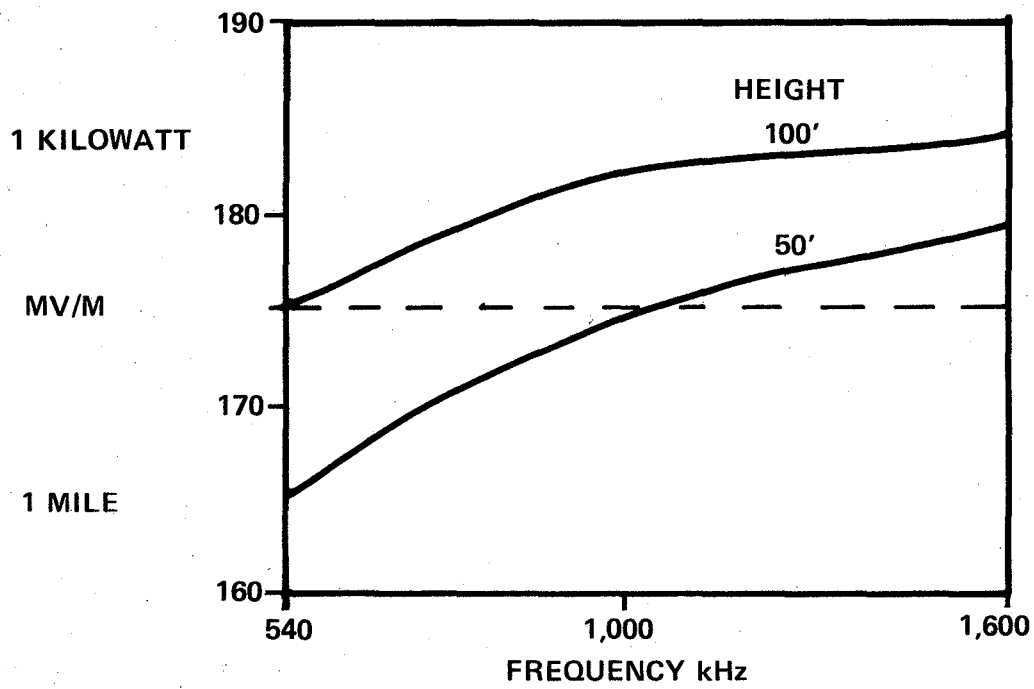


Figure 12 Paron Field Intensity

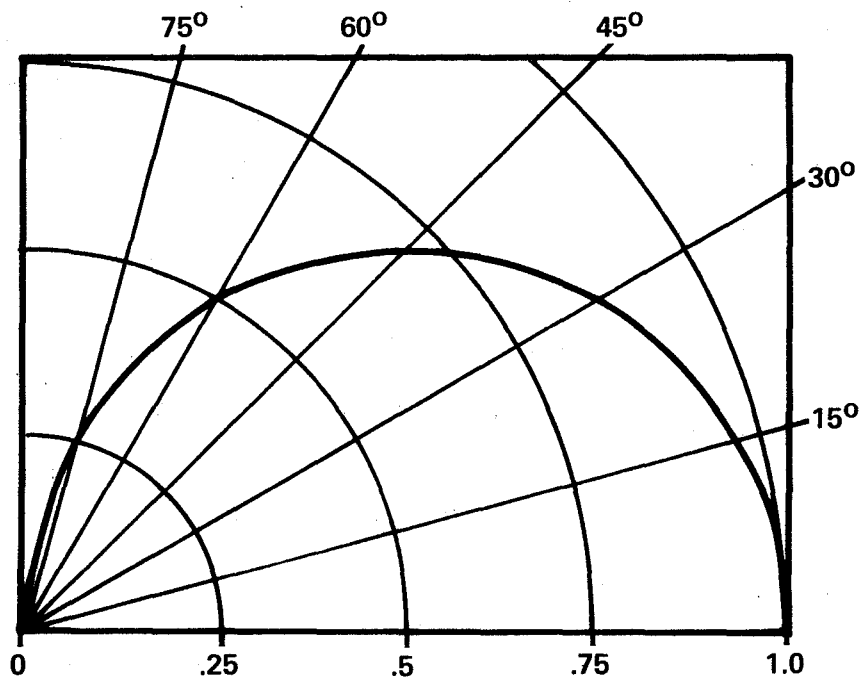


Figure 13 Vertical Radiation Pattern

will approach 186.3 mV/m at one mile for all frequencies at short heights.

The vertical radiation pattern for short or zero height PARAN's is shown in Figure 13. It is the same as that for a short monopole, since it is contained within a one radian cube. For the same reason the horizontal plane pattern is non-directional within plus or minus 0.1 dB.

The bandwidth also approaches a sixteen-to-one improvement and this can be seen by considering the four elements as current filaments on the surface of a thick cylinder as shown in Figure 14. If the four towers were lifted from ground and fed from a point at the geometrical center the radiation resistance here would be exactly that for a single tower of the same height and no improvement in efficiency would result. The four circuits in parallel have one fourth the radiation of each of the elements. This is a basic concept upon which the mutual impedance between antennas is developed.

The same principle applies to the reactance of the system as shown in Figure 15. The four reactances in parallel produce one fourth the reactance of the elements however the mutual reactances are absent for the reason shown in Figure 7. Here we have a four to one decrease in reactance and with a four to one increase in resistance due to current distribution the Q of the circuit has been reduced almost sixteen-to-one. This explains a fundamental reason behind the bandwidth improvement of thick radiators.

The power capability of the PARAN system is primarily due to its voltage limitation at the lowest frequency of operation. Using 15 ohms as the practical radiation resistance and -J300 ohms reactance at 500 kilohertz the current for 50,000 watts is (12,500W per element)

$$I = \sqrt{\frac{12,500}{15}} = 29 \text{ Amperes}$$

$$E = 29 \times 300 = 8,700 \text{ Volts (carrier)}$$

$$E \text{ (Modulated Peak)} = 8.700 \times 2 \times 1.41 = 25 \text{ kV}$$

# THE PERIMETER CURRENT ANTENNA (PARAN)

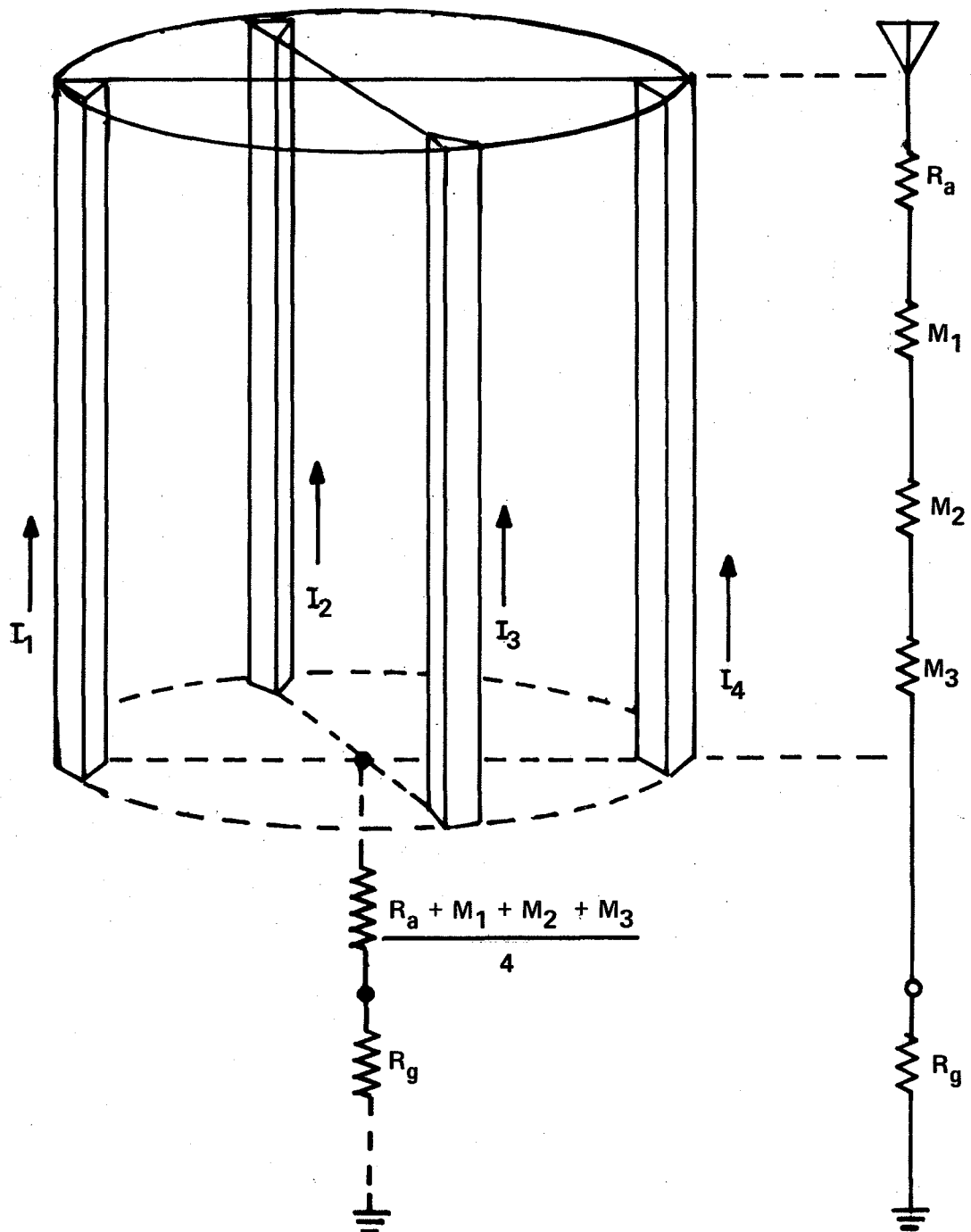


Figure 14 Convolution Into A Thick Monopole

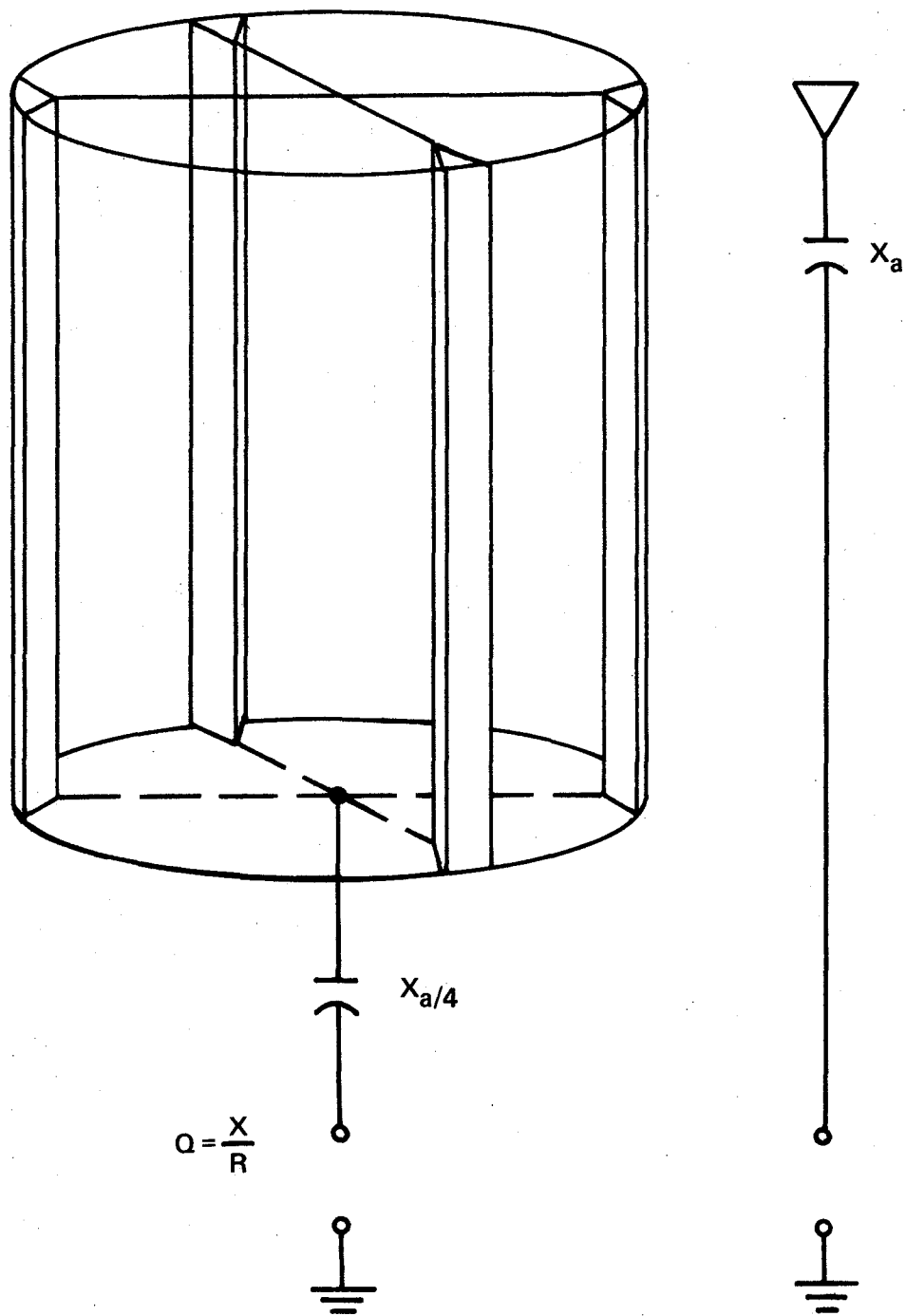


Figure 15 Bandwidth Of Thick Antennas



The values over the frequency range of interest are shown in Figure 16.

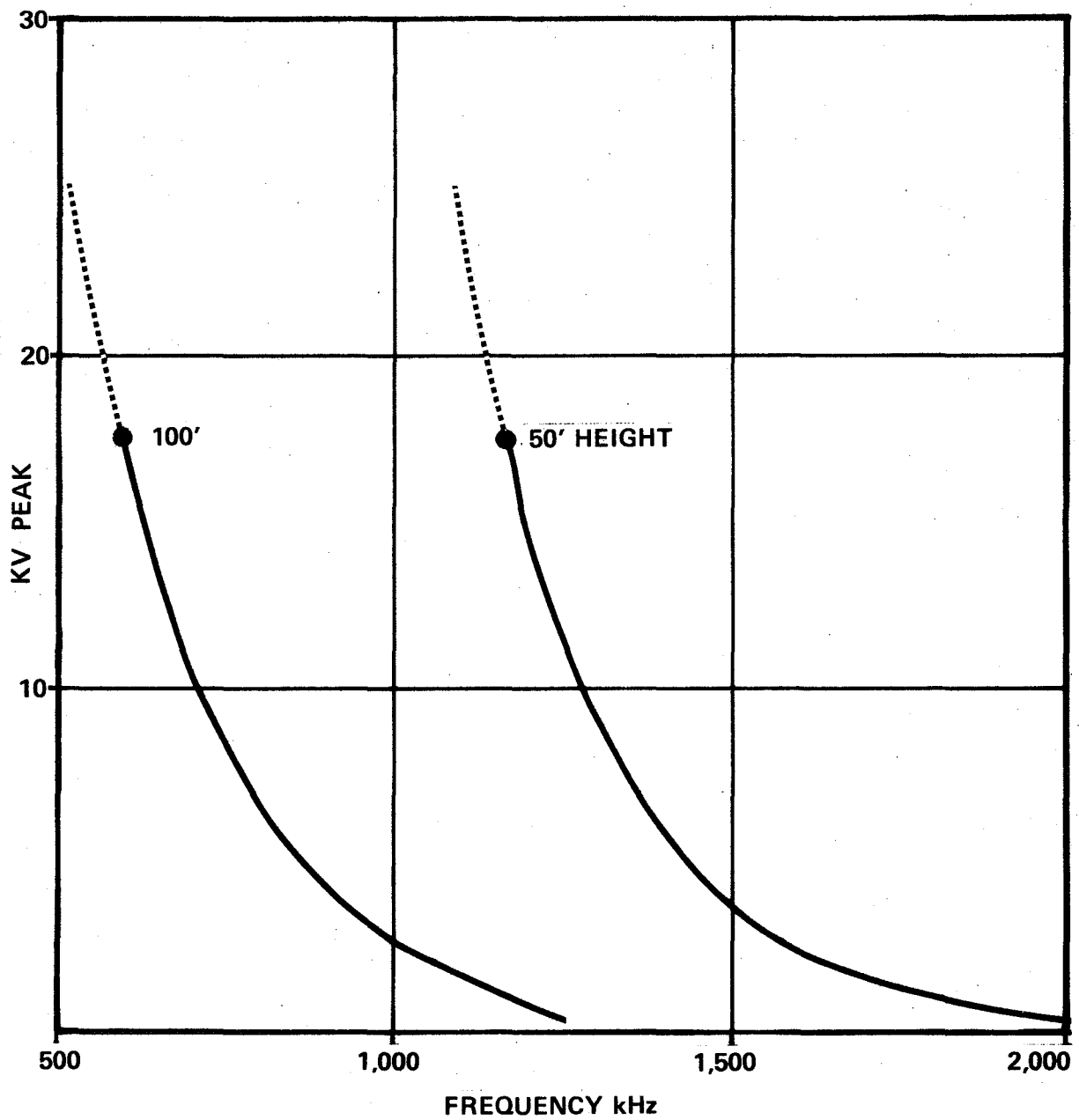
One of the first questions that has been asked is about the use of the PARAN in directional antenna systems.

The complex problem of sky wave radiation must be worked out as a unique problem in each application. This is a task for broadcasters and/or their engineering consultants. Directional systems with PARAN elements are quite feasible if attention is paid to all of the problems involved.

The sky wave radiation from the top hat alone on the PARAN antenna has been calculated for its lowest frequency of operation and is shown in Figure 17 for one kilowatt of power. The maximum radiation value is 1.2 mV/m at one mile and this can be added to Figure 13 where the field is 186.3 mV/m at one mile on the ground. It represents about one half of one percent increase in radiation at a vertical angle of 50 degrees from a phase center on the ground at the geometric center of the PARAN set.

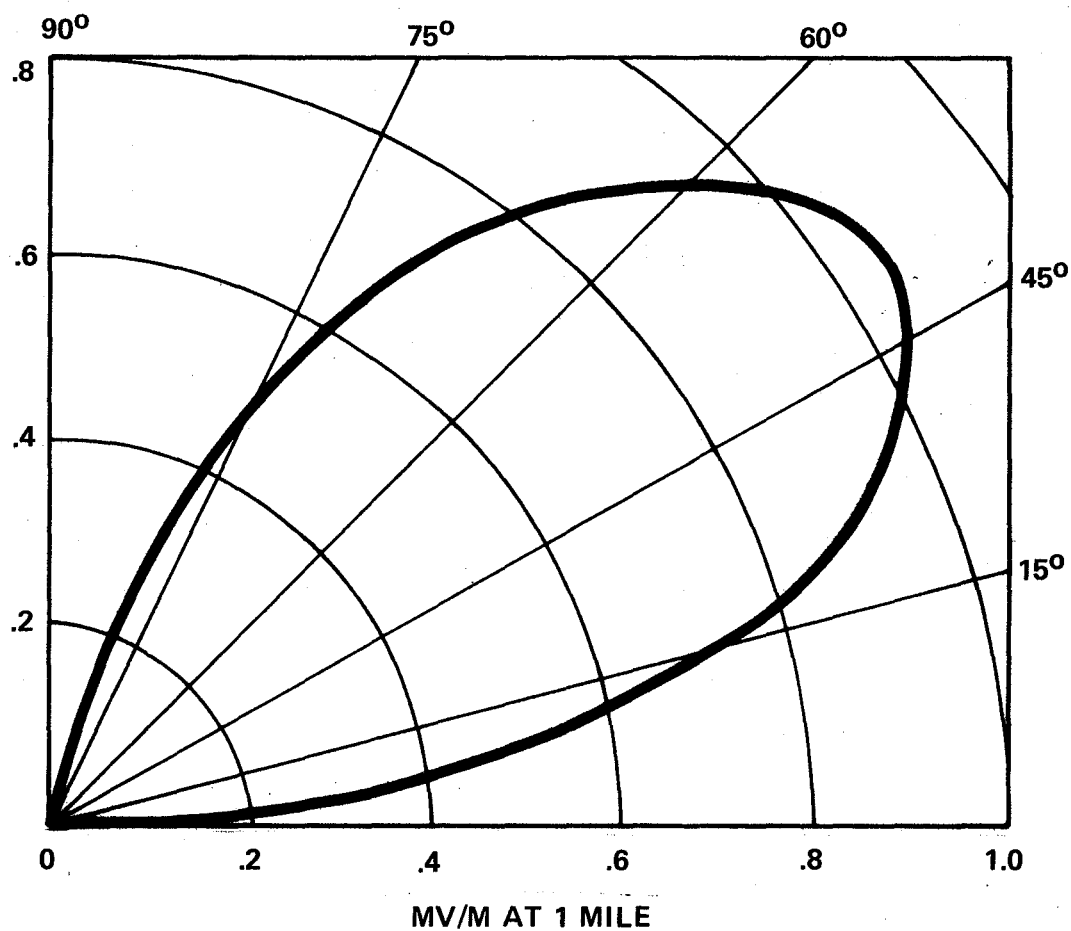
When used as one element in a directional array the vector sum of the top hat components from all of the top hats will take on the pattern of the directional array. The resultant will continue to be a small component increase in the same order of magnitude. The parameters are easily programmed and can be included in computer solutions to directional systems.

In large spaced arrays where the mutual impedance between sets of PARAN's representing tower locations is almost equal for all elements of the set, then four element PARAN's as shown here should be quite feasible depending upon the protection problem. Keep in mind that two tower PARAN's may be used for a potential eight-to-one improvement in efficiency. With normal two tower directional arrays the two element PARAN can be oriented at right angles to the tower line ensuring symmetry of mutual impedances and closer spacings may be used. We offer these as tools for the ingenuity of broadcast engineers.



M4-3(12)

Figure 16 Paran Antenna Voltage 50kW - 100% Modulation



1 KILOWATT OF POWER

M4-3(13)

FIGURE 17 SUM OF RADIATION COMPONENTS FROM THE PARAN TOP HAT

Monitoring the amplitude and phase from a set of PARAN's can be done at the geometric center of a set, or if the application warrants sampling loops on all towers with a phase meter reading the vector sum of a set.

A number of PARAN fifty kilowatt antennas are in broadcast use overseas. They have also been sold to the United States Government for other purposes. The basic principles of antenna theory can be used to properly engineer the total system for conformance with the FCC Rules and Regulations as they apply to broadcasting in the United States. Two basic 4 element models are offered which are 50 and 100 feet high. The system can be extended to even lower heights with the use of more elements if the need arises.

# Installing New Ground Systems

by Thomas Vernon

**Harrisburg PA** Many small market AM stations that were part of the boon in the '60s are approaching 30 years of age. Those that haven't seen much antenna system maintenance may be experiencing problems with erratic antenna resistance readings, poor efficiency and spotty signal coverage that always improves right after it rains.

These symptoms almost always point to a badly deteriorated ground system. Many small market stations cannot afford to hire a consulting firm to install a new system. Rest assured however,

that savvy small market engineers can do a credible job themselves with proper planning and preparation.

## STATION SKETCHES

The first thing to do is find out what sort of ground system is supposed to be in place. Check your station license. Typically it will specify a 23'x23' ground screen with 120 copper radials spaced 3' apart.

The next step is to go out to the trans-

mitter site and see what's there. If the system was installed more than 20 years ago, there may be little left to find. The ravages of time and occasional copper thieves take their toll.

Careful excavation with a shovel and pick axe may reveal deteriorated or broken strapping, a rotted ground screen,

wholesalers, and cut into 2- or 4-inch strapping at a sheet metal shop for less than the normal price of strapping.

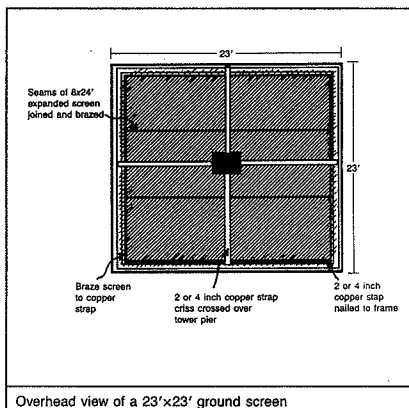
You must make sure however, that the material is 99% copper and not a copper/tin alloy as is sometimes used in roofing.

Although many types of wire have been used in radials, #10 soft drawn copper is the preferred type. Hard drawn wire may break as it is plowed into the ground, particularly in rocky soils.

Traditionally, silver solder has been used on all connections. Cadwelding is now the preferred method, as it makes a better bond and is much more affordable than silver solder.

Copper pop rivets are useful for joining sections of strapping together prior to soldering.

To plow radials into the ground, a tractor with a single sub-soiler plow will be required. A sub-soiler blade is capable of burying the wire 8 to 10 inches deep. When such a plow is located, it will have to be modified for inserting radials into



or poorly spliced radials. Buried radials may be easily located with a field strength meter and headphones.

There's no way around it: Putting in a ground system the right way is a costly venture. The following suggestions may help in getting the right materials quickly and at a favorable cost.

First, only use the largest broadcast supply distributors. They are able to buy copper at volume discounts and usually offer better prices than smaller operations can. Some materials can be purchased and fabricated locally at considerable savings without compromising quality. Copper can be purchased in 25'x1 3/4' sections from roofing

the ground.

There are two methods of plowing radials into the ground. In the first, the spool of wire is located at the tower and the loose end attached to the plow. In this case, all that is required is that a 1/4-inch hole be drilled through the toe of the blade.

### Guard against breakage

If you are working in an extremely rocky area, pulling the wire through the ground in this manner may cause numerous problems with wire breakage. Since the wire is being pulled the entire length of the trench, there is quite a bit of friction. Add a few sharp rocks, and the wire is easily cut or damaged. In this situation, a different approach is required.

The second method involves mounting the spool of wire on the tractor, while the loose end is attached to a secure point near the tower base. Obviously this takes more modifications to the plow, but it also greatly reduces friction and breakage problems. The reel is secured to the plow by means of a length of pipe attached to the plow with "U" bolts.

The devices used to secure weights to the ends of barbells are useful in keeping the reel centered on the pipe. A piece of conduit is welded on to the back of the blade for the wire to pass through, and a pulley may be attached to the frame to reduce friction. Access to welding equipment and some improvisations will go a long way in creating a device that works.

### Sweat equity

With all the materials and equipment collected, it's time to begin work. Plan on having two or three able-bodied assistants for the duration of the project. You'll need them.

Measure the length of the radials from the tower and mark out the circumference. One easy way to do this is with a measured length of wire attached near the tower base. With this wire stretched taught, walk around the tower marking the distance with spray paint on the

(continued on page 28)

## QEI QEI QEI QEI QEI QEI QEI QEI QEI QEI

# W H Y Q E I ?

### 24 Hours.



Our 24 hour service hotline number is 609-728-2020.

Call us toll free at 800-334-9154 for all the facts on QEI "New Reliabilities" FM transmitters from 1kw to 30 kw.

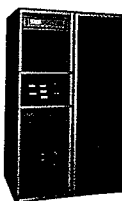
### Power Up.



With our FMQ 3.5/5/10 kW or 20/30 kW FM transmitters, you can upgrade power in the field.

Call us toll free at 800-334-9154 for all the facts on QEI "New Reliabilities" FM transmitters from 1kw to 30 kw.

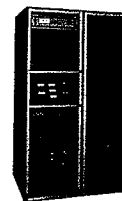
### Single Phase 30 kW.



Our new FMQ 30000B is the only 30 kW transmitter available with a single phase power supply.

Call us toll free at 800-334-9154 for all the facts on QEI "New Reliabilities" FM transmitters from 1kw to 30 kw.

### Less is More.



All of QEI's FM transmitters have no plate blockers or sliding contacts.

Call us toll free at 800-334-9154 for all the facts on QEI "New Reliabilities" FM transmitters from 1kw to 30 kw.

### Free.



Our FREE spares kits include every solid state component of the transmitter, exciter and remote control.

Call us toll free at 800-334-9154 for all the facts on QEI "New Reliabilities" FM transmitters from 1kw to 30 kw.

### The Longest.



Our PA tube warranty is the longest in the business — 15,000 hours.

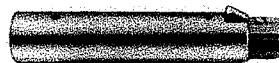
Call us toll free at 800-334-9154 for all the facts on QEI "New Reliabilities" FM transmitters from 1kw to 30 kw.

QEI CORPORATION  
ONE AIRPORT DRIVE • P.O. BOX D • WILLIAMSTOWN, N.J. 08094

TEL (609) 728-2020 • FAX (609) 629-1751

## GOT A FIELD PROBLEM ?

GET A SESCOM  
IL OR TR SERIES



IN-LINE TRANSFORMERS  
PADS OR FILTERS  
SOLVE YOUR MATCHING  
PROBLEM

47 UNITS TO SOLVE  
YOUR EXACT PROBLEM

XLR'S TO XLR'S  
XLR'S TO PHONE  
MINI PHONE  
RCA  
RCA'S TO RCA'S

SEND FOR FREE CATALOG

SESCOM INC.

2100 WARD DR.  
HENDERSON NV 89015 U.S.A.  
702-563-3400, 800-634-3407, FAX 702-563-4828

QUALITY • ENGINEERING • INNOVATION

# Your Ground System

(continued from page 22)

ground or with occasional wooden stakes. Make sure you'll have some sort of temporary ground for the transmitter while the work is being done. Four 8' lightning rods located at the corners of the transmitter building are better than no ground at all.

Next, remove all of the existing ground system. Be as thorough as possible. If any of the old wiring is left in place it can short out the new system resulting in pattern instability and an inefficient system.

Measure the 23x23 area around the tower base and make sure that it's level. Remove any remaining vegetation and thoroughly treat the area with commercial weed killer or large quantities of rock salt. This will prevent the possibility of vegetation growing up through your new screen and damaging it.

Now you're ready to begin plowing radials into the ground. Remember that

you'll have 30 wires coming into each side and they should be spaced 6-to-8 inches apart. The first few radials may be a little rough, but once you develop a system the remainder will go in with relative ease.

One suggestion if you're working in a rocky area: Make a dry run before plowing in a radial. In this way you'll discover rocks and other obstructions in the path and can remove them before the second run when the wire is inserted. This may take a little more time, but will result in fewer broken wires.

Be sure to start each run about two feet within the 23 foot square to insure there will be enough slack.

## Building a frame

With all the radials in place, a frame for the ground screen can be constructed. Treated 4x4 lumber is used for the 23 foot frame. Use stakes or what-

ever means are appropriate to secure the frame and prevent twisting.

Fold all the radials out over the frame, leaving about a foot of slack on all wires. Fill the area with 3/4 inch of gravel. Ten tons of gravel is sufficient.

Put the two pieces of strapping that run over the tower base in place. You will have to fold the strap to go over the tower base. Two-inch strap is sufficient for power levels up to 1 kW, while 4-inch strap is used for 5 kW and above.

Attach strapping to the top of the frame. Copper roofing nails are ideal for this if you can find them. For areas where radials intersect the transmitter building, strapping is run around the building with radials attached to either side. All equipment inside the building is grounded to this strap.

Transmitters and equipment racks are attached by soldering a strap to the chassis under the rear door. Remove all paint in the area to be soldered. A welding torch may be necessary to generate enough heat for a good connection.

The radials are now soldered to the strap on top of the frame at 6- to 8-inch

intervals. You may wish to place a piece of scrap metal in the area where you are soldering, so the torch does not set the frame on fire.

Screening comes in 8x24 foot sections, which should be carefully unrolled in place. Wear gloves for this operation, as the edges are razor sharp. Tack the sections in place. Carefully measure and make a cutout for the concrete pier. Overlap sections by 1 1/2 inches. Join the sections together by twisting the overlapped areas together. Solder all of these joints. The screen is now soldered to the frame at 6-inch intervals.

With the ground system in place, a fence must be erected around the outside perimeter. A wooden fence is preferred. Be sure to work with the contractor who installs the fence to be sure that the post holes don't cut through any radials.

By following the steps outlined above, you should be able to install a quality ground system yourself.

■ ■ ■

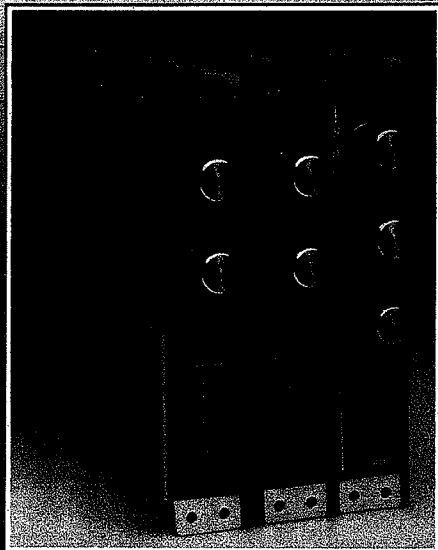
Tom Vernon, a regular RW columnist, divides his time among broadcast consulting, computers and instructional technology. He can be reached at 717-367-1151.

## TURBO CHARGE

### Your Optimod™ 8100 with CALIFORNIA DIGITAL DIGIMOD 2000™

**D**IGIMOD 2000™ A 3 circuit card package transforms a standard OPTIMOD 8100™ into a multi band, digitally controlled processor, delivering maximum, competitive processing when using compact disc and R-Dat.

Call your favorite dealer for price and availability.



*California Digital*  
Audio Systems

#### DEALER LIST:

- BROADCASTERS GENERAL STORE:**  
Ocala, FL (904) 622-9058  
Marietta, GA (404) 425-0630  
Carol Stream, IL (708) 231-7120  
Arlington, TX (817) 275-1380
- BROADCAST EQUIPMENT SALES:**  
Jackson, MS (601) 857-8573

DISTRIBUTED BY: Family Marketing Group  
DEALER INQUIRIES INVITED...904-622-2779

## Digital Displays

(continued from page 19)

the flow of light from the display.

Unlike the LED, LCDs can contain numerous more displays. They are even now used to produce the picture on pocket-sized television sets.

LCDs can also produce white letters on a dark background. This is known as the dynamically scattered LCD. Another type of nematic fluid and no polarizers are used to achieve this display.

### Vacuum fluorescent display

Another method of displaying information from small computers is the vacuum fluorescent display. This device operates similarly to the triode vacuum tube. A schematic illustration is found in Figure 3.

Vacuum fluorescent (VF) character displays consist of a single cathode producing electrons. The "plates" or positive voltage levels where electrons are collected are the character elements.

The plates are coated with zinc oxide. This is a fluorescent material and when electrons strike it, a blue-green glow is produced. The grid is used to erase the display from the screen when no longer needed.

Vacuum fluorescent displays are quite popular even though they employ a much older technology. They consume very little power, have a long life and a fast response time. Color displays can also be produced when filters are used.

This concludes the 12-part *Introduction to Digital Electronics* course. A multiple choice test and an answer sheet will be mailed to you by 16 July.

Please mail the answer sheet back no later than August 15th.

■ ■ ■

Ed Montgomery currently is an electronics teacher at Thomas A. Edison High School in Fairfax County. He has taught broadcast engineering at Northern Virginia Community College and worked as broadcast engineer for several radio stations.

# A Lesson in License Challenge

(continued from previous page)

cially in the latter portion of the license term), the licensee was still entitled to a "renewal expectancy." As a result, the FCC concluded that, while it was a "close" case, the incumbent should win.

## Court appeal

On appeal, though, the Court had other ideas. First, the Court found that the FCC had acted arbitrarily in granting a "renewal expectancy" and in thereby essentially ignoring the downturn in the incumbent's performance.

The Court noted that the "renewal expectancy" is supposed to be a predictive device. That is, such an expectancy is to be awarded to those licensees whose past performance indicates likely strong future performance. Here, analysis of the incumbent's past performance revealed a "strong downward trend," suggesting anything but a likely strong future performance.

With respect to the R-rated material, the Court indicated

that, in granting the incumbent's renewal, the Commission could not properly ignore that material. Accordingly, the Court sent the case back to the FCC with instructions to redo the renewal expectancy analysis with particular emphasis on the incumbent's performance at the end of the license term and to consider further the matter of "renewal expectancy."

The Court's action sent an important message to broadcasters. However, that message may have been lost as a result

of the not unexpected fascination of the obscenity aspect of the case, which tended to attract more attention than the more mundane renewal expectancy aspect.

## The risk

But think about this: How many broadcasters do you know who actually air full frontal nudity and graphic depictions of sex acts? Probably not many, if any at all. By contrast, every broadcast licensee has to file renewal applica-

tions and thus runs the risk of a comparative challenge in which the station's continued operation could hinge totally on the concept of "renewal expectancy."

The primary teaching of the Court's opinion appears that, if a licensee's responsiveness to community needs through non-entertainment programming has decreased, decreased, and permanently, over the course of a license term, that licensee may not be entitled to a "renewal expectancy." Without

such an expectancy, it is much more difficult to prevail in a comparative renewal proceeding.

Because all broadcasters are technically subject to potential comparative challenge at renewal time, the Court's treatment of the renewal expectancy could and should have attracted the lion's share of attention. In case you missed this case, you may want to discuss it, and its implications for your own operation, with your communications counsel.

Harry Cole is a partner in the Washington DC-based law firm of Bechtel & Cole, Chartered. He can be reached at 202-833-4190.

## DAB In Canada

(continued from page 15)

information that can't be heard and by allowing audio noise to rise to just below the point of perception.

Under consideration is the following plan to implement DAB pending successful test results and spectrum availability: It would be introduced sometime between 1995 and 2000. Priority for assigning DAB channels would be given to existing AM and FM stations. Any additional channels would be made available to other applicants.

DAB would be primarily terrestrially based, but direct broadcast satellite service would be available for remote areas and for national programming services to all areas.

DAB would simulcast with the AM and FM stations until there was a high penetration of DAB receivers. Then, AM and FM operation would cease.

DAB is seen as resolving, once and for all, competition problems between AM and FM. If the operations are turned off, I guess it would.

Steve Crowley is a registered professional engineer with the consulting firm of du Trail, Lundin & Rackley, Inc., 1019 19th Street, N.W., Third Floor, Washington, DC, 20036. He can be reached at 202-223-6700. Or by FAX at 202-466-2042.

## Get the box that makes On-air Magic...

### Eventide's H3000B Ultra-Harmonizer.

Introducing radio's most colorful black box.

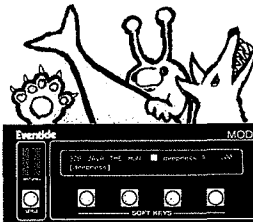


Shimmerish Sweep Reverb program—one of 70+ Eventide Broadcast Ultra-Harmonizer® digital audio effects you can use "right out of the box." Just turn the H3000B on, and it'll turn your listeners on.

**RADIO'S MOST COLORFUL BLACK BOX**  
EVENTIDE INC.  
ONE ALSAN WAY  
LITTLE FERRY, NJ 07643  
TEL: 201-641-1200 • TWX: 710-991-8715 • FAX: 201-641-1640

**Eventide**  
the next step

Morning zoo-in-a-box.

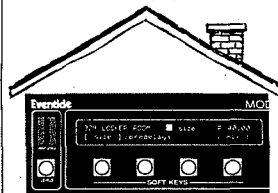


Java The Hun vocal shifter—one of 70+ Broadcast Ultra-Harmonizer® digital effects designed to let you dial up pre-programmed insanity. It's easy to afford the broadcast-engineered H3000B's power and flexibility; ask your Eventide distributor.

**RADIO'S MOST COLORFUL BLACK BOX**  
EVENTIDE INC.  
ONE ALSAN WAY  
LITTLE FERRY, NJ 07643  
TEL: 201-641-1200 • TWX: 710-991-8715 • FAX: 201-641-1640

**Eventide**  
the next step

Running out of room? Plenty of rooms in here.

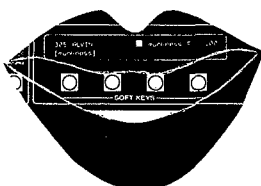


Locker Room reverb/echo—one of 70+ broadcast-engineered H3000B audio effects you can use "right out of the box." The powerful and versatile Broadcast Ultra-Harmonizer® is also amazingly affordable—put it to work for you.

**RADIO'S MOST COLORFUL BLACK BOX**  
EVENTIDE INC.  
ONE ALSAN WAY  
LITTLE FERRY, NJ 07643  
TEL: 201-641-1200 • TWX: 710-991-8715 • FAX: 201-641-1640

**Eventide**  
the next step

The effects are all digital. The grins are only natural.

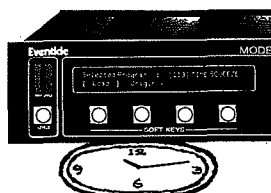


Alvin vocal shift program—one of 70+ Eventide Broadcast Ultra-Harmonizer® digital audio effects designed to stretch your imagination (and your smile). And when you have fun, so do your listeners.

**RADIO'S MOST COLORFUL BLACK BOX**  
EVENTIDE INC.  
ONE ALSAN WAY  
LITTLE FERRY, NJ 07643  
TEL: 201-641-1200 • TWX: 710-991-8715 • FAX: 201-641-1640

**Eventide**  
the next step

Pressed for time? Press directly below.

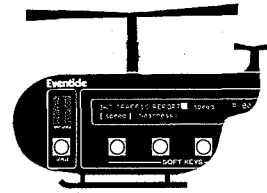


TimeSqueeze™ automatic stereo time compression/expansion—one of 70+ Broadcast Ultra-Harmonizer® digital audio effects designed to make you more effective. The H3000B: never before has so little money done so much for your station's sound.

**RADIO'S MOST COLORFUL BLACK BOX**  
EVENTIDE INC.  
ONE ALSAN WAY  
LITTLE FERRY, NJ 07643  
TEL: 201-641-1200 • TWX: 710-991-8715 • FAX: 201-641-1640

**Eventide**  
the next step

Audio effects designed to make your staff more effective.



Traffic Report voice filter with "copter effect"—one of 70+ Broadcast Ultra-Harmonizer® digital audio effects. Put the "special effects department in a box" to work call your Eventide distributor.

**RADIO'S MOST COLORFUL BLACK BOX**  
EVENTIDE INC.  
ONE ALSAN WAY  
LITTLE FERRY, NJ 07643  
TEL: 201-641-1200 • TWX: 710-991-8715 • FAX: 201-641-1640

**Eventide**  
the next step

Circle 97 On Reader Service Card

# ENGINEERING REPORT

## E-288 Summary Radio Issues

- AM Receivers
- Digital Audio Broadcasting
- Low Profile AM Antenna Project
- NRSC Activities Update
- STL Authorization Deadline Extended

## Television Issues

- ATV and HDTV Exhibits at 1990 Convention
- FCC ACATS Update
- ATTC Update

## General Issues

- 1990 NAB Broadcast Engineering Conference
- FCC Terminates Proceedings Without Action
- FCC Declines to Preempt State, Local RF Regulations
- FCC Violation Round-up

## Digital Audio Broadcasting

NAB will sponsor a demonstration of the European EBU/DAB-147 digital audio broadcasting system at the NAB Convention in Atlanta. The system was developed to allow multipath-free mobile reception of digital audio transmissions. (See the previous Engineering Report for more information.) The NAB '90 showing is expected to include a booth demonstration of DAB hardware. System developers will be present to answer questions about development progress and mobile test results. Additional mobile tests are planned for five cities in Canada, with the tests to be conducted later this year. For more information, contact Stan Salek, NAB Science & Technology, at (202) 429-5391.

## Low Profile AM Antenna Project

The second stage of the computer modeling on the low profile antenna project is underway. Engineers at AGL, Inc are in the process of modifying the Numerical Electromagnetics Code (NEC) to optimize the antenna model for a given gain and bandwidth as it analyzes the antenna's emissions characteristics. This is the first step in the process of developing a viable model for a low profile antenna. The NEC is a computer program which predicts the behavior of radiating structures.

The objective of this project is to develop a standardized mathematical model from which engineers can design low profile AM antennas. Science and Technology has specified that the antenna should be physically small (a maximum of 50 feet in height) economical, easy to install and operate in population centers (on a warehouse or building roof) and have a stable radi-

ation pattern. Such an antenna could enable some Daytimers to increase coverage and possibly operate at night by moving their facilities closer to the population center of the station's licensed community. ✓

## NRSC Activities Update

The NRSC has approved the circulation for comment of a third voluntary standards proposal. The document, titled "Performance Recommendations for AM Receivers," addresses minimum operational performance for NRSC AM radios. To comply with the standard, receivers must be capable of audio response to 7.5 KHz, without harmonic distortion exceeding two percent. The NRSC prepared this document to augment the NRSC-1 audio standard, providing radio receiver manufacturers with more detailed design guideline information.

On FM radio issues, the NRSC Multipath Working Group is currently investigating a laboratory test plan that could isolate the effects of transmission system components on multipath distortion. The Composite Studies Working Group is studying the effects of subcarriers and system overshoot on total RF occupied bandwidth, as well as whether different types of FM receiver decoders are less susceptible to adjacent channel interference.

For more information on NRSC activities, contact Stan Salek at (202) 429-5391.

## STL Authorization Deadline Extended

New rules that were to have taken effect on July 1, 1990 have been pushed back by the FCC to July 1, 1993, giving stations and manufacturers an additional time to comply. Per FCC Rule 74.550, all STL equipment operating in the 944-952 MHz band was to have been FCC authorized by July 1, 1990. The Rule was enacted in 1985 to foster an anticipated shift to narrowband channels of 300 kHz (for FM composite links) and 200 kHz (for discrete channels). For more information, call Stan Salek, (202) 429-5391.

*See Engineering Report, page 36*

## AM Receivers

Several new radio receivers were shown at the recent Consumer Electronics Show that offer improved performance to AM reception. Both DENON and Philips showed NRSC-compatible tuners, intended to be incorporated into home stereo systems. The DENON unit, model TU-660 will be available from dealers in February.

Also, Taiwan-based SANGEAN showed an AM Stereo/FM Stereo pocket-sized headphone radio, the model SR-66. The unit is available in quantity from both SANGEAN and U.S. dealers, at a single piece price of about \$33. They can be reached directly by writing SANGEAN America, Inc., 9060 Telstar Ave., Suite #202, El Monte, CA 91731. U.S. dealer information can be obtained from Steve Kravitz, Motorola, at (708) 576-0554. NAB staff contact: Stan Salek, (202) 429-5391.



manner. It is possible in this way to realize an approximately nondirectional characteristic in the horizontal plane, while marked directivity in the vertical is maintained. Directional characteristics for a typical case are shown in Fig. 54. Such polyphase arrangements are very flexible, since by simple changes in the individual array it is possible to vary the directional characteristics in the horizontal plane in almost any manner desired.

**20. Ring Antenna Systems.**<sup>1</sup>—Marked directivity in the vertical plane combined with a substantially circular pattern in a horizontal plane can be obtained by arranging short vertical radiators in concentric rings and providing a uniform progressive phase shift between adjacent antennas in the individual rings such that the total phase shift around the circumference of each ring is the same and is a whole number of cycles.

Two types of such ring antenna systems have especially desirable properties. The first, termed the  $J_0$  type, consists of a multiplicity of concentric rings, with all antennas in the same ring having the same phase. The other, termed the  $J_n$  type, has only a single ring, but with the total phase shift around the ring being  $n$  cycles, where  $n$  is an integer not less than 1.

The design of a  $J_0$  antenna is carried out as follows: First, an integer  $m$  is selected that will give the desired power gain when substituted in the approximate relation

$$\text{Power gain} \cong 1.17 \sqrt{m - 0.5} \quad (44)$$

This power gain is expressed with respect to a short vertical grounded antenna, and assumes that the radiators of which the ring array is composed are likewise short vertical radiators. The value of  $m$  obtained in this way then determines a value of the quantity  $k'\rho_0$  according to the relation

$$k'\rho_0 = \pi(m - 0.25) \quad (45)$$

The quantity  $k'$  is defined by the relation

$$k' = \frac{2\pi}{\lambda} S \quad (46)$$

where

$$S = 1 + \frac{1.8}{k'\rho_0 - \frac{\pi}{4}} \quad (47)$$

The radius  $\rho$  of a ring is then made such that  $J_0(k'\rho)$  is a maximum, corresponding to

$$\rho \cong 0.62 \frac{\lambda}{S} + \frac{p\lambda}{2S} \text{ wave lengths} \quad (48)$$

where  $p$  has the value 0 for the first ring, 1 for the second ring, 2 for the third ring, etc., and the outer ring in the array is the one for which the radius  $\rho$  is a little less than  $k'\rho_0$ . There is also a central antenna. The number of antennas in each ring should be not less than  $1 + k'\rho_0/S$ . The total current in each ring, when the current in the center antenna is taken as unity, will then be 2.00 for the first ring, 2.9 for the second

<sup>1</sup> W. W. Hansen, and J. R. Woodyard, A New Principle in Directional Antenna Design, *Proc. I.R.E.*, Vol. 26, p. 233, March, 1938; W. W. Hansen and L. M. Hollingsworth, Design of "Flat-shooting" Antenna Arrays, *Proc. I.R.E.*, Vol. 27, p. 137, February, 1939; H. Chierix, Antennes a Rayonnement Zenithal Réduit, *L'Onde électrique*, Vol. 15, p. 440, July, 1936. See also U. S. Patent 2,218,487, Oct. 15 1940, issued to W. W. Hansen and F. E. Terman.

... among the antennas in the ring, and the phases of successive rings differ by exactly  $180^\circ$ . An example of a  $J_0$  antenna system is given in Fig. 55.

The  $J_n$  antenna is designed by first selecting the total number of cycles  $n$  of phase shift around the ring to give the desired gain, according to the approximate equation

$$\text{Power gain} = 0.752 \sqrt{n + 1.5} \quad (49)$$

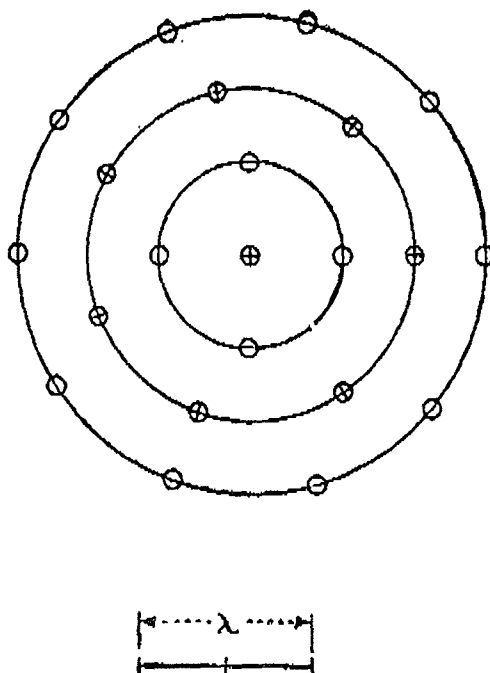


FIG. 55.—Plan view of  $J_0$  antenna array with  $m = 4$ , having a gain of 2.3. The circles represent array elements, those with a (−) inside having the current flowing  $180^\circ$  out of phase with the currents in the antennas marked (+). The radii of the successive rings are  $0.52\lambda$ ,  $0.95\lambda$  and  $1.39\lambda$ , and the relative currents in the individual antennas are 1, 0.50, 0.41, and 0.36 for the successive rings.

This assumes that the array is composed of short vertical radiators, and gives the power gain with respect to a single such radiator. The minimum number of radiators required is  $2n + 3$ . With fewer than this, the radiation pattern in the horizontal plane will not be circular. The radius  $\rho$  of the ring must be small enough to satisfy the relation  $(2\pi\rho/\lambda)^2 \ll 4$ . The exact value of the radius is otherwise immaterial except for the fact that the smaller the radius the lower will be the radiation resistance, and hence the more difficult it becomes to reduce the other losses sufficiently to provide an efficient radiating system. The  $J_n$  antenna is characterized by a directivity in a vertical plane that has no minor lobes, as shown in Fig. 56.

Comparison of the characteristics of the  $J_0$  and  $J_n$  arrays indicates that the latter is preferable when high gain is desired, whereas the former becomes more economical with moderate gains. The transition point at which the multiple-ring arrangement has approximately the same desirability as the single ring occurs when  $(k'\rho_0)/S$  is in the range 6.65 to 10.

**21. Antenna Systems Involving Plane Reflectors.** *Systems Employing a Single Flat Reflector.*—In ultra-high-frequency work, a flat conducting sheet, usually of copper, is often placed near an antenna system to modify the field pattern and increase the gain. Such a reflector acts in the same as a perfectly conducting earth, and its effect can be analyzed in the same way.

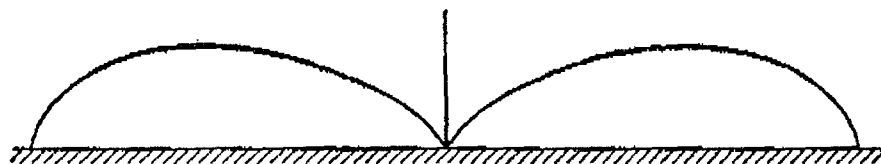


FIG. 56.—Field produced in a vertical plane by a single-ring antenna for  $n = 5$ , corresponding to a gain of 2.1.

The simplest arrangement involving a flat reflector of this type consists of a half-wave antenna adjacent to and parallel with a copper sheet or screen. In such an arrangement, the spacing between the antenna and the reflector is preferably of the

<sup>1</sup> These total relative currents in each ring are proportional to the areas under the successive loops of the function  $\rho J_0(k'\rho)$ , with each ring of antennas being identified with the corresponding loop of the Bessel function.

in the plane of the loop that is approximately circular, as shown in Fig. 53b. This is obtained from the field patterns of the individual antennas by noting that the individual radiations in any particular direction are in time quadrature, and so combine to give a resultant that is the square root of the sum of the squares of the individual radiations in that direction.

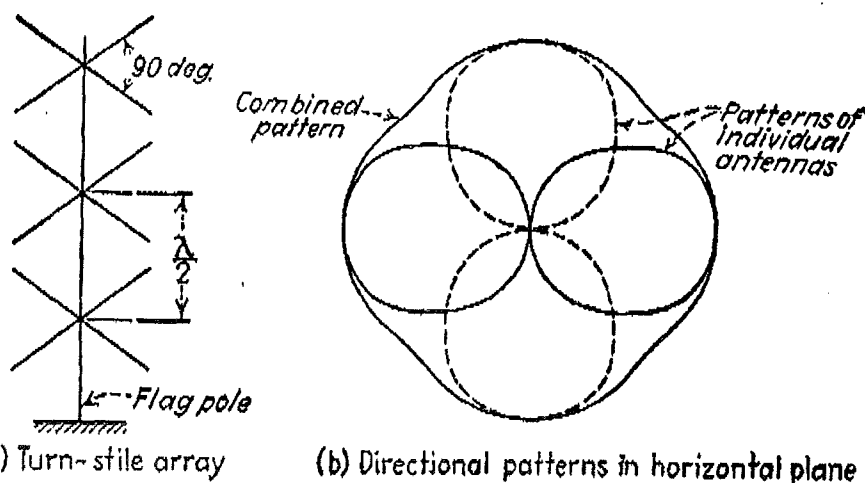


FIG. 53.—Stacked array of turnstile antenna systems, together with directional patterns in horizontal plane.

Turnstile antennas are sometimes arranged in an array in which a number of individual turnstiles in a horizontal plane are arranged one above the other in a broadside array, in which the line of the array is vertical, as shown in Fig. 53a. This gives approximately uniform radiation in all horizontal directions, but provides directivity in a vertical plane.

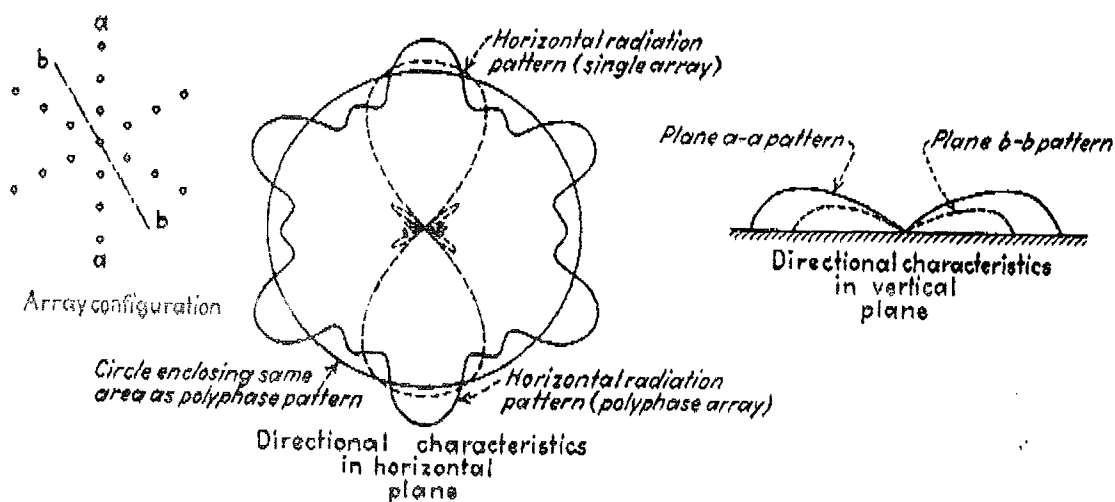
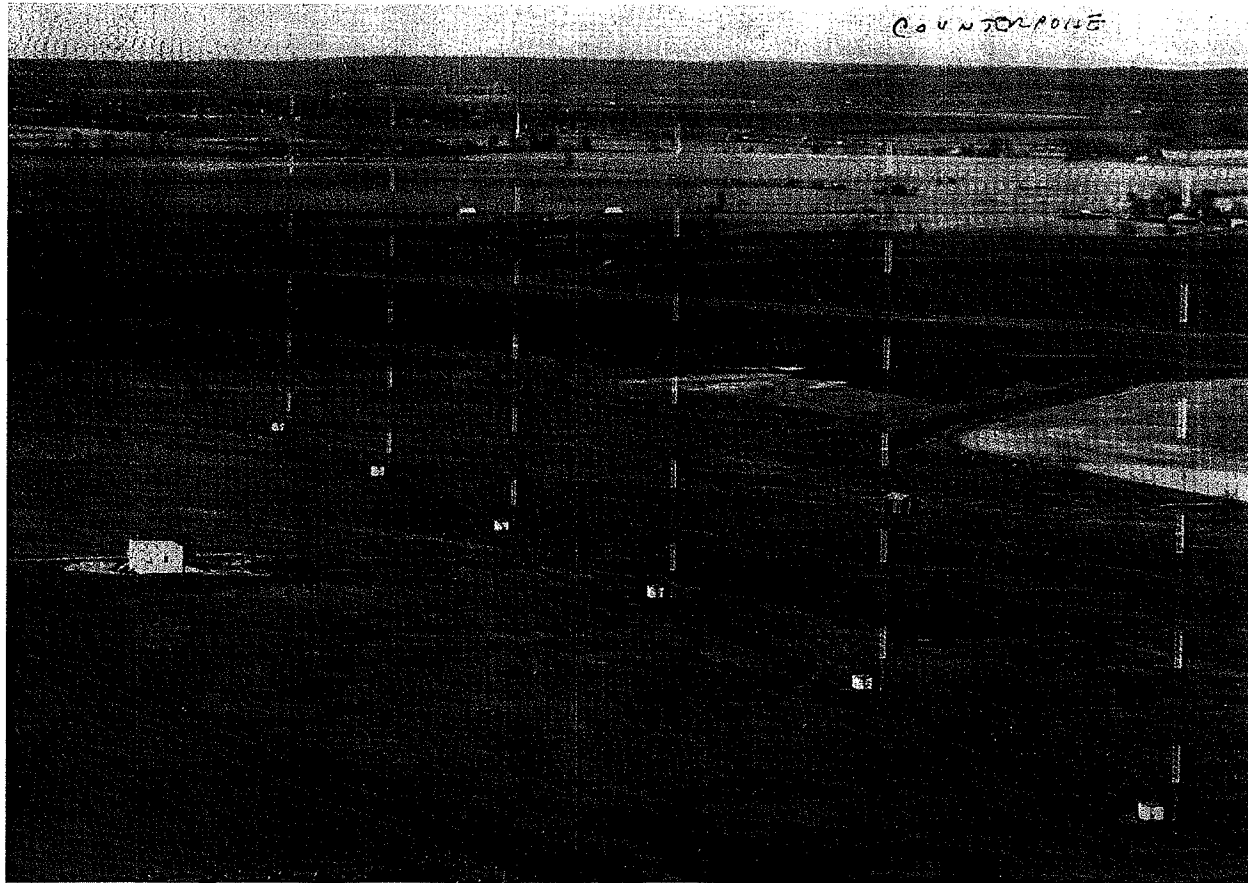


FIG. 54.—Polyphase antenna array that concentrates radiation along the horizontal without requiring a high pole structure. Varying the angle between the lines of antennas or modifying the arrangement of antennas within a line, etc., makes it possible to control the horizontal and vertical patterns.

*Polyphase Antenna Arrays.*<sup>1</sup>—Marked directivity in a vertical plane can be obtained at broadcast and lower frequencies by using a large number of short vertical radiators in a polyphase array, as illustrated in Fig. 54. Here short vertical radiators are arranged at regular intervals in linear arrays, a number of such linear arrays are arranged as shown, and then the various linear arrays are excited in a polyphase

<sup>1</sup> Such arrangements have been proposed by Terman, *op. cit.*, p. 678.



#### Antenna System

The directional antenna system for the new KTBS was designed and adjusted by the consulting firm of A. Earl Cullum, Jr. of Dallas. The array (Fig. 5) is a six tower "in line" type with four of the towers used for daytime operation and all six in service at night time. The towers are 378 feet high and spaced about 530 feet which means that the end towers of the array are approximately one half mile apart. The towers were furnished by the International Derrick and Equipment Company and were erected by the Andrews Company of Ft. Worth. A four-section RCA Pylon FM antenna was mounted on top of Number 3 tower. The combined height of this Number 3 tower and Pylon is 378 feet.

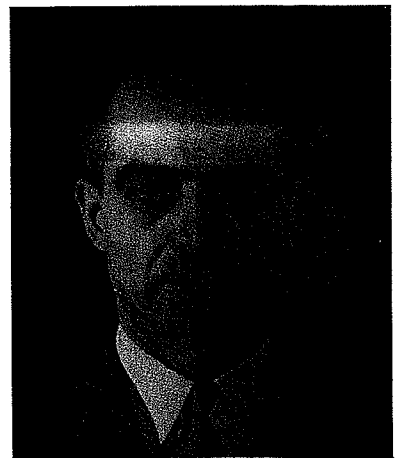
Since a rather "tight" pattern was involved the array was constructed according to a very rigid specification in order to obtain the highest degree of stability possible. Every precaution was taken to insure permanence of all joints, bonds and electrical connections. Mechanically all towers and ground systems are symmetrical with the exception of the one radiator

which is made up of a shortened tower plus the FM Pylon. All underground joints and all connections between heavy members above ground were made with silver solder or brazed and welded. In ad-

dition to the bond straps furnished by the tower manufacturer for "jumping" the butt joints on the towers the lighting conduits were bonded to the towers at 10-foot intervals throughout the tower lengths.

#### ABOUT THE AUTHOR

W. M. (BILL) WITTY, the author of this article, needs no introduction to most readers of BROADCAST NEWS. For nearly twenty years he has been intimately associated with the broadcasting industry in the southwest—first as RCA's field sales engineer for the area, and more recently as a consulting engineer in his own right. Leaving the perhaps more glamorous field of allocations engineering to others, Bill has specialized in "facilities engineering"—i.e., the planning and supervision of plant installations, particularly those involving complicated and extensive antenna or equipment problems. The KTBS transmitter plant was one of these. The accompanying article—printed in Bill's own modest words—makes no attempt to glamorize this job. However, BROADCAST NEWS readers familiar with this type of installation will quickly recognize it as the work of an expert.



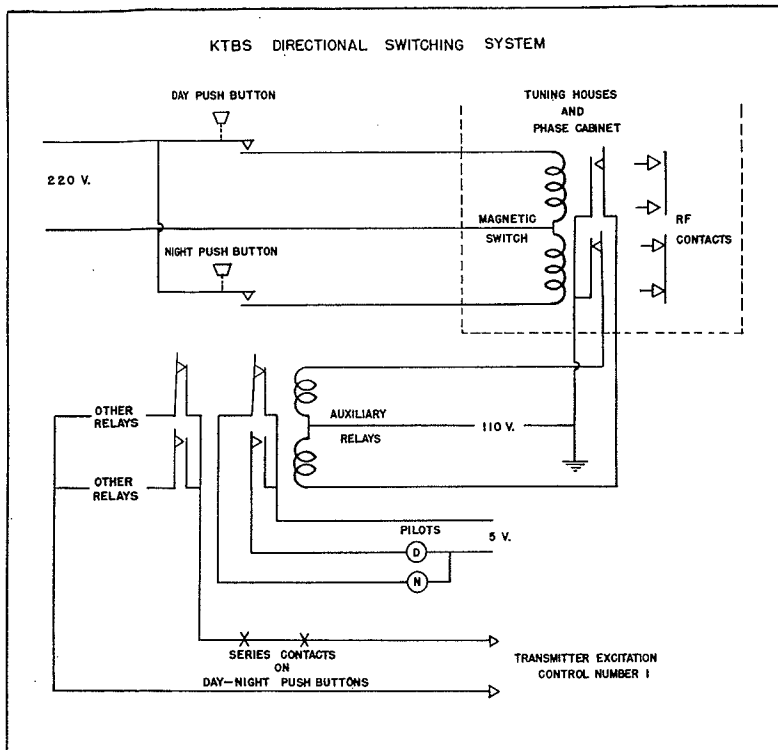


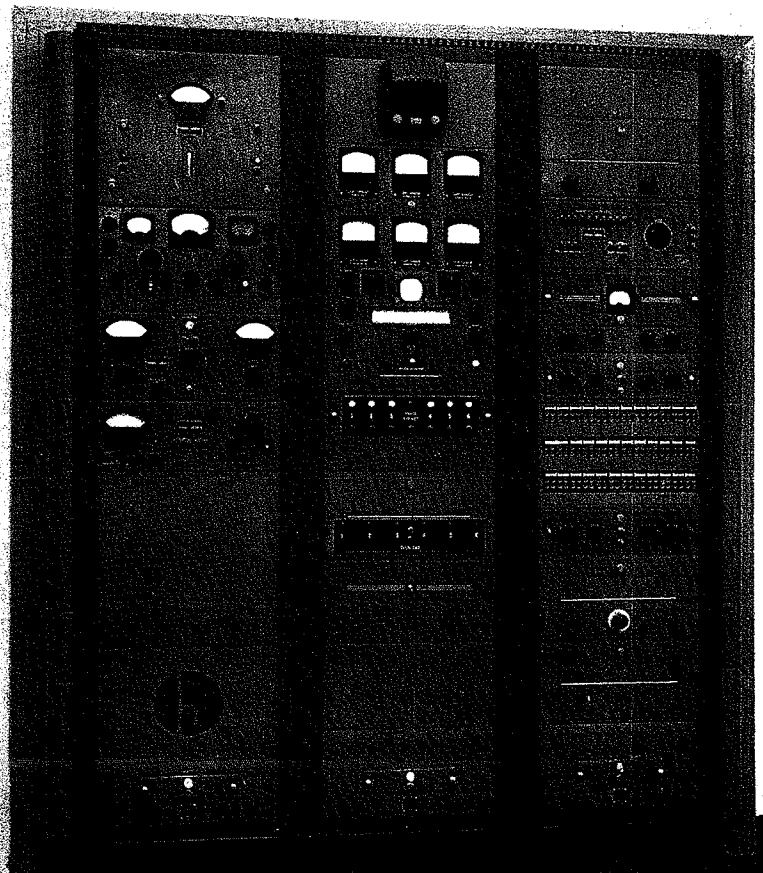
FIG. 12 (left). Simplified schematic of the KTBS directional switching system. Push buttons on the phasing cabinet operate contactors in the phasing cabinet and in the six antenna tuning houses. Back contacts operate signal lights in the transmitter room and prevent excitation from being applied until all contactors have closed.

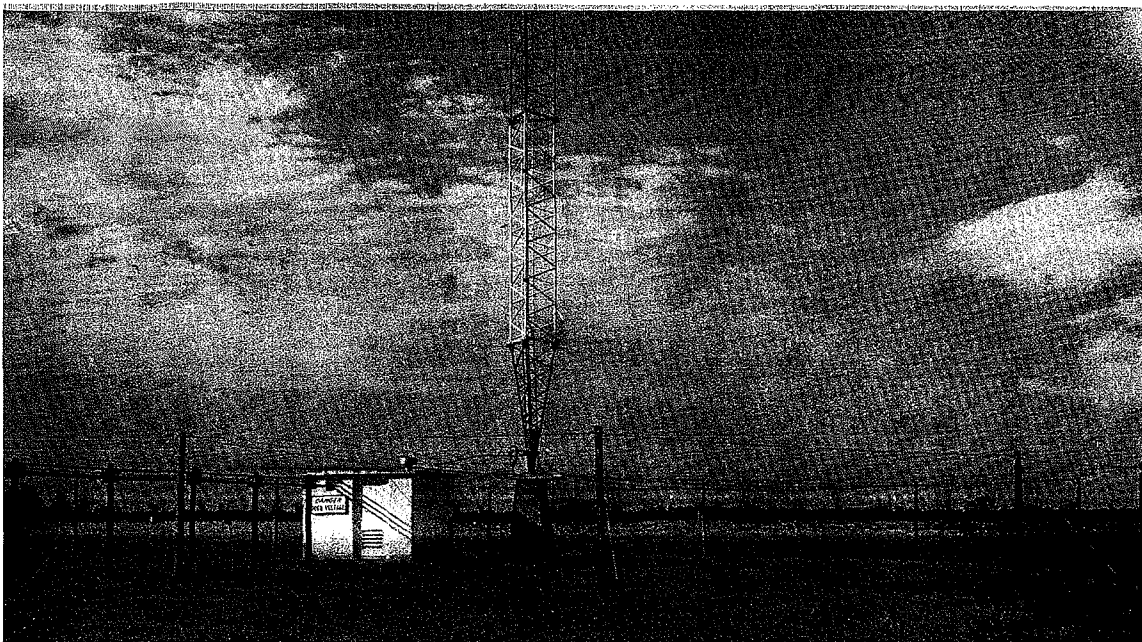
### Directional Switching System

KTBS's directional system consists actually of two separate and complete systems, so far as phasing and power dividing equipments are concerned. The daytime pattern is obtained with one set of networks, transmission lines and four of the six towers. The nighttime pattern utilizes another set of networks, lines and all six of the towers. Switching between the two modes of operation twice each day is accomplished by means of solenoid type switches located in each of the tuning houses and in the phase cabinet in the transmitter building (Fig. 12). Seven of these switches are actuated from two push buttons located on the front of the phase cabinet in the transmitter building. Each of the seven switches is provided with back contacts which actuate auxiliary relays in the transmitter building that have one set of contacts to operate pilot lights and another set to close the transmitter excitation control circuit. Extra series contacts on the push buttons also break the transmitter excitation control circuit. The excitation control in this instance is the plate supply to the transmitter crystal oscillator.

With this arrangement it is virtually impossible to switch the antenna system with carrier power "on". Also if one of the remote solenoid switches fails to go over its pilot light will indicate in which tuning house the trouble is and it is not possible to put the carrier back on until this switch has properly closed. All of the switches must be in one of the two positions—that is—day position or night position before carrier power can be restored. The operator is able to manually hold off excitation until all lights are on for one position, thus indicating that the remote switches are all clear. Should he inadvertently release the push button before all of the switches have cleared the auxiliary relays will prevent excitation from being restored.

FIG. 13 (left). These three racks are built into the right wall of the transmitter room. The left-hand rack contains frequency and modulation monitors and distortion measuring equipment; the center rack the antenna meters, the phase monitor and the contactor signal lights; the right-hand rack contains the audio input equipment.





#### Ground System

The type of ground system installed at KTBS, to some extent, departs from the conventional form of buried radial system. The KTBS ground system does have 120 buried radials 300 feet long around each tower, but these do not come all the way in to the tower base insulators. Rather, these radials terminate at an underground circular bond strap 100 feet in diameter around the edge of the overhead system. The overhead system (Fig. 7) is supported by anchored poles—12 at each tower—and is 8 feet above the ground level. It consists of 120 radials drawn tautly and

soldered between a central ring (Fig. 8) mounted around the top of the tower foundation and a large copper cable supported by the twelve poles (Fig. 9) around the 100-foot circle. This outer cable is, in turn, bonded to the underground circular bond strap by means of 4-inch copper strip running down and tacked to each pole. Since the tuning houses are beneath the ground system, connections to the tuning house equipment from the ground system, as well as from the antenna, are made through the roof of the tuning houses.

This type of design insures maximum stability of antenna impedance since there

can be no foreign material of changeable nature such as vegetation, water or soil within the field of the antenna at the point which is most critical and where the current is highest.

The individual tower ground systems were connected together by means of a buried 4 inch copper strip running the full length of the array. Also transverse 4-inch copper strips were placed at halfway intervals between all of the towers and any ground radials that were traversed were silver soldered to these strips. The central transverse strip extends to the transmitter

FIG. 9 (below). Close-up view of one of the anchored poles supporting the overhead ground screen. Note compression spring which provides compensation for expansion due to temperature changes.

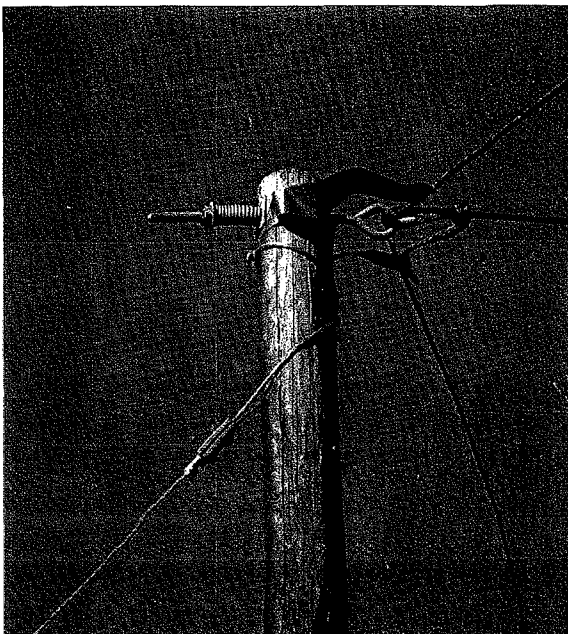


FIG. 10 (below). This is a close-up view of the central ring to which the 120 radials of the elevated ground screen are carefully braised. The ring, in turn, is connected by copper straps to the bonding about the tower base.

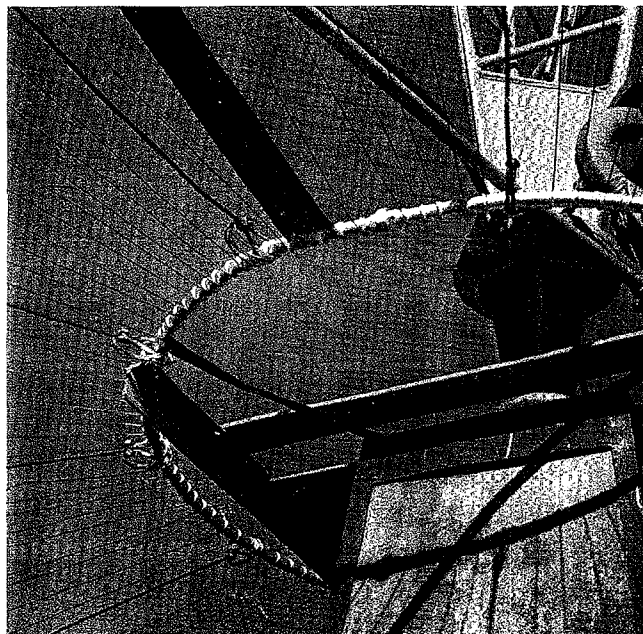


FIG. 7 (opposite page). Overall view of the elevated ground screen installed around each of the KTBS towers. This arrangement provides a stable antenna impedance because changes in vegetation or ground water in the critical area around the base are minimized.

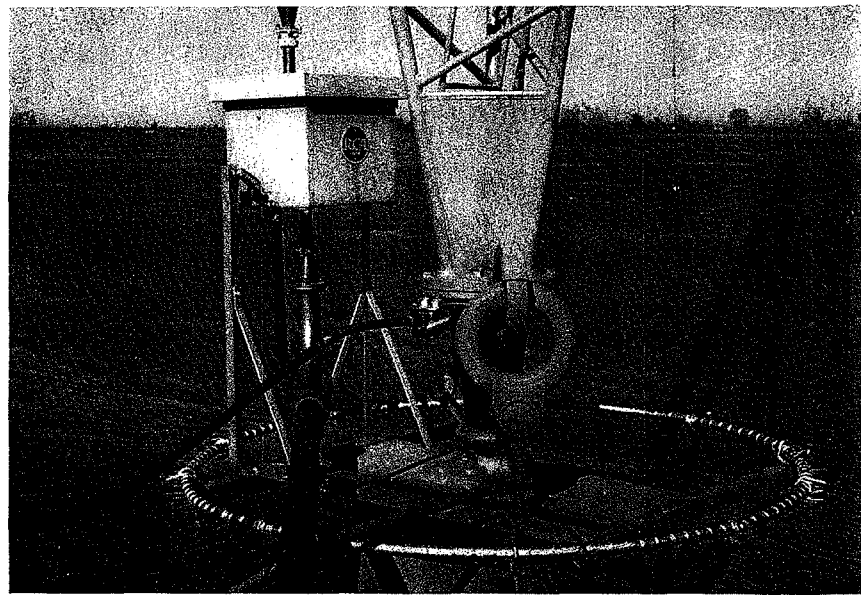


FIG. 8 (right). This close-up view of the base of one tower shows the BAF-4A FM Isolation Unit (in square box) and the Austin Transformer (large open coils) used to isolate the tower lightning circuits.

building and is connected to the ground terminals of all the transmitting equipment.

Other copper strips were buried along the line of transmission line poles between the transmitter building and towers Number 3 and Number 4. All transmission lines, conduits, and sampling lines were bonded to these buried strips at each pole, which are spaced at 10-foot intervals. Along the runs between the towers these ground connections are made at 30-foot intervals.

#### Tower Lighting System

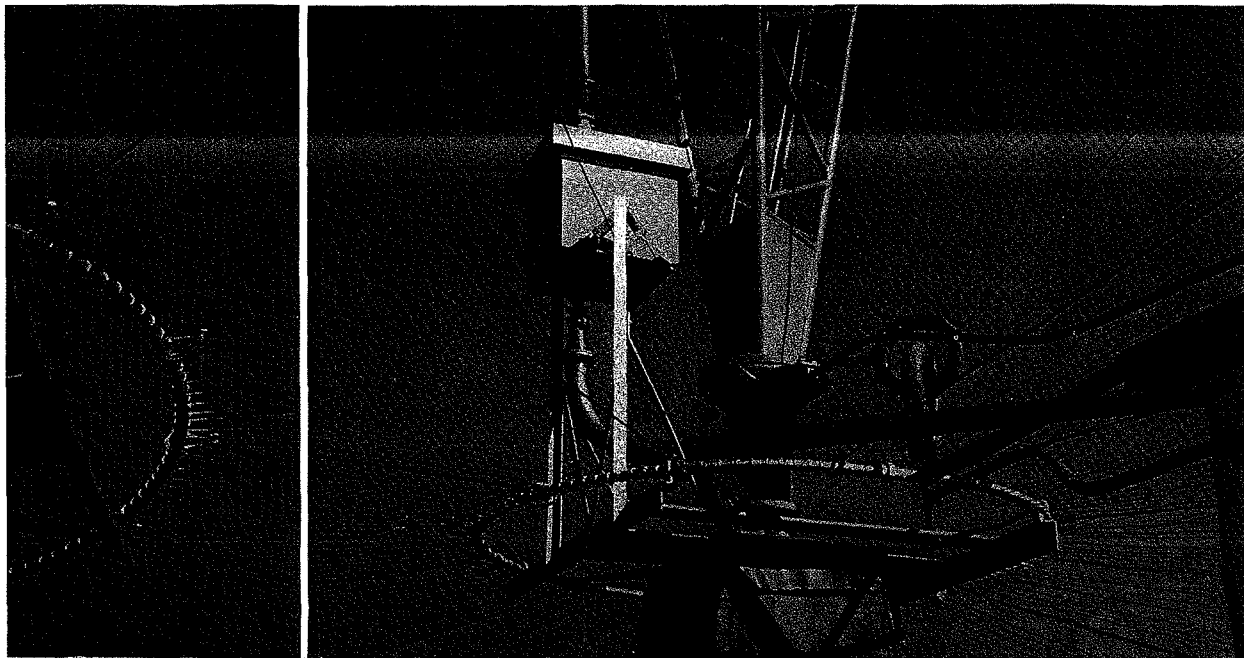
In many directional antenna systems the 1000 watt beacons mounted on each

tower in accordance with CAA requirements are flashed by means of individual flashers of the non-synchronous type installed on each tower. The speed of the motor in this type flasher varies a slight amount with the result that the lights on a multi-element array occasionally get "in step". If this occurs with as many as six elements a rather heavy demand is made on the power service and the line voltage will fluctuate to the extent that it is sometimes difficult to operate measuring equipment in a station during nighttime hours.

At KTBS a central flasher was installed in the transmitter building and the three

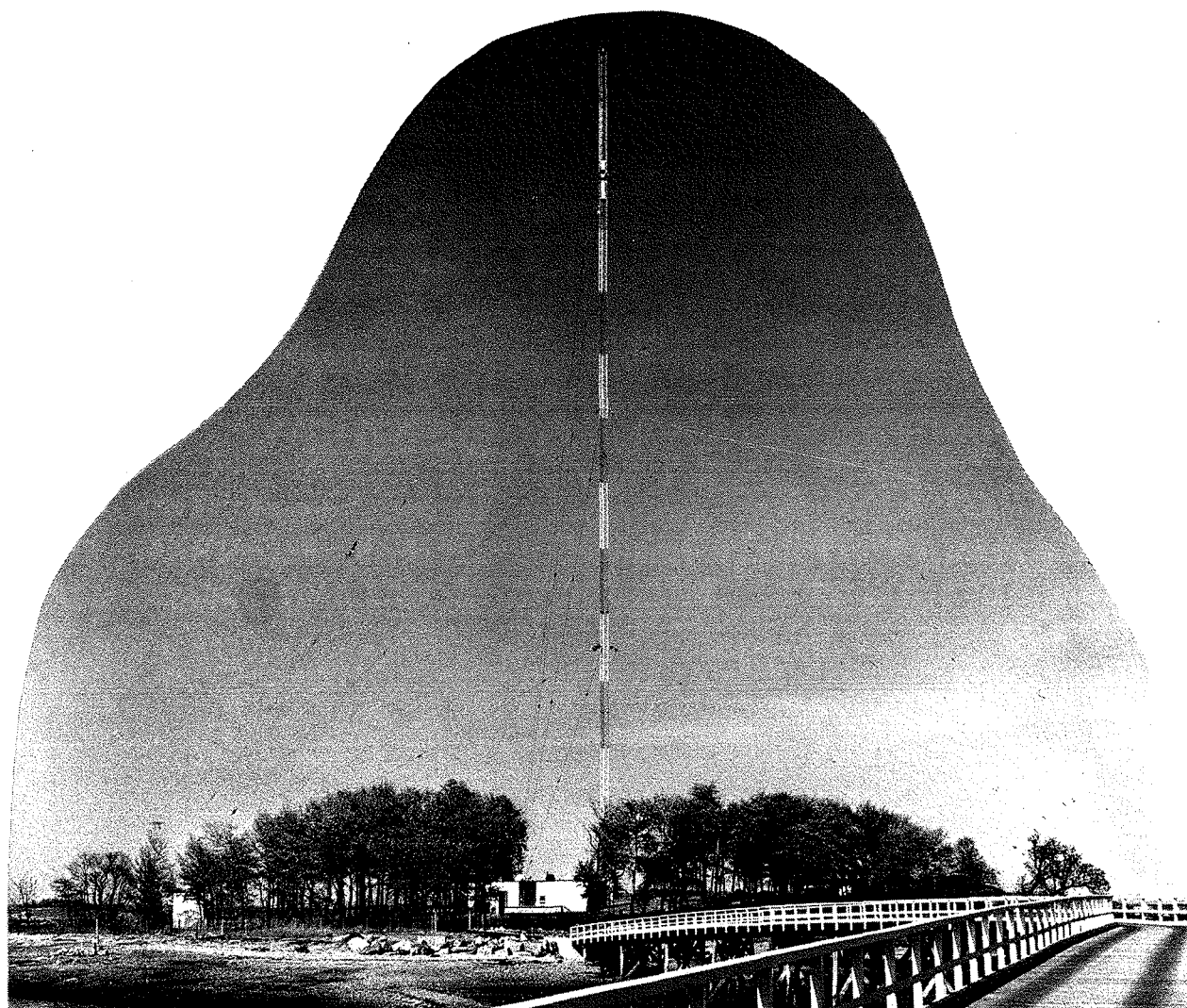
phase power service divided among the six towers in such a manner that a nearly constant lighting load is presented at all times. The flasher consists of a synchronous motor geared to rotate a cam shaft at 36 R.P.M. Six adjustable split cams are mounted on the shaft and arranged to operate individual mercury type switches that control the lighting voltage to each tower. This arrangement enables the desired lighting sequence of the towers to be obtained and the split cams permit accurate adjustment of the 2:1 light-to-darkness ratio required by the CAA.

FIG. 11 (below). This view of the tower base shows the connections between the tower and the doghouse (lower right corner). The large concentric line is the FM feed line which runs directly to the BAF-4A Isolation Unit in the square box at the top left of this picture. Note that the isolation unit is mounted on springs in order to provide for differential expansion of the FM line which runs up the tower.





# **WNBC-WCBS SHARED ANTENNA SYSTEM**



***Presented at The 18th Annual NAB  
Engineering Conference  
April 7, 1964***

**LESTER A. LOONEY, Formerly  
MANAGER, TRANSMITTER ENG.  
NATIONAL BROADCASTING CO.**

**OGDEN L. PRESTHOLDT  
DIRECTOR OF ENGINEERING  
CBS RADIO DIVISION**



### WNBC-WCBS SHARED ANTENNA SYSTEM

In order to improve the service from WNBC, the National Broadcasting Company station in New York, a change in transmitter location was desired. After some search an island of about six acres known as High Island in Long Island Sound was obtained. The island is close to shore and accessible by bridge in the Borough of the Bronx in New York City. This location, being near sea level, had the advantage of permitting a higher antenna as well as a ground system extending into salt water.

The transmitter of WCBS, the Columbia Broadcasting System station in New York, was located on Columbia Island about one and one half miles from High Island. This Island was reached only by boat, and as remote control was anticipated, it was desirable to provide easier access to the transmitter. There had been occasions during winter ice conditions and storms when Columbia Island was isolated for a day or more. As good transmitter locations are not plentiful in the vicinity of New York City, it was natural to consider a joint project on High Island. After some study it was agreed that NBC and CBS together would plan, design, and construct, complete new transmitting stations using a common antenna. The two stations are both Class 1A with powers of 50 KW. WNBC operates on 660 kc/s and WCBS on 880 kc/s. The frequency separation, one being three fourths of the other, seemed sufficient to insure successful operation into a single antenna.

FCC construction permits when obtained, contained specifications for both stations that the antenna height must not exceed 549 feet above mean sea level, that the unattenuated field intensity at one mile, based on 1 KW antenna input, must be at least 225 millivolts per meter, and that any spurious radiations resulting from cross modulation be held to non-interfering levels.

Considering the ground elevation, the antenna height became about 528 feet above ground. The theoretical no-loss performance of a plain vertical antenna of this height is only 206 mv/m at 660 kc/s and 228 mv/m at 880 kc/s. It was then obvious that some increase in efficiency would be necessary at 880 kc/s to compensate for losses and that an appreciable

increase would be necessary for 660 kc/s. To obtain the increase, a top loaded and reactance sectionalized antenna tower was indicated. To determine the optimum degree of top loading, position of tower sectionalizing and reactance insertion, the RCA Laboratories were engaged to model the antenna.

With the physical data arrived at, the antenna was specified as shown in Figure 1. The tower has a triangular constant cross-section,  $4\frac{1}{2}$  feet on a face, is sectionalized with a single pedestal type insulator about 85 feet from the top and guyed at four levels. The set of guys attached to the top of the tower (unlike the others) have no insulators at the tower, and are electrically bonded to the tower. The upper sections of these guys are therefore used for top loading to increase the electrical height of the tower. A suitable reactance is connected between the upper and lower sections of the tower to control the effective electrical height.

Vertical plane radiation patterns obtained from the model, indicated that a field of about 246 mv/m at one mile might be realized for one KW radiated power. The value was approximately the same for both frequencies. This meant that on the basis of 50 KW input to the antenna, the required field would be obtainable with about 42 KW radiated power, leaving 8 KW available to supply the system losses and any tolerance in the modeling data.

To provide additional information, a mathematical model was prepared for each frequency and arranged to program a computer, with variables of top loading, current distribution, (which would be obtained by variation of the sectionalizing reactance) and estimated values of tower ohmic resistance. These computations indicated a trend of increased field with reduced length of guy top loading, other variables being held constant. This results from using guys for top loading instead of the so called "HAT" of structural steel. The guy loading, while quite desirable from a structural viewpoint, has a vertical component which modifies the effective current distribution of the very top portion of the antenna. It was obvious, however, that appreciable reduction in top loading would result in excessive values of sectionalizing reactance necessary to maintain a suitable current distribution on the tower. This would cause high sectionalizing voltages and losses in the reactance network. The guy top loading was finally set at a length of about 120 feet. There would be some effective

extension of this value due to the capacity of extra large insulators at the ends of the loading sections.

The antenna system was constructed in accordance with the above values. The design was based on 50 lbs./sq.ft. on flats for wind loading and the tower is constructed from 30 foot welded sections. In view of the voltages anticipated from the operation of two 50 KW transmitters (the peak voltages add arithmetically) three exceptionally large guy insulators were used at the ends of the guy sections used for top loading. The remaining insulators were spaced in an attempt to minimize guy currents and equalize insulator voltages. Considering that the antenna was to be used for two separate transmitters with the increased complexity in the networks for matching, isolation, and sectionalizing, it was felt advisable to have an auxiliary antenna with its own networks. For this use, a bottom segment of one of the top guys cables was made 200 feet in length with the top end terminated in large insulators and a corona ring. Although only the lower power auxiliary transmitters would be used on this antenna, the peak voltage at the upper end calculated to be well over 100 KV. All guys were fabricated from one inch diameter Alumoweld cables. Each strand in the cable is of steel with a thick aluminum covering providing good conductivity for the current carrying portions.

The tower being sectionalized and top loaded has a higher loop current than would be found in an equivalent unloaded antenna. Because of this higher loop current, conduction losses in the steel tower might have become significant. As a precaution, we obtained the cooperation of the tower fabricator in the control of the galvanizing process and obtained a galvanized coat thicker than normal.

An efficient ground system was designed and installed, starting with a conventional expanded copper mesh ground screen about 40 feet square around the tower base. From this screen 120 radials of one inch wide buried copper ribbon were extended approximately one fourth wave length to the island shore line. Further extension of the radials was by #2-0 stranded copper cable to a point where at least 50 feet was immersed in salt water. The ends were anchored by securing to concrete blocks.

At this stage, base impedance and tower current distribution measurements were made, on one frequency at a time, using various amounts of a temporary simple coil for the 660 kc/s reactance at the sectionalizing point, and a short circuit

or capacitor for 880 kc/s. Field intensity measurements were next made to determine the antenna performance as well as to exactly confirm the optimum value of sectionalizing reactance for each frequency. This work was performed with the advantage of daylight while the two stations were still in operation at the old locations, by permission from the FCC to use a test power of 50 watts on the frequencies of 640, 680, 860 and 900 kc/s. Advantage was taken of the water of Long Island Sound bordering on the station to use a boat in making radial measurements in several directions. This method was faster and produced more consistent data than could be obtained on land with short radials in the built up city area. The boat was run on a radial starting from and ending with a fix. Speed was maintained as near constant as possible, with the start, finish, and measurement times recorded. An example of these measurements is shown on Figure 2. From these, as well as measurements on land, it was confirmed that the antenna would meet the required radiation efficiency. The sectionalizing reactances required, were determined at 180 ohms inductive for 660 kc/s and 50 ohms capacitive for 880 kc/s. The tower current distribution placed the minimum at about 23 degrees above the ground. The widely differing reactances were due to insufficient height for the low frequency, while at the high frequency the antenna with the top loading, was somewhat too high.

It was now necessary to consider a design for the permanent sectionalizing reactance. This component is of particular interest because of the two-frequency requirements and the necessity to avoid large losses. Several networks had been considered which would supply the separately required reactances. With the precise values now in hand the networks shown in Figure 3 were re-examined. #1 is the simplest, however, calculations indicated that the coil current would exceed 400 amperes and the loss at 660 kc/s would be about 6 KW. The reactance slope, or variation against frequency in the band  $\pm 10$  KC would also be excessive. The base impedance of a loaded antenna varies more rapidly with frequency than that of a simple antenna. Using a sectionalizing reactance such as is necessary for two frequencies causes a still steeper base impedance variation and results in concern for the proper loading and low distortion operation of the transmitter. These characteristics were sufficient to reject #1 network. The other three networks, by proper choice of values can all be made to exhibit nearly equal and acceptable amounts of loss and reactance slopes. #2 however, develops a peak voltage well over 100 KV

across the capacitor, and #3 an effective current of 200 amperes in  $L_1$ . Voltages were computed for full modulation and the current for no modulation condition. These characteristics do not make for easy design, and in addition these two circuits would be critical to adjust, especially if it became necessary to do so after installation high up in the tower. #4 network provided a very happy compromise. The voltages and currents are not uncomfortable for design purposes and the adjustments, even after installation, can be made straight forward. At this point it should be explained that the provision for getting a power circuit past the tower sectionalizing to supply the top beacon had already been made. Previous measurements had shown that running power circuits up through the tubing of a sectionalizing coil and the consequent short circuiting of unused turns for adjustment, would reduce appreciably the effective  $Q$  of the coil. Therefore an insulating transformer such as is commonly used at the tower base was installed at the sectionalizing level to supply the top beacon. The operation of #4 network can best be seen in Figure 4.  $L_1 C_1$  is made anti-resonant at 660 kc/s so that for practical purposes, all the sectionalizing current at that frequency flows in  $L_3$ . Thus with  $L_3$  alone connected, it may be adjusted to the proper value by reference to the antenna base impedance determined during the tests. With the other leg of the network added, and an approximate value of  $L_2$  in use,  $L_1 C_1$  may then be adjusted for the same base impedance as obtained before. The frequency may then be changed to 880 kc/s and  $L_2$  adjusted for the base impedance determined for that frequency.

Figure 5 shows the way in which the network was installed in the tower. A 5 foot open face section above the sectionalizing insulator made room for a shield cabinet containing  $L_3$  and a 10 foot space below the insulator was provided for a double compartment cabinet for  $L_1 C_1$  and  $L_2$ . As there is very little circulating current between the two legs of the network they are individually connected between the tower sections. The shield cabinets are constructed of one eighth inch thick aluminum with welded seams and ventilating louvres with baffles to minimize rain entrance. The doors have special RF bonding and weather strips. The coils for the network were specified so that there would be a minimum of unused turns and as good a  $Q$  factor as feasible. Before installing the coils in the cabinets the  $Q$ 's were carefully measured by plotting resonance curves for each frequency.  $Q$ 's between 900 and 1000 were found. When the coils were installed in the

shield cabinets the Q's dropped to about 600. On the basis of a 600 Q the network loss computed at about 1500 watts for each frequency. The capacitors for  $C_1$  are multiple vacuum units, three of which are variable. They are rated at 60 KV. The network provides a DC path for static drain and a ball gap across the sectionalizing insulator supplies protection to the network from lightning. The single sectionalizing insulator minimizes stray capacity between tower sections. It is equipped with a rain shield and was especially designed to tolerate a small amount of rocking, which can occur during high winds.

The pictures Figures 6 and 7, show  $L_3$  mounted in the upper cabinet, and  $L_1$ ,  $C_1$ ,  $L_2$  mounted in the lower cabinet. The cabinets were painted with Day Glo, the same as the two top orange sections of the tower. This paint, having florescent characteristics, provides increased visibility during daylight.

Figure 8 illustrates the effect on the antenna base resistance of using a two frequency sectionalizing reactance network instead of a simple coil as would be used in the case of the antenna being built for one station. The base resistance around 660 kc/s was measured using only the coil  $L_3$  at the section and again when the entire network was connected. There is an increase in slope of about 1.3 over a 20 KC band when the complete network is connected. It may be noticed that the two plots cross at the carrier frequency.

Figure 9 illustrates the measured current distribution on the tower at 640 kc/s. The complete curve was obtained with a sectionalizing reactance of zero and indicates only the tower current. That is, the current in the guy loading and the effect of it is not shown. The partial curves show the locations of the current minimum for sectionalizing reactance values of j140 and j190 ohms.

Although some trouble was experienced initially with inadequate electrical bonding at the cabinet door edges, there has been no difficulty to date with the sectionalizing network proper. The antenna system as a whole is performing satisfactorily.

During the early stages of the project, we became aware of many serious problems relating to the design of the isolating and coupling networks. The general performance criteria we originally had in mind were not reducible to specific performance standards until several network designs had been studied in detail.

General problems relating to network losses were of particular concern in this instance because the circuitry required to provide the unusually high isolation necessary between these transmitters could very easily result in excessive losses. A second important factor relating to circuit performance dealt with the problem of maintaining reasonably constant load impedance over the bandwidth being transmitted. In normal installations, this requirement does not impose any special design requirements, but under some circumstances, the impedance bandwidth problem may become controlling in network design. A further requirement was that the coupling and isolating network for each station be capable of being disconnected from the antenna system in the event of failure in one network so that the other station could continue operation in normal fashion and that the station in trouble would be able to work in perfect safety on the network which had suffered a failure.

Past experience has established that a transmitter using a Class "C" final amplifier and having stray R.F. energy in its tank circuit will generate cross modulation products as though the amplifier behaved as a mixer with 25-30 db loss. If these spurious emissions fall on or near frequencies that are used by other services, it has been found that these spurious emissions in 50 kw plants must be kept at least 120 db below the level of the fundamental. Both the sum and difference frequencies were in use within 100 miles of the transmitting site; therefore, these first order effects had to be effectively removed. The net isolation required was such that attenuations in the order of 100 db at carrier frequency had to be obtained and, consequently, all networks had to be enclosed in well-shielded cabinets.

These problems in terms of defining the performance of the coupling and isolating networks indicated to us that a reasonably complete design of the networks would be necessary before specifications for the network could be written; consequently, we designed these networks ourselves.

Base impedance data from the model measurement work indicated that there could be impedance bandwidth problems. These data from the model work indicated that the antenna impedance would be significantly worse than that specified in EIA Standard TR-101-A for normal load impedance and that actual tests on transmitter performance should be made. An analysis of Class "C" amplifier performance indicates that the optimum load impedance as a function of bandwidth should be the equivalent of a dissipative parallel resonant circuit. Both NBC and CBS arranged for tests to determine transmitter performance into the then expected load impedance. These tests indicated that both the RCA BTA-50H and the G.E. BT-50-A transmitters would meet frequency response and distortion specifications with the expected load impedance if that impedance characteristic was properly oriented. The foregoing transmitter performance experiments also verified the fact that impedance bandwidth characteristics of other natures would not provide the same overall performance.

If the load impedance would be made reasonably constant over a frequency range significantly in excess of the bandwidth to be transmitted, transmitter performance could be further improved and overall operation significantly stabilized. These performance measurements indicated that serious consideration should be given to antenna coupling circuit design which would provide broad band impedance control in the same fashion as that provided by compensation used in television antennas.

The actual antenna impedance, as a function of frequency, was determined around both operating frequencies during the antenna tuning process. These data indicated that the impedance bandwidth problem was worse than that anticipated from the model measurements; a graph of these data is presented on Figure 10. Since suitable performance of the system was directly related to the proper matching of this impedance characteristic to the transmitter, considerable effort was devoted to the optimizing of these matching networks.

Consider for the moment a simple antenna whose resistance is constant and whose reactance varies as a series resonant L-C circuit. The terminal admittance and equivalent circuit of this antenna is shown in Figure 11 a, b. Suppose now, we put a reactive network across these input terminals, (Figure 11 b) and try to improve the admittance match thereby. Assume that the network in parallel with the antenna is a parallel L-C



network resonant to the carrier frequency. The effect at frequency  $f_1$ , a lower side band frequency, will be that of transforming the admittance from the original value to a new value, along a constant conductance path as shown on the Smith chart of Figure 11 a. Similarly, the admittance at carrier frequency is not changed; and the admittance at  $f_2$ , an upper side band frequency, is also improved. It may be seen that for moderate impedance bandwidth problems a significant improvement can be made by proper choice of the L-C ratio of the compensating network. It may also be seen that for impedance mismatches that are sufficiently severe such as that for  $f_3$  on Figure 11 a, that the reactive compensation network no longer offers a significant improvement. Our impedance bandwidth problem was severe enough to warrant a study of more effective methods of compensation.

Previous experiments had indicated that compensating networks using a dissipative element were capable of providing better overall driving point impedance characteristics. The circuit of Figure 11 c is such a network. This compensating circuit will add both susceptance and conductance to the antenna admittance as shown by the transformation of the  $f_1$  admittance on the Smith chart of Figure 11 a. A brief analysis of this type of network indicated that it provided two principal functions: (1) that of absorbing the energy reflected by the admittance mismatch at the side band frequencies and (2) that of providing relatively broad band constant load impedance for the transmitter. Since both of these conditions fit the required performance objective, dissipative compensating networks were considered to provide satisfactory system performance.

The foregoing detailed circuit requirements were applied to the design of suitable isolating and coupling networks, Figure 12 shows the final networks. Since the base impedance was capacitive at both frequencies, a common antenna loading coil  $L_a$  performed a common tuning function and reduced the undesired voltages across both the isolating networks. The remainder of the circuit in Figure 12 may be described as follows: The first network at the antenna end of the circuit is an L or a T network for matching the antenna impedance to the transmission line; some of the circuit elements in these networks are rejection traps tuned to the undesired frequency. The T network at the transmission line end is a phase shift network to properly orient the load impedance to the optimum position at the plates of the final Class "C" amplifier. Calculations indicated that two traps would provide

adequate isolation and, therefore, the third element could be used for other purposes.

A very low L-C ratio parallel resonant circuit connected in shunt to ground will provide an excellent filter to limit the generation and radiation of spurious frequencies. Calculations established that the antenna impedance could be properly transformed by the first series arm of the WCBS T network so that this shunt L-C network could also act as a reactive compensating network as previously described. These two functions, compensation and filtering, are performed by the shunt network in the WCBS circuit. (It was not practical to incorporate this feature in the WNBC side of the network.) A limited amount of compensation was provided for WCBS by this method. Further compensation of either the dissipative or non-dissipative type can be added, if needed, at this same point. On the WNBC side, the first T network was required to properly orient the impedance characteristic for compensation, and provision was made for compensation at the end of that network. Figure 13 is a photograph of the WCBS network; note particularly that  $L_{13}$  could not readily be made with half the present inductance and twice the diameter of the tubing as would be required for a significant increase in bandwidth impedance compensation. Figure 14 is a photograph of the network feeding the auxiliary antenna; this network provides only isolation and matching at the carrier frequency; no provisions were made here for broad band compensation or proper orientation of the load impedance.

An important consideration was that of obtaining maximum Q in the decoupling networks; properly designed coils for operation at this power level will produce Q's in the 500-1000 range. In a tuned circuit utilizing a coil and condenser in either series or parallel, it is important that the circuit connections also be made to provide minimum loss. No turns may be shorted in the coil; and the circuit should occupy the minimum physical space. Conductor sizes must be adequate for the current to be carried, a value of 20 amperes unmodulated carrier for each inch of circumference was used. Care was taken to make equivalent paths for each condenser, when units were used in parallel. Most of the resonant circuits in the decoupling networks were designed to operate at or near full design inductance. Detailed measurements of Q of these circuits have not been made, but those that were made of the antenna sectionalizing network suggest that Q's in excess of 600 were obtained in actual operation of these networks.

Stringent performance specifications were established for all characteristics of the plant. We believe that these performance criteria have been adequately met.

The transmitting site is almost completely surrounded by the New York urban area. It was not possible to find directions with relatively unobstructed sites for the making of the field strength proof. Therefore, the radials were chosen near the nominal cardinal directions  $0^{\circ}$ ,  $45^{\circ}$ ,  $90^{\circ}$ ,  $135^{\circ}$ , etc. Minor variations of these bearings were made to fit available water navigation paths, parkways or other roads which would provide somewhat improved measuring locations. Four field crews were used each consisting of a driver and engineer. Each crew measured field strength of both stations at each location with careful calibration of the field set for each measurement at each location. Final analysis of these data indicated reasonably uniform radiations in all eight directions on both frequencies and yielding a radiation efficiency of 244 mv/m per kw at 660 kc/s and 256 mv/m per kw at 880 kc/s. These radiation efficiencies are both significantly above the required 225 mv/m per kw. The current minimum on both frequencies had been drawn up to a height sufficient to significantly control fading. As the current minimum is raised on the tower, the magnitude of the current at the loop increases and consequently, losses increase. The resultant radiation efficiencies demonstrate that the construction techniques used have kept the antenna losses to a minimum.

Since the coupling and isolating networks were designed with due consideration to the bandwidth problem, calculations and data were readily available for the values of various elements at side frequencies as well as at carrier frequency. The High Island plant is only a few miles from both old WNBC and WCBS transmitting plants; both stations operate 24 hours a day.

Difficulty was encountered in tuning these networks on the actual operating frequency. Considerable success was obtained in the tuning of these networks for side band frequencies with final trim up on carrier frequency. Figure 15 indicates the approximate normalized impedance characteristic as observed at the final amplifier plates in the WCBS transmitter. A similar impedance frequency characteristic was obtained for WNBC. Since the impedance bandwidth problem is significantly worse at 660 kc/s, a dissipative compensating network along the lines previously described has been built for WNBC's use and is currently under test. Figure 16 indicates

the improvement in impedance characteristic available by this procedure; these measurements were taken at the transmitter output terminals, the impedance there should be similar to a series resonant circuit at that point.

The isolation networks were designed with the intention of reducing spurious signals to an absolute minimum. The approximate difference frequency, 219 kc/s, is used by a low power radio beacon at Teterboro Airport some 15 miles from the transmitter plant. The sum frequency, 1540 kc/s, is used in Philadelphia, Pennsylvania. The two spurious signals, 220 kc/s and 1540 kc/s, which could interfere with these services, are the highest order cross modulation products generated. The success of the installed filters in preventing cross modulation can best be gauged by the fact that both the 219 kc/s and the 1540 kc/s signals can be received with no noticeable interference from the WNBC and WCBS signals, within a quarter mile of the High Island transmitter. As a further demonstration of the isolation between the two transmitters, I asked our operating staff to connect a 500 ohm one tenth watt resistor between plate and ground of the final amplifier of the WCBS transmitter and have WNBC operate with 50 kw. I have that resistor with me; and as you can see, it shows no ill effects from that test. If that resistor had dissipated its rated power under the foregoing test, the isolation would have been 57 db. It may be of interest to note here that during tune up of the antenna system as much as 80 watts of the WCBS Columbia Island signal could be obtained in the High Island antenna system, this represents a natural decoupling of about 28 db between sites spaced 1.75 miles. The original 4 mile spacing between WNBC and WCBS resulted in an isolation of only approximately 35 db. It may thus be seen that significantly better isolation between transmitters has been achieved in the joint plant than existed when the plants were separated.

I am sure that you all realize that a project of this magnitude that has extended over several years has required the cooperation and the diligent efforts of many people in both organizations. Specific credit to all of them would take more time than is warranted, but there are two that I want to especially point out at this time. Mr. William Duttera, our Session Coordinator, who was responsible for the original idea, and continued to participate in the project; and Mr. John Seibert of NBC spent many months following the details of the joint construction as well as the details within the WNBC portion of the plant.

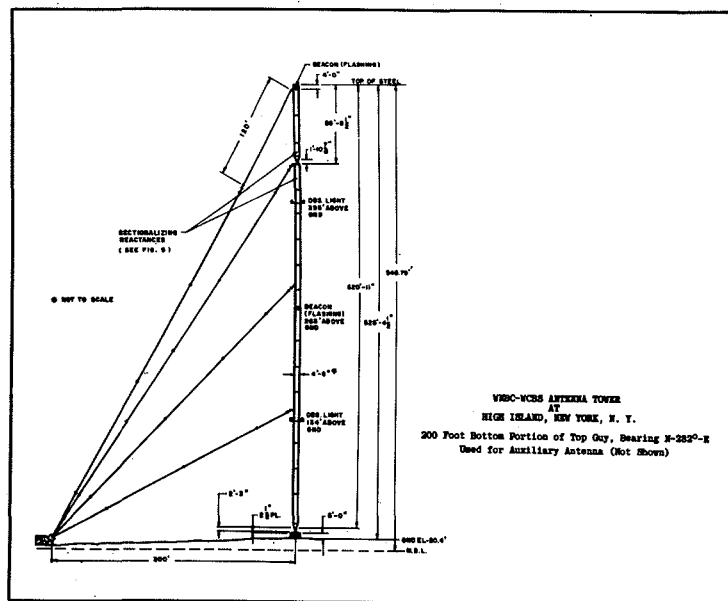


FIGURE 1

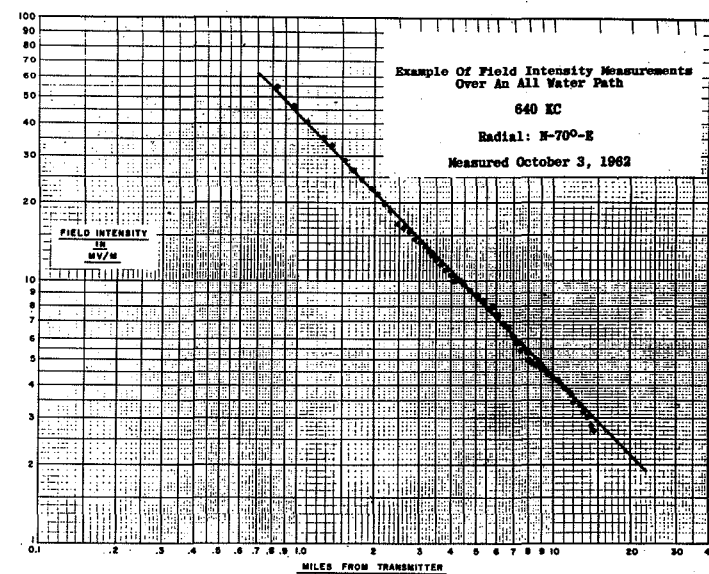


FIGURE 2

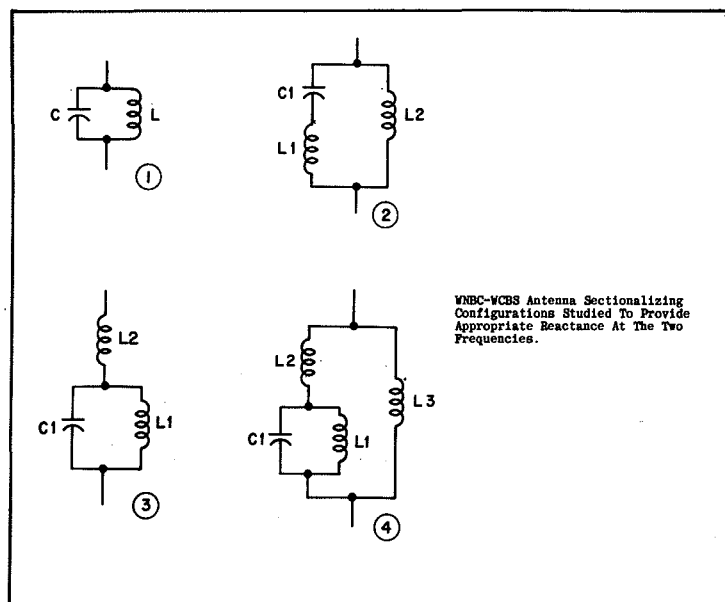


FIGURE 3

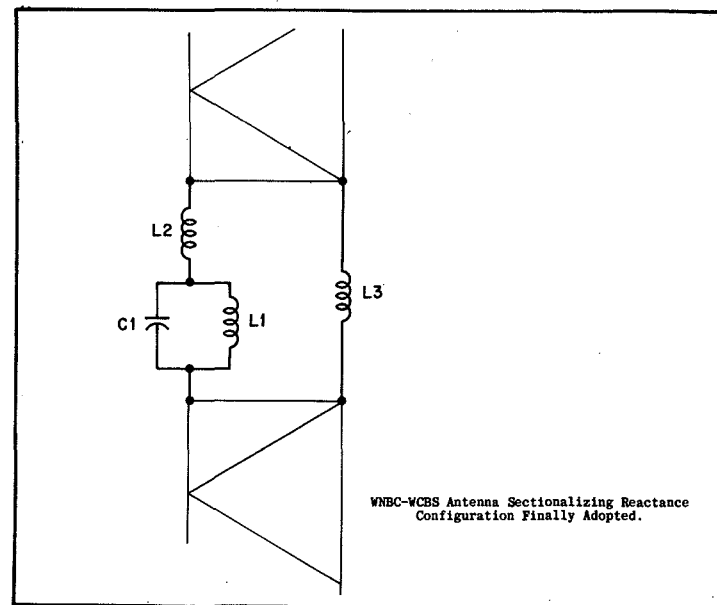


FIGURE 4

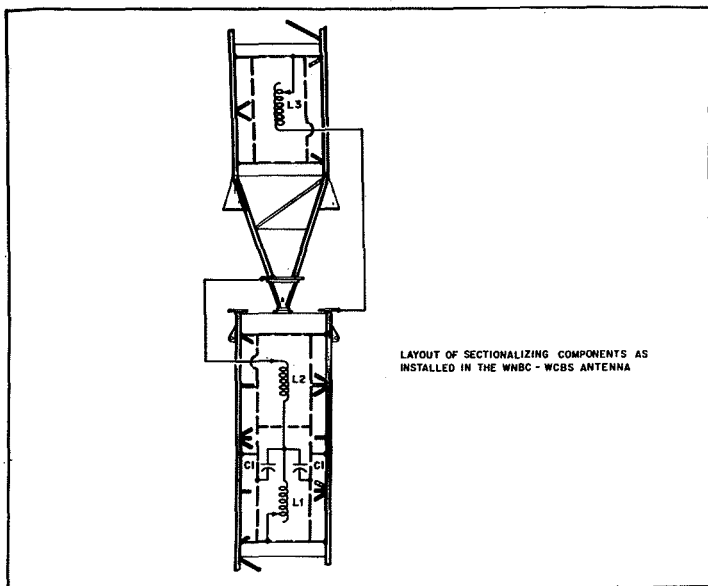


FIGURE 5

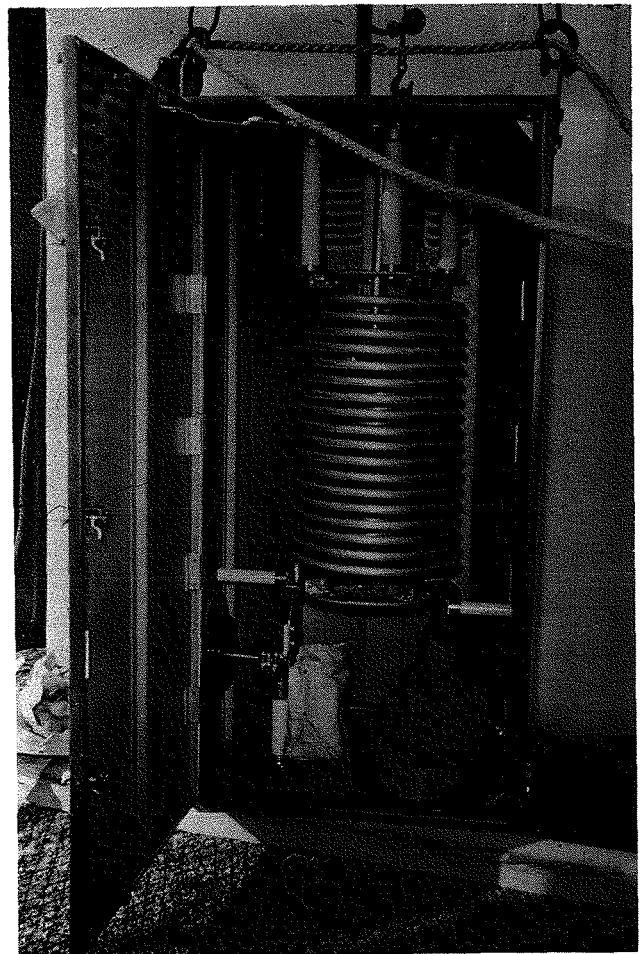


FIGURE 6

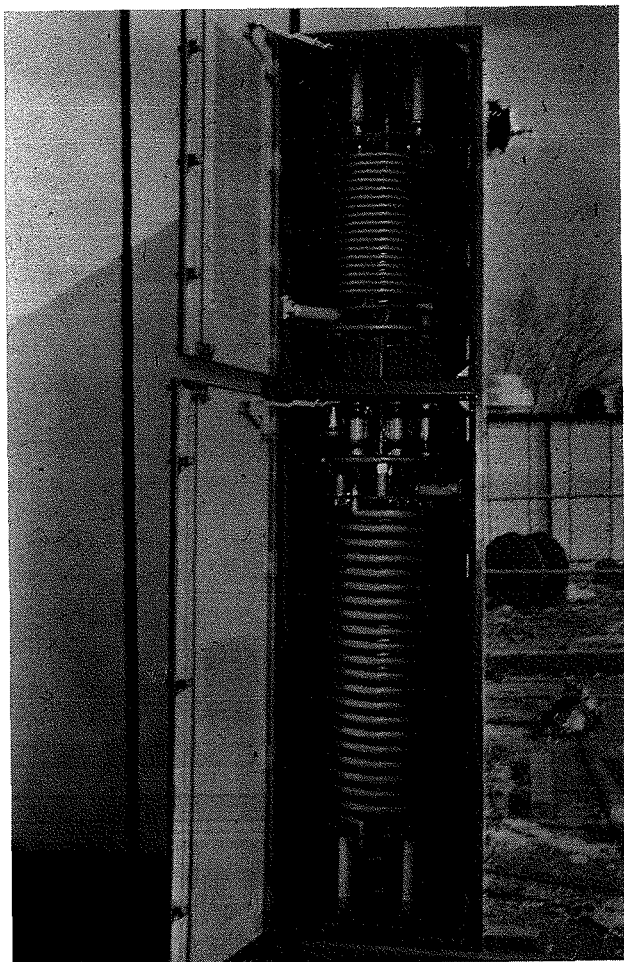


FIGURE 7

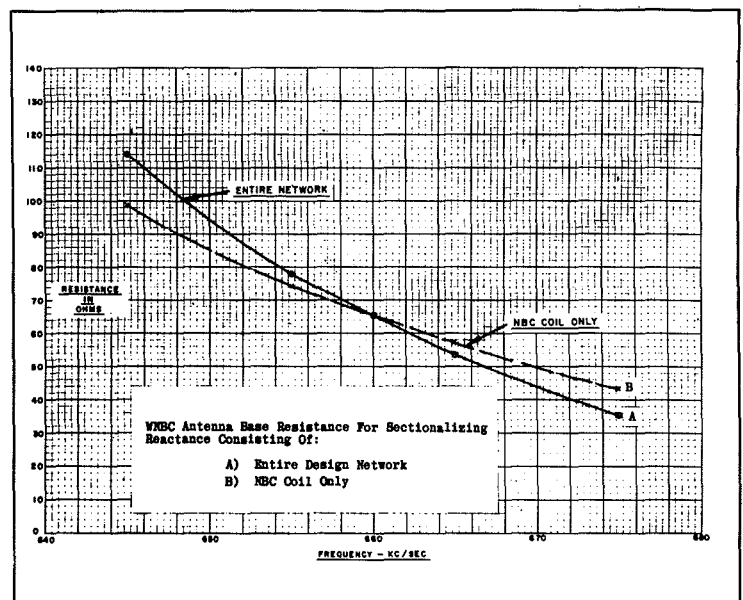


FIGURE 8

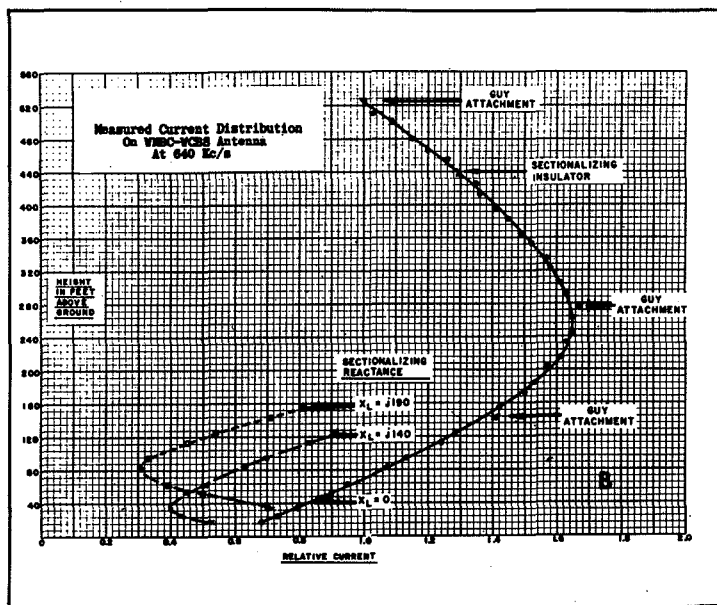


FIGURE 9

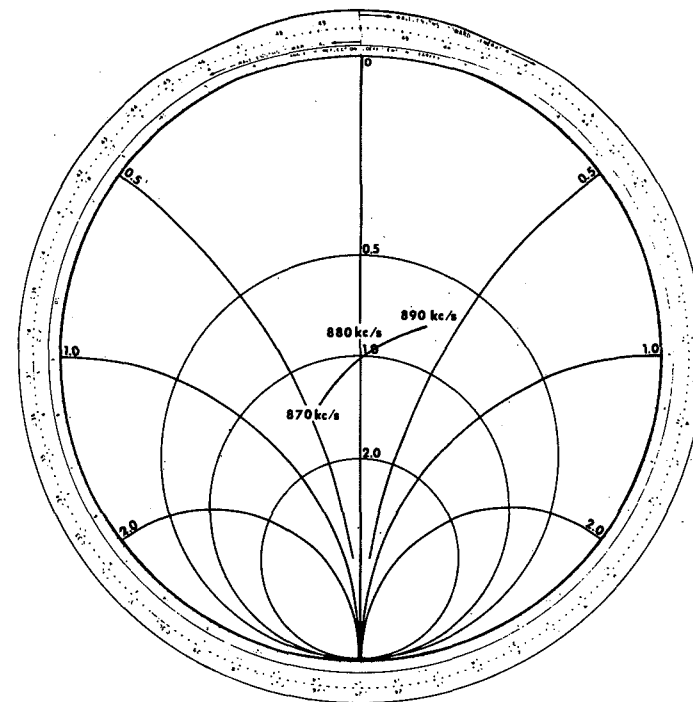


FIGURE 10

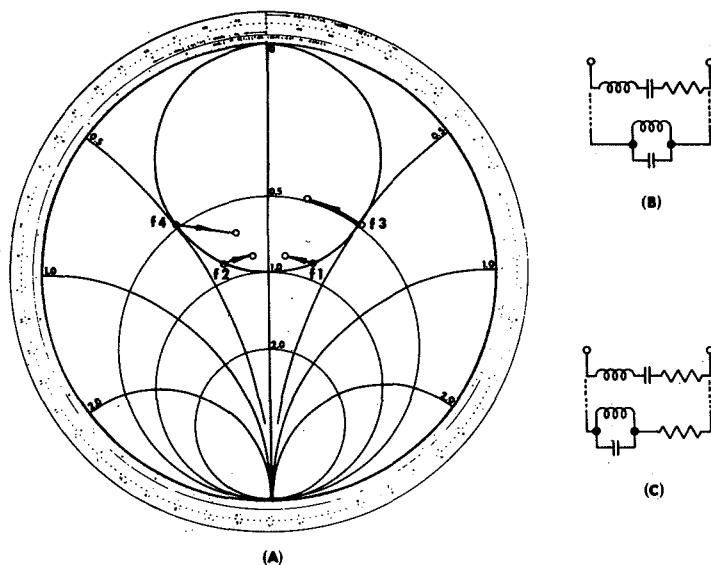
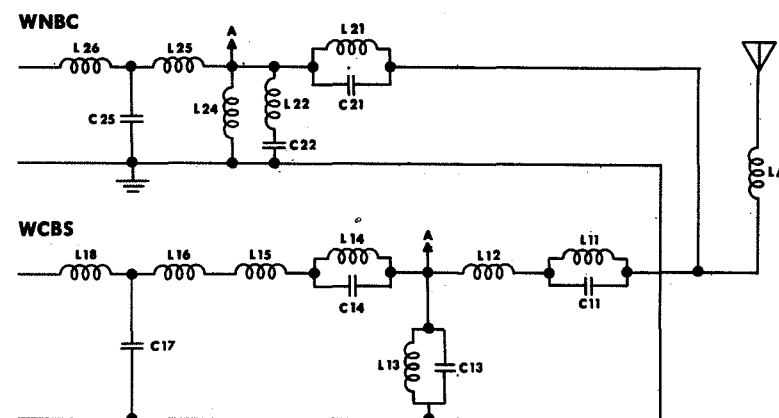


FIGURE 11



COUPLING AND ISOLATING NETWORKS  
FIGURE 12

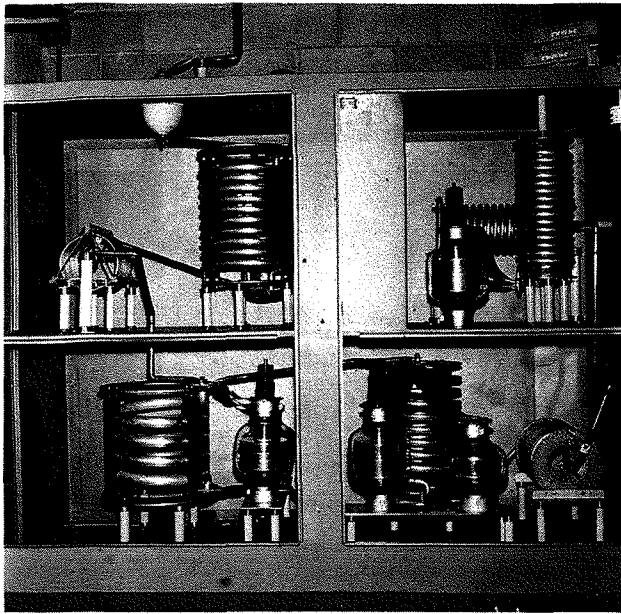


FIGURE 13



FIGURE 14

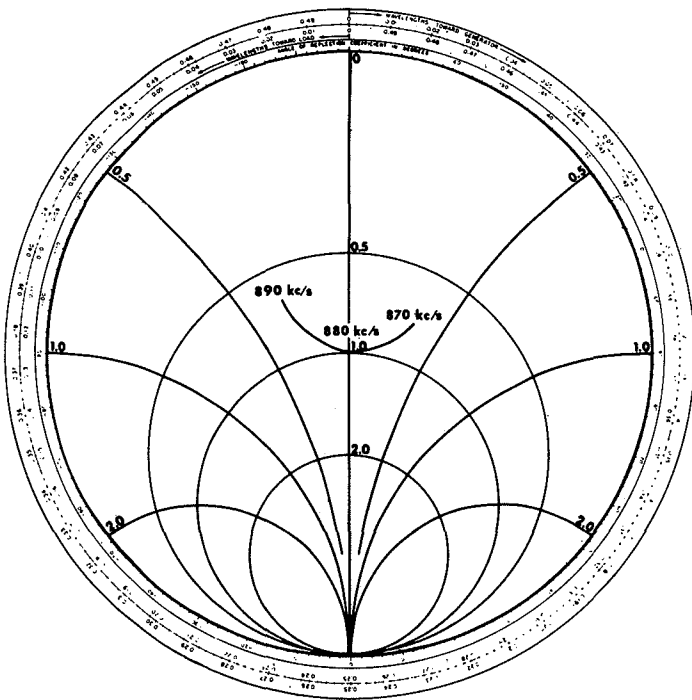


FIGURE 15

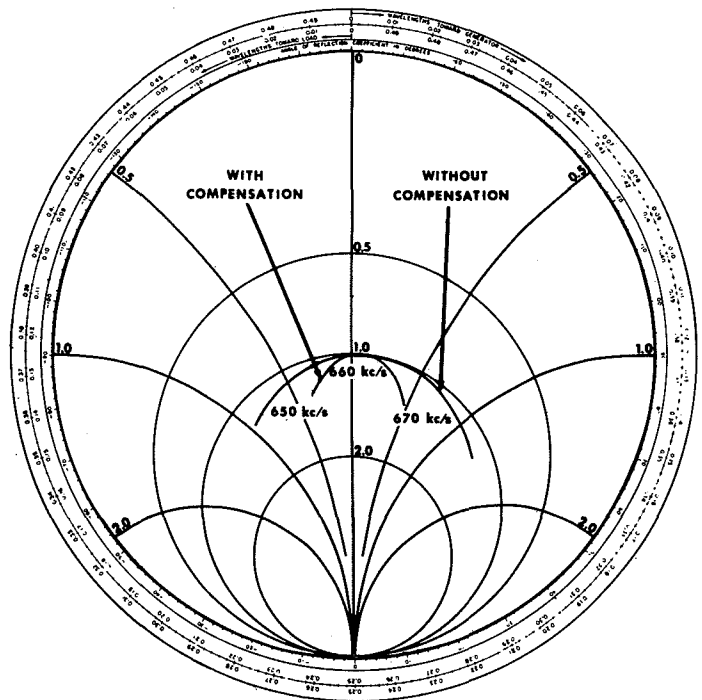


FIGURE 16



# The Effects of Tower Lighting and Isolation Circuits Upon Tower Impedance of Various AM Towers

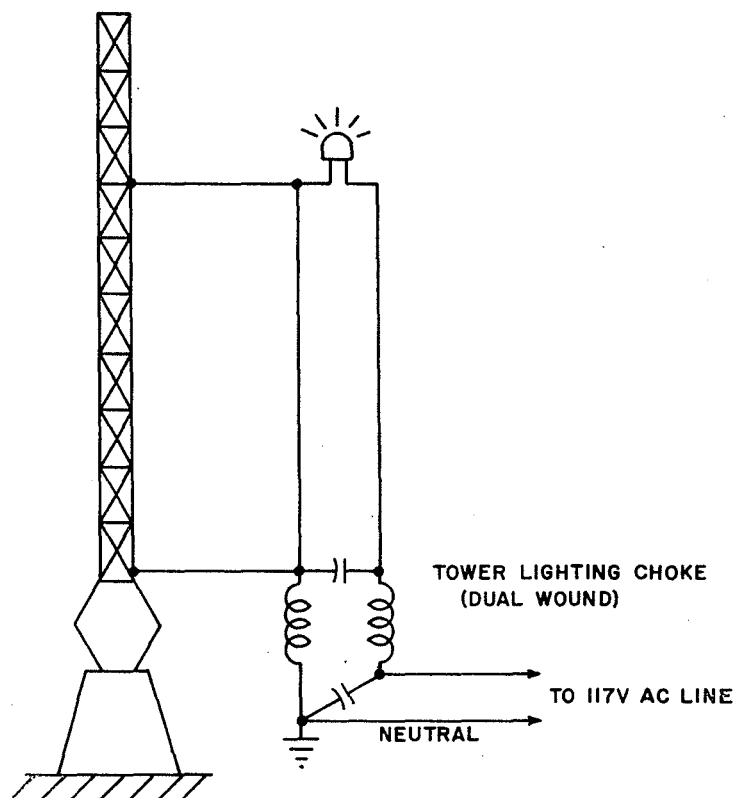


Figure 1—Single choke tower lighting isolation.

Tower lighting isolation circuits often affect the measured antenna impedance of an AM tower. The results of an investigation of this problem are reported.

By VIR N. JAMES\*

PERHAPS some of you have measured antenna impedances and found them to vary when you connected the tower lighting or isolation circuits. Or, perhaps, you have investigated apparent transmitter efficiencies in the range of 90 to 110 per cent. Tower lighting or isolation circuits frequently cause such conditions to exist.

During the course of our consulting work, we had encountered these conditions and antenna resistance changes up to 50 per cent due to the effects of tower lighting isolation circuits. It was, therefore, deemed advisable to investigate these effects in more detail.

To this end, special equipment was set up to measure the antenna impedance of KSTR, Grand Junction, Colo., which operates on an

assigned frequency of 620 kilocycles. Impedance measurements of the KSTR 300-ft. tower over the entire broadcast band provided an opportunity to study the effects of tower isolation circuits for effective antenna heights which varied with frequency from 0.15 to 0.5 wavelength. The investigation consisted of tower impedance measurements without isolation circuits and then with various tower isolation circuits connected.

Tower lighting isolation circuits commonly encountered consist of the following types:

1. A single dual-wound choke. This choke is often supplied in diameters of approximately 5 inches and lengths up to 18 inches with a two-layer winding. One winding connects each side of the ac circuit

to the tower lights. Some chokes are triple wound to accommodate a third tower circuit. A simple schematic showing the connection of a single dual-wound lighting choke is shown in Figure 1.

2. Sometimes two of these chokes are used in tandem. A schematic of tandem chokes is shown in Figure 2. It will be noted that the neutral side of the tower light is shown tied to the tower so that the tower isolation choke functions as a static drain choke.

3. An entirely different means of tower lighting isolation is provided by the transformer isolation type or so-called "Austin" transformer. Transformer isolation is shown in Figure 3.

The tower isolation chokes frequently encountered have a high

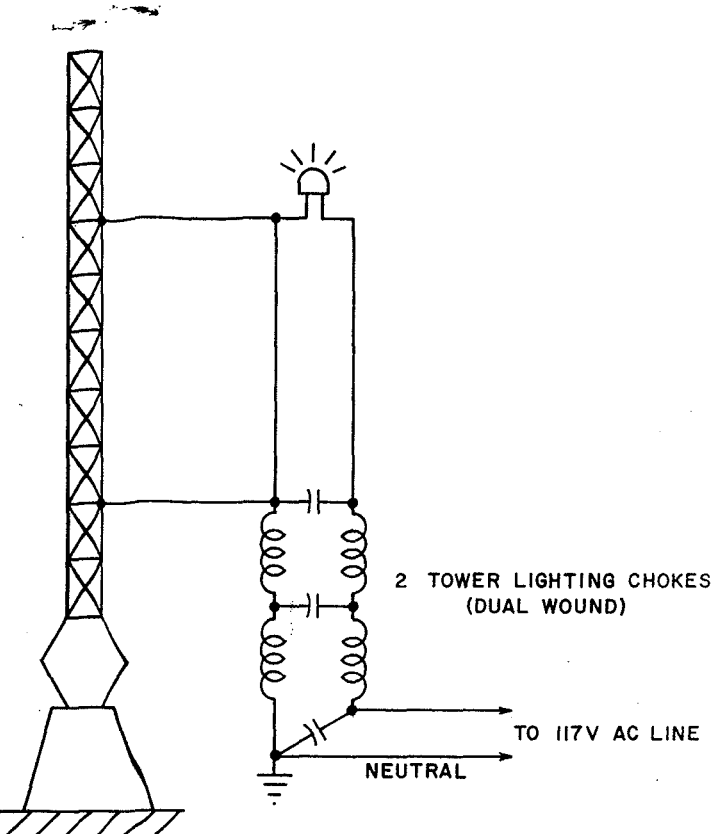


Figure 2—Tandem choke tower lighting isolation.

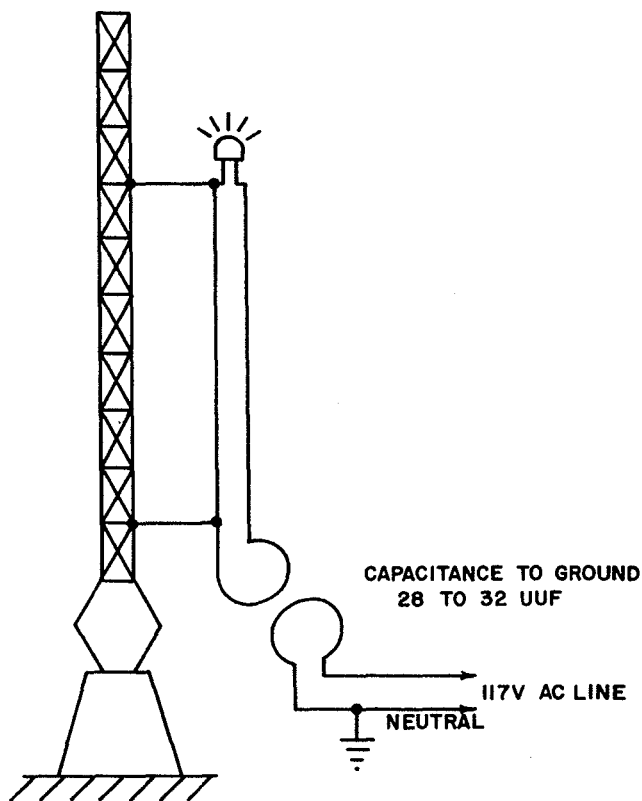


Figure 3—Transformer tower lighting isolation.

\*Consulting Radio Engineer, 232 S. Jasmine, Denver 22, Colo.  
This report was presented at the 14th NAB Engineering Conference.

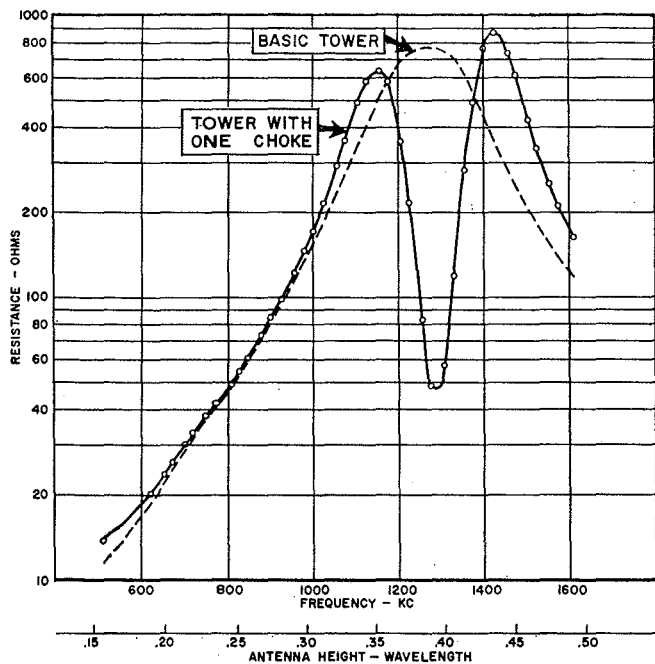


Figure 4—Tower resistance variation 1-choke isolation circuit.

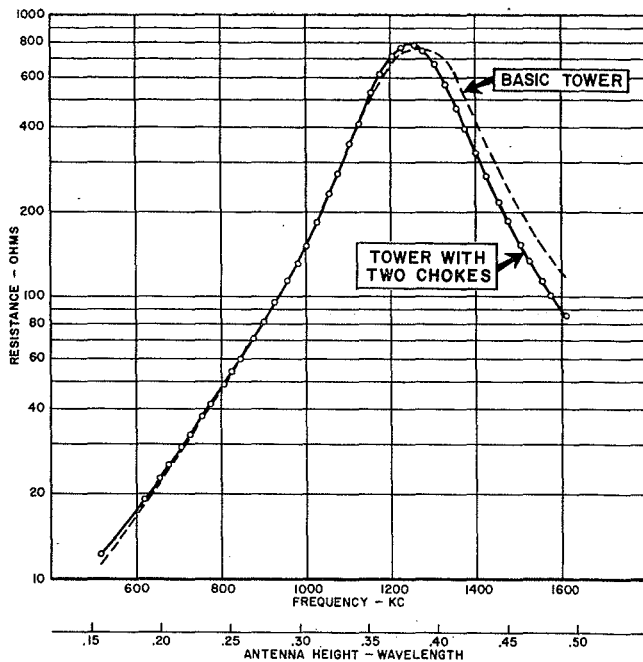


Figure 5—Tower resistance variation 2-choke isolation circuit.

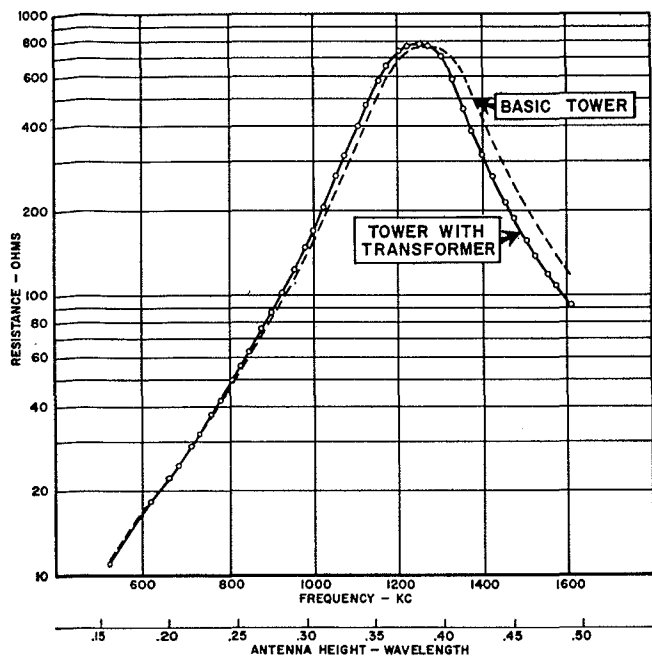


Figure 6—Tower resistance variation transformer isolation circuit.

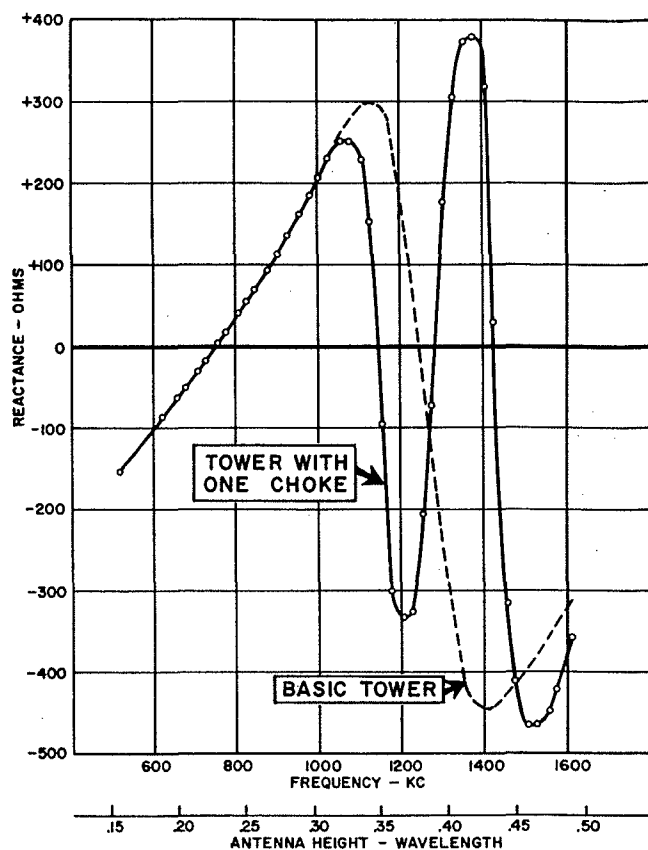


Figure 7—Tower reactance variation 1-choke isolation circuit.

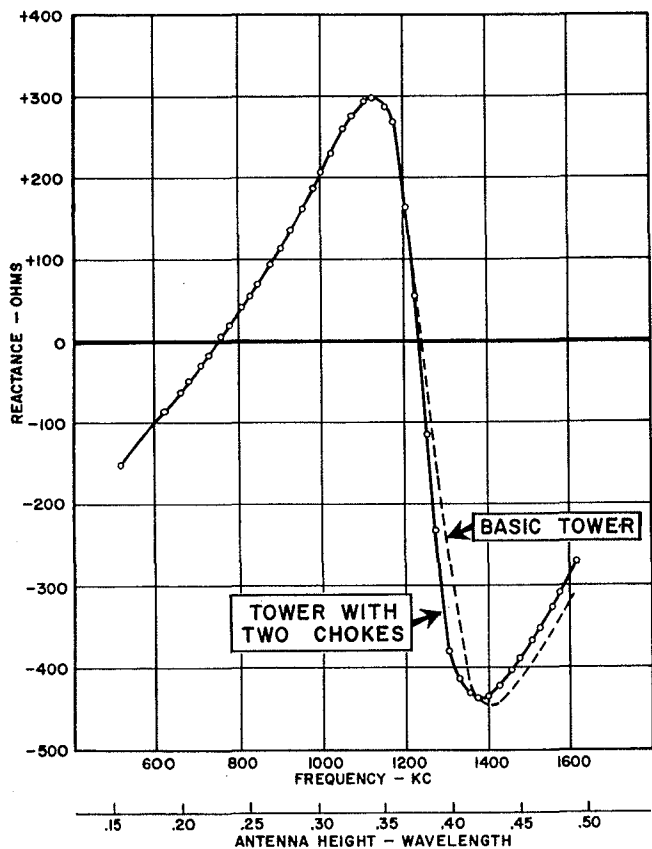


Figure 8—Tower reactance variation 2-choke isolation circuit.

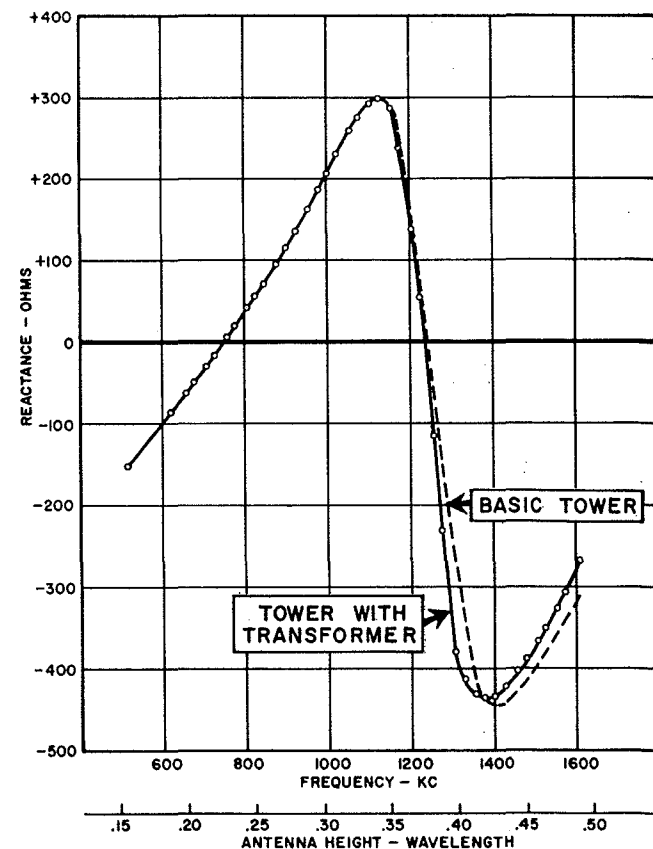


Figure 9—Tower reactance variation transformer isolation circuit.

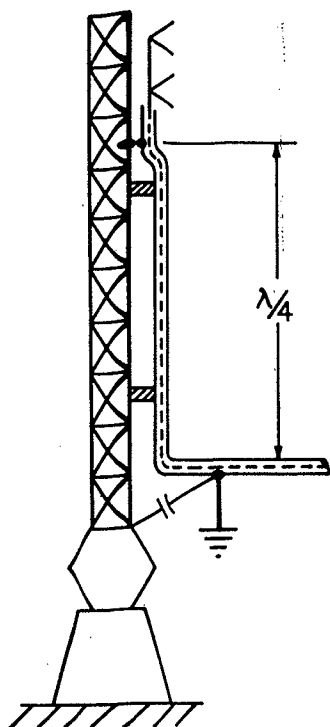


Figure 10—One-fourth-wave line isolation.

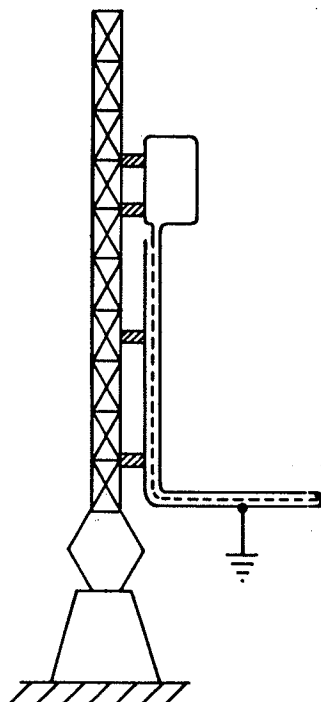


Figure 11 — Insulated sampling loop isolation.

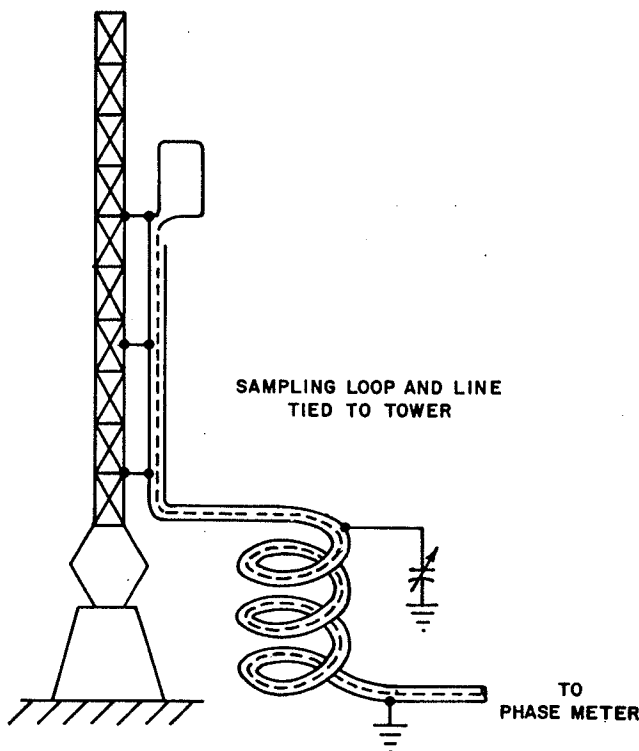


Figure 12—Parallel resonance isolation.

### MEASURED ANTENNA IMPEDANCE KSTR Tower — Height 300 ft.

value of inductance on the order of 350 microhenries. The transformer isolation units consist of a large doughnut-shaped primary winding connected to the 60-cycle power line. The tower lights are supplied with current from a secondary doughnut winding located in the field of the primary but spaced several inches from it.

The effects upon tower impedances of tower lighting chokes may be thought of as a highly inductive circuit with a significant amount of circuit resistance at the R.F. frequency. The effect is further complicated by a distributed capacitance effect. The mathematics for calculating the effects of such tower lighting chokes in the range where the operation is critical is quite difficult. However, their performance may be obtained easily and rapidly with a radio frequency bridge. The transformer isolation circuit, on the other hand, shunts the antenna impedance with a capacitance of approximately 30 micromicrofarads. The effects, therefore, of the transformer isolation is more readily calculated.

(Continued on page 27)

F(KC)	Tower Height Wave Length	Tower Only		2 Chokes		1 Choke		Trans.	
		R	X	R	X	R	X	R	X
517	.158	11.3	-153	12.2	11.8	13.9	13.4	11.0	10.8
620	.189	18.7	-86.7	19.1	18.6	20.1	19.7	18.2	17.9
655	.200	22.2	-63	22.8	21.9	23.7	23.0	20.2	19.9
675	.206	24.6	-50	25.2	24.5	26.0	24.6	24.6	24.0
705	.215	28.1	-30-	29.2	30.0	30	28.7	28.9	28.2
725	.221	31.3	-17.2	32.3	33.0	33	32.9	32	31.0
755	.230	36.5	+5	37.4	36.9	37.9	38.3	37.5	36.9
775	.236	41	19	41.5	41.1	42	43	42	40.8
805	.246	48	41	48.9	48.2	49	50	50	50
825	.252	53.2	55	54	52.8	54.5	54.1	56	55.1
845	.258	60	70	60	58.9	60.2	59.7	62.9	63
875	.267	71	94	71	70.1	73	72.1	76	77
900	.275	82	113	81.5	82.3	84	83	87	87
925	.282	95.7	135	95.2	95.7	98	97.3	102.2	101.6
955	.291	114.5	162	114	113.8	121	120	123.3	123.0
980	.299	134	186	131	132.1	146	145	148	147
1000	.305	153.5	207	151	206	171	208	170	206
1025	.313	185	231	184	230	215	232	206	232
1055	.322	231	261	231	259	290	253	267	259
1075	.328	271.5	275	272	275	359	252	312	274
1105	.337	340	294	350	294	490	229	400	283
1125	.343	400	299	410	299	580	254	475	278
1155	.352	496	292	530	287	633	-95	580	240
1175	.359	575	268	620	238	580	-300	655	149
1205	.368	690	164	720	138	353	-332	740	-7
1225	.374	730	90.8	767	55	214	-326	770	-109
1255	.383	760	-50	787	-116	83.3	-205	782	-222
1275	.389	765	-146	750	-232	48.1	-71.4	770	-290
1305	.398	750	-263	668	-380	57.3	+177	712	-374
1330	.406	700	-330	565	-414	119	306	590	-420
1355	.414	603	-416	465	-431	281	374	460	-439
1375	.420	515	-438	394	-436	493	380	383	-440
1400	.427	435	-444	325	-435	760	318	315	-434
1425	.435	350	-442	269	-422	862	29	265	-421
1455	.444	285	-428	218	-403	730	-316	214	-403
1475	.450	249	-415	187	-389	607	-410	189	-389
1505	.459	207	-395	153	-367	423	-465	158	-368
1525	.466	182.2	-380	134	-351	336	-464	139	-352
1555	.475	154	-356	114	-326	251	-448	119	-329
1575	.481	138	-339	101	-308	210	-421	108	-311
1610	.491	117.2	-311	86	-269	163	-357	92	-280

**Mississippi**  
Jackson  
Ellington Radio, Inc.  
FL 3-2769

**Missouri**  
Kansas City  
Burstin-Applebee Company  
Baltimore 1-1155

**St. Louis**  
Graybar Electric Company  
Jefferson 1-4700

**New Hampshire**  
Concord  
Evans Radio  
Capital 5-3358

**New Jersey**  
Camden  
General Radio Supply Co.  
WO 4-8560 (in Phila.: WA 2-7037)

**New Mexico**  
Alamogordo  
Radio Specialties Company, Inc.  
Hemlock 7-0307

**Albuquerque**  
Radio Specialties Company, Inc.  
AM 8-3901

**New York**  
Buffalo  
Genesee Radio & Parts Co., Inc.  
DElaware 9661  
Wehle Electronics Inc.  
TL 4-3270

**Mineola, Long Island**  
Arrow Electronics, Inc.  
Pioneer 6-8686

**New York City**  
H. L. Dalis, Inc.  
EMpire 1-1100  
Milo Electronics Corporation  
BEekman 3-2980  
Sun Radio & Electronics Co., Inc.  
OREgon 5-8600  
Terminal Electronics, Inc.  
CHelsea 3-5200

**Ohio**  
Cincinnati  
United Radio Inc.  
CHerry 1-6530

**Cleveland**  
Main Line Cleveland, Inc.  
EXpress 1-4944  
Pioneer Electronic Supply Co.  
SUperior 1-9411

**Columbus**  
Buckeye Electronic Distributors, Inc.  
CA 8-3265

**Dayton**  
Srepcos, Inc.  
BALdwin 4-3871

**Oklahoma**  
Tulsa  
S & S Radio Supply  
LU 2-7173

**Oregon**  
Portland  
Lou Johnson Company, Inc.  
CAPital 2-9551

**Pennsylvania**  
Philadelphia  
Almo Radio Company  
WALnut 2-5918  
Radio Electric Service Co.  
WALnut 5-5840

**Pittsburgh**  
Marks Parts Company  
FAirfax 1-3700

**Reading**  
The George D. Barbey Co., Inc.  
FR 6-7451

**Tennessee**  
Knoxville  
Bondurant Brothers Company  
3-9144

**Texas**  
Dallas  
Graybar Electric Company  
Riverside 2-6451

**Houston**  
Busacker Electronic Equipment Co.  
JACKson 6-4661  
Harrison Equipment Company  
CAPitol 4-9131

**Utah**  
Salt Lake City  
Standard Supply Company  
EL 5-2971

**Virginia**  
Norfolk  
Priest Electronics  
MA 7-4534

**Washington**  
Seattle  
Western Electronic Company  
AT 4-0200

**West Virginia**  
Bluefield  
Meyers Electronics, Inc.  
DAvenport 5-9151

**Wisconsin**  
Milwaukee  
Electronic Expeditors, Inc.  
WOodruff 4-8820

## TOWER IMPEDANCE

### Starts on page 4

culated. It should be noted that transformer isolation does not provide a static drain. This must be added.

The measurements of the KSTR tower were made under the following conditions:

A. No lighting isolation.

B. One tower lighting choke.

C. Two tower lighting chokes in tandem.

D. Tower shunted by a 30 micro-microfarads capacitor to simulate the transformer isolation.

The measurements of the KSTR tower with the various forms of tower lighting isolation described above were performed using a General Radio type 916-AL radio frequency bridge. The signal generator consisted of a very stable master oscillator followed by a power amplifier to isolate the effects of the bridge on the oscillator. A built-in electronic voltage regulator maintained the oscillator frequency and output very stable. The detector consisted of a very selective, well shielded, superheterodyne receiver. The switching arrangement was set up to disconnect the tower lighting circuits or to permit connecting one choke, two chokes in tandem, or the shunt capacitance.

Figure 4 is a plot of the base tower resistance for the entire broadcast band as shown by a broken curve. The solid curve is a plot of the resistance obtained with a single dual-wound tower lighting choke connected. It will be noted that the tower resistance showed a maximum change from 765 ohms down to 48 ohms at a frequency of 1275 kilocycles, corresponding to a tower height of approximately 0.4 wavelengths. This represents a *drastic* change of 93.8 per cent. It is to be noted that the variation of tower resistance within the one quarter wave region was fairly small.

In Figure 5 it will be seen that when two tower lighting chokes were used in tandem, a great deal less change in antenna resistance occurred. In fact over a broad band from 0.25 to 0.35 wavelength of tower height close agreement was obtained with basic tower resistance.

Figure 6 shows how transformer

isolation affects tower resistance. This system proved inferior to the two chokes in tandem, although vastly superior to the single choke commonly utilized. Very little change in antenna resistance occurred over only a small range of approximately .2 to .25 wavelength antenna height. At all other antenna heights, the transformer caused a significant change in measured antenna resistance. While the effect upon tower reactance may not be as significant as tower resistance for non-direction operation, it is quite important in directional antenna work.

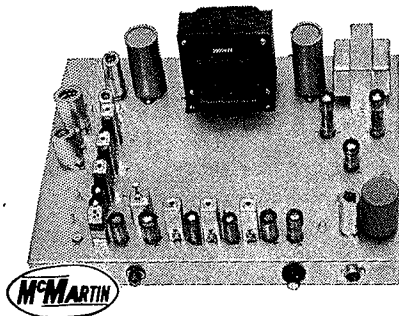
Figure 7 shows the effect upon the measured tower reactance of a single tower lighting choke isolation circuit. Again the tower reactance without any isolation circuit is shown as a dashed curve. The tower reactance obtained with a single choke connected in the tower lighting circuit is shown by the solid curve. Here the effect is exceedingly great. For instance, at 1375 kilocycles corresponding to an antenna height of approximately .420 wavelength, the reactance changed from a negative 438 ohms up to a positive 380 ohms. This change of 818 ohms represents a percentage change of 187 per cent. Again, the use of two chokes in tandem greatly reduces the adverse effect of the tower lighting circuit upon the measured true reactance, as shown in Figure 8. Similarly, Figure 9 illustrates the effect of transformer isolation upon the tower reactance. Again, the isolation transformer, while radically better than a single choke, measured inferior to the two chokes in tandem.

It may be noted, however, that in critical areas of tower height considerable resistance and reactance variations occurred with the use of these types of tower lighting isolation circuits.

Other forms of isolation are normally used to prevent loss of radio frequency power in AM towers, when other radio services share the same tower. Figure 10 illustrates a circuit which isolates an FM antenna from an AM tower. Here the outer conductor of the coax line is tied to the tower near the top while a length of line of approximately one-quarter wave length long (at the AM frequency) is insulated from the tower. A capacitor is frequently

# Beautiful Signals

**HANDLED with CARE**



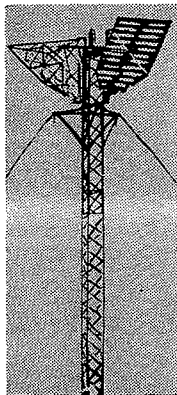
## MULTIPLEX RECEIVERS

Better sound sells FM on main carrier and subs. Better sales result with carefully engineered and reliable receiving equipment. At Continental rigid quality control and extreme manufacturing care guarantees you and your listeners the finest reception . . . whatever your requirements.

Lease (without down payment) and Lease Purchase Plans available.

Write or call

**CONTINENTAL MANUFACTURING, INC.**  
1612 California Street - Omaha, Nebr.



## TOWERS REFLECTORS BUILDINGS

- FIXED
- PORTABLE

Complete installations for all communications purposes



**CONSTRUCTION CO.**  
2737 HAWKEYE DR. SIOUX CITY, IOWA

*Tower Fabricators  
and Erectors  
the World Over!*

MAIL TODAY! FOR 1960 CATALOG!  
TOWER CONSTRUCTION CO.  
2747 HAWKEYE DRIVE  
SIOUX CITY, IOWA

NAME: \_\_\_\_\_

ADDRESS: \_\_\_\_\_

CITY: \_\_\_\_\_

ST: \_\_\_\_\_

connected from the base of the tower to the coax outer conductor at the point where it is also connected to ground. This length of insulated line, together with the tower, forms a one-quarter wave resonant circuit having the top end shorted with resulting high impedance at the open lower end. This high impedance formed by the one-quarter wave stub serves to isolate FM or TV service from the AM tower. In practice the grounding point and/or the top point, which is tied to the tower, is moved until the measured AM antenna impedance shows that it is unaffected by the presence of the FM or other service.

In Figure 11 a sampling loop is isolated from the tower merely by insulation. This type of sampling loop isolation is frequently utilized in simple two-tower directional antenna systems. However, frequently it has been found that insulated sampling loops appreciably change the measured antenna impedance, often due to a significant capacitance coupling effect. Several cases of radical pattern distortion have been encountered even in simple two-tower directionals.

Figure 12 illustrates a parallel resonant type of isolation for sampling loops. In this system one side of the pickup loop and the outer conductor of the coax line is tied to the tower. Indeed, the line is bonded to the tower at frequent intervals. At the base of the tower, the coax line is connected to a large coil formed by the coaxial cable. This coaxial coil must be tuned close to resonance if the tower impedance is to be unaltered by the pickup loop. It has been found that improper tuning of such tank circuits permits attainment of wide variations of tower impedances. However, where these circuits are properly tuned, no undesirable effects have been encountered.

Although time did not permit, nor did the manufacturer care to supply a tunable resonant choke for tower lighting isolation, nevertheless, this form may be entirely satisfactory.

**Conclusion:** Regardless of the type of tower isolation circuit employed, the performance must be thoroughly checked. It is hoped that the broadcast equipment suppliers will make more suitable isolation circuit systems available.

## SINE SQUARED

Starts on page 12

ponent) is different from the modulation (chrominance component), they will not register and the difference in delay may be easily determined. Further, this same presentation shows whether the frequency response of the system is flat since again complete registry should occur.

### Linearity Testing

As indicated earlier the  $\sin^2$  technique may be used for linearity testing. This is perhaps misleading and still the technique makes use of conventional  $\sin^2$  shaping filters so it is included for the sake of completeness.

The conventional signal used for testing linearity is the stair step. Usually ten steps are used. For the proposed test the number of steps is first reduced to five and the signal is introduced into the system. At the output the signal is differentiated so that spikes all having a common base result. This signal is fed into a  $\sin^2$  pulse shaping filter so as to bandwidth limit the noise and is then presented on an oscilloscope. It is a simple matter to see whether all five pulses have identical amplitude (the case for perfect linearity).

The shaping filter should be such as to produce a 2.75 usec h.a.d. pulse in the conventional manner. The response is 6 db down at 182 kc/s and zero 364 kc/s. If more steps are used it becomes necessary to use narrower pulses which in turn have wider bandwidth and consequently introduces more noise with consequent error.

### Conclusions

As was indicated at the beginning this paper is intended as a survey of the uses of the  $\sin^2$  pulse; to try to show where it may provide more direct means of evaluating circuits; and finally to establish techniques for general picture enhancement. The equipment for some uses is complex, for others it is relatively simple. There is, however, a great amount of material available in the literature and more will doubtless appear. In broad perspective the  $\sin^2$  pulse is a powerful tool. It can reveal many deficiencies. It requires a certain amount of education and experience to appreciate its full potential.

# THE FOLDED UNIPOLE ANTENNA FOR AM

By JOHN H. MULLANEY\*

**T**HIS article will discuss a method for reducing the physical height of an antenna system without seriously impairing its electrical characteristics. This will be accomplished by use of folded-unipole antenna theory. Present day techniques dictate that in order to reduce the physical size of an antenna system and still obtain a reasonable efficiency, inductive or capacitive loading be utilized in order to change the current distribution of the array. It will be shown that by grounding a vertical structure and folding back one or more conductors parallel to the side of the structure, it is possible to obtain a wide range of resonant radiation resistances by varying the ratio of the diameter of the folded back conductor in relation to the tower. It will also be shown that a top-loaded folded-unipole antenna can obtain a wide range of resonant radiation resistances and at the same time obtain a band-width many times greater than the same antenna without loading and use of the folded-unipole method of feed.

Series-fed vertical antennas are commonly used in standard broadcast service today. Some stations use a shunt-fed antenna, but the great majority are series-fed. The folded-unipole antenna could be called a modification of the standard shunt-fed system. Instead of having a slant wire leaving the tower at an angle of approximately  $45^\circ$  (as used for shunt-fed

systems), the folded-unipole antenna has wires (one or more can be used) attached to the tower at a pre-determined height, supported by stand-off insulators, and run parallel to the sides of the tower to its base. The tower is grounded at its base—that is, no base insulator is used. These folds, or wires, are joined together at the base and driven at this point through an impedance matching network. Depending upon the type of folded-unipole antenna used, the wires may be connected to the tower at the top and/or at pre-determined levels along the tower (shorting stubs).

The folded-unipole antenna has the advantage of not requiring a base insulator, lighting chokes, or isolation transformers. It provides better protection against lightning, due to the fact that the antenna is grounded. In addition, the folded-unipole antenna, on a comparison basis, will develop a somewhat higher radiation efficiency, particularly for towers of the order of  $45^\circ$  to  $60^\circ$  high. The band-width for the folded-unipole antenna is also superior to that of a series or shunt-fed antenna system. The folded-unipole has an additional advantage over a series or a shunt-fed system in that it will operate with a much shorter ground system and still produce approximately the same effective field.

Basically speaking, a folded-unipole antenna can

\*Consulting Engineer, 2000 P St., N. W., Washington 6, D. C.

# BROADCASTING

The advantages of using a folded antenna for broadcast include the elimination of the base insulator, lightning choke, and isolation transformer, higher radiation efficiency, wide bandwidth, adjustable radiation resistance, and the use of a shorter ground system. These and other factors dealing with the design and construction of the folded unipole AM radiator are described in this article.

be visualized as a half-wave folded-dipole perpendicular to the ground and cut in half. The following discussion will briefly treat the theory of and results obtained from this type of antenna system.

## Theory of Folded-Unipole Antenna

To readily understand the folded-unipole antenna and its use in feeding a grounded tower, let's take a quick look at some basic transmission line theory. We know that a transmission line which is less than  $90^\circ$  in length and shorted at its far end will appear inductive at its input terminals. If this line is increased in length so that it equals a quarter wave, it will appear to be a parallel resonant circuit at its input. That is, it will appear to have very high impedance.

Figure 1 illustrates a one fold, folded-unipole antenna. In order to determine its input impedance, let us assume a generator voltage ( $e$ ) and then find the current ( $I$ ) flowing in the lower end of element  $d_1$  as illustrated in Figure 1. Roberts (Input Impedance of a Folded Dipole, R.C.A. Review, Volume 8, No. 2, June, 1947, W. Van B. Roberts) has outlined a method for analysis of a folded-unipole antenna.

Referring to Figure 2, it should be noted that Generator A is opposing Generator C, with respect

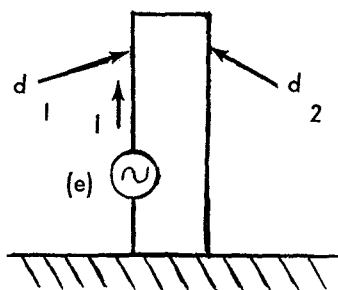


Figure 1. A one fold, folded unipole antenna.

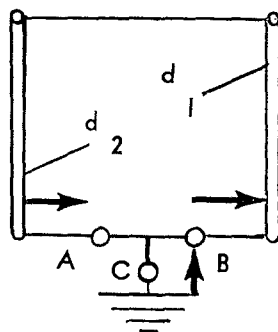


Figure 2.

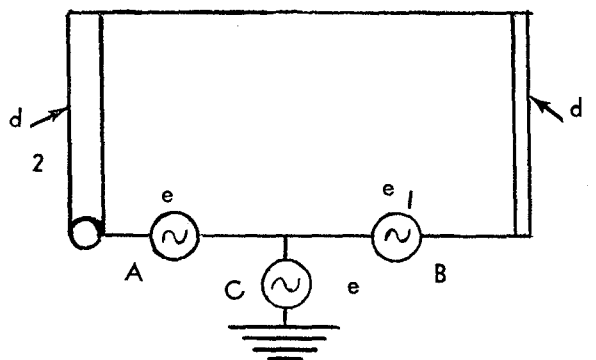


Figure 3. The folded unipole antenna with unequal size conductors.



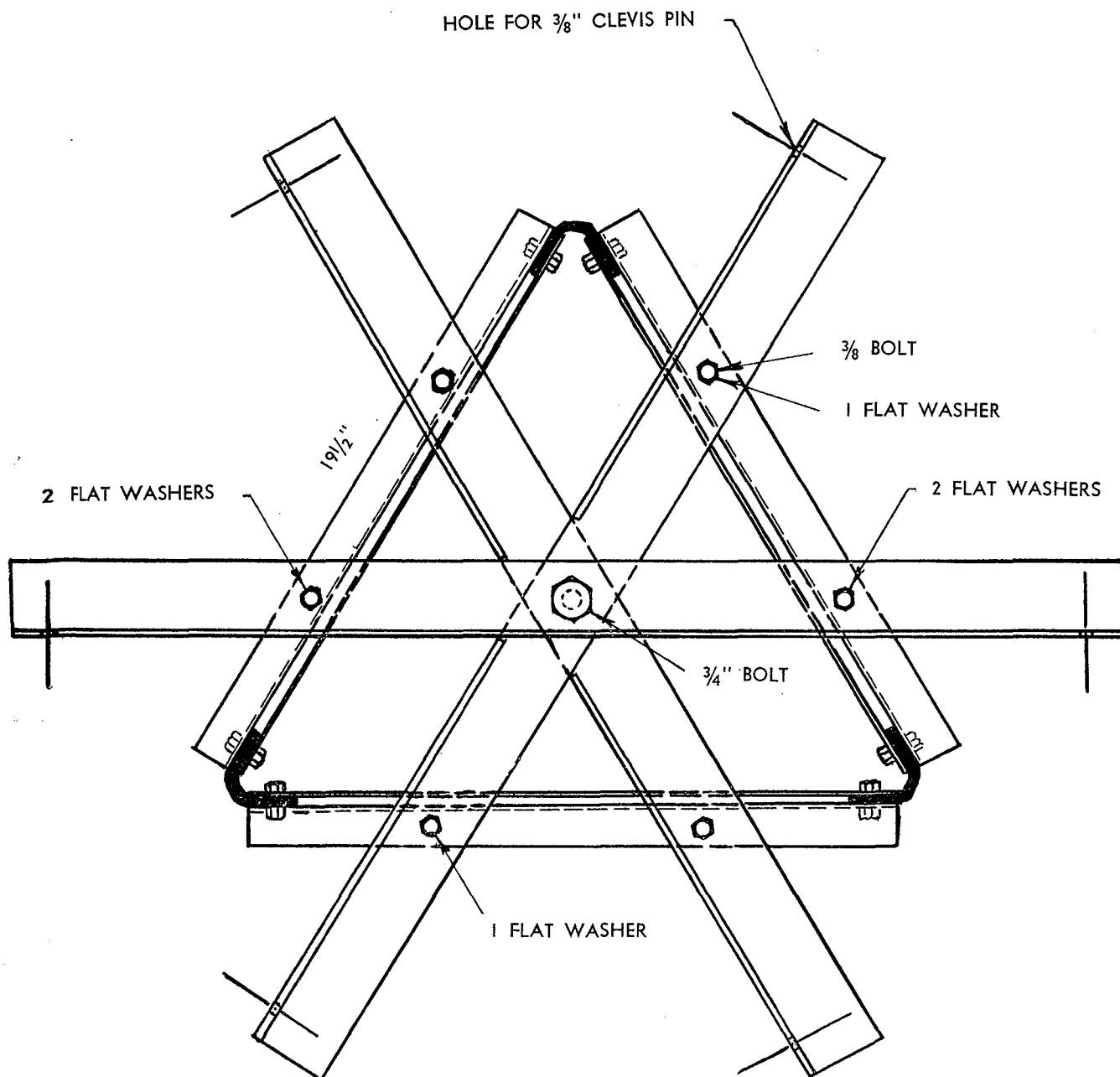


Figure 4. Top view of a uniform cross-section, guyed tower rigged for a six wirefolded-unipole antenna.

to the lower end of element  $d_2$ . Thus, element  $d_2$  is grounded so far as any voltage is concerned.

Generators B and C impress a voltage,  $2E$ , on the lower end of element  $d_1$ ; therefore, Figure 2 is equivalent to Figure 1. Our reason for using three generators is that it is fairly easy to determine the current developed by each generator and then by the principle of superposition, add these currents to obtain the actual current in the lower end of element  $d_1$ .

Let's go a little further and first assume that there is no voltage (for the moment) in the lower generator. There is then only the voltage  $2E$  acting between the lower ends of  $d_1$  and  $d_2$ . Inasmuch as elements  $d_1$  and  $d_2$  form a  $90^\circ$  transmission line, shorted at the far end, their impedance is very high; consequently, only a small current will flow into element  $d_1$ . Next, assume there is voltage only

in Generator C. Then, since the lower ends of  $d_1$  and  $d_2$  are shorted together (by the zero internal impedance of A and B), the two elements act as a simple  $90^\circ$  radiator made up of two elements connected in parallel. If  $R$  is the radiation resistance of this radiator, Generator C will supply a total current equal to  $E/R$  to this composite antenna, but by symmetry, this current divides equally between  $d_1$  and  $d_2$ , so that the current entering element  $d_1$  is:

$$I_1 = \frac{\frac{1}{2} E}{R} \quad (1)$$

Thus, if Generators A, B and C are all working at once, the voltage impressed on element  $d_1$  is  $2E$ , while the current entering it is  $\frac{1}{2} E/R$  plus a very small amount produced by Generators A and B working above. The input resistance of element  $d_1$ , being the ratio of voltage impressed to resulting current flow, is therefore approximately  $4R$ . If the two ele-

elements are close together, the value of resistance will be different from that of a single radiator, and the impedance multiplication due to folding is approximately four.

The impedance transformation can be expressed as follows:

$$\text{The impedance transformation} = \frac{Z_1}{Z_0} = (1 + n)^2 \quad (2)$$

Where:

$Z_1$  = input impedance of the folded-unipole antenna.

$Z_0$  = input impedance of a single antenna.

$$n = \text{current ratio} = \frac{I_2}{I_1} = 1$$

Up to this point, we have discussed equal size conductors, that is the diameter of the tower and the fold is the same. However, with the introduction of the transformation ratio, as noted in (2), we are now prepared to discuss the operation of a folded-unipole antenna with unequal diameter conductors. Figure 3 illustrates the folded-unipole antenna with unequal size conductors.

Generators A and C are alike in order to put zero voltage on element  $d_2$ , but Generator B must now be so chosen that no current will flow through Generator C when it is not producing voltage. The determination of this voltage ( $e_1$ ) is one of the two essentials to the solution of the problem. The other is to determine how the current produced by Generator C, acting above, divides between elements  $d_1$  and  $d_2$ . This problem becomes extremely complex because of the non-symmetry of the elements and there are several methods which can be used to solve the problem. "Guertler" (Impedance Transformation in Folded-dipole, Proceedings of the IRE, September 1950) demonstrates a method for determining this voltage. "Roberts" has also demonstrated methods for determining this voltage. We will use the electrostatic or capacitive method discussed by Roberts, since this method appears to offer the most promise for a simple solution. Briefly, this theory states that the current will divide directly as the ratio of the capacities of the elements, while the voltage ratio will be the inverse of the capacity ratio. To solve our problem then, we must assign undefined capacities,  $c_1$  and  $c_2$  to elements  $d_1$  and  $d_2$ . Then:

$$\frac{e}{e_1} = \frac{c_1}{c_2} \quad (3)$$

The current entering element  $d_1$  is the total current produced by Generator C acting alone multiplied by:

$$c_1 / (c_1 + c_2) \quad (4)$$

Neglecting the very small current produced by Generators A and B acting alone, as already discussed for equal elements, the total current due to Generator C alone is:

$$\frac{e}{R} \quad (5)$$

Where  $R$  = radiation resistance of the two elements connected in parallel.

The driving point impedance of the antenna is:

$$\frac{(e + e_1)}{\text{the current entering } d_1} \quad (6)$$

Thus, it is readily proven that the driving point impedance is:

$$\frac{R(1 + c_2^2)}{c_1} \quad (7)$$

The foregoing method of determination indicates that the impedance step up ratio depends upon the ratio of the elements' diameters, being inversely proportional to the diameter of the excited fold or element and directly proportional to the diameter of the grounded element. The spacing between the tower and fold is not extremely critical, but does determine, to some extent, the impedance transformation ratio. Although this type of antenna has good band-width, its band-width characteristics will be decreased if a transformation ratio of greater than approximately ten is attempted by means of the spacing ratio. It has been found that the best way to increase the band-width of the antenna is to increase the number of folds.

The electrostatic or capacitive method outlined by Roberts is primarily a physicist's approach to a solution of the folded-unipole antenna. It can be shown that the impedance transformation ratio for a folded unipole antenna where unequal diameters are used is:

$$\text{Transformation ratio} = \frac{(1 + Z_1)^2}{Z_2} \quad (8)$$

Where:

$Z_1$  = the characteristic impedance of a transmission line made up of the smaller of the two conductor diameters spaced the center to center distance of the two conductors in the antenna.

$Z_2$  = the characteristic impedance of a transmission line made up of two conductors the size of the larger of the two.

The above equation assumes that the power will be fed to the smaller conductor (fold). That is, the feed line from the transmitter is connected in series with the fold (fold's diameter always assumed smaller than tower's) so that an impedance step-up of greater than four will be achieved.

The magnitudes for  $Z_1$  and  $Z_2$  of equation (8) for uniform cross-section conductors can be determined from standard transmission line formulas.

During the past five years, numerous experimental measurements have been made on different types of folded-unipole antennas for broadcast use. Our ex-

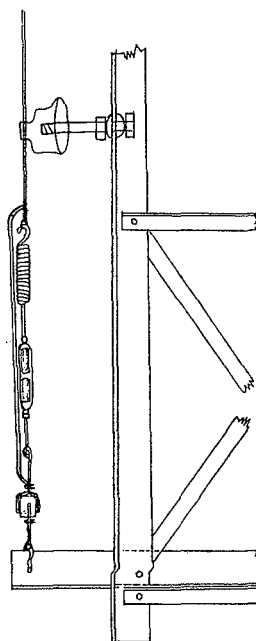
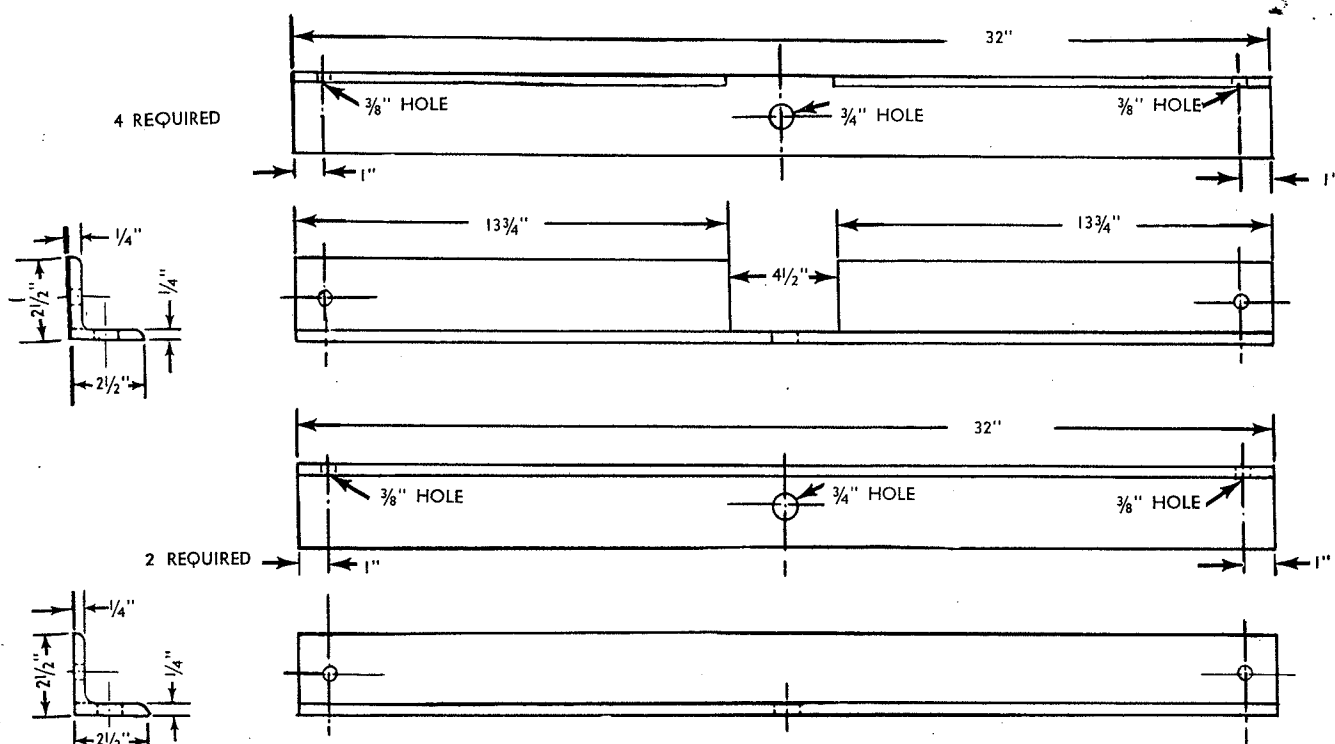


Figure 5. Details of the fold attachment at the tower's base.



NOTE: OVERALL LENGTH IS FOR TYPICAL GUYED TOWER. LENGTH MAY VARY DUE TO CROSS SECTION. HOLE SIZES ARE STANDARD.

Figure 6. Detailed drawing of the crossarms.

perience indicates that the average height of a non-directional broadcast antenna will vary somewhere between 150 and 300 ft. Inasmuch as the change in frequency from the low end to the high end of the broadcast band is approximately three to one and if we assume that the height of the broadcast antenna is not higher than  $90^\circ$  and six driven folds are used on the tower without any shorting stubs, the following empirical expression may be used to obtain the impedance of a folded-unipole antenna:

$$Z_{fu} = 3.6 (Z_{11}) \quad (9)$$

Where:

$Z_{fu}$  = base impedance of the folded-unipole in ohms.

$Z_{11}$  = base self-impedance in ohms for the tower height under consideration.

3.6 = empirical constant determined from measurements.

Equation (9) assumes that the folded-unipole antenna is approximately  $90^\circ$  and has not been resonated by use of shorting stubs (that is, wires connected between each of the folds to the tower at predetermined levels, based on impedance measurements at the base of the tower).

In normal practice, it is desirable to resonate the folded-unipole antenna by means of shorting stubs. These stubs are actually short circuits connected between each of the folds to the tower at some point below the top of the tower. The actual location for these shorting stubs must be determined experimentally. To do this, first measure the tower with the shorting stubs at the very top. Then have a tower rigger move the shorting stubs down until  $j0$  is measured at the base. It should be noted that a folded-unipole antenna will initially measure  $+j$ . Consequently, if the shorting stubs are moved down the tower too far, the measured reactance sign will change to a minus, indicating that the antenna has gone

through resonance. Hence, this means that the shorting stubs should be moved up until  $j0$  is obtained. This condition is theoretically referred to as first resonance. At resonance,  $Z = R$ ; hence, the following empirical expression may be used for obtaining the resistance of a folded-unipole antenna at first resonance:

$$Z_{fu} = 7.3 (R_{11}) \quad (10)$$

Where:

$Z_{fu}$  = base impedance or resistance for folded-unipole at first resonance (ohms).

$R_{11}$  = self-base resistance of tower (ohms).

7.3 = empirical constant determined from measurements.

### Practical Aspects of Folded-Unipole Antennas

So far, we have discussed how to determine the impedance for a folded-unipole antenna, assuming it had six folds, but no information has been given with regard to the practical construction of this type of antenna. Equations (9) and (10) were developed from measurements of what we call our standard broadcast folded-unipole antenna.

Figure 4 is a top view of a uniform cross-section, guyed tower rigged for a six wire folded-unipole antenna.

Figure 5 is a drawing indicating the details of the fold attachment at the tower's base.

Figure 6 is a detail drawing of the cross-arms or spider.

Figure 7 is a bill of materials for a typical folded-unipole antenna installation on a uniform cross-section guyed tower.

Figure 8 is a plot of impedance measurements obtained on a 200 ft. tower with six folds at 1570 KC. This tower is 0.319 wave lengths or approximately  $115^\circ$  high and would be expected to have a self-impedance ( $Z_{11}$ ) of  $155 j260$ ; however, when it is

converted to a folded-unipole antenna and the folded-unipole shorting stubs have been adjusted to obtain  $j0$  or resonance at the base, the resistance is multiplied up to 1.170 ohms. This is a transformation ratio of 7.55. In order to transform this impedance to 50 ohms  $j0$  (transmission line impedance), an "L" or "T" type of network may be used. We prefer to use a modified version of an "L" network (See Figure 10) and treat the transmission line resistance as a series resistance of a parallel network at resonance.

The following formulas may be used to determine  $X_1$  and  $X_c$  for an "L" network:

$$Z_{fu} = \frac{X_1}{R_1} + R_1 \quad (11)$$

$$X_c = X_1 + \frac{R_1^2}{X_1} \quad (12)$$

$$X_1 = \sqrt{(R_1 Z_{fu}) - (R_1)^2} \quad (13)$$

The following data furnishes complete information for the construction of a typical standard broadcast folded-unipole antenna.

Where:

$Z_{fu}$  = measured base impedance of folded-unipole at resonance (ohms).

$R_1$  = transmission line impedance (ohms).

$X_1$  = reactance of series coil (ohms).

$X_c$  = reactance of shunt condenser (ohms).

Using the foregoing formulas, a modified L network was used to match the impedance shown in Figure 8. Figure 9 is a plot of coupling impedance obtained for this antenna system.

In order to determine the current in the antenna, an ammeter may be placed in either the transmission line output (input to modified L network) or the

output of the network (input to the folded-unipole) or at both locations for determining power. The F.C.C. will allow the meter to be placed at either location and to be used for direct measurement of power. Where a folded-unipole antenna is operated at first resonance, it is recommended that the antenna ammeter be placed in the input to the network so that a larger scale ammeter can be used. It should be noted that inasmuch as the antenna is adjusted to  $j0$ , line current is a true indication of power.

Figure 11 is a plot of the measured resistance and reactance for a folded-unipole antenna (resonated) which is 70° in height at 800 KC. This antenna would be expected to have a base impedance (when measured without folded-unipole rigging) of  $31 + j9$ . Examination of Figure 11 shows that this antenna (folded-unipole rigged and resonated) has a feed point impedance of  $230 \pm j0$ . An impedance match from 50 ohm line to this impedance can be readily obtained by use of an "L" or "T" coupling network.

### Current Distribution On A Folded-Unipole Antenna

During the writer's experiments with folded-unipole antennas in 1949 and 1950 for the United States Air Force, it was determined by measurement that the current distribution on a folded-unipole antenna is the same as that of a base insulated antenna of identical height. D. L. Waidelech has proven ("General Folded-dipole Antenna Design," Communications, April 1949) that the current distribution on a folded-dipole antenna is the same as that of a simple dipole antenna. Inasmuch as a folded-unipole is basically  $1/2$

FIGURE 7

### Bill of Materials for Folded-Unipole Antenna Installation For Uniform Cross-Section Guyed Tower

1. 6 pieces of angle iron (Figure 6).
2. 2 each  $3/4"$  x  $1 3/4"$  bolts and 2 lock washers.
3. 12 each  $3/8"$  x  $1 1/2"$  bolts and 12 lock washers.
4. 12 flat washers  $7/16"$  I.D. maximum O.D.
5. 12 each  $3/8"$  Clevis Shackle.
6. 6 turnbuckles  $1/2"$  bolts or larger.
7. 3 pieces of copper strap 6" wide (long enough to ground antenna at base).
8. 24 wire clamps suitable to attach shorting straps to antenna (aluminum deadend clamps).
9. 6 folds—No. 4 NCSR, stranded aluminum wire—total length equal to 6 times tower's height plus 25' additional.
10. 6 egg type strain insulators—to insulate folds at base of antenna 3" diameter or better.
11. 36 stand-off insulators (placed at 30' intervals on tower adjacent to folds) (Jocelyn Cross Arm Pin and 15 KV Insulator).
12. 1 variable vacuum capacitor 10/1000 uuF or equivalent 15 KV, 45 amperes (suggest Jennings type).
13. 1 variable inductor 0/60 microhenries—appropriate to handle 1 KW power (suggest Gates, Johnson, or Multronics type coil).
14. 6 springs 4"-6" long.
15. 1 Weston or equivalent R.F. ammeter 0-6 amps (for 1 KW installations).
16. 1 remote antenna ammeter unit.
17. Tuning unit cabinet with bowl feed thru for output connection.
18. Miscellaneous:  
Solder, brazing rod and torches, flux, polyethylene tape, hand tools, and small parts to mount inductor and variable capacitor. Also needed to facilitate the measurements, adequate extension lights and a rough support for the measuring equipment to provide access to the antenna tuner unit.

*Note: All hardware to be galvanized or painted with aluminum paint. Dissimilar metal clamps recommended for use between tower and aluminum wire.*

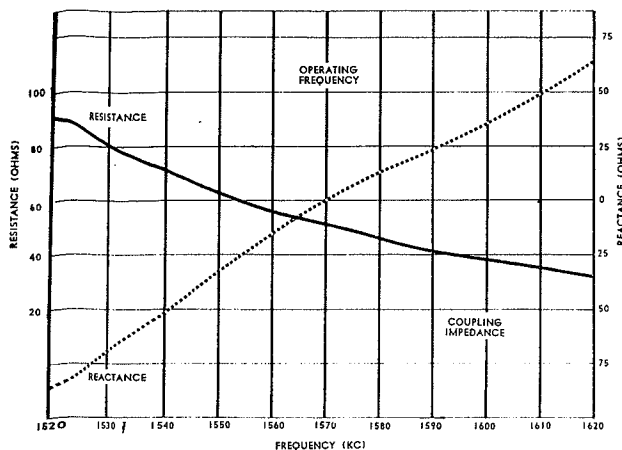


Figure 8. Impedance measurements obtained on a 200 ft. tower with six folds at 1570 KC.

of a folded-dipole antenna, it follows that the current distribution of a folded-unipole would be the same as that of a simple unipole. Further, Schelkunoff ("Antennas Theory and Practice," Wiley) has shown that the current distribution for a folded-dipole is the same as that of a simple dipole of similar length.

Numerous field intensity measurements have been made during the past five years on folded-unipole antennas to determine their current distribution and effective *Erms*. Measurements have been made on series-fed antennas before converting to folded-unipole and then comparison measurements made to demonstrate that the current distribution and effective fields are similar for both antennas. It can therefore be concluded that the current distribution of a folded-unipole type of antenna will be the same as that of a simple base insulated series-fed antenna.

#### Band-Width Considerations

The band-width of an antenna depends upon its base impedance and the rate with which its reactance changes with frequency. The band-width is considered to be the frequency band within which the power is equal to or greater than one-half the power at resonance. Expressed in equation form:

$$\Delta f = \frac{2R\alpha}{\frac{dx}{df}} \quad (14)$$

Where:

- $\Delta f$  = band-width in kilocycles between half-power points.
- $R\alpha$  = measured antenna resistance in ohms.
- $\frac{dx}{df}$  = slope of reactance curve at resonant frequency.

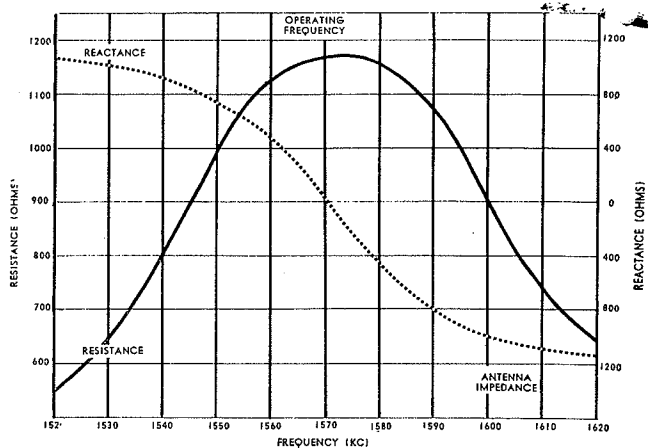


Figure 9. Plot of coupling impedance.

The effective band-width will be doubled when the generator is matched to the antenna circuit. The *Q* of a folded-unipole antenna can be determined from the equation:

$$Q = \frac{f_0}{\Delta f} \quad (15)$$

Where:

$f_0$  = operating frequency in kilocycles.

$\Delta f$  = band-width of antenna in kilocycles.

Our experiments indicate that a folded-unipole antenna has a much more desirable band-width characteristic than an equal height series-fed antenna.

#### Top-Loaded Folded-Unipole Antennas

For very short towers, advantage may be taken of top-loading to increase the effective height of a folded-unipole antenna.

Our experience indicates that the simplest and most effective means for top-loading a folded-unipole antenna is to connect the top three guy wires to the tower, adjust them to a given physical length and then inter-connecting them at the lower end to simulate a pyramid. Experimental data indicates that the following expression can be used to compute the length of guy wires necessary to obtain a given amount of top-loading:

$$G_{\text{eff}}^0 = \frac{TL^0 + G_{11}^0}{0.705} \quad (16)$$

Where:

$G_{\text{eff}}$  = desired electrical tower height in degrees.

$TL^0$  = desired top-loading in degrees.

$G_{11}$  = electrical height of tower without top-loading in degrees.

0.705 = empirical constant.

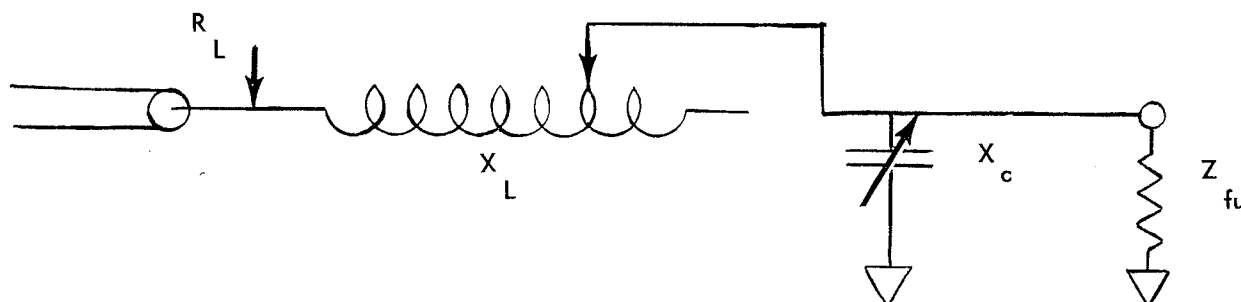


Figure 10. Schematic of "L" type impedance transforming network.

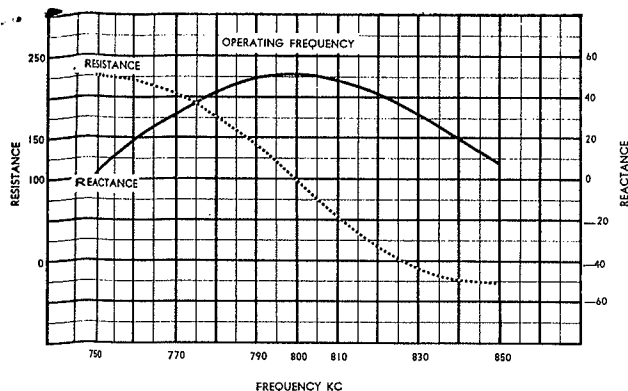


Figure 11. Plot of the measured resistance and reactance for a folded-unipole antenna 70 degrees in height at 800 KC.

Figure 12 is a plot of the measured resistance and reactance for a folded-unipole antenna (resonated) which is 69.5° in height at 1000 KC and has been top-loaded an additional 15.5° to given an electrical height of 85°. This antenna would be expected to have a base impedance of  $39 + j40$  (when measured without folded-unipole rigging but with top-loading). Figure 12 shows that this antenna (folded-unipole) rigged and resonated) has a feed point impedance of  $350 \pm j0$ . An appropriate impedance transformer should be used to match this antenna impedance to a transmission line.

### Second Resonance for Folded-Unipole Antennas

A folded-unipole antenna can obtain a wide range of resonant radiation resistance by varying the ratio of the diameters of the folded conductors to the diameter of the tower. The radiation resistance varies as the square of the height and if the transformation ratio is raised enough, the height of the antenna can be reduced, the limit being the point where ground losses consume a prohibitive percentage of the power.

For practical operation a short antenna should have a resistance of at least 50 ohms. Unfortunately short series-fed antennas in the range of 45° to 60° do not approach this value; consequently, this type of antenna has excessive losses. In these ranges, the use of a top-loaded folded-unipole antenna is extremely desirable, inasmuch as these antennas can be operated at first or second resonance. For second resonance, a top-loaded folded-unipole has a length of approximately one-half that of a folded-unipole at first resonance. This is the same as saying that if a folded-unipole antenna had a length of approximately 90° (electrical), we would expect second resonance to occur at approximately one-half this length or 45°. The base impedance for a top-loaded folded-unipole antenna at second resonance can be expressed as:

$$R_{2r} = 1580$$

$$\left[ \frac{h_{2r}}{2r} \times \frac{\log 4S^2/d_1 d_2}{\log 2S/d_2} \right]^2 \quad (17)$$

Where:

$R_{2r}$  = resistance of folded-unipole at second resonance (ohms).  
 $h_{2r}$  = height at second resonance.

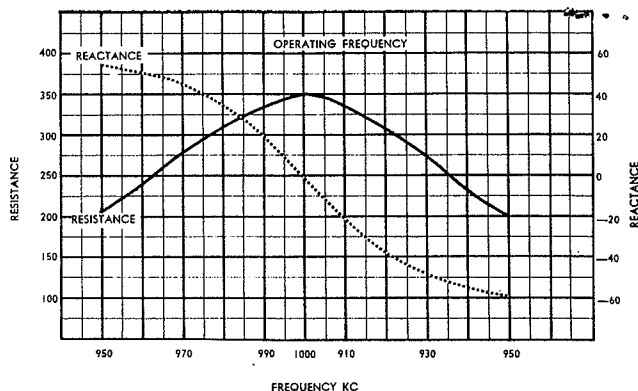


Figure 12. Plot of resistance and reactance for a folded-unipole antenna which is 69.5 degrees in height at 1000 KC and has been top-loaded an additional 15.5 degrees to simulate electrical height of 85 degrees.

$2r$  = wave length at second resonance (same units as  $h_{2r}$ ).  
 $S$  = spacing, center to center, of tower to fold.  
 $d_1$  = fold diameter.  
 $d_2$  = tower diameter.  
 $S$ ,  $d_1$  and  $d_2$  should be expressed in the same units.

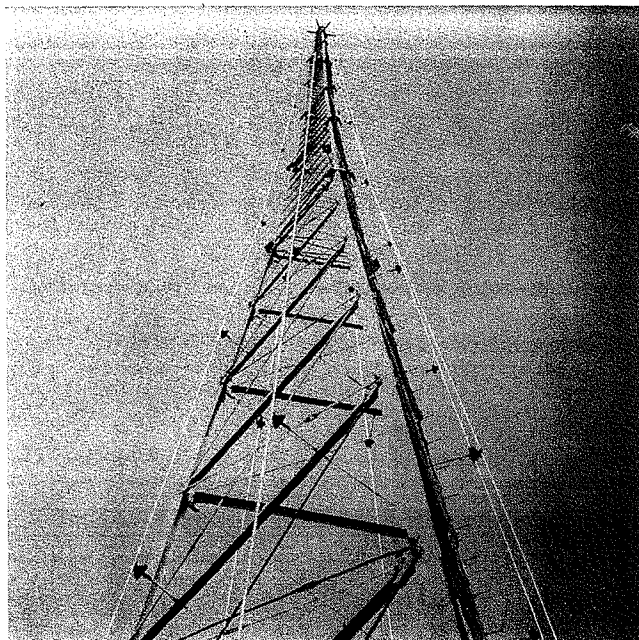
It should be noted that "log<sub>10</sub>" or "loge" can be used, inasmuch as a ratio is expressed in equation (17).

It should be noted that the operation of a folded-unipole at second resonance is similar to that at first resonance; however, the ratio of the diameter of the folds to the tower's diameter and the spacing is much more critical.

### Unattenuated Field Intensity

It has been observed experimentally that a folded-unipole antenna will develop a higher unattenuated field intensity than the same equivalent height series-fed antenna system. The increase in field intensity varies between approximately two to ten per cent. The greatest increase in field intensity is experienced on short antennas in the range 45° to 75°.

This paper was presented at the 14th Annual NAB Engineering Conference.



Rooftop installation of folded-unipole antenna system at WAKE, Atlanta, Ga.

EFFECTS OF TOWER LIGHTING AND  
ISOLATION CIRCUITS UPON THE IMPEDANCE  
OF VARIOUS AM TOWERS

14TH NAB  
BROADCAST ENGINEERING CONFERENCE  
CHICAGO, ILLINOIS  
MARCH 1960

*Vir N. James*

CONSULTING RADIO ENGINEERS

1316 S. KEARNEY, DENVER 22, COLORADO SKYline 6-1603

## THE EFFECTS OF TOWER LIGHTING AND ISOLATION CIRCUITS UPON TOWER IMPEDANCE OF VARIOUS AM TOWERS

PERHAPS SOME OF YOU HAVE MEASURED ANTENNA IMPEDANCES AND FOUND THEM TO VARY WHEN YOU CONNECTED THE TOWER LIGHTING OR ISOLATION CIRCUITS. OR, PERHAPS, YOU HAVE INVESTIGATED APPARENT TRANSMITTER EFFICIENCIES IN THE RANGE OF 90 TO 110%. TOWER LIGHTING OR ISOLATION CIRCUITS FREQUENTLY CAUSE SUCH CONDITIONS TO EXIST.

DURING THE COURSE OF OUR CONSULTING WORK, WE HAD ENCOUNTERED THESE CONDITIONS AND ANTENNA RESISTANCE CHANGES UP TO 50% DUE TO THE EFFECTS OF TOWER LIGHTING ISOLATION CIRCUITS. IT WAS, THEREFORE, DEEMED ADVISABLE TO INVESTIGATE THESE EFFECTS IN MORE DETAIL.

TO THIS END, SPECIAL EQUIPMENT WAS SET UP TO MEASURE THE ANTENNA IMPEDANCE OF KSTR, GRAND JUNCTION, COLORADO, WHICH OPERATES ON AN ASSIGNED FREQUENCY OF 620 KILOCYCLES. IMPEDANCE MEASUREMENTS OF THE KSTR 300 FOOT TOWER OVER THE ENTIRE BROADCAST BAND, PROVIDED AN OPPORTUNITY TO STUDY THE EFFECTS OF TOWER ISOLATION CIRCUITS FOR EFFECTIVE ANTENNA HEIGHTS WHICH VARIED WITH FREQUENCY FROM 0.15 TO 0.5 WAVELENGTH. THE INVESTIGATION CONSISTED OF TOWER IMPEDANCE MEASUREMENTS WITHOUT ISOLATION CIRCUITS AND THEN WITH VARIOUS TOWER ISOLATION CIRCUITS CONNECTED.

TOWER LIGHTING ISOLATION CIRCUITS COMMONLY ENCOUNTERED CONSIST OF THE FOLLOWING TYPES:

1. A SINGLE DUAL-WOUND CHOKE. THIS CHOKE IS OFTEN SUPPLIED IN DIAMETERS OF APPROXIMATELY 5 INCHES AND LENGTHS UP TO 18 INCHES WITH A TWO LAYER WINDING. ONE WINDING CONNECTS EACH SIDE OF THE AC CIRCUIT TO THE TOWER LIGHTS. SOME CHOKES ARE TRIPLE WOUND TO ACCOMMODATE A THIRD TOWER CIRCUIT. A SIMPLE SCHEMATIC SHOWING THE CONNECTION OF A SINGLE DUAL-WOUND LIGHTING CHOKE IS SHOWN IN FIGURE 1.



2. SOMETIMES TWO OF THESE CHOKES ARE USED IN TANDEM. A SCHEMATIC OF TANDEM CHOKES IS SHOWN IN FIGURE 2. IT WILL BE NOTED THAT THE NEUTRAL SIDE OF THE TOWER LIGHT IS SHOWN TIED TO THE TOWER SO THAT THE TOWER ISOLATION CHOKES FUNCTIONS AS A STATIC DRAIN CHOKES.

3. AN ENTIRELY DIFFERENT MEANS OF TOWER LIGHTING ISOLATION IS PROVIDED BY THE TRANSFORMER ISOLATION TYPE OR SO-CALLED "AUSTIN" TRANSFORMER. TRANSFORMER ISOLATION IS SHOWN IN FIGURE 3.

THE TOWER ISOLATION CHOKES FREQUENTLY ENCOUNTERED HAVE A HIGH VALUE OF INDUCTANCE ON THE ORDER OF 350 MICROHENRIES. THE TRANSFORMER ISOLATION UNITS CONSIST OF A LARGE DOUGHNUT SHAPED PRIMARY WINDING CONNECTED TO THE 60 CYCLE POWER LINE. THE TOWER LIGHTS ARE SUPPLIED WITH CURRENT FROM A SECONDARY DOUGHNUT WINDING LOCATED IN THE FIELD OF THE PRIMARY BUT SPACED SEVERAL INCHES FROM IT.

THE EFFECTS UPON TOWER IMPEDANCES OF TOWER LIGHTING CHOKES MAY BE THOUGHT OF AS A HIGHLY INDUCTIVE CIRCUIT WITH A SIGNIFICANT AMOUNT OF CIRCUIT RESISTANCE AT THE R.F. FREQUENCY. THE EFFECT IS FURTHER COMPLICATED BY A DISTRIBUTED CAPACITANCE EFFECT. THE MATHEMATICS FOR CALCULATING THE EFFECTS OF SUCH TOWER LIGHTING CHOKES IN THE RANGE WHERE THE OPERATION IS CRITICAL, IS QUITE DIFFICULT. HOWEVER, THEIR PERFORMANCE MAY BE OBTAINED EASILY AND RAPIDLY WITH A RADIO FREQUENCY BRIDGE. THE TRANSFORMER ISOLATION CIRCUIT ON THE OTHER HAND SHUNTS THE ANTENNA IMPEDANCE WITH A CAPACITANCE OF APPROXIMATELY 30 MICROMICROFARADS. THE EFFECTS, THEREFORE, OF THE TRANSFORMER ISOLATION IS MORE READILY CALCULATED. IT SHOULD BE NOTED THAT TRANSFORMER ISOLATION DOES NOT PROVIDE A STATIC DRAIN. THIS MUST BE ADDED.

THE MEASUREMENTS OF THE KSTR TOWER WERE MADE UNDER THE FOLLOWING CONDITIONS:

A. NO LIGHTING ISOLATION

- B. ONE TOWER LIGHTING CHOKE
- C. TWO TOWER LIGHTING CHOKES IN TANDEM
- D. TOWER SHUNTED BY A 30 MICROMICROFARADS CAPACITOR TO SIMULATE THE TRANSFORMER ISOLATION.

THE MEASUREMENTS OF THE KSTR TOWER WITH THE VARIOUS FORMS OF TOWER LIGHTING ISOLATION DESCRIBED ABOVE, WERE PERFORMED USING A GENERAL RADIO TYPE 916-AL RADIO FREQUENCY BRIDGE. THE SIGNAL GENERATOR CONSISTED OF A VERY STABLE MASTER OSCILLATOR FOLLOWED BY A POWER AMPLIFIER TO ISOLATE THE EFFECTS OF THE BRIDGE ON THE OSCILLATOR. A BUILT-IN ELECTRONIC VOLTAGE REGULATOR MAINTAINED THE OSCILLATOR FREQUENCY AND OUTPUT VERY STABLE. THE DETECTOR CONSISTED OF A VERY SELECTIVE, WELL SHEILDED, SUPERHETERODYNE RECEIVER. THE SWITCHING ARRANGEMENT WAS SET UP TO DISCONNECT THE TOWER LIGHTING CIRCUITS OR TO PERMIT CONNECTING ONE CHOKE, TWO CHOKES IN TANDEM, OR THE SHUNT CAPACITANCE.

FIGURE 4 IS A PLOT OF THE BASE TOWER RESISTANCE FOR THE ENTIRE BROADCAST BAND AS SHOWN BY A BROKEN CURVE. THE SOLID CURVE IS A PLOT OF THE RESISTANCE OBTAINED WITH A SINGLE DUAL-WOUND TOWER LIGHTING CHOKE CONNECTED. IT WILL BE NOTED THAT THE TOWER RESISTANCE SHOWED A MAXIMUM CHANGE FROM 765 OHMS DOWN TO 48 OHMS AT A FREQUENCY OF 1275 KILOCYCLES, CORRESPONDING TO A TOWER HEIGHT OF APPROXIMATELY 0.4 WAVELENGTHS. THIS REPRESENTS A DRASTIC CHANGE OF 93.8%. IT IS TO BE NOTED THAT THE VARIATION OF TOWER RESISTANCE WITHIN THE ONE QUARTER WAVE REGION WAS FAIRLY SMALL.

IN FIGURE 5 IT WILL BE SEEN THAT WHEN TWO TOWER LIGHTING CHOKES WERE USED IN TANDEM, A GREAT DEAL LESS CHANGE IN ANTENNA RESISTANCE OCCURRED. IN FACT OVER A BROAD BAND FROM 0.25 TO 0.35 WAVELENGTH OF TOWER HEIGHT CLOSE AGREEMENT WAS OBTAINED WITH BASIC TOWER RESISTANCE.

FIGURE 6 SHOWS HOW TRANSFORMER ISOLATION EFFECTS TOWER RESISTANCE. THIS SYSTEM PROVED INFERIOR TO THE TWO CHOKES IN TANDEM, ALTHOUGH VASTLY SUPERIOR TO THE SINGLE CHOKE COMMONLY UTILIZED. VERY LITTLE CHANGE IN

ANTENNA RESISTANCE OCCURRED OVER ONLY A SMALL RANGE OF APPROXIMATELY .2 TO .25 WAVELENGTH ANTENNA HEIGHT. AT ALL OTHER ANTENNA HEIGHTS, THE TRANSFORMER CAUSED A SIGNIFICANT CHANGE IN MEASURED ANTENNA RESISTANCE. WHILE THE EFFECT UPON TOWER REACTANCE MAY NOT BE AS SIGNIFICANT AS TOWER RESISTANCE FOR NON-DIRECTION OPERATION, IT IS QUITE IMPORTANT IN DIRECTIONAL ANTENNA WORK. FIGURE 7 SHOWS THE EFFECT UPON THE MEASURED TOWER REACTANCE OF A SINGLE TOWER LIGHTING CHOKE ISOLATION CIRCUIT. AGAIN THE TOWER REACTANCE WITHOUT ANY ISOLATION CIRCUIT IS SHOWN AS A DASHED CURVE. THE TOWER REACTANCE OBTAINED WITH A SINGLE CHOKE CONNECTED IN THE TOWER LIGHTING CIRCUIT IS SHOWN BY THE SOLID CURVE. HERE THE EFFECT IS EXCEEDINGLY GREAT. FOR INSTANCE, AT 1375 KILOCYCLES CORRESPONDING TO AN ANTENNA HEIGHT OF APPROXIMATELY .420 WAVELENGTH, THE REACTANCE CHANGED FROM A NEGATIVE 438 OHMS UP TO A POSITIVE 380 OHMS. THIS CHANGE OF 818 OHMS REPRESENTS A PERCENTAGE CHANGE OF 187%. AGAIN, THE USE OF TWO CHOKES IN TANDEM GREATLY REDUCES THE ADVERSE EFFECT OF THE TOWER LIGHTING CIRCUIT UPON THE MEASURED TRUE REACTANCE, AS SHOWN IN FIGURE 8. SIMILARLY, FIGURE 9 ILLUSTRATES THE EFFECT OF TRANSFORMER ISOLATION UPON THE TOWER REACTANCE. AGAIN, THE ISOLATION TRANSFORMER, WHILE RADICALLY BETTER THAN A SINGLE CHOKE, MEASURED INFERIOR TO THE TWO CHOKES IN TANDEM.

IT MAY BE NOTED, HOWEVER, THAT IN CRITICAL AREAS OF TOWER HEIGHT CONSIDERABLE RESISTANCE AND REACTANCE VARIATIONS OCCURRED WITH THE USE OF THESE TYPES OF TOWER LIGHTING ISOLATION CIRCUITS.

OTHER FORMS OF ISOLATION ARE NORMALLY USED TO PREVENT LOSS OF RADIO FREQUENCY POWER IN AM TOWERS, WHEN OTHER RADIO SERVICES SHARE THE SAME TOWER. FIGURE 10 ILLUSTRATES A CIRCUIT WHICH ISOLATES A FM ANTENNA FROM AN AM TOWER. HERE THE OUTER CONDUCTOR OF THE COAX LINE IS TIED TO THE TOWER NEAR THE TOP WHILE A LENGTH OF LINE OF APPROXIMATELY ONE QUARTER WAVE LENGTH LONG (AT

THE AM FREQUENCY) IS INSULATED FROM THE TOWER. A CAPACITOR IS FREQUENTLY CONNECTED FROM THE BASE OF THE TOWER TO THE COAX OUTER CONDUCTOR AT THE POINT WHERE IT IS ALSO CONNECTED TO GROUND. THIS LENGTH OF INSULATED LINE, TOGETHER WITH THE TOWER, FORMS A ONE-QUARTER WAVE RESONANT CIRCUIT HAVING THE TOP END SHORTED WITH RESULTING HIGH IMPEDANCE AT THE OPEN LOWER END. THIS HIGH IMPEDANCE FORMED BY THE ONE-QUARTER WAVE STUB SERVES TO ISOLATE FM OR TV SERVICE FROM THE AM TOWER. IN PRACTICE THE GROUNDING POINT AND/OR THE TOP POINT, WHICH IS TIED TO THE TOWER, IS MOVED UNTIL THE MEASURED AM ANTENNA IMPEDANCE SHOWS THAT IT IS UNAFFECTED BY THE PRESENCE OF THE FM OR OTHER SERVICE.

IN FIGURE 11 A SAMPLING LOOP IS ISOLATED FROM THE TOWER MERELY BY INSULATION. THIS TYPE OF SAMPLING LOOP ISOLATION IS FREQUENTLY UTILIZED IN SINGLE TOWER NON-DIRECTIONAL ANTENNA SYSTEMS. HOWEVER, FREQUENTLY IT HAS BEEN FOUND THAT INSULATED SAMPLING LOOPS APPRECIABLY CHANGE THE MEASURED ANTENNA IMPEDANCE, OFTEN DUE TO A SIGNIFICANT CAPACITANCE COUPLING EFFECT. SEVERAL CASES OF RADICAL PATTERN DISTORTION HAVE BEEN ENCOUNTERED EVEN IN SIMPLE TWO TOWER DIRECTIONALS. FIGURE 12 ILLUSTRATES A PARALLEL RESONANT TYPE OF ISOLATION FOR SAMPLING LOOPS. IN THIS SYSTEM ONE SIDE OF THE PICKUP LOOP AND THE OUTER CONDUCTOR OF THE COAX LINE IS TIED TO THE TOWER. INDEED, THE LINE IS BONDED TO THE TOWER AT FREQUENT INTERVALS. AT THE BASE OF THE TOWER, THE COAX LINE IS CONNECTED TO A LARGE COIL FORMED BY THE COAXIAL CABLE. THIS COAXIAL COIL MUST BE TUNED CLOSE TO RESONANCE IF THE TOWER IMPEDANCE IS TO BE UNALTERED BY THE PICKUP LOOP. IT HAS BEEN FOUND THAT IMPROPER TUNING OF SUCH TANK CIRCUITS PERMITS ATTAINMENT OF WIDE VARIATIONS OF TOWER IMPEDANCES. HOWEVER, WHERE THESE CIRCUITS ARE PROPERLY TUNED, NO UNDESIRABLE EFFECTS HAVE BEEN ENCOUNTERED.

ALTHOUGH TIME DID NOT PERMIT, NOR DID THE MANUFACTURER CARE TO  
SUPPLY A TUNABLE RESONANT CHOKE FOR TOWER LIGHTING ISOLATION, NEVERTHELESS,  
THIS FORM MAY BE ENTIRELY SATISFACTORY.

CONCLUSION:

REGARDLESS OF THE TYPE OF TOWER ISOLATION CIRCUIT EMPLOYED, THE  
PERFORMANCE MUST BE THOROUGHLY CHECKED. IT IS HOPED THAT THE BROADCAST  
EQUIPMENT SUPPLYERS WILL MAKE MORE SUITABLE ISOLATION CIRCUIT SYSTEMS  
AVAILABLE.

  
VIR N. JAMES

VIR N. JAMES, CONSULTING RADIO ENGINEERS, DENVER, COLO., MARCH, 1960

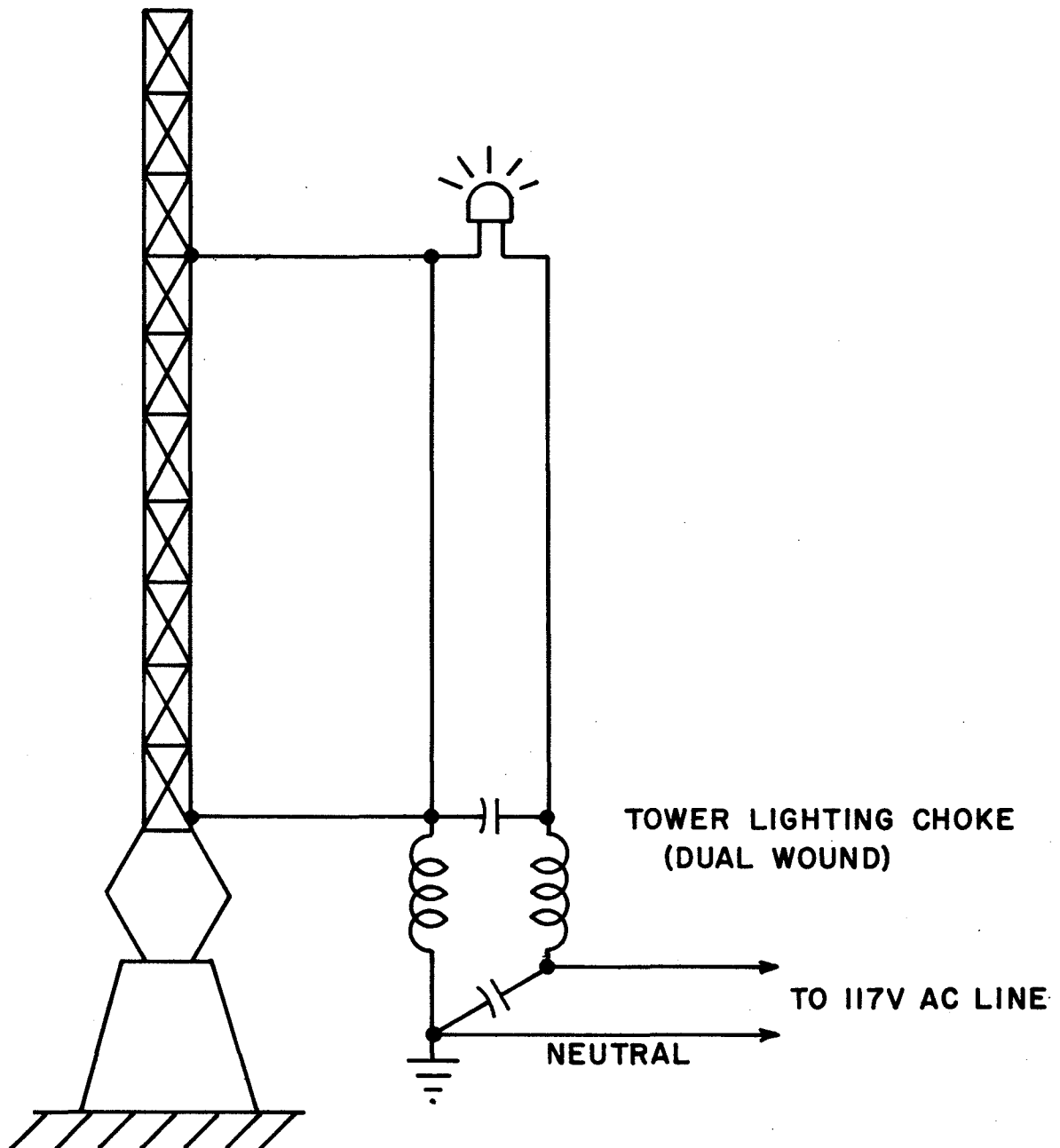
MEASURED ANTENNA IMPEDANCE

KSTR TOWER - HEIGHT 300'

F(KC)	TOWER HEIGHT WAVE LENGTH	<u>TOWER ONLY</u>		<u>2 CHOKES</u>		<u>1 CHOKE</u>		<u>TRANS.</u>	
		<u>R</u>	<u>X</u>	<u>R</u>	<u>X</u>	<u>R</u>	<u>X</u>	<u>R</u>	<u>X</u>
517	.158	11.3	-153	12.2	11.8	13.9	13.4	11.0	10.8
620	.189	18.7	-86.7	19.1	18.6	20.1	19.7	18.2	17.9
655	.200	22.2	-63	22.8	21.9	23.7	23.0	20.2	19.9
675	.206	24.6	-50	25.2	24.5	26.0	24.6	24.6	24.0
705	.215	28.1	-30	29.2	30.0	30	28.7	28.9	28.2
725	.221	31.3	-17.2	32.3	33.0	33	32.9	32	31.0
755	.230	36.5	+5	37.4	36.9	37.9	38.3	37.5	36.9
775	.236	41	19	41.5	41.1	42	43	42	40.8
805	.246	48	41	48.9	48.2	49	50	50	50
825	.252	53.2	55	54	52.8	54.5	54.1	56	55.1
845	.258	60	70	60	58.9	60.2	59.7	62.9	63
875	.267	71	94	71	70.1	73	72.1	76	77
900	.275	82	113	81.5	82.3	84	83	87	87
925	.282	95.7	135	95.2	95.7	98	97.3	102.2	101.6
955	.291	114.5	162	114	113.8	121	120	123.3	123.0
980	.299	134	186	131	132.1	146	145	148	147
1000	.305	153.5	207	151	206	171	208	170	206
1025	.313	185	231	184	230	215	232	206	232
1055	.322	231	261	231	259	290	253	267	259
1075	.328	271.5	275	272	275	359	252	312	274
1105	.337	340	294	350	294	490	229	400	283
1125	.343	400	299	410	299	580	254	475	278
1155	.352	496	292	530	287	633	-95	580	240
1175	.359	575	268	620	238	580	-300	655	149
1205	.368	690	164	720	138	353	-332	740	-7
1225	.374	730	90.8	767	55	214	-326	770	-109
1255	.383	760	-50	787	-116	83.3	-205	782	-222
1275	.389	765	-146	750	-232	48.1	-71.4	770	-290
1305	.398	750	-263	668	-380	57.3	+177	712	-374
1330	.406	700	-330	565	-414	119	306	590	-420
1355	.414	603	-416	465	-431	281	374	460	-439
1375	.420	515	-438	394	-436	493	380	383	-440
1400	.427	435	-444	325	-435	760	318	315	-434
1425	.435	350	-442	269	-422	862	29	265	-421
1455	.444	285	-428	218	-403	730	-316	214	-403
1475	.450	249	-415	187	-389	607	-410	189	-389
1505	.459	207	-395	153	-367	423	-465	158	-368
1525	.466	182.2	-380	134	-351	336	-464	139	-352
1555	.475	154	-356	114	-326	251	-448	119	-329
1575	.481	138	-339	101	-308	210	-421	108	-311
1610	.491	117.2	-311	86	-269	163	-357	92	-280

VIR N. JAMES, CONSULTING RADIO ENGINEERS, DENVER, COLO., MARCH, 1960.

# SINGLE CHOKE TOWER LIGHTING ISOLATION



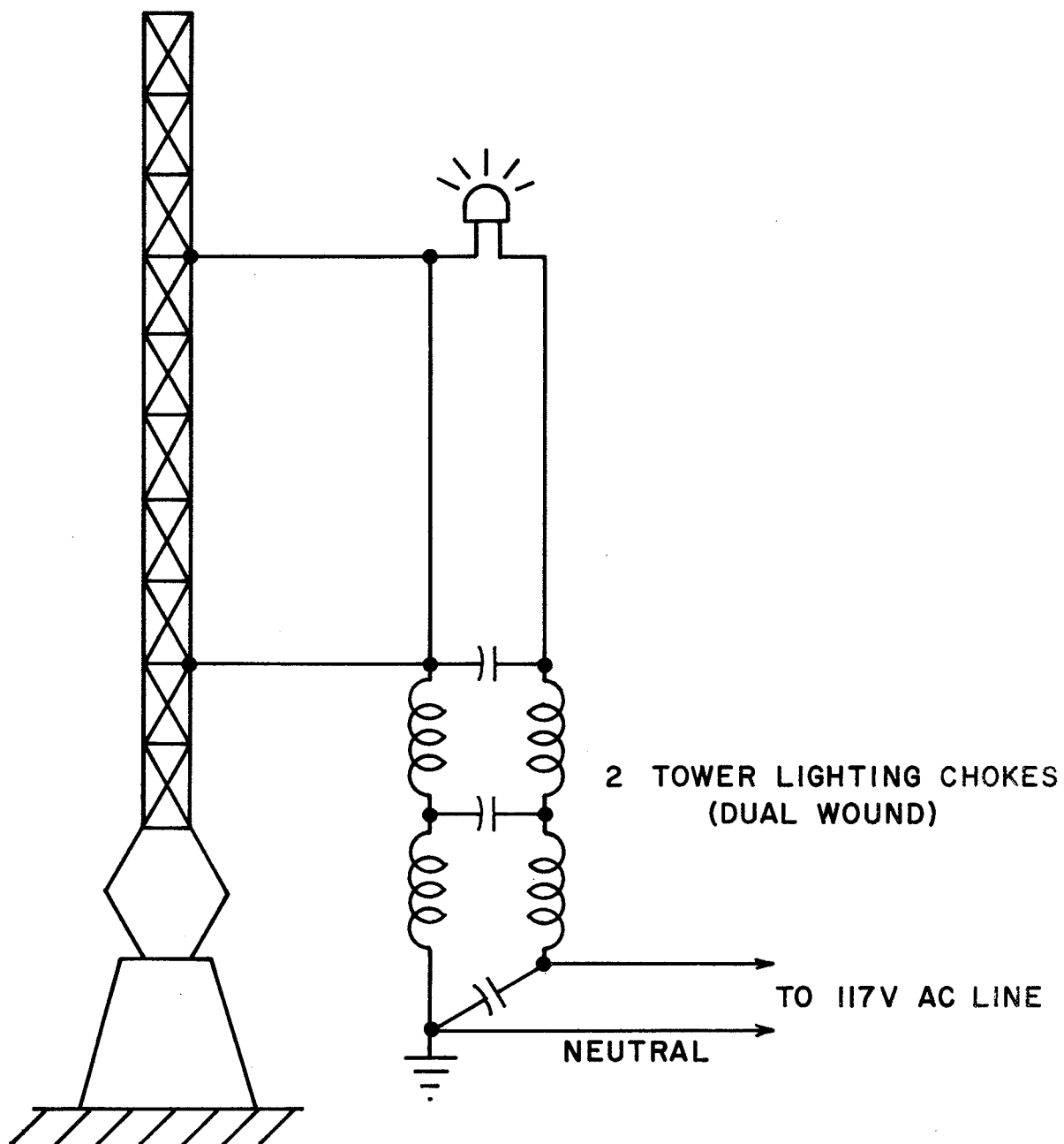
*Vir N. James*

CONSULTING RADIO ENGINEERS

1316 S. KEARNEY, DENVER 22, COLORADO SKYline 6-1603

FIGURE 1  
MARCH 1960

# TANDEM CHOKES TOWER LIGHTING ISOLATION



*Vir N. James*

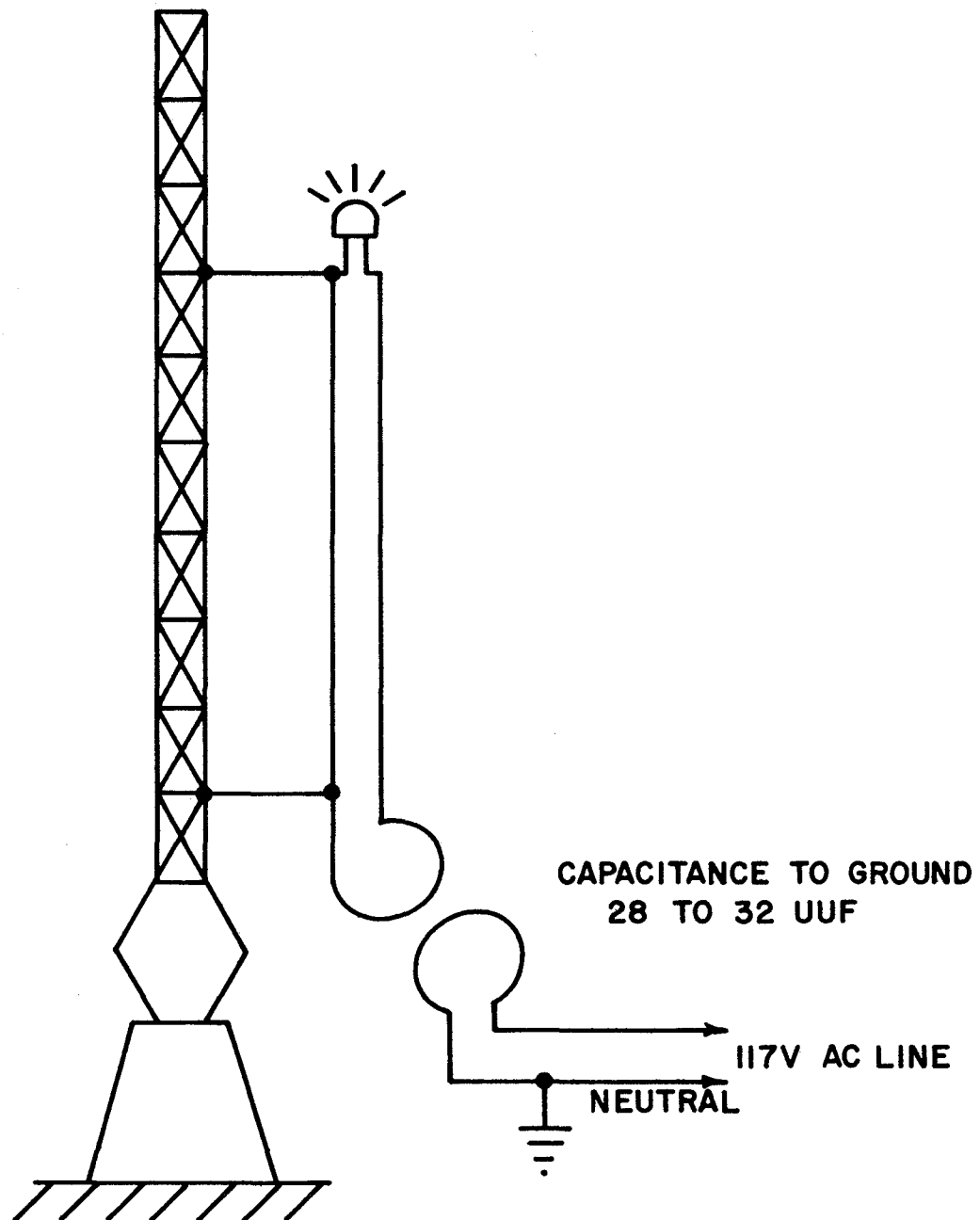
CONSULTING RADIO ENGINEERS

1316 S. KEARNEY, DENVER 22, COLORADO SKYLINE 6-1603

FIGURE 2  
MARCH 1960



# TRANSFORMER TOWER LIGHTING ISOLATION



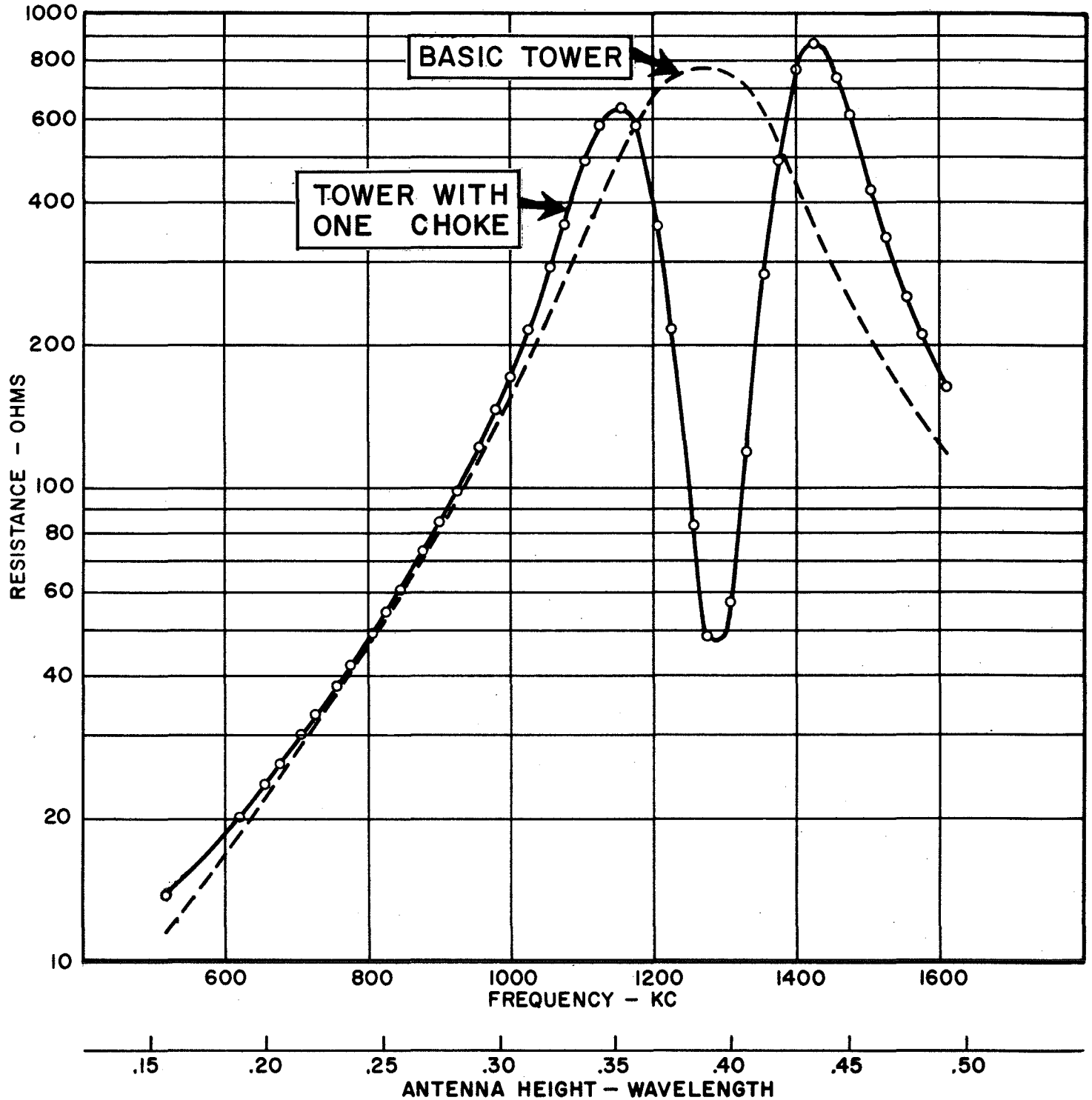
*Vir N. James*

CONSULTING RADIO ENGINEERS

1316 S. KEARNEY, DENVER 22, COLORADO SKyline 6-1603

FIGURE 3  
MARCH 1960

# TOWER RESISTANCE VARIATION I-CHOKE ISOLATION CIRCUIT



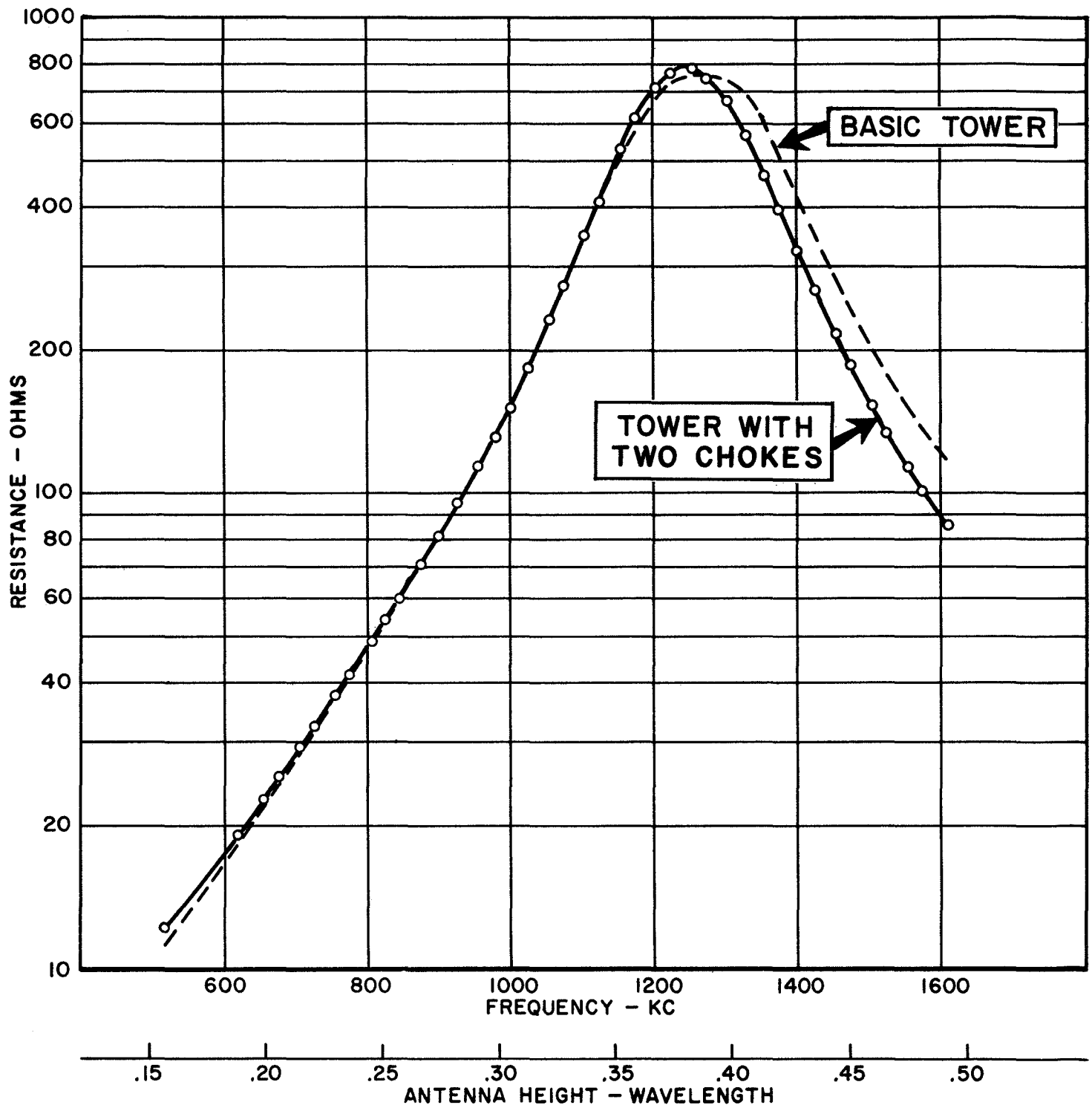
*Vir N. James*

CONSULTING RADIO ENGINEERS

1316 S. KEARNEY, DENVER 22, COLORADO Skyline 6-1603

FIGURE 4  
MARCH 1960

# TOWER RESISTANCE VARIATION 2-CHOKE ISOLATION CIRCUIT



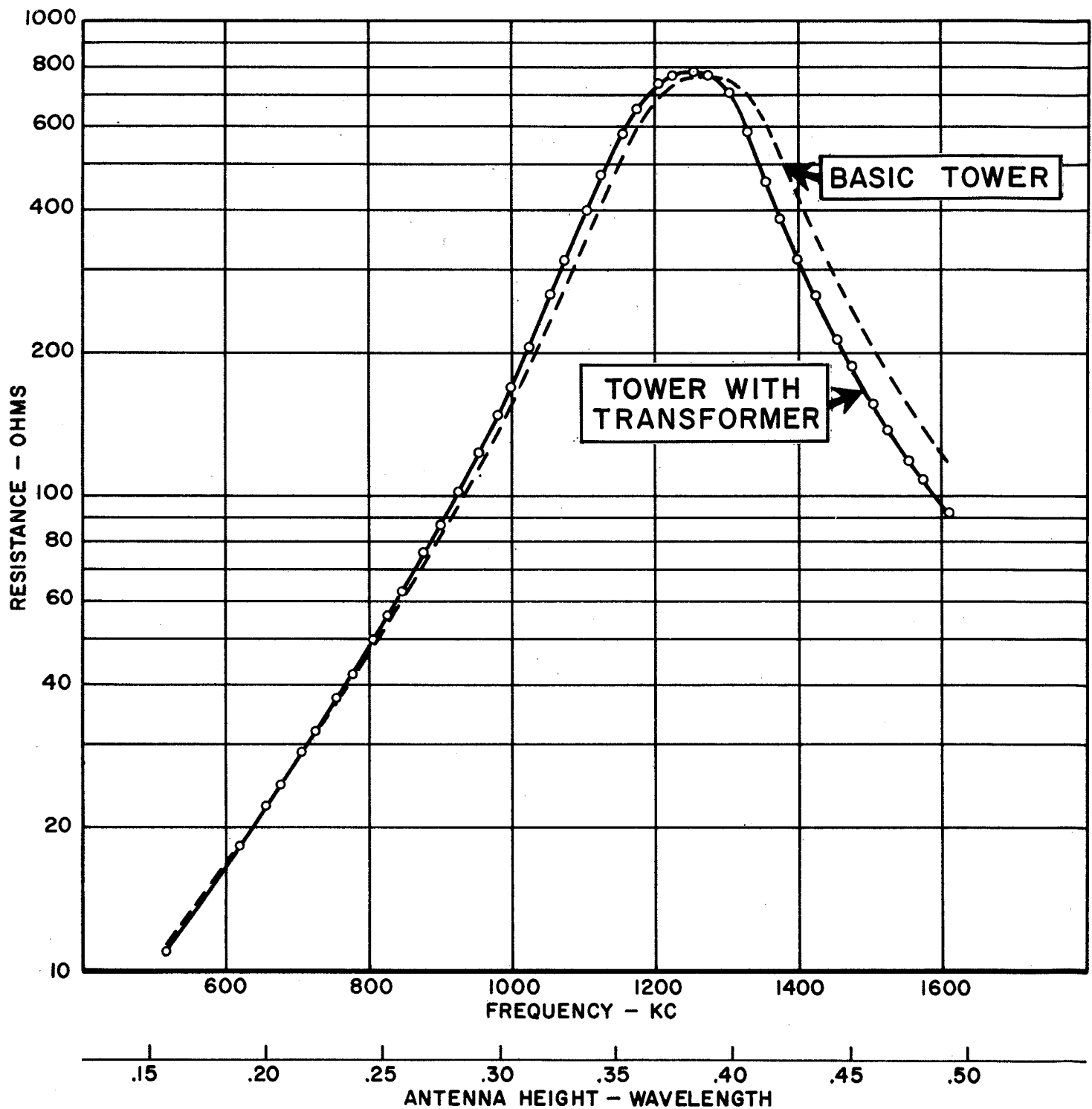
*Vir N. James*

CONSULTING RADIO ENGINEERS

1316 S. KEARNEY, DENVER 22, COLORADO Skyline 6-1603

FIGURE 5  
MARCH 1960

# TOWER RESISTANCE VARIATION TRANSFORMER ISOLATION CIRCUIT



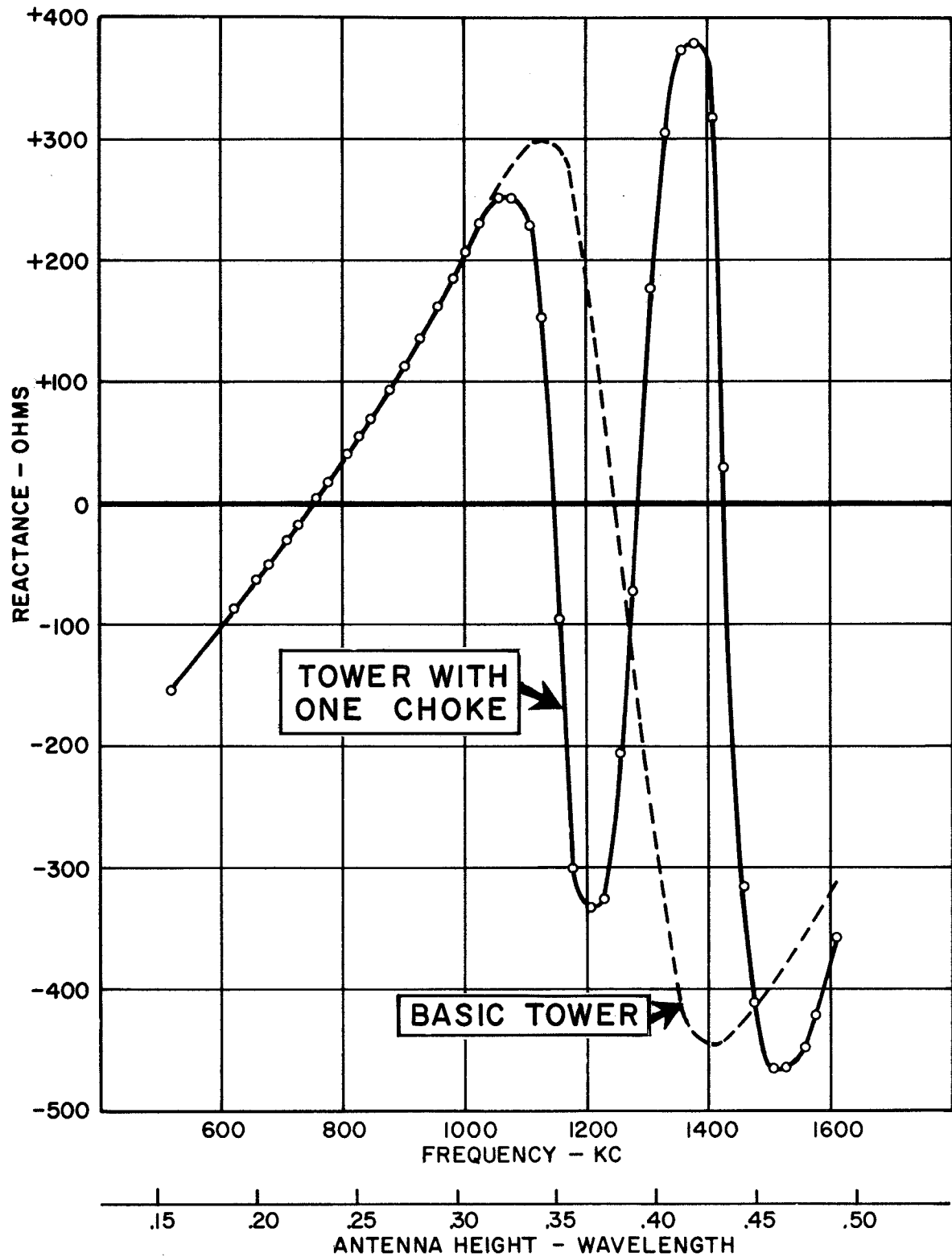
*Vir N. James*

CONSULTING RADIO ENGINEERS

1316 S. KEARNEY, DENVER 22, COLORADO Skyline 6-1603

FIGURE 6  
MARCH 1960

# TOWER REACTANCE VARIATION I-CHOKE ISOLATION CIRCUIT



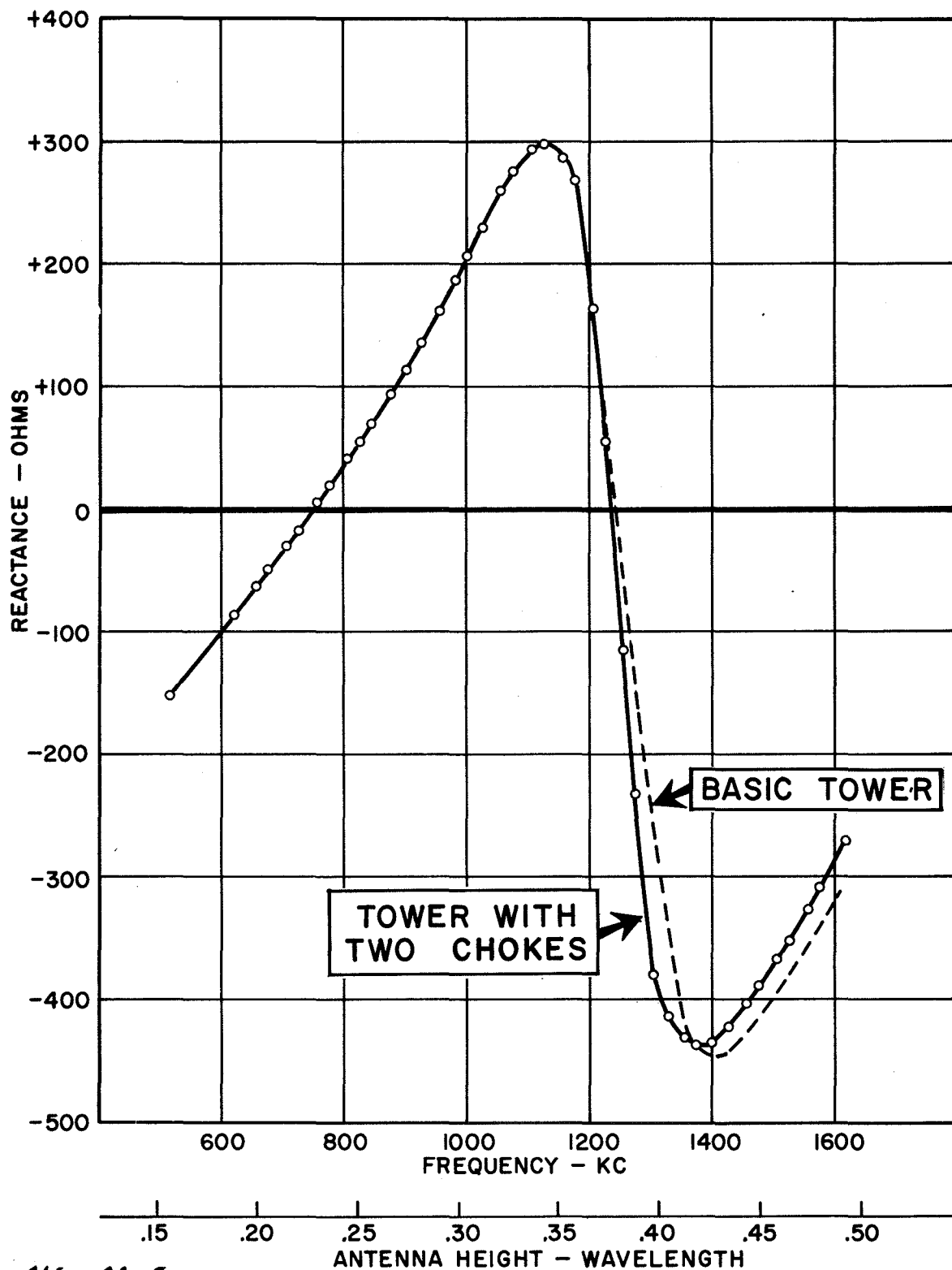
*Vir N. James*

CONSULTING RADIO ENGINEERS

1316 S. KEARNEY, DENVER 22, COLORADO Skyline 6-1603

FIGURE 7  
MARCH 1960

# TOWER REACTANCE VARIATION 2-CHOKE ISOLATION CIRCUIT



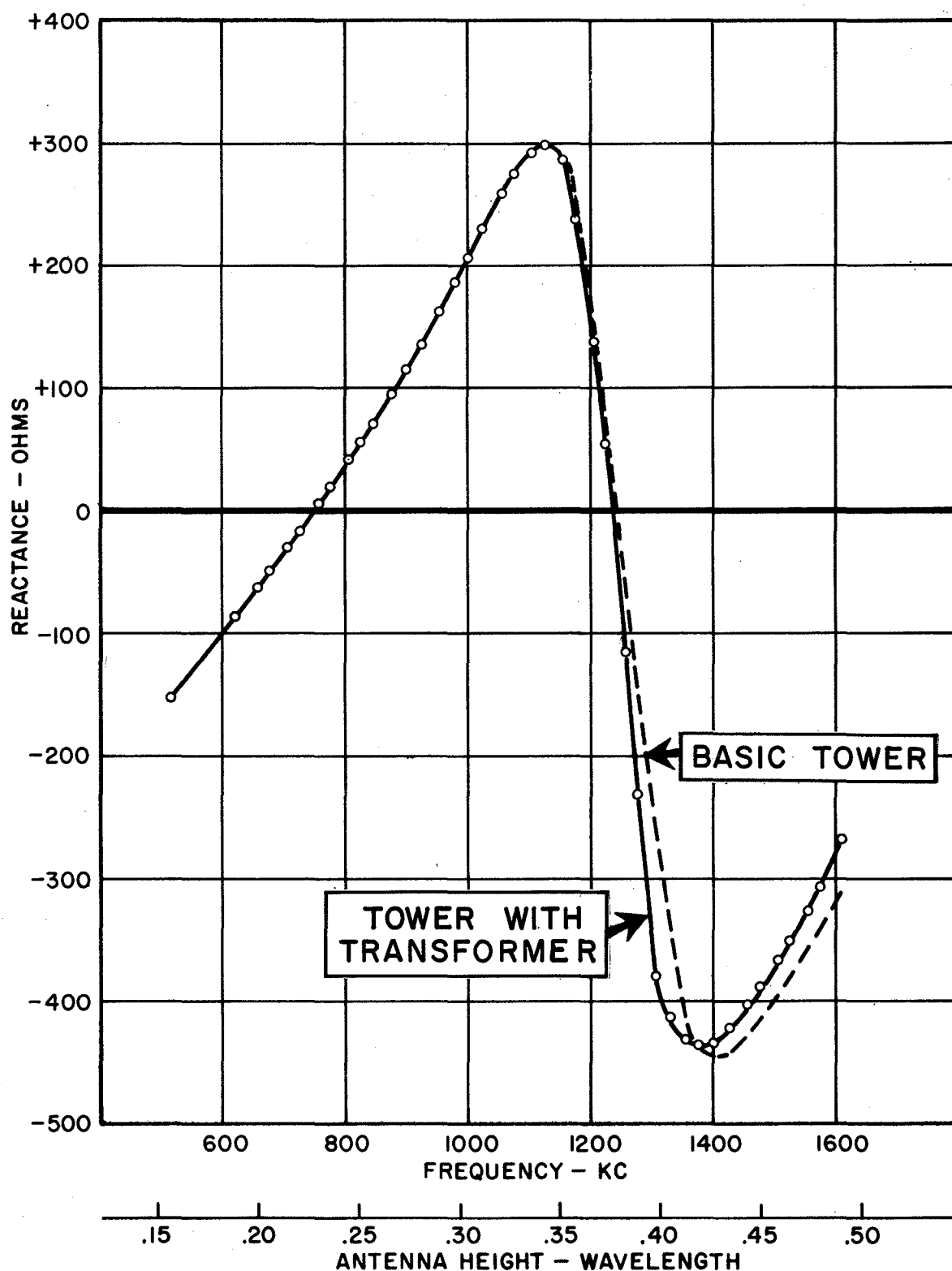
*Vir N. James*

CONSULTING RADIO ENGINEERS

1316 S. KEARNEY, DENVER 22, COLORADO SKYLINE 6-1603

FIGURE 8  
MARCH 1960

# TOWER REACTANCE VARIATION TRANSFORMER ISOLATION CIRCUIT



*Vir N. James*

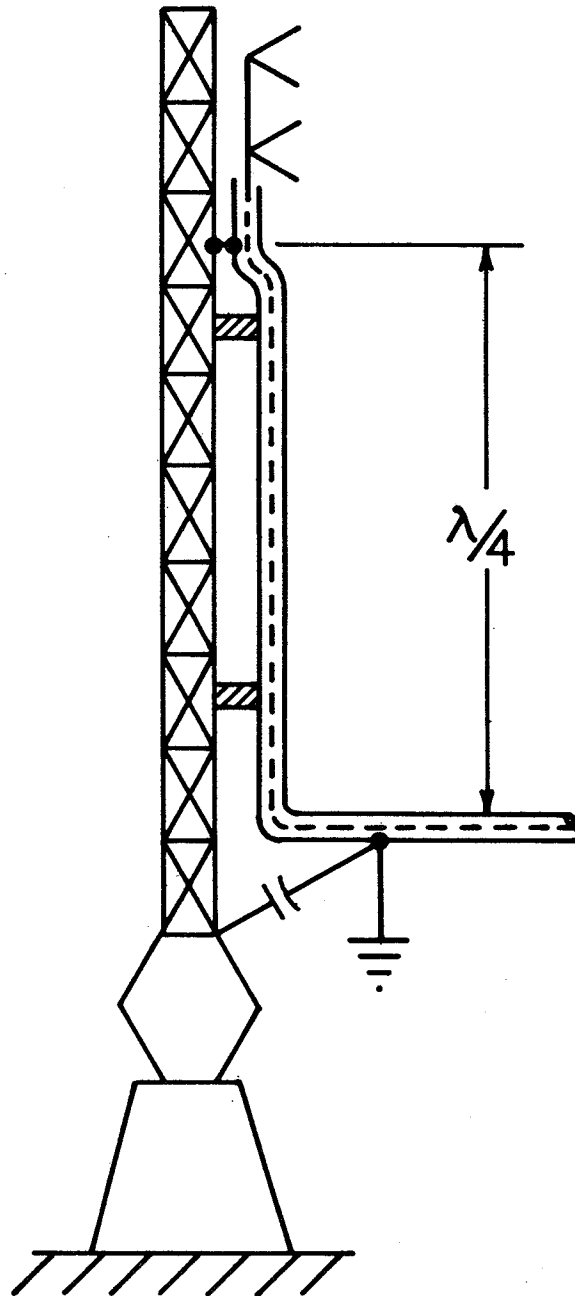
CONSULTING RADIO ENGINEERS

1316 S. KEARNEY, DENVER 22, COLORADO Skyline 6-1603

FIGURE 9

MARCH 1960

## 1/4-WAVE LINE ISOLATION



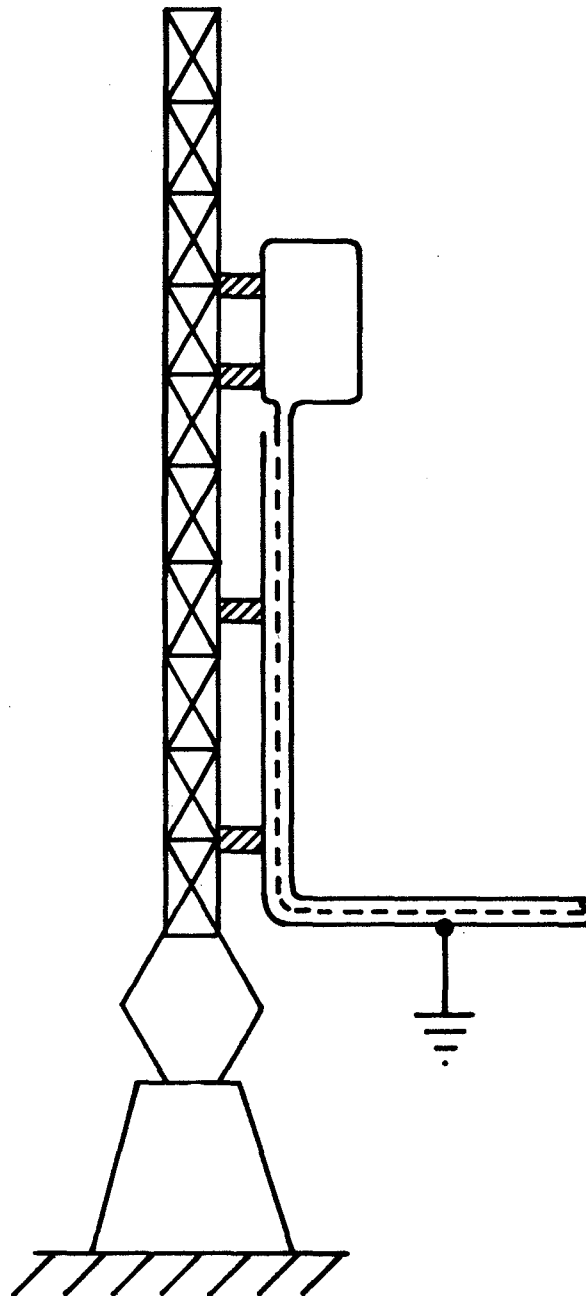
*Vir N. James*  
CONSULTING RADIO ENGINEERS

1316 S. KEARNEY, DENVER 22, COLORADO SKyline 6-1603

FIGURE 10  
MARCH 1960



# INSULATED SAMPLING LOOP ISOLATION



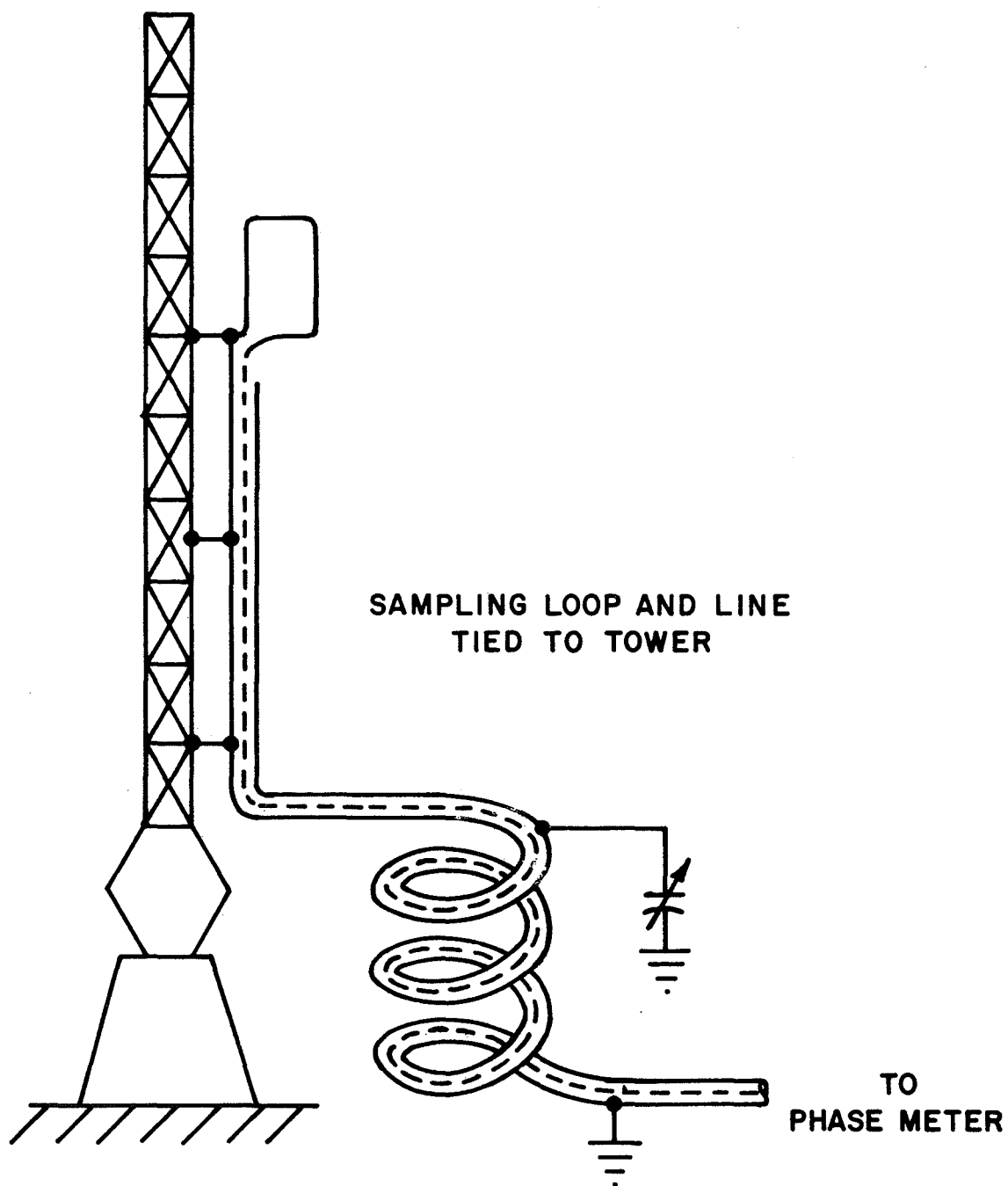
*Vir N. James*

CONSULTING RADIO ENGINEERS

1316 S. KEARNEY, DENVER 22, COLORADO SKyline 6-1603

FIGURE 11  
MARCH 1960

# PARALLEL RESONANCE ISOLATION



*Vir N. James*

CONSULTING RADIO ENGINEERS

1316 S. KEARNEY, DENVER 22, COLORADO Skyline 6-1603

FIGURE 12  
MARCH 1960

4/13/85  
Hansen

# THE EFFECT OF A QUARTER WAVELENGTH STUB ON MEDIUM WAVE ANTENNAS

Jerry M. Westberg

Harris Corporation, Broadcast Transmission Division

Quincy, Illinois

When an FM antenna is mounted on a medium wave tower, the coax must cross the base insulator of the tower. One popular method of crossing the base insulator with coax, is to have the coax insulated from the tower one quarter wavelength up the tower.

There is a common assumption that the performance of an antenna will not be affected by the bonding of coax one quarter wavelength up on a medium wave antenna (hereafter referred to as a quarter wavelength stub). It can be shown by measured and theoretical data that this assumption is not true. The base impedance of a 204° tower was measured before and after the installation of a quarter wavelength stub. The base impedance was then measured off-frequency to determine an equivalent Q for the two antennas. The equation used to compute equivalent Q is as follows:

$$Q_e = \frac{F}{2\Delta F} \left( \sqrt{VSWR} - \frac{1}{\sqrt{VSWR}} \right)$$

F = Frequency

$\Delta F$  = Frequency change from F

VSWR = VSWR caused by change in frequency

The base impedance of the tower changed from 58-J138 Ohms to 98-J281 Ohms. The equivalent Q of the antenna increased from 9.2 to 15.3.

The antenna was then modeled using a "method of moments" technique. For the analysis, an antenna and coax radius of .48 and .02 degrees, respectively, were used. The center-to-center separation of the antenna and coax is 1.14 degrees. The results were comparable to the measured data. The predicted impedances before and after the installation of a quarter wavelength stub are 54-J204 and 80-J379, respectively. The equivalent Q for each case was computed to be 13.9 and 18.4.

### VARY TOWER HEIGHT

Seven other antennas of different height were modeled. The same radii and separation was used. Base impedances and equivalent Qs were calculated for each antenna with and without a quarter wavelength stub. The results are found in table 1 below. These data are pictured on figures 1-3.

TABLE 1

TOWER HEIGHT (DEGREES)	IMPEDANCE OF TOWER (OHMS)	Q <sub>e</sub>	IMPEDANCE OF TOWER WITH STUB (OHMS)	Q <sub>e</sub>
92	65 + J77	5.2	310 + J136	4.6
102	104 + J144	4.7	473 - J424	4.7
122	308 + J297	3.9	548 - J589	6.8
143	836 + J19	4.1	328 - J631	9.1
163	398 - J493	5.3	198 - J569	11.6
184	126 - J343	8.9	123 - J484	14.6
194	79 - J269	11.2	98 - J434	16.4
204	54 - J204	13.9	80 - J379	18.4

Tower radius .48°

Stub radius .02°

Separation 1.14°

### VARY BONDING POINT

The equivalent Q of every antenna (except for 102° and 92°) was increased with the addition of a quarter wavelength stub. The distance from the ground to the point where the coax is bonded to the tower was adjusted and the results were recorded. The results are found in tables 2-6 below.

TABLE 2. 204 DEGREE TOWER

BONDING DISTANCE FROM GROUND (DEGREES)	IMPEDANCE OF TOWER WITH STUB (OHMS)	Q <sub>e</sub>
112	27 - J213	23.4
102	44 - J278	20.3
92	80 - J379	18.4
82	183 - J573	17.0
71	809 - J1011	15.5
66	2067 - J131	14.6
61	1011 + J1078	15.2

TABLE 3. 184 DEGREE TOWER

BONDING DISTANCE FROM GROUND (DEGREES)	IMPEDANCE OF TOWER WITH STUB (OHMS)	Q <sub>e</sub>
92	123 - J484	14.6
82	381 - J801	12.6
71	2075 - J290	11.4
66	1072 + J1036	10.9
61	384 + J828	12.2

TABLE 4. 143 DEGREE TOWER

BONDING DISTANCE FROM GROUND (DEGREES)	IMPEDANCE OF TOWER WITH STUB (OHMS)	Q <sub>e</sub>
92	328 - J631	9.1
82	1248 - J594	7.5
76	1428 - J295	7.0
71	791 + J768	7.3
66	391 + J658	7.4

TABLE 5. 102 DEGREE TOWER

BONDING DISTANCE FROM GROUND (DEGREES)	IMPEDANCE OF TOWER WITH STUB (OHMS)	Q <sub>e</sub>
92	473 - J424	4.7
87	630 - J344	4.0
82	588 + J226	4.3

TABLE 6. 92 DEGREE TOWER

BONDING DISTANCE FROM GROUND (DEGREES)	IMPEDANCE OF TOWER WITH STUB (OHMS)	Q <sub>e</sub>
92	310 + J136	4.6
82	179 + J146	4.8

The base impedance of a 209 degree tower was measured. The tower has a 1" electrical conduit and 7/8" coax insulated from the tower one quarter wavelength up the tower. The base impedance of the tower with a quarter wavelength stub is 74 - J263 ohms. The equivalent Q of the antenna is 19.8.

The coax and conduit were then bonded to the tower at different heights. The tower base impedance was swept each time the bonding strap was moved and an equivalent Q was computed. The results are found in table 7 below.

TABLE 7. MEASURED 209 DEGREE TOWER

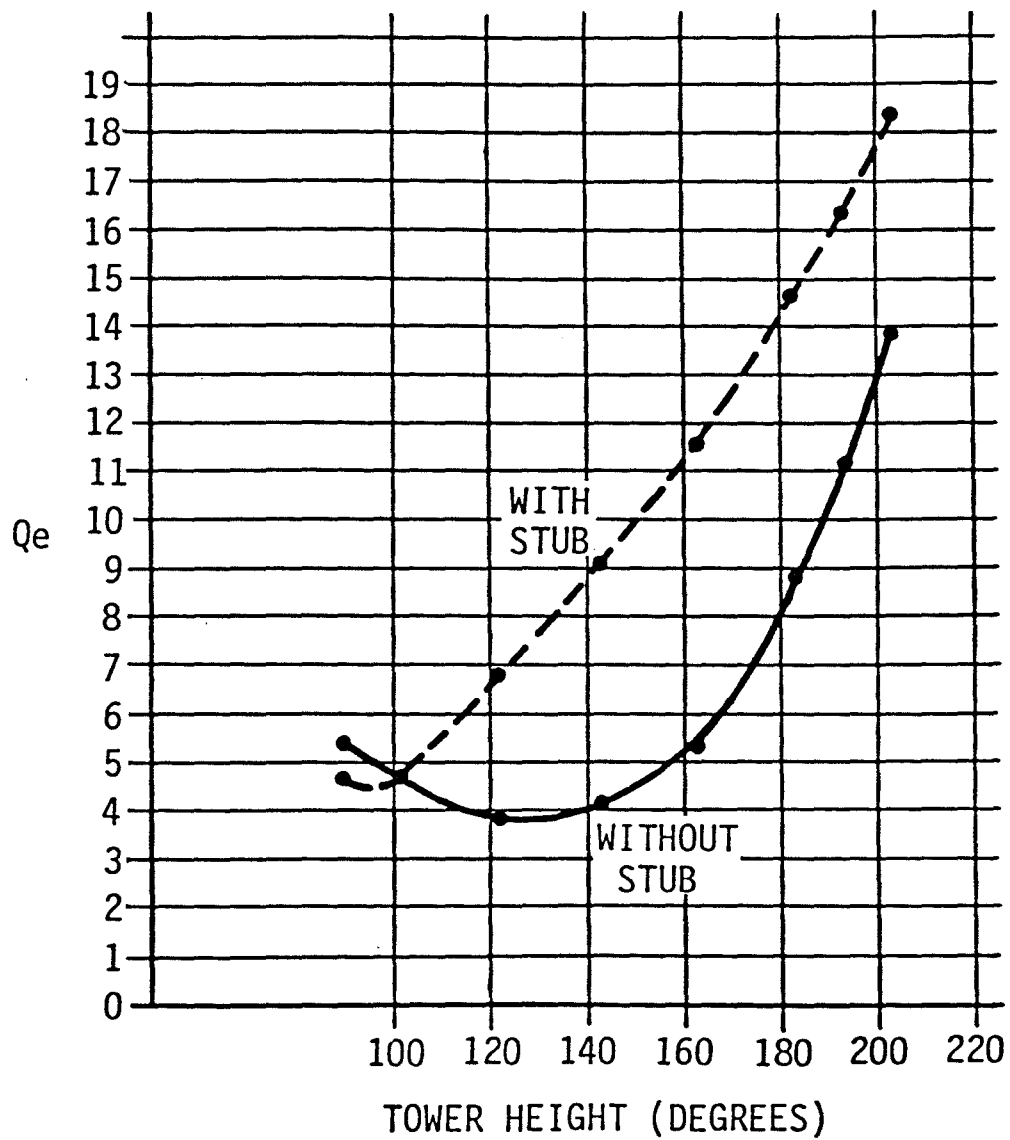
BONDING DISTANCE FROM GROUND (DEGREES)	IMPEDANCE OF TOWER WITH STUB (OHMS)	Q <sub>e</sub>
90	74 - J263	19.8
80	114 - J332	18.4
75	149 - J375	17.4
70	209 - J446	16.2
65	310 - J520	15.8
60	529 - J586	14.9
55	919 - J533	15.4
45	595 + J658	15.5

CONCLUSION

The impedance of a medium wave antenna is affected by the presence of a quarter wavelength stub. The magnitude of change in impedance depends on the tower height.

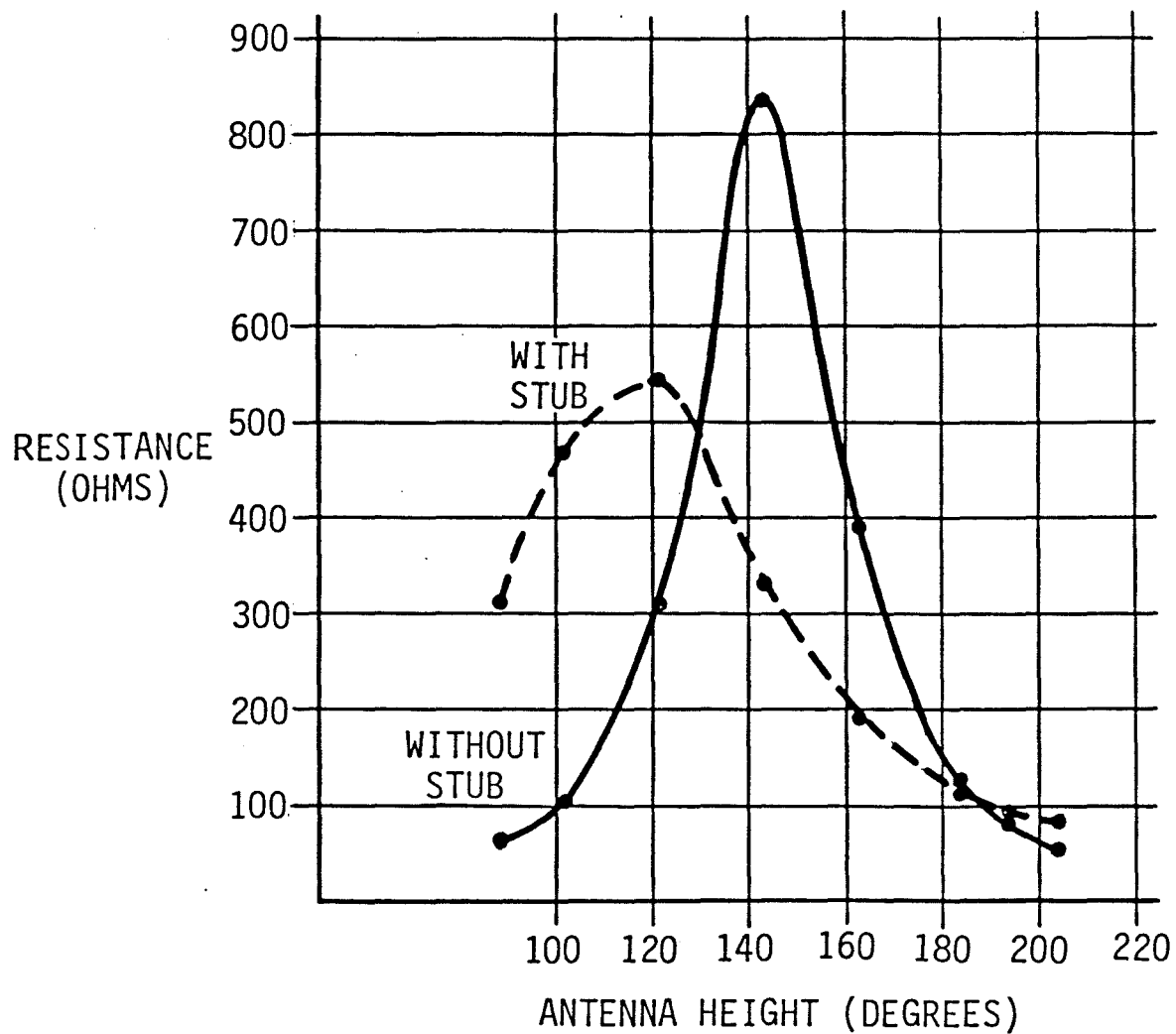
The bandwidth of an antenna is influenced by the presence of a quarter wavelength stub. For tower heights above 102 degrees the data suggest that the stub adversely affects the bandwidth of the antenna. The presence of a quarter wavelength stub will increase the bandwidth of a medium wave antenna for heights less than 102°.

The bandwidth of the antenna with a quarter wavelength stub may be improved by adjusting the height above ground where the stub is bonded to the tower. For maximum bandwidth the bonding point of the stub varied from 66° for a 204° tower to 90° for a 92° tower. It should also be noted that the maximum bandwidth point of attachment appears to occur when the tower base impedance is close to resonance. This provides a good benchmark for field adjustment. The bonding point of the stub to the tower may be lowered until the base impedance of the tower is resonant.



Tower radius .48 degrees  
Stub radius .02 degrees  
Separation 1.14 degrees

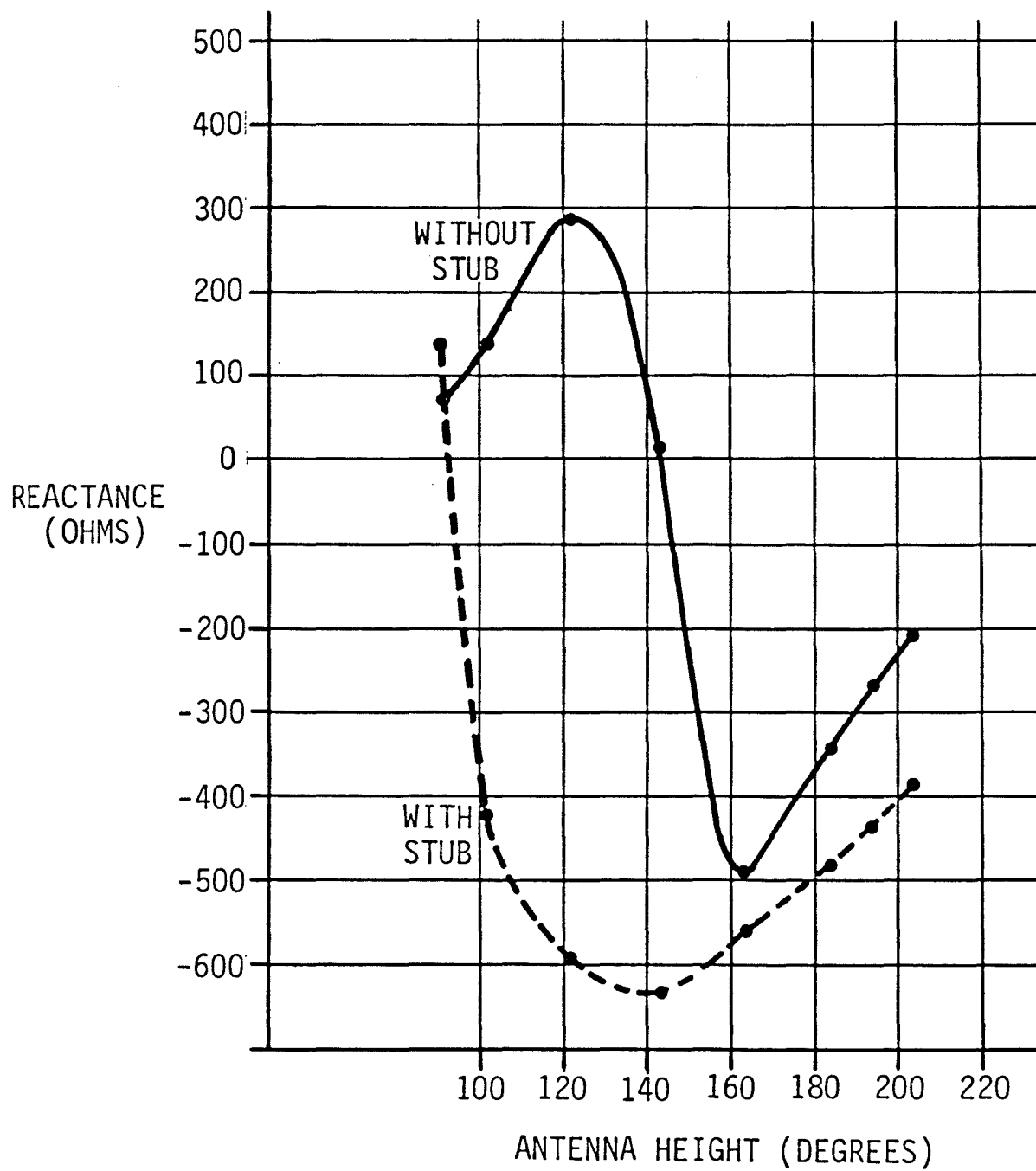
Figure 1. Equivalent Q vs Tower Height  
With and Without a Quarter Wavelength Stub



Tower radius .48 degrees  
Stub radius .02 degrees  
Separation 1.14 degrees

Figure 2. Resistance vs Tower Height  
With and Without a Quarter Wavelength Stub





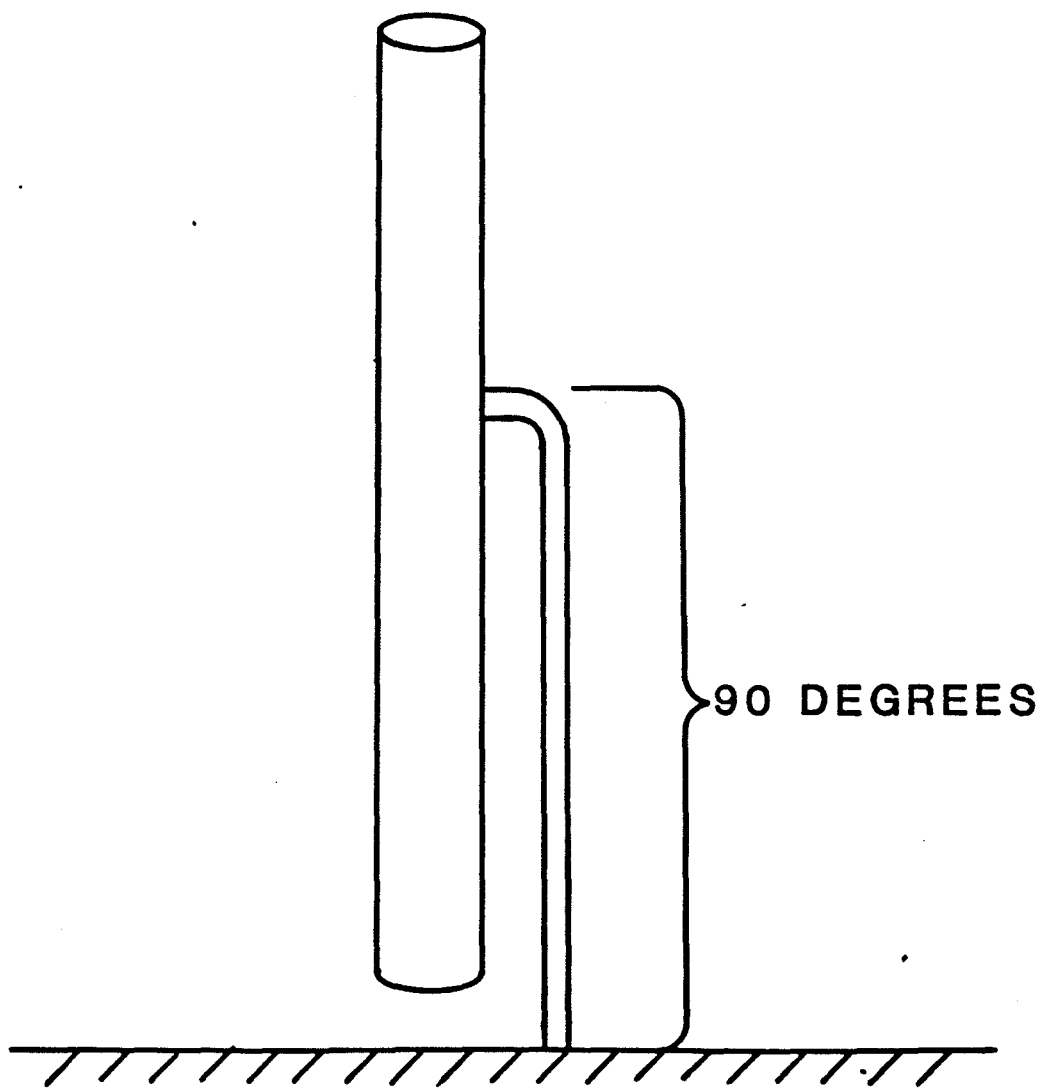
Tower radius .48 degrees  
 Stub radius .02 degrees  
 Separation 1.14 degrees

Figure 3. Reactance vs Tower Height  
 With and Without a Quarter Wavelength Stub

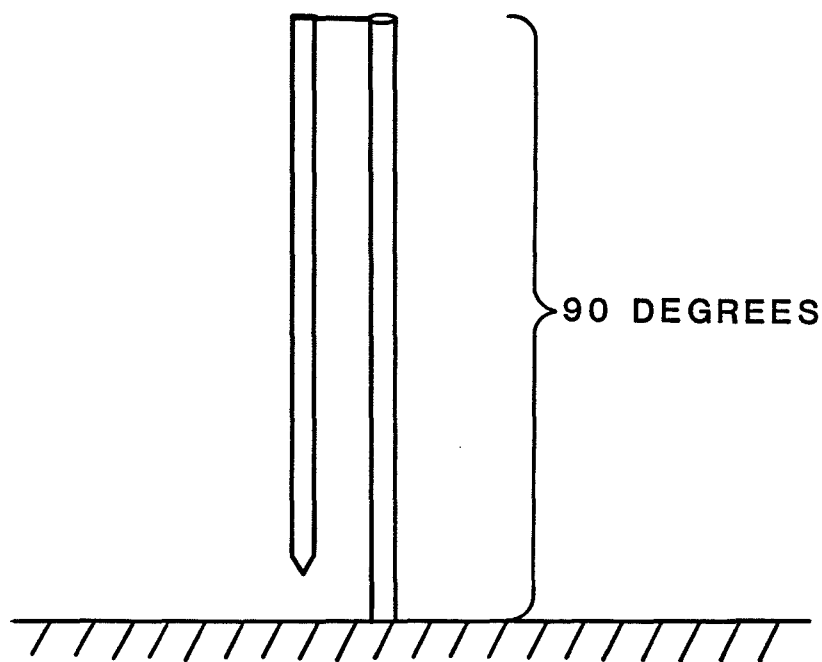
#### REFERENCES

Dah-Cheng Kuo and Bradley J. Strait, Improved Programs for Analysis of Radiation and Scattering by Configurations of Arbitrarily Bent Thin Wires (Department of Electrical and Computer Engineering, Syracuse University, Syracuse, New York 13210)(AFCRL-72-0051).

Warren L. Stutzman and Gary A. Thiele, Antenna Theory and Design (John Wiley & Sons, Inc., 1981) pp. 205-212.

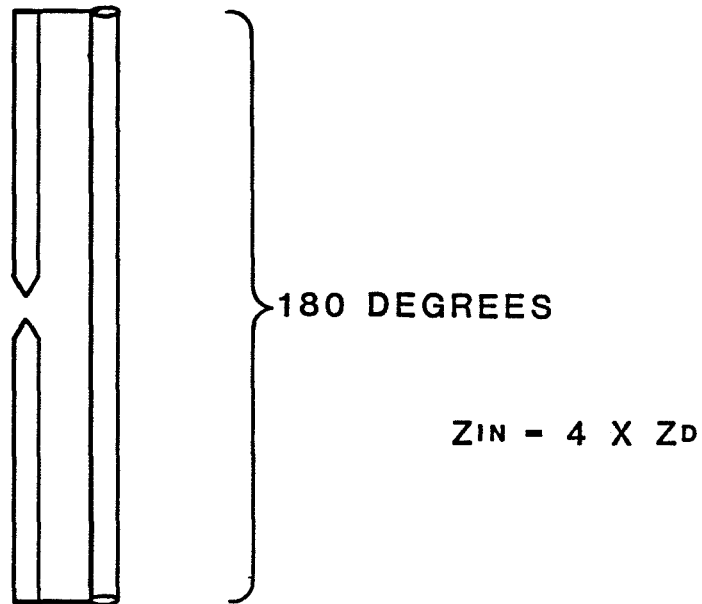


03730



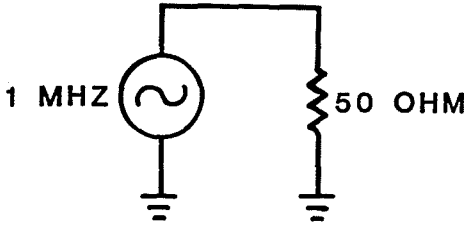
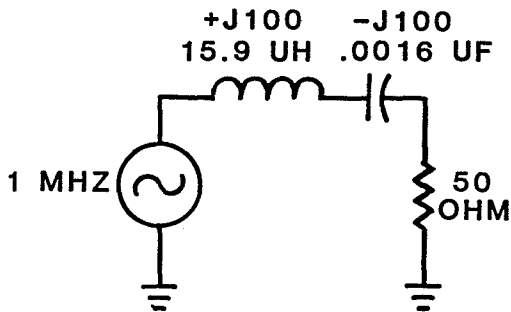
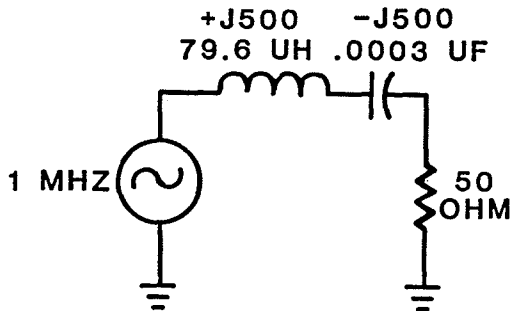
90 DEGREE MONOPOLE WITH  
QUARTER WAVELENGTH STUB

03783



REFLECTION OF MONOPOLE  
IS A FOLDED DIPOLE

003930

CIRCUIT	IMPEDANCE $\pm 10$ KHZ	VSWR $\pm 10$ KHZ	ACTUAL Q
	$50 + j0$ OHMS	1:1	0
	$50 \pm j2.5$ OHMS	1.05:1	2
	$50 \pm j10$ OHMS	1.2:1	10

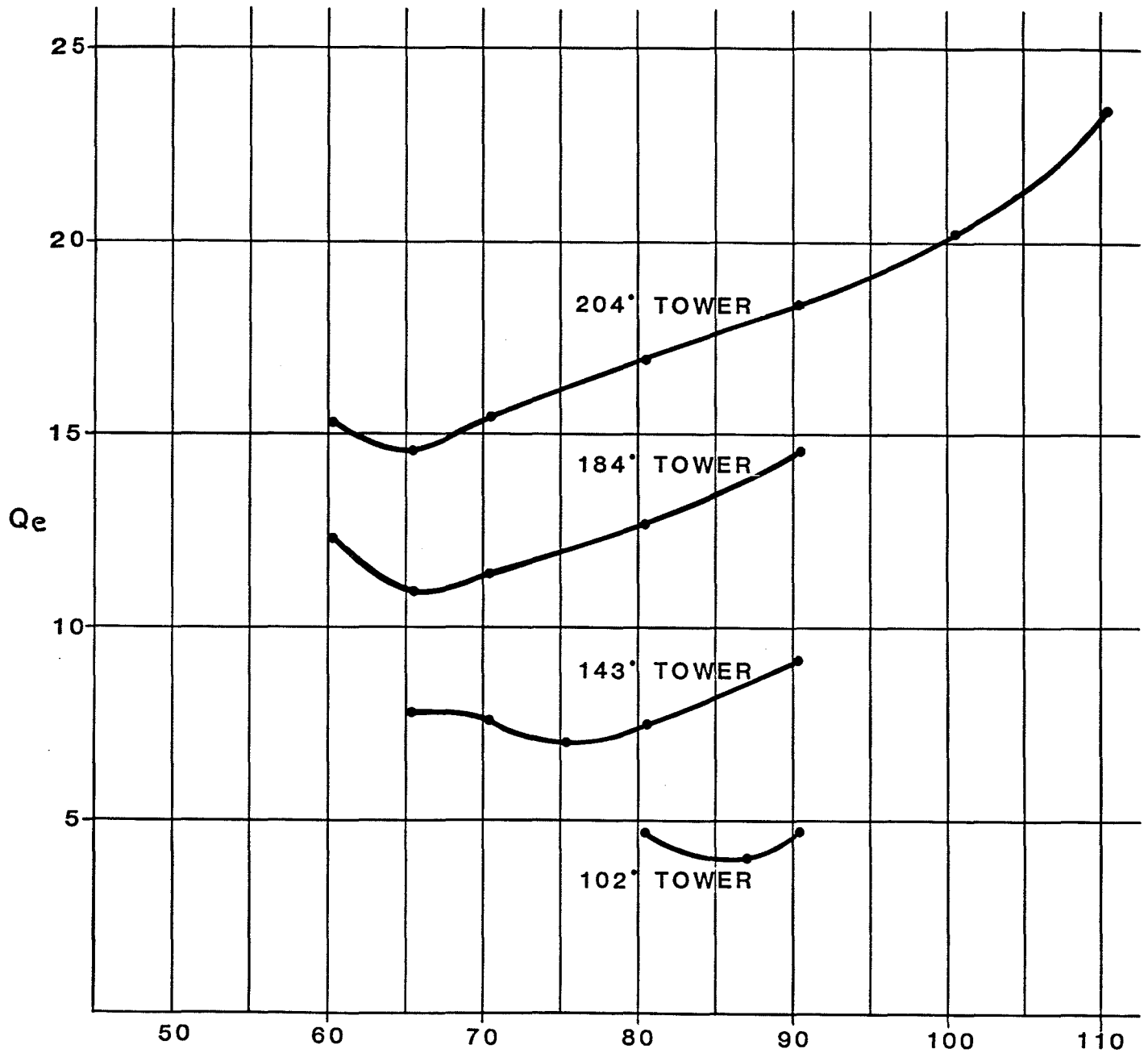
WASG 204° TOWER

	WITHOUT STUB		WITH STUB	
	MEASURED	PREDICTED	MEASURED	PREDICTED
Q <sub>E</sub>	9.2	13.9	15.3	18.4
Z	58 - J138	54 - J204	98 - J281	80 - J379

WVLN 148° TOWER

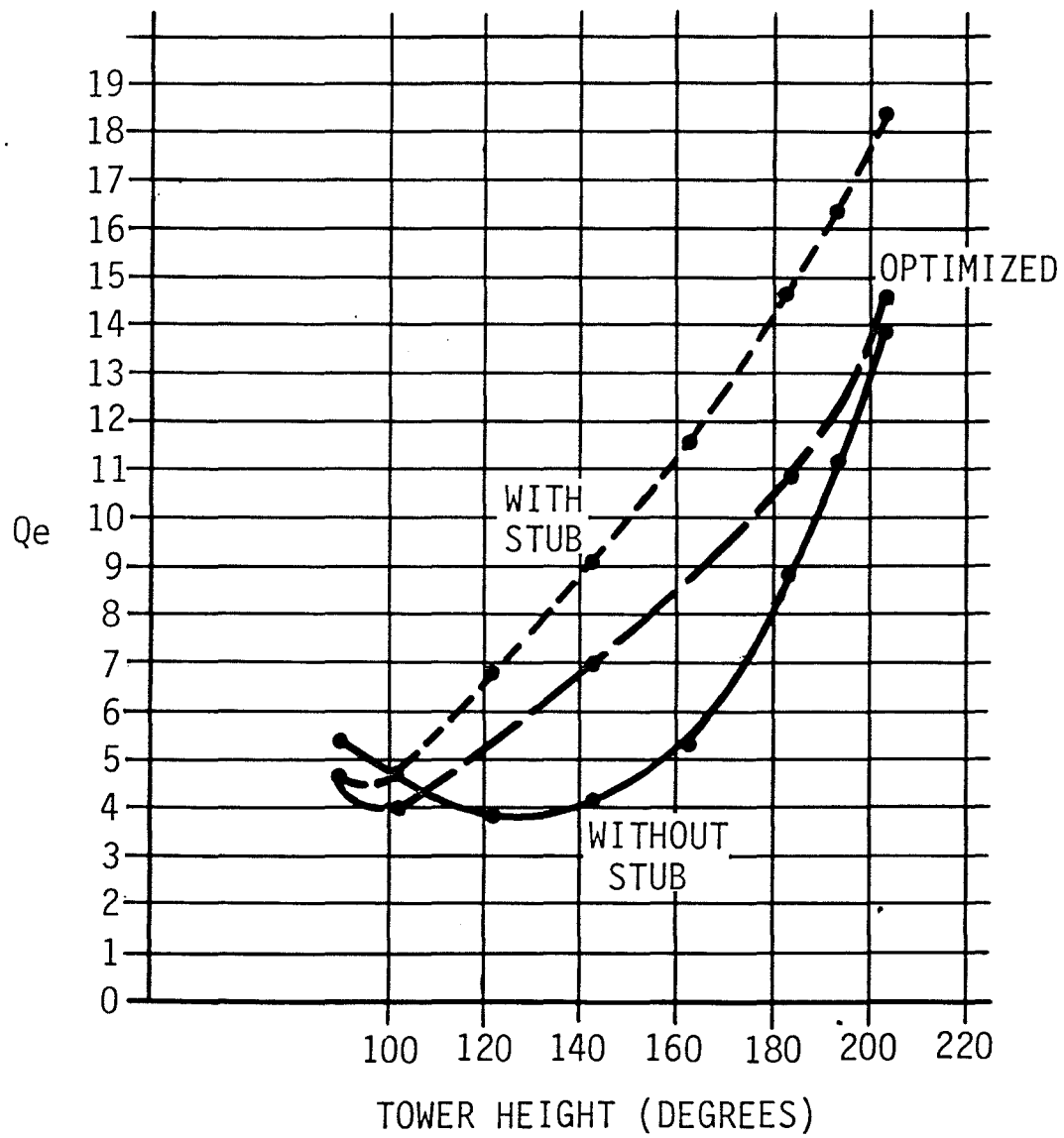
	WITHOUT STUB		WITH STUB	
	MEASURED	PREDICTED	MEASURED	PREDICTED
Q <sub>E</sub>	-	4.1	12.5	11.1
Z	-	823 - J216	252 - J433	247 - J560

00730



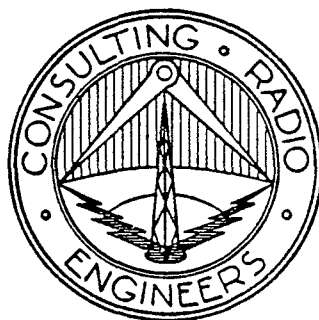
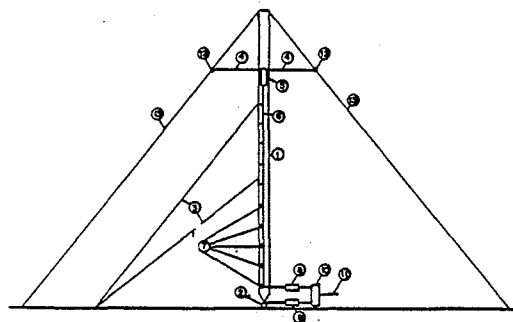
HEIGHT ABOVE GROUND WHERE STUB  
IS BONDED TO THE TOWER (DEGREES)





9/20/85  
AM  
ANTENNAS

A NEW DIMENSION  
FOR THE DESIGN OF  
MEDIUM WAVE ANTENNAS



Copyright, 1985, A. D. Ring & Associates, P. C.  
PRESENTED BY OGDEN PRESTHOLDT  
AT THE IEEE  
35th ANNUAL BROADCAST SYMPOSIUM  
SEPTEMBER 20, 1985

A. D. RING & ASSOCIATES, P.C.

WASHINGTON, D.C.

# A NEW DIMENSION FOR THE DESIGN OF MEDIUM WAVE ANTENNAS

## I INTRODUCTION AND SUMMARY

In the medium wave (AM radio) band directional antennas are frequently used both to provide service to specified areas and to minimize interference to other radio stations. There are two basic modes of propagation which occur at these frequencies. During both the daytime and nighttime a ground wave signal is propagated. Further, during the nighttime a second method of propagation occurs, a signal is reflected from the ionosphere and returns to the earth at greater distances with significantly less attenuation than that suffered by the ground wave. Conventional directional antennas suppress both the ground wave and the sky wave and consequently some desired ground wave service may be lost in order to minimize the sky wave interference to other stations.

It is proposed to use a combination of vertical, horizontal and diagonal antenna segments to obtain significant separate control over the ground wave and sky wave radiation. These various antenna segments will have to be excited with carefully chosen current amplitudes and phases in order to obtain this control. It has been found that the currents and phases associated with "Tee" or "L" antennas as used in the past have not provided this choice of amplitude and phase.

In order to illustrate this concept a model vertical antenna with a center fed horizontal antenna centered above the mid height of the vertical antenna will be described. It is shown that the model and other antennas utilizing this principle can provide improved ground wave service and better sky wave protection that can be obtained with the use of vertical antennas alone.

## II MODEL ANTENNA

Figure 1 is a set of cartesian and spherical coordinates chosen to describe the model and its radiation characteristics. The ground plane is the X-Y plane and the positive Z direction is toward the zenith. The positive R direction is out from the origin, positive Theta is away from the zenith (Z axis), and positive Psi is counter clockwise from the X axis.

Figure 2 shows the principle features of the model. A typical 190 degree base fed vertical antenna tower (#1), base insulator (#2) and support guy cables (#3) is shown. At the 145 degree height a center fed horizontal antenna (#4) is shown. It is oriented parallel to the Y axis. Its ends would be supported by insulators (#12) and an auxiliary set of transparent guy cables at a 45 degree angle (#13) thus making each half of the antenna 45 degrees in length. The horizontal element would be fed from a balanced feed network (#5) supported in the tower. This network would be fed by a

coaxial transmission line (#6) supported inside the tower and insulated (#7) from the tower for the bottom 90 degrees. A power and phase control network (#8) would feed the transmission line for the horizontal antenna. A conventional matching network (#9) would be provided for the vertical antenna. A typical combining network (#10) would be used to combine the antennas for a common feed line (#11).

### III CALCULATION OF RADIATION

The radiation from such an antenna can be analyzed by separately developing the equations for the total radiation from each of the elements. For this analysis sinusoidal current distribution is assumed. The far field was calculated by the integration of the antenna current elements and their images for each antenna segment.

There is only a Theta component of the electric field for a vertical antenna, it is given by the following equation:

$$E(\theta) = \frac{60I(l_v)}{R(\theta)} \sin(\theta) [\cos(Bh \cos(\theta)) - \cos(Bh)] \quad (1) \text{ Volts per meter}$$

Where  $I(l_v)$  = vertical antenna loop current in amperes  
 (its phase is assumed to be zero)  
 $R(\theta)$  = distance to observation point in meters

Bh = electrical height of the vertical antenna  
 Th = the angle Theta

Using the same procedure the Theta and Psi fields (there is no radial component) from the horizontal wire are given by the following equations:

$$E(Th) = - \frac{120 I(lh) [(F1)(M1)(M2)(M3)]}{R(0)[1 - \sin(Th)\sin(Psi)]} \quad (2) \text{ Volts per meter}$$

$$E(Psi) = - \frac{120 I(lh) [(F1)(M1)(M4)(M3)]}{R(0)[1 - \sin(Th)\sin(Psi)]} \quad (3) \text{ Volts per meter}$$

Where I(lh) = the magnitude of the loop current in the horizontal wire

Ph = the phase of the loop current  
 F1 =  $\cos(Ph) + j\sin(Ph)$   
 M1 =  $\sin(Ba\cos(Th))$   
 M2 =  $\cos(Th)\sin(Psi)$   
 M3 =  $\cos(Bl)\sin(Th)\sin(Psi) - \cos(Bl)$   
 M4 =  $\cos(Th)\cos(Psi)$   
 Ba = the electrical height of the horizontal wire  
 Bl = the electrical half length of the horizontal wire

Note that the  $E(\theta)$  components in equations 1 and 2 are in time quadrature, this may be the reason that the concept was not previously discovered!

#### IV CALCULATION OF CONIC SECTIONS

The radiation from the model antenna is best described with the use of a series of conic sections. A computer program was written to perform the necessary calculations. By means of a hemispherical integration the total power flow for both the  $\theta$  and  $\psi$  components of field were summed up and a multiplication factor established to correct the assumed currents so that the radiated fields would be in mV/m at one kilometer for one watt.

In the model it is assumed that the vertical antenna has a loop current of 1.00 at a phase of 0 degrees. The horizontal antenna has a loop current of 5.00 at a phase of 90 degrees. In this example the calibration factor was found to be 0.06875. Thus the actual currents would be 0.06875 amperes for the vertical antenna and 0.3438 amperes for the horizontal antenna.

Pertinent conic sections were then drawn by the computer for the model antenna. In the following conic section graphs it is assumed that each antenna is operating with the current that is necessary for the combined system to radiate one watt.

Figure 3 shows the conic sections for the  $E(\Theta)$  component from the vertical antenna alone, as expected they all show an omnidirectional pattern. Note that  $\Theta = 90$  degrees corresponds to an angle of elevation of zero.

Figure 4 shows the conic sections for the  $E(\Theta)$  component from the horizontal antenna only. At an azimuth or  $\Psi$  angle of 0 and 180 degrees there is no  $E(\Theta)$  component because that direction is at right angles to the horizontal wire. Also at an azimuth of 90 and 270 degrees (the direction of the horizontal wire) the  $\Theta$  radiation is zero on the ground ( $\Theta=90$ ) and goes through a maximum at  $\Theta$  approximately 30 degrees.

Figure 5 shows the conic sections for the  $E(\Psi)$  component from the horizontal antenna. Note that this is the only  $E(\Psi)$  component so it is also the total  $e(\Psi)$  component.

Figure 6 shows the conic sections for the total  $E(\Theta)$  field. For  $\Theta = 90$  degrees (on the ground) the field is omnidirectional. As the angle of elevation increases ( $\Theta$  decreases) the  $E(\Theta)$  component first decreases, goes through zero and then increases.

#### V ALLOCATIONS IMPACT

Figure 7 illustrates two AM stations service areas under several different operating conditions. They operate with a power of 1 kW utilizing 190 degree vertical antennas on 1000



kHz separated by 260 miles in an area where the conductivity is 10 mmhos per meter and the dielectric constant is 15. The illustration shows to approximate scale the daytime ground wave service, the nighttime service as it would be limited by sky wave interference with the vertical antenna only and the improved night time service that would result from the use of the model antenna with the horizontal element.

Figure 8 shows the ground wave field strength versus distance from both the vertical antenna alone and with the addition of the horizontal antenna and the interference producing sky wave signal of the other station.

The station is protected during the daytime to its 0.43 mV/m ground wave contour. Its 0.5 mV/m contour occurs at 60.5 miles. At night with the same power and antennas the interference limit is to the approximate 6.8 mV/m contour which occurs at 17 miles.

Now with the model antenna which has a horizontal antenna added with the appropriate current amplitude and phase the nighttime limit is reduced to the approximate 1.3 mV/m contour which now occurs at 33 miles. To obtain this change in vertical pattern from the model a ratio of horizontal loop current to vertical antenna current of 5/1 is required. A phase of +90 degrees was required assuming that the horizontal wire was parallel to the line joining the stations and that the reference of zero degrees corresponds to current flow toward the other station.

For the same input power to the combined antenna system this addition of the horizontal antenna reduced the RMS of the ground wave to 65 percent of its former value. In spite of this reduction in ground wave efficiency the service radius is nearly doubled.

Figure 9 shows the behavior of several examples of the use of the horizontal wire in antennas. All are oriented and adjusted to fit the allocation situation outlined above and to protect a second station 260 miles in the 90 degree direction. The top of the figure shows 5 different model antennas. PA is the example just described. PB is a typical two element directional antenna using 90 degree towers. PC is a directional antenna consisting of two 135 degree elements with a horizontal wire on one vertical antenna. PD is another two element antenna with 90 degree towers. PE is another single tower example with the vertical antenna 135 degrees in height. The graph on the left shows the vertical radiation pattern of each of these antennas in the 90 degree direction. The graph on the right is the horizontal radiation pattern for each antenna with a radiated power of one watt.

These examples are offered for illustrative purposes only and are not intended to represent the optimum that can be achieved with the proposed antenna concept.

## VI CONCLUSIONS

An antenna system consisting of both vertical and horizontal radiating elements has been described. It truly adds another dimension or perhaps several dimensions to the design of medium wave antennas. It is not yet known how versatile the system will eventually be but it is anticipated that it will permit new stations to be added to the spectrum, for existing stations to improve their local service and to result in reduced interference to many stations.

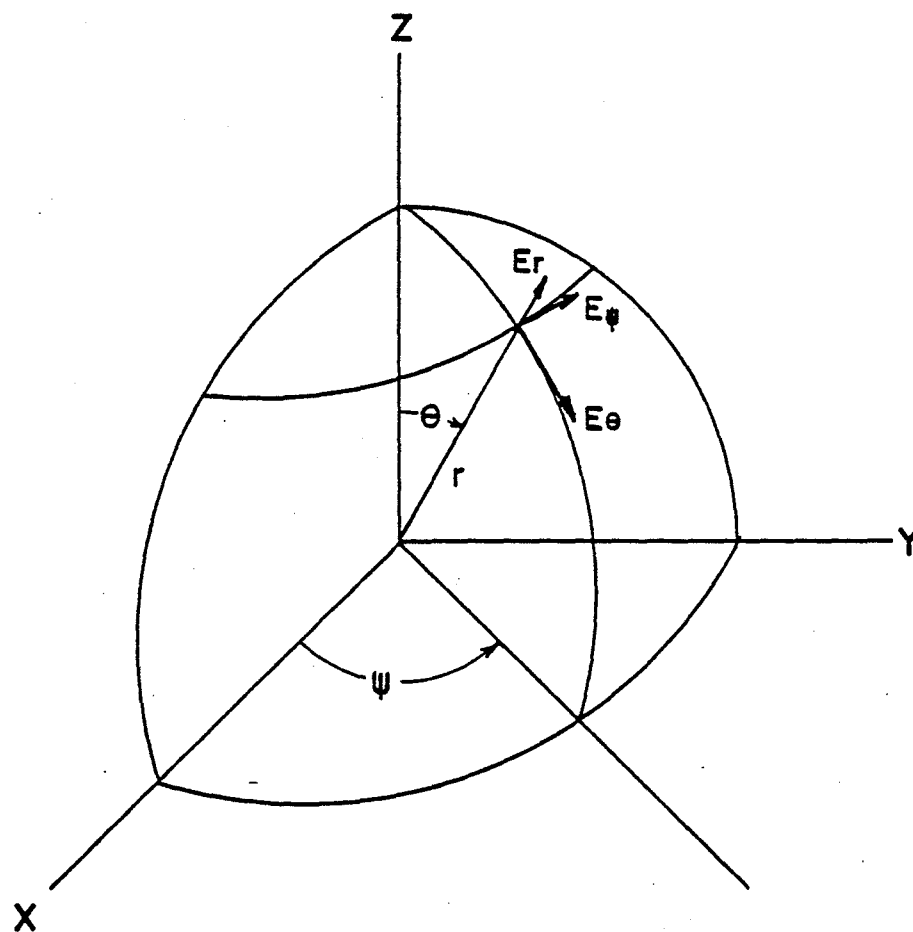


FIGURE 1

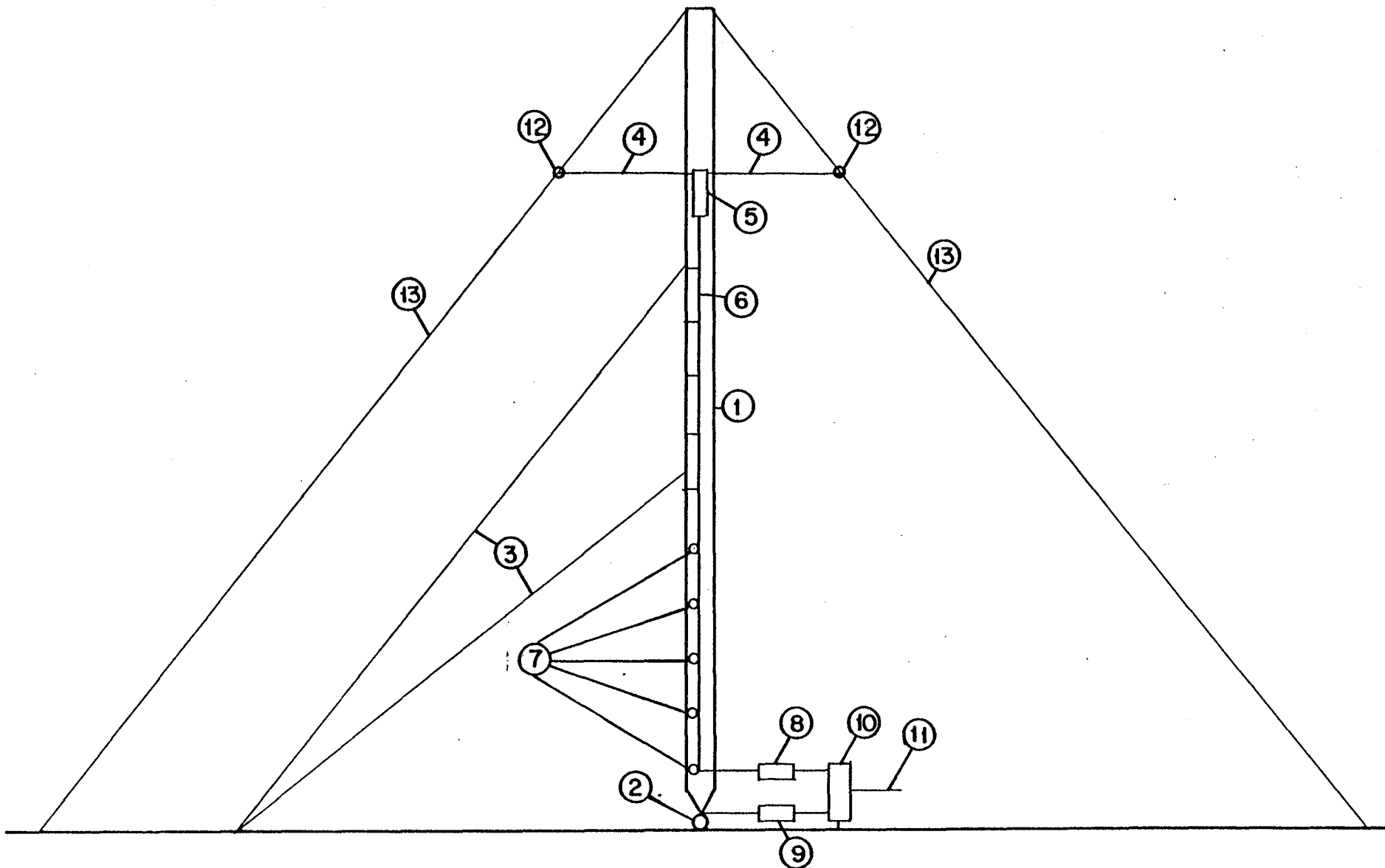
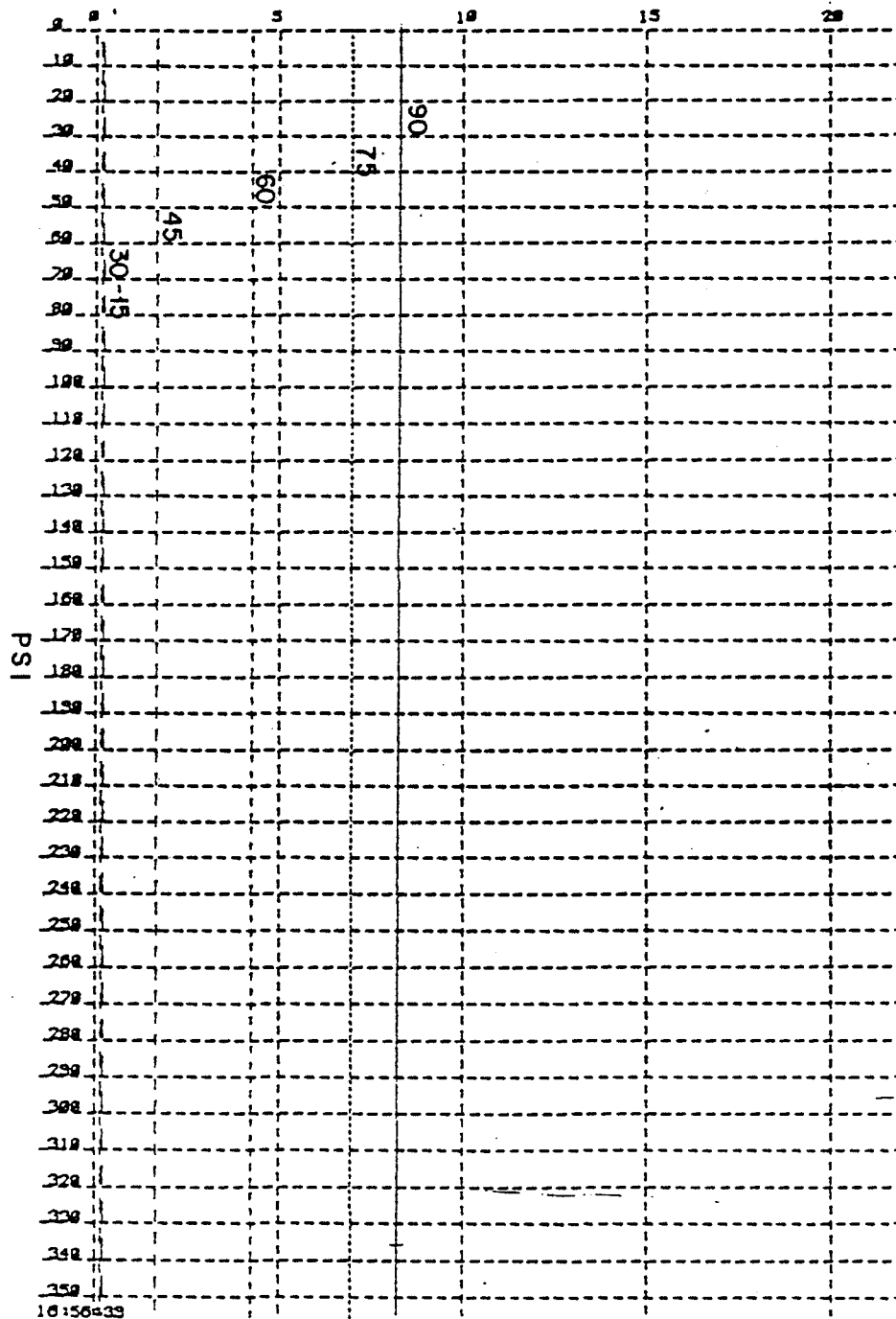


FIGURE 2

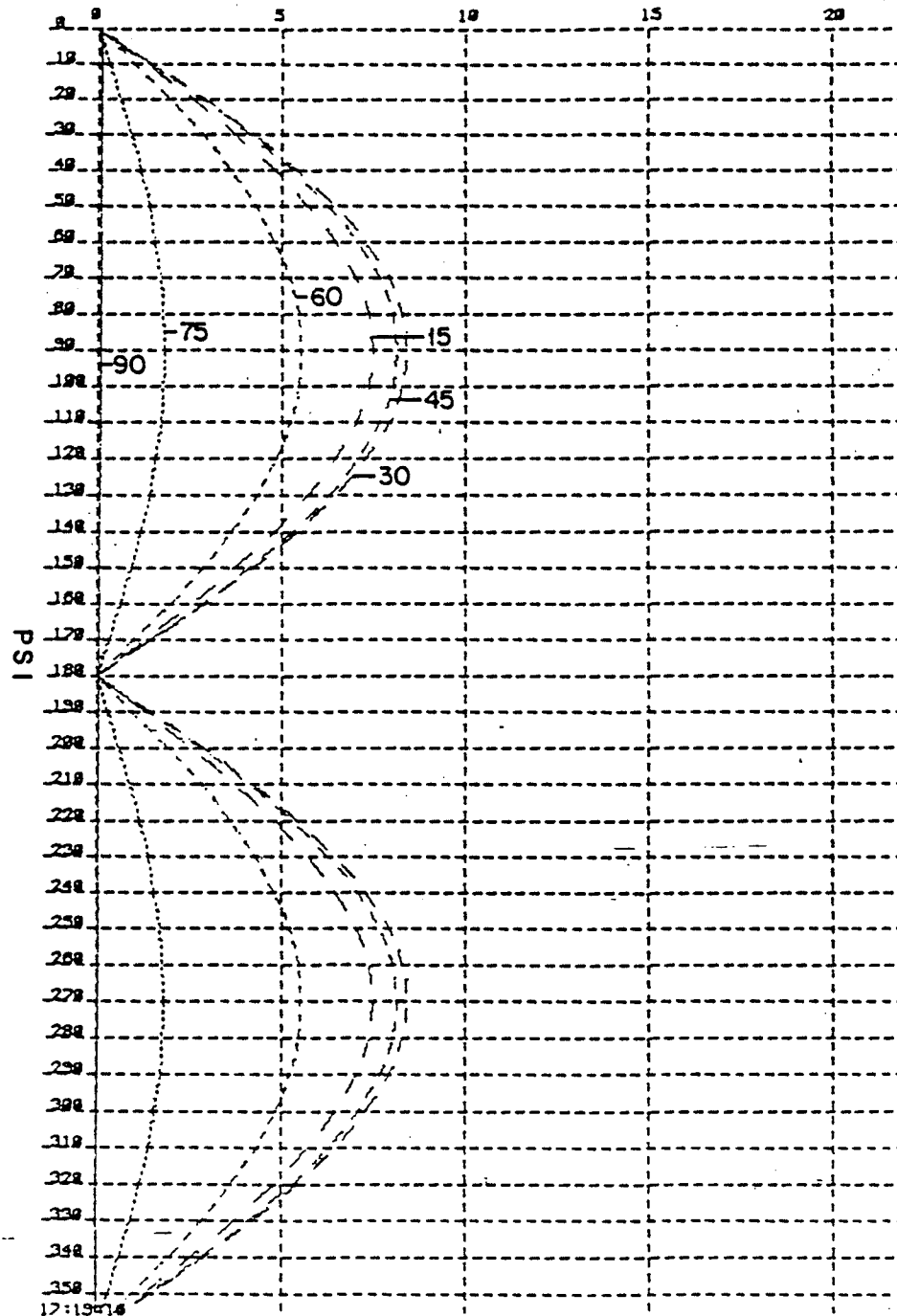
CONIC SECTIONS  
 PARAMETER IS THETA  
 mV/m AT 1 Km. FOR 1 Watt



E (TH) FOR VERTICAL ANTENNA

FIGURE 3

CONIC SECTIONS  
 PARAMETER IS THETA  
 mV/m AT 1 Km. FOR 1 Watt



E (TH) FOR HORIZONTAL ANTENNA

FIGURE 4

CONIC SECTIONS  
 PARAMETER IS THETA  
 mV/m AT 1 Km. FOR 1 Watt

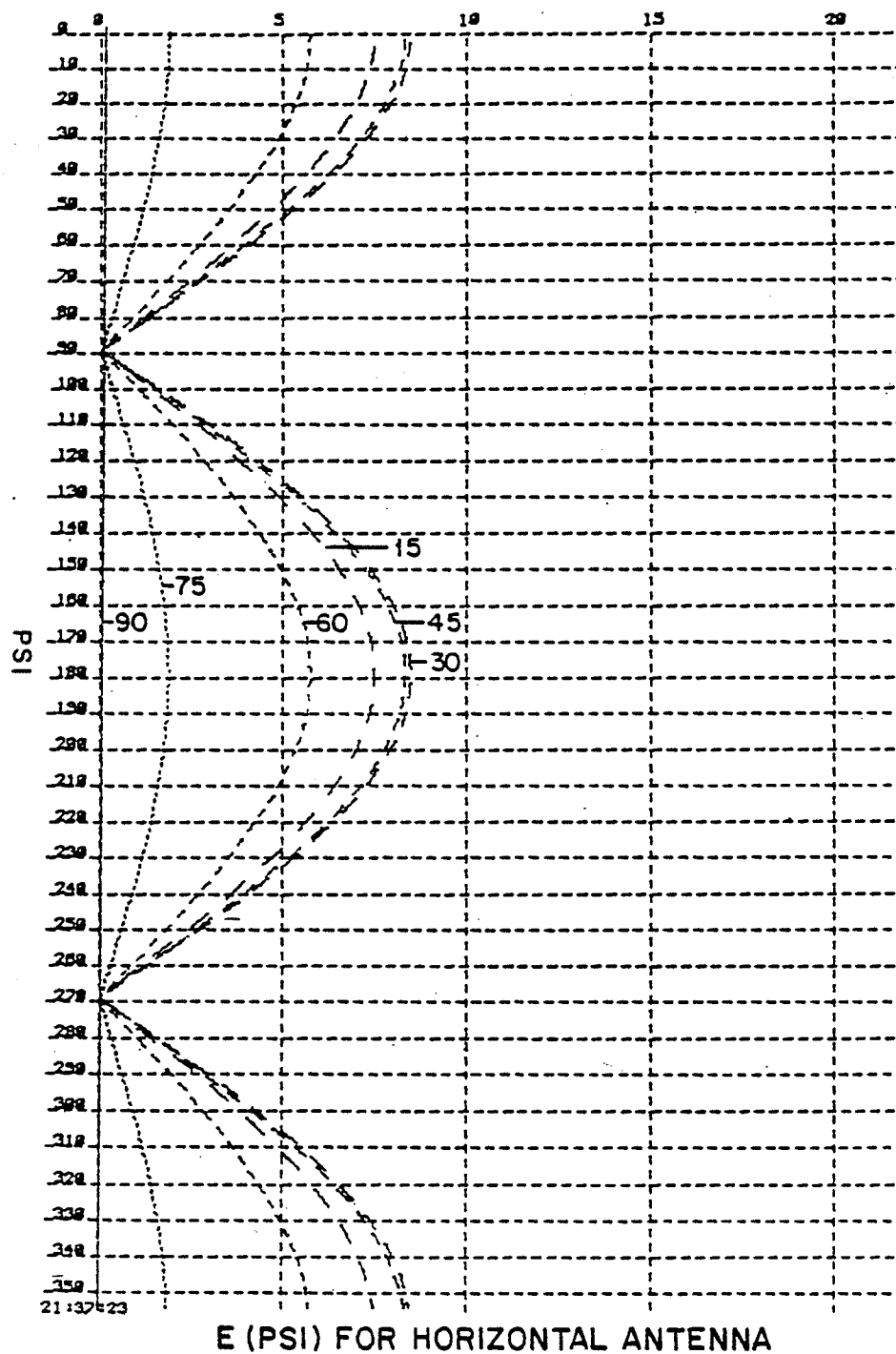


FIGURE 5



CONIC SECTIONS  
 PARAMETER IS THETA  
 mV/m AT 1 Km. FOR 1 Watt

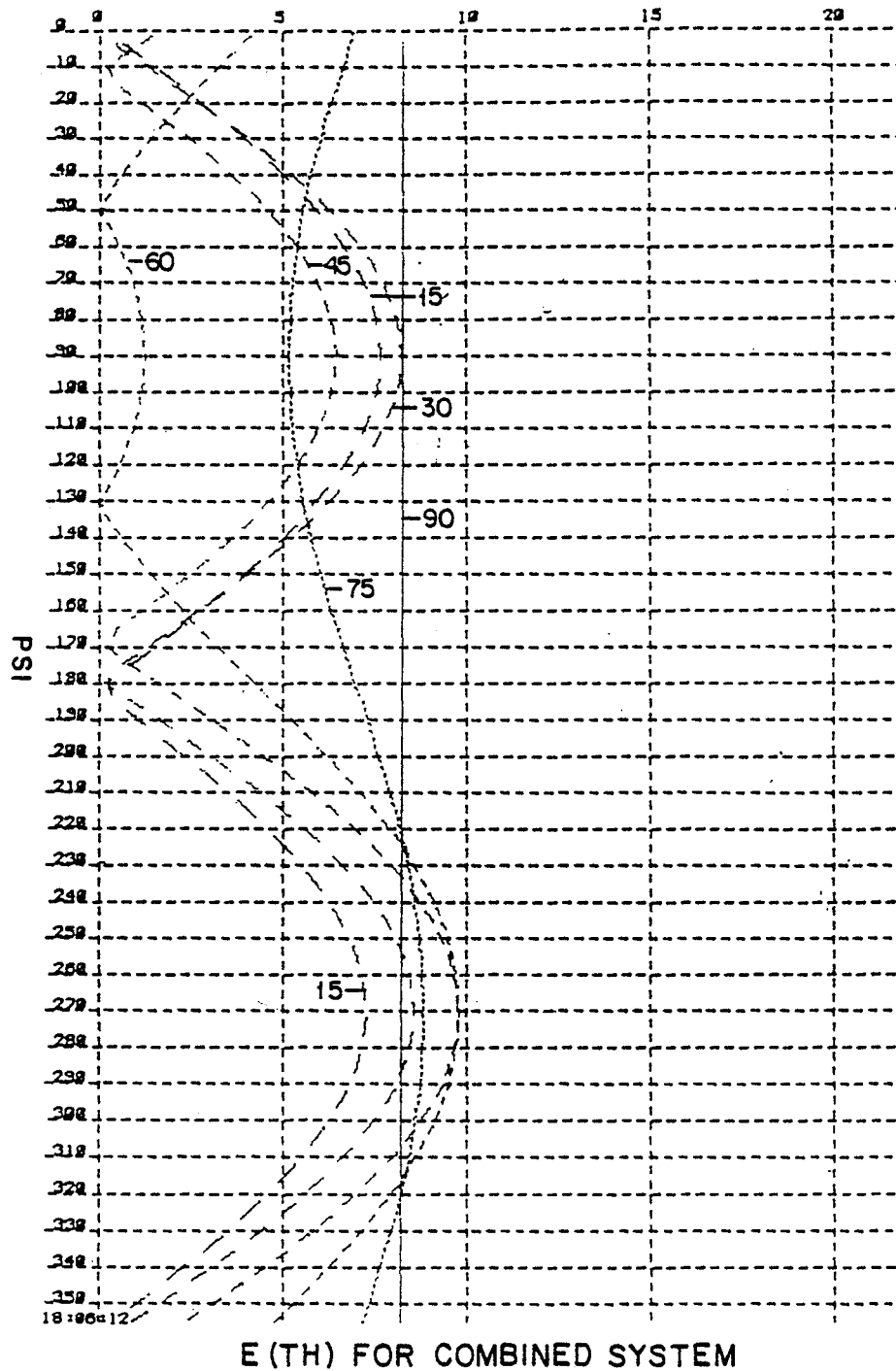


FIGURE 6

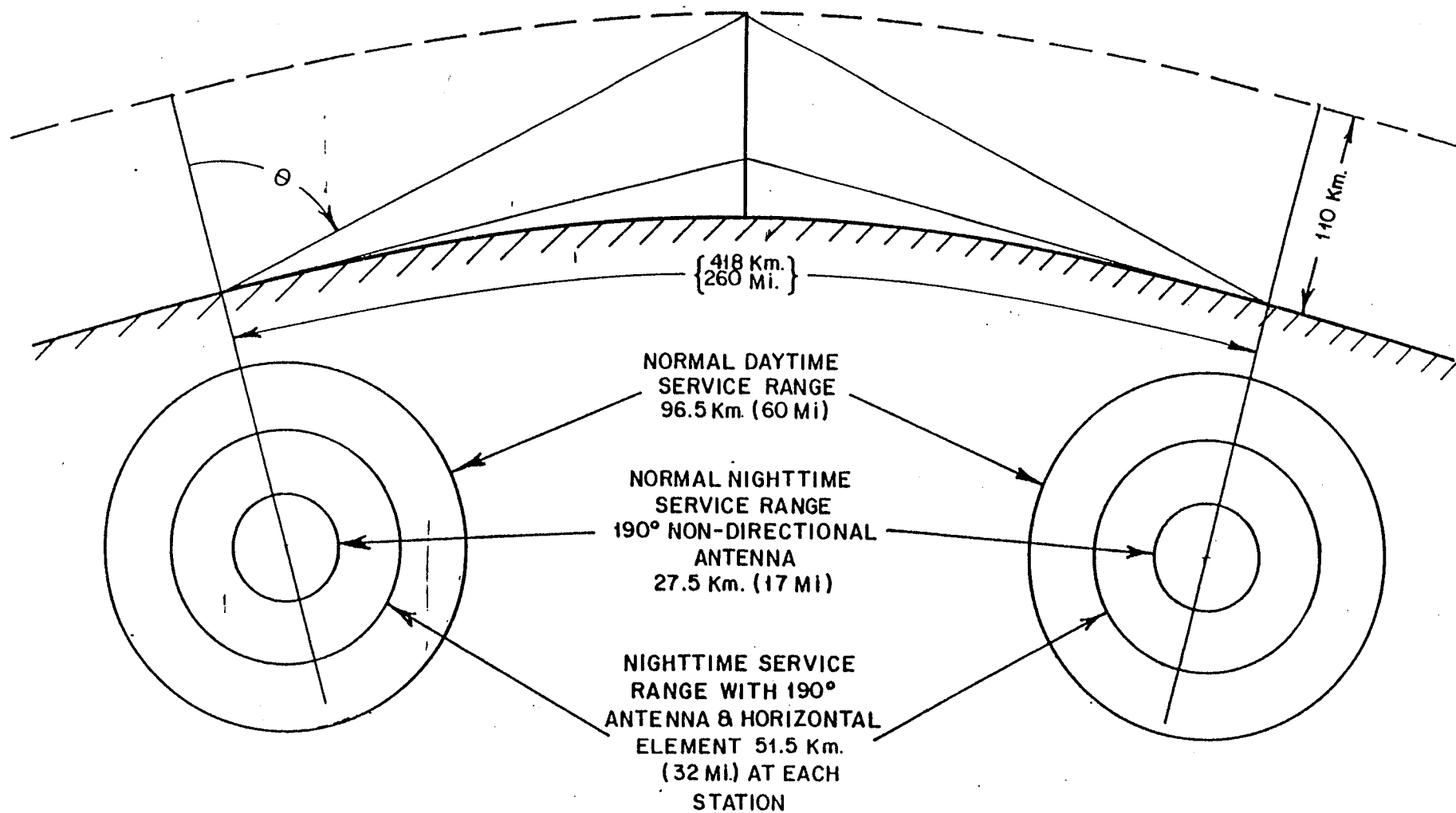
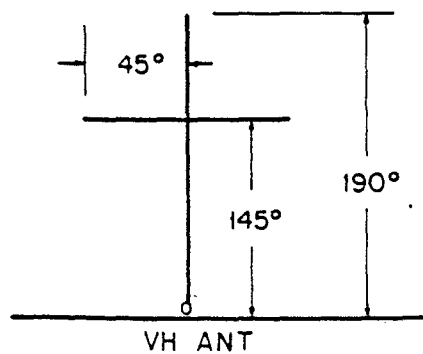
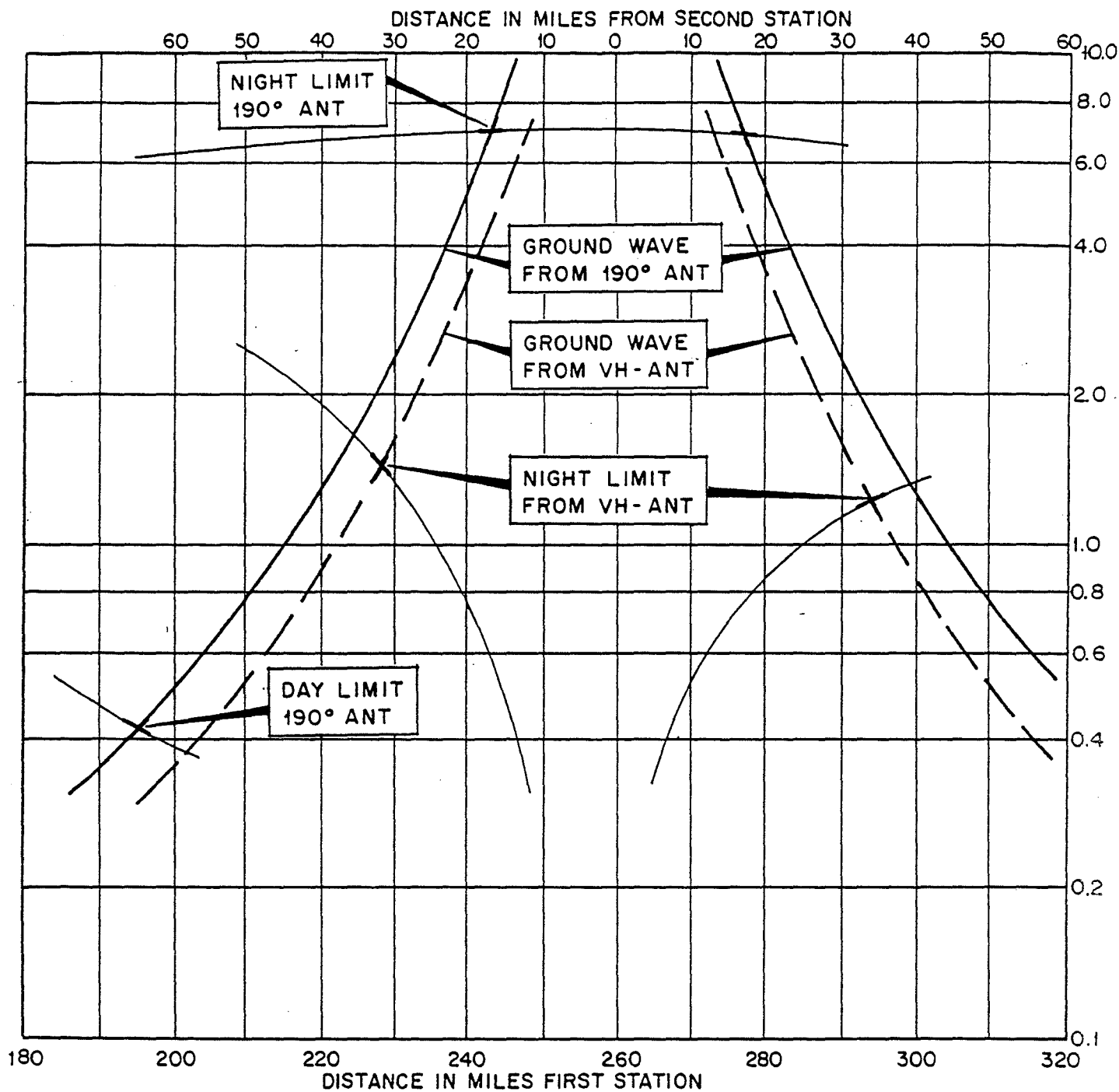


FIGURE 7



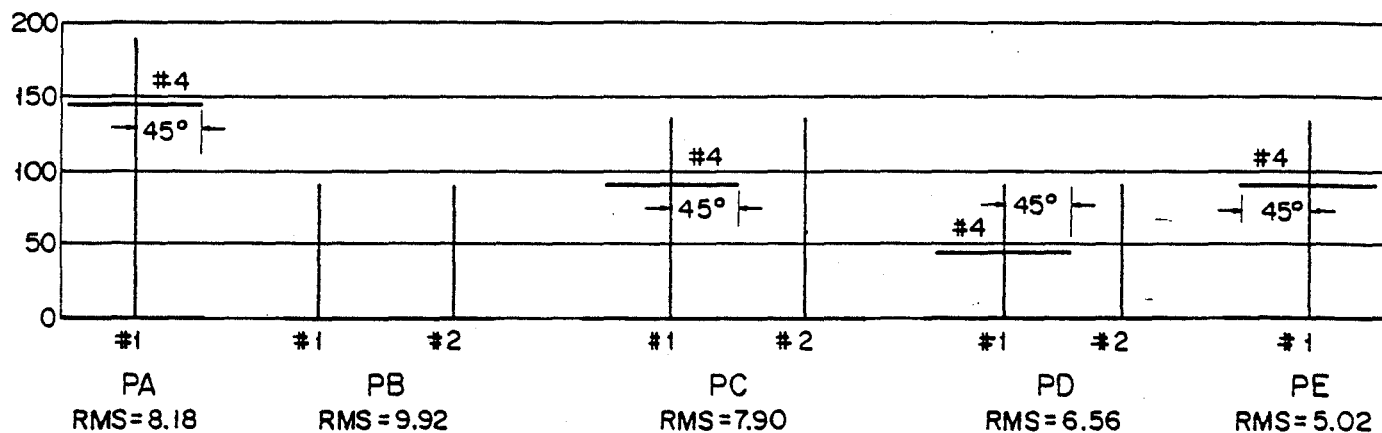
VERTICAL ANTENNA 1/0°

HORIZONTAL ANTENNA 5/90°

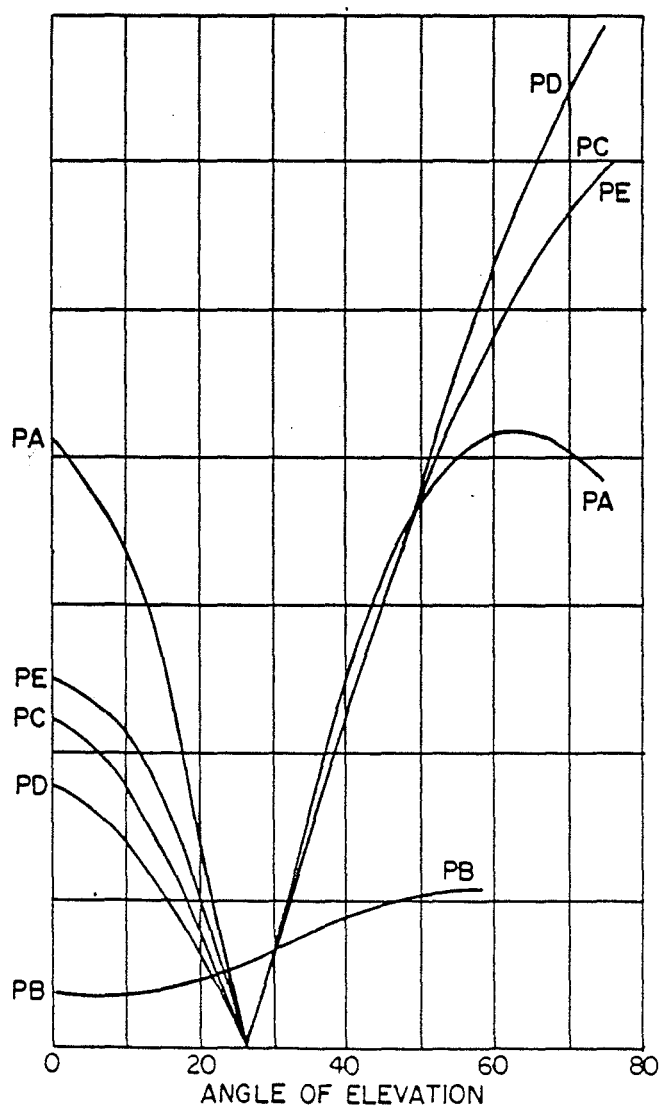
FIGURE 8

# FIGURE 9

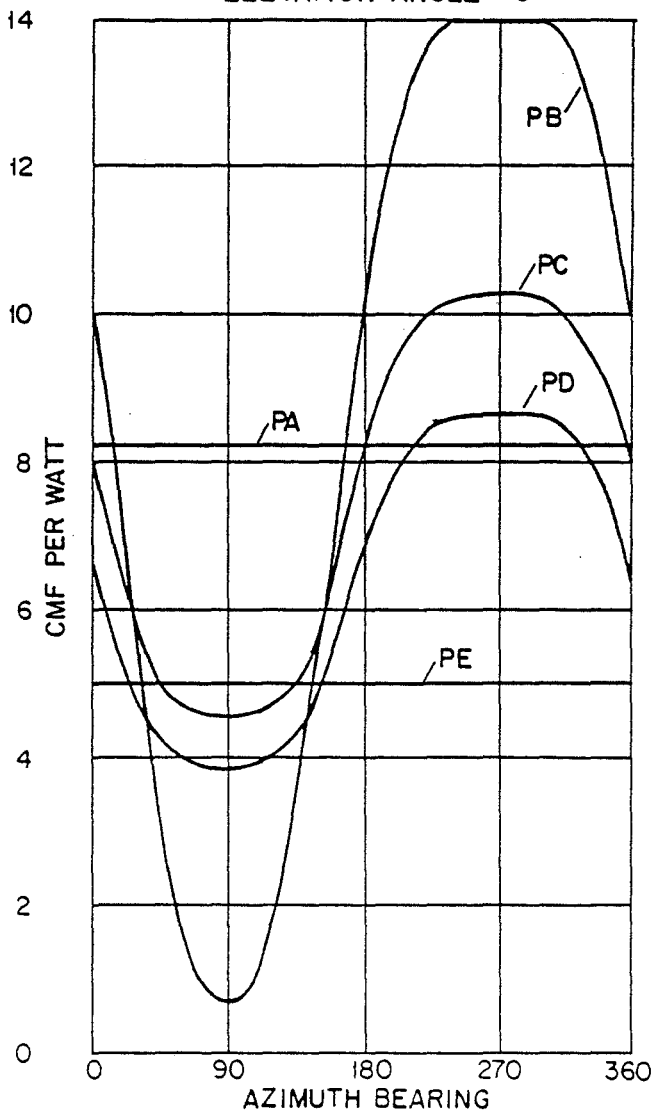
#1	$1/Q$	$1/Q$	$1/Q$	$1/Q$	$1/Q$
#2		$0.9/90$	$0.4/90$	$0.4/90$	
#4	$5.0/90$		$5.0/253$	$6.0/253$	$7.7/90$



## VERTICAL PATTERNS HORIZONTAL BEARING = 90°



## HORIZONTAL PATTERNS ELEVATION ANGLE = 0



1/20/86

Antennas - AM.

## THE PROBLEM

Radio communications services which depend upon the propagation of a groundwave along the earth's surface may experience severe interference problems due to the reflection of signals on their own or related frequencies from ionized layers in the earth's upper atmosphere (the ionosphere). For example, stations operating in the Standard (Medium Frequency) Broadcast Band suffer greatly from such skywave interference.

In general, the interfering signals can originate in either the same radiating system as that which generates the desired ground-wave, or from other stations located perhaps many hundreds of miles away. In the first case, the interfering signal, being of the same frequency as the desired (groundwave) signal, and bearing the same modulation, can cause severe variations of amplitude and phase of the received signal. This interference, generally known as selective fading, can seriously limit the useful range of a facility by causing severe distortion of the demodulated (audio) signal or by causing the amplitude of the received signal to drop below local noise levels.

The second case, caused by sources other than the source of the desired groundwave, can be even more disruptive, since the interfering signal(s) bear modulation different from that of the desired signal.

Both types of interference would be made more tolerable if a

transmitting antenna could be designed to as to reduce, relative to the desired surface wave, that portion of the radiated energy which travels outward and upward to reflect from the ionosphere.

#### DEFICIENCIES AND/OR LIMITATIONS OF KNOWN PRIOR ART

Efforts to design such an antenna generally depend upon achieving some specific distribution of current and phase so as to shape the radiation pattern in the vertical plane. (That is, to "squeeze" the radiated signal pattern down as close as possible to the horizontal plane.)

Such attempts have met with varying degrees of success. In general, it appears that attempts to drastically improve the vertical plane radiation characteristics of short (e.g., one half wavelength or less) radiators have not been particularly successful.

Some larger radiating structures (for example, the Franklin Antenna) do give good performance and are capable of generating strong ground waves while providing considerable suppression of skyward radiation over at least a range of vertical angles. Such designs, however, do not provide as much suppression of skyward radiation as is desirable over as wide a range of vertical angles as is needed. Further, these structures are generally quite expensive to build and maintain.

#### CONCEPTUAL DESCRIPTION OF THE ANTI-SKYYWAVE ANTENNA

The following paragraphs describe the theory behind an antenna structure intended to be capable of generating strong ground waves

while radiating only limited amounts of energy skyward.

This discussion is the essence of theoretical research and experimentation on the subject, spread over a period of several years. Only one of the several approaches which have been investigated will be discussed.

The following is in terms of AM Broadcast practices and problems, but the ideas apply to other services which depend upon the surface wave.

Consider a vertical current-carrying conductor above the earth, which is an imperfectly conducting dielectric material. If this vertically-oriented conductor is located near the surface, (as is the case with the typical AM broadcast antenna), two distinct far-field waves are generated. One, the skyward wave, is of the form:

$$\text{EQUATION 1) } E_{\text{SPACE}} = j30\beta Idl \cos\phi \left( \frac{e^{-j\beta R_1}}{R_1} + \frac{R_v e^{-j\beta R_2}}{R_2} \right)$$

The other, the surface wave (or "ground wave") has the form:

$$\text{EQUATION 2) } E_{\text{SURFACE}} = j30\beta Idl (1-R_v) \frac{e^{-j\beta R_2}}{R_2} \\ \times \sqrt{1 - 2\kappa^2 + (\cos^2\phi)\kappa^2 \left(1 + \frac{\sin^2\phi}{2}\right)^2}$$

With the geometry as show in Figure 1 and :

EQUATION 3)  $\mu^2 = 1/(E_r + jX)$

EQUATION 4)  $X = \frac{1.8 \times 10^4 G_{\text{MH/METER}}}{f_{\text{MHz}}}$

EQUATION 5)  $\beta = 2\pi/\lambda$   $G = \text{CONDUCTIVITY OF EARTH (MH/METER)}$

EQUATION 6)  $F = \left\{ 1 - j\sqrt{\pi\omega} e^{-\omega} [\text{erfc}(j\sqrt{\omega})] \right\}$   $E_r = \epsilon/\epsilon_y = \text{RELATIVE DIELECTRIC CONSTANT OF EARTH}$

EQUATION 7)  $\omega = \frac{j\beta R \mu^2 (1 - \mu^2 \cos^2 \phi)}{2} \left[ 1 + \frac{\sin \psi}{\mu \sqrt{1 - \mu^2 \cos^2 \phi}} \right]^2$

EQUATION 8)  $\text{erfc}(j\sqrt{\omega}) = \frac{2}{\omega} \int_{j\sqrt{\omega}}^{\infty} e^{-v^2} dv$

The skyward field has a relative magnitude as a function of the vertical angle ( $U$ ) similar to that shown in Figure 2.

The magnitude of this field is zero at both the zenith ( $\phi = 90$  Deg.) and at the horizontal plane ( $\phi = 0$  Deg.). The zero (null) at the zenith follows from the direction of current flow in the conductor and the geometry. The null at the horizontal plane is due to the fact that the two terms in Equation 1), which describe the contributions from the source ( $R_1$ ) and from its image ( $R_2$ ) are equal in magnitude. However, the vertical coefficient of reflection,  $R_v$ , has a unique value of -1.0 at the horizontal plane. Thus, complete cancellation of these two terms occurs at  $\phi = 0$ .



The vertical coefficient of reflection varies rapidly, in both magnitude and phase, as a function of  $\psi$ . A rough graph of magnitude and phase of  $R_v$  vs.  $\psi$  for a typical earth material is shown in Figures 3-A and 3-B.

The maximum magnitude in the skyward field pattern of a short vertical radiator in the medium frequency broadcast band generally occurs about 25 to 30 degrees above the horizontal.

This skyward energy is, of course, that which travels outward and upward and, upon reflection from the ionosphere, returns to earth to possibly create interference.

The surface wave, on the other hand, appears to result only from the image, not from the source itself. (Note that there is no term dependent upon  $R_1$  in the surface wave equation - EQUATION 2).)

The term  $(1-R_v)$  has the unique value of 2.0 at the horizontal plane, because (as discussed above) the vertical coefficient of reflection has the unique value of -1.0 at the angle  $\psi=0$  Deg. Because of the manner in which  $R_v$  varies with  $\psi$  and the behavior of the surface wave attenuation term,  $F$ , the surface wave field decreases rapidly with height above the surface, and in no practical case is it a source of (broadcast band) ionosphere-reflected interfering signals.

The surface wave has a vertical plane pattern generally similar to that shown in in Figure 4. The precise vertical plane pattern

naturally depends upon radiator height (length), current distribution, earth constants, etc.

Figures 5-A and 5-B are sketches of the proposed antenna design. A base fed monopole (a quarter wavelength or so in height), operating over a conventional ground system consisting of perhaps 120 buried copper radial ground wires about one quarter wave in length, forms one important element of the system. Disposed around the base of the conventional monopole are several short (one-thirtieth of a wavelength or so) base-fed radiating elements. Around the entire array of monopole and short radiators is a circular electric screen, about one thirtieth of a wavelength high and at a distance of about one quarter wave from the monopole.

At a far-field observation point on the earth's surface, such as  $P_1$ , the electric screen acts to impede the illumination of the surface of the earth by the collection of short radiators. Thus, the screen, in concert with other design factors, decreases the ability of the short radiators to generate a strong surface wave. At appreciable angles above the horizon, however, the geometry of the structure permits more and more of the current carrying length of the short radiators to become effective in radiating a skyward field (e.g., points  $P_2$  and  $P_3$ ).

The number and placement of the short radiators, together with their height and the height of the circular electric screen ("fence") can be so designed as to provide a very close match in both amplitude and phase to the skyward radiation from the taller

base-fed monopole. By appropriate adjustment of the phase and magnitude of the currents flowing in the short radiators, this skyward radiation can be made to very nearly cancel the skyward radiation of the taller monopole over wide ranges of vertical angles. Since the screen, acting with the ground system, has a drastic effect upon the ability of the short radiators to generate a surface wave, while only modestly affecting the surface wave characteristics of the taller monopole, a strong ground wave results, even though the skyward radiation is severely curtailed.

More than one short radiator is used simply to aid in obtaining the desired radiation pattern (both in amplitude and in phase) from the short sources, and to achieve a gain in efficiency through mutual impedance effects. Further, the effective length of the short radiators should be increased by top-loading or other appropriate techniques.

This antenna design should result in greatly increased ground wave signal strengths (per unit of input power) as compared with that obtained with conventional antenna systems. The fields so generated are on the order of twice those usually obtained in practice, but exact values are greatly influenced by frequency, antenna system design, and the electrical characteristics of the earth.

#### PRESENT STATE OF DEVELOPMENT

A reasonably complete mathematical (computer) model of the new antenna concept has been implemented. Variables permitted by the

computer model include frequency, dimensions of the radiating elements (and the number of elements in the ring of low-profile radiators), the conductivity and dielectric constant of the ground screen and of the surrounding earth, the radius and height of the circular electric screen, and so on. Thus, it is possible to (at least partially) verify the model by comparing the results for well-established cases before proceeding on to the complete design. For example, Figures 6-A through 6-D present vertical section ("slices") for conventional base-fed antennas of height 90, 135, 180 and 225 electrical degrees, respectively, operating over a perfectly conductive earth (that is, the usual assumption in broadcast antenna design practice).

As expected, no surface wave is present in the perfectly conductive case. The field strengths (stated in terms of mV/m at one Kilometer for one kilowatt of radiated power for all cases presented herewith) agree with those computed for these heights of radiator using other computational approaches.

Figure 1a of Section 73.190 of the FCC's Rules and Regulations ("the Class I Curve") has been digitized, in order that some comparison of the nighttime interference generating characteristics of various antenna designs can be made. The second graph on each of the above (and following) figures presents the computed interference contribution (per kW of radiated power) as a function of distance (km).

Figures 7-A through 7-D correspond to Figures 6-A through 6-D,

except that finite (and typical) values of conductivity and dielectric constant have been taken into account. Here, a significant portion of the energy exists in the form of a surface wave. (In broad terms, something on the order of 90 percent of the radiated energy goes into the skyward flow, for typical broadcast AM antenna systems.)

The surface wave has the rather interesting characteristic of traveling outward and downward from the source. In addition to the vertical electric field component (which is to be expected, since the electric current flows in a vertical direction in the radiator), there is a horizontal component of electric field, parallel to the surface of the earth. Since the earth has a finite conductivity, there is a flow of energy downward into the earth, which accounts for the greatly increased attenuation of the surface wave as compared with the skyward wave.

#### COMPUTED PERFORMANCE OF ASWA

FIGURES 8-A through 8-D present computed skyward and surface wave fields for the same ASWA antenna systems whose central (tall) radiator is 90, 135, 180 and 225 deg. in height, respectively. As above, the calculated skywave interference contributions are also shown. (Following standard broadcast engineering practice, the interference values shown are based upon a 20:1 ratio of desired to undesired signal strengths.)

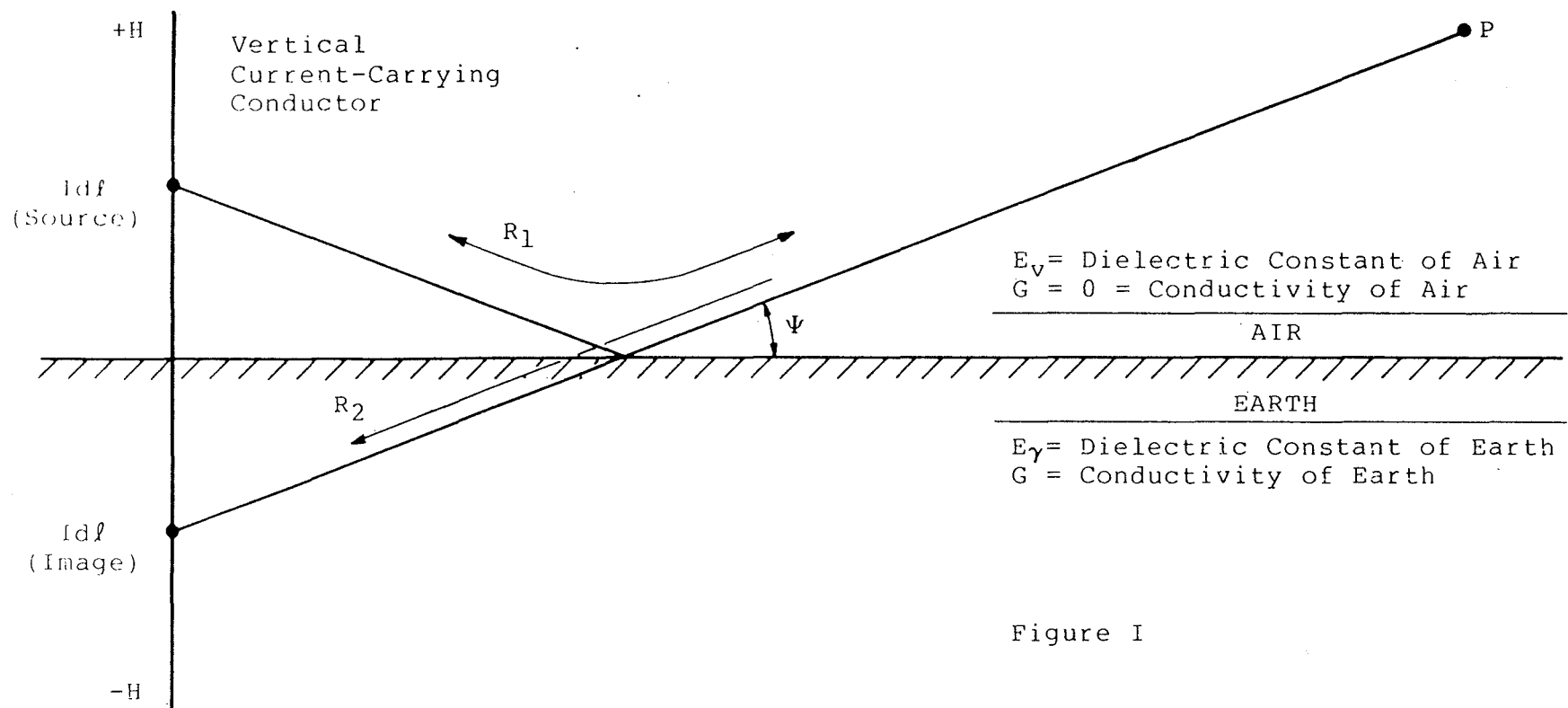


Figure I

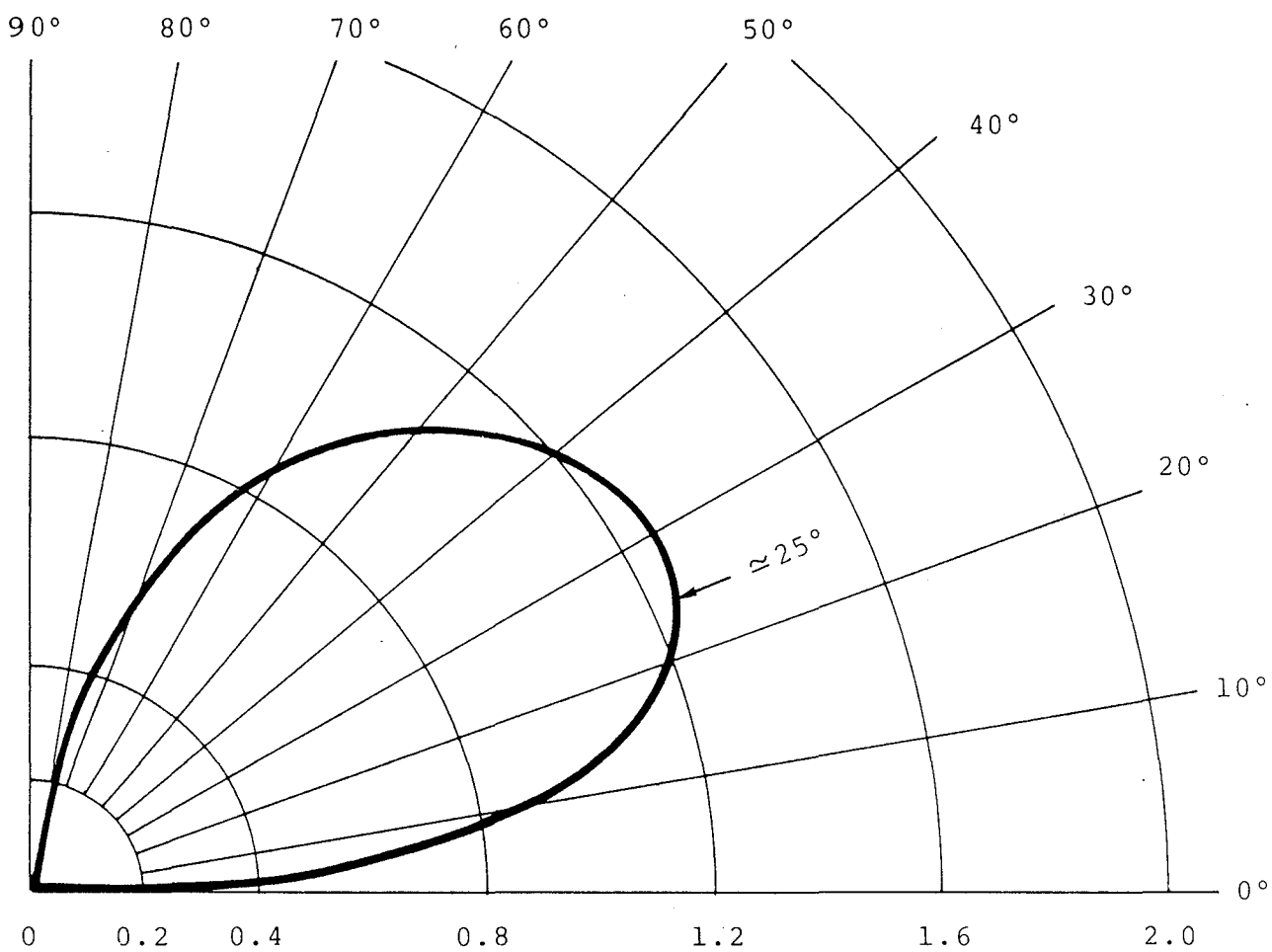


Figure II

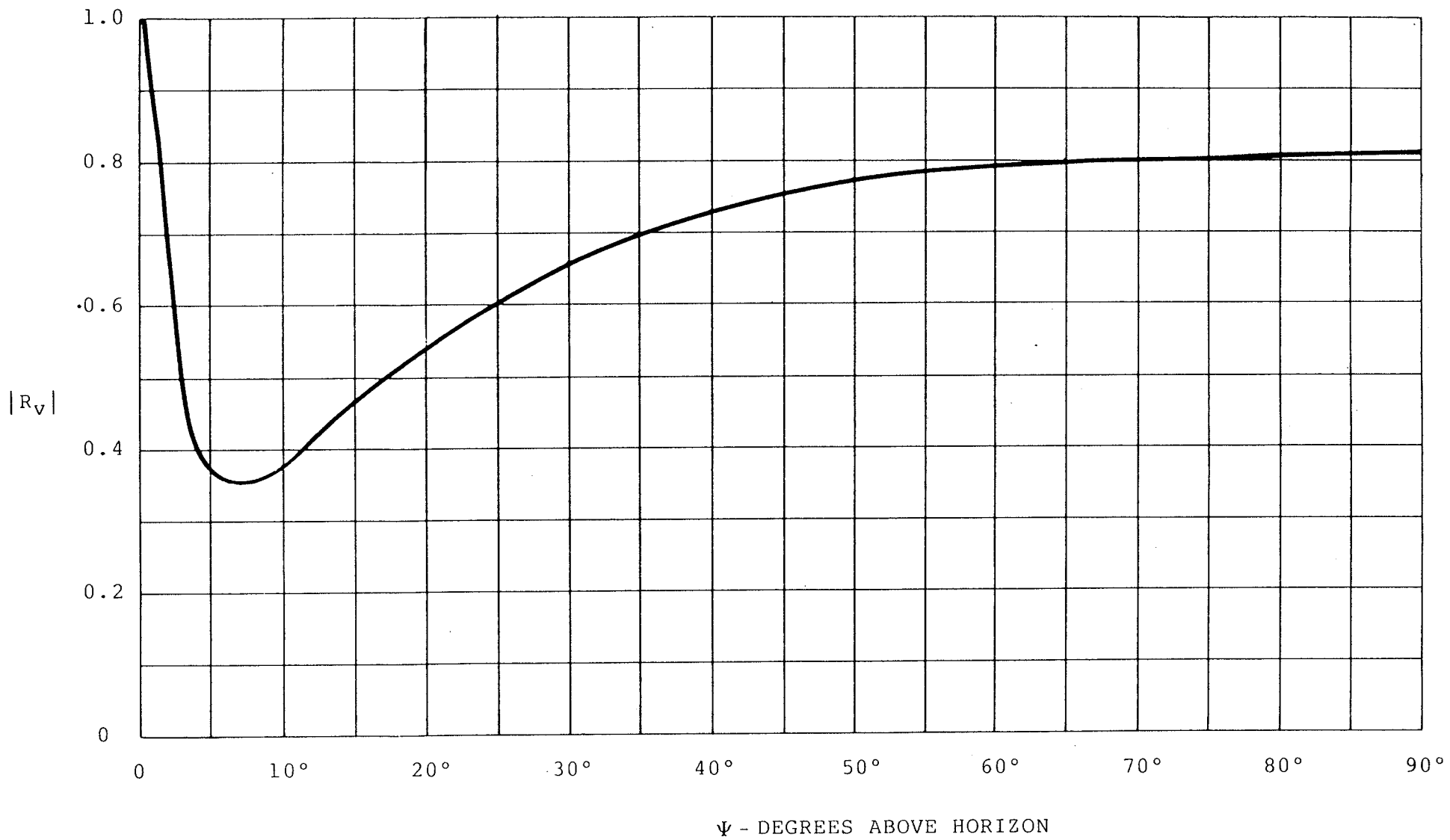


Figure III-A



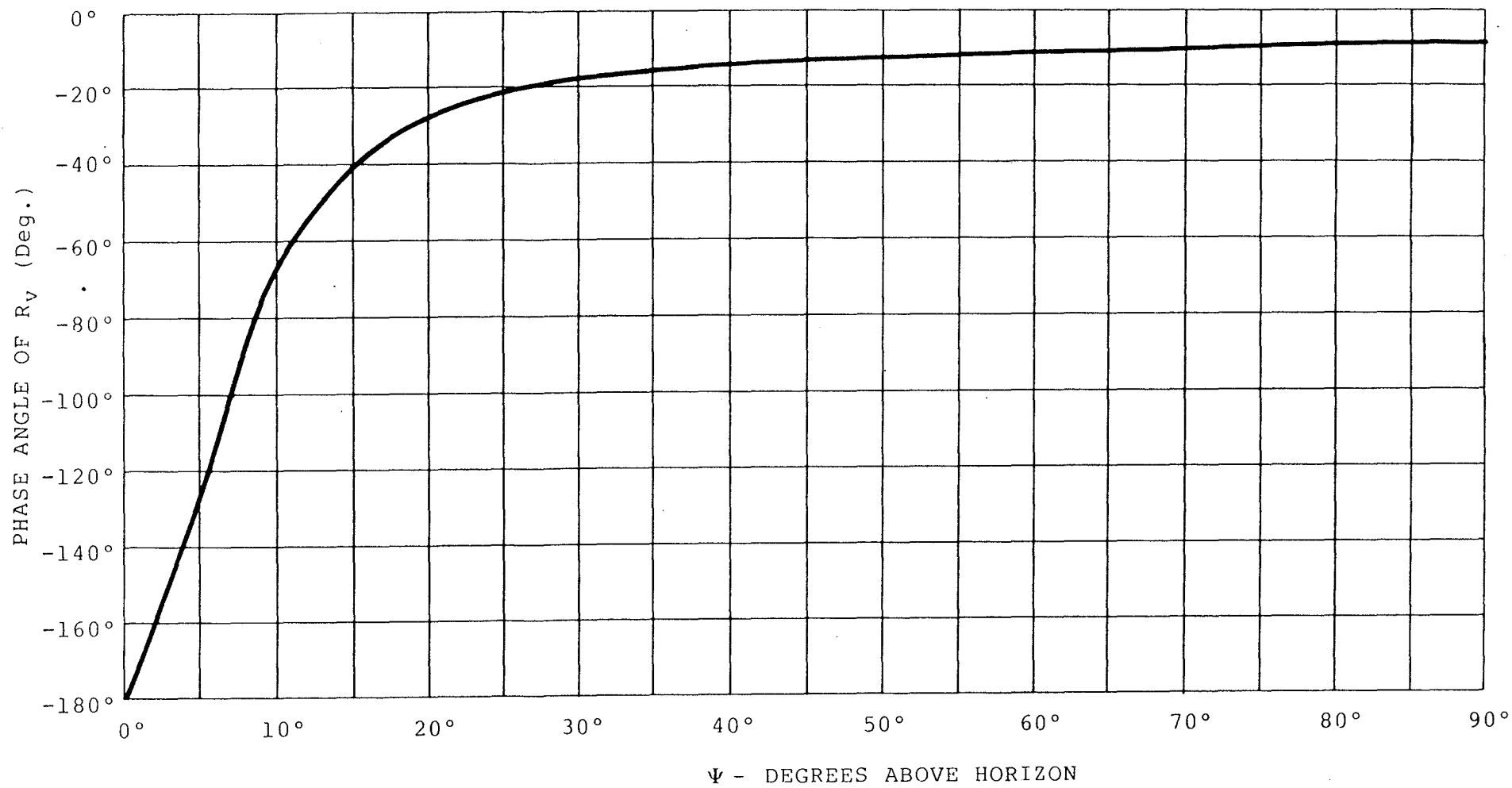


Figure III-B

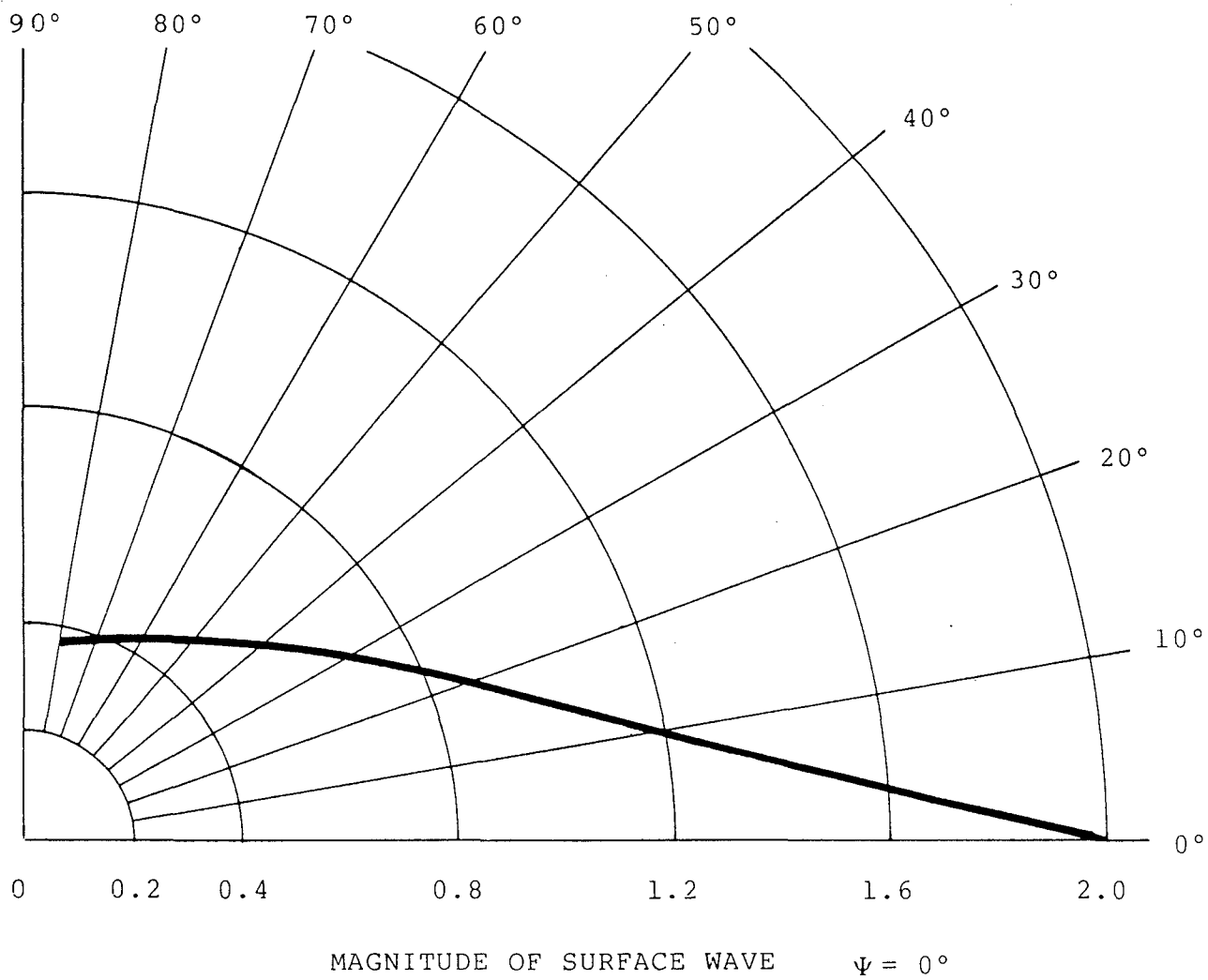
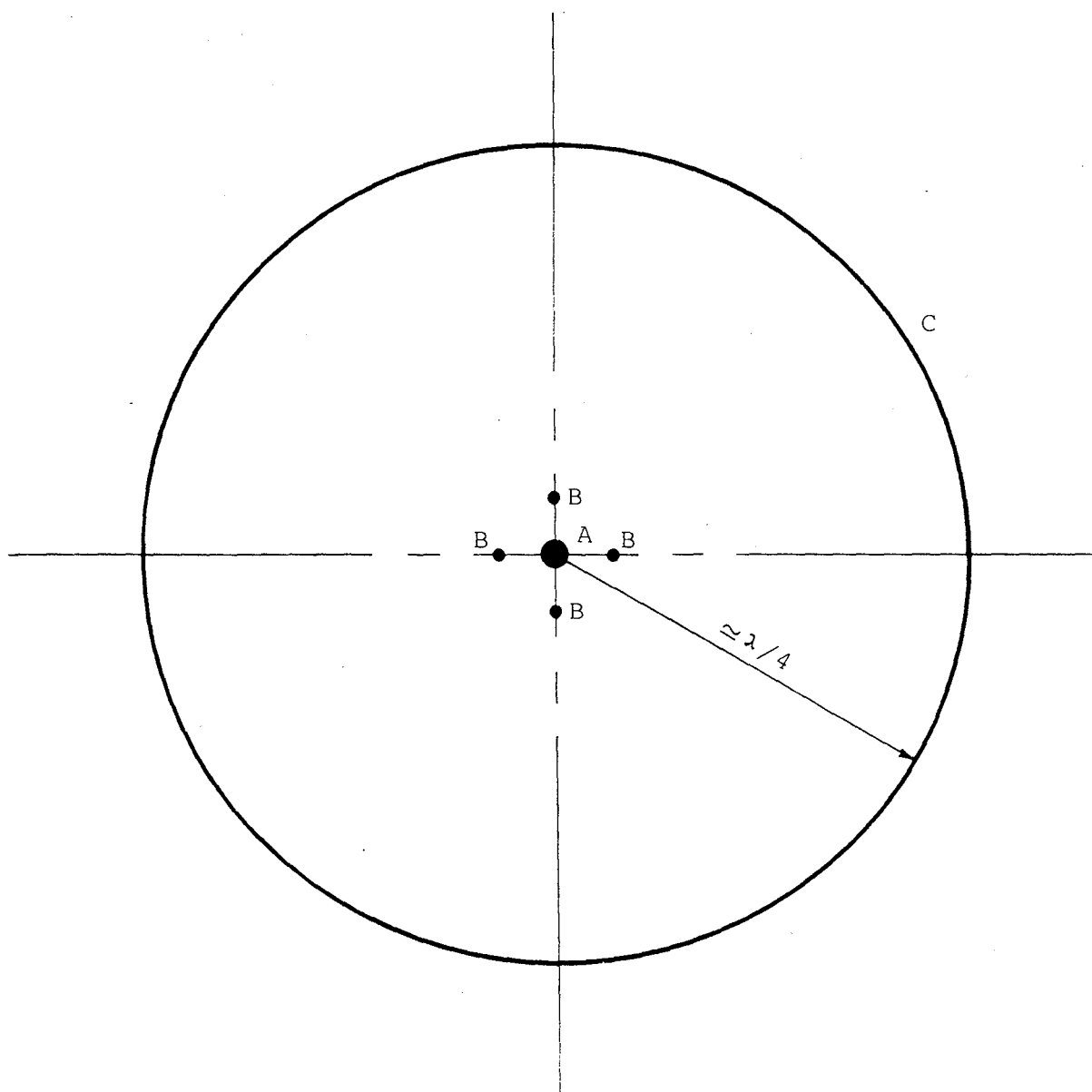


Figure IV



- A). Vertical Base-fed  
Monopole - Height  $\approx \lambda/4 - \lambda/2$
- B). Collection of Short Base-fed  
Vertical Conductors - About  $10^\circ$  in Height
- C). Electric Screen - About  $10^\circ$  in Height

Figure V-A

Base-Fed  
Monopole  
( $\approx \lambda/4 - \lambda/2$  High)

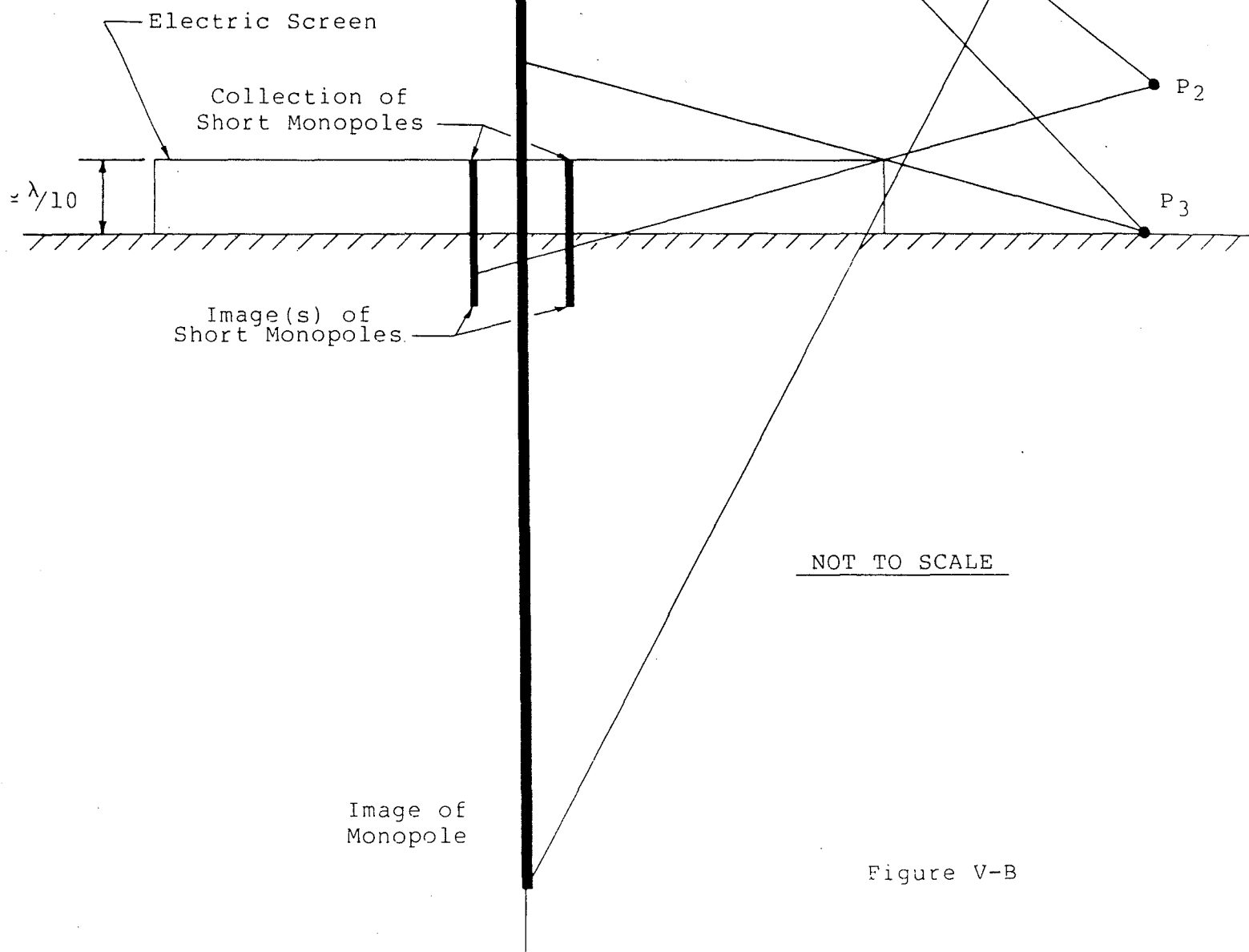
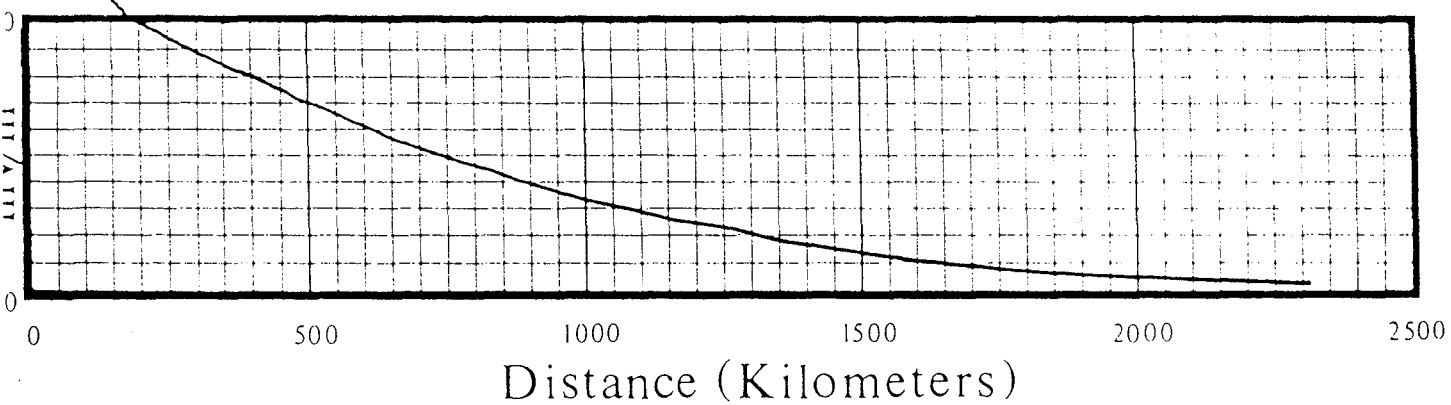
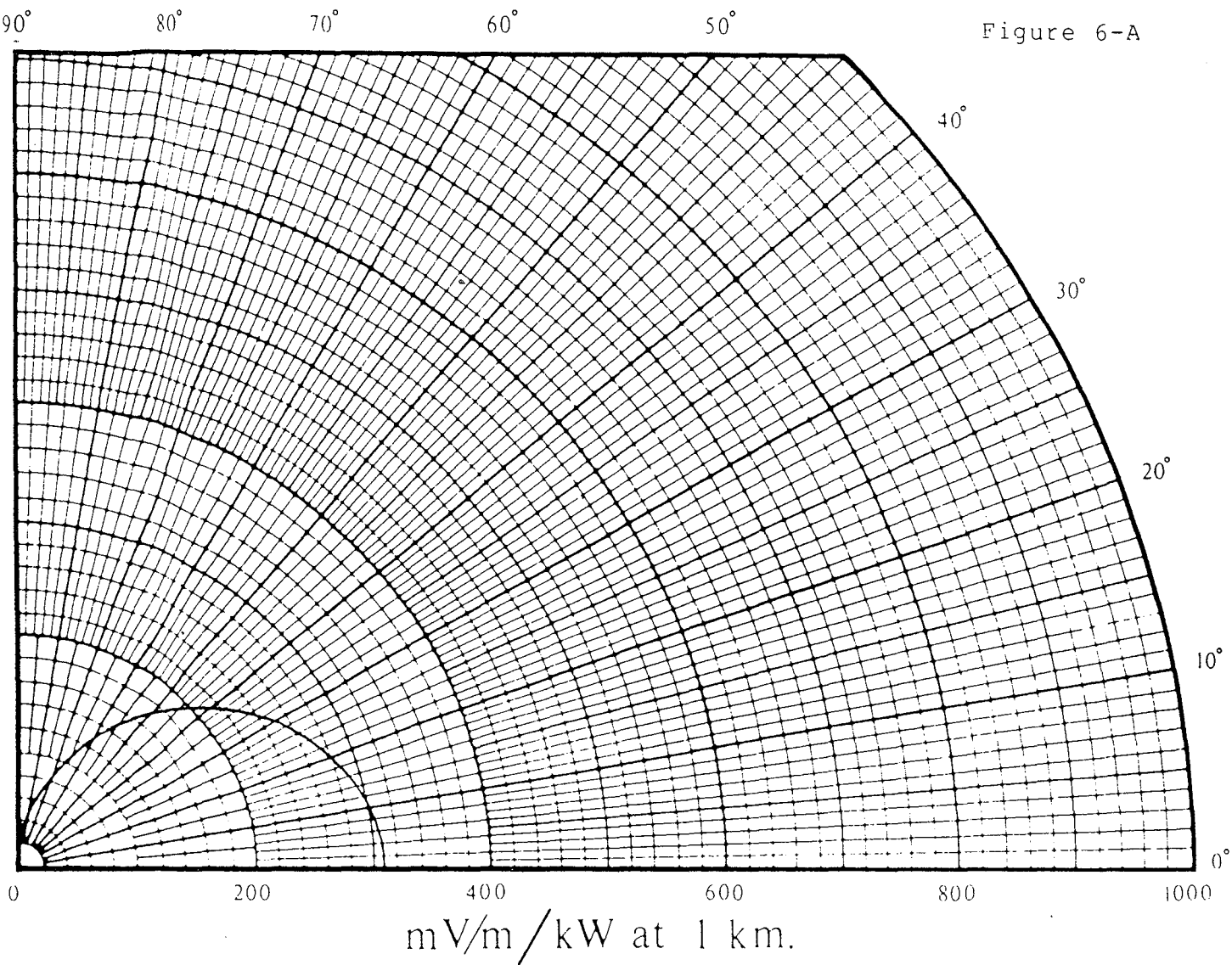


Figure V-B



DATE/TIME 4-JAN-1986 10:51:22  
 GROUND SCREEN (DEG.) 90.0  
 GS CONDUCTIVITY (MHOS) 0.10E+09  
 EARTH CONDUCTIVITY 0.10E+09

FREQUENCY (MHZ.) 1.000  
 GS DIELECTRIC CONSTANT 15.0  
 EARTH DIELECTRIC CONSTANT 15.0  
 MONOPOLE HEIGHT (DEG.) 90.00

MONOPOLE LOOP (AMP.) 5.22

90°

80°

70°

60°

50°

Figure 6-B

40°

30°

20°

10°

0°

0

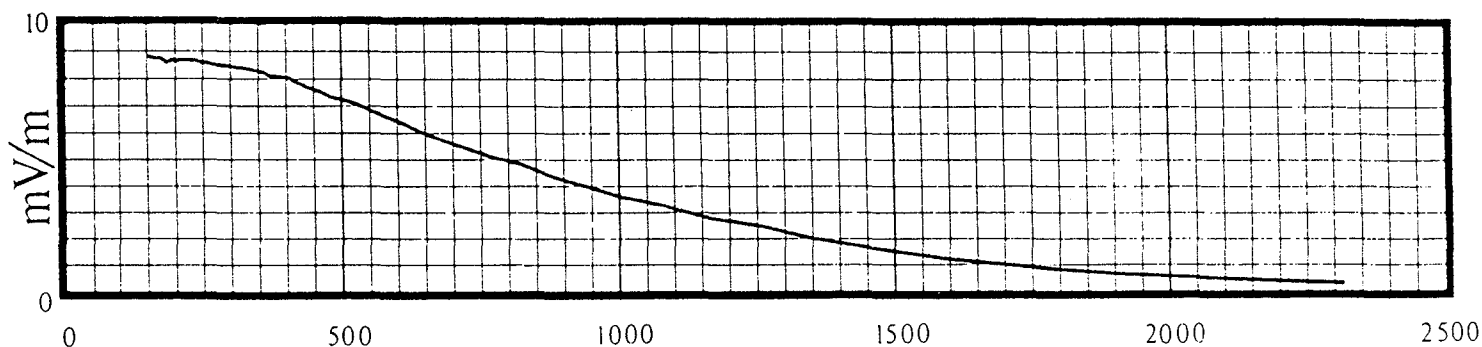
200

400

600

800

1000

 $\text{mV/m/kW at 1 km.}$ 

Distance (Kilometers)

DATE/TIME 4-JAN-1986 11:06:11

GROUND SCREEN (DEG.) 90.0

GS CONDUCTIVITY (MHOS) 0.10E+09

EARTH CONDUCTIVITY 0.10E+09

FREQUENCY (MHZ.) 1.000

GS DIELECTRIC CONSTANT 15.0

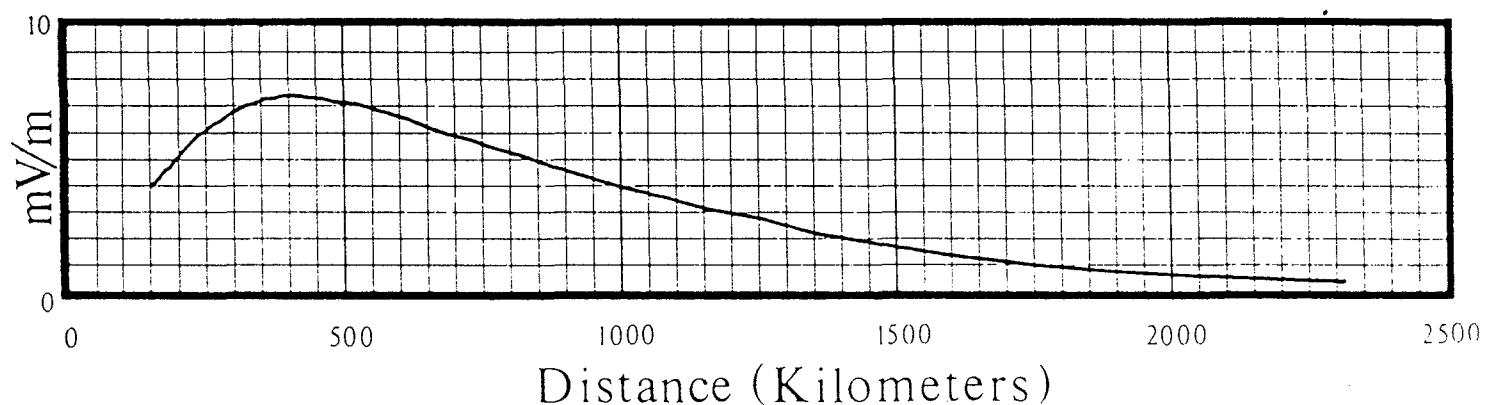
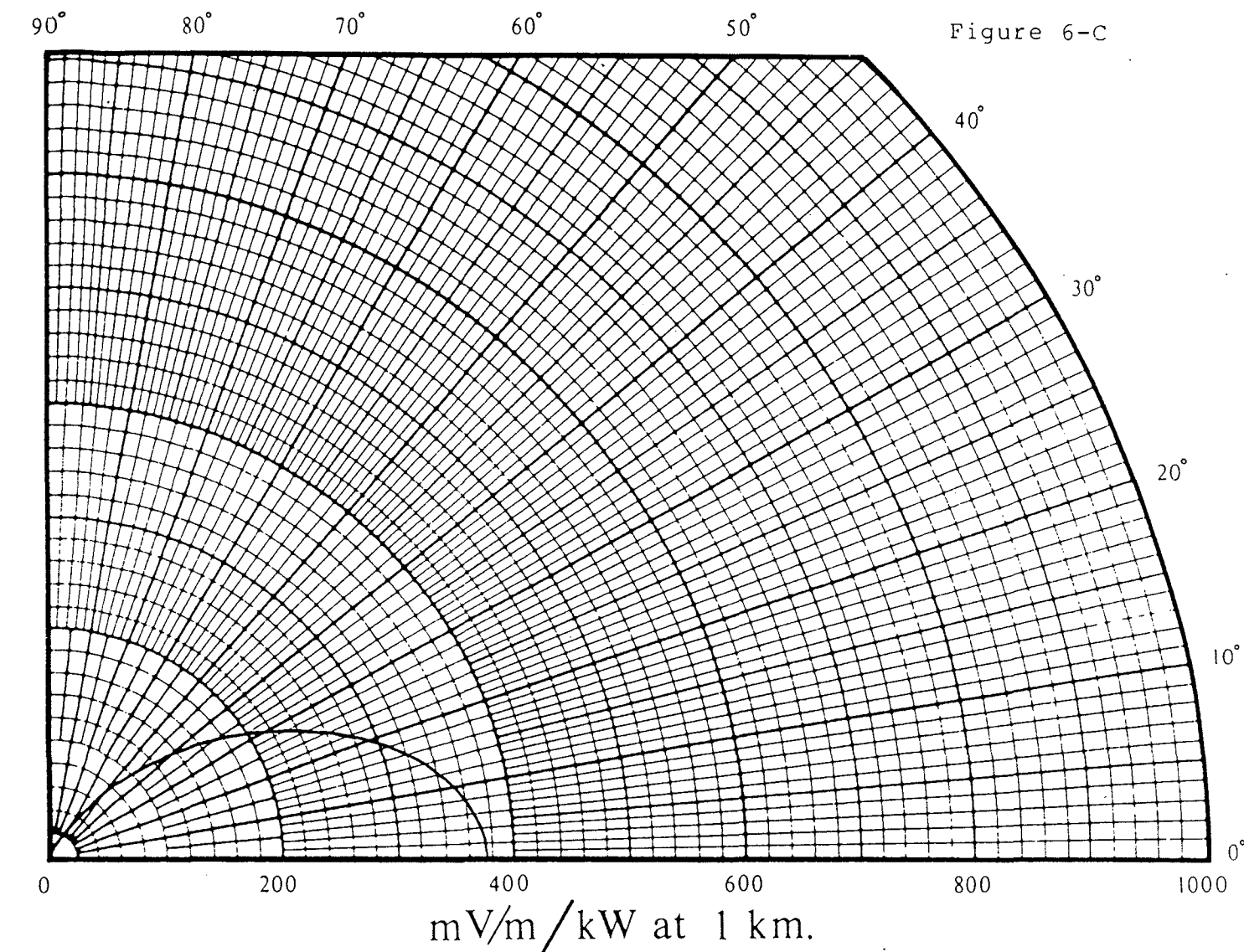
EARTH DIELECTRIC CONSTANT 15.0

MONOPOLE HEIGHT (DEG.) 135.00

MONOPOLE LOOP (AMP.) 3.28

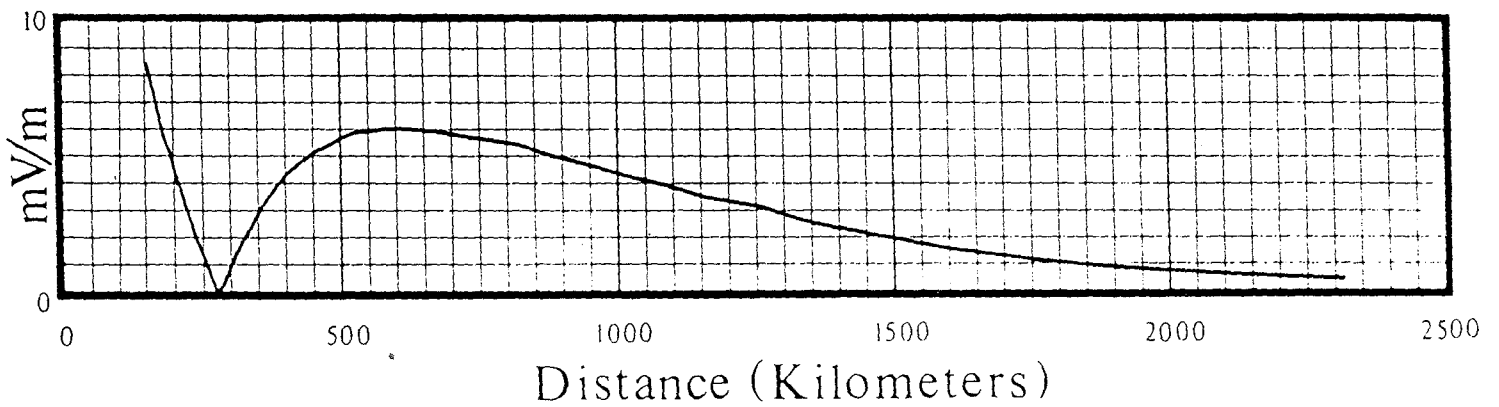
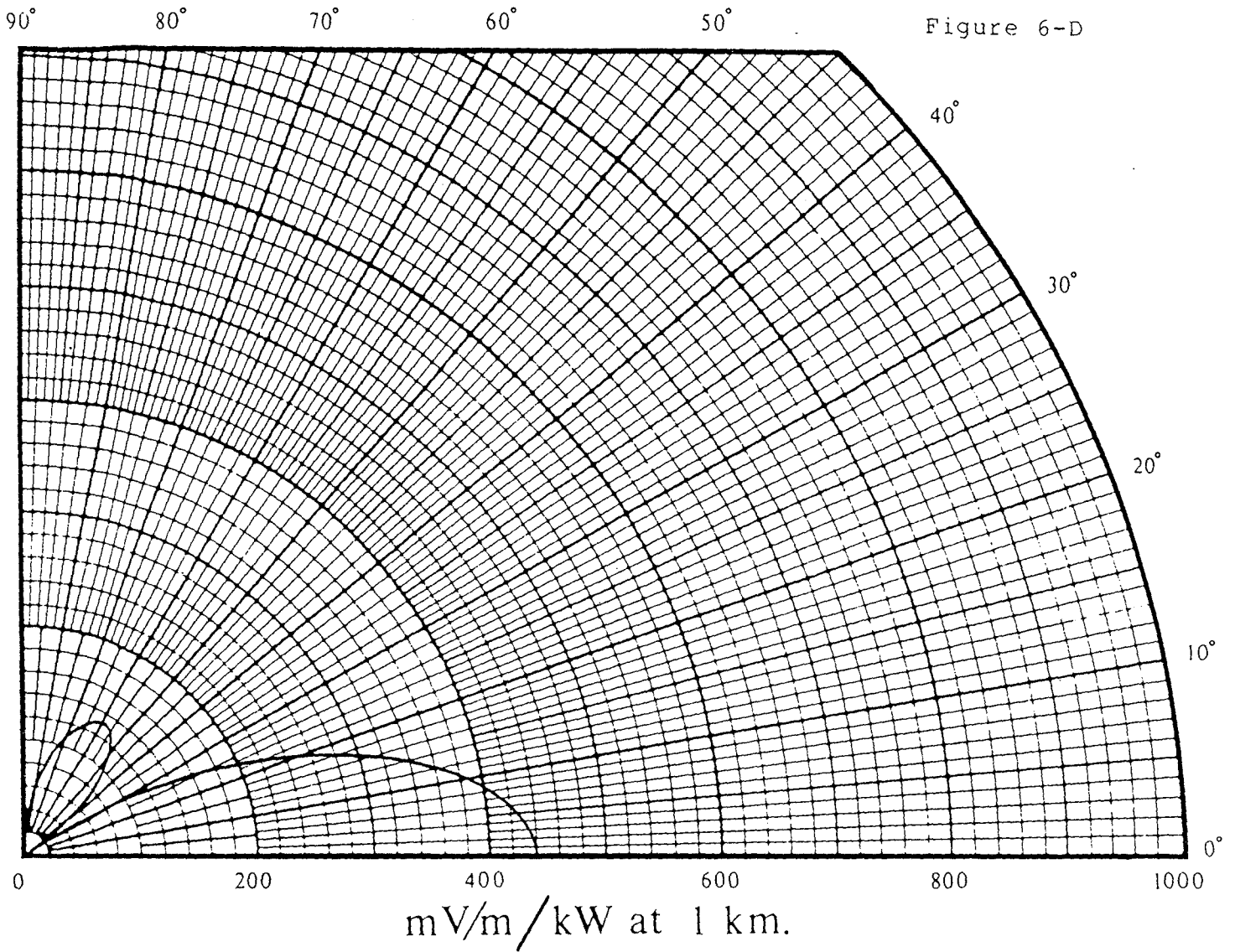
Richard L. Biby, P.E.

Figure 6-C



DATE/TIME	4-JAN-1986 11:00:28	FREQUENCY (MHZ.)	1.000
GROUND SCREEN (DEG.)	90.0	GS DIELECTRIC CONSTANT	15.0
GS CONDUCTIVITY (MHOS)	0.10E+09	EARTH DIELECTRIC CONSTANT	15.0
EARTH CONDUCTIVITY	0.10E+09	MONOPOLE HEIGHT (DEG.)	180.00

MONOPOLE LOOP (AMP.) 3.17



DATE/TIME 4-JAN-1986 11:08:36  
 GROUND SCREEN (DEG.) 90.0  
 GS CONDUCTIVITY (MHOS) 0.10E+09  
 EARTH CONDUCTIVITY 0.10E+09

FREQUENCY (MHZ.) 1.000  
 GS DIELECTRIC CONSTANT 15.0  
 EARTH DIELECTRIC CONSTANT 15.0  
 MONOPOLE HEIGHT (DEG.) 225.00

MONOPOLE LOOP (AMP.) 4.33



90°

80°

70°

60°

50°

Figure 7-A

40°

30°

20°

10°

0°

0

200

400

600

800

1000

mV/m/kW at 1 km.

mV/m

10

0

0

500

1000

1500

2000

2500

Distance (Kilometers)

DATE/TIME 4-JAN-1986 11:12:26  
 GROUND SCREEN (DEG.) 90.0  
 GS CONDUCTIVITY (MHOS) 0.10E+09  
 EARTH CONDUCTIVITY 0.40E-02

FREQUENCY (MHZ.) 1.000  
 GS DIELECTRIC CONSTANT 15.0  
 EARTH DIELECTRIC CONSTANT 15.0  
 MONOPOLE HEIGHT (DEG.) 90.00

MONOPOLE LOOP (AMP.) 5.92

Richard L. Blevins

90°

80°

70°

60°

50°

Figure 7-B

40°

30°

20°

10°

0°

0

200

400

600

800

1000

 $\text{mV/m/kW at 1 km.}$  $\text{mV/m}$ 

10

0

0

500

1000

1500

2000

2500

Distance (Kilometers)

DATE/TIME 4-JAN-1986 11:16:09  
GROUND SCREEN (DEG.) 90.0  
GS CONDUCTIVITY (MHOS) 0.10E+09  
EARTH CONDUCTIVITY 0.40E-02

FREQUENCY (MHZ.) 1.000  
GS DIELECTRIC CONSTANT 15.0  
EARTH DIELECTRIC CONSTANT 15.0  
MONOPOLE HEIGHT (DEG.) 135.00

MONOPOLE LOOP (AMP.) 3.92

Richard L. Biby, P.E.

90°

80°

70°

60°

50°

Figure 7-C

40°

30°

20°

10°

0°

0

200

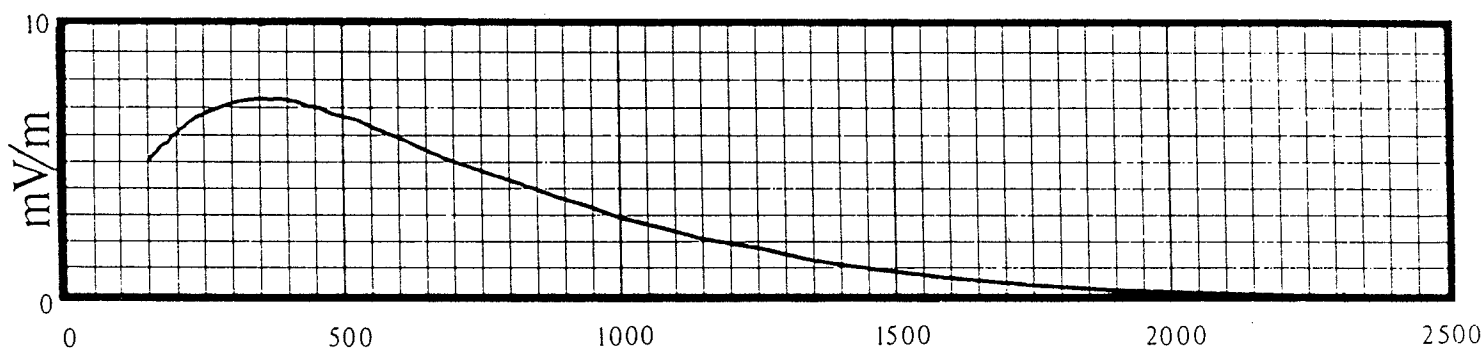
400

600

800

1000

mV/m/kW at 1 km.



Distance (Kilometers)

DATE/TIME 4-JAN-1986 11:21:30  
 GROUND SCREEN (DEG.) 90.0  
 GS CONDUCTIVITY (MHOS) 0.10E+09  
 EARTH CONDUCTIVITY 0.40E-02

FREQUENCY (MHZ.) 1.000  
 GS DIELECTRIC CONSTANT 15.0  
 EARTH DIELECTRIC CONSTANT 15.0  
 MONOPOLE HEIGHT (DEG.) 180.00

MONOPOLE LOOP (AMP.) 4.03

Richard L. Biby, P. E.

90°

80°

70°

60°

50°

Figure 7-D

40°

30°

20°

10°

0°

0

200

400

600

800

1000

mV/m/kW at 1 km.

mV/m

10

0

0

500

1000

1500

2000

2500

Distance (Kilometers)

DATE/TIME 4-JAN-1986 11:24:29

GROUND SCREEN (DEG.) 90.0

GS CONDUCTIVITY (MHOS) 0.10E+09

EARTH CONDUCTIVITY 0.40E-02

FREQUENCY (MHZ.) 1.000

GS DIELECTRIC CONSTANT 15.0

EARTH DIELECTRIC CONSTANT 15.0

MONOPOLE HEIGHT (DEG.) 225.00

MONOPOLE LOOP (AMP.) 5.32

Richard L. Biby, P.E.

90°

80°

70°

60°

50°

Figure 8-A

40°

30°

20°

10°

0°

0

200

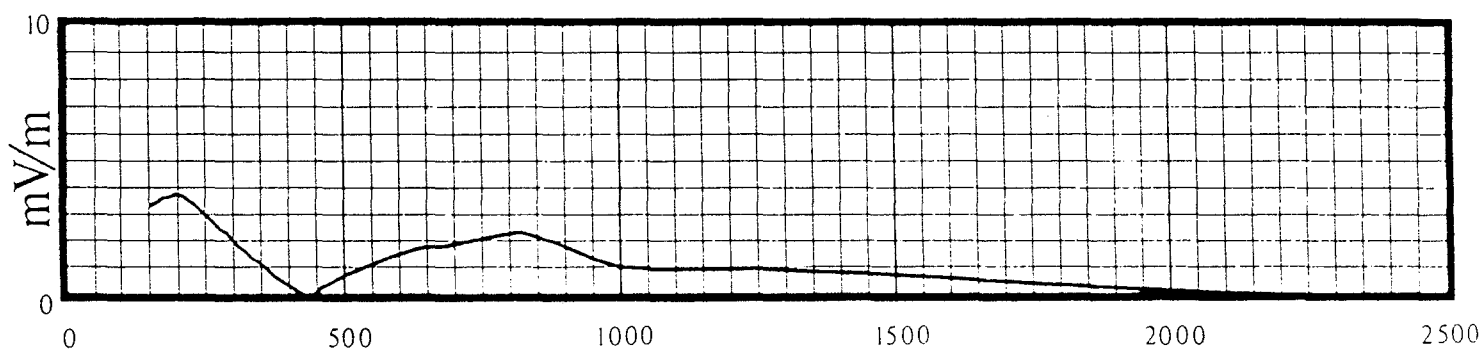
400

600

800

1000

mV/m/kW at 1 km.



Distance (Kilometers)

DATE/TIME 4-JAN-1986 11:37:26  
 GROUND SCREEN (DEG.) 90.0  
 GS CONDUCTIVITY (MHOS) 0.10E+09  
 EARTH CONDUCTIVITY 0.40E-02  
 RING HEIGHT (DEG.) 10.0  
 NULL (DEG. ABOVE HOR.) 25  
 MONOPOLE LOOP (AMP.) 18.04

FREQUENCY (MHZ.) 1.000  
 GS DIELECTRIC CONSTANT 15.0  
 EARTH DIELECTRIC CONSTANT 15.0  
 MONOPOLE HEIGHT (DEG.) 90.00  
 RING RADIUS (DEG.) 5.0  
 SCREEN HEIGHT (DEG.) 10.0  
 RING ELEMENTS (AMP.) 10.24

Richard L. Biby, P.E.

90°

80°

70°

60°

50°

Figure 8-B

40°

30°

20°

10°

0°

0

200

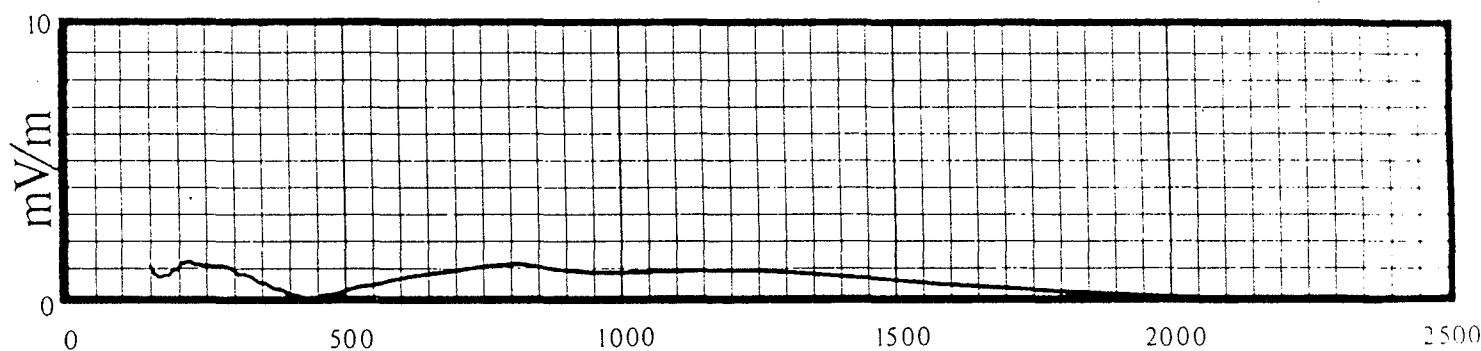
400

600

800

1000

mV/m/kW at 1 km.



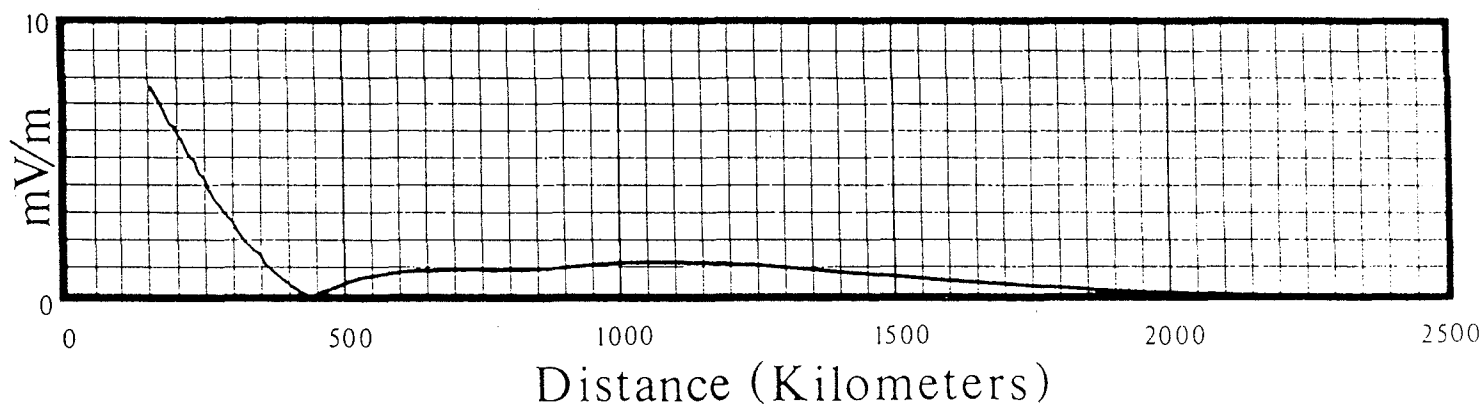
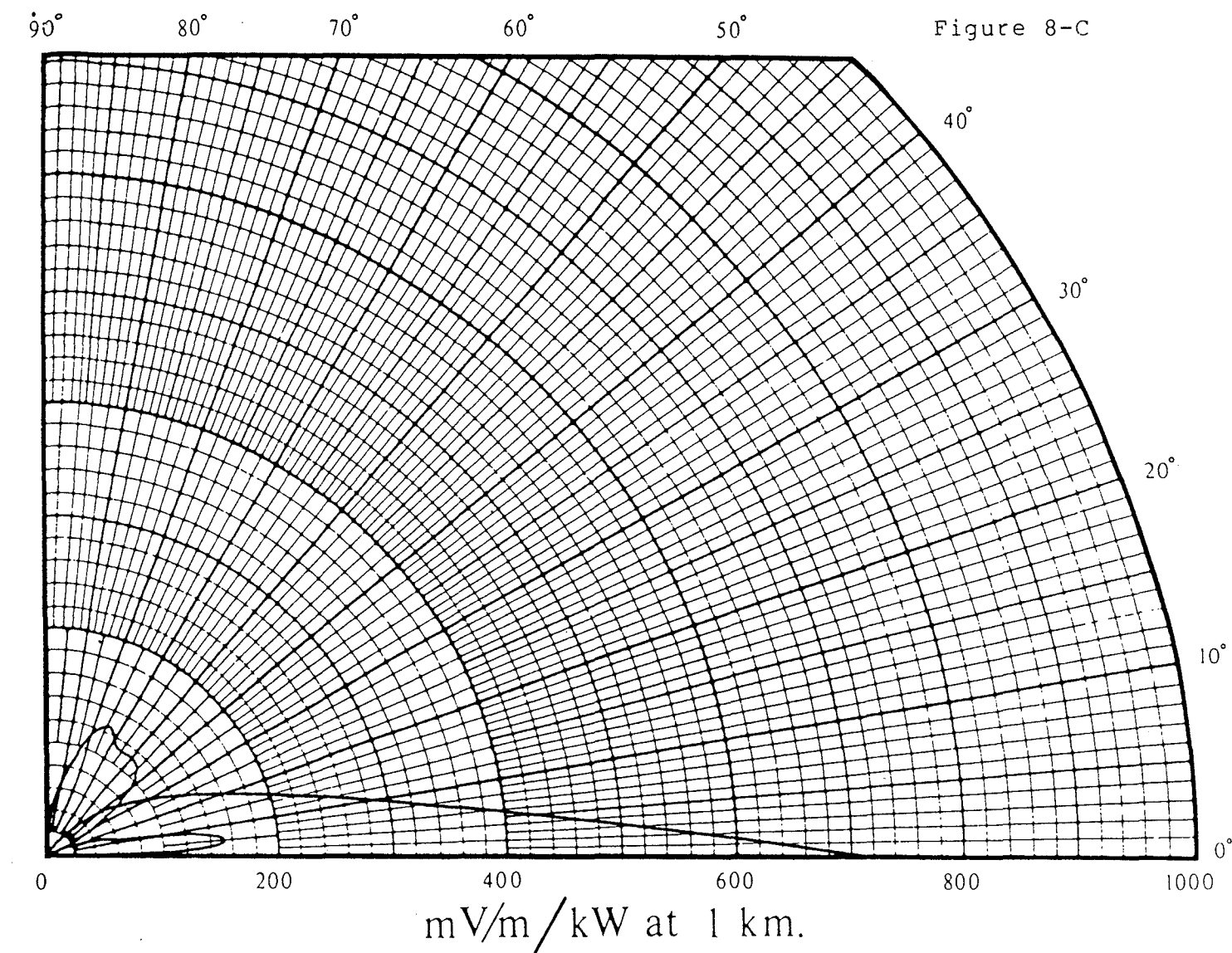
Distance (Kilometers)

DATE/TIME 4-JAN-1986 11:40:35  
 GROUND SCREEN (DEG.) 90.0  
 GS CONDUCTIVITY (MHOS) 0.10E+09  
 EARTH CONDUCTIVITY 0.40E-02  
 RING HEIGHT (DEG.) 10.0  
 NULL (DEG. ABOVE HOR.) 25  
 MONOPOLE LOOP (AMP.) 8.72

FREQUENCY (MHZ.) 1.000  
 GS DIELECTRIC CONSTANT 15.0  
 EARTH DIELECTRIC CONSTANT 15.0  
 MONOPOLE HEIGHT (DEG.) 135.00  
 RING RADIUS (DEG.) 5.0  
 SCREEN HEIGHT (DEG.) 10.0  
 RING ELEMENTS (AMP.) 7.30

Richard L. Bell, P.E.

Figure 8-C



DATE/TIME	5-JAN-1986 04:35:22	FREQUENCY (MHZ.)	1.000
GROUND SCREEN (DEG.)	90.0	GS DIELECTRIC CONSTANT	15.0
GS CONDUCTIVITY (MHOS)	0.10E+09	EARTH DIELECTRIC CONSTANT	15.0
EARTH CONDUCTIVITY	0.40E-02	MONOPOLE HEIGHT (DEG.)	180.00
RING HEIGHT (DEG.)	10.0	RING RADIUS (DEG.)	5.0
NULL (DEG. ABOVE HOR.)	25	SCREEN HEIGHT (DEG.)	10.0
MONOPOLE LOOP (AMP.)	6.09	RING ELEMENTS (AMP.)	4.64



90°

80°

70°

60°

50°

Figure 8-D

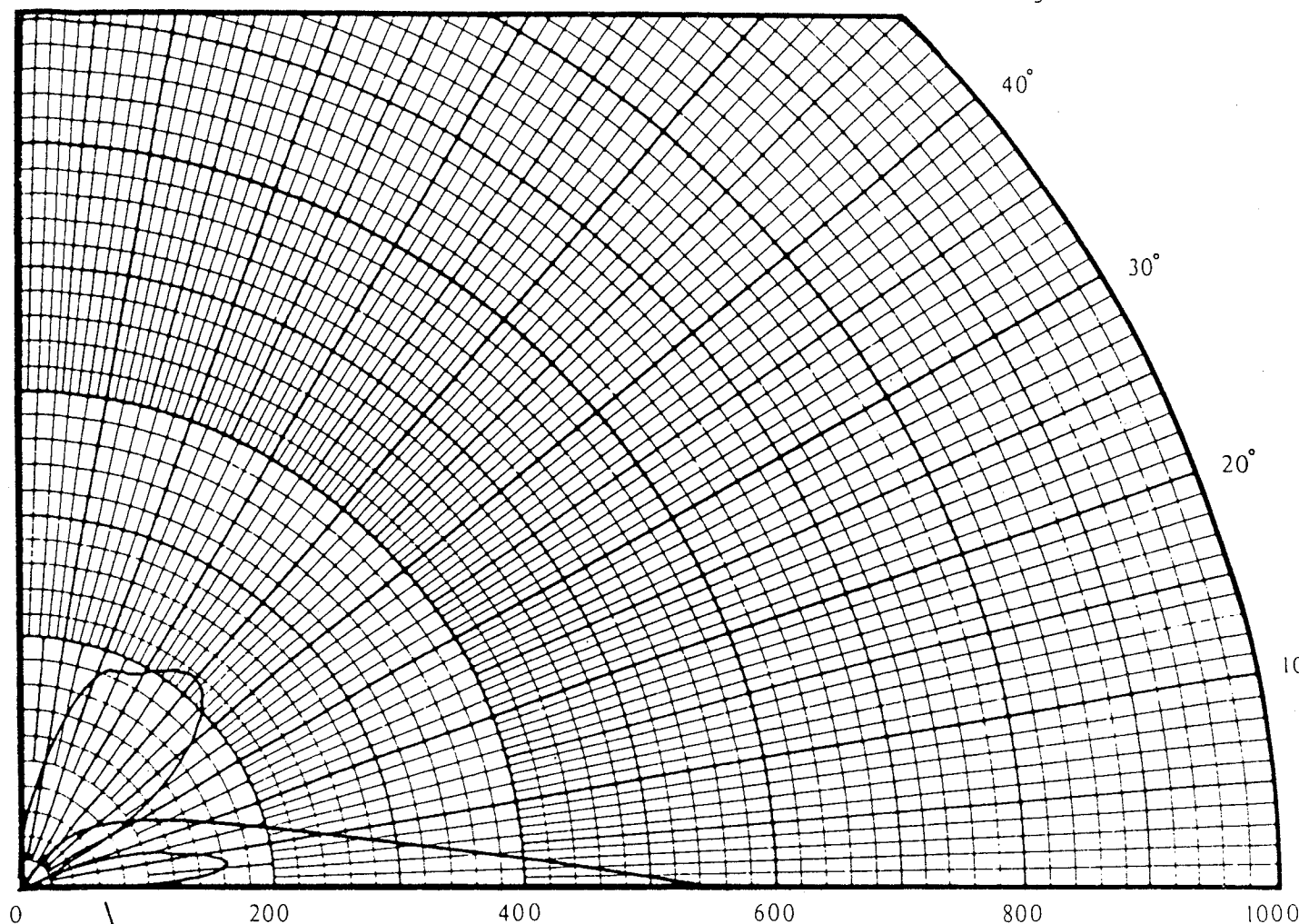
40°

30°

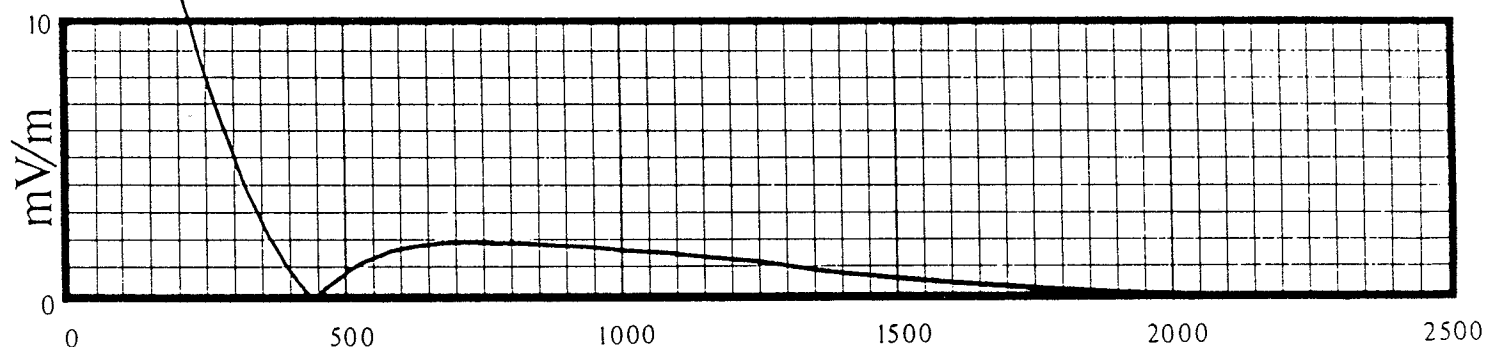
20°

10°

0°



mV/m/kW at 1 km.



Distance (Kilometers)

DATE/TIME 5-JAN-1986 04:39:37  
 GROUND SCREEN (DEG.) 90.0  
 GS CONDUCTIVITY (MHOS) 0.10E+09  
 EARTH CONDUCTIVITY 0.40E-02  
 RING HEIGHT (DEG.) 10.0  
 NULL (DEG. ABOVE HOR.) 25  
 MONOPOLE LOOP (AMP.) 5.21

FREQUENCY (MHZ.) 1.000  
 GS DIELECTRIC CONSTANT 15.0  
 EARTH DIELECTRIC CONSTANT 15.0  
 MONOPOLE HEIGHT (DEG.) 225.00  
 RING RADIUS (DEG.) 5.0  
 SCREEN HEIGHT (DEG.) 10.0  
 RING ELEMENTS (AMP.) 1.58



90°

80°

70°

60°

50°

Figure 9-A

40°

30°

20°

10°

0°

0

200

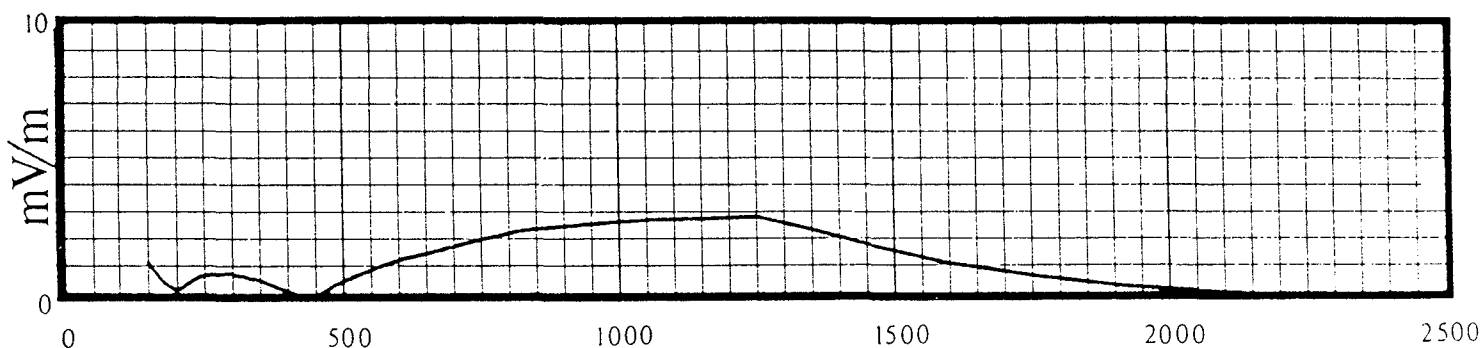
400

600

800

1000

mV/m/kW at 1 km.



Distance (Kilometers)

DATE/TIME 5-JAN-1986 04:43:44  
 GROUND SCREEN (DEG.) 90.0  
 GS CONDUCTIVITY (MHOS) 0.10E+09  
 EARTH CONDUCTIVITY 0.40E-02  
 RING HEIGHT (DEG.) 10.0  
 NULL (DEG. ABOVE HOR.) 25  
 MONOPOLE LOOP (AMP.) 19.97

FREQUENCY (MHZ.) 1.000  
 GS DIELECTRIC CONSTANT 15.0  
 EARTH DIELECTRIC CONSTANT 15.0  
 MONOPOLE HEIGHT (DEG.) 90.00  
 RING RADIUS (DEG.) 5.0  
 RING ELEMENTS (AMP.) 12.69

Richard L. Biby, P.E.

90°

80°

70°

60°

50°

Figure 9-B

40°

30°

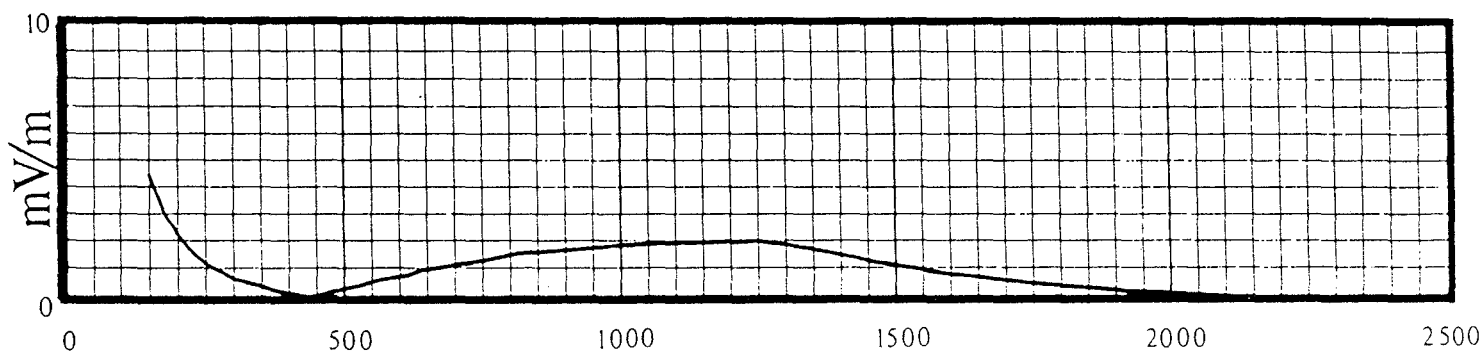
20°

10°

0°

0 200 400 600 800 1000

mV/m/kW at 1 km.



Distance (Kilometers)

DATE/TIME	5-JAN-1986 04:49:24	FREQUENCY (MHZ.)	1.000
GROUND SCREEN (DEG.)	90.0	GS DIELECTRIC CONSTANT	15.0
GS CONDUCTIVITY (MHOS)	0.10E+09	EARTH DIELECTRIC CONSTANT	15.0
EARTH CONDUCTIVITY	0.40E-02	MONOPOLE HEIGHT (DEG.)	135.00
RING HEIGHT (DEG.)	10.0	RING RADIUS (DEG.)	5.0
NULL (DEG. ABOVE HOR.)	25		
MONOPOLE LOOP (AMP.)	10.15	RING ELEMENTS (AMP.)	9.38

Richard L. Biby, P.E.

90°

80°

70°

60°

50°

Figure 9-C

40°

30°

20°

10°

0°

0

200

400

600

800

1000

mV/m/kW at 1 km.

mV/m

10

0

0

500

1000

1500

2000

2500

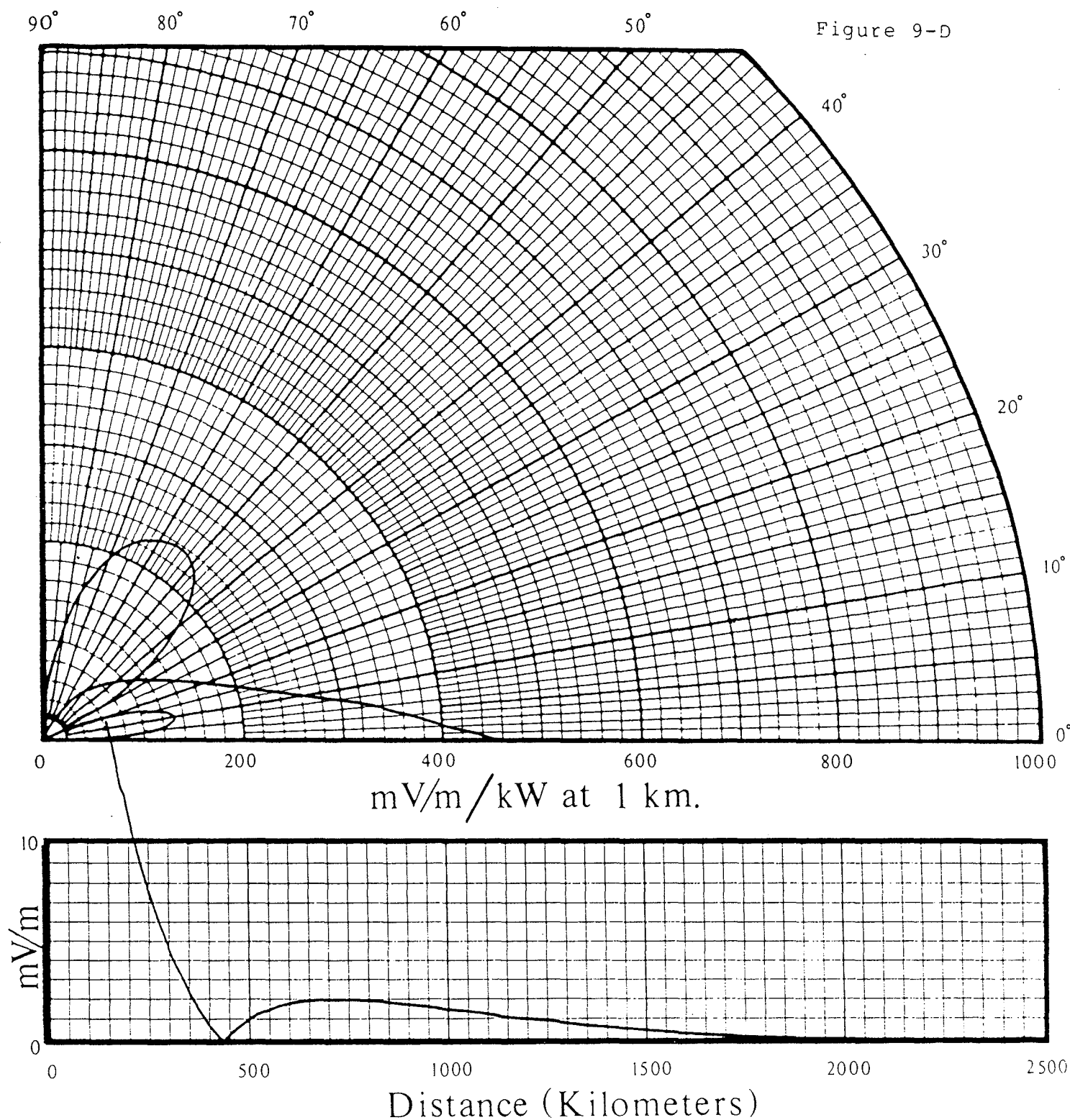
Distance (Kilometers)

DATE/TIME 5-JAN-1986 04:52:26  
 GROUND SCREEN (DEG.) 90.0  
 GS CONDUCTIVITY (MHOS) 0.10E+09  
 EARTH CONDUCTIVITY 0.40E-02  
 RING HEIGHT (DEG.) 10.0  
 NULL (DEG. ABOVE HOR.) 25  
 MONOPOLE LOOP (AMP.) 7.13

FREQUENCY (MHZ.) 1.000  
 GS DIELECTRIC CONSTANT 15.0  
 EARTH DIELECTRIC CONSTANT 15.0  
 MONOPOLE HEIGHT (DEG.) 180.00  
 RING RADIUS (DEG.) 5.0  
 RING ELEMENTS (AMP.) 5.82

Richard L. Bobb, P.E.

Figure 9-D



DATE/TIME	5-JAN-1986 04:57:18	FREQUENCY (MHZ.)	1.000
GROUND SCREEN (DEG.)	90.0	GS DIELECTRIC CONSTANT	15.0
GS CONDUCTIVITY (MHOS)	0.10E+09	EARTH DIELECTRIC CONSTANT	15.0
EARTH CONDUCTIVITY	0.40E-02	MONOPOLE HEIGHT (DEG.)	225.00
RING HEIGHT (DEG.)	10.0	RING RADIUS (DEG.)	5.0
NULL (DEG. ABOVE HOR.)	25		
MONOPOLE LOOP (AMP.)	5.68	RING ELEMENTS (AMP.)	1.68

90°

80°

70°

60°

50°

Figure 10-A

40°

30°

20°

10°

0°

0

200

400

600

800

1000

mV/m/kW at 1 km.

mV/m

10

0

0

500

1000

1500

2000

2500

Distance (Kilometers)

DATE/TIME 5-JAN-1986 05:02:01

GROUND SCREEN (DEG.) 90.0

GS CONDUCTIVITY (MHOS) 0.10E+09

EARTH CONDUCTIVITY 0.40E-02

RING HEIGHT (DEG.) 10.0

NULL (DEG. ABOVE HOR.) 15

MONOPOLE LOOP (AMP.) 20.41

FREQUENCY (MHZ.) 1.000

GS DIELECTRIC CONSTANT 15.0

EARTH DIELECTRIC CONSTANT 15.0

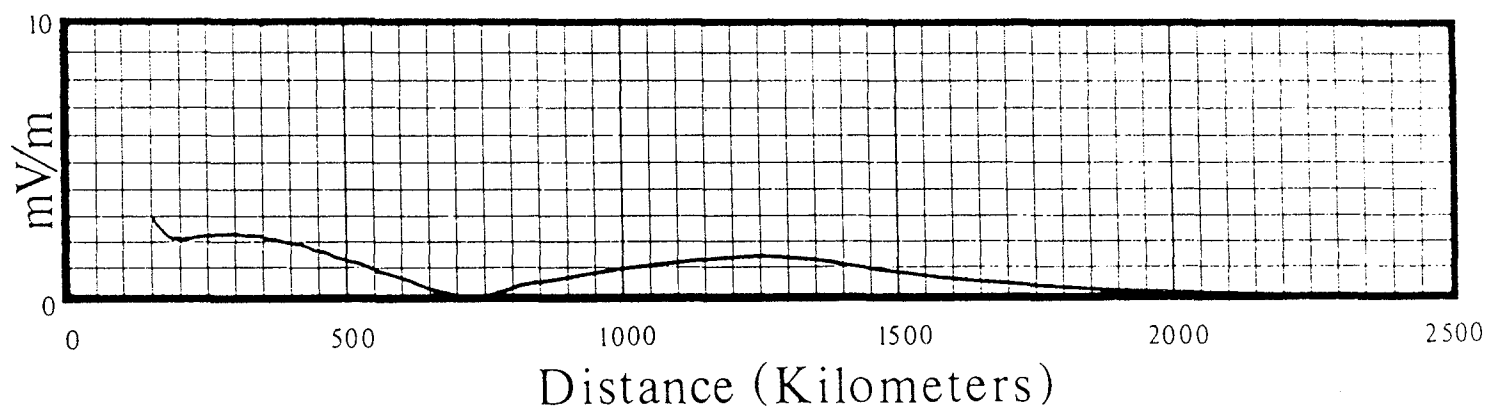
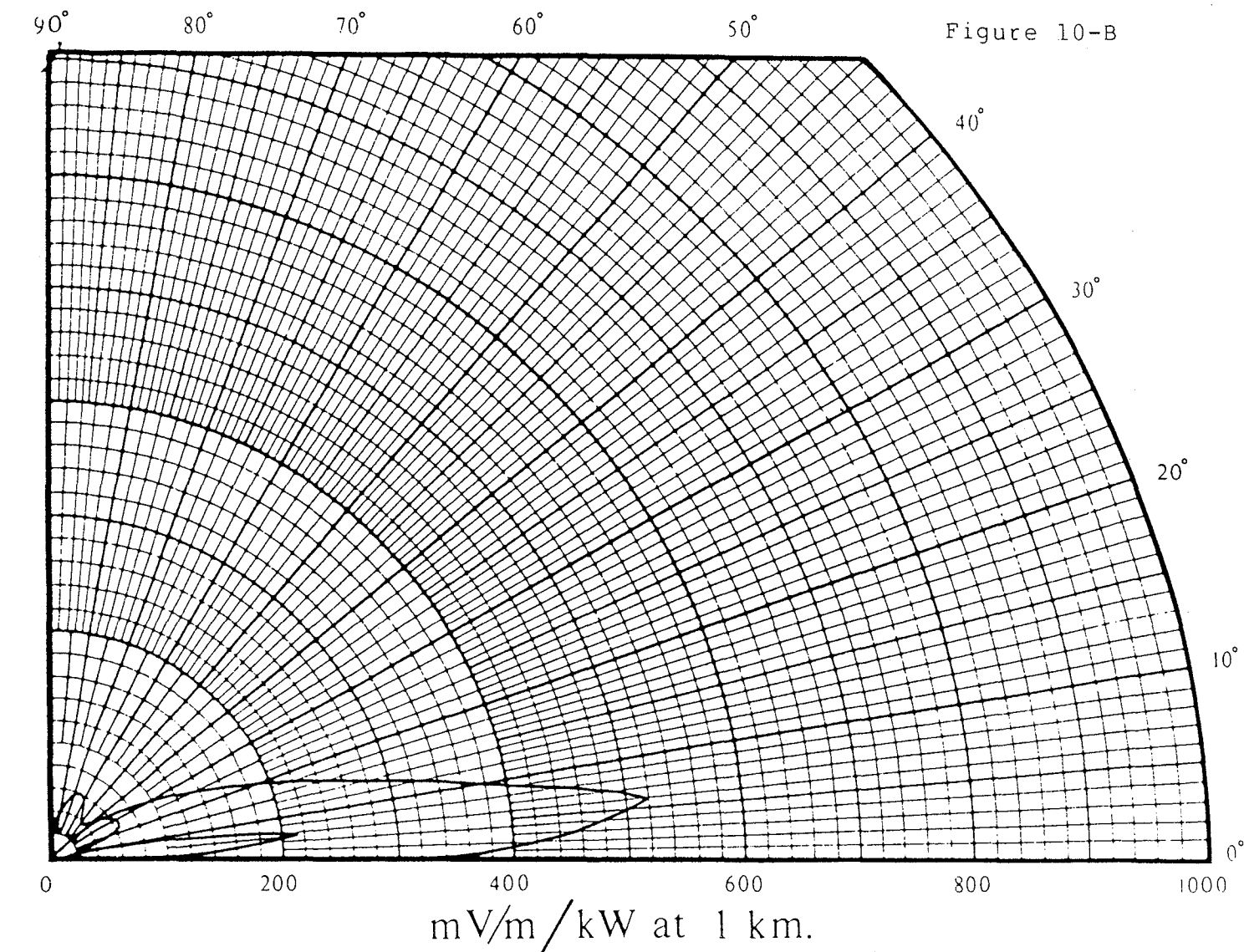
MONOPOLE HEIGHT (DEG.) 90.00

RING RADIUS (DEG.) 5.0

RING ELEMENTS (AMP.) 11.71

Richard L. Biby, P.E.

Figure 10-B



DATE/TIME	5-JAN-1986 05:06:44	FREQUENCY (MHZ.)	1.000
GROUND SCREEN (DEG.)	90.0	GS DIELECTRIC CONSTANT	15.0
GS CONDUCTIVITY (MHOS)	0.10E+09	EARTH DIELECTRIC CONSTANT	15.0
EARTH CONDUCTIVITY	0.40E-02	MONOPOLE HEIGHT (DEG.)	135.00
RING HEIGHT (DEG.)	10.0	RING RADIUS (DEG.)	5.0
NULL (DEG. ABOVE HOR.)	15		
MONOPOLE LOOP (AMP.)	10.31	RING ELEMENTS (AMP.)	8.92

90°

80°

70°

60°

50°

Figure 10-C

40°

30°

20°

10°

0°

0

200

400

600

800

1000

mV/m/kW at 1 km.

mV/m

10

0

0

500

1000

1500

2000

2500

Distance (Kilometers)

DATE/TIME 5-JAN-1986 05:11:39  
 GROUND SCREEN (DEG.) 90.0  
 GS CONDUCTIVITY (MHOS) 0.10E+09  
 EARTH CONDUCTIVITY 0.40E-02  
 RING HEIGHT (DEG.) 10.0  
 NULL (DEG. ABOVE HOR.) 15  
 MONOPOLE LOOP (AMP.) 7.07

FREQUENCY (MHZ.) 1.000  
 GS DIELECTRIC CONSTANT 15.0  
 EARTH DIELECTRIC CONSTANT 15.0  
 MONOPOLE HEIGHT (DEG.) 180.00  
 RING RADIUS (DEG.) 5.0  
 RING ELEMENTS (AMP.) 6.04

Richard L. Biby, P.E.



90°

80°

70°

60°

50°

Figure 10-D

40°

30°

20°

10°

0°

0

200

400

600

800

1000

mV/m/kW at 1 km.

mV/m

10

0

500

1000

1500

2000

2500

Distance (Kilometers)

DATE/TIME 5-JAN-1986 05:16:08

GROUND SCREEN (DEG.) 90.0

GS CONDUCTIVITY (MHOS) 0.10E+09

EARTH CONDUCTIVITY 0.40E-02

RING HEIGHT (DEG.) 10.0

NULL (DEG. ABOVE HOR.) 15

MONOPOLE LOOP (AMP.) 5.27

FREQUENCY (MHZ.) 1.000

GS DIELECTRIC CONSTANT 15.0

EARTH DIELECTRIC CONSTANT 15.0

MONOPOLE HEIGHT (DEG.) 225.00

RING RADIUS (DEG.) 5.0

RING ELEMENTS (AMP.) 2.69

Richard L. Blevins, P.E.



# AM Antenna Design: The New Wave?

*Relaxed regulations and improved technologies are beginning to make AM's future sound better.*

By Hugh Aldersey-Williams

**T**he AM industry has been thrown into turmoil by recent moves both in technology and in regulatory areas.

For its part, the FCC has outlined regulatory changes it would like to see in AM broadcasting. The changes would improve AM's competitive position with regard to FM transmission, which has been received rather more favorably in recent years.

### Night and day

While the FCC has been relaxing its regulations, the NAB has been seeking to improve AM antenna technology. The principal problem that hampers the success of AM transmissions is signal interference arising from the antenna signal strength profile (Figure 1a). Existing antenna designs generate signals having two components.

The groundwave is directed from the antenna to the horizon. The stronger it is, the wider the coverage of that broadcasting station. The skywave, on the other hand, is directed more vertically, and would not matter but for the fact that its signal is reflected by the earth's ionosphere back towards the surface. This can cause "selective fading"—severe ampli-

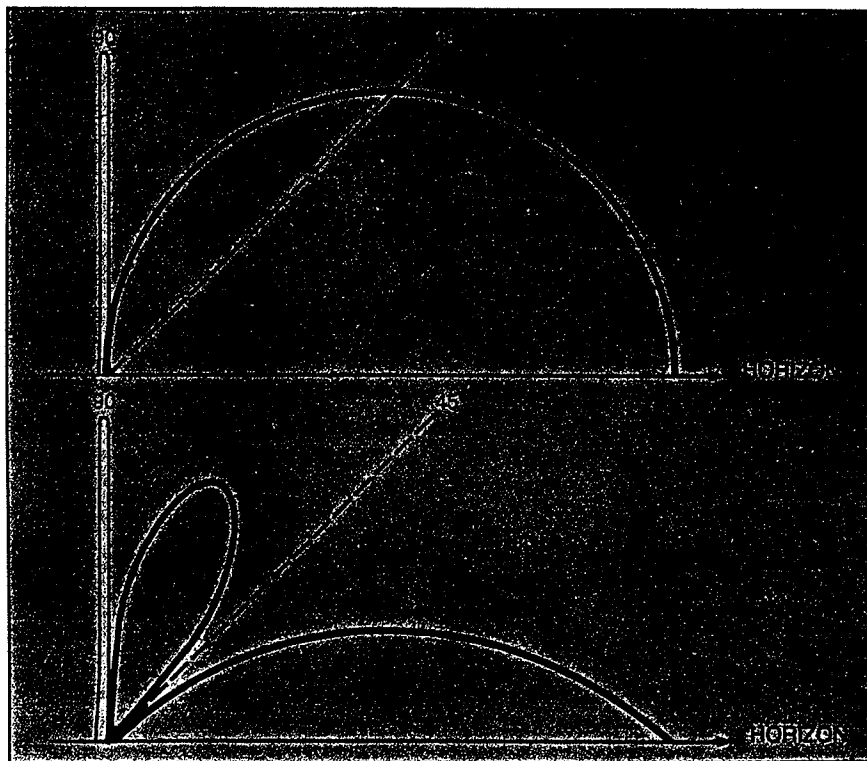


Figure 1. Signal strength versus departure angle for a) typical AM antenna; b) new design antenna. Note the relative increase in signal strength at the horizon (groundwave) and the decrease at 45 degrees (skywave).

tude and phase distortion or even disappearance into noise—of one broadcast signal, as well as interference between stations with signals that are close in frequencies even though they may be hundreds of miles apart. At night, the

ionosphere reflects radio waves even more strongly than it does during the day, making many AM services unusable after dark. Efforts to increase the groundwave signal strength produce a concomitant increase in the skywave,

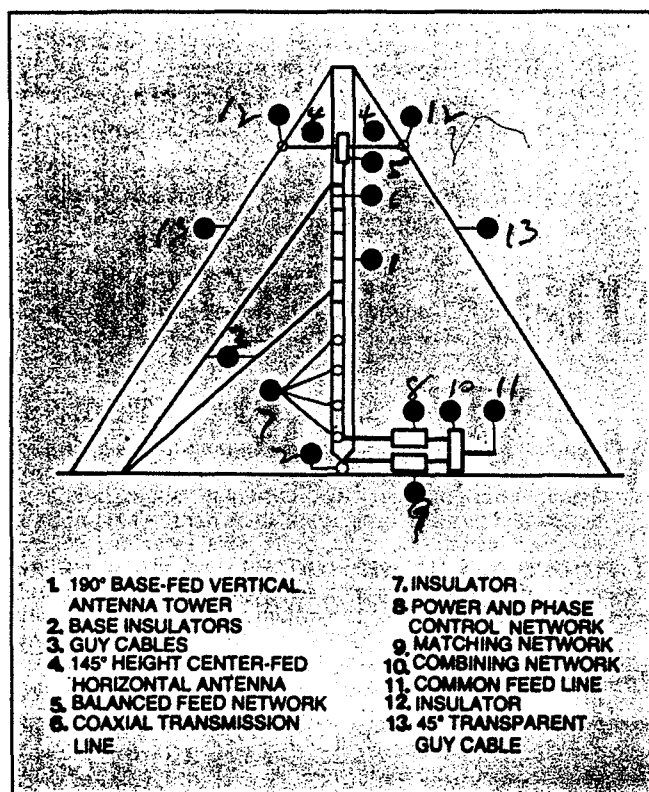


Figure 2. Design of Prestholdt's AM antenna comprising horizontal, vertical, and diagonal antenna elements.

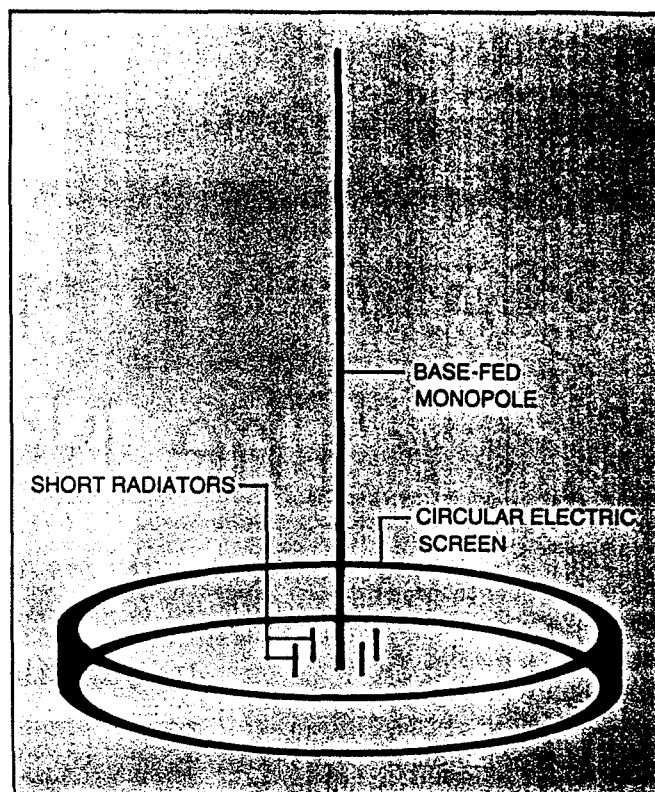


Figure 3. Design of Biby's AM antenna showing the central monopole, four short radiators, and the circular electric screen.

merely exacerbating the problem of interference. In a typical AM broadcast antenna system, perhaps only 10 percent of the radiated energy goes into the groundwave.

Previous attempts to devise an antenna design with a stronger groundwave but a weaker skywave have not been very successful. Larger radiating structures have been able to generate stronger groundwaves while suppressing the skywave component, but this has not been possible with short radiators (shorter than half a wavelength). Successes have been limited by the comparative expense of the antenna designs and the fact that they did not suppress the skywave signal over the full range of vertical angles necessary to cut interference to an acceptable level.

Now, the NAB has authorized the construction and testing of two new antenna designs, which represent the most promising move in the technology of the field for years. "This is a major undertak-

ing for the association," says NAB president Eddie Fritts, "one which we expect to have a significant impact on AM radio. The result should be a clearer, louder, better quality sound for AM."

In a field 40 miles west of Washington, DC, next month, ground will be broken for the prototypes, developed independently by two engineering consultancies. Construction of the antennas is expected to take one year, and field testing and proof of performance will take another year. Tests will be conducted on the unused 100 kHz available on AM.

The engineers responsible for the projects stress that both designs currently only exist on paper and have not yet been proven in any way. Nonetheless, theoretical predictions have been sufficiently optimistic for the NAB to give its backing. "A significant increase in AM service would result if these antennas are successful and implemented by AM broadcasters," says the NAB.

The new designs work essential-

ly by combining a number of antennas at one location. The overall signal obtained by adding the individual signals from each antenna in the array is expected to provide more independent control over the skywave and groundwave component signals. Suitable adjustment of the component antennas could then minimize the skywave signal and simultaneously increase the horizon signal strength of the groundwave (Figure 1b).

### Antenna segments

The first public announcement of a design, one of those now being investigated by the NAB, was announced at the September 1985 IEEE Annual Broadcast Symposium by Ogden Prestholdt, a retired partner of A.D. Ring and Associates. It comprises vertical, horizontal, and diagonal antenna segments. These segments are designed to be excited with carefully chosen current amplitudes and phases to obtain an overall radiation distribution with a sup-

## RF Engineering

AM Antenna Design

pressed skywave. Using separately driven diagonal as well as vertical and horizontal segments provides a selection of amplitudes and phases than has been possible with the "T" and "L" antennas tried in the past, says Prestholdt.

The design was conceived when it was realized that "vertical polarization isn't necessarily generated only by a vertical wire," says Prestholdt. A possible configuration of Prestholdt's design is shown in Figure 2. It comprises a typical 190 degree base-fed vertical tower with a base insulator and guy cables. At the 145 degree height, there is a center-fed horizontal antenna oriented parallel to the y-axis and supported at its ends by insulators and an auxiliary set of transparent guy cables at a 45 degree angle. Thus, each half of the antenna is 45 degrees in length. The horizontal element would be fed from a balanced feed network supported in the tower which is in turn fed by a coaxial transmission line supported inside the tower and insulated, for isolation, from it for the lower 90 degrees.

Prestholdt calculates the radiation distribution—described in a series of conic sections—from the prototype antenna by first developing a mathematical description of the total radiation from a short current element using a computer. Then, the far-field—both skywave and groundwave—is calculated by integrating the antenna current elements and their images for each antenna segment. The component due to the vertical antenna only varies with the angle of elevation and is in that direction, while the horizontal signal is a function of both elevation and bearing from the antenna and has components in both of these directions. The elevation components are found to be in time quadrature—i.e., these signals from the horizontal and vertical antennas are 90 degrees out of phase when the antenna currents are in phase. By selecting appropriate signal amplitudes the skywave component can then be minimized.

A typical configuration of two

# "No more halftime headaches..."

"This new Telex headset is so light and comfortable I can finally leave my aspirin home. And, my engineer says I sound great!"

*Charlie Jones*

The newest Telex "Sportscaster" boom mic headset has the pros in the broadcast booth talking. Good news about the model PH-24 is spreading quickly among veteran sports announcers like network television sports announcer Charlie Jones. Imagine, a professional broadcast headset with full studio-quality, electret condenser microphone and optimum earphone receiver performance weighing a mere 2½ oz. (less cord).



Includes effective windscreen and push-to-quiet switch. For complete information about this and other professional headsets from Telex, write to Telex Communications, Inc., 9600 Aldrich Avenue South, Minneapolis, MN 55420. For quick information, call toll free **800-328-3771** or in Minnesota call (612) 887-5550.



Charlie Jones, nationally known network television sports announcer.

## RF Engineering

### AM Antenna Design

distant antennas of the new design might reduce the RMS of the groundwave significantly from its value for conventional vertical antennas. But, Prestholdt reports, the AM transmission service radius can be approximately doubled because of the reduced level of interference between the two antennas. "It is not yet known how versatile the system will eventually be," says Prestholdt, "but it is anticipated that it will permit new stations to be added to the spectrum, for existing stations to improve their local service and to result in reduced interference to many stations."

### Short radiators

The second proposed antenna comes from Richard Biby of Communications Engineering Services. It will be described in detail in a paper at the NAB conference in April. The design centers on a base-fed monopole of about a quarter of a wavelength in height. This operates over a conventional ground system comprising approximately 120 buried copper radial ground wires of the same length as the monopole. Around the base of the monopole are distributed a number of shorter ( $\frac{1}{30}$  wavelength) base-fed radiating elements. These short radiators and the central monopole are enclosed by a circular electric screen also about  $\frac{1}{30}$  wavelength high and roughly a quarter of a wavelength from the monopole (Figure 3). Biby says that "this is not a super-gain scheme—the performance of the antenna is critically dependent on the imperfect conducting characteristic of the earth."

The screen in the layout serves to cancel the creation of a strong groundwave by the short radiators, but does not prevent them from radiating a strong skywave at angles above the horizon. Judicious positioning of the screen and the short radiators allows the skywaves from the central monopole and from the short radiators to be closely matched in phase and amplitude. Then, adjustment of the short radiator currents can

cancel the two skywaves over a range of vertical angles. The circular electric screen only has a small effect on the groundwave component from the monopole.

"This antenna design," says Biby, "should result in greatly increased groundwave signal strengths per unit of input power as compared with that obtained with conventional antenna systems." Biby's computer model of the new antenna concept allows for variation of a number of details that affect the radiation strength at vertical and horizontal angles from the antenna. These variables on the computer model include frequency, the number and dimensions of radiating elements, conductivity, and dielectric constant of the screen and the earth. Biby is able to compare results for well-established designs for verification of the model before using it to predict an optimum new antenna configuration.

### For the future

Both Biby and Prestholdt are confident that their computer modeling of their antennas' performance will be verified when the antennas are up and running in early 1987. For the moment, however, they emphasize that they have only these theoretical predictions.

Nonetheless, their experiments are being followed with interest by the parties that stand to benefit. Biby and Prestholdt have been receiving attention from a number of companies, which do not wish to be named. Michael Rau, the NAB's engineer coordinating the field study, also says a lot of interest is being shown by the broadcast community—engineers, consultants, and managers.

Such interest, while encouraging, is a little premature with first tests not due to start for at least a year. The NAB is, however, maintaining a mailing list for those who wish to be updated on progress and for volunteer AM engineers interested in performing the necessary skywave field measurements over the period of the test.

BM/E

You could  
**WIN!**  
**\$1000**

by answering three simple questions about a new product we've introduced in an ad which appears on a previous page in this issue.

We're anxious for you to see what makes this new boom mic headset different from the rest. So, we're willing to put your name into a \$1000 drawing if you'll answer three simple questions about the PH-24. (Here's a hint. The answers are contained in the ad.)

**Question 1**—What TYPE of boom mic is used to produce the full studio quality sound discussed in the ad?

**Question 2**—How LIGHT (in ounces) is this lightweight headset?

**Question 3**—What HALFTIME PROBLEM has network sports announcer Charlie Jones eliminated since he began using the PH-24?

Hurry! Only those correctly answered entries post-marked before Feb. 28, 1986 will be used in a random drawing held on March 14, 1986. The drawing will be performed by a neutral party. Employees and families of Telex or this publication will not be eligible. Winner will be notified by mail, and the winner's name and address will be available to anyone upon request.

Void where prohibited by law.

**"No more halftime headaches..."**



Send answers to:

**Telex Communications, Inc.**  
Headset Drawing  
9600 Aldrich Avenue South  
Minneapolis, MN 55420

**Answer 1:** \_\_\_\_\_

**Answer 2:** \_\_\_\_\_

**Answer 3:** \_\_\_\_\_

NAME \_\_\_\_\_

COMPANY \_\_\_\_\_

ADDRESS \_\_\_\_\_

CITY \_\_\_\_\_

STATE \_\_\_\_\_ ZIP \_\_\_\_\_ **BME 2-86**

JOHN H. MULLANEY  
CONSULTING RADIO ENGINEERS

ENGINEERING COMMENTS PREPARED ON BEHALF OF RADIO STATION WKBO CONCERNING  
THE APPLICATION OF RADIO STATION WFEC TO MOVE TRANSMITTER SITE

August 9 , 1976

JOHN H. MULLANEY  
CONSULTING RADIO ENGINEERS

State of Maryland                    )  
                                      )  
County of Montgomery                ) SS:  
                                      )  
Potomac                                )

John H. Mullaney, being first duly sworn upon oath, deposes & states that he is a registered professional engineer in the state of Maryland & the District of Columbia, & his qualifications are known to the Federal Communications Commission. Affiant states that he has been retained by Harrea Broadcasters, Inc., licensee of radio station WKBO who operate on 1230 KHz at Harrisburg, Penna., to prepare comments in regard to the application of Scott Broadcasting Corporation, licensee of radio station WFEC who operate on 1400 KHz at Harrisburg, Penna., on the possible interference such application might create to the operation of WKBO because of the close separation of antennas.

Affiant states that the computations & exhibits contained herein were made by him personally & all facts reported herein are true of his own knowledge, except where stated to be on information or belief, & as to those facts, he believes them to be true.

/S/ John H. Mullaney  
John H. Mullaney, P.E.  
Maryland #5314 ( S E A L )

Subscribed & sworn to before me this 9 th day of August 1976.

/S/ Joyce A. Mullaney  
Joyce A. Mullaney,  
Notary Public

( S E A L )

My Commission Expires: July 1, 1976.

ENGINEERING COMMENTS PREPARED ON BEHALF OF RADIO STATION WKBO CONCERNING  
THE APPLICATION OF RADIO STATION WFEC TO MOVE TRANSMITTER SITE

I. General:

This office has been retained by Harrea Broadcasters, Inc., licensee of radio station WKBO of Harrisburg, Penna. WKBO operates on 1230 KHz with 1-0.25 KW U using a 150' grounded folded-unipole antenna. We were retained to study an application filed on July 8, 1976 by Scott Broadcasting Corp., licensee of radio station WFEC who operate on 1400 KHz, 1-0.25 KW U to move their transmitter site within 370' of the present antenna system of WKBO. Our study has been directed to determining if the close proximity of the WFEC antenna would create interference to WKBO & make any recommendations to protect the operation of WKBO.

We have determined that the proposed operation of WFEC has a high probability of creating re-radiation of WKBO's signal & thereby distorting its radiation pattern. In addition there is a possibility of cross-modulation being set up between the two stations.

WFEC is presently located approximately 2,630' from the WKBO antenna on a true bearing of 22.46°. Their proposed move would locate the WFEC antenna approximately 370' away on a true bearing of 123.28°. Filters are now installed at the WKBO installation to prevent any cross-modulation or re-radiation of the WFEC & WCMB(1460 KHz 5 KW DA-N) signals.

It is not the position of WKBO that it is impossible for WFEC to prevent interference to WKBO's non-directional pattern nor eliminate any inter-modulation, but rather that because of the extremely close spacing of the two antennas, the fact that both will be grounded folded unipole types, & the frequency separation is only 170 KHz, that it will be a very difficult problem to solve. WFEC's engineering statement does not appear to be aware of the magnitude of the problem inasmuch as they do not furnish details regarding exactly how they propose to handle the matter. WKBO feels that special conditions should be assigned to any construction permit granted WFEC for this site.

II. Engineering Discussion:

A. WFEC Proposed Antenna System:

The proposed antenna will be located at the southern tip of City Island, just south of Penn Central Railroad bridge. The geographic coordinates are:

N. Lat.	40° 15' 19"
W. Long.	76° 56' 04"

The WKBO antenna is located at geographic coordinates of:

Page 2,      Engineering Comments Cont:

N. Lat.      40° 15' 11"  
W. Long.      76° 53' 08"

The distance between antennas is 0.0701 miles or 370'. The true bearing from WKBO to the proposed WFEC antenna is 123.28°.

WFEC proposes to use a grounded folded-unipole antenna 175' tall, which is equivalent to a height of 89.7° at 1400 KHz & 78.75° at 1230 KHz. The proposed ground system will be abbreviated & the power input to the antenna will be adjusted so as to produce an unattenuated efficiency of 150 mv/m/KW at one mile. Although the cross section of the tower has not been stated one would expect a tower with a width of 18" to 36". The folds would be spaced anywhere from 18" to 36", & the radius of the fold wires would be on the order of 0.125".

Figures 1 & 2 are tabulations of computer runs for a 175' folded-unipole antenna system with the parameters shown.

Figure 1 furnishes information for a tower with an 18" side, fold spaced 24", radius of fold wire 0.125" at 1400 KHz. It will be noted that the current transformation ratio is 4.397, while the characteristic impedance of the transmission line portion of the antenna is approximately 409 Ohms. If this antenna is to be adjusted for a 50 Ohm feed-point, the three shorting stubs on the tower must be located approximately 103' from the base of the tower.

Figure 2 furnishes the same type of information as shown in Figure 1 except the dimensions of the tower width have been changed to 24". The current transformation ratio is slightly higher with a value of 5.236, while the characteristic impedance of the transmission line is slightly lower with a value of approximately 403 Ohms.

Figure 3 & 4 are computer tabulations for the same 175' tower but this time the frequency has been changed to 1230 KHz. The purpose of making this run was to determine what the WFEC tower would look like at 1230 KHz the operating frequency of WKBO.

A study of figures 3 & 4 indicates that for an 18" width tower with the stub at the top of the tower one would expect to measure an impedance of approximately 307 -j216 Ohms; while for the same conditions but for a 24" tower the expected measured impedance would be approximately 400 -j200 Ohms. If the WFEC tower had been stubbed to obtain an approximate 50 Ohm feed-point resistance at 1400 KHz for Figures 1 & 2, the equivalent impedances at 1230 KHz would be 114 j198 & 79 j182 Ohms. The exact value of impedance at either frequency can vary depending upon lead length, distance up tower folds are terminated, & any variations in parameters.

A series-pass, parallel-reject type of network can be used in the antenna lead to the coupling unit to prevent the majority of inter-modulation between carriers; however it will not keep incident fields from either



Page 3,            Engineering Comments Cont:

antenna system from being induced in the tower structure which is grounded. It therefore will be quite difficult to design a filter system that will prevent fields from being re-radiated by each tower at the other stations frequency. The reason for this is the fact that each tower is a folded-unipole, & grounded & unless each antenna can be adjusted to have a very high impedance at the other stations frequency currents will flow in each antenna & prevent proper isolation. The use of networks in the folds is possible but these networks even considering the low power of both stations would have to have components capable of handling high currents.

The attached Appendix illustrates the method of determining the impedance of a folded-unipole antenna. It has been used to set up the computer program used to obtain the tabulations shown on Figures 1 through 4.

#### B. Distortion to WKBO Antenna System:

We are concerned with the problem of the WFEK re-radiating the signal of WKBO & creating distortion to our non-directional pattern. In order to determine what effect if any the WFEK antenna would have on the WKBO antenna system we have determined the re-radiated field using the following expression:

$$E_r = 37.25 \left[ \frac{(1 - \cos G)}{\sin^2 G} (\sin^2 (G/2)) (\lambda/\pi) (E_i/Z_b) \right]$$

Where:

$E_r$  = re-radiated field in mv/m

$G$  = height of re-radiating structure(our case 78.75°)

$\lambda$  = wavelengths in meters

$E_i$  = incident field in volts per meter at re-radiator where  
 $E_i = 1/d (E_o) \times 10^{-3}$  volts per meter(our case  $1/0701 \times 150 \times 10^{-3} = 2.1398$  volts per meter.

37.25 = Factor

$Z_b$  = base impedance of re-radiator after determining equivalent termination impedance at re-radiating frequency(our case 47.79)

Substituting in the above equation we obtain a re-radiated field of 43.615 mv/m. The spacing between the two towers is 370' or 166.56° at 1230 KHz. The field ratio for tower #2(WFEK tower) is  $43.615/150 = 0.2908$ . (the re-radiated field divided by unattenuated field of WKBO system at 1230 KHz). The time space phasing for the #2 tower will be equal to the actual spacing between the towers plus 180° for the reversal on the tower. This equals -13.44°. The orientation of the array will be 123.28°. The field & phase for the WKBO tower is taken as 1 at an angle of 0°. For purposes of computation we will use a Standard Pattern; however the difference between a Theoretical & Standard pattern is only 5% & has no bearing on this discussion. Now substituting the known parameters in the General Case directional antenna design formulae we obtain the tabulation of

Page 4,                      Engineering Comments Cont:

Figure 5. Figure 6 is a plot of the directional pattern created by the location of the WFEC tower along with a comparison to the non-directional pattern for WKBO.

It should be noted that WKBO will also re-radiate the 1400 KHz signal of WFEC & distort their non-directional pattern. The results of this distortion is not shown in this engineering statement.

C. Suggested Conditions For Any Construction Permit:

Inasmuch as WKBO is required to limit its efficiency to 150 mv/m at one mile in order to prevent interference to co-channel stations, & also maintain necessary filters to prevent cross-modulation or signal reradiation to radio station WCMB on 1460 KHz at Harrisburg, Penna, & also cooperate with the licensee of radio station WFEC to prevent any such cross-modulation or signal reradiation it follows that any change in the present existing conditions (no re-radiation or cross-modulation between stations) could cause WKBO to cause re-radiation, cross-modulation, & co-channel interference to other stations. In view of this it is respectively submitted that WFEC if given a construction permit should have the following conditions assigned:

"The authority granted herein is subject to the following conditions:"

1. Before program tests are authorized, permittee shall submit to the Commission sufficient field intensity measurements made on Station WKBO, Harrisburg, Pa., to satisfactorily demonstrate that the WKBO radiation pattern has not changed as a result of permittee's construction. The minimum required measurements made prior & subsequent to said construction shall include at least ten(10) consecutive points on at least eight radials. Permittee shall assume responsibility for all costs involved in complying with this condition.
2. Permittee assume the responsibility for installation & adjustment of necessary equipment in its & WKBO's antenna system to prevent adverse affects on WKBO, Harrisburg, Pa., due to cross-modulation or signal reradiation. Permittee will also assume the responsibility for installation & adjustment of necessary equipment in its & WCMB's antenna system to prevent adverse affects on WCMB, Harrisburg, Pa., due to cross-modulation or signal reradiation. Permittee shall assume responsibility for all costs involved in complying with this condition.

It is assumed that the Commission would also require WFEC to demonstrate by means of field intensity measurements on their own operation that they have obtained an inverse distance field at one mile of 150 mv/m, & their pattern is substantially non-directional.

Page 5,            Engineering Comments Cont:

D. The Matter of Cross-Modulation:

WKBO now maintains filters to prevent cross-modulation between WKBO & WFEC. It is assumed that WFEC also maintains such filters inasmuch as no problems have been noted with WFEC operating at their present location. The probability of increasing this potential for interference is self evident & needs no amplification at this time.

III. Summary:

It has been demonstrated that the proposed move of WFEC could create serious distortion problems to the WKBO antenna system let alone their own proposed operation. Affiants is aware that by use of filters it is quite likely that re-radiation of the WKBO non-directional operation can be eliminated. It also follows that by use of proper filters cross-modulation can also be eliminated or reduced to an acceptable level; however because of the close spacing of the two antenna systems & the fact that both towers are grounded & fed by the folded-unipole technique sets up a condition that could make it extremely difficult to prevent re-radiation of each of the stations signals by the other stations antenna system. The matter of obtaining a good bandwidth for proper modulation can also become a problem if filters or high Q techniques are used to try & de-tune the systems at the other operating frequency. Operating two antennas within 170 KHz at a spacing of 370' is not considered good engineering & unless strict conditions are placed on any construction by WFEC, their proposed operation could cause WKBO to have a distorted non-directional pattern, so much so, that interference is created to other radio stations. A serious reduction in bandwidth would distort the modulation quality of the WKBO signal, which in turn could affect their ability to sell time.

Affiants believes that sufficient reasons have been setforth to demonstrate that any authority to construct to WFEC should be subject as a minimum to the conditions suggested.

/S/ John H. Mullaney

John H. Mullaney, P.E.  
Maryland #5314

August 9, 1976.

( S E A L )

# FIGURE 1

JOHN H. MULLANEY  
CONSULTING RADIO ENGINEERS

SIDE OF TOWER IN INCHES ? 18  
SEPARATION OF FOLDS FROM TOWER IN INCHES ? 24  
RADIUS OF FOLD IN INCHES ? .125

CURRENT TRANSFORMATION RATIO 4.397

HEIGHT OF TOWER IN FEET ? 175  
FREQUENCY IN KHZ ? 1400

CHARACTERISTIC IMPEDANCE OF TRANSMISSION LINE 409.278 OHMS

LOSS RESISTANCE OF TOWER IN OHMS ? 1  
BASE INDUCTANCE IN MICRO HENRIES ? 0  
DISTANCE FROM TOP OF TOWER  
TO STUB IN FEET (START,STOP,STEP) ? 0,175,5,

DISTANCE OF STUB FROM TOP BOTTOM		RESISTANCE	REACTANCE
0.000	175.000	222.953	119.077
5.000	170.000	205.495	129.060
10.000	165.000	188.284	136.022
15.000	160.000	171.738	140.420
20.000	155.000	156.115	142.699
25.000	150.000	141.550	143.265
30.000	145.000	128.091	142.469
35.000	140.000	115.729	140.602
40.000	135.000	104.418	137.906
45.000	130.000	94.096	134.570
50.000	125.000	84.686	130.749
55.000	120.000	76.114	126.559
60.000	115.000	68.304	122.095
65.000	110.000	61.185	117.427
70.000	105.000	54.692	112.609
75.000	100.000	48.764	107.682

Page 2, Figure 1 Cont:

80.000	95.000	43.349	102.677
85.000	90.000	38.400	97.616
90.000	85.000	33.872	92.514
95.000	80.000	29.731	87.382
100.000	75.000	25.943	82.225
105.000	70.000	22.480	77.048
110.000	65.000	19.318	71.850
115.000	60.000	16.436	66.630
120.000	55.000	13.816	61.384
125.000	50.000	11.443	56.109
130.000	45.000	9.307	50.797
135.000	40.000	7.398	45.443
140.000	35.000	5.708	40.039
145.000	30.000	4.235	34.576
150.000	25.000	2.975	29.044
155.000	20.000	1.930	23.435
160.000	15.000	1.102	17.737
165.000	10.000	0.498	11.939
170.000	5.000	0.127	6.031
175.000	0.000	0.000	0.000

# FIGURE 2

JOHN H. MULLANEY  
CONSULTING RADIO ENGINEERS

SIDE OF TOWER IN INCHES ? 24  
SEPARATION OF FOLDS FROM TOWER IN INCHES ? 24  
RADIUS OF FOLD IN INCHES ? .125

CURRENT TRANSFORMATION RATIO 5.236

HEIGHT OF TOWER IN FEET ? 175  
FREQUENCY IN KHZ ? 1400

CHARACTERISTIC IMPEDANCE OF TRANSMISSION LINE 403.493 OHMS

LOSS RESISTANCE OF TOWER IN OHMS ? 1  
BASE INDUCTANCE IN MICRO HENRIES ? 0  
DISTANCE FROM TOP OF TOWER  
TO STUB IN FEET (START,STOP,STEP) ? 0,175,5,

DISTANCE OF STUB FROM TOP	DISTANCE OF STUB FROM BOTTOM	RESISTANCE	REACTANCE
0.000	175.000	275.515	149.043
5.000	170.000	248.214	163.674
10.000	165.000	221.769	172.626
15.000	160.000	197.072	177.054
20.000	155.000	174.548	178.036
25.000	150.000	154.320	176.480
30.000	145.000	136.324	173.108
35.000	140.000	120.400	168.473
40.000	135.000	106.344	162.986
45.000	130.000	93.947	156.947
50.000	125.000	83.004	150.570
55.000	120.000	73.330	144.009
60.000	115.000	64.763	137.370
65.000	110.000	57.156	130.724
70.000	105.000	50.387	124.121
75.000	100.000	44.349	117.591
80.000	95.000	38.950	111.152
85.000	90.000	34.114	104.812
90.000	85.000	29.773	98.575
95.000	80.000	25.873	92.439
100.000	75.000	22.364	86.397

Page 2,      Figure 2 Cont:

105.000	70.000	19.206	80.444
110.000	65.000	16.365	74.569
115.000	60.000	13.812	68.763
120.000	55.000	11.522	63.014
125.000	50.000	9.475	57.311
130.000	45.000	7.653	51.642
135.000	40.000	6.042	45.994
140.000	35.000	4.633	40.356
145.000	30.000	3.416	34.713
150.000	25.000	2.386	29.052
155.000	20.000	1.539	23.361
160.000	15.000	0.874	17.625
165.000	10.000	0.393	11.830
170.000	5.000	0.100	5.960
175.000	0.000	0.000	0.000

# FIGURE 3

JOHN H. MULLANEY  
CONSULTING RADIO ENGINEERS

SIDE OF TOWER IN INCHES ? 18  
SEPARATION OF FOLDS FROM TOWER IN INCHES ? 24  
RADIUS OF FOLD IN INCHES ? .125

CURRENT TRANSFORMATION RATIO 4.397

HEIGHT OF TOWER IN FEET ? 175  
FREQUENCY IN KHZ ? 1230

CHARACTERISTIC IMPEDANCE OF TRANSMISSION LINE 409.278 OHMS

LOSS RESISTANCE OF TOWER IN OHMS ? 1  
BASE INDUCTANCE IN MICRO HENRIES ? 0  
DISTANCE FROM TOP OF TOWER  
TO STUB IN FEET (START,STOP,STEP) ? 0,175,5,

DISTANCE OF STUB FROM TOP BOTTOM		RESISTANCE	REACTANCE
0.000	175.000	307.184	-215.650
5.000	170.000	348.007	-196.159
10.000	165.000	389.070	-164.445
15.000	160.000	425.566	-118.521
20.000	155.000	450.883	-58.890
25.000	150.000	458.360	9.918
30.000	145.000	444.349	79.505
35.000	140.000	410.550	140.416
40.000	135.000	363.395	185.978
45.000	130.000	310.905	214.269
50.000	125.000	259.637	227.270
55.000	120.000	213.471	228.741
60.000	115.000	173.932	222.505
65.000	110.000	141.063	211.635
70.000	105.000	114.189	198.305
75.000	100.000	92.391	183.935
80.000	95.000	74.761	169.394
85.000	90.000	60.496	155.184
90.000	85.000	48.929	141.575



Page 2,

Figure 3 Cont:

95.000	80.000	39.523	128.694
100.000	75.000	31.849	116.579
105.000	70.000	25.570	105.224
110.000	65.000	20.421	94.591
115.000	60.000	16.191	84.632
120.000	55.000	12.715	75.294
125.000	50.000	9.862	66.521
130.000	45.000	7.525	58.260
135.000	40.000	5.622	50.462
140.000	35.000	4.084	43.081
145.000	30.000	2.856	36.074
150.000	25.000	1.893	29.404
155.000	20.000	1.160	23.036
160.000	15.000	0.627	16.939
165.000	10.000	0.268	11.084
170.000	5.000	0.065	5.445
175.000	0.000	0.000	0.000

**FIGURE 4****JOHN H. MULLANEY**  
**CONSULTING RADIO ENGINEERS**

SIDE OF TOWER IN INCHES ? 24  
SEPARATION OF FOLDS FROM TOWER IN INCHES ? 24  
RADIUS OF FOLD IN INCHES ? .125

CURRENT TRANSFORMATION RATIO      5.236

HEIGHT OF TOWER IN FEET ? 175  
FREQUENCY IN KHZ ? 1230

CHARACTERISTIC IMPEDANCE OF TRANSMISSION LINE      403.493 OHMS

LOSS RESISTANCE OF TOWER IN OHMS ? 1  
BASE INDUCTANCE IN MICRO HENRIES ? 0  
DISTANCE FROM TOP OF TOWER  
TO STUB IN FEET (START,STOP,STEP) ? 0,175,5,

DISTANCE OF STUB FROM TOP	DISTANCE OF STUB FROM BOTTOM	RESISTANCE	REACTANCE
0.000	175.000	401.074	-199.936
5.000	170.000	447.411	-154.470
10.000	165.000	483.458	-91.413
15.000	160.000	500.310	-14.713
20.000	155.000	491.858	66.106
25.000	150.000	458.628	138.978
30.000	145.000	407.850	194.643
35.000	140.000	349.482	229.919
40.000	135.000	291.881	246.906
45.000	130.000	239.979	250.155
50.000	125.000	195.680	244.325
55.000	120.000	159.023	233.112
60.000	115.000	129.178	219.084
65.000	110.000	105.051	203.882
70.000	105.000	85.577	188.490
75.000	100.000	69.830	173.466
80.000	95.000	57.053	159.103
85.000	90.000	46.640	145.531
90.000	85.000	38.115	132.790
95.000	80.000	31.105	120.864

Page 2,

Figure 4 Cont:

100.000	75.000	25.318	109.713
105.000	70.000	20.525	99.281
110.000	65.000	16.546	89.507
115.000	60.000	13.237	80.332
120.000	55.000	10.485	71.698
125.000	50.000	8.200	63.551
130.000	45.000	6.307	55.842
135.000	40.000	4.748	48.527
140.000	35.000	3.474	41.563
145.000	30.000	2.447	34.916
150.000	25.000	1.633	28.551
155.000	20.000	1.007	22.438
160.000	15.000	0.548	16.550
165.000	10.000	0.236	10.862
170.000	5.000	0.057	5.353
175.000	0.000	0.000	0.000

# FIGURE 5

JOHN H. MULLANEY  
CONSULTING RADIO ENGINEERS

## EFFECT OF WFEC ON WKBO ANTENNA SYSTEM.

FREQUENCY 1230 KHZ

POWER

0.702 KW

### TABULATION OF ANTENNA PARAMETERS

TOWER NUMBER	ORIENTATION DEGREES	SPACING DEGREES	FEET	FIELD RATIO	PHASING DEGREES
1	0.000	0.000	0.000	1.000	0.000
2	123.280	166.560	369.972	0.291	-13.440

TOWER NUMBER	HEIGHT DEGREES	FEET	SIDE OF TOWER
1	67.500	149.935	32.000
2	78.750	174.924	18.000

TOWER NUMBER	N-DA FIELDS AT ONE MILE 1 KILOWATT	702.000 WATTS
-----------------	---------------------------------------	---------------

1	190.862	159.915
2	192.659	161.420

	THEORETICAL	STANDARD
RSS	158.020	165.921
RMS	148.373	155.792
RSS/RMS RATIO	1.065	1.065
K	151.734	159.321

TABULATION OF STANDARD HORIZONTAL PATTERN

TRUE BEAR.	FIELD MV/M	TRUE BEAR.	FIELD MV/M	TRUE BEAR.	FIELD MV/M	TRUE BEAR.	FIELD MV/M
0.0	154.199	90.0	137.554	180.0	175.037	270.0	120.170
5.0	164.169	95.0	132.076	185.0	183.537	275.0	116.938
10.0	174.087	100.0	127.757	190.0	191.226	280.0	114.918
15.0	183.403	105.0	124.527	195.0	197.642	285.0	113.812
20.0	191.591	110.0	122.261	200.0	202.378	290.0	113.311
25.0	198.195	115.0	120.822	205.0	205.112	295.0	113.144
30.0	202.854	120.0	120.090	210.0	205.636	300.0	113.114
35.0	205.330	125.0	119.994	215.0	203.869	305.0	113.114
40.0	205.519	130.0	120.522	220.0	199.871	310.0	113.127
45.0	203.458	135.0	121.730	225.0	193.841	315.0	113.233
50.0	199.317	140.0	123.723	230.0	186.102	320.0	113.605
55.0	193.385	145.0	126.637	235.0	177.084	325.0	114.490
60.0	186.046	150.0	130.606	240.0	167.295	330.0	116.191
65.0	177.747	155.0	135.720	245.0	157.282	335.0	119.016
70.0	168.966	160.0	141.988	250.0	147.590	340.0	123.221
75.0	160.172	165.0	149.317	255.0	138.714	345.0	128.949
80.0	151.790	170.0	157.495	260.0	131.049	350.0	136.178
85.0	144.169	175.0	166.203	265.0	124.843	355.0	144.712

The directional antenna pattern was developed by using the General Case design formulae & adjusting the pattern for Standard computations in accordance with the Commission Rules.

DIRECTIONAL ANTENNA DESIGN FORMULAE  
(General Case)

Formulae Used:

$$E = K \sum_{k=1}^N F(\theta)_k M_k \frac{\Psi_k + S_k \cos(\phi - A_k) \cos \theta}{\quad} \quad (1)$$

$$K = \text{RMS} / \left[ \sum_{j=1, k=1}^N M_j M_k \cos(\Psi_{jk}) J_0(S_{jk}) \right]^{1/2} \quad (2)$$

$$F(\theta)_k = \frac{\cos(G_k \sin \theta) - \cos G_k}{\cos \theta (1 - \cos G_k)} \quad (3)$$

Page 3, Figure 5 Cont:

Where:

$E$  = Unattenuated field intensity in mv/m at one mile

$K$  = A constant to convert unit pattern values to unattenuated field intensity in mv/m at one mile

$F(\theta)_k$  = The vertical radiating characteristics of kth antenna as defined by formula (3) above.

$N$  = Number of towers

$\phi$  = Azimuth angle from reference line of the array

RMS = Effective field of the directional pattern

$J_0$  = Bessel function, zero order, of tower spacing

$\theta$  = Angle above the horizontal

$A_k$  = Azimuth angle measured clockwise from the reference line of the array to a line drawn from the reference point through the kth tower

$G_k$  = Height of the kth antenna in electrical degrees

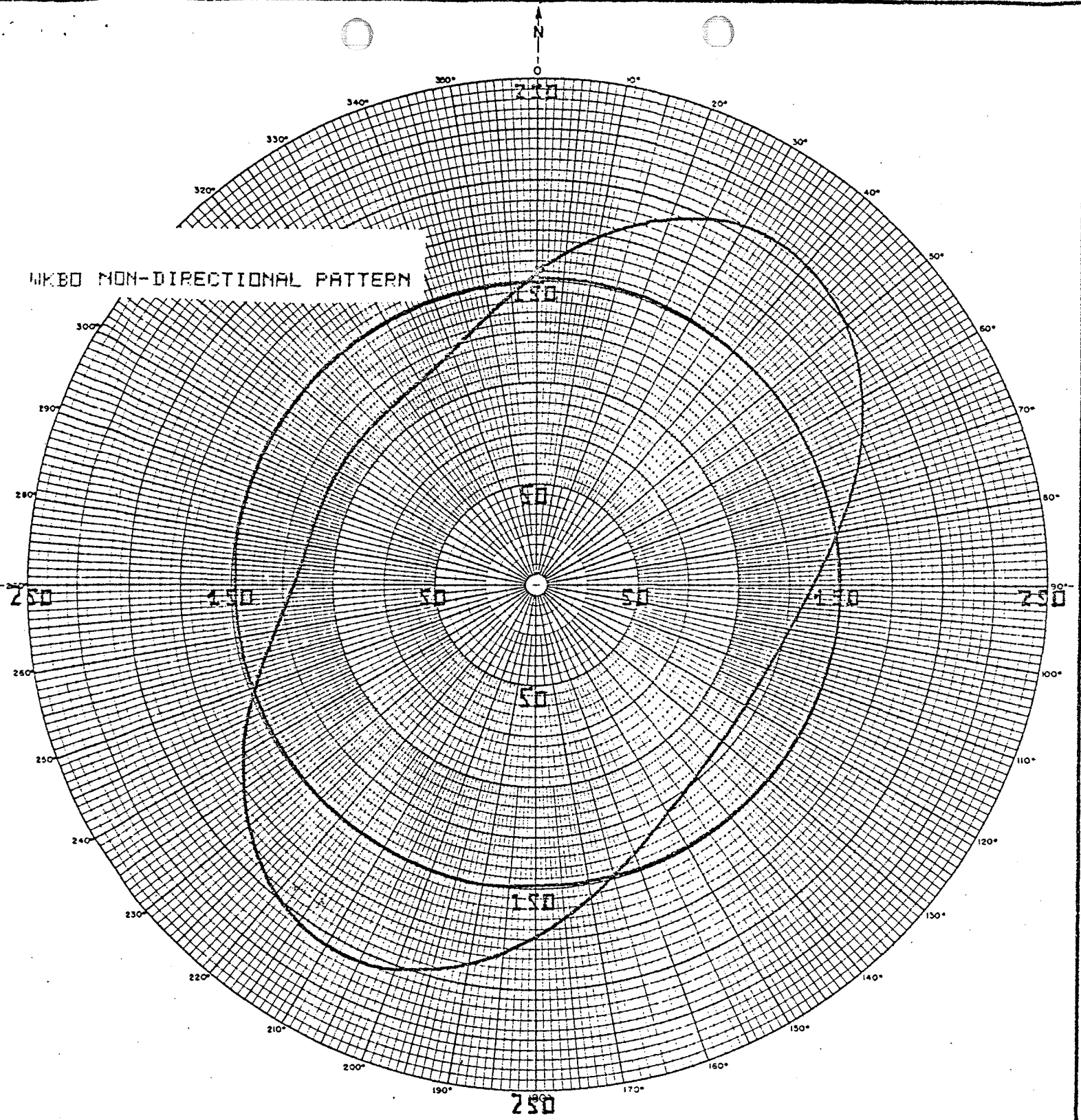
$M_k$  = Relative field ratio of the kth tower

$\Psi_k$  = Relative phase angle of field radiated from kth tower

$S_k$  = Spacing of the kth tower from the reference point

$S_{jk}$  = Spacing between towers j and k

$\Psi_{jk}$  = Relative phase between the fields radiated from j and k.



TITLE : EFFECT OF WFEC ON WKBO ANTENNA SYSTEM.

FREQ : 1230.

POWER : 0.70

# TWRS. : 2

RMS : 155.8

RSS : 165.9

**JOHN H. MULLANEY**  
CONSULTING  
RADIO ENGINEERS  
POTOMAC, MARYLAND.

**FIGURE 6**

APPENDIX

METHOD OF DETERMINING FOLDED UNIPOLE DRIVE POINT IMPEDANCE:

I. Introduction:

The folded-unipole antenna for standard broadcast use was introduced to the industry by John H. Mullaney, P.E. in 1956. An article entitled "The Folded Unipole Antenna For AM Broadcasting", by affiant was printed in December 1960 in Broadcasting Engineering. Since that time your affiant has used this type of antenna in not only non-directional but directional applications for standard broadcast stations. The mathematical approaches to the solution of a folded-unipole problem have been expanded by your affiant & it is now possible to predicate with reasonable accuracy the expected impedance for these antennas. The following discussion setstforth the salient factors used in the determination of the base impedance.

II. Engineering Discussion:

A. Drive Point Impedance Formula:

$$Z_D = Z_1 \parallel Z_2 - Z_3$$

$$Z_1 = (1+n)^2 Z_i + n(1+n) Z_B$$

$$Z_2 = Z_L + (1+n) Z_B$$

$$Z_3 = n Z_B$$

$n$  = current transformation ratio

$$Z_B = j 2\pi f L$$

$Z_L$  = impedance of transmission line mode.

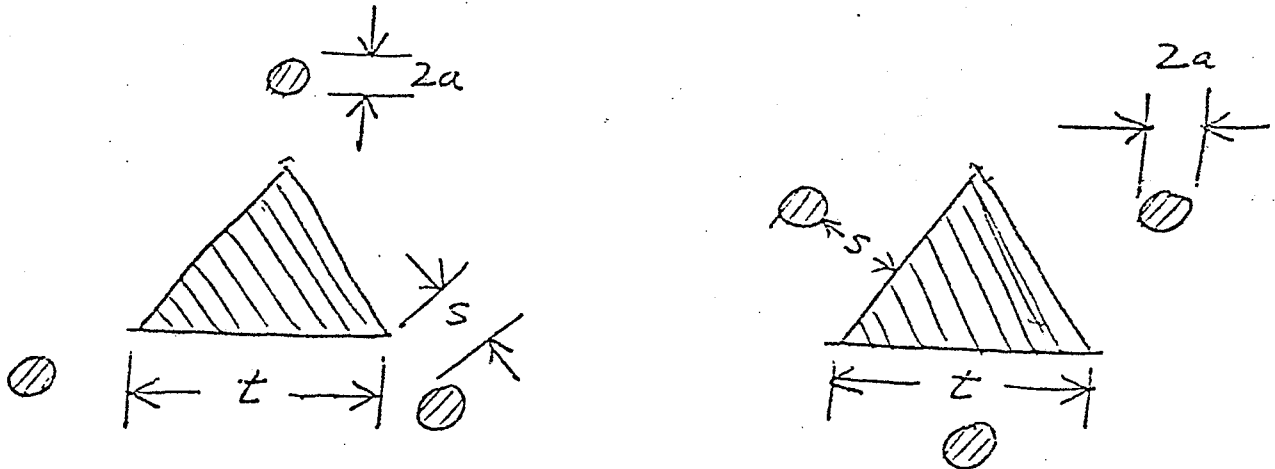
$L$  = base inductance



Page 2, Folded-Unipole Cont:

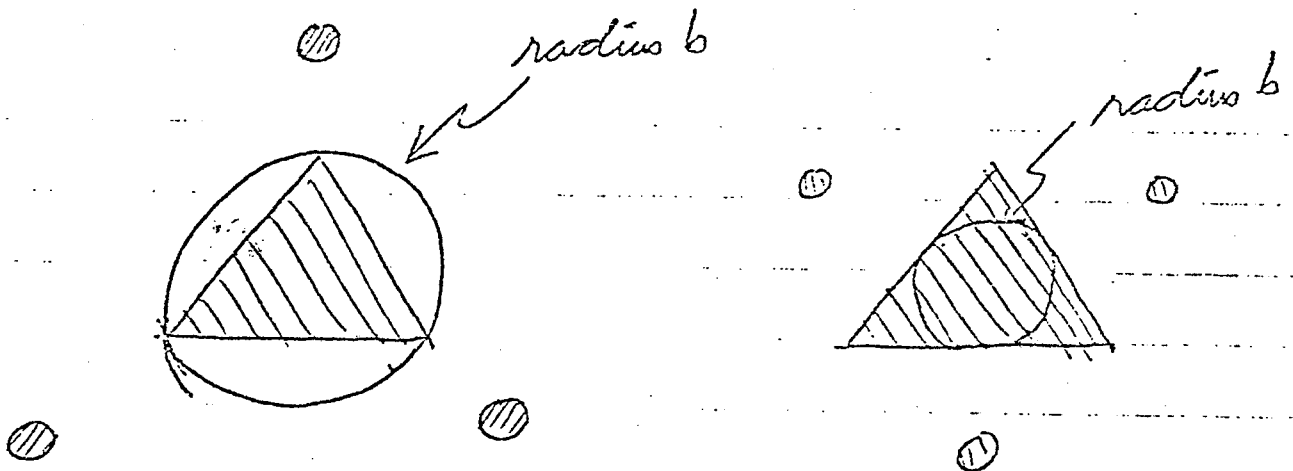
B. Calculation of Current Transformation Ratio:

Two types of cross sections are given consideration:



$a$  = radius of fold  
 $t$  = side of tower  
 $s$  = separation of fold from tower

For purposes of calculation, replace the triangles by circles of the appropriate diameter:



$$b = t/\sqrt{3}$$

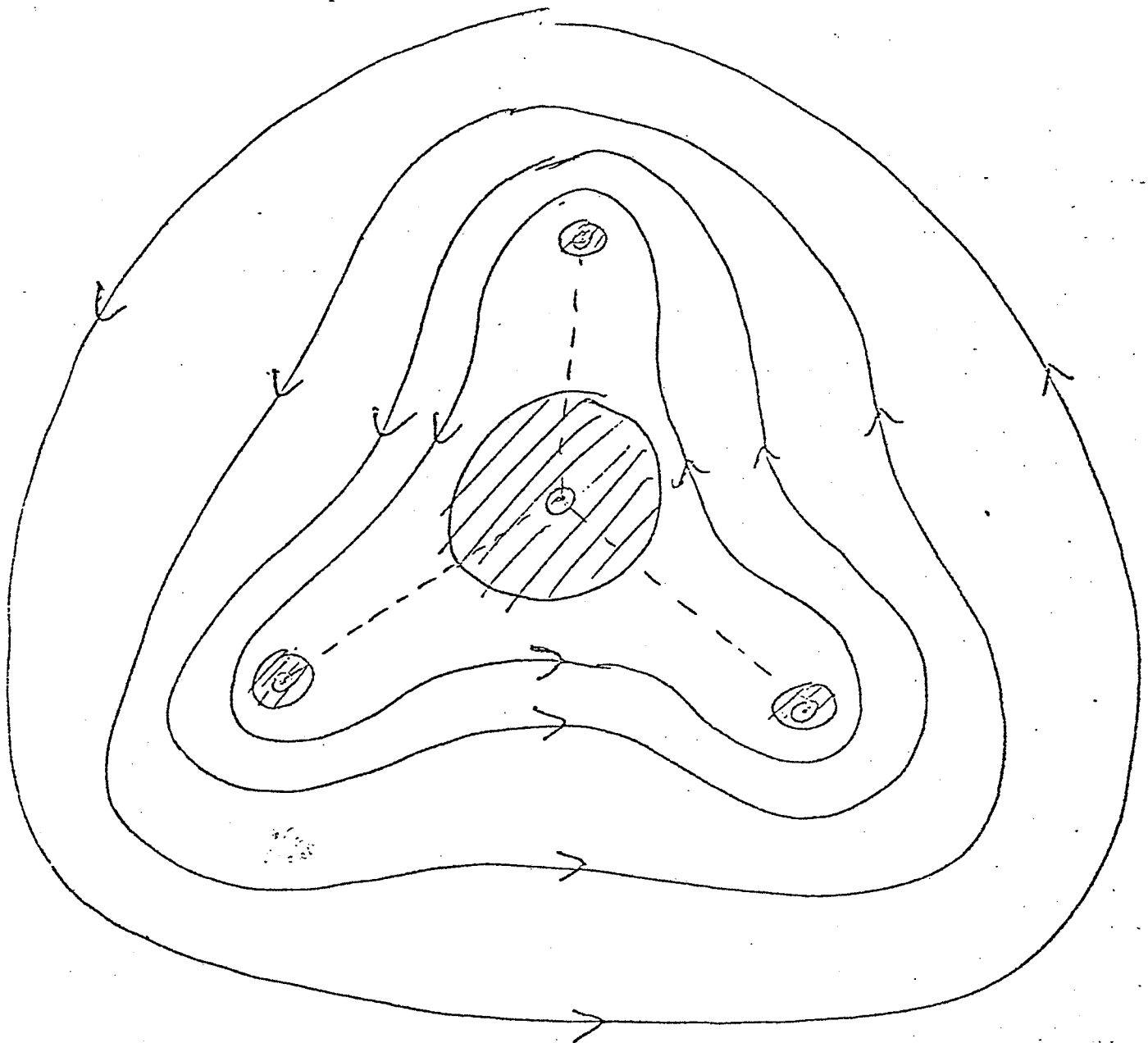
$$b = t/4$$

The equivalent radius is chosen so that the separation of the fold from the tower remains unchanged.

C. Magnetic Field:

Page 3 is a sketch of the magnetic field around a folded-unipole tower.

Page 3, Folded-Unipole Cont:

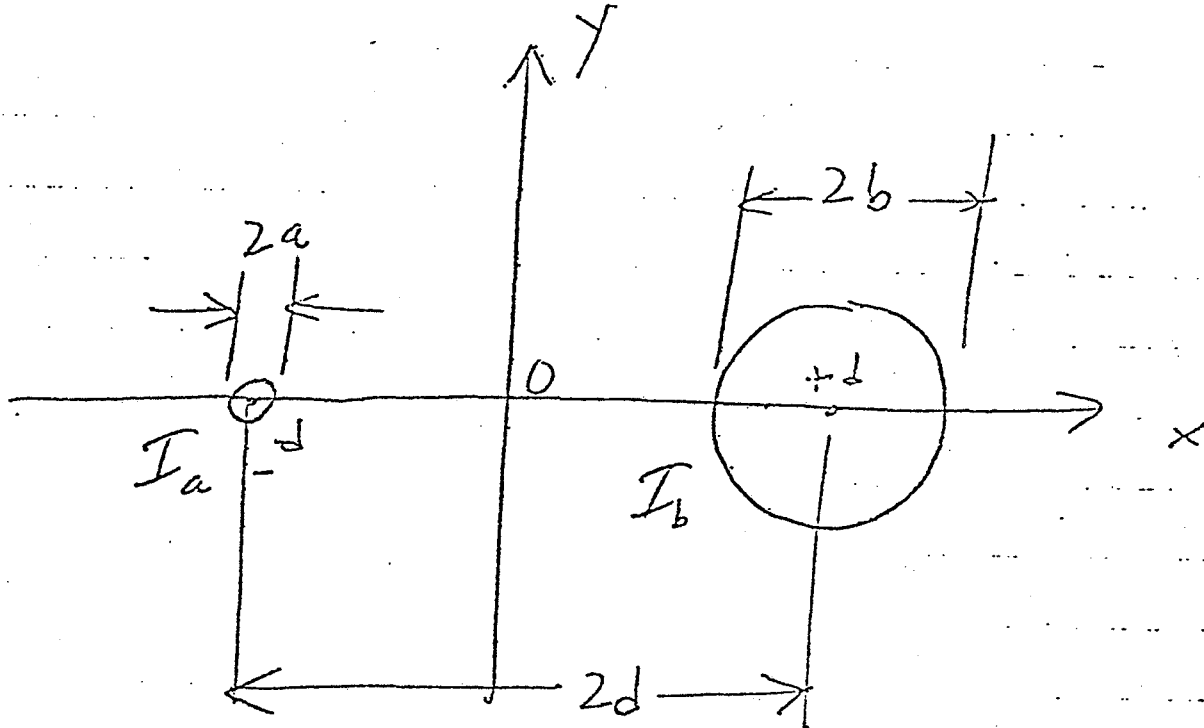


Physical principle: No flux linked between conductors.

Page 4,      Folded-Unipole Cont:

D. Simplified Problem:

Going further the fold & the tower can be represented as:



The linked flux can be expressed as:

$$\begin{aligned}\phi &= \frac{\mu_0}{2\pi} \int_{-d+a}^{d-b} \left( \frac{I_a}{x+d} - \frac{I_b}{d-x} \right) dx \\ &= \frac{\mu_0}{2\pi} \left[ I_a \ln(x+d) + I_b \ln(d-x) \right]_{-d+a}^{d-b} \\ &= \frac{\mu_0}{2\pi} \left[ I_a \ln\left(\frac{2d-b}{a}\right) + I_b \ln\left(\frac{b}{2d-a}\right) \right]\end{aligned}$$

Page 5.      Folded-Unipole Cont:

Require  $\phi = 0$ , then:

$$I_a \ln \frac{2d-b}{a} = I_b \ln \frac{2d-a}{b}$$

$$\frac{I_b}{I_a} = \frac{\ln \left( \frac{2d-b}{a} \right)}{\ln \left( \frac{2d-a}{b} \right)}$$

Since there are three folds, the current transformation ratio is one third of the ratio of  $I_b$  to  $I_a$ , hence:

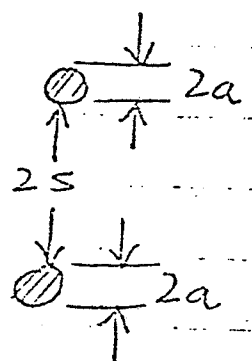
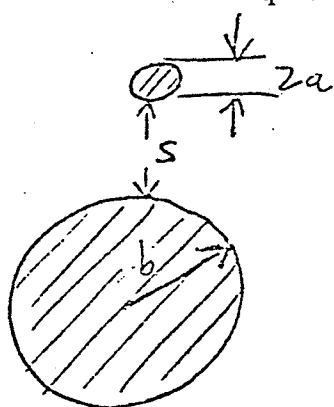
$$n = \frac{1}{3} \frac{\ln \left( \frac{2d-b}{a} \right)}{\ln \left( \frac{2d-a}{b} \right)}$$

Page 6,      Folded-Unipole Cont:

E. Calculation of Transmission Line Impedance:

The transmission line impedance for a folded-unipole antenna which is equivalent to a two conductor transmission line of unequal diameters can be determined as follows:

Equivalent cross sections:



The Characteristic impedances is then:

$$Z_0 = 60 \ln \frac{(a+b+s)^2}{ab}, \quad Z_0 = 120 \ln \frac{2a+s}{a}$$

Since there are three folds:

$$Z_L = j \frac{1}{3} Z_0 \tan G$$

F. Summary:

The equations setforth in this Appendix have been used to write a computer program to determine the base impedance of a three fold folded-unipole antenna system. Figures 1 through 4 present data concerning the WKBO-WFEC problem.

Power Ratio

K&E 10 X 10 TO 1/2 INCH 7 X 10 INCHES KEUFFEL & ESSER CO. MADE IN U.S.A.

10000 6000000

$X_L = j150$

$j150 \rightarrow E, 46 1320$

Make HP65 Card. 2/17/81

Power Ratio

CP

E

$X_L$

$150$

E

1.0

$150$

$500 + j0$

0.5

Rel Power = 0.235  $\angle -14^\circ$  ( $X_L = 500 \Omega$ )  
 $jX = j1A$

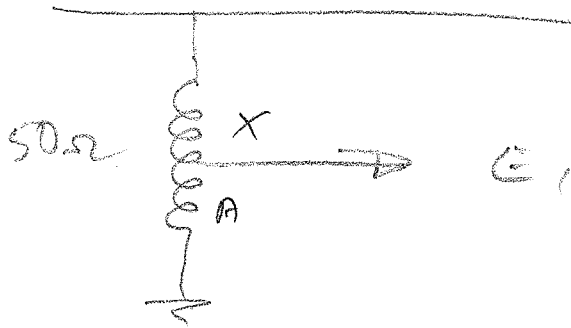
Rel Power = 0.200  $\angle -26.6^\circ$  ( $X_L = 1000 \Omega$ )  
 $jX = j1A$

Rel Power = 0.150  $\angle -37.6^\circ$  ( $X_L = 1500 \Omega$ )  
 $jX = j1A$

POWER DIVIDER PHASE SHIFTER

0° 10° 20° 30° 40° 50°

2/17/81

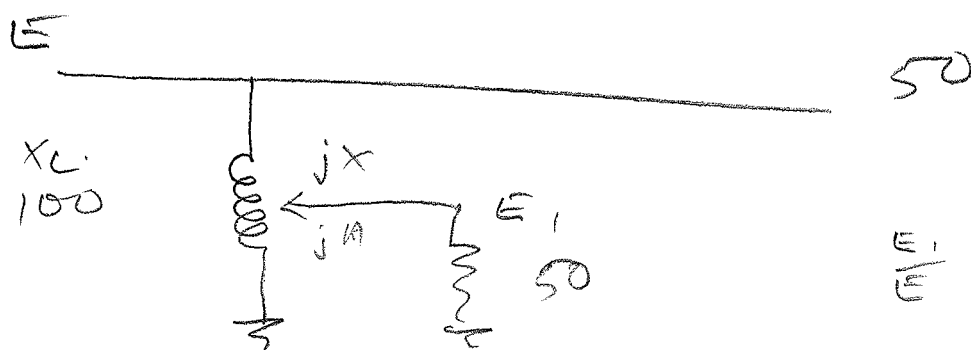


$$\frac{E_1}{E} = \frac{50 A}{-XA + j(A+X) 50}$$

$$= \frac{50 A}{-XA + j 2500}$$

$\frac{A}{25}$	$\frac{X}{25}$	$\frac{E_1}{E}$		
25	25	$\frac{1250}{2577} \angle 90$ $\frac{106}{106}$	.485 $\angle -14$	(Power Rel = .235)
30	20	$\frac{1500}{2571} \angle 90$ $\frac{103.5}{103.5}$	.583 $\angle -13.5$	(.340)
20	30	$\frac{1000}{2571} \angle 90$ $\frac{107.5}{107.5}$	.389 $\angle -13.5$	(.151)
35	15	$\frac{1750}{2554} \angle 90$ $\frac{101.9}{101.9}$	.685 $\angle -11.9$	(.469)
20	10	$\frac{2000}{2532} \angle 90$ $\frac{99.1}{99.1}$	.790 $\angle -9.1$	(.624)
45	5	$\frac{2250}{2510} \angle 90$ $\frac{95.1}{95.1}$	.896 $\angle -5.1$	(.802)
15	35	$\frac{750}{2564} \angle 90$ $\frac{101.9}{101.9}$	.294 $\angle -11.9$	(.086)
10	40	$\frac{500}{2532} \angle 90$ $\frac{99.1}{99.1}$	.197 $\angle -9.1$	(.039)

2/17/81

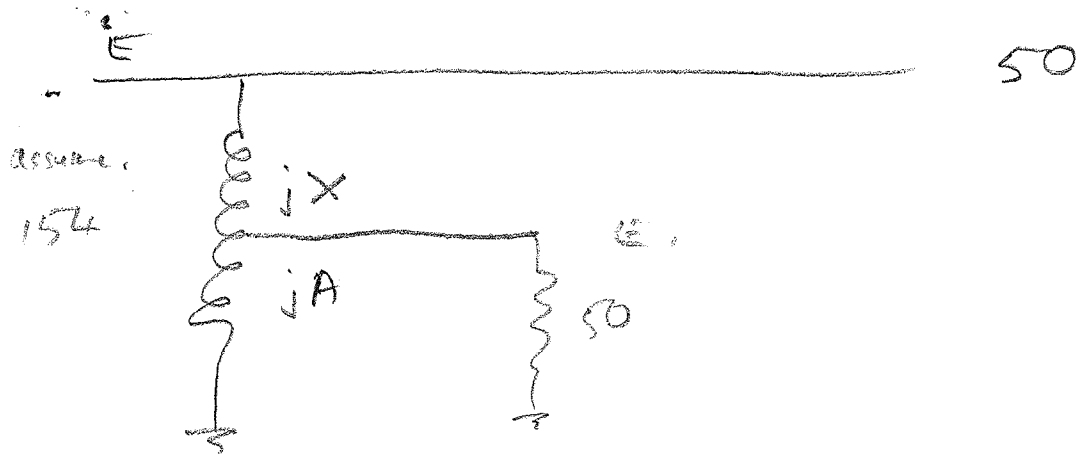


$$\frac{E_1}{E} = \frac{50 \cdot A \angle 90^\circ}{-XA + j(A+X)}$$

$$\frac{E_1}{E} = \frac{50 \cdot A \angle 90^\circ}{-XA + j 50 \cdot 100}$$

A	X	$\frac{E_1}{E}$			
50	50	$\frac{2500 \angle 90}{-2500 + j 5000}$	$= \frac{2500 \angle 90}{5590 \angle 116.6}$	$= .447$	$\angle -26.6$
				Rel. Power = 0.200	
75	25	$\frac{3750 \angle 90}{-1875 + j 5000}$	$= \frac{3750 \angle 90}{5340 \angle 110.6}$	$= .710$	$\angle -20.6$
				Rel. Power = 0.504	
85	15	$\frac{4250 \angle 90}{-1275 + j 5000}$	$= \frac{4250 \angle 90}{5160 \angle 104.3}$	$= .824$	$\angle -14.3$
				Rel. Power = .678	
92	8	$\frac{4600 \angle 90}{-736 + j 5000}$	$= \frac{4600 \angle 90}{5054 \angle 98.4}$	$= .910$	$\angle -8.4$
				Rel. Power = .828	
60	40	$\frac{3000 \angle 90}{-2400 + j 5000}$	$= \frac{3000 \angle 90}{5546 \angle 115.6}$	$= .541$	$\angle -25.6$
				Rel. Power = .293	
40	60	$\frac{2000 \angle 90}{-2400 + j 5000}$	$= \frac{2000 \angle 90}{5546 \angle 115.6}$	$= .361$	$\angle -25.6$
				Rel. Power = .130	
25	75	$\frac{1250 \angle 90}{-1875 + j 5000}$	$= \frac{1250 \angle 90}{5340 \angle 110.6}$	$= .234$	$\angle -20.6$
				Rel. Power = .055	
20	80	$\frac{1000 \angle 90}{-1600 + j 5000}$	$= \frac{1000 \angle 90}{5250 \angle 107.5}$	$= .190$	$\angle -17.7$
				Rel. Power = .036	





$$\frac{E_1}{E} = \frac{50 \cdot A \angle 90^\circ}{-XA + j(50A + 50X)} = \frac{50 \cdot A \angle 90^\circ}{-XA + j50 \cdot 154 \angle (A+X)}$$

$\frac{A}{77}$	$\frac{X}{77}$	$\frac{E_1/E}{\frac{3850 \angle 90}{-5929 + j7700}}$
----------------	----------------	--

$$= \frac{3850 \angle 90}{9718 \angle 127.6} = .396 \angle -37.6^\circ$$

(Rel. Power = .157)

$\frac{A}{100}$	$\frac{X}{54}$	$\frac{5000 \angle 90}{-5400 + j7700}$
-----------------	----------------	--

$$= \frac{5000 \angle 90}{9405 \angle 125^\circ} = .532 \angle -35^\circ$$

(Rel. Power = .283)

$\frac{A}{120}$	$\frac{X}{34}$	$\frac{6000 \angle 90}{-4080 + j7700}$
-----------------	----------------	--

$$= \frac{6000 \angle 90}{8714 \angle 118} = .689 \angle -28^\circ$$

(Rel. power = .474)

$\frac{A}{130}$	$\frac{X}{24}$	$\frac{6500 \angle 90}{-3120 + j7700}$
-----------------	----------------	--

$$= \frac{6500 \angle 90}{8308 \angle 112} = .782 \angle -22^\circ$$

(Rel Power = .612)

$\frac{A}{140}$	$\frac{X}{14}$	$\frac{7000 \angle 90}{-1960 + j7700}$
-----------------	----------------	--

$$= \frac{7000 \angle 90}{7946 \angle 104.3} = .881 \angle -14.3^\circ$$

(Rel power = .776)

$\frac{A}{148}$	$\frac{X}{6}$	$\frac{7400 \angle 90}{-888 + j7700}$
-----------------	---------------	---------------------------------------

$$= \frac{7400 \angle 90}{7751 \angle 96.6} = .955 \angle -6.6^\circ$$

(Rel. Power = .911)

$\frac{A}{54}$	$\frac{X}{180}$	$\frac{2700 \angle 90}{-5400 + j7700}$
$\frac{A}{34}$	$\frac{X}{120}$	$\frac{1700 \angle 90}{-4080 + j7700}$

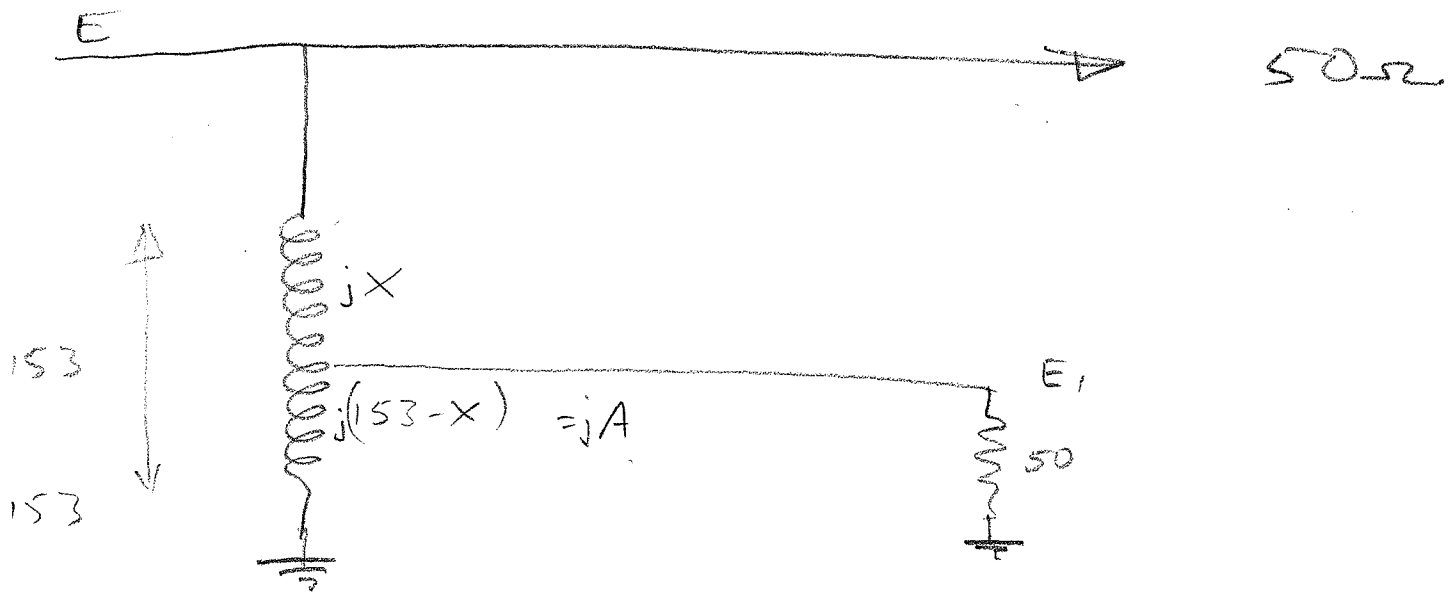
$$= \frac{2700 \angle 90}{9405 \angle 125^\circ} = .287 \angle -35^\circ$$

(Rel. Power = .082)

$$= \frac{1700 \angle 90}{8714 \angle 118} = .195 \angle -28^\circ$$

(Rel. Power = .078)

2/17/81



$$\frac{E_1}{E} = \left[ \frac{50j(153-X)}{50 + j(153-X)} \right] + jX$$

let

$$= \frac{50j(153-X)}{50j(153-X) + jX[50 + j(153-X)]}$$

$$= \frac{jA \cdot 50}{jA \cdot 50 + jX[50 + jA]}$$

$$= \frac{jA \cdot 50}{jA \cdot 50 - XA + jX50} = \frac{50A \angle 90^\circ}{-XA + j(A \cdot 50 + X50)}$$

# Elevated Vertical Antenna Systems

Is your vertical-antenna system performance up to snuff? If not, maybe it needs a lift—in elevation above ground, that is!

By Al Christman, KB8I  
Electrical Engineering Dept  
Grove City College  
Grove City, PA 16127

For many years, standard broadcast stations have used vertical monopoles (towers) as transmitting antennas. These monopoles are required by the FCC to have extensive ground systems, usually consisting of 120 or more buried radial wires that are used to simulate a perfectly conducting image plane beneath the monopole. The length of the radials is generally  $\frac{1}{4}\lambda$ , although longer radials are often used. Electromagnetic energy leaving a radiator travels through space until reaching the earth's surface, where it flows through the soil to the radials, and then back to the antenna feed point.

## Background

The FCC mandate requiring the use of many buried radials is apparently based upon the findings of three RCA engineers: Brown, Lewis and Epstein. These men carried out extensive tests on buried-wire radial ground systems in the mid-1930s and published their results in a now-classic paper in the *Proceedings of the Institute of Radio Engineers*.<sup>1</sup> In this 1937 paper, a single test was performed wherein the radials were laid

upon the surface of the earth rather than buried in the soil. The conclusion was that "this ground system is about as good as an equal number of buried wires."<sup>2</sup> The experimenters' normal procedure was to bury the wires to a depth of about 6 inches.<sup>3</sup> Although this work was done at a frequency of 3 MHz, the results were quickly applied by AM broadcasters to their own part of the spectrum (540-1600 kHz), and buried radials have been used in AM-broadcast antenna systems ever since.

I recently studied elevated vertical antenna systems to determine how well they perform compared to conventional ground-mounted systems. My computer-modeling results indicate that an elevated vertical monopole antenna with four elevated horizontal radials provides more power gain at low elevation angles than does a conventional ground-mounted monopole with 120 buried radials.

The frequency of operation for my analyses was 3.8 MHz, and I used ground constants  $\sigma$  (conductivity) and  $\epsilon_r$  (relative permittivity) that simulate average-soil electrical parameters. The computer program I used for this work was NEC-GSD, a *Method of Moments* code developed by engineers

at the Lawrence Livermore National Laboratory.

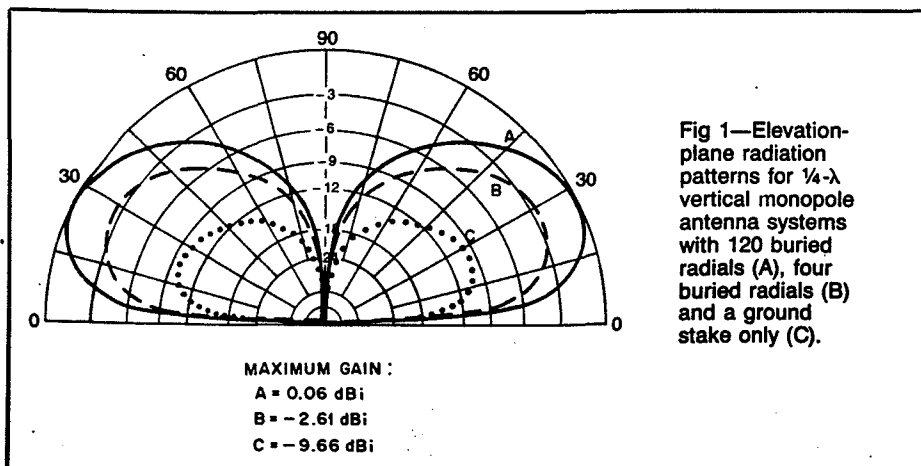
In agreement with the findings of Arch Doty, K8CFU, I believe that the use of elevated, rather than buried, radials provides superior performance, because it allows the collection of electromagnetic energy in the form of *displacement currents*, rather than forcing *conduction currents* to flow through lossy earth.<sup>4</sup>

## The Computer Analysis

The first step I took was to determine what effects, if any, would be caused by changing the depth at which the ground radials were buried. I used NEC-GSD to model a  $\frac{1}{4}\lambda$  vertical monopole with 120 buried  $\frac{1}{4}\lambda$  radials. The operating frequency was 3.8 MHz, and I modeled the system with average ground ( $\sigma = 0.003$  S/m and  $\epsilon_r = 13$ ).<sup>5</sup>

For the NEC model, the antenna was constructed of no. 12 wire (radius = 1 mm) and metal conductivities were adjusted to simulate an aluminum monopole mounted on a 2-foot steel ground stake with copper radials. As the burial depth of the radials was increased from 2 to 6 inches, the power gain of the antenna decreased only slightly (see Table 1), as did the ground-wave field strength. (Note that the reactive portion of the input impedance may be altered by adjusting the length of the monopole or by making it thicker in relation to the radials.) I used the vertical-monopole antenna system with 120 radials buried 2 inches deep as a reference standard for comparison with the other antenna systems discussed in this article.

I repeated the procedure described above using four buried radials, rather than 120. The results are given in Table 2. As before, slightly lower power gains and field strengths were calculated as radial depth increased. Compared to the 120-radial cases, monopoles with only four buried radials have much higher ground losses, as evidenced by



<sup>1</sup>Notes appear on p 42.

Table 1

## Power Gain and Electric Field Strength for Vertical Monopole Antennas with 120 Buried Radials

Elevation angle (degrees)	Calculated power gain (dBi)		
	120 radials buried 2 in.	120 radials buried 4 in.	120 radials buried 6 in.
0	-∞	-∞	-∞
5	-6.14	-6.15	-6.16
10	-2.40	-2.41	-2.42
15	-0.86	-0.87	-0.88
20	-0.17	-0.18	-0.19
25	+0.06	+0.04	+0.03
30	-0.02	-0.03	-0.04
40	-0.83	-0.84	-0.85
50	-2.37	-2.37	-2.37
60	-4.68	-4.69	-4.69
70	-8.13	-8.14	-8.14
80	-14.13	-14.14	-14.14
90	-158.38	-158.45	-158.51
Vertical electric field strength (mV/m)	33.16	33.10	33.06
Input impedance (ohms)	39.87 + j22.0	40.18 + j22.49	40.44 + j23.02

Table 2

## Calculated Power Gain and Electric Field Strength for Vertical Monopole Antennas with 4 Buried Radials

Elevation angle (degrees)	Calculated power gain (dBi)		
	4 radials buried 2 in.	4 radials buried 4 in.	4 radials buried 6 in.
0	-∞	-∞	-∞
5	-8.82	-8.84	-8.85
10	-5.08	-5.10	-5.11
15	-3.54	-3.56	-3.58
20	-2.85	-2.87	-2.89
25	-2.62	-2.65	-2.66
30	-2.70	-2.72	-2.74
40	-3.52	-3.54	-3.55
50	-5.06	-5.08	-5.10
60	-7.37	-7.40	-7.42
70	-10.83	-10.86	-10.87
80	-16.84	-16.86	-16.88
90	-169.74	-169.99	-170.17
Vertical electric field strength (mV/m)	24.37	24.31	24.27
Input impedance (ohms)	74.48 + j33.69	74.73 + j34.04	74.93 + j34.39

Table 3

## Calculated Power Gain and Electric Field Strength for Elevated Vertical Monopole Antenna Systems

Elevation angle (degrees)	Calculated power gain (dBi)					
	4 radials height = 5 ft	4 radials height = 10 ft	4 radials height = 15 ft	4 radials height = 20 ft	4 radials height = 25 ft	4 radials height = 30 ft
0	-∞	-∞	-∞	-∞	-∞	-∞
5	-6.40	-6.22	-6.09	-5.97	-5.82	-5.60
10	-2.69	-2.53	-2.43	-2.34	-2.23	-2.06
15	-1.19	-1.08	-1.03	-1.00	-0.96	-0.85
20	-0.56	-0.50	-0.53	-0.59	-0.64	-0.64
25	-0.41	-0.43	-0.54	-0.71	-0.89	-1.02
30	-0.57	-0.68	-0.91	-1.22	-1.56	-1.87
40	-1.59	-1.93	-2.45	-3.13	-3.92	-4.71
50	-3.38	-3.99	-4.88	-6.05	-7.46	-8.87
60	-5.94	-6.85	-8.15	-9.92	-12.06	-13.72
70	-9.61	-10.80	-12.50	-14.87	-17.55	-18.05
80	-15.77	-17.15	-19.16	-21.97	-24.67	-23.45
90	-157.37	-154.72	-152.32	-150.20	-148.37	-146.88
Vertical electric field strength (mV/m)	32.19	32.94	33.49	34.00	34.66	35.55
Input impedance (ohms)	38.64 + j8.60	36.06 + j3.37	3.77 + j0.59	31.35 - j1.17	28.82 - j2.05	26.51 - j2.08

reductions in gain and field strength, and by increases in input resistance. Much of the power radiated by the 120-radial antennas is now wasted heating the soil in the four-radial systems. Variations in azimuth-plane gain were negligible (0.01 dB or less).

The elevation-plane radiation patterns for vertical monopole antennas with 120 radials, four radials and no radials (ground stake only) are shown in Fig 1. The pattern shape remains essentially constant, but the pattern size (gain) depends upon the quality of the ground system. All of the vertical electric field

strengths in the tables were normalized for an applied power of 1 kW at the feed points of the antennas, and were calculated at a distance of 1 mile and a height of 5 feet above ground. [This normalization procedure allows the pattern values for the different antenna configurations to be compared directly at any given elevation angle—Ed.] At this height the electric field is almost entirely surface wave (ground wave) rather than sky wave. I concluded from this comparison that if radials must be buried, more radials are better than a few radials in order to minimize losses. Also,

it's helpful to keep buried radials as close as possible to the ground surface.

The next system configuration I modeled was a vertical monopole radiator with four horizontal radials—all elevated above the earth's surface. I found that low-angle power gain and field strength increase as the height of the antenna system is increased. Also, the gain at somewhat higher angles decreases as the antenna is raised (see Table 3). Note that the power gain at take-off angles below 15° increases continually as the antenna height is raised from 5 feet to 30 feet, but the gain at a take-off angle

of 20° reaches a maximum value at a height of around 10 feet, and then decreases as the antenna is moved higher.

Compared with the reference 120-buried-radial system, the four-radial elevated antenna system reaches parity (equivalent performance to the reference) at low angles at a height of about 15 feet above the surface of the earth. If the antenna is raised further, a secondary high-angle lobe will develop as the antenna height approaches  $\frac{1}{4} \lambda$ ; gain at very low angles continues to increase. Variations in azimuth-plane gain are quite small, even with only four radials in the antenna system.

#### Antenna-System Geometry

The physical layout of the basic

elevated-radial antenna system I modeled is shown in Fig 2. The monopole and the outer ends of the radials are supported by conductive masts. The height of the radial-support masts is the same as the elevation of the radials above ground, but these masts are separated laterally from the tips of the radials by six inches. The central mast supports the monopole, and it is also the same height as the radials. Each mast is attached to a two-foot-long ground stake that is driven fully into the earth.

The masts and ground stakes are made of steel, the radials are copper, and the monopole is constructed of aluminum, as before. All conductors are no. 12. The four radials are electrically connected directly to the top of the central mast,

but are insulated from all other support structures. The outer conductor of the coaxial cable is also connected to the four radials at the top of the center mast.

This antenna arrangement allows significant current to flow on the central mast, so I also modeled the system with a slightly different feed-point design. In this second elevated-radial model, I isolated the central mast from the radials in order to reduce current flow on the mast.<sup>6</sup> As shown in Table 4, the isolated antenna system yields a small improvement in ground-wave field strength values, and more power gain at low elevation angles. There is only a slight change in feed-point impedance. Fig 3 shows the elevation-plane radiation pattern for an isolated four-radial

Table 4

Calculated Power Gain and Electric Field Strength for Isolated Elevated Vertical Monopole Antenna Systems

Elevation angle (degrees)	Calculated power gain (dBi)					
	4 radials height = 5 ft	4 radials height = 10 ft	4 radials height = 15 ft	4 radials height = 20 ft	4 radials height = 25 ft	4 radials height = 30 ft
0	-∞	-∞	-∞	-∞	-∞	-∞
5	-6.33	-6.01	-5.74	-5.50	-5.27	-5.06
10	-2.62	-2.32	-2.08	-1.87	-1.67	-1.50
15	-1.12	-0.87	-0.67	-0.51	-0.37	-0.26
20	-0.49	-0.30	-0.16	-0.07	-0.02	+0.01
25	-0.33	-0.21	-0.16	-0.17	-0.22	-0.32
30	-0.49	-0.46	-0.52	-0.64	-0.82	-1.08
40	-1.51	-1.70	-2.01	-2.44	-2.99	-3.66
50	-3.29	-3.74	-4.37	-5.20	-6.23	-7.48
60	-5.85	-6.58	-7.57	-8.85	-10.43	-12.21
70	-9.52	-10.50	-11.83	-13.55	-15.58	-17.30
80	-15.67	-16.84	-18.41	-20.44	-22.65	-23.65
90	-157.35	-154.72	-152.47	-150.61	-149.07	-147.80
Vertical electric field strength (mV/m)	32.47	33.71	34.82	35.86	36.86	37.82
Input impedance (ohms)	38.19 + j8.46	35.06 + j3.52	32.59 + j1.38	30.54 + j0.26	28.74 - j0.35	27.15 - j0.64

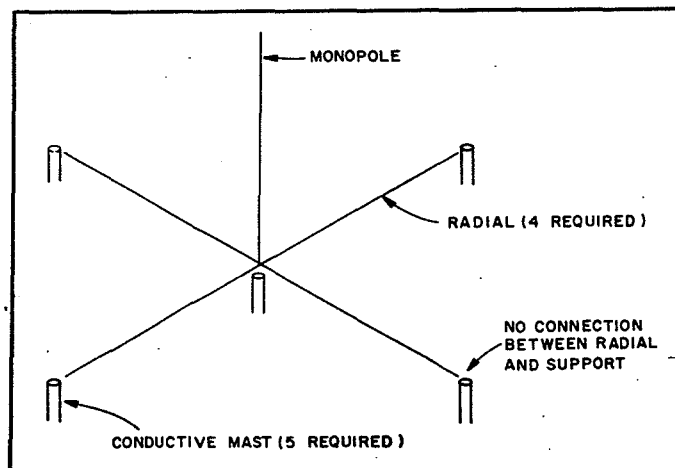


Fig 2—Physical layout of a four-radial, elevated vertical-monopole antenna.

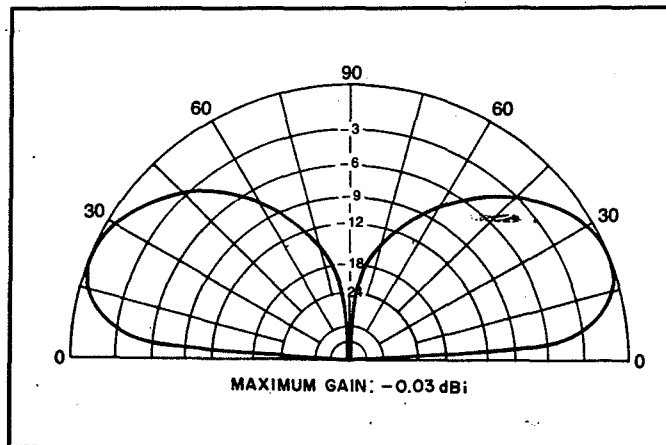


Fig 3—Elevation-plane radiation pattern for a four-radial, elevated vertical-monopole antenna isolated from the support mast (feed-point height = 15 feet).

Table 5

Calculated Power Gain and Electric Field Strength for Isolated Vertical Antenna Systems with 4 Shortened Radials and/or Shortened Monopoles

Elevation angle (degrees)	Calculated power gain (dBi)		
	1/8- $\lambda$ monopole 1/8- $\lambda$ radials	1/8- $\lambda$ monopole 1/4- $\lambda$ radials	1/4- $\lambda$ monopole 1/8- $\lambda$ radials
0	- $\infty$	- $\infty$	- $\infty$
5	-6.88	-6.44	-6.20
10	-3.15	-2.74	-2.53
15	-1.62	-1.27	-1.09
20	-0.95	-0.67	-0.54
25	-0.74	-0.55	-0.49
30	-0.84	-0.77	-0.77
40	-1.71	-1.94	-2.09
50	-3.32	-3.93	-4.22
60	-5.72	-6.75	-7.14
70	-9.25	-10.66	-11.13
80	-15.31	-17.01	-17.51
90	-154.24	-146.52	-160.29
Vertical electric field strength (mV/m)	30.44	32.05	33.02
Input impedance (ohms)	8.25 -j653.45	7.0 -j541.76	36.32 -j136.61

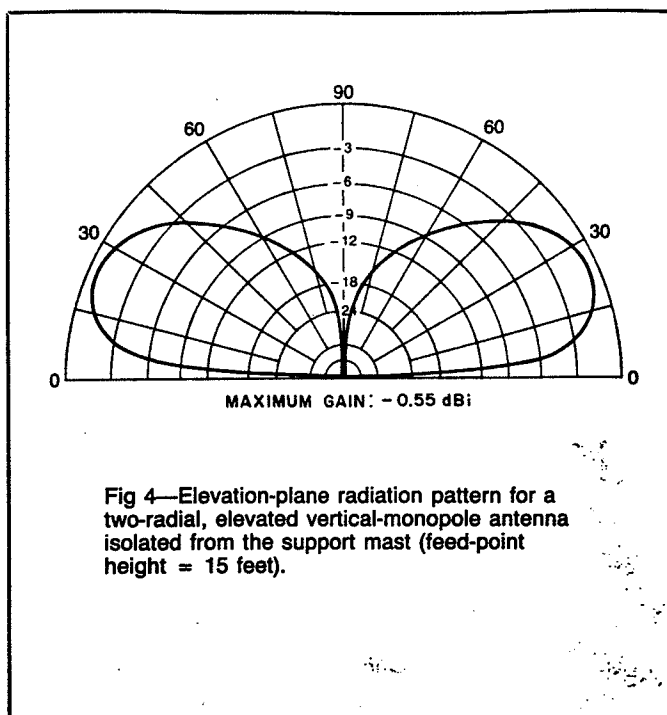


Fig 4—Elevation-plane radiation pattern for a two-radial, elevated vertical-monopole antenna isolated from the support mast (feed-point height = 15 feet).

Table 6

Calculated Power Gain and Electric Field Strength for Isolated Vertical Antenna Systems with 2 Radials

Elevation angle (degrees)	Calculated power gain (dBi)					
	1/8- $\lambda$ monopole 1/8- $\lambda$ radials			1/8- $\lambda$ monopole 1/4- $\lambda$ radials		
	Azimuth angle (degrees)			Azimuth angle (degrees)		
	0	45	90	0	45	90
0	- $\infty$	- $\infty$	- $\infty$	- $\infty$	- $\infty$	- $\infty$
5	-7.13	-7.05	-6.96	-7.75	-7.59	-7.32
10	-3.41	-3.31	-3.22	-4.09	-3.87	-3.58
15	-1.89	-1.78	-1.67	-2.68	-2.37	-2.04
20	-1.24	-1.11	-0.98	-2.17	-1.74	-1.35
25	-1.05	-0.90	-0.74	-2.18	-1.59	-1.11
30	-1.18	-0.99	-0.81	-2.54	-1.77	-1.18
40	-2.13	-1.86	-1.60	-4.09	-2.83	-1.98
50	-3.83	-3.46	-3.13	-6.52	-4.66	-3.51
60	-6.32	-5.85	-5.43	-9.75	-7.26	-5.83
70	-9.93	-9.37	-8.88	-13.96	-10.95	-9.28
80	-16.05	-15.42	-14.88	-20.41	-17.11	-15.29
90	-151.54	-151.54	-151.54	-144.30	-144.30	-144.30
Vertical electric field strength (mV/m)	29.61	29.87	30.16	27.59	27.96	28.88
Input impedance (ohms)	8.63 -j780.88			9.20 -j544.24		

Perhaps surprisingly, the best performer of this group is a 1/4- $\lambda$  monopole with four 1/8- $\lambda$  radials. This configuration provides more signal strength than the other variations, and also has an input impedance closer to 50  $\Omega$ . [Note that this configuration provides the best performance of the *modified* configurations, but does not perform as well as a full-size elevated 1/4- $\lambda$  radiator with four 1/4- $\lambda$  elevated radials—Ed.]

To find out what impact on system effectiveness would be suffered by reducing the three-dimensional antenna system to two dimensions, I next modeled elevated-radial monopole antenna systems with only two radials. The results are shown in Tables 6 and 7. The 1/4- $\lambda$  monopole with two 1/4- $\lambda$  radials appears to be the best in this group, and is actually superior to the best of the four-radial "half-pints" previously described (in Table 5). The elevation-plane radiation pattern for this antenna configuration is shown in Fig 4.

Jack Belrose, VE2CV, suggested that I model some "Field-Day Special" antennas using an elevated monopole with just a single radial. The results are presented in Tables 8 and 9. These hybrids put out a mix of vertically and horizontally polarized radiation. They produce both low- and high-angle radiation, and exhibit front-to-back ratios as high as 12 to 15 dB at some takeoff angles. The full-size version (1/4- $\lambda$  elements) appears to work the best, and its feed-point impedance is much more favorable for 50- $\Omega$  feed lines than the rest of the

antenna system at a height of 15 feet.

#### Modifications to the Basic Elevated-Radial System

As I've shown, the performance of the full-size, isolated, elevated antenna system consisting of a 1/4- $\lambda$  monopole and four 1/4- $\lambda$  radials at a height of 15

feet is competitive with a conventional 120-buried-radial, ground-mounted antenna. This section describes the results of modeling exercises I conducted with various combinations of shortened monopoles and/or radials. Table 5 shows what can be achieved with a mixture of 1/4- and 1/8- $\lambda$  elements.

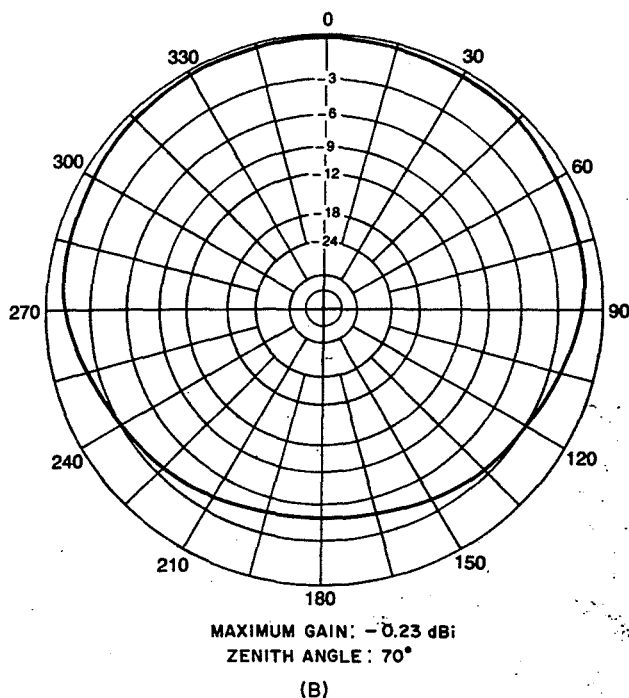
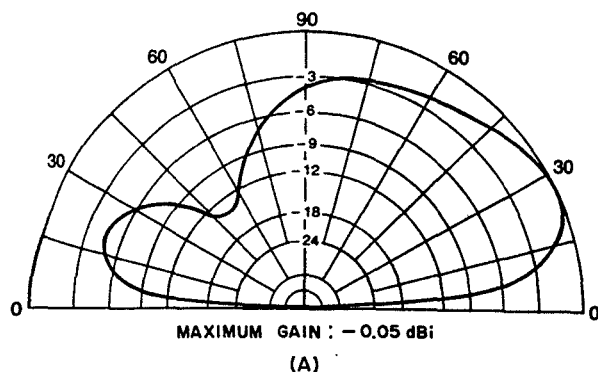


Fig 5—Elevation-plane (A) and azimuth-plane (B) radiation patterns for a one-radial, elevated vertical-monopole antenna isolated from the support mast (height = 15 feet).

bunch. Fig 5 shows the radiation patterns of this antenna.

#### Arrays

Many hams use phased-vertical arrays for 80-meter DXing, and elevated-radial antenna systems should lend themselves nicely to such applications. Table 10 lists power-gain and field-strength values for both the two-element end-fire (cardioid) array and the very popular four-square array, when constructed from individual four-elevated-radial building blocks. These antenna-system configurations are shown in Figs 6 and 7, and the patterns are shown in Figs 8 and 9.

#### Soil Types

As the electrical quality of the soil becomes worse, an elevated-radial antenna system must be raised progressively higher above the earth in order to reach performance on par with that of the reference 120-buried-radial vertical monopole. If the soil is very highly conductive, the reverse is true. At AM broadcast frequencies (1 MHz), my modeling studies have shown that adequate heights are 10 feet for very good soil, 16 feet for average soil and 23 feet for very poor soil.

This reveals another interesting aspect of using the elevated-radial technique: as the operating frequency decreases, the height at which system performance

Table 7

Calculated Power Gain and Electric Field Strength for Isolated Vertical Antenna Systems with 2 Radials

Elevation angle (degrees)	Calculated power gain (dBi)					
	1/4-λ monopole 1/8-λ radials			1/4-λ monopole 1/4-λ radials		
	Azimuth angle (degrees)			Azimuth angle (degrees)		
	0	45	90	0	45	90
0	-∞	-∞	-∞	-∞	-∞	-∞
5	-6.29	-6.25	-6.21	-6.12	-6.03	-5.90
10	-2.61	-2.57	-2.53	-2.48	-2.36	-2.22
15	-1.18	-1.13	-1.09	-1.10	-0.95	-0.78
20	-0.64	-0.58	-0.53	-0.64	-0.43	-0.22
25	-0.60	-0.53	-0.46	-0.69	-0.42	-0.16
30	-0.90	-0.81	-0.73	-1.12	-0.77	-0.44
40	-2.26	-2.13	-2.00	-2.81	-2.22	-1.72
50	-4.43	-4.25	-4.07	-5.43	-4.53	-3.81
60	-7.41	-7.16	-6.93	-8.90	-7.63	-6.68
70	-11.45	-11.14	-10.86	-13.40	-11.78	-10.63
80	-17.87	-17.52	-17.19	-20.11	-18.26	-16.97
90	-157.65	-157.65	-157.65	-149.71	-149.71	-149.71
Vertical electric field strength (mV/m)	32.72	32.84	32.97	33.35	33.67	34.15
Input impedance (ohms)	36.81 -j263.26			34.92 +j0.83		

approaches that of the reference-standard system also increases for a given soil type. In other words, an elevated-radial 160-meter antenna would have to be higher above the earth than its 80-meter equivalent in order to obtain

comparable performance over the same ground.

#### Summary

My studies on vertical monopole antennas using the NEC-GSD computer

Table 8

## Calculated Power Gain and Electric Field Strength for Isolated Vertical Antenna Systems with 1 Radial

Elevation angle angle (degrees)	Calculated power gain (dBi)							
	1/4- $\lambda$ monopole 1/4- $\lambda$ radial				1/4- $\lambda$ monopole 1/8- $\lambda$ radial			
	Azimuth angle (degrees)				Azimuth angle (degrees)			
	0	45	90	180	0	45	90	180
0	- $\infty$	- $\infty$	- $\infty$	- $\infty$	- $\infty$	- $\infty$	- $\infty$	- $\infty$
5	-6.07	-6.25	-7.30	-9.52	-5.91	-6.08	-6.60	-7.53
10	-2.36	-2.52	-3.55	-5.96	-2.21	-2.38	-2.90	-3.88
15	-0.87	-1.00	-2.01	-4.75	-0.74	-0.91	-1.44	-2.49
20	-0.23	-0.33	-1.33	-4.54	-0.14	-0.30	-0.86	-2.02
25	-0.05	-0.11	-1.09	-4.97	-0.01	-0.17	-0.76	-2.08
30	-0.14	-0.16	-1.14	-5.92	-0.19	-0.36	-0.99	-2.51
40	-0.76	-0.71	-1.69	-9.36	-1.17	-1.36	-2.12	-4.24
50	-1.55	-1.49	-2.49	-13.82	-2.70	-2.93	-3.89	-7.02
60	-2.19	-2.20	-3.20	-11.80	-4.54	-4.85	-6.07	-10.72
70	-2.64	-2.77	-3.65	-7.82	-6.55	-6.94	-8.37	-14.10
80	-3.12	-3.28	-3.86	-5.35	-8.69	-9.08	-10.31	-13.70
90	-3.92	-3.92	-3.92	-3.92	-11.12	-11.12	-11.12	-11.12
Vertical electric field strength (mV/m)	33.21	32.43	28.69	22.90	33.98	33.35	31.49	28.52
Input impedance (ohms)	49.56 +j16.56				40.65 -j485.47			

code indicate that a radiator elevated 10 to 20 feet above ground and having only four elevated horizontal radials can out-perform a ground-mounted monopole with 120 buried radials. At 3.8 MHz, an elevation height of about 15 feet is adequate for average soil, while a lower height is satisfactory for shorter wavelengths. Higher elevation above ground is necessary over soil with poorer

electrical characteristics and at lower operating frequencies.

I will be doing field studies to verify the computer predictions (preliminary tests during Field Day showed very promising results). If the information gathered from NEC is correct, the construction cost and complexity of effective vertical-monopole antenna systems

can be greatly reduced over that of comparable buried-radial systems now widely in use. At the same time, ease of installation and low-angle gain will be increased. The elevated-radial technique appears to be equally valid in the medium-frequency broadcast band and at the lower end of the HF range, so perhaps the ground-plane vertical is "the antenna for all bands"!

Table 9

## Calculated Power Gain and Electric Field Strength for Isolated Vertical Antenna Systems with 1 Radial

Elevation angle (degrees)	Calculated power gain (dBi)							
	1/8- $\lambda$ monopole 1/8- $\lambda$ radial				1/8- $\lambda$ monopole 1/4- $\lambda$ radial			
	Azimuth angle (degrees)				Azimuth angle (degrees)			
	0	45	90	180	0	45	90	180
0	- $\infty$	- $\infty$	- $\infty$	- $\infty$	- $\infty$	- $\infty$	- $\infty$	- $\infty$
5	-8.54	-8.88	-10.84	-17.05	-6.96	-7.28	-8.33	-10.58
10	-4.76	-5.01	-6.79	-13.72	-3.19	-3.50	-4.54	-6.90
15	-3.13	-3.29	-4.88	-12.93	-1.61	-1.90	-2.92	-5.47
20	-2.31	-2.36	-3.75	-13.42	-0.85	-1.12	-2.14	-4.93
25	-1.86	-1.80	-3.00	-14.95	-0.52	-0.77	-1.79	-4.90
30	-1.63	-1.46	-2.48	-17.44	-0.46	-0.69	-1.71	-5.21
40	-1.41	-1.10	-1.82	-17.11	-0.83	-1.03	-2.08	-6.55
50	-1.19	-0.87	-1.42	-10.19	-1.58	-1.78	-2.88	-8.36
60	-0.88	-0.69	-1.16	-5.93	-2.52	-2.75	-3.89	-9.51
70	-0.59	-0.56	-0.99	-3.32	-3.56	-3.82	-4.91	-8.99
80	-0.52	-0.59	-0.89	-1.72	-4.68	-4.92	-5.68	-7.49
90	-0.85	-0.85	-0.85	-0.85	-5.97	-5.97	-5.97	-5.97
Vertical electric field strength (mV/m)	24.75	23.45	18.09	9.90	29.95	28.79	25.48	20.18
Input impedance (ohms)	23.49 -j527.41				12.22 -j1004.27			



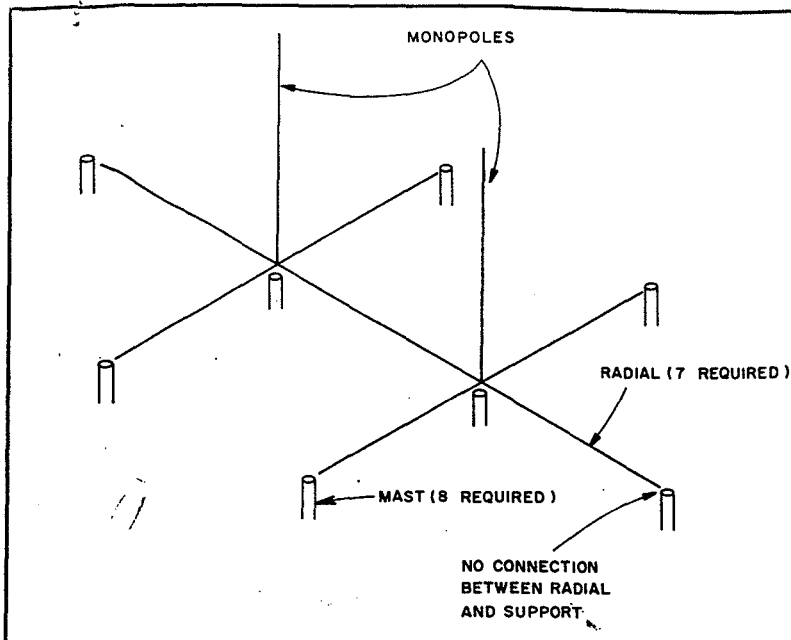


Fig 6—Physical layout of an elevated, two-element phased-vertical array (feed-point height = 15 feet).

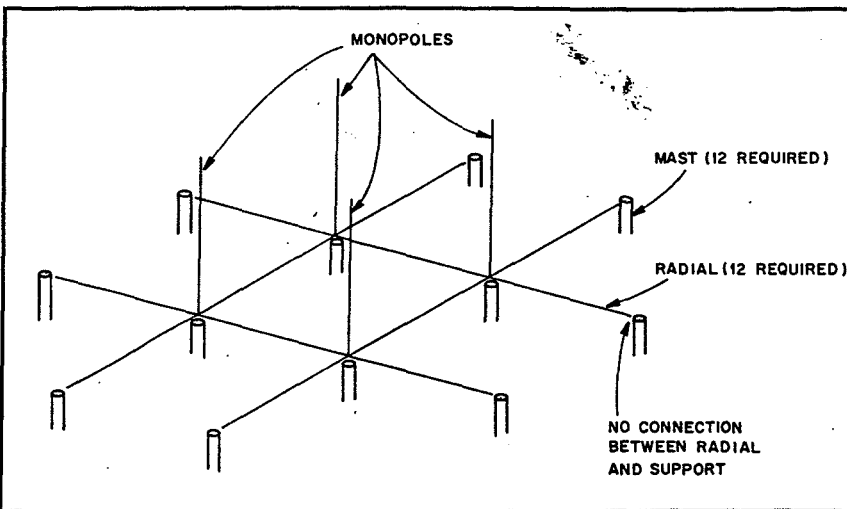
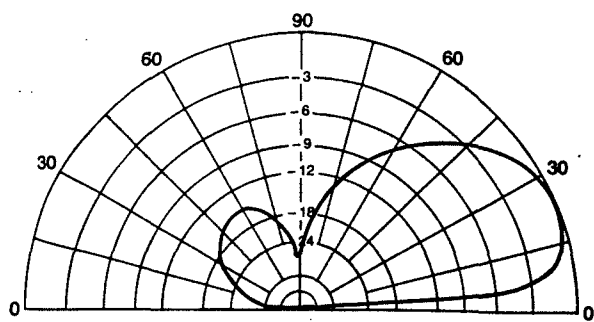


Fig 7—Physical layout of an elevated, four-square phased-vertical array (feed-point height = 15 feet).

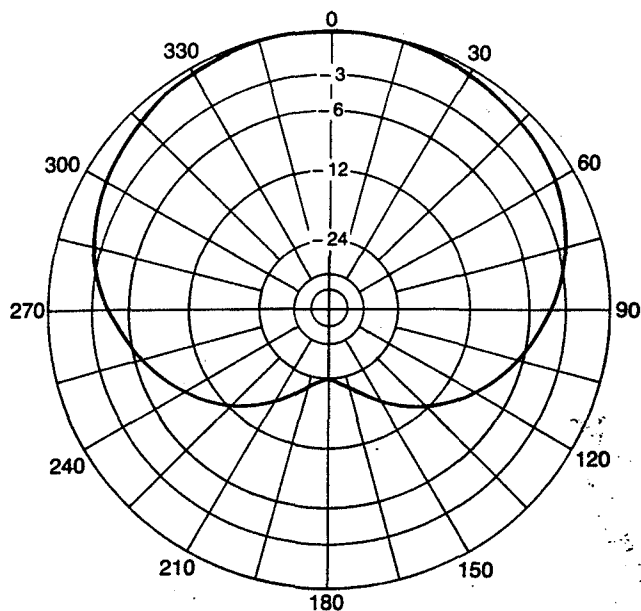
**Table 10**  
**Calculated Power Gain and Electric Field Strength for Isolated Phased-Vertical Antenna Systems**

Elevation angle (degrees)	2-element cardioid array					4-element 4-square array			
	Azimuth angle (degrees)					Azimuth angle (degrees)			
	0	45	90	180	45	90	135	225	
0	-∞	-∞	-∞	-∞	-∞	-∞	-∞	-∞	
5	-2.45	-2.96	-6.18	-32.85	-0.50	-3.29	-13.87	-37.32	
10	+1.23	+0.69	-2.53	-27.61	+3.16	+0.39	-9.94	-33.19	
15	2.66	2.07	-1.16	-23.74	4.54	1.82	-8.15	-31.06	
20	3.20	2.55	-0.70	-20.42	5.03	2.36	-7.17	-29.65	
25	3.23	2.51	-0.76	-17.68	5.00	2.40	-6.61	-28.67	
30	2.92	2.10	-1.20	-15.51	4.63	2.11	-6.33	-28.00	
40	+1.51	+0.47	-2.91	-12.70	3.17	+0.85	-6.33	-26.44	
50	-0.76	-2.06	-5.57	-11.57	+1.08	-0.94	-6.71	-22.02	
60	-3.87	-5.40	-9.11	-11.93	-1.29	-2.89	-7.10	-16.70	
70	-8.01	-9.69	-13.60	-13.99	-3.61	-4.66	-7.35	-12.58	
80	-14.06	-15.65	-19.44	-19.06	-5.65	-6.17	-7.48	-9.66	
90	-25.00	-25.00	-25.00	-25.00	-7.53	-7.53	-7.53	-7.53	
Vertical electric field strength (mV/m)	51.39	48.35	32.99	1.89	64.86	46.34	12.90	0.81	
Input impedance (ohms)	19.61	+j7.41	51.07	+j33.71	9.68 +j2.78	36.8 -j4.47	36.8 -j4.47	66.62 +j47.2	



MAXIMUM GAIN: 3.26 dBi  
AZIMUTH ANGLE: 90°

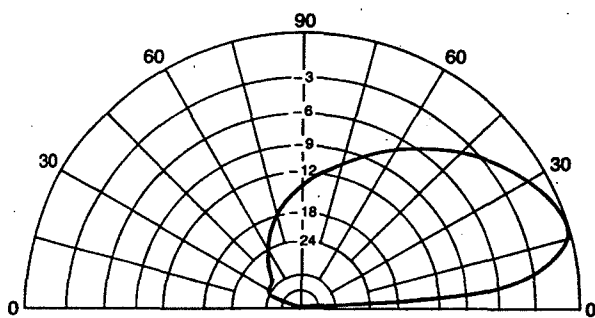
(A)



MAXIMUM GAIN: 3.20 dBi  
ZENITH ANGLE: 70°

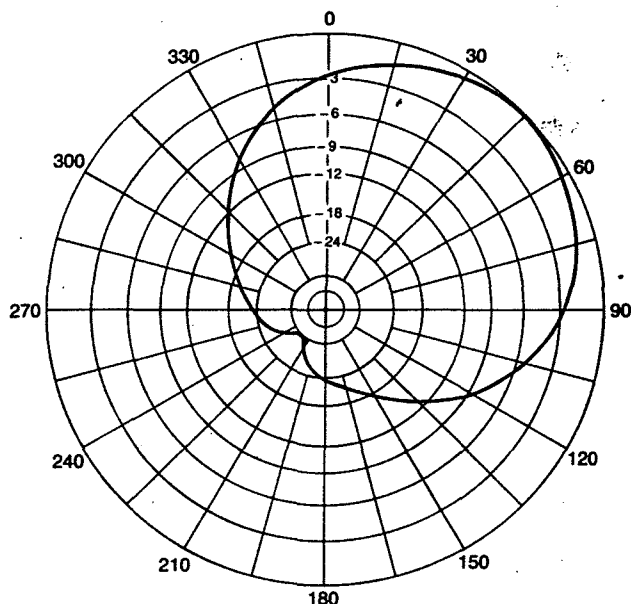
(B)

Fig 8—Elevation-plane (A) and azimuth-plane (B) radiation patterns for an elevated, two-element phased-vertical array (feed-point height = 15 feet).



MAXIMUM GAIN: 5.07 dBi  
AZIMUTH ANGLE: 45°

(A)



MAXIMUM GAIN: 5.03 dBi  
ZENITH ANGLE: 70°

(B)

Fig 9—Elevation-plane (A) and azimuth-plane (B) radiation patterns for an elevated, four-square phased-vertical array (feed-point height = 15 feet).

#### Notes

<sup>1</sup>G. H. Brown, R. F. Lewis and J. Epstein, "Ground Systems as a Factor in Antenna Efficiency," *Proceedings of the Institute of Radio Engineers*, Vol 25, No. 6, Jun 1937, pp 753-787.

<sup>2</sup>"Ground Systems . . .," p 784.

<sup>3</sup>"Ground Systems . . .," p 769.

<sup>4</sup>A. Doty, "Improving Vertical Antenna Efficiency," *CQ*, Apr 1984, pp 24-31.

<sup>5</sup>G. Hagn, SRI International, Arlington, VA, private communication.

<sup>6</sup>Because the coaxial transmission line feeding power to the antenna must extend vertically along the center mast, some means of preventing the flow of antenna current on the outer surface of the cable shield must be used to isolate the feed line from the vertical support structure. This can be done by using a transformer at the feed point, or by placing suitable ferrite material around the outside of the transmission line (a choke balun).

#### Reference

A. M. Christman, "Vertical Monopoles with Elevated Ground Systems," *Proceedings of the Third Annual Review of Progress in Applied Computational Electromagnetics*, Naval Postgraduate School, Monterey, CA, March 1987.

Al Christman has been a licensed Amateur Radio operator since 1974. Al earned BS and MS degrees in mineral preparation and mining engineering at Penn State University, and BSEE

and MSEE degrees at West Virginia University. He has served on the faculties of Mt Vernon Nazarene College (teaching physics and electronics) and Ohio University (teaching courses in the EE program). Al's career has included stints as a chemical engineer (while he was serving in the US Army) and as a mining engineer for US Steel Corp. Al is presently a PhD candidate in the electrical and computer engineering program at Ohio University, Athens, Ohio.

In addition to his amateur license, Al holds an FCC General Class Radiotelephone Operator's license and spent several years as an FM broadcast engineer and consultant.

# UNDERSTANDING ELEVATED VERTICAL ANTENNAS

*Useful information about a popular antenna type*

---

I live on a small lot that limits my options for antennas. I'm also an avid DXer who *needs* the lowest possible radiation angle. A vertical antenna was an obvious choice to satisfy my needs. After working and listening to many DX stations who were using a vertical or GP (ground plane) antenna, mostly Europeans, I considered three possible configurations:

- 1) ground mounted quarter wave
- 2) elevated quarter wave or ground plane
- 3) half wave (including the popular Cushcraft "R" series)

I consulted antenna books by Kraus,<sup>1</sup> Orr,<sup>2</sup> Moxon,<sup>3</sup> and the ARRL,<sup>4</sup> and used MININEC<sup>5</sup> to compute the relative performance of various designs. I chose a conductivity of 4 mS/meter and a dielectric constant of 13 for all the calculations in this article. Vertical antenna performance varies greatly with ground characteristics, so the data presented here should only be used for comparison purposes. The MININEC-computed impedances and gains aren't accurate because the effect of ground on the antenna currents isn't taken into account; however, the data are adequate for comparison purposes. The elevation plots presented for quarter-wave verticals with two elevated radials were computed with 0 degrees perpendicular to the plane of the antenna and radials.

A ground-mounted vertical with 30 or more radials would be a great choice for all around

operating, as illustrated in **Figure 1**. Unfortunately, I have a small yard, blockage from our two story stucco house would be excessive, and I'd have to put a fence around the antenna to protect the kids and dog—so I ruled out the ground-mounted vertical design. This narrowed the field to an elevated quarter or half-wave vertical. **Figure 1** shows the relative performance of a quarter-wave vertical 8 feet above ground and a half-wave vertical with its center 20 feet high. The remainder of this article summarizes what I learned as a result of my personal experience and by using MININEC/NEC analysis on both these antenna types.

I couldn't find an aesthetically pleasing arrangement for radials on my roof, so I purchased a Cushcraft R4—which is a half-wave design using traps for 20, 15, 12, and 10 meters. It has a built-in counterpoise consisting of a series inductor and 4 short stainless steel radials at the base. The R4 was a big improvement over my dipole for DXing on 20 meters. I computed the performance of the R4 on my roof by simulating it as a vertical dipole with its center 30 feet off ground. The results shown in **Figure 2** are very interesting. The antenna has a fairly broad second lobe, which can be viewed as a plus because it increases the angular coverage of the antenna, or a minus because the higher angle lobes may increase the QRM from local stations. Chapter 3, Figure 15 of *The ARRL Antenna Book*, 16th edition, shows the effect of height on a ground plane

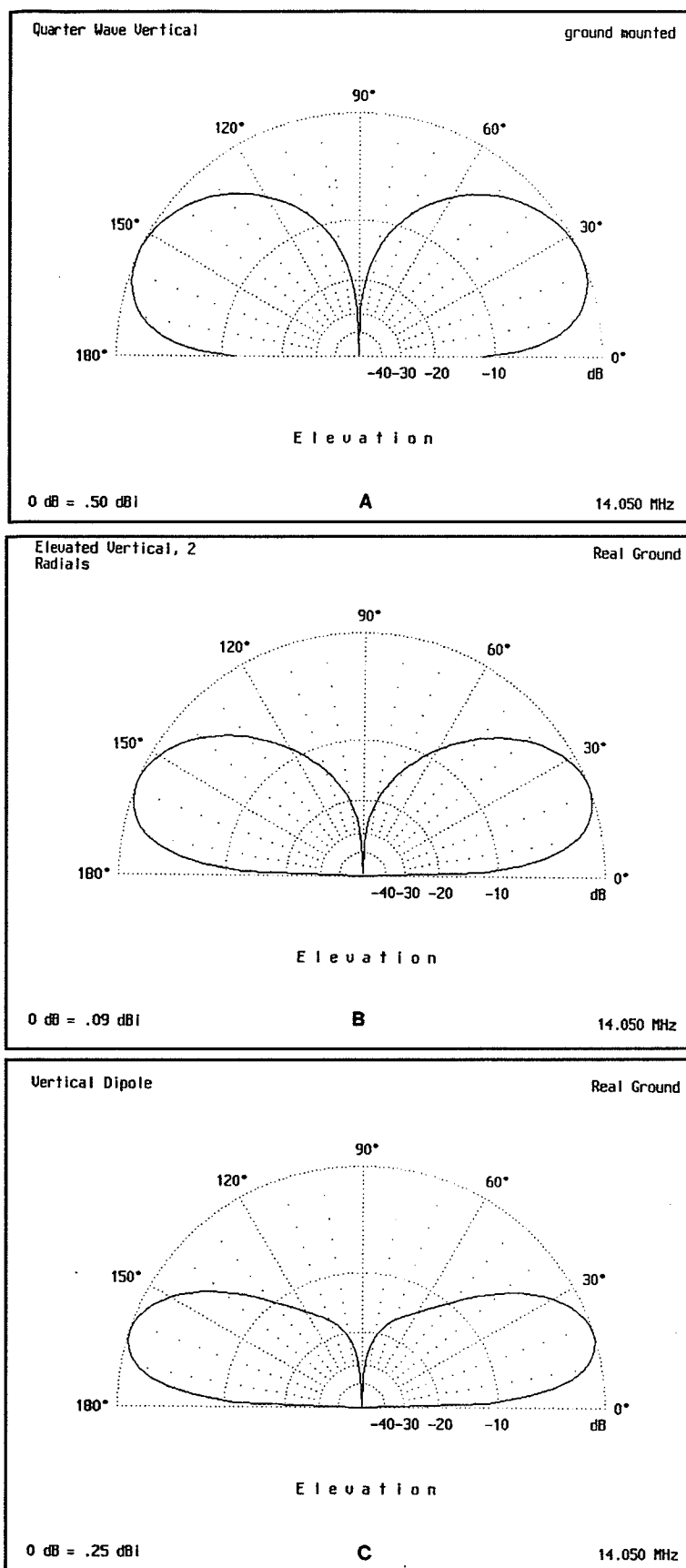


Figure 1. Relative performance of (A) ground-mounted quarter wave, (B) elevated quarter wave (or ground plane), and (C) half-wave vertical antennas.

antenna. This is very close to the same results for the vertical dipole. If your goal is strictly DXing, you need not mount the antenna with its center higher than 1/4 wavelength above ground. For this half-wave equivalent antenna, that means the base will be close to the ground.

Al Christman, KB8I, published an interesting article in *QST* on elevated vertical antennas.<sup>6</sup> He showed that good performance could be obtained with only 2 radials. A comparison of a vertical mounted 20 feet high with 2 and 4 radials is shown in Figure 3. The antenna with 2 radials has an azimuthal asymmetry of only 0.25 dB—hardly worth worrying about. I used NEC<sup>7</sup> to analyze the performance of verticals with 2 and 4 radials at lower height. NEC computed the effects of ground on the antenna currents and produced accurate impedance and gain results. These results are shown in Figure 4; again, no appreciable difference can be seen. I was pleasantly surprised, but subsequent investigation turned up a potential problem with the 2-radial design that I couldn't ignore.

Les Moxon, G6XN, included an interesting discussion on short, coil-loaded radials in his excellent book *HF Antennas for All Locations*. He mentions the effect of radial imbalance on vertical antenna performance. Radial imbalance may be caused by wire length differences or as a result of unequal loading due to nearby objects like a house, wiring, plumbing, or antennas. The effect created when 1 radial is 6 inches long and the other 6 inches short is shown in Figure 5; this is only  $\pm 2.7$  degrees on 20 meters. The resulting pattern with its high angle lobe may not be suspected by the operator in his shack because the SWR is not always sensitive to these imbalances and is generally tuned during antenna installation. This effect is not observed at very low heights, like 2 feet. Another example, with which I have personal operating experience, is a 40-meter elevated vertical (up 20 feet) with 2 radials spread out on the roof. I was never happy with the performance of this antenna, which was worse for DX than my dipole up only 40 feet. The analysis shown in Figure 6 clearly shows a significant low angle gain degradation (3 dB or more at 10 degrees) for the same small radial imbalance. Quarter-wave wire radials run close to a house roof are good candidates for coupling or loading-induced imbalances.

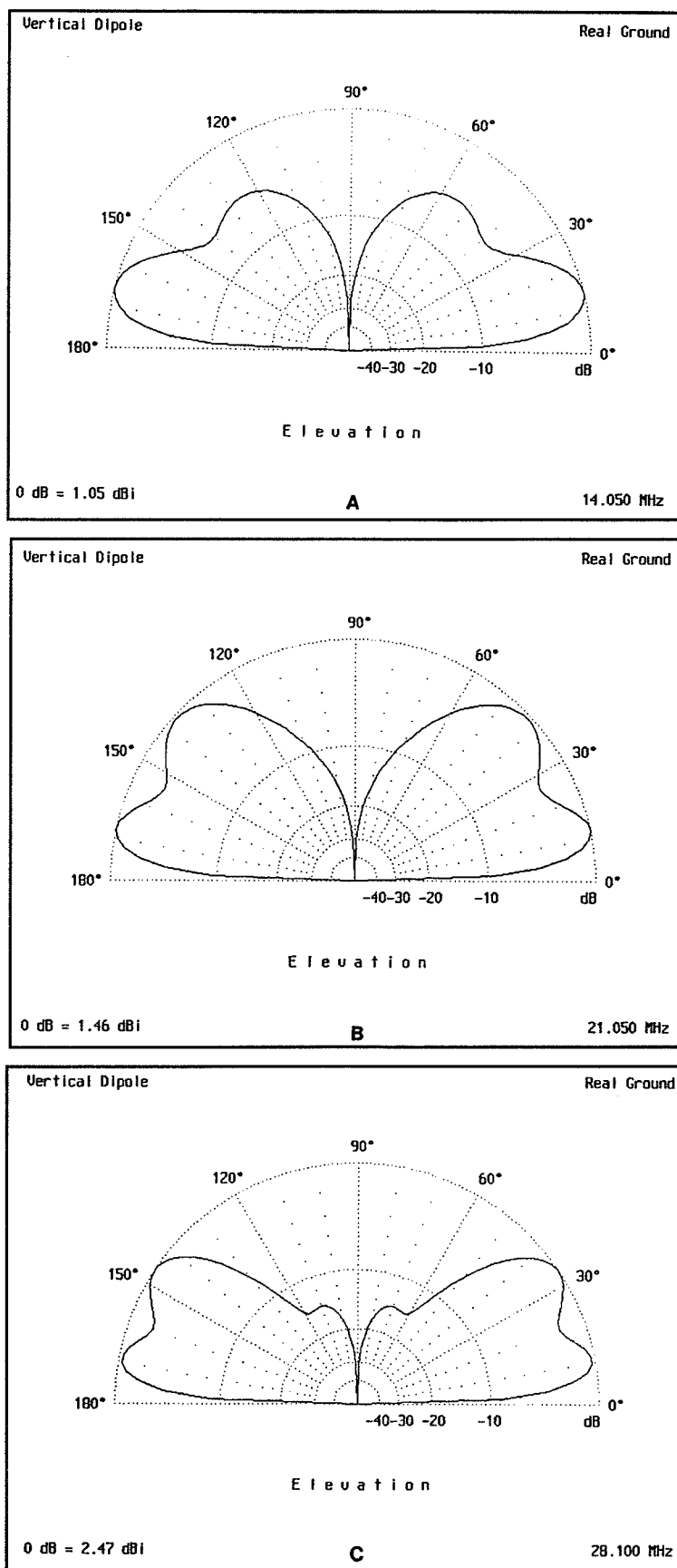
Moxon's solution to this problem is to use short, coil-loaded radials. A MININEC analysis confirmed his design. Vertical antenna performance with radial lengths of 60 degrees or less was insensitive to radial imbalances. I read of a low-band station that used coax radials with good luck.<sup>8</sup> A quarter-wave length of coax with a velocity factor of 0.66 is 60 degrees long on the outside of the shield. A quarter-wave open

circuit stub looks like a short at the feed end and, because it is less than 60 degrees long on the outside, it won't cause pattern distortion if the radial pair is imbalanced. I trimmed a pair of RG-213 radials for 30 meters using a dip meter and installed them on a roof-mounted WARC-band vertical. I simply connected the center conductor of the coax radial to the feed-line coax ground and left the shield open. I could have connected the radial shields together, but saw no reason to do so. The results were as expected and the antenna tuned the same as it had with 2 wire radials. I then cut pairs of coax radials for my roof-mounted 40/80/160 meter multiband vertical and replaced the wire radials. Again, the antenna tuned as before and even seemed to work better. I dressed the coax neatly around the edges of the roof. This made my wife happy, and I no longer have to worry about tripping over the wire radials I have running every which way on the roof!

I've been doing some 80-meter antenna comparisons over the past few months. My inverted vee is only 40 feet up at the apex, but it outperforms my vertical on most DX stations. I believe part of the reason for this is the enhanced signal-to-noise ratio provided by the inverted vee, but even strong DX signals were often weaker on the vertical. The performance improved significantly after I added 2 additional coax radials to the vertical for 80 meters. I think the pattern may have been skewed because the radials weren't in a straight line and didn't provide good field cancellation, but I'm not certain. All I know is 4 radials work better than 2 in this situation.

The radiation resistance of an elevated vertical depends on the height above ground. Close to the ground, the quarter-wave design has about one half the resistance of a dipole as expected (i.e.,  $\approx 36$  ohms). As the antenna is elevated, the radiation resistance drops and becomes 18 ohms when far from ground. Moxon gives an excellent explanation of this effect.<sup>9</sup> His article "Ground Planes, Radial Systems, and Asymmetric Dipoles," is must reading for anyone seriously considering an elevated vertical antenna. My NEC radiation resistance calculations (shown in **Figure 7**) agree very closely with those presented in Moxon's article. These results show that even for a vertical with 2 radials mounted 1 foot above ground, the loss resistance is less than 3 ohms. This corresponds to an efficiency of 92 percent, which is better than all but the most extensive ground-mounted systems.

Elevated vertical antennas are good performers when properly installed. The feedpoint impedance can be raised to 50 ohms using the old "ground plane" technique of sloping the radials down toward the ground. A better way to



**Figure 2.** Performance of a vertical dipole with its center up 30 feet on (A) 20, (B) 15, and (C) 10 meters.

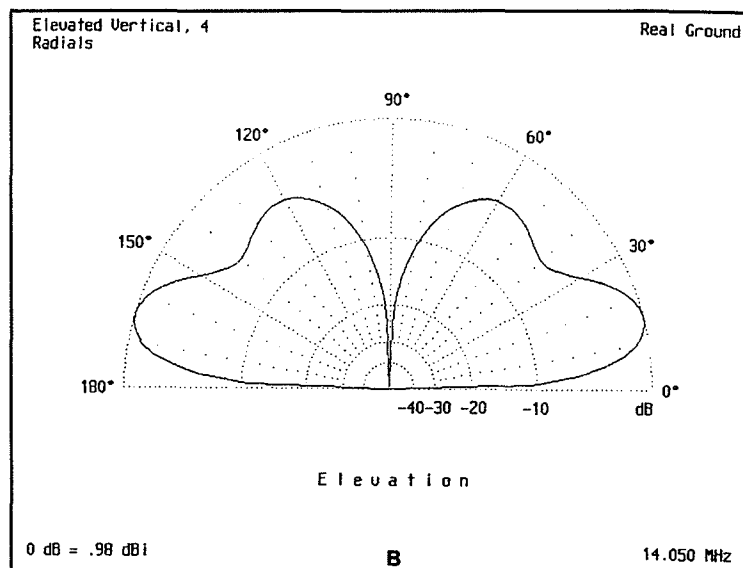
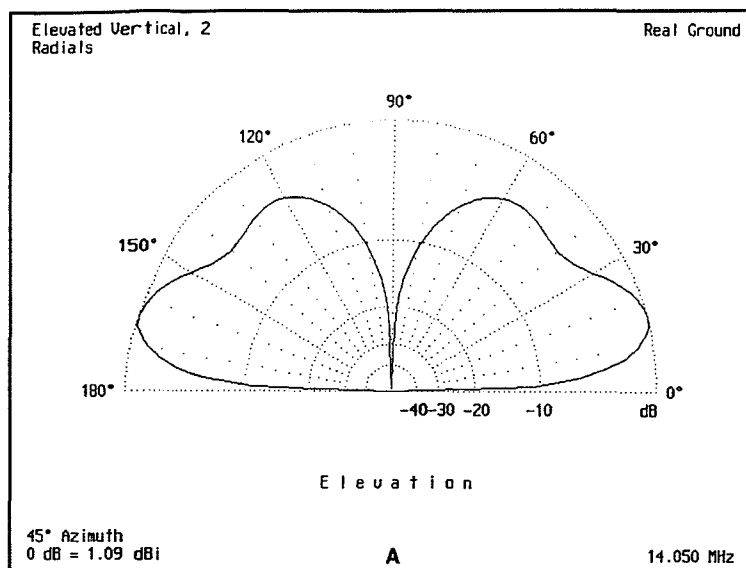


Figure 3. Comparison of elevated quarter-wave verticals with (A) 2 radials and (B) 4 radials.

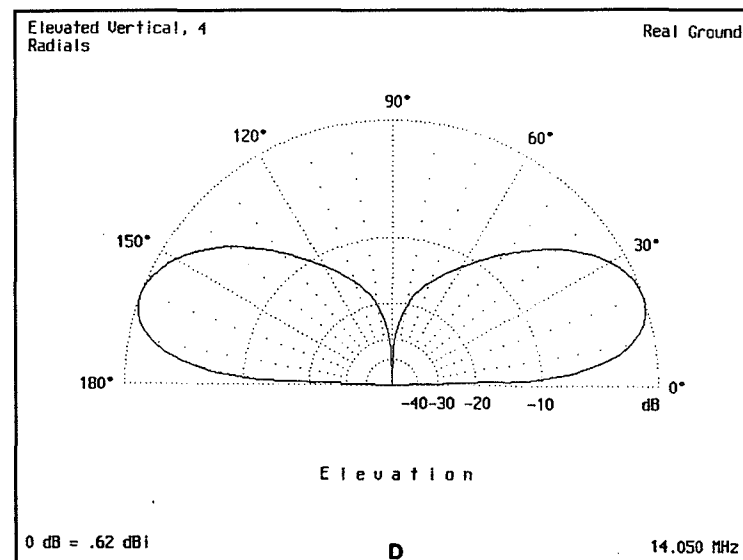
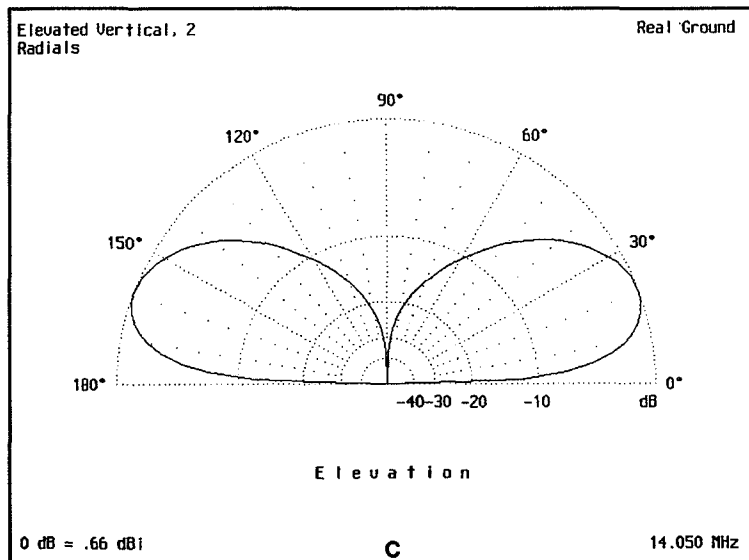
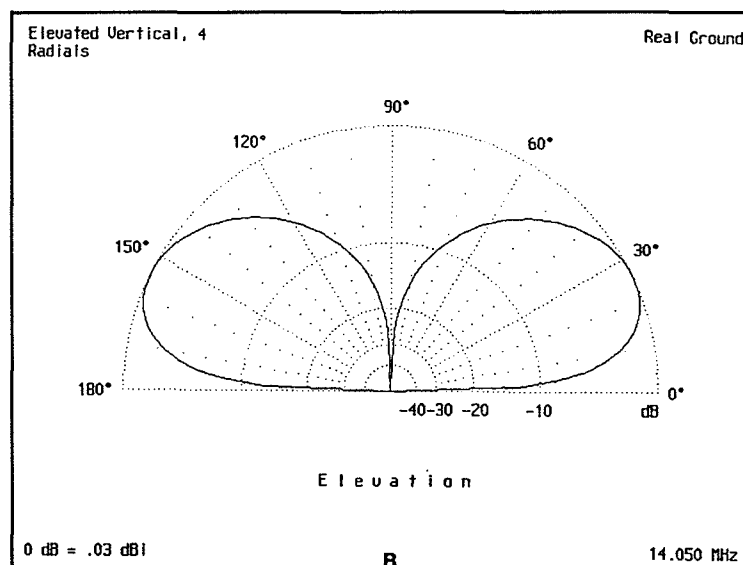
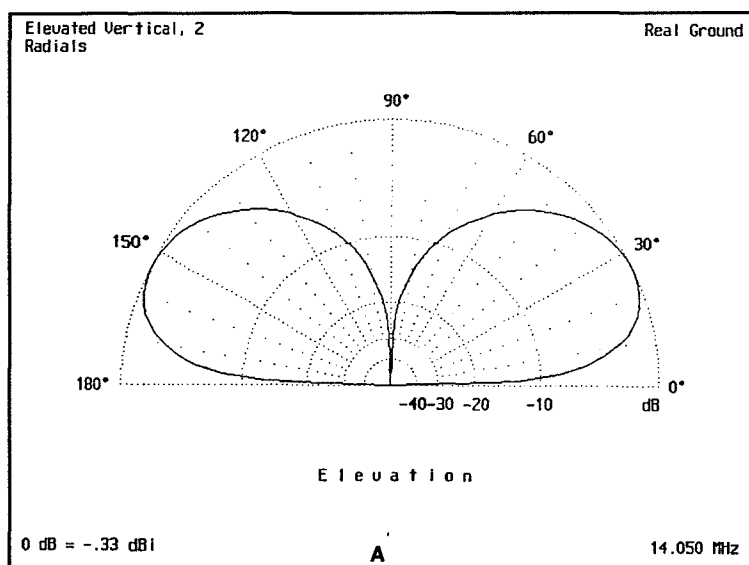


Figure 4. Performance comparison of elevated vertical antennas at low height (A) up 2 feet, 2 radials, (B) up 2 feet, 4 radials, (C) up 10 feet, 2 radials, and (D) up 10 feet, 4 radials.

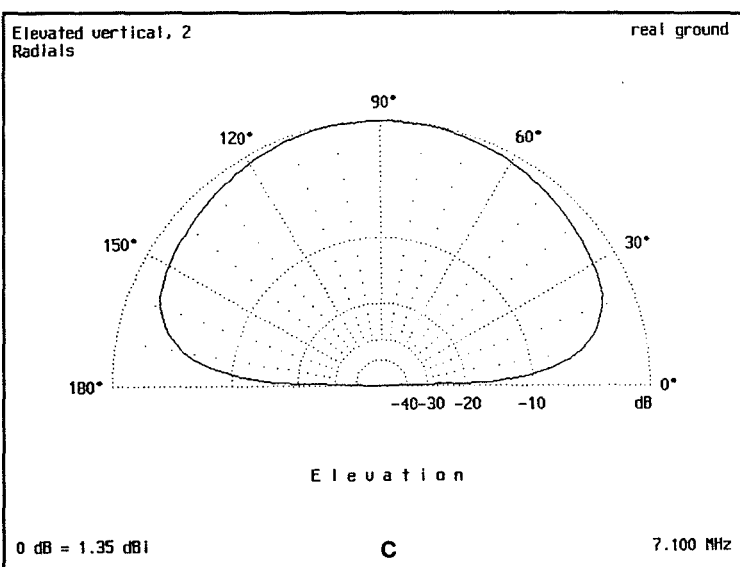
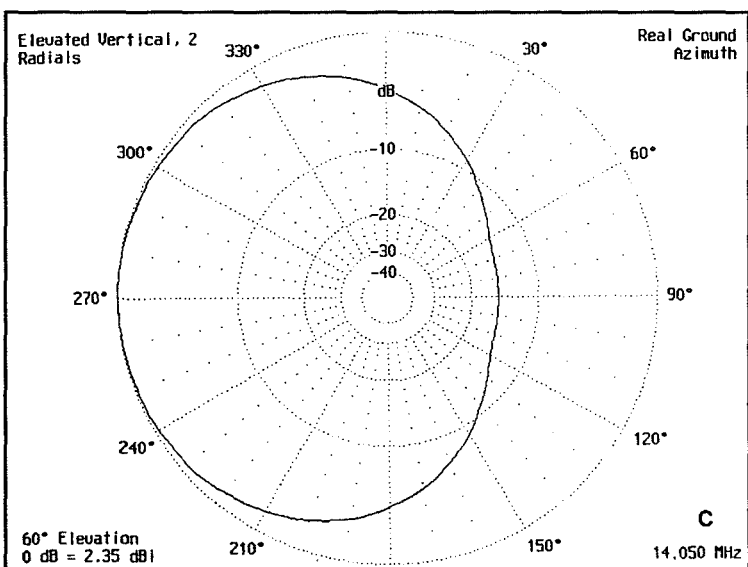
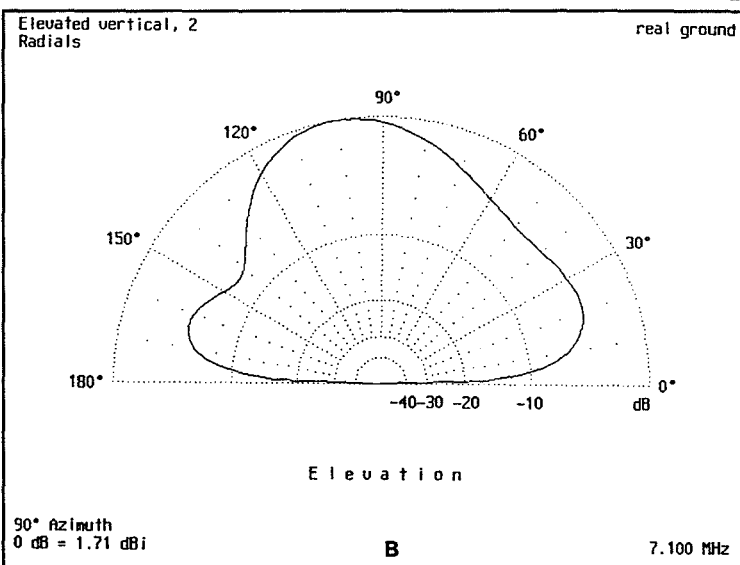
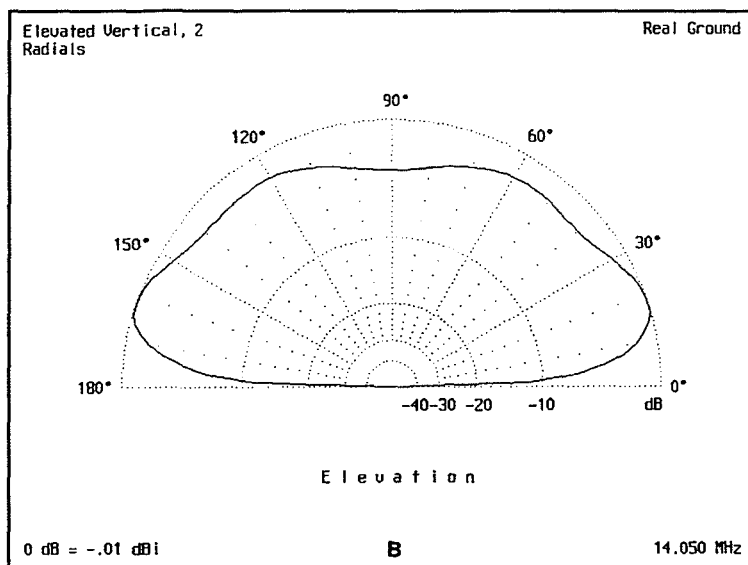
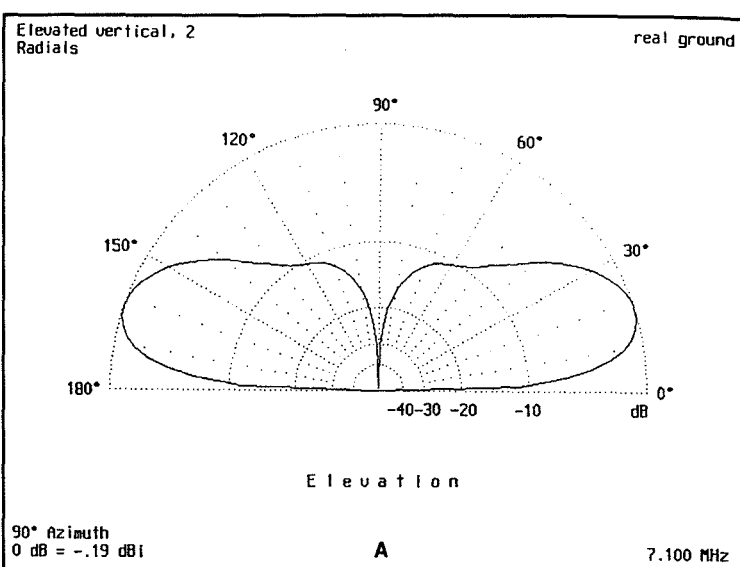
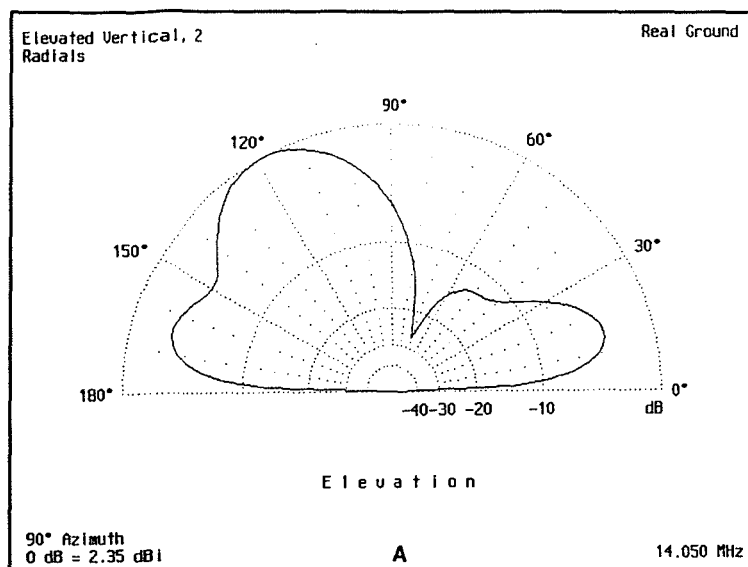


Figure 5. Twenty-meter vertical elevated 20 feet with 2 radials imbalanced  $\pm 2.7$  degrees. (A) Worst case elevation pattern at 90 degrees azimuth, (B) elevation pattern at 0 degrees azimuth, and (C) azimuth pattern at 60 degrees elevation.

Figure 6. Forty-meter vertical elevated 20 feet with (A) 2 balanced radials, (B) 2 unbalanced radials, and (C) 2 unbalanced radials for azimuths of 90 degrees and 0 degrees, respectively.

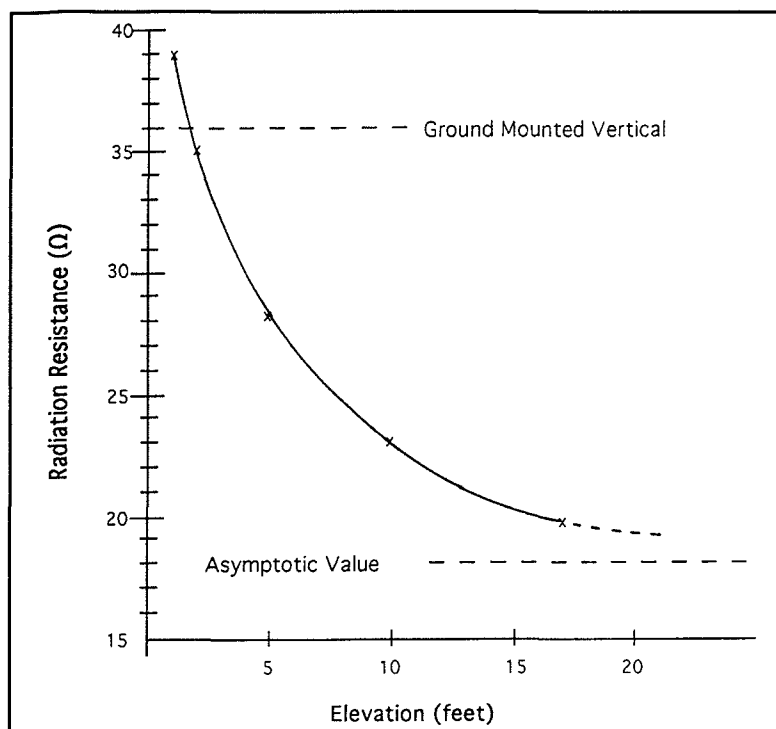


Figure 7. Radiation resistance versus height above ground for a 20-meter, 2-radial vertical.

obtain a 50-ohm match is to use a transmission line transformer. Jerry Sevick, W2FMI, has published many low-impedance designs in the past few years.<sup>10</sup> Sevick's transformers are available commercially from Amidon Associates.\* I hope this article has provided some useful data for elevated vertical antenna users.

\*Amidon Associates, Inc., 2216 East Gladwick Street, Dominguez Hills, California 90220.

#### REFERENCES

1. J. Krauss, *Antennas*, McGraw-Hill, New York, 1988.
2. W. Orr and S. Cowan, *All About Vertical Antennas*, Radio Publications, Inc., Lake Bluff, Illinois 1988.
3. L. Moxon, *HF Antennas for All Locations*, Radio Society of Great Britain, Herts, England, 1993.
4. G. Hall, Editor, *The ARRL Antenna Book*, 16th edition, American Radio Relay League, Newington, Connecticut, 1991.
5. Brian Beezley, K6STI, AO 6.0, 507-1/2 Taylor Street, Vista, California 92084.
6. A. Christman, "Elevated Vertical Antenna Systems," *QST*, August 1988, pages 35-42.
7. Brian Beezley, K6STI, NEC 1.0, ibid.
8. W. Orr, "Radio FUNDamentals," *CQ*, June 1992, pages 57-58.
9. L. Moxon, "Ground Planes, Radial Systems, and Asymmetric Dipoles," *The ARRL Antenna Compendium*, Volume 3, 1992, pages 19-27.
10. J. Sevick, "The Ultimate Multimatch Unun," *CQ*, August 1993, pages 15-19.

## PRODUCT INFORMATION

### New Analog Devices Brochure

Analog Devices offers a 24-page brochure that describes their latest fixed- and floating-point DSPs (digital signal processors), and 16-bit codecs, as well as chipset solutions for sound, fax/modem and combination sound/modem designs. An overview of DSP architectures includes the new SHARC (Super Harvard ARchitecture Computer) DSP with a 4-megabit on-chip SRAM and "glueless" interface for multi-processor applications. A second member of the SHARC family offers 2-mega-bits of memory, and future memory variants are on the way. Also included is an overview of the company's software and hardware tools for application development; tools include GNU C Compilers and C Debuggers. FFT benchmarks are provided to indicate performance for routine DSP functions. Mixed-Signal Processors are also discussed for use in high-volume, cost-sensitive applications where the DSP, codec, and all data and program memory are included on a single tightly integrated chip.

*Digital Signal Processing* is available at no charge, and can be requested through Analog Devices' Literature Center; refer to publication number G1633a; phone: 617-461-3881.

### AD8300 DAC From Analog Devices

Analog Devices' AD8300 is a 12-bit voltage-output DAC (digital-to-analog converter) that operates from a single 3-V supply. It requires no external components and integrates a converter, reference, and output amplifier into a compact SO-8 or 8-pin DIP package. The AD8300's internal reference is adjusted to give an analog output of 0.5 mV/bit (2.0475 V full scale). The output amplifier can swing to either supply rail (true single-supply rail-to-rail operation), and is capable of sourcing or sinking up to 5 mA. With a minimum supply voltage of 2.7 V, the AD8300 can operate from battery supplies, even in cold weather or at the end of battery life. It can also be used in traditional 5-V logic systems.

Operation is specified over the -40° to +85°C temperature range. The AD8300 is housed in either a compact SO-8 or 8-pin DIP package.

For further information, contact: Analog Devices, Inc., 181 Ballardvale Street, Wilmington, MA 01887 (phone: 617-937-1428; fax: 617-821-4273).





# FOLDED UNIPOLE ANTENNA KITS

FOR  
AM BROADCAST STATIONS

UP-300 A/B  
UP-600 A/B  
530-1600 KHZ

## GIVE YOUR STATION:

- BETTER SOUND
- BETTER EFFICIENCY
- LIGHTNING PROTECTION
- REVENUE FROM CATV, TWO-WAY, FM
- AN EMERGENCY ANTENNA

## - FEATURES -

UP-300 AND UP-600 SYSTEMS are designed specifically for AM Broadcast operation and afford the broadcaster significant advantages in efficiency, lightning protection, bandwidth, and FM feedline isolation when compared to most conventional "series-fed" antennas.

**ADVANCED CONSTRUCTION.** An advanced "delta" tension assembly is employed to maintain mechanical and electrical stability, even in hurricane winds. These unipoles are nominally rated to 50,000 watts, 100% modulated, in specific applications. The UP-300 and UP-600 series unipoles are designed using the latest fiberglass and epoxied plastics for superb insulation and stability.

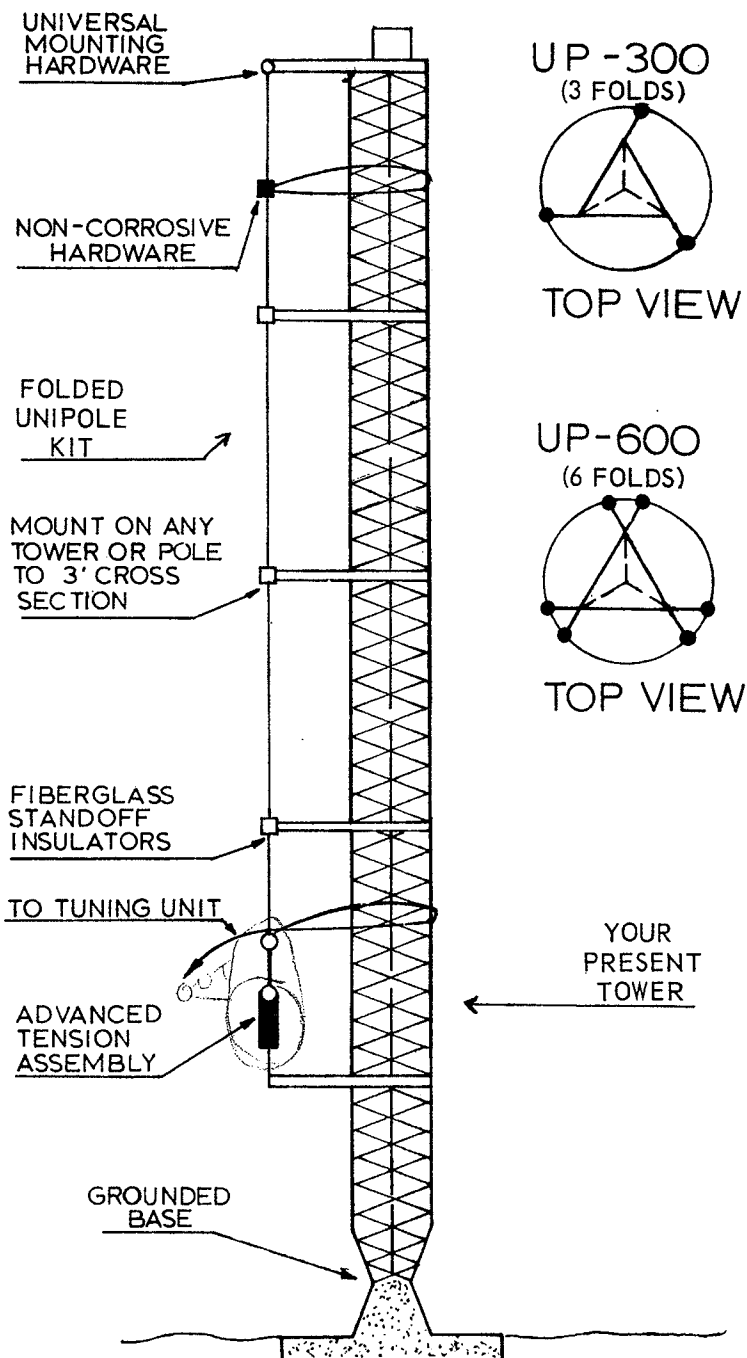
**FAST INSTALLATION.** A universal mounting system permits unparalleled rapid installation on towers from 12" to 36" face dimension and with leg diameters from 1" to 3". Tower loads are small and installation is feasible on most AM broadcast towers.

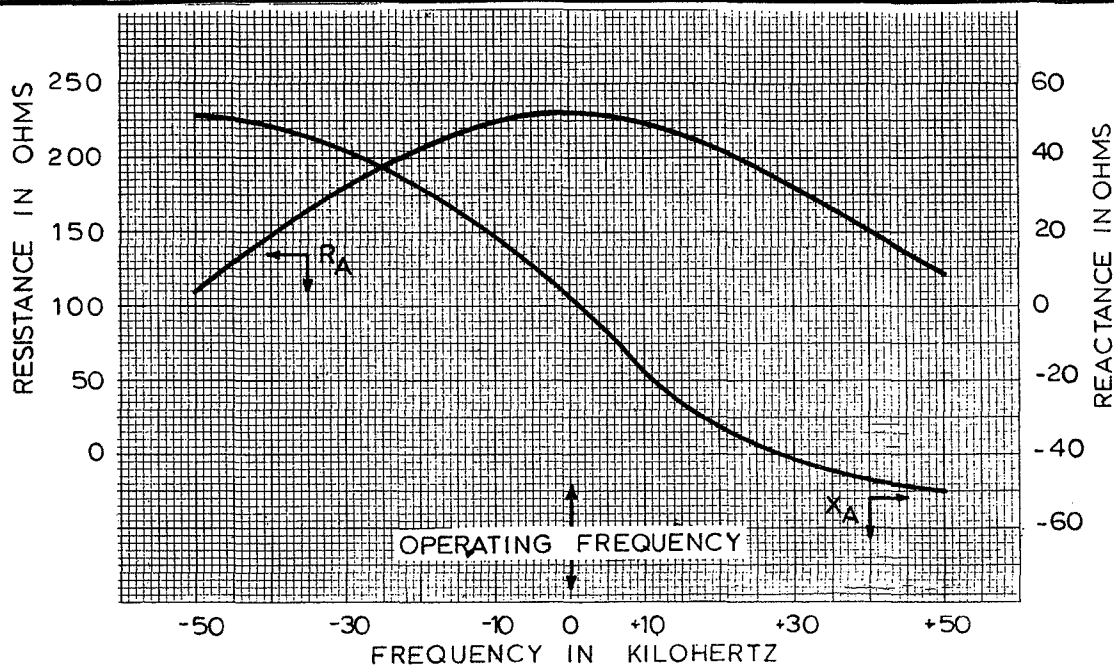
**FLEXIBLE ANTENNA IMPEDANCE SELECTION** is assured as resistance and reactance parameters seen at the feedpoint are variable about each axis by physical unipole adjustment. Existing tuning houses can frequently be used with little modification.

**FCC APPROVAL.** The FCC routinely approves many applications by letter for folded unipole installations on non-directional towers. Ordinarily, no fee is involved.

**APPLICATIONS.** The UP-300 A/B may be used in virtually all unipole applications. However, where high power capability is required, or where electrically short antennas are to be fed, the UP-600 A/B is indicated. Special models are available for self-supporting and large cross-section towers.

## SINGLE FACE VIEW (ONE FOLD SHOWN)





Typical Impedance Curve  $\frac{1}{4}$  wavelength Tower.

### WHY THE FOLDED UNIPOLE?

- 1. EFFICIENCY.** The radiation model of the folded unipole configuration is an identity with that of the "series-fed" antenna. Therefore, the unipole gains efficiency from more effective matching and impedance transformation rather than modification of the radiation pattern. More optimum base impedances materially reduce losses in turning units and in marginal and deteriorated ground systems, increasing radiated field toward theoretical values.
- 2. BANDWIDTH.** Certain antenna configurations, although matched at carrier frequency, cause substantial mismatches at higher audio sideband frequencies. In such cases, the superior bandwidth of the folded unipole optimally matches the transmitter over the whole audio range, resulting in clear, sharp maximum modulation for better coverage and penetration.
- 3. LIGHTNING PROTECTION.** "Series-fed" antennas must rely on spark gaps to shunt lightning discharges to ground, frequently after equipment damage is done. During folded unipole installation, however, the tower is bonded directly to the ground radials with a heavy copper strap. This provided a direct lightning ground and a high level of protection to transmission gear.
- 4. ISOLATION.** Since the folded unipole equipped tower base is at RF ground potential, no lightning chokes, FM "Bazooka" sections, or two-way isocouplers are ever required. Instead, transmission lines and conduits are bonded directly to the tower. This makes it convenient for broadcasters to lease tower space for FM, two-way, and CATV antennas, or to improve their own system range with higher two-way or STL antennas.
- 5. EMERGENCY ANTENNAS.** The high effectiveness of the folded unipole in the absence of a good ground system indicates its use for standby antenna systems where a large tower and ground system is not economical.

### MECHANICAL ELECTRICAL DATA

	UP - 300 A/B	UP - 600 A/B
Frequency Range:	530 - 1600 KHZ	530 - 1600 KHZ
Power Rating:	10,000 Watts *	50,000 Watts *
Impedance Range:	10 - $300\Omega \pm j 200\Omega$ *	10 - $300\Omega \pm j 150\Omega$ *
Lightning Protection:	DC Ground	DC Ground
Windload (100 mph):	300 # (136 Kg) *	600 # (372 Kg) *
Download:	500 # (225 Kg) *	1000 # (450 Kg) *
Weight:	125 # (57 Kg) *	250 # (114 Kg) *
Insulation:	Epoxy - Fiberglass	Epoxy - Fiberglass

\* Typical  $\frac{1}{4}$  wavelength tower installation 1250 KHZ

### ORDERING INFORMATION

UP - 300 A/B (Note; "A" usually supplied 530 - 1200 KHZ, "B" from 1210 - 1600 KHZ,, subject to specific application)  
UP - 600 A/B

Specify: FREQUENCY, TOWER TYPE, TOWER HEIGHT, SPECIAL CONSIDERATIONS (FM ANTENNAS, CALL LETTERS, ETC.), COPY LAST ANTENNA GRAPH



LBA SYSTEMS, LTD.

DIVISION: LAWRENCE BEHR ASSOCIATES, INC.

P. O. Box 3313 - Greenville, N. C. 27834 - 919-758-4509

a 10 to 15 cps beat, is 1% or less. At 5:1 the error is about 1.3%, at 4:1 about 2.2%, and at 3:1 approximately 3.6%. Thus by applying these correction factors, reliable measurements can be obtained at ratios as low as 3:1.

In making these measurements, it is essential to mount the field meter on a tripod. It is also necessary to interrupt the carrier and to shift the frequency of the desired station only. It is not necessary to make any changes in the operation of the undesired station. I might point out that the error is always going to make readings higher than those in the absence of interference.

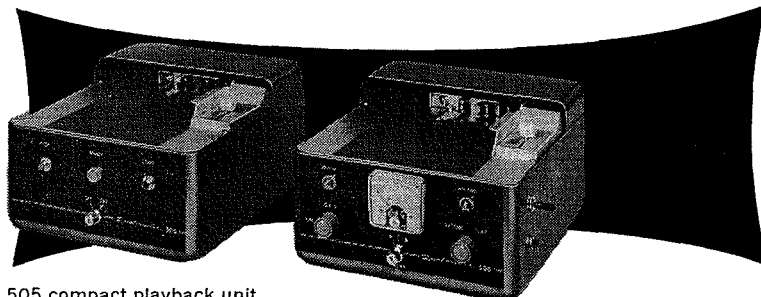
This idea is not new. Prior to World War II the FCC considered operating co-channel stations with slight carrier offsets to aid allocation. As mentioned above, this would eliminate the fading or beating of signals in the area between stations. However, since stability of crystal oscillators was not good enough at the time, this system was not incorporated into the Rules.

Among the uses of this technique are allocation measurements in areas where interference would be received; tune-up adjustments on directional patterns at night, during the experimental hours when sky-wave signals are present; measurements of Class IV stations service areas during heavy interference.

This technique is quite simple to employ. We set up the field meter at the edge of the interference zone. Then, by two-way radio or telephone adjust the frequency of the desired station transmitter until a very slow beat is observed on the field meter. At this point the two signals are almost synchronous. The operator notes the frequency deviation read on the frequency monitor at the station, and changes the transmitter frequency accordingly up or down 10 to 15 cps. At this point the needle on the field meter will stop swinging and a steady reading will be obtained. If a swinging or slight flutter is noticed during the day, the frequency of one of the two stations has probably shifted and the above steps can be repeated.

In summary, this technique is believed to be 100% reliable and has been verified by the author in both controlled tests and actual field work. ▲

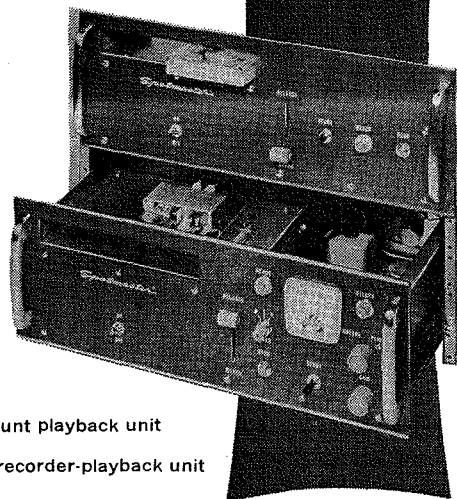
# The Standard of QUALITY



505 compact playback unit

500 compact recorder-playback unit

There's a lot of get-up-and-go packed into SPOTMASTER compact and rack mount cartridge tape recorders. Engineered for compactness, reliability and low maintenance—they do more work more efficiently than any other system. Whether your station is big and forward looking or—for now—just forward looking, write or call us, and ask about our complete line of SPOTMASTER cartridge tape equipment. For the Standard of Quality in cartridge equipment—ask for SPOTMASTER—more broadcasters around the World do.



505R rack mount playback unit

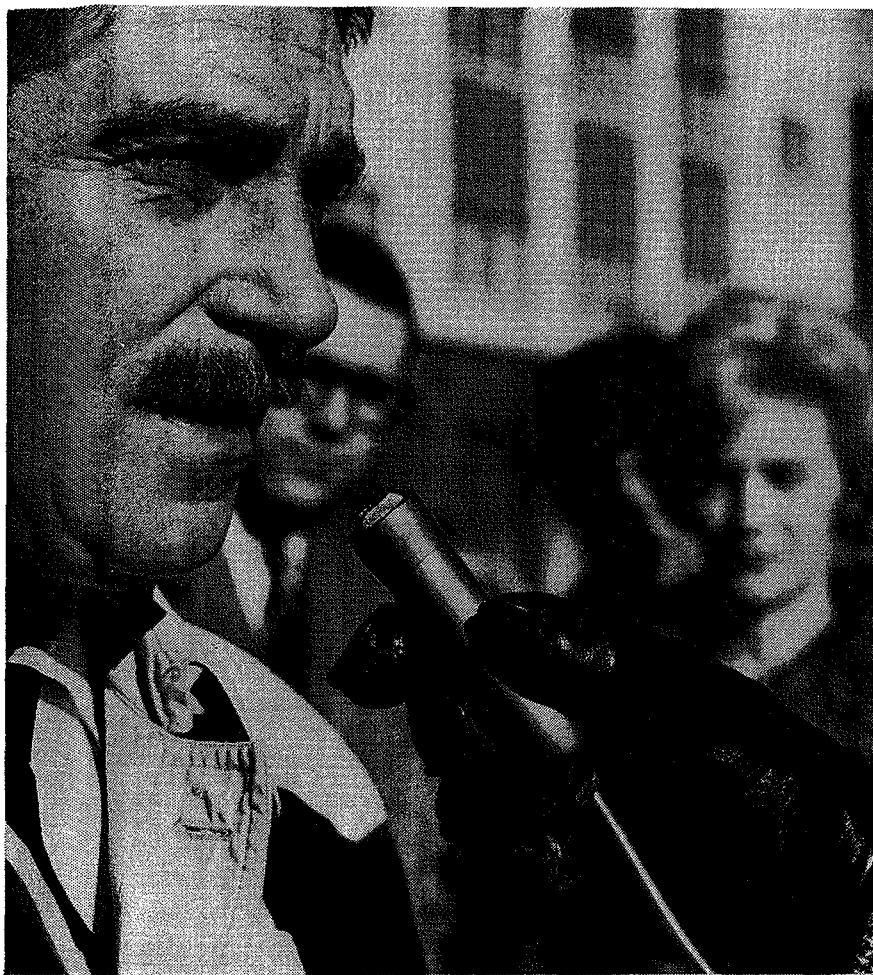
500R rack mount recorder-playback unit

## BROADCAST ELECTRONICS, INC.

8800 BROOKVILLE RD. SILVER SPRING, MARYLAND, JU 8-4983

SOLD NATIONALLY BY: **VISUAL ELECTRONICS**

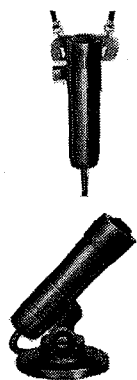
356 W. 40th St., N. Y., N. Y., CANADA • Northern Electric Co Ltd  
250 Sidney St., Belleville, Ontario.



## THE TURNER MODEL 58 STUDIO MICROPHONE

*For broadcasting excellence inside or outside the studio*

Designed for TV and broadcast use, the Model 58 has been specially engineered by Turner to withstand heat, rough handling and humidity. This modestly-priced microphone is rugged enough for sports remotes, studio or outside interviews, panel shows—anywhere freedom and mobility are required: yet it gives the quality performance you expect from stationary studio microphones.



The Model 58 is 4" long, weighs only 3½ ounces. Complete with lavalier; or it can be adapted to a desk or floor stand. Level (RETMA) -149 db. Response 60-13,000 cps. Allows a choice of either hi impedance or 150 ohms selected at the free end of the cable. Model 58A: combination 50 or 200 ohms selected the same way. Net price \$34.20. For complete specifications, write:



**THE TURNER MICROPHONE COMPANY**

909 17th Street N.E., Cedar Rapids, Iowa

IN CANADA: Tri-Tel Associates, 81 Sheppard Ave. West, Willowdale, Ontario.  
EXPORT: Ad Auriema, Inc., 85 Broad St., New York 4, N. Y.

Circle Item 16 on Tech Data Card

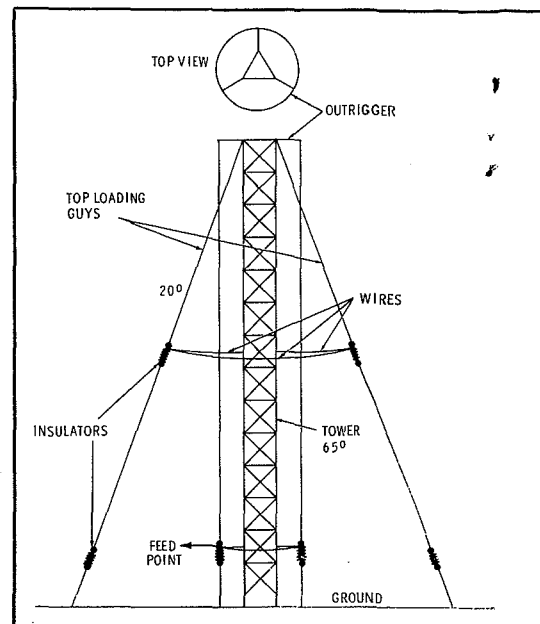


Fig. 2. Top-loaded folded unipole antenna.

### Q and Bandwidth

Probably, Q alone is not of great interest to the average engineer, although it does reflect the quality factor of the antenna. For a folded unipole, Q can be defined as:

$$\frac{F_o}{F_b}$$

where,

$F_o$  is the operating frequency in kilocycles,

$F_b$  is the bandwidth of the antenna in kilocycles.

Bandwidth, the difference in kc between the half-power points, can be calculated from:

$$BW = \frac{2R\alpha}{\frac{dx}{df}}$$

where,

$R_a$  is the antenna resistance,

$\frac{dx}{df}$  — is the reactance slope at resonance.

### Top Loading

The most effective combination is top loading with a folded unipole antenna. A very common practice in top loading (when it is not desired to build a bird cage or top-hat-ring) is to use the loading system at hand—the guy wires!

Fig. 2 shows a typical top loaded antenna. The three guys of the top section are connected directly to the tower with an insulator inserted at the desired distance down the guy loading wire. At the bot-

tom of this upper section a wire is connected to each guy, forming a complete ring around the antenna at the insulator height. This additional electrical length (to the height of the tower) produces higher efficiency. The effective height can be calculated as follows:

$$H^{\circ}eff = \frac{Lt^{\circ} + H\alpha^{\circ}}{0.705}$$

where,

$H^{\circ}eff$  is the desired effective electrical height,

$Lt^{\circ}$  is the chosen top loading,

$H\alpha^{\circ}$  is the existing tower height without top loading,

0.705 is an experimental constant.<sup>1</sup>

### Folded Unipole Impedance

From what has been said about the folded-unipole antenna, it may have become apparent that it is really a modified transmission line shorted at one end. This, in turn, indicates it is possible to tune the antenna with shorting bars. In practice, to resonate a folded unipole so that  $Z$  equals  $R$ , a fairly simple procedure is followed.

Under normal conditions when

no shorting bars are used, the folded unipole will reactance measure  $+j$ ; at resonance this will become  $j0$ . To achieve  $j0$  it is only necessary to measure the reactance and then attach shorting bars between the vertical wires and the tower, noting the new reactance value each time the bars are moved. If  $j$  becomes negative, you have placed the bars too far down; go up again until  $j$  equals zero. At this point the tower is in resonance for the operating frequency. This condition is known as **first resonance**.

An interesting aspect of folded-unipole antennas is the fact that because  $j$  is always zero at resonance the line current is an exact function of the power in the antenna; thus, the measured antenna resistance and indicated antenna current in the formula  $P = I^2R$  give accurate value of power.

In general, the gain in radiation efficiency obtained through the use of an antenna between  $65$  and  $120^{\circ}$  is not very great compared with the increased cost. However, one aspect of very short antennas (assuming the FCC Rules regarding minimum efficiency are met) is sometimes overlooked.

The shorter an antenna is, the lower its radiation resistance, and the higher its reactance becomes; at the same time bandwidth is relatively small.

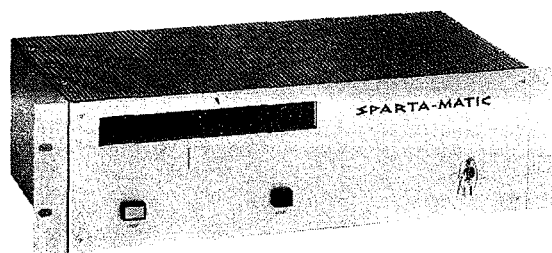
The problems involved in the use of very short antennas involve DC and RF losses. For example, if the antenna radiation resistance is low, it may become comparable to that of the ground system; so ground system losses approach the radiation obtained.

A very high antenna reactance requires an equally high reactance in the tuning unit. This results in an appreciable loss, and the radiating system dissipates valuable RF in an undesirable manner.

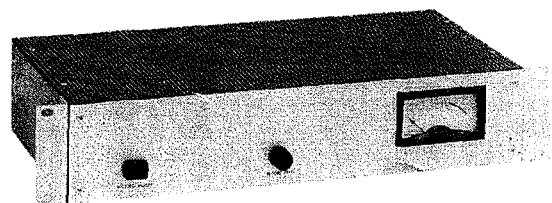
In the case of a folded unipole antenna, it is not unusual to have an antenna resistance and reactance of  $250$  ohms and  $j0$ . This simplifies the tuning problem, and results in an installation where the resistance of a less efficient ground system (and hence its losses) become very small with respect to the power radiated. ▲

<sup>1</sup>"The Folded Unipole Antenna for Broadcast Use," presented by John H. Mullaney at the 1960 NAB Engineering Conference.

## SPARTA-MATIC



300P — \$495.00



300R — \$230.00

### SETTING THE STANDARD FOR CARTRIDGE TAPE

The SPARTA-MATIC 300 series cartridge tape system is receiving enthusiastic acclaim by broadcasters everywhere! Offering outstanding improvements in all areas, the SPARTA-MATIC 300P playback unit and its companion 300R record amplifier, contain all the features you have been waiting for:

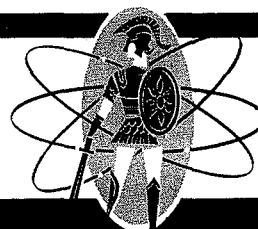
- Continuous Duty Rated
- Compact, Modern, Functional Design
- Laminated Tape Heads
- Proven Reliability
- Table Top, Custom or Rack Mounting (Rack Mounting Illustrated)
- Improved Tone Burst Cueing
- Plug in Relays and Modules
- Solid State Design

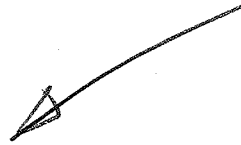
All this and much more is yours with the new leader . . . SPARTA-MATIC. Dependable quality that every broadcaster can afford. The sophisticate of cartridge tape: the SPARTA-MATIC 300 series.

Call, Write or Wire Today for Guaranteed Satisfaction Offer.

## SPARTA ELECTRONIC CORPORATION

6450 FREEPORT BOULEVARD • SACRAMENTO 22, CALIFORNIA • GA 1-2070





The Folded Unipole Antenna for Broadcast

Presented by: John H. Mullaney

Consulting Radio Engineer

Washington, D. C.

Tuesday, April 5, 1960

14th Annual NAB Engineering Conference

Chicago, Illinois

THE FOLDED-UNIPOLE ANTENNA FOR BROADCAST

I - INTRODUCTION:

This paper will discuss a method for reducing the physical height of an antenna system without seriously impairing its electrical characteristics. This will be accomplished by use of folded-unipole antenna theory. Present day techniques dictate that in order to reduce the physical size of an antenna system and still obtain a reasonable efficiency, inductive or capacitive loading be utilized in order to change the current distribution of the array. It will be shown that by grounding a vertical structure and folding back one or more conductors parallel to the side of the structure, it is possible to obtain a wide range of resonant radiation resistances by varying the ratio of the diameter of the folded back conductor in relation to the tower. It will also be shown that a top-loaded folded-unipole antenna can obtain a wide range of resonant radiation resistances and at the same time obtain a band-width many times greater than the same antenna without loading and use of the folded-unipole method of feed.

Series-fed vertical antennas are commonly used in standard broadcast service today. Some stations use a shunt-fed antenna, but the great majority are series-fed. The folded-unipole antenna could be called a modification of the standard shunt-fed system. Instead of having a slant wire leaving the tower at an angle of approximately  $45^{\circ}$  (as used for shunt-fed systems), the folded-unipole antenna has wires (one or more can be used) attached to the tower at a pre-determined height, supported by stand-off insulators, and run parallel to the sides of the tower to its base. The tower is grounded at its base--that is, no base insulator is used. These folds, or wires, are joined together at the base and driven at this point through an impedance matching network. Depending upon the type of folded-unipole antenna used, the wires may be connected to the tower at the top and/or at pre-determined levels along the tower (shorting stubs).

The folded-unipole antenna has the advantage of not requiring a base insulator, lightning chokes, or isolation transformers. It provides better protection against lightning, due to the fact that the antenna is grounded. In addition, the folded-unipole antenna, on a comparison basis, will develop a somewhat higher radiation efficiency, particularly for towers of the order of  $45^{\circ}$  to  $60^{\circ}$  high. The band-width for the folded-unipole antenna is also superior to that of a series or shunt-fed antenna system. The folded-unipole has an additional advantage over a series or a shunt-fed system in that it will operate with a much shorter ground system and still produce approximately the same effective field.

Basically speaking, a folded-unipole antenna can be visualized as a half-wave folded-dipole perpendicular to the ground and cut in half. The following discussion will briefly treat the theory of and results obtained from this type of antenna system.

II - THEORY OF FOLDED-UNIPOLE ANTENNA:

A - General:

To readily understand the folded-unipole antenna and its use in feeding a grounded tower, let's take a quick look at some basic transmission line

## II - THEORY OF FOLDED-UNIPOLE ANTENNA (CONTINUED):

### A - General (Continued):

theory. We know that a transmission line which is less than  $90^\circ$  in length and shorted at its far end will appear inductive at its input terminals. If this line is increased in length so that it equals a quarter wave, it will appear to be a parallel resonant circuit at its input. That is, it will appear to have very high impedance.

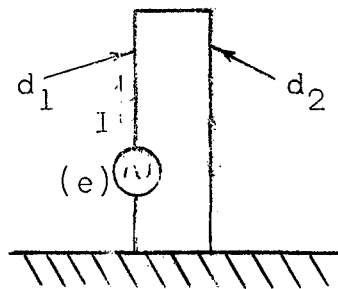


FIGURE 1

Figure 1 illustrates a one fold, folded-unipole antenna. In order to determine its input impedance, let us assume a generator voltage (e) and then find the current (I) flowing in the lower end of element  $d_1$  as illustrated in Figure 1. Roberts (Input Impedance of a Folded Dipole, R.C.A. Review, Volume 8, No. 2, June, 1947, W. Van B. Roberts) has outlined a method for analysis of a folded-unipole antenna. Figure 1 then becomes:

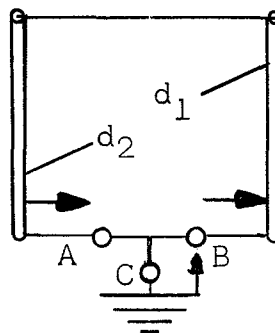


FIGURE 2

Referring to Figure 2, it should be noted that Generator A is opposing Generator C, with respect to the lower end of element  $d_2$ . Thus, element  $d_2$  is grounded so far as any voltage is concerned.



## II - THEORY OF FOLDED-UNIPOLE ANTENNA (CONTINUED):

### A - General (Continued):

Generators B and C impress a voltage,  $2E$ , on the lower end of element  $d_1$ ; therefore, Figure 2 is equivalent to Figure 1. Our reason for using three generators is that it is fairly easy to determine the current developed by each generator and then by the principal of superposition, add these currents to obtain the actual current in the lower end of element  $d_1$ .

Let's go a little further and first assume that there is no voltage (for the moment) in the lower generator. There is then only the voltage  $2E$  acting between the lower ends of  $d_1$  and  $d_2$ . Inasmuch as elements  $d_1$  and  $d_2$  form a  $90^\circ$  transmission line, shorted at the far end, their impedance is very high; consequently, only a small current will flow into element  $d_1$ . Next, assume there is voltage only in Generator C. Then, since the lower ends of  $d_1$  and  $d_2$  are shorted together (by the zero internal impedance of A and B), the two elements act as a simple  $90^\circ$  radiator made up of two elements connected in parallel. If  $R$  is the radiation resistance of this radiator, Generator C will supply a total current equal to  $E/R$  to this composite antenna, but by symmetry, this current divides equally between  $d_1$  and  $d_2$ , so that the current entering element  $d_1$  is:

$$I_1 = \frac{1/2 E}{R} \quad (1)$$

Thus, if Generators A, B and C are well working at once, the voltage impressed on element  $d_1$  is  $2E$ , while the current entering it is  $1/2 E/R$  plus a very small amount produced by Generators A and B working above. The input resistance of element  $d_1$ , being the ratio of voltage impressed to resulting current flow, is therefore approximately  $4R$ . If the two elements are close together, the value of resistance will be different from that of a single radiator, and the impedance multiplication due to folding is approximately four.

The impedance transformation can be expressed as follows:

$$\text{The impedance transformation} = \frac{Z_1}{Z_0} = (1 + n)^2 \quad (2)$$

Where:

$Z_1$  = input impedance of the folded-unipole antenna.

$Z_0$  = input impedance of a single antenna.

$n$  = current ratio  $\frac{I_2}{I_1} = 1$

Up to this point, we have discussed equal size conductors, that is the diameter of the tower and the fold is the same. However, with the introduction of the transformation ratio, as noted in (2) above, we are

## II - THEORY OF FOLDED-UNIPOLE ANTENNA (CONTINUED):

### A - General (Continued):

now prepared to discuss the operation of a folded-unipole antenna with unequal diameter conductors. Figure 3 illustrates the folded-unipole antenna with unequal size conductors.

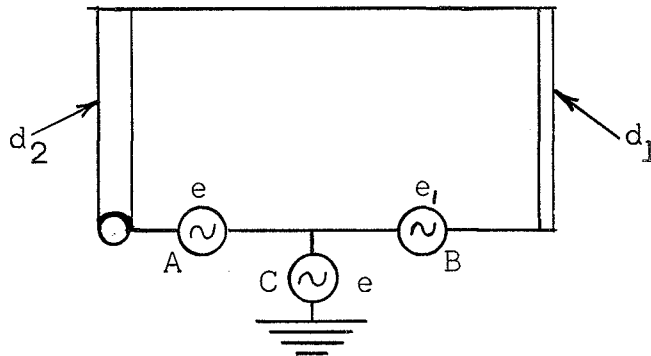


FIGURE 3

Generators A and C are alike in order to put zero voltage on element  $d_2$ , but Generator B must now be so chosen that no current will flow through Generator C when it is not producing voltage. The determination of this voltage ( $e_1$ ) is one of the two essentials to the solution of the problem. The other is to determine how the current produced by Generator C, acting above, divides between elements  $d_1$  and  $d_2$ . This problem becomes extremely complex because of the non-symmetry of the elements and there are several methods which can be used to solve the problem. "Guertler" (Impedance Transformation in Folded-dipole, Proceedings of the IRE, September 1950) demonstrates a method for determining this voltage. "Roberts" has also demonstrated methods for determining this voltage. We will use the electrostatic or capacitive method discussed by Roberts, since this method appears to offer the most promise for a simple solution. Briefly, this theory states that the current will divide directly as the ratio of the capacities of the elements, while the voltage ratio will be the inverse of the capacity ratio. To solve our problem then, we must assign undefined capacities,  $c_1$  and  $c_2$  to elements  $d_1$  and  $d_2$ . Then:

$$\frac{e}{e_1} = \frac{c_1}{c_2} \quad (3)$$

The current entering element  $d_1$  is the total current produced by Generator C acting alone multiplied by:

$$c_1 / (c_1 + c_2) \quad (4)$$

Neglecting the very small current produced by Generators A and B acting alone, as already discussed for equal elements, the total current due to Generator C alone is:

$$\frac{e}{R} \quad (5)$$

## II - THEORY OF FOLDED-UNIPOLE ANTENNA (CONTINUED):

### A - General (Continued):

Where R = radiation resistance of the two elements connected in parallel.

The driving point impedance of the antenna is:

$$\frac{(e + e_1)}{\text{the current entering } d_1} \quad (6)$$

Thus, it is readily proven that the driving point impedance is:

$$R \frac{(1 + c_2)^2}{c_1} \quad (7)$$

The above method of determination indicates that the impedance step up ratio depends upon the ratio of the elements' diameters, being inversely proportional to the diameter of the excited fold or element and directly proportional to the diameter of the grounded element. The spacing between the tower and fold is not extremely critical, but does determine, to some extent, the impedance transformation ratio. Although this type of antenna has good band-width, its band-width characteristics will be decreased if a transformation ratio of greater than approximately ten is attempted by means of the spacing ratio. It has been found that the best way to increase the band-width of the antenna is to increase the number of folds.

The electrostatic or capacitive method outlined by Roberts is primarily a physicist's approach to a solution of the folded-unipole antenna. It can be shown that the impedance transformation ratio for a folded-unipole antenna where unequal diameters are used is:

$$\text{Transformation ratio} = \frac{(1 + Z_1)^2}{Z_2} \quad (8)$$

Where:

$Z_1$  = the characteristic impedance of a transmission line made up of the smaller of the two conductor diameters spaced the center to center distance of the two conductors in the antenna.

$Z_2$  = the characteristic impedance of a transmission line made up of two conductors the size of the larger of the two.

The above equation assumes that the power will be fed to the smaller conductor (fold). That is, the feed line from the transmitter is connected in series with the fold (fold's diameter always assumed smaller than tower's) so that an impedance step-up of greater than four will be achieved.

The magnitudes for  $Z_1$  and  $Z_2$  of equation (8) for uniform cross-section conductors can be determined from standard transmission line formulas.

## II - THEORY OF FOLDED-UNIPOLE ANTENNA (CONTINUED):

### A - General (Continued):

During the last five years, numerous experimental measurements have been made on different types of folded-unipole antennas for broadcast use. Our experience indicates that the average height of a non-directional broadcast antenna will vary somewhere between 150 and 300'. Inasmuch as the change in frequency from the low end to the high end of the broadcast band is approximately three to one and if we assume that the height of the broadcast antenna is not higher than 90° and six driven folds are used on the tower without any shorting stubs, the following empirical expression may be used to obtain the impedance of a folded-unipole antenna:

$$Z_{fu} = 3.6 (Z_{11}) \quad (9)$$

Where:

$Z_{fu}$  = base impedance of the folded-unipole in ohms.

$Z_{11}$  = base self-impedance in ohms for the tower height under consideration.

3.6 = empirical constant determined from measurements.

Equation (9) assumes that the folded-unipole antenna is approximately 90° and has not been resonated by use of shorting stubs. (that is, wires connected between each of the folds to the tower at pre-determined levels, based on impedance measurements at the base of the tower).

In normal practice, it is desirable to resonate the folded-unipole antenna by means of shorting stubs. These stubs are actually short circuits connected between each of the folds to the tower at some point below the top of the tower. The actual location for these shorting stubs must be determined experimentally. To do this, first measure the tower with the shorting stubs at the very top. Then have a tower rigger move the shorting stubs down until  $j0$  is measured at the base. It should be noted that a folded-unipole antenna will initially measure  $+j$ . Consequently, if the shorting stubs are moved down the tower too far, the measured reactance sign will change to a minus, indicating that the antenna has gone through resonance. Hence, this means that the shorting stubs should be moved up until  $j0$  is obtained. This condition is theoretically referred to as first resonance. At resonance,  $Z = R$ ; hence, the following empirical expression may be used for obtaining the resistance of a folded-unipole antenna at first resonance:

$$Z_{fu} = 7.3 (R_{11}) \quad (10)$$

Where:

$Z_{fu}$  = base impedance or resistance for folded-unipole at first resonance (ohms).

$R_{11}$  = self-base resistance of tower (ohms)

7.3 = empirical constant determined from measurements.

### III - PRACTICAL ASPECTS OF FOLDED-UNIPOLE ANTENNAS:

So far, we have discussed how to determine the impedance for a folded-unipole antenna, assuming it had six folds, but no information has been given with regard to the practical construction of this type of antenna. Equations (9) and (10) were developed from measurements of what we call our standard broadcast folded-unipole antenna.

Figure 4 is a top view of a uniform cross-section, guyed tower rigged for a six wire folded-unipole antenna.

Figure 5 is a drawing indicating the details of the fold attachment at the tower's base.

Figure 6 is a detail drawing of the cross-arms or spider.

Figure 7 is a bill of materials for a typical folded-unipole antenna installation on a uniform cross-section guyed tower.

Figure 8 is a plot of impedance measurements obtained on a 200' tower with six folds at 1570 KC. This tower is 0.319 wave lengths or approximately 115° high and would be expected to have a self-impedance ( $Z_{11}$ ) of 155 j260; however, when it is converted to a folded-unipole antenna and the folded-unipole shorting stubs have been adjusted to obtain j0 or resonance at the base, the resistance is multiplied up to 1,170 ohms. This is a transformation ratio of 7.55. In order to transform this impedance to 50 ohms j0 (transmission line impedance), an "L" or "T" type of network may be used. We prefer to use a modified version of an "L" network (See Figure 10) and treat the transmission line resistance as a series resistance of a parallel network at resonance.

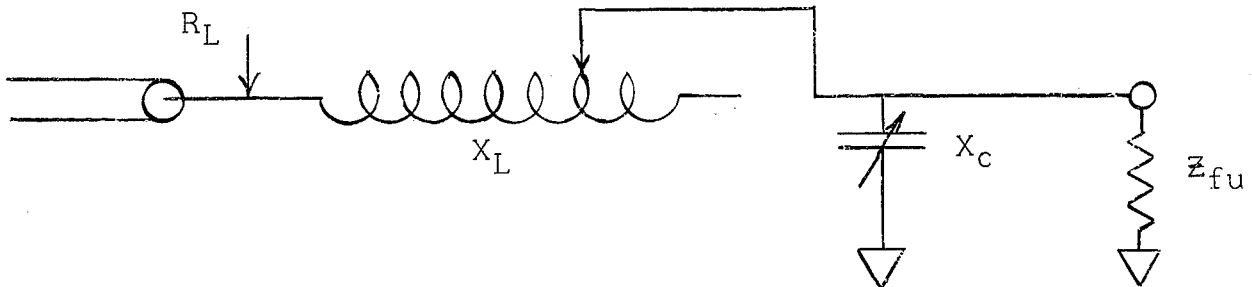


FIGURE 10  
(Schematic of "L" type impedance transforming network)

The following formulas may be used to determine  $X_L$  and  $X_C$  for an "L" network:

$$Z_{fu} = \frac{X_L}{R_L} + R_L \quad (11)$$

$$X_C = X_L + \frac{R_L^2}{X_L} \quad (12)$$

$$X_L = \sqrt{(R_L Z_{fu}) - (R_L)^2} \quad (13)$$

The following data furnishes complete information for the construction of a typical standard broadcast folded-unipole antenna.

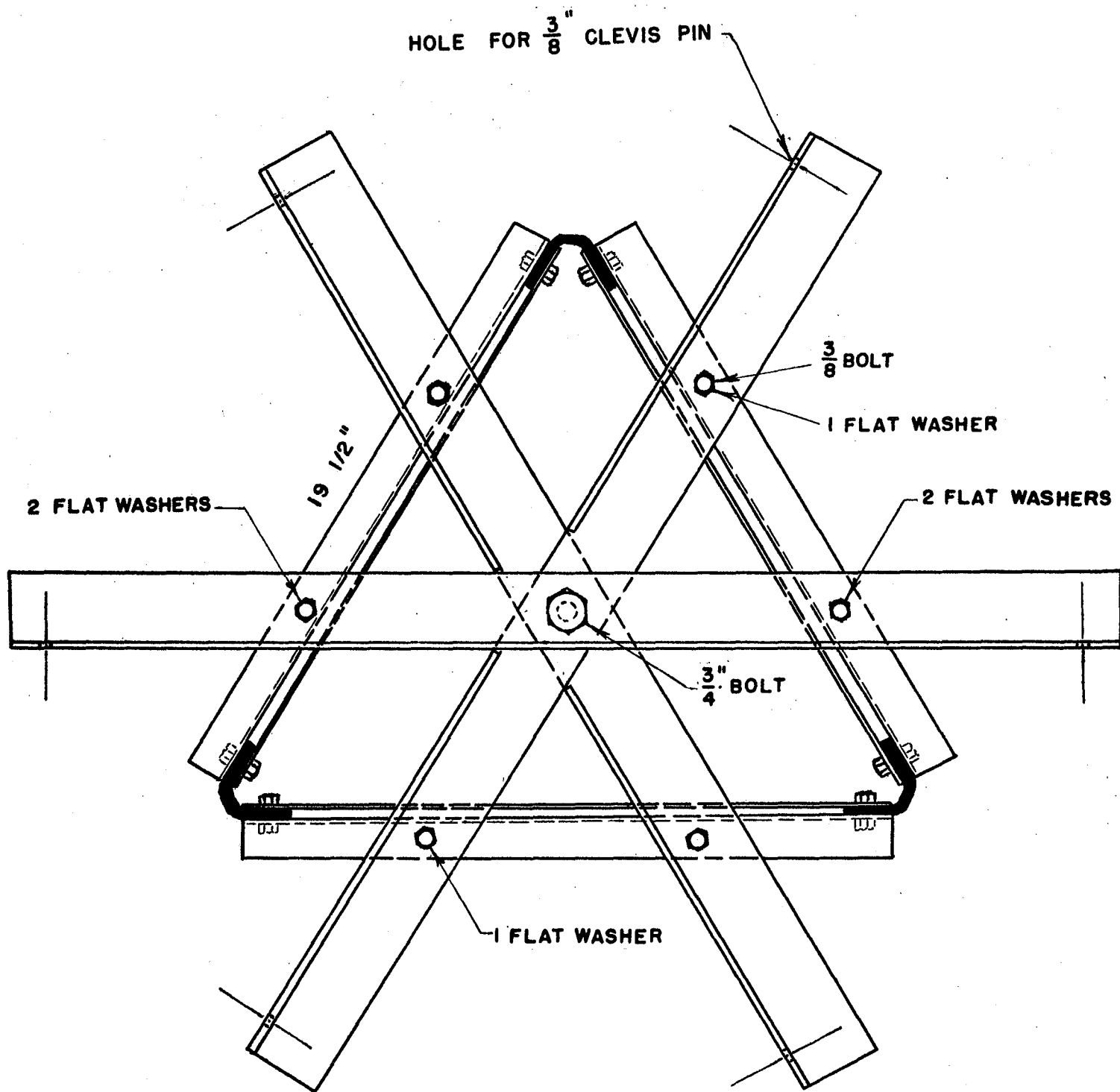


FIGURE 4

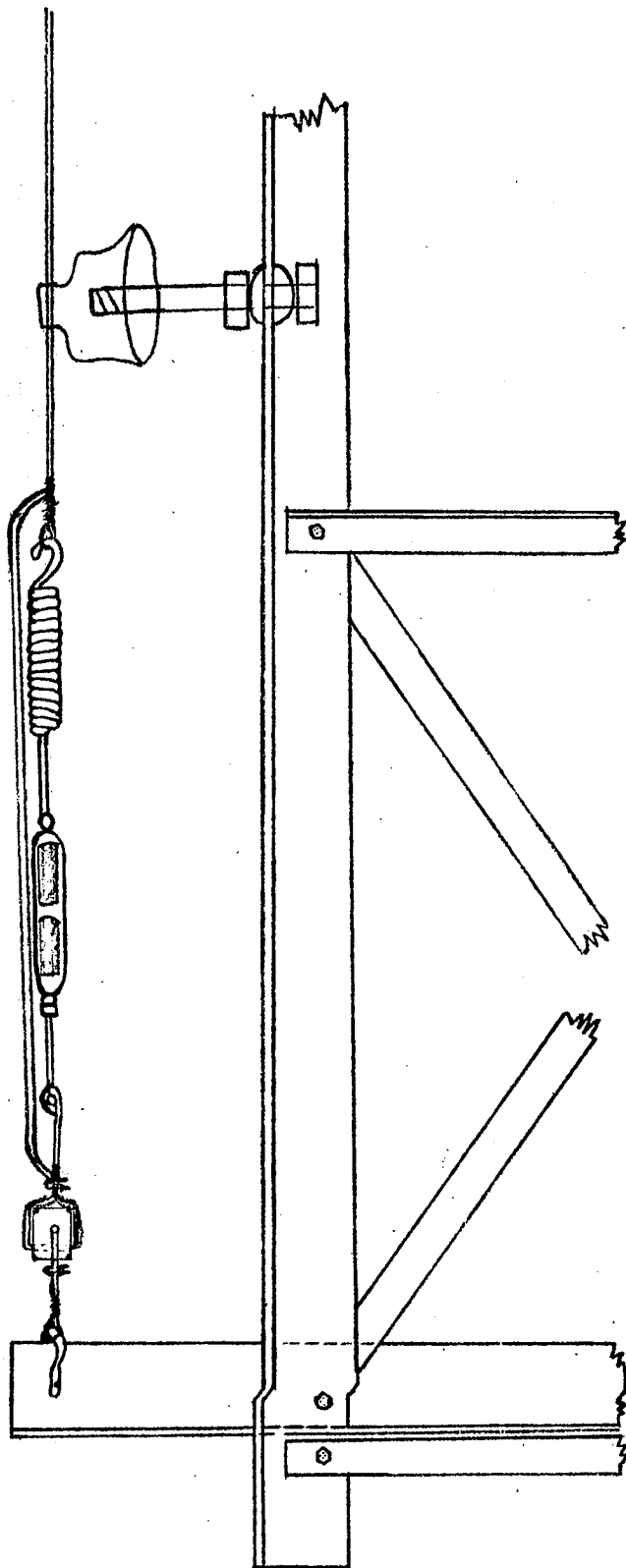
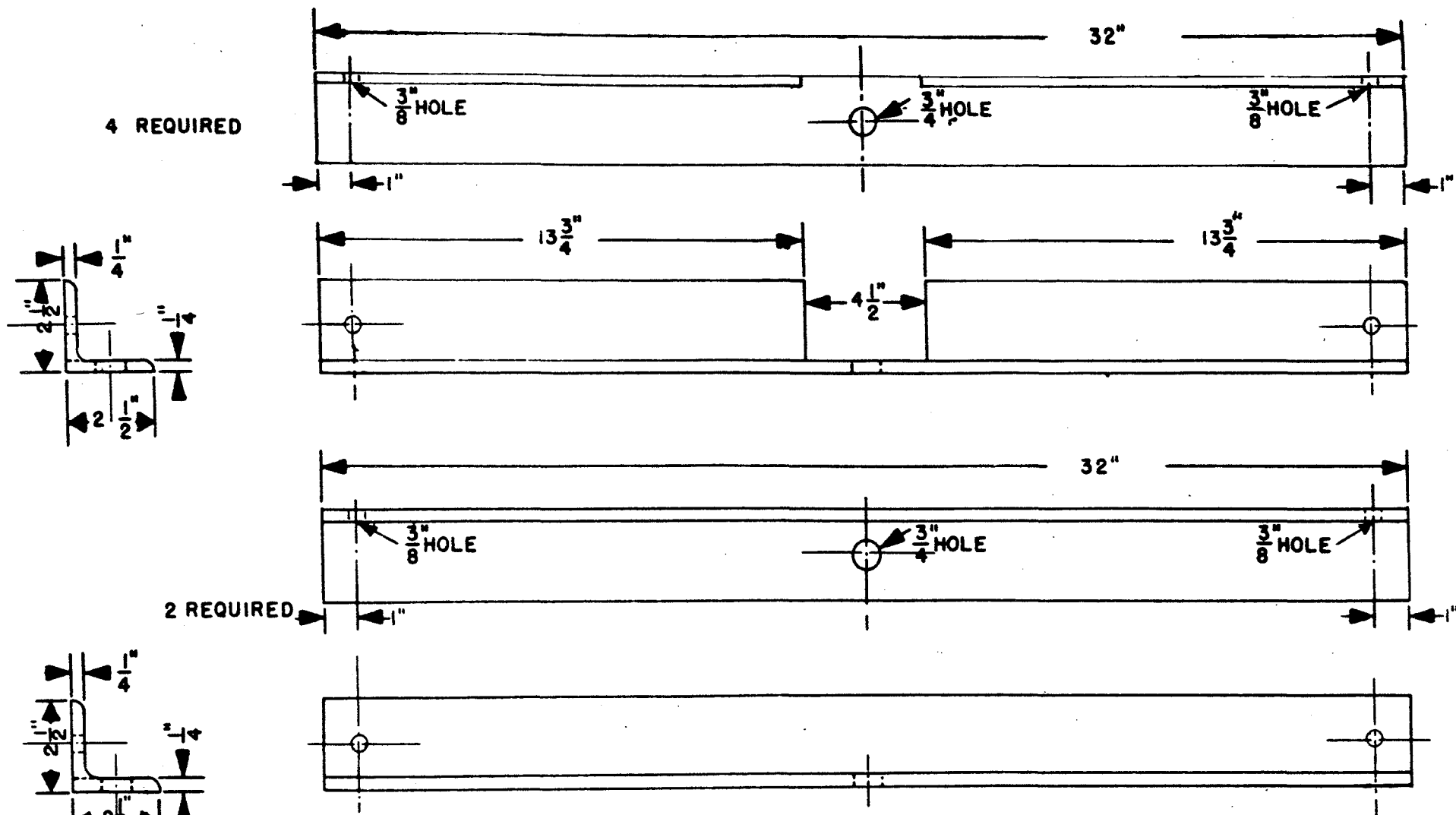


FIGURE 5  
DETAILS OF FOLD  
ATTACHMENT AT TOWER BASE



NOTE: OVERALL LENGTH IS  
FOR TYPICAL GUYED  
TOWER. LENGTH MAY  
VARY DUE TO CROSS  
SECTION. HOLE SIZES  
ARE STANDARD.

FIGURE 6



FIGURE 7

BILL OF MATERIALS FOR FOLDED-UNIPOLE ANTENNA INSTALLATION  
FOR UNIFORM CROSS-SECTION GUYED TOWER

1. 6 pieces of angle iron (Figure 6).
2. 2 each 3/4" x 1 3/4" bolts and 2 lock washers.
3. 12 each 3/8" x 1 1/2" bolts and 12 lock washers.
4. 12 flat washers 7/16" I.D. maximum O.D.
5. 12 each 3/8" Clevis Shackle.
6. 6 turnbuckles 1/2" bolts or larger.
7. 3 pieces of copper strap 6" wide (long enough to ground antenna at base).
8. 24 wire clamps suitable to attach shorting straps to antenna (aluminum deadend clamps).
9. 6 folds - #4 NCSR, stranded aluminum wire - total length equal to 6 times tower's height plus 25' additional.
10. 6 egg type strain insulators - to insulate folds at base of antenna 3" diameter or better.
11. 36 stand-off insulators (placed at 30' intervals on tower adjacent to folds) (Jocelyn Cross Arm Pin and 15 KV Insulator).
12. 1 variable vacuum capacitor 10/1000 uuF or equivalent 15 KV, 45 amperes (suggest Jennings type).
13. 1 variable inductor 0/60 microhenries - appropriate to handle 1 KW power (suggest Gates, Johnson, or Multronics type coil).
14. 6 springs 4" - 6" long.
15. 1 Weston or equivalent R.F. ammeter 0-6 amps (for 1 KW installations).
16. 1 remote antenna ammeter unit.
17. Tuning unit cabinet with bowl feed thru for output connection.
18. Miscellaneous:

Solder, brazing rod and torches, flux, polyethelene tape, hand tools, and small parts to mount inductor and variable capacitor. Also needed to facilitate the measurements, adequate extension lights and a rough support for the measuring equipment to provide access to the antenna tuner unit.

Note: All hardware to be galvanized or painted with aluminum paint. Dissimilar metal clamps recommended for use between tower and aluminum wire.

### III - PRACTICAL ASPECTS OF FOLDED-UNIPOLE ANTENNAS (CONTINUED):

Where:

$Z_{fu}$  = measured base impedance of folded-unipole at resonance (ohms).

$R_1$  = transmission line impedance (ohms).

$X_1$  = reactance of series coil (ohms).

$X_c$  - reactance of shunt condenser (ohms).

Using the above formulas, a modified L network was used to match the impedance shown in Figure 8. Figure 9 is a plot of coupling impedance obtained for this antenna system.

In order to determine the current in the antenna, an ammeter may be placed in either the transmission line output (input to modified L network) or the output of the network (input to the folded-unipole) or at both locations for determining power. The F.C.C. will allow the meter to be placed at either location and to be used for direct measurement of power. Where a folded-unipole antenna is operated at first resonance, it is recommended that the antenna ammeter be placed in the input to the network so that a larger scale ammeter can be used. It should be noted that inasmuch as the antenna is adjusted to  $j0$ , line current is a true indication of power.

Figure 11 is a plot of the measured resistance and reactance for a folded-unipole antenna (resonated) which is  $70^0$  in height at 800 KC. This antenna would be expected to have a base impedance (when measured without folded-unipole rigging) of  $31 + j9$ . Examination of Figure 11 shows that this antenna (folded-unipole rigged and resonated) has a feed point impedance of  $230 \pm j0$ . An impedance match from 50 ohm line to this impedance can be readily obtained by use of an "L" or "T" coupling network.

### IV - CURRENT DISTRIBUTION ON A FOLDED-UNIPOLE ANTENNA:

During the writer's experiments with folded-unipole antennas in 1949 and 1950 for the United States Air Force, it was determined by measurement that the current distribution on a folded-unipole antenna is the same as that of a base insulated antenna of identical height. D. L. Waidelech has proven ("General Folded-dipole Antenna Design", Communications, April 1949) that the current distribution on a folded-dipole antenna is the same as that of a simple dipole antenna. Inasmuch as a folded-unipole is basically  $1/2$  of a folded-dipole antenna, it follows that the current distribution of a folded-unipole would be the same as that of a simple unipole. Further, Schelkunoff (Antennas "Theory and Practice", Wiley) has shown that the current distribution for a folded-dipole is the same as that of a simple dipole of similar length.

Numerous field intensity measurements have been made during the last five years on folded-unipole antennas to determine their current distribution and effective  $E_{rms}$ . Measurements have been made on series-fed antennas before converting to folded-unipole and then comparison measurements made to demonstrate that the current distribution and effective fields are similar for both antennas. It can therefore be concluded that the current distribution of a folded-unipole type of antenna will be the same as that of a simple base insulated series-fed antenna.

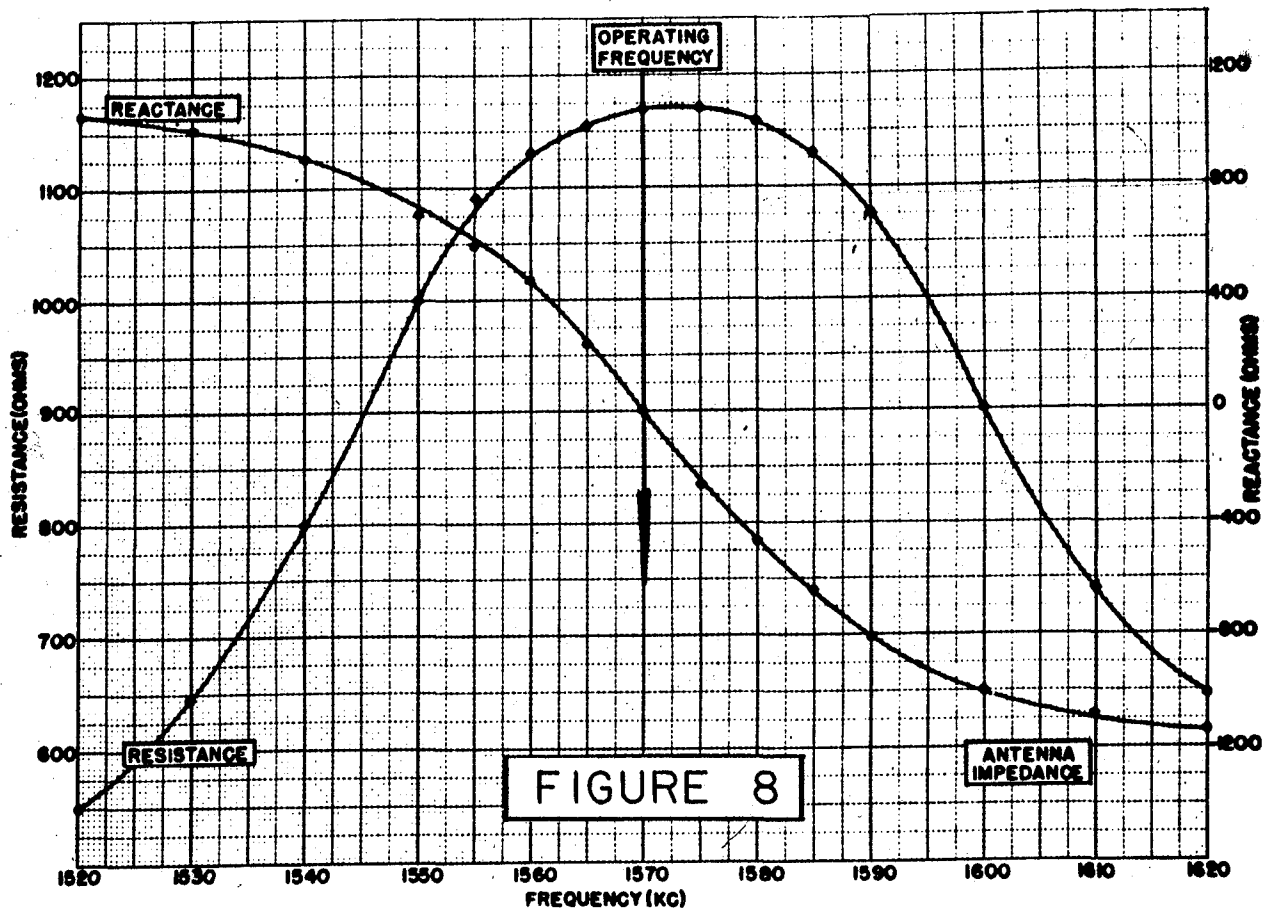


FIGURE 8

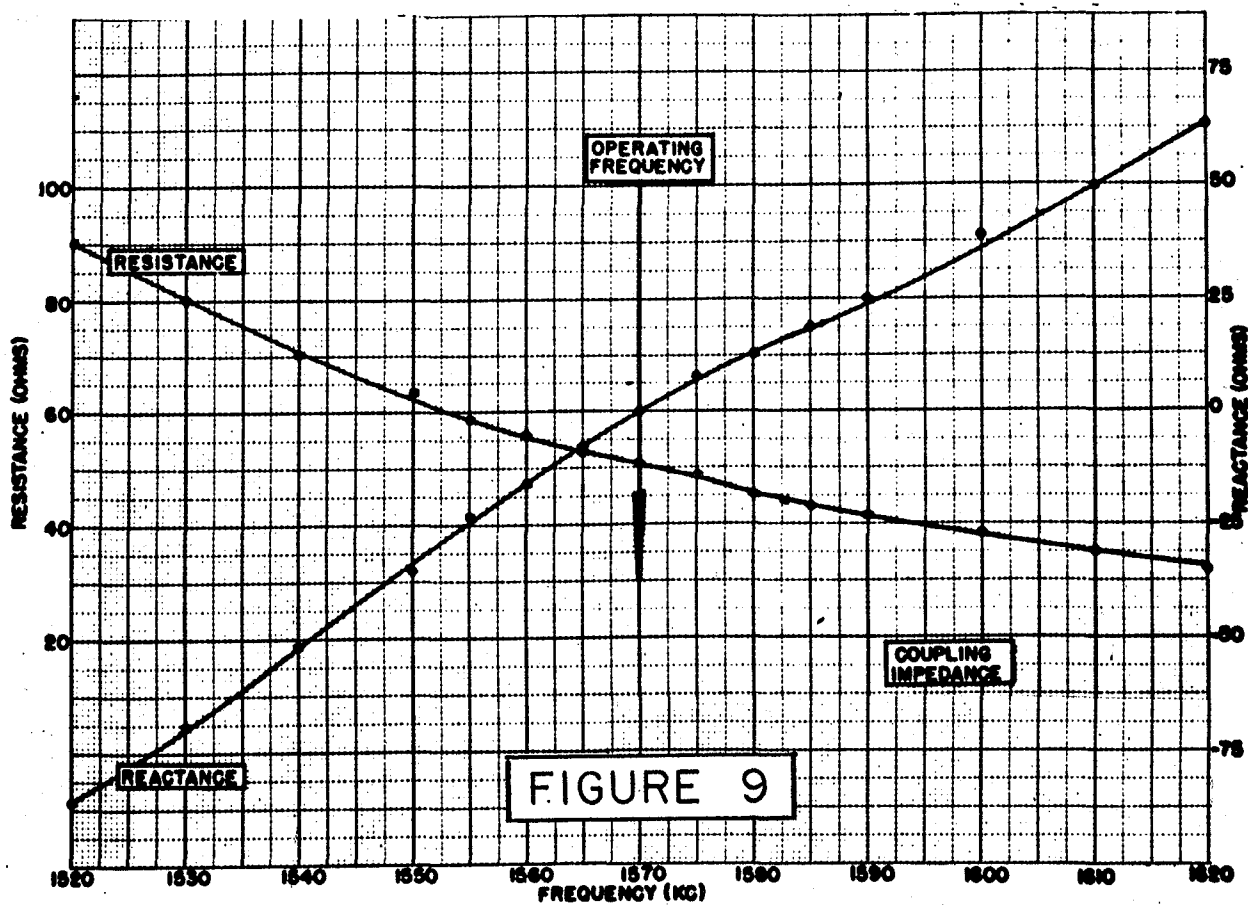


FIGURE 9

## V - BAND-WIDTH CONSIDERATIONS:

The band-width of an antenna depends upon its base impedance and the rate with which its reactance changes with frequency. The band-width is considered to be the frequency band within which the power is equal to or greater than one-half the power at resonance. Expressed in equation form:

$$\Delta f = \frac{2R_a}{\frac{dx}{df}} \quad (14)$$

Where:

$\Delta f$  = band-width in kilocycles between half-power points.

$R_a$  = measured antenna resistance in ohms.

$\frac{dx}{df}$  = slope of reactance curve at resonant frequency.

The effective band-width will be doubled when the generator is matched to the antenna circuit. The Q of a folded-unipole antenna can be determined from the equation:

$$Q = \frac{f_o}{\Delta f} \quad (15)$$

Where:

$f_o$  = operating frequency in kilocycles

$\Delta f$  = band-width of antenna in kilocycles

Our experiments indicate that a folded-unipole antenna has a much more desirable band-width characteristic than an equal height series-fed antenna.

## VI - TOP-LOADED FOLDED-UNIPOLE ANTENNAS:

For very short towers, advantage may be taken of top-loading to increase the effective height of a folded-unipole antenna.

Our experience indicates that the simplest and most effective means for top-loading a folded-unipole antenna is to connect the top three guy wires to the tower, adjust them to a given physical length and then inter-connecting them at the lower end to simulate a pyramid. Experimental data indicates that the following expression can be used to compute the length of guy wires necessary to obtain a given amount of top-loading:

$$G_{eff}^0 = \frac{TL^0}{0.705} + G_{11}^0 \quad (16)$$

Where:

$G_{eff}$  = desired electrical tower height in degrees.

$TL^0$  = desired top-loading in degrees

$G_{11}$  = electrical height of tower without top-loading in degrees.

VI - TOP-LOADED FOLDED-UNIPOLE ANTENNAS (CONTINUED):

0.705 = empirical constant.

Figure 12 is a plot of the measured resistance and reactance for a folded-unipole antenna (resonated) which is 69.5° in height at 1000 KC and has been top-loaded an additional 15.5° to given an electrical height of 85°. This antenna would be expected to have a base impedance of 39 +j40 (when measured without folded-unipole rigging but with top-loading). Figure 12 shows that this antenna (folded-unipole) rigged and resonated) has a feed point impedance of 350 ± j0. An appropriate impedance transformer should be used to match this antenna impedance to a transmission line.

VII - SECOND RESONANCE FOR FOLDED-UNIPOLE ANTENNAS:

A folded-unipole antenna can obtain a wide range of resonant radiation resistance by varying the ratio of the diameters of the folded conductors to the diameter of the tower. The radiation resistance varies as the square of the height and if the transformation ratio is raised enough, the height of the antenna can be reduced, the limit being the point where ground losses consume a prohibitive percentage of the power.

For practical operation a short antenna should have a resistance of at least 50 ohms. Unfortunately short series-fed antennas in the range of 45° to 60° do not approach this value; consequently, this type of antenna has excessive losses. In these ranges, the use of a top-loaded folded-unipole antenna is extremely desirable, inasmuch as these antennas can be operated at first or second resonance. For second resonance, a top-loaded folded-unipole has a length of approximately one-half that of a folded-unipole at first resonance. This is the same as saying that if a folded-unipole antenna had a length of approximately 90° (electrical), we would expect second resonance to occur at approximately one-half this length or 45°. The base impedance for a top-loaded folded-unipole antenna at second resonance can be expressed as:

$$R_{2r} = 1580 \left[ \frac{h_{2r}}{2r} \times \frac{\log 4S^2/d_1 d_2}{\log 2S/d_2} \right]^2 \quad (17)$$

Where:

$R_{2r}$  = resistance of folded-unipole at second resonance (ohms).

$h_{2r}$  = height at second resonance.

$2r$  = wavelength at second resonance (same units as  $h_{2r}$ ).

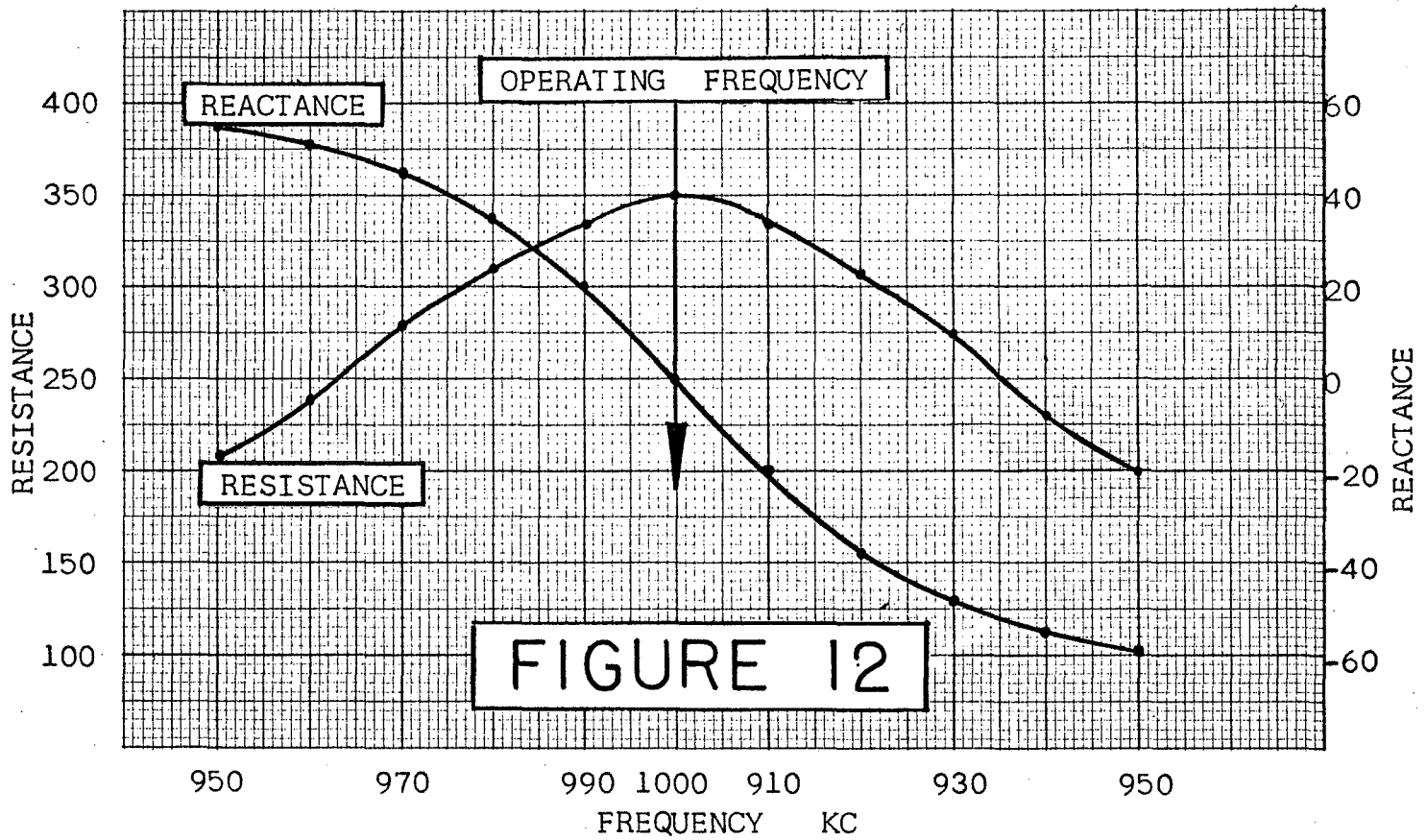
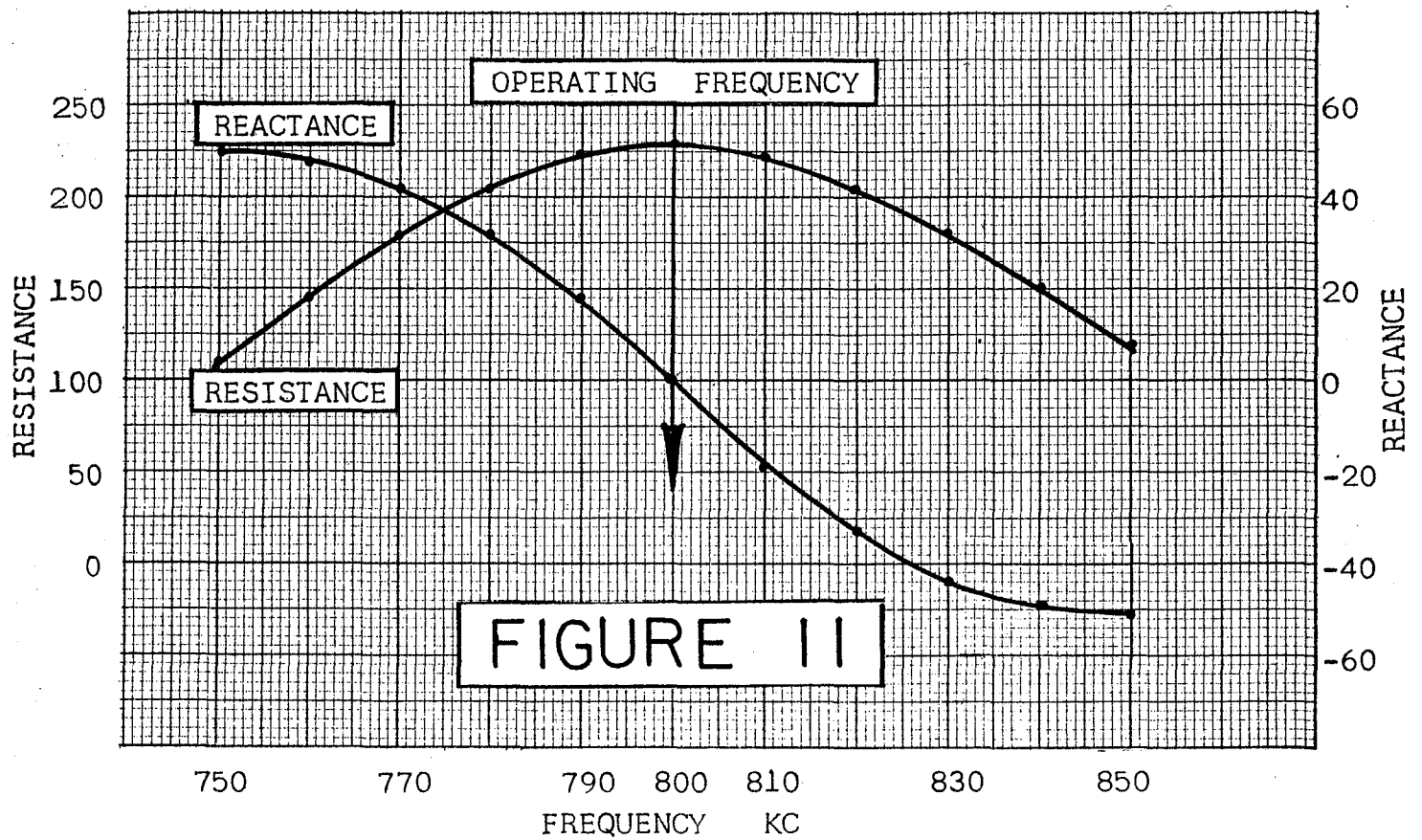
$S$  = spacing, center to center, of tower to fold.

$d_1$  = fold diameter.

$d_2$  = tower diameter.

$S$ ,  $d_1$  and  $d_2$  should be expressed in the same units.

It should be noted that "log<sub>10</sub>" or "log<sub>e</sub>" can be used, inasmuch as a ratio is expressed in equation (17).



VII - SECOND RESONANCE FOR FOLDED-UNIPOLE ANTENNAS (CONTINUED):

It should be noted that the operation of a folded-unipole at second resonance is similar to that at first resonance; however, the ratio of the diameter of the folds to the tower's diameter and the spacing is much more critical.

VIII - UNATTENUATED FIELD INTENSITY:

It has been observed experimentally that a folded-unipole antenna will develop a higher unattenuated field intensity than the same equivalent height series-fed antenna system. The increase in field intensity varies between approximately two to ten percent. The greatest increase in field intensity is experienced on short antennas in the range  $45^{\circ}$  to  $75^{\circ}$ .

IX - ACKNOWLEDGMENT:

The author wishes to express his appreciation to Peter V. Gureckis, Milton A. Chambers, Harold B. Rothrock, John R. McKenna and the entire Mullaney engineering staff for their assistance in preparing this paper.

# Static voltages on the guy insulators of m.f. and l.f. broadcast tower antennas

Professor J. V. SURUTKA, D.Sc.\*

and

D. M. VELIČKOVIĆ, D.Sc.†

## SUMMARY

A new approximate method for calculating the static voltages on the guy insulators of m.f. and l.f. broadcast tower antennas is given. The method is based on an integral-equation technique, where the integral equation is solved by the so-called point matching method; the unknown charge densities are approximated by polynomials. The polynomial expansion provides very significant advantages, primarily because it leads to the integrals in closed form, and because it requires a very low order of polynomial. A numerical example is given to illustrate the method.

\* Department of Electrical Engineering, University of Belgrade, PO Box 816, 11001 Belgrade, Yugoslavia.

† Department of Electronics, University of Niš, 18000 Niš, Yugoslavia.

## 1 Introduction

The overcrowding of medium and low frequency bands and resulting interference in the European broadcasting area often force broadcasting organizations to increase the powers of their transmitters and powers of the order of 1000 kW are not infrequent both in Europe and in neighbouring countries. In this connexion the problems concerning the voltages and insulating material of broadcast tower antennas as well as the methods of calculating these voltages are becoming again of growing importance.

The first thorough study of radio-frequency voltages appearing on the insulators of guy ropes was made in 1939 in the classical paper by Brown<sup>1</sup>. Though the voltages resulting from the electrostatic field during thunderstorms have not been theoretically treated in Brown's paper, he pointed to these voltages as a cause liable to produce sparks across the guy insulators. Once the static voltage has broken the gap, the r.f. voltage maintains the arc even if it were much less than the voltage required to start the arc. In order to overcome these difficulties Brown proposed the use of high-resistance leaks across the guy insulators which could clear up all troubles due to the static charge. However, according to widespread experience, a direct or near stroke of lightning may destroy the leak resistors entirely. At any rate, a quantitative knowledge of the static voltages and the methods for their determination deserve to be investigated.

In a recent paper Bruger<sup>2</sup> has given an interesting method for calculating both the r.f. and static voltages on the guy insulators. As stressed by the author himself, in this method emphasis was laid on the clarity and easy applicability, instead of on extreme precision.

The purpose of the present paper is to develop a more accurate, but conceptually simple method for calculating the static voltages on the guy insulators. Essentially, the method is based on an integral equation technique, where the integral equation is approximately solved by the so-called point-matching method.<sup>3</sup> The unknown sub-integral functions, representing in the present case the charge densities per unit length of conductors, can be approximated by functional series of convenient functions with unknown coefficients. In this paper, however, a polynomial approximation is adopted. Besides the conceptual simplicity, the polynomial expansion offers very significant advantages in the necessary computational work on the electronic computer. Apart from the fact that the true distribution function can be well approximated by a low-order polynomial, the polynomial approximation leads to integrals which, by means of the recurrent formulas, can be reduced to elementary integrals.

## 2 Static Field in the Vicinity of the Antenna Tower

Most of the m.f. and l.f. transmitting antennas are built in the form of guyed steel towers of uniform cross-section. For the purpose of analysis they can be approximated by cylinders<sup>4</sup> of equivalent radius  $a$ . The supporting guy wire-ropes are broken up at several points by insulators. In addition to the r.f. voltages induced in the guy sections, before and during thunderstorms, the



insulators are exposed to high quasi-static voltages produced by very strong atmospheric electric fields. For the sake of simplicity we assume that this field is static and, in the absence of the antenna tower, is homogeneous having a vertical field strength  $E_0$ .

As the first step in determining the static voltages on the guy insulators, the resultant field in the vicinity of the tower has to be calculated. In this calculation, the presence of the guys could be ignored, because induced charges on them are too small to affect appreciably the charge distribution along the tower. The validity of this assumption will be checked numerically in Section 4. Since the base of the antenna tower is earthed through the static drain coil, the tower is at the static potential of the ground, which is taken as a reference. In order to avoid dealing with an infinite ground plane, the method of images will be used. So, the ground plane is replaced by the electrical image of the cylinder representing the antenna tower. Both the antenna cylinder and its image, with height  $h$  and radius  $a$ , are shown in Fig. 1. The  $z$ -axis of cylindrical co-ordinates  $r, \phi, z$ , coincides with the axis of the cylinders.

Let the unknown charge density per unit length of the antenna cylinder be denoted by  $q(z)$ . According to the method of images the following symmetry condition must be fulfilled:

$$q(-z) = -q(z). \quad (1)$$

If we denote

$$\phi_0 = -E_0 z \quad (2)$$

the scalar potential of the unperturbed atmospheric electric field and by  $\phi_i$  the scalar potential created by the induced charges on the antenna, the initial equation expressing the boundary condition for potential has the form

$$\phi_0 + \phi_i = 0 \quad \left|_{r=a, -h \leq z \leq h} \right. \quad (3)$$

Since  $h \gg a$ , in calculating the potential  $\phi_i$  at a point  $P(r \geq a, z)$  it can be assumed that the induced charges are localized on the axis of the cylindrical conductor. So, we have

$$\phi_i = \frac{1}{4\pi\epsilon_0} \int_{-h}^h \frac{q(z') dz'}{\sqrt{r^2 + (z - z')^2}}. \quad (4)$$

Introducing equations (4) and (2) into equation (3), and taking into account the symmetry condition (1), we obtain the fundamental integral equation in the form

$$\int_{-h}^h \frac{q(z') dz'}{\sqrt{a^2 + (z - z')^2}} - \int_0^h \frac{q(z') dz'}{\sqrt{a^2 + (z + z')^2}} = 4\pi\epsilon_0 E_0 z. \quad (5)$$

This equation is automatically satisfied for  $z = 0$ .

Solving equation (5), the unknown charge distribution can be determined and, consequently, the resultant potential is

$$\phi = \phi_0 + \phi_i. \quad (6)$$

Although an exact method for solving equation (5) does not exist, there are several methods for solving it approximately. A simple, but very general approximate method is the above mentioned point-matching method. According to this method the unknown charge distribu-

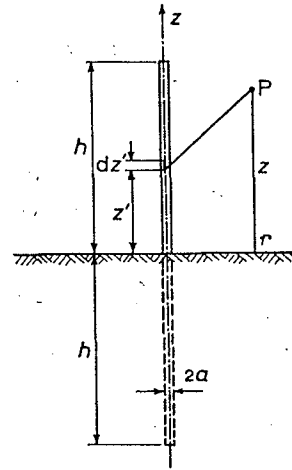


Fig. 1. Cylinder representing the antenna tower and its image.

tion can be approximated by a finite functional series with unknown coefficients. These coefficients can be determined by satisfying the integral equation at a sufficient number of points along the conductor. Though the basic functions in the form of rectangular and triangular pulses are in common use, we will choose the polynomial series. In solving equation (5) the polynomial series have an outstanding advantage because they lead to the integrals which are reducible to the elementary ones. On the other hand, polynomials of relatively low order approximate the charge distribution in a very satisfactory manner. So, using polynomials, both the number of integrals and, especially, the computation time for their evaluation are extremely favourable.

In order to make further analysis irrespective of the height  $h$  of the tower, let us first normalize all the lengths, so that

$$u = z/h; \quad u' = z'/h; \quad A = a/h \quad (7)$$

and, consequently

$$q(z') = dQ/dz' = q(u')/h. \quad (8)$$

With the new, normalized coordinates the integral equation (5) can be written in the form

$$\int_0^1 \frac{q(u') du'}{\sqrt{A^2 + (u - u')^2}} - \int_0^1 \frac{q(u') du'}{\sqrt{A^2 + (u + u')^2}} = 4\pi\epsilon_0 E_0 h^2 u. \quad (9)$$

Let us now approximate the unknown charge density function by the polynomial

$$q(u') = \sum_{n=1}^N B_n u'^n \quad u' \geq 0, \quad (10)$$

where  $N$  is the order of the polynomial and  $B_n$  are the coefficients to be determined. The constant term  $B_0$  is set equal to zero because the polynomial (10) must satisfy

$$q(0) = 0, \quad (11)$$

imposed by the symmetry condition (1).

With the charge density distribution function (10), equation (9) becomes

$$\sum_{n=1}^N B_n J_n(u) = 4\pi\epsilon_0 E_0 h^2 u \quad (12)$$

where

$$J_n(u) = P_n(u) - P_n(-u), \quad (13)$$

and

$$P_n(u) = \int_0^1 \frac{u'^n du'}{\sqrt{A^2 + (u-u')^2}}. \quad (14)$$

The integrals (14), for different values of  $n$ , can be reduced to elementary integrals:

$$\begin{aligned} &= \operatorname{arcsinh} \{(1-u)A + \operatorname{arcsinh}(u/A), \text{ for } n = 0 \\ P_n(u) &= \sqrt{A^2 + (1-u)^2} - \sqrt{A^2 + u^2} + uP_0(u), \text{ for } n = 1 \\ &= \{\sqrt{A^2 + (1-u)^2} + (2n-1)uP_{n-1}(u) \\ &\quad - (n-1)(A^2 + u^2)P_{n-2}(u)\}/n, \text{ for } n \geq 2. \end{aligned} \quad (15)$$

In order to determine  $N$  unknown coefficients  $B_n$  of the charge density function (10), we take  $N$  convenient points  $u_i$  along the antenna cylinder and stipulate that equation (12) be satisfied at these points. So, we get a system of  $N$  linear equations in  $N$  unknowns  $B_n$ :

$$\sum_{n=1}^N B_n J_n(u_i) = 4\pi\epsilon_0 E_0 h^2 u_i, \quad i = 1, 2, \dots, N. \quad (16)$$

Although the choice of points  $u_i$  is arbitrary, it is quite natural to select them equidistantly, i.e.

$$u_i = i/(N+1), \quad i = 1, 2, \dots, N. \quad (17)$$

The end-point  $u = 1$  is excluded because the function  $q(u)$  is discontinuous there; the point  $u = 0$  is already taken into account by (11).

By solving system (16) we get unknown coefficients  $B_n$ , and finally determine the charge density function (10). The resultant potential  $\phi$  in the vicinity of the antenna tower can be calculated from equation (6). In final form, we can write

$$\phi = \frac{1}{4\pi\epsilon_0 h} \sum_{n=1}^N B_n \{P_n(u, R) - P_n(-u, R)\} - E_0 hu, \quad (18)$$

where  $P_n(u, R)$  is obtained from  $P_n(u)$  by substituting  $A$  for  $R = r/h$ ;  $r$  and  $z = uh$  are cylindrical coordinates of the point wherein the potential is to be calculated.

If necessary, the cylindrical components of the field strength can be calculated by means of the formulae given in the Appendix.

### 3 Static Voltages on the Guy Insulators

Essentially, the same method will be used in determining the static voltages on the insulators of guy wire-ropes.

In order to fix the notation, a sectionalized antenna guy with its electrical image is shown in Fig. 2. There are  $M$  guy sections having lengths  $d_m$ ,  $m = 1, 2, \dots, M$ , and a radius  $b$ . The first guy section is directly anchored to the ground, without an insulator. Let a new coordinate system,  $x-y-z$ , be introduced and positioned in such a way that the  $z$ -axis coincides with the axis of the guy, and  $x$ -axis lies in the ground plane. The distances along the image of the guy are measured by the coordinate  $t$ , whose origin coincides with the origin of the  $x-y-z$  system.

The charge density distribution function  $q(z)$  along the guy sections, as well as the voltages  $V_m$  on the guy insulators are determined by solving numerically a system of integral equations. These equations are derived by making the following simplifying suppositions:

- (i) The charge distribution on the antenna tower is not disturbed by the presence of the guys. (This will be fully justified later by comparing the calculated charge densities per unit length on the tower and on the guys.)
- (ii) Mutual effects between the guys are negligible and can be ignored.
- (iii) The induced charges are localized on the axes of the guy sections.

Accordingly, the potential at a point  $P(x, y, z)$  in the presence of only one guy can be written as the sum

$$\phi = \phi_0 + \phi_i + \phi_g + \phi_{gi} \quad (19)$$

where

$\phi_0$  is the scalar potential of the unperturbed atmospheric electric field, given by (2) (note the change of the coordinates);

$\phi_i$  is the potential created by induced charges on the antenna tower and its image, the guys being neglected;

$\phi_g$  is the potential due to the induced charge on the guy;

$\phi_{gi}$  is the potential due to the charge on the guy-image.

According to the notation in Fig. 2, the two latter potentials can be written as follows:

$$\phi_g = \frac{1}{4\pi\epsilon_0} \int_0^d \frac{q_g(z') dz'}{\sqrt{x^2 + y^2 + (z-z')^2}} \quad (20)$$

$$\phi_{gi} = \frac{1}{4\pi\epsilon_0} \int_0^d \frac{q_{gi}(t) dt}{\sqrt{x^2 + y^2 + z^2 + t^2 - 2t \times (z \cos 2\theta + x \sin 2\theta)}} \quad (21)$$

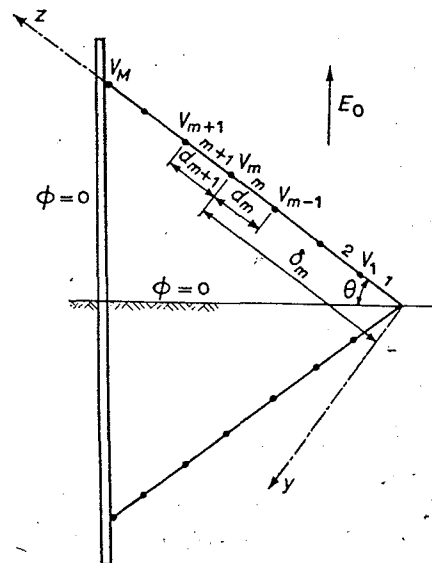


Fig. 2. A sectionalized antenna guy with its electrical image.

where

$$d = \sum_{m=1}^M d_m \quad (22)$$

is the total length of the guy,  $q_g(z')$  and  $q_{gi}(t)$  are the charge densities on the guy and its image, respectively. For  $t = z'$

$$q_{gi}(t) = -q_g(z'). \quad (23)$$

At a point  $P(x = 0, y = b, z)$  on the surface of the guy, equation (19) can be put in the form:

$$\phi = \phi_0(P) + \phi_i(P) + \frac{1}{4\pi\epsilon_0} \int_0^d \frac{q_g(z') dz'}{\sqrt{b^2 + (z - z')^2}} - \frac{1}{4\pi\epsilon_0} \int_0^d \frac{q_g(z') dz'}{\sqrt{b^2 + z^2 + z'^2 - 2zz' \cos 2\theta}} \quad (24)$$

Since the total charge on a section of the guy must be equal to zero (except for the section  $m = 1$ , which is directly connected to the ground), the function  $q_g(z')$  is discontinuous and as a rule changes the algebraic sign at points where the guy is broken by insulators. For that reason the function  $q_g(z')$  should be replaced by  $M$  functions  $q_m(z')$ , each valid for a separate section.

According to the boundary condition for potential, the potential  $\phi$  defined by equation (24) must have a particular constant value along each section:

$$\phi = \begin{cases} \Phi_1 & \text{for } 0 < z < \delta_1 = d_1 \\ \Phi_2 & \text{for } \delta_1 < z < \delta_2 \\ \vdots & \vdots \\ \Phi_m & \text{for } \delta_{m-1} < z < \delta_m \\ \vdots & \vdots \\ \Phi_M & \text{for } \delta_{M-1} < z < \delta_M \end{cases} \quad (25)$$

where

$$\delta_m = \sum_{i=1}^m d_i \quad (26)$$

The  $M-1$  unknown potentials, from  $\Phi_2$  through  $\Phi_M$ , are to be determined. Once the potentials  $\Phi_m$  have been known, the voltages  $V_m$  on the insulators can be calculated by using the formula

$$V_m = \Phi_m - \Phi_{m+1} \quad (27)$$

Since the potential of the tower is equal to zero,  $V_m = \Phi_m$ .

In order to calculate the unknown potentials  $\Phi_m$ , let us approximate the charge distribution functions  $q_m(z')$  by polynomials of the  $N$ -th order:

$$q_m(z') = \sum_{n=0}^N A_{mn} \left[ \frac{z' - \delta_m + d_m}{d_m} \right]^n, \quad m = 1, 2, \dots, M. \quad (28)$$

Since  $q_1(0) = 0$ , the constant term on the first section ( $m = 1$ ) is

$$A_{10} = 0. \quad (29)$$

In addition to the distributed charge  $q_m(z)$ , there are the lumped charges  $Q_m$  and  $-Q_{m-1}$  on the ends of each section. These charges are localized on the metal holders of the insulators and have the values

$$\begin{aligned} Q_m &= CV_m = C(\Phi_m - \Phi_{m+1}) \\ Q_{m-1} &= CV_{m-1} = C(\Phi_{m-1} - \Phi_m) \end{aligned} \quad (30)$$

where  $C$  is the insulator self-capacitance in farads.

Since the total charge on each section ( $m \neq 1$ ) must be equal to zero, the charges  $Q_m$ ,  $-Q_{m-1}$  and  $q_m(z')$  satisfy the condition

$$\int_{\delta_{m-1}}^{\delta_m} q_m(z') dz' + Q_m - Q_{m-1} = 0, \quad (31)$$

$$\text{i.e. } \sum_{n=0}^N A_{mn} d_m / (n+1) + C(2\Phi_m - \Phi_{m+1} - \Phi_{m-1}) = 0, \quad m = 2, 3, \dots, M. \quad (32)$$

With equations (28) and (25), equation (24) gives a system of  $M$  integral equations:

$$\begin{aligned} \Phi_m &= \phi_0(z) + \phi_i(z) + \frac{1}{4\pi\epsilon_0} \times \\ &\times \sum_{m=1}^M \sum_{n=0}^N \left\{ \int_{\delta_{m-1}}^{\delta_m} \frac{A_{mn} \{(z' - \delta_m + d_m)/d_m\}^n dz'}{\sqrt{b^2 + (z - z')^2}} - \right. \\ &\quad \left. - \int_{\delta_{m-1}}^{\delta_m} \frac{A_{mn} \{(z' - \delta_m + d_m)/d_m\}^n dz'}{\sqrt{b^2 + z^2 + z'^2 - 2zz' \cos 2\theta}} \right\} \\ &\quad \delta_m - d_m < z < \delta_m, \quad m = 1, 2, \dots, M. \end{aligned} \quad (33)$$

If we introduce the normalized co-ordinates, defined by

$$u' = (z' - \delta_m + d_m)/d_m, \quad u = z/d, \quad (34)$$

the equation (33) can be put in a simpler form:

$$\begin{aligned} \Phi_m &= \phi_0(ud) + \phi_i(ud) + \frac{1}{4\pi\epsilon_0 d} \times \\ &\times \sum_{m=1}^M d_m \sum_{n=0}^N A_{mn} \left[ \int_0^{1/\rho_1} \frac{u'^n du'}{\sqrt{\rho_1}} - \int_0^{1/\rho_2} \frac{u'^n du'}{\sqrt{\rho_2}} \right] \\ &\quad (\delta_m - d_m)/d < u < \delta_m/d, \quad m = 1, 2, \dots, M, \end{aligned} \quad (35)$$

where

$$\rho_1 = (b/d)^2 + \{u - u'd_m/d - (\delta_m - d_m)/d\}^2 \quad (36)$$

$$\rho_2 = (b/d)^2 + u^2 + \{(u'd_m + \delta_m - d_m)/d\}^2 - 2u\{(u'd_m + \delta_m - d_m)/d\} \cos 2\theta. \quad (37)$$

The integrals of the type

$$J_n = \int_0^1 \frac{u'^n du'}{\sqrt{\rho}}, \quad \rho = \alpha + \beta u' + \gamma u'^2, \quad (38)$$

appearing in equation (35), can be calculated by the following formulae:

$$J_n = \begin{cases} \frac{1}{\sqrt{\gamma}} \ln \frac{2\sqrt{\gamma\rho(1)} + 2\gamma + \beta}{2\sqrt{\gamma\rho(0)} + \beta} & \text{for } n = 0 \\ \frac{\sqrt{\rho(1)} - \sqrt{\rho(0)} - 0.5\beta J_0}{\gamma} & \text{for } n = 1 \\ \frac{J_{n-1} - (n-1)\alpha J_{n-2}}{n\gamma} & \text{for } n \geq 2 \end{cases} \quad (39)$$

where

$$\gamma > 0, \quad \rho(0) = \alpha, \quad \rho(1) = \alpha + \beta + \gamma.$$

The following unknown constants will now be determined:

$M-1$  potentials  $\Phi_m$  on sections  $m = 2, 3, \dots, M$  ( $\Phi_1 = 0$ );

$M(N+1)$  coefficients  $A_{mn}$ .

Since the coefficients  $A_{mn}$  are subject to  $M$  conditions defined by equations (29) and (32), the remaining

Table 1  
The ratio  $E_z/E_r$  for different values of  $N$

$z/h$	$N = 2$	$N = 3$	$N = 5$	$N = 10$	$N = 15$
0.1	$1.368 \times 10^{-4}$	$3.110 \times 10^{-4}$	$3.992 \times 10^{-4}$	$6.768 \times 10^{-5}$	$1.636 \times 10^{-6}$
0.2	$5.685 \times 10^{-4}$	$3.566 \times 10^{-4}$	$1.263 \times 10^{-4}$	$6.956 \times 10^{-6}$	$3.151 \times 10^{-7}$
0.3	$3.387 \times 10^{-4}$	$6.402 \times 10^{-6}$	$7.996 \times 10^{-6}$	$1.401 \times 10^{-6}$	$1.794 \times 10^{-7}$
0.4	$5.590 \times 10^{-5}$	$1.542 \times 10^{-4}$	$2.601 \times 10^{-5}$	$4.431 \times 10^{-7}$	$2.472 \times 10^{-7}$
0.5	$3.571 \times 10^{-4}$	$3.776 \times 10^{-5}$	$7.123 \times 10^{-5}$	$1.901 \times 10^{-7}$	$9.197 \times 10^{-8}$
0.6	$3.460 \times 10^{-4}$	$2.131 \times 10^{-4}$	$2.743 \times 10^{-6}$	$8.866 \times 10^{-8}$	$6.664 \times 10^{-8}$
0.7	$3.266 \times 10^{-4}$	$2.261 \times 10^{-4}$	$2.142 \times 10^{-4}$	$1.812 \times 10^{-6}$	$8.031 \times 10^{-7}$
0.8	$2.551 \times 10^{-3}$	$1.006 \times 10^{-3}$	$1.848 \times 10^{-4}$	$1.613 \times 10^{-5}$	$9.266 \times 10^{-6}$
0.9	$1.044 \times 10^{-2}$	$7.838 \times 10^{-3}$	$5.619 \times 10^{-3}$	$3.465 \times 10^{-4}$	$1.943 \times 10^{-4}$

$M(N+1)-1$  necessary equations are obtained by satisfying equations (35) in  $M(N+1)-1$  points along the sections. On the first section we select  $N$  matching points and on all other sections  $N+1$  points each. These points can be chosen arbitrarily, but none at the ends of the sections. If the selected points are equidistant on a section, their co-ordinates  $z_i$  are determined by

$$z_i = id_1/(N+1) \quad i = 1, 2, \dots, N \quad \text{for } m = 1 \quad (40)$$

$$z_i = \delta_{m-1} + id_m/(N+2) \quad i = 1, 2, \dots, N+1 \quad \text{for } m = 2, \dots, M. \quad (41)$$

Dividing equations (40) and (41) by  $d$  we obtain the normalized co-ordinates  $u_i$ .

By solving  $(M-1)+M(N+1)$  linear equations, the unknowns  $\Phi_m$  and  $A_{mn}$  can be calculated. The voltages  $V_m$  are obtained by equation (27).

#### 4 Numerical Example and Conclusion

In order to illustrate the theory and to draw some practical conclusions, the charge densities and static guy-insulator voltages will be calculated for the antenna of the main m.f. transmitter of Radio Beograd. This is a guyed steel tower with triangular cross-section, having a height of 235 m and an equivalent radius  $a$  of 0.7 m. The tower is guyed by 3 sets of 3 guy wires attached to the tower at three different heights and inclined at an angle of  $45^\circ$  with respect to the ground plane. In horizontal projection the guy-wires are laid out  $120^\circ$  apart. The radius of wires  $b$  is 14 mm. The arrangement of the guy sections in the vertical plane as well as the necessary notation are shown in Fig. 3. The insulator capacitance is about 50 pF.

Applying the method described in Section 2, the potential in the tower vicinity was first calculated. For checking the convergence and accuracy of results with respect to the order of the polynomial used, the fulfilment of the boundary condition on the antenna cylinder surface was verified. The ratio of the tangential field component,  $E_z$ , and radial component,  $E_r$ , seems to be very suitable criterion for that. That is why the ratio  $E_z/E_r$  was calculated for different values of  $N$  and it is presented in Table 1. It is surprising that even a polynomial of the order as low as  $N = 2$  fulfils the boundary condition very well. The equipotential lines, relevant to an

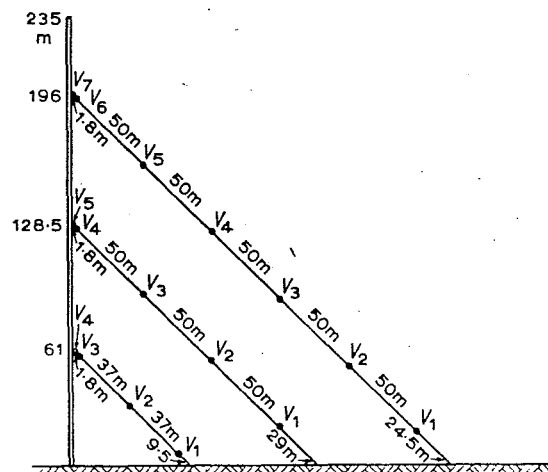


Fig. 3. Arrangement of the guy sections of the antenna tower of the main m.f. transmitter of Radio Beograd.

unperturbed field strength  $E_0 = 100$  V/m and  $N = 5$ , are shown in Fig. 4.

The charge density per unit length of the tower for  $E_0 = 100$  V/m and for different values of  $N$  is presented in Table 2.

Table 2  
The charge density  $q(z)$  along the tower in  $10^{-9}$  C/m  
( $E_0 = 100$  V/m,  $a/h = 0.002978$ )

$z/h$	0.0	0.1	0.2	0.3	0.4	0.5	0.6	0.7	0.8	0.9	1.0
$N = 2$	0	23	46	71	96	122	149	176	204	234	263
$N = 5$	0	23	47	71	95	120	147	175	209	251	307
$N = 20$	0	23	47	71	95	120	146	174	207	250	407

The results for  $z/h = 1$  should be disregarded because the top of the tower is a point of discontinuity.

The voltages on guy insulators, for  $E_0 = 100$  V/m,  $C = 50$  pF and for the second- and fifth-order polynomial approximation of the charge density on guy sections, are shown in Table 3. (The charge density on the tower is approximated by a polynomial of the fifth-order.)

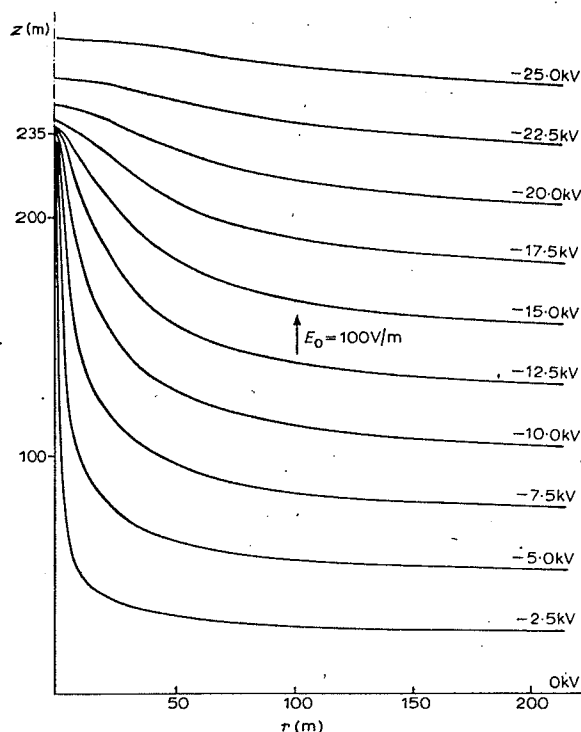


Fig. 4. Equipotential lines in the vicinity of the antenna cylinder;  $h = 235$  m,  $a/h = 0.002978$  and  $E_0 = 100$  V/m.

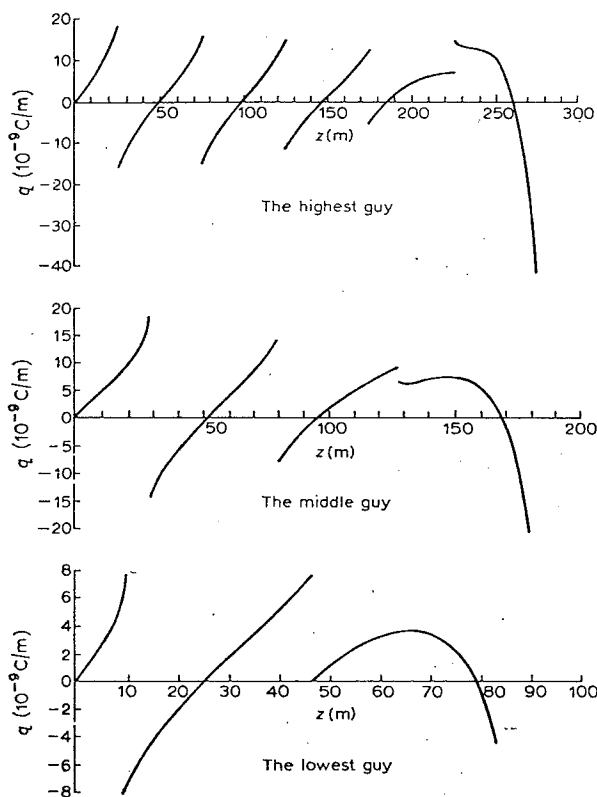


Fig. 5. Charge density per unit length along the guys from Fig. 3;  $E_0 = 100$  V/m,  $C = 50$  pF and  $N = 5$ .

Table 3

Voltages on guy-insulators,  $V_m$ , in kV  
( $E_0 = 100$  V/m,  $C = 50$  pF)

	$V_1$	$V_2$	$V_3$	$V_4$	$V_5$	$V_6$	$V_7$
THE HIGHEST GUY							
$N = 2$	3.225	3.060	2.682	1.790	1.077	5.500	4.181
$N = 5$	3.223	3.057	2.675	1.768	1.144	5.398	4.181
THE MIDDLE GUY							
$N = 2$	3.092	2.235	0.161	2.994	2.495		
$N = 5$	3.084	2.220	0.120	2.930	2.495		
THE LOWEST GUY							
$N = 2$	1.271	0.636	0.768	1.139			
$N = 5$	1.263	0.619	0.744	1.139			

In order to estimate the effects of the insulator capacitance, the same voltages were calculated for  $C = 0$ . These values are given in Table 4.

Table 4

Voltages on guy-insulators,  $V_m$ , in kV  
( $E_0 = 100$  V/m,  $C = 0$ )

	$V_1$	$V_2$	$V_3$	$V_4$	$V_5$	$V_6$	$V_7$
THE HIGHEST GUY							
$N = 2$	3.268	3.108	2.784	2.102	0.385	6.696	4.181
$N = 5$	3.259	3.106	2.780	2.087	0.443	6.608	4.181
approx.	3.272	3.122	2.811	2.184	0.139	7.343	4.181
THE MIDDLE GUY							
$N = 2$	3.245	2.435	0.597	3.782	2.495		
$N = 5$	3.231	2.426	0.562	3.725	2.495		
approx.	3.282	2.493	0.933	4.213	2.495		
THE LOWEST GUY							
$N = 2$	1.409	0.956	1.226	1.139			
$N = 5$	1.400	0.939	1.200	1.139			
approx.	1.445	1.121	1.427	1.139			

In addition to the values of voltages corresponding to  $N = 2$  and  $N = 5$ , the third approximate value ('approx.') of the voltage is given in Table 4. This value is defined as the difference between the potentials in the mid-points of two adjacent sections in the physical absence of the guys. These potentials are those calculated in Section 2, i.e.  $\phi_0 + \phi_i$ . It is interesting to note a very good overall agreement between these approximate values and those calculated by the present method for  $C = 0$ , except for the minimum values of the voltages.

The curves in Fig. 5 represent the charge density distribution functions along the three guys from Fig. 3, corresponding to  $E_0 = 100$  V/m,  $C = 50$  pF and  $N = 5$ . It is to be noted that the maximum value of the charge density on the guys is at least an order of magnitude smaller than the average charge density on the tower. This justifies the assumption that the guys do not affect appreciably the charge distribution along the tower.

In the foregoing examples all the voltages and charge densities are calculated under the assumption of a relatively low field strength  $E_0 = 100$  V/m, which is a

representative value for calm weather conditions. However, immediately before and during thunderstorms this value can be exceeded by ten or even a hundred times. According to Müller-Hillebrand<sup>5</sup>, maximal field strength of 3–5 kV/m is typical, and very rarely exceeds 10 kV/m. Similar data can be found in the paper by Simpson and Scrase,<sup>6</sup> who quote values of 5–10 kV/m.

In order to point out the significance of the static voltages, we shall compare these voltages, corresponding to a moderate static field strength  $E_0 = 1$  kV/m, with the measured r.f. voltages for the same antenna. The results are shown in Table 5. The r.f. voltages correspond to an unmodulated r.f. power of 400 kW.

**Table 5**  
Static and r.f. voltages on guy insulators, in kV.  
( $E_0 = 1$  kV/m,  $C = 50$  pF; r.f. power 400 kW)

	$V_1$	$V_2$	$V_3$	$V_4$	$V_5$	$V_6 + V_7$
THE HIGHEST GUY						
Static	32.23	30.57	26.75	17.68	11.44	95.79
r.f.	0.5	1.2	1.3	1.4	2.0	9.8
THE MIDDLE GUY						
	$V_1$	$V_2$	$V_3$	$V_4 + V_5$		
Static	30.84	22.20	1.20	54.25		
r.f.	1.8	2.0	1.9	3.3		
THE LOWEST GUY						
	$V_1$	$V_2$	$V_3 + V_4$			
Static	12.63	6.19	18.83			
r.f.	1.8	4.9	11.8			

The method explained in this paper can, of course, be applied to antenna towers consisting of several sections of different, but uniform cross-section.

## 5 Acknowledgment

This work was in part supported by the Serbian National Research Foundation.

## 6 References

1. Brown, G. H., 'A consideration of the radio frequency voltages encountered by the insulating material of broadcast tower antennae', *Proc. IRE*, 27, pp. 566–78, September 1939.
2. Bruger, P., 'Pardunenisolation der Mittelwellenantenne Langenberg des Westdeutschen Rundfunks', *Rundfunktech. Mitt. (Germany)*, 13, pp. 235–43, May 1969.

3. Harrington, R. F., 'Field Computation by Moment Methods' (Macmillan, London 1968).
4. King, R. W. P., 'The Theory of Linear Antennas', p. 20 (Harvard University Press, Cambridge, Mass., 1956).
5. Müller-Hillebrand, D., 'Zur Physik der Blitzentladung', *Elektrotech. Z.-A., (Germany)*, 82, pp. 232–48, August 1961.
6. Simpson, G. and Scrase, F. J., 'The distribution of electricity in thunderclouds', *Proc. R. Soc. Lond., Series A*, 161, No. 906, p. 309, 1937.

## 7 Appendix

The cylindrical components of the field strength in the vicinity of the tower (the guys are ignored) can be calculated by means of the following formulae:

$$E_z = E_0 + \frac{1}{4\pi\epsilon_0 h^2} \sum_{n=1}^N B_n [nP_{n-1}(u, R) + nP_{n-1}(-u, R) - \{R^2 + (u-1)^2\}^{-\frac{1}{2}} - \{R^2 + (u+1)^2\}^{-\frac{1}{2}}], \quad (42)$$

$$E_r = \frac{1}{4\pi\epsilon_0 h^2} \sum_{n=1}^N B_n \{T_n(u, R) - T_n(-u, R)\}, \quad (43)$$

where

$$T_n(u, R) = \int_0^1 \frac{u'^n du'}{\{R^2 + (u-u')^2\}^{\frac{1}{2}}}$$

$$= \frac{1-u}{R^2 \sqrt{R^2 + (u-1)^2}} + \frac{u}{R^2 \sqrt{R^2 + u^2}} \quad \text{for } n=0$$

$$= \frac{\sqrt{R^2 + u^2}}{R^2} - \frac{(R^2 + u^2 - u)}{R^2 \sqrt{R^2 + (u+1)^2}} \quad \text{for } n=1$$

$$= \frac{u \sqrt{R^2 + u^2}}{R^2} - \frac{\{R^2 - u^2 + (R^2 + u^2)u\}}{R^2 \sqrt{R^2 + (u-1)^2}} + P_0(u, R) \quad \text{for } n=2$$

$$= \frac{[\{R^2 + (u-1)^2\}^{-\frac{1}{2}} + u(2n-3)T_{n-1}(u, R) - (n-1)(R^2 + u^2)T_{n-2}(u, R)]}{n-2} \quad \text{for } n > 3$$

$$(44)$$

Manuscript first received by the Institution on 24th April 1973 and in final form on 14th September 1973. (Paper No. 1558/Com. 184.)

© The Institution of Electronic and Radio Engineers, 1973

# SUMMARY OF STANDARD REFERENCE ANTENNAS

TYPE OF ANTENNA	VERTICAL PATTERN SHAPE	MV/M FOR 1 WATT AT 1 MILE $E_0$	MV/M FOR 1 KW AT 1 MILE $E_0$	POWER GAIN $g$	db GAIN $G$	TYPE OF ANTENNA	VERTICAL PATTERN SHAPE	MV/M FOR 1 WATT AT 1 MILE $E_0$	MV/M FOR 1 KW AT 1 MILE $E_0$	POWER GAIN $g$	db GAIN $G$
UNIFORM SPHERICAL RADIATOR		3,402	107.6	1	0	UNIFORM HEMISPHERICAL RADIATOR		4,811	152.1	2	3,010
CURRENT ELEMENT		4,167	131.8	1.5	1.761	VERTICAL CURRENT ELEMENT		5,893	186.3	3	4,771
HALF WAVE ANTENNA		4,358	137.8	1.641	2.151	QUARTER WAVE VERTICAL ANTENNA		6,163	194.9	3,282	5,161
0.622 $\lambda$ ANTENNA		4,472	141.4	1.728	2.375	0.311 $\lambda$ VERTICAL ANTENNA		6,324	200	3,456	5,386
TWO END ON HALF WAVE IN PHASE ANTENNA		5,283	167.1	2.411	3.822	HALF WAVE VERTICAL ANTENNA		7,471	236.2	4,822	6,832

## Standard Reference Antennas\*

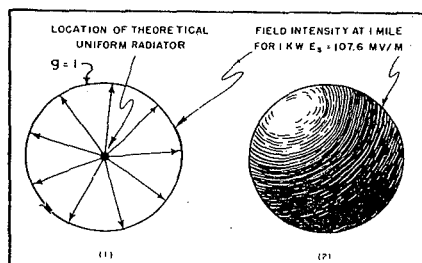
by CARL E. SMITH<sup>1</sup>

Vice President, In Charge of Engineering,  
United Broadcasting Company

THE UNIFORM OMNIDIRECTIONAL (spherical) or isotropic radiator, in free space, has been adopted as the *standard reference antenna* (Figure 1) because it has no directivity. This

Figure 1

A pattern of a uniform radiator which is the theoretical standard reference antenna. At left appears a cross-sectional view of a spherical pattern which has a field intensity gain of 1, a power gain of 1 ( $g=1$ ) and a decibel gain of 0 ( $G=0$ ). At right appears a spherical radiation pattern surface of a uniform or isotropic radiator.



### Characteristics of the Omnidirectional Uniform Spherical Radiator, Used as the Standard Theoretical Reference, and the Uniform Hemispherical Radiator Used as a Standard of Directivity and For Computation of Gain and Efficiency.

standard, which has come into rather common use in recent years, is defined as a theoretical antenna which radiates waves having the same field intensity in all directions. Actually such a radiator can not be realized, because all antennas have directional properties. In the case of acoustic waves, this standard is represented by a sphere pulsating radially.

The figure of merit or efficiency of all other antennas can be compared with this basic standard, and other secondary standards for free space

may be selected and used as convenience demands; Table 1 (above).

#### Uniform Hemispherical Radiator

If a uniform radiator is placed at the surface of a perfectly conducting plane, all of the power must be radiated in the hemisphere above the surface of the earth, as shown in Figure 2. For a given power source, the power flow will have twice the intensity of a uniform radiator in free

(Continued on page 38)

\*From the author's book on *Directional Antennas*, published by the Cleveland Institute of Radio Electronics. The book treats in detail several methods of determining directional antenna efficiency, in addition to a systematization of over 15,000 directional antenna patterns.

<sup>1</sup>Also president of the Cleveland Institute of Radio Electronics.

More than  
**2000**  
up-to-the-minute  
**RADIO and ELECTRONIC**  
**PARTS**  
in this just-off-the-press  
**ICA CATALOG**  
Standard Items  
NEW ITEMS  
New Prices

**It's Free!**

SEND FOR YOUR COPY TODAY

**ICA**  
MERCHANDISER

A beautiful floor unit-70" high, 34" wide.

Sturdily constructed of steel and plywood.

Write and let us tell you how to get one of these handsome self-service units FREE

**insuline**  
CORPORATION OF AMERICA  
Insuline Building - Long Island City 1, New York  
More than a quarter-century of Quality production

## Reference Antennas

(Continued from page 20)

space, hence the power gain is said to be 2.

This antenna can be considered as a standard for determining the directivity of antennas located on the surface of the earth, such as broadcasting antennas. It is particularly useful in the computation of the gain and efficiency of directional antenna systems.

### Directivity Definitions

On the basis of equal powers, the *directivity* or *directive gain* of a given antenna can be defined as the ratio of the maximum power flow intensity to the power flow intensity of a uniform radiator, when the total power output of both sources are equal:

$$g = \frac{P_m}{P_s} \quad (\text{equal powers}) \quad (1)$$

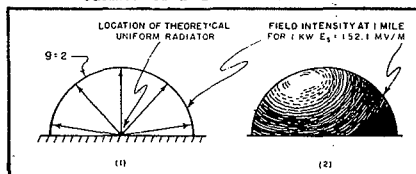
Where:  $g$  = directivity or power gain,

$P_m$  = maximum power flow intensity from the directional antenna radiating 1 kw of power,

$P_s$  = uniform power flow intensity from the standard reference antenna radiating 1 kw of power.

Figure 2

Pattern of a uniform radiator at the surface of a perfect reflecting earth. At left is a cross-sectional view of a hemispherical pattern, which has a field intensity gain of 1.4, a power gain of  $g=2$ , and a decibel gain of  $G=3.01$ . At right is the hemispherical radiation pattern surface of a uniform radiator.



Or, in terms of field intensities the power gain can be determined by:

$$g = \left[ \frac{E_m}{E_s} \right]^2 \quad (\text{equal powers}) \quad (2)$$

Where:  $g$  = directivity or power gain,

$E_m$  = maximum field intensity in mv/m from the directional antenna at 1 mile, for 1 kw of radiated power,

$E_s$  = field intensity (107.6 mv/m) from a uniform spherical radiator at 1 mile, for 1 kw of radiated power.

On the basis of equal field intensities the directivity can be determined by taking the ratio of the power radiated, when the maximum field intensity of the directional antenna is made equal to the field intensity of a uniform spherical radiator:

$$g = \frac{P_s}{P_r} \quad (\text{equal field intensities}) \quad (3)$$

Where:  $g$  = directivity or power gain,

$P_s$  = power radiated (1 kw) from a uniform spherical radiator to produce a given field intensity of  $E_s$  (107.6 mv/m) at 1 mile,

$P_r$  = power radiated from the directional antenna to produce the same given maximum field intensity  $E_m$  (107.6 mv/m) at 1 mile.

On the basis of decibels, the gain can be computed from:

$$G = 10 \log g \quad (4)$$

Where:  $G$  = decibels directive gain,  
 $g$  = directivity or power gain.



## ... For Dependable Commercial Service

Designed for the rigors of commercial service in all types of radio communication . . . broadcast, mobile, aircraft, police. Precision made for utmost in stability, dependability, trouble-free operation. Calibrated within .005 per cent of specified frequency . . . range 1.5 to 10.5 MC. Temp. coefficient less than 2 cycles per megacycle per degree centigrade. Weighs less than 3/4 ounce. Gasket sealed against contamination and moisture. Meets FCC requirements for all above services. See your jobber—Petersen Radio Company, Inc., 2800 W. Broadway, Council Bluffs, Iowa. (Telephone 2760.)

**PR Precision CRYSTALS**

## Electronic Research & Mfg. Corp.

A Service to INDUSTRY

Development and Construction of  
Electronic Equipment for Any Application

1420 E. 25th St., Cleveland 14, O. - Ph.: SU. 1958

## WHEN YOU CHANGE YOUR ADDRESS

Be sure to notify the Subscription Department of COMMUNICATIONS, 52 Vanderbilt Avenue, New York 17, N. Y., giving the old as well as the new address, and do this at least four weeks in advance. The Post Office Department does not forward magazines unless you pay additional postage, and we cannot duplicate copies mailed to the old address. We ask your cooperation.



# A-M / F-M Installation

finished with celotex board and the ceiling with acoustical tile. The cement floor was covered with cork which, in addition to absorbing vibrations set up by the transmitter, has a high coefficient of sound absorption.

Openings were provided in the concrete floor for wiring and ventilating the transmitter. Grills were installed above the transmitter in conjunction with an exhaust fan overhead. A housing was provided at the bottom of the transmitter containing two fans which pull air through spun glass filters, thereby assuring an abundance of circulating air.

Standards of good engineering practice were followed in the installation of the ground system, which consists of a copper ground mesh screen 48' by 48', silver soldered to 120 radials 210' in length. All radials were silver soldered to a driven ground at their ends.

For our f-m system we used a four-section pylon<sup>2</sup> with a total overall length of 54'. In hoisting the pylon a fifty-foot boom was attached, first to the 154' a-m tower and guyed. This was the main fulcrum for raising the pylon. A sling was thrown around the pylon ten feet from the center of gravity enabling the boom to hoist it above the lever of the a-m tower. After about two hours of hoisting the pylon 154', the four-bay unit was in place.

The distance between the transmitter building and the tower base is 190'. The transmitter line is supported by thirteen 10' towers which in turn support a six-wire a-m transmission line. A 1½" coaxial f-m transmission line

**Cinder Block Building, Housing Transmitter, Located in Pennsylvania Woodland Area, 830 Feet Above Sea Level. Four Section F-M Pylon Erected Atop 154 Foot A-M Tower.**

**by WILLIS N. WEAVER and N. CARL KITCHEN**

**Chief Engineer**

**Continuity Director**

**WNOW, York, Penna.**

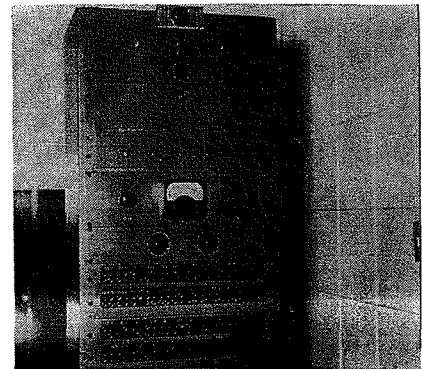
and 1½" conduit carry tower lighting, remote monitoring meter and utility lighting circuits. Expansion joints are used on the 1½" conduit, which is broken at 60' intervals for the insertion of vapor-proof lights along the catwalk.

At present, we have two studios with facilities to run shows from the control room either by an announcer or engineer. There is also a remote control room which was included in the event that separate programs for f-m are required. The large studio is 35' by 50' and uses a polycylindrical acoustical treatment, while the smaller studio, 22' by 30', uses a diagonal treatment.

The audio rack consists of four jack strips and enough auxiliary equipment to run the control room without the consolette. All mixer inputs appear

on the audio rack to facilitate operation.

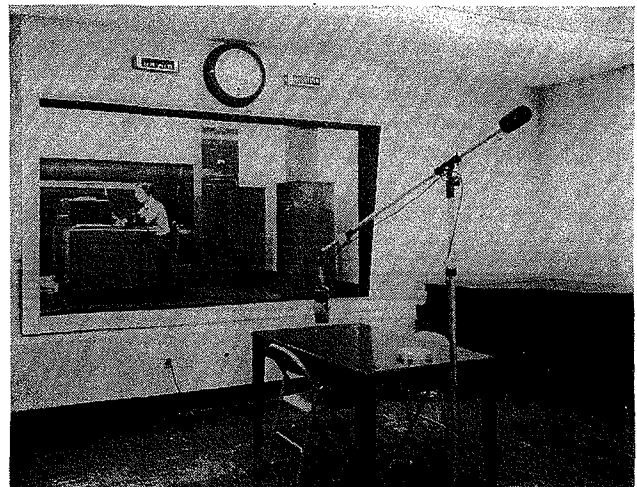
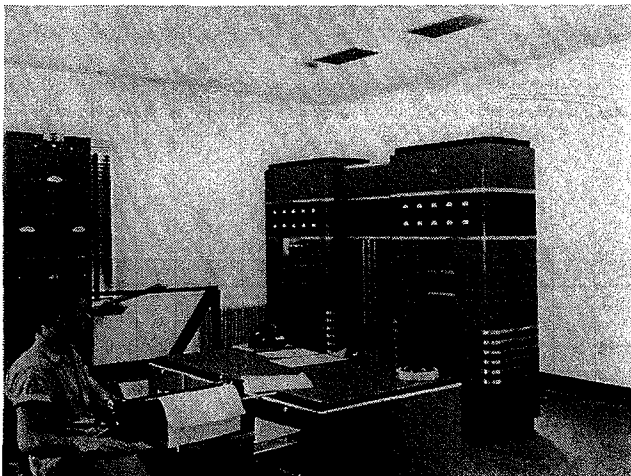
All offices are equipped with speakers and can be fed individual programs originating in the studios or on turntables. Normally they are fed from a separate amplifier bridged across the program bus.



The patchboard panel in the control room.

<sup>1</sup>RCA 1-kw transmitters. <sup>2</sup>RCA.

Left: A view of the a-m transmitter. Note vent grills in ceiling. Right: View of studio A and control room.



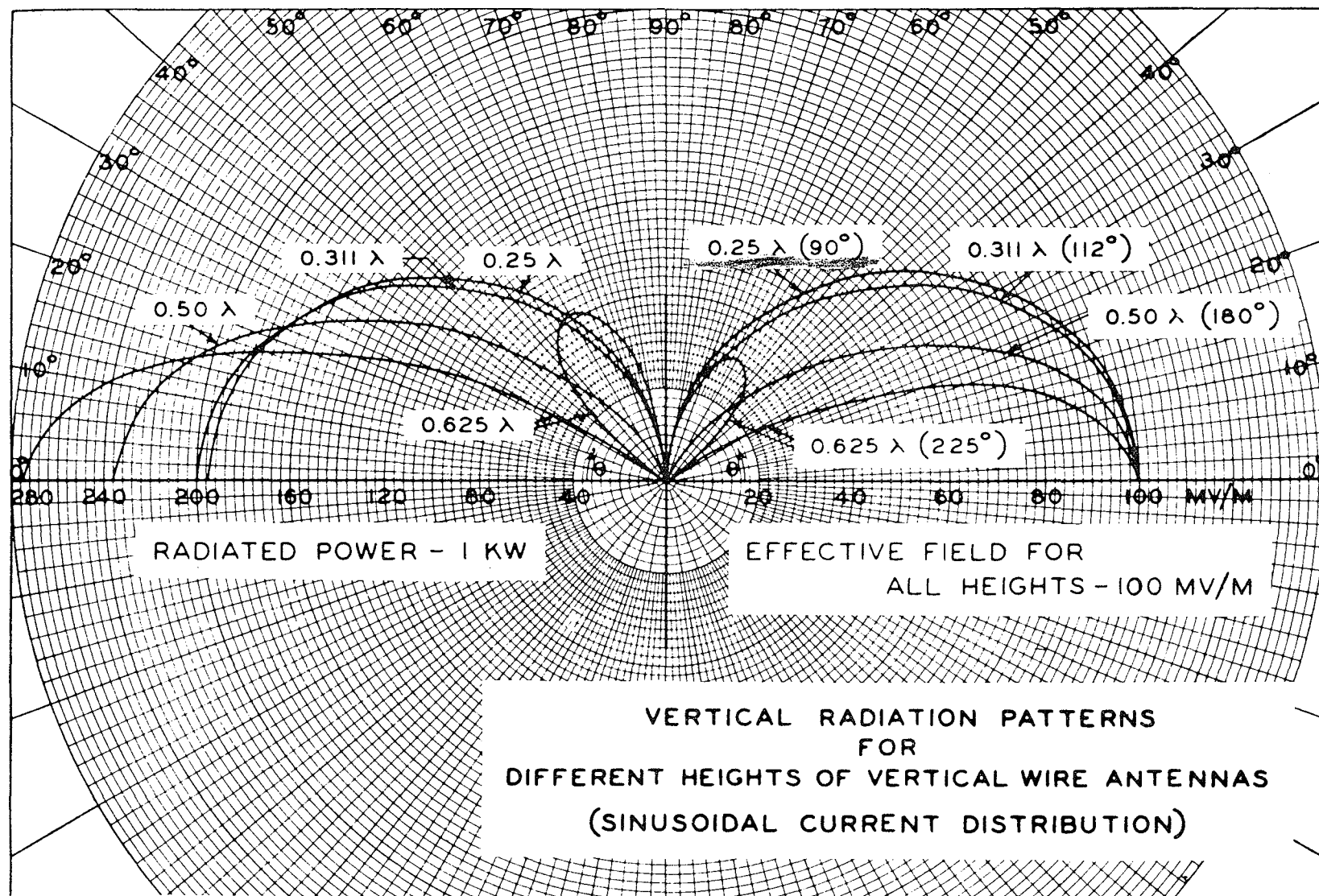


Figure 1

Figure 2

9723

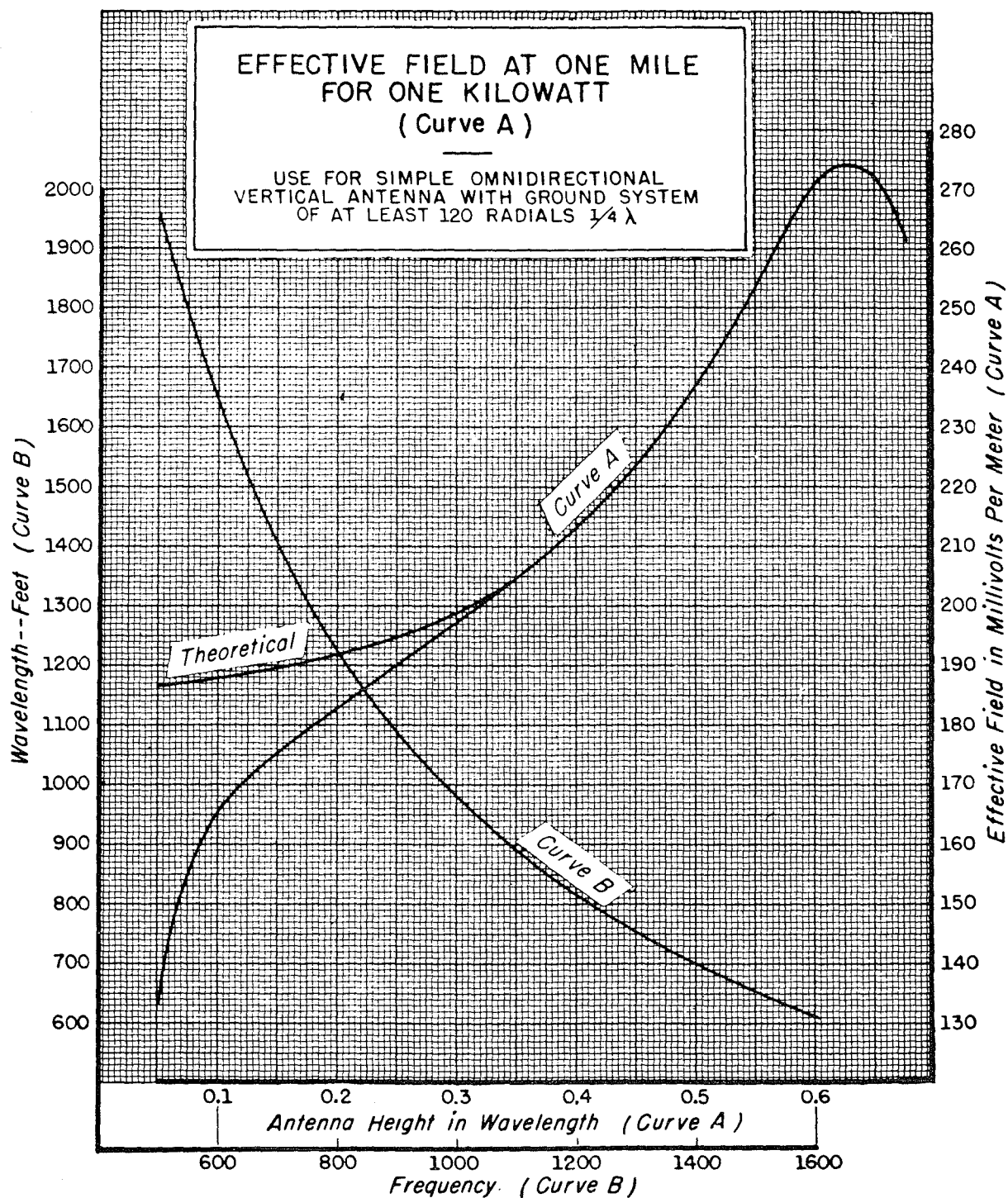


Figure 3

TABLE I  
SUMMARY OF STANDARD REFERENCE ANTENNAS

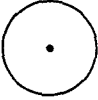

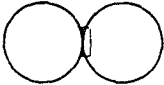
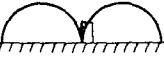






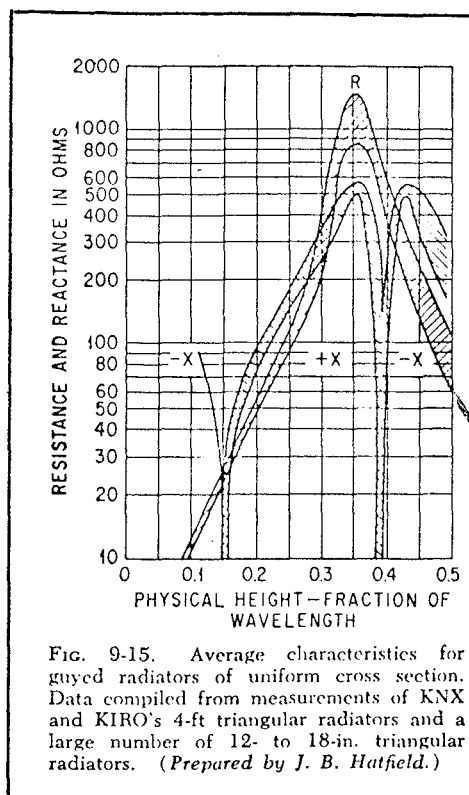
TYPE OF ANTENNA	VERTICAL PATTERN SHAPE	MV/M FOR 1 WATT AT 1 MILE $E_0$	MV/M FOR 1 KW AT 1 MILE $E_0$	POWER GAIN $g$	db GAIN $G$	TYPE OF ANTENNA	VERTICAL PATTERN SHAPE	MV/M FOR 1 WATT AT 1 MILE $E_0$	MV/M FOR 1 KW AT 1 MILE $E_0$	POWER GAIN $g$	db GAIN $G$
UNIFORM SPHERICAL RADIATOR		3.402	107.6	1	0	UNIFORM HEMISPHERICAL RADIATOR		4.811	152.1	2	3.010
CURRENT ELEMENT		4.167	131.8	1.5	1.761	VERTICAL CURRENT ELEMENT		5.893	186.3	3	4.771
HALF WAVE ANTENNA		4.358	137.8	1.641	2.151	QUARTER WAVE VERTICAL ANTENNA		6.163	194.9	3.282	5.161
0.622 $\lambda$ ANTENNA		4.472	141.4	1.728	2.375	0.311 $\lambda$ VERTICAL ANTENNA		6.324	200	3.456	5.386
TWO END ON HALF WAVE IN PHASE ANTENNA		5.283	167.1	2.411	3.822	HALF WAVE VERTICAL ANTENNA		7.471	236.2	4.822	6.832

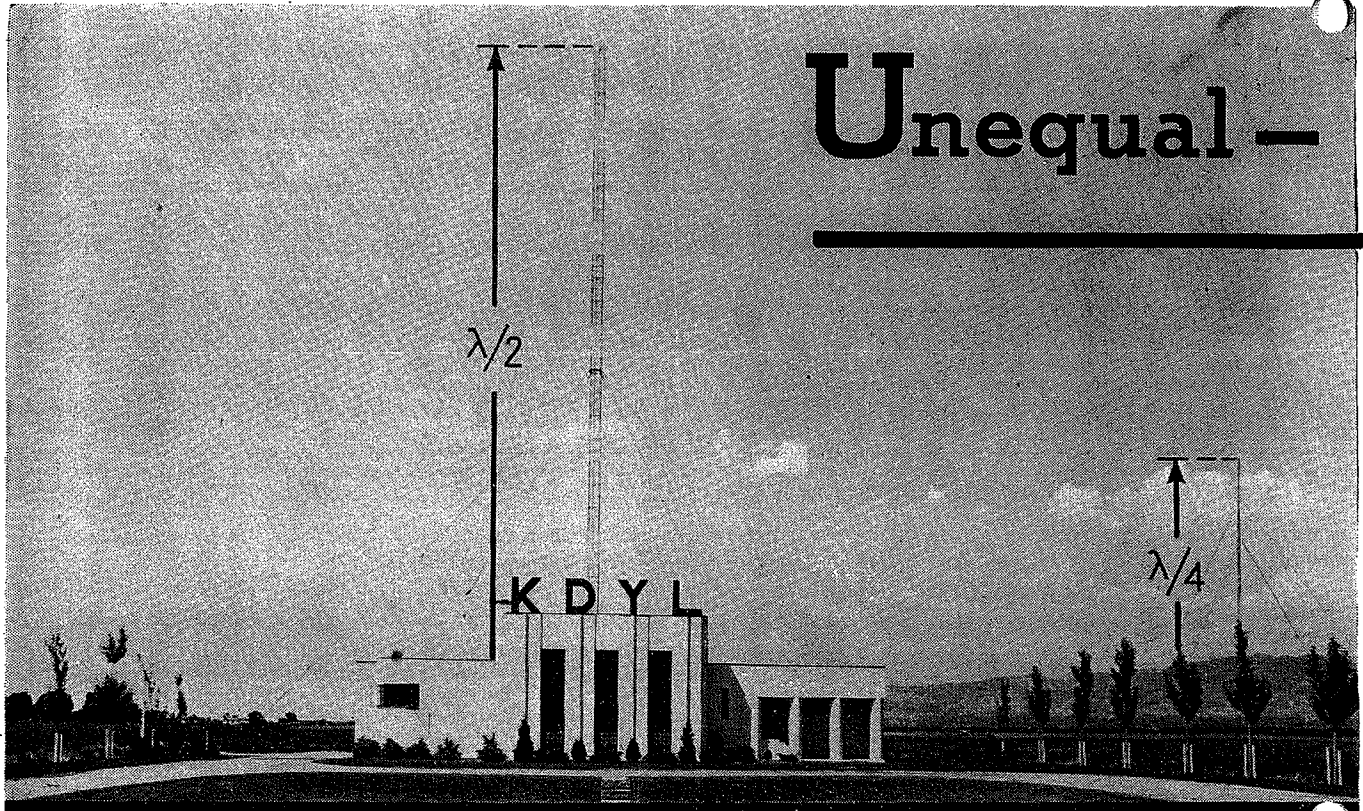
Figure 4

Base operating Impedances  
Reactance and Resistance, Single Tower Antenna  
Guyed Radiators of uniform cross-section



# ADJUSTING

## Unequal —



This two-tower directional array of station KDYL, with the main tower (behind the building) exactly twice the height of the other tower (at the right), is used as an example to illustrate the two methods developed by the authors for adjusting currents and phases to secure a desired nonsymmetrical radiation pattern

**T**HE directional antenna array which has been in operation at radio station KDYL since the summer of 1941 is of somewhat unusual design, in that the two towers are of unequal height, with a large spacing between the towers. At the same time, the coupling and phasing networks were somewhat unorthodox. These factors, together with the rather diversified nature of the terrain, made an antenna problem of real interest to an antenna engineer. It is the purpose of this paper to relate the procedure followed in properly adjusting the array to obtain the required radiation pattern.

### The Antenna Problem at KDYL

Prior to the installation of the array at KDYL, this station operated with a single nondirectional tower 400 feet in height, approximately one-half wave at the operating frequency. It was decided to use a second tower 200 feet in height to make up the directional array. By using

this shorter tower, several thousand dollars were saved. The additional sky wave which would result by using a quarter-wave tower working in conjunction with a half-wave tower was desirable since the country surrounding Salt Lake City is mountainous, and the ground wave is highly attenuated.

It was felt, after three years of experience with the operation of the single half-wave tower, that it did not fit the requirements of broadcasting in Utah. High-angle radiation is vitally necessary in this part of the country, where the ground wave attenuates rapidly and the night sky wave provides a service to sections of the state which would have no service at all if dependent on ground wave transmission alone.

Figure 1 shows the desired horizontal polar diagram. The towers are located on a somewhat east-west line, with a tower spacing of 0.65 wave-lengths (233 electrical deg.) Tower No. 2 lies to the east of tower

No. 1. If the two antennas were identical, desired shape of the horizontal pattern would be obtained if the current in tower No. 2 were 0.6 of that in No. 1, and if the current in No. 2 lagged the current in No. 1 by 45 deg. If the horizontal angle  $\phi$  is measured counter-clockwise from the east line of towers as shown on Fig. 1, the shape of the horizontal field pattern is given by

$$F_{\phi} = \frac{1 + 0.6 \angle -45^{\circ} + 233^{\circ} \cos \phi}{1.6} \quad (1)$$

where

$$\bar{I}_2 = 0.6 \bar{I}_1 \angle -45^{\circ} \quad (2)$$

This horizontal radiation diagram is replotted in Cartesian coordinates in Fig. 2. This was done for greater ease of comparison with other similar patterns in the work about to be described. This type of pattern in Cartesian coordinates gives greater detail in the null points than when plotted in polar coordinates.

The relation shown in Eq. (2) is predicated on the assumption that



# Tower Broadcast Arrays

When towers of unequal height are used in a broadcast directional array, adjustments are complicated by the fact that magnitudes and phases of base currents may differ from those of the radiated fields. Two methods are presented for minimizing cut-and-try adjustments, one involving simple field strength measurements and the other using model antennas

the towers are identical, so that the fields produced by each tower at a point in the horizontal plane lying on the perpendicular bisector of the line of towers have the same respective phase relations with the base currents of the towers and bear the same proportionality factor. When the towers are of unequal height, equal

currents at the bases of the two antennas may produce greatly unequal fields. Furthermore, with the base currents in phase, the two fields produced at this point may be distinctly out of phase.

## Analysis for Unequal Towers

An explanation of this effect may

be found by referring to Fig. 3. This picture should be regarded as entirely qualitative, but illustrative of the phenomena in question. The current along an antenna may be regarded as made up of a main current wave traveling up the tower, retarding in phase as it travels and decreasing exponentially in value. A second

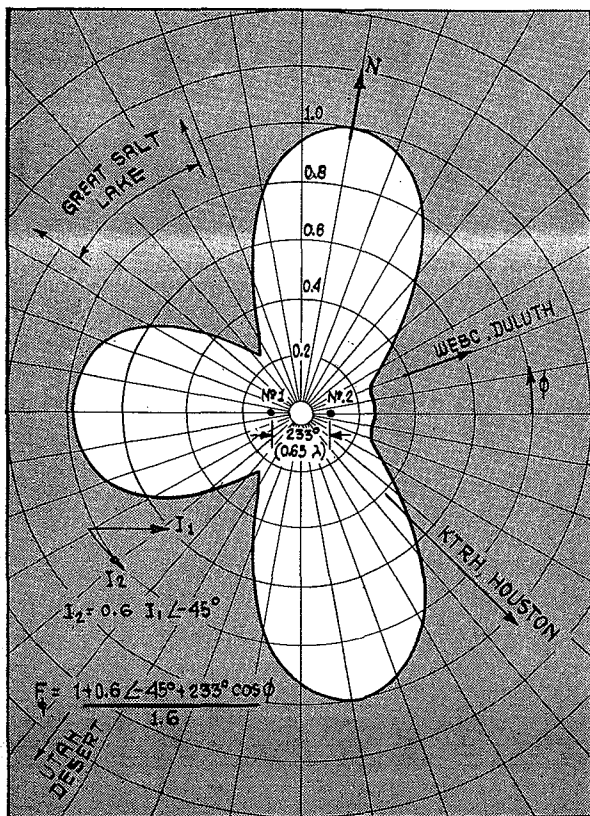


FIG. 1—Radiation pattern desired for KDYL in Salt Lake City, with nulls on two other 1320-kc stations and on two nearby sparsely populated areas, the Great Salt Lake and the Utah desert

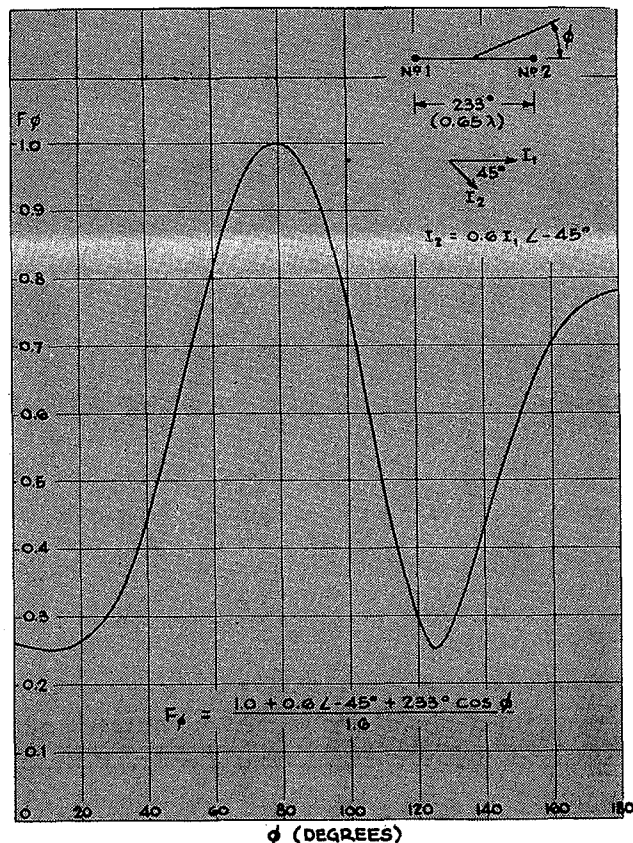
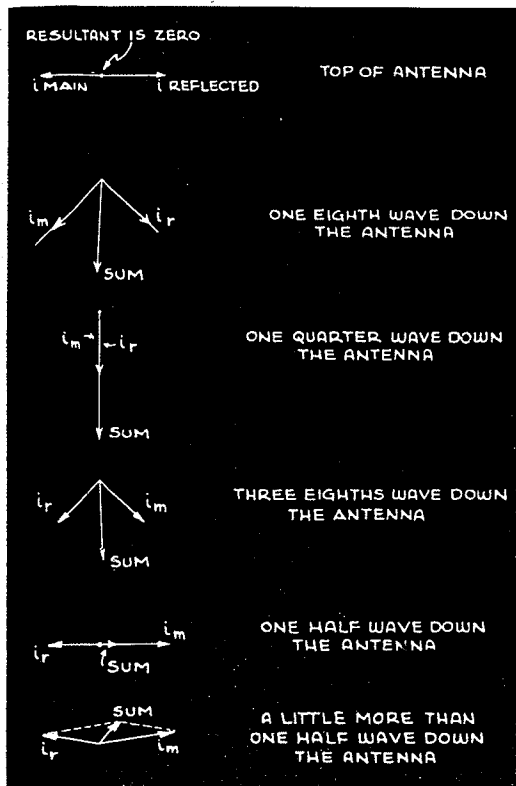


FIG. 2—Upper half of the radiation pattern of Fig. 1, replotted in Cartesian coordinates with degrees measured counterclockwise from the horizontal line extending to the right through the towers

FIG. 3 (BELOW)—Vector diagrams illustrating how the total current in a tower changes in phase at different points on the tower



reflected current wave travels down the tower, again retarding in phase and decreasing exponentially in value.

At the top of the antenna, where the total current must be zero, the two current waves are equal in magnitude and exactly out of phase so that the vector sum of the currents is zero. As we travel down the antenna, the total current, shown as the vector sum in Fig. 3, changes phase very little until we reach the region about one-half wave from the top of the antenna, where the phase shifts about 90 deg. As we proceed still further, the phase shifts another 90 deg., so that the current in this region is almost 180 deg. out of phase with the current near the top of the antenna.

Figure 4 shows the current magnitude and phase angle as a function of the distance from the top of the antenna. It is shown that for a tower which is only one-quarter wave tall (90 deg.) the current all along the tower, including the base current, has essentially constant phase, so that the radiated field bears a simple phase relation with the current at the base of the tower. However, if the tower is close to one-half wave in

height (180 deg.), the current along most of the tower is substantially constant in phase, but the base current is very much out of phase with most of the current along the tower. The phase of the radiated field will be essentially determined by the large currents in the neighborhood of one-quarter wave from the top of the tower, so that the phase relation between base current and the radiated field may be a complicated and critical relation.

In the actual installation, one is then confronted with the problem of deciding just what magnitude and phase of base currents to use. This decision is important since the currents will be metered by ammeters placed in the lead at the base of the tower and by a phase monitor whose pickup coils are coupled to the same lead.

#### Choice of Three Methods

It seems that three separate means of adjusting the array could be followed. First one might simply guess at the desired networks needed, set up the system and examine the field pattern obtained. Then adjustments

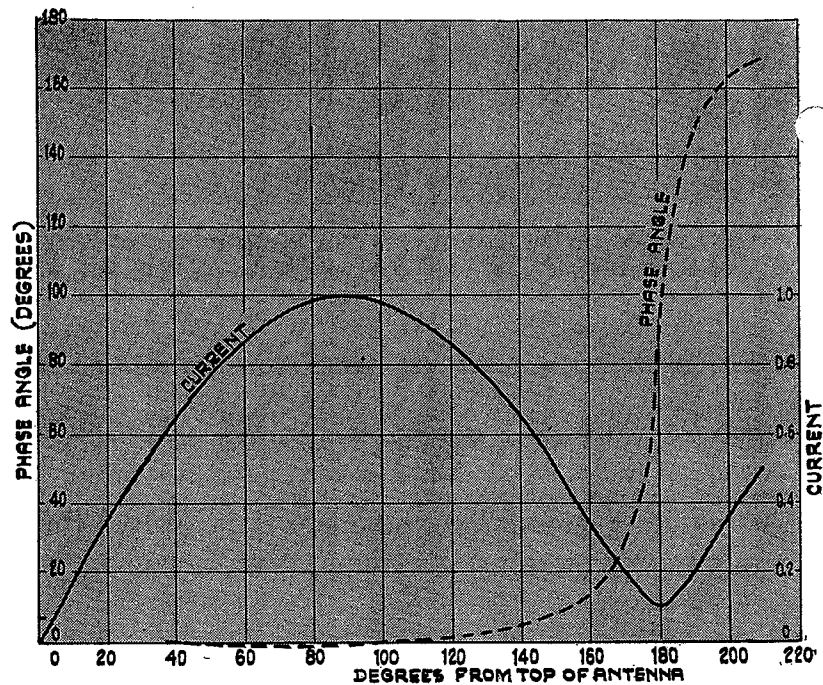


FIG. 4 (ABOVE)—Variation of magnitude and phase angle of total tower current with distance from the top of the tower

FIG. 5 (RIGHT) — Measuring points (A, B and C) used in the field measurement method, with each tower in turn being energized

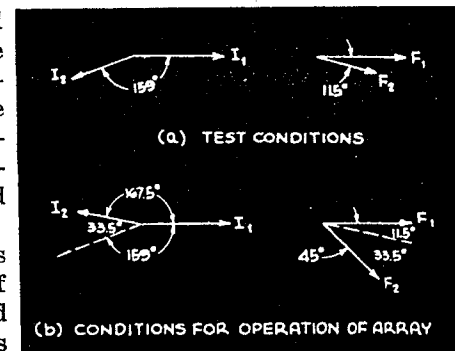
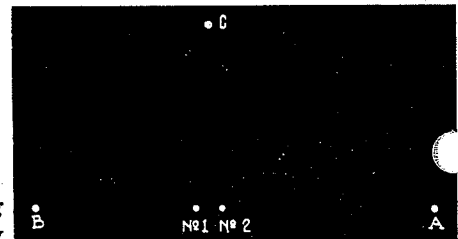


FIG. 6—Vector diagrams showing results of the initial calculations made with the measured values of field strength

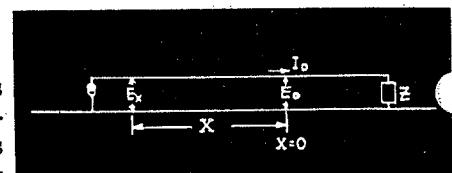


FIG. 7—Terminated transmission line upon which Eq. (16) and (17) are based



to correct the pattern could be made, which soon degenerates into a good deal of cut-and-try with the coupling and phasing networks. This first procedure requires a great deal of time, much trudging around the countryside with a field intensity meter, and the patience of Job<sup>1</sup>.

As a second means of adjustment, one might consider placing the phase monitor pickup coil on the tall tower about half-way up the tower, so that the correct phase would be monitored. This does eliminate the uncertainty of phase monitoring, but makes necessary the use of an extra trap circuit to bring signal from this coil to the phase monitor across the base insulator. To assist in establishing base current phase relationships for use in designing phasing networks, it is then necessary to place another phase monitor pickup coil at the base of the tower and measure the phase between the base current and the current at the middle of the antenna. This system was not used because of the mechanical difficulties of mounting the upper coil on the tower as well as the necessity of the trap circuit already mentioned.

The third possible means is that followed by the authors, in which the necessary relations were established from field measurements and were verified by the use of model antennas.

### Field Measurements

After the transmission lines to the two towers were completed, arrangements were made so that a small amount of power could be fed to either tower. Then a clear spot of ground on the line of towers and about three miles east of the array was selected and a field intensity meter located there. This is point A in Fig. 5. The distance to this point is unimportant as long as the distance from the array to point A is of the order of 20 times or more than the spacing between towers.

Since tower No. 2 is about one-quarter wave in height and therefore resonant if grounded, this tower was floated on its base insulator so that it would be distinctly out of tune. Then tower No. 1 was fed with a small amount of current. In this case, it was possible to get 3.0 amp into this tower. With the current held at this value, the field intensity at point A was measured, and found to be 78.0 mv

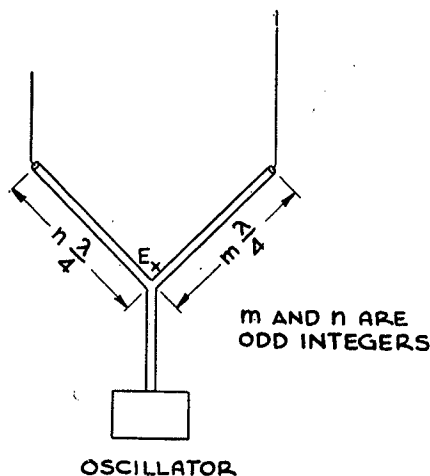


FIG. 8—Method of feeding model antennas

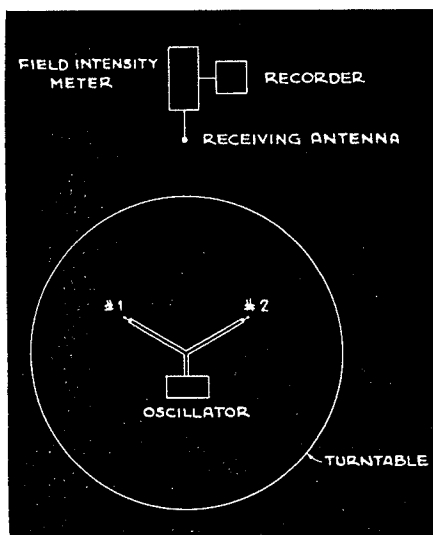


FIG. 9—Relationship of rotatable model antennas to measuring equipment

per meter. Thus,  $I_1$  is 3.0 amp and  $F_{A,1}$  (field at A due to current in No. 1) is 78.0 mv per meter. Thus,  $I_{A,1}$  is 3.0 amp and  $F_{A,1}$  (field at A due to current in No. 1) is 78.0 mv per meter.

The field at A is directly proportional to the current in the antenna, so that

$$F_{A,1} = K_{A,1} I_1, \text{ or} \quad (3)$$

$$K_{A,1} = \frac{F_{A,1}}{I_1} = \frac{78.0}{3.0} = 26.0 \text{ mv per meter at point A for 1 amp in No. 1} \quad (4)$$

No. 1 was then grounded to throw it out of action, and No. 2 was fed with 3.8 amp. The field at A was now found to be 65.0 mv per meter. Then  $I_2$  is 3.8 amp,  $F_{A,2}$  is 65.0 mv per meter, and

$$F_{A,2} = K_{A,2} I_2. \quad (5)$$

$$K_{A,2} = \frac{F_{A,2}}{I_2} = \frac{65.0}{3.8} = 17.1 \text{ mv per meter at point A for 1 amp in No. 2} \quad (6)$$

To meet the desired conditions implied by Eq. (2),

$$F_{A,2} = 0.6 F_{A,1} \quad (7)$$

Substituting Eq. (3) and (5) in (7), we obtain

$$K_{A,2} I_2 = 0.6 K_{A,1} I_1, \text{ or} \quad (8)$$

$$I_2 = \frac{0.6 K_{A,1}}{K_{A,2}} I_1 = 0.912 I_1 \quad (9)$$

We have thus found that to obtain the desired field pattern of the directional array, Eq. (9) must be satisfied.

Similar measurements at point B, Fig. 5 yield

$$K_{B,1} = 24.0 \text{ mv per meter at point B for 1 amp in No. 1} \quad (10)$$

$$K_{B,2} = 15.78 \text{ mv per meter at point B for 1 amp in No. 2} \quad (11)$$

Point B is about the same distance from the array as point A, but need not be equal to it, and again the distance need not be measured. These values serve as a check on Eq. (9) and yield

$$I_2 = \frac{0.6 K_{B,1}}{K_{B,2}} I_1 = 0.912 I_1 \quad (12)$$

The next step in the procedure is that of determining the correct phase angle of the base currents. No. 2 tower was measured and found to have a resistance of 69.0 ohms and an inductive reactance of 147.0 ohms. A capacitor with a reactance of 147.0 ohms was placed from the bottom of the tower to ground, with an ammeter in the lead from the tower to the capacitor. Thus tower No. 2 was tuned to resonance.

Power was then fed to tower No. 1. With the current in No. 1 equal to 6.5 amp, it was found that the current in No. 2 was 2.6 amp. Then the phase relation between these two currents was measured with an RCA Type 300-A Phase Monitor\*, and it was found that the current in No. 2 lagged the current in No. 1 by 159 deg. The fields at the measuring points were again measured. The following data has thus been accumulated:

$I_1$	= 6.5 amp
$I_2$	= 2.6 amp
$F_A$	= 140 mv per meter
$F_B$	= 144 mv per meter
$\phi$	= 233 deg
$K_{A,1}$	= 26.0 mv per meter per amp
$K_{A,2}$	= 17.1 mv per meter per amp
$K_{B,1}$	= 24.0 mv per meter per amp
$K_{B,2}$	= 15.78 mv per meter per amp

When the above values are substituted in Eq. (7a) and (8a) in the Appendix, we find  $\sin \Delta = -0.1935$ , and  $\cos \Delta = 0.965$ , so  $\Delta$  equals  $-11.5$  degrees.

The results of these calculations are shown at (a) in Fig. 6. At the time that the current  $I_2$  lagged  $I_1$  by

\* Brown, George H., and Swift, Gilbert, A Radio-Frequency Phase Meter with Many Uses, *Broadcast News*, p. 8, July, 1938.

<sup>1</sup> Job, i, 1-22; ii, 1-13.

159 deg., the field  $F_2$  lagged the field  $F_1$  by 11.5 deg. The results of turning  $F_2$  clockwise until it lags  $F_1$  by 45 deg. are shown at (b) in Fig. 6. This turning of  $F_2$  is accompanied by a turning of  $I_1$  through the same angle, so that we see that  $I_2$  actually leads  $I_1$  by 167.5 deg. when the fields are in the phase relation which will yield the desired field pattern. Thus, from this relation and Eq. (9), when

$$\bar{F}_2 = 0.6 \bar{F}_1 \angle -45^\circ \quad (13)$$

the base currents in the array must be related by

$$\bar{I}_2 = 0.912 \bar{I}_1 \angle +167.5^\circ \quad (14)$$

#### Model Antenna Measurements

To verify the conclusions reached by actual field measurements, models of the two KDYL towers were constructed. In order that the field pattern measured in the models might be of use in furnishing information, it was necessary that the base current relations be known. A simple property of transmission lines made this possible. Figure 7 shows a transmission line terminated in an arbitrary impedance, and fed with a generator at the other end. At some point ( $x=0$ ), we designate the current and voltage as  $\bar{I}_0$  and  $\bar{E}_0$ . Then at a point  $x$  units toward the generator the voltage is

$$\bar{E}_x = \bar{E}_0 \cos\left(\frac{2\pi x}{\lambda}\right) + j\bar{I}_0 Z_c \sin\left(\frac{2\pi x}{\lambda}\right) \quad (15)$$

where  $Z_c$  is the characteristic impedance of the line and  $\lambda$  is the wavelength. When  $x = \lambda/4$ ,

$$\bar{E}_x = j\bar{I}_0 Z_c \quad (16)$$

and when  $x = 3\lambda/4$ ,

$$\bar{E}_x = -j\bar{I}_0 Z_c \quad (17)$$

Stated more simply, the voltage at a point on a transmission line is equal to the product of the characteristic impedance and the current at another point which is an odd number of quarter waves further along the line. The voltage and current are in time quadrature. The ratio of current to voltage and the phase relation is independent of the value of the load impedance or the standing wave relationship on the line.

The model antennas were then fed from an oscillator by means of the concentric transmission lines shown in Fig. 8. In this figure,  $E_x$  is the common voltage at the junction of the transmission lines. Thus, if the two lines are each odd multiples of a quarter wave in length, and are equal in length, the two antenna currents will be forced to be equal in magnitude and in phase with each other, even though the antennas have widely different impedances and large mutual impedance exists be-

tween the antennas. If the two lines are each odd multiples of a quarter wave in length and differ in length by one-half wave, the currents in the antennas will then be equal in magnitude, but will be directly out of phase with each other (180 deg.).

The arrangement of Fig. 8 was placed on a rotating metal plate or turntable. A receiving antenna, field intensity meter, and an Esterline-Angus recorder were placed a good many wavelengths away from the transmitting antenna system, as shown in Fig. 9. The field intensity was thus recorded as a function of angle of rotation of the transmitting antenna system.

With the antennas fed with equal and in-phase currents, the broken curve of Fig. 10 was obtained. A number of field intensity ratios and phase angles were substituted in the field intensity equation to find the best fit with the theoretical curve. The solid curve on Fig. 10 represents the best fit, obtained from the formula

$$\frac{1 - 0.65 \angle -30^\circ + 233^\circ \cos \phi}{1.65}$$

When the antennas were fed directly out-of-phase and with equal currents, the broken curve of Fig. 11 was obtained. The best fit was obtained from

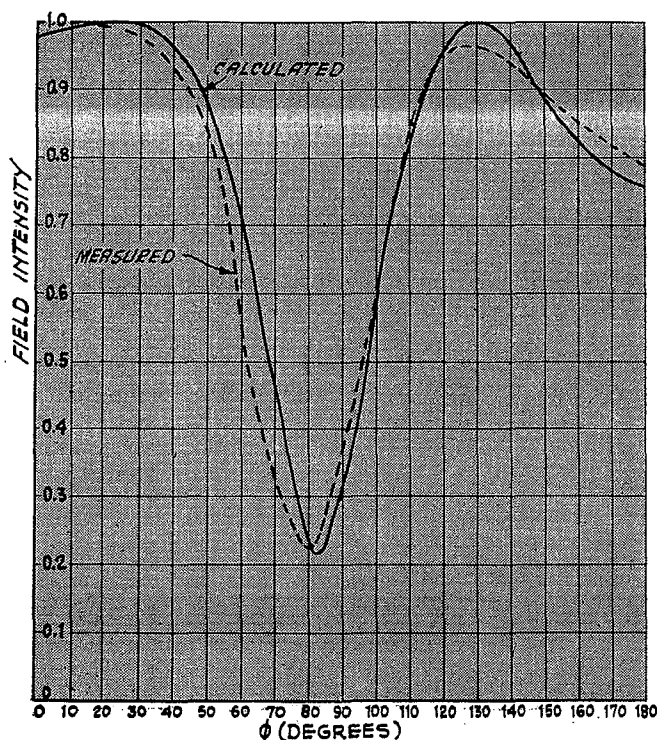


FIG. 10—Measured curve obtained when rotating model antennas were fed with in-phase equal currents, and best obtainable calculated curve

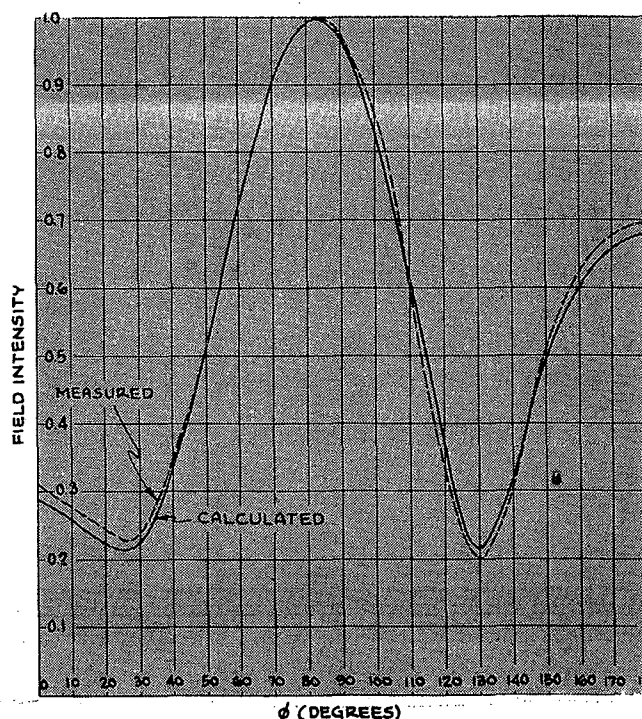


FIG. 11—Measured curve obtained when rotating model antennas were fed with out-of-phase equal currents, and best possible calculated curve

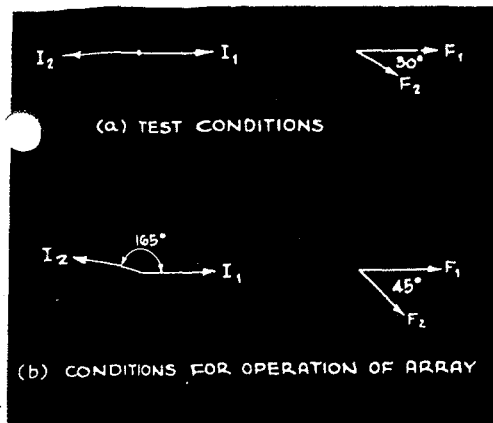


FIG. 12—Vector diagrams for model antenna method

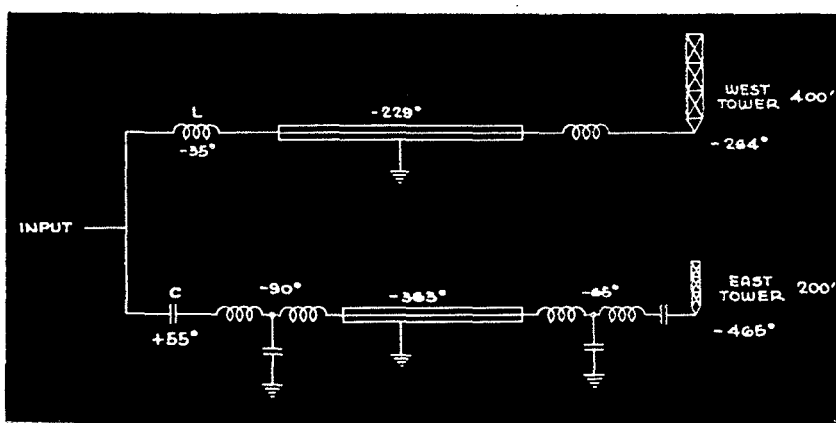


FIG. 13—Complete phasing and coupling finally used at KDYL

$$\frac{1 + 0.65 \angle -30^\circ + 233^\circ \cos \phi}{1.65}$$

This gives us the information that when  $\bar{I}_2 = \bar{I}_1 \angle -180^\circ$ , the effective radiating fields were  $\bar{F}_2 = 0.65 \bar{F}_1 \angle -30^\circ$ . These conditions are shown at (a) in Fig. 12. As was done earlier in the paper, we turn  $F_2$  in a clockwise direction until the desired 45-deg. angle is obtained between the fields. For this condition, we find that  $I_2$  leads  $I_1$  by 165 deg.

Since we desire the field ratio to be 1, and we have found that equal currents yield a field ratio of 0.65, the necessary current ratio is 0.6/0.65 or 0.923.

Thus, for operation of the array, we find that the base current condition shall be

$$I_2 = 0.923 I_1 \angle +165^\circ \quad (18)$$

#### Phasing and Impedance-Matching Circuits

The data previously obtained was sufficient to yield the mutual impedance between the antennas. With tower No. 2 resonated and grounded, and with tower No. 1 fed directly,

$$-\bar{I}_1 \bar{Z}_m = \bar{I}_2 R_{2,2} \quad (19)$$

Since  $\bar{I}_1$  is 6.5 amp at zero deg. phase angle,  $\bar{I}_2$  is 2.6 amp at  $-159$  deg., and  $R_{2,2}$  is the self resistance of tower No. 2 and is 69.0 ohms, we find that  $\bar{Z}_m$ , the mutual impedance between the antennas, is  $27.6 \angle +21^\circ$ .

Our next step is to determine the impedance of each antenna when the array is fed with the desired current ratio and phase angle. We postulate that the currents will be related by the relation

$$\bar{I}_2 = 0.912 \bar{I}_1 \angle +167.5^\circ$$

Then the impedance of tower No. 1 during operation of the array is

$$\bar{Z}_1 = \frac{V_1}{I_1} = R_{1,1} + jX_{1,1} + \frac{\bar{I}_2}{\bar{I}_1} \bar{Z}_m \quad (20)$$

Here  $R_{1,1}$ , the self resistance of No. 1, is 96.5 ohms, and  $X_{1,1}$ , the self reactance of No. 1, is  $-165.0$  ohms. When these values are inserted in Eq. (20) we find that

$$\bar{Z}_1 = 71.7 - j168.8 \text{ ohms} \quad (21)$$

Also,  $R_{2,2}$ , the self resistance of No. 2, is 69.0 ohms, and  $X_{2,2}$ , the self reactance of No. 2, is  $+147.0$  ohms, so the impedance of tower No. 2 during operation of the array is

$$\bar{Z}_2 = \frac{V_2}{I_2} = R_{2,2} + jX_{2,2} + \frac{\bar{I}_1}{\bar{I}_2} \bar{Z}_m = 44.0 + j130.3 \text{ ohms} \quad (22)$$

Since the array is fed with concentric transmission lines which have a characteristic impedance of 70 ohms, tower No. 1 was matched to its transmission line by the simple method of inserting a single inductance coil in series with the antenna to cancel out the capacitive reactance of 168.8 ohms. The effective resistance of No. 1 was so close to 70 ohms that a resistance-changing network was not considered necessary. A T network was placed at tower No. 2 to convert the impedance  $Z_2$  to a pure resistance of 70 ohms. This network

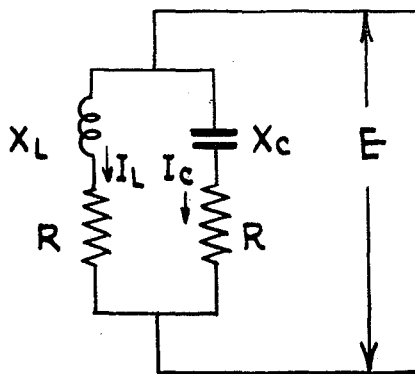


FIG. 14—Simple power-dividing network

introduced a phase delay of 65 deg. The complete phasing and coupling system is shown in Fig. 13. The 90-deg. lagging network at the input of the transmission line leading to tower No. 2 was used simply for phase shift, with no impedance conversion.

The inductance  $L$  and capacitance  $C$  in this diagram form an interesting yet simple power-dividing network. Its operation may best be described by referring to the circuit of Fig. 14. The two resistors  $R$  in this case each represent the 70-ohm loads furnished by the transmission lines and their associated networks. The reactance of the capacitor may be selected at random. We will designate the relative value with respect to  $R$  as  $M$ , so that

$$X_C = MR \quad (23)$$

Our remaining condition is that when once the capacitance has been set at a selected value, the inductance will be set to have the value

$$X_L = R/M \quad (24)$$

Then

$$\bar{I}_L = \frac{\bar{E}}{R + jX_L} = \frac{\bar{E}}{R + jR/M} = \frac{M\bar{E}}{MR + jR} \quad (25)$$

$$\bar{I}_C = \frac{\bar{E}}{R - jX_C} = \frac{\bar{E}}{R - jMR} = \frac{j\bar{E}}{MR + jR} \quad (26)$$

Dividing Eq. (25) by Eq. (26),

$$\bar{I}_L / \bar{I}_C = -jM \quad (27)$$

Thus we see that the current in the inductive arm always lags the current in the capacitive arm by 90 deg., and is  $M$  times in magnitude. This allows us to vary the power division between towers without changing the phase of the currents.

Another useful property of this  
(Continued on page 288)

# Broadcast Arrays

(Continued from page 123)

circuit it is revealed by adding Eq. (25) and Eq. (26) :

$$\bar{I}_L + \bar{I}_C = \frac{(M + j) \bar{E}}{MR + jR} = \frac{\bar{E}}{R} \quad (28)$$

This equation shows that, as long as Eq. (23) and Eq. (24) are satisfied, the input impedance of the circuit is a pure resistance of value  $R$ .

The power flowing into the inductive branch (power into tower No. 1) is

$$P_1 = I_L^2 R \quad (29)$$

while the power into the capacitive branch (power into tower No. 2) is

$$P_2 = I_C^2 R \quad (30)$$

or, dividing Eq. (29) by Eq. (30),

$$I_L/I_C = M = \sqrt{P_1/P_2} \quad (31)$$

But, from Eq. (21),

$$P_1 = 71.7 I_L^2 \quad (32)$$

and from Eq. (22) and the fact that  $I_2 = 0.912 I_1$ ,

$$P_2 = 44.0 I_2^2 = 36.6 I_L^2 \quad (33)$$

Dividing Eq. (32) by Eq. (33),

$$P_1/P_2 = 1.96 \quad (34)$$

so that Eq. (31) yields  $M = 1.4$ , and with  $R$  equal to the characteristic impedance of the transmission lines (70 ohms), the series capacitive reactance is 98.0 ohms, while the series inductive reactance is 50.0 ohms. When the circuit of Fig. 13 was installed, impedance measurements were made at the common feed point with the results shown in Fig. 15.

When these components were in-

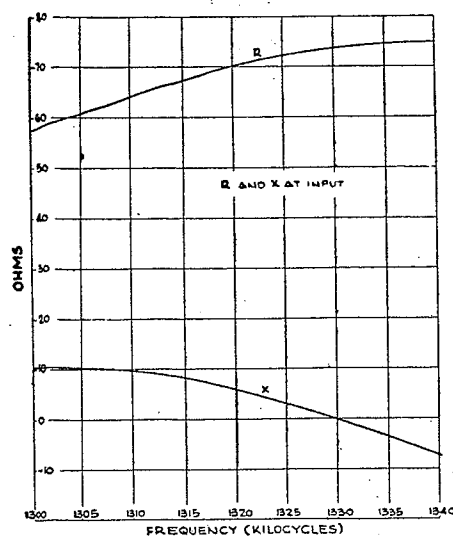


FIG. 15—Results of impedance measurements at the common feed point in Fig. 13 for frequencies on each side of the assigned frequency of 1320 kc

stalled, it was found that the current relations were

$$\bar{I}_2 = 0.88 \bar{I}_1 \angle +160^\circ \quad (35)$$

While these values were not in exact agreement with those predicted by the two methods described in this paper, it was known from calculation that the desired pattern could be obtained with this experimental relation. Accordingly, it was decided to measure the field intensity pattern before proceeding with fine adjustments. It was found that the pattern obtained was so close to the desired pattern that no further adjustments were necessary.

## Measured Field Intensity Pattern

While the mountains and rocky terrain around Salt Lake City are the cause of very high attenuation, there are also present some of the most highly conductive areas to be found anywhere. This highly conductive area lies to the northwest of Salt Lake City, and is caused by the lake itself and the several thousands of square miles of dried-up lake bed, rich in mineral salts. As a result, any particular type of directional pattern soon loses its identity, since the high attenuation to the east and south and the high conductivity to the northwest and west stretch and constrict the pattern all out of its original shape. In fact, the extremes of conductivity and attenuation are such that no directional pattern can remain looking like a directional pattern when measured on a radius of around 100 miles. As a practical result, the benefit derived from the use of a directional array is that the sky wave in the direction of co-channel stations has been reduced, thus permitting the use of higher transmitter power. There is, of course, the added consideration that in certain strategic directions, the high-angle radiation is increased. This helps provide a service in sections where the ground wave dies out rapidly.

Another point noted in proof-of-performance measurements was that measurements made on the east radials at distances up to about one and one-half miles from the towers showed less signal intensity than was indicated by the projection of the curve joining intensity measurements made further away, and conversely that measurements on the west radials showed just the reverse of this effect. These effects are

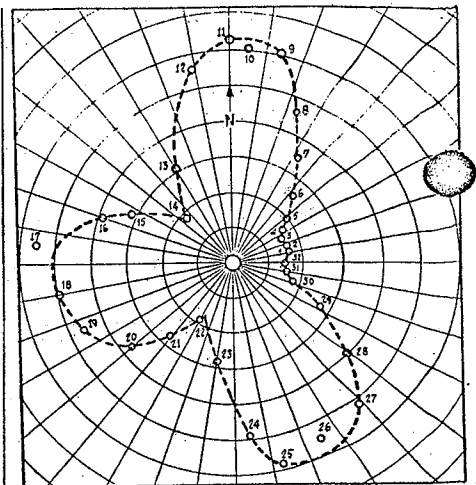


FIG. 16—Final measured polar radiation pattern obtained after antennas of KDYL were adjusted according to the procedures in this article. Compare with the initially desired pattern in Fig. 1

caused by the fact that the towers are spaced sufficiently that at distances of less than one and one-half miles the reciprocal distances from the measuring set to the two towers are unequal. Another contributing factor is the fact that Salt Lake City is located in a saucer-shaped valley with the transmitter near the lowest point. The differences in elevation are such that in a great many parts of the city it is possible to get a direct airline signal from the transmitter. Since the city lies toward the north and east of the transmitter site, where the ground level rises continuously, it is not possible to evaluate the true conductivity in these directions by radial field intensity measurements.

To overcome these effects and to obtain a horizontal field intensity pattern which was a function of the array constants and not of the terrain, it was decided to follow a comparison procedure. The first step was to float tower No. 2 and to feed tower No. 1 with 5 kw of power. Then field intensity measurements were made at 32 selected locations at various angles about the array. Each location was approximately two and one-half miles from the array. It was not necessary to measure the distance. It was only necessary that the point selected be far enough away so that the free space pattern could shape itself. Then the array was fed in the desired manner and the fields again measured at these selected points. At each particular point, the directional field intensity was then divided by the nondirectional field

intensity to secure a ratio which could be plotted to show the directional pattern. The results are shown in Fig. 16. Comparison with Fig. 1 shows that the desired pattern has been obtained.

#### Conclusion

The results obtained at radio station KDYL show that either the method of measuring fields of the actual array or the model method may be used to furnish data for designing the phasing and matching networks. The model method may appeal in some cases because the measurements may be made before the actual towers are erected. Also, where one tower is between 0.3 and 0.4 wavelength tall, neither grounding nor floating of this tower will entirely remove it from the picture when the field intensity per ampere factor of the remaining antenna is being measured on the actual antenna system.

On the model antenna system, either tower can be removed at will. However, the use of models requires a large area clear of obstructions, as well as a high-frequency oscillator, receiver, recorder and turntable. If all of this equipment is not readily available, one may be strongly attracted to the method of measuring field intensities on the actual array.

#### Appendix

Determination of the Effective Field Phase Angle from Field Intensity Measurements:

The field intensity at measuring point A (Fig. 5) is

$\bar{F}_A = \bar{I}_1 K_{A,1} + \bar{I}_2 K_{A,2} \angle + \Delta + kd$  (1a)  
and the field at measuring point B is

$\bar{F}_B = \bar{I}_1 K_{B,1} + \bar{I}_2 K_{B,2} \angle + \Delta - kd$  (2a)  
where  $\Delta$  is the angle by which the field from tower 2 leads the field from tower 1,  $d$  is the spacing between the towers,  $\lambda$  is free space wavelength, and  $kd$  is  $2\pi d/\lambda$  radians or  $360 d/\lambda$  deg. Then

$$F_A^2 = (I_1 K_{A,1})^2 + (I_2 K_{A,2})^2 + 2I_1 I_2 K_{A,1} K_{A,2} \cos(\Delta + kd) \quad (3a)$$

$$F_B^2 = (I_1 K_{B,1})^2 + (I_2 K_{B,2})^2 + 2I_1 I_2 K_{B,1} K_{B,2} \cos(\Delta - kd) \quad (4a)$$

Rewriting these equations, we obtain

$$\begin{aligned} \cos(\Delta + kd) &= \cos \Delta \cos kd - \sin \Delta \sin kd \\ \frac{F_A^2 - (I_1 K_{A,1})^2 - (I_2 K_{A,2})^2}{2I_1 I_2 K_{A,1} K_{A,2}} &= \end{aligned} \quad (5a)$$

$$\begin{aligned} \cos(\Delta - kd) &= \cos \Delta \cos kd + \sin \Delta \sin kd \\ \frac{F_B^2 - (I_1 K_{B,1})^2 - (I_2 K_{B,2})^2}{2I_1 I_2 K_{B,1} K_{B,2}} &= \end{aligned} \quad (6a)$$

Adding Eq. (5a) to Eq. (6a),

$$\begin{aligned} \cos \Delta \cos kd &= \frac{[F_B^2 - (I_1 K_{B,1})^2 - (I_2 K_{B,2})^2] + [F_A^2 - (I_1 K_{A,1})^2 - (I_2 K_{A,2})^2]}{4I_1 I_2 K_{B,2} K_{B,1}} \quad (7a) \end{aligned}$$

Subtracting Eq. (5a) from Eq. (6a),

$$\begin{aligned} \sin \Delta \sin kd &= \frac{[F_B^2 - (I_1 K_{B,1})^2 - (I_2 K_{B,2})^2] - [F_A^2 - (I_1 K_{A,1})^2 - (I_2 K_{A,2})^2]}{4I_1 I_2 K_{A,2} K_{A,1}} \quad (8a) \end{aligned}$$

These two equations may be used to find the sine and the cosine of the angle  $\Delta$ . The two equations are needed to determine the correct quadrant. When the spacing between the antennas is an odd multiple of 90 deg., Eq. (7a) disintegrates, and Eq. (8a) alone is useful. Under this condition, we may determine the sine of the angle  $\Delta$ , but we need further information to establish the correct quadrant. To find the quadrant, we must establish another measuring point, C, on a line which is perpendicular to the line of towers. At this point, the field intensity is given by the relation

$$F_C^2 = (I_1 K_{C,1})^2 + (I_2 K_{C,2})^2 + 2I_1 I_2 K_{C,2} K_{C,1} \cos \Delta \quad (9a)$$

or

$$\cos \Delta = \frac{F_C^2 - (I_1 K_{C,1})^2 - (I_2 K_{C,2})^2}{2I_1 I_2 K_{C,2} K_{C,1}} \quad (10a)$$

The angle  $\Delta$  is then determined by Eq. (8a) and Eq. (10a).

Another unfortunate case is that in which the towers are spaced an even multiple of 180 deg. apart. Then Eq. (8a) is useless. In this event, the measuring points A and B should each be displaced from the line of towers by an angle  $\phi$ . Then Eq. (7a) and Eq. (8a) may be used directly, except that  $kd \cos \phi$  is first substituted for  $kd$ .

# Adjustment of DIRECTIONAL ANTENNAS

A method of measuring resistance and reactance values at radio frequencies with an ordinary 3-inch cathode-ray oscilloscope while full power is being fed to the broadcast antenna. Width and height measurements of an elliptical pattern give the required constants

By **WILLIAM S. DUTTERA**

*Engineering Department  
National Broadcasting Company  
New York City*

**I**N the alignment of directional antennas there arise two types of problems. The first is that of securing the proper phase relations and amplitude relations between the various antenna currents. The second is that of tuning each antenna to match its transmission line, so no standing waves exist on the line.

The methods of arriving at proper phasing and current ratios are as varied as the number of engineers engaged in tuning directional antennas. It is not proposed to discuss this subject here, but instead to deal with the second part of the problem. Specifically, this involves determining the resistance and reactance which each transmission line sees at its antenna. The engineer wants to know if the line is "working" into too high or too low resistance, how much reactance is present and

whether this reactance is inductive or capacitive.

In some cases, particularly with antennas less than about 120 degrees high, it is possible to calculate the line termination networks with reasonable accuracy by a combination of ordinary measurements and proper application of circuit theory. With high antennas having distorted current distribution, or with a combination of high and low antennas, accurate calculations are not possible. It has heretofore been necessary in these cases to obtain final circuit adjustment by what almost becomes a trial and error method.

It must be noted that it is impossible to measure, by normal methods, the impedance of an antenna as a working part of a directional system. The measurement must necessarily be made without disturbing the system, under the condition of partial or full power. It is in this manner that the cathode-ray tube measurements to be described are made.

## Method Used in 60-cycle Circuits

In 60-cycle single-phase power circuits the load impedance can be found with meters measuring volts, amperes and power factor, connected as shown in Fig. 1. In brief, one

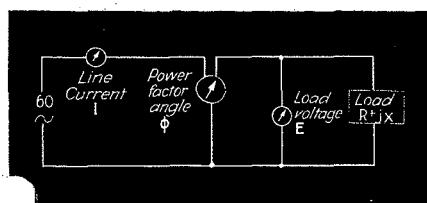
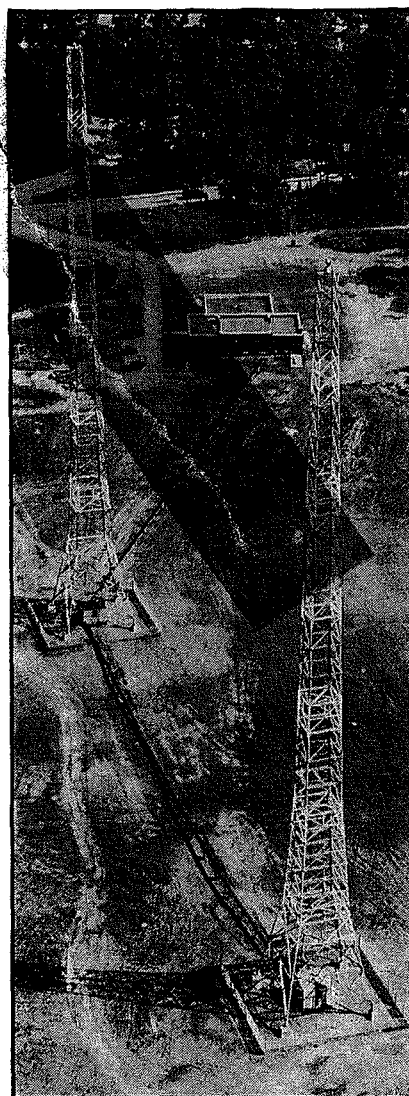


FIG. 1—Standard method of measuring the resistance and reactance of a load at power frequencies, using ordinary meters



This two-tower directional antenna system of station WEAJ in Port Washington, Long Island has been adjusted by the cathode-ray method described in this article. Two oscilloscopes were used, one in each under-the-tower tuning house

current flowing in the power factor meter is proportional to the phase and magnitude of the load current, and the other current is proportional to the phase and magnitude of the load voltage. The resultant action of the fields of these two currents upon a vane produces a displacement of the vane. A pointer attached to the vane indicates directly the phase angle between load current and voltage.

With  $E$ ,  $I$  and the phase angle  $\phi$  known, the resistance  $R$  and  $X$  are obtained from the following basic formulas:

$$R = \frac{E}{I} \cos \phi \quad X = \frac{E}{I} \sin \phi$$



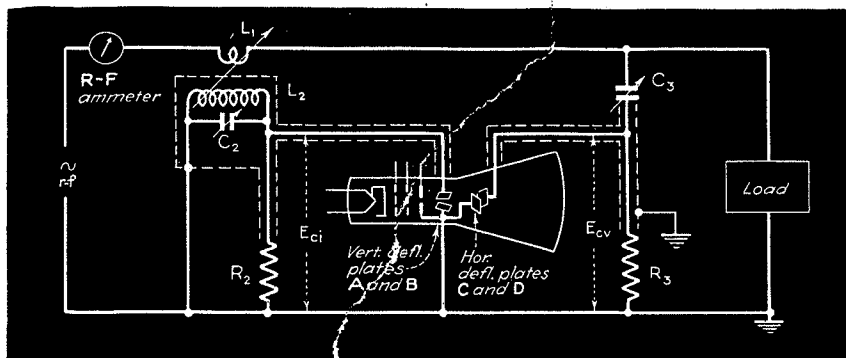


FIG. 2—Circuit for measuring the resistance and reactance of a load at radio frequencies under operating conditions. The cathode-ray tube may be part of an ordinary three-inch cathode-ray oscilloscope

### Cathode-ray Tube Method

In the r-f version of the procedure for determining load impedance, a cathode-ray tube is substituted for the voltmeter, ammeter, and power factor meter, as shown in Fig. 2. In this case it is simpler to use voltages instead of currents. A cathode-ray tube with electrostatic deflecting plates is chosen. A voltage proportional to the amplitude and phase of the load voltage is taken from voltage divider  $C_3R_3$  and applied to horizontal deflecting plates  $C$  and  $D$ . A voltage proportional to the amplitude and phase of the line current is secured from a well-shielded transformer  $L_1L_2$  and applied to vertical deflecting plates  $A$  and  $B$ .

Initially, the voltages applied to the two sets of deflecting plates are adjusted so that when the load is a pure resistance of known value the pattern on the tube is a circle of convenient size. Any other load then gives an ellipse, the orientation and dimensions of which permit calculation of the load constants.

Condenser  $C_3$  permits reducing the r-f voltage applied to the horizontal deflecting plates, and at the same time serves with  $R_3$  to provide approximately 90-deg. phase shift. The voltage due to line current is adjusted by varying the coupling between the primary and secondary of the transformer. It has been found in practice that no coil is necessary in the primary, since sufficient deflection generally can be obtained by coupling to the bus feeding the terminating equipment.

### Analysis of Circuit Relations

It can be shown that when secondary circuit  $L_2C_2$  is tuned to resonance, the following relation based on the simplified equivalent circuit in Fig.

3 will provide a sufficiently close approximation to actual conditions:

$$E_{ci} = E'_{ci} = -jI_2 X_2 = I_0 X_{12} X'_2 / R_1 \quad (1)$$

Here  $E_{ci}$  is the voltage on the cathode-ray tube due to the load current  $I_0$ . This means the cathode-ray tube voltage  $E_{ci}$  is in phase with the load current.

The load voltage part of the circuit is as shown in Fig. 4. In this case,

$$E_{cv} = E_0 R_3 \left[ \frac{R_3}{R_3^2 + X_c^2} + j \frac{X_c}{R_3^2 + X_c^2} \right] = E_0 R_3 K \angle \theta \quad (2)$$

where  $E_{cv}$  is the voltage on the cathode-ray tube due to the load voltage, and

$$\theta = \tan^{-1}(X_c/R_3)$$

In Fig. 5 is a vector representation of the cathode-ray tube voltages resulting from the load current and load voltage when the load is a pure resistance. A circular pattern is obtained on the cathode-ray tube screen when capacity  $C_2$  in Fig. 2 is adjusted until voltage vector  $E_{ci}$  takes the position designated as  $E''_{ci}$ . This adjustment is necessary for calibration because  $E_{cv}$  is not fully 90 deg. ahead of load voltage  $E_0$  ( $R_3C_3$  does not provide a full 90-deg. shift in phase). Adjusting  $C_2$

makes the vertical deflecting plate voltage  $E''_{ci}$  lag  $E_{cv}$  by 90 deg., and adjusting the coupling between  $L_1$  and  $L_2$  makes these voltages equal.

### Analysis of The Cathode-ray Pattern

It is well known that if equal voltages 90 deg. out of phase are applied to a cathode-ray tube the pattern will be a circle. If the voltages are unequal but 90 deg. out of phase the pattern will be an ellipse with its major axis on either the  $x$  or  $y$  axis, depending upon which set of deflecting plates has the larger voltage. If the phasing is other than 90 deg., the major axis of the ellipse will assume an intermediate position somewhere between 0 and 90 deg. with respect to the  $x$  axis.

An example of a general pattern is shown in Fig. 6. It is obtained with voltage  $E_{ci}$  (that due to the current) acting on the vertical deflecting plates, and voltage  $E_{cv}$  (that due to the load voltage) acting on the horizontal deflecting plates, as is shown in Fig. 2. The center of the ellipse is at 0. The ellipse intercepts the  $x$  axis at points separated by distance  $A$ . The total deflection along the  $x$  axis is  $A$  and the total deflection along the  $y$  axis is  $B$ . It can be shown that when this pattern is obtained from a given load under the operating conditions described above, the impedance of the load is

$$Z = \frac{R A_1}{B} \pm j R \frac{A}{B} \sqrt{1 - \left(\frac{A_1}{R}\right)^2} \quad (3)$$

Here,  $R$  is the load resistance which gives a circular pattern. The first term of this equation is the resistance of the load under operating conditions, and the second term is similarly the reactance of the load.

It will be noted that the reactive term has a plus or minus sign. If the cathode-ray tube connections are

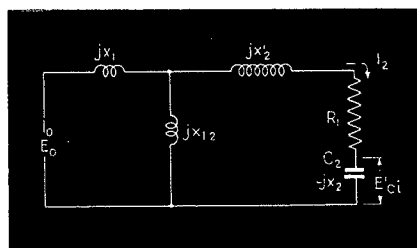


FIG. 3—Equivalent circuit for the current section of the cathode-ray measuring circuit. The voltage drop across the condenser depends on the load current value

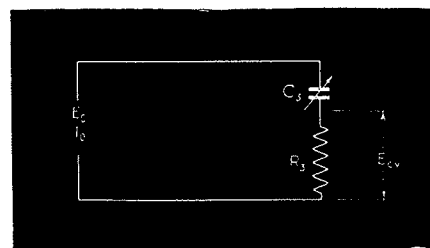


FIG. 4—Equivalent circuit for the voltage section is identical to the actual circuit since it is simply an r-f voltage divider connected across the load

so made that with a capacitive load the major axis of the ellipse is in the first and third quadrants, the sign of the reactive term is negative. It will be assumed that this is the case in the following examples. It will also be assumed that  $R$  is equal to 75 ohms. Patterns for four different types of loads, with resulting resistance and reactance values based on these assumptions, appear in Fig. 7.

### The Practical Application

In a normal application the tuning equipment which matches an antenna to its transmission line corresponds to the load shown in Fig. 2. The simplest method of adjusting  $L_2C_2$  and  $C_2$  involves starting with any one antenna and tuning its matching equipment so that it presents a resistive load  $R$  of the correct value for proper termination of the transmission line. This antenna only is then fed from the transmitter with approximately the same power it will carry when it is a part of the directional system. The condenser  $C_2$  is now varied until about half of full-scale deflection is obtained on the screen of the cathode-ray tube. Next,  $C_2$  is adjusted so that the major axis of the ellipse is along either the  $x$  or  $y$  axis, depending upon the relative voltages. Finally, the coupling between  $L_1$  and  $L_2$  is adjusted so that a circular pattern is obtained. This constitutes the calibration of the equipment. If similar equipment is used at all the radiators, the same procedure is followed at each.

All radiators are now fed together, and the three measurements indicated in Fig. 6 are made on the elliptical pattern of each antenna. From this data, the resistance and reactance of each antenna are calculated as previously explained.

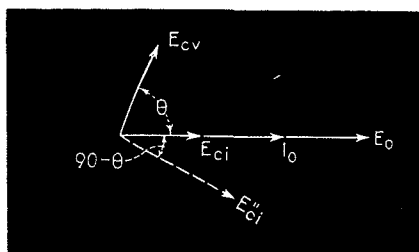


FIG. 5—The circular pattern required for calibration is obtained by detuning  $L_2C_2$  until the deflecting plate voltages are equal and 90 degrees out of phase

Coil  $L_2$  should be well shielded electrostatically, so it is excited only by the intended field due to line current. Likewise,  $C_2$  and its associated connections should not be subject to extraneous electrostatic fields. In order to assure this result, it is preferable to use coaxial leads for all connections shown with shielding in Fig. 2.

Resistors  $R_2$  and  $R_3$  in Fig. 2 are of arbitrary value. When these resistors are 200 ohms each, the power consumed by the measuring equipment is of the order of 25 watts. This is ordinarily low enough so that the equipment may be removed without any noticeable effect on the directional system. The values of  $R_2$  and  $R_3$  may be increased considerably in order to reduce power consumption.

Some types of cathode-ray oscilloscopes may have to be modified by the installation of r-f jacks on the sides of the unit, to permit short leads directly to the deflecting plates (internal amplifiers in the oscilloscope are not used.) Special provisions may also have to be made for the spot-centering voltages.

Where a cross-ruled scale is not provided with the oscilloscope, transparent graph paper will prove satisfactory and may be fastened to the face of the tube. This permits reading dimensional values directly without a ruler; units of measurement are unimportant so long as all three values are in the same units.

The true r-f power being fed to the antenna or load may readily be determined in this cathode-ray method if an r-f ammeter is inserted in the circuit, as shown in Fig. 2. Multiplying the resistive component of the load impedance by the square of the current reading gives the power.

In this application the degree of

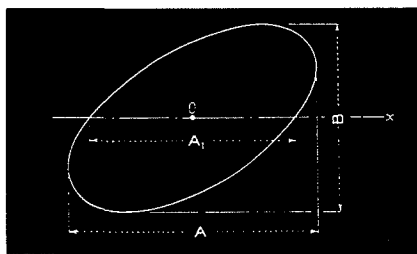


FIG. 6—Typical pattern. Resistance and reactance values are found by measuring lengths  $A$ ,  $A_1$  and  $B$  and substituting the results in equation 3

accuracy required is not very great. Consequently, such sources of inaccuracy as non-linear deflection or observational errors in reading the values of  $A$ ,  $A_1$  and  $B$  are not of a serious magnitude. A three-inch tube has been found to be satisfactory, but it is entirely feasible to obtain greater accuracy if needed.

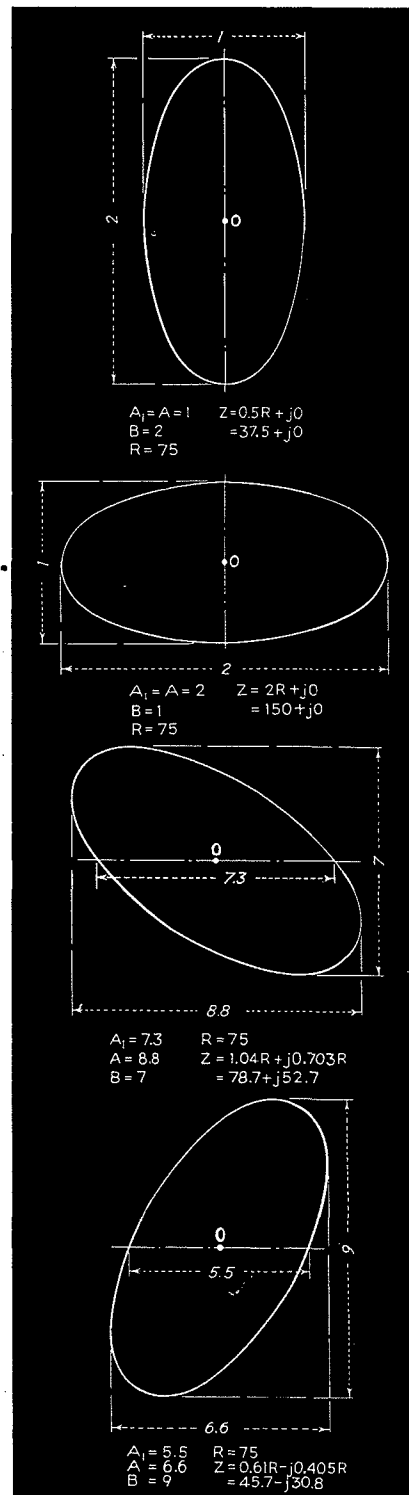
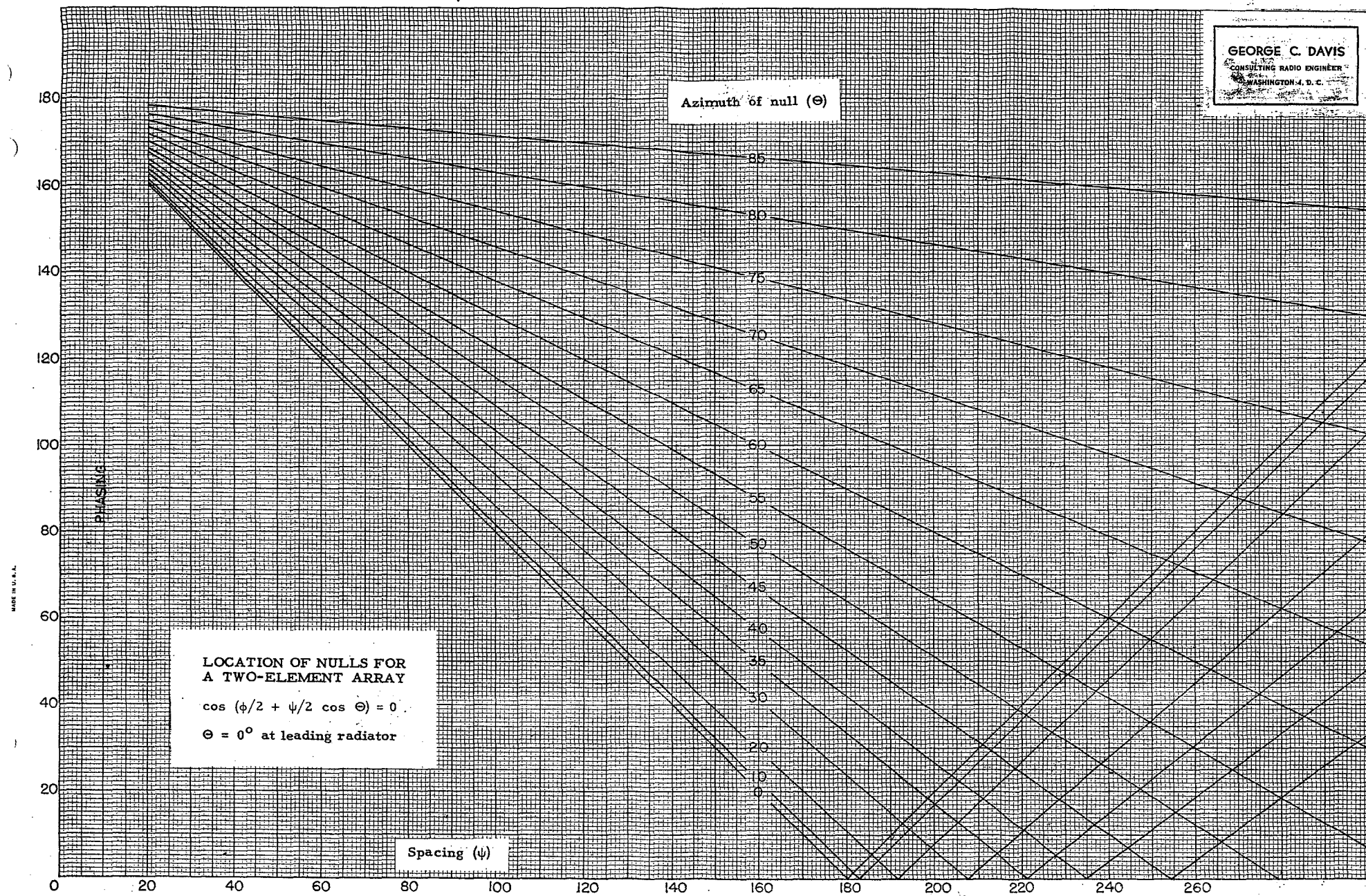


FIG. 7—Examples of cathode-ray patterns and corresponding r-f impedance values



GEORGE C. DAVIS  
CONSULTING RADIO ENGINEER  
WASHINGTON 4, D. C.



# Location of nulls

GEORGE C. DAVIS  
CONSULTING RADIO ENGINEER  
WASHINGTON, D. C.

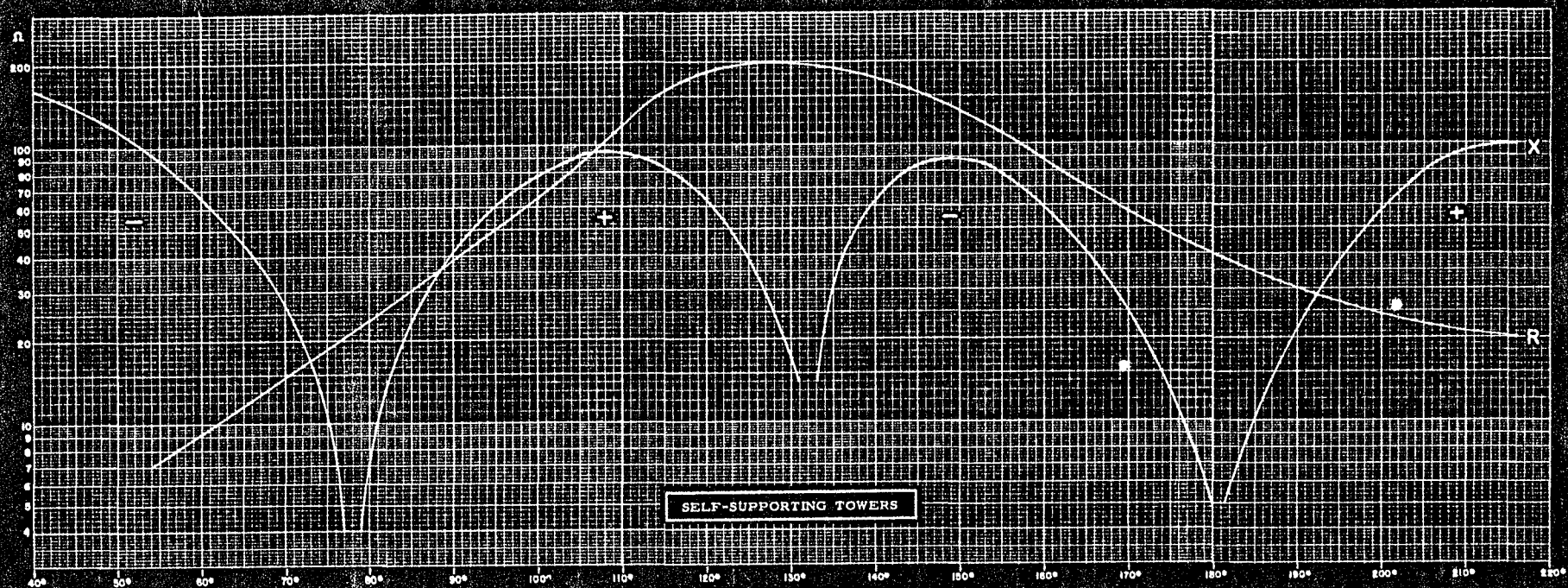
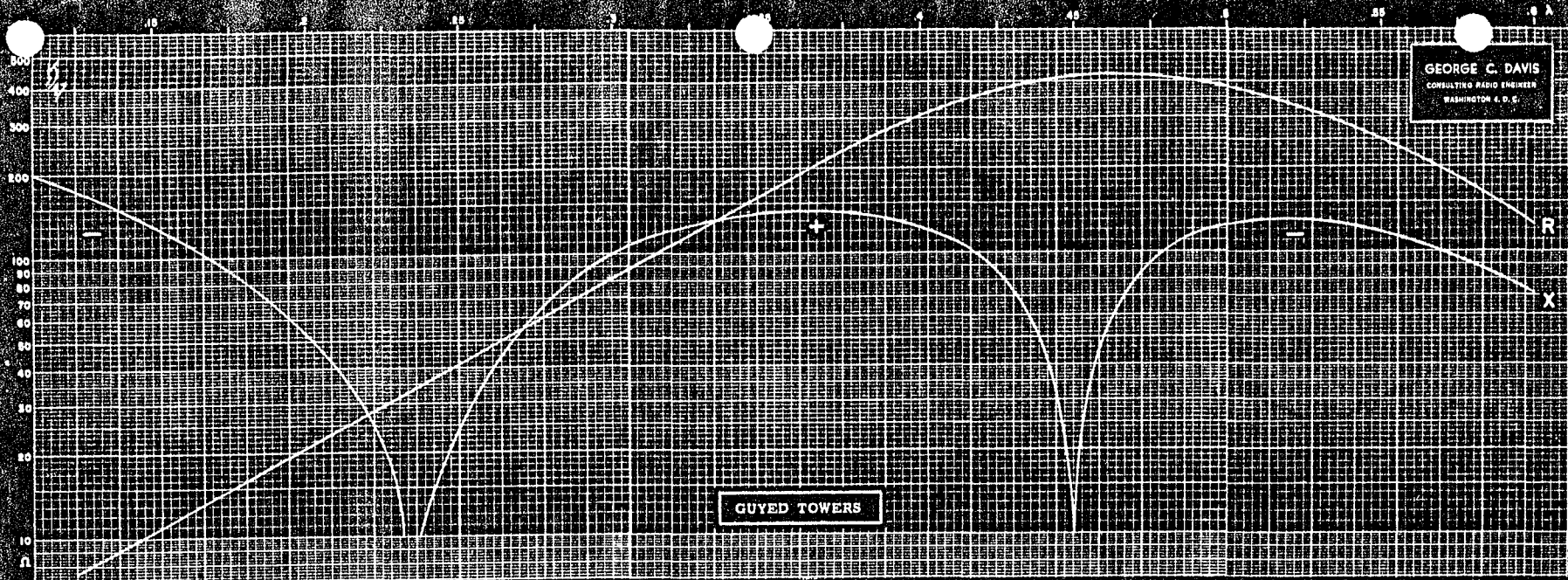
Azimuth of null ( $\Theta$ )

Phasing ( $\phi$ )

LOCATION OF NULLS FOR  
A TWO-ELEMENT ARRAY  
 $\cos(\phi/2 + \psi/2 \cos \Theta) = 0$   
 $\Theta = 0^\circ$  at leading radiator

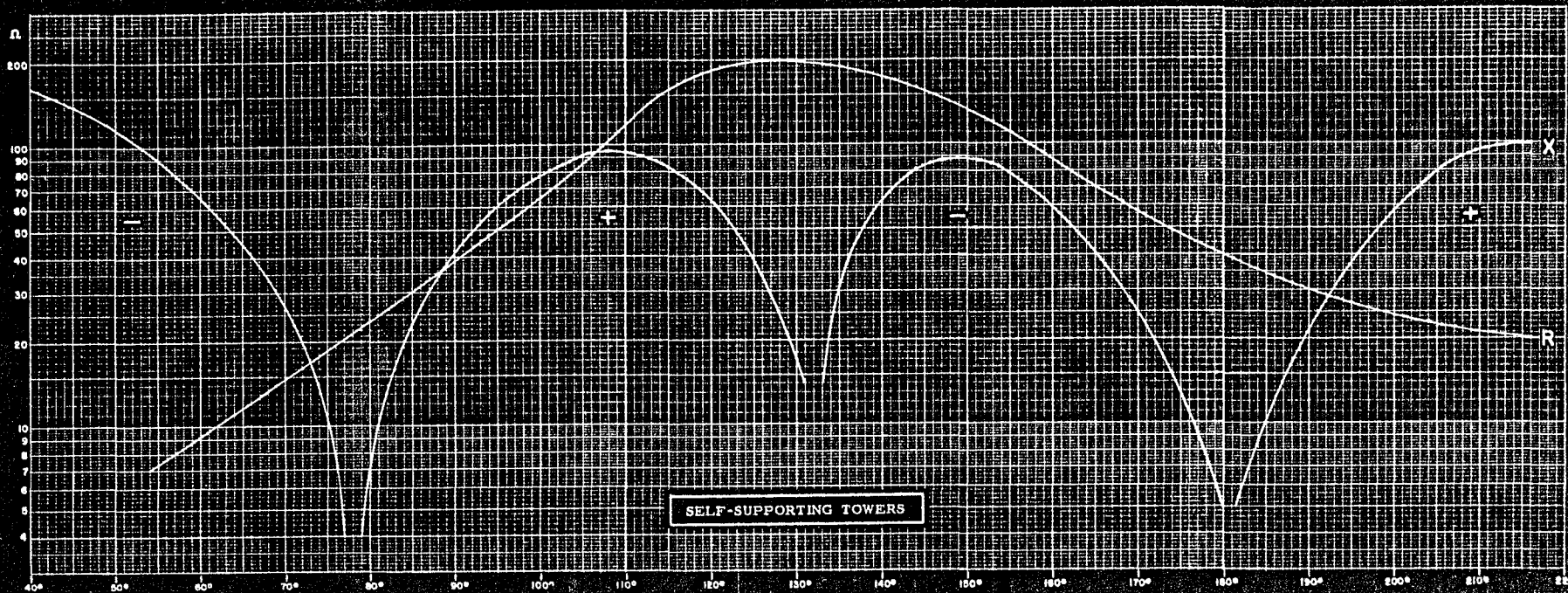
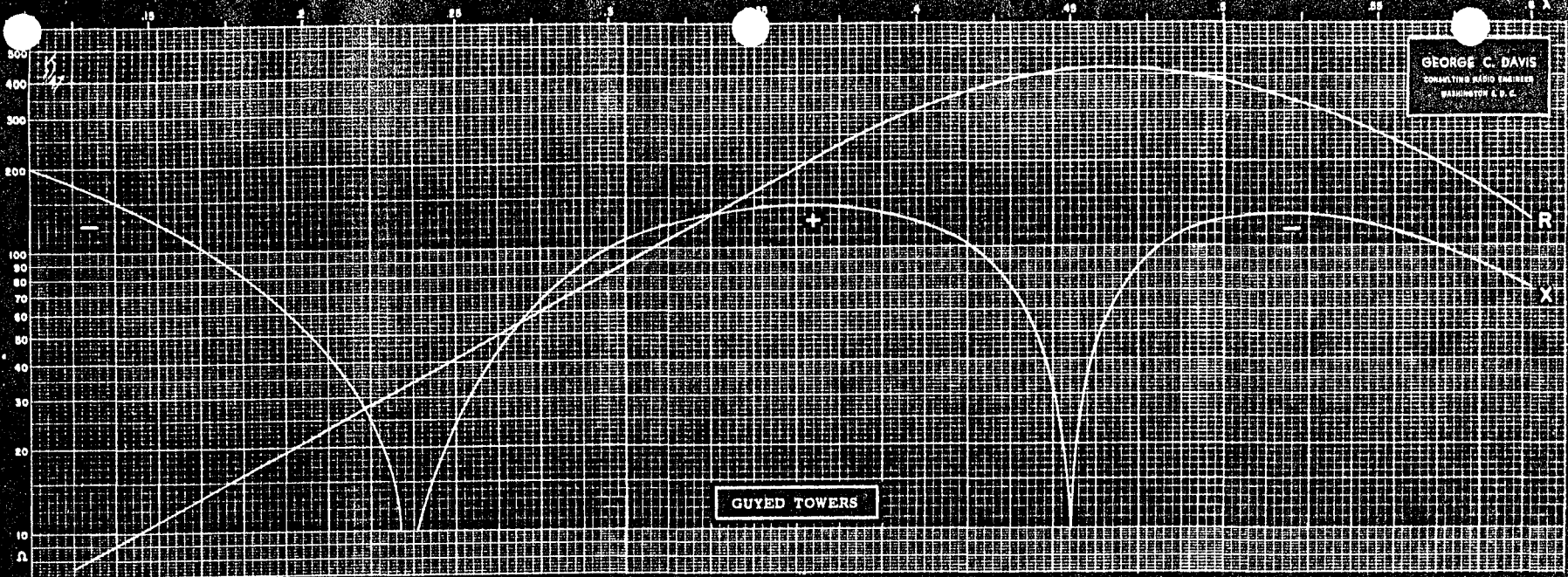
Spacing ( $\psi$ )





GRAPH OF RESISTANCE AND  
REACTANCE VERSUS TOWER HEIGHT  
(Based on I.R.E. Curves)

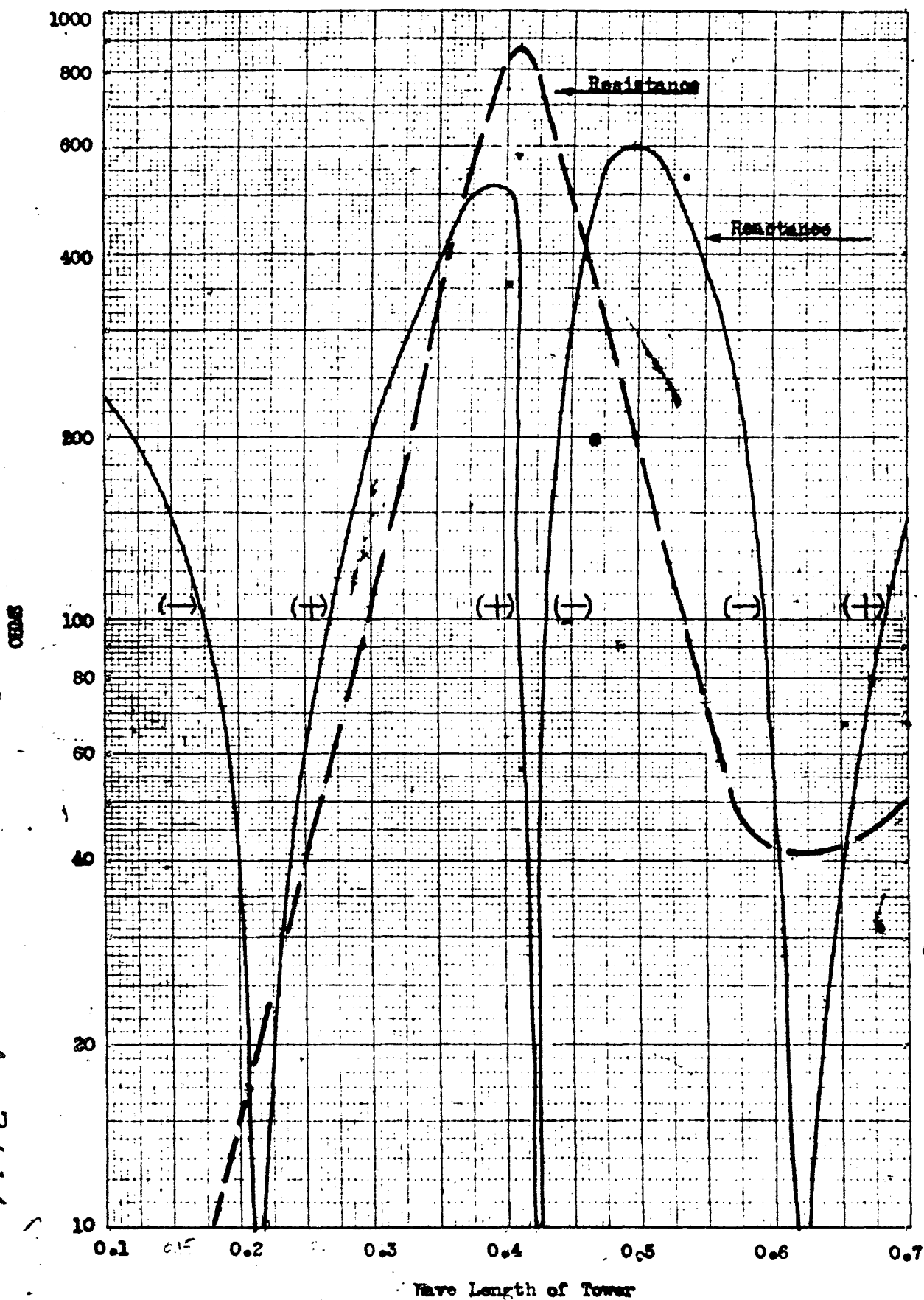
GEORGE C. DAVIS  
CONSULTING RADIO ENGINEER  
WASHINGTON, D. C.



GRAPH OF RESISTANCE AND  
REACTANCE VERSUS TOWER HEIGHT  
(Based on I.R.E. Curves)

# RADIATION RESISTANCE AND REACTANCE OF WINCHARGER RADIO TOWERS

A-3114



A-3114

# Retuning The Directional Antenna

**Don't lose sleep or get grey hairs over DA arrays that go astray. Retune and refile as outlined here.**

By Barry Atwood

THERE COMES A TIME in the life of many directional antenna arrays when, despite careful maintenance, the system no longer does what it was designed to do. The array simply fails to provide specified values of field intensity at one or more monitoring points.

The problem results from a change in the environment of the system, which encompasses not only the immediate vicinity of the array, but the entire coverage area. When excessive fields are noted, the station engineer usually tries to restore the monitoring point field intensity to normal by adjusting the antenna parameters, as close as possible, to the values specified on the station license. This usually does not work, since the conditions that existed when the array was first installed are no longer present. It thus becomes necessary to retune the antenna system.

The many articles covering the design of directional antenna systems prove to be of little value in the readjustment of an existing array. However, the method outlined, sometimes with slight variations, has been used by many consulting engineers in the final adjustment of an array after the design values have been established. Rare, indeed, is the directional antenna system that works exactly as designed with the original computed values. The refined "cut-and-try" procedure set forth in this article has no connection with any existing array, or any type of array, but rather serves to illustrate the principles involved.

## First, Check The Monitoring System

Before proceeding with any actual retuning,

**Barry Atwood** is chief engineer, WBKY-FM, University of Kentucky at Lexington.

test carefully to make sure that the monitoring system is functioning properly. The first thing is to be certain that you are in the exact location specified for the monitoring point. Most descriptions of monitor point locations pinpoint the location as an exact, specific number of feet from some fixed object, such as a road marker or telephone pole. Measure off the distance exactly, since an error of only 10 feet or so can cause an erroneous reading, particularly in deep null locations.

The second step is to check for correct antenna parameters. Check the station license, and make sure that the values of common point current, antenna phasing, and antenna base current ratios are as specified by the license. After you have verified that all of the antenna system parameters are correct, you should establish that the common point impedance is of the correct value. Actual measurements are best, but an approximate check can be made by computing the operating power by the indirect method.

Next, check the accuracy of the antenna base and common point ammeters. A meter of known accuracy should be inserted in series with each meter and a comparison of the two readings made.

The antenna phase monitor should also be checked. To do this, first remove all of the antenna sampling lines except for the line connected to the reference tower. Then, connect a capacitor (.01  $\mu$ F or so) from the reference tower input jack of the monitor to the next input jack. Set up the phase monitor to read the phase angle between the two inputs. You should read a 90° phase difference.

Now check the field intensity meter. This can be accomplished by direct comparison with another meter, preferably one that has been recently calibrated by the factory.

The last thing to be checked is to make sure that the monitoring points which yield high values of field intensity have not gone "bad." This is done by making field intensity measurements at other points on the radial to see how they compare with the readings obtained in the same locations during the original proof.

A very careful check should also be made of the antenna ground system. Usually, a fault in the ground system will cause the field intensity to drop at all monitoring locations since this type of fault reduces the antenna efficiency. However, a break in the main ground buss to one tower, or faults in the radials around one tower, may upset the pattern. If all of these checks prove positive, the only way to reduce the monitoring point field intensity is to retune the antenna system.

## Next, Get FCC Clearance, Prepare Work Sheets

Before proceeding with any actual tuning, it will be necessary to obtain the authority of the FCC. A telegram should be sent to the FCC in Washington, D.C., requesting authority to operate the antenna system at variance from licensed



parameters to facilitate retuning. Once this authority is granted, the telegram from the FCC is posted alongside the station license and you are ready to proceed with actual retuning.

First, prepare a work sheet such as shown in Fig. 1. The work sheet illustrated is for a three tower array with four monitoring points. Any array configuration and number of monitoring points can be accommodated. The first six vertical columns list the phasor control settings. The first three relate to the phasor current controls, and the next three relate to the phasing controls. For example, "1A" refers to the tower number one current control on the phasor, "2A" is for the tower number two current control, and so on. A two tower array would have only four columns for phasor controls, an array with four towers would have eight, and so forth.

The *horizontal* row, fourth from the top, lists the present dial settings of the phasor controls, since most phasors have some form of counter dial on the controls. After the entries for phasor controls, entries are made for monitoring points. Be sure to list *all* of the monitoring points specified by the station license. Under the location of each monitor point, list the maximum permissible field intensity in mV/m for that point. In the fourth horizontal row, list the readings obtained at these points. In this example, the reading obtained at the first monitoring point is above limits. The reading is 27 mV/m, and the maximum permitted is 18 mV/m. The object in this example is to reduce the field intensity at monitoring point number one to below 18 mV/m.

Under each column entry for phasor controls, is an entry of "cw" and "ccw." These describe the movements that will be made of each control, first in a clockwise direction, then in a counterclockwise direction. The object of the game is to move each phasor control first one way and then the other, and observe the changes that occur in field intensity at each monitoring point location. Under each monitor point entry, there is a space to record the change in field intensity that occurs as the number one tower current control is varied in a clockwise direction. Just below that entry, there is a space to record the change as the tower number one current control is varied in a counterclockwise direction, and so on for each phasor control and monitor point. The exact procedure to be used will be detailed later. Some phasors do not have any controls for the reference tower in the system, since the other controls can be varied with reference to this tower. If this is the case with your phasor, simply omit the entries for this tower.

### Obtain Needed Equipment

Before you start to turn the phasor controls, make sure you have the necessary equipment. You already have a field intensity meter and have tested it to assure yourself it is accurate. Do obtain fresh batteries for the instrument, since it will be in use quite a bit.

An accurate impedance bridge of some sort is also necessary, since readjustment of the array will change the common point impedance. The handiest type of bridge to have is the inline, operating impedance bridge. It is best to try to gain access to a standard rf impedance bridge, signal generator, and detector combination. It may be impossible to return to the original value of common point impedance, and it will be necessary to run new impedance curves in this case.

You should have some form of two-way radio system for communication between the transmitter phasor site and the various monitor points. For this type of operation, two engineers are required, one at the phasor controls, the other at the monitor points. One man can do the job without a two-way radio, but it takes a lot more time, particularly with a large array and many monitor points. If you obtain a two-way radio system, one unit should be set up at the transmitter site in some convenient location so that the transmitter engineer can converse by radio and manipulate the phasor controls. The second unit should be installed in a car. The mobile unit is then driven to the various monitoring point locations. Don't forget to keep a log of the transmissions made over the two way radio as required!

### Some Initial Considerations

Before taking off in the car for the first monitor point, a few facts should be kept in mind. The first thing to consider is the change that will occur in the common point impedance as the phasor controls are varied. It will be necessary, therefore, to determine the operating power by the indirect method for the time being, and the transmitter engineer must keep a close watch over the power output. He should determine the plate current required for the normal power output of the transmitter, and disregard the reading of the common point meter.

Another factor to consider is the weather. Rain has an adverse effect on many directional antenna systems. Even after a rain, the array may exhibit some instability until the area has thoroughly dried out. It is best to start actual retuning only after you have some insurance of favorable weather conditions.

The last factor to consider is the time of day that field intensity measurements are made. Measurements should be made only within the period of from two hours after sunrise to two hours before sunset. Skywave interference may preclude valid readings at other than these times, particularly when dealing with very low values of field intensity. This type of interference increases very rapidly after sunset. If the station is licensed for operation with a nighttime power less than that of the daytime power, adjustment should be made on high power. (This assumes that the actual phasor configuration is the same for both day and night operation, and only the transmitter power is changed, since both day and night patterns are dependent on the same phasor

PHASOR CONTROLS						MONITOR POINTS			
CURRENT			PHASING			#1 160°	#2 175°	#3 185°	#4 210°
1A	2A	3A	1φ	2φ	3φ	18.0 mv/m	7.0 mv/m	34.5 mv/m	22.0 mv/m
3425	5029	4096	6395	2435	7253	27.0	5.2	29.6	19.1
CW									
CCW									
	CW								
	CCW								
		CW							
		CCW							
			CW						
			CCW						
				CW					
				CCW					
					CW				
					CCW				

Fig 1 (left). Sample worksheet with initial conditions filled in.

Fig 2 (left below). Examples of data entered. No 2 phase control ccw one turn brings field intensity to within required readings.

Fig 3 (below). Log listing all new parameters.

PHASOR CONTROLS						MONITOR POINTS			
CURRENT			PHASING			#1 160°	#2 175°	#3 185°	#4 210°
1A	2A	3A	1φ	2φ	3φ	18.0 mv/m	7.0 mv/m	34.5 mv/m	22.0 mv/m
3425	5029	4096	6395	2435	7253	27.0	5.2	29.6	19.1
CW						25.8	5.0	28.0	19.3
CCW						27.2	5.3	28.9	18.3
	CW					26.2	5.9	29.0	18.0
	CCW					24.1	6.0	28.7	16.9
		CW				22.9	5.6	27.0	19.5
		CCW				24.0	6.6	26.8	20.1
			CW			16.3	7.5	27.3	18.9
			CCW			31.2	9.6	30.5	21.3
				CW		19.5	6.3	30.1	21.6
				CCW		15.1	5.0	28.3	18.5
					CW	29.6	9.8	36.6	25.3
					CCW	21.6	8.3	32.1	21.6

ORIGINAL READINGS						11/6/66
1A	2A	3A	1φ	2φ	3φ	
3425	5029	4096	6395	1435	7253	
TUNED TO						
1A	2A	3A	1φ	2φ	3φ	
3425	5029	4125	6395	1435	6283	
ADJUSTED TO BRING 1/3 BASE CURRENT						
RATIO AND 1/3 PHASE INTO LIMITS						
O.E.R.						



settings.) In the event the station uses a different pattern shape (not to be confused with pattern size) for day and night operation, this procedure will have to be performed twice, once for each pattern. Such a system would have two separate phasors, or a switching system to change phasor components. For stations that are nondirectional during the day, and directional at night, adjustments will have to be made on the directional antenna system at the nighttime power, but during the day.

#### The Actual Tuning Procedure

With the transmitter engineer at the phasor controls and two-way radio, the field operator should proceed to the first monitor point. The car should be driven as close as possible to the actual point of measurement and a reading taken. Now, set the field intensity meter on the roof, or hood of the car, and rotate the meter for maximum pickup, as in making normal field measurements. (The meter should be placed somewhere on the car that will permit the operator to watch the meter and converse with the transmitter engineer over the two-way radio.) Adjust the gain control of the meter to give the same reading as was obtained on foot at the exact monitor position.

The field operator now instructs the transmitter engineer to vary the first phasor current control one turn in the clockwise direction. When the control has been moved to this position, the transmitter engineer informs the field operator that the move has been made. The field operator now enters the field intensity reading in the appropriate place on the work sheet.

For example, let us assume that the field operator has gone to the first monitor point and measured 27 mV/m. This reading is entered under monitor point number one on the work sheet as shown in Fig. 2. The field operator then instructs the transmitter engineer to move the tower number one phasor current control one turn in the clockwise direction. Now, let us assume that after the transmitter engineer has made this move, that the field operator now reads 25.8 mV/m. He would then enter this reading directly below the original reading of 27 mV/m as shown in Fig. 2.

After the reading has been logged for the first move, the field operator instructs the transmitter engineer to move the first current control one turn in the counterclockwise direction from the original position. (This actually requires him to move the control two turns in the counterclockwise direction, since the object is to get one turn counterclockwise past the original setting of the control.)

After recording the ccw readings, the field operator now instructs the transmitter engineer to return the control to the original setting. (This would be one turn in the clockwise direction.) The field operator should now verify that the field intensity is the same value as originally read. For the example given in Fig. 2, the reading

should return to 27 mV/m. The reason for this check, is that some phasor controls may exhibit some backlash and may not return to the exact same spot on the coil, even though the counter dials indicate the same reading. If this occurs,

Fig. 4. Work sheet for antenna proof of performance measurements.

215° loc #	day orig	day 1966	day ratio	nite orig	nite 1966	nite ratio
1102	125	118	.944	56	42.5	.759
1103	73	73	1.0	32	42.8	1.34
1104	82	73	.89	35	30.9	.883
1105	55	51	.928	23	22.8	.992
1106	69	69	1.0	30	28.5	.861
1107	42	42	1.0	26	26	1.0
1108	36	22	.613	23.2	16.3	.704
overall radial average			.942			.966
daytime measurements made 9/20/66						
nighttime measurements made 9/23/66						
220° loc #						
1201						
1202						
1203						
1204						
1205						
1206						
1207						

return to this value.

If it is not possible to return to the original value, try to choose some value that will give some leeway for future adjustment in the position of the coil taps. Also, try to choose some value that you can live with, that is to say, a value that yields a convenient figure of common point current. Be sure that this new value of common point current will fall within the range of the common point ammeter as required by FCC rules. If a new value of common point impedance is established, it will be necessary to obtain authorization from the FCC to determine operating power by the indirect method, pending approval of the new common point impedance measurement report.

### Determine New Parameters

With the common point impedance adjusted, and the antenna tuned to the new values, it would be wise to make up some type of table listing all of the new parameters. This list should include the measured common point impedance, common point current for direct method of power measurement, transmitter plate voltage and current, antenna phase monitor readings, remote meter readings, and antenna base current readings.

It is best to take an average of several base current readings for each tower, taken every hour or so over a period of several days, and establish this average of each tower as the base current.

COMMON POINT IMPEDANCE

STATION CALL & LOCATION:  
 POWER, MODE OF OPERATION AND FREQUENCY:  
 DATE OF MEASUREMENT:

**Fig. 5** Impedance characteristic plot.

January, 1968 — BM/E

This chart should also list the limits for all parameters. It will also be found helpful to maintain a running log of any future phasor adjustments. A stenographer's note pad is quite handy for this purpose. Readings of phasor control settings should be entered in this book before any adjustments are made. The phasor dial readings after adjustment should also be entered, along with the date, explanation of why the phasor was adjusted, and the initials of the engineer who made the adjustments. This log will provide the station engineer with some means of accurately returning to original phasor settings, should anything go wrong. It is a good idea to log any adjustments that are made of the common point impedance, or of antenna tuning units. Fig. 3 illustrates one format for such a log.

### Running the Proof

With the array in final adjustment, it will now be necessary to run a "skeleton" proof of performance of the antenna system to prove that the pattern is basically unchanged. Field intensity measurements will have to be made on at least five consecutive points on each radial. These measurements will have to be made in the same locations as measured in the original antenna proof of performance. It is best to make at least seven measurements, since some readings may prove to be invalid and have to be discarded.

A work sheet such as shown in Fig. 4 should be prepared. Graph paper with one-quarter-inch squares is ideal for this form. In the left hand column, list the radial bearing, and the location numbers obtained from the original proof. Vertical columns should be established to list readings obtained in the original proof, and the present readings for each pattern. The average of the original and the present readings should be noted for each location, and the overall average for the entire radial should also be tabulated. Some locations may yield an average which is abnormally high or low, but these readings may be discarded, so long as you end up with readings for at least five consecutive points. After all of the radials are measured, the average of each radial should be checked. If the average of two or more radials falls outside the limits of 0.8 to 1.2, further retuning will be necessary. This is rather unlikely, however. As illustrated in Fig. 4, the reading obtained at location number 1108 on the 215° radial was discarded, since it would upset the average.

The dates that the readings are made should also be entered on the work sheet. Remember to make all field intensity measurements within the period of from two hours after sunrise to two hours before sunset. Before starting out each day, make measurements at the monitoring point locations to insure that the adjustment of the array has not shifted.

After all of the radials have been run, tabulate the overall average of all the radials. This is the average of all the radial averages. After the

skeleton proof is completed, the common point impedance curves should be run. This step can be omitted if it was found possible to return to the original value of common point impedance. The impedance should be measured at the station frequency in steps of 5 kHz out to 30 kHz, either side of the station frequency. These measurements should be compiled in columnar form, and curves of the impedance characteristic plotted as shown in Fig. 5.

### Compiling the Proof

After all of the necessary data has been taken, it should be assembled into neat order. The skeleton proof of performance should be submitted as one report, and the common point impedance as a separate report. These reports may be submitted in the form of three-ring notebook. The skeleton proof, and the common point impedance report should contain a signed and notarized affidavit, signed by the engineer who made the measurements. This affidavit should contain the qualifications of the engineer who made the measurements, a statement that he made the measurements, and his relationship to the station.

The next page of each report should contain a description of the method used in making the measurements, the name of the manufacturers of the instruments used, and the rated accuracy. The date, accuracy, and by whom each instrument was last calibrated, along with the serial number of each instrument should also be included.

The next page of the skeleton proof should contain a tabulation of all the antenna and transmitter final stage parameters. The skeleton proof is then completed with a separate page for the readings of each radial, including all of the information shown in Fig. 4. Readings of abnormal averages should be omitted from the report.

The final page of the antenna skeleton proof of performance is a tabulation of the field intensity at all of the monitoring point locations. The common point impedance report is then completed with a tabulation of the measured impedance at each frequency, and a graph of the tabulated data as shown in Fig. 5.

### File for Modified License

After all of the reports are completed, the station should file for a modified station license. This is done on FCC Form 302. This form and all reports must be filed in triplicate. ●

Before you can retune you may have to detune powerline poles and other structures. An article on the subject will appear in a forthcoming issue.

# Design Charts for Low-Frequency Antenna Efficiency

*Nomograms help estimate conversion  
efficiency from transmitter to radiated power*

By GEORGE J. MONSER,

American Electronic Labs,  
Lansdale, Pennsylvania

IN LOW-FREQUENCY SYSTEM DESIGN, a knowledge of the radiation capability of the antenna is necessary. The designer must be able to predict the conversion efficiency from transmitter output power to useful radiated power, compatible with the information bandwidth. The nomograms in Fig. 2 and 3 help estimate this conversion efficiency. They should be regarded as an extension of an earlier reference sheet.<sup>1</sup>

Figure 1A illustrates a technique for coupling the electrically short antenna to the final output stage of the transmitter.

Given a certain antenna size, operating frequency and bandwidth requirement, the technique finds attainable conversion efficiency. Conversely, for a given transmitter capability, radiated power and information bandwidth, the technique finds conversion efficiency and antenna

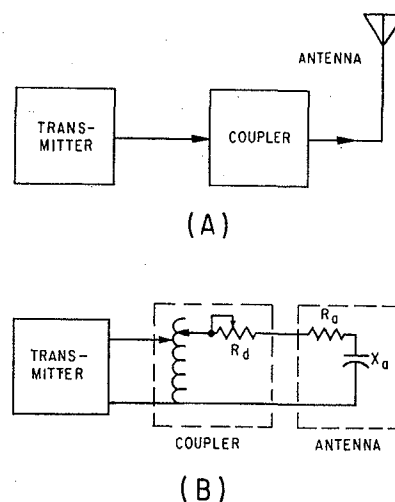


FIG. 1—Block diagram shows coupling of final output stage of transmitter to the electrically short antenna

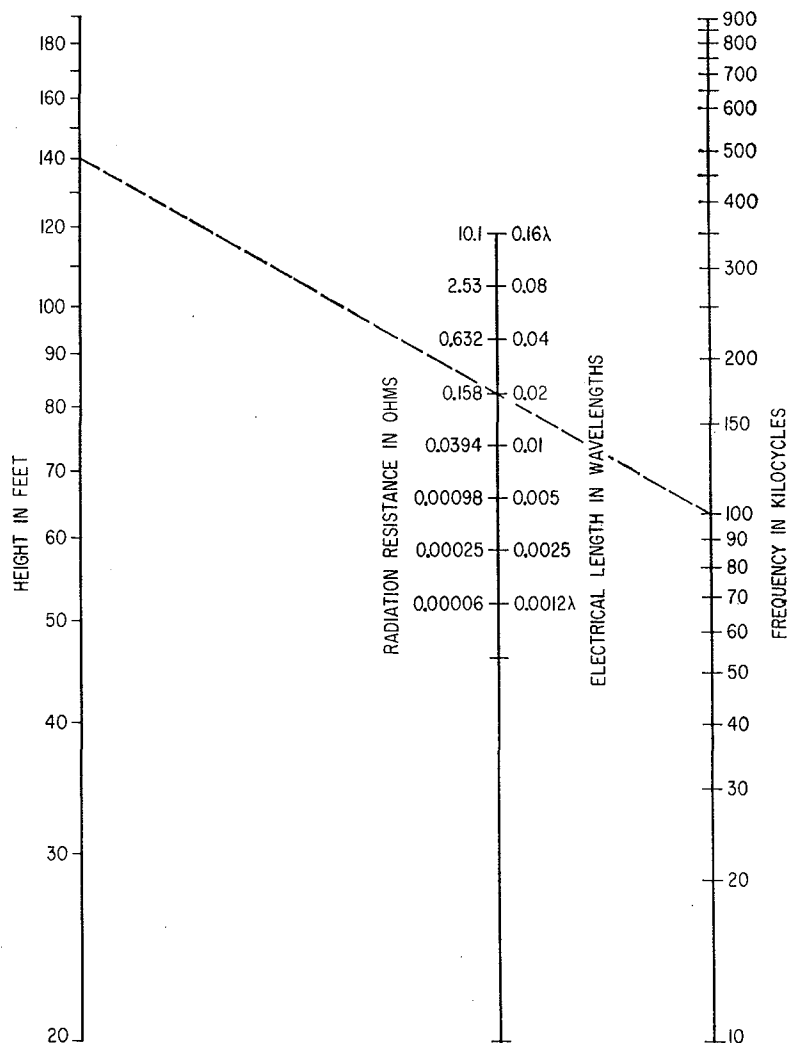


FIG. 2—Radiation resistance nomogram for vertical short monopole antenna, valid for lengths up to 0.1 wavelength

size in a given case.

Under the tuned condition in Fig. 1B, the reactance of the tuner is adjusted to equal the antenna reactance, and  $Q = f_o/BW \equiv X_a/R$ , where  $f_o$  is the operating frequency,  $BW$  the circuit bandwidth,  $X_a$  the antenna reactance at frequency  $f_o$ ,  $R = R_a + R_d$  the total circuit resistance,  $R_a$  the radiation resistance and  $R_d$  the added dissipative resistance.

To use the equation, antenna reactance is expressed as  $X_a = 31.9 (\lambda/h)$  where  $(\lambda/h)$  is the reciprocal of the antenna electrical length. This was derived and presented in Fig. 4 of Reference 1. It is valid for short, thin vertical monopoles, that is, when electrical length is less than  $\lambda/16$  and for height-to-radius ratios 60 to 90.

Normalized bandwidth  $\beta = BW/f_o = (R_d/31.9) (h/\lambda) + 12.6 (h/\lambda)^3$ . Normalized efficiency of conversion  $\eta = R_a/(R_a + R_d) \equiv 12.6 (h/\lambda)^3/\beta$ .

The nomograms relating the variables of these equations are given in Fig. 2 and 3. On each nomogram is a reference construction line.

As an example of a problem solution, suppose that 4 watts of radiated power are required, and a bandwidth of 3 Kc is required. Assume the transmitter output at 100 Kc is 1,000 watts. Size of the vertical stub antenna is to be determined, assuming no antenna top loading.

First compute normalized bandwidth,  $\beta = 0.03$ , or 3 percent.

Next compute efficiency  $\eta = P_{\text{radiated}}/P_{\text{input}} = 0.004$ , or 0.4 percent.

Enter Fig. 2 with these values and read  $h/\lambda = 0.02$ , and  $R_a = 0.16$  ohms.

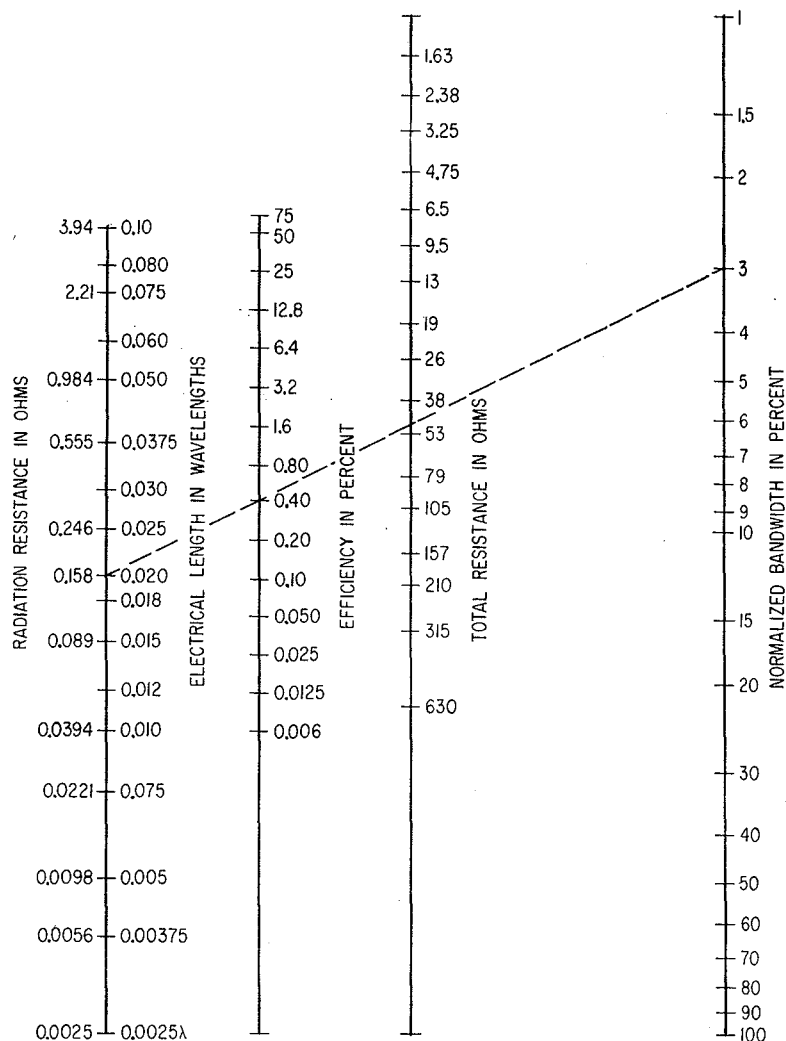


FIG. 3—Nomogram for determining efficiency in percent of short monopole antenna, valid for lengths up to 0.1 wavelength

Enter Fig. 3 with this value and the operating frequency, 100 Kc, and read the antenna height as 140 feet. The total circuit resistance can be estimated from Fig. 2 as  $R \approx 40$  ohms.

Entries into the nomograms can be made in different order, depending on the known and desired information. Approximations were made in the deriva-

tion, restricting usage to electrical lengths less than  $\lambda/16$  and thin vertical antennas. Accepting a small loss in accuracy, electrical lengths up to  $0.1 \lambda$  can be considered.

#### REFERENCE

- (1) G. J. Monser, Design Charts for Low-Frequency Antennas, *ELECTRONICS*, 26, p 86, Mar. 18, 1960.

# Effect of Feed on Pattern of Wire Antennas

Measured radiation patterns for straight wire antennas of various lengths from a half wavelength to three wavelengths and fed at various points are presented herewith. They show that feed point affects the number, orientation, and magnitude of the lobes

By  
**D. C. GLECKNER**

*Antenna Laboratory  
The Ohio State University Research  
Foundation  
Columbus, Ohio*

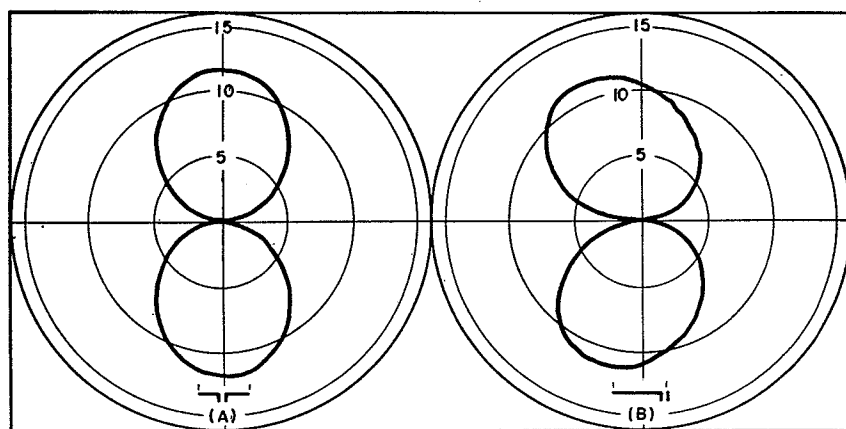


FIG. 1—Radiation from a half-wavelength antenna. Antenna outline with each pattern shows feed point; outline marked off in half wavelengths

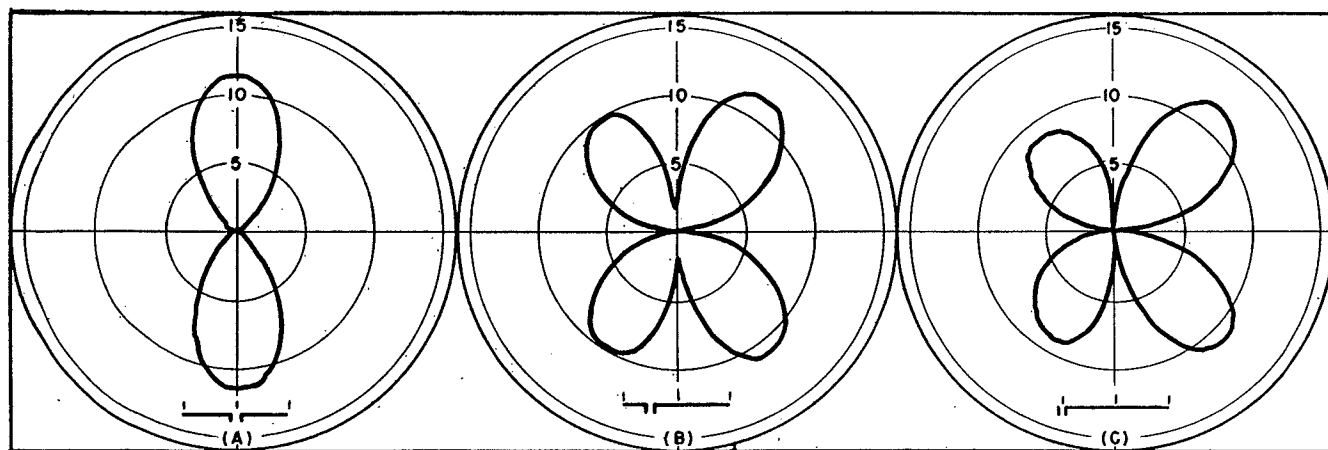


FIG. 2—Shape of field strength pattern of an antenna one-wavelength long depends on the location of the feed point

**R**ADIATION PATTERNS of wire antennas one-half wavelength or longer are dependent on the position of feed used to excite the antenna. There has been considerable confusion in published handbooks

as to just how a certain length antenna is fed to get the desired pattern. This investigation was made to determine the effects of the position of feed upon the pattern of wire antennas.

No attempt will be made to explain the results except to state that the current distribution differs appreciably from a sinusoidal distribution for certain off-center feeds.

Because the pattern of a single

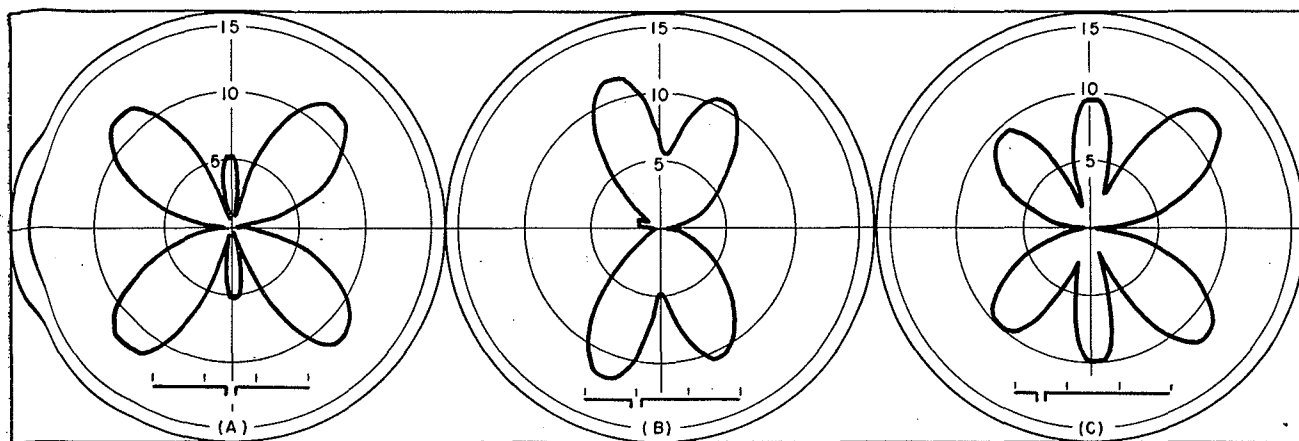


FIG. 3—Filed strength patterns of a one and one-half wavelength antenna for four different feed positions

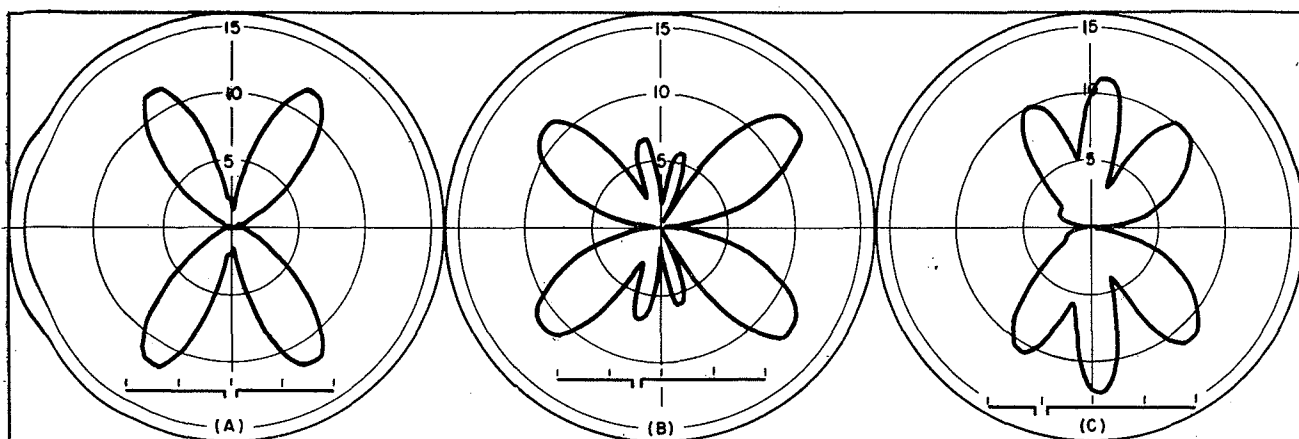


FIG. 4—Radiation patterns of a two-wavelength antenna showing effect of moving feed position from center to one end

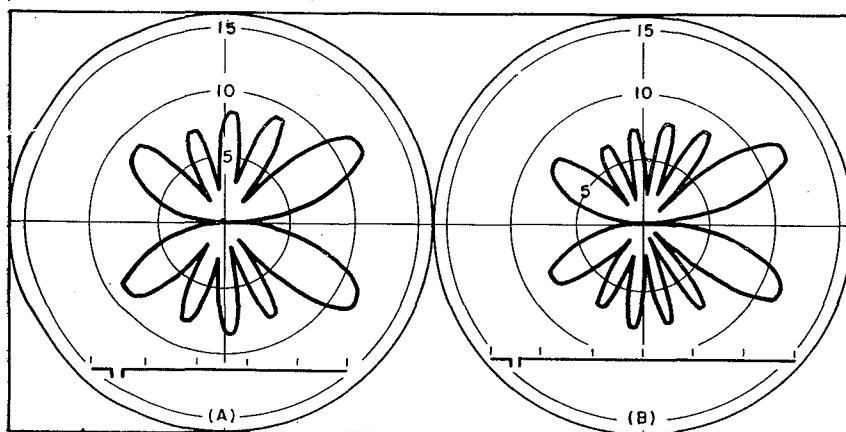


FIG. 5—Radiation from long wire antennas

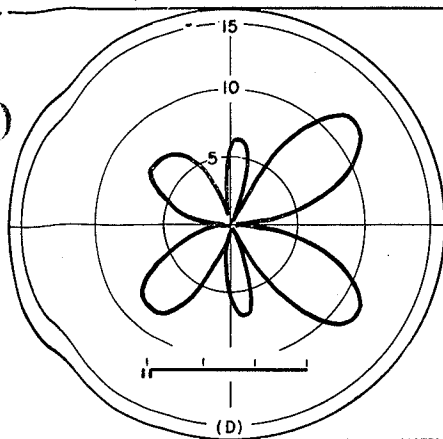
fed wire antenna is independent of the impedance match between it and the receiver or transmitter, it was not necessary to have a perfect impedance match between the antenna and the detector. However, the receiver had a coaxial feed and, therefore, a balance to unbalance trans-

former had to be used. In order to preserve the balance, it was necessary to have a partial impedance match. In the case of high impedance feeds (end feeds or feeds an even number of half wavelengths from the end) a quarter wave section of parallel wire transmission

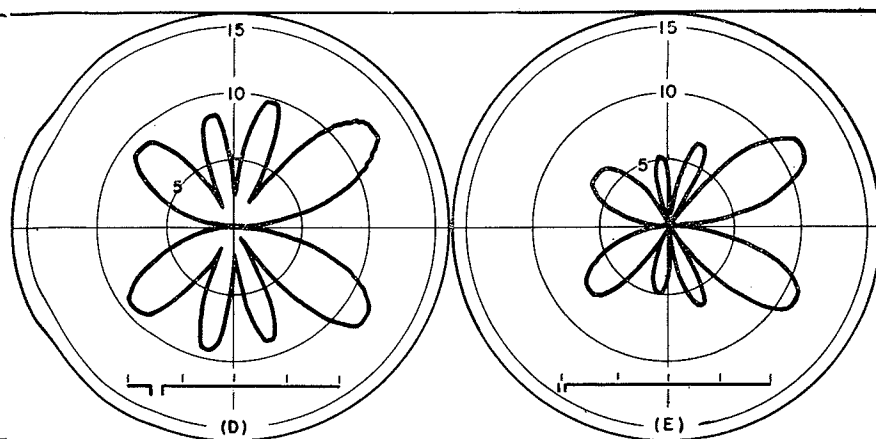
line was inserted between the antenna and the balancing unit.

The field strength patterns that are shown in the accompanying figures were measured by using scale models of the antennas at 10 and 20 cm. This method of measuring field strength patterns was used by the Antenna Laboratory of the Ohio State University Research Foundation during World War II for the determination of aircraft antenna characteristics (see *ELECTRONICS* cover, May 1947).

The equipment used to measure these patterns consisted of an electro-magnetic transmitting horn, a rotating table upon which a hollow vertical plywood shaft was fastened, the antenna to be measured being mounted on top of the shaft and supported by polystyrene rods when necessary. The antenna to be measured was then a receiving antenna. A Littelfuse bolometer was used as the detector. The pat-



The full wavelength antenna was measured using a balanced voltage feed at the center of the antenna. The two half-wavelength portions of the antenna then have in-phase antenna currents flowing on them. The pattern obtained using this feed point is shown in Fig. 2A. The feed point was moved one-quarter wavelength off center and fed with a balanced current feed. The pattern (Fig. 2B) was nearly that which is usually published for a full wavelength antenna. However, the two lobes of energy on the same



terns were continuously recorded by means of a selsyn system between the rotating table and shaft and the recording table. A concentric line lighthouse tube oscillator and a 10 cm two-cavity klystron were used as transmitting sources.

#### Measurements

The patterns of the half wavelength antenna shown in Figure 1 were taken using first a balanced current feed at the center of the half wavelength and then a voltage feed at the end of the half wavelength wire. (Each diagram has an illustration of its antenna, marked in half wavelengths.) It was apparent that the current distribution on the half wavelength antenna is not sinusoidal when it was end fed. With end feeding the lobes are displaced 15 to 20 degrees from their position when the half wavelength wire was center fed.

side of the wire are not equal in amplitude, but were present at about the published angle of 54 degrees. The minimum differed in amplitude from those obtained when the same length was end fed. When the full wavelength wire was end fed with a voltage feed, the lobes on both sides of the wire closest to the fed end of the antenna were reduced in amplitude even more than when the feed point was a quarter wavelength from the end of the wire, as seen in Fig. 2C.

A one and one-half wavelength wire was measured for center feed, Fig. 3A, one-quarter wavelength off center, Fig. 3B, one-half wavelength off center, Fig. 3C, and end fed, Fig. 3D. It is interesting to note the differences in amplitude of the broadside lobes and that the position of the large lobes off the free end of the end fed wire are slightly closer than the corresponding lobes for other feed points.

A two wavelength wire was measured using a balanced voltage feed at the center, (Fig. 4A), a current feed one-quarter wavelength off center (Fig. 4B), a voltage feed a half wavelength off center (Fig. 4C), a current feed three-quarters wavelength off center (Fig. 4D), and end fed with a voltage type feed (Fig. 4E). Different distributions must be present on the antenna for different feeds and the current distributions apparently are not sinusoidal even for the balanced center feed since the broadside minima are not complete. The pattern with the feed one-quarter wavelength off center (Fig. 4B), indicates that current distributions on each half of the wire were not identical let alone sinusoidal. When the wire was fed one-half wavelength off center (Fig. 4C), the minima were not complete and of different values due to the unbalanced current distribution along the antenna.

When the wire was fed three-quarters wavelength off center (Fig. 4D), the current distribution was again different from that when the antenna was end fed (Fig. 4E), as it was for the same types of feeds using the three-half wavelengths antenna (Fig. 3). The large lobes off the free end of the wire were again closer to the wire when the two-wavelength antenna was fed three-quarter wavelength off center, (Fig. 4D), than when the wire was fed one-quarter wavelength from the end (Fig. 4E).

Also shown in Figure 5 are the patterns of longer wires, namely, two and one-half wavelengths and three wavelengths long. Time did not permit further measurements. The minima were not complete as was shown before for similar type feeds used on shorter lengths of wire. Similar effects of non-sinusoidal current distributions were present when unterminated rhombic and V antennas were measured.

This investigation was prompted by discussion between C. H. Page and G. H. Brown at the I.R.E. 1947 Winter Convention in New York City, of the effect of the diameter of the antenna on the pattern when various positions of feeds are used.



# Phasing Networks

Graphical methods are applied to the design of phase-shifting and impedance-matching networks required to distribute power properly in directional antennas. Compared to conventional network analysis the vector method results in economy of circuit components and simplified design procedure

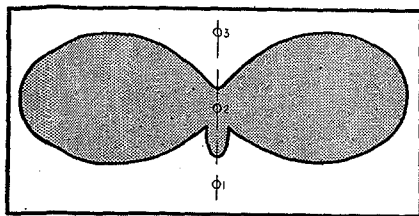


FIG. 1—Desired radiation pattern, which can be produced by the antenna array of Fig. 2

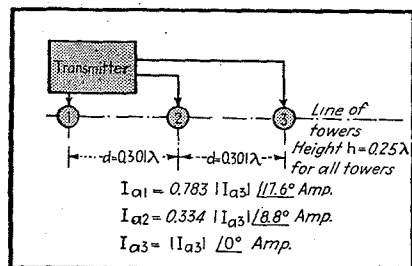


FIG. 2—Antenna array required to produce the radiation pattern of Fig. 1

By C. RUSSELL COX

Chief Engineer, Andrew Company  
Chicago, Illinois

VECTOR synthesis is a convenient mathematical tool which is very helpful to the designer of r-f phase-shifting and impedance-matching networks for the directional arrays used by many broadcast stations. Not only does this combination graphical and mechanical technique afford a clear understanding of the operation of a-c circuits, but it can also be used to "synthesize" network designs which display great simplicity when compared to circuits determined by ordinary methods. Problems in the design of phasing net-

works for directional antenna arrays are particularly susceptible to solution by vector methods.

## Principles of Vector Synthesis

In general, the synthesis of a network by vector manipulation usually reduces to the following problem: Given a pair of vectors  $I_1$  and  $E_1$ , representing the current through and the voltage across an impedance, it is required to establish a circuit which will transform  $I_1$  and  $E_1$  into another pair of vectors,  $I_2$  and  $E_2$ . The latter pair of vectors is usually specified by the conditions of the problem.†

When the input and output impedances  $R_1$  and  $R_2$  between which the network must operate are known, the two currents are related by a simple law which equates input and output powers:

$$I_1^2 R_1 = I_2^2 R_2$$

The method of designing a network by vector synthesis may be most easily outlined by means of a specific example. To illustrate the general method, let it be required to design phasing networks suitable for providing currents of the desired magnitude and phase to three vertical radiators, in order to produce the radiation pattern shown in Fig. 1.

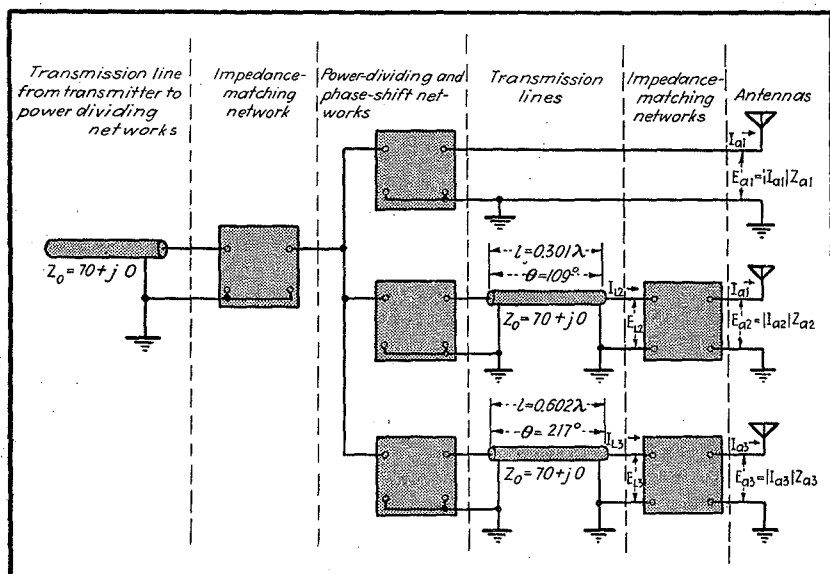


FIG. 3—Block diagram of system of networks and transmission lines for feeding antennas with the currents and voltages necessary to produce directional radiation pattern

† If the circuit is free from dissipation the second pair of vectors is subject to the restriction.

$$\frac{1}{2} (E_1 I_1^* + E_1 I_1) = \frac{1}{2} (E_2 I_2^* + E_2 I_2)$$

in which the asterisk (\*) denotes the conjugate function. This equation states that the network must neither create nor destroy power.

# for Broadcast Arrays

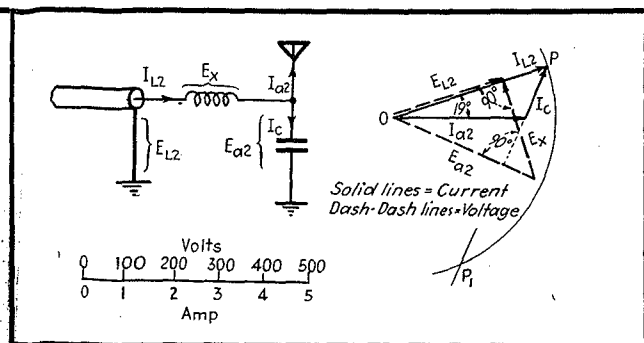
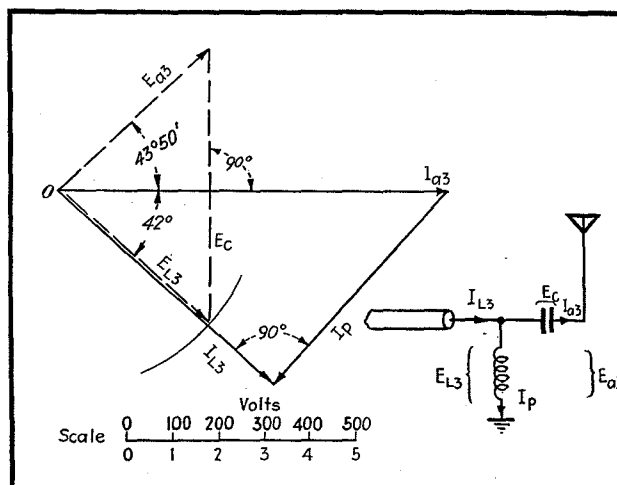


FIG. 4—L-type network for matching impedance of transmission line to impedance of antenna 2, with vector diagram from which design of the network is derived

FIG. 5 (RIGHT)—Impedance-matching network of the L-type for matching antenna 3 to a 70-ohm transmission line. Vector diagram illustrates method of designing this circuit



An analysis of this radiation pattern reveals that the towers must be  $0.25 \lambda$  high, separated by a distance  $0.301 \lambda$ , and fed with currents whose magnitudes and relative phases are as given in Fig. 2. A block diagram showing the elements of a suitable system of networks to produce the desired radiation pattern is shown in Fig. 3.

The problem at hand is now to design, by methods of vector synthesis, impedance-matching networks between the transmission lines and the antennas, power-dividing and phase-shift networks, and the impedance-matching circuit which connects the transmission line from the transmitter to the three power-dividing and phase-shift networks. (It should be noted from Fig. 2 that antenna 1 is located at the transmitter and consequently does not require a transmission line, as do the other two antennas.)

## Example of Vector Synthesis

To design a feed system for the array of Fig. 3, it is necessary to start at the antennas and work back through each network and transmission line toward the transmitter. The conditions of the problem yield the following information regarding antenna currents, impedances, and powers:

$$I_{a1} = 6.7/17.6^\circ \text{ amperes}$$

$$I_{a2} = 2.86/8.8^\circ \text{ amperes}$$

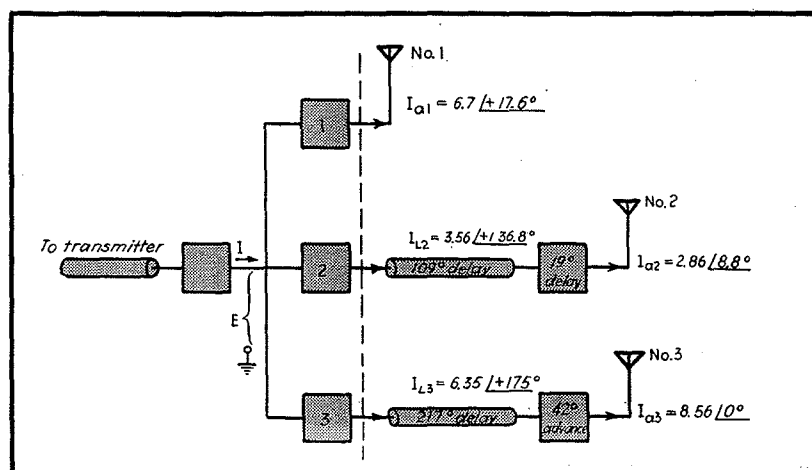


FIG. 6—Block design illustrating the summary of phase shifts occurring between the power-dividing networks and the antenna

$$I_{a3} = 8.56/0^\circ \text{ amperes}$$

$$Z_{a1} = 28.7 + j39 = 48.4/53.67^\circ \text{ ohms}$$

$$Z_{a2} = 108 - j45 = 117/-22.63^\circ$$

$$Z_{a3} = 38.5 + j37 = 53.5/43.83^\circ$$

$$P_{a1} = 1290 \text{ watts}$$

$$P_{a2} = 890 \text{ watts}$$

$$P_{a3} = 2820 \text{ watts}$$

where  $I_{a1}$ ,  $I_{a2}$ , and  $I_{a3}$  are currents in antennas 1, 2, and 3 respectively, and the angles represent phases relative to that of  $I_{a3}$ . The quantities  $Z_{a1}$ ,  $Z_{a2}$ , and  $Z_{a3}$  are the impedances of antennas 1, 2, and 3, respectively, and  $P_{a1}$ ,  $P_{a2}$ , and  $P_{a3}$  are the powers in antennas 1, 2, and 3, respectively.

From this data the voltage applied to the antennas and the currents in the transmission lines (whose impedance is  $Z_o = 70 + j0$ ) can be determined as follows:

$$E_{a1} = |I_{a1}| Z_{a1} = 6.7 \times 48.4/53.67^\circ = 324/53.67^\circ \text{ volts}$$

$$E_{a2} = |I_{a2}| Z_{a2} = 2.86 \times 117/-22.63^\circ = 335/-22.63^\circ \text{ volts}$$

$$E_{a3} = |I_{a3}| Z_{a3} = 8.56 \times 53.5/43.83^\circ = 458/43.83^\circ \text{ volts}$$

$$I_{L2} = \sqrt{P_{a2}/Z_o} = \sqrt{890/70} = 3.56 \text{ amp.}$$

$$I_{L3} = \sqrt{P_{a3}/Z_o} = \sqrt{2820/70} = 6.35 \text{ amp.}$$

$$E_{L2} = Z_o I_{L2} = 70 \times 3.56 = 250 \text{ volts}$$

$$E_{L3} = Z_o I_{L3} = 70 \times 6.35 = 444 \text{ volts}$$

where  $E_{a1}$ ,  $E_{a2}$ , and  $E_{a3}$  are the voltages applied to antennas 1, 2, and 3 respectively and the phase angle of each voltage is referred to the corresponding antenna current as a reference,  $I_{L2}$  and  $I_{L3}$  are the magnitudes of the currents in the transmission lines feeding antennas 2 and 3, and  $E_{L2}$  and  $E_{L3}$  are the mag-

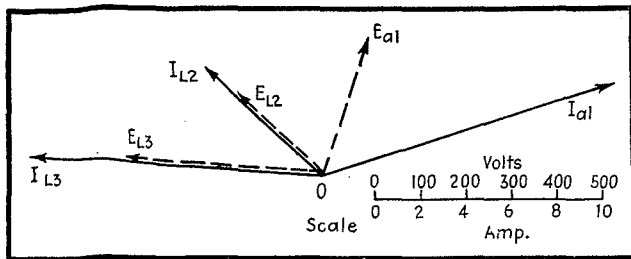


FIG. 7—Vector diagram of voltages and currents which must be produced by phase-shifting and power-dividing networks

FIG. 9—Vector diagram for input circuits →

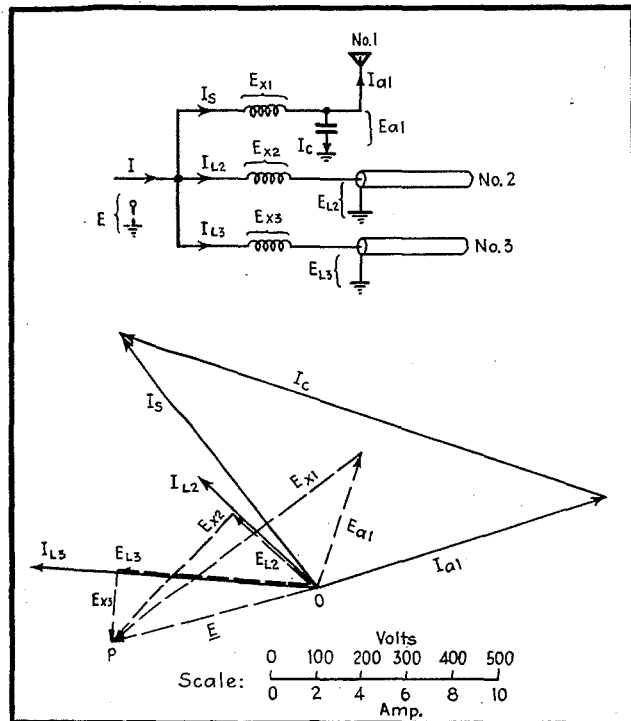
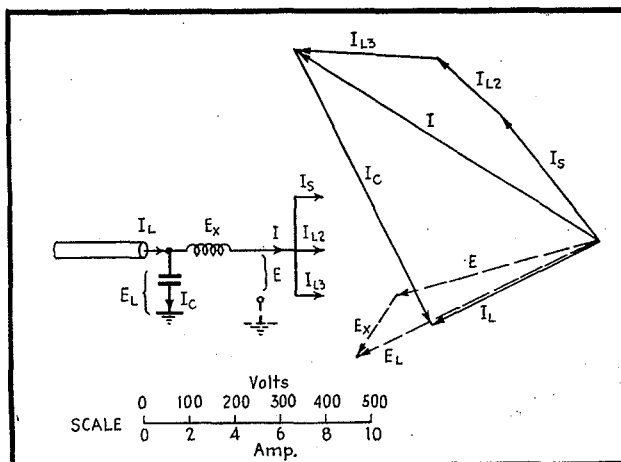
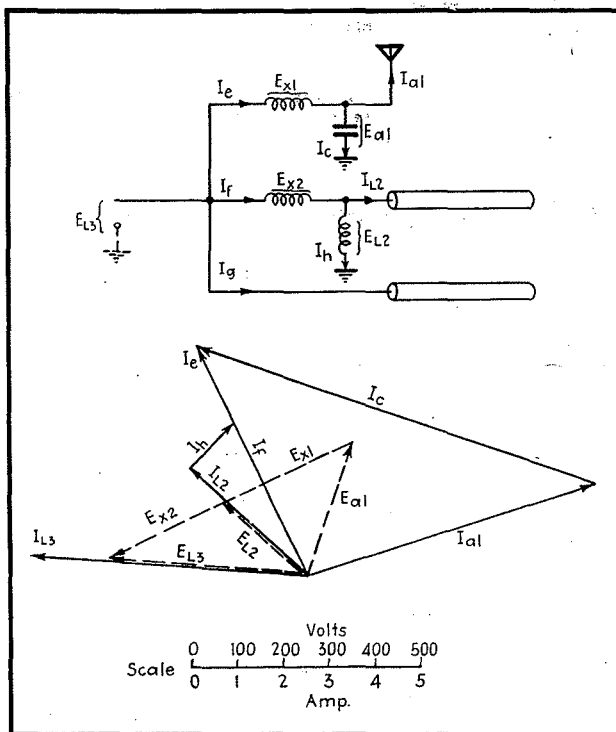


FIG. 8—Synthesis of phasing and power-dividing networks

FIG. 10—Alternative design of phasing networks →



nitudes of the voltages across these transmission lines. With this data, the impedance-matching networks between the transmission lines and the antennas can now be designed.

#### Design of Network for Matching Impedances

The sketch in Fig. 4 illustrates the synthesis of a network for matching the line impedance of  $Z_o = 70 \angle 0^\circ$  ohms to the center antenna impedance of  $117 \angle -22.63^\circ$  ohms. We begin by drawing a vector of length 2.86 units to represent the antenna current  $I_{a2}$ . This vector can be drawn in any conven-

ient direction but since it is used as the reference vector, it will be drawn along the x-axis. To some suitable voltage scale, the vector for the antenna voltage  $E_{a2}$ , at an angle of  $-22.63^\circ$  with respect to  $I_{a2}$ , can also be drawn.

An  $L$  network of the type shown will give the impedance transformation. For such a network, Kirchhoff's law for branching currents must be satisfied, i.e.,  $I_{L2} = I_{a2} + I_e$ , where  $I_e$  is the current through the capacitor. Therefore the tips of  $I_{L2}$  and  $I_e$  must coincide at some point  $P$  which lies on a circle of radius  $I_{L2} = 3.56$ , drawn from 0

(zero) as a center. Since the current through a reactance forms a 90-deg angle with the voltage across it, we may lay out  $I_e$  at right angles to  $E_{a2}$ , and the intersection of  $I_e$  with the circle locates the point  $P$ .

The potential  $E_{L2}$  must equal the sum of  $E_e$  and  $E_{a2}$ . Therefore, the tail of  $E_e$  must lie on the tip of  $E_{a2}$ , and the direction of  $E_e$  is normal to the current  $I_{L2}$  through the inductance. The magnitude of  $E_e$  is determined by the point of intersection with  $I_{L2}$ , and the voltage triangle is completed by drawing  $E_{L2}$  from 0 (zero) to the point of in-

tersection of  $E_s$  with current  $I_{L2}$ . Because  $I_c$  leads  $E_{a2}$  by 90 deg, the parallel reactance must be that due to a capacitance. Similarly, since  $E_s$  leads  $I_{L2}$  by 90 deg, the series reactance must be that due to an inductance. The magnitudes of the required reactances are obtained by dividing the length of a vector representing voltage across a reactance by the length of the corresponding current vector, i.e.,  $X_L = E_s/I_{L2}$ , and  $X_c = E_{a2}/I_c$ .

The network of Fig. 4 is a delay network because  $I_{a2}$  lags behind  $I_{L2}$ . Had we chosen to extend  $I_c$  in the opposite direction, intersecting the circle at  $P_1$ , a phase-advance network would have been obtained.

#### Choice of Configuration

The choice between the phase-advance and the phase-delay configuration is purely a matter of convenience. Any impedance transformation problem may be solved by either network. However, in designing the matching circuit for antenna 3 we choose the phase-advance network because this choice happens to simplify design of the phasing networks. We begin the construction of the vector diagram for antenna 3 (Fig. 5) by drawing vectors  $I_{a3}$  and  $E_{a3}$ . The series capacitor introduces a voltage  $E_c$  which adds to  $E_{a3}$ , but in a direction normal to  $I_{a3}$ . Then, a circle of radius  $E_{L3}$  locates the tip of  $E_c$ , and the vector  $I_{L3}$ , whose length is known, is drawn through the point of intersection. The vector  $I_p$ ,

drawn normal to and lagging  $I_{L3}$ , completes the construction.

#### Phasing Networks

A summary of the phase shifts in the lines and antenna tuning units is given in Fig. 6. Each of the two transmission lines introduces a delay (in degrees) of  $\theta = 360 l/\lambda$ , where  $l$  is the length of the line and  $\lambda$  is the wavelength. For  $\lambda = 0.301$  the delay is 109 deg, and for  $\lambda = 0.602$  the delay is 217 deg. The apparatus to the left of the dotted line in Fig. 6 is required to divide the transmitter power into three parts and distribute it among the three antennas with the required phase angles and amplitudes. Figure 7 represents the three voltages and currents leaving the phasing apparatus at the dotted lines of Fig. 6.

The remaining problem is that of selecting a voltage vector  $E$  which can be rotated and transformed by means of three separate reactance networks to produce  $E_{a1}$ ,  $E_{L2}$ , and  $E_{L3}$ . An important point is that the vector  $E$  may be of any magnitude and of any phase, and we may therefore select  $E$  to suit our own convenience. Referring to Fig. 8 we see that reactances in series with transmission lines 2 and 3 produce voltage vectors  $E_{x2}$  and  $E_{x3}$  which intersect at  $P$ . The vector  $E$ , drawn from 0 (zero) to  $P$ , is then a convenient vector to represent the input voltage.

Since the antenna current  $I_{a1}$  is far removed in direction from  $E$ ,

it is necessary to obtain somehow a new current  $I_c$  that is at least within 90 deg. of  $E$ . This is accomplished by introducing a parallel capacitance across antenna  $I_c$ , producing the current  $I_c$  leading  $E_{a1}$  by 90 deg. An inductance in series with  $I_c$  introduces a voltage vector  $E_{x1}$ , drawn from the tip of  $E_{a1}$  by 90 deg. An inductance in  $I_c$  perpendicular to  $E_{a1}$  we have satisfied all the conditions of the problem.

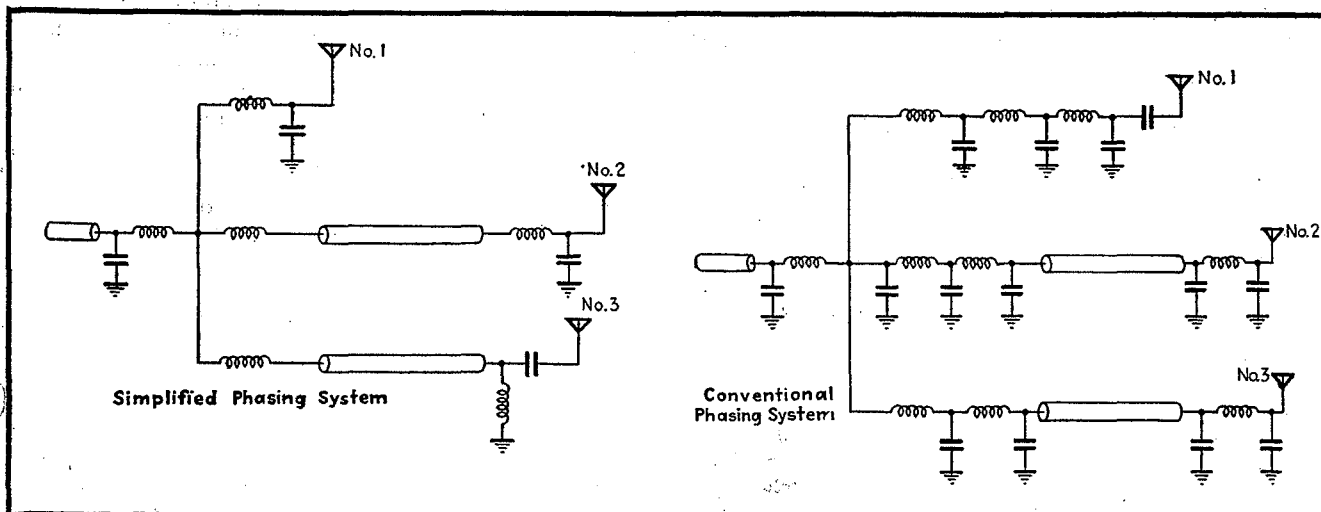
#### Input Circuit

An input circuit, to provide a load impedance of  $70 + j0$  ohms for the transmitter, is illustrated in Fig. 9. The total current  $I$  is obtained by adding vectorially the three branch currents  $I_s$ ,  $I_{L2}$  and  $I_{L3}$ . By adding a series inductance to produce  $E_s$ , and a parallel capacitance to produce  $I_c$ , the voltage and current triangles are all properly completed.

#### Alternative Solution

In an earlier paragraph, it was stated that any voltage vector  $E$  (Fig. 8) could be selected when designing the phasing networks. Suppose, for instance, that antenna 3 is thought to be the dominant element in the array and that we wish to do all the tuning in the networks feeding antennas 1 and 2. Then,  $E_{L3}$  is the input voltage, as shown in Fig. 10. The design in this case follows the same principles established in previous examples.

Completed simplified system of networks designed by vector synthesis, and equivalent system of networks designed by conventional methods



# Design Charts for Low-Frequency Antennas

By **GEORGE J. MONSER**, Staff Engineer, Military Electronics Div., Motorola Inc., Scottsdale, Arizona

PROPAGATION of radio waves at lf and vlf is characterized by a high degree of stability and by the long range of useful signal transmission. One limitation that deters greater usage is the antenna size necessary to efficiently radiate power.

This article presents nomograms helpful in estimating the radiation capability of electrically-short antennas once the antenna current is specified.

For an electrically short base-driven antenna as shown in Fig. 1A, the radiation resistance is

$$R_a \doteq 10 G_o^2 \quad (1)$$

(valid when  $G_o < 0.785$  radians)

where  $G_o$  is the electrical height in radians.

Since  $G_o = 2\pi h/\lambda$ , in which  $h$  is the antenna height and  $\lambda$  is the wavelength in the same units

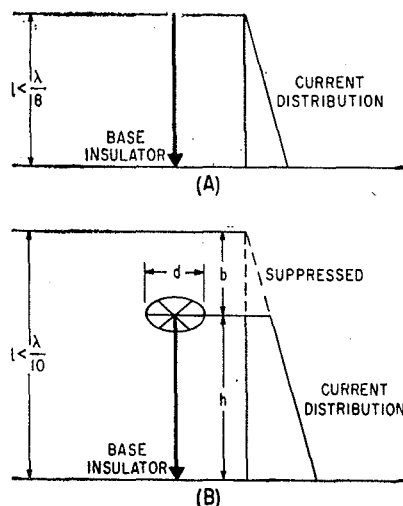


FIG. 1—Stub antenna (A) and stub antenna with top loading (B)

as  $h$ ,

$$R_a = 4.06 \times 10^{-10} h^2 f^2 \quad (2)$$

when  $h$  is the antenna height in feet and  $f$  is the frequency in Kc.

Equation (2) is shown graphically in Fig. 2.

For an electrically short base-driven antenna, top loaded with a flat horizontal disk as shown

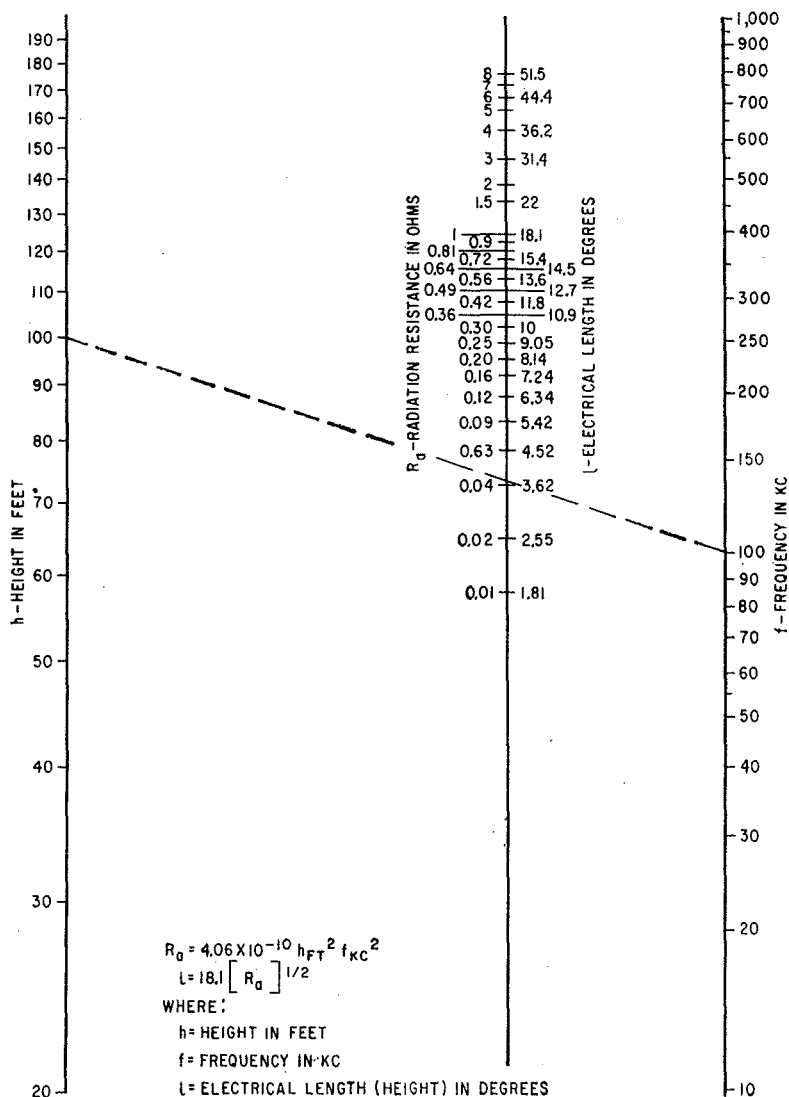


FIG. 2—Stub antenna chart valid for electrical lengths less than  $\lambda/8$

in Fig. 1B, the radiation resistance is

$$R_a = 1,578 \left( \frac{h}{\lambda} \right)^2 \left\{ 1 - \left[ \frac{h}{(h+b)} \right] + \frac{1}{2} \left[ \frac{h}{(h+b)} \right]^2 \right\} \quad (3)$$

valid for  $(h+b) < 0.1 \lambda$  where  $b$  is the increase in height due to the top-loading disk and  $\lambda$  is the wavelength;  $h$ ,  $b$  and  $\lambda$  are expressed in the same units.

To use equation (3) in this form requires considerable computation. A more useful relationship would be

$$R_a = g(f, h, d) \quad (4)$$

where  $f$  is the frequency,  $h$  is the height of the stub and  $d$  is the diameter of the disk.

An approximate functional relationship for equation (4) is found by  $X_a = Z_o \cot(2\pi h/\lambda)$  which is the stub reactance at  $f_1$ ;  $X_b = 1/2\pi f_1 C_2$  which is the top loading disk reactance at  $f_1$ ; and  $Z_o = 60 [\ln(h/a) - 1]$  is the characteristic impedance for the stub transmission line; where  $C_2$  is the capacitance (0.35

pF) of the disk (remote from earth),  $d_a$  is the diameter of the disk in centimeters,  $h$  is the height of the stub and  $a$  is the effective radius of the stub in the same units as  $h$ .

From the equation for the characteristic impedance of a stub transmission line, note that  $Z_o = 200$  ohms for the restricted range  $60 < (h/a) < 90$ . From the equation for stub reactance at  $f_1$ ,

$$X_a = Z_o \left( \frac{\lambda}{2\pi h} \right) = 300 \times 10^3 / hf = K_a / hf \quad (5)$$

where  $h$  is the stub height in feet and  $f$  is the frequency in Kc.

From the equation for the top loading disk reactance at  $f_1$ ,

$$X_b = 150 \times 10^3 / df = K_b / df \quad (6)$$

where  $d$  is the diameter of the disk in feet and  $f$  is the frequency in Kc.

For the short line,

$$h/(h+b) = X_c/X_a \quad (7)$$

where  $X_a$  is the stub reactance

and  $X_c = X_a X_b / (X_a + X_b)$  is the stub input reactance with top loading.

Using equations (5) through (7),

$$h/(h+b) = X_c/X_a = 1/(1+\alpha) \quad (8)$$

where

$$\alpha = K_a d / K_b h = 2(d/h).$$

With the aid of the above development, Eq. (3) is reformed yielding

$$R_a = 4.06 \times 10^{-10} h^2 f^2 \phi^2 \quad (9)$$

where  $\phi = (h/(h+b)) - 2 = (1/(1+\alpha)) - 2$ ,

$h$  is the stub height in feet and  $f$  is the frequency in Kc.

Figure 3 relates the variables in Eq. (9) for two different  $d/h$  ratios. The percentage increase in length for the two  $d/h$  ratios has also been indicated.

Figure 4 relates the variables in Eq. (5).

#### REFERENCE

- (1) J. S. Belrose, et al, The Engineering of Communication Systems for Low Radio Frequencies. *Proc IRE*, p 661, May 1959.

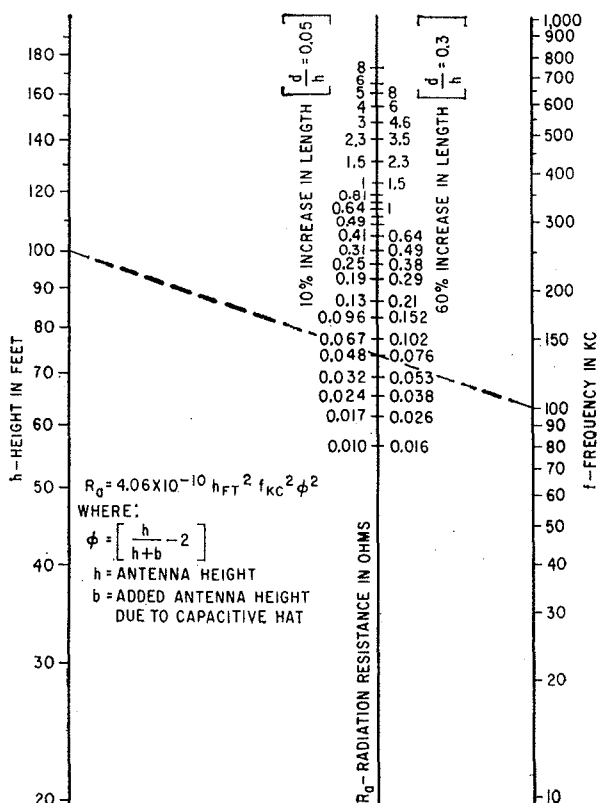


FIG. 3—Stub antenna with two different  $d/h$  ratios for flat-top loading valid for  $h+b < \lambda/10$

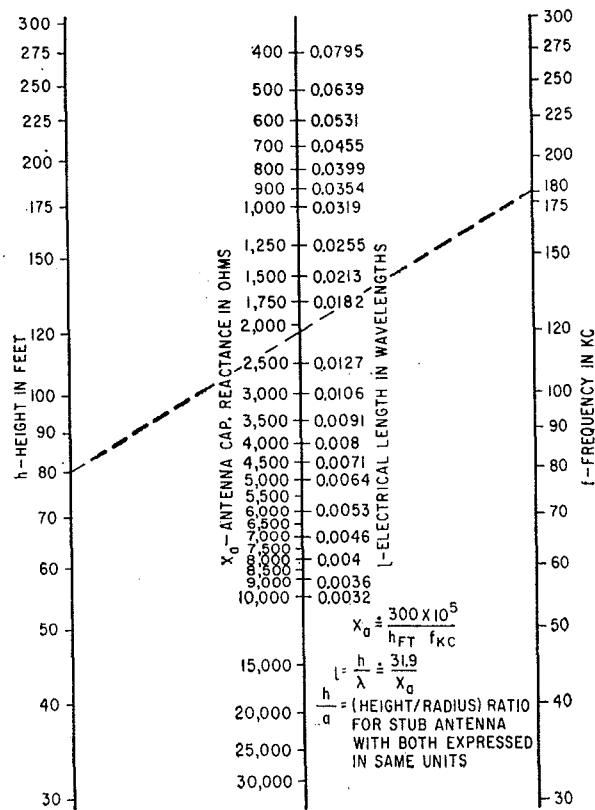
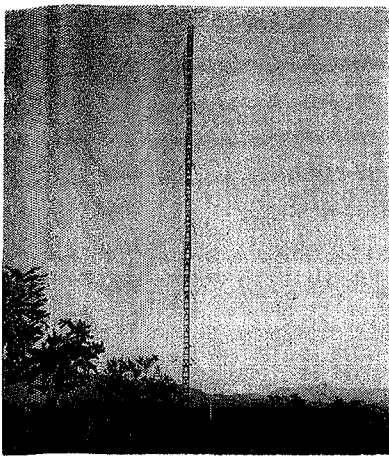
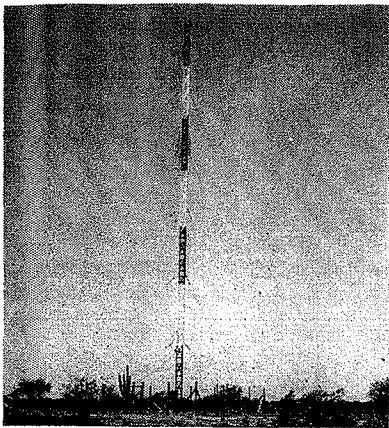


FIG. 4—Stub antenna reactance chart valid for electrical lengths  $< \lambda/16$  and for  $60 < (h/2) < 90$



Low frequency antennas with umbrella top hat: arrangement (A) shows apex angle 63 degrees



Arrangement (B) has angle apex of 44 degrees

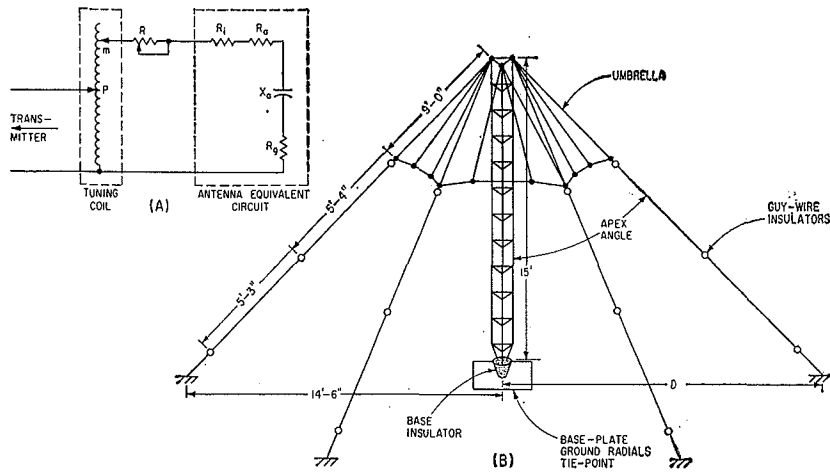


FIG. 1—Antenna equivalent circuit, upon which analysis is based (A), and simplified layout of scale-model antenna (B)

# Antenna Design for

Half-wave antennas, although efficient radiators, may be several miles long for very low frequency operation.

Here are design criteria for electrically short antennas with high radiation efficiency, plus data from test antennas

By GEORGE J. MONSER  
and WALLACE D. SABIN,

Motorola Inc.,  
Military Electronics Division,  
Scottsdale, Arizona.

A SIMPLIFIED analysis is developed, in which it is shown that for maximum radiation efficiency for specified bandwidth, the ratio of the radiation resistance to antenna reactance slope at the operating frequency should be maximized. Test data supporting the theory is given for two base-feed radiators: a  $\frac{1}{16}$  scale model evaluated at 1.5 Mc, and a 150-foot unit evaluated at 150 Kc. While the test data is restricted to these two units, the basic precepts are general and can be applied to the design of any electrically short vertical radiator.

Radiation efficiency provides a convenient means for measuring the radiation capability of the antenna, since it relates the radiated power to the antenna input power. The

antenna must of course be suitably coupled to the transmitter, and coupler loss should be included in the definition.

For the arrangement illustrated in Fig. 1B, percentage radiation efficiency is given by

$$\eta_R = \frac{R_a}{R_{loop}} \times 100 \quad (1)$$

Where:  $R_a$  = antenna radiation resistance referred to the base (or driving point),  $R_{loop} = R_a + R_g + R_i + R_t + R$ ,  $R_g$  = equivalent ground loss resistance,  $R_i$  = equivalent base insulator loss resistance,  $R_t$  = base tuning coil resistance, and  $R$  = broadbanding dissipative resistance.

Maximum efficiency occurs when  $R_a$  is maximum and  $R_{loop}$  minimum. A limit on the reduction of  $R_{loop}$  is set by the required radiation bandwidth. Thus

$$Q = \frac{f_o}{2R_{loop}} \left| \frac{dX}{df} \right|_{f_o} = \frac{f_o}{R_{loop}} \left| \frac{dX_a}{df} \right|_{f_o}$$

where  $dX/df|_{f_o}$  = net reactance slope evaluated at  $f_o$ ,  $dX_a/df|_{f_o}$  = antenna reactance slope evaluated at  $f_o$ , and  $f_o$  = frequency for which net reactance  $X = Q$ .

Substituting into Eq. 1

$$\eta_R = \left[ \frac{R_a}{\left( \frac{f_o}{Q} \right) \left| \frac{dX_a}{df} \right|_{f_o}} \right] \times 100 \quad (2)$$

Either quantity within the brackets may be used to calculate radiation efficiency. Equation 2 shows that for a particular bandwidth (BW), a maximization of the

$R_a / \left| \frac{dX_a}{df} \right|_{f_o}$  ratio is required.

Radiation resistance provides a convenient concept for relating radiated power to the antenna driving current. For an electrically short monopole, the radiation re-

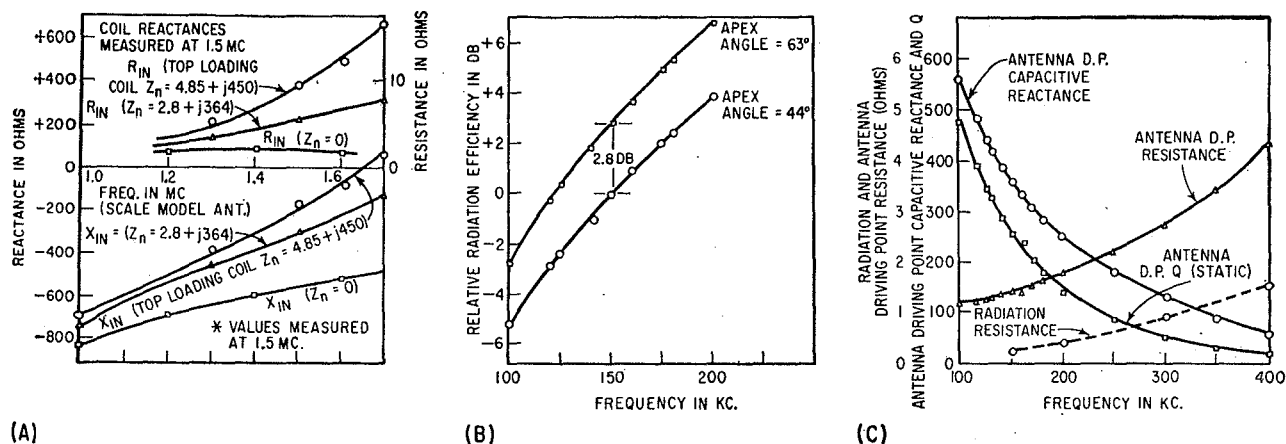


FIG. 2—Scale model impedance curves for range of top-loading coil reactances (A); efficiency versus frequency for the 150-ft antenna with guy-wire top-hat (B); driving point resistance and reactance of 150-ft antenna versus frequency for top-hat apex angle of 63 degrees (C)

## Maximum L-F Radiation

sistance (referred to the base) is  $R_a = 40\pi^2 (h/\lambda)^2$  (3) Where  $h$  = height of vertical radiator and  $\lambda$  = wavelength expressed in same units as  $h$ .

Equation 3 can be extended to include the effect of top-loading.

For a short monopole, top-loaded with a nonradiating capacitive top-hat, the radiation resistance becomes

$$R_a = 1,578 \left( \frac{h}{\lambda} \right)^2 \left[ 1 - \frac{h}{h+b} + (1/4) \left( \frac{h}{h+b} \right)^2 \right] \quad (4)$$

Provided  $(h+b) < 0.1\lambda$ , where  $h$  = length of vertical radiator,  $b$  = equivalent additional vertical length resulting from the top-loading,  $\lambda$  = wavelength expressed in same units as  $h$ .

For a short monopole, with a combined top-load consisting of a coil in series with the hat, no known simple expression exists for calculating radiation resistance. However, when the reactance of the top-loading coil is much less than the reactance of the top-hat, the effect is analogous to increasing  $b$  slightly in Eq. 4.

The reactance of the monopole (stub) is  $X_a = -Z_o \cot(2\pi h/\lambda)$  (5)

where  $Z_o = 60 [\ln(h/p) - 1]$  = characteristics impedance of the stub considered to be a transmission line,  $h$  = antenna height,  $\lambda = c/f$  = wavelength in the same units

as  $h$ ,  $p$  = equivalent radius of stub in the same units as  $h$ ,  $c$  = speed of light,  $f$  = frequency.

Under the following restrictions of  $h/\lambda < 0.1$  and  $60 < h/p < 90$  the reactance equation becomes  $X_a = K_a/hf$  where  $K_a = -Z_o c/2\pi$  = a constant. The antenna slope reactance is therefore

$$\frac{dX_a}{df} = \frac{K_a}{hf^2} \quad (6)$$

In similar fashion for the top-loaded antenna

$$X_a' = \frac{\beta K_a}{hf^a} \quad (7)$$

Where  $K_a$ ,  $h$ , and  $f$  are as defined for equation (5),  $\beta$  = coefficient due to top-loading,  $a$  = exponent for the frequency term and  $dX_a'/df = aK_a/hf^{a+1}$

The exponent  $a$  is close to unity for the capacitive top-hat. For combined top-loading, the exponent may approach 10.

Several methods are available for controlling or modifying the performance of base-driven vertical antennas.

The following techniques are examples: (a) guy-wire capacitive top-loading, (b) flat-disk capacitive top-loading, (c) combined top-loading, where a coil is inserted between the top of the tower and the top-hat.

Figure 1B shows a sketch of the scale model antenna. In this figure, the umbrella or guy-wire top-hat length is specified for maximum radiation resistance. To establish

this length, tests similar to those performed by Smith and Johnson<sup>1</sup> were conducted. The improvement in radiation capability was referenced to this configuration.

Observe in Fig. 1B, that if the apex angle approaches 90 degrees, the umbrella top-hat becomes electrically equivalent to a flat-top. The effect of increasing the apex angle has recently been reviewed in the literature<sup>3</sup>. To verify published data, two apex angles (44 and 63 degrees) were checked. Smeby<sup>2</sup> showed in an earlier paper that the effect of top-hat current on useful radiation becomes less pronounced with larger apex angles and that a further reduction in the effect of top-hat current would be obtained by folding back the top-hat. For the Smith and Johnson antenna, he indicated that theoretically about 1 db improvement in radiation capability would result, if the top-hat was folded back.

Table I summarizes the results for the different arrangements investigated using the scale model antenna.

Additional insight into the performance characteristics listed in Table I may be had by observing Fig. 2A and Table II. Figure 2A shows the antenna input impedance components for the scale model plotted as a function of frequency. Three different top-loading coil impedances ( $Z_n$ ) are indicated. For  $Z_n$ ,



TABLE I—Efficiency Varies Widely With Antenna Configuration







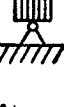
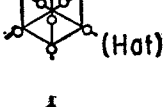
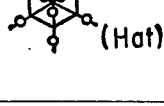
Type	Arrangement	Configuration	Efficiency (Percent)
1	Stub Antenna (No-Top Loading)		15
2	Type 1—With Umbrella (Capacitive Top-Loading) Apex Angle = 44°		53
3	Type 2—With Coil Inserted Between Stub and Top-Hat		72
4	Stub Antenna With 3 Outriggers		14
5	Stub Antenna With 6 Outriggers		24
6	Stub Antenna With 6 Outriggers And Umbrella Top-Loading Apex Angle = 44°		51
7	Stub Antenna With 6 Outriggers And Umbrella Top-Loading Apex Angle = 63°		75
8	Stub Antenna With 6 Outriggers And Folded Back Umbrella Top-Hat Apex Angle = 63°	 (Hat)	78
9	Same Unit As Type 8—With Top-Hat Extended For $\eta_R$ (Max.)	 (Hat)	92

TABLE II—Reactance Equations For Different Antenna Arrangements

Antenna Identification	Reactance Equation	Equation Valid For Frequencies Between
Type 2	$855 f_{mc}^{-1.06}$	1-2 Mc
Type 7	$700 f_{mc}^{-1.06}$	1-2 Mc
Type 7	$595 f_{mc}^{-1.06}$	1-2 Mc
Top hat extended one section— Apex angle 63°		
Type 7	$505 f_{mc}^{-1.06}$	1-2 Mc
Top hat extended two sections— Apex angle 63°		
Type 8	$700 f_{mc}^{-1.06}$	1-2 Mc
Type 3 <sup>a</sup>	$740 f_{mc}^{-1.6}$	1-1.5 Mc
Type 3 <sup>a</sup>	$1290 f_{mc}^{-3.4}$	1.4-1.6 Mc
Type 3 <sup>a</sup>	$19100 f_{mc}^{-9.2}$	1.6-1.8 Mc
1/10 scale model antenna— 5 foot radius disk top hat	$1110 f_{mc}^{-1.09}$	1-2 Mc

<sup>a</sup>  $X_n = 363$  ohms at 1.5 Mc (top loading coil)

= 0, the unit is simply an umbrella top-loaded unit. Observe that with increased top-loading-coil reactance  $X_n$ , the input reactance decreases and the reactance slope at the operating frequency increases.

Table II summarizes the reactance data for a number of different top-loading conditions considered in Table I. In Table II, reactance curves similar to those shown in Fig. 2A were reduced to equation form over the range of interest. Observe that with the exception of the combined top-loading case, the reactance exponent is close to unity, so that the effect on radiation efficiency indicated by Eq. 2 is small. However, for combined top-loading, this is not the case. It was found that only about 1 db improvement in radiation efficiency over the type 2 unit could be obtained with this type of loading, even though the driving point antenna reactance could be greatly reduced.

The greatest improvement noted during the scale model tests was between the type 2 unit and the type 9 unit (see Table I), where a 2.4-db improvement in radiation was measured. Accordingly, the 150-foot antenna performance was first measured as a type 2 unit, and then as a type 9 unit. The data was treated similarly to that outlined for the model, and the improvement in radiation efficiency was found to be about 2.8-db. This value was then checked by computing efficiency using Eq. 2. Figure 2B shows the results of this effort.

Figure 2C shows the final antenna design values. In this figure, driving-point impedance components, radiation resistance, and Q-static ( $X_{DP}/R_{DP}$ ) are sketched as a function of frequency.

Field test data presented in this article were obtained while performing work on Contract DA 36-039-SC-78020.

## REFERENCES

- (1) C. E. Smith and E. M. Johnson, Performance of Short Antennas, *Proc IRE*, Oct. 1947.
- (2) L. C. Smeby, Short Antenna Characteristics—Theoretical, *Proc. IRE*, Oct. 1949.
- (3) J. S. Belrose, et al., The Engineering of Communication Systems for Low Radio Frequencies, *Proc. IRE*, Part I, p 661, May 1959.
- (4) E. C. Jordan, "Electromagnetic Waves and Radiating Systems," Prentice-Hall, Inc., N. Y. 1950.
- (5) D. S. Bond, "Radio Direction Finders," p 221, McGraw-Hill Book Co., Inc., N. Y.
- (6) E. E. Terman and J. M. Pettit, "Electronic Measurements," p 405, McGraw-Hill Book Co., Inc., N. Y.

# LOW IMPEDANCE FOR BROADCAST RECEIVERS

Using a large low-impedance loop antenna improves pickup over that of a smaller high-impedance loop. Design of transformer for optimum coupling of low-impedance loop to grid of first stage is described. Curves give conditions for maximum gain

By L. O. VLADIMIR

Receiver Division  
General Electric Co.  
Bridgeport, Conn.

**L**OW-IMPEDANCE LOOP antennas have been used for some time in direction finders, and just prior to the war were beginning to find favor in home receivers. They are of particular value in large console models where advantage can be taken of available area to install efficient antennas.

In addition, low-impedance loop antennas are stable. That is, their inductance will ordinarily not change with age and humidity as much as will that of high-impedance loops. Placement of leads from loop to receiver is not as critical for low-impedance loops as for high-impedance loops. Also, the low-impedance loop is easier to manufacture than the high-impedance loop because its inductance need not be adjusted to within such narrow limits; normal manufacturing variations can be compensated with the antenna trimmer. Of course the coupling transformer must be closely adjusted, but

this is standard procedure in coil manufacture.

## Coupling Transformer

The heart of the low-impedance loop antenna is the step-up transformer that couples the loop to the grid of the r-f or mixer tube. The characteristic of this circuit is given by the expression, derived in Appendix I

$$\text{Gain} = kQ_s(L_{BQ}/L_L)^{1/2} \times [m(1+m-mk^2)/(1+m)]^{1/2} \times (1+m+2mk^2)^{-1} \quad (1)$$

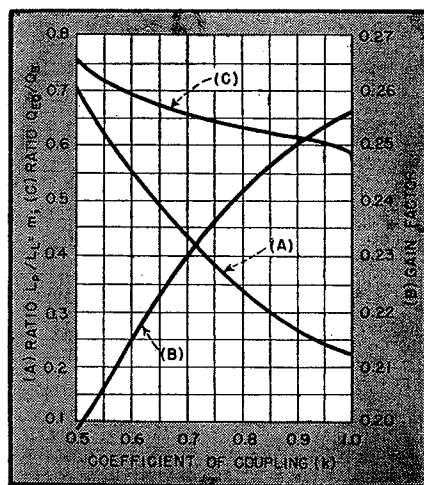


FIG. 2—Curve (A): Inductance ratio as a function of coupling coefficient for maximum gain. Curve (B): Gain factor as a function of coupling coefficient for optimum inductance ratio. Curve (C): Ratio of Q's for optimum inductance ratio varies with coupling coefficient

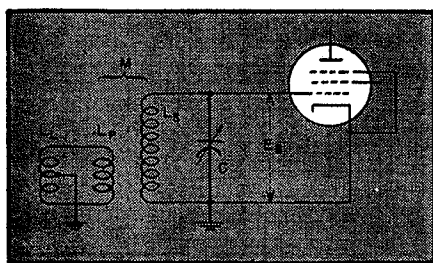


FIG. 1—Low-impedance loop antenna is coupled by step-up transformer to input of first stage

in which the significance of the terms is shown in Fig. 1 and Table I.

In the schematic diagram of Fig. 1, the inductance  $L_L$  is the loop, which can or cannot be center-tapped. Neither case will affect the results because capacitance coupling between primary and secondary windings is very small compared to inductive coupling.

Equation 1 will be analysed to determine the optimum design of the coupling transformer and to compare merits of the low-impedance loop to those of the high-impedance loop.

## Optimum Gain

Of primary interest in determining maximum gain of the coupling transformer is the magnitude of the quantity  $m$  in Eq. 1. Because the values  $L_{BQ}$ ,  $L_L$  and  $Q_s$  are roughly fixed by other design considerations, we specifically wish to substitute various values of  $k$  in Eq. 1 to find what value  $m$  must be for maximum gain. While the maximum point could be found by differentiating this equation, the resultant derivative is a sixth order equation and extremely difficult to handle. Accordingly the information was obtained graphically and is shown by curve (A) in Fig. 2.

Knowing the realizable coefficient of coupling which we can obtain in our transformer design, we can find

# LOOP ANTENNA

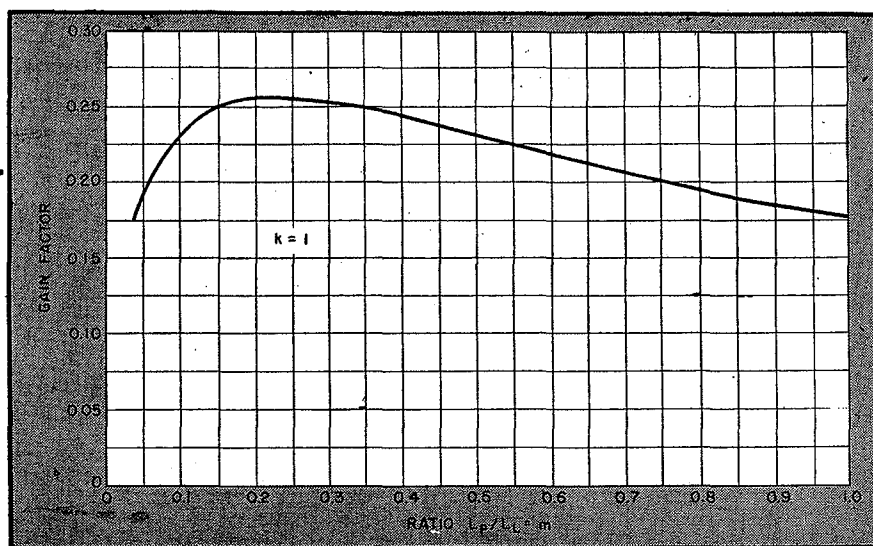


FIG. 3—Gain factor as a function of inductance ratio for constant coupling coefficient shows a broad maximum

$m$  directly. From this value of  $m$  and the loop inductance  $L_L$  we can find the required primary inductance  $L_P$ . Inasmuch as the quantity  $L_{sq}$  is fixed by tuning considerations, only the quantity

$$k[m(1+m-mk^2)/(1+m)]^{1/2} \times (1+m+2mk^2)^{-1}$$

of Eq. 1 can be varied freely. Call this quantity the *gain factor* and plot it against  $k$  as shown by curve (B) in Fig. 2.

Obviously  $k$  should be as large as possible for maximum gain, but the difference in performance between a coil having a  $k$  of 85 percent and one having a  $k$  of 95 percent hardly justifies extraordinary or costly precautions to obtain the higher coupling coefficient. Small powdered-iron core coils normally can be made with a  $k$  of 85 percent. Such a design is usually satisfactory from both cost and performance standpoints. The addition of powdered-iron cups surrounding the coils may bring  $k$  to over 90 percent, but the additional cost is considerable. If a coil is designed without powdered-iron, the coupling coefficient usually obtainable hardly justifies the degradation in performance.

The curve of gain factor as a function of  $m$ , allowing  $k$  to remain constant, shows the maximum to be rather broad as illustrated in Fig. 3. Thus with  $k$  fixed at unity,  $m$  can

have any value from 0.17 to 0.3 without noticeable loss in gain. Curves for other values of  $k$  can be plotted.

## Conductor Size

It is usually of interest to estimate the overall total  $Q$  of the coil in the circuit. The ratio of this value  $Q_{BQ}$  to  $Q_s$  is plotted as curve (C) in Fig. 2 against coupling coefficient. This ratio holds for values of  $m$  to give maximum gain as shown in curve (A) in Fig. 2, and the assumptions are the same as were made in the calculations for that curve, namely that  $Q_L$  equals  $Q_P$  and the total primary quality (i.e., of  $L_L$  and  $L_P$  combined) equals one-half  $Q_s$ .

The choice of conductor size for  $L_L$ ,  $L_P$ , and  $L_s$  is the determining factor in fixing selectivity and must therefore be carefully considered by the designer. When an iron core is used, the secondary can be properly wound with 5/41, 7/41, or 10/44 sse litz wire, and excellent secondary quality thus obtained. Either the loop antenna is constructed of heavy copper wire (No. 10 B&S gage or larger) or it may be made of flat copper ribbon. Such copper ribbon should usually be at least 0.01-inch thick to give satisfactory loop quality. A fairly typical large console loop constructed of  $\frac{3}{8}$ -inch wide flat copper ribbon 0.01-inch thick showed  $Q$  measurements of 100 at 600 kc and 175 at

Table I—Symbols Used in Text

$A$	: Area in square meters of loop antenna (Eq. 2)
$\alpha$	: Algebraic factor, introduced in Appendix II, $\alpha = (1+m)/m$ , see $m$
$E$	: Potential; $E_L$ induced into loop antenna, $E_g$ developed across grid of first tube
$k$	: Coefficient of coupling between transformer windings, see $M$
$L$	: Inductance; $L_L$ of loop antenna, $L_P$ of transformer primary, $L_s$ of transformer secondary, $L_{sq}$ as given in Eq. 5
$\lambda$	: Wavelength in meters (Eq. 2)
$M$	: Mutual inductance between transformer windings: $M = k(L_P L_s)^{1/2}$
$m$	: Ratio of transformer primary inductance to loop antenna inductance, $m = L_P/L_L$ , introduced in Appendix I, value for maximum gain given in Fig. 2
$N$	: Number of turns in loop antenna (Eq. 2)
$Q$	: Quality; $Q_L$ of loop antenna, $Q_P$ of transformer primary, $Q_s$ of transformer secondary, $Q_{sq}$ as given in Eq. 4
$R$	: Resistance; $R_L$ of loop antenna, $R_P$ of transformer primary, $R_s$ of transformer secondary, $R_{sq}$ as given in Eq. 6
$V$	: Voltage picked up by loop in a field of one volt per meter (Eq. 2)
For quantities not listed here, see Fig. 1, 4, and 5.	

1,400 kc, before the chassis was mounted in the cabinet.

The choice of conductor for the primary winding of the transformer is more difficult. A tabulation of quality obtained in a nine-turn solenoid such as would be used for the primary winding, wound on a 0.43-inch outside diameter Bakelite form through which was placed a 3/8-inch diameter iron core, is given in Table II.

From this table it would appear that No. 28 F. (single coat of vinyl-acetal insulation) solid wire is a good conductor to use. However, there are other factors which must be taken into account. The primary winding being closely associated with the secondary, in order to obtain close coupling, causes a pronounced loss in quality due to eddy currents induced in the primary conductor.

Due to the high cost of 20/44 or 30/44 litz wire, a suitable compromise may often be found in some such size as 10/41 litz. It should be noted that conductor cross-sectional area is of importance in determining inductor quality as well as the multistranding. Thus 10/41 litz will give better quality than 10/44, and 7/41 litz is usually preferable to 10/44 litz for the same reason, at least as far as the primary winding is concerned.

#### Comparison of Loops

We now have sufficient information to compare mathematically the performance of a low-impedance loop with that of a high-impedance loop. In designing a receiver it was decided to change from an average-sized high-impedance loop mounted underneath the shelf of a console to a low-impedance loop mounted on a frame within the console cabinet. The frame was swiveled to allow some adjustment of position, but was only slightly smaller in area than the inside of the console.

Voltage pickup of a high-impedance loop in a field of one volt per meter is given by<sup>1</sup>

$$V = 2\pi NA/\lambda \quad (2)$$

The figure of merit of the loop is equal to Eq. 2 multiplied by the loop quality  $Q_L$ .

The high-impedance loop which had been used had an inductance of 200  $\mu$ h (as determined by tracking considerations). Dimensions were

Table II—Quality of Coil Obtained With Different Wires

Wire Type	Frequency in kc		
	1,400	1,000	600
7/41 litz	65	45	35
10/41 litz	73	52	40
20/44 litz	80	53	42
30/44 litz	100	73	57
No. 34 F.	45	32	25
No. 28 F.	67	52	45

10.5 by 8.5 inches, and there were 19 turns. At 1,000 kc, 300 meters, the figure of merit, Eq. 2 times  $Q_L$ , equals 2.77.

In the case of the low-impedance loop, the voltage pickup is obtained by Eq. 2 as before, but the figure of merit is this expression multiplied by the gain of the coupling transformer given by Eq. 1. This gain is derived from known constants of the coupling transformer and the loop inductance. For this case where the equivalent inductance must remain 200  $\mu$ h because we will use the same tuning gang, and the antenna inductance will equal 8.4  $\mu$ h (the inductance of a two-turn loop whose dimensions are 21 by 30 inches), the gain is given by  $Q_s(L_{BQ}/L_L)^{1/2}$  times the gain factor. For a  $k$  of 85 percent from curve (B) in Fig. 2 the gain factor is 0.246, and because  $Q_s$  of the coil under consideration is 140 at 1,000 kc, the gain is 168. The figure of merit, Eq. 2 times this gain, equals 2.87.

Thus we have improved the figure of merit of the pickup system although we had to increase the area from 0.058 square meters to 0.408 square meters to do so. It is to be noted that a number of refinements such as spacing between turns of the loop and space factor<sup>2</sup> have been neglected, but results check reasonably well with measurement.

DERIVATION of Eq. 1, upon which the transformer design depends, is based on simple circuit theory. However, because the steps of the derivation indicate the function of the circuit and the limitations of the final design equation, the derivation is given. As will be recognized, the results are applicable to transformer couplings used in other applications than that considered here.

#### Appendix I

The equivalent circuit of Fig. 1 is as shown in Fig. 4A.<sup>3</sup> We are to find the ratio of  $E_g$  to  $E_L$ , the gain of the network. Let us lump  $R_L$  plus  $R_p$  and  $R_s$  into one equivalent resistance  $R_{BQ}$  which we shall place in the secondary circuit as in Fig. 4B.

By Thévenin's theorem we can write

$$E_{AB} = \frac{\omega M E_L}{\omega(L_L + L_P - M + M)} = \frac{M E_L}{L_L + L_P}$$

At resonance

$$I_c = \frac{M E_L / (L_L + L_P)}{R_{BQ}} = \frac{M E_L}{(L_L + L_P) R_{BQ}}$$

And

$$E_g = \frac{1}{\omega C} \times \frac{M E_L}{(L_L + L_P) R_{BQ}}$$

Because at resonance the total inductive reactance as seen at the grid of the tube is equal to the capacitive reactance, we can replace  $1/\omega C$  with  $\omega L_{BQ}$ , which is the combined reactances of  $L_s$ ,  $L_P$ , and  $L_L$  when connected as shown. Thus

$$E_g = \omega L_{BQ} \times \frac{M E_L}{(L_L + L_P) R_{BQ}}$$

But  $\omega L_{BQ}/R_{BQ} = Q_{BQ}$ , and because  $M = k(L_P L_s)^{1/2}$  we can write

$$\frac{E_g}{E_L} = \frac{M Q_{BQ}}{L_L + L_P}$$

or

$$\text{Gain} = \frac{k(L_P L_s)^{1/2} Q_{BQ}}{L_L + L_P}$$

Although this expression gives the gain of the coupling transformer, it does not clearly indicate the manner in which the transformer constants affect its gain. To convert this equation into a more informative form we proceed as follows:

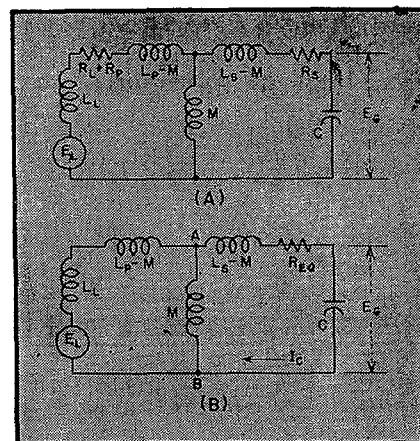


FIG. 4—(A) Equivalent circuit of Fig. 1 can be further simplified to that at (B)

The primary inductance will always be dependent on the inductance of the antenna loop, so let us choose some arbitrary constant which will be the ratio of these inductances. In fact, it is the value of this ratio which gives maximum gain which we wish to find. Therefore, define  $L_P = mL_L$ , then

$$\text{Gain} = kQ_{sq} \sqrt{\frac{L_s}{L_L}} \times \frac{\sqrt{m}}{1+m} \quad (3)$$

This equation is quite valid, but the equivalent quality is not directly known, although it can be measured by connecting a Q-meter across the secondary winding with the primary winding connected to the antenna loop. Also it will not be the value of the secondary inductance which will be known when a design is calculated, but the value of the equivalent inductance, because that is fixed by the value of the tuning capacitance and the required tuning range. Therefore this equation will be modified to an expression in terms of the equivalent inductance and the quality of the secondary coil alone, for these are the quantities which are usually known.

In Appendix II the equivalent inductance is found to be

$$L_{sq} = L_s \frac{1+m-mk^2}{1+m}$$

In Appendix III the equivalent resistance is found to be

$$R_{sq} = R_s \frac{1+m+2mk^2}{1+m}$$

From these results, and because  $Q_{sq} = \omega L_{sq}/R_{sq}$  and  $Q_s = \omega L_s/R_s$  the equivalent quality is

$$Q_{sq} = Q_s \frac{1+m-mk^2}{1+m+2mk^2} \quad (4)$$

Substituting into Eq. 3 this expression for the equivalent quality and writing  $L_s$  in terms of  $L_{sq}$ , we obtain the design equation

$$\text{Gain} = kQ_s (L_{sq}/L_L)^{1/2} \times [m(1+m-mk^2)/(1+m)]^{1/2} \times (1+m+2mk^2)^{-1}$$

#### Appendix II

To determine the equivalent inductance of the coupling transformer and loop antenna we write from Fig. 4B the inductance to the left of points A-B as

$$\frac{(L_L + L_P - M)M}{L_L + L_P - M + M}$$

This quantity can be simplified using the previously defined relation that  $L_P = mL_L$ , and by defining  $(1 +$

$m)/m = \alpha$ , and using the relation  $M = k(L_P L_s)^{1/2}$  to the expression

$$\frac{\alpha k(L_P L_s)^{1/2} - k^2 L_s}{\alpha}$$

The inductance to the right of points A-B in Fig. 4B is likewise simplified to the expression

$$L_s - k(L_P L_s)^{1/2}$$

Note that the mutual inductance between points A and B has been considered as a parallel branch of the inductance to the left of A-B. The total equivalent inductance across the tuning capacitance is the sum of these two inductances, thus

$$L_{sq} = \frac{\alpha k(L_P L_s)^{1/2} - k^2 L_s}{\alpha} + L_s - k(L_P L_s)^{1/2} = \frac{L_s(\alpha - k^2)}{\alpha}$$

Substituting the expression in  $m$  for which  $\alpha$  stands gives

$$L_{sq} = L_s \frac{1+m-mk^2}{1+m} \quad (5)$$

#### Appendix III

Likewise, to determine the equivalent resistance of the coupling transformer and loop antenna we simplify the circuit of Fig. 4A to that of Fig. 5A. This simplification is done by considering such a circuit as that at Fig. 5B which we wish to replace with an equivalent series circuit. The impedance seen to the left of terminals C-D is

$$\frac{j\omega L_D(R_C + j\omega L_C)}{R_C + j\omega L_C + j\omega L_D}$$

The real terms are the only ones of interest at present because we wish to find an equivalent resistance for  $R_L$ . Call this equivalent resistance  $R_C'$ , then

$$R_C' = (R_C \omega^2 L_D^2) / (R_C^2 + \omega^2 L_C^2 + 2\omega^2 L_C L_D + \omega^2 L_D^2)$$

In the denominator, the  $R_C^2$  term is small compared with the other terms, therefore the expression can be simplified to

$$R_C' = R_C \left( \frac{L_D}{L_C + L_D} \right)^2$$

Because the circuits under discussion have reasonably high quality ( $Q > 40$ ), the inductances can be combined without regard to their resistances. Therefore we can replace the circuit shown in Fig. 5B with the equivalent series circuit shown in Fig. 5C. In this manner we obtain the circuit of Fig. 5A.

Assume that  $Q_L$  equals  $Q_P$ , then  $R_L = R_P/m$  and total primary resistance is  $R_P + R_P/m$  or  $R_P(1+m)/m$ , which is the primary resistance of the circuit shown in Fig. 4A. The

equivalent primary resistance for the circuit of Fig. 5A is

$$R_P \frac{1+m}{m} \left( \frac{M}{L_L + L_P} \right)^2$$

Let us call this expression  $R_P'$ , and use the previously given relations  $(1+m)m = \alpha$ ,  $mL_L = L_P$ , and  $M = k(L_P L_s)^{1/2}$  to simplify it to

$$R_P' = R_P(k^2 L_s / \alpha L_P)$$

Let us also assume that the combined quality of the loop and primary inductances is one half the quality of the secondary inductance. On the average this condition usually exists. The combined quality of loop and primary inductance will be designated by  $Q_P'$ ; then  $2Q_P' = Q_s$ , or  $2\omega L_P/R_P = \omega L_s/R_s$ , so that we have  $R_P = 2L_P R_s / L_s$ , which when substituted into the foregoing gives

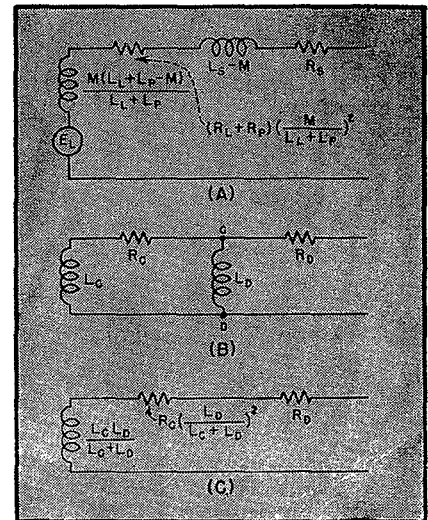


FIG. 5—Equivalent resistance is found from circuit at (A), which is derived from that at Fig. 4A by steps shown here at (B) and (C)

$$R_P' = \frac{2L_P R_s}{L_s} \times \frac{k^2 L_s}{\alpha L_P}$$

If we add  $R_s$  to this value we obtain the total equivalent resistance which we were seeking, thus

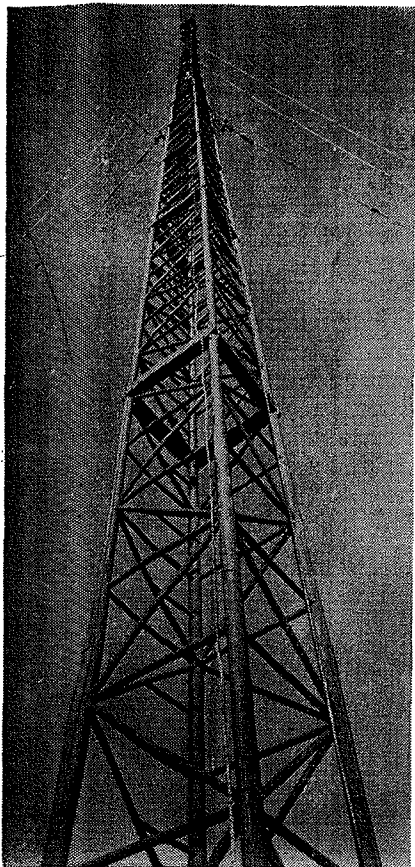
$$R_{sq} = R_P' + R_s = \frac{R_s(2k^2 + \alpha)}{\alpha}$$

Substituting the expression in  $m$  for which  $\alpha$  stands gives

$$R_{sq} = R_s \frac{1+m+2mk^2}{1+m} \quad (6)$$

#### REFERENCES

- (1) Terman, F. E., "Radio Engineers' Handbook", McGraw-Hill Book Co., Inc., New York 1943, p. 813, Eq. 40.
- (2) Taylor, P. B., Theory of Loop Antenna with Leakage between Turns, *Proc. I. R. E.*, Dec. 1937, p. 1574.
- (3) Everitt, W. L., "Communication Engineering", McGraw-Hill Book Co., Inc., Chapter VII.
- (4) Bachman, W. S., Loop-Antenna Coupling-Transformer Design *Proc. I. R. E.*, Dec. 1945.



Radio Frankfurt loop-fed antenna under construction

# Antifading Broadcast Antenna

The service area of a broadcast transmitter within which interference between ground and sky-wave components does not occur can be extended by reduction of high-angle radiation from the antenna. Use of a sectional mast with an insulator cancels the progressive wave usually found on fabricated towers

By **HELMUT BRUECKMANN**

*Consultant  
Signal Corps Engineering Laboratories  
Fort Monmouth, N. J.*

**T**HE RECEPTION of a broadcast station in the frequency range 0.5 to 1.6 mc is frequently affected by fading at relatively short distances, especially at night. This kind of fading, which results from interference of ground and sky wave, is observed at distances of about 50 to 100 miles or more. It causes linear and nonlinear distortion at the receiver, sometimes to an extent which completely spoils a high-quality radio program, even with AVC in the receiver. This effect is true also for a high-power station, the signal from which is strong enough to overcome r-f noise. As a result, a considerable part of the potential coverage area of many radio stations suffers from poor reception. In order to achieve an undisturbed primary coverage as large as possible, especially at night time, many high-power radio

stations have been equipped with antifading antennas. However, not all of them have been successful.

In 1930, German broadcast stations started to use a single vertical wire or metal rope hung in the axis of a self-supporting wooden tower with a height in the order of half a wavelength and excited electrically at the base. Experience with this kind of antenna in respect to reduction of fading was good. In some cases, the undisturbed night-time primary coverage was increased by 100 percent in area, compared to an antenna with a height of one-quarter wavelength or less. However, the maintenance of the wooden tower proved to be expensive and difficult, and many towers were destroyed by fire or storm. In time they were replaced by self-radiating steel towers which were fed at the base in the same manner as the one-wire antennas. These steel towers were much cheaper, easier to maintain and less subject to hazards. However, they

were disappointing in respect to reduction of fading.

Beginning in 1936, several investigators showed that this effect was due to the progressive voltage-current wave along the tower which is superimposed on the standing voltage-current wave as shown in Fig. 1A. This progressive wave carries the energy which is radiated by each element of the antenna or dissipated by losses. In a thin conductor like the one-wire antenna, the progressive wave is small compared to the standing wave and, therefore, the radiation of the progressive wave is almost negligible. In a thick conductor like a steel tower, this is no longer true. The vertical radiation pattern of a simple vertical antenna with height  $H = 0.585 \lambda$  is shown in Fig. 1B,  $H = 210^\circ$  curves 1, 2 and 3, for different values of  $K$ .

The distance for which ground and sky wave are equal and, therefore, fading is worst is strongly affected by such modification of the radiation pattern, as illustrated in

Table I—Characteristics of Antenna Operating at 1,195 kc

	Loop-fed			Base-fed
Length of stub in feet between grounded tap and base of mast	58.7	55.1	52.0	*
Height in feet of the current node above ground	-0.8	8.8	16.8	11
Elevation angle in degrees of null of vertical radiation pattern	90	62	54	65
Gain in db in the horizontal direction due to pattern (calculated)	2.15	2.40	2.61	—
Input impedance in ohms of the coaxial transmission line	100-j51	84+j37	27+j35	*
Antenna efficiency in percent, including matching network	73	67	62	73
Losses in stub in percent of the input power	3	10	12	*
Heat losses in percent along the mast (calculated)	0.7	0.6	0.7	0.7
Losses in percent in coaxial transmission line inside mast	1.4	1.4	4.2	*
Ratio of current in percent at current node and at current loop	—	2.9	2.7	26
Voltage in kv across base insulator	5.9	8.3	10.2	9.5
Voltage in kv across sectional-mast insulator	5.7	4.4	6.9	**
Maximum voltage in kv across coaxial transmission line inside mast	6.8	8.0	13.0	*
Standing-wave ratio in coaxial transmission line inside mast	2.2	2.5	7.9	—

\* Disconnected  
 \*\* Shorted  
 Voltages are for 100 kw rms unmodulated power input.

Fig. 1C. The ground-wave intensity is based on measurements with a certain station as an example. The sky-wave intensity is calculated for perfect reflection from the E-layer as an arbitrary basis of comparison. It is apparent that the distance for which ground and sky wave are equal is reduced considerably with a base-fed mast antenna, compared to a thin vertical radiator, namely from about 135 miles to about 105 miles. This reduction corresponds to a decrease in undisturbed area of 40 percent.

### Principle of New Antenna

Around 1940, the author suggested that the shaft of the mast be broken up by an insulator somewhere in its upper part, and that it be excited electrically at this sectional-mast insulator. Although this idea was not in itself new, nobody up to that time had mentioned the advantages of this idea in respect to antifading action.

Disregarding the physical problem of transmitting power to the

sectional-mast insulator, by tentatively locating the current source at this point, the basic idea can be illustrated as shown in Fig. 1D. In respect to current distribution, the upper part of the mast works as an open one-wire line and the lower part as a one-wire line terminated by an inductance. According to the flow of energy there is a progressive wave superimposed on the standing wave in each part of the mast, traveling upward in the upper part and downward in the lower part. Each of the two progressive waves is, near the current source, about half as strong as in the case of excitation at the base. The radiation components originating from them cancel each other at least partially because of the opposite direction of the progressive waves. For the sake of brevity, this kind of antenna may be called the loop-fed antenna, in contrast to the base-fed antenna.

As shown in Fig. 2, the current distribution in the lower part of the mast depends upon the induct-

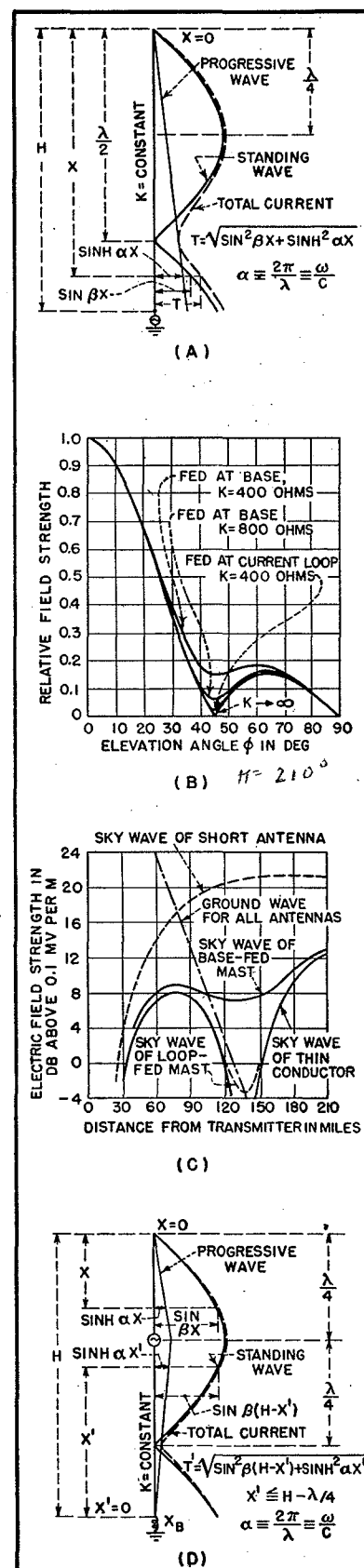


FIG. 1—(A) standing, progressive and total current waves on radiator fed at base, (B) vertical pattern of vertical 0.585-wavelength radiator, (C) sky and ground-wave field strengths, and (D) standing, progressive and total current waves on center-fed radiator



ance which is connected between the base of the mast and ground. This means that the vertical radiation pattern can be controlled by varying this inductance. In order to have a pattern suitable for reduction of fading, it is not necessary to have a current loop at the sectional-mast insulator. Actually a current distribution similar to that in Fig. 2B is more favorable because it allows reduction of the total height of the mast, which can be as low as 0.4 wavelength. Since the inductance at the base can be adjusted conveniently, it is possible to adapt the antenna during operation to a change in ionospheric conditions, as it happens, for example, during spring and fall.

A simple way to feed the antenna at the sectional-mast insulator is shown in Fig. 3A. A coaxial r-f cable is wound as a big coil. Its outer conductor is connected between the base of the mast and ground, representing the inductance mentioned above. The inner conductor of this cable is continued through the inside of the lower part of the mast and insulated from it up to the lower end of the upper part of the mast. This continuation of the inner conductor and the mast itself form a coaxial transmission line, with the mast as the outer conductor. A current equal in phase and magnitude and opposite in direction to the current in the inner conductor flows on the inner surface of the lower part of the

mast. No radiation originates therefrom. At the sectional-mast insulator, this current goes around the rim of the mast shaft and continues on the outside surface.

Normally, a tuning and matching network would be introduced at the sectional-mast insulation between the antenna terminals and the coaxial cable. However, in this case it is not necessary. On that part of the coaxial transmission line which is formed by the mast itself and the inner conductor, even a high standing-wave ratio does not matter, both from the standpoints of power losses and break-down voltage of the insulators, because of the great dimensions available. Therefore, it is sufficient to have a matching and tuning network at the lower end of the lower part of the mast shaft where it can be operated conveniently. Even more convenient, the matching network can be installed at the grounded end of the coil of coaxial cable.

In order to determine how much the loop-fed antenna actually improves sky-wave suppression, field strength measurements by airplane were made with a 330-foot high antenna model operated at 1,640 kc. For an elevation angle of 43 degrees, the field strength was reduced by about 14 db compared to the base-fed antenna, and by 23 db compared to a simple short antenna. In effect, the loop-fed mast is about equal to, if not better than, the base-fed one-wire antenna in

respect to the sky-wave suppression.

The calculated field strength of the reflected sky wave as a function of the distance, when based on the measured pattern, is shown in Fig. 1C. According to this diagram, the undisturbed primary coverage at night time is increased considerably; namely, by about 30 percent in radius or 68 percent in area, compared to a base-fed mast.

### Radio Frankfort Antenna

The first broadcast transmitter which was to have obtained a permanent version of the loop-fed antenna was the 100-kw station in Berlin, Germany. The war prevented this and, instead, such an antenna was erected in 1946 for the 100-kw station in Frankfort-on-Main. Meanwhile, the antenna originally planned for Berlin is thought to have been erected also.

The antenna for Radio Frankfort is a 402-foot steel tower with uniform square cross section. The sectional-mast insulator is at a height of 269 feet so that the upper part of the tower is 133 feet long. The construction of this sectional-mast insulator is similar to that used for station WMAQ.

At the time of the erection in 1947, it was a problem to provide for the necessary inductance between the lower end of the mast shaft and the ground system. This inductance could not be established by a coaxial cable wound into a coil, as indicated in Fig. 3A, because there was no 100-kw cable available. Instead, sections of another mast of identical construction were used to build a kind of short-circuited stub. They are hung up horizontally by strain insulators at a distance of 20 inches above the ground in such a way that they form one big loop with a diameter of 64 feet, as shown in Fig. 3B. One end of this stub is connected to the base of the antenna, the other end is grounded. By moving the tap for the ground connection along the stub, the reactance that is effective between the base of the antenna and ground can be varied conveniently, providing a simple means of adjusting the current distribution along the antenna and, consequently, the vertical radiation pattern.

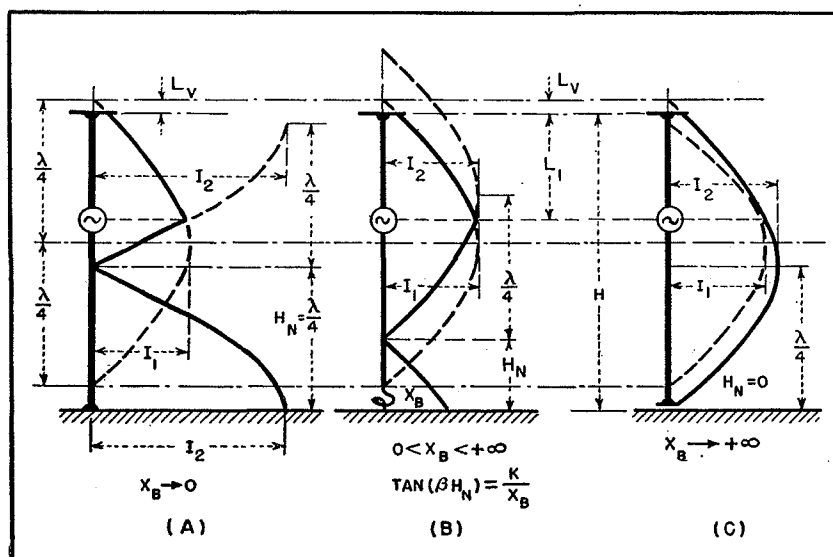


FIG. 2—Effect of variation of series impedance  $X_B$  at base of loop-fed antenna on current distribution



In the axis of this stub, the same kind of copper rope as used in the axis of the mast is hung up by strain insulators. At the base of the antenna, it is connected directly to the copper rope in the axis of the antenna. At the other end it is connected to a matching and tuning network. In this way the coaxial transmission line represented by the copper rope inside the antenna and the mast shaft is continued to the point where the outer conductor is grounded. In view of the high voltage-rating of this coaxial transmission line inside the stub, there is no danger of flashing over, even with a high standing-wave-ratio. Therefore, the matching and tuning network could be installed outside the mast shaft in a small tuning house.

The actual performance of this antenna was measured for three different settings of the tap for the ground connection on the stub corresponding to three different radiation patterns. Some of the results are listed in Table I. A total antenna efficiency of 73, 67 and 62 percent was obtained corresponding to a total loss of 1.4, 1.7, and 2.1 db respectively, a relatively high efficiency considering the inexpensive ground system used and the high frequency of 1.2 mc. Even with these losses, the ground-wave field strength is greater than that of a quarter-wave antenna with an efficiency of 100 percent.

### Power Losses

About 1.4 to 4.2 percent of the input power was found to be dissipated in the coaxial transmission line inside the tower. This is not too much considering that this coaxial line has a high standing-wave ratio. Another 3 to 12 percent of the input power is lost in the stub. This is due to the low characteristic impedance of the stub, only 62 ohms, which is unfavorable but could not be avoided because of lack of material. Without restriction in material, the losses could have been made much smaller. The balance of about 10 percent loss probably is due chiefly to ground losses. Equally satisfactory are the voltage ratings of the antenna.

Preliminary field strength re-

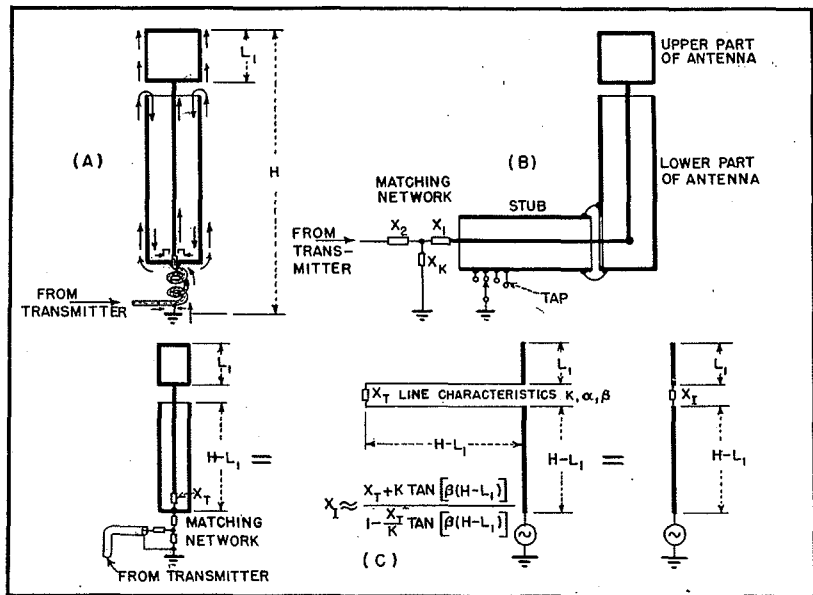


FIG. 3—(A) current flow in loop-fed antenna, (B) loop-fed antenna with matching network outside mast, and (C) equivalent circuit of loop-fed antenna operated as base-fed type.

cordings at night time, at a distance where the fading with a simple quarter-wavelength antenna at the transmitter previously had been serious, showed that the fading at Radio Frankfort is much smaller than the signal of another station equipped with a quarter-wave antenna located at the same place and with almost the same frequency. Final tests have not yet been made in respect to the area undisturbed by fading.

The new antenna also has advantages in respect to its usable frequency range. Full benefit of its antifading action can be obtained in a frequency range of about  $\pm 20$  percent of the frequency for which it is designed, without any alteration of the antenna itself, just by properly adjusting the tap for the ground connection on the stub. If the antenna is required to operate at a frequency outside of this range, it can be used as a base-fed antenna with the coaxial cable inside the mast working as a stub, shown in Fig. 3C. With this mode of excitation, and with a suitable reactance  $X_T$  between the inner conductor and the lower end of the mast, the radiation efficiency at low frequencies is higher than with a simple steel tower because its effective height can be increased by making the input impedance of the coaxial cable

inside the mast at the sectional-mast insulator inductive. At higher frequencies the sectional-mast insulator can be used to decrease the electrical height of the antenna in order to obtain a more suitable vertical radiation pattern by making the input impedance of the coaxial cable capacitive. It is also possible to operate the antenna as a simple base-fed mast by short-circuiting the sectional-mast insulator. This possibility may be useful in case of trouble with this insulator.

Acknowledgment is made of the help furnished by Messrs. Gerwig and Graziadei and others involved in the development of the antenna which was carried out under the supervision of the author in the Forschungsanstalt der Deutschen Reichspost, Berlin, Germany.

Valuable help in antenna measurements was afforded by Messrs. Haberkant and Behne, employees of Radio Frankfort.

Interest and encouragement were given by R. J. Condon, AMG, and Lt. L. C. Heinzman, then chief engineer of Radio Frankfort.

### BIBLIOGRAPHY

- Stuart Ballantine, High Quality Radio Broadcasting, *Proc. IRE*, 22, p 564, 1934.
- R. F. Guy, Notes on Broadcast Antenna Developments, *RCA Review*, p 39, April 1937.

# Resistance-Capacitance FILTER CHART

Values of  $R$  and  $C$  for both low-pass and high-pass filters are given in terms of the amount of rejection desired at any given frequency from 1 millicycle to 1,000 megacycles.

Chart also gives the reactance of a capacitor at any frequency

**R**ESISTANCE-CAPACITANCE filters are frequently used when a sharp cutoff characteristic is not required and, in the low-pass case, when the voltage drop across the series resistor can be tolerated. Applications of the low-pass  $R$ - $C$  filter include decoupling from a common power supply for a multistage vacuum-tube amplifier, smoothing filters for power supplies when a large voltage drop across the filter is not objectionable, and inexpensive hash filters to attenuate high-frequency disturbances on electrical leads. High-pass  $R$ - $C$  filters are often used as interstage coupling networks.

The circuits of Fig. 1 show the  $R$ - $C$  low-pass and high-pass filter connected to an a-c generator. The generator resistance is assumed to be negligible compared with  $R$ , and d-c voltages are omitted for the purposes of an a-c analysis.  $R$  and  $C$  form a voltage divider, and the complex output voltage is given by

$$\text{Low-pass: } E_o = \frac{-jX_c E_i}{R - jX_c} \quad (1a)$$

$$\text{High-pass: } E_o = \frac{R E_i}{R - jX_c} \quad (1b)$$

By **ERNEST FRANK**

*Sperry Gyroscope Co.  
Garden City, N. Y.*

The magnitude of the ratio of  $E_i$  to  $E_o$  is

$$\text{Low-pass: } \left| \frac{E_i}{E_o} \right| = \sqrt{1 + \left( \frac{R}{X_c} \right)^2} \quad (2a)$$

$$\text{High-pass: } \left| \frac{E_i}{E_o} \right| = \sqrt{1 + \left( \frac{X_c}{R} \right)^2} \quad (2b)$$

Solving the above equations for the generator frequency  $f$  gives

$$\text{Low-pass: } f = \frac{1}{2\pi RC} \sqrt{\left| \frac{E_i}{E_o} \right|^2 - 1} \quad (3a)$$

$$\text{High-pass: } f = \frac{1}{2\pi RC} \sqrt{\left| \frac{E_i}{E_o} \right|^2 - 1} \quad (3b)$$

When the reactance of  $C$  is equal to  $R$ , the ratio  $|E_i/E_o|$  is equal to  $\sqrt{2}$ . This condition occurs at a frequency  $f_s$  that is equal to  $1/2\pi RC$  and corresponds to the frequency at which the output voltage is 3 db down from the input voltage, ignoring impedance levels ( $\text{db} = 20 \log_{10} |E_o/E_i|$ ). Therefore

$$\text{Low-pass: } f = f_s \sqrt{\left| \frac{E_i}{E_o} \right|^2 - 1} \quad (4a)$$

$$\text{High-pass: } f = f_s \frac{1}{\sqrt{\left| \frac{E_i}{E_o} \right|^2 - 1}} \quad (4b)$$

In low-pass applications the ratio  $|E_i/E_o|$  is often selected to be 10 or greater. Therefore, Eq. (4a) becomes

$$f \approx f_s \left| \frac{E_i}{E_o} \right| ; \left| \frac{E_i}{E_o} \right| \geq 10 \quad (5)$$

because  $|E_i/E_o|^2 \gg 1$ . The value of  $f$  is given to an accuracy of about 1 percent by Eq. (5) when  $|E_i/E_o| = 10$ . When  $|E_i/E_o| = 100$ ,  $f$  is given to an accuracy of about 0.1 percent. The error resulting from the use of Eq. (5) is in the pessimistic direction since the true value of  $f$ , obtained from Eq. (4a), is always smaller than the value of  $f$  given by Eq. (5).

## Use of Chart

In high-pass applications, the value of  $f_s$  is usually of primary interest, and is given by  $f_s = 1/2\pi RC$ . The chart in Fig. 2 enables  $f_s$  to be read directly in one operation for a given value of  $R$  and  $C$  in either the low-pass or high-pass case. When a value of  $|E_i/E_o|$  equal to or greater than 10 is desired in the low-pass case, the value of  $f_s$  determined from the chart can be multiplied by  $|E_i/E_o|$ . The chart can also be used to determine the reactance of a capacitor at any frequency. The following examples illustrate the use of the chart.

## Example 1

A plate decoupling  $R$ - $C$  filter must attenuate frequencies above 50 cps by a voltage ratio of 10:1. The value of  $R$  cannot exceed 4,000 ohms to avoid an excessive loss in d-c voltage. What value of  $C$  is required? From Eq. (5),  $f_s = 50/10 = 5$  cps. From the chart, draw a

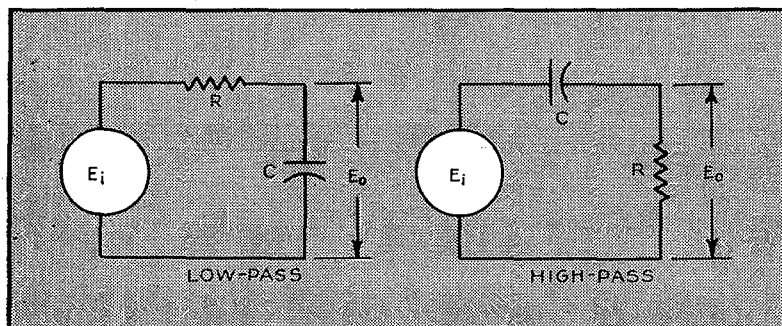


FIG. 1—Low- and high-pass  $R$ - $C$  filters shown connected to a-c generator

A and G.

To get reliable indications of antenna current, the stray capacitance of the input terminal and of  $C_1$  to ground must be reduced to as low a value as possible. Careful arrangement of the elements of the network, together with a short input lead, will increase the accuracy of power output measurements.

There are several precautions to be taken in connection with the design, construction, and use of the artificial antenna described here.

The various components of the network must be carefully chosen to give satisfactory service. This caution is particularly applicable to capacitor  $C_1$  which may be subjected to extremely high r-f potential, even with low-power transmitters. For example, at two megacycles, a transmitter which produces 20 watts in an antenna resistance of three ohms causes a current of 2.57 amperes rms to flow. Using the value of  $C_1$  in our typical case, 69.9  $\mu\text{mf}$ , the current in  $C_1$  would be 2.25 am-

peres. The peak voltage across  $C_1$  with 100-percent modulation is  $2 \times 1.4 \times 1140 \times 2.25 = 7,160$  volts.

In conclusion, while the antenna network presented here falls considerably short of perfection, it does have a substantial field of usefulness from an engineering point of view. The effort consumed by its design and construction is small indeed when one considers the amount of time which can be saved in the development and testing of multi-frequency transmitters.

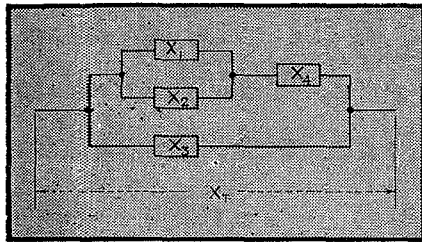


FIG. 5—Assumed circuit from which reactive network is developed

#### Appendix I Simulation of Reactance Curve

Neglect the resistance in the circuit. The reactive portion of the simulated antenna can be represented by Fig. 5. The total circuit reactance is

$$X_T = \frac{X_1 X_2 X_3 + X_3 X_4 (X_1 + X_2)}{X_1 X_2 + X_4 (X_1 + X_2) + X_3 (X_1 + X_2)} \quad (5)$$

$$\begin{aligned} \text{let } X_1 &= +\omega L_2 \\ X_2 &= -1/\omega C_5 \\ X_3 &= -1/\omega C_3 \\ X_4 &= -1/\omega C_4 \end{aligned}$$

Substituting these values into Eq. (5) gives

$$X_T = \frac{\omega^2 L_2 (C_4 + C_5) - 1}{\omega C_3 [1 - \omega^2 L_2 (C_4 + C_5)] - \omega C_4 (\omega^2 L_2 C_5 - 1)} \quad (6)$$

when  $\omega = \omega_2$ ,  $X_T = 0$

$$\omega_2^2 L_2 (C_4 + C_5) - 1 = 0 \quad (7)$$

when  $\omega = \omega_3$ ,  $X_T = \text{infinity}$

$$C_3 [1 - \omega_3^2 L_2 (C_4 + C_5)] - C_4 (\omega_3^2 L_2 C_5 - 1) = 0 \quad (8)$$

when  $\omega = \omega_1$ ,  $X_T = X_1$

$$X_1 = \frac{\omega_1^2 L_2 (C_4 + C_5) - 1}{\omega_1 C_3 [1 - \omega_1^2 L_2 (C_4 + C_5)] - \omega_1 C_4 (\omega_1^2 L_2 C_5 - 1)} \quad (9)$$

Equations (7), (8), and (9) are now solved simultaneously for unknowns  $C_4$ ,  $C_5$ , and  $L_2$ , giving the equations of Table II.

#### Appendix II Simulation of Resistance Curve

In the network of Fig. 6A the equivalent series resistance,  $R_s$ , as shown at Fig. 6B is a function of the branch reactance  $X_1$  which in turn is some function of frequency; thus

$$R_s = \frac{(R_1 R_2) (R_1 + R_2) + R_2 X_1^2}{(R_1 + R_2)^2 + X_1^2} \quad (10)$$

This circuit is satisfactory for our purpose because the equivalent series reactance  $X_s$  can at all times be made small compared to either the total series resistance or the total series reactance. This total series reactance includes the reactance developed in Appendix I. We are primarily concerned with the duplication of a resistance variation. The magnitude and importance of  $X_s$  is considered elsewhere.

The minimum value of  $R_s$  in Eq. (10) occurs when  $X_1 = 0$  and  $R_s = R_0 = R_1 R_2 / (R_1 + R_2)$ . If Eq. (10) is solved for  $X_1$ , we obtain

$$X_1 = \pm \left[ \frac{(R_1 R_2) (R_1 + R_2) - R_s (R_1 + R_2)^2}{R_s - R_0} \right]^{1/2} \quad (11)$$

From the condition for a minimum value of  $R_s$ ,  $R_1 = R_0 R_2 / (R_2 - R_0)$ , which, substituted into Eq. (11), gives

$$X_1 = \left( \frac{R_2^2}{R_2 - R_0} \right) \left[ \frac{R_0 - R_s}{R_s - R_2} \right]^{1/2} \quad (12)$$

Now if in Fig. 6A,  $X_1$  assumes the configuration of Fig. 6C.

$$X_1 = \frac{1 - \omega^2 L_1 (C_1 + C_2)}{\omega C_1 (\omega^2 L_1 C_2 - 1)}$$

Substituting this value of  $X_1$  into Eq. (12) yields

$$\frac{1 - \omega^2 L_1 (C_1 + C_2)}{\omega C_1 (\omega^2 L_1 C_2 - 1)} =$$

$$\frac{R_2^2}{R_1 - R_0} \left[ \frac{R_0 - R_s}{R_s - R_2} \right]^{1/2} \quad (13)$$

If  $\omega_1$  is the angular frequency at which the  $L_1 C_2$  loop is in parallel resonance, that is:  $L_1 C_2 = 1/\omega_1^2$ , and similarly, if  $\omega_2$  is the angular frequency at which the circuit of Fig. 6C is in series resonance so that  $L_1 (C_1 + C_2) = 1/\omega_2^2$ , Eq. (13) can be written in terms of resonant and antiresonant angular velocities.

There are three unknowns in this resultant equation, namely,  $R_s$ ,  $\omega$ , and  $C_1$ . If three conditions are known, a corresponding number of simultaneous equations can be set up. The most convenient boundary conditions are the two limit frequencies and one intermediate frequency, and the corresponding antenna resistances. Using these values to solve this equation gives the design equations of Table III.

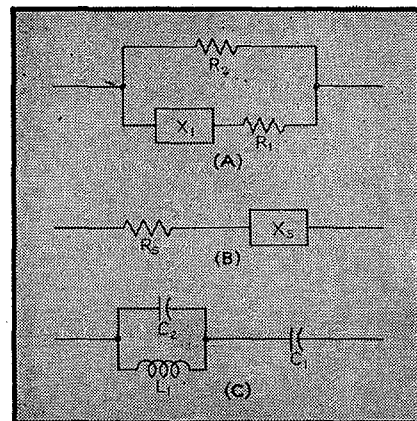


FIG. 6—Circuit from which resistive network is developed: (A) the assumed circuit, (B) the equivalent series circuit, and (C) the final design

particular example, the reactance error at any frequency is less than two percent.

To complete the sample calculations, the significant resistance values of the given antenna with reference to Fig. 3B are:  $R_{s1} = 3.2$  ohms,  $f_1 = 2$  mc or  $\omega_1 = 2\pi (2 \times 10^6)$ ,  $R_o = 2.7$  ohms,  $f_2 = 4$  mc or  $\omega_2 = 2\pi (4 \times 10^6)$ ,  $R_{s5} = 6$  ohms,  $f_5 = 7.5$  mc or  $\omega_5 = 2\pi (7.5 \times 10^6)$ ,  $R_{s3} = 11.5$  ohms, and  $f_3 = 9$  mc or  $\omega_3 = 2\pi (9 \times 10^6)$ .

Substitution of the preceding constants into the equations of Table III gives  $R_2 = 11.8$  ohms,  $f_4 = 9.275$  mc,  $C_1 = 0.0135$   $\mu$ f,  $L_1 = 0.1197$   $\mu$ h,  $C_2 = .00247$   $\mu$ f, and  $R_1 = 3.42$  ohms.

If these values are substituted in the equation for  $R_s$  and the resultant values plotted against frequency, the lower curve of Fig. 4 is obtained.

The actual artificial antenna is the series combination of the resistive and reactive networks.

#### Reactance Error due to Resistance Network

Lumping the reactive elements of the resistance network of Fig. 2C into a single reactance  $X_1$ , we find that the reactance of the resistance network is

$$X_s = X_1 R_2^2 / [(R_1 + R_2)^2 + X_1^2] \quad (1)$$

To find the greatest value that  $X_s$  can ever reach, differentiate Eq. (1) with respect to  $X_1$

$$\frac{d(X_s)}{dX_1} = \frac{[(R_1 + R_2)^2 + X_1^2] R_2^2 - (X_1 R_2^2) 2X_1}{[(R_1 + R_2)^2 + X_1^2]^2}$$

Setting the numerator equal to zero, and solving for  $X_1$

$$X_1 = R_1 + R_2 \quad (2)$$

Substituting Eq. (2) into Eq. (1)

$$X_{smax} = R_2^2 / 2 (R_1 + R_2) \quad (3)$$

In a typical case where  $R_2 = 11.8$  ohms and  $R_1 = 3.42$  ohms, the maximum value of  $X_s$  is 4.56 ohms inductive. Substituting Eq. (2) in Eq. (10) from Appendix II gives

$$R_s = \frac{R_2 (R_2 + 2R_1)}{2 (R_1 + R_2)} \quad (4)$$

Using the same numerical values for  $R_1$  and  $R_2$ ,  $R_s = 7.2$  ohms.

Referring to the antenna resistance curve of Fig. 4B, we see that  $R_s = 7.2$  ohms at a frequency of 7.9 mc. At this frequency the antenna reactance is  $-j100$  ohms.

Thus, in the given example, the maximum error introduced by the reactance of the resistance variation circuit occurs at 7.9 mc and has a value of  $X_{smax}/X_A = 4.56/100 = 4.56$  percent.

#### Antenna Operation

The simulative network discussed in this paper is, strictly speaking, only an approximation of the antenna which it is intended to replace. At any frequency the simulated reactance and resistance will differ from the actual values by a finite amount. The magnitude of these discrepancies will vary depending on the antenna, but in general it will be found that the reactance curve can be made to match within two percent, while the resistance may deviate as much as ten

percent from the true value.

Effect of mismatch on the tuning of the transmitter output circuits may for all practical purposes be neglected. However, the setting of the coupling control, being sensitive to the resistive component of the antenna impedance, will differ slightly at some points from its position when working into an actual antenna.

The network may be used for measuring power output if a radio-frequency ammeter is connected in series with the circuit. The power output is  $P = I_A^2 R_s$  where  $P$  is power output in watts,  $I_A$  is amperes rms, and  $R_s$  is equivalent series resistance of entire network. The value of  $R_s$  at each frequency should be determined by measurement on either a Q meter or a suitable r-f bridge, between terminals

TABLE III—RESISTANCE NETWORK DESIGN EQUATIONS

Units in farads, henrys, cycles, and ohms.

(1) Solve for  $R_2$  from the following equation, using given values from the antenna to be duplicated

$$\pm N [A (R_2 - R_{s5})]^{1/2} \mp M [F (R_2 - R_{s1})]^{1/2} = (N - M) [R_2 - R_{s3}]^{1/2}$$

$$\text{where } A = \frac{(R_{s3} - R_o) / (R_{s5} - R_o)}{\left[ \frac{\omega_5 (\omega_2^2 - \omega_5^2)}{\omega_3 (\omega_2^2 - \omega_5^2)} \right]^2}$$

$$F = \frac{(R_{s3} - R_o) / (R_{s1} - R_o)}{\left[ \frac{\omega_1 (\omega_2^2 - \omega_3^2)}{\omega_3 (\omega_2^2 - \omega_1^2)} \right]^2}$$

$$M = \omega_5^2 - \omega_3^2$$

$$N = \omega_1^2 - \omega_3^2$$

(2) Having found  $R_2$ , solve for  $\omega_4$  from

$$\omega_4 = [(\pm \omega_5^2 B - \omega_3^2) / (B - 1)]^{1/2}$$

$$\text{where } B = \left[ \frac{R_2 - R_{s3}}{A (R_2 - R_{s5})} \right]^{1/2}$$

$$(3) C_1 = \left( \frac{\omega_2^2 - \omega_5^2}{\omega_5^2 - \omega_3^2} \right) \left( \frac{\omega_4^2}{\omega_2^2 \omega_5 R} \right)$$

$$\text{where } R = \frac{R_2^2}{R_2 - R_o} \left[ \frac{R_{s5} - R_o}{R_2 - R_{s5}} \right]^{1/2}$$

$$(4) L_1 = (\omega_4^2 - \omega_2^2) / \omega_4^2 \omega_2^2 C_1$$

$$(5) C_2 = 1 / \omega_4^2 L_1$$

$$(6) R_1 = R_o R_2 / (R_2 - R_o)$$

(7) To check accuracy of the calculated components, plot  $R_s$  vs angular velocity from the following equation and compare this curve with the given antenna resistance curve

$$R_s = \frac{(R_1 R_2) (R_1 + R_2) + R_2 X_B^2}{(R_1 + R_2)^2 + X_B^2}$$

$$\text{where } X_B = (-1/2 \pi f C_1) + \frac{2 \pi f L_1}{1 + (4 \pi^2 f^2 L_1 C_2)}$$

TABLE II—REACTANCE NETWORK DESIGN EQUATIONS

Units are in farads, henrys, cycles, and ohms.

1) Assume a value for  $C_3$

$$(2) C_s = \frac{(\omega_2^2 - \omega_1^2) (-X_1 \omega_1 C_3 - 1) - X_1 C_3 \omega_1 (\omega_3^2 - \omega_2^2)}{X_1 (\omega_1 \omega_3^2 - \omega_1^3)}$$

where  $C_s = C_4 C_5 / (C_4 + C_5)$

$\omega_1$  — angular velocity at lower limit

$\omega_2$  — quarter-wavelength angular velocity

$\omega_3$  — half-wavelength angular velocity

$X_1$  — antenna reactance at  $\omega_1$  (proper sign must be used for  $X_1$  when substituting into equation)

$$(3) C_4 = C_s (\omega_3 / \omega_2)^2 - C_3 (\omega_2 L \omega_3)^2 / \omega_2^2$$

$$(4) C_5 = C_s C_4 / (C_4 - C_s)$$

$$5) L_2 = 1 / \omega_2^2 (C_4 + C_5)$$

Note: (A) If  $\omega_3$  is unspecified it can be assumed to be  $1.67 \omega_2$ , as stated in Table I (5); (B) The  $Q$  of  $L_2$  should be as high as possible, at least 300; (C) Distributed capacitance of  $L_2$  should be subtracted from the calculated value of  $C_5$  to determine the physical value for  $C_5$ .

(6) To check accuracy of computed components, plot  $X_s$  vs angular velocity from the following equation, and compare this curve with the given antenna reactance curve

$$X_s = \frac{\omega^2 L_2 (C_4 + C_5) - 1}{\omega C_3 [1 - \omega^2 L_2 (C_4 + C_5)] - \omega C_4 (\omega^2 L_2 C_5 - 1)}$$

responding frequency characteristic is shown in Fig. 3A.

The problem is to select values of  $C_3$ ,  $C_4$ ,  $C_5$ , and  $L_2$  to yield a reactance variation which duplicates that of any given antenna. While  $C_3$  is theoretically unnecessary to obtain the simulated curve, in practice it was found that the stray capacitance from the antenna terminal to ground introduced a large error in reactance at the low-frequency end of the band. Using a controlled value of  $C_3$  eliminates the effect of this unavoidable capacitance. Thus some value is selected for  $C_3$  greater than the supposed stray capacitance to ground and if the final capacitance to ground is smaller than the assumed value, a trimmer capacitor can be inserted to make up the difference. A practical value for  $C_3$  is about  $10 \mu\mu\text{f}$ .

Design equations for this reactance network are derived in Appendix I and summarized in Table II.

In a similar manner, the network

of Fig. 2C provides the required resistance variation. Design equations for this network are derived in Appendix II and summarized in Table III. The quantities referred to in this table are made clear by Table I and Fig. 3B.

#### Example of Network Design

Pertinent data concerning the reactive characteristics of an antenna is: Lower limit frequency = 2 mc, reactance at lower limit frequency =  $-j 930$ , quarter-wave frequency = 9.3 mc, and half-wave frequency = 15.5 mc.

From this data, values for substitution into Table II are:  $\omega_1 = 2\pi (2 \times 10^6)$ ,  $\omega_2 = 2\pi (9.3 \times 10^6)$ ,  $\omega_3 = 2\pi (15.5 \times 10^6)$ ,  $X_1 = -930$ , and let  $C_3 = 10 \times 10^{-12}$ . Solving for the reactive network components, we obtain  $C_s = 20.3 \mu\mu\text{f}$ ,  $C_4 = 69.9 \mu\mu\text{f}$ ,  $C_5 = 28.7 \mu\mu\text{f}$ , and  $L_2 = 2.96 \mu\text{h}$ .

If these values are substituted into the equation for  $X_s$  and react-

ance plotted against frequency, the upper curve of Fig. 4 is obtained. Checking the value of  $X_s$  against actual antenna reactance at any frequency shows that the error at any point is well within the limits of engineering accuracy. In this

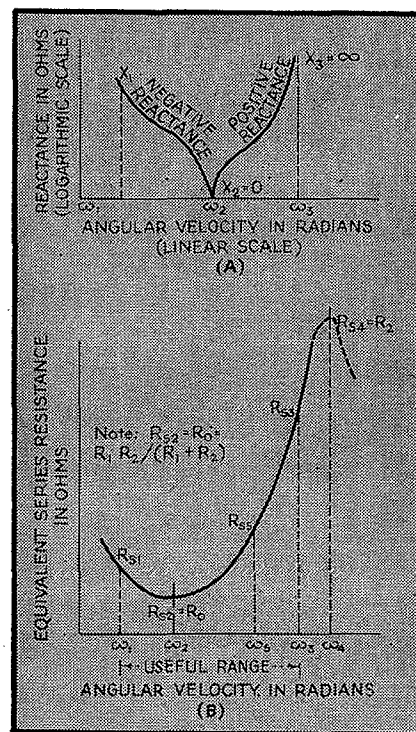


FIG. 3—Critical frequencies and their associated reactances (A) and resistances (B) of the antenna to be simulated are used to obtain values for the artificial antenna elements

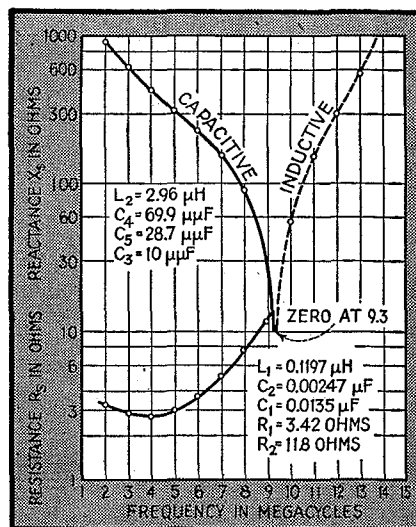


FIG. 4—An artificial antenna built from the design equations was tested and had these reactive and resistive characteristics; compare with Fig. 1

# ANTENNA

Design of a two-terminal, lumped-constant network that simulates, within a specified frequency band, the impedance variations of a single-wire antenna. The resulting artificial antenna can be used for tuning transmitters and for power measurements

per values of resistance and either inductive or capacitive reactance in series.

If  $I_A$  is the current flowing in the artificial antenna circuit, the power output of the transmitter would be  $P = I_A^2 R_s$ . If the values of  $X_s$  and  $R_s$  are correctly chosen,  $P$  will be true power output of the transmitter into the actual antenna at the same frequency.

## Single Series Circuits

Using fixed  $R$ - $C$  and  $L$ - $C$  combinations to simulate the antenna is accurate and simple, but lacks flexibility where a continuous frequency band must be covered. The circuit consists of either a fixed capacitor or coil in series with a non-reactive resistor. The constants of the inductor or capacitor and resistor are calculated from the given antenna reactance, radiation resistance, and frequency.

The fixed resistance is made equal to the antenna resistance. The series capacitance is  $C_s = 1/2\pi f X_A$  where  $X_A$  is negative. For positive values of  $X_A$  the antenna is inductive and  $L_s = X_A/2\pi f$ .

To provide an arrangement that is easier to work with when the frequency is frequently changed, the reactive and resistive components are made adjustable as, for example, a variable capacitor in series with a carbon composition resistor. When the antenna is inductive, a variable inductor is substituted for the capacitor. To further increase the versatility of the artificial antenna, both an inductor and a capacitor can be included in the series circuit, and a switch provided to short the unwanted element.

Although these adjustable circuits are theoretically sound, they seldom are satisfactory over a wide frequency range. In addition to their stray capacitance to ground, adjustable inductors have a high distributed capacitance. This may give rise to spurious resonances. Variable capacitors of high maximum capacitance must be extremely large to withstand the high r-f potentials.

Not only are there practical electrical difficulties, but there are the operational disadvantages which require the manipulation of two controls for each change in output frequency. An error in setting of either the reactor or resistor results in unreliable measurements and a loss of time in rechecking results.

## Composite Series Circuits

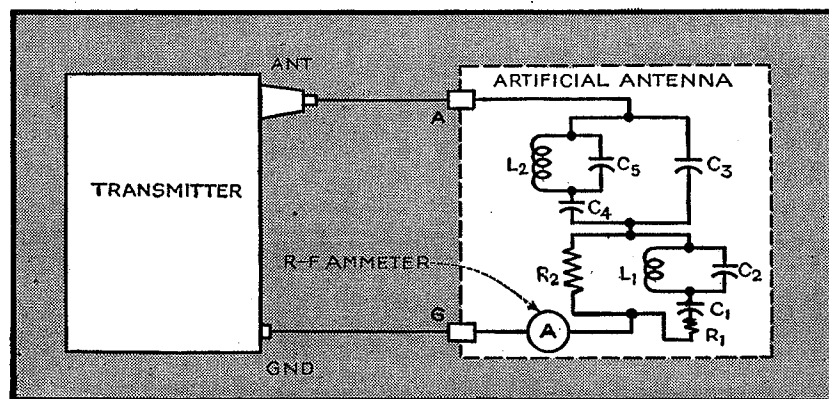
In contrast to the foregoing circuits that utilize variable components, the proposed artificial antenna is composed of fixed elements. When these elements are properly chosen, the reactance and resistance seen

at the terminals of the network (Fig. 2A) will match those of the actual antenna at every frequency within the assumed limits.

It is the plan of this paper to treat each portion separately and finally to show how they are connected in series to form the desired circuit. The portion marked  $X_s$  will automatically duplicate the series reactance of the given antenna, while  $R_s$  will produce the resistance variation with frequency. Although in practice it is not possible to isolate resistance and reactance completely, it is assumed that the equivalent series resistance of the reactance section is low enough to be negligible and the equivalent series reactance of the resistance section can be disregarded in comparison with that contributed by the reactive circuit.

## Network Equations

A combination of reactances which can have an equivalent series reactance variation with frequency similar to that shown in Fig. 1 is represented in Fig. 2B. The cor-



An r-f ammeter can be included in the artificial antenna for power measurements. Stray capacitances must be held to a minimum



# ARTIFICIAL

**A**RTIFICIAL ANTENNAS are necessary for testing variable-frequency radio equipment under conditions closely approximating those encountered in service. It is impractical to use an actual antenna in laboratory tests because radiated energy must be kept at a minimum, and it is usually inconvenient to precisely duplicate an antenna which is used in a special application such as on aircraft.

Although artificial antennas are used for both transmitters and receivers, the complexity of the antenna matching problem is not the same for both classes of equipment. This difference arises mainly because most receiver antenna circuits are untuned while transmitter output circuits, to deliver maximum power to the radiator, must be closely adjusted at each frequency. Because of the greater relative importance of the latter problem, this paper will concern itself with transmitting rather than receiving antennas.

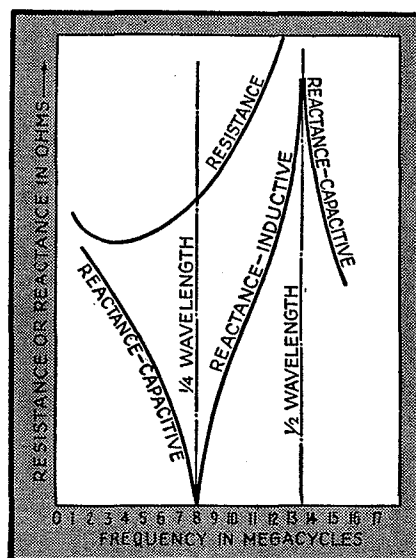
Need for a greatly improved artificial antenna for transmitters became apparent during the author's experience in the design and testing of aircraft communication transmitters in the medium to high-frequency band. Types of dummy load in wide use for this purpose,

**TABLE I—MINIMUM REQUIRED DATA FOR ARTIFICIAL ANTENNA DESIGN**

- (1) Reactance and resistance at the lower frequency limit.
- (2) Quarter-wavelength frequency and resistance.
- (3) Resistance at some critical frequency between upper frequency limit and quarter-wavelength frequency.
- (4) Resistance at the upper frequency limit.
- (5) Half-wavelength frequency. (If this frequency is not known, it can be assumed to be approximately 1.67 times the quarter-wavelength frequency. This constant is empirical and was selected as an average during a study of many fixed, single-wire antennas.)

By **SIDNEY WALD**

*Advanced Development Engineer  
RCA Victor Division  
Radio Corporation of America  
Camden, N. J.*

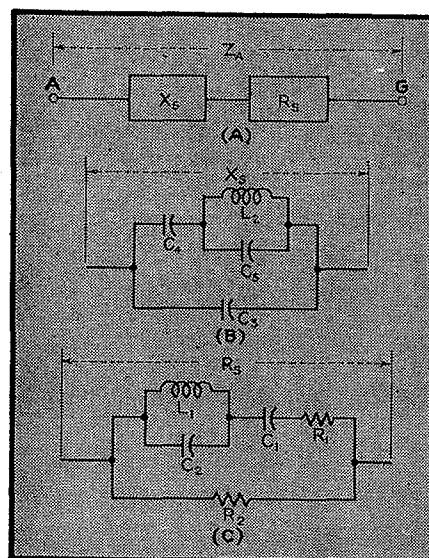


**FIG. 1—Typical impedance variation of an antenna of fixed length when the frequency is varied, showing reactance variation as a tangent function of frequency**

while perfectly satisfactory for use at a single frequency, resulted in much loss of time and were excessively bulky when applied to equipment having a frequency range of one to ten megacycles. To speed up variable-frequency tests, which at times had to be performed under reduced atmospheric pressure to simulate high-altitude flight conditions, a fixed network was designed which matched the actual antenna both for resistance and reactance at all frequencies.

## Basis for Design

While theoretical considerations in this paper are general, this discussion is limited to a band from approximately one to twenty mc. The antenna for which an equivalent circuit is desired is the single-conductor type operating against a ground. The configuration of the wire may be horizontal, vertical,



**FIG. 2—(A) Antenna impedance can be represented by variable series reactance and resistance. (B) The reactance component and (C) the resistance component can be simulated by lumped constants**

straight, or folded V. The quarter-wave resonant frequency of such a radiator usually lies between 5 and 10 mc. The characteristics of the antenna which must be known are given in Table I. A typical impedance characteristic is shown in Fig. 1.

To properly evaluate various requirements of a good dummy antenna, it is necessary to understand the way in which the impedance of an actual antenna varies with frequency. The equivalent circuit of an antenna is that of a series reactance  $X_s$  and series resistance  $R_s$  as shown in Fig. 2A. These two components of impedance change with frequency. The variations of  $X_s$  and  $R_s$  with frequency given in Fig. 1 apply to all types of antennas where size and geometry remain fixed, while the frequency is changed. To simulate such an antenna at a given frequency it is only necessary to connect the pro-

tions for military equipment involve much more difficult operating conditions, namely, temperatures ranging from  $-50^{\circ}$  to  $185^{\circ}\text{F}$  and humidities up to 100 percent prevailing in many cases over most of the year. Yet the designers of airborne and ground communication and electronic equipment demand the same high degree of performance over this greater temperature range and under these more damaging humidity conditions.

New capacitor designs for ground signal equipment, which normally uses low frequencies and relatively large capacitance units, required potting in hermetically-sealed containers. New designs for radio equipment, which uses the smaller molded units, required the introduction of new processes for stabilization over the wide temperature range and new materials for sealing the terminals in order to protect units from humidity.

A typical manufacturing and design problem was the change required to assure conformance with a severe humidity requirement placed on molded capacitors which were used on special military equipment. It was necessary at the start to check 100 percent of the molded mica capacitors. Subsequently, experiments proved that Neoprene cement applied to the leads greatly improved the yield

of capacitors and reduced the inspection costs. Further investigation showed that solutions of Vinylite VMCH and XYNC were even more effective in sealing the units against humidity and were easy to apply.

Manufacturing experience has shown that relatively poor stability and high values of temperature coefficient will result with the best quality of mica unless proper precautions are taken in the assembly, processing and molding of the units. Manufacturing methods were worked out to assure high stability with temperature and time for molded mica capacitors covering capacitances up to 20,000  $\mu\text{mf}$ . Some of these are made to a capacitance tolerance of  $\pm$  (0.5 percent +  $1\mu\text{mf}$ ), have a temperature coefficient of less than 15 parts per million per degree Fahrenheit over the temperature range of  $-50^{\circ}$  to  $+185^{\circ}\text{F}$ , and retrace to within 0.05 percent of the initial capacitance after repeated thermal cycling over this range. Such capacitors are being made because critical electronic equipment will not operate precisely without them.

#### Use of Mica Substitutes

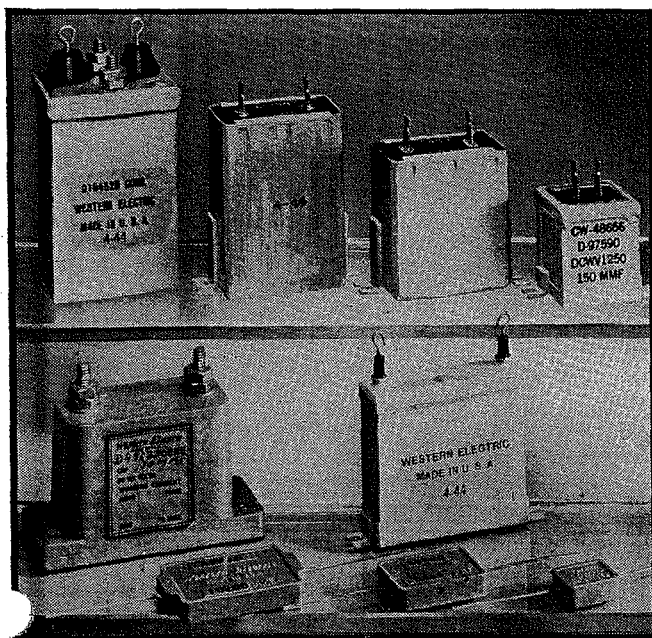
In view of some of the problems and processes discussed above, a brief statement concerning the use of paper and other

types of capacitors as alternates may be in order. The development and application of small molded, mineral-oil filled capacitors has been accomplished to a considerable extent. Designs have been devised and are in production that are both mechanically and electrically interchangeable with the mica types.

As has been well publicized, many synthetic micas have been developed and have helped insofar as they could replace mica in capacitors for special applications. However, to date none of the available alternative dielectric materials compare favorably in all characteristics with mica—even with the lower grades of mica that remain practically untouched.

Continued effort to make certain that the lower grades of mica are used wherever the requirements permit, and that the available stocks are processed with the great care this precious material deserves, will go far toward assuring an adequate supply of mica capacitors.

The improvements in the processes and facilities for manufacturing mica capacitors reported above are to a large extent based upon the unified efforts of the engineering staffs of the Western Electric Company and Bell Telephone Laboratories, which the author gratefully acknowledges.

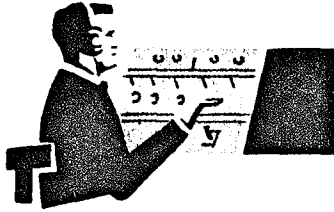


Representative examples of the nine types of molded and potted mica capacitors now being made by Western Electric



Adjusting finished silvered mica capacitors to exact capacitance value by scraping silver from the top lamination





# THE ENGINEER'S CORNER

FROM THE ENGINEERING DEPARTMENT OF THE NATIONAL ASSOCIATION OF BROADCASTERS  
1771 N STREET, N.W., WASHINGTON D. C. 20036 DECATUR 2-9300



## - TECHNICAL TALK -

### FUNDAMENTALS OF STANDARD BROADCAST ANTENNAS

Barnett F. Goldberg, P. E.  
Broadcast Engineering Consultant  
Columbia, S. C.

#### Introduction

Antennas are the basic components of any electronic system which depends upon free space as the propagation medium. The antenna is the connecting link between free space and the transmitter-receiver units of radio communications system. As such, it plays an essential role in determining the characteristics of the system in which it is used.

In many radio communication systems, such as those designed for navigational or direction-finding purposes, the operational characteristics of the system are designed around the directive properties of the antenna itself, while in other systems, such as that of the typical omnidirectional one-tower broadcast station, the antenna serves simply to efficiently radiate energy in all directions in order to provide a reasonably uniform groundwave coverage pattern.

In other broadcast systems, the antenna may be required to have additional properties such as highly directional horizontal pattern, while in still other cases both the vertical and horizontal patterns must be shaped to achieve certain types of coverage requirements and/or to eliminate interference to other broadcast stations on the same and adjacent channels.

Regardless of the particular system application, all antennas have certain basic properties in common and it is the purpose of this paper to discuss these "fundamentals" which are most often of particular interest to the fulltime Broadcast Engineer.

*Correct  
on Rm 5.  
in manuscript*

### Pertinent Antenna System Properties

The properties of standard broadcast antennas which are of maximum interest to the Broadcast Engineer are an antenna's (1) Horizontal and Vertical Radiation Pattern (2) its Circuitual Efficiency (3) its Peak and RMS Gain and (4) its Base and Common Point impedance. For passive linear antennas, which embraces all broadcast antenna systems, these properties are identical for either transmitting or receiving use, and as a direct consequence of the reciprocity theorem, we can expect any of these antenna systems to exhibit the same properties in the receiving mode as it does when used as a transmitting antenna. To those of you in the audience who have ever undertaken an antenna resistance measurement employing the RF Bridge Method, using a receiver and associated oscillator, this reciprocity action will be readily recognized!

### Horizontal Radiation Pattern

The horizontal radiation pattern of a standard broadcast antenna is probably one of its most basic properties in that it determines in concert with the station's output power what coverage will obtain for the station. For this reason it is the property that is usually specified first in a discussion of selecting among available broadcast antenna systems, especially in the Daytime or as we Consultants say, the Groundwave Case.

The basic radiation pattern of a Single Tower Broadcast Antenna System is omnidirectional in the Horizontal Plane, subject to only minor variations in circularity which arise from ground system considerations, method of feed, such as the shunt slant-wire feed, etc. The omnidirectional characteristic obtains from the fact that the radio frequency current flowing in the vertical tower element induces an equal radiation and induction field in all azimuths about the tower's periphery. By equal I do not mean equal in the sense of electric field intensity magnitude but rather equal in relative radiation strengths, as regard the respective azimuthal components.

Broadcast Antenna systems employing more than one active tower usually display horizontal directivity determined by the spacing, current ratios and relative phase magnitude of the currents supplied to the various tower elements.

Directional, multi-element antennas are used in two principal applications at Standard Broadcast Stations. They serve in the Daytime case to orient coverage towards desirable areas of population and to eliminate groundwave interference between and among stations on co and adjacent channels.

During the Night-time Broadcast hours such arrays are employed to suppress undersirable skywave interference among stations on a common channel and to some extent also to direct coverage contours into certain land areas where specified grades of Broadcast Service, i.e. Field Intensities, are required to meet particular Commission Technical Standards.

Directional Antennas also find application in certain "Transitional Time" or "Critical Hours " cases, time periods during which Class II Stations must protect their Class I co-channel occupants against undesirable Daytime Skywave Interference.

It is pertinent at this point to cite a fact not generally appreciated among some Broadcast Technicians to the effect that any antenna system which is horizontally directive will be directive also in the zenith or vertical plane. Please note the distinction "directive in the vertical plane" with the degree of vertical directivity different in the various azimuths about the array's center but related to the horizontal or azimuthal directivity.

We shall discuss this vertical directivity in more detail later on but it is important to introduce its concept at this point inasmuch as it is a factor in the design of Night-time directional antenna systems, where often the vertical radiation patterns with azimuth are of more singular importance than are the resultant groundwave horizontal patterns which are obtained in these designs. In fact, it is safe to say that the groundwave pattern is more the consequence of a required vertical directivity pattern vs specified azimuth than is any usual Night-time requirement on groundwave horizontal directivity alone!

Summing up our observations on antenna horizontal directivity then we should note that during the Daytime Case the principal use of a horizontally directive antenna obtains usually for the purpose of controlling groundwave interference and/or coverage criteria while for the Night-time case the use of a directive antenna lies in the Antenna's ability to produce certain required vertical patterns which are necessary to suppress radiation via the skywave towards co and adjacent channel stations.

#### Vertical Radiation Pattern

Let us now turn our attention to an antenna system's vertical directivity. Figure 1 of this Paper shows the Vertical Radiation patterns produced by a number of popular antenna systems. Referring to this Figure we can compare a Quarter, Half-wave and other popularly sized vertical radiators with respect to their respective Vertical Radiation patterns.

We should note that for the sake of rendering this comparison most effective we have assumed that all systems radiate the same inverse field in the horizontal plane, that is 100 mv/m at One Mile. In this respect it is particularly pertinent to cite the fact that these antennas have different basic groundwave radiation efficiencies, as we will discuss later, but for the sake of our present discussion, let us assume that we have fed each antenna that amount of power which is required to make it radiate an inverse field of 100 mv/m at One Mile unattenuated (in the Horizontal Plane).

Our immediate attention is called to the fact that comparing all antennas on a common groundwave Inverse Field Basis, the taller antennas radiate a proportionately smaller amount of radiation above the horizontal plane. From this we can deduce that all things being equal, with a constant amount of power flowing into a particular antenna system, the taller structures should be more efficient in the production of a groundwave signal for a given radio frequency power input, which indeed they are!

A second conclusion which obtains from a comparison of the various antennas is the vertical null and secondary lobe effects present in antennas above one-half a wavelength in height. While the explanation of this phenomena requires some mathematics and a knowledge of the current distribution in the taller structures, suffice to say here that structures taller than one-half a wavelength exhibit a vertical directive effect such as would be produced by a series of quarter-wave radiators stacked one on top of another, somewhat in the fashion that Mobile Communications and FM Antennas obtain greater Horizontal Gain over conventional dipole systems through vertical stacking, or what might be more properly called increased vertical aperture.

The singular importance of Figure 1 is to show how antenna vertical dimensions, measured in fractions of a wavelength, affect the distribution of radiated energy in the vertical plane, with the taller structures concentrating a greater amount of this energy in the planes immediately adjacent to the ground plane.

While the majority of us deal with the conventional quarter-wave omnidirectional antenna there are certain situations, especially Class I stations, where the taller structures are used to obtain a desirable "Anti-Fading Characteristic", wherein cancellation of the groundwave signal via outer extremity transitional skywave reflection is avoided by proper design of the station's vertical radiation pattern, even where only a single radiating element is employed as the station's Daytime antenna.

Our previous discussion should sensitize you to the effect of antenna height on antenna vertical directivity and to the use of this vertical directivity to achieve certain desirable coverage characteristics during the transitional times of the Daytime Broadcast day.

We are now ready to look into the question of Antenna efficiency.

#### Antenna Efficiency

The question is often raised as to what is meant by the term Antenna Root Mean Square (RMS) Field Intensity, especially as the term is used in ordinary Broadcast consulting work where it is usually expressed in Millivolts per Meter Unattenuated at One Mile for a specified Antenna Input Power, usually One Kilowatt.

All antenna systems are referenced to some common rating base for the purpose of evaluating their respective performance. We of the Broadcast fraternity often speak of a particular antenna system as radiating so many Millivolts per Meter Unattenuated at One Mile for a certain, usually specified Antenna Power input.

Probably such jargon obtains from the constant use of the Commission's Graph of practical Antenna Efficiency, Section 73.190 of the Rules, Graphical figure 8, wherein a presentation is made of typical antenna efficiency vs tower height assuming a standard 120 radial quarter-wave ground system with the various radials distributed uniformly about the single antenna structure's base.

This Commission figure is appended here as Exhibit Figure 2 and if we consult it we shall note that for the typical range of antenna heights, usually from 0.15 to 0.60 wavelength, this efficiency ranges from about a low of 175 mv/m to a high of 274 mv/m unattenuated at One Mile for One Kilowatt of Antenna input.

Most of us familiar with the standard 88 degree tower recognize the figure of 189 mv/m, as taken from this curve, as the average efficiency for the most commonly used single tower AM Radiator.

The mathematical derivation of this curve is quite complex and beyond the scope of this paper; however, suffice to say that understanding how to use this curve is of more practical importance than is an understanding of its derivation for our present purpose.

Returning to Antenna Efficiency, let us turn our attention to a third Graph appended to this Paper, Graph 3 which shows an efficiency comparison among several of the more standard reference and practical antenna systems. Your especial attention is called to the "Uniform Spherical Radiator" which the theorist refers to as an Isotropic or a

Point Source radiator. Such a radiator does not exist in any practical form but you should recognize it as the familiar "light bulb" concept. This is "a reference antenna" which would radiate RF just as a conventional light bulb radiates light spherically in all directions without either vertical or horizontal directivity.

This antenna is seen to produce 107.6 mv/m at One Mile unattenuated in all directions and its significance is that all antenna systems directive in either or both planes can be directly compared with it. Let us make such a comparison by looking at several of the other reference antennas shown in Figure 3. Look for instance at the Half-wave antenna. Here we have an antenna efficiency of 137.8 mv/m and it is important to note that the increase in horizontal gain (not efficiency) obtains from the Half-wave antenna's horizontal and vertical directivity!

Let us now go to a Quarter-wave Vertical Antenna, the third Figure Block on the right-hand side of Figure 3. Here we see for this 90° radiator a theoretical efficiency of 194.9 mv/m for One Kilowatt at One Mile Unattenuated.

How do we compare this with the Commission's 195 mv/m figure? Return to Figure 2, the Commission's Chart and notice that the theoretical efficiency of a Quarter-wave antenna is 195mv/m but a practical antenna system employing 120 Quarterwave ground radials varies downward from this theoretical efficiency by some 6 mv/m, or about 189 mv/m for One Kilowatt of Antenna Input!

It is interesting to note from the comparison of these two Charts just how good modern antenna systems are efficiency-wise. A conventional Quarter-wave antenna system is just short of 97% efficient! The loss in the practical antenna system obtains from the real ground system and other IR losses inherent in it.

Our discussion of the foregoing parameter should demonstrate how antenna systems are compared one to another and to what degree the present state of the art is with respect to overall antenna efficiency.

We are now ready to discuss the phenomena of Antenna Gain external and separate from antenna efficiency in the sense of power input vs power output from a given antenna system.

#### Antenna Gain

The gain of an antenna is a basic property which is frequently used as a figure of merit; however, as we have discussed previously, one must not be misled into believing that Antenna Gain alone is the sole determining factor in an overall antenna system performance.

Antenna gain is commonly defined as the ratio of the maximum radiation intensity in a given direction to the maximum radiation intensity produced in the same direction by a reference antenna with the same power input.

The reference radiator most commonly used is the Isotropic Radiator which we discussed previously; however, it need not be that particular antenna and antenna gain may be given in terms of any conveniently selected reference antenna so long as the reference antenna is clearly stated.

In Broadcast work, the reference most commonly used is the range of vertical antenna efficiency - height characteristics summarized in Section 73.189 (2) (i) through 73.189 (2) (iii) respectively of the Rules. Briefly stated, these allow for Antenna Efficiencies from 150 mv/m minimum for a Class IV station to a minimum of 225 mv/m for a Class I station, based on One Kilowatt of Antenna Power Input to the system.

Since gain is associated with a concentration of radiated energy, high values of gain are correspondingly associated with narrow beamwidths! For antennas with no internal losses, the Gain rating is the same as the antennas' Directivity Factor. However, while Directivity can be computed from either theoretical considerations or from measured radiation patterns, the gain of an antenna is almost always determined by a direct comparison measurement made against some form of a standard reference antenna.

In the directional broadcast array, usually one tower in the array is selected as this standard and the familiar Non-Directional Day-time Antenna Proof of Performance is run from it, as a prerequisite to the later Night-time Directional Proof.

It may be well to insert here the concept of "Effective Antenna Area or Antenna Aperture" as this factor relates to antenna gain. The effective area is of interest when it is desired to compute the energy collected by a particular antenna as this collection would be related to the energy picked up by a reference antenna exposed to the same field intensity level. A little thought here will reveal that antenna aperture is really a measure of antenna gain or the ability of the antenna to intercept a given amount of energy passing through its intercept area.

The above concepts together with our prior discussions of Vertical and Horizontal Patterns, Antenna Efficiency (losses) and Antenna Gain lead us to our final consideration, that of delivering power into and out of an antenna system. Since we are principally Broadcast Engineers, let us confine our discussion to the principle of getting energy into our antenna systems and efficiently radiating it into the areas of principal concern, i.e. along the ground.

214  
New 014

### Antenna Impedance

The input impedance of any antenna system is of considerable importance to the Antenna Systems Engineer since it directly affects the efficiency of energy transfer from the transmitter to the antenna proper.

The overall input impedance of an antenna system depends not only on the impedance of the individual antenna elements comprising the system but on the mutual impedance existing between the elements themselves and the transmission lines and coupling components interconnecting the various system elements.

The overall design of a complex antenna system will therefore be governed as much by these details as by the antenna elements themselves!

If the system is complicated, adequate bandwidth becomes a prime consideration and it is essential that all of the antenna system's components be chosen so that favorable impedance properties exist amongst the various inter-related components. This is sometimes a very difficult problem in which only the experience and ingenuity of an experienced Broadcast Consultant can spell the difference between a successful array and one which is never quite up to par.

While the tune-up of a non-directional antenna system looks deceptively simple, even here, tune-ups attempted with inadequate attention to coupling network details lead invariably to high harmonic emissions, unnecessary losses and unfavorable operating tank circuit constants.

While time does not permit us to go into the subject of antenna impedance matching, let us briefly look at a typical set of antenna base impedance constants as is shown in Figure 4 of this Paper.

Note how the resistance of a short antenna compares with that of a longer antenna. Note too the large capacitive reactance of a short antenna and how as an antenna is lengthened towards One Quarter wavelength, it goes through electrical resonance (pure resistive input) at 88 degrees physical height and then becomes inductively reactive as it is increased beyond 88 physical degrees.

The significance of these single-tower impedance properties sheds some light on why physically short antennas do not enjoy wide acceptance in the Broadcast Industry, not because they are inefficient as radiators but rather because their bandwidths are severely limited by the high reactance values present, coupled with the natural IR losses which obtain in view of the high currents which must of necessity be passed into the antenna to produce the requisite power output from it.



Conclusions and Summary

This paper has attempted to describe and discuss some of the more pertinent properties of Standard Broadcast Antenna systems. While emphasis has been placed on antenna systems specifically designed for the Standard Broadcast Band, much of the technical information given here applies to all types of antenna systems, regardless of the respective antenna's end application.

It is hoped that some of the information and observations presented here have been stimulating and thought provoking to you and that as an end result of this presentation you might be motivated to enlarge your individual understanding of this subject.

XXX